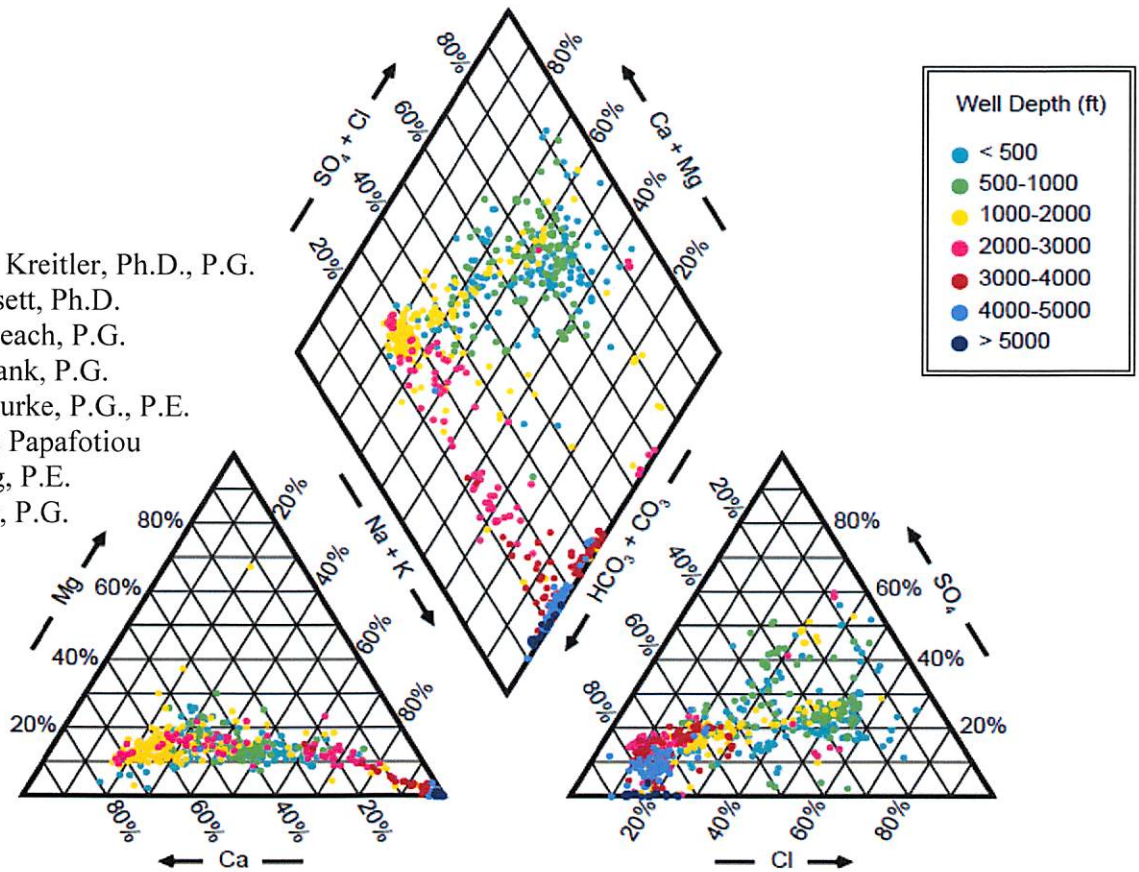


# Evaluation of Hydrochemical and Isotopic Data in Groundwater Management Areas 11, 12 and 13

by  
 Charles W. Kreitler, Ph.D., P.G.  
 Randy Bassett, Ph.D.  
 James A. Beach, P.G.  
 Leigh Symank, P.G.  
 Dave O'Rourke, P.G., P.E.  
 Alexandros Papafotiou  
 John Ewing, P.E.  
 Van Kelley, P.G.



**Texas Water**  
**Development Board**

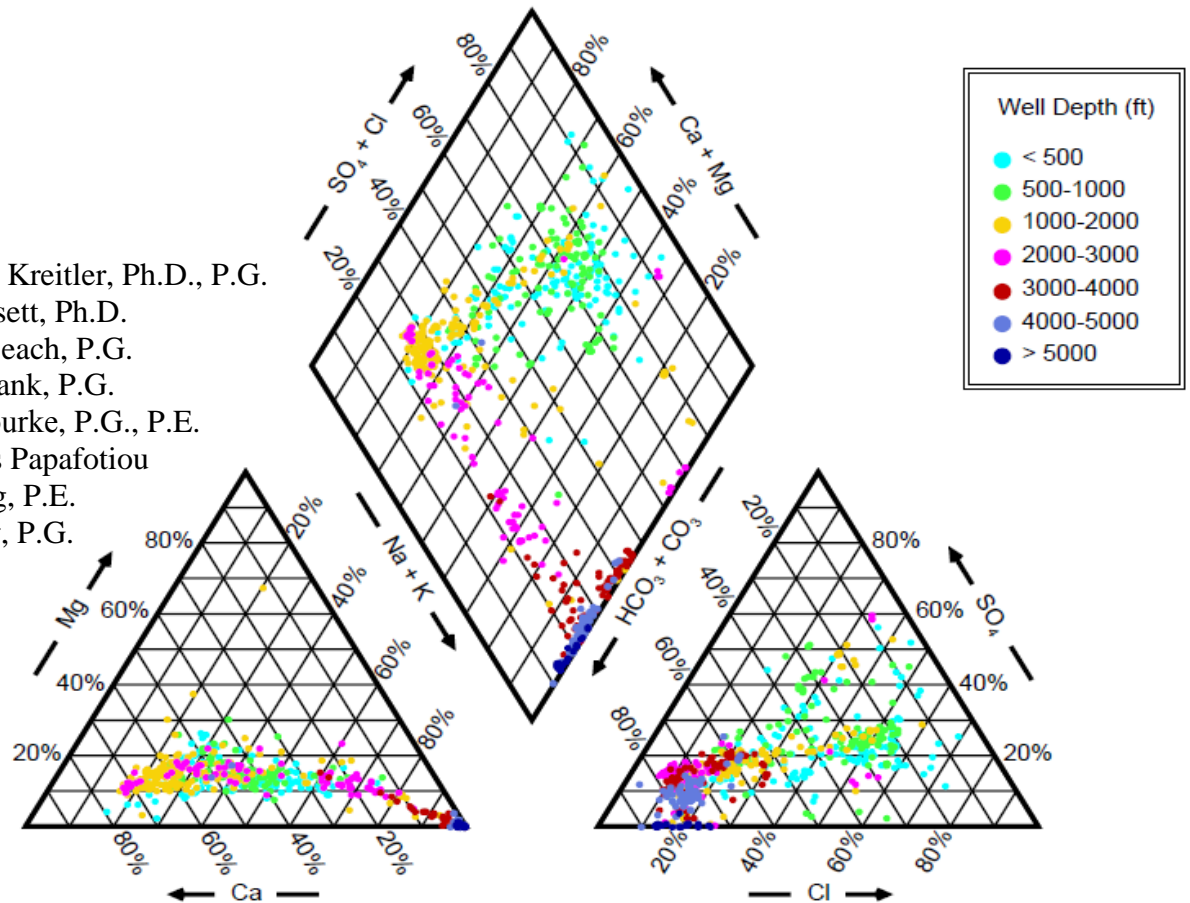
1700 Congress Avenue  
 Austin, Texas 78701

2014 AUG 18 PM 3:10  
 REACT ADMINISTRATION

July 2013

# Evaluation of Hydrochemical and Isotopic Data in Groundwater Management Areas 11, 12 and 13

by  
Charles W. Kreitler, Ph.D., P.G.  
Randy Bassett, Ph.D.  
James A. Beach, P.G.  
Leigh Symank, P.G.  
Dave O'Rourke, P.G., P.E.  
Alexandros Papafotiou  
John Ewing, P.E.  
Van Kelley, P.G.



**Texas Water**  
**Development Board**

1700 Congress Avenue  
Austin, Texas 78701

July 2013

*This page is intentionally blank.*



# Texas Water Development Board

## **Evaluation of Hydrochemical and Isotopic Data in Groundwater Management Areas 11, 12 and 13**

by  
Charles W. Kreitler, Ph.D., P.G.  
James A. Beach, P.G.  
Leigh Symank, P.G.  
Dave O'Rourke, P.G., P.E.  
LBG-Guyton Associates

Randy Basset, Ph.D.  
Tetra Tech

Alexandros Papafotiou  
John Ewing, P.E.  
Van Kelley, P.G.  
Intera

July 2013

*This page is intentionally blank.*

## Geoscientist and Engineering Seal

This report documents the work of the following Licensed Texas Geoscientists and Licensed Texas Professional Engineers:

Charlie W. Kreitler, Ph.D., P.G.

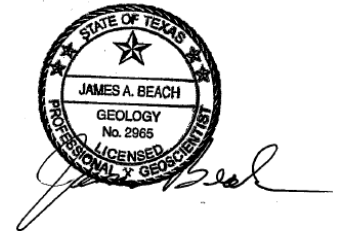
Dr. Kreitler was responsible for hydrochemical and isotope analysis and oversight of the project.

*Charles W. Kreitler*



James A. Beach, P.G.

Mr. Beach was the Project Manager and responsible for evaluating how the hydrochemical and isotope results affect conceptual models of the GAMs.



David O'Rourke, P.G., P.E.

Mr. O'Rourke organized and directed the field sampling effort to collect primary groundwater chemistry data to support the project.



John E. Ewing, P.E.

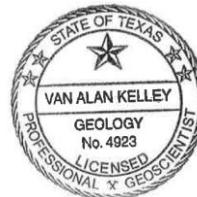
Mr. Ewing was responsible for performing GAM runs.



*J. E. Ewing*

Van A. Kelley, P.G.

Mr. Kelley provided guidance and oversight of GAM runs.



*Van Kelley*

*This page is intentionally blank.*

## Table of Contents

1	Executive Summary .....	1
2	Introduction .....	7
3	Study Area .....	11
4	Data Evaluation .....	17
4.1	TWDB Groundwater Database .....	17
4.2	Newly Collected Data .....	18
5	Hydrogeologic Setting.....	21
5.1	Hydrostratigraphy .....	22
5.2	Regional Groundwater Flow .....	26
5.3	Recharge to Discharge .....	30
5.4	Hydraulic Properties .....	31
5.5	Overview and Summary .....	32
6	Hydrochemical and Isotopic Approach to Understanding Aquifer Dynamics.....	33
7	Hydrochemical and Isotopic Evaluation .....	41
7.1	Northeast Transect .....	42
7.1.1	General Geochemical Trends.....	42
7.1.2	Geochemical Modeling.....	100
7.2	Central Transect .....	115
7.2.1	General Geochemical Trends.....	124
7.2.2	Geochemical Modeling.....	187
7.3	Gonzales Transect.....	197
7.3.1	General Geochemical Trends.....	197
7.3.2	Geochemical Modeling.....	250
7.4	South Transect .....	270
7.4.1	General Geochemical Trends.....	270
7.4.2	Geochemical Modeling.....	330
7.4.3	Brackish Lower Wilcox Group.....	350
8	Numerical Modeling for Central and Gonzales Transects .....	363
8.1	Overview of Existing Models .....	363
8.1.1	Yegua-Jackson Aquifer Groundwater Availability Model .....	365
8.1.2	Queen City and Sparta Aquifers Groundwater Availability Model.....	369
8.2	Model Extraction and Design .....	373
8.2.1	Development of the Gonzales Transect Model.....	375
8.2.2	Development of the Central Transect Model.....	378
8.3	Modeling Approach .....	382
8.4	Gonzales Transect Model .....	392
8.4.1	Results of Flow Simulations .....	392
8.4.2	Age and Sensitivity Analysis .....	402
8.5	Central Transect Model.....	413
8.5.1	Results of Flow Simulations .....	413
8.5.2	Age and Sensitivity Analysis .....	424
8.6	Modeling Discussion .....	435
9	Conclusions .....	439
10	Acknowledgements .....	445
11	References .....	447

*This page is intentionally blank.*

## List of Figures

Figure 2-1.	Location of the major aquifer in Groundwater Management Areas (GMAs) 11, 12 and 13.	8
Figure 2-2.	Location of the minor aquifers in Groundwater Management Areas (GMAs) 11, 12 and 13.	9
Figure 2-3.	Location of the existing TWDB Groundwater Availability Models in Groundwater Management Areas (GMAs) 11, 12 and 13.	10
Figure 3-1.	Groundwater Management Areas and counties that contain the data for the study area transects.	13
Figure 3-2.	Cross-section in Brazos and Robertson counties showing dipping nature of the Carrizo-Wilcox Aquifer and other Texas coastal aquifer systems (Note: transects B-B' through F-F' are not addressed in this study).	14
Figure 3-3.	Average annual precipitation in Texas (PRISM, 2000).	15
Figure 5-1.	Map of major faults and structural features for the Texas Coastal Plain and East Texas Embayment. Faults modified from Ewing (1990). Structure axes modified from Guevara and Garcia (1972), Galloway (1982), and Galloway and others (2000).	22
Figure 5-2.	Generalized stratigraphic section for the Carrizo-Wilcox Aquifer in Texas (after Ayers and Lewis, 1985; Hamlin, 1988; Kaiser and others, 1978).	26
Figure 5-3.	Simulated drawdown from the predevelopment to 1990 in the Carrizo-Wilcox Aquifer (Deeds and others, 2009).	29
Figure 7-1.	Data distribution of wells with outcrop and downdip extent (up to 3,000 milligrams per liter total dissolved solids) of the Carrizo-Wilcox, Queen City, Sparta, and Yegua-Jackson aquifers in the Northeast Transect, Groundwater Management Area 11.	46
Figure 7-2.	Well depths measured from land surface in feet in the Carrizo-Wilcox Aquifer, Northeast Transect, Groundwater Management Area (GMA) 11.	47
Figure 7-3.	Potentiometric surface of the Carrizo-Wilcox Aquifer (1936-1976) (Figure 13 from Fogg and Kreitler, 1982).	48
Figure 7-4.	Piper diagram showing chemistry of the Carrizo-Wilcox Aquifer wells in the Northeast Transect by well depth measured from land surface in feet (ft).	49
Figure 7-5.	Bicarbonate ( $\text{HCO}_3$ ) versus sodium (Na) measured in milliequivalents per liter (meq/L), Carrizo-Wilcox Aquifer, Northeast Transect, Groundwater Management Area 11.	50
Figure 7-6.	Sodium (Na) versus calcium (Ca) measured in milliequivalents per liter (meq/L), Carrizo-Wilcox Aquifer, Northeast Transect, Groundwater Management Area 11.	50
Figure 7-7.	Bicarbonate ( $\text{HCO}_3$ ) versus calcium (Ca) measured in milliequivalents per liter (meq/L), Carrizo-Wilcox Aquifer, Northeast Transect, Groundwater Management Area 11.	51
Figure 7-8.	pH versus bicarbonate ( $\text{HCO}_3$ ) measured in milliequivalents per liter (meq/L), Carrizo-Wilcox Aquifer, Northeast Transect, Groundwater Management Area 11.	51
Figure 7-9.	pH versus sodium (Na) measured in milliequivalents per liter (meq/L), Carrizo-Wilcox Aquifer, Northeast Transect, Groundwater Management Area 11.	52
Figure 7-10.	Sulfate ( $\text{SO}_4$ ) versus bicarbonate ( $\text{HCO}_3$ ) measured in milliequivalents per liter (meq/L), Carrizo-Wilcox Aquifer, Northeast Transect, Groundwater Management Area 11.	52
Figure 7-11.	Chloride (Cl) versus sodium (Na) measured in milliequivalents per liter (meq/L), Carrizo-Wilcox Aquifer, Northeast Transect, Groundwater Management Area 11.	53
Figure 7-12.	Chloride (Cl) versus bicarbonate ( $\text{HCO}_3$ ) measured in milliequivalents per liter (meq/L), Carrizo-Wilcox Aquifer, Northeast Transect, Groundwater Management Area 11.	53

Figure 7-13. Depth measured from land surface in feet (ft) versus sulfate (SO <sub>4</sub> ) measured in milliequivalents per liter (meq/L), Carrizo-Wilcox Aquifer, Northeast Transect, Groundwater Management Area 11.....	54
Figure 7-14. Depth measured from land surface in feet (ft) versus calcium (Ca) measured in milliequivalents per liter (meq/L), Carrizo-Wilcox Aquifer, Northeast Transect, Groundwater Management Area 11.....	54
Figure 7-15. Calcium concentrations measured in milliequivalents per liter (meq/L) in the Carrizo-Wilcox Aquifer, Northeast Transect, Groundwater Management Area (GMA) 11.....	55
Figure 7-16. Depth measured from land surface in feet (ft) versus bicarbonate (HCO <sub>3</sub> ) measured in milliequivalents per liter (meq/L), Carrizo-Wilcox Aquifer, Northeast Transect, Groundwater Management Area 11.....	56
Figure 7-17. Depth measured from land surface in feet (ft) versus pH, Carrizo-Wilcox Aquifer, Northeast Transect, Groundwater Management Area 11.....	56
Figure 7-18. Depth measured from land surface in feet (ft) versus sodium (Na) measured in milliequivalents per liter (meq/L), Carrizo-Wilcox Aquifer, Northeast Transect, Groundwater Management Area 11.....	57
Figure 7-19. Depth measured from land surface in feet (ft) versus chloride (Cl) measured in milliequivalents per liter (meq/L), Carrizo-Wilcox Aquifer, Northeast Transect, Groundwater Management Area 11.....	57
Figure 7-20. Depth measured from land surface in feet (ft) versus total dissolved solids (TDS) measured in parts per million (ppm), Carrizo-Wilcox Aquifer, Northeast Transect, Groundwater Management Area 11.....	58
Figure 7-21. Well depths measured from land surface in feet in the Queen City Aquifer, Northeast Transect, Groundwater Management Area (GMA) 11.....	62
Figure 7-22. Water level elevations from 1970 to 2010 measured in feet above mean sea level (ft AMSL) in the Queen City Aquifer, Northeast Transect, Groundwater Management Area (GMA) 11.	63
Figure 7-23. Piper diagram showing chemistry of the Queen City Aquifer wells in the Northeast Transect by well depth measured from land surface in feet (ft).....	64
Figure 7-24. Bicarbonate (HCO <sub>3</sub> ) versus sodium (Na) measured in milliequivalents per liter (meq/L), Queen City Aquifer, Northeast Transect, Groundwater Management Area 11.....	65
Figure 7-25. Sodium (Na) versus calcium (Ca) measured in milliequivalents per liter (meq/L), Queen City Aquifer, Northeast Transect, Groundwater Management Area 11.....	65
Figure 7-26. Bicarbonate (HCO <sub>3</sub> ) versus calcium (Ca) measured in milliequivalents per liter (meq/L), Queen City Aquifer, Northeast Transect, Groundwater Management Area 11.....	66
Figure 7-27. pH versus bicarbonate (HCO <sub>3</sub> ) measured in milliequivalents per liter (meq/L), Queen City Aquifer, Northeast Transect, Groundwater Management Area 11.....	66
Figure 7-28. pH versus sodium (Na) measured in milliequivalents per liter (meq/L), Queen City Aquifer, Northeast Transect, Groundwater Management Area 11.....	67
Figure 7-29. Chloride (Cl) versus sodium (Na) measured in milliequivalents per liter (meq/L), Queen City Aquifer, Northeast Transect, Groundwater Management Area 11.....	67
Figure 7-30. Chloride (Cl) versus bicarbonate (HCO <sub>3</sub> ) measured in milliequivalents per liter (meq/L), Queen City Aquifer, Northeast Transect, Groundwater Management Area 11.....	68
Figure 7-31. Sulfate (SO <sub>4</sub> ) versus bicarbonate (HCO <sub>3</sub> ) measured in milliequivalents per liter (meq/L), Queen City Aquifer, Northeast Transect, Groundwater Management Area 11.....	68

Figure 7-32. Depth measured from land surface in feet (ft) versus nitrate (NO <sub>3</sub> ) measured in milligrams per liter (mg/L), Queen City Aquifer, Northeast Transect, Groundwater Management Area 11.	69
Figure 7-33. Depth measured from land surface in feet (ft) versus sulfate (SO <sub>4</sub> ) measured in milliequivalents per liter (meq/L), Queen City Aquifer, Northeast Transect, Groundwater Management Area 11.	69
Figure 7-34. Depth measured from land surface in feet (ft) versus calcium (Ca) measured in milliequivalents per liter (meq/L), Queen City Aquifer, Northeast Transect, Groundwater Management Area 11.	70
Figure 7-35. Calcium concentrations measured in milliequivalents per liter (meq/L) in the Queen City Aquifer, Northeast Transect, Groundwater Management Area (GMA) 11.	71
Figure 7-36. Depth measured from land surface in feet (ft) versus pH, Queen City Aquifer, Northeast Transect, Groundwater Management Area (GMA) 11.	72
Figure 7-37. Depth measured from land surface in feet (ft) versus bicarbonate (HCO <sub>3</sub> ) measured in milliequivalents per liter (meq/L), Queen City Aquifer, Northeast Transect, Groundwater Management Area 11.	72
Figure 7-38. Depth measured from land surface in feet (ft) versus sodium (Na) measured in milliequivalents per liter (meq/L), Queen City Aquifer, Northeast Transect, Groundwater Management Area 11.	73
Figure 7-39. Depth measured from land surface in feet (ft) versus chloride (Cl) measured in milliequivalents per liter (meq/L), Queen City Aquifer, Northeast Transect, Groundwater Management Area 11.	73
Figure 7-40. Depth measured from land surface in feet (ft) versus total dissolved solids (TDS) measured in parts per million (ppm), Queen City Aquifer, Northeast Transect, Groundwater Management Area 11.	74
Figure 7-41. Well depths measured from land surface in feet in the Sparta Aquifer, Northeast Transect, Groundwater Management Area (GMA) 11.	77
Figure 7-42. Water level elevations from 1960 to 2010 measured in feet above mean sea level (ft AMSL) in the Sparta Aquifer, Northeast Transect, Groundwater Management Area (GMA) 11.	78
Figure 7-43. Piper diagram showing chemistry of the Sparta Aquifer wells in the Northeast Transect by well depth measured from land surface in feet (ft).	79
Figure 7-44. Bicarbonate (HCO <sub>3</sub> ) versus sodium (Na) measured in milliequivalents per liter (meq/L), Sparta Aquifer, Northeast Transect, Groundwater Management Area 11.	80
Figure 7-45. Sodium (Na) versus calcium (Ca) measured in milliequivalents per liter (meq/L), Sparta Aquifer, Northeast Transect, Groundwater Management Area 11.	80
Figure 7-46. Bicarbonate (HCO <sub>3</sub> ) versus calcium (Ca) measured in milliequivalents per liter (meq/L), Sparta Aquifer, Northeast Transect, Groundwater Management Area 11.	81
Figure 7-47. pH versus bicarbonate (HCO <sub>3</sub> ) measured in milliequivalents per liter (meq/L), Sparta Aquifer, Northeast Transect, Groundwater Management Area 11.	81
Figure 7-48. pH versus sodium (Na) measured in milliequivalents per liter (meq/L), Sparta Aquifer, Northeast Transect, Groundwater Management Area 11.	82
Figure 7-49. Chloride (Cl) versus sodium (Na) measured in milliequivalents per liter (meq/L), Sparta Aquifer, Northeast Transect, Groundwater Management Area 11.	82
Figure 7-50. Chloride (Cl) versus bicarbonate (HCO <sub>3</sub> ) measured in milliequivalents per liter (meq/L), Sparta Aquifer, Northeast Transect, Groundwater Management Area 11.	83

Figure 7-51. Sulfate (SO <sub>4</sub> ) versus bicarbonate (HCO <sub>3</sub> ) measured in milliequivalents per liter (meq/L), Sparta Aquifer, Northeast Transect, Groundwater Management Area 11.....	83
Figure 7-52. Depth measured from land surface in feet (ft) versus nitrate (NO <sub>3</sub> ) measured in milligrams per liter (mg/L), Sparta Aquifer, Northeast Transect, Groundwater Management Area 11.	84
Figure 7-53. Depth measured from land surface in feet (ft) versus sulfate (SO <sub>4</sub> ) measured in milliequivalents per liter (meq/L), Sparta Aquifer, Northeast Transect, Groundwater Management Area 11.....	84
Figure 7-54. Depth measured from land surface in feet (ft) versus calcium (Ca) measured in milliequivalents per liter (meq/L), Sparta Aquifer, Northeast Transect, Groundwater Management Area 11.....	85
Figure 7-55. Depth measured from land surface in feet (ft) versus sodium (Na) measured in milliequivalents per liter (meq/L), Sparta Aquifer, Northeast Transect, Groundwater Management Area 11.....	85
Figure 7-56. Depth(measured from land surface in feet (ft) versus pH, Sparta Aquifer, Northeast Transect, Groundwater Management Area 11. ....	86
Figure 7-57. Depth measured from land surface in feet (ft) versus chloride (Cl) measured in milliequivalents per liter (meq/L), Sparta Aquifer, Northeast Transect, Groundwater Management Area 11.....	86
Figure 7-58. Depth measured from land surface in feet (ft) versus total dissolved solids (TDS) measured in parts per million (ppm), Sparta Aquifer, Northeast Transect, Groundwater Management Area 11.....	87
Figure 7-59. Well depths measured from land surface in feet in the Yegua Formation of the Yegua-Jackson Aquifer, Northeast Transect, Groundwater Management Area (GMA) 11.....	90
Figure 7-60. Water level elevations from 1975 to 2010 measured in feet above mean seal level (ft AMSL) in the Yegua Formation of the Yegua-Jackson wells, Northeast Transect, Groundwater Management Area (GMA) 11.....	91
Figure 7-61. Piper diagram showing chemistry of Yegua Formation of the Yegua-Jackson Aquifer wells in the Northeast Transect by well depth measured from land surface in feet (ft)..	92
Figure 7-62. Bicarbonate (HCO <sub>3</sub> ) versus sodium (Na) measured in milliequivalents per liter (meq/L), Yegua Formation of the Yegua-Jackson Aquifer, Northeast Transect, Groundwater Management Area 11.....	93
Figure 7-63. Sodium (Na) versus calcium (Ca) measured in milliequivalents per liter (meq/L), Yegua Formation of the Yegua-Jackson Aquifer, Northeast Transect, Groundwater Management Area 11.	93
Figure 7-64. Bicarbonate (HCO <sub>3</sub> ) versus calcium (Ca) measured in milliequivalents per liter (meq/L), Yegua Formation of the Yegua-Jackson Aquifer, Northeast Transect, Groundwater Management Area 11.....	94
Figure 7-65. pH versus bicarbonate (HCO <sub>3</sub> ) measured in milliequivalents per liter (meq/L), Yegua Formation of the Yegua-Jackson Aquifer, Northeast Transect, Groundwater Management Area 11.	94
Figure 7-66. pH versus sodium (Na) measured in milliequivalents per liter (meq/L), Yegua Formation of the Yegua-Jackson Aquifer, Northeast Transect, Groundwater Management Area 11.	95

Figure 7-67. Chloride (Cl) versus sodium (Na) measured in milliequivalents per liter (meq/L), Yegua Formation of the Yegua-Jackson Aquifer, Northeast Transect, Groundwater Management Area 11.	95
Figure 7-68. Chloride (Cl) versus bicarbonate (HCO <sub>3</sub> ) measured in milliequivalents per liter (meq/L), Yegua Formation of the Yegua-Jackson Aquifer, Northeast Transect, Groundwater Management Area 11.	96
Figure 7-69. Sulfate (SO <sub>4</sub> ) versus bicarbonate (HCO <sub>3</sub> ) measured in milliequivalents per liter (meq/L), Yegua Formation of the Yegua-Jackson Aquifer, Northeast Transect, Groundwater Management Area 11.	96
Figure 7-70. Depth measured from land surface in feet (ft) versus bicarbonate (HCO <sub>3</sub> ) measured in milliequivalents per liter (meq/L), Yegua Formation of the Yegua-Jackson Aquifer, Northeast Transect, Groundwater Management Area 11.	97
Figure 7-71. Depth measured from land surface in feet (ft) versus sulfate (SO <sub>4</sub> ) measured in milliequivalents per liter (meq/L), Yegua Formation of the Yegua-Jackson Aquifer, Northeast Transect, Groundwater Management Area 11.	97
Figure 7-72. Depth measured from land surface in feet (ft) versus calcium (Ca) measured in milliequivalents per liter (meq/L), Yegua Formation of the Yegua-Jackson Aquifer, Northeast Transect, Groundwater Management Area 11.	98
Figure 7-73. Depth measured from land surface in feet (ft) versus pH, Yegua Formation of the Yegua-Jackson Aquifer, Northeast Transect, Groundwater Management Area 11.	98
Figure 7-74. Depth measured from land surface in feet (ft) versus sodium (Na) measured in milliequivalents per liter (meq/L), Yegua Formation of the Yegua-Jackson Aquifer, Northeast Transect, Groundwater Management Area 11.	99
Figure 7-75. Depth measured from land surface in feet (ft) versus chloride (Cl) measured in milliequivalents per liter (meq/L), Yegua Formation of the Yegua-Jackson Aquifer, Northeast Transect, Groundwater Management Area 11.	99
Figure 7-76. Depth measured from land surface in feet (ft) versus total dissolved solids (TDS) measured in parts per million (ppm), Yegua Formation of the Yegua-Jackson Aquifer, Northeast Transect, Groundwater Management Area 11.	100
Figure 7-77. Map view of all well locations and Transects 1 and 2 in the Northeast Transect.	107
Figure 7-78. Transect 1 from wells in the Carrizo-Wilcox Aquifer outcrop to Well 3.	108
Figure 7-79. Transect 2 from the Carrizo-Wilcox Aquifer outcrop to Wells 5 through 9.	109
Figure 7-80. Sodium, alkalinity and chloride with distance from the outcrop.	110
Figure 7-81. Calcium, potassium and magnesium with distance from the outcrop.	111
Figure 7-82. pH, carbon-13 and carbon-14 with distance from the outcrop.	112
Figure 7-83. Northeast Transect cross section with calcium analytical data measured in milliequivalents per liter (meq/L).	113
Figure 7-84. Northeast Transect cross section with sodium analytical data measured in milliequivalents per liter (meq/L).	114
Figure 7-85. Data distribution of wells with outcrop and downdip extent (up to 3,000 milligrams per liter total dissolved solids) of the Carrizo-Wilcox, Queen City, Sparta, Yegua-Jackson and Brazos River Alluvium aquifers in the Central Transect, Groundwater Management Area (GMA) 12.	116
Figure 7-86. Central Transect sampled well locations, Groundwater Management Area (GMA) 12.	121

Figure 7-87. Cross-section A-A' in dip direction of the Central Transect, Groundwater Management Area 12.....	122
Figure 7-88. Cross-section B-B' in strike direction of the Central Transect, Groundwater Management Area 12.....	123
Figure 7-89. Well depths measured from land surface in feet in the Wilcox Group of the Carrizo-Wilcox Aquifer, Central Transect, Groundwater Management Area (GMA) 12.....	127
Figure 7-90. Potentiometric surface of the Wilcox Group of the Carrizo-Wilcox Aquifer using water level data measured in feet above mean sea level (ft AMSL) from 1990 to 2011 in the Central Transect, Groundwater Management Area 12.....	128
Figure 7-91. Piper diagram showing chemistry of Wilcox Group of the Carrizo-Wilcox Aquifer wells in the Central Transect by well depth measured from land surface in feet (ft)....	129
Figure 7-92. Bicarbonate ( $\text{HCO}_3$ ) versus sodium (Na) measured in milliequivalents per liter (meq/L), Wilcox Group of the Carrizo-Wilcox Aquifer, Central Transect, Groundwater Management Area 12.....	130
Figure 7-93. Sodium (Na) versus calcium (Ca) measured in milliequivalents per liter (meq/L), Wilcox Group of the Carrizo-Wilcox Aquifer, Central Transect, Groundwater Management Area 12.	130
Figure 7-94. Bicarbonate ( $\text{HCO}_3$ ) versus calcium (Ca) measured in milliequivalents per liter (meq/L), Wilcox Group of the Carrizo-Wilcox Aquifer, Central Transect, Groundwater Management Area 12.....	131
Figure 7-95. pH versus bicarbonate ( $\text{HCO}_3$ ) measured in milliequivalents per liter (meq/L), Wilcox Group of the Carrizo-Wilcox Aquifer, Central Transect, Groundwater Management Area (GMA) 12.	131
Figure 7-96. pH versus sodium (Na) measured in milliequivalents per liter (meq/L), Wilcox Group of the Carrizo-Wilcox Aquifer, Central Transect, Groundwater Management Area 12.	132
Figure 7-97. Sulfate ( $\text{SO}_4$ ) versus bicarbonate ( $\text{HCO}_3$ ) measured in milliequivalents per liter (meq/L), Wilcox Group of the Carrizo-Wilcox Aquifer, Central Transect, Groundwater Management Area 12.....	132
Figure 7-98. Chloride (Cl) versus sodium (Na measured in milliequivalents per liter (meq/L)), Wilcox Group of the Carrizo-Wilcox Aquifer, Central Transect, Groundwater Management Area 12.	133
Figure 7-99. Chloride (Cl) versus bicarbonate ( $\text{HCO}_3$ ) measured in milliequivalents per liter (meq/L), Wilcox Group of the Carrizo-Wilcox Aquifer, Central Transect, Groundwater Management Area 12.....	133
Figure 7-100. Depth measured from land surface in feet (ft) versus nitrate ( $\text{NO}_3$ ) measured in milligrams per liter (mg/L), Wilcox Group of the Carrizo-Wilcox Aquifer, Central Transect, Groundwater Management Area 12.....	134
Figure 7-101. Depth measured from land surface in feet (ft) versus sulfate ( $\text{SO}_4$ ) measured in milliequivalents per liter (meq/L), Wilcox Group of the Carrizo-Wilcox Aquifer, Central Transect, Groundwater Management Area 12.....	134
Figure 7-102. Depth measured from land surface in feet (ft) versus calcium (Ca) measured in milliequivalents per liter (meq/L), Wilcox Group of the Carrizo-Wilcox Aquifer, Central Transect, Groundwater Management Area 12.....	135
Figure 7-103. Calcium concentrations measured in milliequivalents per liter (meq/L) in the Wilcox Group of the Carrizo-Wilcox Aquifer, Central Transect, Groundwater Management Area (GMA) 12.	136

Figure 7-104. Depth measured from land surface in feet (ft) versus bicarbonate ( $\text{HCO}_3$ ) measured in milliequivalents per liter (meq/L), Wilcox Group of the Carrizo-Wilcox Aquifer, Central Transect, Groundwater Management Area 12. ....	137
Figure 7-105. Depth measured from land surface in feet (ft) versus pH, Wilcox Group of the Carrizo-Wilcox Aquifer, Central Transect, Groundwater Management Area 12. ....	137
Figure 7-106. pH in the Wilcox Group of the Carrizo-Wilcox Aquifer, Central Transect, Groundwater Management Areas (GMA) 12. ....	138
Figure 7-107. Depth measured from land surface in feet (ft) versus sodium (Na) measured in milliequivalents per liter (meq/L), Wilcox Group of the Carrizo-Wilcox Aquifer, Central Transect, Groundwater Management Area 12. ....	139
Figure 7-108. Depth measured from land surface in feet (ft) versus chloride (Cl) measured in milliequivalents per liter (meq/L), Wilcox Group of the Carrizo-Wilcox Aquifer, Central Transect, Groundwater Management Area 12. ....	139
Figure 7-109. Depth measured from land surface in feet (ft) versus total dissolved solids (TDS) measured in parts per million (ppm), Wilcox Group of the Carrizo-Wilcox Aquifer, Central Transect, Groundwater Management Area 12. ....	140
Figure 7-110. Well depths measured from land surface in feet in the Queen City Aquifer, Central Transect, Groundwater Management Area (GMA) 12. ....	143
Figure 7-111. Potentiometric surface of the Queen City Aquifer using water level data measured in feet above mean sea level (ft AMSL) from 1990 to 2011 in the Central Transect, Groundwater Management Area (GMA) 12. ....	144
Figure 7-112. Piper diagram showing chemistry of the Queen City Aquifer wells in Central Transect by well depth measured from land surface in feet (ft). ....	145
Figure 7-113. Bicarbonate ( $\text{HCO}_3$ ) versus sodium (Na) measured in milliequivalents per liter (meq/L), Queen City Aquifer, Central Transect, Groundwater Management Area 12. ....	146
Figure 7-114. Sodium (Na) versus calcium (Ca) measured in milliequivalents per liter (meq/L), Queen City Aquifer, Central Transect, Groundwater Management Area 12. ....	146
Figure 7-115. Bicarbonate ( $\text{HCO}_3$ ) versus calcium (Ca) measured in milliequivalents per liter (meq/L), Queen City Aquifer, Central Transect, Groundwater Management Area 12. ....	147
Figure 7-116. pH versus bicarbonate ( $\text{HCO}_3$ ) measured in milliequivalents per liter (meq/L), Queen City Aquifer, Central Transect, Groundwater Management Area 12. ....	147
Figure 7-117. pH versus sodium (Na) measured in milliequivalents per liter (meq/L), Queen City Aquifer, Central Transect, Groundwater Management Area 12. ....	148
Figure 7-118. Sulfate ( $\text{SO}_4$ ) versus bicarbonate ( $\text{HCO}_3$ ) measured in milliequivalents per liter (meq/L), Queen City Aquifer, Central Transect, Groundwater Management Area 12. ....	148
Figure 7-119. Chloride (Cl) versus sodium (Na) measured in milliequivalents per liter (meq/L), Queen City Aquifer, Central Transect, Groundwater Management Area 12. ....	149
Figure 7-120. Chloride (Cl) versus bicarbonate ( $\text{HCO}_3$ ) measured in milliequivalents per liter (meq/L), Queen City Aquifer, Central Transect, Groundwater Management Area 12. ....	149
Figure 7-121. Depth measured from land surface in feet (ft) versus nitrate ( $\text{NO}_3$ ) measured in milligrams per liter (mg/L), Queen City Aquifer, Central Transect, Groundwater Management Area 12. ....	150
Figure 7-122. Depth measured from land surface in feet (ft) versus sulfate ( $\text{SO}_4$ ) measured in milliequivalents per liter (meq/L), Queen City Aquifer, Central Transect, Groundwater Management Area 12. ....	150

Figure 7-123. Depth measured from land surface in feet (ft) versus calcium (Ca) measured in milliequivalents per liter (meq/L), Queen City Aquifer, Central Transect, Groundwater Management Area 12.....	151
Figure 7-124. Depth measured from land surface in feet (ft) versus bicarbonate ( $\text{HCO}_3$ ) measured in milliequivalents per liter (meq/L), Queen City Aquifer, Central Transect, Groundwater Management Area 12.....	151
Figure 7-125. Depth measured from land surface in feet (ft) versus sodium (Na) measured in milliequivalents per liter (meq/L), Queen City Aquifer, Central Transect, Groundwater Management Area 12.....	152
Figure 7-126. Depth measured from land surface in feet (ft) versus pH, Queen City Aquifer, Central Transect, Groundwater Management Area 12.....	152
Figure 7-127. Depth measured from land surface in feet (ft) versus chloride (Cl) measured in milliequivalents per liter (meq/L), Queen City Aquifer, Central Transect, Groundwater Management Area 12.....	153
Figure 7-128. Depth measured from land surface in feet (ft) versus total dissolved solids (TDS) measure in parts per million (ppm), Queen City Aquifer, Central Transect, Groundwater Management Area 12.....	153
Figure 7-129. Well depths measured from land surface in feet in the Sparta Aquifer, Central Transect, Groundwater Management Area (GMA) 12.....	156
Figure 7-130. Potentiometric surface of the Sparta Aquifer using water level data measured in feet above mean sea level (ft AMSL) from 1990 to 2011 in the Central Transect, Groundwater Management Area 12.....	157
Figure 7-131. Piper diagram showing chemistry of the Sparta Aquifer wells in the Central Transect by well depth measured from land surface measured in feet (ft).....	158
Figure 7-132. Bicarbonate ( $\text{HCO}_3$ ) versus sodium (Na) measured in milliequivalents per liter (meq/L), Sparta Aquifer, Central Transect, Groundwater Management Area 12.....	159
Figure 7-133. Sodium (Na) versus calcium (Ca) measured in milliequivalents per liter (meq/L), Sparta Aquifer, Central Transect, Groundwater Management Area 12.....	159
Figure 7-134. Bicarbonate ( $\text{HCO}_3$ ) versus calcium (Ca) measured in milliequivalents per liter (meq/L), Sparta Aquifer, Central Transect, Groundwater Management Area 12.....	160
Figure 7-135. pH versus bicarbonate ( $\text{HCO}_3$ ) measured in milliequivalents per liter (meq/L), Sparta Aquifer, Central Transect, Groundwater Management Area 12.....	160
Figure 7-136. pH versus sodium (Na) measured in milliequivalents per liter (meq/L), Sparta Aquifer, Central Transect, Groundwater Management Area 12.....	161
Figure 7-137. Sulfate ( $\text{SO}_4$ ) versus bicarbonate ( $\text{HCO}_3$ ) measured in milliequivalents per liter (meq/L), Sparta Aquifer, Central Transect, Groundwater Management Area 12.....	161
Figure 7-138. Chloride (Cl) versus sodium (Na) measured in milliequivalents per liter (meq/L), Sparta Aquifer, Central Transect, Groundwater Management Area 12.....	162
Figure 7-139. Chloride (Cl) versus bicarbonate ( $\text{HCO}_3$ ) measured in milliequivalents per liter (meq/L), Sparta Aquifer, Central Transect, Groundwater Management Area 12.....	162
Figure 7-140. Depth measured from land surface in feet (ft) versus sulfate ( $\text{SO}_4$ ) measured in milliequivalents per liter (meq/L), Sparta Aquifer, Central Transect, Groundwater Management Area 12.....	163
Figure 7-141. Depth measured from land surface in feet (ft) versus calcium (Ca) measured in milliequivalents per liter (meq/L), Sparta Aquifer, Central Transect, Groundwater Management Area 12.....	163

Figure 7-142. Depth measured from land surface in feet (ft) versus bicarbonate ( $\text{HCO}_3$ ) measured in milliequivalents per liter (meq/L), Sparta Aquifer, Central Transect, Groundwater Management Area 12.	164
Figure 7-143. Depth measured from land surface in feet (ft) versus sodium (Na) measured in milliequivalents per liter (meq/L), Sparta Aquifer, Central Transect, Groundwater Management Area 12.	164
Figure 7-144. Depth measured from land surface in feet (ft) versus pH, Sparta Aquifer, Central Transect, Groundwater Management Area 12.	165
Figure 7-145. Depth measured from land surface in feet (ft) versus chloride (Cl) measured in milliequivalents per liter (meq/L), Sparta Aquifer, Central Transect, Groundwater Management Area 12.	165
Figure 7-146. Depth measured from land surface in feet (ft) versus total dissolved solids (TDS) measured in parts per million (ppm), Sparta Aquifer, Central Transect, Groundwater Management Area 12.	166
Figure 7-147. Well depths measured from land surface in feet in the Yegua-Jackson Aquifer, Central Transect, Groundwater Management Area (GMA) 12.	169
Figure 7-148. Potentiometric surface of the Yegua-Jackson Aquifer using water level data measured in feet above mean sea level (ft AMSL) from 1980 to 2011 in the Central Transect, Groundwater Management Area 12.	170
Figure 7-149. Piper diagram showing chemistry of the Yegua-Jackson Aquifer wells in the Central Transect by well depth measured from land surface in feet (ft).	171
Figure 7-150. Bicarbonate ( $\text{HCO}_3$ ) versus sodium (Na) measured in milliequivalents per liter (meq/L), Yegua-Jackson Aquifer, Central Transect, Groundwater Management Area 12.	172
Figure 7-151. Sodium (Na) versus calcium (Ca) measured in milliequivalents per liter (meq/L), Yegua-Jackson Aquifer, Central Transect, Groundwater Management Area 12.	172
Figure 7-152. Bicarbonate ( $\text{HCO}_3$ ) versus calcium (Ca) measured in milliequivalents per liter (meq/L), Yegua-Jackson Aquifer, Central Transect, Groundwater Management Area 12.	173
Figure 7-153. pH versus bicarbonate ( $\text{HCO}_3$ ) measured in milliequivalents per liter (meq/L), Yegua-Jackson Aquifer, Central Transect, Groundwater Management Area 12.	173
Figure 7-154. pH versus sodium (Na measured in milliequivalents per liter (meq/L)), Yegua-Jackson Aquifer, Central Transect, Groundwater Management Area 12.	174
Figure 7-155. Sulfate ( $\text{SO}_4$ ) versus bicarbonate ( $\text{HCO}_3$ ) measured in milliequivalents per liter (meq/L), Yegua-Jackson Aquifer, Central Transect, Groundwater Management Area 12.	174
Figure 7-156. Chloride (Cl) versus sodium (Na) measured in milliequivalents per liter (meq/L), Yegua-Jackson Aquifer, Central Transect, Groundwater Management Area 12.	175
Figure 7-157. Depth measured from land surface in feet (ft) versus sulfate ( $\text{SO}_4$ ) measured in milliequivalents per liter (meq/L), Yegua-Jackson Aquifer, Central Transect, Groundwater Management Area 12.	175
Figure 7-158. Depth measured from land surface in feet (ft) versus calcium (Ca) measured in milliequivalents per liter (meq/L), Yegua-Jackson Aquifer, Central Transect, Groundwater Management Area 12.	176
Figure 7-159. Depth measured from land surface in feet (ft) versus sodium (Na) measured in milliequivalents per liter (meq/L), Yegua-Jackson Aquifer, Central Transect, Groundwater Management Area 12.	176

Figure 7-160. Depth measured from land surface in feet (ft) versus chloride (Cl) measured in milliequivalents per liter (meq/L), Yegua-Jackson Aquifer, Central Transect, Groundwater Management Area 12. ....	177
Figure 7-161. Depth measured from land surface versus total dissolved solids (TDS) measured in parts per million (ppm), Yegua-Jackson Aquifer, Central Transect, Groundwater Management Area 12. ....	177
Figure 7-162. Well depths measured from land surface in feet in the Brazos River Alluvium Aquifer, Central Transect, Groundwater Management Area (GMA) 12. ....	180
Figure 7-163. Potentiometric surface of the Brazos River Alluvium Aquifer using water well data measured in feet above mean sea level (ft AMSL) from 1990 to 2011 in the Central Transect, Groundwater Management Area 12. ....	181
Figure 7-164. Piper diagram showing chemistry of the Brazos River Alluvium Aquifer wells in the Central Transect by well depth measured from land surface measured in feet (ft). ....	182
Figure 7-165. Bicarbonate ( $\text{HCO}_3$ ) versus sodium (Na) measured in milliequivalents per liter (meq/L), Brazos River Alluvium Aquifer, Central Transect, Groundwater Management Area 12. ....	183
Figure 7-166. Sodium (Na) versus calcium (Ca) measured in milliequivalents per liter (meq/L), Brazos River Alluvium Aquifer, Central Transect, Groundwater Management Area 12. ....	183
Figure 7-167. Bicarbonate ( $\text{HCO}_3$ ) versus calcium (Ca) measured in milliequivalents per liter (meq/L), Brazos River Alluvium Aquifer, Central Transect, Groundwater Management Area 12. ....	184
Figure 7-168. Sulfate ( $\text{SO}_4$ ) versus bicarbonate ( $\text{HCO}_3$ ) measured in milliequivalents per liter (meq/L), Brazos River Alluvium Aquifer, Central Transect, Groundwater Management Area 12. ....	184
Figure 7-169. Chloride (Cl) versus sodium (Na) measured in milliequivalents per liter (meq/L), Brazos River Alluvium Aquifer, Central Transect, Groundwater Management Area 12. ....	185
Figure 7-170. Chloride (Cl) versus sulfate ( $\text{SO}_4$ ) measured in milliequivalents per liter (meq/L), Brazos River Alluvium Aquifer, Central Transect, Groundwater Management Area 12. ....	185
Figure 7-171. Magnesium (Mg) versus calcium (Ca) measured in milliequivalents per liter (meq/L), Brazos River Alluvium Aquifer, Central Transect, Groundwater Management Area 12. ....	186
Figure 7-172. Sulfate ( $\text{SO}_4$ ) versus calcium (Ca) measured in milliequivalents per liter (meq/L), Brazos River Alluvium Aquifer, Central Transect, Groundwater Management Area 12. ....	186
Figure 7-173. Relative concentrations of major anions and total dissolved solids in the evolution of the Simsboro Formation (Wilcox Group) of the Carrizo-Wilcox Aquifer along this transect. ....	191
Figure 7-174. Relative concentrations of major cation in the evolution of the Simsboro Formation (Wilcox Group) of the Carrizo-Wilcox Aquifer along this transect. ....	192
Figure 7-175. Stable isotope values and methane mole percent of fixed gas in the Simsboro Formation (Wilcox Group) of the Carrizo-Wilcox Aquifer along this transect. ....	193
Figure 7-176. Relative measured radiocarbon age in the evolution of the Simsboro Formation (Wilcox Group) of the Carrizo-Wilcox Aquifer along this transect. ....	194
Figure 7-177. Central Transect cross section with sodium analytical data measured in milliequivalents per liter (meq/L). ....	195
Figure 7-178. Central Transect cross section with carbon-14 analytical data measured in percent modern carbon. ....	196

Figure 7-179. Data distribution of wells with outcrop and downdip extent (up to 3,000 milliequivalents per liter total dissolved solids) of the Carrizo-Wilcox, Queen City, Sparta and Yegua-Jackson aquifers in the Gonzales Transect Groundwater Management Area (GMA) 13.	201
Figure 7-180. Gonzales Transect sampled well locations, Groundwater Management Area (GMA) 13.	202
Figure 7-181. Cross-section A-A' in dip direction of the Gonzales Transect, Groundwater Management Area 13.	203
Figure 7-182. Well depths measured from land surface in feet (ft) in the Carrizo Sand Formation of the Carrizo-Wilcox Aquifer, Gonzales Transect, Groundwater Management Area (GMA) 13.	204
Figure 7-183. Potentiometric surface of the Carrizo Sand Formation of the Carrizo-Wilcox Aquifer using water level data measured in feet above mean sea level (ft AMSL) from 1931 to 2010 in the Gonzales Transect, Groundwater Management Area (GMA) 13.	205
Figure 7-184. Depth to water in flowing and non-flowing wells in the Carrizo Sand Formation of the Carrizo-Wilcox Aquifer, Gonzales Transect, Groundwater Management Area (GMA) 13.	206
Figure 7-185. Piper diagram showing chemistry of the Carrizo Sand Formation of the Carrizo-Wilcox Aquifer wells in the Gonzales Transect by well depth measured from land surface in feet (ft).	207
Figure 7-186. Bicarbonate ( $\text{HCO}_3$ ) versus sodium (Na) measured in milliequivalents per liter (meq/L), Carrizo Sand Formation of the Carrizo-Wilcox Aquifer, Gonzales Transect, Groundwater Management Area 13.	208
Figure 7-187. Sodium (Na) versus calcium (Ca) measured in milliequivalents per liter (meq/L), Carrizo Sand Formation of the Carrizo-Wilcox Aquifer, Gonzales Transect, Groundwater Management Area 13.	208
Figure 7-188. Bicarbonate ( $\text{HCO}_3$ ) versus calcium (Ca) measured in milliequivalents per liter (meq/L), Carrizo Sand Formation of the Carrizo-Wilcox Aquifer, Gonzales Transect, Groundwater Management Area 13.	209
Figure 7-189. pH versus bicarbonate ( $\text{HCO}_3$ ) measured in milliequivalents per liter (meq/L), Carrizo Sand Formation of the Carrizo-Wilcox Aquifer, Gonzales Transect, Groundwater Management Area 13.	209
Figure 7-190. pH versus sodium (Na) measured in milliequivalents per liter (meq/L), Carrizo Sand Formation of the Carrizo-Wilcox Aquifer, Gonzales Transect, Groundwater Management Area 13.	210
Figure 7-191. Sulfate ( $\text{SO}_4$ ) versus bicarbonate ( $\text{HCO}_3$ ) measured in milliequivalents per liter (meq/L), Carrizo Sand Formation of the Carrizo-Wilcox Aquifer, Gonzales Transect, Groundwater Management Area 13.	210
Figure 7-192. Chloride (Cl) versus sodium (Na) measured in milliequivalents per liter (meq/L), Carrizo Sand Formation of the Carrizo-Wilcox Aquifer, Gonzales Transect, Groundwater Management Area 13.	211
Figure 7-193. Chloride (Cl) versus bicarbonate ( $\text{HCO}_3$ ) measured in milliequivalents per liter (meq/L), Carrizo Sand Formation of the Carrizo-Wilcox Aquifer, Gonzales Transect, Groundwater Management Area 13.	211

Figure 7-194. Depth measured from land surface in feet (ft) versus sulfate (SO <sub>4</sub> ) measured in milliequivalents per liter (meq/L), Carrizo Sand Formation of the Carrizo-Wilcox Aquifer, Gonzales Transect, Groundwater Management Area 13. ....	212
Figure 7-195. Depth measured from land surface in feet (ft) versus calcium (Ca) measured in milliequivalents per liter (meq/L), Carrizo Sand Formation of the Carrizo-Wilcox Aquifer, Gonzales Transect, Groundwater Management Area 13. ....	212
Figure 7-196. Calcium concentrations measured in milliequivalents per liter (meq/L) in the Carrizo Sand Formation of the Carrizo-Wilcox Aquifer, Gonzales Transect, Groundwater Management Area (GMA) 13. ....	213
Figure 7-197. Depth measured from land surface in feet (ft) versus sodium (Na) measured in milliequivalents per liter (meq/L), Carrizo Sand Formation of the Carrizo-Wilcox Aquifer, Gonzales Transect, Groundwater Management Area 13. ....	214
Figure 7-198. Depth measured from land surface in feet (ft) versus bicarbonate (HCO <sub>3</sub> ) measured in milliequivalents per liter (meq/L), Carrizo Sand Formation of the Carrizo-Wilcox Aquifer, Gonzales Transect, Groundwater Management Area 13. ....	214
Figure 7-199. Bicarbonate (HCO <sub>3</sub> ) concentrations measured in milliequivalents per liter (meq/L) in the Carrizo Sand Formation of the Carrizo-Wilcox Aquifer, Gonzales Transect, Groundwater Management Area (GMA) 13. ....	215
Figure 7-200. Depth measured from land surface in feet (ft) versus pH, Carrizo Sand Formation of the Carrizo-Wilcox Aquifer, Gonzales Transect, Groundwater Management Area 13. ....	216
Figure 7-201. pH in the Carrizo Sand Formation of the Carrizo-Wilcox Aquifer, Gonzales Transect, Groundwater Management Area (GMA) 13. ....	217
Figure 7-202. Depth measured from land surface versus chloride (Cl) measured in milliequivalents per liter (meq/L), Carrizo Sand Formation of the Carrizo-Wilcox Aquifer, Gonzales Transect, Groundwater Management Area 13. ....	218
Figure 7-203. Chloride (Cl) concentrations measured in milliequivalents per liter (meq/L) in the Carrizo Sand Formation of the Carrizo-Wilcox Aquifer, Gonzales Transect, Groundwater Management Area 13. ....	219
Figure 7-204. Depth measured from land surface in feet (ft) versus total dissolved solids (TDS) measured in parts per million (ppm), Carrizo Sand Formation of the Carrizo-Wilcox Aquifer, Gonzales Transect, Groundwater Management Area 13. ....	220
Figure 7-205. Well depths measured from land surface in feet in the Queen City Aquifer, Gonzales Transect, Groundwater Management Area (GMA) 13. ....	222
Figure 7-206. Potentiometric surface of the Queen City Aquifer using water level data measured in feet above mean sea level (ft AMSL) from 1980 to 2011 in the Gonzales Transect, Groundwater Management Area 13. ....	223
Figure 7-207. Piper diagram showing chemistry of the Queen City Aquifer wells in the Gonzales Transect by well depth measured from land surface in feet (ft). ....	224
Figure 7-208. Bicarbonate (HCO <sub>3</sub> ) versus sodium (Na) measured in milliequivalents per liter (meq/L), Queen City Aquifer, Gonzales Transect, Groundwater Management Area 13. ....	225
Figure 7-209. Sodium (Na) versus calcium (Ca) measured in milliequivalents per liter (meq/L), Queen City Aquifer, Gonzales Transect, Groundwater Management Area 13. ....	225
Figure 7-210. Chloride (Cl) versus sodium (Na) measured in milliequivalents per liter (meq/L), Queen City Aquifer, Gonzales Transect, Groundwater Management Area 13. ....	226
Figure 7-211. Well depths measured from land surface in feet in the Sparta Aquifer, Gonzales Transect, Groundwater Management Area (GMA) 13. ....	228

Figure 7-212. Potentiometric surface of the Sparta Aquifer using water level data measured in feet above mean sea level (ft AMSL) from 1980 to 2011 in the Gonzales Transect, Groundwater Management Area (GMA) 13.....	229
Figure 7-213. Piper diagram showing chemistry of the Sparta Aquifer wells in the Gonzales Transect by well depth measured from land surface in feet (ft). .....	230
Figure 7-214. Bicarbonate (HCO <sub>3</sub> ) versus sodium (Na) measured in milliequivalents per liter (meq/L), Sparta Aquifer, Gonzales Transect, Groundwater Management Area 13. ....	231
Figure 7-215. Sodium (Na) versus calcium (Ca) measured in milliequivalents per liter (meq/L), Sparta Aquifer, Gonzales Transect, Groundwater Management Area 13. ....	231
Figure 7-216. Chloride (Cl) versus sodium (Na) measured in milliequivalents per liter (meq/L), Sparta Aquifer, Gonzales Transect, Groundwater Management Area 13. ....	232
Figure 7-217. Depth measured from land surface in feet (ft) versus chloride (Cl) measured in milliequivalents per liter (meq/L), Sparta Aquifer, Gonzales Transect, Groundwater Management Area 13. ....	232
Figure 7-218. Depth measured from land surface in feet (ft) versus total dissolved solids (TDS) measured in parts per million (ppm), Sparta Aquifer, Gonzales Transect, Groundwater Management Area 13.....	233
Figure 7-219. Well depths measured from land surface in feet in the Yegua-Jackson Aquifer, Gonzales Transect, Groundwater Management Area (GMA) 13.....	235
Figure 7-220. Potentiometric surface of the Yegua-Jackson Aquifer using water level data measured in feet above mean sea level (ft AMSL) from 1921 to 2002 in the Gonzales Transect, Groundwater Management Area (GMA) 13.....	236
Figure 7-221. Piper diagram showing chemistry of the Yegua-Jackson Aquifer wells in the Gonzales Transect by well depth measured from land surface in feet (ft). .....	237
Figure 7-222. Bicarbonate (HCO <sub>3</sub> ) versus sodium (Na) measured in milliequivalents per liter (meq/L), Yegua-Jackson Aquifer, Gonzales Transect, Groundwater Management Area 13. ....	238
Figure 7-223. Chloride (Cl) versus sodium (Na) measured in milliequivalents per liter (meq/L), Yegua-Jackson Aquifer, Gonzales Transect, Groundwater Management Area 13. ....	238
Figure 7-224. Depth measured from land surface in feet (ft) versus total dissolved solids (TDS) measure din parts per million (ppm), Yegua-Jackson Aquifer, Gonzales Transect, Groundwater Management Area 13.....	239
Figure 7-225. Piper diagram showing chemistry of all the San Antonio Water System well nests in the Gonzales Transect by aquifer.....	245
Figure 7-226. Piper diagram showing chemistry of the San Antonio Water System well Nest 2 in the Gonzales Transect. ....	246
Figure 7-227. Piper diagram showing chemistry of the San Antonio Water System well Nest 3 in the Gonzales Transect.....	247
Figure 7-228. Piper diagram showing chemistry of the San Antonio Water System well Nest 4 in the Gonzales Transect.....	248
Figure 7-229. Depth measured in feet (ft) versus δ <sup>13</sup> C, San Antonio Water System well nests, Gonzales Transect, Groundwater Management Area 13.....	249
Figure 7-230. Depth measured in feet (ft) versus carbon-14 percent modern ( <sup>14</sup> C %), San Antonio Water System well nests, Gonzales Transect, Groundwater Management Area 13.....	249
Figure 7-231. Gonzales Transect sampled well locations, Groundwater Management Area (GMA) 13. ....	257

Figure 7-232. Potentiometric surface of the Carrizo Sand Formation portion of the Carrizo-Wilcox Aquifer using water level data measured in feet above mean sea level (ft AMSL) in the Gonzales Transect, Groundwater Management Area (GMA) 13. ....	258
Figure 7-233. Regional compositional changes in the Carrizo Sand Formation portion of the Carrizo-Wilcox Aquifer using the existing TWDB database. ....	259
Figure 7-234. Regional compositional changes in the Carrizo Sand Formation portion of the Carrizo-Wilcox Aquifer using the existing TWDB database. ....	260
Figure 7-235. Anion concentrations along Transect 1 that includes Transect 2 wells indicated by the region between the dashed lines with (left) and excluded Transect 2 wells (right). ....	261
Figure 7-236. Cation concentrations along Transect 1 that in the first case includes the Transect 2 wells indicated by the region between the dashed lines (left) and excludes the Transect 2 wells (right). ....	262
Figure 7-237. Sulfate concentrations and sulfur isotope values along the profile by well with (left) and without (right) Transect 2 wells. ....	263
Figure 7-238. Methane mole percent of dissolved gas and the methane isotopic values. ....	264
Figure 7-239. Chloride (Cl) concentration measured in milliequivalents per liter (meq/L) in all four aquifers with transect distance from model well number 1 (Wilcox Group recharge area). ....	265
Figure 7-240. The comparison of total dissolved solids (TDS) measured in milligrams per liter (mg/L) content with transect distance among the four aquifers in the transect. ....	265
Figure 7-241. The comparison of $\delta^{13}\text{C}$ of the total dissolved carbon with transect distance among the four aquifers in the transect. ....	266
Figure 7-242. The comparison of $^{14}\text{C}_{\text{OBS}}$ years before present of total dissolved carbon with transect distance among the four aquifers in the transect (compare with Table 7-5 and Table 7-6 for $^{14}\text{C}_{\text{ADJ}}$ ). ....	266
Figure 7-243. Gonzales Transect cross section with sodium analytical data. ....	268
Figure 7-244. Gonzales Transect cross section with carbon-14 analytical data. ....	269
Figure 7-245. Data distribution of wells with outcrop and downdip extent (up to 3,000 milligrams per liter total dissolved solids) of the Carrizo Sand Formation portion of the Carrizo-Wilcox Aquifer, Queen City, Sparta and Yegua-Jackson aquifers in the South Transect. ....	274
Figure 7-246. Well depths measured from land surface in feet in the Carrizo Sand Formation portion of the Carrizo-Wilcox Aquifer, South Transect, Groundwater Management Area (GMA) 13. ....	275
Figure 7-247. Water level elevations from 1929 to 2010 measured in feet above mean sea level (ft AMSL) in the Carrizo Sand Formation portion of the Carrizo-Wilcox Aquifer, South Transect, Groundwater Management Area (GMA) 13. ....	276
Figure 7-248. Carrizo Sand Formation portion of the Carrizo-Wilcox Aquifer faults in Charlotte, Jourdanton and Pleasanton Trough, Atascosa County, Texas (from Hargis, 2009). .	277
Figure 7-249. Piper diagram showing chemistry of the Carrizo Sand Formation portion of the Carrizo-Wilcox Aquifer wells in the South Transect by well depth measured from land surface in feet (ft). ....	278
Figure 7-250. Bicarbonate ( $\text{HCO}_3$ ) versus sodium (Na) measured in milliequivalents per liter (meq/L), Carrizo Sand Formation portion of the Carrizo-Wilcox Aquifer, South Transect, Groundwater Management Area 13. ....	279

Figure 7-251. Sodium (Na) versus calcium (Ca) measured in milliequivalents per liter (meq/L), Carrizo Sand Formation portion of the Carrizo-Wilcox Aquifer, South Transect, Groundwater Management Area 13.....	279
Figure 7-252. Bicarbonate (HCO <sub>3</sub> ) versus calcium (Ca) measured in milliequivalents per liter (meq/L), Carrizo Sand Formation portion of the Carrizo-Wilcox Aquifer, South Transect, Groundwater Management Area 13.....	280
Figure 7-253. pH versus bicarbonate (HCO <sub>3</sub> ) measured in milliequivalents per liter (meq/L), Carrizo Sand Formation portion of the Carrizo-Wilcox Aquifer, South Transect, Groundwater Management Area 13.....	280
Figure 7-254. pH versus sodium (Na) measured in milliequivalents per liter (meq/L), Carrizo Sand Formation portion of the Carrizo-Wilcox Aquifer, South Transect, Groundwater Management Area 13.....	281
Figure 7-255. Sulfate (SO <sub>4</sub> ) versus bicarbonate (HCO <sub>3</sub> ) measured in milliequivalents per liter (meq/L), Carrizo Sand Formation portion of the Carrizo-Wilcox Aquifer, South Transect, Groundwater Management Area 13.....	281
Figure 7-256. Chloride (Cl) versus sodium (Na) measured in milliequivalents per liter (meq/L), Carrizo Sand Formation portion of the Carrizo-Wilcox Aquifer, South Transect, Groundwater Management Area 13.....	282
Figure 7-257. Chloride (Cl) versus bicarbonate (HCO <sub>3</sub> ) measured in milliequivalents per liter (meq/L), Carrizo Sand Formation portion of the Carrizo-Wilcox Aquifer, South Transect, Groundwater Management Area 13.....	282
Figure 7-258. Depth measured from land surface in feet (ft) versus sulfate (SO <sub>4</sub> ) measured in milliequivalents per liter (meq/L), Carrizo Sand Formation portion of the Carrizo-Wilcox Aquifer, South Transect, Groundwater Management Area 13.....	283
Figure 7-259. Depth measured from land surface in feet (ft) versus calcium (Ca) measured in milliequivalents per liter (meq/L), Carrizo Sand Formation portion of the Carrizo-Wilcox Aquifer, South Transect, Groundwater Management Area 13.....	283
Figure 7-260. Calcium concentrations measured in milliequivalents per liter (meq/L) in the Carrizo Sand Formation portion of the Carrizo-Wilcox Aquifer, South Transect, Groundwater Management Area (GMA) 13.....	284
Figure 7-261. Depth measured from land surface in feet (ft) versus sodium (Na) measured in milliequivalents per liter (meq/L), Carrizo Sand Formation portion of the Carrizo-Wilcox Aquifer, South Transect, Groundwater Management Area 13.....	285
Figure 7-262. Depth measured from land surface versus bicarbonate (HCO <sub>3</sub> ) measured in milliequivalents per liter (meq/L), Carrizo Sand Formation portion of the Carrizo-Wilcox Aquifer, South Transect, Groundwater Management Area 13.....	285
Figure 7-263. Bicarbonate concentrations measured in milliequivalents per liter (meq/L) in the Carrizo Sand Formation portion of the Carrizo-Wilcox Aquifer, South Transect, Groundwater Management Area (GMA) 13.....	286
Figure 7-264. Depth measured from land surface in feet (ft) versus pH, Carrizo Sand Formation portion of the Carrizo-Wilcox Aquifer, South Transect, Groundwater Management Area 13.....	287
Figure 7-265. pH concentrations in the Carrizo Sand Formation portion of the Carrizo-Wilcox Aquifer, South Transect, Groundwater Management Area (GMA) 13.....	288
Figure 7-266. Sodium concentrations measured in milliequivalents per liter (meq/L) in the Carrizo Sand Formation portion of the Carrizo-Wilcox Aquifer, South Transect, Groundwater Management Area (GMA) 13.....	289

Figure 7-267. Depth measured from land surface versus chloride (Cl) measured in milliequivalents per liter (meq/L), Carrizo Sand Formation portion of the Carrizo-Wilcox Aquifer, South Transect, Groundwater Management Area 13. ....	290
Figure 7-268. Chloride concentrations measured in milliequivalents per liter (meq/L) in the Carrizo Sand Formation portion of the Carrizo-Wilcox Aquifer, South Transect, Groundwater Management Area (GMA) 13. ....	291
Figure 7-269. Depth measured from land surface measured in feet (ft) versus total dissolved solids measured in parts per million (ppm), Carrizo Sand Formation portion of the Carrizo-Wilcox Aquifer, South Transect, Groundwater Management Area 13. ....	292
Figure 7-270. Total dissolved solids measured in parts per million (ppm) in the Carrizo Sand Formation portion of the Carrizo-Wilcox Aquifer, South Transect, Groundwater Management Area (GMA) 13. ....	293
Figure 7-271. Well depths measured from land surface in feet in the Queen City Aquifer, South Transect, Groundwater Management Area (GMA) 13. ....	297
Figure 7-272. Water level elevations from 1971 to 2011 measured in feet above mean sea level (ft AMSL) in the Queen City Aquifer, South Transect, Groundwater Management Area (GMA) 13. ....	298
Figure 7-273. Piper diagram showing chemistry of the Queen City Aquifer wells in the South Transect by well depth measured from land surface in feet (ft). ....	299
Figure 7-274. Bicarbonate (HCO <sub>3</sub> ) versus sodium (Na) measured in milliequivalents per liter (meq/L), Queen City Aquifer, South Transect, Groundwater Management Area 13. ....	300
Figure 7-275. Sodium (Na) versus calcium (Ca) measured in milliequivalents per liter (meq/L), Queen City Aquifer, South Transect, Groundwater Management Area 13. ....	300
Figure 7-276. Bicarbonate (HCO <sub>3</sub> ) versus calcium (Ca) measured in milliequivalents per liter (meq/L), Queen City Aquifer, South Transect, Groundwater Management Area 13. ....	301
Figure 7-277. pH versus bicarbonate (HCO <sub>3</sub> ) measured in milliequivalents per liter (meq/L), Queen City Aquifer, South Transect, Groundwater Management Area 13. ....	301
Figure 7-278. pH versus sodium (Na) measured in milliequivalents per liter (meq/L), Queen City Aquifer, South Transect, Groundwater Management Area 13. ....	302
Figure 7-279. Sulfate (SO <sub>4</sub> ) versus bicarbonate (HCO <sub>3</sub> ) measured in milliequivalents per liter (meq/L), Queen City Aquifer, South Transect, Groundwater Management Area 13. ....	302
Figure 7-280. Sodium (Na) versus chloride (Cl) measured in milliequivalents per liter (meq/L), Queen City Aquifer, South Transect, Groundwater Management Area 13. ....	303
Figure 7-281. Chloride (Cl) versus bicarbonate (HCO <sub>3</sub> ) measured in milliequivalents per liter (meq/L), Queen City Aquifer, South Transect, Groundwater Management Area 13. ....	303
Figure 7-282. Depth measured from land surface in feet (ft) versus sulfate (SO <sub>4</sub> ) measured in milliequivalents per liter (meq/L), Queen City Aquifer, South Transect, Groundwater Management Area 13. ....	304
Figure 7-283. Sulfate concentrations measured in milliequivalents per liter (meq/L) in the Queen City Aquifer, South Transect, Groundwater Management Area (GMA) 13. ....	305
Figure 7-284. Depth measured from land surface in feet (ft) versus calcium (Ca) measured in milliequivalents per liter (meq/L), Queen City Aquifer, South Transect, Groundwater Management Area 13. ....	306
Figure 7-285. Calcium concentrations measured in milliequivalents per liter (meq/L) in the Queen City Aquifer, South Transect, Groundwater Management Area (GMA) 13. ....	307

Figure 7-286. Depth measured from land surface in feet (ft) versus bicarbonate ( $\text{HCO}_3$ ) measured in milliequivalents per liter (meq/L), Queen City Aquifer, South Transect, Groundwater Management Area 13.....	308
Figure 7-287. Bicarbonate concentrations measured in milliequivalents per liter (meq/L) in the Queen City Aquifer, South Transect, Groundwater Management Area (GMA) 13.....	309
Figure 7-288. Depth measured from land surface in feet (ft) versus pH, Queen City Aquifer, South Transect, Groundwater Management Area 13.....	310
Figure 7-289. Depth measured from land surface in feet (ft) versus sodium (Na) measured in milliequivalents per liter (meq/L), Queen City Aquifer, South Transect, Groundwater Management Area 13.....	310
Figure 7-290. Depth measured from land surface in feet (ft) versus chloride (Cl) measured in milliequivalents per liter (meq/L), Queen City Aquifer, South Transect, Groundwater Management Area 13.....	311
Figure 7-291. Depth measured from land surface in feet (ft) versus total dissolved solids (TDS) measured in parts per million (ppm), Queen City Aquifer, South Transect, Groundwater Management Area 13.....	311
Figure 7-292. Well depths measured in feet from land surface in the Sparta Aquifer, South Transect, Groundwater Management Area (GMA) 13.....	314
Figure 7-293. Water level elevations from 1942 to 2010 measured in feet above mean sea level (ft AMSL) in the Sparta Aquifer, South Transect, Groundwater Management Area (GMA) 13.	315
Figure 7-294. Piper diagram showing chemistry of the Sparta Aquifer wells in the South Transect by well depth measured from land surface in feet (ft). .....	316
Figure 7-295. Bicarbonate ( $\text{HCO}_3$ ) versus sodium (Na) measured in milliequivalents per liter (meq/L), Sparta Aquifer, South Transect, Groundwater Management Area 13.....	317
Figure 7-296. Sodium (Na) versus calcium (Ca) measured in milliequivalents per liter (meq/L), Sparta Aquifer, South Transect, Groundwater Management Area 13.....	317
Figure 7-297. Bicarbonate ( $\text{HCO}_3$ ) versus calcium (Ca) measured in milliequivalents per liter (meq/L), Sparta Aquifer, South Transect, Groundwater Management Area 13.....	318
Figure 7-298. pH versus bicarbonate ( $\text{HCO}_3$ ) measured in milliequivalents per liter (meq/L), Sparta Aquifer, South Transect, Groundwater Management Area 13.....	318
Figure 7-299. Sulfate ( $\text{SO}_4$ ) versus bicarbonate ( $\text{HCO}_3$ ) measured in milliequivalents per liter (meq/L), Sparta Aquifer, South Transect, Groundwater Management Area 13.....	319
Figure 7-300. Chloride (Cl) versus sodium (Na) measured in milliequivalents per liter (meq/L), Sparta Aquifer, South Transect, Groundwater Management Area 13.....	319
Figure 7-301. Depth measured from land surface in feet (ft) versus sulfate ( $\text{SO}_4$ ) measured in milliequivalents per liter (meq/L), Sparta Aquifer, South Transect, Groundwater Management Area 13.	320
Figure 7-302. Depth measured from land surface in feet (ft) versus calcium (Ca) measured in milliequivalents per liter (meq/L), Sparta Aquifer, South Transect, Groundwater Management Area 13.	320
Figure 7-303. Depth measured from land surface in feet (ft) versus bicarbonate ( $\text{HCO}_3$ ) measured in milliequivalents per liter (meq/L), Sparta Aquifer, South Transect, Groundwater Management Area 13.....	321

Figure 7-304. Depth measured from land surface in feet (ft) versus sodium (Na) measured in milliequivalents per liter (meq/L), Sparta Aquifer, South Transect, Groundwater Management Area 13.	321
Figure 7-305. Depth measured from land surface in feet (ft) versus chloride (Cl) measured in milliequivalents per liter (meq/L), Sparta Aquifer, South Transect, Groundwater Management Area 13.	322
Figure 7-306. Depth measured from land surface in feet (ft) versus total dissolved solids (TDS) measured in parts per million (ppm), Sparta Aquifer, South Transect, Groundwater Management Area (GMA) 13.	322
Figure 7-307. Well depths measured from land surface in feet in the Yegua-Jackson Aquifer, South Transect, Groundwater Management Area (GMA) 13.	325
Figure 7-308. Water level elevations from 1921 to 2010 measured in feet above mean sea level (ft AMSL) in the Yegua-Jackson Aquifer, South Transect, Groundwater Management Area (GMA) 13.	326
Figure 7-309. Piper diagram showing chemistry of the Yegua-Jackson Aquifer in the South Transect by well depth measured from land surface in feet (ft).	327
Figure 7-310. Sodium (Na) versus calcium (Ca) measured in milliequivalents per liter (meq/L), Yegua-Jackson Aquifer, South Transect, Groundwater Management Area 13.	328
Figure 7-311. Chloride (Cl) versus sodium (Na) measured in milliequivalents per liter (meq/L), Yegua-Jackson Aquifer, South Transect, Groundwater Management Area 13.	328
Figure 7-312. Depth measured from land surface in feet (ft) versus calcium (Ca) measured in milliequivalents per liter (meq/L), Yegua-Jackson Aquifer, South Transect, Groundwater Management Area 13.	329
Figure 7-313. Depth measured from land surface versus chloride (Cl) measured in milliequivalents per liter (meq/L), Yegua-Jackson Aquifer, South Transect, Groundwater Management Area 13.	329
Figure 7-314. Depth measured from land surface in feet (ft) versus total dissolved solids (TDS) measured in parts per million (ppm), Yegua-Jackson Aquifer, South Transect, Groundwater Management Area 13.	330
Figure 7-315. Study area showing locations of wells used in geochemical modeling (Pearson and White, 1967).	332
Figure 7-316. Ages of groundwater in the Carrizo Sand Formation portion of the Carrizo-Wilcox Aquifer (Figure 5 from Pearson and White (1967)).	333
Figure 7-317. Groundwater elevation contours, model transect lines and corrected groundwater ages.	339
Figure 7-318. Concentrations measured in milligrams per liter (mg/L) of major geochemical constituents of alkalinity, calcium, chloride, magnesium, sodium and sulfate as a function of distance along the transect line measured in miles (mi).	340
Figure 7-319. Sodium, chloride and alkalinity concentrations measured in milligrams per liter (mg/L) as a function of distance along the transect line in wells used for NETPATH modeling.	341
Figure 7-320. Calcium, magnesium and sulfate concentrations measured in milligrams per liter (mg/L) as a function of distance along the transect line in wells used for NETPATH modeling.	342
Figure 7-321. Vertical profile along Transect line 1 showing well, well screen depths and inferred and potential water flow pathways.	343

Figure 7-322. Vertical profile along Transect line 2 showing well, well screen depths and inferred and potential groundwater flow pathways. ....	347
Figure 7-323. Vertical profile along Transect line 3 showing well, well screen depths and inferred and potential groundwater flow pathways. ....	348
Figure 7-324. Vertical profile along Transect line 4 showing well, well screen depths and inferred and potential groundwater flow pathways. ....	349
Figure 7-325. Location map for the brackish Lower Wilcox Group wells sampled in 2012 in Bexar and Atascosa counties. ....	356
Figure 7-326. Location map for the brackish Lower Wilcox Group wells sampled in 2012 in Bexar, Atascosa and Webb counties. ....	357
Figure 7-327. Cross-section A-A' of wells sampled in the brackish Lower Wilcox Group in 2012 in Bexar and Atascosa counties. ....	358
Figure 7-328. Piper diagram for the brackish Lower Wilcox Group wells. ....	359
Figure 7-329. Concentrations of major cations measured in milligrams per liter (mg/L), anions and total dissolved solids with respect to well location in the transect. ....	360
Figure 7-330. Stable isotopes along the transect. ....	361
Figure 8-1. Location of the three Groundwater Availability Models for the Sparta, Queen City and Carrizo-Wilcox aquifers (top) and the Groundwater Availability Model for the Yegua-Jackson Aquifer (bottom). ....	364
Figure 8-2. Plan-view of spatial grid and outline of active cells in the Groundwater Availability Model for the Yegua-Jackson Aquifer (Deeds and others, 2010). ....	366
Figure 8-3. Cross-section of hydrogeologic units and corresponding layer indexes in the Groundwater Availability Model for the Yegua-Jackson Aquifer (Deeds and others, 2010). ...	367
Figure 8-4. Qualitative profile and model conceptualization of the Groundwater Availability Model for the Yegua-Jackson Aquifer (from Deeds and others, 2010). ....	368
Figure 8-5. Spatial grid plan-views and model boundaries of the Groundwater Availability Models for the southern portion of the Sparta, Queen City and Carrizo-Wilcox aquifers (top) and central portion of the Sparta, Queen City and Carrizo-Wilcox aquifers (bottom) (Kelley and others, 2004). ...	371
Figure 8-6. Qualitative profile and model conceptualization of the Groundwater Availability Models for the Sparta, Queen City and Carrizo-Wilcox aquifers (from Kelley and others, 2004). ...	372
Figure 8-7. Locations of the Gonzales (GUA) and Central Transect (BRA) lines compared to three-dimensional spatial grid plan-views of the Groundwater Availability Model for the Yegua-Jackson Aquifer (YEG), southern portion of the Sparta, Queen City and Carrizo-Wilcox aquifers (QCSP_S) and central portion of the Sparta, Queen City and Carrizo-Wilcox aquifers (QCSP_C) (coordinates in Groundwater Availability Model projection). ....	374
Figure 8-8. Extraction of the Yegua-Jackson Aquifer and Queen City and Sparta aquifers cross-sections by intercepting the Gonzales Transect Model line with the three-dimensional spatial grids used in the Yegua-Jackson Aquifer and Queen City and Sparta aquifers Groundwater Availability Models. The two cross-sections are consequently combined to create the Guadalupe transect model. ....	376
Figure 8-9. The Yegua-Jackson Aquifer and Queen City and Sparta aquifers cross-sections extracted from the three-dimensional Groundwater Availability Models (left) compared to the resulting Gonzales Transect Model model (right): distributions of layer indexes (top), horizontal conductivity (middle) and leakance (bottom). ....	377

Figure 8-10.	Boundary conditions used in the Gonzlaes Model Transect model. ....	378
Figure 8-11.	Extraction of the Yegua-Jackson Aquifer and the Queen City and Sparta aquifers cross-sections by intercepting the Central Transect Model line to the three-dimensional spatial grids used in the Yegua-Jackson Aquifer and the Queen City and Sparta aquifers Groundwater Availability Models. The two cross-sections are consequently combined to create the Central Transect Model model. ....	380
Figure 8-12.	The Yegua-Jackson Aquifer and the Queen City and Sparta aquifers cross-sections extracted from the three-dimensional Groundwater Availability Models (left) compared to the resulting Central Transect Model model (right): distributions of layer indexes (top), horizontal conductivity (middle) and leakance (bottom). ....	381
Figure 8-13.	Boundary conditions used in the Central Transect Model model. ....	382
Figure 8-14.	Delineation of areas used for the outcrop mass balance using the Guadalupe River and the Brazos River basins. The basins are subsequently cropped to the outcrop locations. ....	387
Figure 8-15.	Formation outcrops in the Groundwater Availability Models for the Yegua-Jackson Aquifer, southern portion of the Queen City, Sparta and Carrizo-Wilcox aquifers and central portion of the Queen City, Sparta and Carrizo-Wilcox aquifers and river basins cropped to the outcrops. ....	388
Figure 8-16.	Extraction of fluxes from the Upper Wilcox outcrop in the Brazos basin area (top) and fluxes from the Carrizo-Wilcox Aquifer outcrop in the Guadalupe basin area (bottom). ....	389
Figure 8-17.	Comparison of transverse lateral flow to vertical flow through the general head boundary conditions for the models of the Sparta, Queen City and Carrizo-Wilcox aquifers in the Gonzales (top) and the central (bottom) cross-sections. ....	391
Figure 8-18.	Comparison of hydraulic heads predicted with the three-dimensional models of the Yegua-Jackson Aquifer and southern portion of the Sparta, Queen City and Carrizo-Wilcox aquifers (top) to those predicted with the Gonzales Transect model (bottom). ....	395
Figure 8-19.	Cells corresponding to water level measurements (top) based on projections of well locations to the Gonzales Transect model (bottom, left), and cross-plots between measurements and heads modeled with the 3D (bottom, middle) and the 2D models (bottom, right). State well number (TWDB database), measured water level and corresponding aquifer are indicated next to the well locations. ....	396
Figure 8-20.	Cross-plots of hydraulic heads modeled with the three-dimensional Groundwater Availability Models and the Gonzales Transect model at locations selected as representative for deep and shallow parts of the modeled formations. ....	397
Figure 8-21.	Comparison of hydraulic heads between the Gonzales Transect model and Groundwater Availability Models: plots of relative error versus depth for the Yegua-Jackson Aquifer (top) and the Sparta, Queen City and Carrizo-Wilcox aquifers (bottom). ....	399
Figure 8-22.	Illustration of the conceptual difference in boundary conditions used in the three-dimensional models and the two-dimensional transect: the original Yegua-Jackson Aquifer Groundwater Availability Model treats the base of the Lower Yegua unit as a no-flow boundary whereas in the transect model water flows in vertically through the Cook Mountain Formation. Similarly, the Queen City and Sparta Aquifers Groundwater Availability Model treats the Sparta Aquifer unit as a general head boundary whereas hydraulic heads in the Sparta Aquifer unit of the transect model depend strongly on recharge and general head boundary conditions imposed at the outcrop and the Catahoula. ....	401

Figure 8-23.	Portions of the Gonzales transect model corresponding to extended (A) and, original (B) layers from the Queen City and Sparta aquifers Groundwater Availability Models and layers from the Yegua-Jackson Aquifer Groundwater Availability Model (C).....	402
Figure 8-24.	Groundwater ages and particle pathlines computed with the reference simulation of the Gonzales Transect model.....	406
Figure 8-25.	Model cells corresponding to water age measurements projected locations and depths in the Gonzales Transect. ....	409
Figure 8-26.	Water age sensitivity to layer horizontal conductivity, Gonzales Transect model. 410	
Figure 8-27.	Water age sensitivity to layer leakance, Gonzales Transect model. ....	411
Figure 8-28.	Water age sensitivity to recharge at layer outcrop, Gonzales Transect model.	412
Figure 8-29.	Comparison of hydraulic heads predicted with the three-dimensional models of the Yegua-Jackson Aquifer and the central portion of the Sparta, Queen City and Carrizo-Wilcox aquifers cross sections (top) to those predicted with the Central Transect model (bottom).....	416
Figure 8-30.	Cells corresponding to water level measurements (top) based on projections of well locations to the Central Transect model (bottom, left), and cross-plots between measurements and heads modeled with the 3D (bottom, middle) and the 2D models (bottom, right). State well number (TWDB database), measured water level and corresponding aquifer are indicated next to the well locations.....	417
Figure 8-31.	Cross-plots of hydraulic heads modeled with the three-dimensional Groundwater Availability Models and the Central Transect model at locations selected as representative for deep and shallow parts of the modeled formations.....	419
Figure 8-32.	Comparison of hydraulic heads between Central Transect model and Groundwater Availability Models: plots of relative error versus depth for the Yegua-Jackson Aquifer (top) and the Sparta, Queen City and Carrizo-Wilcox aquifers (bottom). ....	421
Figure 8-33.	Illustration of conceptual differences in the boundary conditions used in the 3D models and the 2D transect: the original Yegua-Jackson Aquifer Groundwater Availability Model treats the base of the Lower Yegua unit as a no-flow boundary whereas, in the transect model, water flows in vertically through the Cook Mountain Formation. Similarly, the Queen City Sparta Aquifers Groundwater Availability Model treats the Sparta Aquifer unit as a general head boundary whereas hydraulic heads in the Sparta Aquifer unit of the transect model depend strongly on recharge and general head boundary conditions imposed at the outcrop and the Catahoula.	423
Figure 8-34.	Portions of the Central Transect model corresponding to extended (A) and original Queen City and Sparta aquifers Groundwater Availability Model layers (B) and the Yegua-Jackson Aquifer Groundwater Availability Model layers (C). ....	424
Figure 8-35.	Groundwater ages (in years) and particle pathlines computed with the reference simulation of the Central Transect model. ....	428
Figure 8-36.	Model cells corresponding to water age measurements projected locations and depths in the Central Transect.....	431
Figure 8-37.	Water age sensitivity to layer horizontal conductivity, Central Transect model. 432	
Figure 8-38.	Water age sensitivity to layer leakance, Central Transect model. ....	433
Figure 8-39.	Water age sensitivity to recharge at layer outcrop, Central Transect model.....	434

## List of Tables

Table 5-1.	Summary of mean hydraulic conductivity values (feet/day). .....	31
Table 7-1.	Summary of results for groundwater age estimates. ....	106
Table 7-2.	Chemical and isotopic results from samples collected in Brazos, Burleson, Milam and Robertson counties in 2012. ....	117
Table 7-3.	Summary of age estimates for the Wilcox Group of the Carrizo-Wilcox Aquifer. ....	190
Table 7-4.	Chemical and isotopic results from samples collected in the Gonzales Transect during 2012. ....	241
Table 7-5.	Summary of results for the Carrizo Sand Formation portion of the Carrizo-Wilcox Aquifer groundwater age estimates from geochemical modeling <sup>(6)</sup> . ....	256
Table 7-6.	Summary of results for the Queen City and Sparta aquifer groundwater age estimates. ....	267
Table 7-7.	Summary of results for groundwater age estimates from geochemical modeling. ....	344
Table 7-8.	Results of modeling reaction paths. ....	345
Table 7-9.	Selected chemical constituents for the brackish test and monitor wells (Kreitler and Morrison, 2009). ....	354
Table 7-10.	Chemical and isotopic composition of the brackish Lower Wilcox Group water samples. ....	355
Table 7-11.	Summary of results for the brackish Lower Wilcox Group groundwater age estimates. ....	362
Table 7-12.	Summary of results for the brackish Lower Wilcox Group groundwater pH and saturation indices. ....	362
Table 8-1.	Generalized stratigraphic profile for the Carrizo-Wilcox, Queen City, Sparta (QCSP) and Yegua-Jackson (YEG) aquifers in the investigated area. ....	363
Table 8-2.	Locations of the first grid cell at the outcrop and last grid cell at the down-dip boundary in the two transect lines at Texas Groundwater Availability Model coordinates. ....	374
Table 8-3.	IBOUND indexes, number of active cells, mean layer horizontal conductivity and leakance in the Gonzales Transect Model model. ....	378
Table 8-4.	IBOUND indexes, number of active cells, mean layer horizontal conductivity and leakance in the Central Transect Model model. ....	382
Table 8-5.	Mass balance derived for the investigated areas of the Guadalupe and the Brazos River basin. ....	390
Table 8-6.	Calibrated parameters for the Gonzales and the Central Transect models. ....	391
Table 8-7.	State wells with available water level measurements near the Gonzales Transect mode coordinates, measured water levels and modeled heads at cells corresponding to well locations and depths. ....	396
Table 8-8.	Selected model cells and their hydraulic heads used for comparison between the Gonzales Transect model and the three-dimensional Yegua-Jackson Aquifer and southern portion of the Queen City and Sparta aquifers models. ....	398
Table 8-9.	Overview of recharge assigned to outcrop cells per layer in the Gonzales Transect model. Red colors indicate dried-out cells where recharge is transferred to the cells of the underlying layer. ....	400
Table 8-10.	Percentage of water balance that occurs in the deep portions where the Queen City and Sparta aquifers Groundwater Availability Models layers were extended in the Gonzales Transect model. Vertical flows correspond to the sum of absolute values of flows through the bottom face of the model cells in the corresponding portion of the model (A, B, and C).	

Horizontal flows correspond to the sum of absolute values of flows through the right face of the model cells in the corresponding portion of the model (A, B, and C)..... 402

Table 8-11. Overview of water age sensitivity runs carried out with the Gonzales Transect model. 407

Table 8-12. Overview of wells with available water age measurements and comparison to water ages modeled using particle tracking in the Gonzales Transect. .... 408

Table 8-13. State wells with available water level measurements near the Central Transect model coordinates, measured water levels and modeled heads at cells corresponding to well locations and depths..... 418

Table 8-14. Selected model cells and their hydraulic heads used for comparison between the Central Transect model and the three-dimensional model Groundwater Availability Models. . 420

Table 8-15. Overview of recharge assigned to outcrop cells per layer in the Central Transect model. Red colors indicate dried-out cells where recharge is transferred to the cells of the underlying layer. .... 422

Table 8-16. Percentage of the water balance that occurs in the deep portions where the Queen City and Sparta aquifers Groundwater Availability Model layers were extended in the Central Transect model. Vertical flows correspond to the sum of absolute values of flows through the bottom face of the model cells in the corresponding portion of the model (A, B, and C). Horizontal flows correspond to the sum of absolute values of flows through the right face of the model cells in the corresponding portion of the model (A, B, and C). .... 424

Table 8-17. Overview of water age sensitivity runs carried out with the Central Transect model. 429

Table 8-18. Overview of wells with available water age measurements and comparison to water age modeled using particle tracking in the Brazos transect. .... 430

## **List of Appendices**

- Appendix A Chemical Analysis  
(Includes Data Collected Previously by TWDB & New Data Collected During  
This Study) - Electronic Deliverables Only
- Appendix B Field Notes and Lab Reports - Electronic Deliverables Only

*This page is intentionally blank.*

## 1 Executive Summary

The Texas Water Development Board (TWDB) has collected hydrochemical and isotope data in Groundwater Management Areas 11, 12 and 13 for over a decade. Prior to this study, a comprehensive assessment of this data has not been completed. The TWDB has several Groundwater Availability Models located throughout Groundwater Management Areas 11, 12 and 13 and the existing data offered an opportunity to evaluate the hydrochemical and isotope data to see if it was consistent with the conceptual models for the aquifer systems and the Groundwater Availability Models in the study area. In addition to evaluating the existing data, new data were also collected in selected areas to help evaluate the existing conceptual models and to support ongoing Groundwater Availability Model development and refining efforts.

Hydrochemical and isotope data were evaluated in four varying transect areas: The Northeast, Central, Gonzales, and South Transects for the Carrizo-Wilcox, Queen City, Sparta, Yegua-Jackson and Brazos River Alluvium aquifers. The first step of the process was to assimilate, review and integrate the water chemistry data for these aquifers from the TWDB groundwater database. The second step was to collect additional hydrochemical and isotope data from recently constructed brackish wells, primarily to develop a better understanding of the age of these waters. The hydrochemical and isotope data were evaluated by assessing chemical evolution of the groundwater with depth and age; comparison of the ratios of various constituents such as calcium and bicarbonate, sodium and chloride and others; geochemical modeling using NETPATH; and by using Piper diagrams. In addition, two-dimensional, cross-section groundwater flow models were constructed to estimate travel times from the aquifer outcrops to downdip areas as a means of comparison to the groundwater age estimated from isotopic data.

The most common types of water chemistry in the major and minor aquifers in Groundwater Management Areas 11, 12 and 13 are sodium-bicarbonate type water, sodium-sulfate-chloride type water and calcium-magnesium-sodium-bicarbonate. The occurrence of sodium-bicarbonate type water is common in Tertiary-aged aquifers (Carrizo-Wilcox, Queen City and Sparta) along the Texas Gulf Coast from east Texas to central Texas. The Yegua-Jackson does not typically contain sodium-bicarbonate water, but rather a sodium-sulfate-chloride water. The Brazos River Alluvium Aquifer in Groundwater Management Area 12 is a mixed cation (calcium-magnesium-sodium) bicarbonate type water.

In the higher rainfall regions (northeast Texas) the sodium-bicarbonate waters originate as a calcium-magnesium-chloride-sulfate in and/or near the outcrop (recharge zone) and as they flow into the deeper confined sections these aquifers “evolve” to a sodium-bicarbonate water. Though the sodium-bicarbonate type waters are common in these aquifers, some exceptions are noted. For instance, in south Texas the Queen City Aquifer (Gonzales Transect) does not evolve to a bicarbonate-dominated water and the Sparta Aquifer in the Gonzales and South transects remains a chloride-sulfate type water. These three aquifers in their different transects in south Texas are underlain by the very fresh sodium-bicarbonate water in the Carrizo Sand Formation portion of the Carrizo-Wilcox Aquifer. Comparison of the water chemistry from these aquifers does not support the concept of significant leakage of the underlying Carrizo Sand Formation portion of the Carrizo-Wilcox Aquifer into these aquifers. Rather, each aquifer seems to have somewhat distinct hydrochemical signatures that are not indicative of significant mixing.

The Yegua-Jackson Aquifer from central Texas to south Texas is predominantly a sodium-chloride-sulfate type water. Groundwater production is primarily in the outcrop and not downdip. The source of this possible chemical signature is not known, but it has not been significantly impacted by the leakage of deeper sodium-bicarbonate water. The total dissolved solids for the groundwater in the Yegua-Jackson Aquifer is often higher than underlying aquifers. Thus, we conclude that the underlying aquifers are not leaking significant quantities of groundwater into the Yegua-Jackson Aquifer and causing lower total dissolved solids waters.

The Brazos River Alluvium Aquifer along the Brazos River in Groundwater Management Area 12 has a calcium-magnesium-bicarbonate composition. None of the Tertiary-aged aquifers beneath the Brazos River Alluvium Aquifer, that is, the Carrizo-Wilcox, Queen City, Sparta or Yegua-Jackson have that type of water either in their subcrop immediately beneath the Brazos River Alluvium Aquifer or within their confined section beneath the alluvium. These formations have either a calcium-magnesium-chloride-sulfate in the outcrop or sodium-bicarbonate water downdip (e.g., Carrizo-Wilcox Aquifer). There is no evidence in the water chemistry to support significant upward leakage from deeper Tertiary-aged aquifers into the Brazos River Alluvium Aquifers.

The water chemistry from the three nests of San Antonio Water System's wells in Gonzales County further documents the lack of significant cross-formational flow between the Carrizo Sand Formation portion of the Carrizo-Wilcox Aquifer, the Queen City Aquifer and the Sparta Aquifer. The hydrochemical and isotope data from these nests of wells is consistent with the other data for the respective aquifer zone, but significantly different from the other aquifers in the transect.

The carbon-14 ages of groundwater are generally younger in the outcrop and older downdip in the confined section of an aquifer. A corrected estimate of the age of water requires knowing more than just the activity of carbon-14. The corrected carbon-14 dates in this report were estimated either with an isotopic signature correction technique ( $\delta^{13}\text{C}$ , a measure of the ratio of stable isotopes carbon-13 to carbon-12) or the combination of  $\delta^{13}\text{C}$  and geochemical modeling. Most of the efforts in age dating of the water were for the Carrizo-Wilcox Aquifer in the Northeast Transect, the Wilcox Group of the Carrizo-Wilcox Aquifer in the Central Transect, the Carrizo Sand Formation portion of the Carrizo-Wilcox Aquifer in the Gonzales and South transects because the geochemical reactions were better understood in those areas. Groundwater age in the outcrop was typically modern and increased in the downdip wells to an inferred age greater than 40,000 years before present because the samples contained no measurable carbon-14 (Figure 5-2). The Carrizo-Wilcox Aquifer to the Yegua-Jackson Aquifer generally contains old water. Comparison of the carbon-14 ages of the Carrizo Sand Formation portion of the Carrizo-Wilcox Aquifer waters in the Gonzales Transect and in the South Transect indicate that both transects have a gradual increase in age from the outcrop to measurable carbon-14 values at intermediate depths to very low carbon-14 in the deepest wells. However, the carbon-14 ages as the wells in the Central Transect get old (20,000 years plus) immediately (4 miles) downdip from the outcrop.

A comparison of the downdip extent of the higher calcium for the Gonzales and South transects versus the Central Transect is similar to the carbon-14 age distribution just discussed. In the Gonzales and South transects, higher calcium concentrations are observed about 20 miles downdip from the outcrop. For the Central Transect, the higher calcium concentrations occur primarily in the outcrop and not downdip in the confined section. A hydrogeologic implication to

this difference in carbon-14 age estimates and the downdip measurement of calcium between the South and Central transects is that the Carrizo Sand Formation groundwater in the South Transect is actively flowing from the outcrop into the deep subsurface. In the Central Transect, much of the active flow may be contained to the outcrop with discharge to the numerous streams and rivers that cross or headwater in the outcrop. There may only be limited flow into the deeper confined parts of the aquifer. Although it is uncertain whether or not the higher historical pumping in the South Transect is a factor in this difference, it is unlikely that relatively recent pumping would have a significant impact on the overall chemistry or groundwater age throughout the South Transect.

This concept of more recharge flowing to the confined section of the aquifer in south Texas is counterintuitive to the idea of more precipitation and less evapotranspiration in east Texas than in south Texas. In addition, it is doubtful that pumping in South Texas is causing a significant increase of induced recharge into the Carrizo Sand Formation of the Carrizo-Wilcox Aquifer. The higher transmissivities for the Carrizo Sand Formation portion of the Carrizo-Wilcox Aquifer in south Texas than for the Wilcox Group of the Carrizo-Wilcox Aquifer (north of the Colorado River) may permit more recharge to occur into the deeper subsurface in south Texas and more lateral flow in the outcrop to occur in central and east Texas.

Groundwater is flowing from the outcrop into the subsurface of the Carrizo Sand Formation portion of the Carrizo-Wilcox Aquifer for the Gonzales and the South transects. This observation is based on the potentiometric surface, the presence of elevated calcium in the confined section and the gradual increase in carbon-14 ages. Although there is no obvious geochemical evidence for significant cross formation flow from deeper units to shallower units, groundwater is flowing from the outcrop to downdip zones. This finding creates a paradox of how to discharge the buildup of groundwater at depth when it intersects the deep saline water that appear to be flowing up the structural dip from deeper geo-pressured zone. Unfortunately, no wells exist at a depth which would help to answer this question in the context of this study. The amount of cross-formational flow that occurs in the aquifer is an important consideration in appropriately calibrating the Groundwater Availability Models, especially the steady-state model. The importance of these flows is probably less significant in the context of regional water planning and overall assessment of regional impacts on time scales less than a hundred years. That is not to say that vertical flow under pumping conditions is not important, but rather that the usefulness of the Groundwater Availability Models in a predictive capacity is not completely diminished because of this uncertainty. If a large wellfield is constructed in the downdip section, water level measurements after production begins will allow for appropriate adjustments of vertical permeability in the model to improve the predictive capability of the Groundwater Availability Model. These modifications might be better characterized as parameter adjustments rather than conceptual model changes, but until such observation data are available, it is uncertain how much the conceptual model might need to be modified. The hydrochemical and isotope data available for this study were not appropriate for such quantitative assessments.

The water chemistry in the Carrizo Sand Formation wells in Bexar and Atascosa counties appears unique in comparison to other aquifers studied in this project. The sodium-sulfate water type for the brackish wells is similar only to waters in the Yegua-Jackson Aquifer. The carbon-14 percent modern indicates old water in both the outcrop and downdip. No chemical or isotopic evolution is observed for the water chemistry as was observed in the other aquifers in this study.

Two-dimensional transect models of the Carrizo-Wilcox, Queen City, Sparta and Yegua-Jackson aquifers were developed to assess groundwater ages and downgradient movement of water in the Guadalupe River and the Brazos River basins. The transect models were developed based on structure and data extracted from the existing three-dimensional Groundwater Availability Models. In an attempt to estimate the average simulated deep recharge for the transect models, the Groundwater Availability Models were used to assess the mass balance at the aquifer outcrops delineated in both river basins. This analysis indicated that net recharge calculated locally at the transect outcrops cannot adequately reproduce the flow conditions in the subsurface, as these are dictated by three-dimensional flow patterns imposed by the boundary conditions and flow gradients on a regional scale. Instead, the transect models were calibrated to observed heads by adjusting net recharge and without altering the hydraulic properties from the original Groundwater Availability Models.

The analyses of mass balances from the two-dimensional transect models showed that the flow patterns are dictated by the boundary conditions. This cross-formational vertical flow is imposed by the no-flow boundary conditions at the bottom of the models and at the down-dip edge of the transect model domain. Analysis of the mass balance further showed that the amount of flow occurring in portions of the transects that extended after extraction from the original Groundwater Availability Models to connect the aquifers is small compared to the overall flow in the transects. The associated uncertainty with this modification is negligible. However, because the conceptualization of vertical flow through the Cook Mountain Formation layer is simulated differently between the two Groundwater Availability Models, no combined model will be able to match flows in both Groundwater Availability Models simultaneously. In other words, the Groundwater Availability Models disagree with one another. Because the transect models combine both Groundwater Availability Models, their results will invariably differ from one or both of the Groundwater Availability Models.

There is a clear discrepancy between the simulated groundwater ages in the three-dimensional Groundwater Availability Models for the Carrizo-Wilcox, Queen City and Sparta aquifers and that in the two-dimensional models. This results from the explicit incorporation of the overlying Yegua-Jackson Aquifer units in the two-dimensional model. There is also a big difference between the simulated ages from the two-dimensional models and the ages determined from isotopic analysis. Generally, the carbon-14 ages for the Carrizo-Wilcox Aquifer, as an example, were less than 40,000 years, but the simulated ages from the two-dimensional models was one to three orders of magnitude greater than that. One explanation for this discrepancy may be due to the hydrologic conditions which resulted in the observed groundwater ages. Harrison and Summa (1991) show that past conditions affecting the entire Gulf Coast Aquifer system can result in deeper penetration of meteoric water into the down-dip portions of the aquifers than that expected under current conditions. Harrison and Summa (1991) also estimate that the recent development of geopressures which restrict the penetration of meteoric water under current conditions were not present in Miocene and earlier times when a smaller compactional force allowed deeper invasion of meteoric water. Given that sea levels during the last glacial low stand (18,000 years before present) were approximately 130 meters lower than present levels and 40 to 50 meters lower just 10,000 years ago, a significantly greater penetration of meteoric water could be expected than under present conditions.

The factors discussed above provide some insight into the potential factors for the discrepancy between the groundwater age estimated from the 2-dimensional transect models and the isotopic

data. Factors include inappropriate modeling assumptions (e.g., steady-state flow systems, simulation of complex 3-dimensional systems with a 2-dimensional transect model, etc.), uncertainty in parameters and/or boundary conditions, and the complexity of sea level changes and the dynamics of geopressurization. This modeling confirms that there are limitations for all Groundwater Availability Models and that these limitations should be seriously considered in all applications.

The results of this study generally confirm the conceptual models for the Queen City and Sparta and Yegua-Jackson Groundwater Availability Models. However, there are some questions that have not been answered by evaluating the hydrochemical and isotopic data. First, due to lack of sufficient and/or appropriate deep wells for sampling, the downdip flow conditions in all the aquifers are still somewhat uncertain. The estimates of groundwater age generally confirm the conceptual model assumption that recharge occurs on the outcrop of the aquifers and that some portion of that recharge moves downdip over time. However, the nature of the flow deep in the aquifers is still not fully understood and this study has not provided any hard evidence regarding the conceptualization of the downdip boundary condition for the aquifers.

The amount of cross-formational flow that occurs in the aquifer is an important consideration in appropriately calibrating the Groundwater Availability Models, especially the steady-state model. The importance of these flows is probably less significant in the context of regional water planning and overall assessment of regional impacts on time scales less than a hundred years. That is not to say that vertical flow under pumping conditions is not important, but rather that the usefulness of the Groundwater Availability Models in a predictive capacity is not completely diminished because of this uncertainty. If a large wellfield is constructed in the downdip section, water level measurements after production begins will allow for appropriate adjustments of permeability and storage properties in the model to improve the predictive capability of the Groundwater Availability Model. These modifications might be better characterized as parameter adjustments rather than conceptual model changes, and until such observation data are available, it is uncertain how much the conceptual model might need to be modified. The hydrochemical and isotope data available for this study were not appropriate for such determinations.

The study confirms a basic tenet of groundwater modeling - that model conceptualization and development should not be undertaken without first understanding the objective of the modeling. In addition, if modeling objectives change over time or if different questions need to be answered with the models, it may be necessary to refine the conceptual models upon which the Groundwater Availability Model is based.

*This page is intentionally blank.*

## 2 Introduction

In January 2011, the TWDB contracted with LBG-Guyton Associates to evaluate the hydrochemical and isotopic data in Groundwater Management Areas 11, 12 and 13. The goal of the study was to assess how these data might change the conceptual models for the TWDB Groundwater Availability Models in the study area. Specifically, the hope was to assess the general assumptions of the Groundwater Availability Model conceptual models and boundary conditions to see if results from the evaluation of hydrochemical and isotope data would help make the models more representative of the aquifer system. LBG-Guyton Associates teamed with Geochemical Technologies Inc., Intera, Baer Engineering, C-tech Corp., and San Antonio Testing Laboratories to complete the project. LBG-Guyton Associates managed the project and was responsible for the assessment of hydrochemical and isotope data. Geochemical Technologies (Randy Bassett, Ph.D.) was responsible for the geochemical modeling with NETPATH and Intera was responsible for 2-dimensional cross-sectional modeling. C-tech Corporation developed 3-dimensional visualizations of the aquifers in the study area and Baer Engineering supported the field sampling effort. San Antonio Testing Laboratories completed some of the chemical analysis of the groundwater samples.

The TWDB has collected hydrochemical and isotope data in Groundwater Management Areas 11, 12 and 13 for over a decade (TWDB, 2013). Prior to this study, a comprehensive assessment of this data has not been undertaken. Because the TWDB has several Groundwater Availability Models located throughout Groundwater Management Areas 11, 12 and 13, the existing hydrochemical and isotope data offered a great opportunity to evaluate the conceptual models for the aquifer systems and the Groundwater Availability Models in the study area. In addition to evaluating the existing data, new data were also collected in selected areas and analyzed to help evaluate the existing conceptual models and to support ongoing Groundwater Availability Model development efforts for minor aquifers.

The major aquifer in Groundwater Management Areas 11, 12 and 13 is the Carrizo-Wilcox Aquifer, as shown in Figure 2-1. Major aquifer Groundwater Availability Models were originally developed for the southern portion of the Sparta, Queen City and Carrizo-Wilcox aquifers (Deeds and others, 2003); central portion of the Sparta, Queen City and Carrizo-Wilcox aquifers (Dutton and others, 2003); and northern portion the Sparta, Queen City and Carrizo-Wilcox aquifers (Fryar and others, 2003).

The minor aquifers in Groundwater Management Areas 11, 12 and 13 include the Brazos River Alluvium, Sparta, Queen City, and Yegua-Jackson as shown in Figure 2-2. The Sparta and Queen City aquifers were incorporated as additional layers to the three previously developed Carrizo-Wilcox Aquifer Groundwater Availability Models (Kelley and others, 2004). In addition, a Groundwater Availability Model for the Yegua-Jackson Aquifer was developed (Deeds and others, 2010). Figure 2-3 shows the model boundaries for the Groundwater Availability Models in Groundwater Management Areas 11, 12 and 13.

New groundwater chemical data were collected along three transects within the study area. Samples were collected from each of the aquifers within Groundwater Management Areas 11, 12 and 13. In addition, existing data along two other transects were evaluated for this study. All newly collected primary data and existing published data were reviewed for the purpose of evaluating existing conceptual models for the aquifers in the study area.

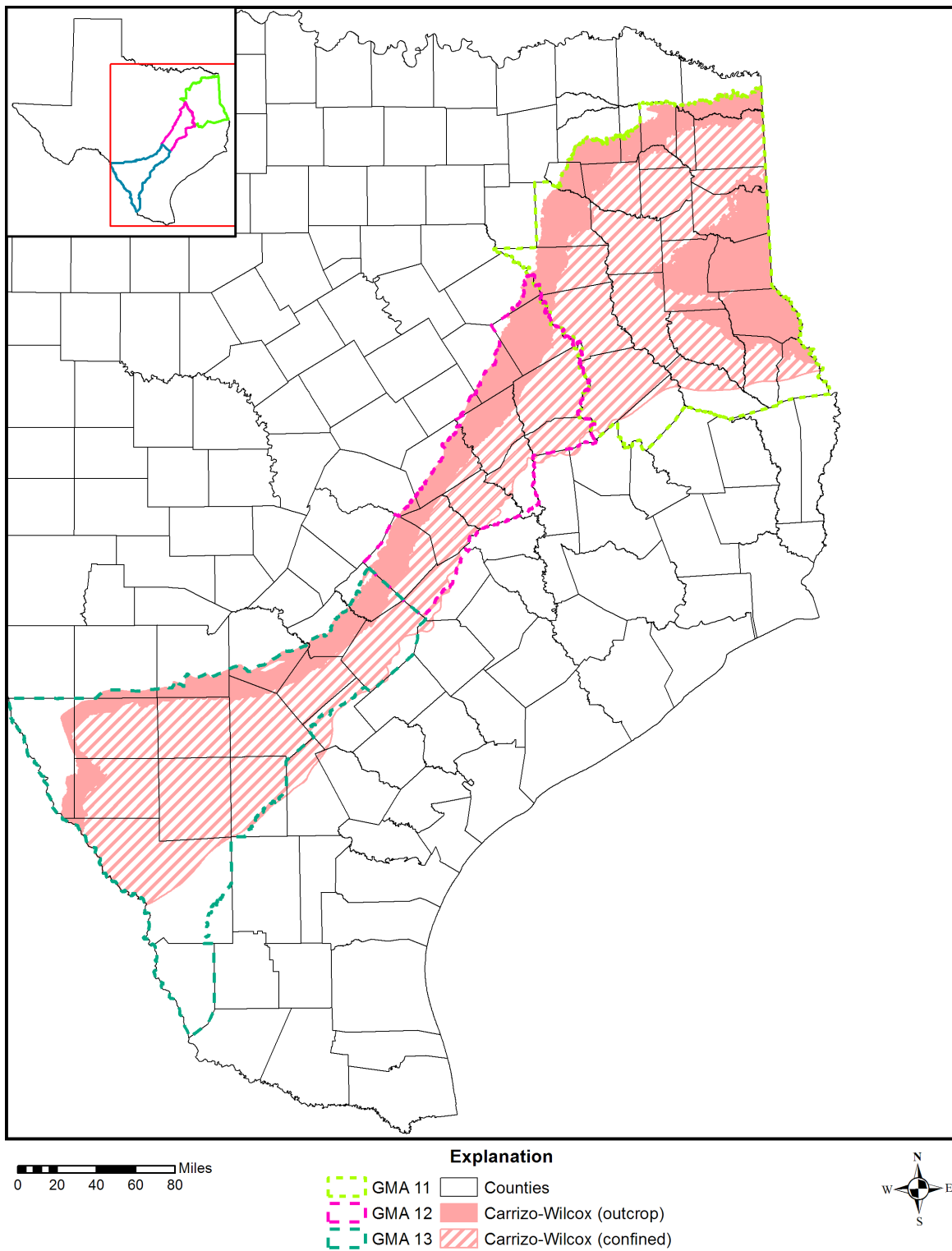


Figure 2-1. Location of the major aquifer in Groundwater Management Areas (GMAs) 11, 12 and 13.

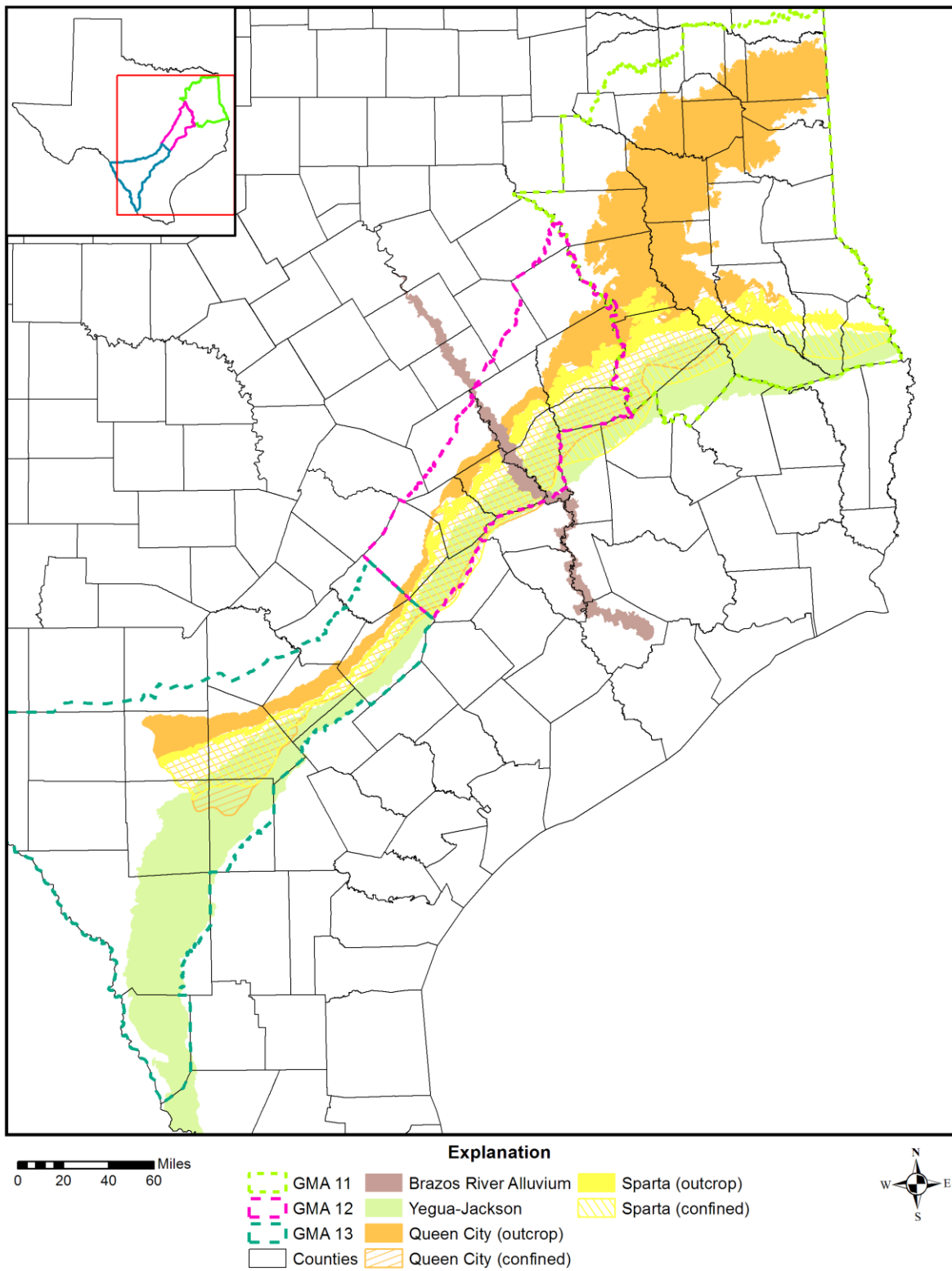
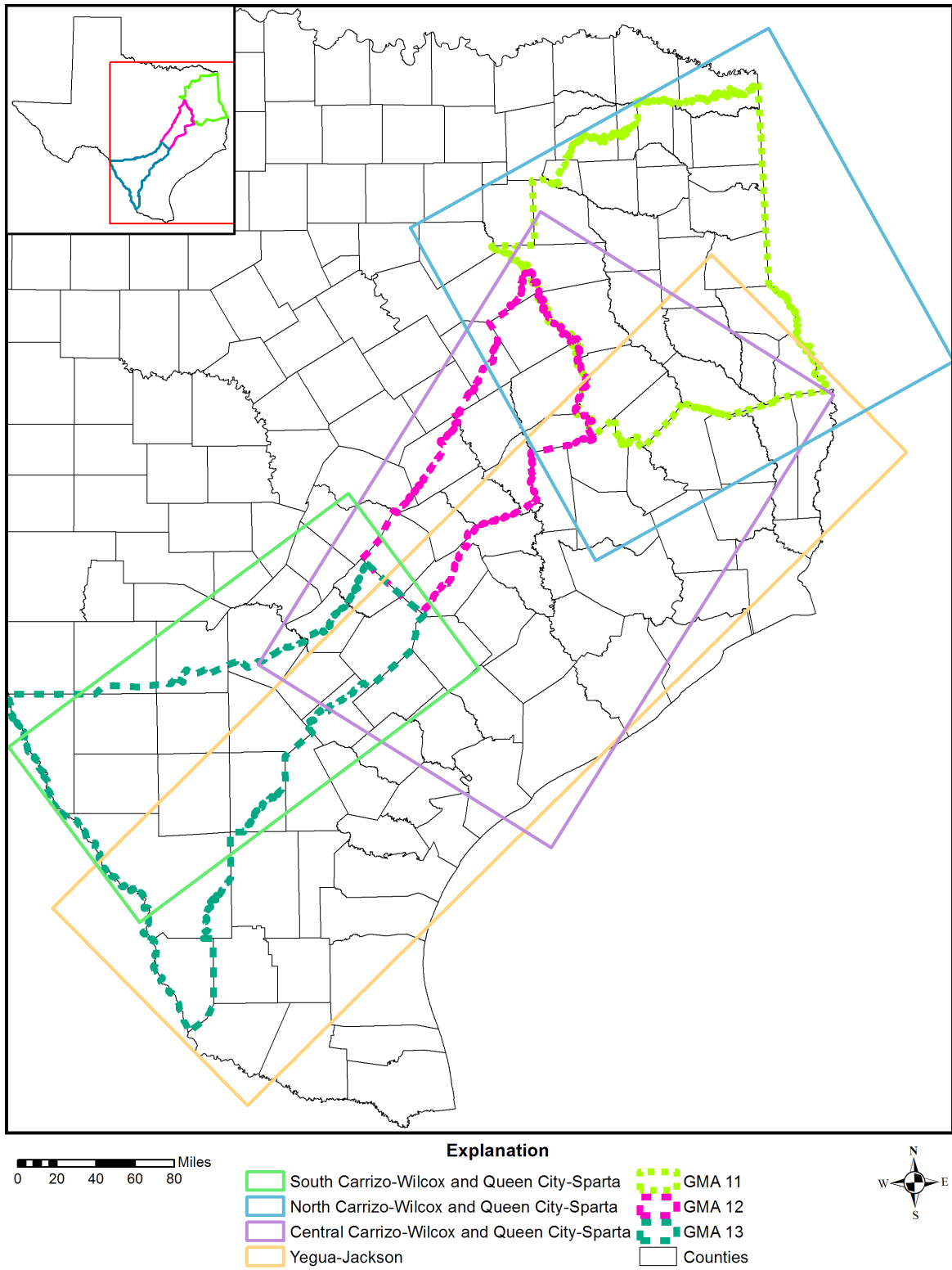


Figure 2-2. Location of the minor aquifers in Groundwater Management Areas (GMAs) 11, 12 and 13.



**Figure 2-3. Location of the existing TWDB Groundwater Availability Models in Groundwater Management Areas (GMAs) 11, 12 and 13.**

### 3 Study Area

The geographic area for this study includes Groundwater Management Areas 11, 12 and 13 (Figure 3-1) and includes the Tertiary-age aquifers of the Carrizo Sand Formation portion of the Carrizo-Wilcox Aquifer (south Texas), the Wilcox Group of the Carrizo-Wilcox Aquifer (central Texas), the Carrizo-Wilcox Aquifer (northeast Texas) and the Queen City, the Sparta and the Yegua-Jackson aquifers. The area also includes the Brazos River Alluvium Aquifer. Figure 3-2 shows the stratigraphic section along the Brazos River in Robertson and Brazos counties.

Geographically, the study area extends from Louisiana to the Rio Grande along the Mexico border. Within this very large area the hydrogeologic setting can vary significantly. Precipitation varies across the three Groundwater Management Areas (Figure 3-3). In Groundwater Management Area 11, average precipitation can be over 50 inches, whereas annual precipitation in Groundwater Management Area 13 can be less than 20 inches. This wide range of precipitation significantly alters the potential amount of recharge across the three Groundwater Management Areas.

Sanford and Selnik (2013) estimated that the fraction of precipitation lost to evapotranspiration could be as little as 50 to 60 percent in east Texas, whereas, the fraction of precipitation lost to evapotranspiration in south Texas could be as high as 90 percent. Permeability between geographic areas and formations also vary significantly.

The Carrizo Sand and the Simsboro Formation, which comprise two distinct units within the greater Carrizo-Wilcox Aquifer, are the most productive aquifers in the study area. The Carrizo Sand extends throughout the entire study area from Mexico to Louisiana, while the Simsboro Formation is limited to the central part of the study area, between the Colorado and Trinity rivers. Both the Carrizo Sand and the Simsboro Formation contain hundreds of feet of vertically continuous and laterally extensive productive sands and gravels. Many wells screened in these aquifers are capable of producing in excess of 1,000 gallons per minute.

The Queen City and the Sparta aquifers are both designated by the TWDB as minor aquifers that are separated by the Weches Formation confining unit. Neither of these aquifers is recognized southwest of the Frio River by the TWDB, because they are replaced with the equivalently-aged Laredo Formation and El Pico Clay, which are unsuitable for significant groundwater production. The Queen City Aquifer is significantly thicker than the Sparta Aquifer. The greatest thickness of the Queen City Aquifer (exceeding 2,000 feet at depth) occurs in the southwest part of the study area. The Sparta Aquifer, by contrast, exhibits its greatest thickness (500 to 700 feet) in the northeast part of the study area, near (and beyond) the Louisiana border.

The Yegua-Jackson Aquifer extends from the Mexico border to the Louisiana border. It is generally the least productive of the aquifers evaluated in this study. Like the Queen City and Sparta aquifers, it has not been significantly developed throughout the study area. Unlike these other aquifers, the Yegua-Jackson Aquifer does not have any significant amount of usable quality groundwater in the confined downdip section of the aquifer. Groundwater use is restricted almost completely to the outcrop area, and so the defined aquifer is limited to the combined outcrops of the Yegua Formation and/or Jackson Group of the Yegua-Jackson Aquifer. The Cook Mountain Formation provides hydraulic separation from the underlying Sparta Sand.

To evaluate the hydrochemistry for this large geographic area (Groundwater Management Areas 11, 12 and 13) with its varying geology and climate (potential recharge), four test areas (transects) were evaluated from northeast Texas to south Texas to see if there were significant differences in the hydrochemistry in the major and minor aquifers in each region (Figure 3-1). The four test areas are:

1. Northeast Transect, which includes Henderson, Anderson and Houston counties in northeast Texas. This area includes the Carrizo-Wilcox, Queen City, Sparta and Yegua Formation of the Yegua-Jackson aquifers. This transect includes an area previously evaluated by Kreitler and Pass (1980) and Kreitler and Wuerch (1981) with some preliminary carbon-14 estimates for the age of the groundwater.
2. Central Transect, which includes Brazos, Burleson, Milam and Robertson counties. This area includes the Wilcox Group of the Carrizo-Wilcox, Queen City, Sparta, Yegua-Jackson and Brazos River Alluvium aquifers. This transect follows the Brazos River.
3. Gonzales Transect, which includes Guadalupe, Gonzales and Caldwell counties. This area includes the Carrizo Sand Formation portion of the Carrizo-Wilcox, Queen City, Sparta and Yegua-Jackson aquifers.
4. South Transect, which includes Bexar, Atascosa and McMullen counties. This area includes the Carrizo Sand Formation portion of the Carrizo-Wilcox, Queen City, Sparta and Yegua-Jackson aquifers, the same set of aquifers as in the Gonzales Transect. This transect includes the area previously evaluated by Pearson (1966) to determine carbon-14 ages of groundwater in the Carrizo-Wilcox Aquifer.

Brackish groundwater is another important component of the hydrogeology in Groundwater Management Areas 11, 12 and 13. Brackish groundwater is defined as having total dissolved solids from 1,000 to 10,000 milligrams per liter. LBG-Guyton Associates (2003) mapped extensive brackish groundwater resources in Groundwater Management Areas 11, 12 and 13. San Antonio Water System is currently developing the brackish groundwater from the Carrizo-Wilcox Aquifer in southern Bexar County. Little is known about the detailed chemistry and the origin of the water in the brackish aquifers. Five wells screened in the brackish Carrizo-Wilcox Aquifer in southern Bexar and northern Atascosa counties were sampled and analyzed. In addition, a Class II injection well that was screened in the Carrizo-Wilcox Aquifer in northern Webb County was tested as a possible end member for the South Transect. The well location map for this brackish aquifer analysis is included in a later section on the results of this testing.

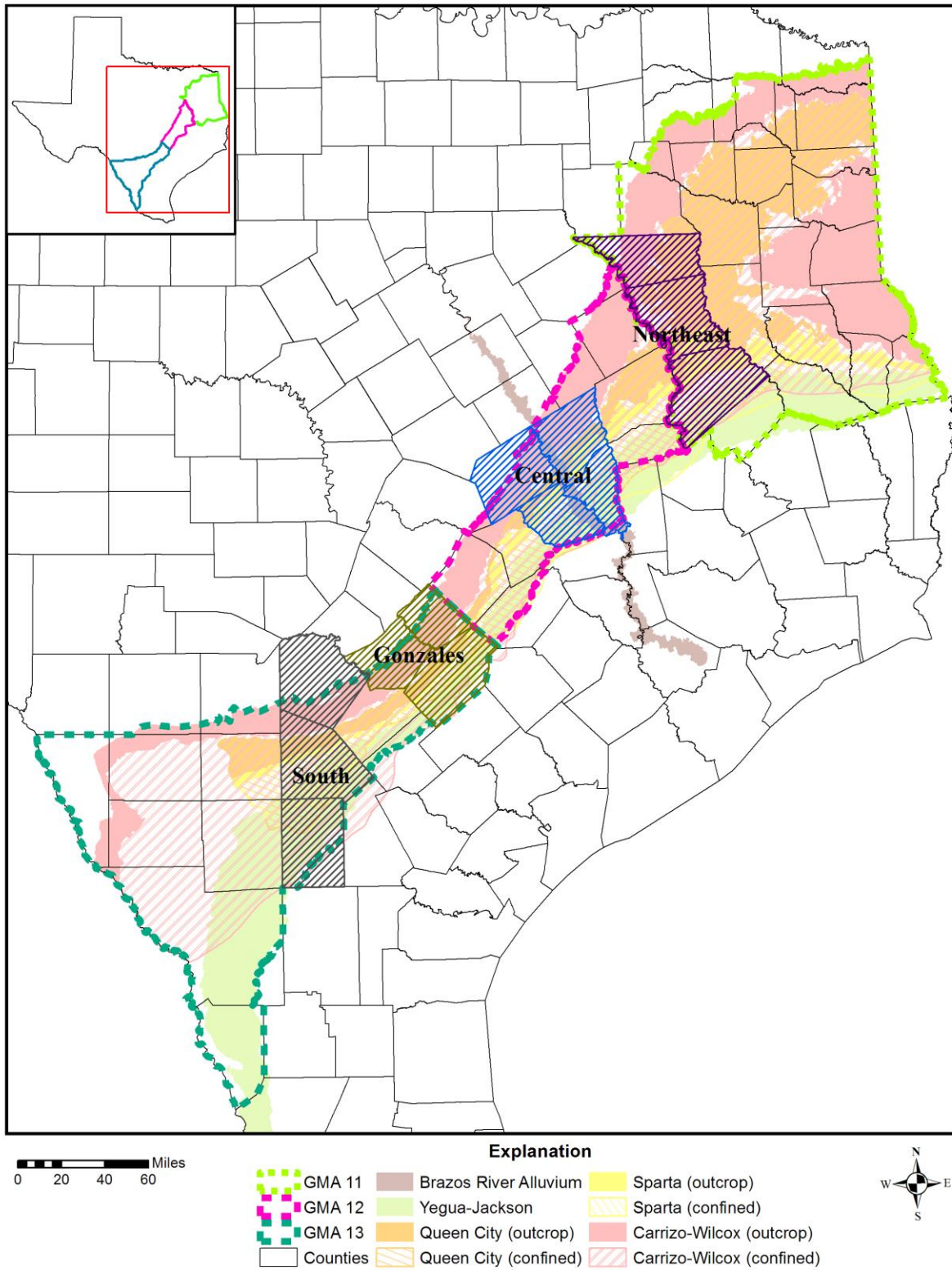


**Figure 3-1. Groundwater Management Areas and counties that contain the data for the study area transects.**

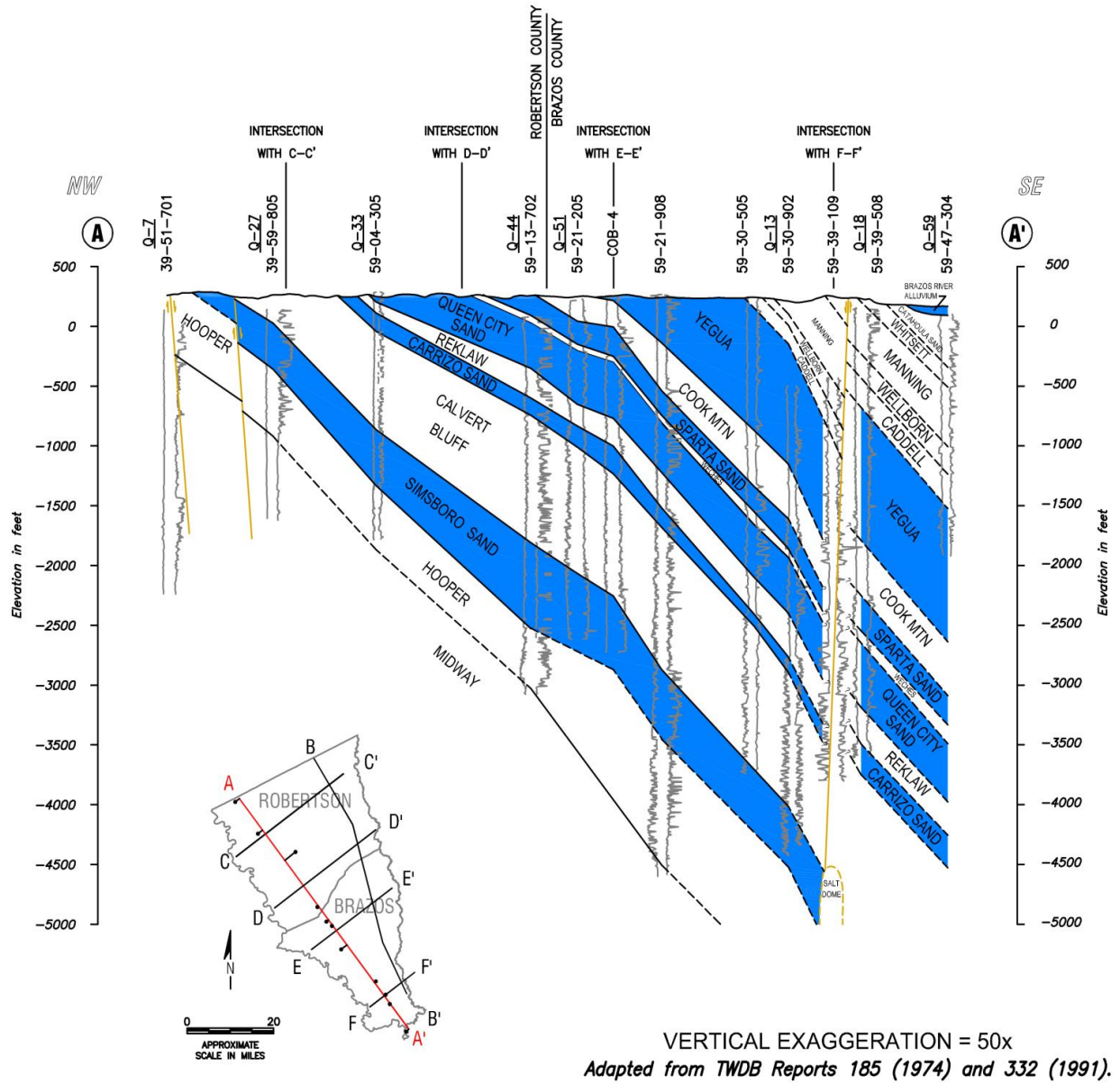


Figure 3-2. Cross-section in Brazos and Robertson counties showing dipping nature of the Carrizo-Wilcox Aquifer and other Texas coastal aquifer systems (Note: transects B-B' through F-F' are not addressed in this study).

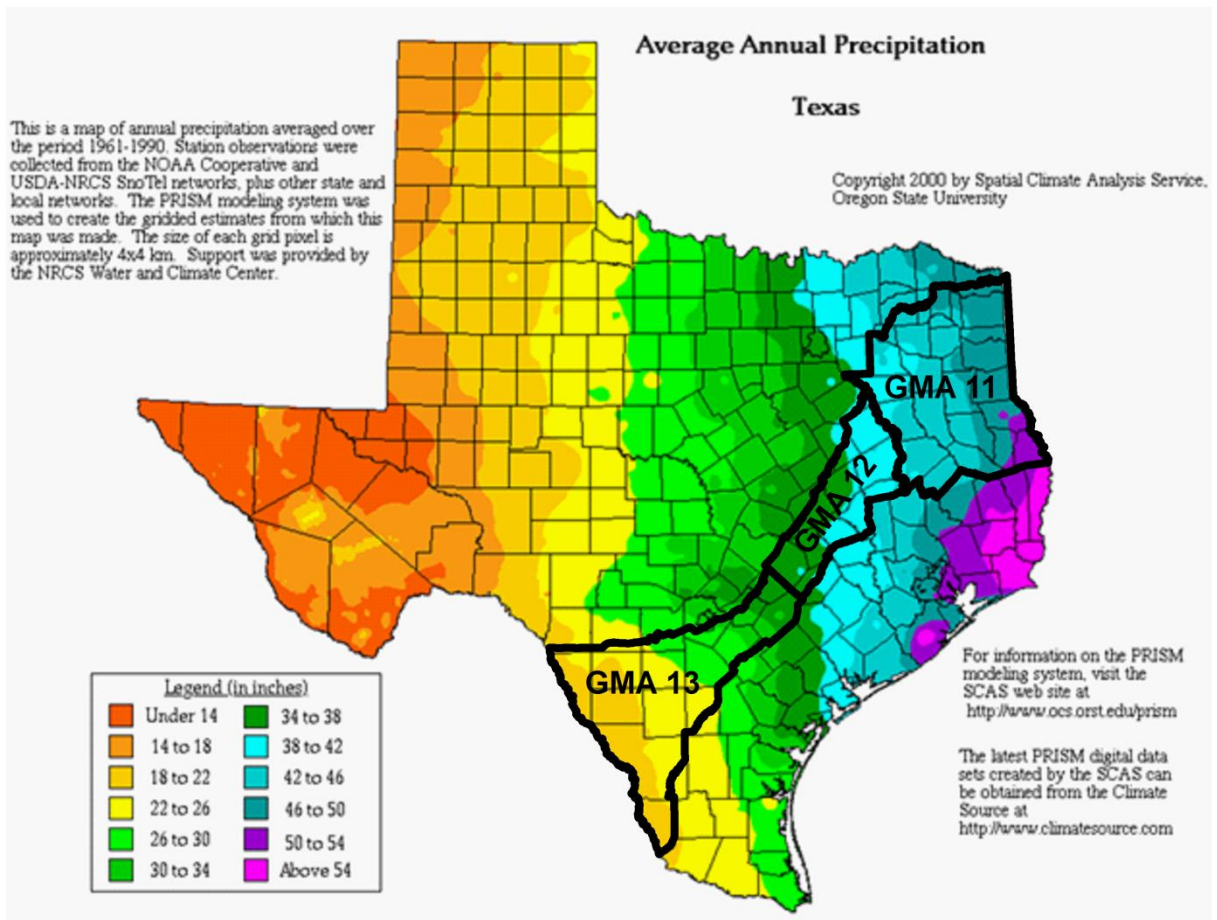


Figure 3-3. Average annual precipitation in Texas (PRISM, 2000).

*This page is intentionally blank.*

## 4 Data Evaluation

Data evaluation of the hydrochemistry in Groundwater Management Areas 11, 12 and 13 is for the Carrizo-Wilcox, Queen City, Sparta, Yegua-Jackson and Brazos River Alluvium aquifers. Collection and evaluation were a two-step process. The first step was the download, review and integration of the water chemistry data for these aquifers in the TWDB electronic groundwater database. A very large database is available for these aquifers. The second step was to collect additional chemical data for two of these transects, plus a set of recently constructed brackish tests and production wells, primarily to develop a better understanding of the age of these waters.

### 4.1 TWDB Groundwater Database

Step one was a download for quality assurance and quality control review of available data from the TWDB electronic groundwater database (2013). The TWDB groundwater data for major and minor aquifers in Groundwater Management Areas 11, 12 and 13 were reviewed for correctness. The types of well data reviewed included latitude and longitude, water levels, water chemistry and isotopes. The number of wells and analyses reviewed is shown below. Locations of groundwater data for all aquifers were mapped for Groundwater Management Areas 11, 12 and 13. All TWDB data used in this report are compiled in Appendix A.

Data were corrected, when possible, otherwise they were not used in the analysis. The final data sets meet the following criteria:

1. All wells have total depth estimate or documented completion intervals, springs were deleted because a specific aquifer designation was not assigned;
2. All sites have location accuracies of + 1 minute or better;
3. No wells have aquifer codes such as “UNKNOWN” or “NON\_APPLICABLE”;
4. Only publishable water level measurements were used;
5. All water levels readings that plot below the bottom of the borehole were excluded;
6. All water quality analyses with charge balance outside + 5 percent were excluded.

Final data sets by aquifer of best available data were then used for the analyses of TWDB data in this report. A summary of the data used are shown below:

#### Well Data

- 15,067 well locations total, of which
- 651 had no well depths (springs excluded)

#### Latitude/Longitude Accuracy

- 11,252 wells had coordinates accurate to 1 second or better
- 1,960 wells had coordinates accurate from 1 to 5 seconds
- 1,247 wells had coordinates accurate from 5 to 10 seconds
- 58 wells had coordinates accurate from 10 seconds to 1 minute
- 550 had coordinates accurate from 1 to  $\pm 2\frac{1}{2}$  minutes or undocumented

#### Water Levels

- 69,835 publishable readings total, of which
- 144 measurements in 58 individual wells were below bottom of well

#### Major Ions

- 6,543 analyses total, of which
- 1,605 largely followed established field sampling protocols
- 3,251 have not followed sampling protocols entirely (older analyses)
- 1,596 had undocumented field sampling protocols
- 195 not balanced within 5%
- Chemical data are presented in tables and figures either as mg/L or meg/l.

#### Isotopes

- 585 analyses total (most of these are radium-226 and radium-228)
- No errors were found

## 4.2 Newly Collected Data

In addition to evaluating existing water quality data in the TWDB database, LBG-Guyton Associates planned and executed a significant field effort to generate primary groundwater chemistry data specifically to support this project. As mentioned previously, and discussed in detail in Section 7, excellent data sets exist from previous work in the Northeast Transect and the South Transect. Therefore, for the purpose of identifying candidate wells to sample for this project, the focus was placed on the areas in which previous data are lacking. In the Central and Gonzales transects, LBG-Guyton Associates tried to identify wells to sample in each major and minor aquifer crossed by the transect line. In the South Transect, previous data sets emphasized the Carrizo Sand Formation. For this project, all wells sampled along the South Transect screened the brackish Lower Wilcox Group portion of the Carrizo-Wilcox Aquifer.

In the Central Transect, 23 wells were sampled from wells screening the Carrizo-Wilcox, Queen City, Sparta, Yegua-Jackson and Brazos River Alluvium aquifers. In the Gonzales Transect, 23 wells were sampled from wells screening the Carrizo-Wilcox, Queen City, and Sparta aquifers. In the South Transect six wells were sampled; five from the brackish Lower Wilcox Group in Bexar and Atascosa counties and one sample from an oil and gas injection well screened in the Carrizo-Wilcox in Webb County. All chemical analyses present in table format are included in Section 7.2, Section 7.3 and Section 7.4 as well as in Appendix A. All field notes and other associated documents are included in Appendix B.

LBG-Guyton Associates and Baer Engineering performed the sampling of the wells identified for the field program. Sampling was performed in accordance with details set forth in the document “LBG-Guyton Sampling and Analysis Plan, GMA 11, 12, 13 Geochemical Evaluation”, included with the electronic deliverables for this report. Most of the wells sampled were either Public Water Supply wells or domestic supply wells, which are regularly pumped, and therefore do not require purging prior to sampling. Sampling activities were coordinated with the owners and operators of the wells. Temperature, conductivity, and pH were measured in the field using calibrated field meters a minimum of three times until measurements were

stabilized. Field notes, photographs of the wells sampled, and a summary of all field measurements is provided with the electronic deliverables for this report. Samples were submitted to San Antonio Testing Laboratory for general chemistry analysis, to Zymax Laboratory for fixed and hydrocarbon gas composition and carbon and hydrogen isotopes, to University of Arizona Laboratory for isotopes of sulfate, and to Beta Analytical laboratory for radiometric dating analysis. Two duplicate samples were collected as part of the field program.

*This page is intentionally blank.*

## 5 Hydrogeologic Setting

The major aquifer supplying Groundwater Management Areas 11, 12 and 13 is the Carrizo-Wilcox Aquifer. Minor aquifers include the Sparta, Queen City, Yegua-Jackson and Brazos River Alluvium. These aquifers are all comprised of Tertiary-age sedimentary sequences of coarse-grained materials comprising aquifers and finer grained materials comprising aquitards, all of which crop out in a wide band roughly parallel to the Texas coast. In the southern and central parts of the study area, the formations dip seaward at approximately one to two degrees. The thickness of each formation increases downdip. In the northern part of the study area, the Sabine Uplift area results in two separate structural domains, one which dips toward the coast and one in which the formations dip to the north toward the axis of the East Texas Basin.

The major structural features that affect the hydrogeology of the study area are displayed in Figure 5-1. In the northern part of the study area, the Sabine Uplift results in two separate structural domains, one which dips toward the coast and one in which the formations dip to the north toward the axis of the East Texas Embayment. In the southern portion of the study area, the updip extent of the Tertiary-aged sedimentary sequences is the Balcones Fault Zone, which separates these formations from older Cretaceous limestone deposits. Throughout most of the north part of the study area the Karnes, Milano, Mexia and the Talco fault zones approximate the updip extent of the Eocene sediments, although the southern extent of the Karnes, Milano and Mexia zone intersects the Eocene sediments. The Wilcox growth fault zone exists in a broad zone downdip of the Carrizo-Wilcox Aquifer, approximately parallel to the coast and the outcrop zone. The San Marcos Arch is a broad regional anticline with an axis perpendicular to the coast line through Gonzales County that separates the Rio Grande Embayment to the southwest from the Houston Embayment to the northeast. The Sabine Uplift is a significant structural feature in East Texas. Its presence can be seen in the outcrop patterns of the Carrizo-Wilcox Aquifer rocks, since the structural uplift has resulted in the erosion of younger formations in this area.

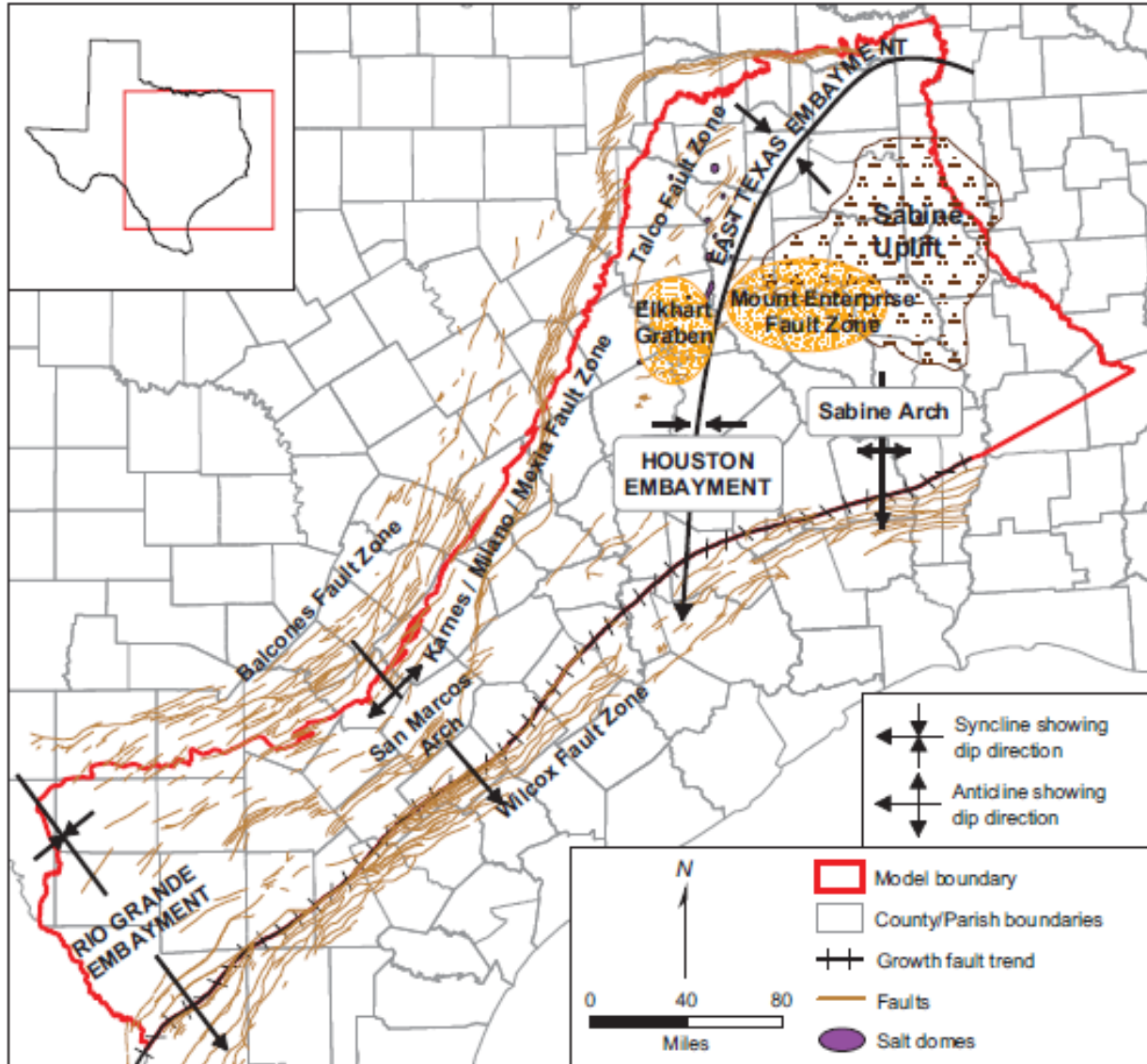


Figure 5-1. Map of major faults and structural features for the Texas Coastal Plain and East Texas Embayment. Faults modified from Ewing (1990). Structure axes modified from Guevara and Garcia (1972), Galloway (1982), and Galloway and others (2000).

## 5.1 Hydrostratigraphy

In the study area, six geologic formations are considered to be significant aquifers by the TWDB. From bottom to top these aquifers are the Wilcox Group, the Carrizo Sand, the Queen City Sand, the Sparta Sand, the Brazos River Alluvium Aquifer and the Yegua-Jackson Aquifer (Figure 5-2). The Carrizo-Wilcox Aquifer is jointly considered to be one of nine major aquifers in Texas as by the TWDB. The Queen City, Sparta, Yegua-Jackson and Brazos River Alluvium aquifers are designated as minor aquifers by the TWDB. The Queen City Sand and the Carrizo Sand are separated by the Reklaw Formation, which is comprised primarily of fine-grained materials and is generally considered to be a confining bed. The Weches Formation, also considered to be a

confining bed, separates the Sparta Sand and the Queen City Sand. The Yegua-Jackson Aquifer is separated from the Sparta Sand by the Cook Mountain Formation.

The character of the different aquifers varies in structure and stratigraphy across the study area. A more detailed description of the individual formations is presented in the following text, and the variations of the primary stratigraphic units across the study area are summarized in Figure 5-2 (from Kelley and others, 2009).

### **Midway Formation**

The Midway Formation is comprised of relatively impermeable marine clays, shales and siltstones. It is not considered to be an aquifer. It is mentioned only because it represents the bottom of the Carrizo-Wilcox Aquifer throughout the study area.

### **Wilcox Group**

The Wilcox Group is a series of fluvial-deltaic sedimentary sequences across the upper Paleocene and lower Eocene. The Wilcox Group is comprised of interbedded sands, clays, and silts, with discontinuous layers of lignite present throughout. The Wilcox Group yields small to large quantities of usable water in the study area (Klemt and others, 1976 and Thorkildsen and Price, 1991).

In Groundwater Management Area 13, recent groundwater modeling efforts have subdivided the Wilcox Group into an upper, middle, and lower section (Deeds and others, 2003), although the use of three model layers in the Wilcox Group is largely adopted so that the layering will correlate to geology in the overlap with the Central Transect (Groundwater Management Area 12), where the Middle Wilcox (Simsboro Formation) is significantly different than the Upper and Lower Wilcox. The Upper Wilcox model layer in this area is very thin, essentially resulting in the modeling of the Wilcox Group as two layers. This is consistent with studies of the Wilcox Group in Bexar, Atascosa, and Wilson counties which indicate that it is more appropriate to represent the Wilcox Group as two layers in this area; an upper layer characterized by predominantly fine-grained material with little potential for groundwater production and the Lower Wilcox contains significantly higher thickness of sand suitable for groundwater production (Hargis, 2009 and LBG-Guyton, 2008).

In Groundwater Management Area 12, in the area between the Colorado River and the Trinity River, the Wilcox Group is mapped as three distinct units; the Hooper, Simsboro and Calvert Bluff formations, from oldest to youngest. The Hooper Formation consists of interbedded shale and sandstone with minor amounts of lignite, and is generally not considered a significant aquifer but is used occasionally, and especially in the outcrop where the Simsboro or Calvert Bluff formations are not present. The Simsboro Formation is primarily a sand unit. It is the primary aquifer in this area and is tapped to produce municipal supply for several cities in the area. The Calvert Bluff Formation is a relatively lower permeability unit consisting of clay and lignite deposits with some sand and largely functions as a leaky aquitard between the Simsboro Formation and the overlying Carrizo Sand.

In Groundwater Management Area 11, in the vicinity of the Sabine Uplift area, the Simsboro Formation ceases to be a distinct and highly productive unit as it is in central Texas (Groundwater Management Area 12). The Wilcox Group is divided informally into a lower and an upper unit (Deeds and others, 2009). As with the modeling efforts in the southern part of the study area, the Wilcox Group is represented as three layers to maintain consistency with the

overlap with the central part of the study area. However, the layer associated with the middle Wilcox is very thin, essentially modeling the Wilcox Group as a two layer system. In many areas, the Upper Wilcox and Carrizo Sand are screened collectively for production. In Marion and Harrison counties, the overlying Reklaw Formation becomes discontinuous and the combined Wilcox Group, Carrizo Sand and Queen City Sand are collectively used (Fogg and Kreitler, 1982).

### **Carrizo Sand**

The Carrizo Sand is the lowest member of the Claiborne Group. It is the most productive aquifer in the southern part of study area (Groundwater Management Area 13). It is primarily composed of permeable medium to coarse sand and gravel and sandstone, with some interbedded silt and clay, and yields moderate to large quantities of fresh to slightly saline water to wells. Total thickness of the Carrizo Sand in the southern study area ranges from about 150 to 1,200 feet (Klemt and others, 1976). The aquifer is thinner to the north, with a reported maximum thickness of 880 feet in the Central Transect (Thorkildsen and Price, 1992), and a total thickness of less than 200 feet in the northern study area in Nacogdoches and Angelina counties (William F. Guyton and Associates, 1970). Inspection of geophysical logs that span the Carrizo Sand indicates three distinct stratigraphic intervals present to varying degrees in most locations. These intervals correspond to differing depositional environments within the Carrizo Sand. Much of the Carrizo Sand is dominated by a bed-load channel system, characterized by significant thickness of coarse sand and gravel typical of fluvial bed load, commonly referred to as the “massive” Carrizo Sand (Hamlin, 1988). Alternatively, areas of mixed alluvial deposits contain more fine-grained materials typical of floodplain deposits, lake deposits, and abandoned channel-fill deposits, and therefore have less desirable hydraulic properties than the massive Carrizo Sand. From central Atascosa County to northeast approximately to the San Marcos Arch, bedload deposits dominate the Carrizo Sand, and therefore the massive Carrizo Sand occurs in nearly the entire thickness. From central to southwest Atascosa County, mixed-alluvial deposits occur with greater frequency, resulting in a lesser proportion of massive Carrizo Sand in this area, and less desirable hydraulic properties (Hamlin, 1988). Hamlin’s study ended in central Gonzales County at the San Marcos Arch. However, a geologic map of the Carrizo Sand thickness produced by Mr. David Thiede, a retired petroleum geologist and former interim director of the Gonzales County Underground Water Conservation District, identifies another area of great thickness in northeastern Gonzales County known as the Yoakum Channel area. A review of Mr. Thiede’s data shows that this area also appears dominated by a bedload fluvial depositional environment, indicated by the thickness of sand and the relative lack of “upper” and “lower” Carrizo intervals and their associated smaller grain sizes and clay and shale interbeds (HDR, 2004).

### **Reklaw Formation**

The Reklaw Formation overlies the Carrizo Sand. It is comprised of clay, shale, fine-grained sandstone and may yield small quantities of water suitable for stock or domestic use. It is conceptually considered as a leaky confining geologic formation that partially restricts the vertical movement of groundwater. It ranges in thickness from about 200 feet to 400 feet throughout the study area (Klemt and others, 1976 and William F. Guyton and Associates, 1970).

### **Queen City Sand**

The Queen City Sand lies conformably atop the Reklaw Formation. In the southern study area it is a thick unit with reported thickness up to 1,400 feet (Klemt and others, 1976), consisting of

interbedded sands and sandy clays, along with clay and shale. In the northern study area, thickness is reported up to 500 feet north and west of the Sabine Uplift (Kelly and others, 2004), while thickness and sand content decreases to the point where no Queen City sands are identifiable in Nacogdoches County (William F. Guyton and Associates, 1970). Review of available geophysical logs does not indicate that a consistent thickness of sand, analogous to the massive Carrizo Sand, is observable in the Queen City Sand throughout the study area. The Queen City Sand is more characterized by smaller stratigraphic intervals of sand and fine-grained material, without a great deal of lateral continuity from one area to the next. To the southwest, the relative abundance of fine-grained material increases as the Queen City Sand becomes interbedded with the El Pico Clay. The TWDB has designated the Frio River as the southern boundary of the Queen City Aquifer, which is classified as a minor aquifer. The increasing presence of clay makes the aquifer less productive in the southwestern portion of Groundwater Management Area 13.

### **Weches Formation**

The Weches Formation overlies the Queen City Sand. It is a thin marine formation consisting chiefly of clay with some sand and limestone. It is approximately 50-200 feet thick in the southern study area (Klemm and others, 1976), and 110 to 240 feet thick in the northern study area (William F. Guyton and Associates, 1970). It is considered to be a confining layer between the Queen City Sand and the Sparta Sand, partially inhibiting vertical movement of groundwater between layers.

### **Sparta Sand**

The Sparta Sand overlies the Weches Formation. It is comprised of interbedded very fine to fine grained sands and clays. It is approximately 40 to 200 feet thick in the southern study area (Klemm and others, 1976), and thickness to nearly 300 feet in the northern study area (William F. Guyton and Associates, 1970). Although it is not as thick as the Queen City Sand, a review of available geophysical logs generally reveals a consistent and identifiable interval of sand thickness of about 50 to 100 feet that is observable laterally through much of the study area (example geophysical logs are included with the electronic deliverables). It yields small to moderate amounts of water to wells, and is classified as a minor aquifer by the TWDB.

### **Cook Mountain Formation**

The Cook Mountain Formation lies above the Sparta Sand and is comprised of fossiliferous clay and shale, with some interbedded sandstone and limestone. The Cook Mountain Formation is not considered to be a significant aquifer by the TWDB. In the context of this report, it is conceptually viewed as a leaky confining unit between the Sparta and Yegua-Jackson aquifers, partially restricting vertical cross-formational movement of water between these aquifers.

### **Yegua-Jackson Aquifer**

The Yegua-Jackson Aquifer is comprised of two different formations; the Yegua Formation is older and the Jackson Group is deposited on top of the Yegua Formation. Both are comprised of alternating unconsolidated sand and clay intervals. Although the TWDB classifies the Yegua-Jackson Aquifer as a minor aquifer, it is primarily used in the outcrop, with very little downdip extent of the formations considered suitable for use as an aquifer (Knox and others, 2009).

### Brazos River Alluvium Aquifer

The Brazos River Alluvium Aquifer is designated as a minor aquifer by the TWDB and occurs in the central part of the study area (Groundwater Management Area 12). The Brazos River Alluvium Aquifer consists of recent unconsolidated fluvial sediments that range in thickness up to about 100 feet in the study area (thicker sequences are observed downstream). Wells in the Brazos River Alluvium Aquifer are used for irrigation, domestic, stock and industrial purposes. Saturated thickness of up to 50 to 60 feet is observed locally across the study area (Cronin and Wilson, 1967). The Brazos River Alluvium Aquifer is comprised of Quaternary sediments that were deposited much more recently than any of the other aquifers previously discussed. As such, this aquifer lies across the top of the outcrop of all the Tertiary-aged aquifers, and may potentially interact with these aquifers.

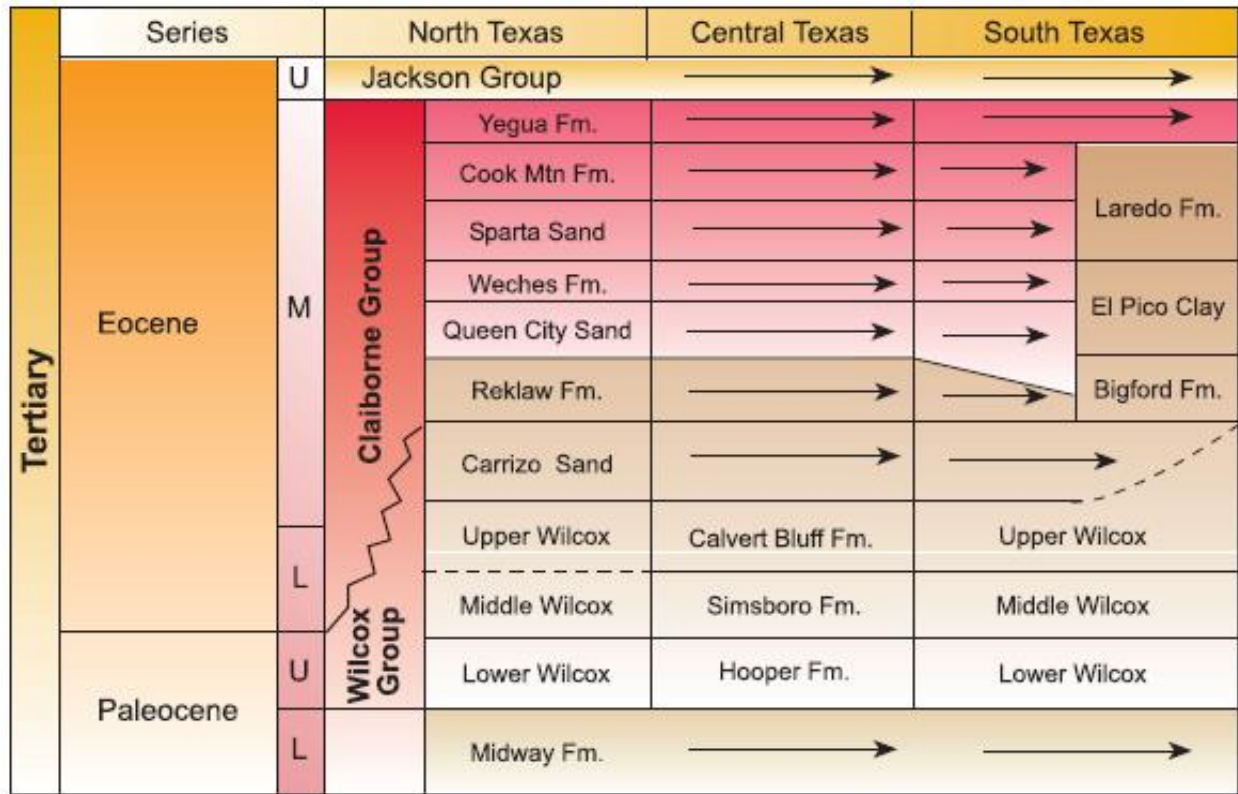


Figure 5-2. Generalized stratigraphic section for the Carrizo-Wilcox Aquifer in Texas (after Ayers and Lewis, 1985; Hamlin, 1988; Kaiser and others, 1978).

### 5.2 Regional Groundwater Flow

In each of the aquifers discussed, there is a characteristic difference between flow direction in the outcrops and flow direction in the downdip sections of the aquifers. The outcrop directly accepts recharge from precipitation. Accordingly, local flow patterns in the outcrop strongly reflect local topography, with the highest water table elevations corresponding to hills and topographically elevated areas, and the lowest water table elevations corresponding to river valleys and stream channels. Under this conceptual model, the flow direction in the outcrop is topographically controlled, flowing from hills and upland areas toward streams and river valleys. In the northern

study area (Groundwater Management Area 11), potentiometric surface maps indicate flow paths from areas of higher elevations toward the Trinity and Sabine rivers; by contrast, flow paths did not converge toward the Neches River in this area (Fogg and Kreitler, 1982). Groundwater also flows from the outcrop into the confined section of the aquifer. Hydraulic gradients in the confined section are lower than the topography-controlled gradients observed in the outcrops, but continue on in a general downdip direction in all of the aquifers in the study area.

### **Historical Groundwater Development**

Major groundwater development projects may cause changes in regional flow patterns if the pumping rates are significant. Significant groundwater pumpage may reduce water levels resulting in cones of depression that can alter the pre-development flow patterns of these aquifers. Historical groundwater development in the region has not occurred at the same rate equally throughout the study area.

The primary purpose for development of the groundwater from the Carrizo Sand in Groundwater Management Area 13 has been for irrigated agriculture. In the early 1930s, farms began heavy pumping in the Winter Garden area of Zavala and Dimmit counties, causing significant drawdowns in this area. In the 1950s and 1960s, irrigation pumpage from the Carrizo Sand Formation increased significantly in Frio, Medina and Atascosa counties. Although the rate of withdrawals in some areas may have leveled off, pumpage continues at relatively high rates in some parts of Groundwater Management Area 13. Irrigation pumpage in Dimmit and Zavala counties has declined from its historical maximum. Groundwater elevation maps produced through the years depict a pronounced cone of depression, with groundwater elevations lower than 200 feet mean sea level, located in the Winter Garden Area (Hamlin, 1988 and McCoy, 1991). Groundwater development of the Carrizo Sand Formation in Wilson, Gonzales and Bastrop counties has been less intense and has not resulted in significant declines in groundwater elevations (HDR, November 2004).

Water level declines of 100 to 200 feet from predevelopment conditions have been observed in the Wilcox Group of the Carrizo-Wilcox Aquifer in Brazos County due to pumping in the Bryan and College Station area to support municipalities around Texas A&M University.

In the northern part of the study area, the Carrizo-Wilcox Aquifer drawdowns greater than 300 feet have been observed due to municipal pumping in Smith, Nacogdoches and Angelina counties. A figure displaying simulated drawdowns in the Carrizo-Wilcox Aquifer is presented as Figure 5-3.

A review of available groundwater elevation data for the Sparta, Queen City and Yegua-Jackson aquifers did not indicate any long-term drawdown trends in these aquifers (HDR, 2004 and Kelley and others, 2009). Although some small municipalities do use these aquifers as a municipal supply and so may experience localized drawdown, there has not been widespread or significant development of the these aquifers such that regional water declines have been observed.

### **Cross-Formational Flow**

Vertical cross-formational flow across the entire area of a confined aquifer is potentially a major source of discharge for an individual aquifer. Its occurrence may be inferred by the vertical difference in potentiometric heads observed in well clusters which are installed at approximately the same location, but screened in different aquifers. In the southern part of the study area, the

vertical flow prior to significant groundwater development is generally upward from the Wilcox Group to the Carrizo Sand to the Queen City Sand to the Sparta Sand to the Yegua Formation. In the northern part of the study area, heads in the Queen City Sand are higher than heads in the Carrizo Sand throughout most of Groundwater Management Area 11 (Fogg and Kreitler, 1982), indicating downward leakage from the Queen City Sand to the Carrizo Sand across the Reklaw Formation. In addition, Fogg & Kreitler (1982) conducted a study of pressure versus depth that indicated that flow within the various strata of the Carrizo-Wilcox Aquifer was primarily downward. However, in the central and southern parts of the study area, heads in the lower units are higher than those in the upper units, indicating upward flow from the deeper older units to the younger, shallower units. The San Antonio Water System installed four well clusters in southwestern Gonzales County that screened the Carrizo Sand, Queen City Sand and Sparta Sand. The differential water level data from these well clusters reveal highest heads in the Carrizo Sand and lowest heads in the Sparta Sand (HDR, May 2004). Paired wells in the Wilcox Group and the Carrizo Sand in southern Bexar County also indicate upward flow (LBG-Guyton, 2008).

Significant groundwater development is capable of reversing the natural pre-development vertical cross-formational flow. This has been observed in the Winter Garden area, where the decline in potentiometric heads associated with irrigation pumping has led to higher heads in the Queen City Sand than in the Carrizo Sand, effectively reversing the pre-development vertical gradient direction in the area (Hamlin, 1988 and Klemm and others, 1976).

Although the direction of vertical cross-formational flow may be inferred from differential potentiometric heads, it is very difficult to quantify from field data the amount of flow that is actually transmitted via this mechanism. Groundwater numerical models provide one method to estimate this component of regional groundwater flow. Groundwater models assume the conservation of mass and energy as an underpinning of the water budget calculations made during model runs. Groundwater model water budgets can be studied to evaluate quantities of cross-formational flow that are not directly observable from field data. Groundwater model studies of the Carrizo-Wilcox Aquifer (Deeds and others, 2009) and Queen City Aquifer (Kelley and others, 2009) have indicated large quantities of cross-formational flow under both pre-development and current conditions. For example, modeling of the southern part of the Carrizo Sand reports that under pre-development conditions, 39,000 acre-feet per year of water flowed out the top of the Carrizo Sand to overlying aquifers, equivalent to 53 percent of all outflow for the layer, exceeding discharge to streams and evapotranspiration combined. By comparison, under year 1999 conditions that reflect significant groundwater pumpage, 57,000 acre-feet year are observed to flow into the Carrizo Sand through the top layer. Carrizo Sand pumpage of 222,000 acre-feet per year has resulted in a net change of 96,000 acre-feet per year of vertical flow, and reversed the vertical gradient direction from net outflow across the top of the aquifer to net inflow. It is also noteworthy that this water budget indicates that over 25 percent of the Carrizo Sand pumpage is supplied by vertical inflow from overlying aquifers. In the southern Sparta Aquifer simulation results it was observed that nearly 84 percent of all discharge from the Sparta Sand layer occurred through cross-formational flow, dwarfing outflows such as discharge to streams or evapotranspiration.

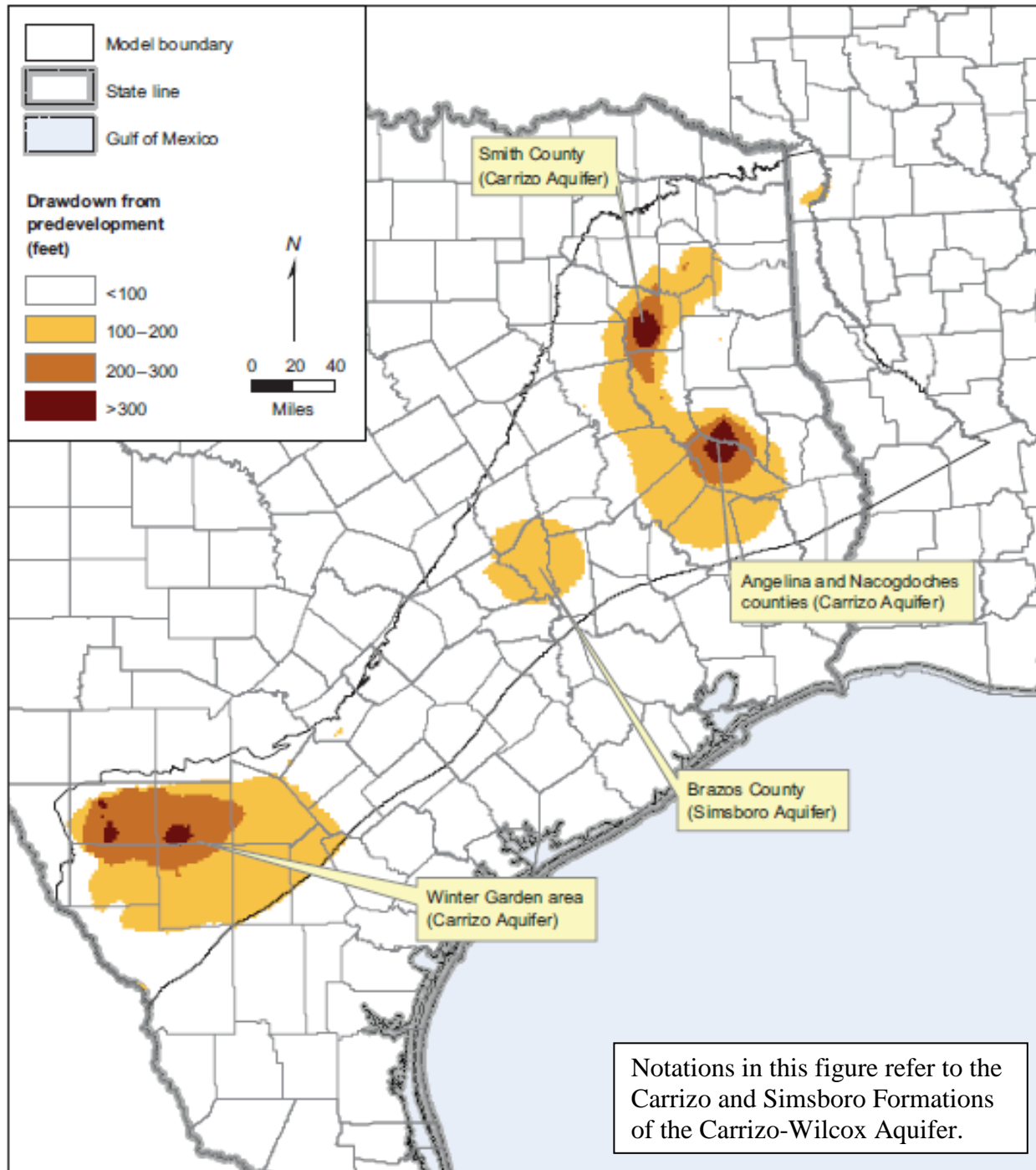


Figure 5-3. Simulated drawdown from the predevelopment to 1990 in the Carrizo-Wilcox Aquifer (Deeds and others, 2009).

### 5.3 Recharge to Discharge

The natural groundwater flow within the subject aquifers is from areas of recharge in the outcrop to areas of discharge. All of the aquifers in the study area display similar patterns of recharge and discharge. The primary source of recharge to all the aquifers is downward percolation of precipitation that falls on the land surface. A portion of the precipitation infiltrates the surface and percolates downward through the unsaturated zone until it reaches the outcrop water table. In general, units comprised of a higher percentage of sand and gravel at the surface will have higher recharge rates. Because most of the aerial recharge has precipitation as its source, recharge is greater in the wetter, northern part of the study area than in the more arid southern part. Estimated Carrizo-Wilcox Aquifer recharge rates are based on a chloride mass balance study that ranged from 0.4 inches per year (two percent of precipitation) in the southwest study area to 4.0 inches per year in the more humid north study area (Reedy and others, 2009). Estimated recharge rates for the Queen City and Sparta aquifers are 0.7 to 1.3 inches per year and 1.3 to 1.5 inches per year, respectively (Kelley and others, 2009). In the Yegua-Jackson Aquifer Groundwater Availability Model, recharge estimates ranged from 0.27 inches per year in the southwest to 1.2 inches per year in the northeast.

Another potential source of recharge and/or discharge is surface water and groundwater interaction with streams as it flows through the outcrop of an aquifer. In the northern part of the study area (Groundwater Management Area 11), most of the perennial streams and rivers are observed to be gaining streams, i.e., stream flow increases as the rivers flow across the outcrops, indicating that the aquifers are discharging to the stream. The Trinity and Sabine rivers appear to be receiving discharge from the Carrizo-Wilcox Aquifer, while evidence appears to indicate that the Neches River is not (Fogg and Kreitler, 1982). Therefore, perennial streams do not serve as a source of recharge in Groundwater Management Areas 11 and 12, although smaller ephemeral stream courses may provide some recharge during storm events. In the central part of the study area, most streams and rivers appear to be receiving discharge from the aquifers as they cross (Saunders, 2009 and HDR, 2004). In the southern part of the study area (Groundwater Management Area 13), conditions are more arid, and some of the streams are losing streams across the Carrizo-Wilcox Aquifer. LBG-Guyton and HDR (1998) estimated that the Nueces and Frio rivers lose approximately 500 acre-feet per year per mile of outcrop, indicating that the surface water flow in these rivers provides a source of recharge to the underlying aquifer. The same study reported that the San Antonio and Atascosa rivers were found to have changed from gaining streams to losing streams in the 1960s and 1970s in response to declining water levels in the outcrop; initially the aquifers discharge to these streams, but now the streams provide recharge to the aquifers. Additionally, this study reported that the San Marcos and Guadalupe rivers were found to be gaining streams, receiving discharge from the aquifers. Slade and others (2002) document gain/loss studies on the Nueces River from 1925 through 1940 that estimate average stream losses of 814 and 653 acre-feet per year per mile of stream.

Of the recharge that is captured in the outcrop, only a fraction moves into the confined portion of the aquifer. The rest travels through various flow paths in the outcrop and may be discharged through stream gains, springs, seeps and evapotranspiration. Deep recharge is a term that refers to the recharge that travels from the outcrop to the confined aquifer. Reedy and others (2009) estimated that for the south, central and northern parts of the study area, approximately 34 percent, six percent and nearly zero percent of the total recharge was transmitted to deep recharge.

## 5.4 Hydraulic Properties

Information on hydraulic properties of the aquifers in the study area are available from many sources, including the Groundwater Availability Model reports for the southern portion of the Sparta, Queen City and Carrizo-Wilcox aquifers (Deeds and others, 2003); central portion of the Sparta, Queen City and Carrizo-Wilcox aquifers (Dutton and others, 2003); and northern portion of the Sparta, Queen City and Carrizo-Wilcox aquifers (Fryar and others, 2003), Queen City and Sparta Aquifers (Kelly and others, 2004) and Yegua-Jackson Aquifer (Deeds and others, 2010). More recently, summary review articles for each of the aquifers in the study were published by the TWDB (Hutchison and others, 2009). This discussion will focus on the property of hydraulic conductivity, which is a measure of the productivity of a formation that is independent of layer thickness. Transmissivity is calculated by multiplying hydraulic conductivity by aquifer thickness.

Estimates of Carrizo-Wilcox Aquifer hydraulic conductivity are presented in Table 5-1 (Deeds and others, 2009). For all 3 parts of the study area, the Carrizo Sand has the highest hydraulic conductivity of the four formations which collectively comprises the Carrizo-Wilcox Aquifer. Even in the central study area, where the Simsboro Formation is considered the most productive aquifer, the Carrizo Sand has a higher hydraulic conductivity. However, the Simsboro Formation's greater thickness in Groundwater Management Area 12 results in a higher transmissivity and thus greater productivity for large capacity wells. Data in Table 5-1 indicates that for the Carrizo-Wilcox Aquifer, the average hydraulic conductivity of all the formations decreases from the southern to the northern study area.

Much less data describing hydraulic conductivity and transmissivity are available for the minor aquifers than for the Carrizo-Wilcox Aquifer. A summary of available data were presented in Kelley and others (2009). The mean of hydraulic conductivity values for the Queen City Sand throughout the study area is 12.7 feet per day. Lateral variability of hydraulic properties is less defined than for the Carrizo-Wilcox Aquifer due to lack of available data. Due to the lack of large capacity wells installed in the Sparta Sand, there is even less data than for the Queen City Sand. The mean hydraulic conductivity for the Sparta Sand throughout the study area was 18.3 feet per day, based on 38 samples (Kelley and others, 2009).

A survey of available data for the Yegua-Jackson Aquifer throughout the study area performed for the Yegua-Jackson Aquifer GAM report revealed data for 41 pumping tests. Hydraulic conductivities ranged from 0.8 feet per day to 22.8 feet per day, with an average value of 7.5 feet per day (Deeds and others, 2010).

**Table 5-1. Summary of mean hydraulic conductivity values (feet/day).**

<b>Region</b>	<b>Carrizo Sand</b>	<b>Upper Wilcox/ Calvert Bluff Formation</b>	<b>Middle Wilcox/ Simsboro Formation</b>	<b>Lower Wilcox/ Hooper Formation</b>
South Texas	44.3	30.7	27.7	13.3
Central Texas	23.6	16.6	16.3	8.3
North Texas	12.2	12.2	8.0	5.5

## 5.5 Overview and Summary

The Carrizo Sand and the Simsboro Formation, which comprise two distinct units within the greater Carrizo-Wilcox Aquifer, are the most productive aquifers in the study area. The Carrizo Sand extends throughout the entire study area from Mexico to Louisiana, while the Simsboro Formation is limited to the central part of the study area, between the Colorado and Trinity rivers. Both the Carrizo Sand and the Simsboro Formation contain hundreds of feet of vertically continuous and laterally extensive productive sands and gravels. Many wells screened in these aquifers are capable of producing in excess of 1,000 gallons per minute. The maximum thickness of sand in the Carrizo Sand occurs in the southern part of the study area in Gonzales, Wilson and Atascosa counties, while the maximum thickness of sand in the Simsboro Formation occurs farther to the north in Lee, Burleson and Brazos counties. In the central study area, where both aquifers are present, they have comparable hydraulic conductivities. However, the Simsboro Formation is the more productive of the two aquifers in this area due to its greater thickness, and by extension, greater total transmissivity.

The Queen City and the Sparta aquifers are both designated by the TWDB as minor aquifers that are separated by the Weches Formation confining unit. Neither of these aquifers is recognized southwest of the Frio River by the TWDB, because they are replaced with the equivalently-aged Laredo Formation and El Pico Clay, which are unsuitable for significant groundwater production. The Queen City Aquifer is significantly thicker than the Sparta Aquifer. The greatest thickness of the Queen City Aquifer (exceeding 2,000 feet at depth) occurs in the southwest part of the study area. The Sparta Aquifer, by contrast, exhibits its greatest thickness (500 to 700 feet) in the northeast part of the study area, near (and beyond) the Louisiana border. Review of available geophysical logs reveals a noticeable difference in the basic character of the two aquifers. The Queen City Aquifer is characterized by far more interbedding of sand and clay strata, with no consistent vertically continuous or laterally extensive thicknesses of sand apparent in the logs. Geophysical logs that include the Sparta Aquifer, by contrast, generally display a more consistent vertically continuous section of clean sand with no significant interbedding of clays or other fine-grained material within (example geophysical logs that display the general characteristics of these aquifers are included with the electronic deliverables). Although the hydraulic conductivity of the Queen City and the Sparta aquifers are comparable, the widespread presence of a continuous sand interval within the Sparta Aquifer may have implications with respect to flow paths and the potential for downdip migration of groundwater.

The Yegua-Jackson Aquifer extends from the Mexico border to the Louisiana border. It is generally the least productive of the aquifers evaluated in this study. Like the Queen City and Sparta aquifers, it has not been significantly developed throughout the study area. Unlike these other aquifers, the Yegua-Jackson Aquifer does not have any significant amount of usable quality groundwater in the confined downdip section of the aquifer. Groundwater use is restricted almost completely to the outcrop area, and so the defined aquifer is limited to the combined outcrops of the Yegua Formation and/or Jackson Group of the Yegua-Jackson Aquifer. The Cook Mountain Formation provides hydraulic separation from the underlying Sparta Sand.

## 6 Hydrochemical and Isotopic Approach to Understanding Aquifer Dynamics

Two different approaches are often used for understanding how groundwater flows within fresh, brackish or saline aquifers. The two approaches are:

1. A hydrologic approach, which is based on potentiometric surface maps, the physical hydrogeologic characteristics of an aquifer or aquitard (such as permeability, porosity and storativity) and the density of the water and the water budget. Groundwater models, such as the TWDB Groundwater Availability Models, are built with these types of data.
2. A hydrochemical approach, which is based on the hydrochemical composition of the water and the geochemical composition of the lithology and mineralogy of the aquifer. As groundwater flows through an aquifer, it will chemically react with the aquifers' rock matrix and often develops a unique chemical signature. For example, chemical composition of groundwater in a limestone aquifer is a calcium-bicarbonate water. The chemical composition of groundwater in a karstic gypsum aquifer typically will be a calcium-sulfate water.

The following paragraphs discuss the hydrochemical approach that was used to guide this study.

An inter-aquifer evaluation occurs if there is flow between two aquifers in which each aquifer contains waters with different chemical compositions. The presence of mixing may be evident in changes in chemical composition. For example, if a groundwater in a gypsum aquifer with a calcium-sulfate water chemistry signature, discharges into a limestone aquifer, elevated concentrations of sulfate may become apparent in the water chemistry of the limestone aquifer. If the higher sulfate values were mapped in only part of the aquifer, then the area of leakage could be identified. Nance (2010) documents the leakage of underlying sulfate-rich brackish groundwater from Triassic and Permian formations into the Cretaceous Antlers Formation on the northwest side of the Edwards-Trinity (Plateau) Aquifer by the occurrence of elevated sulfate and chloride concentrations in the Antlers Formation groundwater. Richter and Kreitler (1993) document numerous other examples of using chemistry to document the mixing of groundwater between two different aquifers. In practical terms groundwater chemistry is often the basis for identifying sources of groundwater contamination. The chemical composition of the groundwater in an aquifer can be a very effective tracer.

The chemical composition of groundwater in an aquifer may also change (evolve) as it flows down the hydraulic gradient from points of recharge to points of discharge within an aquifer (intra-aquifer chemical changes). These chemical changes may occur because of mineral dissolution, oxidation-reduction reactions and temperature and pressure changes. If an aquifer is composed of a limited mineralogy and lithologies, the chemical composition of the water may stabilize relatively quickly as water recharges an aquifer and be of limited value in mapping groundwater flow because the chemistry does not change measurably as the water flows through an aquifer. If, however, an aquifer is composed of a complex mineral assemblage, then multiple chemical reactions may be occurring that result in a continual change in water chemistry as groundwater flows from recharge too deep within an aquifer. Such is the case for the Tertiary-aged sand and clay (shale) aquifers along the U.S. Atlantic and Gulf of Mexico coasts. Groundwaters in these aquifers typically evolve from a variable calcium-magnesium mixed anion (bicarbonate-sulfate-chloride) composition in the outcrop to a sodium-bicarbonate water

downdip and possibly to a sodium-chloride composition at great depths. Because of these regional changes in chemistry, it may be possible to determine directions of groundwater flow (intra-aquifer) as well as possible mixing of waters between aquifers (intra-aquifer).

Foster (1950) first documented the occurrence of sodium-bicarbonate waters in the U.S. Atlantic and Gulf of Mexico aquifers. Since Foster's initial work, the presence and origin of sodium-bicarbonate groundwaters have been documented in other aquifers. Kreitler and others (1977) documented their importance in the Plio-Pleistocene Chicot and Evangeline (coastal plain) aquifers in the Houston, Texas region. Fogg and Kreitler (1982) and Fogg and others (1991) documented their prevalence in the Carrizo-Wilcox and Queen City aquifers in east Texas. Meisler and others (1988) did additional work in understanding the chemical reactions causing the sodium-bicarbonate water in the Atlantic coastal plain. Hamlin (1988) documented the presence of the sodium-bicarbonate water in the Carrizo Sand Formation portion of the Carrizo-Wilcox Aquifer in south Texas. Boghici (2009) documented the general occurrence of sodium-bicarbonate water in the Carrizo-Wilcox Aquifer from east Texas to south Texas.

In a monomineralic aquifer, such as a limestone, the groundwater reacts with a limited number of minerals and results in ubiquitous calcium-bicarbonate chemistry with a pH of about 7. There are minor geochemical changes down a flow path; the water chemistry is of limited value in mapping flow paths. However, in a polymineralic aquifer such as a clayey sandstone, the groundwater reacts simultaneously with several different mineral species. As one reaction approaches saturation, a second reaction with another mineral species may use a product of the first reaction and this may prevent the first reaction from reaching equilibrium. The dissolution of calcite and cation exchange of high cation-exchange capacity clays is an example of two chemical reactions working in opposition to each other. Calcite in sandstone will dissolve until the water is saturated. However, with clay in the aquifer, the calcium from the dissolution of the calcite will be exchanged for sodium. Because of the exchange, the solution becomes under saturated with respect to calcite, and more calcite dissolves. Sodium and bicarbonate concentrations continue to increase to relatively high concentrations because of these simultaneous reactions. In the polymineralic aquifer, the chemical composition of the water will continue to change as it flows through the rock. Mappable changes can be used to indicate directions of flow.

Water chemistry is often plotted on Piper diagrams, graphs or maps. Piper diagrams compare six ionic species within one diagram and provide a snapshot of the water chemistry of an aquifer. Plotting of one ion versus another or one ion versus depth or plotting on a map view frequently can provide important information about the evolution of the water composition and therefore a better understanding of the flow system (Richter and Kreitler, 1993). These types of graphics are used in this report to demonstrate the hydrochemistry and evolution of the chemistry within the aquifer and between aquifers.

The development of sodium bicarbonate water is controlled by two reactions (Foster, 1950):



Reaction (1) states that calcite is dissolved by an acid (in this case, carbonic acid), resulting in calcium and bicarbonate. Reaction (2) states that one mole of calcium will exchange for two moles of sodium on the clays. Magnesium and potassium will also be involved in this reaction. Together, reaction (1) and (2) yield reaction (3).



As these two reactions occur within an aquifer or along a flow path, sodium and bicarbonate will increase to form water with a sodium-bicarbonate composition.

Examination of reaction (3) indicates that other geochemical reactions should be occurring concurrently with the generation of sodium bicarbonate water:

1. Calcium groundwater should become progressively depleted with calcium the farther the water flows through the aquifer. A plot, such as calcium versus depth, may show this to be occurring. A map view of calcium distribution would indicate the groundwaters in the shallow outcrop are high in calcium whereas deeper waters down dip are depleted in calcium. The down dip extent of elevated calcium may be controlled by the amount of sodium-montmorillonite clay in the aquifer and the duration of time for flushing of the sodium off the exchange sites of the clay (Meisler and others, 1988). Calcium from calcite dissolution occurs, but if the calcium is not exchanged for sodium on the clays, there may be deeper down dip presence of dissolved calcium into the aquifer. If there are no available sodium exchange sites, then the development of sodium-bicarbonate waters may not start until deeper in the aquifer and not in the outcrop. The presence of high calcium in the outcrop and low calcium immediately down dip in the confined section may infer that groundwater flow stays predominately in the outcrop where groundwater discharges to streams and rivers that cross or are headwatered in the outcrop. Conversely the presence of calcium down dip into the confined section of an aquifer indicates that groundwater is actively flowing from the outcrop into the confined parts of the aquifer.
2. Initially a sodium-bicarbonate water may be in a closed carbon dioxide system in the outcrop and then deep in the aquifer as an "open" carbon dioxide system. If the aquifer is functioning as a closed system for carbonic acid, then the pH will rise as the sodium and bicarbonate concentrations increase. The dissolution of calcite uses up the carbonic acid, and the hydrogen joins with the carbonate ion, forming bicarbonate. The carbonic acid (dissolved carbon dioxide) is derived primarily from plant decay and respiration in the soil zone. If no additional carbon dioxide is added to the water, the groundwater is considered to be functioning in a closed system. If additional carbon dioxide is being added either by decay of organic material in the aquifer or by an external source of carbon dioxide (deeper gas fields leaking into the aquifer or coalification of organic material), then the aquifer is considered as an open system. A plot of pH versus bicarbonate may show both open and closed conditions in the formations of sodium-bicarbonate waters. In shallow groundwaters, the pH range is approximately five to seven, whereas the deeper water range is from eight to nine. There is an increase of pH with increasing bicarbonate. At high bicarbonate concentrations, bicarbonate appears to increase independently of pH, suggesting that, at greater depths, the aquifer is an open system. In Section 7, several examples of open versus closed systems are evident in the aquifers studied in the different transects. Grossman and others (1986 and 1989) confirmed that the maturation of organic material in the east Texas Tertiary-aged aquifers formed methane and carbon dioxide. This resulted in the addition of bicarbonate in the groundwater. The development of sodium-bicarbonate at depth was therefore in an open carbon system.
3. The pH of a groundwater is also an effective indicator of recharge zones. Low pH waters are typical of recharge areas, and conversely, high pH waters occur in the artesian

section. The pH is a sensitive tracer because a pH change of one unit (for example, from pH five to six) is a change of one order of magnitude of the hydrogen activity. Ionic concentrations generally exhibit increases of no more than two or three times. Recharge areas for an aquifer are characterized by pH values that are lower than those of downdip waters. In the outcrop, recharge waters typically have pH values less than eight and may be as low as five, whereas downdip waters generally have pH values between eight and nine. This is also related to whether the aquifer is open or closed in regards to bicarbonate sources.

4. Nitrate and sulfate ions appear to be reduced in groundwaters as they flow down the hydraulic gradient. Both nitrate and sulfate concentrations decrease with depth. Similarly, higher nitrate and sulfate values exist in the outcrop rather than downdip in the confined section of an aquifer. Reduction of sulfate and nitrate with subsequent oxidation of reduced organics (for example, lignite) can produce bicarbonate but may not be an important reaction for generating bicarbonate in these studied aquifers because the concentrations of nitrate and sulfate appear limited. If sulfate and nitrate reduction and oxidation of organics are an important reaction in generating bicarbonate, then sulfate and nitrate concentrations need to be higher. Groundwater may become more reducing after sulfate and nitrate reduction. Deep sodium-bicarbonate waters commonly contain high bicarbonate content, which suggests coalification of organics in the aquifer, a process that should occur deeper in an aquifer after sulfate and nitrate reductions have occurred.

The general chemical trends established by geochemical evolution of sodium-bicarbonate groundwaters in an aquifer can be used to evaluate flow directions. Waters in the shallow recharge zone of a sandstone aquifer typically have neutral to acidic pH values, high calcium, low sodium, moderate sulfate and nitrate concentrations. The waters in the confined downdip section of the aquifer have higher pH values, low calcium, high sodium, and low sulfate and nitrate concentrations.

In Texas, the generation of sodium bicarbonate waters is typical in Tertiary-aged sandstone aquifers. The longer the water is in the aquifer (or the greater distance of transport), the higher the sodium and bicarbonate concentrations become. Conversely, low-sodium (high-calcium) and low-bicarbonate waters are commonly indicative of recharge waters. By plotting ionic constituents on maps or graphs, the chemical evolution of the water can be discerned, and therefore, the general direction of groundwater flow can be determined.

The geographic distribution of the individual chemical constituents in the development of sodium-bicarbonate waters helps identify recharge zones and downdip confined sections and directions of groundwater flow. It does not, however, indicate rates of flow or indicate ages of groundwater. The measurement of carbon-14 percent modern of the bicarbonate may permit an estimate of the age. Understanding both flow direction and age provides a better hydrochemical understanding of a hydrogeologic model for an aquifer.

Carbon-14 is the radioactive isotope of carbon. It has a half-life of 5,730 (Hem, 1986), that is, one half of its carbon-14 mass decays every 5,730 years. Carbon-14 ages of carbon samples can be estimated to about 40,000 years before present if the original carbon is from an atmospheric source process (e.g., photosynthesis of atmospheric carbon by plants). In groundwater carbon-14 age studies, the carbon-14 of the bicarbonate is measured. Before an age can be estimated, the source of the carbon for the bicarbonate needs to be known. In the case of the sodium-

bicarbonate waters in the Texas coastal plain aquifers, the amount of the non-atmospheric carbon needs to be determined. The formation of sodium-bicarbonate water results in the addition of dead carbon-14, either by dissolution of possible carbonate contents, fragments in the Tertiary-aged aquifer or the addition of carbon dioxide through maturation of Tertiary-aged organic material in the aquifer. Both sources (carbonates and organic material) add dead carbon to the dissolved bicarbonate. The addition of this dead carbon results in a carbon-14 age, which is overestimated (i.e., the water is younger than the apparent carbon-14 age would indicate). Two approaches are used to subtract the amount of bicarbonate which may have been derived from a dead source. The first approach evaluates the  $\delta^{13}\text{C}$  of the bicarbonate of the sample and compares its value to the anticipated  $\delta^{13}\text{C}$  of the original carbon at the beginning of the flow path in the soil zone of the outcrop and to the addition of dead carbon with a known  $\delta^{13}\text{C}$  value (Pearson, 1966 and Pearson and White, 1967). The second and more recent approach uses this  $\delta^{13}\text{C}$  correction approach plus quantification of the evolution of the water geochemistry as it flows along a flow path to the point of sampling within an aquifer (Plummer and others, 1994). Both approaches should provide a younger age than the apparent age where only the radioactive decay half-life is accounted for in estimating an age.

A limited number of studies of carbon-14 and bicarbonate have been previously made on groundwaters in Groundwater Management Areas 11, 12 and 13. Pearson (1966) and Pearson and White (1967) estimated the age of the Carrizo Sand Formation portion of the Carrizo-Wilcox Aquifer groundwater, flowing from its outcrop in Bexar County to depths greater than 4,000 feet, with an age range from modern to ages greater than 28,000 years before present. They corrected the carbon-14 age using a  $\delta^{13}\text{C}$  approach. Kreitler and Pass (1980) estimated uncorrected carbon-14 ages in the Carrizo-Wilcox Aquifer in the Northeast Transect as ranging from about 9,000 years old in the outcrop to 28,000 years old in the confined section. Their age determinations should be considered as maximum ages and approximate in that no correction factor was used to refine their ages. Kreitler and Wuerch (1981) estimated the carbon-14 ages in the Carrizo-Wilcox Aquifer groundwaters around the Oakwood Salt Dome in Leon County from about 2,000 to 23,000 years before present. They used a  $\delta^{13}\text{C}$  correction factor. Kreitler and Senger (1991) estimated the carbon-14 age in the outcrop of the Wilcox Group of the Carrizo-Wilcox Aquifer in the Bastrop, Texas region from 5 wells with a range of about 4,500 years to about 18,000 years. They used a  $\delta^{13}\text{C}$  correction approach. They also found that the more the waters became sodium-bicarbonate types, the older the water became. These four studies estimated the carbon-14 age to be a few thousand years old in the outcrop of the Wilcox Group of the Carrizo-Wilcox Aquifer to about 20,000 to 30,000 years old downdip.

The other geochemical signature evident in the water chemistry of these Tertiary-aged aquifers is the addition of sodium and chloride. In many of the downdip extents of these aquifers, there is often an increase in chloride. The downdip extent of these fresh water aquifers is often based on a 1,000 milligrams per liter, 3,000 milligrams per liter and 10,000 milligrams per liter total dissolved solids line. This line typically is based on an estimate of total dissolved solids from geophysical logs, either the spontaneous potential log or the resistivity logs. It is then inferred that the increase in salinity is from increased concentrations of chloride, but rarely is the inorganic chemical composition evaluated. This study looks specifically at the chemistry in the downdip locations and found that the increases in total dissolved solids were primarily caused by increased alkalinity concentrations and not significant increases in chloride. Chloride was increasing, but the predominant change in total dissolved solids was caused by increased bicarbonates.

The general conceptual model for groundwater flow in the Carrizo-Wilcox, the Queen City, the Sparta and the Yegua-Jackson aquifers is considered to be:

1. Recharge by precipitation on the outcrop.
2. A percentage of groundwater in the outcrop flows to discharge points at topographically low points in the outcrop. These lows may be springs, seeps, creeks and/or rivers.
3. The groundwater that does not discharge in the outcrop flows down the structural dip of these Tertiary-age coastward dipping monoclinial sand aquifers toward the Gulf of Mexico.
4. Discharge of the downdip flowing groundwater is into overlying (or underlying) aquifers by cross-formational flow (Kelley and others, 2009). Flow rates into the downdip confined section are considered to be slower than the short-circuited flow to the streams in the outcrop. Groundwater flow in downdip parts of the aquifers may almost be stagnant.
5. The downdip extent of this confined part of the aquifer has been considered as the interface between updip fresh water and downdip saline water (Dutton and others, 2006).

The balance of groundwater flow between discharge parts in the outcrop versus groundwater flow into the dip confined portions of an aquifer can be tested by determining if there are significant changes in chemistry between outcrop and downdip sections. The downdip sections of the Carrizo-Wilcox Aquifer in Groundwater Management Areas 11, 12 and 13 contain sodium-bicarbonate waters that started as calcium type water and eventually evolved to sodium type water. In the Central Transect (Figure 3-1) the calcium-facies of the Wilcox Group of the Carrizo-Wilcox Aquifer groundwater primarily is in the outcrop but transforms quickly to a sodium type water immediately downdip from the outcrop in the confined sections. There is also a marked difference in carbon-14 percent modern between waters in the outcrop versus waters in the downdip parts of the aquifer. The hydrologic implication is that an active flow system is in the outcrop and the downdip section is more stagnant. In contrast, the higher concentrations of calcium in the groundwater in the Gonzales Transect and South Transect extend much farther into the downdip sections of the Carrizo Sand Formation portion of the Carrizo-Wilcox Aquifer. The hydrologic implication is that the downdip flow of groundwater into the deeper subsurface in the Carrizo Sand Formation in the South Transect is more prevalent than the downdip flow of groundwater in the Wilcox Group in the Central Transect. This appears counter intuitive to the fact that precipitation available for recharge is higher in east Texas than it is in south Texas (Sanford and Selnick, 2013). The difference is considered to be controlled by the very high transmissivities of the Carrizo Sand Formation in south Texas.

The concept of cross-formational flow is another important aspect of this conceptual model. Potentiometric surfaces for some of the Carrizo Sand Formation portion of the Carrizo-Wilcox Aquifer in the Gonzales Transect and the South Transect indicate flow toward the coast, implying the groundwater has to discharge somewhere from the downdip parts of the aquifer. There are, however, no “black holes” in groundwater hydrology. This discharge is considered to be through overlying (or underlying) aquitards into the next vertically adjacent aquifer. Fogg and Kreitler’s (1982) analysis of vertical gradients in the Wilcox Group in east Texas (Northeast Transect) strongly suggests that this process occurs. Kelly and others (2009) argue that cross formational flow between the Queen City Aquifer and the Sparta Aquifer constitutes an

important part of the water budget for these aquifers. The groundwater chemistry in each vertically adjacent aquifer may help determine if there is evidence of leakage from one aquifer to another. Evidence of leakage might be similar in chemistry between the two aquifers. As previously stated, Nance (2010) concluded there was leakage between Permian and Triassic saline formations into the overlying Antlers Formation, based on the similarities in water chemistry between the two aquifer settings. Are there places within the Carrizo-Wilcox, Queen City, Sparta, Yegua-Jackson and Brazos River Alluvium aquifers where the characteristic chemical evolution of sodium-bicarbonate water is altered by the addition of water with a different chemistry such that this chemical is observable? The leakage change hypothesis can be tested by a two-step process: 1) the first step evaluates the evolution of the water chemistry within an aquifer to determine if the evolution of water chemistry can be accounted for solely by intra-aquifer geochemical processes and 2) whether any definable chemical perturbations can be explained by leakage of water of a different chemistry from an adjacent aquifer. One approach to test this hypothesis is to compare the chemistry from nests of wells screened in different formations. This hypothesis was tested with two different approaches. The first approach was in Gonzales County, in the Gonzales Transect, where the San Antonio Water System has three nests of wells. Within each nest, there are three wells individually screened in the Carrizo Sand Formation portion of the Carrizo-Wilcox, the Queen City and the Sparta aquifers. The second approach is a general comparison of the overall chemistry of an overlying aquifer to and underlying aquifer, where flow is to be hypothesized to occur from the deeper aquifer to a shallower aquifer. For example, does the water chemistry in the overlying Queen City, Sparta or Yegua-Jackson aquifers mimic the underlying sodium-bicarbonate water typically seen in the Carrizo Sand Formation portion of the Carrizo-Wilcox Aquifer in south Texas or the Carrizo-Wilcox Aquifer in the middle or northern parts of this Tertiary-aged aquifer system? Or can the chemistry in an aquifer be accounted for by an intra-aquifer geochemical evolution (e.g., development of a sodium-bicarbonate water)?

The interface between updip meteoric water and downdip saline water has been considered relatively narrow and an abrupt boundary (e.g., Klemm and others, 1976). It has also been considered as the boundary between the fresh (less than 1,000) total dissolved solids waters and deeper saline waters associated with the saline to brine section of the Gulf of Mexico sedimentary basin (Dutton and others, 2006).

Geopressured conditions in the deep saline sections have long been considered as causing discharge of saline water toward and into the shallow freshwater aquifer (Galloway, 1982 and Dutton and others, 2006). These 1,000 parts per million and 10,000 parts per million total dissolved solids contour often appears to have been defined with the use of geophysical logs and not by actual water chemistry analyses. Downdip saline waters are typically considered to be chloride type waters, that is, the anions are dominated by the chloride (Kreitler, 1989). The ion use of geophysical logs does not however differentiate whether the increased salinity is caused by increases in chloride or another anion. Because of this, the downdip extent of fresh groundwater as mapped by several geologists in the past could be related to high bicarbonate concentrations and not high chlorides. If the downdip saline sections of these Gulf Coast formations are dominated by bicarbonate type waters, then this 1,000 parts per million total dissolved solids contour may not represent the downdip extent of the fresh water aquifers. It is important to understand how deep the meteoric water actually extends. A review of the water chemistry of the deepest wells may help.

Independent of this evaluation of groundwater flow in the fresh water aquifers in Groundwater Management Areas 11, 12 and 13 is a preliminary hydrochemical evaluation of occurrence of brackish groundwater in the less permeable portions of these aquifers (LBG-Guyton 2003). Limited chemical groundwater data have been collected to determine if and how the brackish sections of these aquifers fit into the overall hydrogeologic picture (e.g., Kreitler and Morrison, 2009).

## 7 Hydrochemical and Isotopic Evaluation

The following sections evaluate the hydrochemical and isotopic data from the TWDB database and new data collected in 2012. New data were collected along two transects, the Central Transect (Groundwater Management Area 12) and the Gonzales Transect (Groundwater Management Area 13) to help evaluate five questions:

1. Are there regional consistent trends in the water chemistry for each aquifer? Do all aquifers in the four transects have sodium-bicarbonate water or are there different types of water in each aquifer? Are there mappable trends in the water chemistry? In addition, what is the best estimate of age of these groundwaters?
2. Does the water chemistry indicate that groundwater flow is most active in the outcrop areas and flow in the downdip parts of these aquifers is relatively stagnant? Does the area or depth of occurrence of the “active” flow vary between aquifers?
3. Is there chemical evidence of cross-formational flow from one aquifer to another?
4. Based on water chemistry analyses what is the deepest downdip extent of these meteoric aquifers?
5. What is the origin of the brackish groundwaters in the aquifer section? Previous research has not been done on the detailed chemistry to better understand the origin of brackish groundwater.

The geochemistry for the four transects (Northeast, Central, Gonzales and South) were evaluated based on the TWDB database (2013), previously collected data and newly collected (2012) chemical and isotopic data. Constituents analyzed for this project included the most relevant, complete, and beneficial datasets, which may not include all ionic or isotopic data available. As an example, the TWDB groundwater database includes oxygen-18, tritium, and deuterium data that were not included in the report because after the initial data analyses, it was determined that no solid conclusions could be drawn for this study.

The aquifers evaluated include the Carrizo-Wilcox Aquifer, the Queen City Aquifer, the Sparta Aquifer and the Yegua-Jackson Aquifer for all four transects. For each transect, there is a general review of each aquifer (data availability, location, well depth and water wells) and then a review of the geochemistry for each aquifer. Where available both the TWDB and recently collected data are reviewed. Historically, the sodium-bicarbonate water is the primary water type seen in the major producing aquifers in Groundwater Management Areas 11, 12 and 13. In that context, each aquifer within the four transects is evaluated to whether they do or do not contain sodium-bicarbonate type water and their chemical evolution. That is, whether the entire pathway from a low pH calcium mixed anion type water evolves to high pH high sodium-bicarbonate water. This may depend upon whether the database for an aquifer includes both outcrop and downdip waters. First, is there pH, calcium, sodium, bicarbonate and sulfate changes that relate to the formation of a sodium-bicarbonate water? Second, are sodium and chloride being added from updip migration of deep saline waters? Piper diagrams, plots of one chemical constituent versus another or depth and maps of specific constituents are used to illustrate the geochemistry and its evolution within an aquifer (intra-aquifer geochemistry) and potential between aquifers (inter-aquifer) as evidence of cross-formational flow. Maps in general are not considered as being as definitive in identifying geochemical changes as other methods of data presentations. The mapping of outcrop versus a downdip confined section is based on the TWDB delineations. An outcrop delineated

area may be ten miles across and 1,000 feet thick. An outcrop area because of its thickness may contain both water table and confined condition with differing chemistry. Discussions of the geochemistry for each aquifer in each transect then follows. Other forms of data presentation, such as a constituent distribution versus depth may better document chemical evolution. Map presentations are therefore only used occasionally to explain geochemical trends. At the end of each transect section is an estimate of the age in the aquifers where adequate carbon-14 data were available. Age estimates focused on the Carrizo-Wilcox in the Northeast Transect, the Wilcox Group of the Carrizo-Wilcox Aquifer in the Central Transect, the Carrizo Sand Formation portion of the Carrizo-Wilcox Aquifer in the Gonzales and South transects. Carbon-14 percent modern values were collected for all wells sampled in 2012. Corrected ages are not made for data in which only limited supporting data were available to provide a corrected value. The presence or absence of significant concentrations of carbon-14 percent modern provides a qualitative evaluation of the age of the waters in these aquifers, which are primarily aquifers other than the Carrizo-Wilcox Aquifer.

For each aquifer in each of the four transects the following sets of figures are included to document the hydrogeology and water chemistry; data distribution, well depth, water levels (either as a potentiometric map or a Geographic Information System representation of water levels), a Piper diagram and a selected set of scatter plots that represent the geochemical reactions associated with the formation of sodium-bicarbonate waters and the addition of sodium and chloride from saline sources into the aquifers. Also included is a brief description of each plot. After this description of each observed chemical trend there is a discussion of the geochemical reactions occurring in that specific aquifer. At the end of each transects' section there is a discussion of the hydrochemistry for all the aquifers and their hydrogeologic signature.

## **7.1 Northeast Transect**

An excellent set of data from the TWDB groundwater database exists for water wells, water chemistry and water levels in the Carrizo-Wilcox, Queen City, Sparta and the Yegua-Jackson aquifers in the Northeast Transect (Figure 7-1) (from oldest to youngest). A three county area of Henderson, Anderson and Houston were selected for more detailed chemical analysis. Preliminary review of the data for this three county area indicated general trends were similar to the trends for the overall East Texas Basin. The Northeast Transect has an annual precipitation range of 38 to 46 inches (Figure 3-3). It is the “wettest” of the four transects studied.

### **7.1.1 General Geochemical Trends**

#### **Carrizo-Wilcox Aquifer**

The Carrizo-Wilcox Aquifer in the Northeast Transect is the most commonly used aquifer in the transect. The Carrizo-Wilcox Aquifer is characterized collectively as a complex mixture of sands and shales. A distinguishable Carrizo-Wilcox Aquifer often overlies the Wilcox Group of the Carrizo-Wilcox Aquifer. Production is primarily from the Wilcox. In the central region (Central Transect), the Wilcox Group is subdivided into the Calvert Bluff, Simsboro and Hooper formations. Because of the sands in the Wilcox Group in the East Texas basin are not as well defined (Fogg and others, 1983) the Wilcox Group is typically not subdivided into three subunits, but treated as a single aquifer.

### Well Depths

Based on Figure 7-2 the well depths are less than 500 feet in the outcrop in Henderson County to 2,000 feet in Houston County in the deep confined section of the aquifer.

### Potentiometric Surface

The Carizo-Wilcox Aquifer's potentiometric surface is approximately 400 feet in elevation in Henderson County and decreases to about 200 feet in southern Houston County (Kelly and others, 2004). Fogg and Kreitler (1982) also mapped the potentiometric surface in the Carrizo-Wilcox Aquifer (Figure 7-3) and provided more detail of water levels within the outcrop. Their map shows more groundwater flow parallel to the strike of the outcrop and towards the rivers that cross the outcrop.

### Piper Diagram

The Piper diagram (Figure 7-4) for the Carrizo-Wilcox Aquifer in the Northeast Transect shows a mixed cation (calcium-magnesium), mixed anion (chloride-sulfate-bicarbonate) type water at shallower depths (less than 500 feet) evolving to a sodium-bicarbonate water with depths greater than 2,000 feet.

### Bicarbonate versus Sodium Plot

A plot of bicarbonate versus sodium (Figure 7-5) for the Carrizo-Wilcox Aquifer data show one primary trend of sodium and bicarbonate increasing at a rate of 1:1 from a point of origin (sodium = 0) where bicarbonate is about two milliequivalents per liter.

### Sodium versus Calcium Plot

A plot of sodium versus calcium (Figure 7-6) shows an inverse relationship between sodium and calcium. At low concentrations of sodium, calcium is independent of sodium. Conversely at low concentrations of calcium, sodium increases independent of calcium.

### Bicarbonate versus Calcium Plot

A plot of bicarbonate versus calcium (Figure 7-7) shows a distribution of data similar to the sodium versus calcium plot (Figure 7-6), that is, an inverse relationship between bicarbonate and calcium.

### pH versus Bicarbonate Plot

The plot of pH versus bicarbonate (Figure 7-8) shows three limbs for the curve. Initially pH rises from about four to about six independent of bicarbonate. For the second limb, pH rises from about six to eight with an increased bicarbonate. The third limb shows increasing bicarbonate independent of pH.

### pH versus Sodium Plot

The plot of pH versus sodium (Figure 7-9) shows a similar distribution of data to the pH versus bicarbonate plot (Figure 7-8). There are low pH values at low sodium values. pH then increases as sodium increases. Sodium then increases independent of pH.

### Sulfate versus Bicarbonate Plot

A plot of sulfate versus bicarbonate (Figure 7-10) shows higher sulfate concentrations for bicarbonate concentrations less than about eight milliequivalents per liter.

### Chloride versus Sodium Plot

The plot of chloride versus sodium (Figure 7-11) shows sodium increasing independent to chloride for nearly all samples. There is a slight upswing of chloride at the highest sodium as is observed for some of the other aquifers that were studied in this project. There are also a few random higher chloride values.

### Chloride versus Bicarbonate Plot

The plot of chloride versus bicarbonate (Figure 7-12) shows bicarbonate increasing independent to chloride until the highest bicarbonate concentrations where there might be a slight increase in chloride.

### Depth versus Sulfate Plot

The plot of depth versus sulfate (Figure 7-13) shows higher random sulfate values at depths shallower than about 750 feet. Sulfate becomes negligible below about 1,700 feet.

### Depth versus Calcium Plot

The plot of depth versus calcium (Figure 7-14) shows high calcium values at depths less than about 250 feet with a small bump at about 750 feet. Calcium becomes negligible at depths greater than 1,000 feet.

### Map of Calcium

The map of calcium (Figure 7-15) in the Carrizo-Wilcox Aquifer shows that nearly all the higher calcium concentrations are in the outcrop.

### Depth versus Bicarbonate Plot

The plot of depth versus bicarbonate (Figure 7-16) shows no trends of the distribution of bicarbonate with depth.

### Depth versus pH Plot

The plot of depth versus pH (Figure 7-17) shows a general increase of pH with greater depth.

### Depth versus Sodium Plot

The plot of depth versus sodium (Figure 7-18) does not show any obvious trends.

### Depth versus Chloride Plot

The plot of depth versus chloride (Figure 7-19) does not show a significant increase in chloride at greater depth as is observed in some other aquifers in other transects. The plot also shows some increased chloride concentrations at shallow depths. These occasional high values are considered to be from anthropogenic sources.

### Depth versus Total Dissolved Solids Plot

Total dissolved solids for the Carrizo-Wilcox Aquifer (Figure 7-20) shows a general increase in total dissolved solids, but is generally less than 1,000 parts per million.

### Discussion

Groundwater in the Carrizo-Wilcox Aquifer in the Northeast Transect is recharged in the outcrop and either discharges in the outcrop or flows into the downdip section of the aquifer. The water

chemistry evolves from a mixed (calcium-magnesium) cation, mixed (chloride-sulfate-bicarbonate) anion type water in the outcrop to a sodium-bicarbonate water downdip. The sodium-bicarbonate waters evolve from a high calcium, low pH, low bicarbonate water in the shallow outcrop to a high pH, low calcium, high sodium, high bicarbonate water downdip. High sulfate waters are primarily in the outcrop. Elevated calcium values are primarily in the outcrop and not downdip.

Figure 7-16 and Figure 7-18 do not show a clear increase in sodium and bicarbonate with depth, although bicarbonate versus sodium (Figure 7-5) shows an excellent correlation. Depth versus calcium (Figure 7-14) shows the loss of calcium with depth. The great thickness of the Carrizo-Wilcox Aquifer complicates the interpretation of the development of the sodium-bicarbonate groundwaters. A chemical analysis from the geographic outcrop may come from a well 500 feet deep and be confined in its hydrogeologic setting. Similarly these sodium-bicarbonate groundwaters may be being ultimately discharged to the streams and/or rivers that cross the outcrop and never flow into the deeper confined section.

The downdip part of the aquifer is denoted by sodium-bicarbonate type waters. Either the direction of groundwater flow is dominated by recharge and discharge in the outcrop and more limited flow to the downdip parts of the aquifer or there are still sodium-calcium exchange sites at the downdip edge of the outcrop as it transitions into the confined section and the water chemistry quickly evolved to a sodium-bicarbonate type water. The corrected carbon-14 ages as the waters become old quickly suggest that the dominant flow in the aquifer stays in the outcrop and flow into the confined section is less.

There is a very limited amount of chloride in the deeper part of the aquifer, suggesting there is no significant discharge of more saline waters from deeper formations into the aquifer. This should be expected since the deeper parts of the Carrizo-Wilcox Aquifer is still in the East Texas basin and do not “transition” into the deeper saline formations as are observed for the Carrizo-Wilcox Aquifer farther to the south.

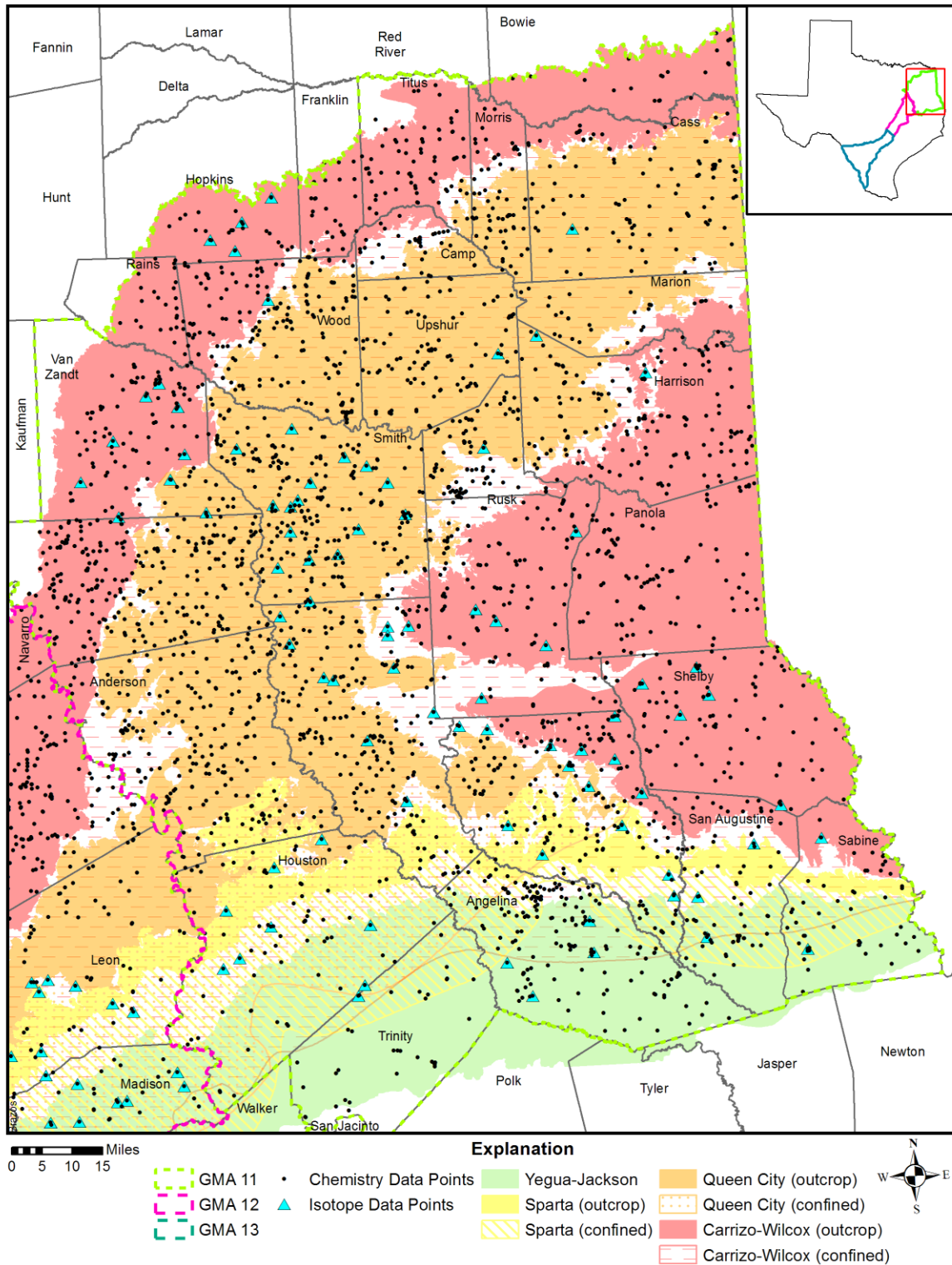


**Figure 7-1. Data distribution of wells with outcrop and downdip extent (up to 3,000 milligrams per liter total dissolved solids) of the Carrizo-Wilcox, Queen City, Sparta, and Yegua-Jackson aquifers in the Northeast Transect, Groundwater Management Area 11.**

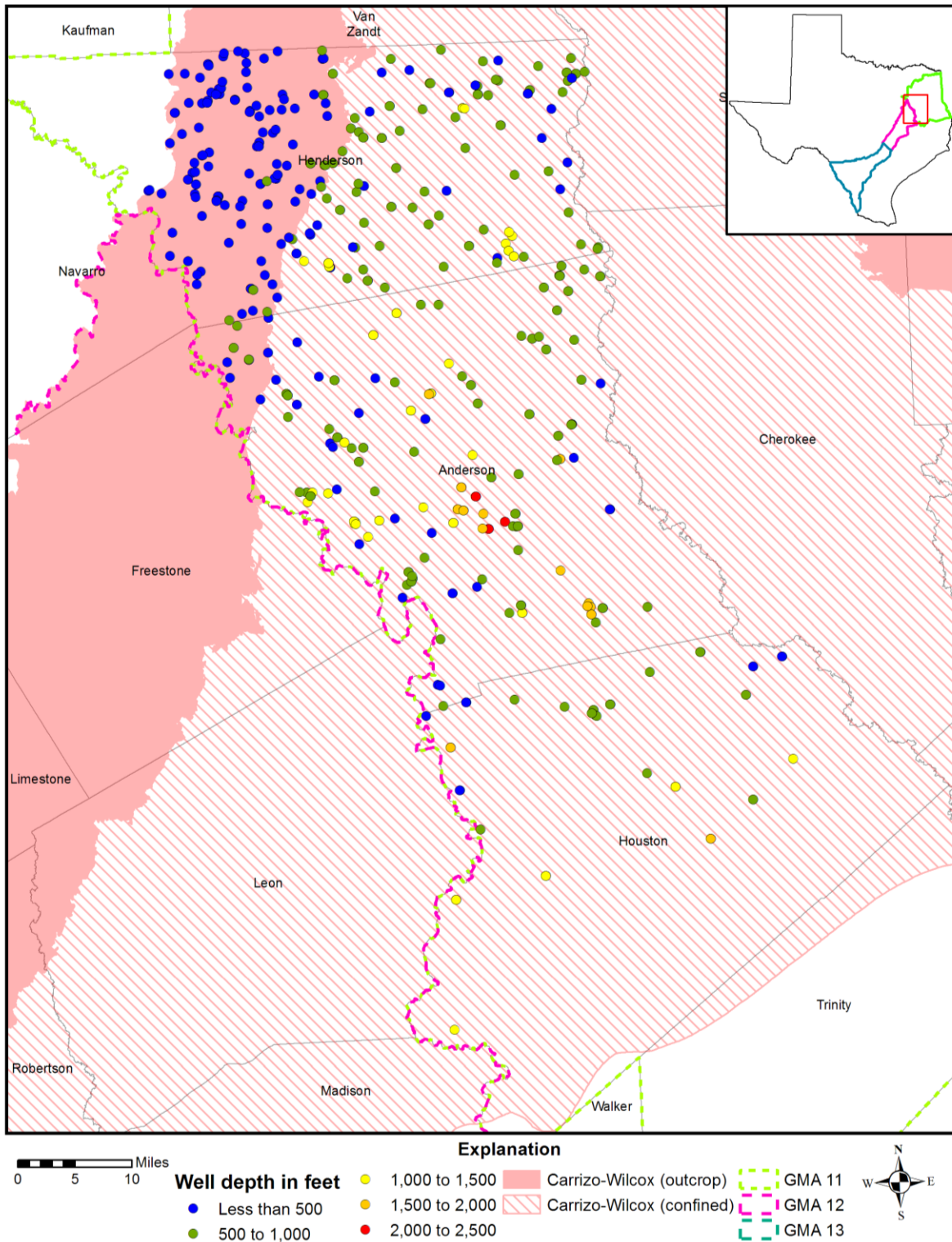


Figure 7-2. Well depths measured from land surface in feet in the Carrizo-Wilcox Aquifer, Northeast Transect, Groundwater Management Area (GMA) 11.

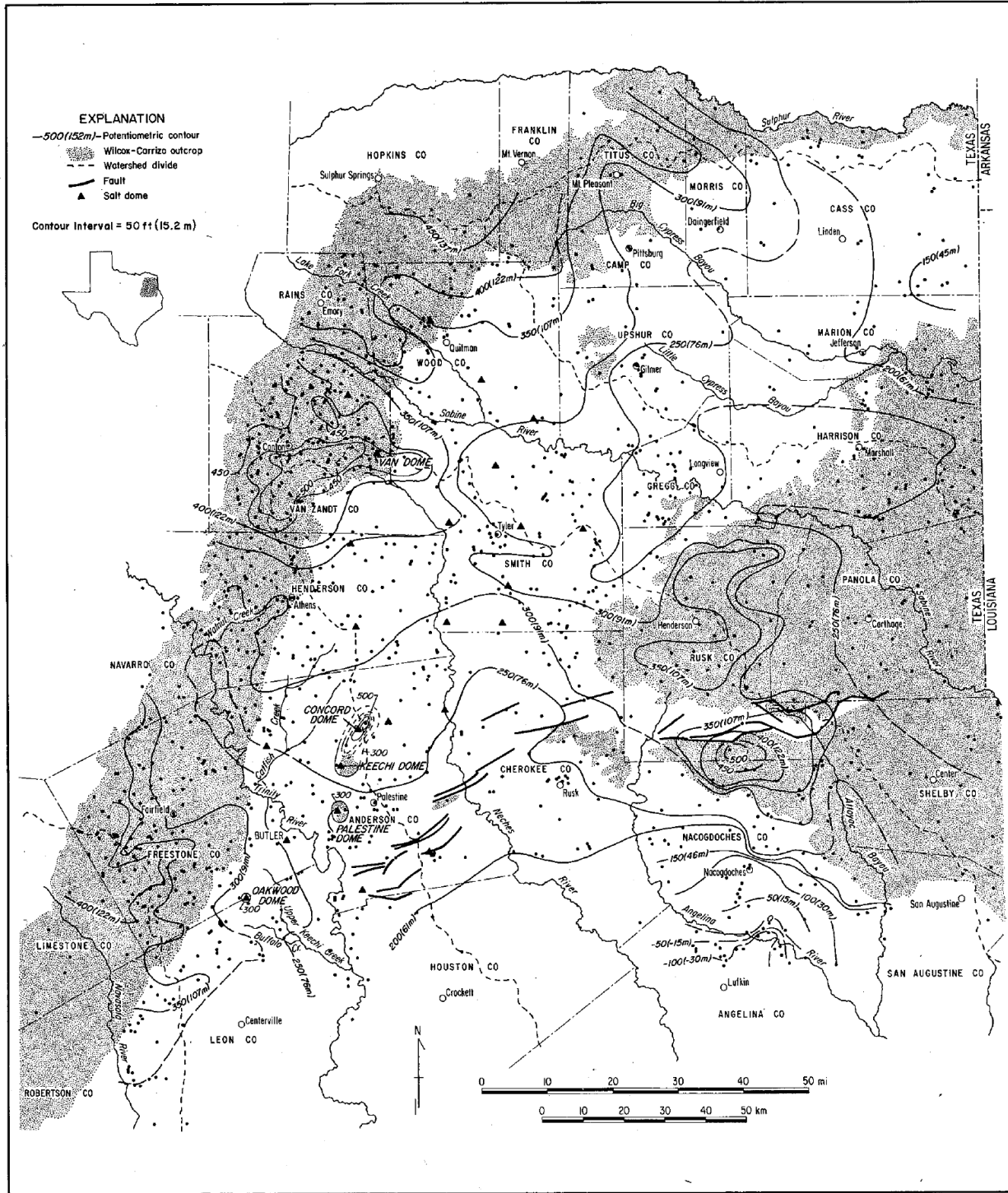


Figure 7-3. Potentiometric surface of the Carrizo-Wilcox Aquifer (1936-1976) (Figure 13 from Fogg and Kretler, 1982).

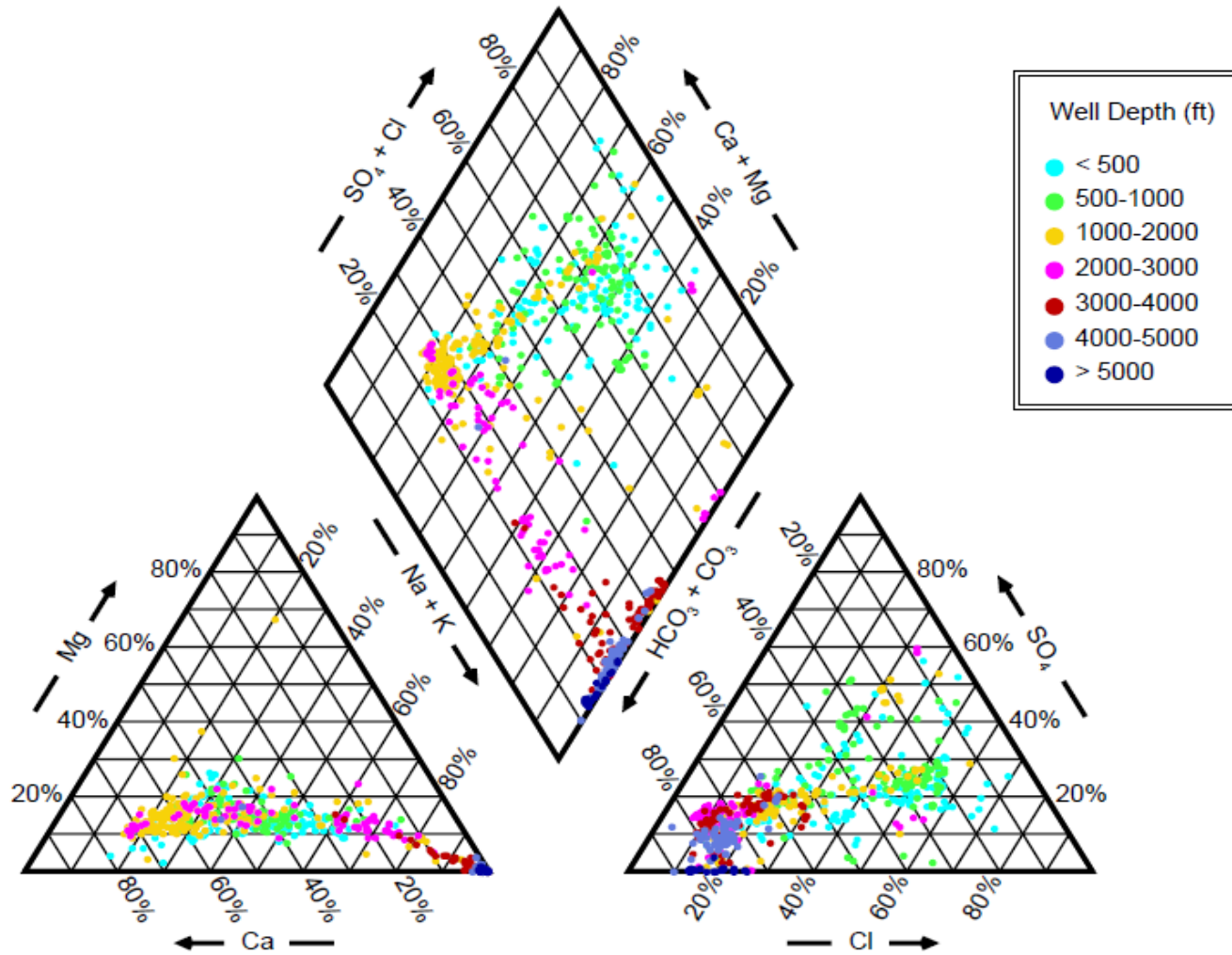


Figure 7-4. Piper diagram showing chemistry of the Carrizo-Wilcox Aquifer wells in the Northeast Transect by well depth measured from land surface in feet (ft).

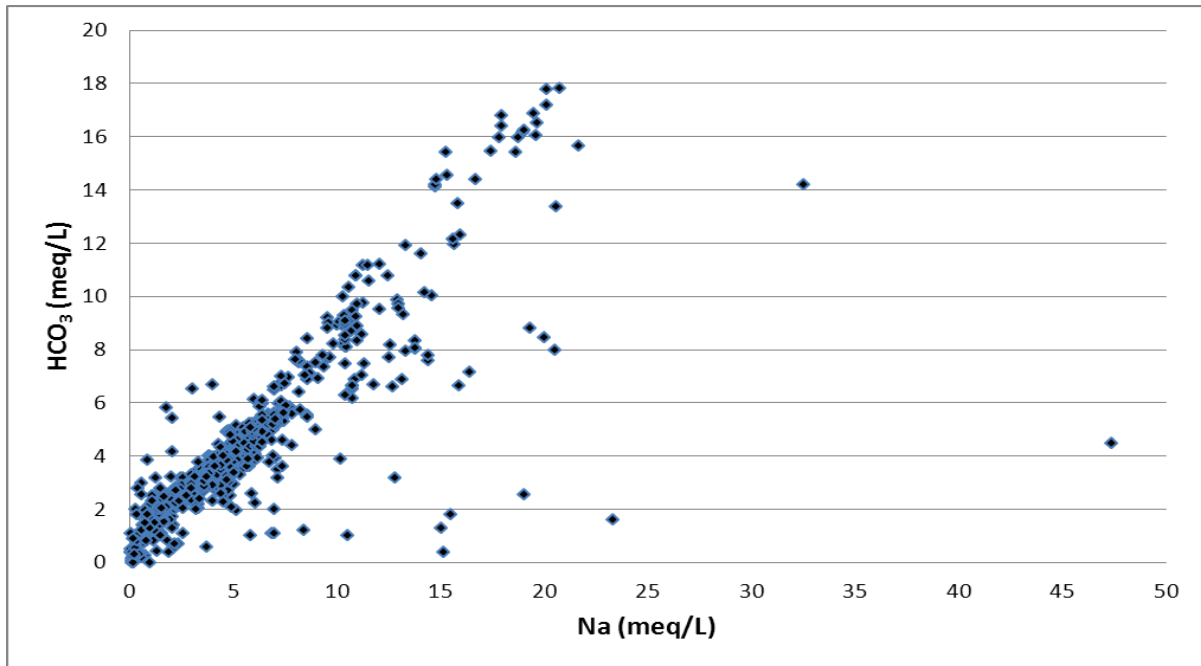


Figure 7-5. Bicarbonate (HCO<sub>3</sub>) versus sodium (Na) measured in milliequivalents per liter (meq/L), Carrizo-Wilcox Aquifer, Northeast Transect, Groundwater Management Area 11.

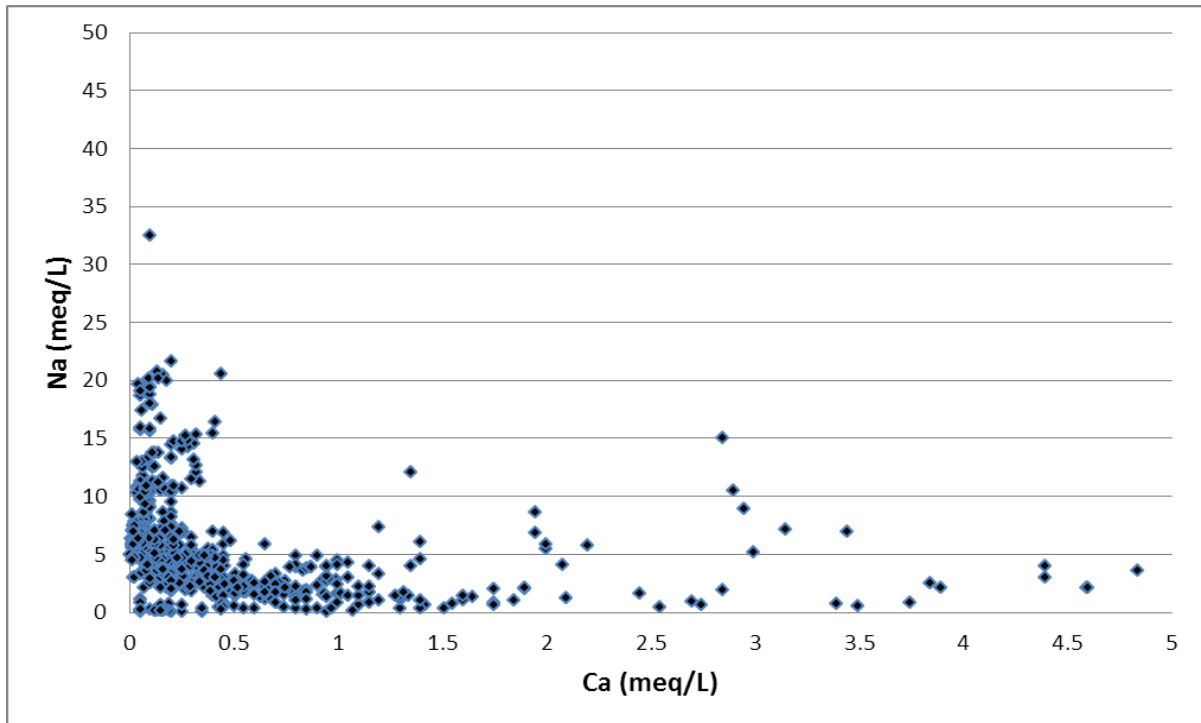


Figure 7-6. Sodium (Na) versus calcium (Ca) measured in milliequivalents per liter (meq/L), Carrizo-Wilcox Aquifer, Northeast Transect, Groundwater Management Area 11.

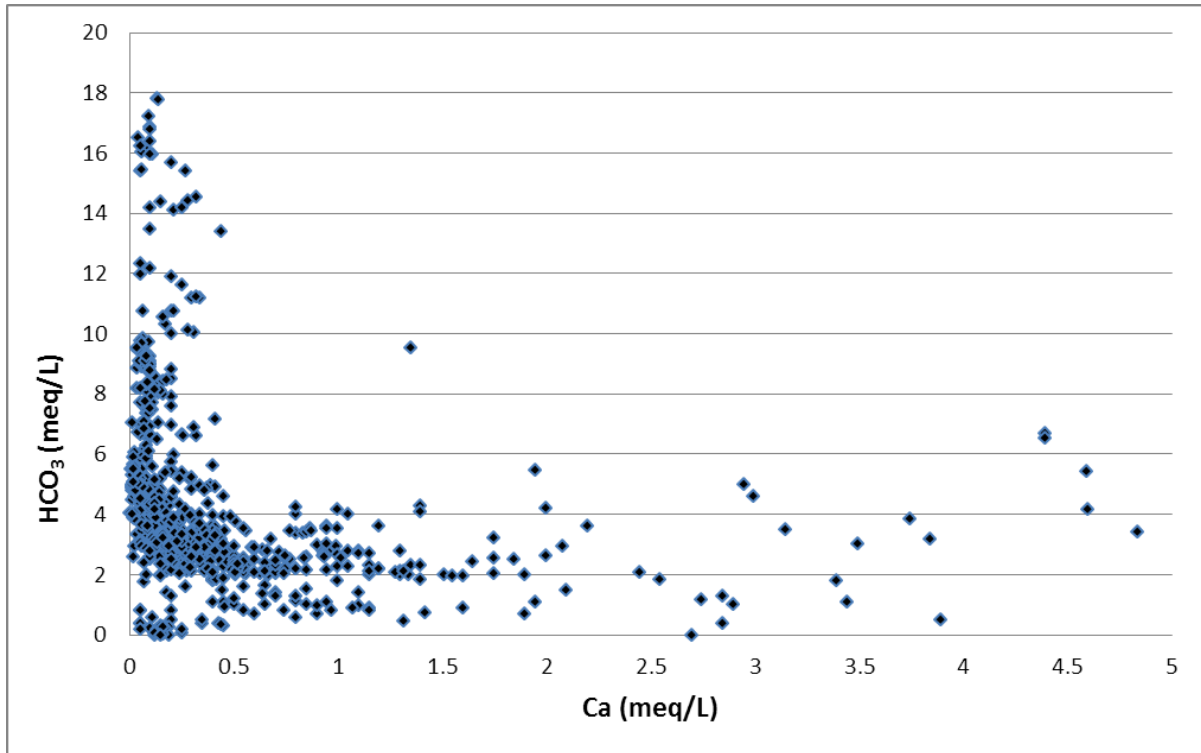


Figure 7-7. Bicarbonate (HCO<sub>3</sub>) versus calcium (Ca) measured in milliequivalents per liter (meq/L), Carrizo-Wilcox Aquifer, Northeast Transect, Groundwater Management Area 11.

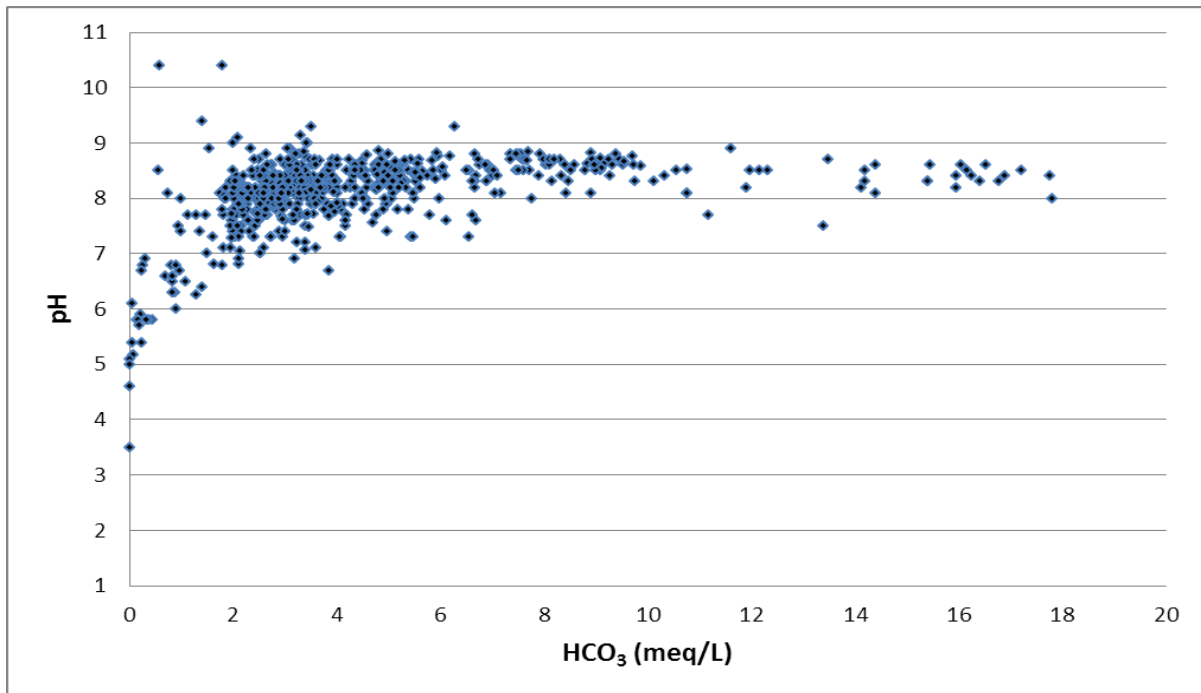


Figure 7-8. pH versus bicarbonate (HCO<sub>3</sub>) measured in milliequivalents per liter (meq/L), Carrizo-Wilcox Aquifer, Northeast Transect, Groundwater Management Area 11.

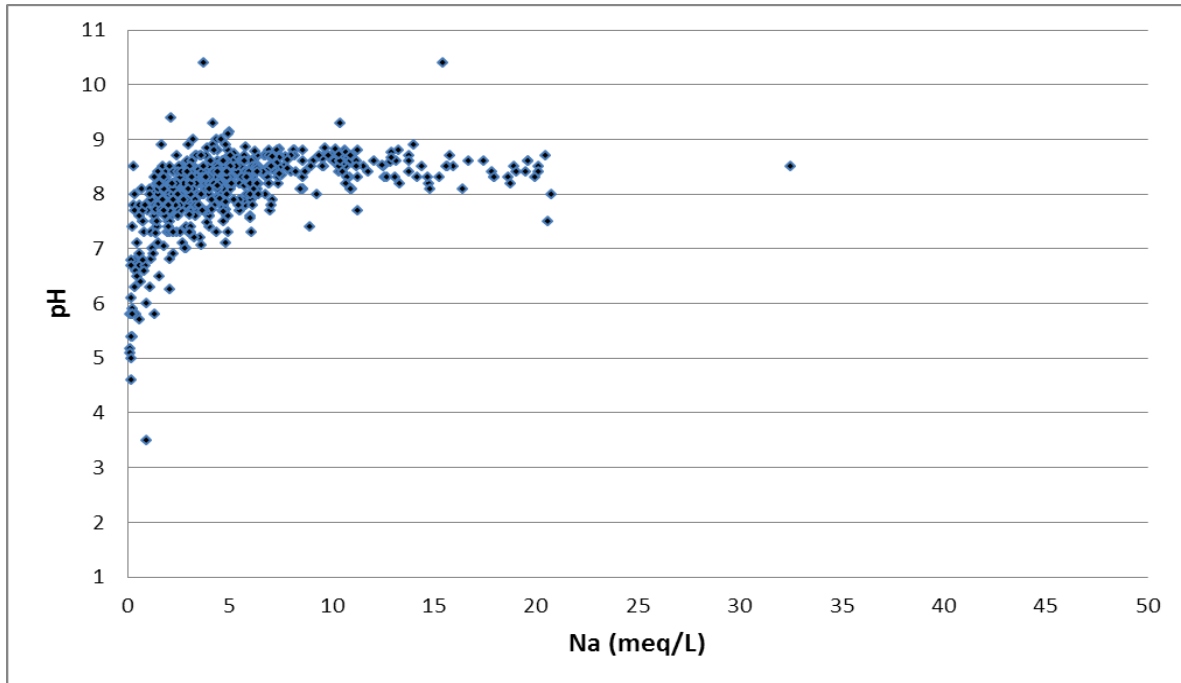


Figure 7-9. pH versus sodium (Na) measured in milliequivalents per liter (meq/L), Carrizo-Wilcox Aquifer, Northeast Transect, Groundwater Management Area 11.

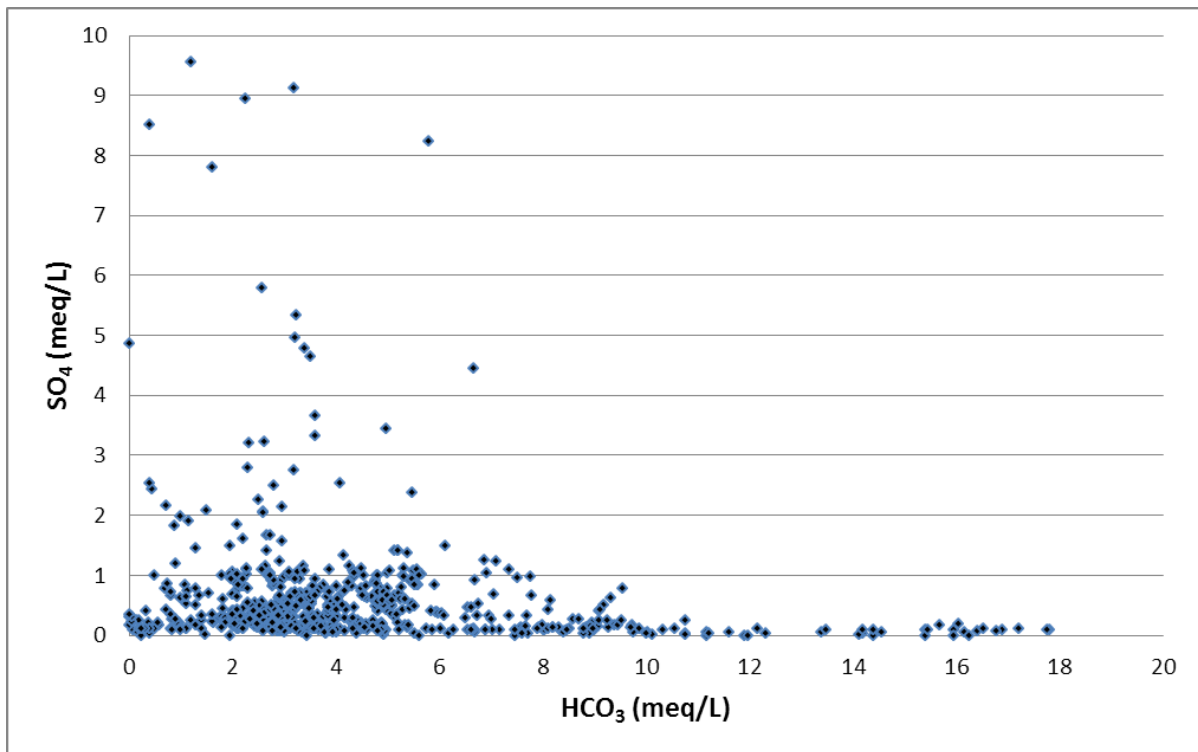


Figure 7-10. Sulfate (SO<sub>4</sub>) versus bicarbonate (HCO<sub>3</sub>) measured in milliequivalents per liter (meq/L), Carrizo-Wilcox Aquifer, Northeast Transect, Groundwater Management Area 11.

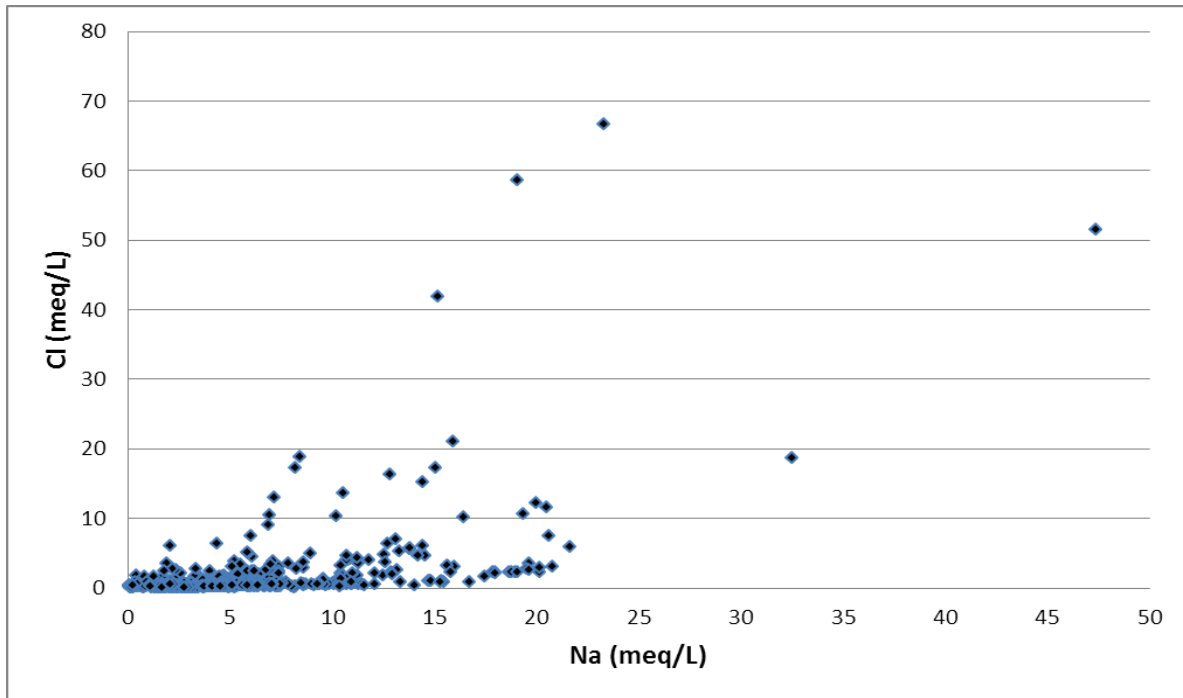


Figure 7-11. Chloride (Cl) versus sodium (Na) measured in milliequivalents per liter (meq/L), Carrizo-Wilcox Aquifer, Northeast Transect, Groundwater Management Area 11.

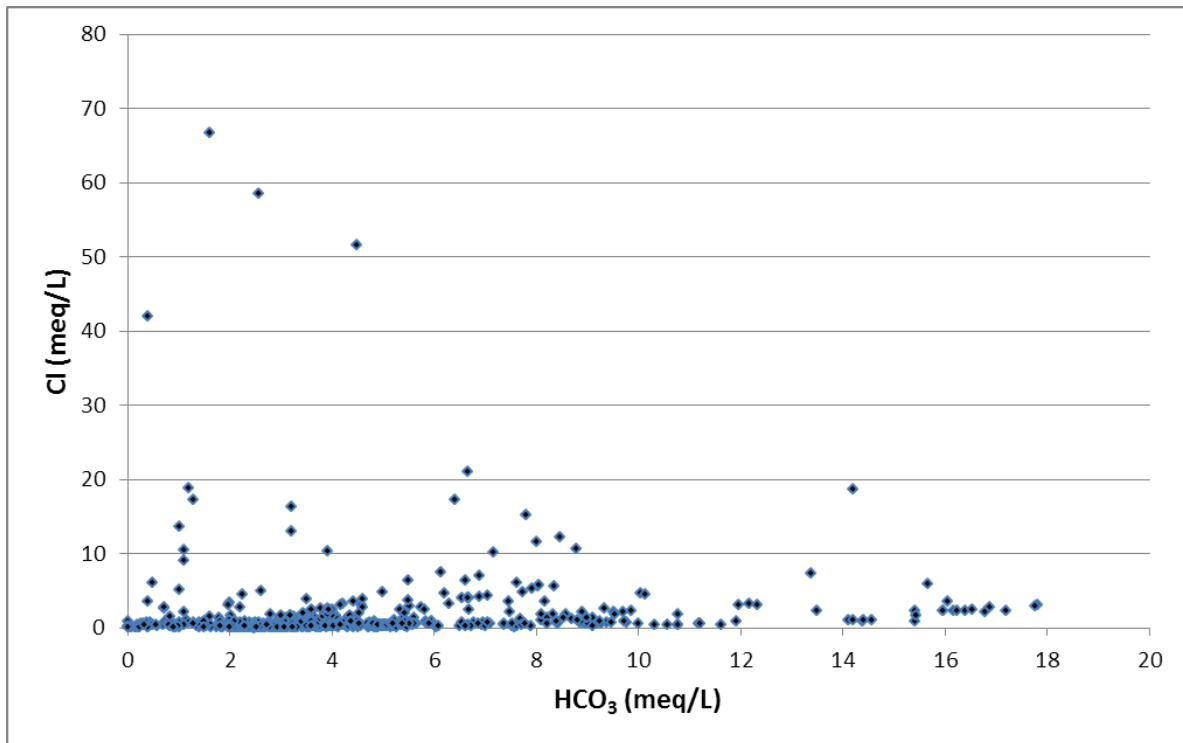
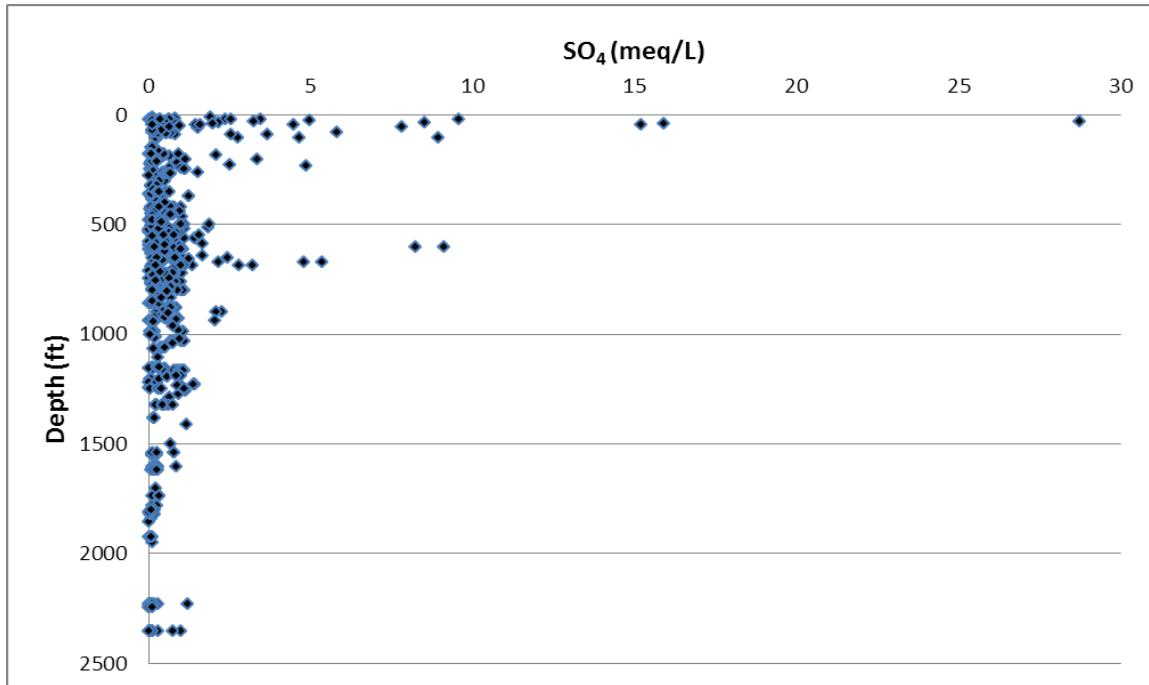
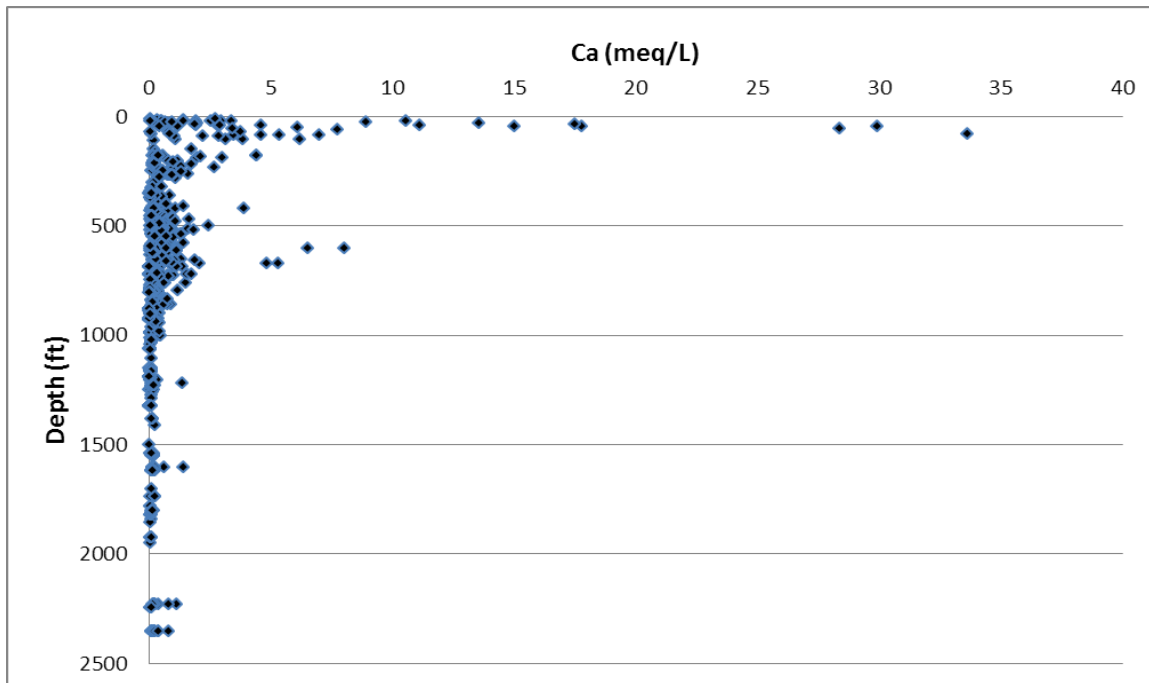


Figure 7-12. Chloride (Cl) versus bicarbonate ( $\text{HCO}_3$ ) measured in milliequivalents per liter (meq/L), Carrizo-Wilcox Aquifer, Northeast Transect, Groundwater Management Area 11.



**Figure 7-13.** Depth measured from land surface in feet (ft) versus sulfate ( $\text{SO}_4$ ) measured in milliequivalents per liter (meq/L), Carrizo-Wilcox Aquifer, Northeast Transect, Groundwater Management Area 11.



**Figure 7-14.** Depth measured from land surface in feet (ft) versus calcium (Ca) measured in milliequivalents per liter (meq/L), Carrizo-Wilcox Aquifer, Northeast Transect, Groundwater Management Area 11.

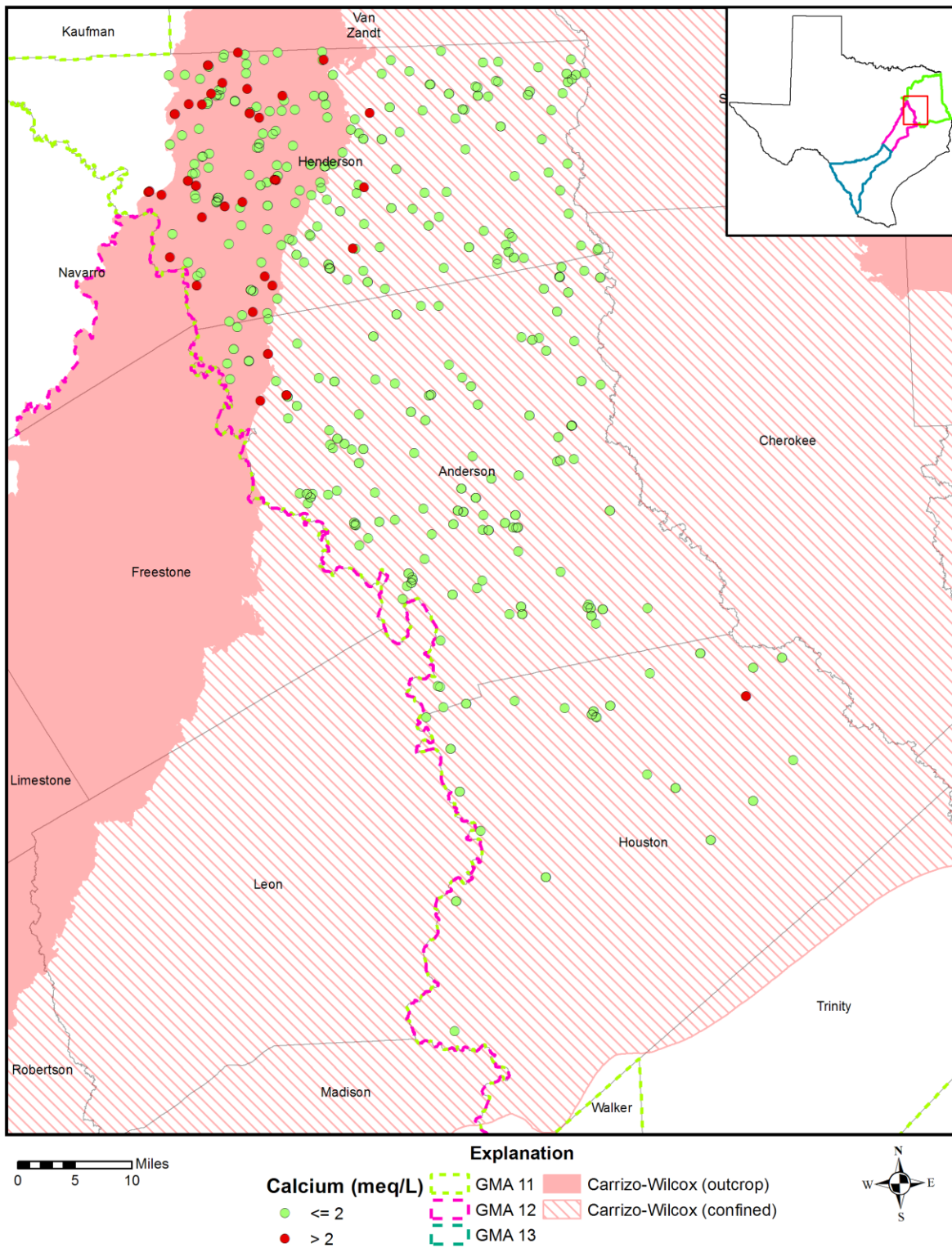


**Figure 7-15. Calcium concentrations measured in milliequivalents per liter (meq/L) in the Carrizo-Wilcox Aquifer, Northeast Transect, Groundwater Management Area (GMA) 11.**

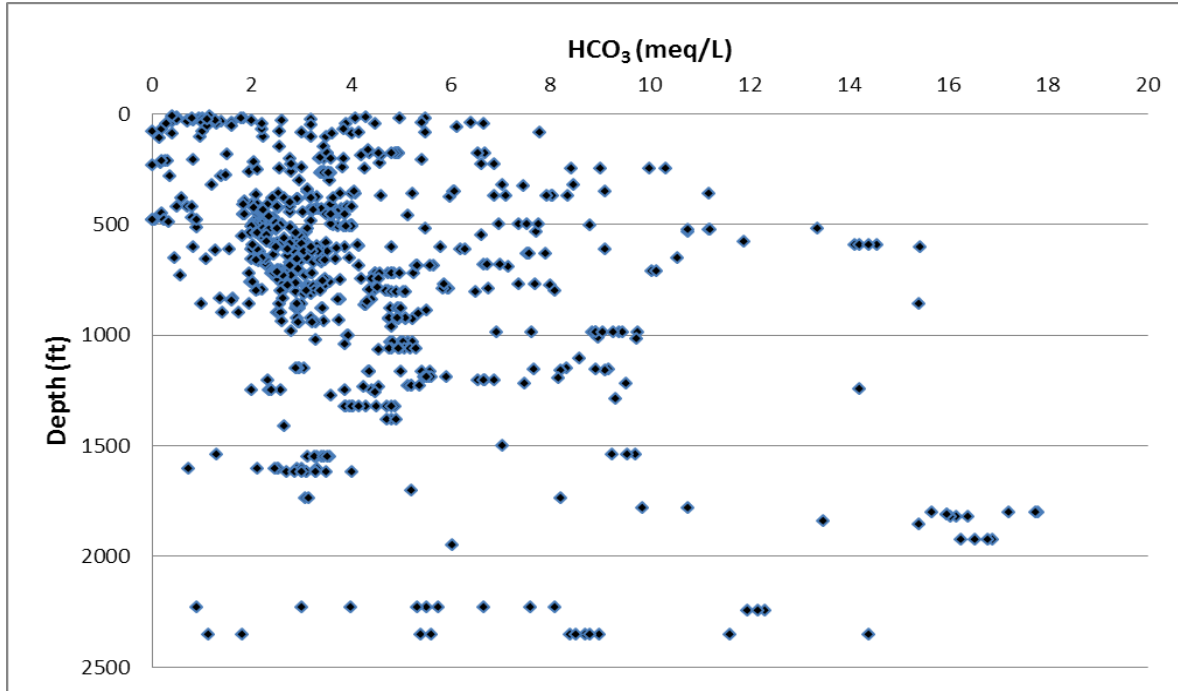


Figure 7-16. Depth measured from land surface in feet (ft) versus bicarbonate (HCO<sub>3</sub>) measured in milliequivalents per liter (meq/L), Carrizo-Wilcox Aquifer, Northeast Transect, Groundwater Management Area 11.

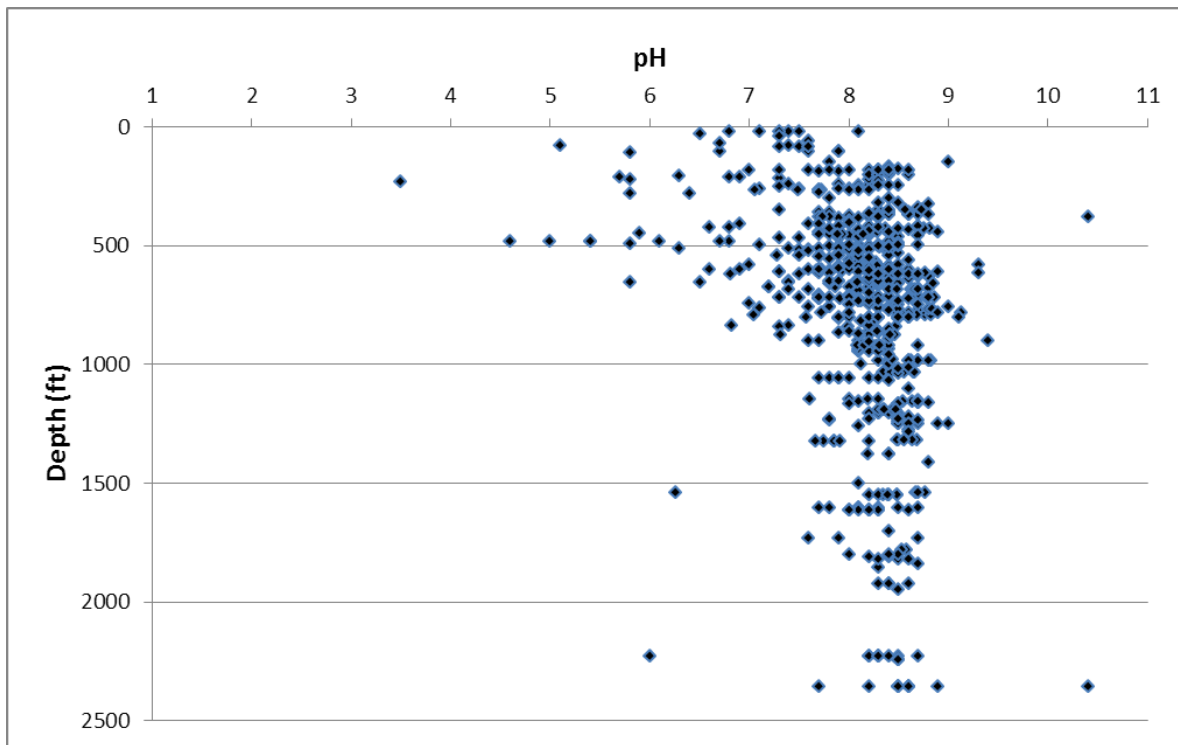
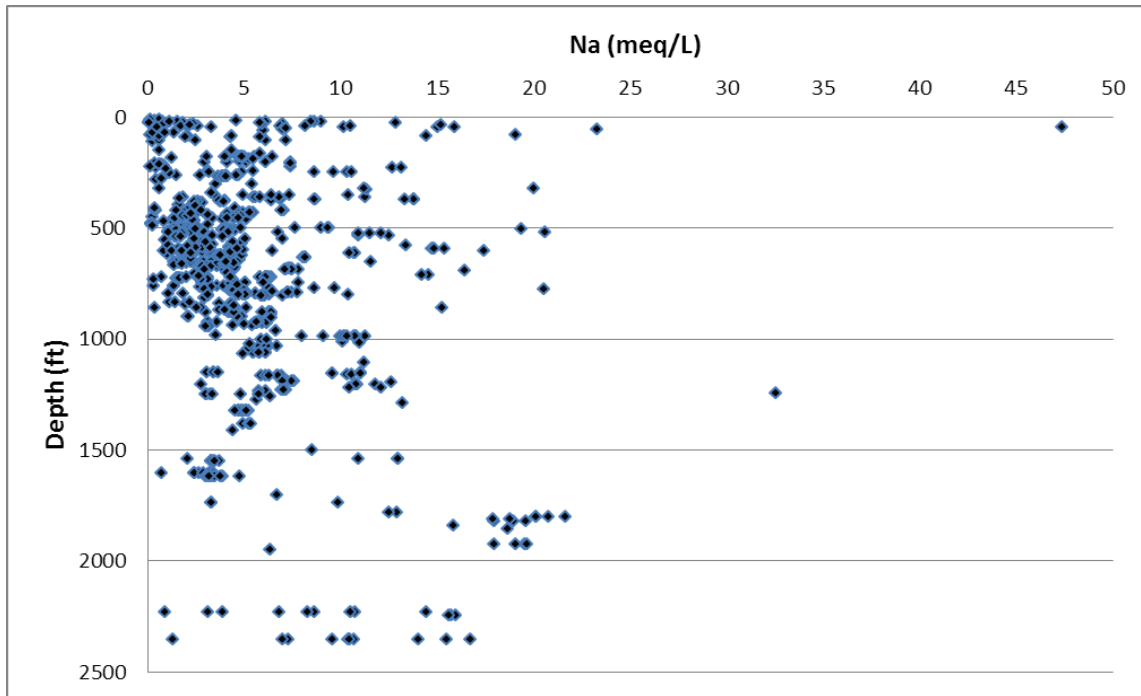
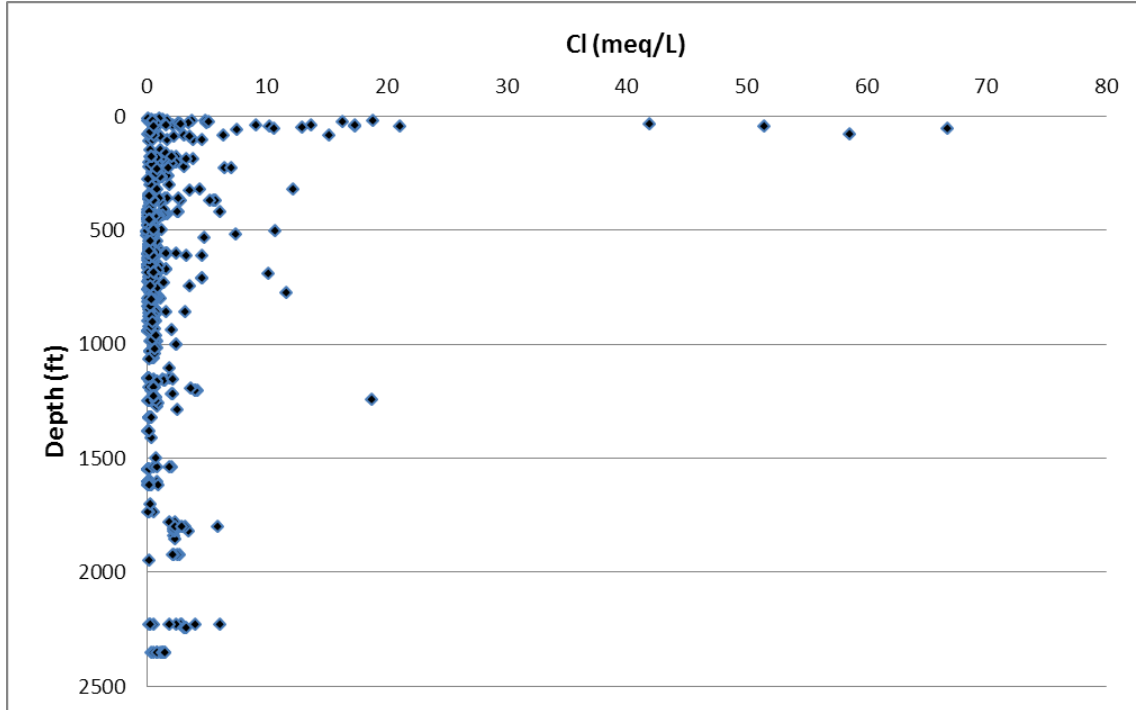


Figure 7-17. Depth measured from land surface in feet (ft) versus pH, Carrizo-Wilcox Aquifer, Northeast Transect, Groundwater Management Area 11.



**Figure 7-18.** Depth measured from land surface in feet (ft) versus sodium (Na) measured in milliequivalents per liter (meq/L), Carrizo-Wilcox Aquifer, Northeast Transect, Groundwater Management Area 11.



**Figure 7-19.** Depth measured from land surface in feet (ft) versus chloride (Cl) measured in milliequivalents per liter (meq/L), Carrizo-Wilcox Aquifer, Northeast Transect, Groundwater Management Area 11.

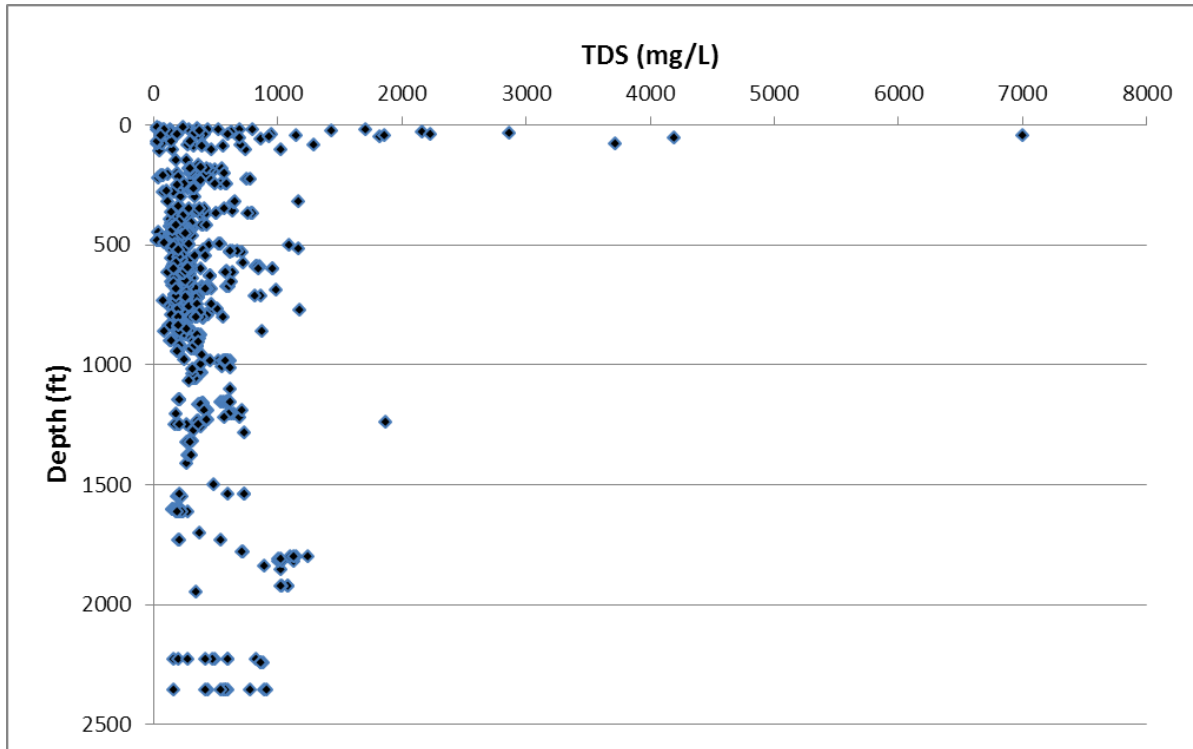


**Figure 7-20.** Depth measured from land surface in feet (ft) versus total dissolved solids (TDS) measured in parts per million (ppm), Carrizo-Wilcox Aquifer, Northeast Transect, Groundwater Management Area 11.

### Queen City Aquifer

The Queen City Aquifer overlies the Carrizo-Wilcox Aquifer and the Reklaw Formation (Figure 5-2). Nearly all the wells are located in the outcrop; only a few wells are screened in the downdip part of the Queen City Aquifer (Figure 7-21).

#### Well Depths

Based on Figure 7-21 the well depths are less than 400 feet in the outcrop and less than 800 feet in downdip sections.

#### Water Level Data

Water levels in the Queen City Aquifer (Figure 7-22) range from approximately 700 feet elevation (1970-2010) in Henderson County and decrease to about 200 feet in the confined section.

#### Piper Diagram

The Piper diagram (Figure 7-23) for the Queen City Aquifer in the Northeast Transect shows a predominantly mixed cation (calcium-magnesium), mixed anion (chloride-sulfate-bicarbonate) type water in the outcrop to a few sodium-bicarbonate water in the downdip confined section of the aquifer.

### Bicarbonate versus Sodium Plot

A plot of bicarbonate versus sodium (Figure 7-24) for the Queen City Aquifer data show two trends: 1) bicarbonate increasing independent of sodium and 2) a trend of sodium and bicarbonate increasing at a rate of 1:1 from a point of origin where bicarbonate is about two milliequivalents per liter.

### Sodium versus Calcium Plot

A plot of sodium versus calcium (Figure 7-25) shows an inverse relationship between sodium and calcium. At low concentrations of sodium, calcium is independent of sodium. Conversely at low concentrations of calcium, sodium increases independent of calcium. Most of the samples are on the calcium limb (in the outcrop).

### Bicarbonate versus Calcium Plot

A plot of bicarbonate versus calcium (Figure 7-26) shows a distribution of data similar to the sodium versus calcium plot (Figure 7-25), that is, an inverse relationship. The calcium limb shows an increase in calcium and bicarbonate at low concentrations.

### pH versus Bicarbonate Plot

The plot of pH versus bicarbonate (Figure 7-27) shows two to three limbs for the curve. Initially pH rises from about four to about six independent of bicarbonate. For the second limb, pH rises from about six to eight with an increasing bicarbonate. The third limb shows increasing bicarbonate independent of pH. The maximum bicarbonate concentrations in the Queen City Aquifer are only about six milliequivalents per liter, whereas maximum bicarbonate in the Carrizo-Wilcox Aquifer is about 18 milliequivalents per liter (Figure 7-5). This lack of high bicarbonate waters may be caused by the fact that most of the Queen City Aquifer wells are in the outcrop.

### pH versus Sodium Plot

The plot of pH versus sodium (Figure 7-28) shows a similar distribution of data to the pH versus bicarbonate plot (Figure 7-27). Most of the water is low sodium type waters whereas, for the underlying Carrizo-Wilcox Aquifer, the maximum sodium concentrations are 18 milliequivalents per liter (Figure 7-9).

### Chloride versus Sodium Plot

The plot of chloride versus sodium (Figure 7-29) shows sodium increasing independent to chloride for nearly all samples.

### Chloride versus Bicarbonate Plot

The plot of chloride versus bicarbonate (Figure 7-30) shows bicarbonate increasing independent to chloride. There are a few high chloride values at very low bicarbonate values.

### Sulfate versus Bicarbonate Plot

The plot of sulfate versus bicarbonate (Figure 7-31) shows higher sulfate concentrations for bicarbonate concentrations less than about one milliequivalents per liter.

#### Depth versus Nitrate Plot

The plot of depth versus nitrate (Figure 7-32) shows several wells at depths less than 100 feet have high nitrate concentrations. At depths greater than about 100 feet, nitrate is negligible.

#### Depth versus Sulfate Plot

The plot of depth versus sulfate (Figure 7-33) shows higher random sulfate values at depths shallower than about 100 feet. Sulfate becomes negligible below about 100 feet.

#### Calcium vs Depth Plot

The plot of calcium versus depth (Figure 7-34) shows high calcium values at depth less than about 400 feet. Calcium becomes negligible at depths greater than 400 feet.

#### Map of Calcium

The map of calcium in the outcrop in the Queen City Aquifer (Figure 7-35) shows that nearly all the higher calcium concentrations are in the outcrop.

#### Depth versus pH Plot

The plot of depth versus pH (Figure 7-36) shows a general increase of pH with greater depth. Most of the samples are in the outcrop.

#### Depth versus Bicarbonate Plot

The plot of depth versus bicarbonate (Figure 7-37) shows a general increase in bicarbonate with depth. Most of the samples are in the outcrop.

#### Depth versus Sodium Plot

The plot of depth versus sodium (Figure 7-38) shows most of the shallow wells are low in sodium. The deeper wells have higher sodium values.

#### Depth versus Chloride Plot

The plot of depth versus chloride (Figure 7-39) does not show an increase in chloride at greater depth as is observed in some other aquifers in the study area. The highest chloride values are in the shallowest wells.

#### Depth versus Total Dissolved Solids Plot

Total dissolved solids for the Queen City Aquifer (Figure 7-40) shows the highest total dissolved solids values are in the shallowest wells.

#### Discussion

Groundwater produced from the Queen City Aquifer in the Northeast Transect is produced primarily from the outcrop. The Piper diagram shows most of the water are of a calcium-sulfate-chloride-bicarbonate type. There are few sodium-bicarbonate values because there are only a few samples from the confined section. This should be expected if we are seeing only the early part of the evolution of sodium-bicarbonate water. The water chemistry also indicates elevated nitrate concentrations. The early stages of the development of a sodium-bicarbonate appear to be occurring in the outcrop of the Queen City Aquifer where a calcium-magnesium, higher sulfate, low sodium and higher nitrate type water is present.

Assessment of the hydrochemical and isotope data in the Northeast Transect generally confirms the overall conceptual model for the Northern Queen City-Sparta GAM. However, the hydrochemical and isotopic data generally do not provide the type of information that allows specific parametric adjustments to improve model calibration.

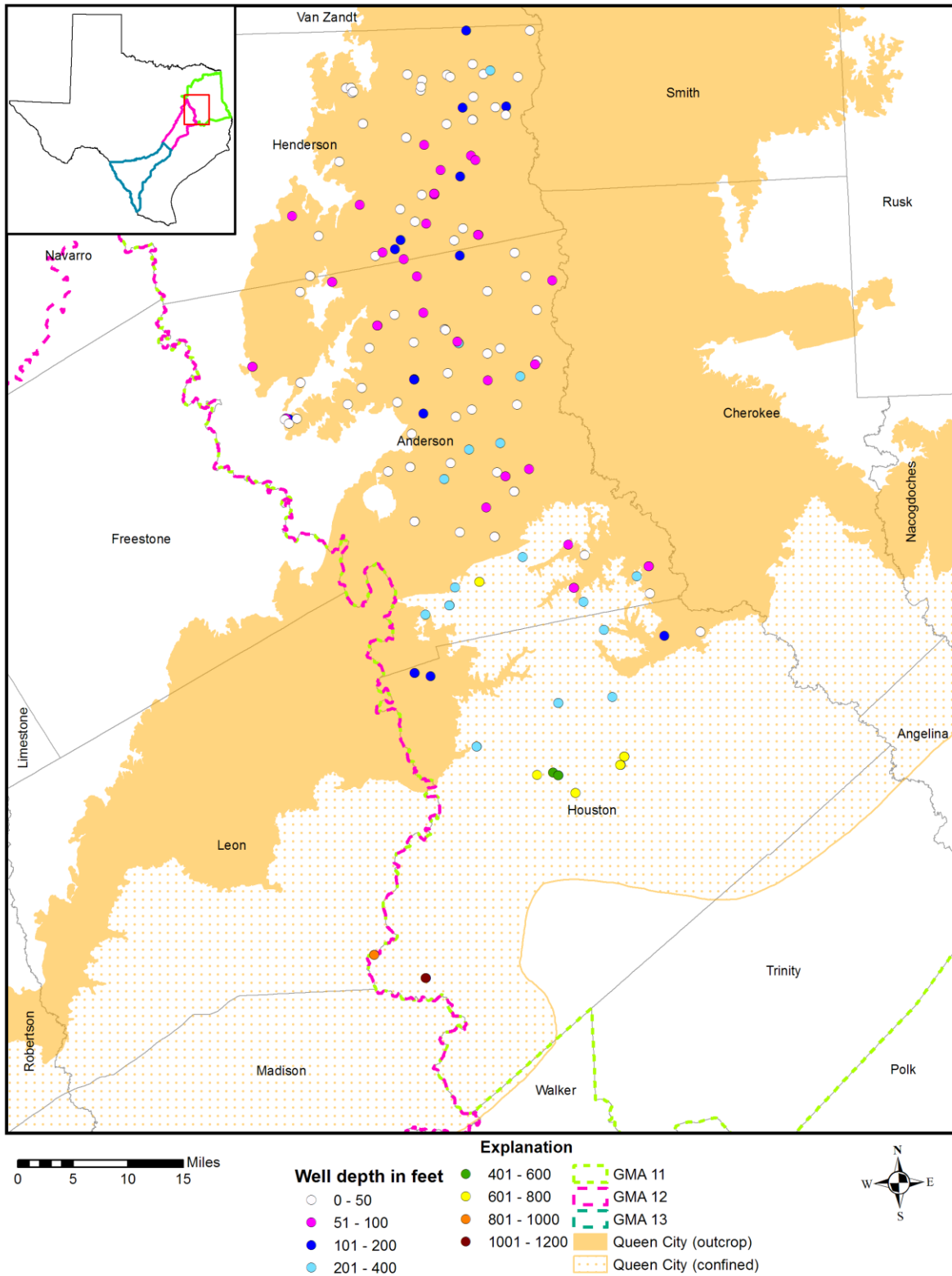


Figure 7-21. Well depths measured from land surface in feet in the Queen City Aquifer, Northeast Transect, Groundwater Management Area (GMA) 11.

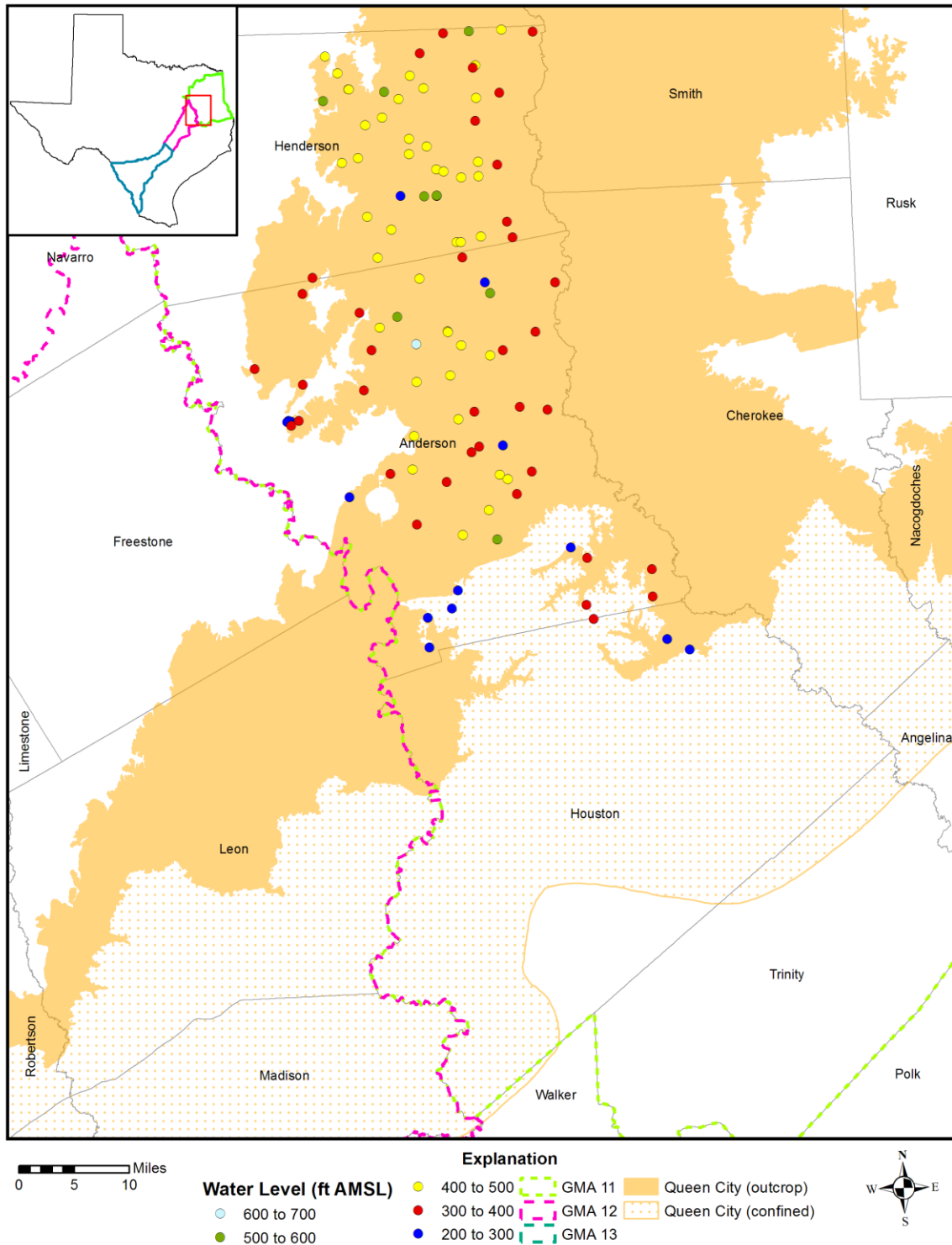


Figure 7-22. Water level elevations from 1970 to 2010 measured in feet above mean sea level (ft AMSL) in the Queen City Aquifer, Northeast Transect, Groundwater Management Area (GMA) 11.

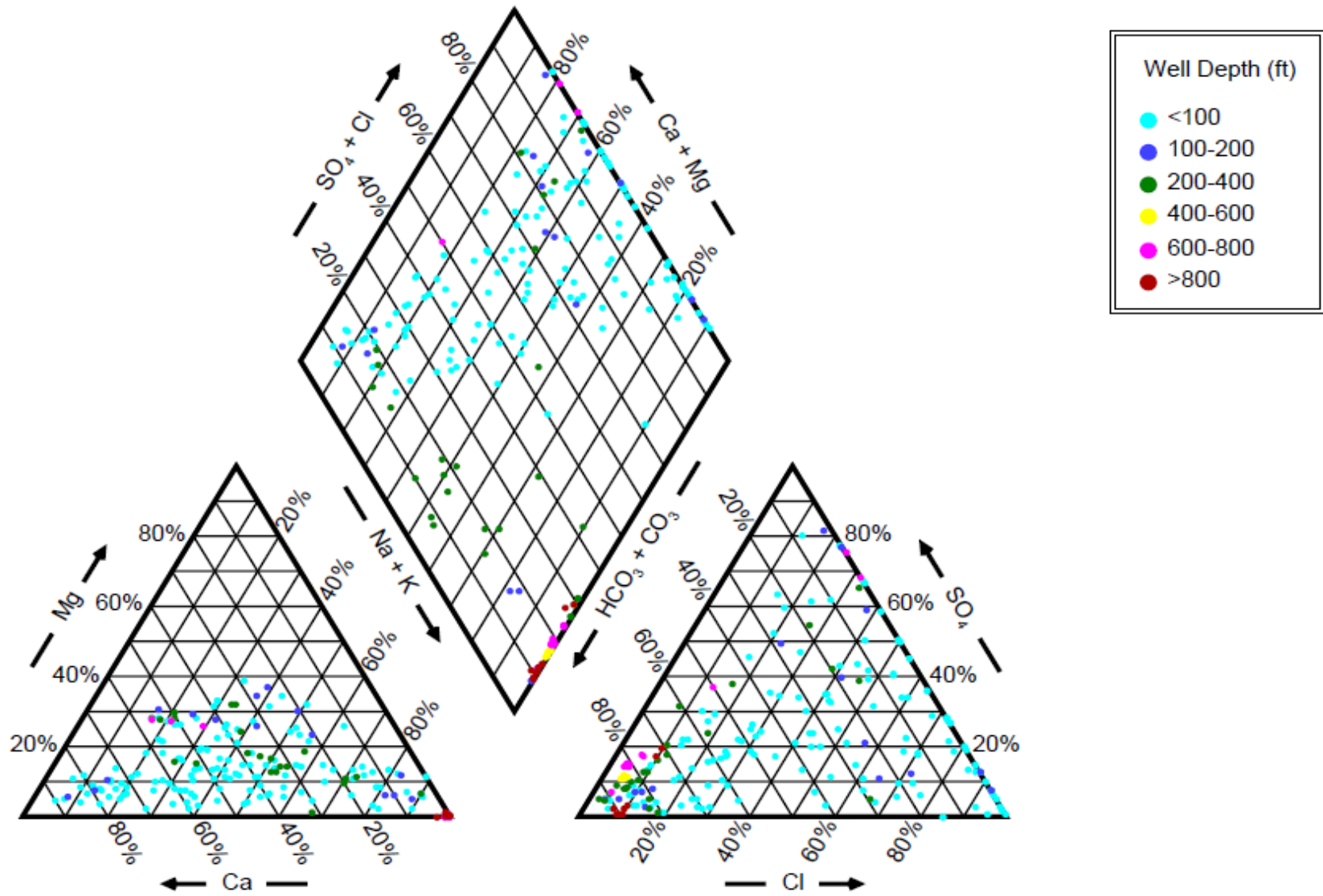


Figure 7-23. Piper diagram showing chemistry of the Queen City Aquifer wells in the Northeast Transect by well depth measured from land surface in feet (ft).

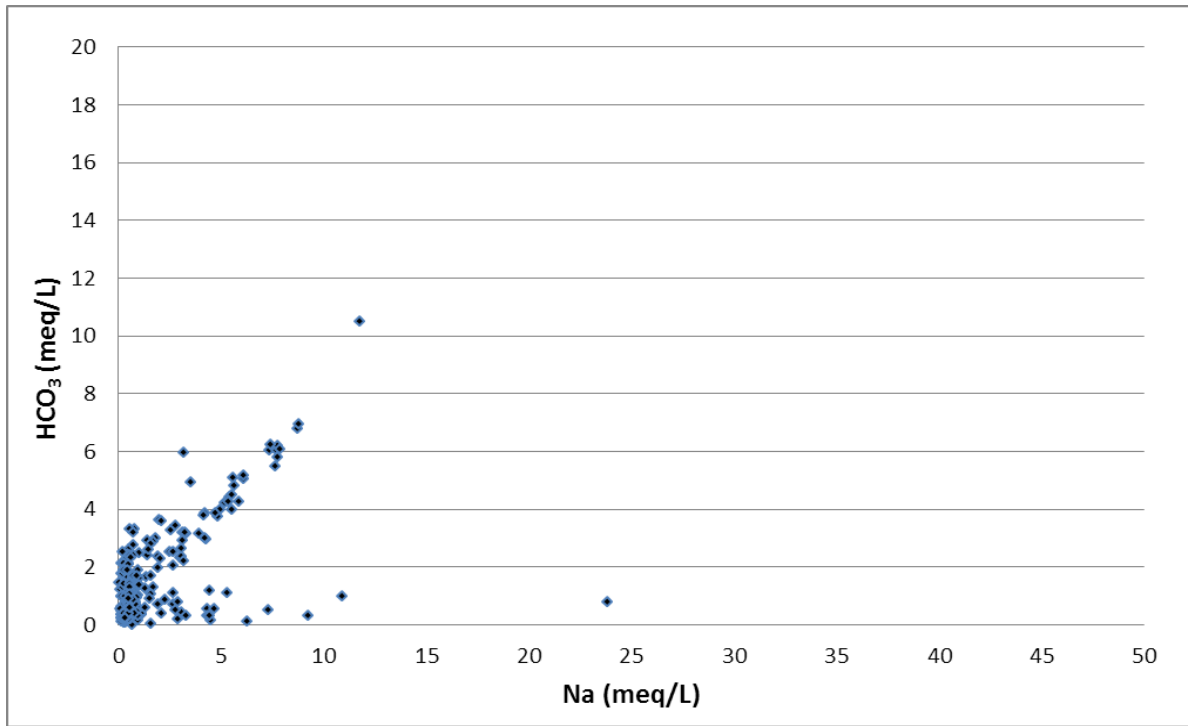


Figure 7-24. Bicarbonate (HCO<sub>3</sub>) versus sodium (Na) measured in milliequivalents per liter (meq/L), Queen City Aquifer, Northeast Transect, Groundwater Management Area 11.

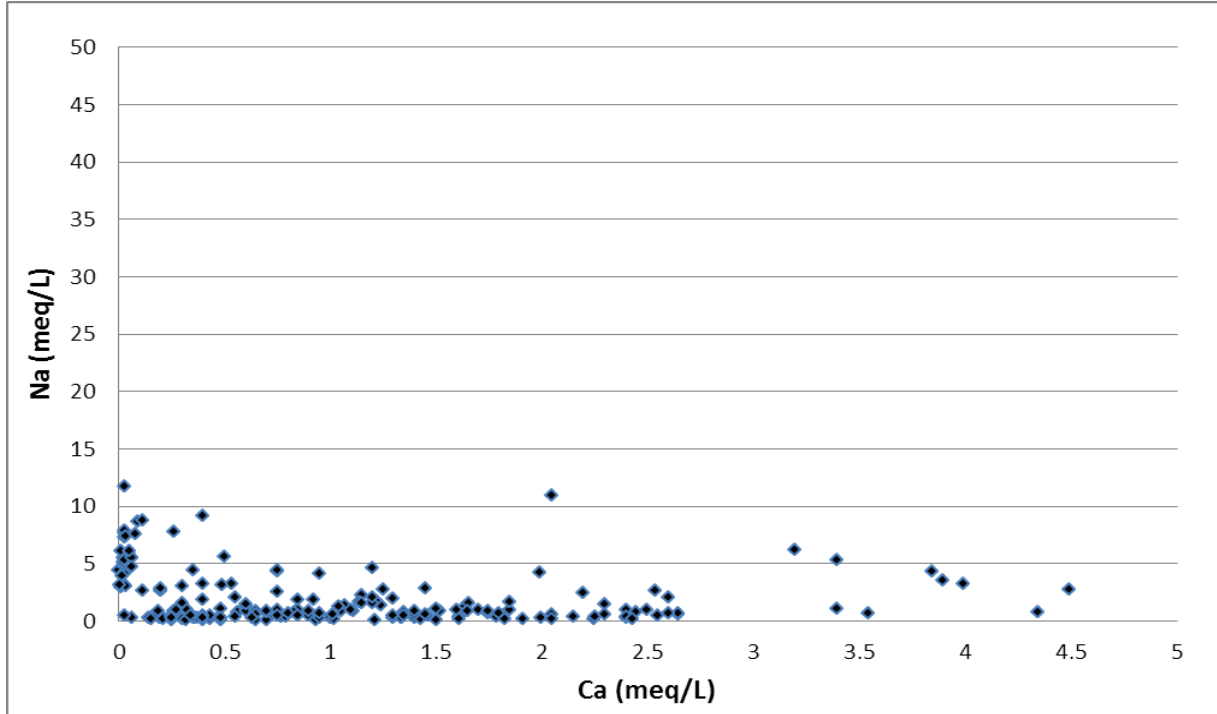


Figure 7-25. Sodium (Na) versus calcium (Ca) measured in milliequivalents per liter (meq/L), Queen City Aquifer, Northeast Transect, Groundwater Management Area 11.

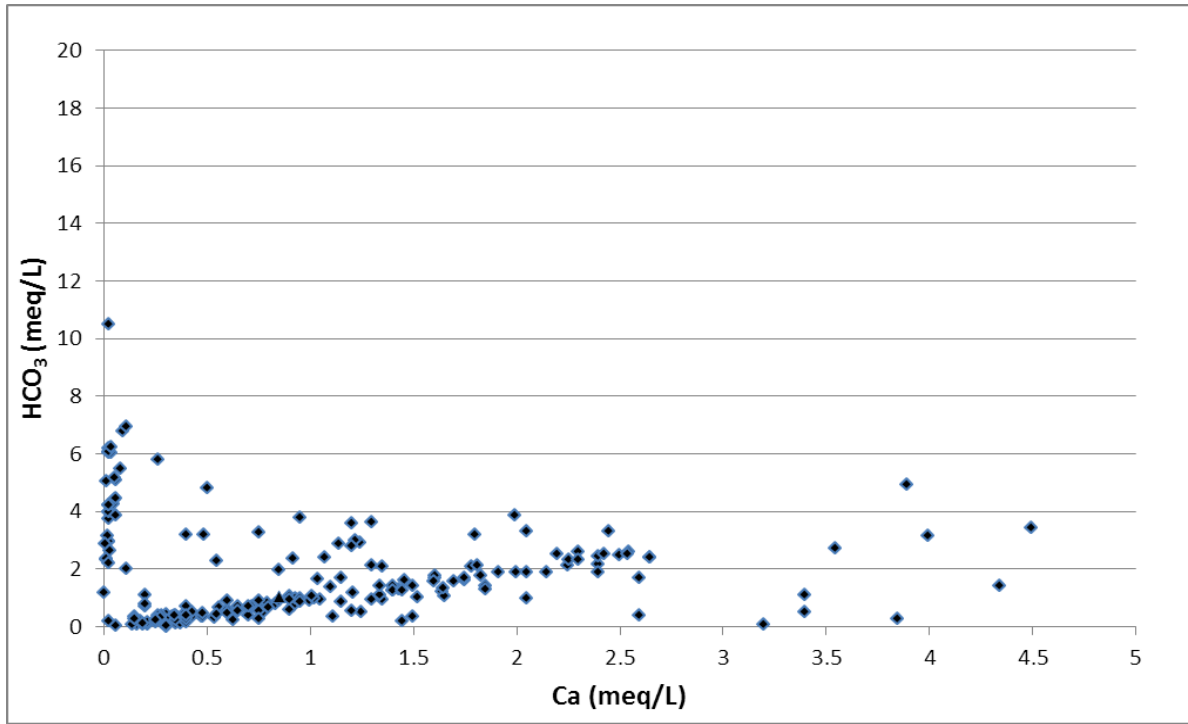


Figure 7-26. Bicarbonate (HCO<sub>3</sub><sup>-</sup>) versus calcium (Ca measured in milliequivalents per liter (meq/L)), Queen City Aquifer, Northeast Transect, Groundwater Management Area 11.

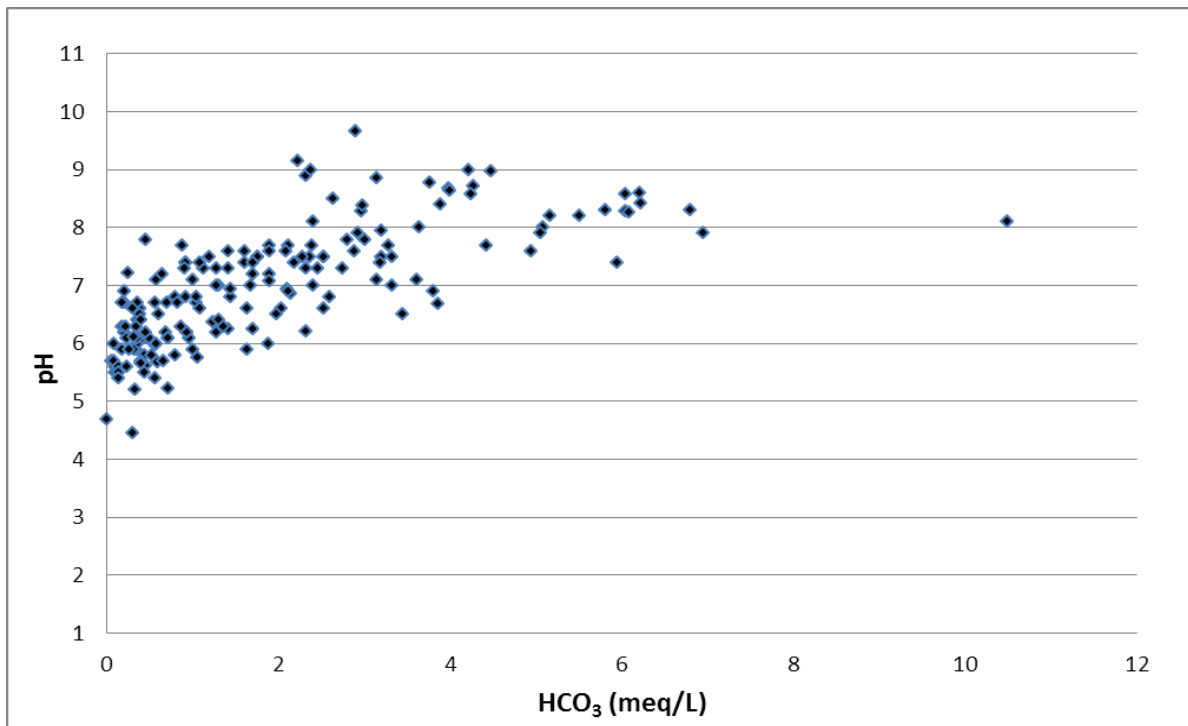


Figure 7-27. pH versus bicarbonate (HCO<sub>3</sub><sup>-</sup>) measured in milliequivalents per liter (meq/L), Queen City Aquifer, Northeast Transect, Groundwater Management Area 11.

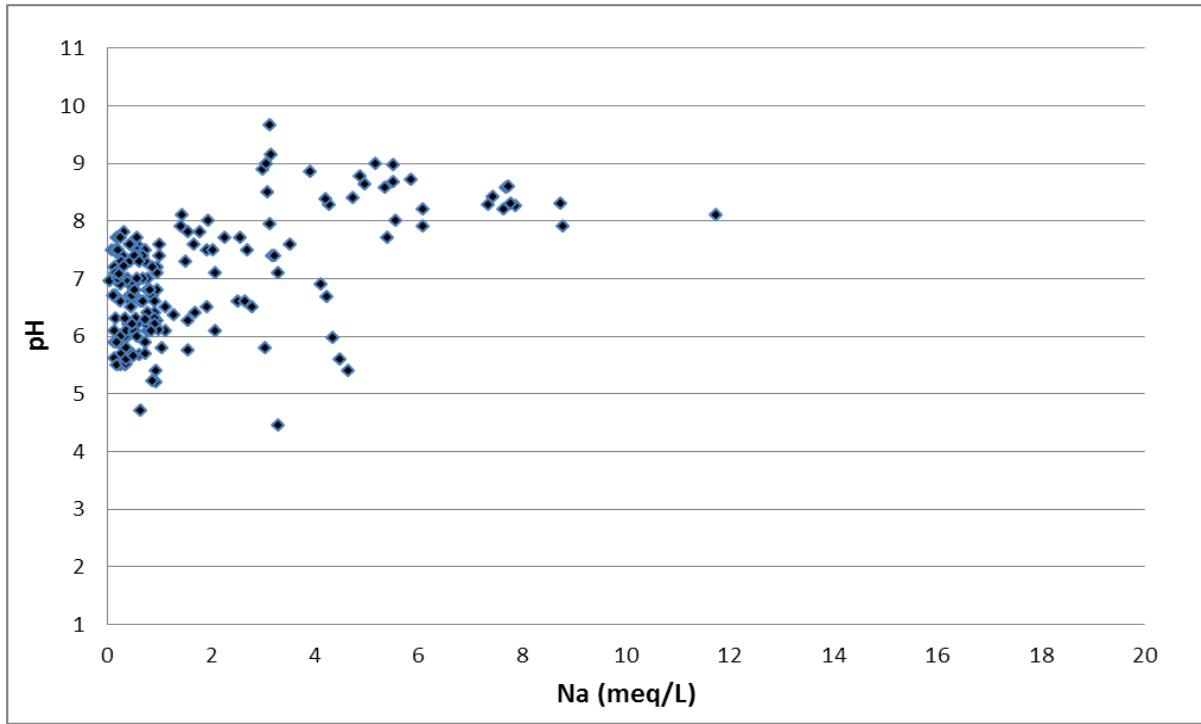


Figure 7-28. pH versus sodium (Na) measured in milliequivalents per liter (meq/L), Queen City Aquifer, Northeast Transect, Groundwater Management Area 11.

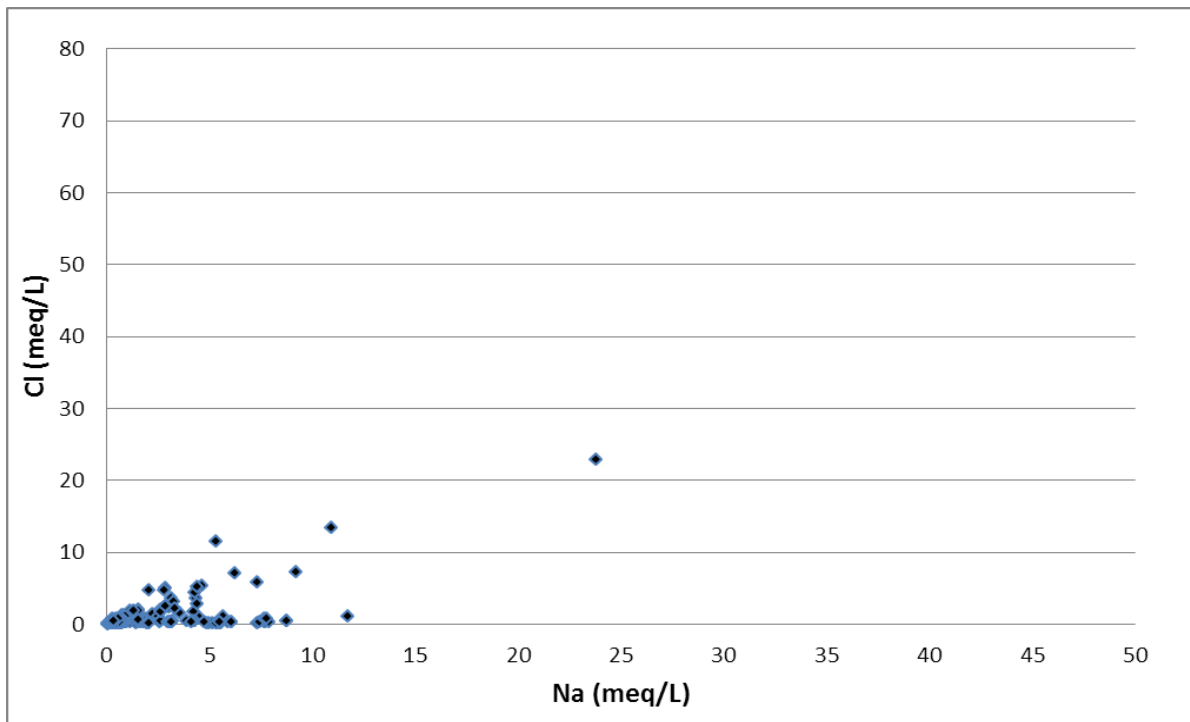


Figure 7-29. Chloride (Cl) versus sodium (Na) measured in milliequivalents per liter (meq/L), Queen City Aquifer, Northeast Transect, Groundwater Management Area 11.

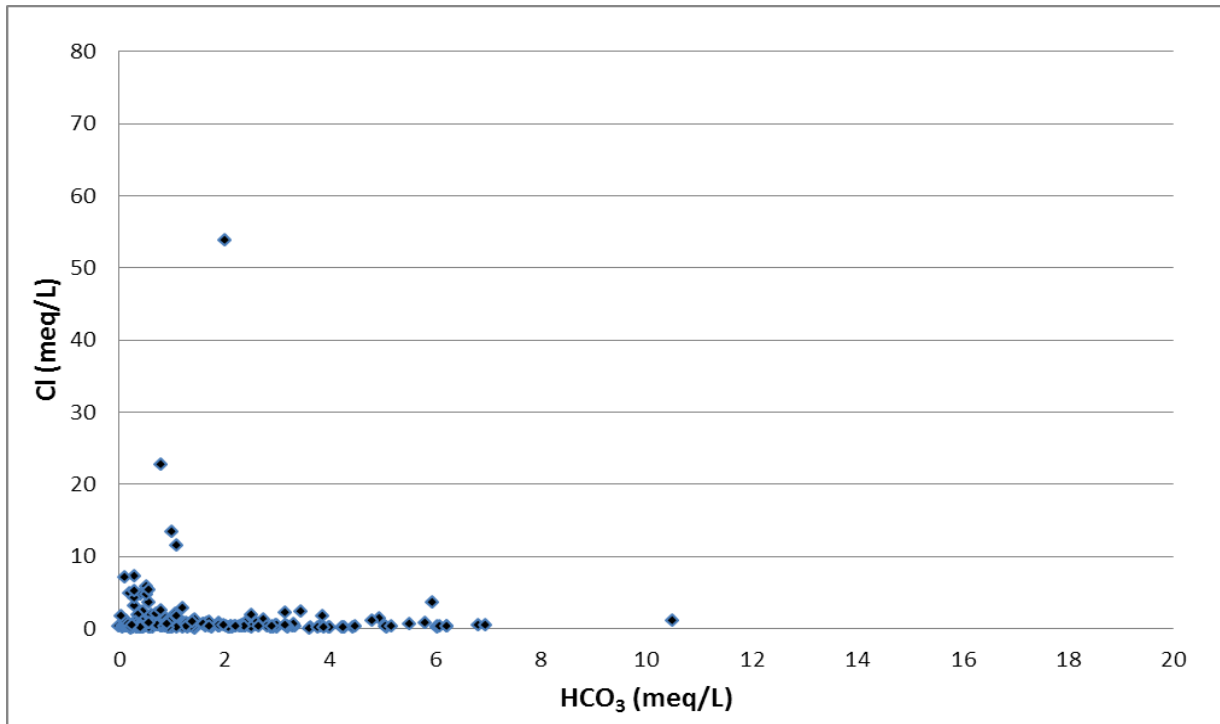


Figure 7-30. Chloride (Cl) versus bicarbonate (HCO<sub>3</sub>) measured in milliequivalents per liter (meq/L), Queen City Aquifer, Northeast Transect, Groundwater Management Area 11.

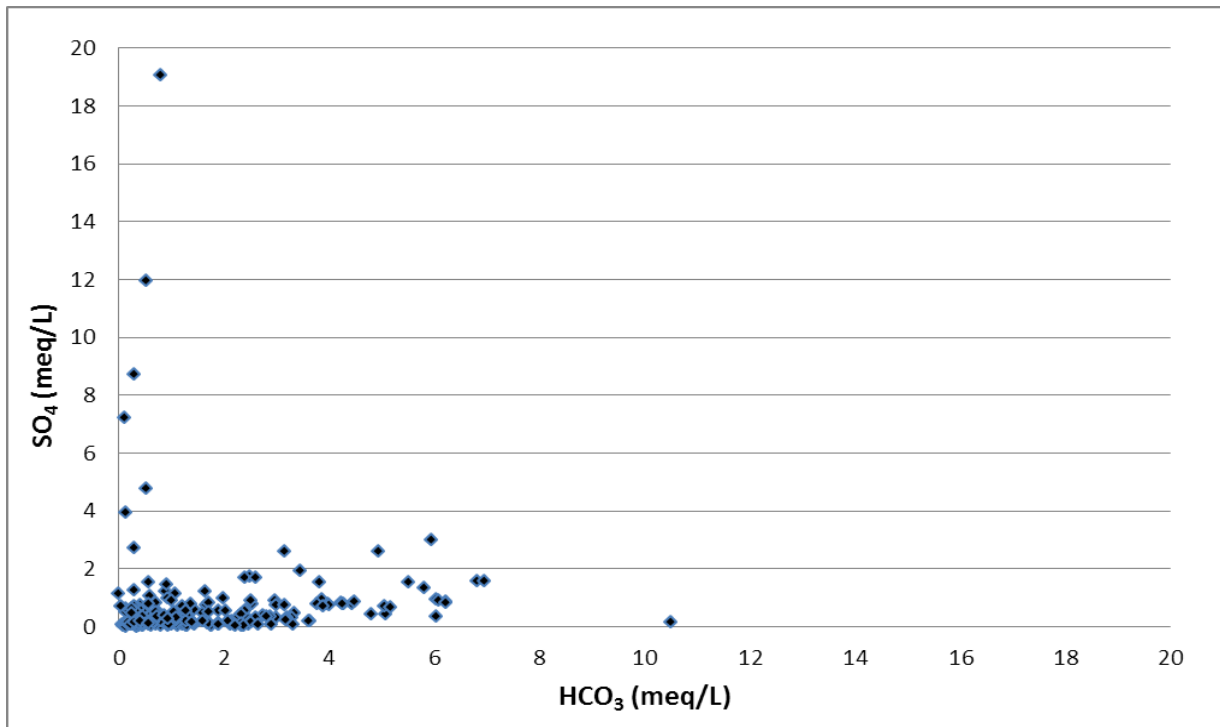


Figure 7-31. Sulfate (SO<sub>4</sub>) versus bicarbonate (HCO<sub>3</sub>) measured in milliequivalents per liter (meq/L), Queen City Aquifer, Northeast Transect, Groundwater Management Area 11.

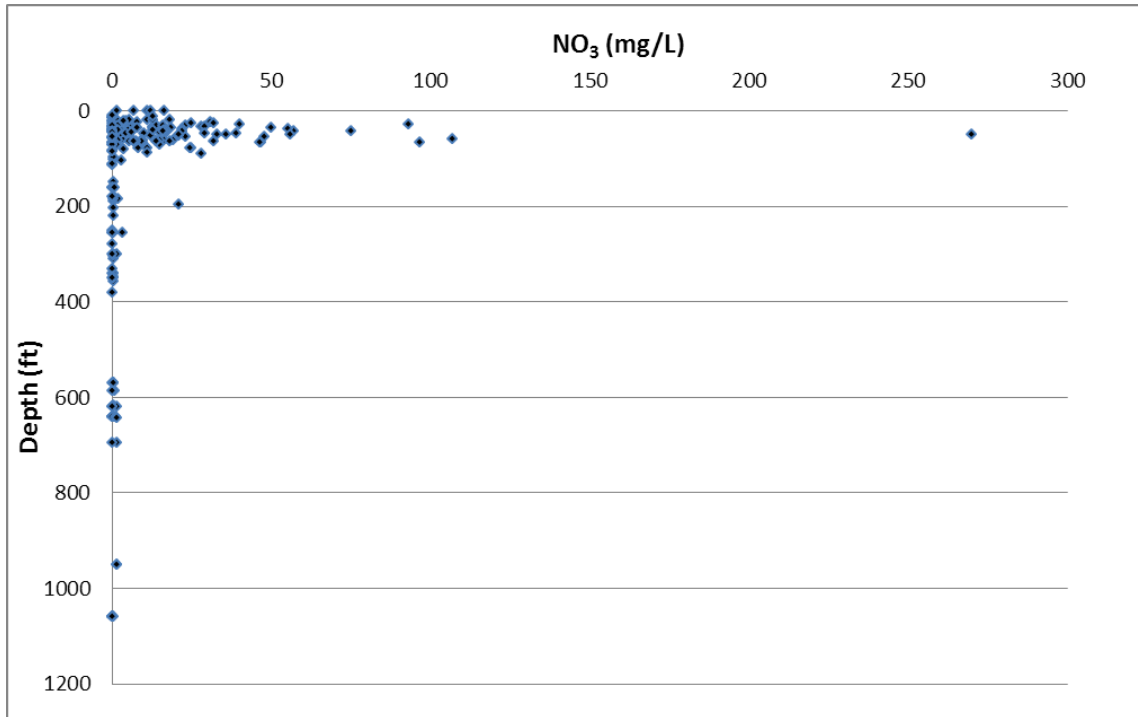


Figure 7-32. Depth measured from land surface in feet (ft) versus nitrate (NO<sub>3</sub>) measured in milligrams per liter (mg/L), Queen City Aquifer, Northeast Transect, Groundwater Management Area 11.

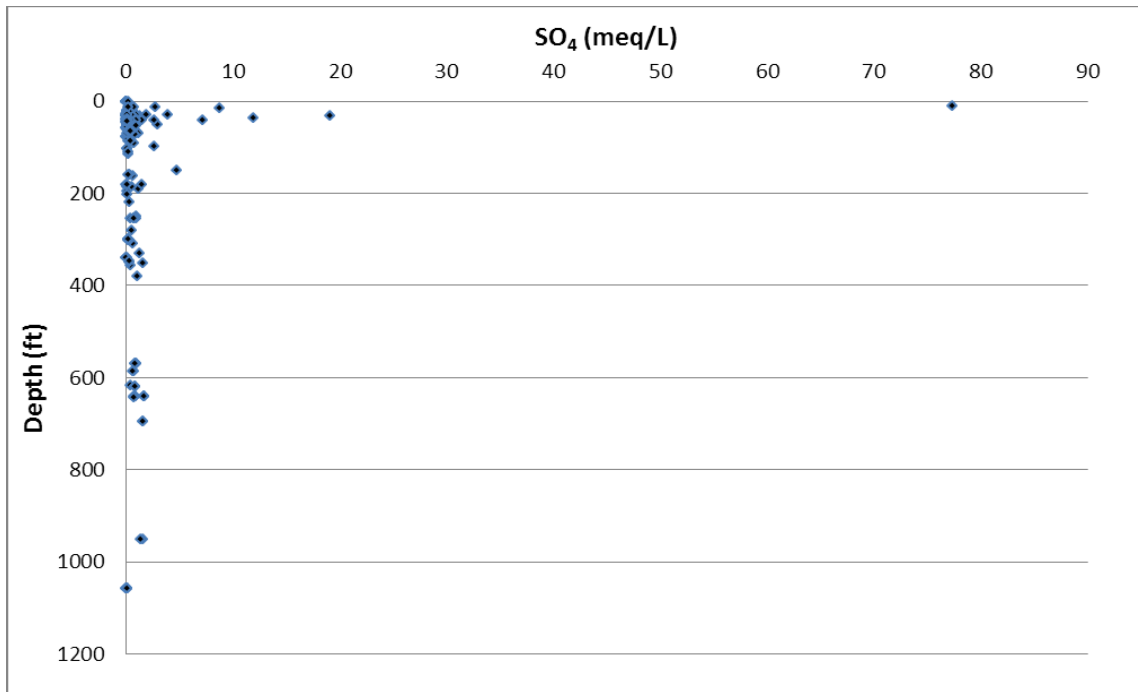
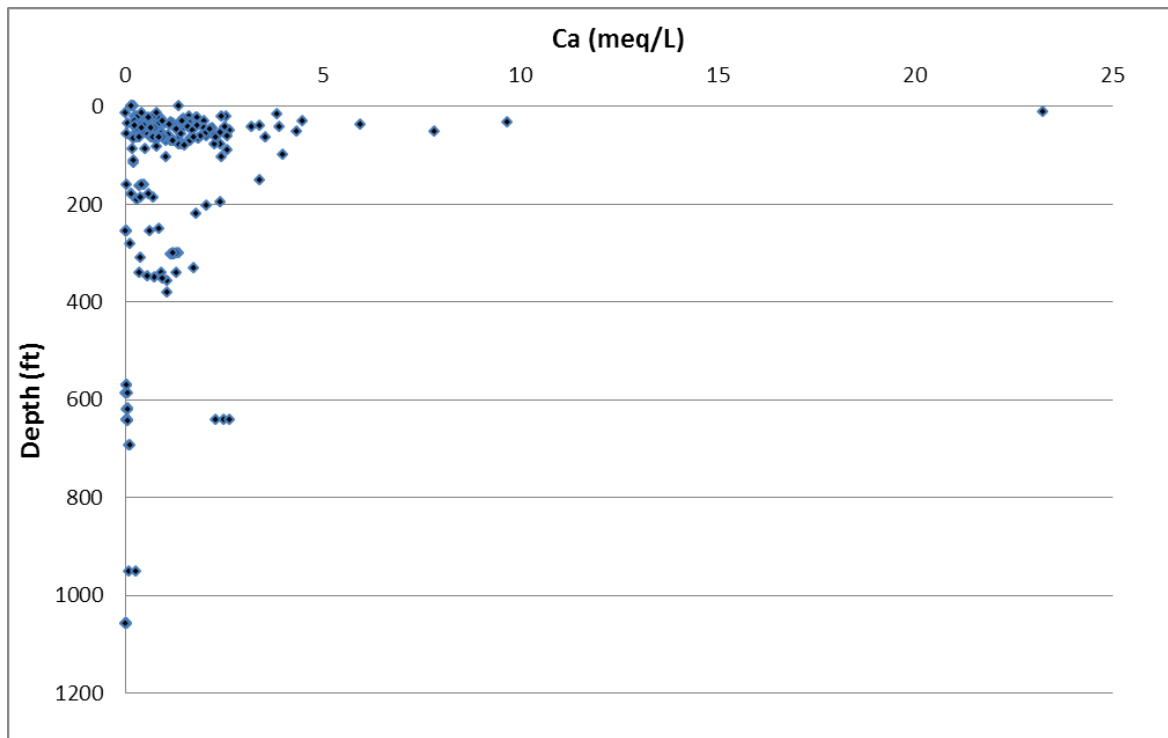


Figure 7-33. Depth measured from land surface in feet (ft) versus sulfate (SO<sub>4</sub>) measured in milliequivalents per liter (meq/L), Queen City Aquifer, Northeast Transect, Groundwater Management Area 11.



**Figure 7-34.** Depth measured from land surface in feet (ft) versus calcium (Ca) measured in milliequivalents per liter (meq/L), Queen City Aquifer, Northeast Transect, Groundwater Management Area 11.

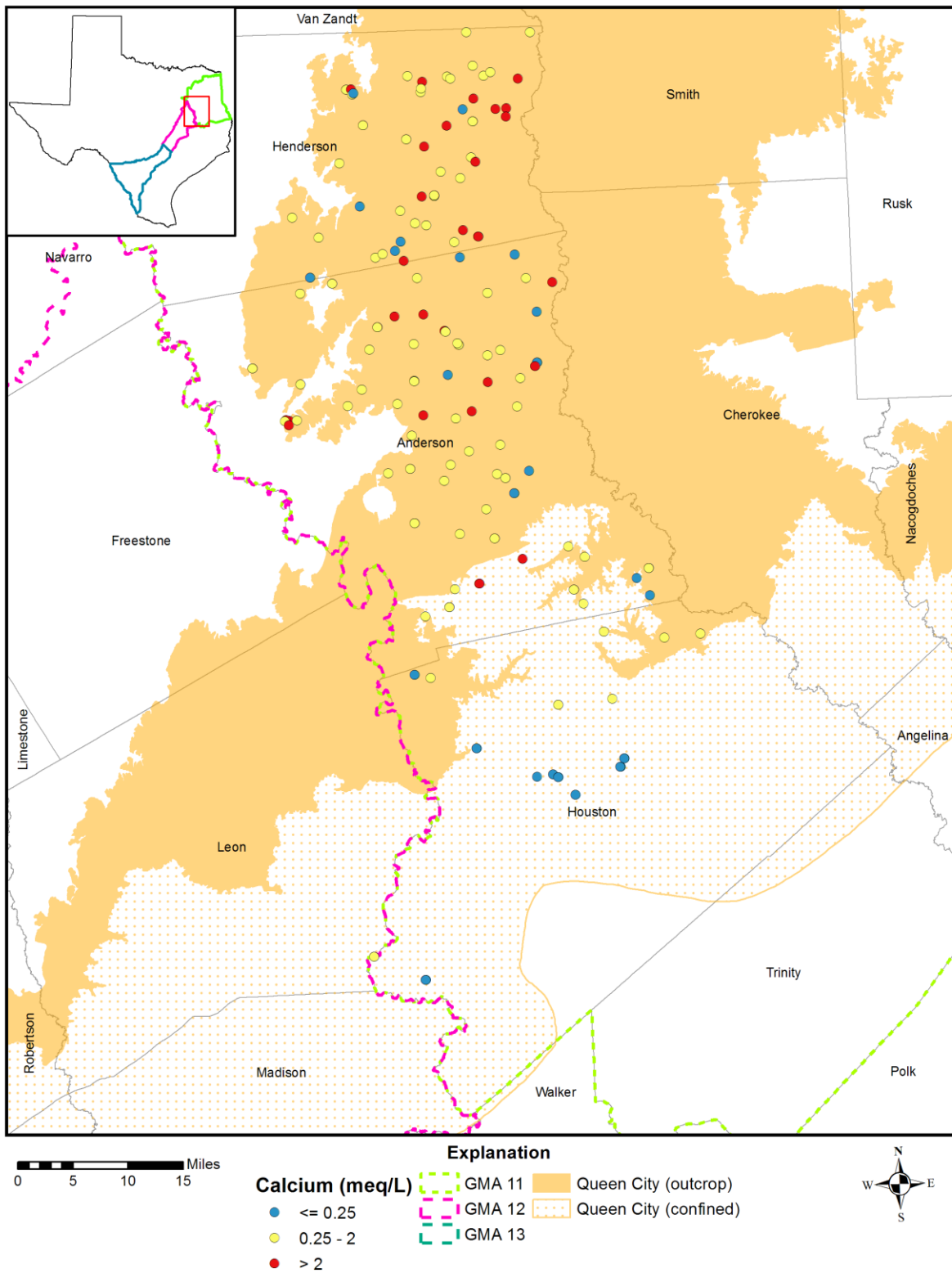


Figure 7-35. Calcium concentrations measured in milliequivalents per liter (meq/L) in the Queen City Aquifer, Northeast Transect, Groundwater Management Area (GMA) 11.

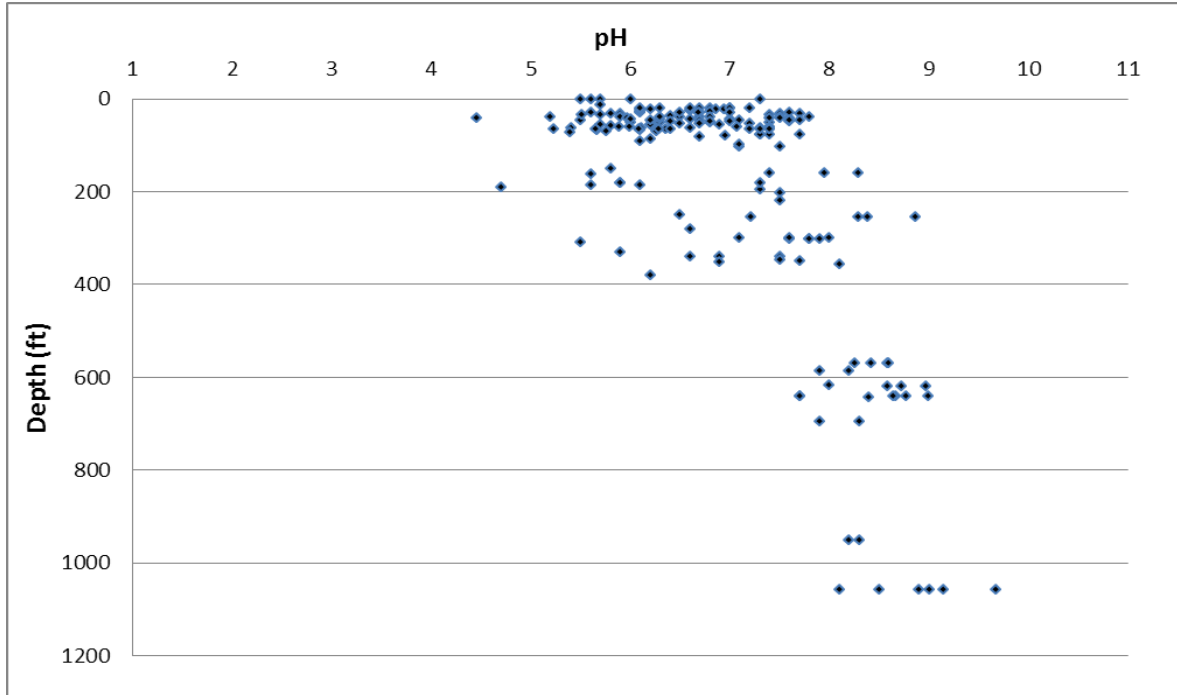


Figure 7-36. Depth measured from land surface in feet (ft) versus pH, Queen City Aquifer, Northeast Transect, Groundwater Management Area (GMA) 11.

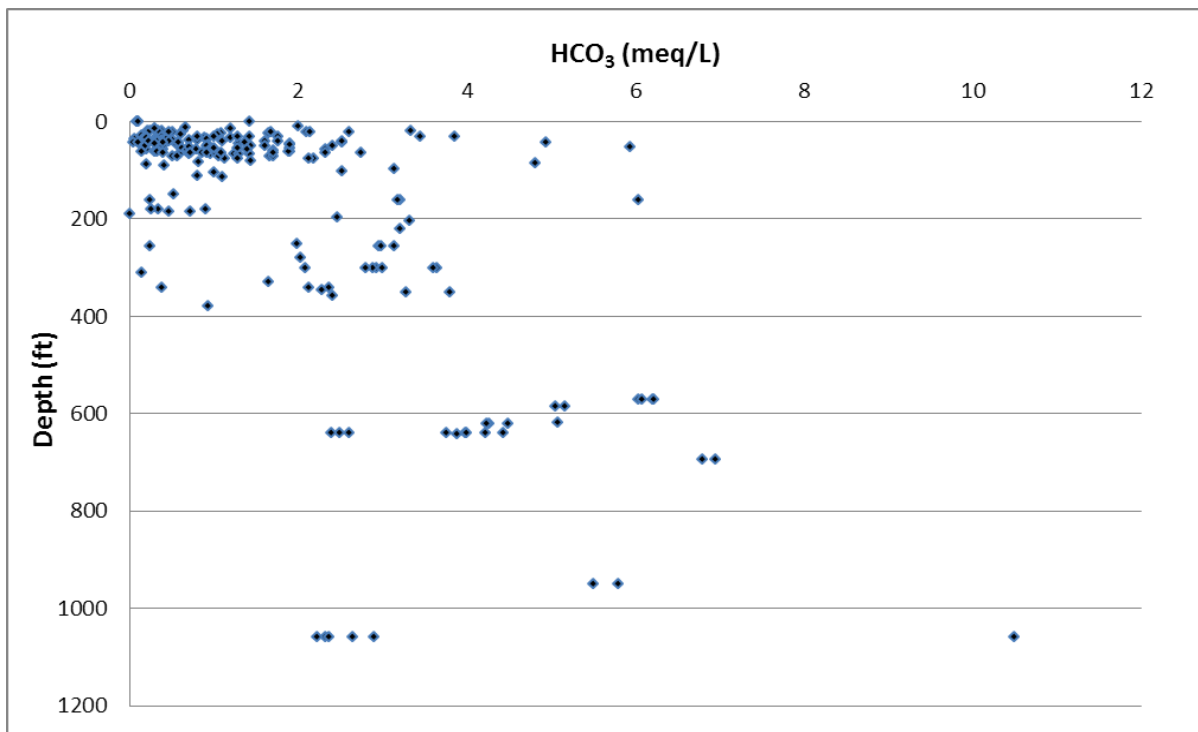


Figure 7-37. Depth measured from land surface in feet (ft) versus bicarbonate (HCO<sub>3</sub>) measured in milliequivalents per liter (meq/L), Queen City Aquifer, Northeast Transect, Groundwater Management Area 11.

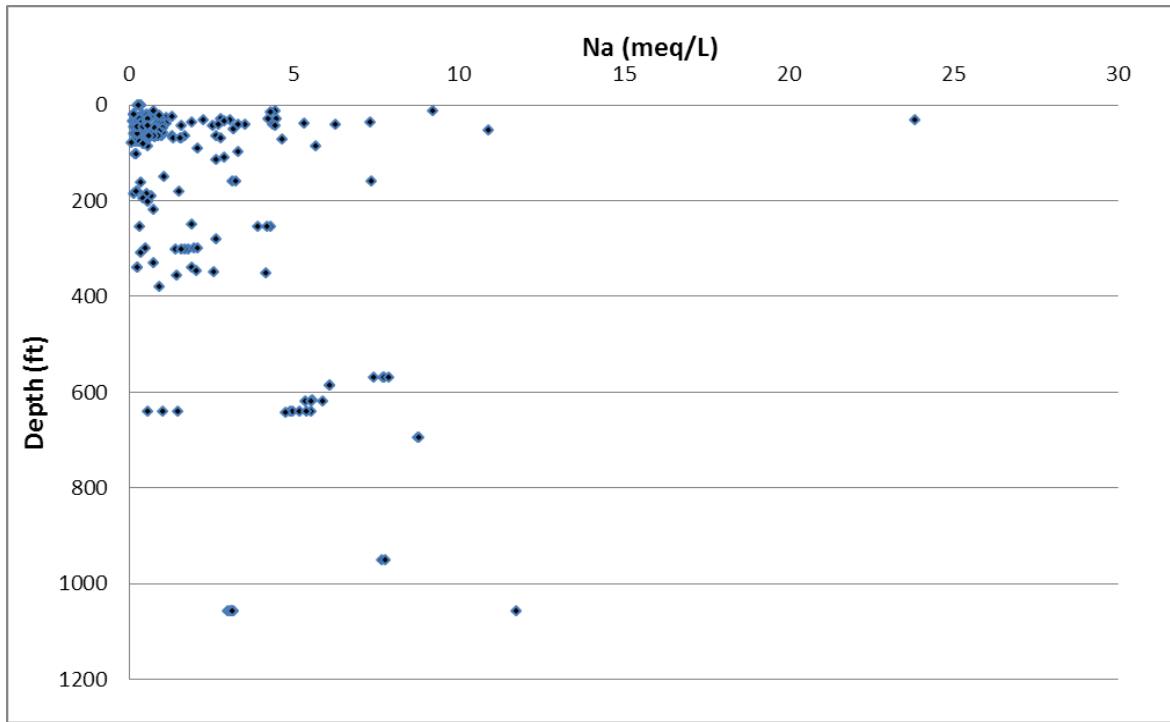


Figure 7-38. Depth measured from land surface in feet (ft) versus sodium (Na) measured in milliequivalents per liter (meq/L), Queen City Aquifer, Northeast Transect, Groundwater Management Area 11.

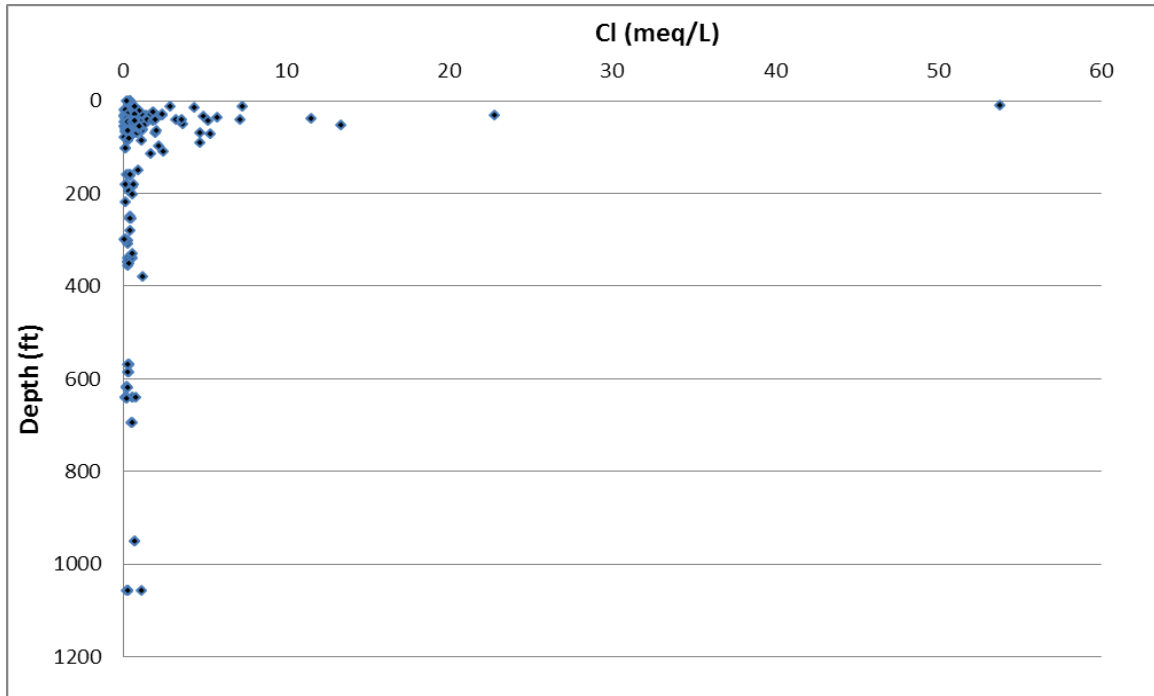
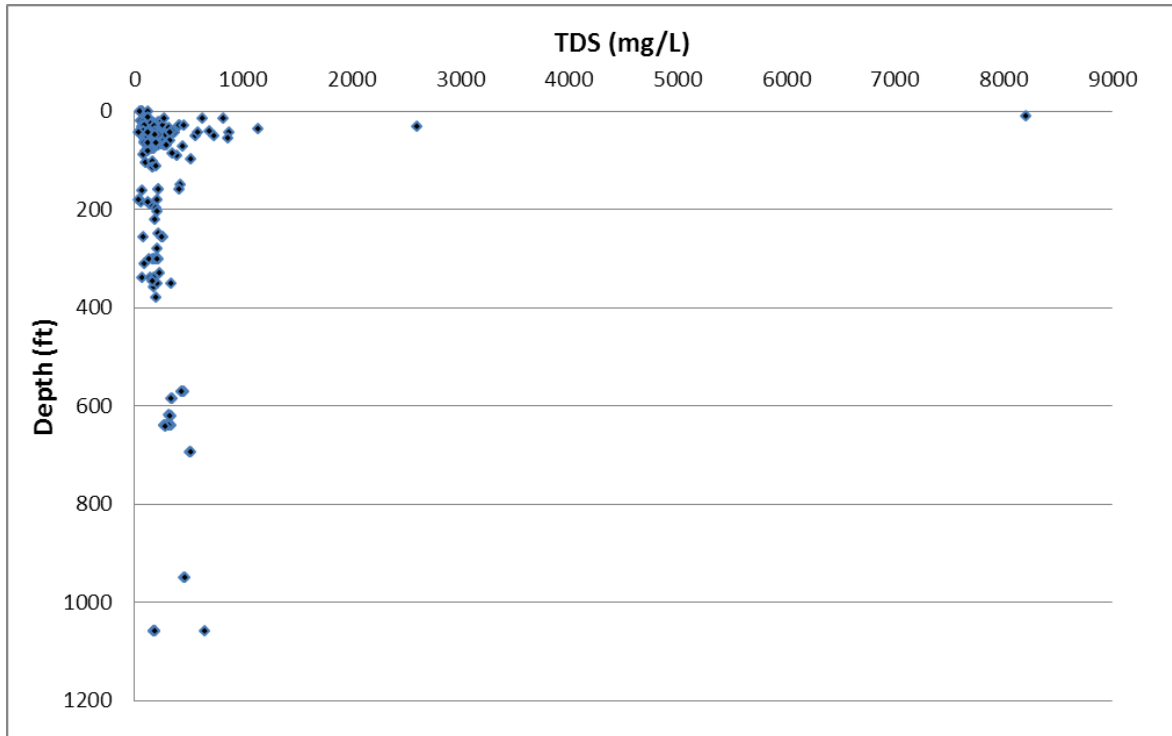


Figure 7-39. Depth measured from land surface in feet (ft) versus chloride (Cl) measured in milliequivalents per liter (meq/L), Queen City Aquifer, Northeast Transect, Groundwater Management Area 11.



**Figure 7-40.** Depth measured from land surface in feet (ft) versus total dissolved solids (TDS) measured in parts per million (ppm), Queen City Aquifer, Northeast Transect, Groundwater Management Area 11.

### Sparta Aquifer

The Sparta Aquifer overlies the Queen City Aquifer, the Carrizo-Wilcox Aquifer and the Weches Formation in Houston County Figure 5-2. A limited TWDB database contains a mix of the Sparta Aquifer well data from outcrop locations.

#### Well Depths

Based on Figure 7-41 the well depths are less than 400 feet in the outcrop and greater than 800 feet in the confined section in Houston County.

#### Water Level Data

Water level elevations (Figure 7-42) from 1960 to 2010 range from 300 to 500 feet in the outcrop and decrease to about 200 feet in the confined section.

#### Piper Diagram

The Piper diagram (Figure 7-43) for the Sparta Aquifer in the Northeast Transect shows a mixed cation (calcium-magnesium-sodium), mixed anion (chloride-sulfate-bicarbonate) type water for shallower depths (less than 400 feet) evolving to a sodium-bicarbonate water with depths greater than 800 feet. The mixed type water chemistry is in the outcrop. The sodium-bicarbonate type waters are in the confined section

#### Bicarbonate versus Sodium Plot

A plot of bicarbonate versus sodium (Figure 7-44) for the Sparta Aquifer data show one primary trend of sodium and bicarbonate increasing at a rate of 1:1.

#### Sodium versus Calcium Plot

A plot of sodium versus calcium (Figure 7-45) shows an inverse relationship between sodium and calcium. At low concentrations of sodium, calcium is independent of sodium. Conversely at low concentrations of calcium, sodium increases independent of calcium.

#### Bicarbonate versus Calcium Plot

A plot of bicarbonate versus calcium (Figure 7-46) shows a distribution of data similar to the sodium versus calcium plot (Figure 7-45), that is, an inverse relationship.

#### pH versus Bicarbonate Plot

The plot of pH versus bicarbonate (Figure 7-47) shows three limbs for the curve. Initially pH rises from about four to about six independent of bicarbonate. For the second limb, pH rises from about six to eight with increasing bicarbonate. The third limb shows increasing bicarbonate independent of pH.

#### pH versus Sodium Plot

The plot of pH versus sodium (Figure 7-48) shows a similar distribution of data to the bicarbonate versus sodium plot (Figure 7-44).

#### Chloride versus Sodium Plot

The plot of chloride versus sodium (Figure 7-49) shows sodium increasing independent to chloride for nearly all samples. There is a slight increase of chloride at the highest sodium.

#### Chloride versus Bicarbonate Plot

The plot of chloride versus bicarbonate (Figure 7-50) shows bicarbonate increasing independent to chloride until the highest bicarbonate concentrations, where there might be a slight increase in chloride.

#### Sulfate versus Bicarbonate Plot

A plot of sulfate versus bicarbonate (Figure 7-51) shows higher sulfate concentrations for bicarbonate concentrations lower than about eight milliequivalents per liter.

#### Depth versus Nitrate Plot

The plot of depth versus nitrate (Figure 7-52) shows several wells at depths less than 100 feet that have high nitrate values.

#### Depth versus Sulfate Plot

The plot of depth versus sulfate (Figure 7-53) shows no significant patterns.

#### Depth versus Calcium Plot

The plot of depth versus calcium (Figure 7-54) shows higher calcium values at depth less than about 800 feet. Calcium is negligible greater than 800 feet.

#### Depth versus Sodium Plot

The plot of depth versus sodium (Figure 7-55) shows increasing sodium with depth.

#### Depth versus pH Plot

The plot of depth versus pH (Figure 7-56) shows a general increase of pH with greater depth.

#### Depth versus Chloride Plot

The plot of depth versus chloride (Figure 7-57) does not show an increase in chloride with depth.

#### Depth versus Total Dissolved Solids Plot

Total dissolved solids for the Sparta Aquifer (Figure 7-58) may show a general increase in total dissolved solids, but it is generally less than 1,000 parts per million. Since chloride is not increasing with depth, the increases are caused by increasing sodium and bicarbonate.

#### Discussion

Groundwater from the Sparta Aquifer, Anderson and Houston counties is from the outcrop and the confined section. In the outcrop, the water chemistry is a mixed cation-anion water. In the confined section of the Sparta Aquifer the water chemistry indicates sodium-bicarbonate type water. The evolution of sodium-bicarbonate water follows a similar path as seen in the underlying Carrizo-Wilcox Aquifer. In both aquifers, chemistry data are available from outcrop and the confined section.

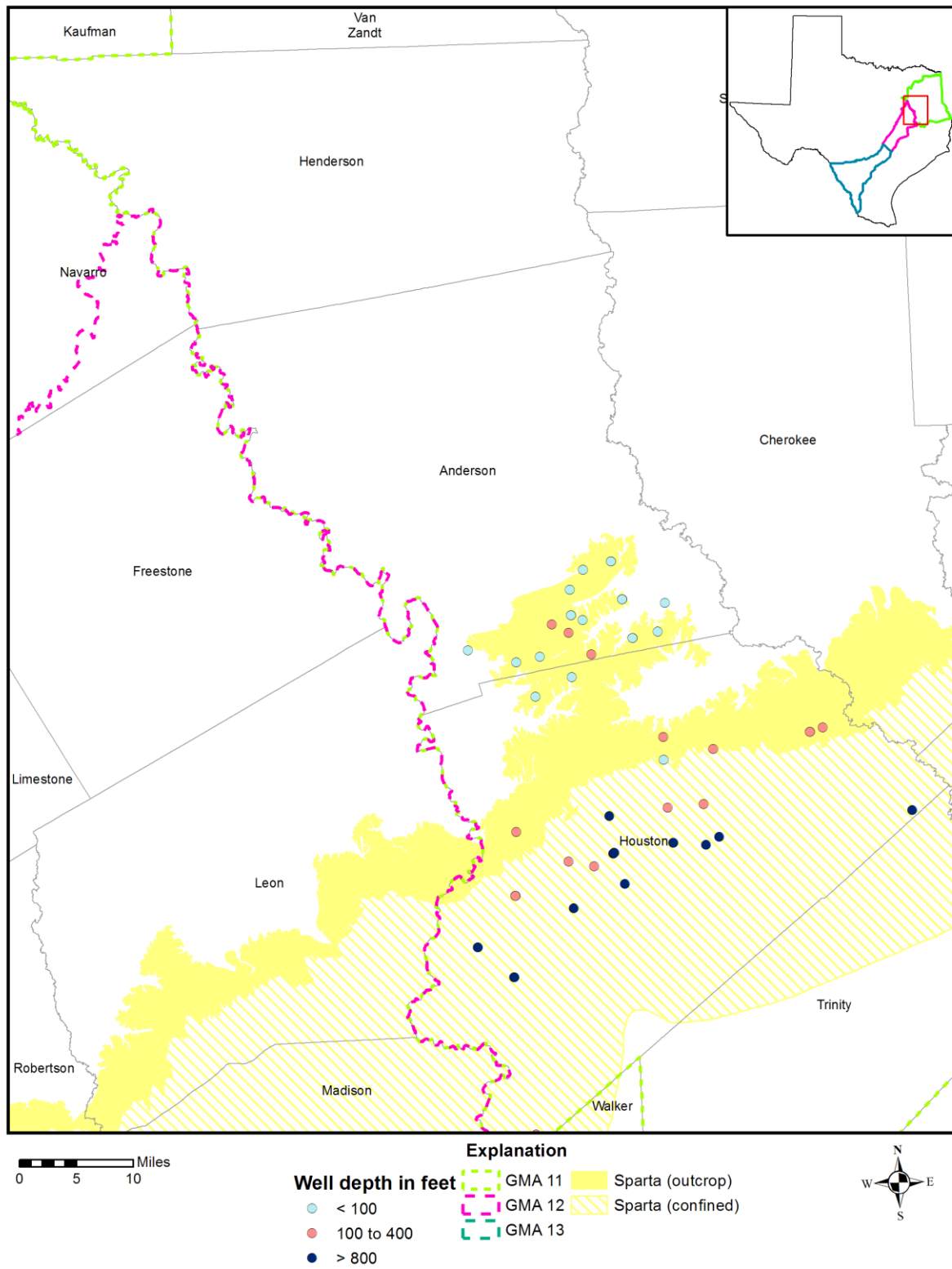


Figure 7-41. Well depths measured from land surface in feet in the Sparta Aquifer, Northeast Transect, Groundwater Management Area (GMA) 11.

Evaluation of Hydrochemical and Isotopic Data in Groundwater Management Areas 11, 12 and 13

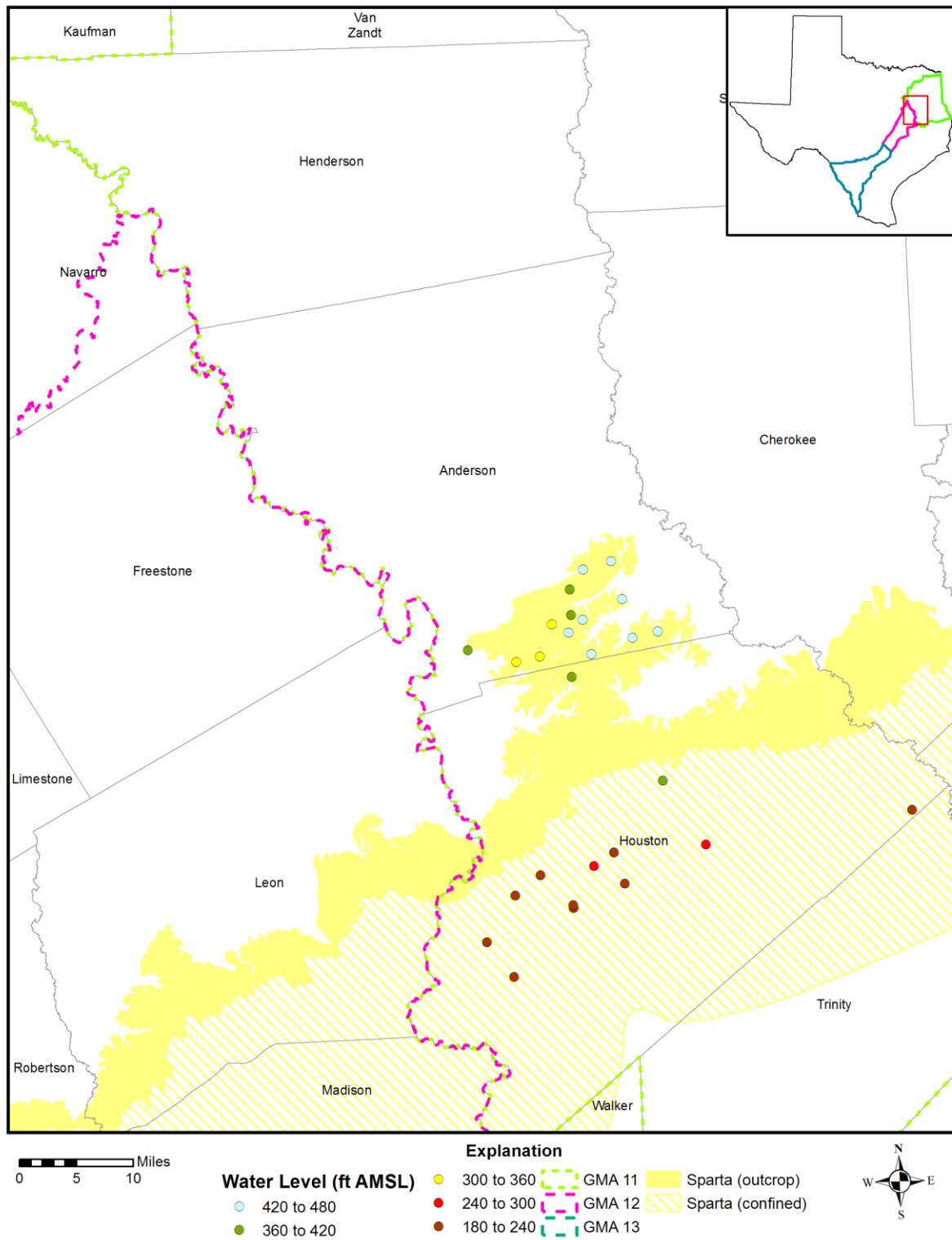


Figure 7-42. Water level elevations from 1960 to 2010 measured in feet above mean sea level (ft AMSL) in the Sparta Aquifer, Northeast Transect, Groundwater Management Area (GMA) 11.

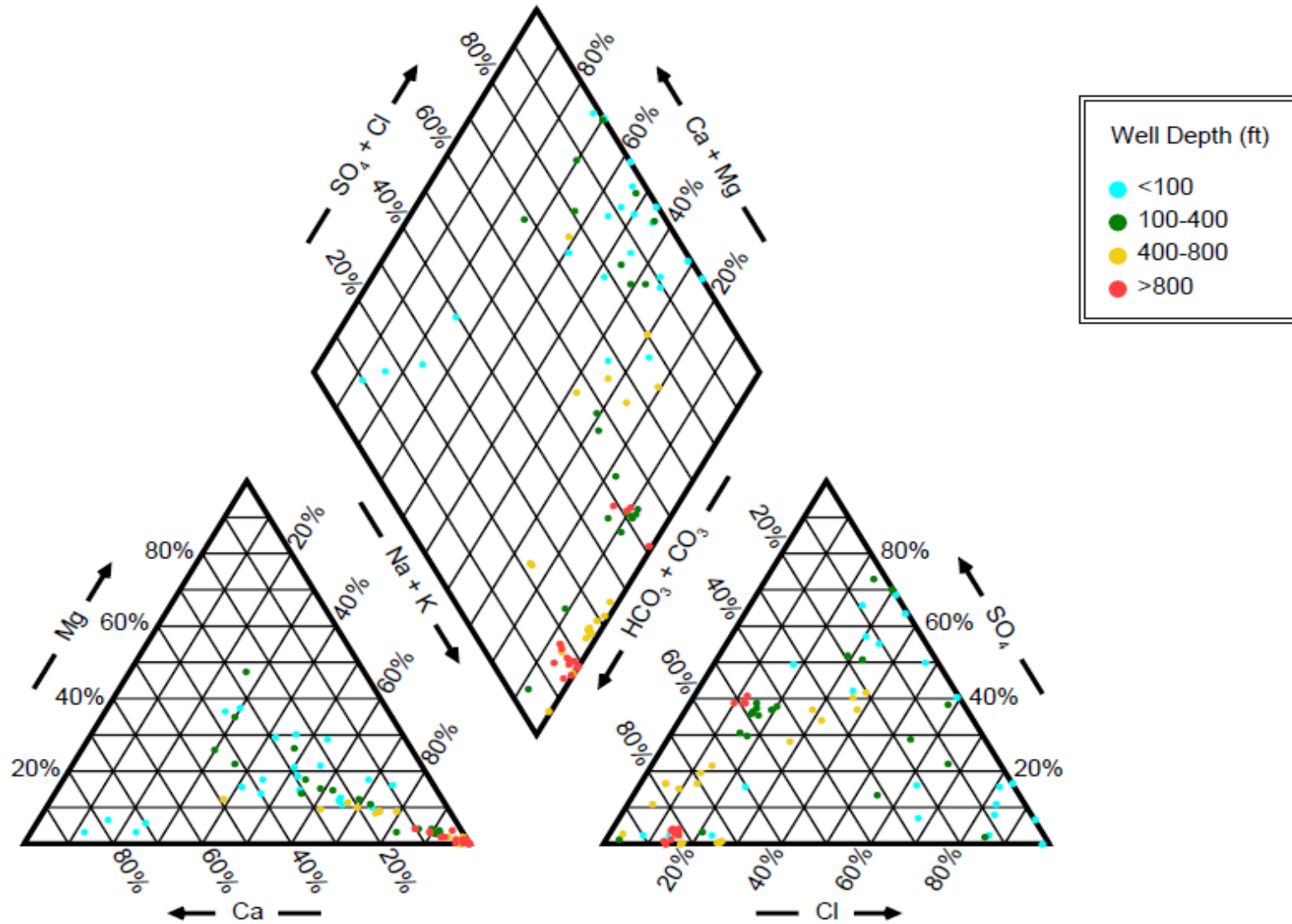


Figure 7-43. Piper diagram showing chemistry of the Sparta Aquifer wells in the Northeast Transect by well depth measured from land surface in feet (ft).

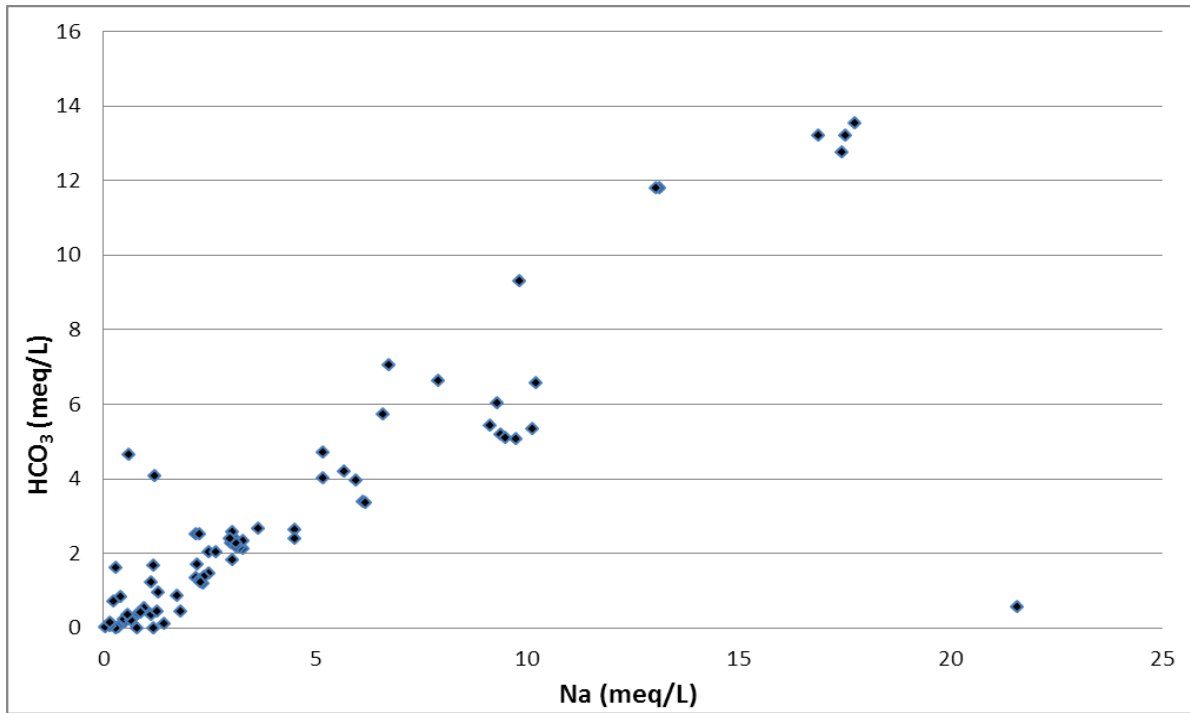


Figure 7-44. Bicarbonate (HCO<sub>3</sub>) versus sodium (Na) measured in milliequivalents per liter (meq/L), Sparta Aquifer, Northeast Transect, Groundwater Management Area 11.

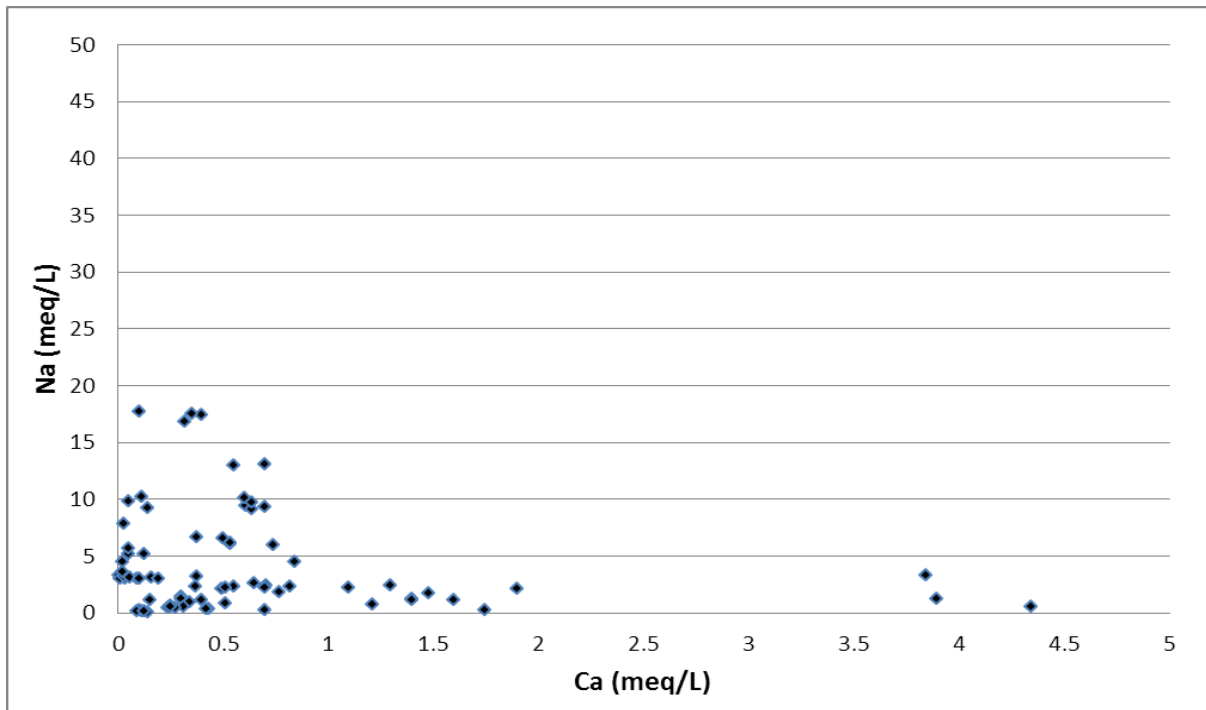


Figure 7-45. Sodium (Na) versus calcium (Ca) measured in milliequivalents per liter (meq/L), Sparta Aquifer, Northeast Transect, Groundwater Management Area 11.

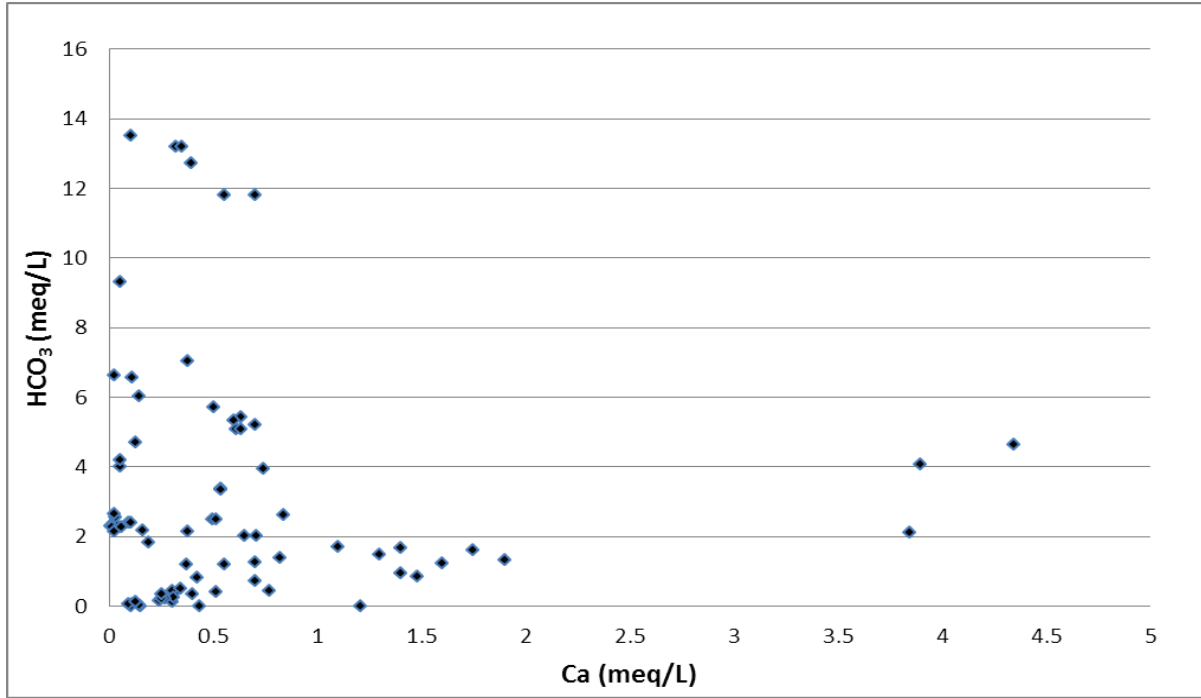


Figure 7-46. Bicarbonate (HCO<sub>3</sub>) versus calcium (Ca) measured in milliequivalents per liter (meq/L), Sparta Aquifer, Northeast Transect, Groundwater Management Area 11.

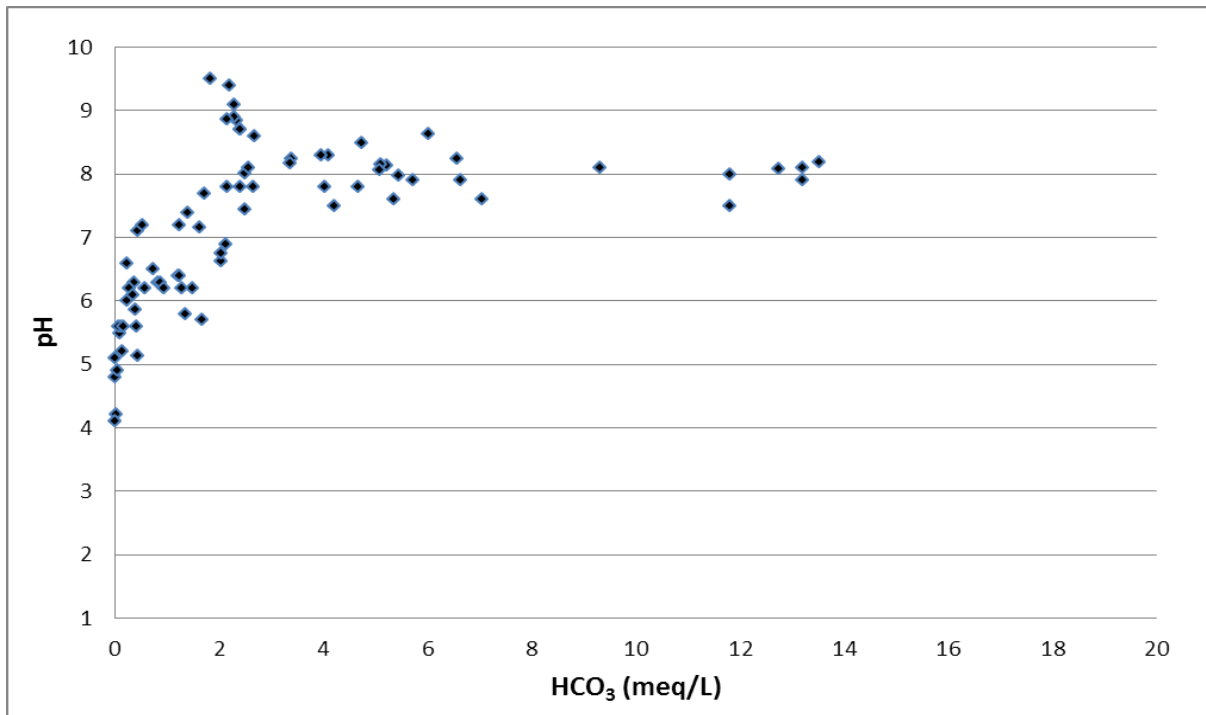


Figure 7-47. pH versus bicarbonate (HCO<sub>3</sub>) measured in milliequivalents per liter (meq/L), Sparta Aquifer, Northeast Transect, Groundwater Management Area 11.

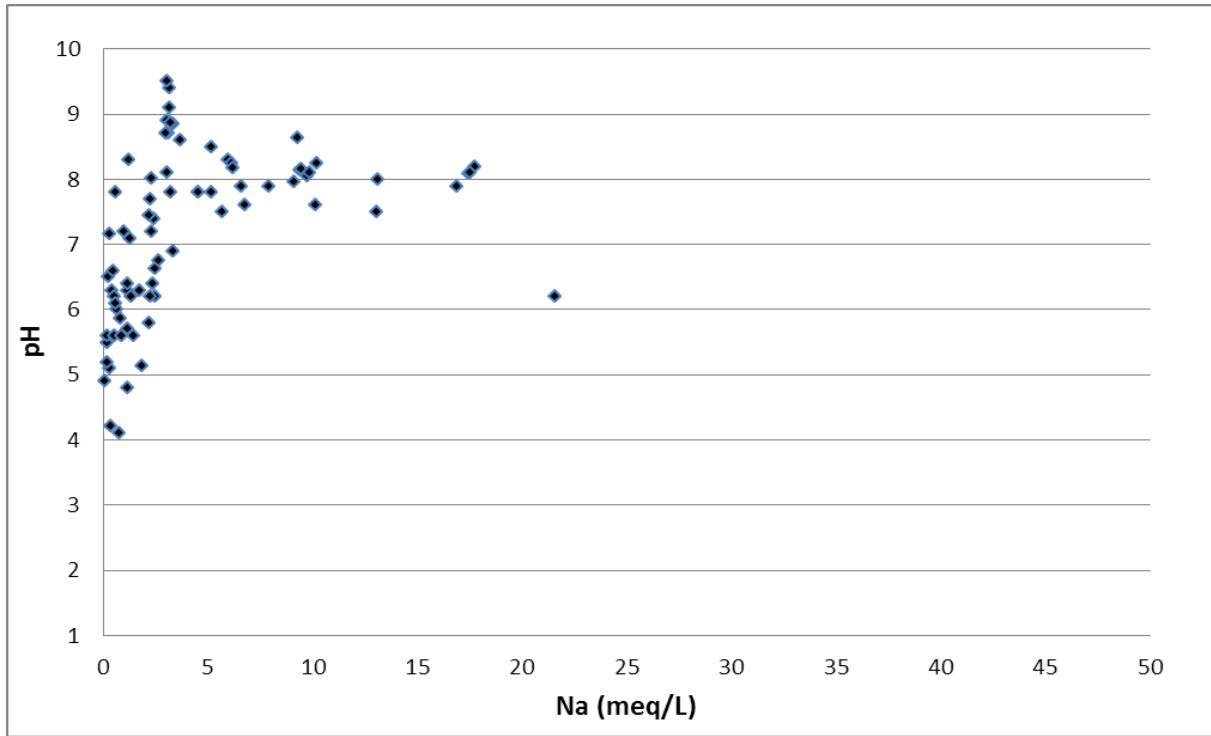


Figure 7-48. pH versus sodium (Na) measured in milliequivalents per liter (meq/L), Sparta Aquifer, Northeast Transect, Groundwater Management Area 11.

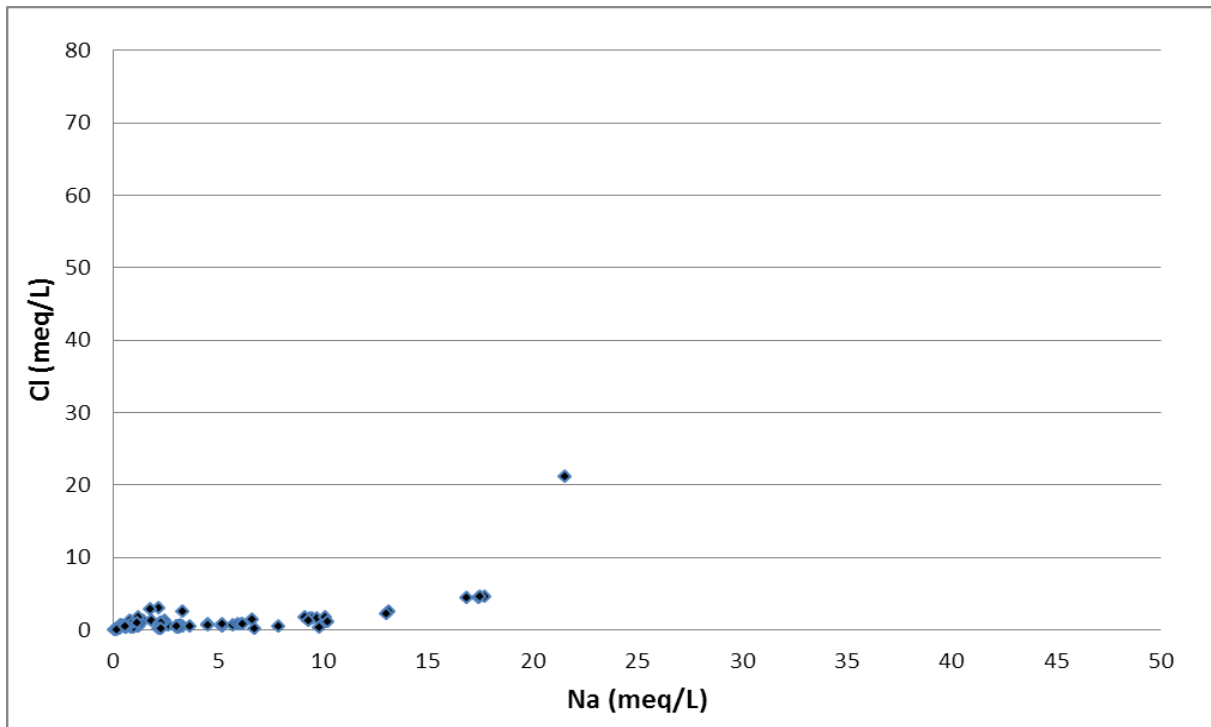


Figure 7-49. Chloride (Cl) versus sodium (Na) measured in milliequivalents per liter (meq/L), Sparta Aquifer, Northeast Transect, Groundwater Management Area 11.

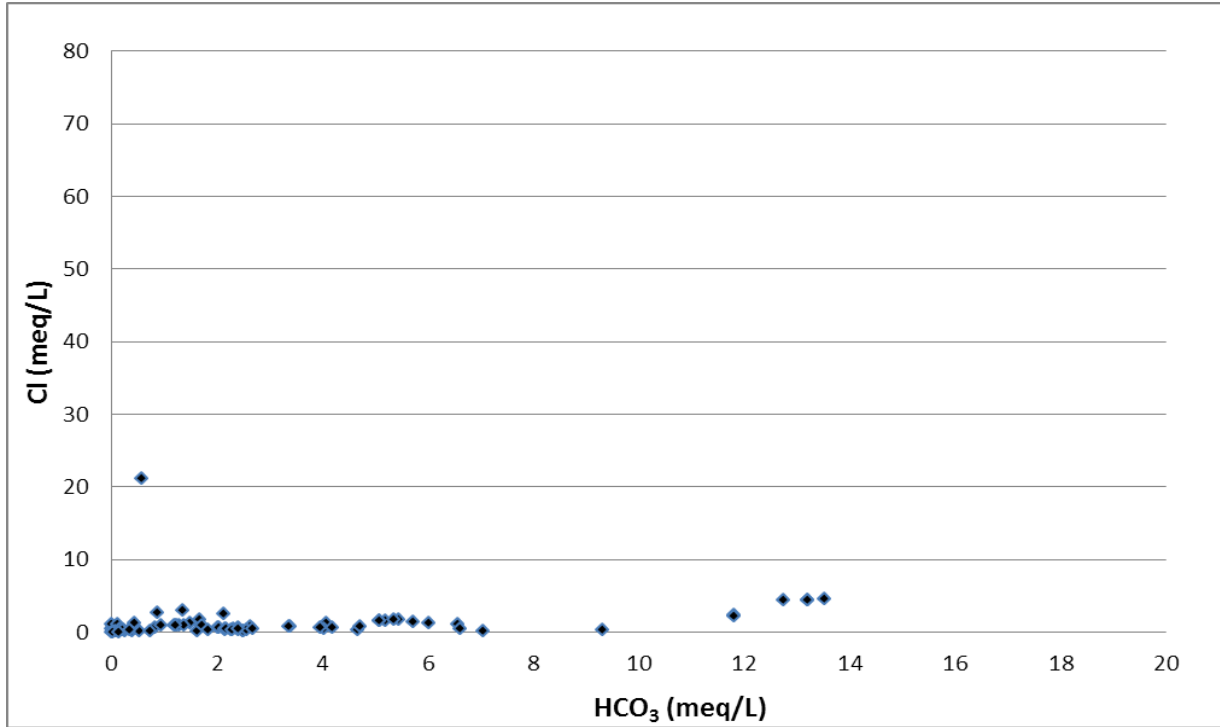


Figure 7-50. Chloride (Cl) versus bicarbonate (HCO<sub>3</sub>) measured in milliequivalents per liter (meq/L), Sparta Aquifer, Northeast Transect, Groundwater Management Area 11.

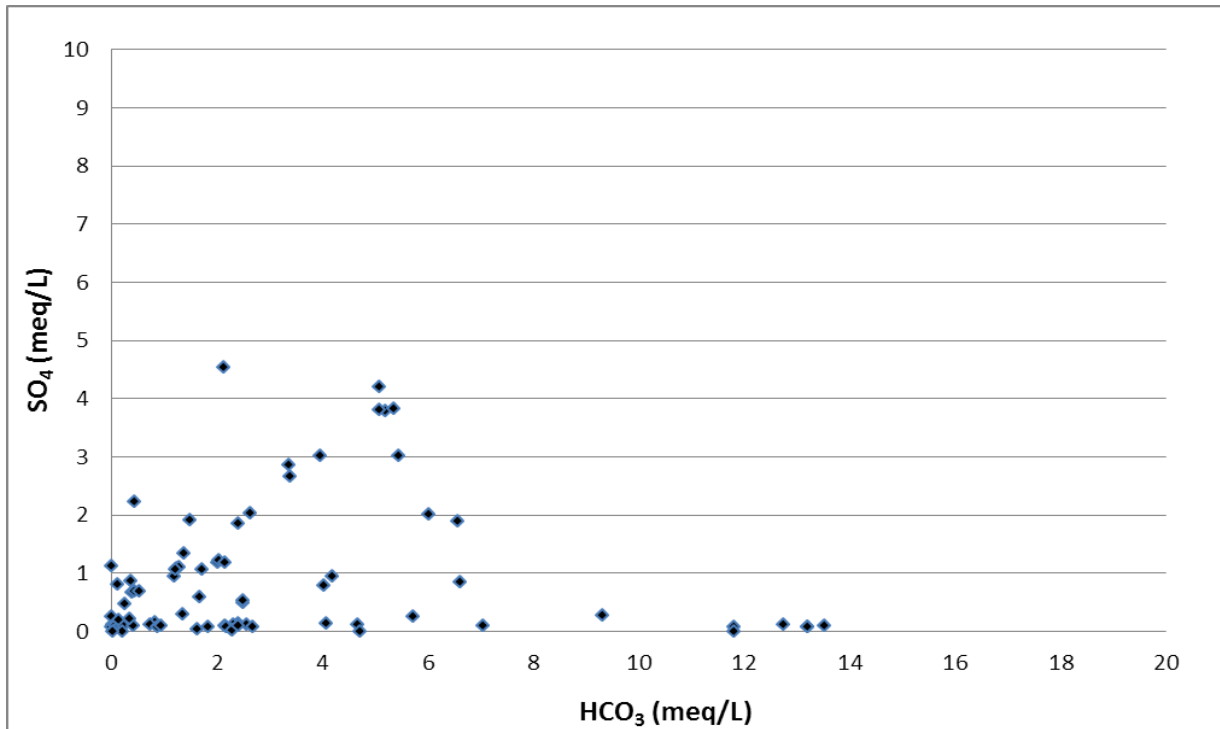


Figure 7-51. Sulfate (SO<sub>4</sub>) versus bicarbonate (HCO<sub>3</sub>) measured in milliequivalents per liter (meq/L), Sparta Aquifer, Northeast Transect, Groundwater Management Area 11.

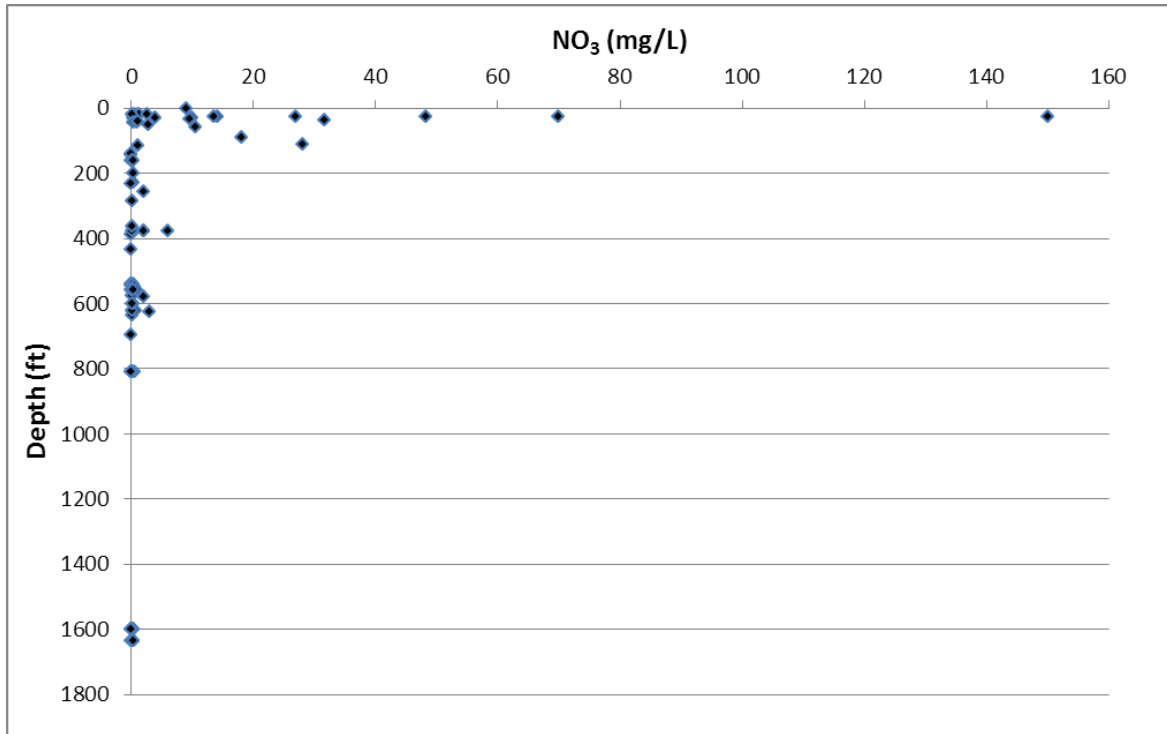


Figure 7-52. Depth measured from land surface in feet (ft) versus nitrate (NO<sub>3</sub>) measured in milligrams per liter (mg/L), Sparta Aquifer, Northeast Transect, Groundwater Management Area 11.

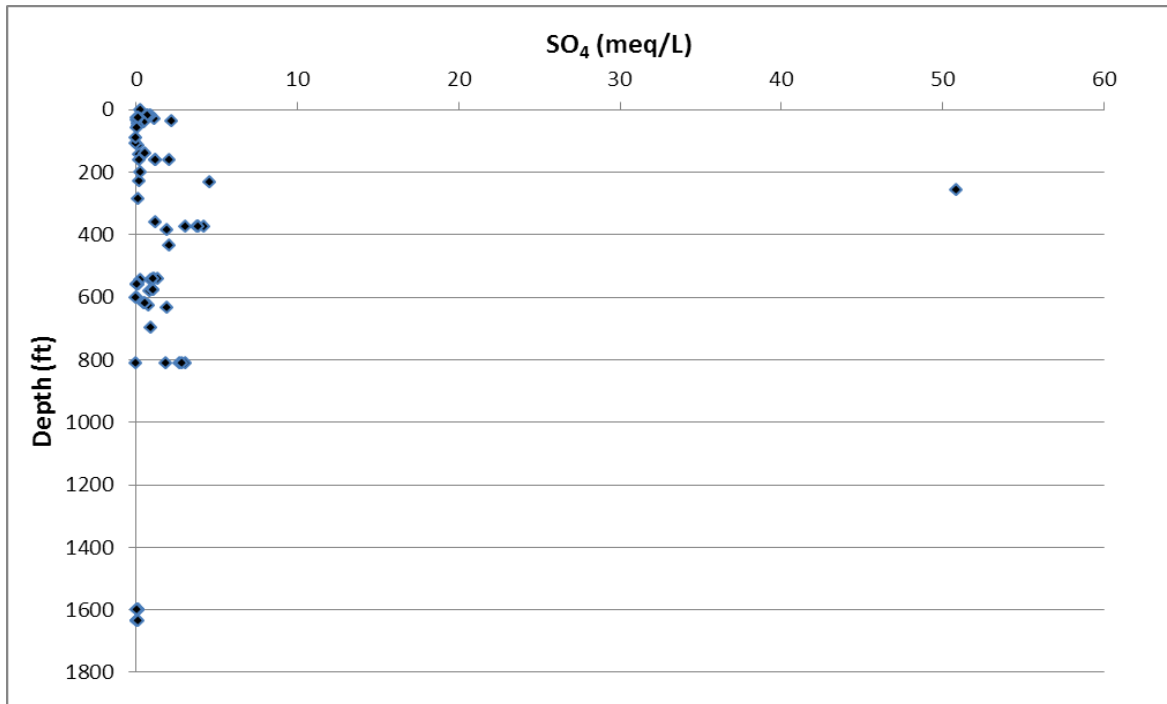


Figure 7-53. Depth measured from land surface in feet (ft) versus sulfate (SO<sub>4</sub>) measured in milliequivalents per liter (meq/L), Sparta Aquifer, Northeast Transect, Groundwater Management Area 11.

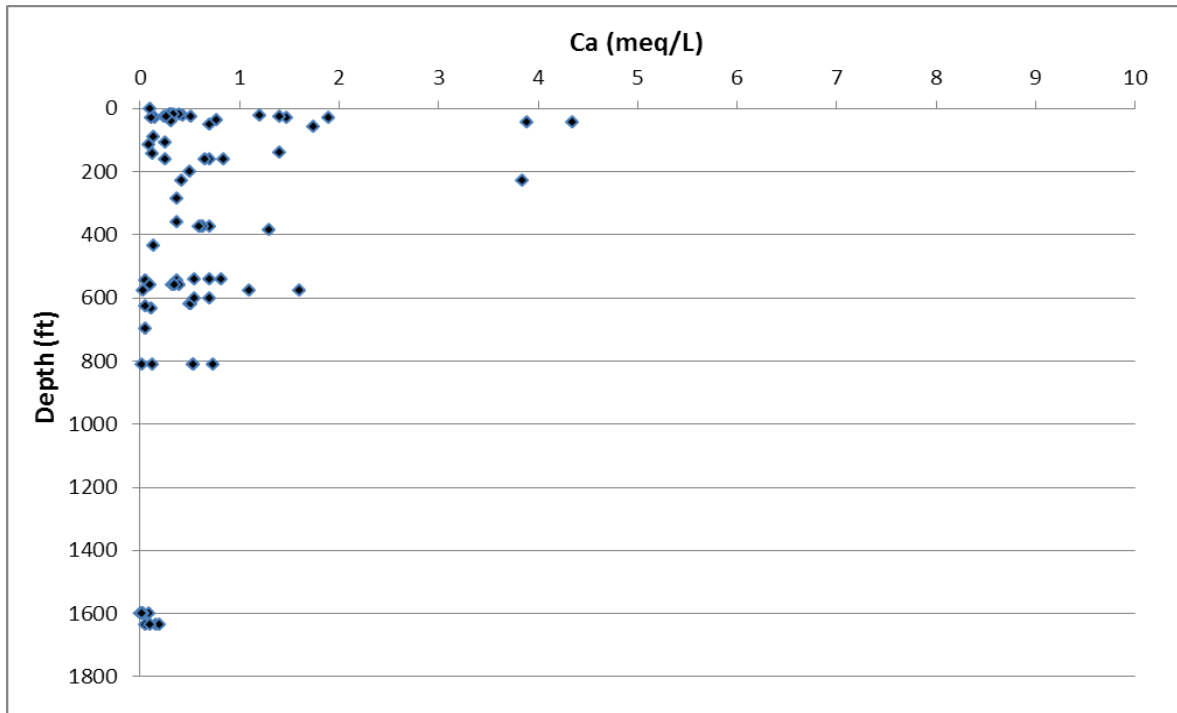


Figure 7-54. Depth measured from land surface in feet (ft) versus calcium (Ca) measured in milliequivalents per liter (meq/L), Sparta Aquifer, Northeast Transect, Groundwater Management Area 11.

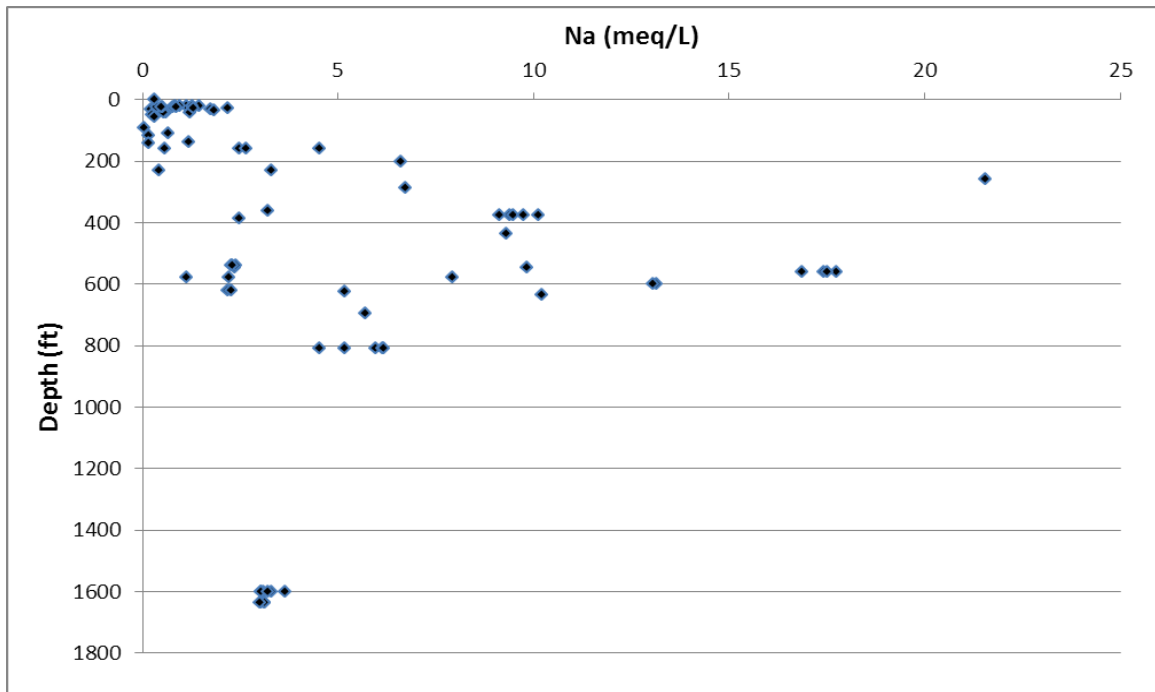


Figure 7-55. Depth measured from land surface in feet (ft) versus sodium (Na) measured in milliequivalents per liter (meq/L), Sparta Aquifer, Northeast Transect, Groundwater Management Area 11.

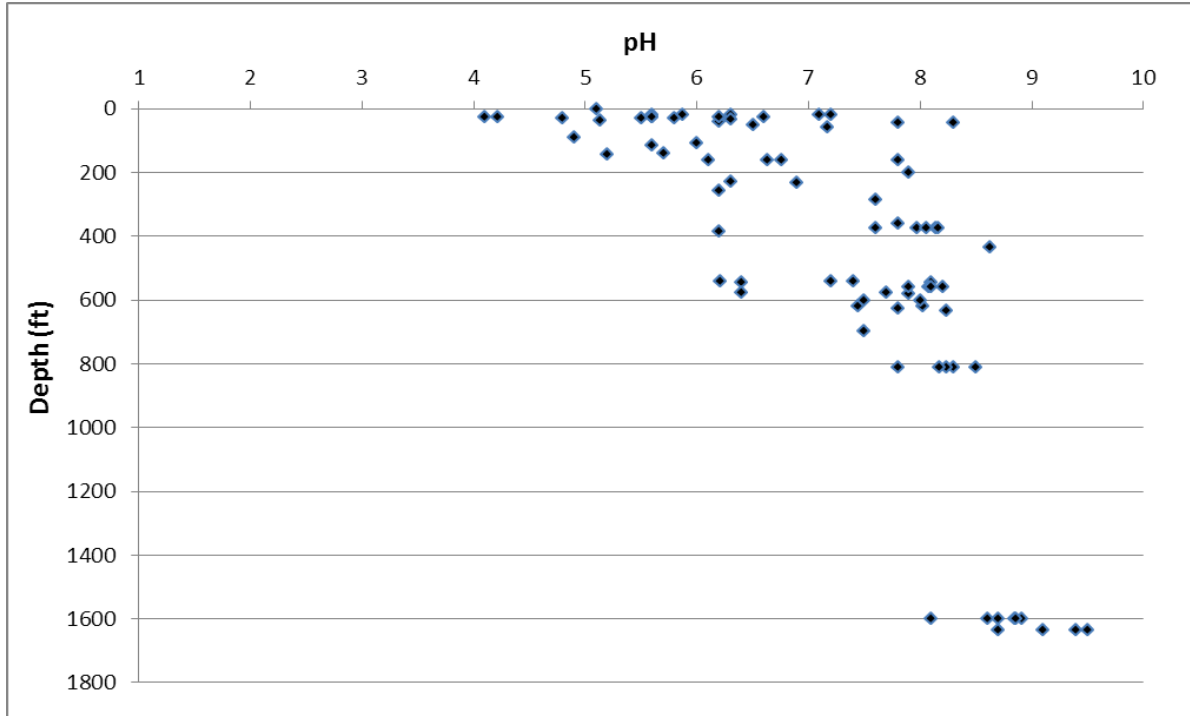


Figure 7-56. Depth(measured from land surface in feet (ft) versus pH, Sparta Aquifer, Northeast Transect, Groundwater Management Area 11.

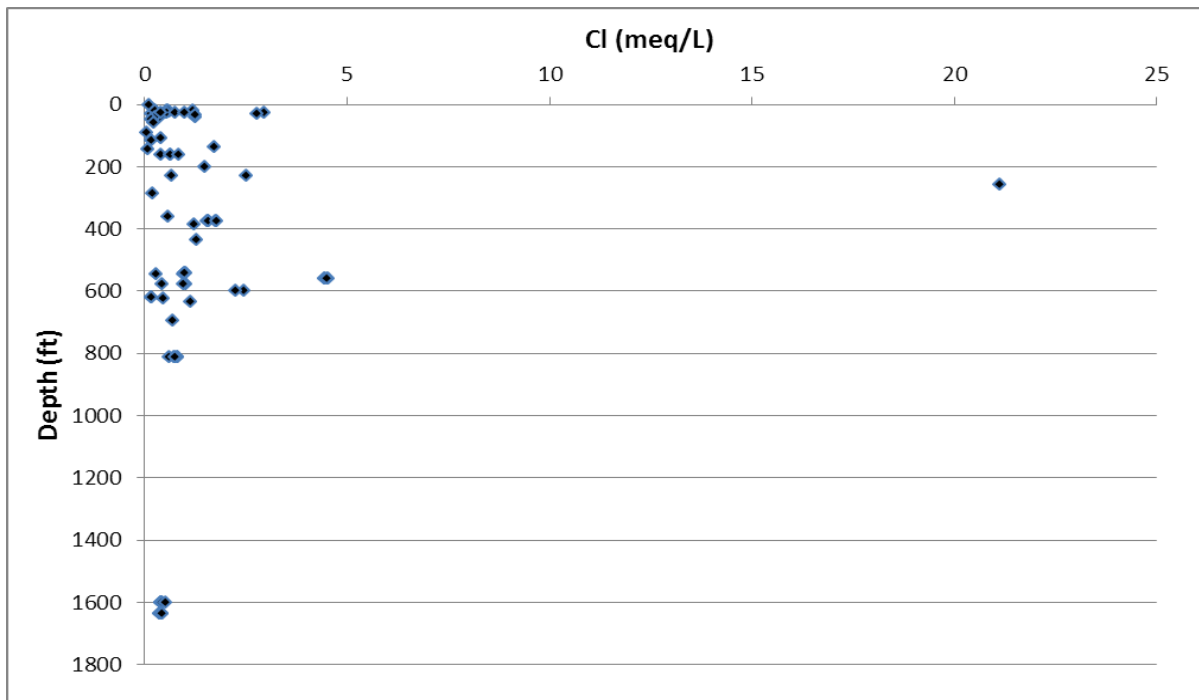
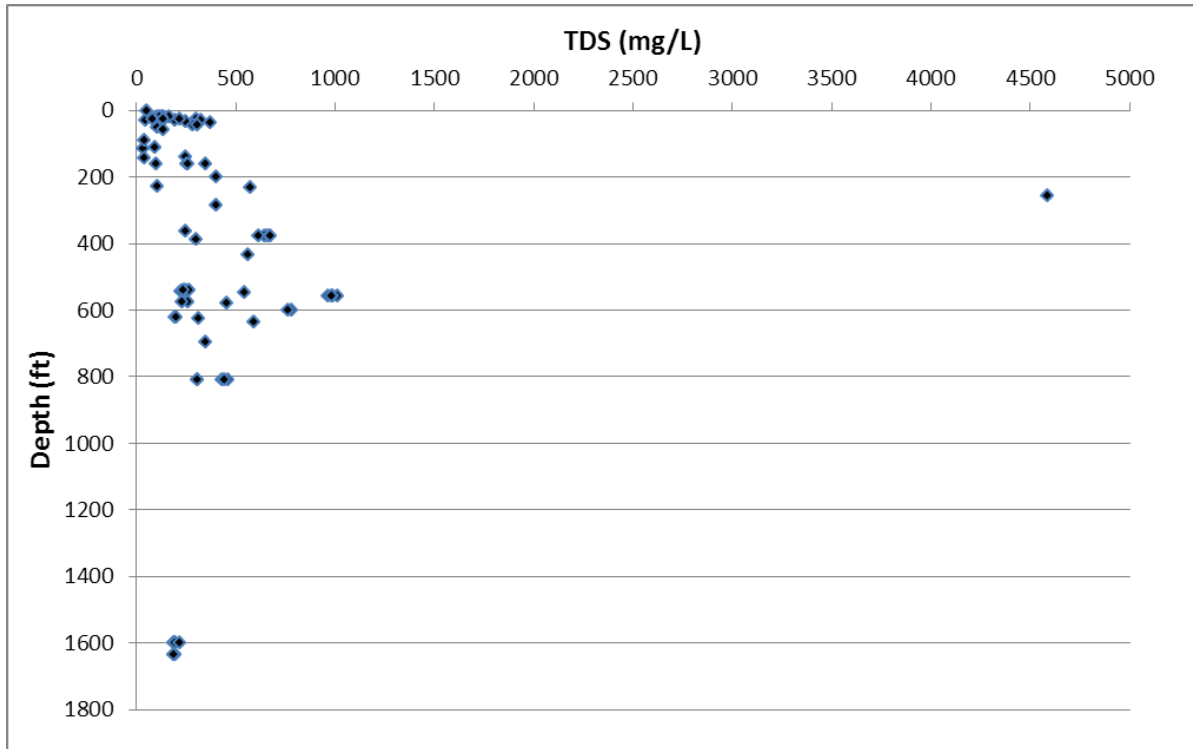


Figure 7-57. Depth measured from land surface in feet (ft) versus chloride (Cl) measured in milliequivalents per liter (meq/L), Sparta Aquifer, Northeast Transect, Groundwater Management Area 11.



**Figure 7-58.** Depth measured from land surface in feet (ft) versus total dissolved solids (TDS) measured in parts per million (ppm), Sparta Aquifer, Northeast Transect, Groundwater Management Area 11.

### **Yegua Formation of the Yegua-Jackson Aquifer**

The Yegua Formation of the Yegua-Jackson Aquifer overlies the Sparta, Queen City and Carrizo-Wilcox aquifers in southern Houston County. There is very limited production from the Yegua Formation of the Yegua-Jackson Aquifer.

#### Well Depths

Based on Figure 7-59 the well depths are typically less than 300 feet in the outcrop. There are no data in the confined part of the formation.

#### Water Level Data

Water levels are about 150 to 250 feet above mean sea level (Figure 7-60).

#### Piper Diagram

The Piper diagram (Figure 7-61) for the Yegua Formation of the Yegua-Jackson Aquifer in the Northeast Transect shows a sodium and mixed anion (chloride-sulfate-bicarbonate) type water where all wells appear to be in the outcrop.

#### Bicarbonate versus Sodium Plot

A plot of bicarbonate versus sodium (Figure 7-62) for the Yegua Formation of the Yegua-Jackson Aquifer data shows one trend of sodium and bicarbonate increasing at a rate of 2:1, sodium to bicarbonate.

Sodium versus Calcium Plot

No correlation is observed (Figure 7-63).

Bicarbonate versus Calcium Plot

No correlation is observed (Figure 7-64).

pH versus Bicarbonate Plot

No correlation is observed (Figure 7-65).

pH versus Sodium Plot

No correlation is observed (Figure 7-66).

Chloride versus Sodium Plot

The plot of chloride versus sodium (Figure 7-67) shows sodium increasing slowly with chloride, for water with sodium concentrations less than ten milliequivalents per liter. Higher chloride concentrations are observed for higher sodium values.

Chloride versus Bicarbonate Plot

The plot of chloride versus bicarbonate (Figure 7-68) shows bicarbonate increasing independent to chloride, for bicarbonate values less than six milliequivalents per liter. At higher bicarbonate concentrations chloride values increase.

Sulfate versus Bicarbonate Plot

A plot of sulfate versus bicarbonate (Figure 7-69) shows higher sulfate concentrations for higher bicarbonate concentrations. This is the inverse of the sulfate versus bicarbonate relationships for the Carrizo-Wilcox and Sparta aquifers (Figure 7-10 and Figure 7-51).

Depth versus Bicarbonate Plot

No correlation is observed (Figure 7-70).

Depth versus Sulfate Plot

No correlation is observed (Figure 7-71).

Depth versus Calcium Plot

No correlation is observed (Figure 7-72).

Depth versus pH Plot

No correlation is observed (Figure 7-73).

Depth versus Sodium Plot

No correlation is observed (Figure 7-74).

Depth versus Chloride Plot

No correlation is observed (Figure 7-75).

Depth versus Total Dissolved Solids Plot

No correlation is observed (Figure 7-77).

### Discussion

The amount of groundwater chemistry from the Yegua Formation of the Yegua-Jackson Aquifer in the Northeast Transect is very limited because of the few wells that produce from it. Groundwater production is from the outcrop and not downdip. From the Piper diagram the water composition is sodium-chloride-bicarbonate-sulfate type water. This water has a general chemical composition dissimilar to the chemistry observed in the Carrizo-Wilcox, the Queen City or the Sparta aquifers in the Northeast Transect. The Yegua Formation of the Yegua-Jackson Aquifer chemistry is generally different for all four transects evaluated in this overall study.

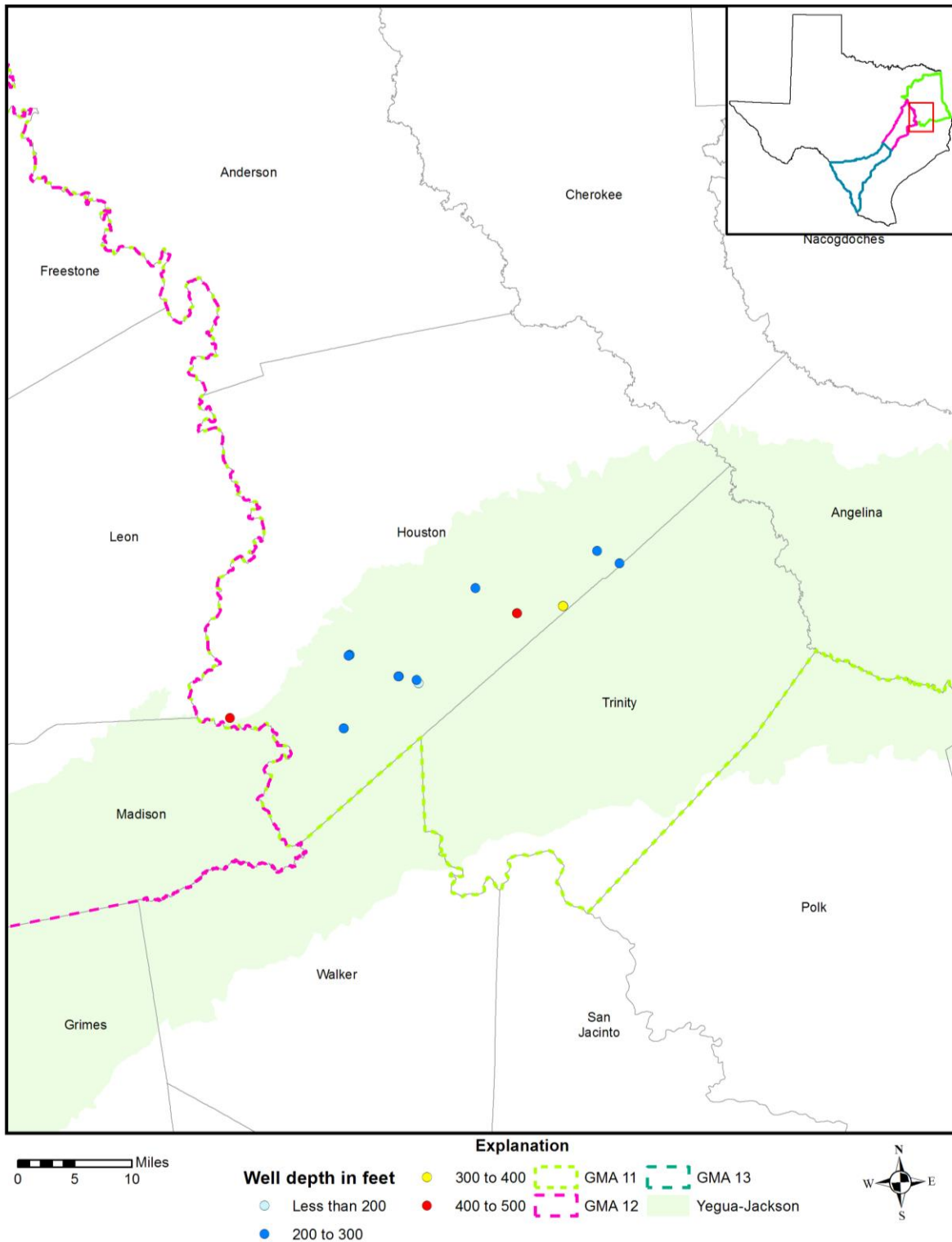


**Figure 7-59.** Well depths measured from land surface in feet in the Yegua Formation of the Yegua-Jackson Aquifer, Northeast Transect, Groundwater Management Area (GMA) 11.

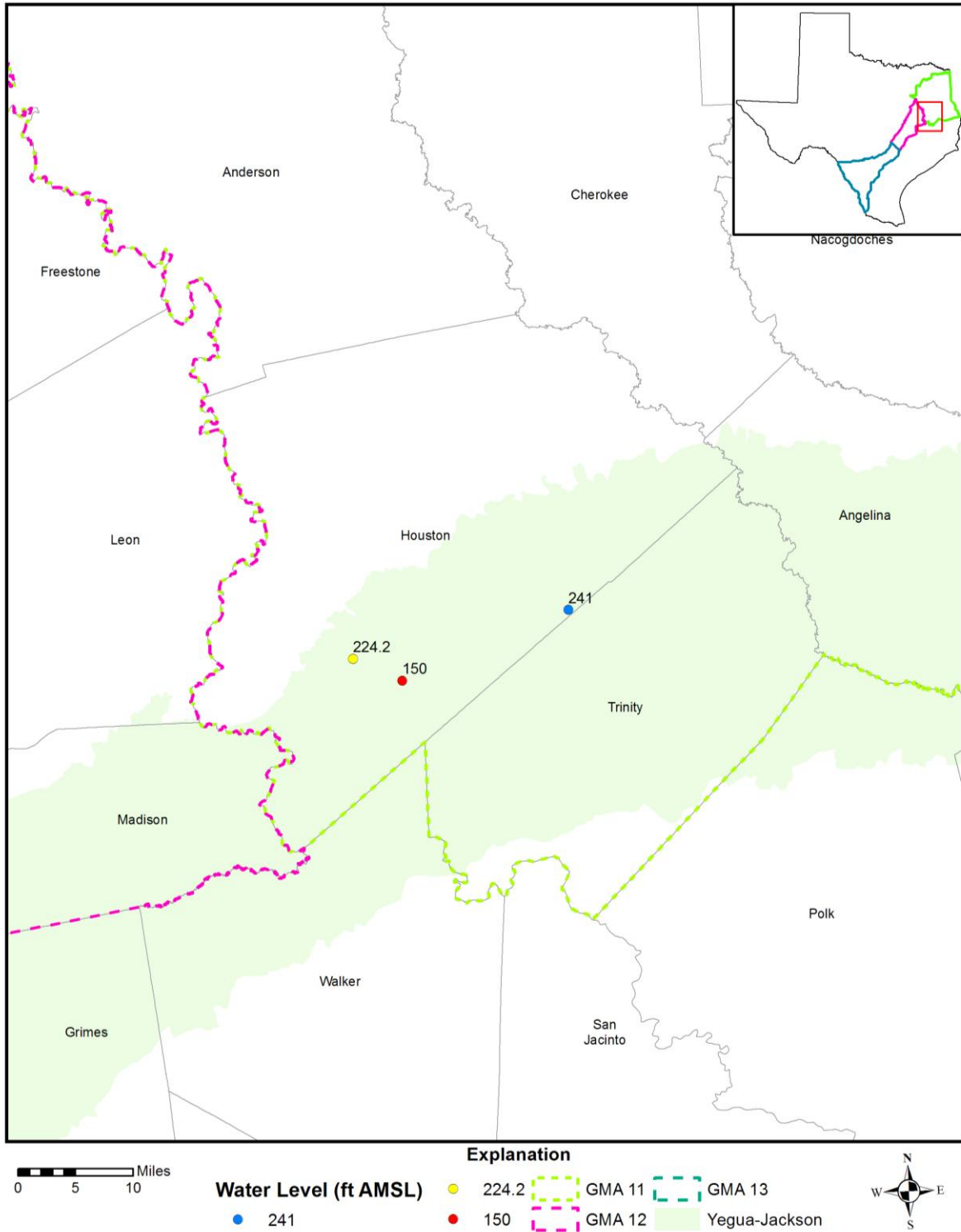


**Figure 7-60.** Water level elevations from 1975 to 2010 measured in feet above mean seal level (ft AMSL) in the Yegua Formation of the Yegua-Jackson wells, Northeast Transect, Groundwater Management Area (GMA) 11.

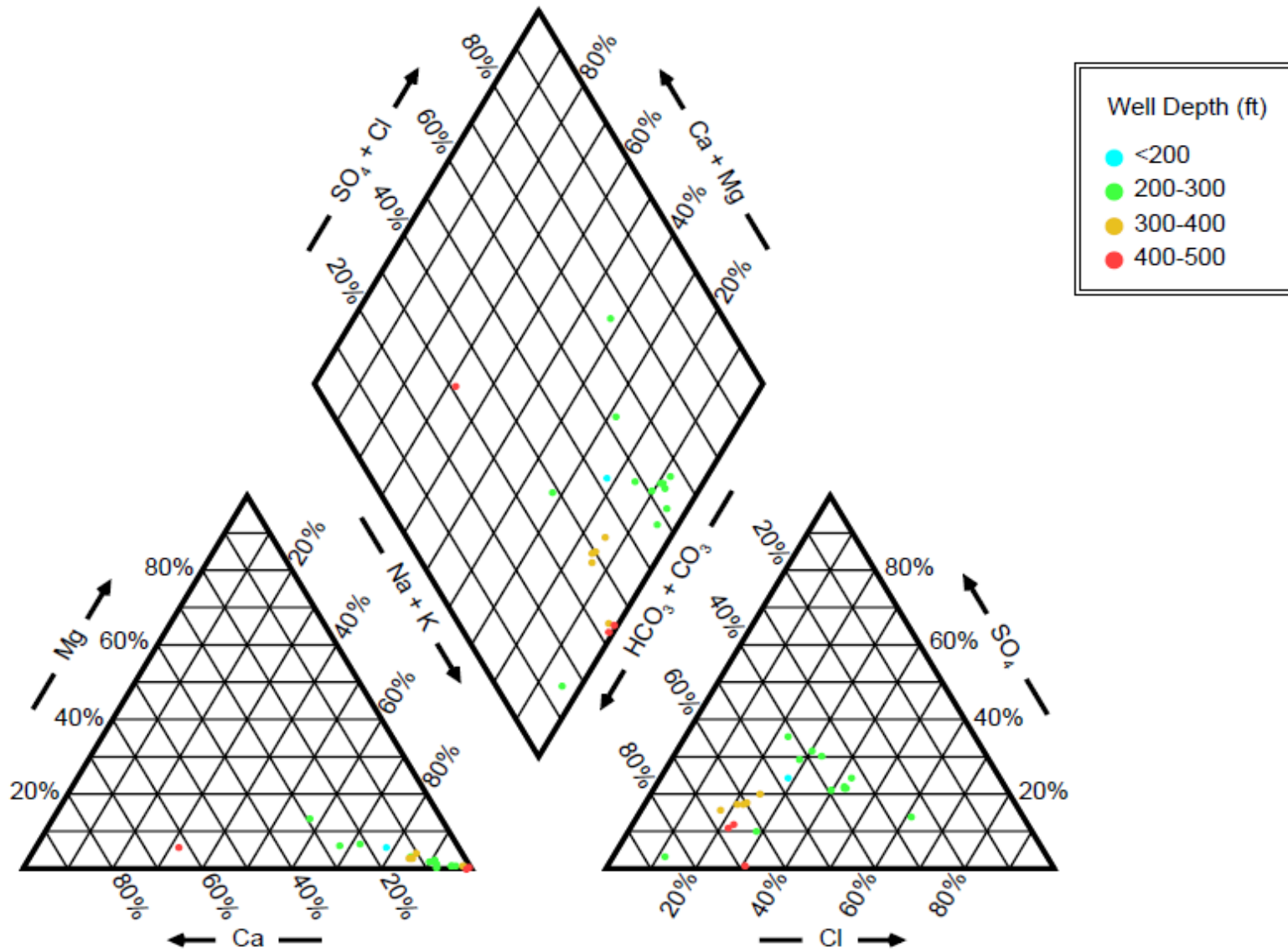


Figure 7-61. Piper diagram showing chemistry of Yegua Formation of the Yegua-Jackson Aquifer wells in the Northeast Transect by well depth measured from land surface in feet (ft).

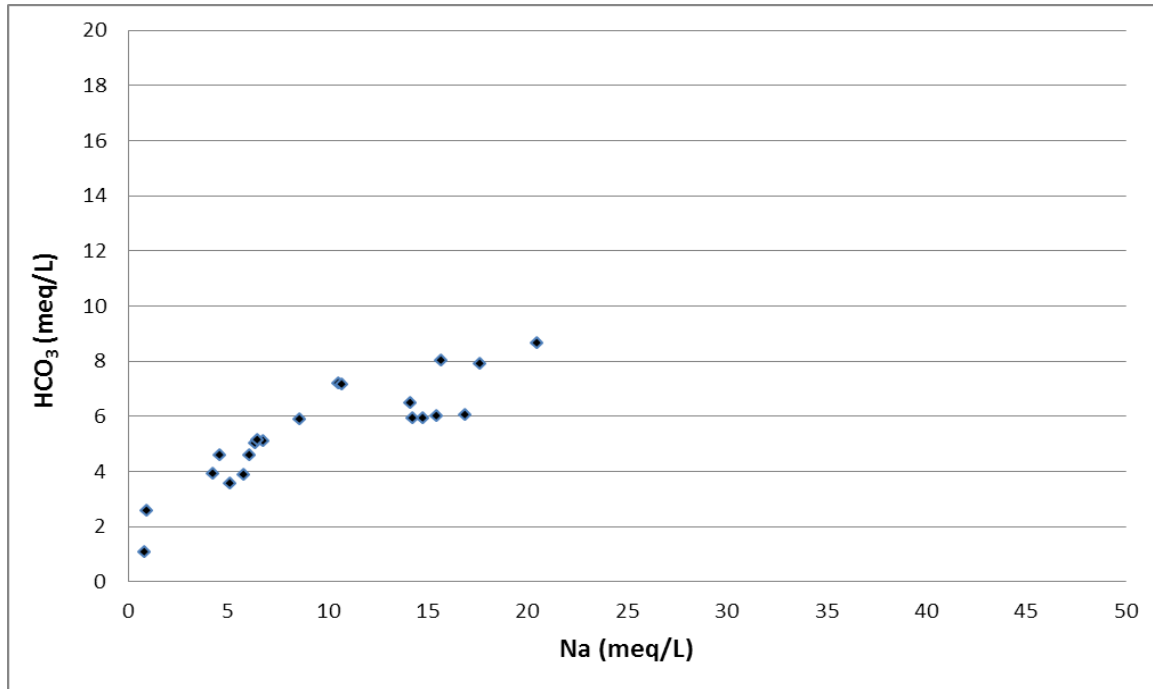


Figure 7-62. Bicarbonate (HCO<sub>3</sub>) versus sodium (Na) measured in milliequivalents per liter (meq/L), Yegua Formation of the Yegua-Jackson Aquifer, Northeast Transect, Groundwater Management Area 11.

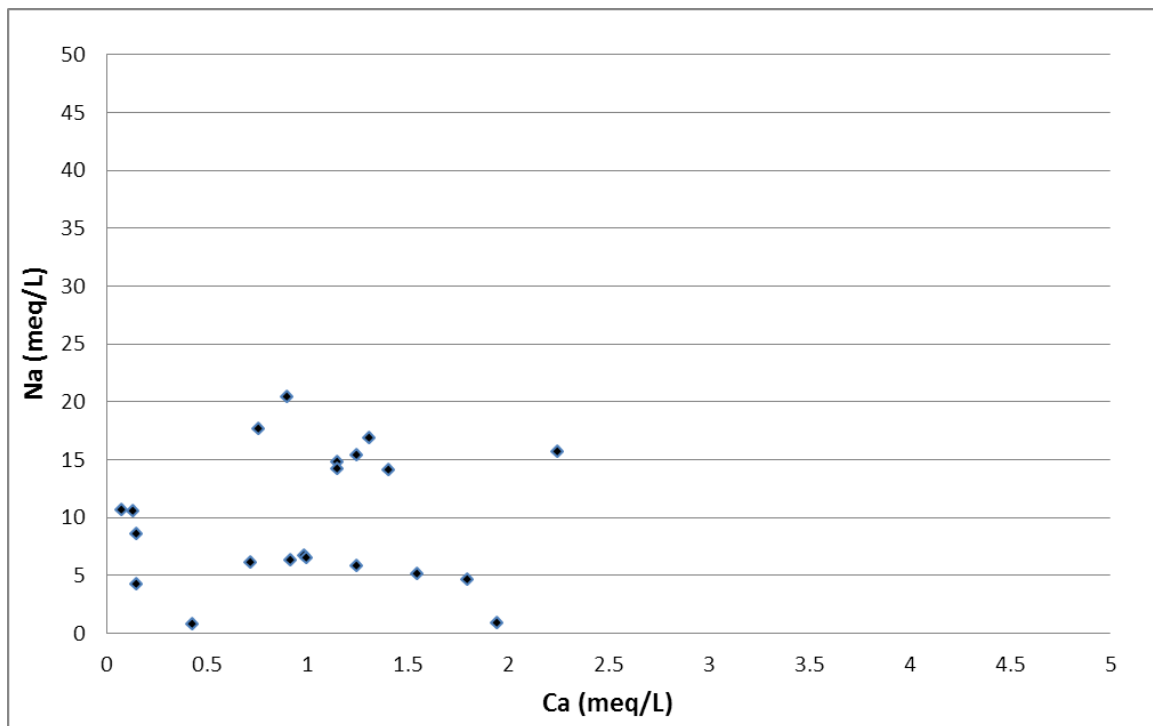


Figure 7-63. Sodium (Na) versus calcium (Ca) measured in milliequivalents per liter (meq/L), Yegua Formation of the Yegua-Jackson Aquifer, Northeast Transect, Groundwater Management Area 11.

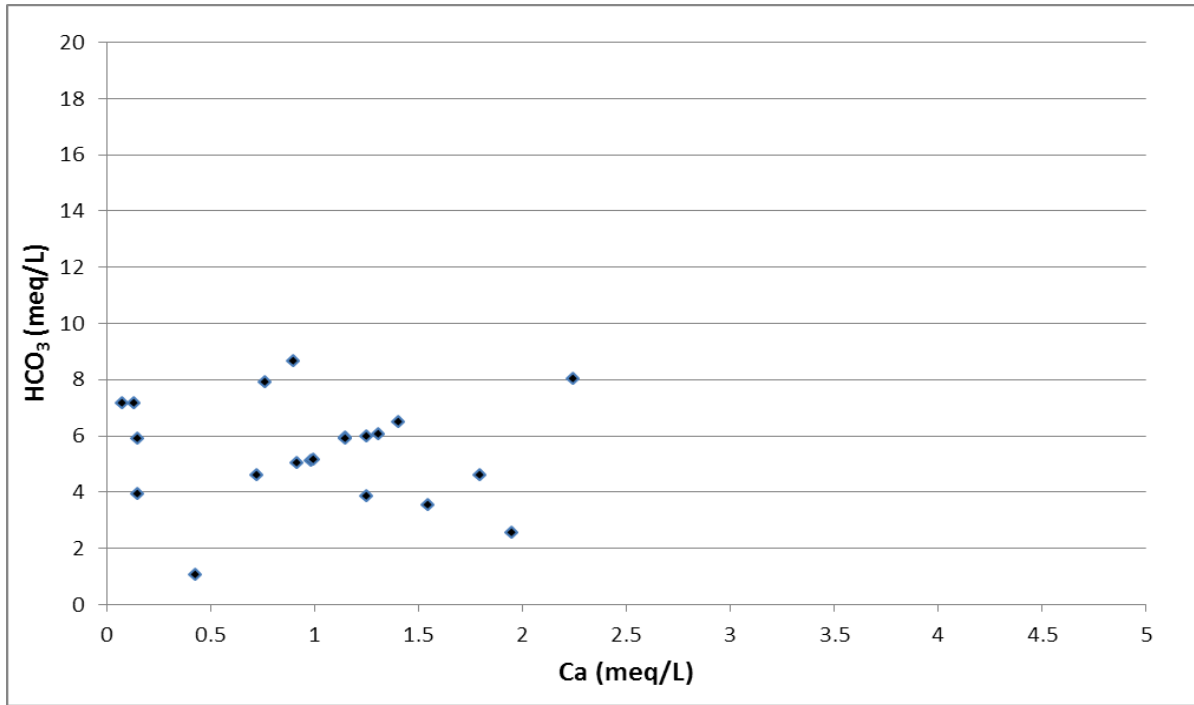


Figure 7-64. Bicarbonate (HCO<sub>3</sub>) versus calcium (Ca) measured in milliequivalents per liter (meq/L), Yegua Formation of the Yegua-Jackson Aquifer, Northeast Transect, Groundwater Management Area 11.

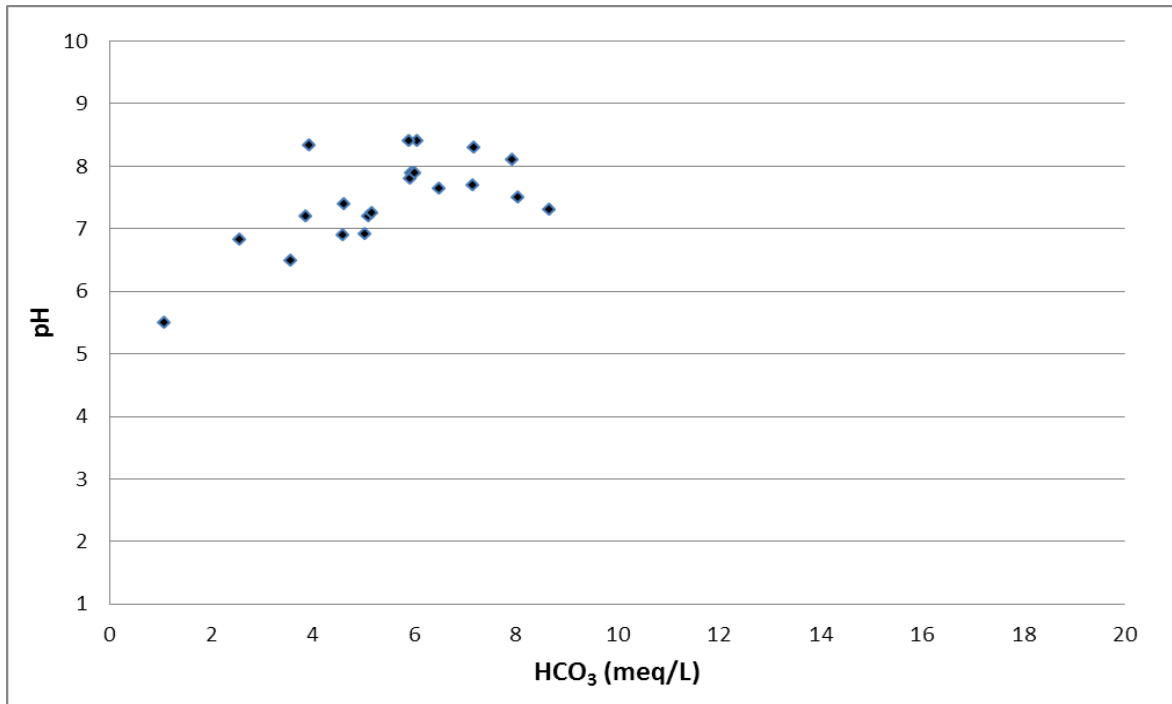


Figure 7-65. pH versus bicarbonate (HCO<sub>3</sub>) measured in milliequivalents per liter (meq/L), Yegua Formation of the Yegua-Jackson Aquifer, Northeast Transect, Groundwater Management Area 11.

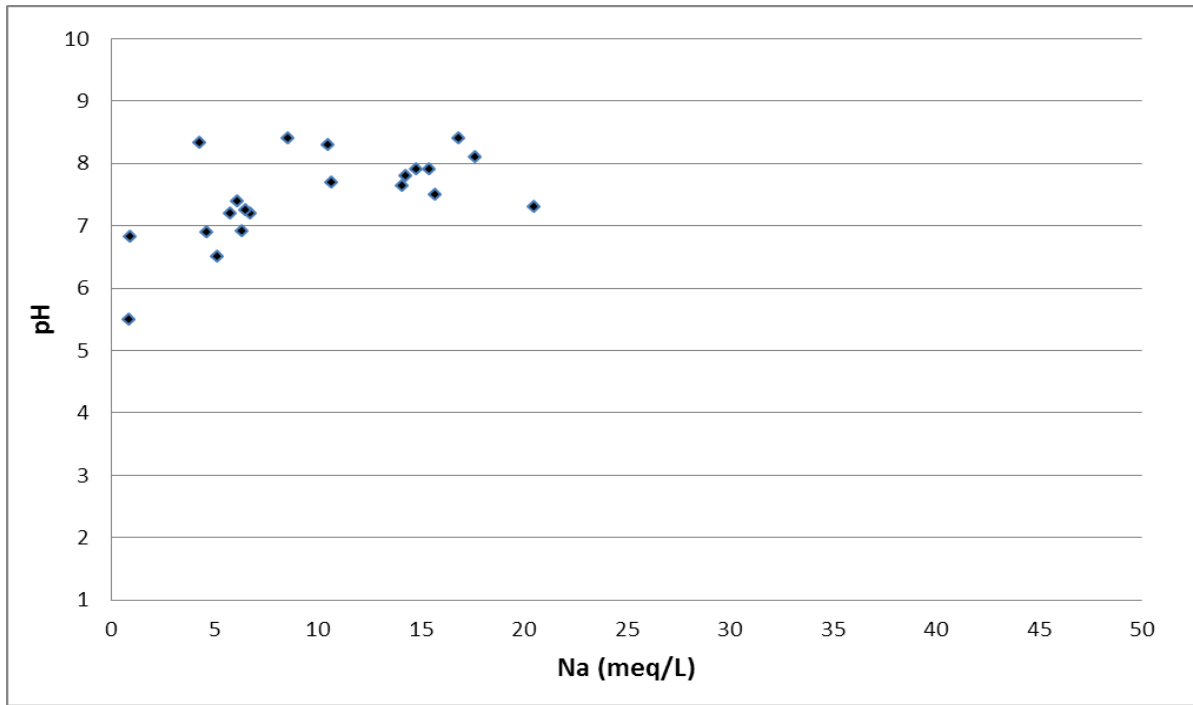


Figure 7-66. pH versus sodium (Na) measured in milliequivalents per liter (meq/L), Yegua Formation of the Yegua-Jackson Aquifer, Northeast Transect, Groundwater Management Area 11.

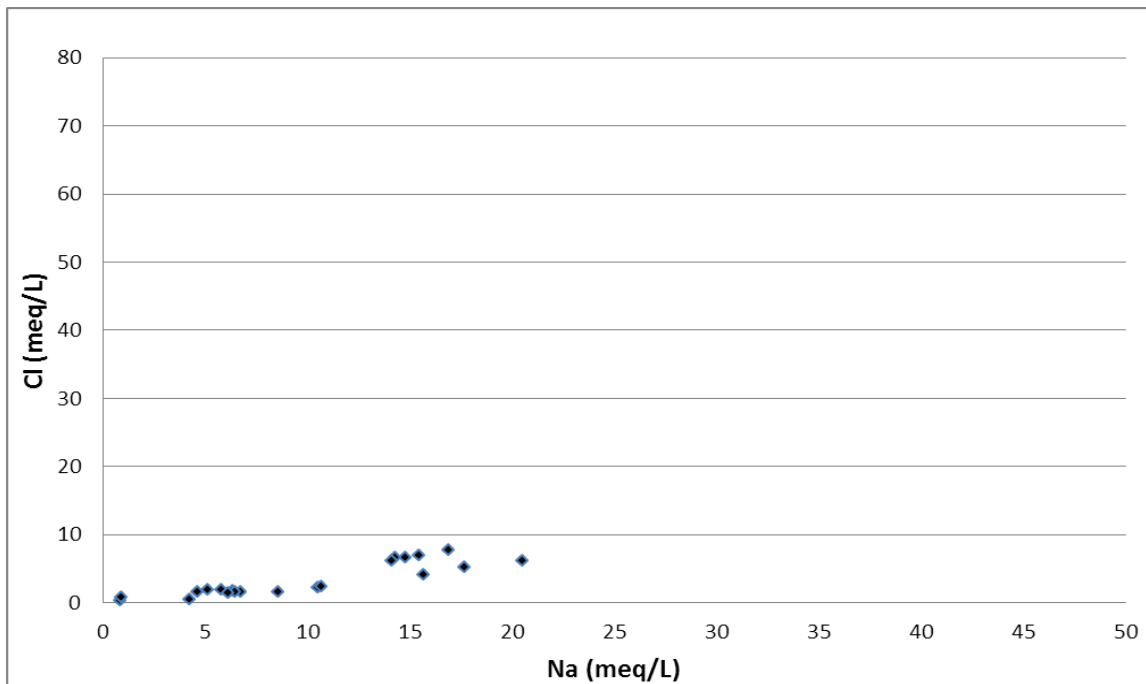


Figure 7-67. Chloride (Cl) versus sodium (Na) measured in milliequivalents per liter (meq/L), Yegua Formation of the Yegua-Jackson Aquifer, Northeast Transect, Groundwater Management Area 11.

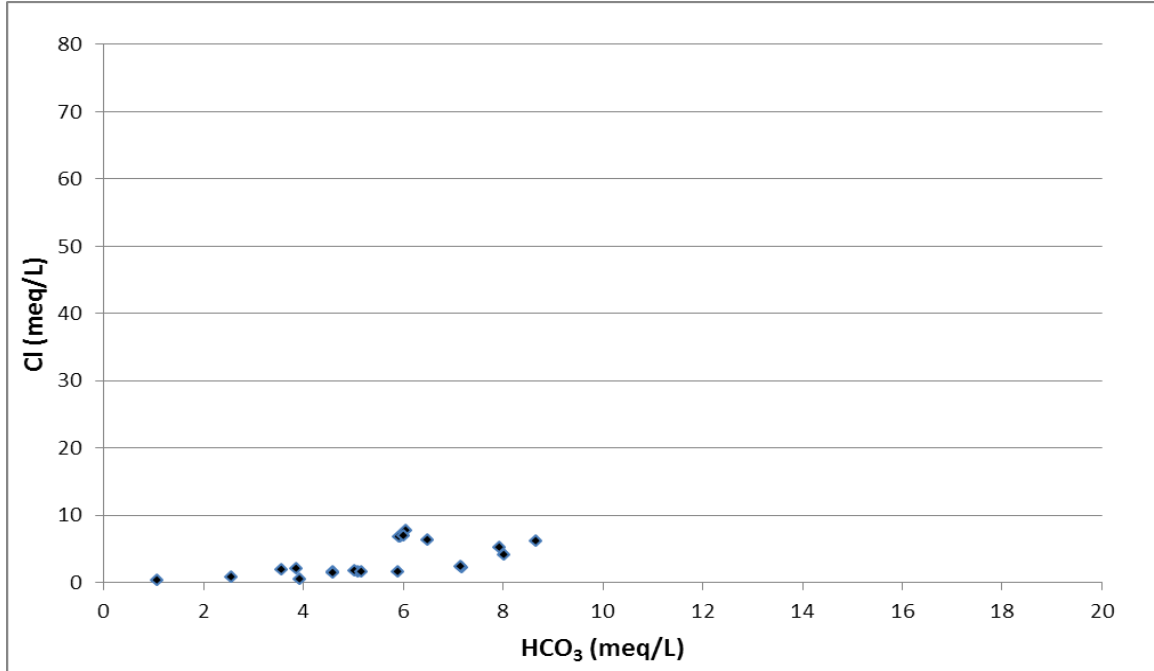


Figure 7-68. Chloride (Cl) versus bicarbonate (HCO<sub>3</sub>) measured in milliequivalents per liter (meq/L), Yegua Formation of the Yegua-Jackson Aquifer, Northeast Transect, Groundwater Management Area 11.

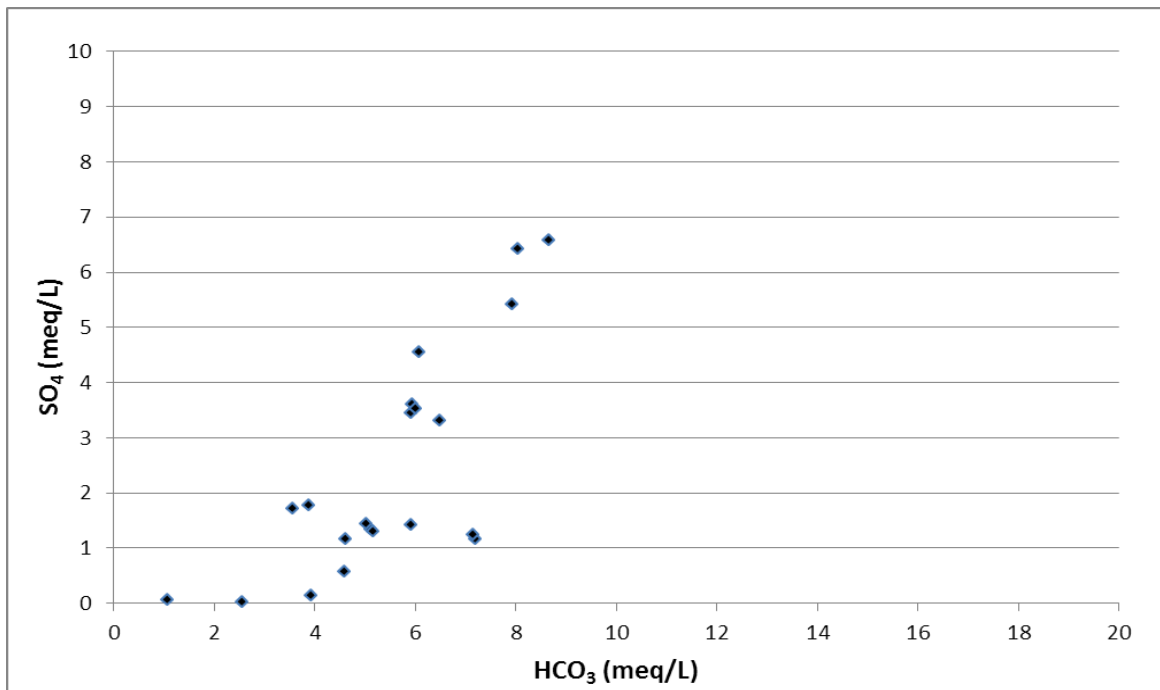
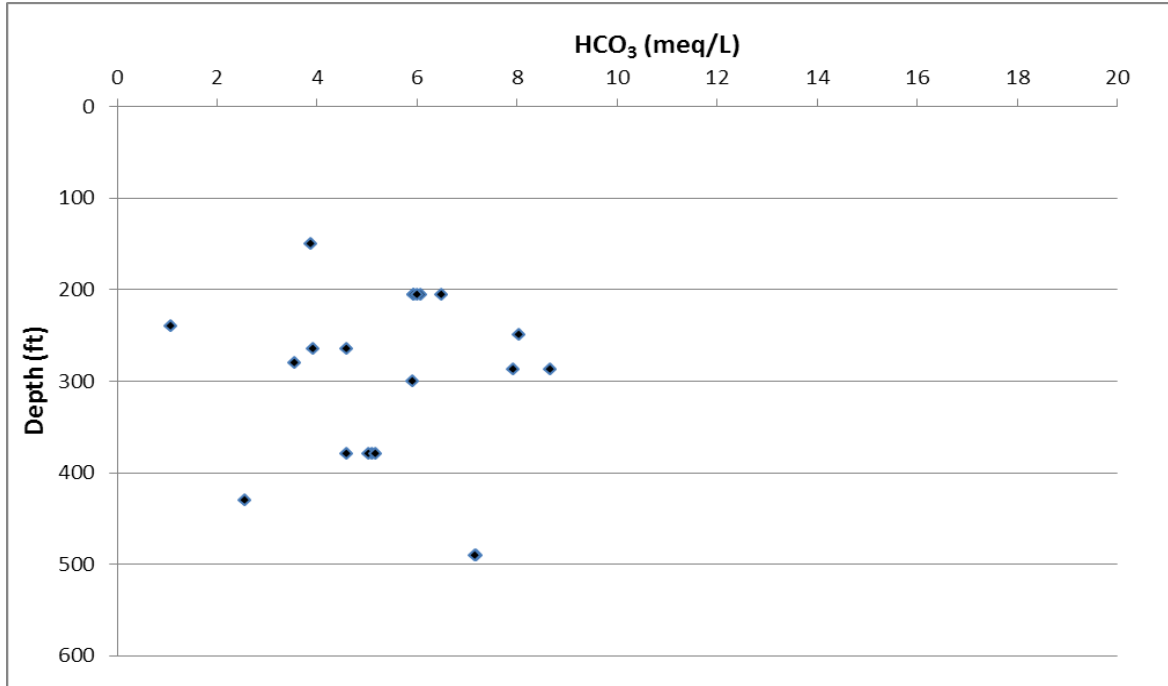
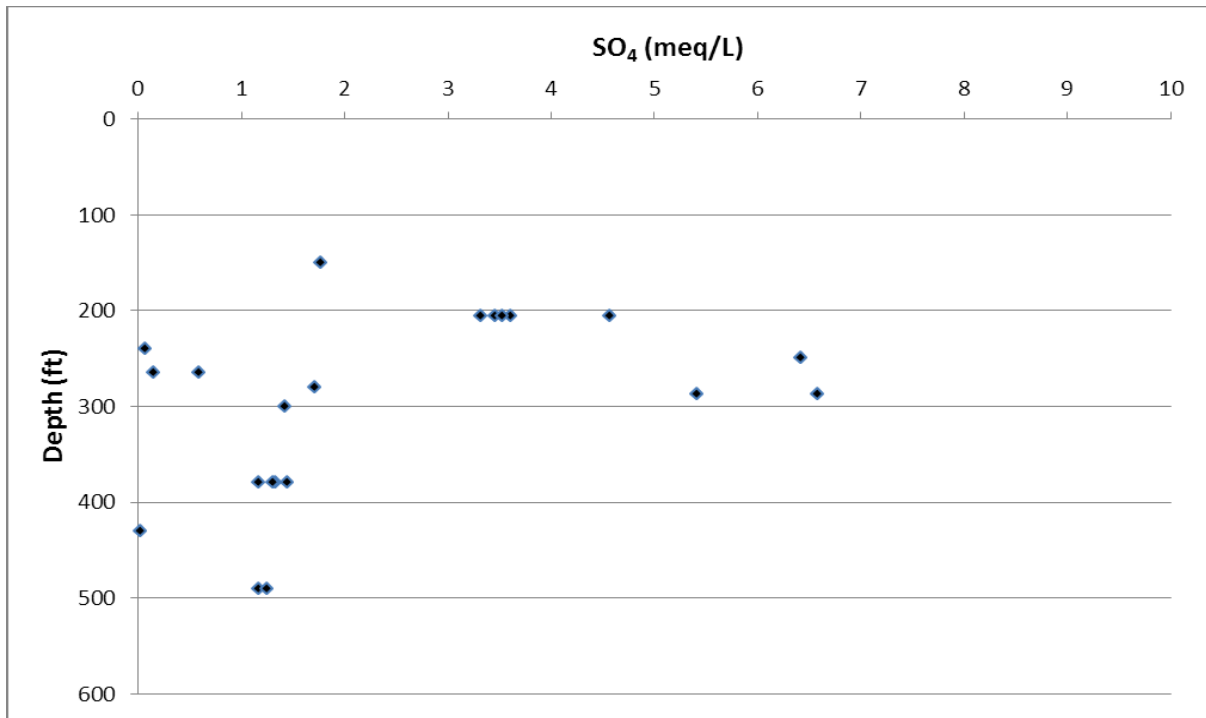


Figure 7-69. Sulfate (SO<sub>4</sub>) versus bicarbonate (HCO<sub>3</sub>) measured in milliequivalents per liter (meq/L), Yegua Formation of the Yegua-Jackson Aquifer, Northeast Transect, Groundwater Management Area 11.



**Figure 7-70.** Depth measured from land surface in feet (ft) versus bicarbonate (HCO<sub>3</sub>) measured in milliequivalents per liter (meq/L), Yegua Formation of the Yegua-Jackson Aquifer, Northeast Transect, Groundwater Management Area 11.



**Figure 7-71.** Depth measured from land surface in feet (ft) versus sulfate (SO<sub>4</sub>) measured in milliequivalents per liter (meq/L), Yegua Formation of the Yegua-Jackson Aquifer, Northeast Transect, Groundwater Management Area 11.

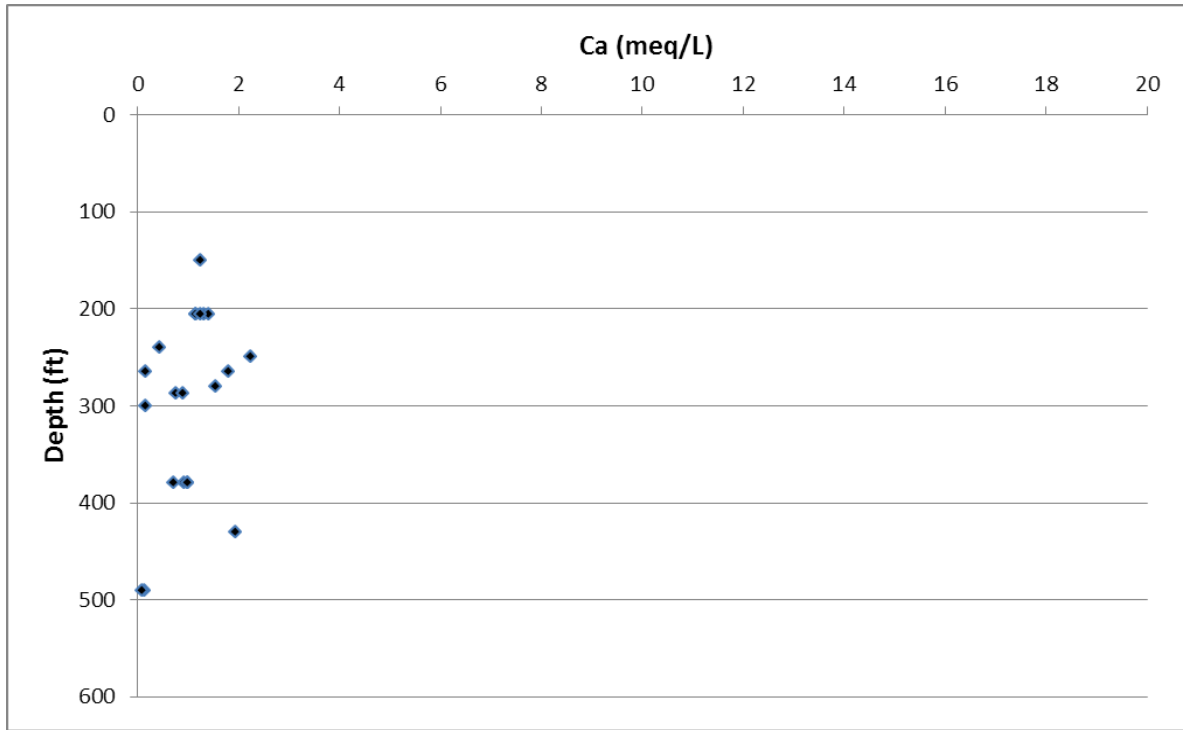


Figure 7-72. Depth measured from land surface in feet (ft) versus calcium (Ca) measured in milliequivalents per liter (meq/L), Yegua Formation of the Yegua-Jackson Aquifer, Northeast Transect, Groundwater Management Area 11.

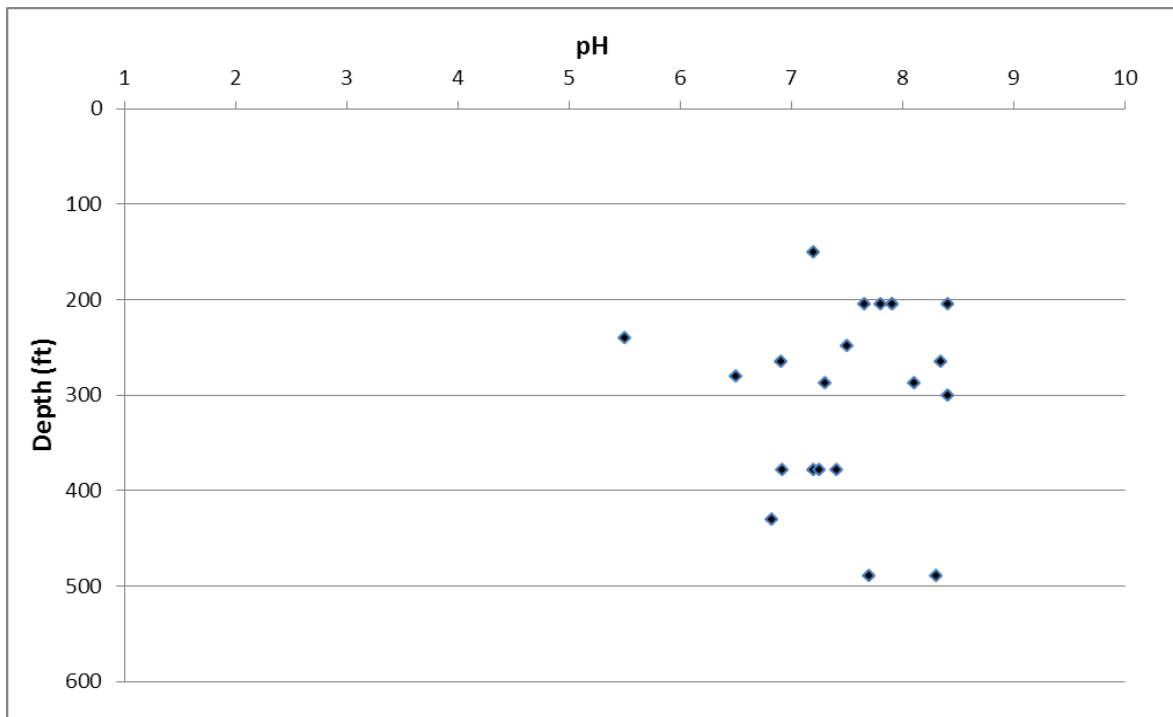
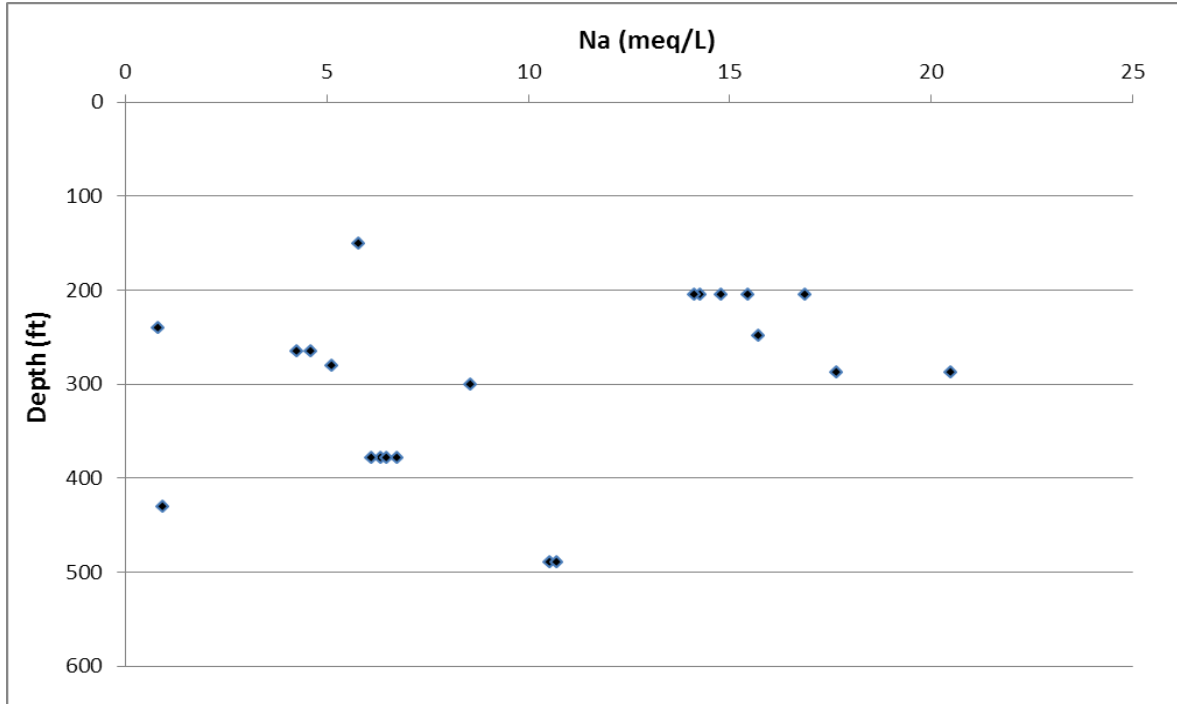
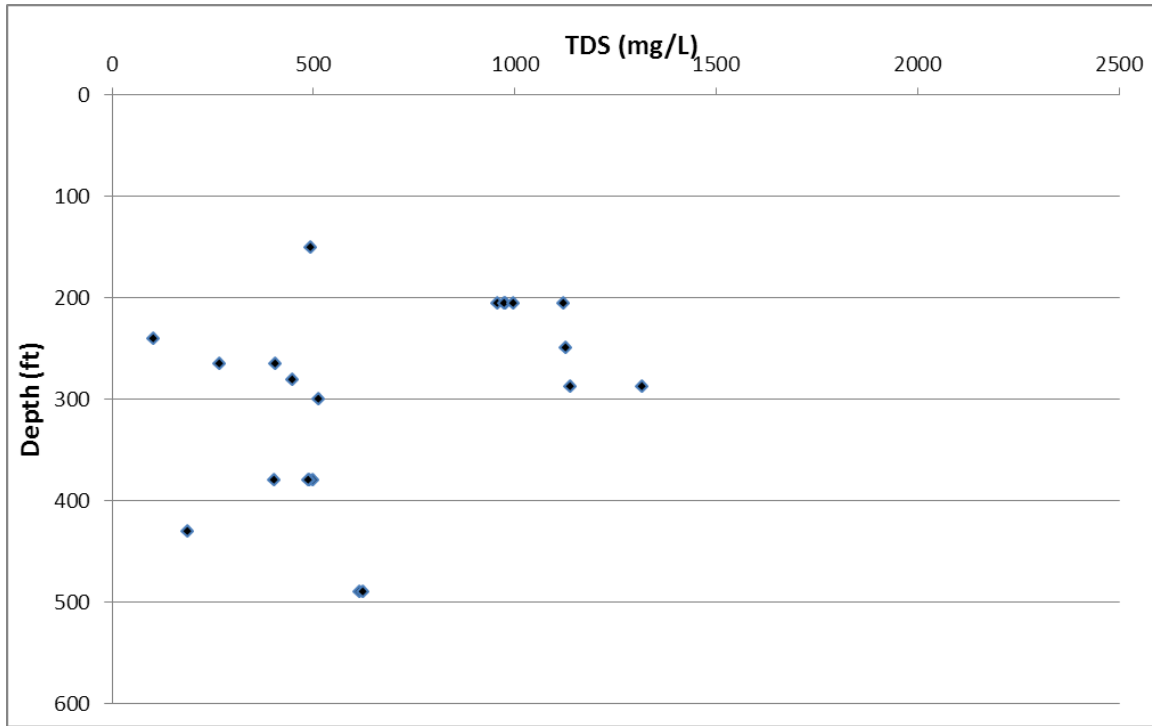


Figure 7-73. Depth measured from land surface in feet (ft) versus pH, Yegua Formation of the Yegua-Jackson Aquifer, Northeast Transect, Groundwater Management Area 11.





**Figure 7-76.** Depth measured from land surface in feet (ft) versus total dissolved solids (TDS) measured in parts per million (ppm), Yegua Formation of the Yegua-Jackson Aquifer, Northeast Transect, Groundwater Management Area 11.

### 7.1.2 Geochemical Modeling

The estimation of the groundwater age in the Carrizo-Wilcox Aquifer along the Northeast Transect is a two-step process. The first step is to quantitatively determine the geochemical evolution of a groundwater as it flows from outcrop to downdip along a flowpath defined by a set of wells with known chemistry. The second step is to calculate a corrected carbon-14 age with this well-defined geochemical pathway. Table 7-1 shows the estimated age of these waters. Transect 1 as shown in Figure 7-77 shows that the Carrizo-Wilcox Aquifer groundwater became rapidly older in the confined section when compared to the outcrop wells.

#### Aquifer Composition

Geochemical modeling for the Northeast Transect is limited to existing chemical and isotopic data collected in 1979 for a hydrogeologic assessment of the Carrizo-Wilcox Aquifer near salt diapirs (Kreitler and Wuerch, 1981). There are a total of 14 radiocarbon and stable carbon isotope analyses for wells in the four adjacent counties of Henderson, Anderson, Houston and Leon (Figure 7-77). Nine of the wells are generally aligned in a northwest to southeast orientation, subparallel to the general direction of flow, as interpreted in the Queen City and Sparta Aquifers GAM (Kelley and others, 2004). These wells all sample the Carrizo-Wilcox Aquifer and represent both the water table and confined sections of the aquifer. The shallowest two wells have depths of 260 and 445 feet below land surface and are located within the outcrop area of the Carrizo-Wilcox Aquifer; the deepest two wells along this transect are from the confined portion of the aquifer and have total depths of 1,840 and 1,810 feet below land surface (Table 7-1, Figure 7-78 and Figure 7-79). The remaining five analyses are in Leon County and

were originally selected for sampling because of proximity to salt diapirs such as the Oakwood Dome. These wells are not aligned along flow lines and are too randomly distributed to consider for this study of groundwater evolution related to regional flow.

The nine aligned wells 1-9 in Transects 1 and 2 (Figure 7-77) were initially considered as representative of an evolutionary transect of shallow recharge water composition that was modified substantially along the flow path by mineral reactions generally well understood for this transect. Others have summarized the compositional changes commonly observed for these Gulf Coast aquifers (Fogg and Kreitler, 1982, Hamlin, 1988 and Henry and others, 1980) as principally changing according to the following sequence:

1. Recharge followed by incorporation of carbon dioxide, with dissolution of calcite, gypsum, or oxidation of pyrite, accompanied by minor reactions with silicate phases.
2. Ion exchange reactions with the fluvial-deltaic and marine clays exchanging calcium for sodium as the dominant reaction.
3. Oxidation of organic material (e.g., lignite) by dissolved oxygen, or through microbial reactions using sulfate or nitrate as the electron acceptor, yielding either carbon dioxide, which dissolves additional calcite, or, depending on the redox conditions, also producing biogenic methane.
4. Evolution of the water results in a progressive increase in pH as calcite dissolves and development of a sodium-bicarbonate composition with low sulfate and chloride concentrations.

These general trends can be seen using the available data from the TWDB database. For example, Figure 7-6 plot is using sodium versus calcium data for the Carrizo-Wilcox Aquifer to illustrate the decrease in calcium with exchange for sodium on the clays. Bicarbonate and sodium concentrations are correlative as the calcium reaction and ion exchange proceeds (Figure 7-5).

For this nine-well transect (Figure 7-77), the chemical trends with distance from the outcrop to the deepest and most distant downgradient wells clearly indicate that the transect does not represent a continuous and progressive chemical evolution of the same water system (Figure 7-80, Figure 7-81 and Figure 7-82). Unfortunately, a chemical analysis was not done for the shallowest well (Well 1, Table 7-1), and only the  $\delta^{13}\text{C}$  and carbon-14 analyses are available; however the first three wells (Wells 1, 2 and 3) seem consistent enough in the isotopic and compositional changes to be plausibly related to the same flow path. Similarly, Wells 5 through 9 show a chemical evolution consistent with the expected conventional understanding for the Carrizo-Wilcox Aquifer.

Comparison of these well locations to the estimated potentiometric surface given in the Queen City and Sparta Aquifers GAM indicates that separating these wells into two flow paths is a reasonable alternative. If the recharge location for Wells 5 through 9 (Transect 2) is farther to the southwest from Wells 1 and 2, then the composition can rather easily be explained. Well 4 (TWDB No. 3803701) does not fit with either transect and is most probably a mixture of water sources; in addition, it is screened shallower than the first transect and deeper than the second. Well radiocarbon age correction for Well 4 can be approximated using the Pearson and White (1967) method, but not as part of either of these two more consistent transects.

It should be noted there is an abrupt decrease in concentration between Well 3 (Transect 1) and Wells 4 and 5 (Transect 2) of sodium, alkalinity, and chloride, three of the most indicative constituents of the compositional evolution (Figure 7-14). It is difficult to conceive of a process that would diminish the chloride, sodium and bicarbonate concentrations downgradient. Chloride concentrations decrease from 142 to 23 milligrams per liter. The more likely scenario is the existence of two flow pathways that are following the same chemical evolutionary process, but are being sampled at different points along the flow path. Clearly the concentration of calcium is diminishing and the sodium and bicarbonate concentrations are rapidly increasing; sulfate and chloride concentrations change minimally over the majority of the flowpath as is commonly observed for this system.

The analytical data required for the original investigation conducted for these wells were limited; consequently there are no fixed gas or hydrocarbon gas analyses, and the only isotopic data are the  $\delta^{13}\text{C}$  and carbon-14 of the dissolved inorganic carbon.

Figure 7-83 displays a graphical cross section along the Northeast Transect, with calcium data posted at the appropriate well location. This figure displays the trend of decreasing calcium with depth that results from cation exchange with the sodium minerals of clays in the aquifer matrix, and visually displays the data trends of calcium with depth that are presented graphically in Figure 7-14.

Figure 7-84 displays a graphical cross section along the Northeast Transect, with sodium data posted at the appropriate well location. The sodium concentrations do not reflect an increasing trend in deeper wells at further distances from the outcrop, as is observed in several of the other aquifers in this study. This figure visually displays the data trends of sodium with depth that are presented graphically in Figure 7-18.

### **Estimation of Age**

Measurement of carbon-14 content of groundwater yields an uncorrected value given in units of decays per minute per gram of carbon and if the carbon is derived from the soil zone where the carbon-14 is fixed from atmospheric sources, then the calculation of age is not as difficult. The complication occurs as the carbon dioxide reacts with carbonate minerals, organic material, etc., which no longer contain carbon-14, but the reaction with these phases changes the mass of carbon dissolved in water. These alterations to carbon content change the apparent or observed age, because it is based on the measurement of carbon-14 in the total dissolved carbon, and thus must be corrected to account for other carbon sources and losses. There are two approaches to estimate groundwater age that best fit the circumstances of the wells in this transect; the first is a simple correction assuming only reaction with calcite along the flowpath (Pearson and White, 1967) and the second is an inverse method using a numerical model to account for all reasonable carbon sources and any contributing chemical reactions (Plummer and others, 1994). The quantity of data available for this transect is large enough that the inverse method of geochemical interpretation and estimation of groundwater age was determined to be most advantageous along transects 1 and 2, but the simplified calcite correction model is required for the other randomly distributed wells, and for the initial well in transect 2.

The inverse method or mass balance approach requires assumptions about the carbon sources in the recharge area and isotopic composition of any reactive carbon sources along the flowpath. Similarly the calcite correction method requires defining the recharge conditions, but only the isotopic composition of calcite. In the original study, all corrections were made using the calcite

correction method. The assumption was made that the  $\delta^{13}\text{C}$  of soil gas carbon dioxide and calcite were -20 ‰ and 0 ‰ respectively, and this assumption is maintained here where the calcite correction method is used for consistency with the original work (Kreitler and Wuerch, 1981). The calcite correction approximation works best if the aquifer is a clean sand with no sources of carbon other than calcite, and no significant incorporation of carbon dioxide beyond the recharge area. The original calculations by Kreitler and Wuerch (1981) represent the only attempts to correct the carbon-14 ages available in the literature for this transect of Texas; the calculations were updated for this study and are included in Table 7-1.

The original measured carbon-14 values and the estimated corrections for all 14 wells are included in Table 7-1. The measured carbon-14 content is given both in carbon-14 activity as percent modern carbon ( $^{14}\text{C}_{\text{OBS}}$  percent modern carbon) and in age as years before present ( $^{14}\text{C}_{\text{OBS}}$  years before present). The correction calculations using the Pearson and White (1967) method result in the ages shown in the tenth column of Table 7-1 as adjusted ages in units of years before present ( $^{14}\text{C}_{\text{ADJ}}$  years before present). All adjusted ages are younger than the measured ages and often are inconsistently corrected and unreasonably younger than the measured carbon-14 content indicates; this can be attributed to the method, which fails to adjust for other reactions along the flow path. For the five wells in Leon County, the corrections may be more reasonable estimates because the wells are close to the Carrizo-Wilcox Aquifer outcrop and less affected by competing reactions. For example, the influence of soil carbon dioxide is reasonably present in the shallow wells of the recharge area, where the aquifer is an open system, and additional carbon dioxide with soil-related carbon-14 is accessible to replace what is consumed in reactions with calcite or silicate minerals. This is the only carbon dioxide considered in the Pearson and White (1967) model. As the groundwater moves downgradient, however, it becomes confined and becomes closed to atmospheric or soil carbon dioxide. Reactions with carbon dioxide and organic material must account for the different isotopic content and absence of new carbon-14 entering the groundwater. This detailed accounting for mass and isotope transfer is done in NETPATH.

Similar to the Pearson and White (1967) approach, the mass balance approach considers the same reactions in the recharge area with carbon dioxide incorporation into the groundwater and dissolution of calcite, but it additionally accounts for ion exchange reactions involving calcium, magnesium, and sodium, as well as the oxidation of lignite or incorporation and loss of carbon dioxide along the flowpath. Secondary reactions of sulfate sources and silicate hydrolysis were considered during modeling and deemed not significant enough to contribute any modification to the age calculation, and were not deemed important for this assessment.

The calculation performed in NETPATH is constrained by two important procedures. First, the change in groundwater composition between wells must be accounted for by reaction with minerals, gasses, or ion exchange. If this difference cannot balance with stoichiometric reactions, then the pathway is not considered correct, either because of incorrect reaction formulation or possibly the effect of mixing with water sources not yet identified. Secondly, the thermodynamic reaction state of minerals must be monitored such that the model does not allow precipitation of a phase which is actually undersaturated. This calculation of thermodynamic reaction state is done as part of the NETPATH approach by using the geochemical equilibrium model WATEQ.

The last two columns in Table 7-1 list the results of the mass balance modeling. For Transect 1, Well 1 is without a chemical analysis and no information is available regarding the location of the well screen, so the inverse method of modeling cannot include that well. The age correction

for recharge to the third well is done using the detailed chemical and isotopic data for Wells 2 and 3. In NETPATH this represents a simulation of chemical changes from the soil zone to Well 2, then accounts for the chemical and isotope changes from Well 2 to Well 3. The estimated age for this reaction path is 16,749 years before present and is a correction from the measured carbon-14 value of 21,260 years before present (Table 7-1). The reactions included in this correction are calcite and carbon dioxide dissolution, ion exchange with calcium, magnesium, sodium and oxidation of lignite.

The model is thermodynamically valid, as it was constrained to provide results only if the computed  $\delta^{13}\text{C}$  of the water matched the measured  $\delta^{13}\text{C}$  at Well 3, and the carbon changes were accounted for by reactions with the identified minerals. The result was an accurate accounting of the change in composition between wells, or the computed  $\delta^{13}\text{C}$  matched the measured  $\delta^{13}\text{C}$  of total dissolved carbon. The correction to a younger age by little more than 20 percent was required, but it was done with exact accounting of the chemical and isotopic compositional changes that are impacting the age correction to any significant degree.

The same procedure was followed for the second transect, though because of the well selection, there are no wells for this transect close enough to the Carrizo-Wilcox Aquifer outcrop, which is needed to better define the recharge circumstances. To circumvent this, the simplified calcite correction method was used for the initial portion of the flowpath from outcrop to Well 5, and then NETPATH was used from Well 5 to Well 9, modeling each well pair in sequence. All computed adjusted ages are given in Table 7-1; all simulations were done using the same constraints as for transect 1 with the exception of adjusting the  $\delta^{13}\text{C}$  of calcite down the flowpath to 2.0 ‰ from 0.0 ‰ to account for changes in carbonate isotope content as the result of dissolution and recrystallization as discussed in Plummer and others (1990).

The success of inverse modeling depends directly on the accuracy and representativeness of the chemical compositions and on selection of the appropriate minerals and phases affecting solute mass transfer. The number of potential models of the system may be numerous; however, they are narrowed by judiciously using thermodynamic and isotopic constraints. For example, phases such as feldspars and quartz will not precipitate from groundwater of intermediate pH in this environment except in minor quantities under a narrow set of circumstances; similarly, clay minerals are extremely insoluble at intermediate pH values. Hydrocarbon gas chemical and isotopic compositions are useful in identifying methanogenesis, and sulfur isotope analyses can identify sulfur sources. These analyses were not available; therefore, these processes were not included in the modeling for the Northeast Transect.

Uncertainties in this process include the possibility of mixing with water from unaccounted for surface water bodies and contamination from unidentified anthropogenic activities. Based on the available data, the observed carbon-14 values were corrected to on average, ages about 25 percent younger, using the mass balance approach, whereas the simplified calcite adjustment was inconsistent in the correction and seemed to overcorrect to an average adjustment of about 40 percent because of omission of important reactions in the aquifer impacting the carbon accounting.

## **Discussion**

The geochemical composition of groundwater in each aquifer in the Northeast Transect is one of three types. In the Carrizo-Wilcox Aquifer and the Sparta Aquifer, the water evolves from a calcium-magnesium-chloride-sulfate-bicarbonate water to a sodium-bicarbonate water as the

water flows from the outcrop to the confined section. In the Queen City Aquifer, production is from the outcrop and chemistry of the water is a calcium-magnesium-chloride-sulfate-bicarbonate type. The chemistry indicates a recharge outcrop setting. In the Yegua Formation of the Yegua-Jackson Aquifer, the waters are from the outcrop and are a sodium mixed anion type. The Yegua Formation waters are chemically different than the underlying aquifers.

Because the chemical compositions of each aquifer are explainable by intra aquifer rock water reactions (based on Piper diagrams and cross plots) there are no anomalous chemical signatures indicating cross-formational leakage from one formation into the other. The chemistry within the Carrizo-Wilcox Aquifer shows a chemical evolution from calcium-magnesium-chloride-sulfate waters in the outcrop to a sodium-bicarbonate water downdip. Although there is some overlap in the Piper diagrams for each water-bearing unit, no cross-formational water from another aquifer is needed to explain its chemistry. The same is true for the Sparta Aquifer where a sodium-bicarbonate water has developed. In the Queen City Aquifer, where production is in the outcrop, the waters have an “outcrop” type signature, and not a sodium-bicarbonate type water if there was cross-formational flow from either the overlying Sparta Aquifer or the underlying Carrizo-Wilcox Aquifer. The Yegua Formation of the Yegua-Jackson Aquifer, has a chemical signature different than the other aquifers underlying it; therefore there is no chemical evidence of cross-formational flow to the Yegua Formation of the Yegua-Jackson Aquifer. The carbon-14 corrected ages increase from younger ages in the outcrop to older ages in the subsurface. The corrected ages are as old as 20,000 years before present.

**Table 7-1. Summary of results for groundwater age estimates.**

<b>Model Well No.</b>	<b>TWDB Well No.</b>	<b>Well Depth (ft)</b>	<b>Aquifer<sup>(1)</sup></b>	<b>Cl (mg/L)</b>	<b>Alk (mg/L)<sup>(2)</sup></b>	<b><math>\delta^{13}\text{C}</math> ‰ (DIC)</b>	<b><sup>14</sup>C<sub>OBS</sub> (pmc)</b>	<b><sup>14</sup>C<sub>OBS</sub> (ybp)</b>	<b><sup>14</sup>C<sub>ADJ</sub> (ybp)<sup>(3)</sup> <i>Pearson &amp; White (1969) All Wells</i></b>	<b><sup>14</sup>C<sub>ADJ</sub> (ybp) <i>Mass Balance Transect 1</i></b>	<b><sup>14</sup>C<sub>ADJ</sub> (ybp) <i>Mass Balance Transect 2</i></b>
1	3449103	260	CWx			-15.6	24.22	11,390	9,394	-	-
2	3449806	445	CWx	38	192	-12.9	32.13	9,120	5,597	-	-
3	3802302	1,206	CWx	142	343	-8.1	7.09	21,260	13,999	16,749	-
4	3803701	1,163	CWx	13	293	-9.0	10.82	17,860	11,464	<sup>(4)</sup>	-
5	3811102	842	CWx	23	80	-14.1	24.71	11,230	8,422	-	8,422
6	3811603	1,550	CWx	3	174	-8.7	9.58	18,840	12,153	-	13,841
7	3819303	1,700	CWx	11	316	-4.7	9.28	19,100	7,467	-	15,283
8	3820604	1,840	CWx	80	710	-3.0	5.42	23,420	8,180	-	15,994
9	3821705	1,810	CWx	80	810	-1.3	3.11	27,890	5,883	-	20,245
10	3834104	190	QC	45.0	236	-15.1	9.58	18,840	14,820	<sup>(4)</sup>	-
11	3598 <sup>(5)</sup>	380	CWx	12.6	34	-18.6	67.48	3,160	2,582	<sup>(4)</sup>	-
12	3654303	691	CWx	38.5	640	-7.2	5.74	22,960	14,753	<sup>(4)</sup>	-
13	3665 <sup>(5)</sup>	640	CWx	27.0	540	-6.3	6.84	21,550	12,200	<sup>(4)</sup>	-
14	3666 <sup>(5)</sup>	482	CWx	34.6	181	-15.5	32.94	8,920	6,890	<sup>(4)</sup>	-

NOTES:

(1) CWx is the Carrizo-Wilcox Aquifer; QC is the Queen City Aquifer.

(2) Alk is the alkalinity as CaCO<sub>3</sub>.

(3) Correction made after Kreitler and Wuerch (1981) using correction factors from Pearson and White (1967).

(4) Wells not consistent with an identified transect in this report.

(5) Sample numbers Kreitler and Wuerch, 1981.

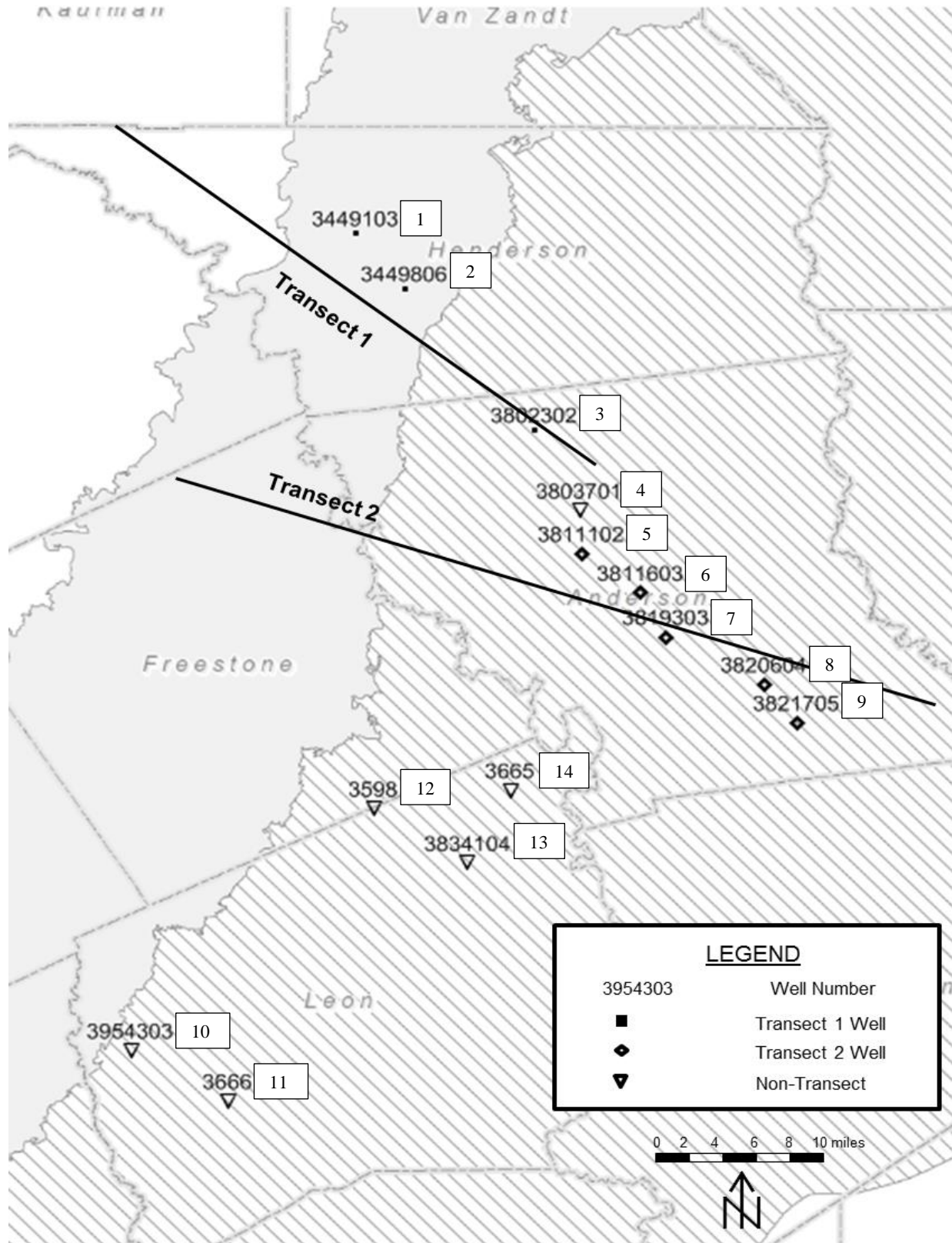


Figure 7-77. Map view of all well locations and Transects 1 and 2 in the Northeast Transect.

Evaluation of Hydrochemical and Isotopic Data in Groundwater Management Areas 11, 12 and 13

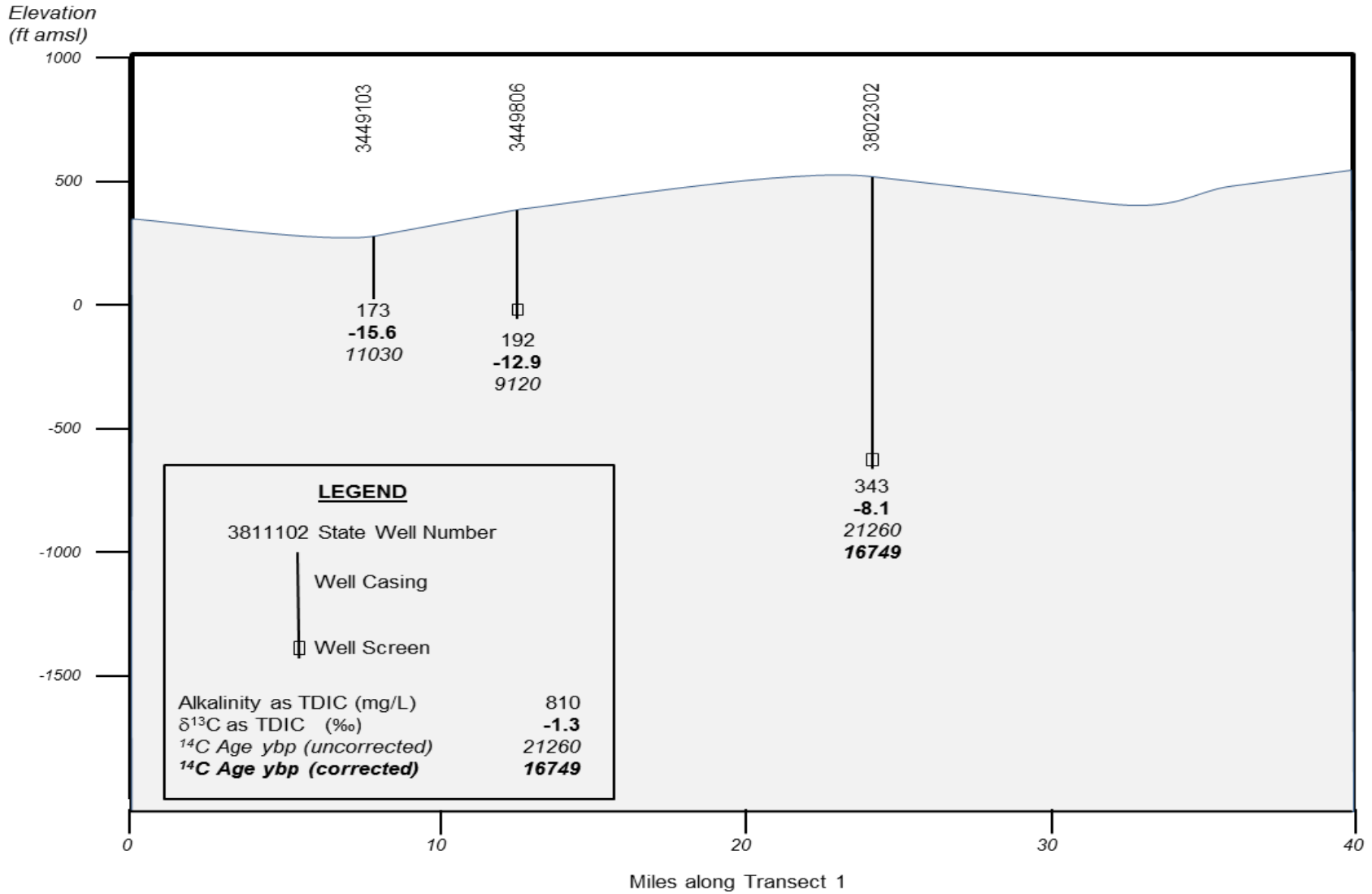


Figure 7-78. Transect 1 from wells in the Carrizo-Wilcox Aquifer outcrop to Well 3.

Evaluation of Hydrochemical and Isotopic Data in Groundwater Management Areas 11, 12 and 13

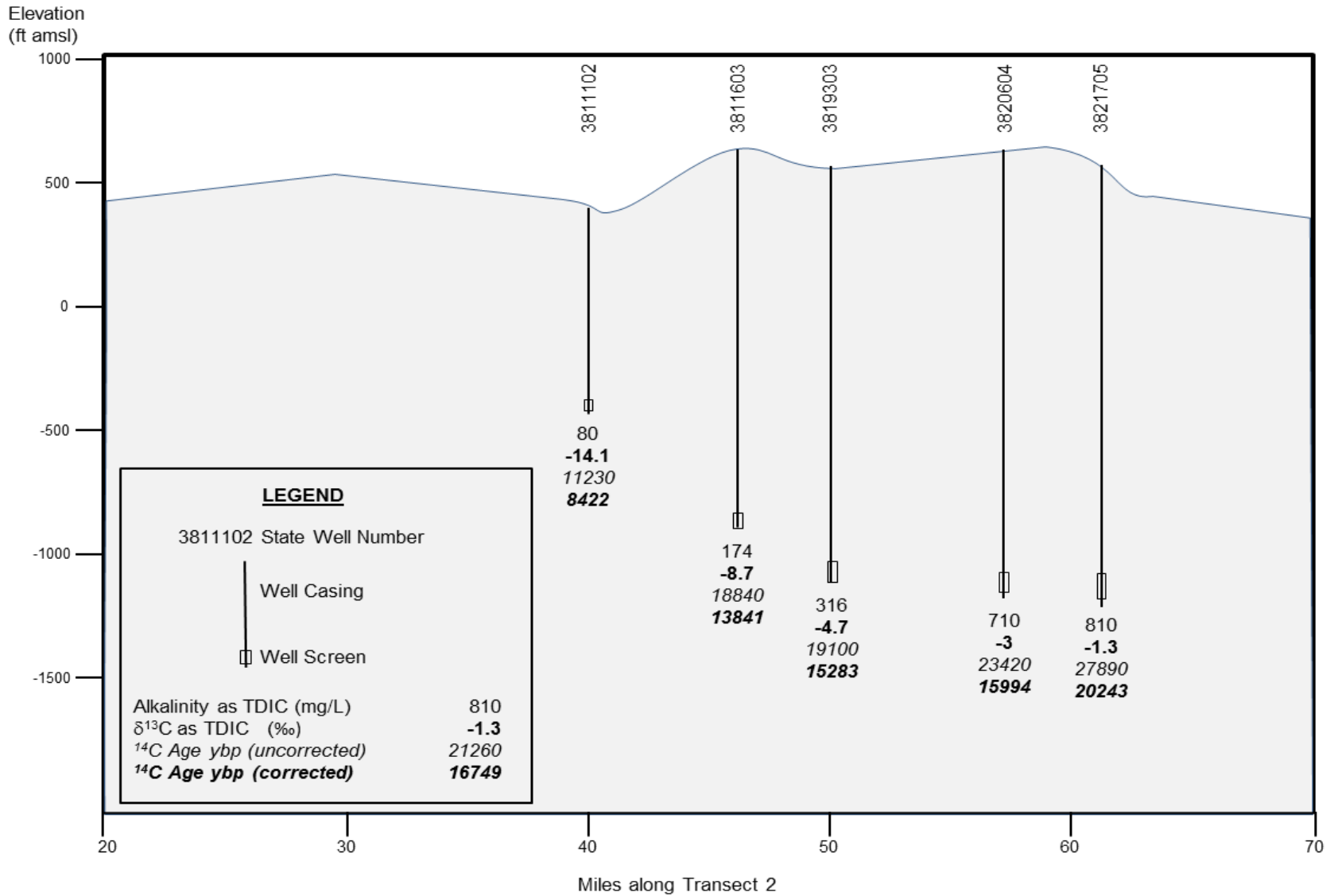


Figure 7-79. Transect 2 from the Carrizo-Wilcox Aquifer outcrop to Wells 5 through 9.

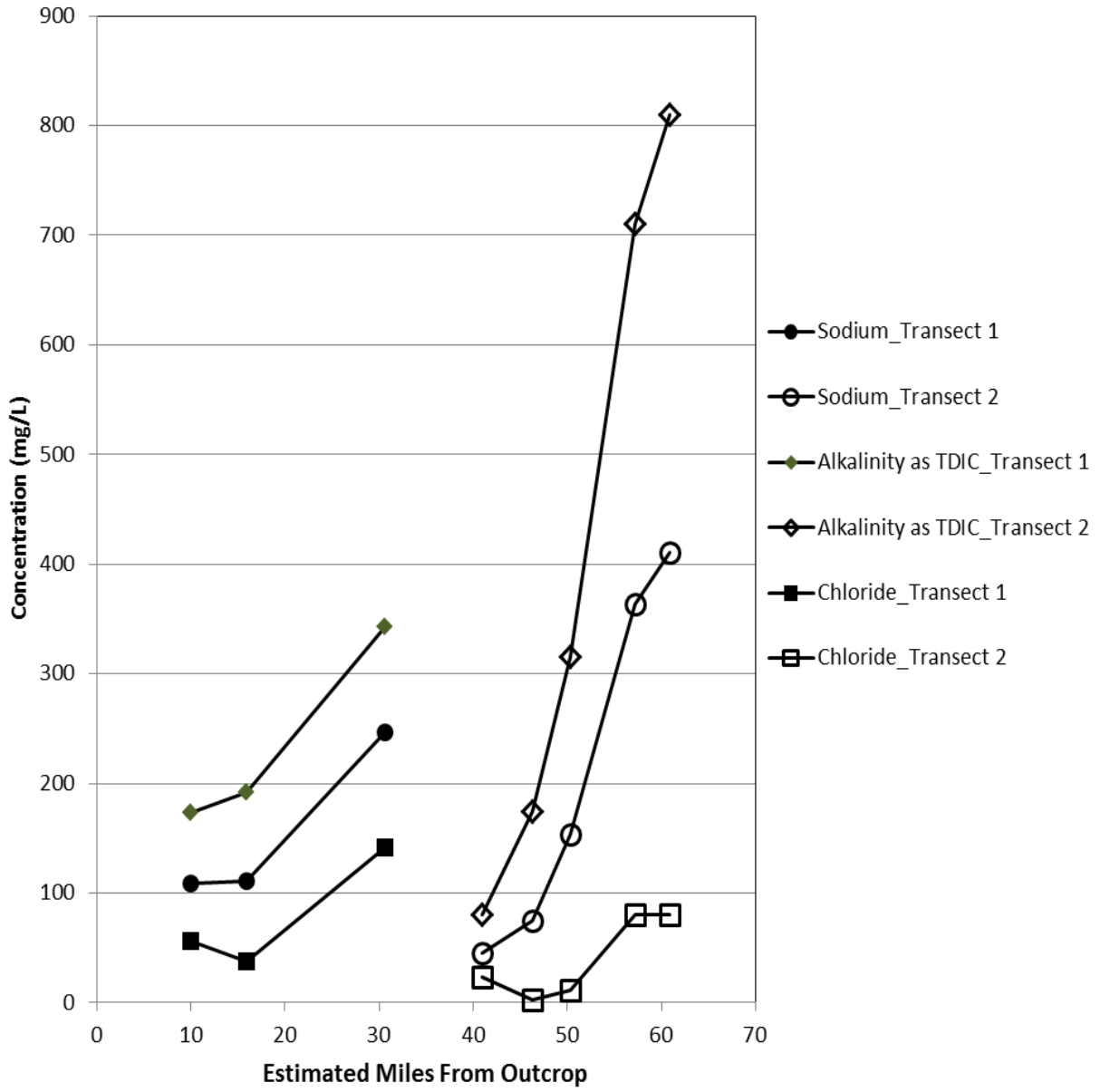


Figure 7-80. Sodium, alkalinity and chloride with distance from the outcrop.

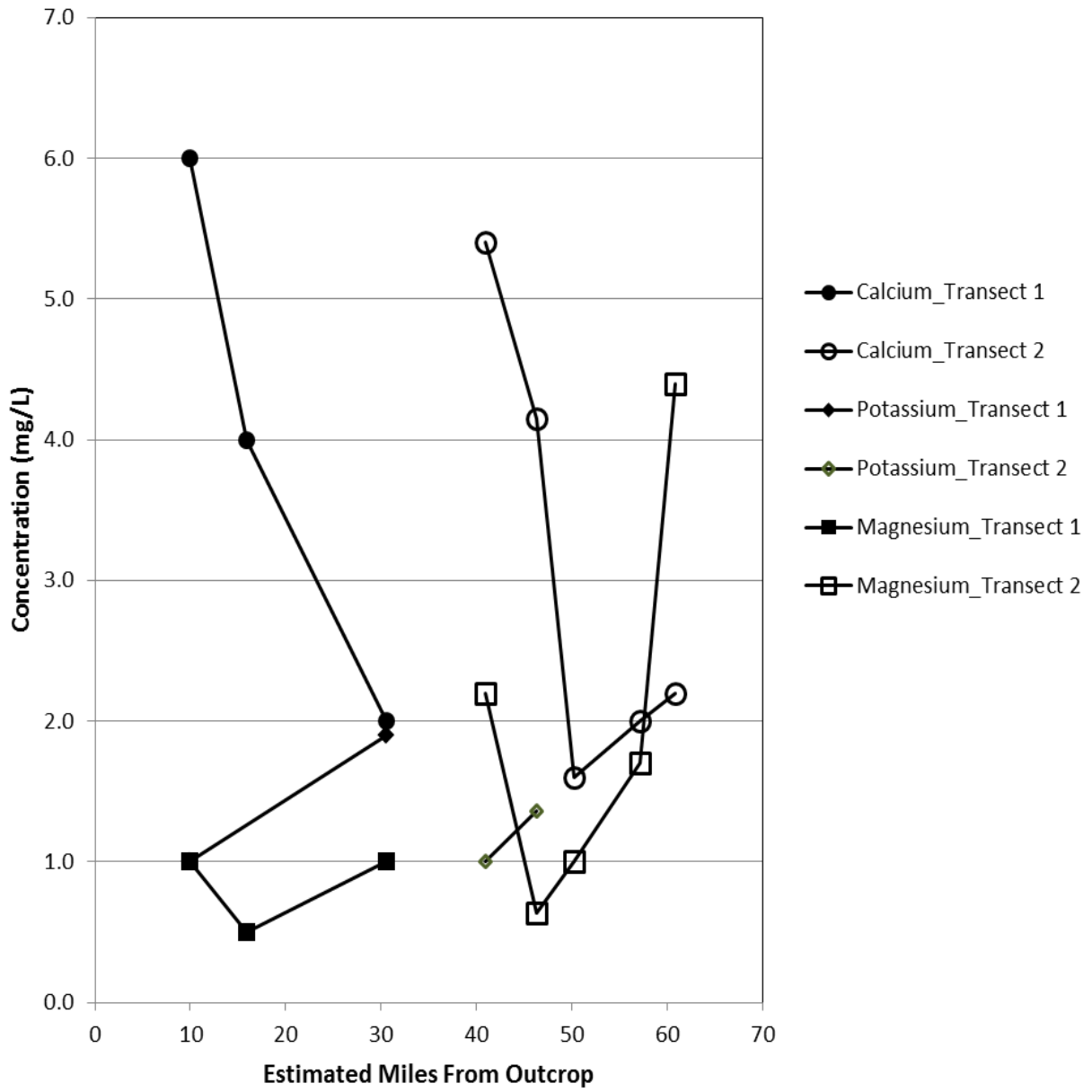


Figure 7-81. Calcium, potassium and magnesium with distance from the outcrop.

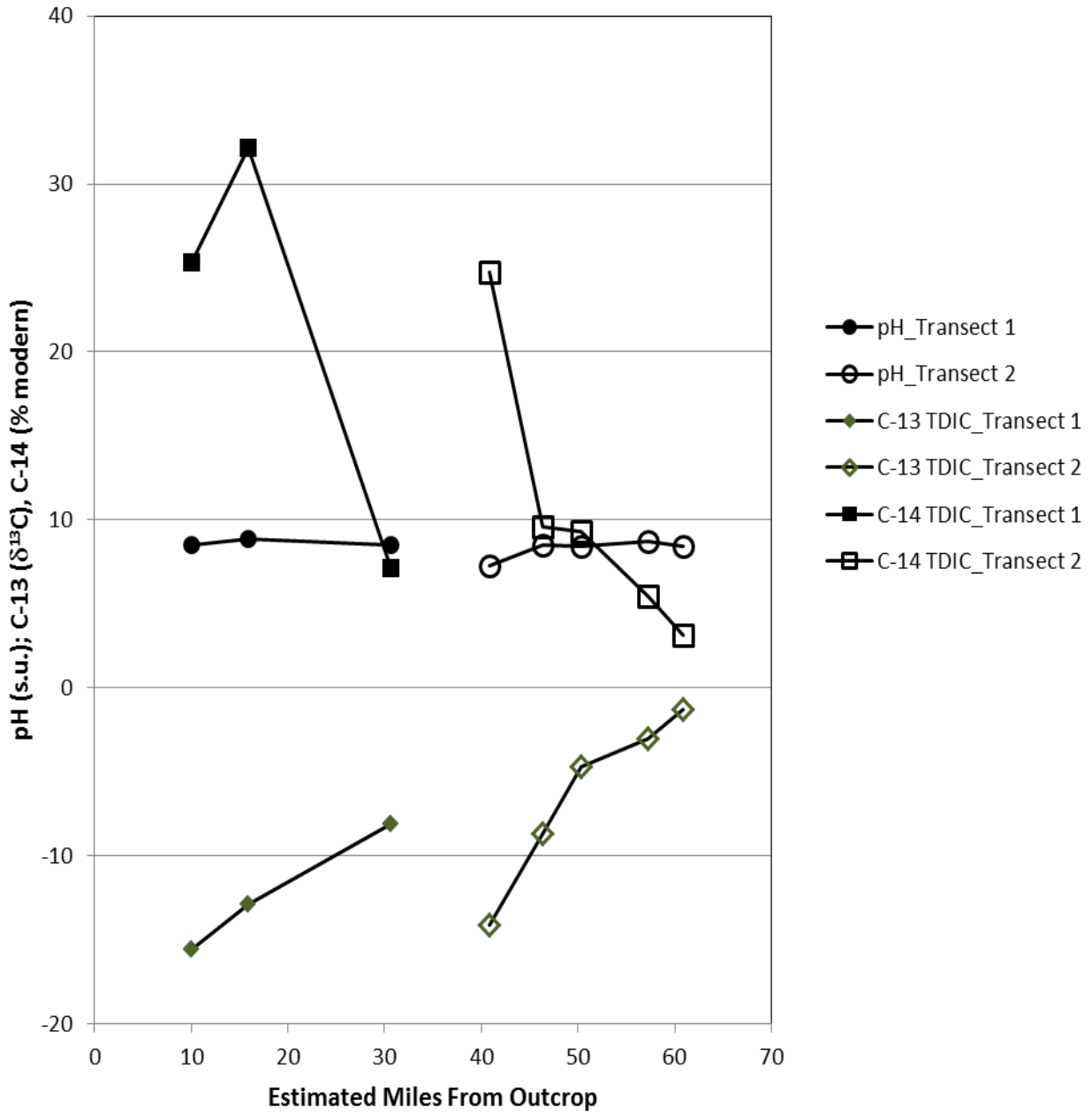


Figure 7-82. pH, carbon-13 and carbon-14 with distance from the outcrop.

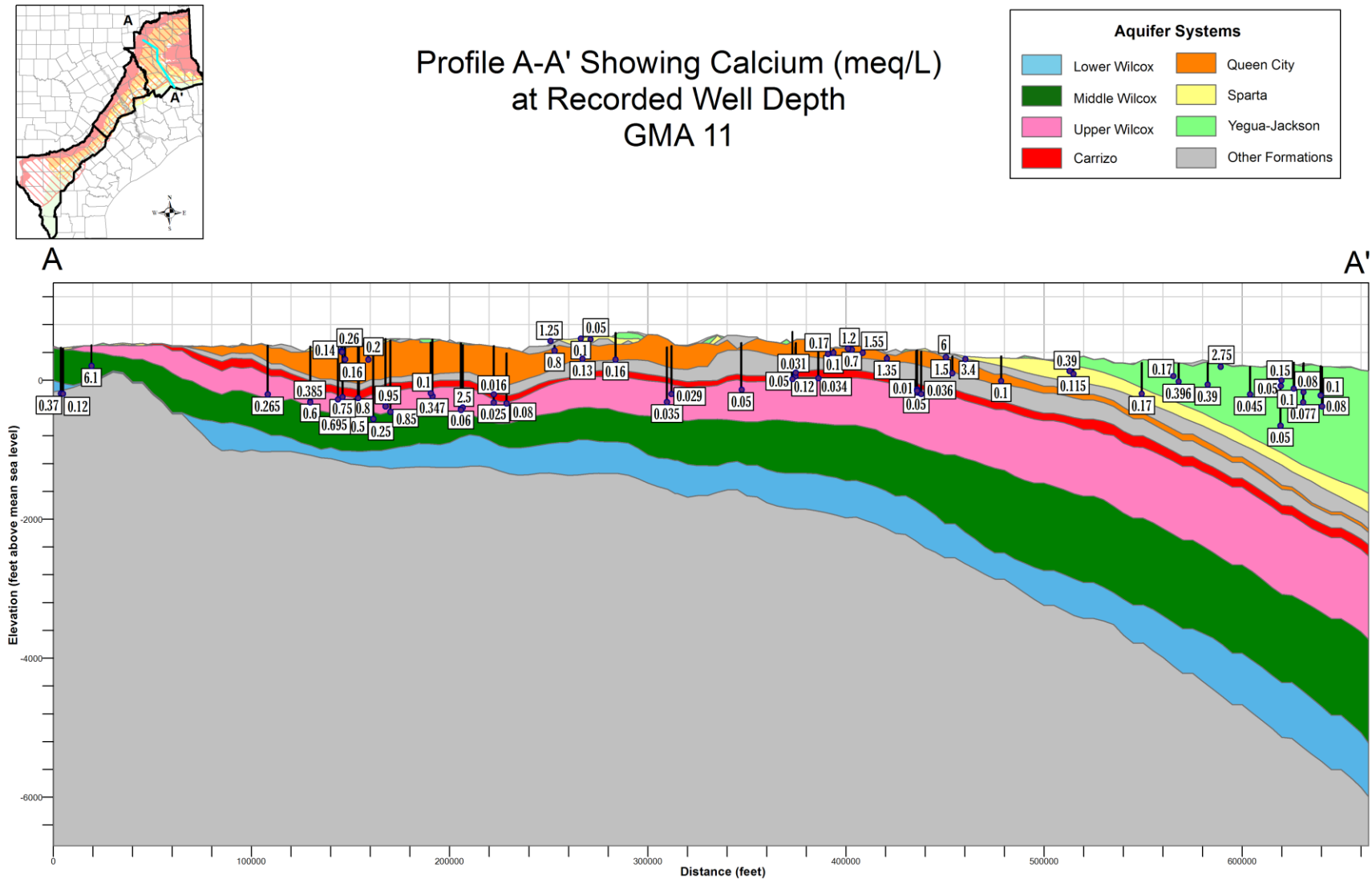


Figure 7-83. Northeast Transect cross section with calcium analytical data measured in milliequivalents per liter (meq/L).

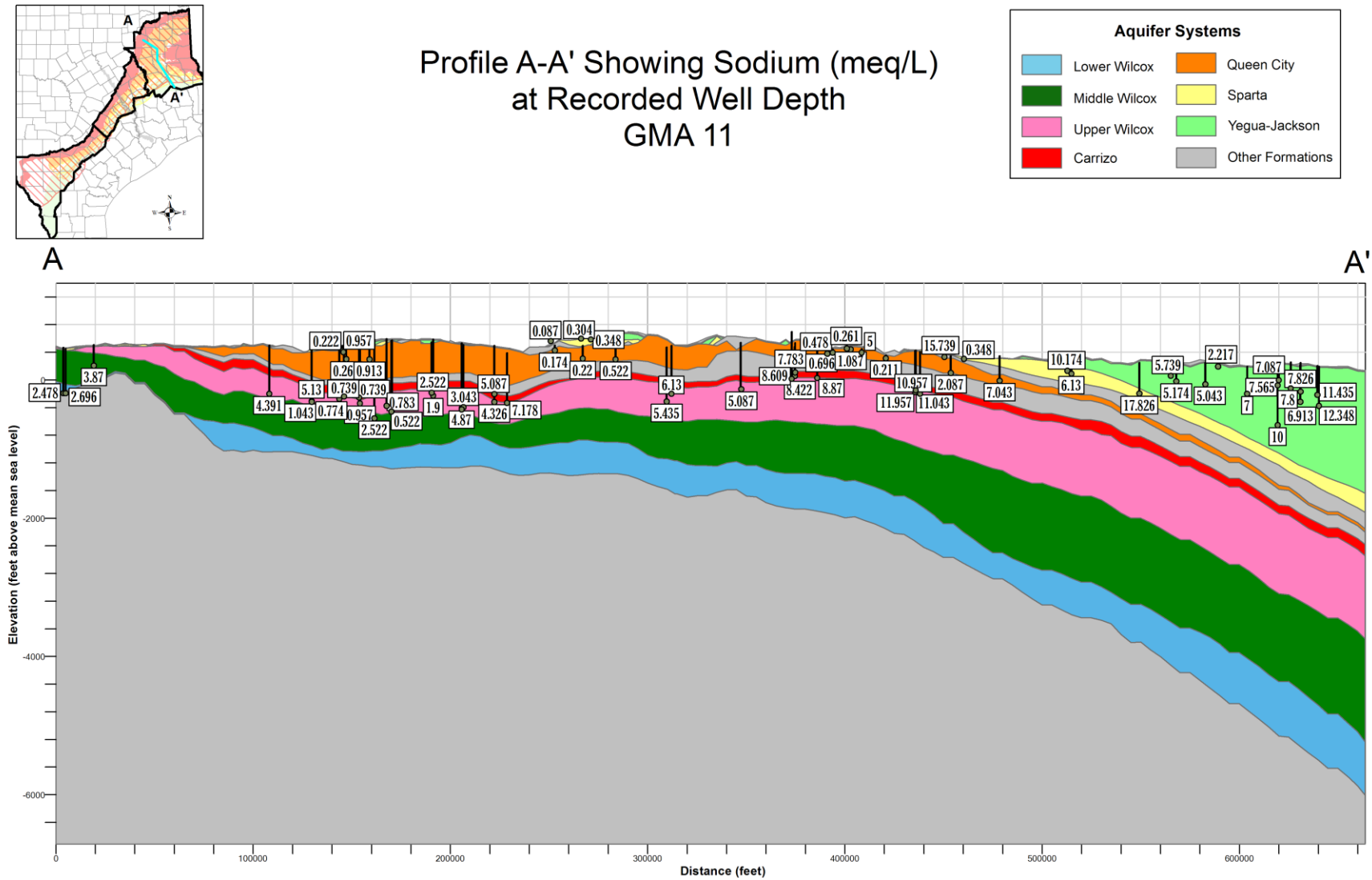
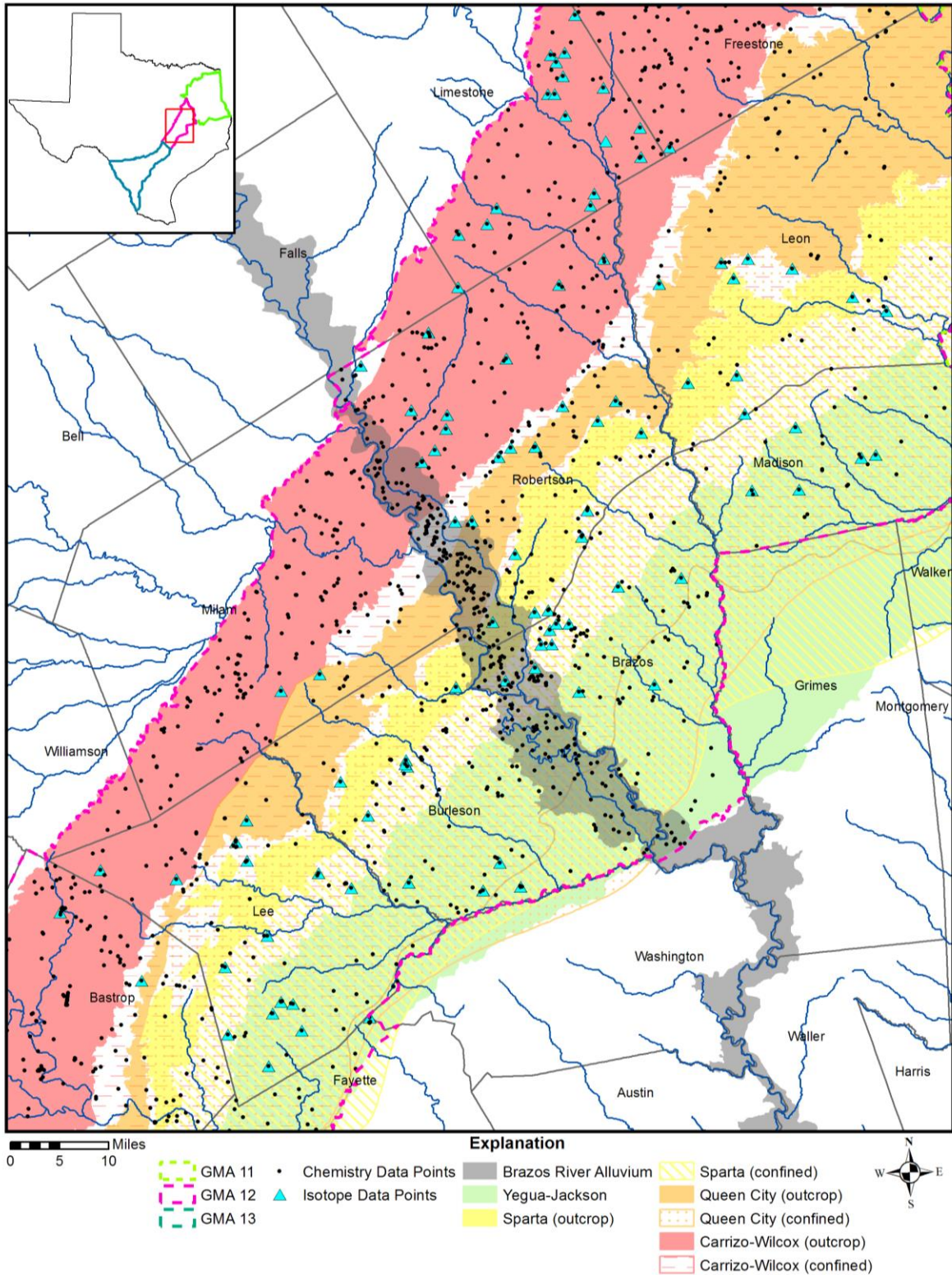


Figure 7-84. Northeast Transect cross section with sodium analytical data measured in milliequivalents per liter (meq/L).

## 7.2 Central Transect

An excellent database from the TWDB groundwater database exists for water wells, water chemistry and water levels in the Carrizo-Wilcox, Queen City, Sparta, Yegua-Jackson and Brazos River Alluvium aquifers in Brazos, Burleson, Milam and Robertson counties. The locations of wells in the TWDB database are shown in Figure 7-86. In addition, twenty-three wells were sampled for this project in 2012 in the Carrizo-Wilcox, Queen City, Sparta, Yegua-Jackson and Brazos River Alluvium aquifers and the Hooper Formation for basic inorganic chemistry, gas chemistry and isotope chemistry. The 2012 chemistry data are in Table 7-2. Locations of the sampled wells are on Figure 7-86. A dip-oriented geologic transect from northwest to southeast with the location of the wells sampled in 2012 is shown in Figure 7-87. The TWDB chemistry data by aquifer are in Appendix A.

A strike-oriented cross section of the Wilcox Group of the Carrizo-Wilcox Aquifer is included in Figure 7-88. In central Texas the Wilcox Group is subdivided into the Calvert Bluff, Simsboro and Hooper formations. The Calvert Bluff Formation is generally considered an aquitard but in outcrop, it may be used for domestic water supply. Similarly the Hooper Formation, the deepest unit in the Wilcox Group, is considered an aquitard, but is occasionally used for water supply where productive sands are found. The major producing section of the Wilcox Group is the middle section, the Simsboro Formation. The sampling of the Wilcox Group in 2012 specifically targeted the Simsboro Formation wells.



**Figure 7-85.** Data distribution of wells with outcrop and downdip extent (up to 3,000 milligrams per liter total dissolved solids) of the Carrizo-Wilcox, Queen City, Sparta, Yegua-Jackson and Brazos River Alluvium aquifers in the Central Transect, Groundwater Management Area (GMA) 12.

Evaluation of Hydrochemical and Isotopic Data in Groundwater Management Areas 11, 12 and 13

**Table 7-2. Chemical and isotopic results from samples collected in Brazos, Burleson, Milam and Robertson counties in 2012.**

Sample Number		BBMR-1	BBMR-2	BBMR-3	BBMR-4	BBMR-5	BBMR-6	
Well Owner		North Milam WSC	Robertson County WSC	Robertson County WSC	City of College Station Col Sta (Carrizo #1)	City of College Station Col Sta (Well #5)	City of College Station Col Sta (Sparta #1)	
Well Number		Well #2	Plant #3	Plant #4				
Well Depth (ft)		315	783	622	1360	2884	540	
Screen Interval * (feet below ground surface)		235-298	680-774	492-612	1120-1340	2364-2862	446-520	
Aquifer		Carrizo-Wilcox	Carrizo-Wilcox	Carrizo-Wilcox	Carrizo	Simsboro	Sparta	
Sample Date		9/11/2012	8/29/2012	8/29/2012	9/20/2012	9/20/2012	9/20/2012	
<b>Stabilized Field Readings</b>		<b>Units</b>						
Temp	°C	23.6	26.2	26.8	29.9	41.7	25.2	
pH		7.56	7	7.32	8.49	8.43	8.95	
Conductivity	µS	700.00	373	335	1442	825	315	
<b>SAT Lab Results: Analyte</b>		<b>Units</b>						
General Chemistry	Total Alkalinity	mg/L	312	104	128	660	320	132.0
	HS <sup>-</sup> (Bisulfide ion)	mg/L	<0.050	<0.050	<0.050	<0.050	<0.050	0.98
	Bromide	mg/L	<0.500	<0.500	<0.500	<0.500	<0.500	<0.500
	Hydrogen Sulfide	mg/L	<0.050	<0.050	<0.050	<0.050	<0.050	0.14
	Fluoride	mg/L	<0.100	0	0.157	0.751	0.278	0.263
	Chloride	mg/L	40	50	24.7	82	40.3	12.6
	Nitrite as N	mg/L	<0.50	<0.50	<0.50	<0.50	<0.50	<0.50
	Nitrate as N	mg/L	<0.50	<0.50	<0.50	<0.50	<0.50	<0.50
	TOC	mg/L	4	2	<1.00	7.40	20.80	4.70
	Sulfate	mg/L	13	17	10.2	<0.50	17.6	<0.50
	Specific Conductance	µmhos/cm	687	419	382	1440	808	310
	TDS	mg/L	407	256	212.0	894.0	516	186
	pH	pH units	8	7	7.25	8.3	7.81	8.83
	pH @ Temperature	°C	12	17	17	15	15	16
	Calcium	mg/L	100	32	31.60	1.76	2.88	<1.00
	Iron	mg/L	1	3	0.811	<0.050	<0.050	<0.050
Magnesium	mg/L	7	6	5.82	<0.500	<0.500	<0.500	
Potassium	mg/L	3	3	4.73	2.32	2.04	<1.00	
Sodium	mg/L	31	25	21.5	354	182	64.8	
<b>Zymax Lab Results: Analyte</b>		<b>Units</b>						
Fixed Gas	O <sub>2</sub> + Ar	% Volume	23.2	12.7	13.8	10.3	14.3	10.4
	N <sub>2</sub>	% Volume	73.6	82.6	84	59.6	84.6	47.8
	CH <sub>4</sub>	% Volume	<0.1	<0.1	<0.1	29.5	0.6	41.8
	CO	% Volume	<0.1	<0.1	<0.1	<0.1	<0.1	<0.1
	CO <sub>2</sub>	% Volume	3.2	4.7	2.3	0.6	0.5	<0.1
<sup>14</sup> C Gas in headspace	C1	ppmv	236.5	23.3	24	See Fixed	See Fixed	See Fixed
	C2	ppmv	5.4	13.2	11.4	188.2	3	213.1
	C3	ppmv	4.2	2.4	2	35.7	4.5	<1.0
	i-C4	ppmv	<1.0	<1.0	<1.0	<1.0	<1.0	<1.0
	n-C4	ppmv	2.7	1.5	1.1	11.5	2.2	<1.0
	i-C5	ppmv	<1.0	<1.0	<1.0	<1.0	<1.0	<1.0
	n-C5	ppmv	<1.0	<1.0	<1.0	<1.0	<1.0	<1.0
Gas in water	C1	µg/L	13.8	1.5	1.3	6078.9	104.2	15,734.2
	C2	µg/L	<1.0	<1.0	<1.0	<1.0	<1.0	14.1
Isotope analysis	C3	µg/L	<1.0	<1.0	<1.0	<1.0	<1.0	<1.0
	δ <sup>13</sup> C <sub>C01</sub>	‰ VPDB	-49.8	ND <sup>2</sup>	ND	-61.6	-54.7	-50.4
	δ <sup>13</sup> C <sub>C02</sub>	‰ VPDB	-15.6	-21.2	-19.1	-14.3	-13.7	ND
	δ <sup>13</sup> C <sub>C03</sub>	‰ VPDB	ND	ND	ND	ND	ND	ND
	δD <sub>C1</sub>	‰ VSMOW	ND	ND	ND	-259	-287	-194
	δD <sub>C2</sub>	‰ VSMOW	ND	ND	ND	ND	ND	ND
	δ <sup>18</sup> O <sub>H2O</sub>	‰ VSMOW	-4.6	-4.8	-4.8	-5.1	-5.2	-5.3
δD <sub>H2O</sub>	‰ VSMOW	-26.1	-26.4	-27.2	-29	-29.8	-29.5	
<b>Beta Lab Results: Analyte</b>		<b>Units</b>						
Radiometric Analysis	Apparent <sup>14</sup> C Age	YBP	2,950	8,920	14,330	41,870	37,830	16,490
	Apparent Age Error	+/- yrs	30	40	60	400	270	60
	<sup>13</sup> C/ <sup>12</sup> C Ratio	‰	-11.2	-19.7	-16.1	-12.3	-5.4	-10.2
	Fraction Modern	%	69.3%	32.9%	16.8%	0.5%	0.9%	12.8%
Fm <sub>dn</sub> Error	+/- %	0.25%	0.16%	0.12%	0.03%	0.03%	0.09%	
<b>U. of AZ Lab Results: Analyte</b>		<b>Units</b>						
Sulfate Isotope	δ <sup>34</sup> S	‰	3.2	-1.1	3.1	9.4	27	Insufficient SO <sub>4</sub>
	δ <sup>18</sup> O (SO <sub>4</sub> )	‰	11.9	16	16.6	None Left	14.8	Insufficient SO <sub>4</sub>

1) Represents top of highest screen interval to bottom of lowest screen interval.  
 ND = Target component's concentration too low to obtain reliable isotope data.

<sup>2</sup> = Laboratory Note: Estimate for target components at low concentrations

<sup>3</sup> = Laboratory Note: Estimate due to low concentration, 3xSTDEV applies

<sup>4</sup> = Laboratory Note: Qualitative measure of hydrocarbon gas during isotope analysis

Evaluation of Hydrochemical and Isotopic Data in Groundwater Management Areas 11, 12 and 13

**Table 7-2. Chemical and isotopic results from samples collected in Brazos, Burleson, Milam and Robertson counties in 2012 (Continued).**

Sample Number		BBMR-7	BBMR-8	BBMR-9	BBMR-10	BBMR-11	BBMR-12	
Well Owner		Clay WSC	Brazos Valley Septic &	D&S Water Co. Lakewood	City of Snook	Texas A&M University	Texas A&M University	
Well Number		Clay WSC Well #1	Water Inc. (Smetana)	Estates (Well #2)	Well #3	Well #7	Well #A7	
Well Depth (ft)		513	730	458	1310	3018	3060	
Screen Interval <sup>1</sup> (feet below ground surface)		468-502	710-730	378-438	144-1284	2490-3010	2742-2990	
Aqualifer		Jackson Group	Queen City	Queen City	Sparto	Simsboro	Simsboro	
Sample Date		9/13/2012	9/20/2012	9/20/2012	9/13/2012	9/18/2012	9/18/2012	
Stabilized Field Readings		Units						
Temp	°C	28.4	26.8	23.8	31.4	42.8	46.2	
pH		7.53	8.31	7.1	8.7	8.27	8.23	
Conductivity	µS	2190	off scale	395	514	865	1056	
SAT Lab Results: Analyte		Units						
General Chemistry	Total Alkalinity	mg/L	580.0	900	96	148	340.0	480
	HS <sup>-</sup> (Bisulfide ion)	mg/L	<0.050	<0.050	<0.050	<0.050	<0.050	<0.050
	Bromide	mg/L	1.44	<0.500	<0.500	<0.500	<0.500	<0.500
	Hydrogen Sulfide	mg/L	<0.050	<0.050	<0.050	<0.050	<0.050	<0.050
	Fluoride	mg/L	1.36	0.806	<0.100	0.311	0.369	<0.100
	Chloride	mg/L	434	132	38.3	33.9	39.5	51.4
	Nitrite as N	mg/L	<0.50	<0.50	<0.50	<0.50	<0.50	<0.50
	Nitrate as N	mg/L	<0.50	<0.50	<0.50	<0.50	<0.50	<0.50
	TOC	mg/L	17.40	3.90	16.90	17.5	9.10	7.1
	Sulfate	mg/L	<0.50	<0.50	28.7	35.2	14.2	<0.50
	Specific Conductance	µmhos/cm	2440	2070	411	505	829	1010
	TDS	mg/L	1440	1260	254	468	520	638
	pH	pH units	7.54	8.36	7.17	8.55	8.3	8.22
	pH @ Temperature	°C	9.6	17	18	9.5	13	13
	Calcium	mg/L	35.5	4.35	4.41	<1.00	3.08	2.97
Iron	mg/L	<0.050	<0.050	0.348	0.14	<0.050	0.132	
Magnesium	mg/L	0.749	1.34	2.1	<0.500	<0.500	<0.500	
Potassium	mg/L	29.6	3.82	3.41	1.23	2.59	3.44	
Sodium	mg/L	558	548	67.8	112	180	210	
Zymax Lab Results: Analyte		Units						
Fixed Gas	O <sub>2</sub> + Ar	% Volume	7.1	9.7	12.5	14.4	15.4	14.4
	N <sub>2</sub>	% Volume	48	85.9	84.5	85.4	82.5	74.3
	CH <sub>4</sub>	% Volume	40.1	3	<0.1	<0.1	1.3	10.6
	CO	% Volume	<0.1	<0.1	<0.1	<0.1	<0.1	<0.1
	CO <sub>2</sub>	% Volume	4.8	1.4	3.1	0.2	0.8	0.7
Gas in headspace	C1	ppmv	See Fixed	See Fixed	See Fixed	132.1	See Fixed	See Fixed
	C2	ppmv	77.8	16.8	<1.0	10.3	7	70.6
	C3	ppmv	7.8	7.7	<1.0	5.8	4.7	14.4
	i-C4	ppmv	<1.0	<1.0	<1.0	<1.0	<1.0	<1.1
	n-C4	ppmv	7	5.3	<1.0	3.1	4.2	5.5
Gas in water	i-C5	ppmv	<1.0	<1.0	<1.0	<1.0	<1.0	<1.0
	n-C5	ppmv	<1.0	<1.0	<1.0	<1.0	<1.0	<1.0
	C1	µg/L	98,656.1	540.3	5.1	9.1	228.7	4300.2
	C2	µg/L	1	<1.0	<1.0	<1.0	<1.0	1.1
	C3	µg/L	<1.0	<1.0	<1.0	<1.0	<1.0	<1.0
Isotope analysis	δ <sup>13</sup> C <sub>C1</sub>	‰ VPDB	-70.2	-55.6	ND	ND	-55.1	-55.4
	δ <sup>13</sup> C <sub>CO2</sub>	‰ VPDB	-19.8	-17.6	-27.9	-22.1	-13.5	-13.3
	δ <sup>13</sup> C <sub>C2</sub>	‰ VPDB	ND	ND	ND	ND	ND	ND
	δD <sub>C1</sub>	‰ VSMOW	-211.2	-280	ND	ND	-302	-305
	δD <sub>C2</sub>	‰ VSMOW	ND	ND	ND	ND	ND	ND
	δ <sup>18</sup> O <sub>H2O</sub>	‰ VSMOW	-4.7	-5	-4.6	-4.9	-5.1	-5
δD <sub>H2O</sub>	‰ VSMOW	-24.3	-27.6	-26.9	-26.4	-29	-27.8	
Beta Lab Results: Analyte		Units						
Radiometric Analysis	Apparent <sup>14</sup> C Age	YBP	> 43,500	35,050	11,200	27,640	25,320	> 43,500
	Apparent Age Error	+/- yrs	0	210	50	140	130	
	<sup>13</sup> C/ <sup>12</sup> C Ratio	‰	-15.2	-17.2	-14.9	-17.4	-11.2	-9.3
	Fraction Modern	%	0.0%	1.3%	24.8%	3.2%	4.3%	0.0%
	Fmdn Error	+/- %	0.00%	0.03%	0.15%	0.06%	0.07%	0.00%
U. of AZ Lab Results: Analyte		Units						
Sulfate Isotope	δ <sup>34</sup> S	‰	Insufficient SO <sub>4</sub>	Insufficient SO <sub>4</sub>	17.2	4	27.4	11.2
	δ <sup>18</sup> O (SO <sub>4</sub> )	‰	Insufficient SO <sub>4</sub>	Insufficient SO <sub>4</sub>	17.5	13.1	15.5	None Left

1) Represents top of highest screen interval to bottom of lowest screen interval.  
 ND = Target component's concentration too low to obtain reliable isotope data.

<sup>a</sup> = Laboratory Note: Estimate for target components at low concentrations

<sup>b</sup> = Laboratory Note: Estimate due to low concentration, 3xSTDEV applies

<sup>c</sup> = Laboratory Note: Qualitative measure of hydrocarbon gas during isotope analysis

Evaluation of Hydrochemical and Isotopic Data in Groundwater Management Areas 11, 12 and 13

**Table 7-2. Chemical and isotopic results from samples collected in Brazos, Burleson, Milam and Robertson counties in 2012 (Continued).**

	Sample Number	BBMR-13	BBMR-14	BBMR-15	BBMR-16	BBMR-17	BBMR-18
	Well Owner	City of Calvert	City of Hearne	City of Bryan	City of Bryan	Brushy WSC	City of Rockdale
	Well Number	Well #4 - Seifert Well	Well #2 San Antonio	Bryan Well #18	Bry Station (Well #4)	Brushy Well #2	Well #10
	Well Depth (ft)	738	1433	2770	2938	3380	380
	Screen Interval <sup>1</sup> (feet below ground surface)	633-738	1260-1418	1418	2416-2918	3120-3360	238-370
	Aquifer	Hooper Fm. <sup>*</sup>	Simsboro	Simsboro	Simsboro	Simsboro	Simsboro
	Sample Date	9/11/2012	9/11/2012	8/29/2012	8/29/2012	9/18/2012	9/11/2012
<b>Stabilized Field Readings</b>		<b>Units</b>					
	Temp	°C	27.8	33.7	41.6	43.2	> 50
	pH		8.3	8.5	8.34	8.33	8.13
	Conductivity	µS	1305	782.0	838	828	off scale
<b>SAT Lab Results: Analyte</b>		<b>Units</b>					
General Chemistry	Total Alkalinity	mg/L	600.0	360	360	324	740.0
	HS <sup>-</sup> (Bisulfide ion)	mg/L	<0.050	<0.050	<0.050	<0.050	<0.050
	Bromide	mg/L	<0.500	<0.500	<0.500	<0.500	<0.500
	Hydrogen Sulfide	mg/L	<0.050	<0.050	<0.050	<0.050	<0.050
	Fluoride	mg/L	<0.100	<0.100	0.337	0.342	1.72
	Chloride	mg/L	94.7	40.5	47.7	46.8	109
	Nitrite as N	mg/L	<0.50	<0.50	<0.50	<0.50	<0.50
	Nitrate as N	mg/L	<0.50	<0.50	<0.50	<0.50	<0.50
	TOC	mg/L	5.20	4.10	3.00	2.8	25.00
	Sulfate	mg/L	<0.50	0.84	60.9	14.7	<0.50
	Specific Conductance	µmhos/cm	1280	755	918	888	1760
	TDS	mg/L	735	442	504	515	922
	pH	pH units	8.42	8.44	8.49	8.43	8.22
	pH @ Temperature	°C	12	12	17	17	18
	Calcium	mg/L	3.53	2.56	3.09	2.78	2.28
Iron	mg/L	<0.050	<0.050	<0.050	<0.050	<0.050	
Magnesium	mg/L	0.933	<0.500	<0.500	<0.500	<0.500	
Potassium	mg/L	3.76	2.12	2.34	2.3	5.92	
Sodium	mg/L	342.0	198	186	193	378	
<b>Zymax Lab Results: Analyte</b>		<b>Units</b>					
Fixed Gas	O <sub>2</sub> + Ar	% Volume	7.6	20.5	12.2	14.6	9.8
	N <sub>2</sub>	% Volume	48.9	79.1	86.1	84	41.1
	CH <sub>4</sub>	% Volume	42.9	<0.1	1.2	0.9	47.3
	CO	% Volume	<0.1	<0.1	<0.1	<0.1	<0.1
	CO <sub>2</sub>	% Volume	0.7	0.4	0.5	0.5	1.8
<sup>13</sup> C Gas in headspace	C1	ppmv	See Fixed	999.4	See Fixed	See Fixed	See Fixed
	C2	ppmv	262.8	6	14.2	11.3	145.0
	C3	ppmv	20	5.1	2.5	2.7	2.1
	i-C4	ppmv	<1.0	<1.0	<1.0	<1.0	<1.0
	n-C4	ppmv	4.9	3.3	1.5	1.9	<1.0
	i-C5	ppmv	<1.0	<1.0	<1.0	<1.0	<1.0
Gas in water	C1	µg/L	15,774.3	84.6	205.7	319.2	12,870.7
	C2	µg/L	1.2	<1.0	<1.0	<1.0	9.6
	C3	µg/L	<1.0	<1.0	<1.0	<1.0	<1.0
Isotope analysis	δ <sup>13</sup> C <sub>C1</sub>	‰ VPDB	-60.2	-53.8	-53.5	-55.0	-52.2
	δ <sup>13</sup> C <sub>C2</sub>	‰ VPDB	-11.4	-13.7	-11.1	-11.3	-6.8
	δ <sup>13</sup> C <sub>C3</sub>	‰ VPDB	ND	ND	ND	ND	ND
	δD <sub>C1</sub>	‰ VSMOW	-294	ND	ND	ND	-295
	δD <sub>C2</sub>	‰ VSMOW	ND	ND	ND	ND	ND
	δ <sup>18</sup> O <sub>H2O</sub>	‰ VSMOW	-5	-5	-5	-5	-5.1
δD <sub>H2O</sub>	‰ VSMOW	-28	-27.4	-29.5	-28.7	-29.1	
<b>Beta Lab Results: Analyte</b>		<b>Units</b>					
Radiometric Analysis	Apparent <sup>14</sup> C Age	YBP	43,070	32,140	> 43,500	39,560	> 43,500
	Apparent Age Error	+/- yrs	520	220		530	30
	<sup>13</sup> C/ <sup>12</sup> C Ratio	‰	-8.2	-11.2	-10.7	-10.5	-6.7
	Fraction Modern	%	0.5%	1.8%	0.0%	0.7%	0.0%
Fmdn Error	+/- %	0.03%	0.05%	0.00%	0.05%	0.00%	
<b>U. of AZ Lab Results: Analyte</b>		<b>Units</b>					
Sulfate Isotope	δ <sup>34</sup> S	‰	8.8	27.3	29.5	29.1	18.5
	δ <sup>18</sup> O (SO <sub>4</sub> )	‰	None Left	None Left	15.8	15.7	None Left

<sup>1</sup> Represents top of highest screen interval to bottom of lowest screen interval.

ND = Target component's concentration too low to obtain reliable isotope data.

<sup>\*</sup> = Hooper Formation of the Comiso-Wilcox aquifer

<sup>a</sup> = Laboratory Note: Estimate for target components at low concentrations

<sup>b</sup> = Laboratory Note: Estimate due to low concentration, 3xSTDEV applies

<sup>c</sup> = Laboratory Note: Qualitative measure of hydrocarbon gas during isotope analysis

**Table 7-2. Chemical and isotopic results from samples collected in Brazos, Burleson, Milam and Robertson counties in 2012 (Continued).**

Sample Number		BBMR-19	BBMR-20	BBMR-21	BBMR-22	BBMR-23	
Well Owner		Texas A&M University	City of Snook	Ramblewood MHP	Texas A&M University	Chance Farm	
Well Number		Well #2	New #2 well	Ramblewood Well #1	Farm Well	TDCJ Buffalo Ranch	
Well Depth (ft)		485	1332	372	72	1506	
Screen Interval <sup>1</sup> (feet below ground surface)		373-473	1278-1311	352-372	52-72	1490-1506	
Aquifer		Sparta	Sparta	Yegua Fm. <sup>*</sup>	Brazos River Alluvium	Sparta	
Sample Date		9/18/2012	9/13/2012	9/18/2012	9/13/2012	9/13/2012	
Stabilized Field Readings		Units					
Temp	°C	25.7	34.7	24.0	meter malfunction	31.1	
pH		8.54	8.52	7.64	7.06	8.40	
Conductivity	µS	1092	812	831	meter malfunction	off scale	
SAT Lab Results: Analyte		Units					
General Chemistry	Total Alkalinity	mg/L	328	284	172	560	380
	HS <sup>-</sup> (Bisulfide ion)	mg/L	0.98	<0.050	<0.050	<0.050	<0.050
	Bromide	mg/L	<0.500	<0.500	<0.500	0.68	<0.500
	Hydrogen Sulfide	mg/L	3.35	<0.050	<0.050	<0.050	<0.050
	Fluoride	mg/L	0.28	0.474	<0.100	0.379	0.531
	Chloride	mg/L	76.6	36.6	114	82.3	127
	Nitrite as N	mg/L	<0.50	<0.50	<0.50	<0.50	<0.50
	Nitrate as N	mg/L	<0.50	<0.50	<0.50	<0.50	<0.50
	TOC	mg/L	6.8	27.10	8.2	<1.00	25.20
	Sulfate	mg/L	72.6	36	52.1	106	257
	Specific Conductance	µmhos/cm	1090	794	851	1430	1870
	TDS	mg/L	614	590	462	954	1170
	pH	pH units	8.53	8.58	7.15	7.06	8.34
	pH @ Temperature	°C	19	9.4	8	9.6	8.7
	Calcium	mg/L	1.06	<1.00	12.5	169	1.23
	Iron	mg/L	<0.050	<0.050	0.203	5.2	0.203
Magnesium	mg/L	<0.500	<0.500	2.24	45.6	<0.500	
Potassium	mg/L	2.56	1.98	5.68	4.76	4.17	
Sodium	mg/L	218	196	170	83.2	430	
Zymax Lab Results: Analyte		Units					
Fixed Gas	O <sub>2</sub> + Ar	% Volume	4.1	19.8	14.3	11.8	14.8
	N <sub>2</sub>	% Volume	86.8	78.5	83.7	74.8	82.7
	CH <sub>4</sub>	% Volume	8.4	1	<0.1	1.2	1.8
	CO	% Volume	<0.1	<0.1	<0.1	<0.1	<0.1
	CO <sub>2</sub>	% Volume	0.6	0.7	2	12.2	0.7
Gas in headspace	C1	ppmv	See Fixed	See Fixed	123.7	See Fixed	See Fixed
	C2	ppmv	101.3	7.8	1.8	6.6	17.3
	C3	ppmv	21.4	6.3	2.9	3.9	5.7
	i-C4	ppmv	<1.0	<1.0	<1.0	<1.1	<1.0
	n-C4	ppmv	4.8	2.5	3.7	6.8	2.4
	i-C5	ppmv	<1.0	<1.0	<1.0	<1.0	<1.0
Gas in water	n-C5	ppmv	<1.0	<1.0	<1.0	<1.0	<1.0
	C1	µg/L	2126.9	294.5	6.1	526.1	279.6
	C2	µg/L	<1.0	<1.0	<1.0	<1.0	<1.0
Isotope analysis	C3	µg/L	<1.0	<1.0	<1.0	<1.0	<1.0
	δ <sup>13</sup> C <sub>C1</sub>	‰ VPDB	-46.6	-60.5	ND	-53.6	-54
	δ <sup>13</sup> C <sub>CO2</sub>	‰ VPDB	-21.3	-12.7	-18.2	-19.9	-19.9
	δ <sup>13</sup> C <sub>C2</sub>	‰ VPDB	ND	ND	ND	ND	ND
	δD <sub>C1</sub>	‰ VSMOW	-272	-327.6	ND	-307.2	-311
	δD <sub>C2</sub>	‰ VSMOW	ND	ND	ND	ND	ND
	δ <sup>18</sup> O <sub>H2O</sub>	‰ VSMOW	-5	-4.9	-4.6	-4.0	-4.9
δD <sub>-20</sub>	‰ VSMOW	-26.6	-26.1	-26.3	-23.1	-27	
Beta Lab Results: Analyte		Units					
Radiometric Analysis	Apparent <sup>14</sup> C Age	YBP	39,770	35,780	14,560	200	42,880
	Apparent Age Error	+/- yrs	380	260	60	30	590
	<sup>13</sup> C/ <sup>12</sup> C Ratio	‰	-17.5	-14.3	-14.5	-15.8	-15.7
	Fraction Modern	%	0.7%	1.2%	16.3%	97.5%	0.5%
	Fmdn Error	+/- %	0.03%	0.04%	0.12%	0.36%	0.03%
U. of AZ Lab Results: Analyte		Units					
Sulfate Isotope	δ <sup>34</sup> S	‰	18.1	4.2	8.6	9.5	5.6
	δ <sup>18</sup> O (SO <sub>4</sub> )	‰	None Left	13.9	15.5	14.2	19.2

<sup>1</sup>) Represents top of highest screen interval to bottom of lowest screen interval.

ND = Target component's concentration too low to obtain reliable isotope data.

<sup>\*</sup> = Yegua Formation of the Yegua-Jackson aquifer

<sup>2</sup> = Laboratory Note: Estimate for target components at low concentrations

<sup>3</sup> = Laboratory Note: Estimate due to low concentration, 3xSTDEV applies

<sup>4</sup> = Laboratory Note: Qualitative measure of hydrocarbon gas during isotope analysis

Evaluation of Hydrochemical and Isotopic Data in Groundwater Management Areas 11, 12 and 13

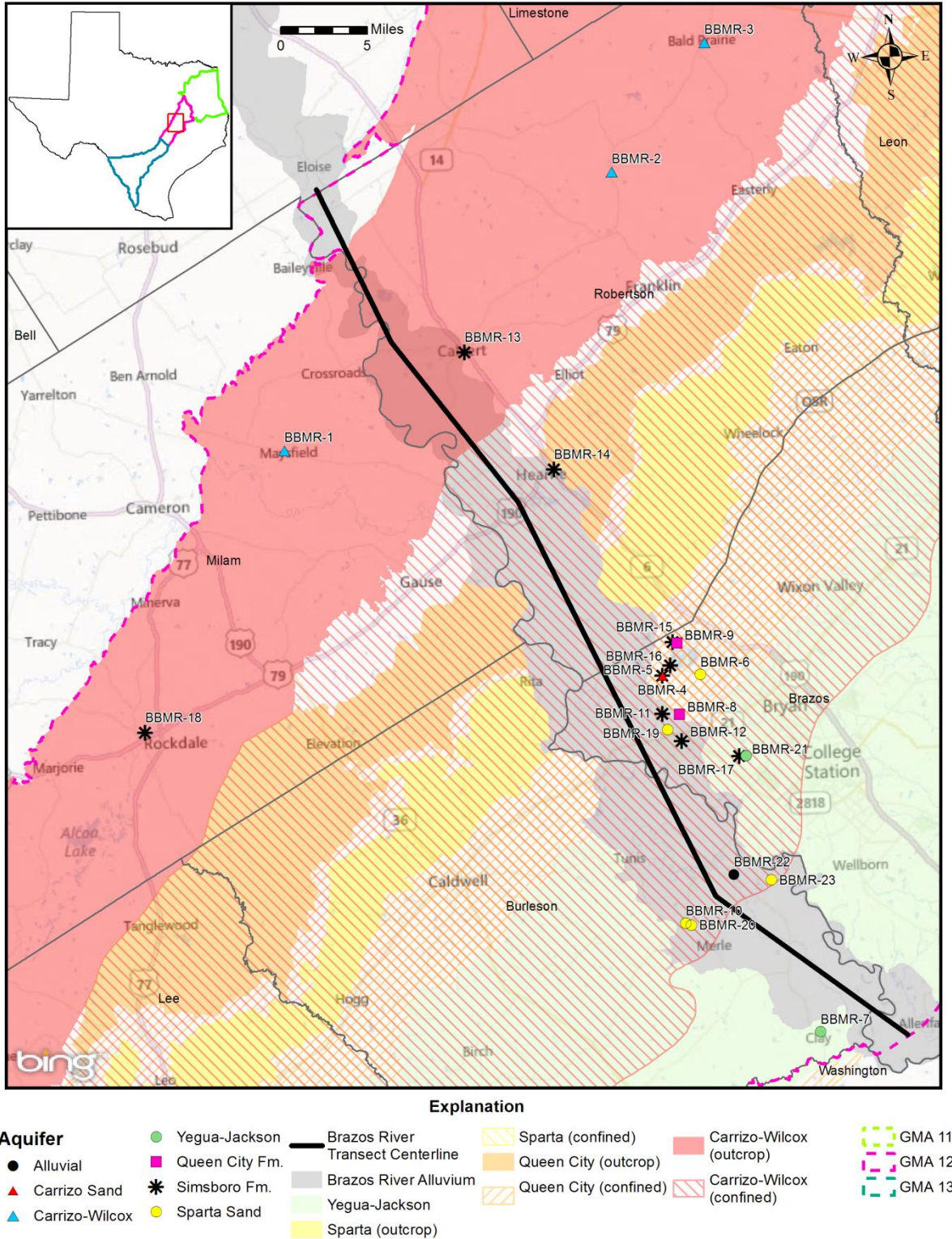
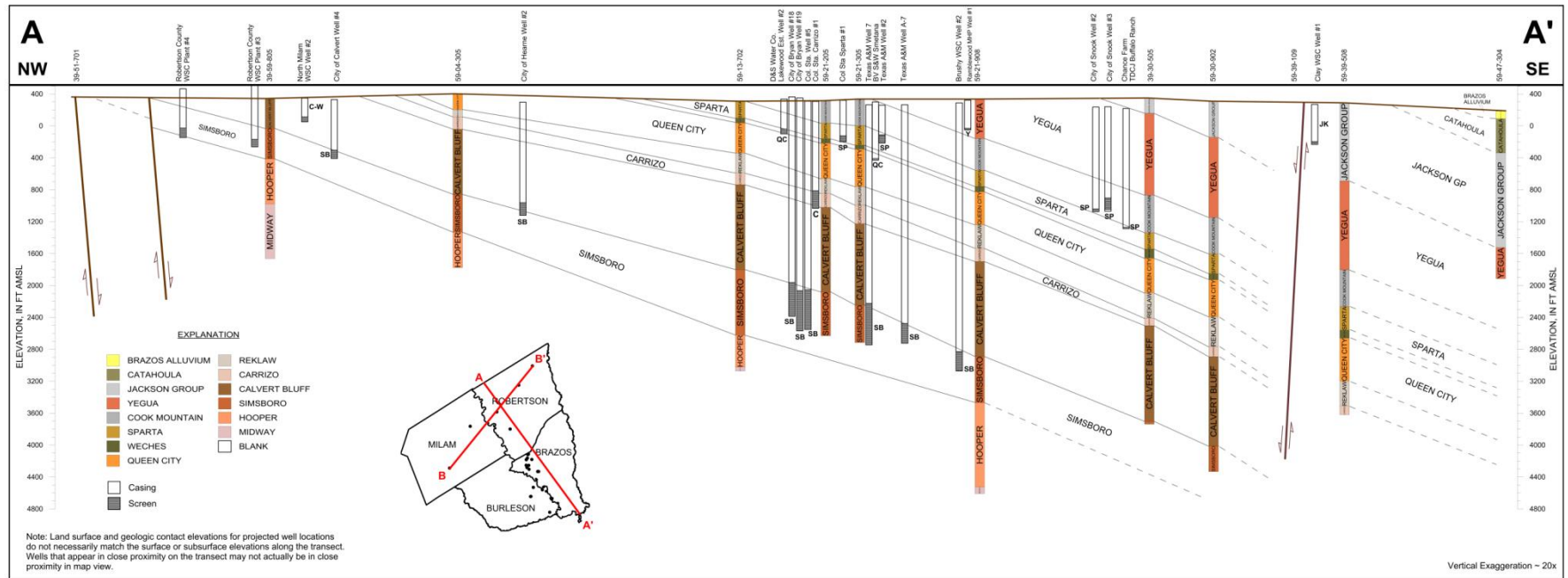


Figure 7-86. Central Transect sampled well locations, Groundwater Management Area (GMA) 12.

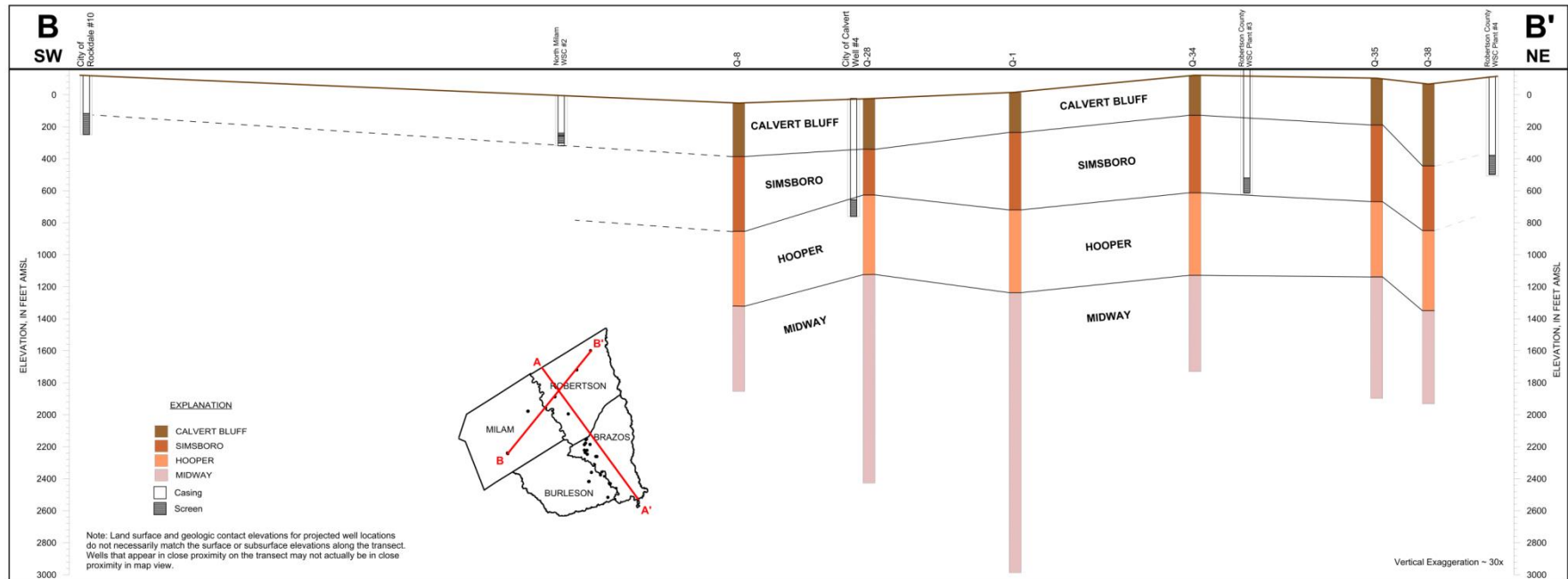
Evaluation of Hydrochemical and Isotopic Data in Groundwater Management Areas 11, 12 and 13



See 'Figure 7-87 BBMR dip section.pdf' for the full-scale version of the cross-section (included as a separate document).

Figure 7-87. Cross-section A-A' in dip direction of the Central Transect, Groundwater Management Area 12.

Evaluation of Hydrochemical and Isotopic Data in Groundwater Management Areas 11, 12 and 13



See 'Figure 7-88 BBMR strike section.pdf' for the full-scale version of the cross-section (included as a separate document).

Figure 7-88. Cross-section B-B' in strike direction of the Central Transect, Groundwater Management Area 12.

### **7.2.1 General Geochemical Trends**

#### **Wilcox Group of the Carrizo-Wilcox Aquifer**

The Wilcox Group of the Carrizo-Wilcox Aquifer is the primary aquifer in Brazos, Burleson, Milam and Robertson counties. An extensive groundwater database is available for the Wilcox Group. The distribution of data is shown on Figure 7-89.

#### Well Depths

Based on Figure 7-89 and the dip-oriented cross section for the transect, well depths in the outcrop can be less than 200 feet and increase to well depths greater than 2,000 feet in east Brazos and Burleson counties. It should be noted that wells further downdip occasionally have a shallower total depth than other wells located updip. This is because the Wilcox Group is a relatively thick section and well depth can vary significantly based on the type and purpose of a well.

#### Potentiometric Surface

The Wilcox Group's potentiometric surface for the transect (based on most recent data) (Figure 7-90) shows water levels in the outcrop as great as 500 feet (above mean sea level) to water levels downdip in Brazos County of about 200 feet or less. From this map two directions of groundwater flow can be inferred: 1) along the strike (northeast to southwest) in the outcrop toward the rivers and creeks and 2) down the structural dip from outcrop into the deep subsurface. Observing only groundwater flow in this map, it should be noted that it is debatable whether or not significant surface water – groundwater interaction exists in the outcrop.

#### Piper Diagram

The Piper diagram for the Wilcox Group (Figure 7-91) in the Central Transect shows a mixed cation (calcium-magnesium-sodium) and mixed anion (sulfate-chloride-bicarbonate) water at shallower depths (less than 500 feet) evolving to a sodium-bicarbonate water at depth.

#### Bicarbonate versus Sodium Plot

A plot of bicarbonate versus sodium (Figure 7-92) for all data (the TWDB data and the 2012 data) shows two trends. For bicarbonate values less than approximately four milliequivalents per liter, bicarbonate increases independent of sodium. For bicarbonate concentrations great than four milliequivalents per liter, both sodium and bicarbonate increase linearly at an approximate ratio of 1:1.

#### Sodium versus Calcium Plot

A plot of sodium versus calcium for all data (Figure 7-93) shows little relationship between sodium and calcium. At low concentrations of sodium, sodium values are independent of calcium. Conversely at low concentrations of calcium, sodium concentrations are independent of calcium.

#### Bicarbonate versus Calcium Plot

A plot of bicarbonate versus calcium (Figure 7-94) shows a distribution of data similar to the pattern of sodium versus calcium (Figure 7-93), calcium and bicarbonate (at low concentrations) appear to increase linearly to about three milliequivalents per liter, calcium then decrease to zero as bicarbonate increases to over 30 milliequivalents per liter.

#### pH versus Bicarbonate Plot

The plot of pH versus bicarbonate (Figure 7-95) shows two limbs to this curve. pH rise from less than five and a half to about eight with increasing bicarbonate. Above a pH of about eight bicarbonate increases independent of pH. The pHs of less than five were not observed for this aquifer, as observed in some of the other aquifers in this project.

#### pH versus Sodium Plot

The plot of pH versus sodium (Figure 7-96) shows a similar distribution of data to the pH versus bicarbonate plot (Figure 7-95).

#### Sulfate versus Bicarbonate Plot

The plot of sulfate versus bicarbonate (Figure 7-97) shows higher sulfate concentrations at bicarbonate concentrations less than ten milliequivalents per liter. There are very low sulfate concentrations at bicarbonate concentrations greater than ten milliequivalents per liter.

#### Chloride versus Sodium Plot

The plot of chloride versus sodium (Figure 7-98) shows three trends: 1) sodium increasing independent of chloride for sodium concentration less than ten milliequivalents per liter, 2) chloride starts increasing slowly at higher sodium concentrations from ten to 30 milliequivalents per liter and 3) a trend of increasing sodium and chloride, starting at low sodium values.

#### Chloride versus Bicarbonate Plot

The plot of chloride versus bicarbonate (Figure 7-99) shows three trends: 1) bicarbonate increases independent of chloride for bicarbonate values from zero to ten milliequivalents per liter, 2) a general increase in both bicarbonate and chloride from bicarbonate concentrations of ten to 20 milliequivalents per liter and 3) a set of higher random chloride values at lower bicarbonate concentrations.

#### Depth versus Nitrate Plot

A plot of depth versus nitrate (Figure 7-100) shows slightly higher nitrate values at shallow depths.

#### Depth versus Sulfate Plot

The plot of depth versus sulfate (Figure 7-101) shows the highest concentrations of sulfate at the shallowest depths and declining to negligible concentrations below 1,500 feet.

#### Depth versus Calcium Plot

The plot of depth versus calcium (Figure 7-102) shows the highest calcium at the shallowest depths in the outcrop at declining to negligible concentrations at depth below 1,500 feet.

#### Map of Calcium

The map of calcium (Figure 7-103) in the Wilcox Group of the Carrizo-Wilcox Aquifer shows calcium concentrations greater than two milliequivalents per liter are in the outcrop or slightly downdip.

#### Depth versus Bicarbonate Plot

The plot of depth versus bicarbonate (Figure 7-104) shows higher bicarbonate concentrations at depth.

#### Depth versus pH Plot

The plot of depth versus pH (Figure 7-105) shows a general increase in pH with depth.

#### Map of pH

The map of pH (Figure 7-106) in the Wilcox Group shows that most of the low pH water (less than seven) sampled is in the outcrop.

#### Depth versus Sodium Plot

The plot of depth versus sodium (Figure 7-107) shows general increases in sodium at depth.

#### Depth versus Chloride Plot

The plot of depth versus chloride (Figure 7-108) shows some higher chloride concentrations at depth less than 250 feet and higher concentrations at depths greater than about 2,000 feet.

#### Depth versus Total Dissolved Solids Plot

The plot of depth versus total dissolved solids (Figure 7-109) shows a general trend of higher total dissolved solids waters at depth. There are some high total dissolved solids values however at shallow depths.

#### Discussion

Groundwaters in the Wilcox Group in the Central Transect both recharges and discharges in the outcrop or flows into the deeper subsurface. The groundwater chemistry evolves from mixed calcium-sodium and sulfate-chloride cation water in the outcrop to a sodium-bicarbonate with some chloride and no sulfate down gradient in the confined section. The earlier part of the flow system is not dominated by sodium-bicarbonate water. The higher calcium waters are restricted to the outcrop (Figure 7-103). The sodium-bicarbonate waters occur mostly in the confined aquifer, but bicarbonate has preponderance over sulfate in the outcrop as well as downdip. The implication is that there is adequate sodium-Montmorillonite in the Wilcox Group to provide exchange sites to replace the dissolved calcium with sodium in the outcrop as well as downdip. The increase in bicarbonate, with no change in pH, suggests that the coalification of organics in the deeper parts is an additional source of bicarbonate. The downdip extent of (1,000 to 3,000 parts per million) salinity is not reached with available wells from TWDB database or the 2012 well sampling. Increases in salinity (total dissolved solids) in the deeper parts of the aquifer are caused primarily by elevated bicarbonate values and not chloride values, although there is a chloride increase at depth. Restriction of the calcium type waters to the outcrop may be caused by faulting in the outcrop area of the Wilcox Group.

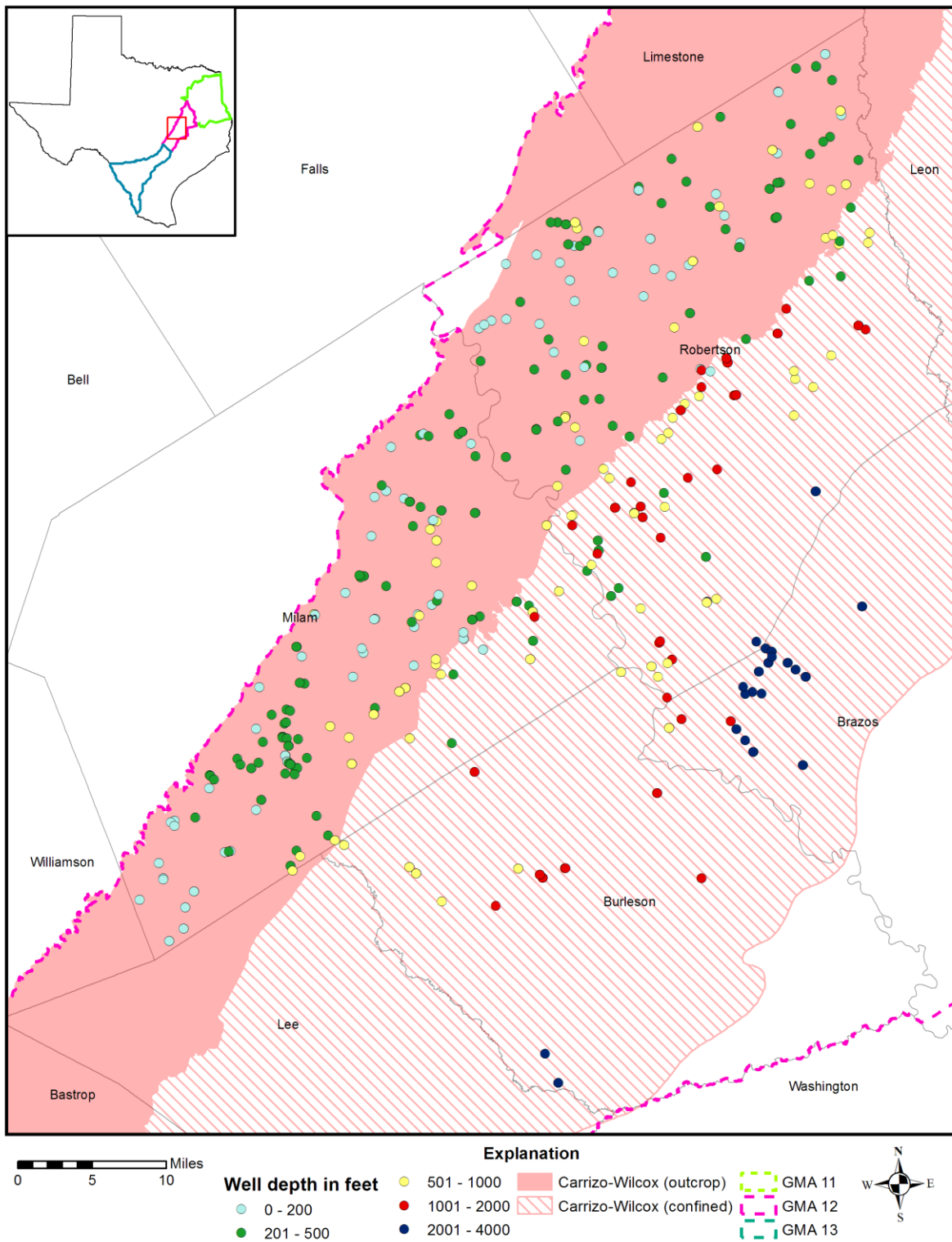


Figure 7-89. Well depths measured from land surface in feet in the Wilcox Group of the Carrizo-Wilcox Aquifer, Central Transect, Groundwater Management Area (GMA) 12.

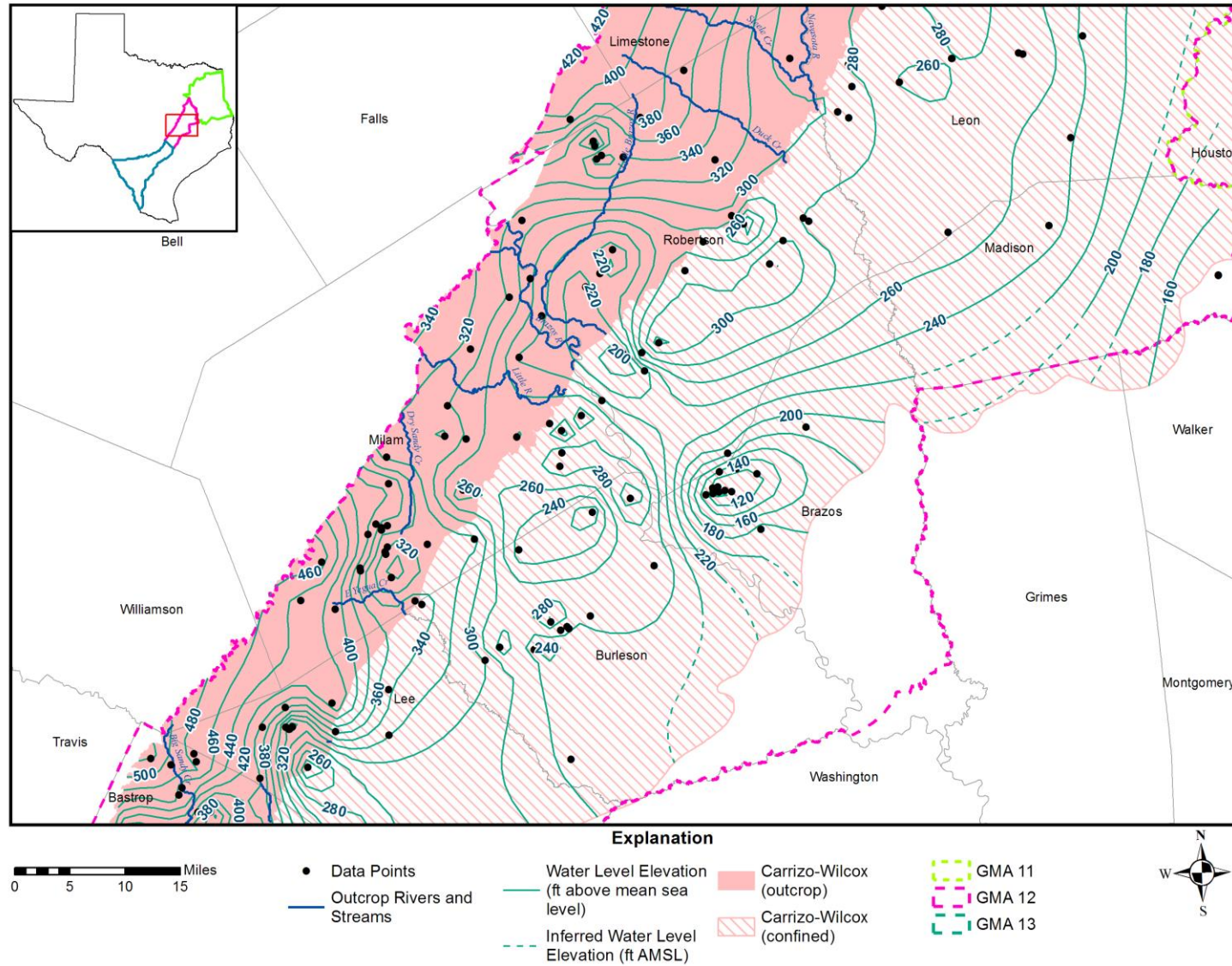


Figure 7-90. Potentiometric surface of the Wilcox Group of the Carrizo-Wilcox Aquifer using water level data measured in feet above mean sea level (ft AMSL) from 1990 to 2011 in the Central Transect, Groundwater Management Area 12.

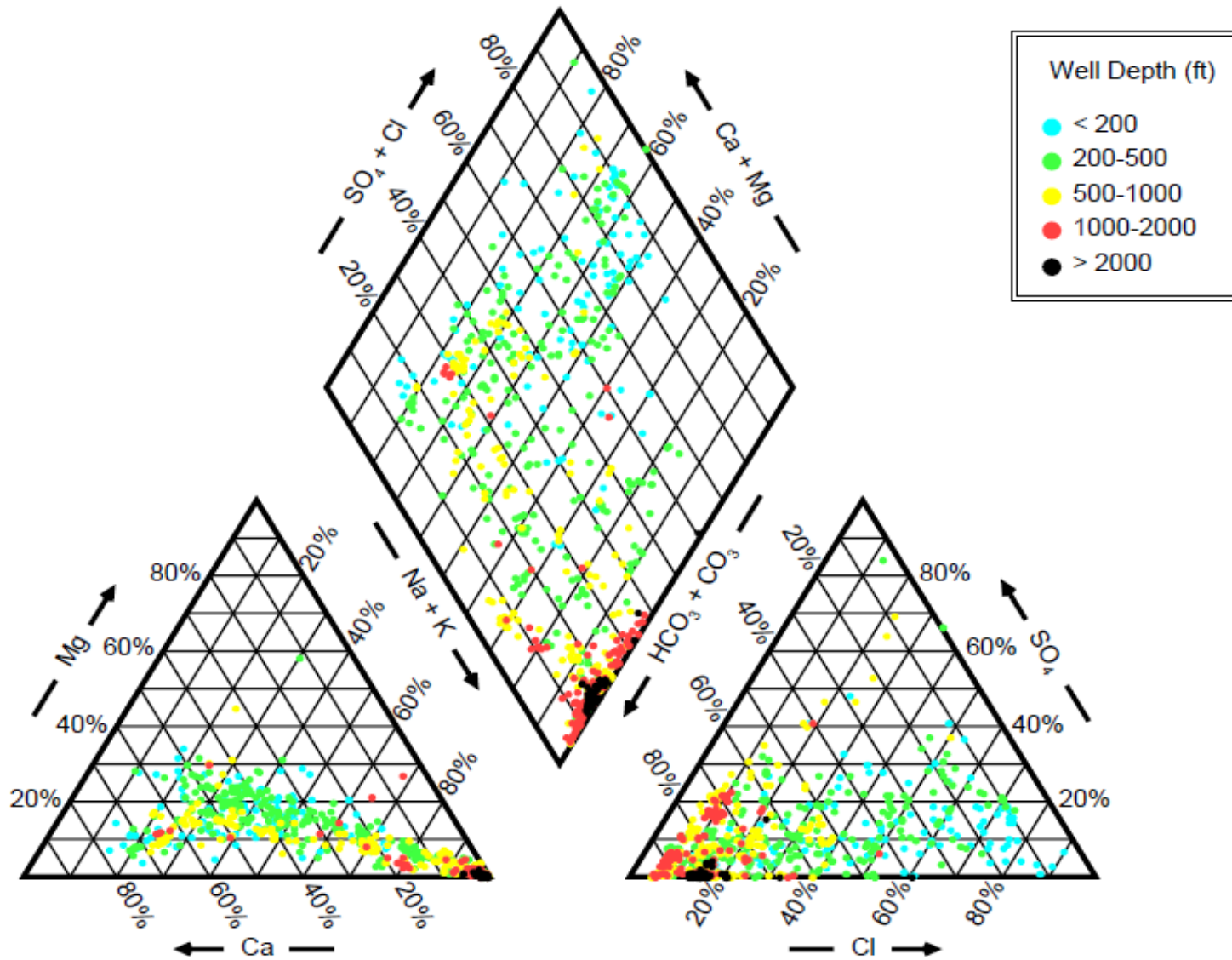


Figure 7-91. Piper diagram showing chemistry of Wilcox Group of the Carrizo-Wilcox Aquifer wells in the Central Transect by well depth measured from land surface in feet (ft).

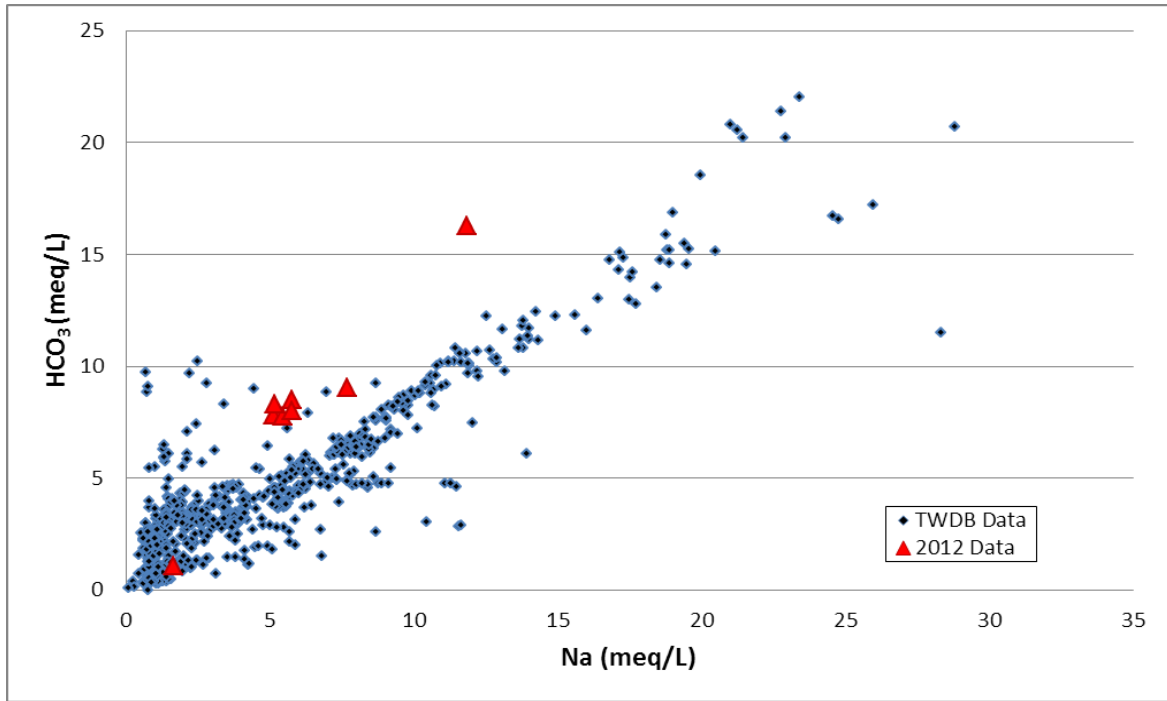


Figure 7-92. Bicarbonate (HCO<sub>3</sub>) versus sodium (Na) measured in milliequivalents per liter (meq/L), Wilcox Group of the Carrizo-Wilcox Aquifer, Central Transect, Groundwater Management Area 12.

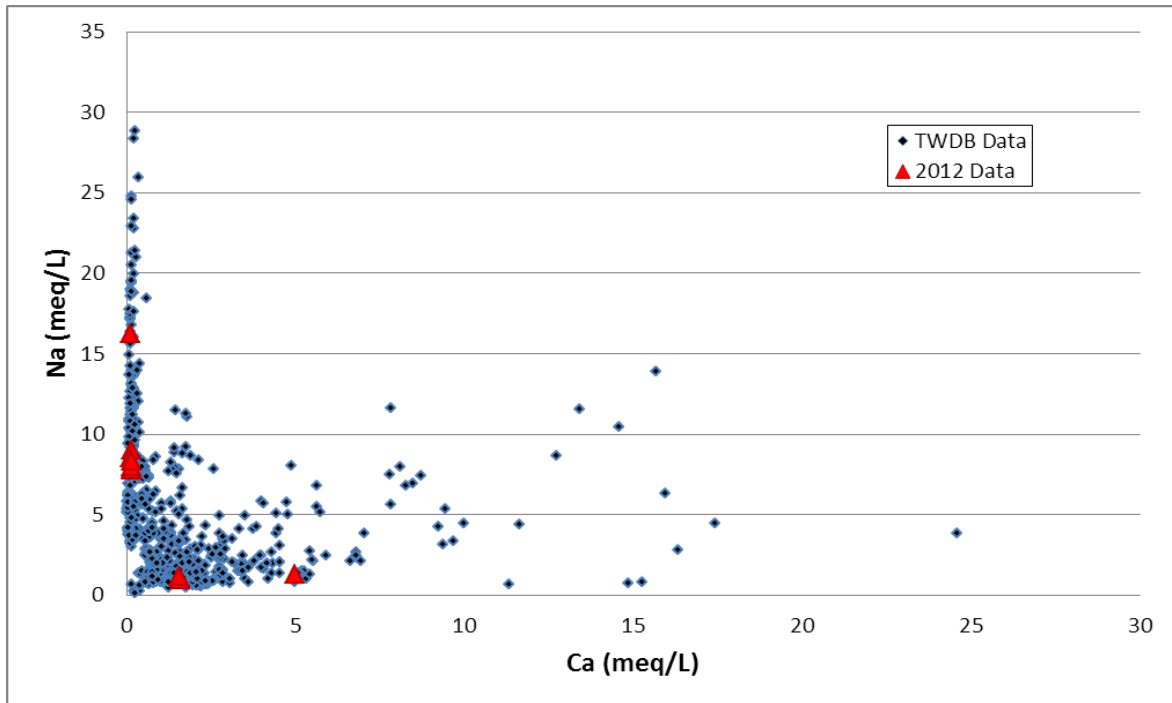


Figure 7-93. Sodium (Na) versus calcium (Ca) measured in milliequivalents per liter (meq/L), Wilcox Group of the Carrizo-Wilcox Aquifer, Central Transect, Groundwater Management Area 12.

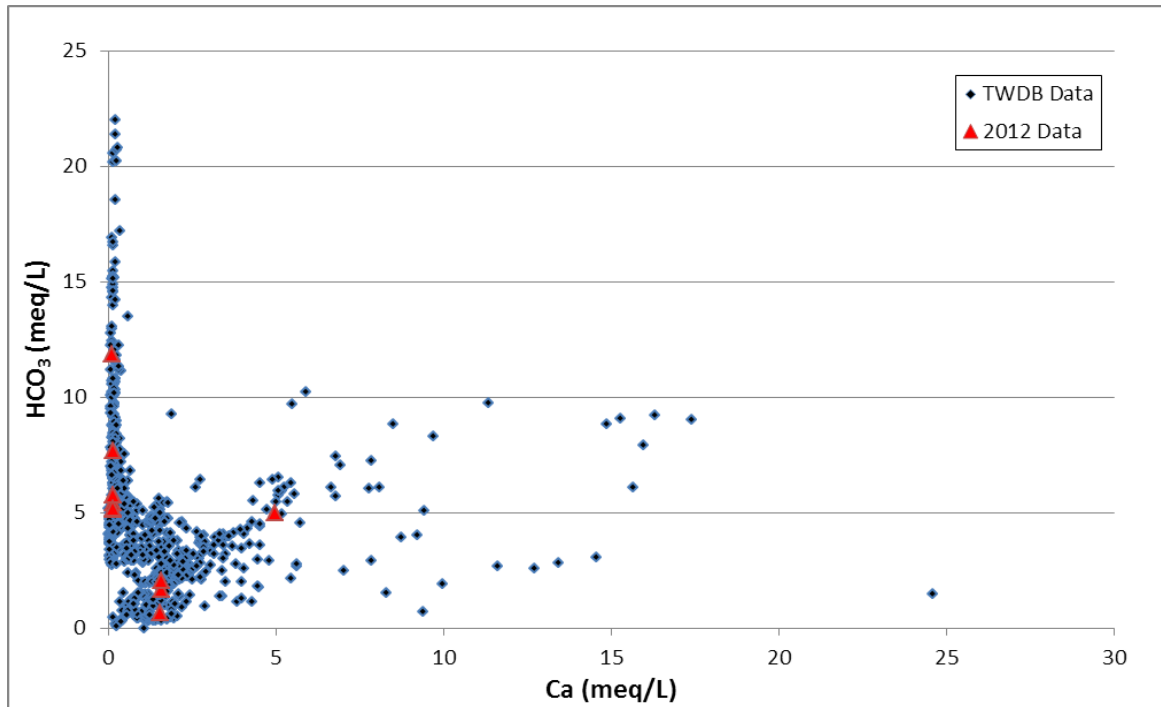


Figure 7-94. Bicarbonate ( $\text{HCO}_3^-$ ) versus calcium (Ca) measured in milliequivalents per liter (meq/L), Wilcox Group of the Carrizo-Wilcox Aquifer, Central Transect, Groundwater Management Area 12.

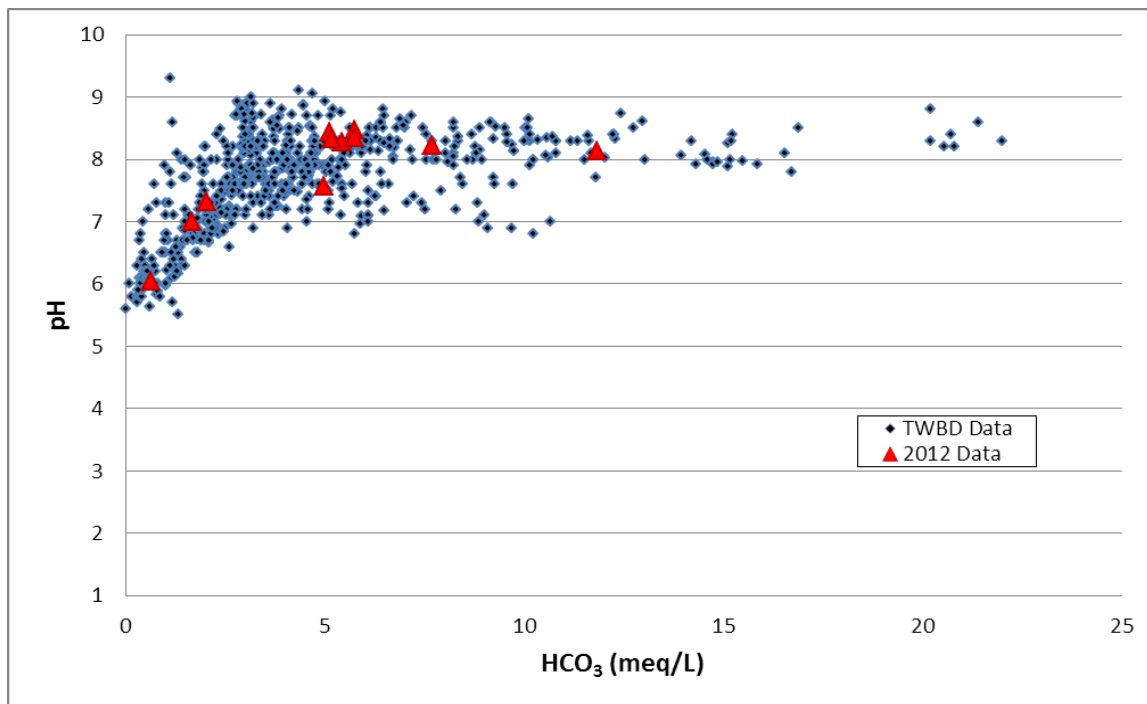


Figure 7-95. pH versus bicarbonate ( $\text{HCO}_3^-$ ) measured in milliequivalents per liter (meq/L), Wilcox Group of the Carrizo-Wilcox Aquifer, Central Transect, Groundwater Management Area (GMA) 12.

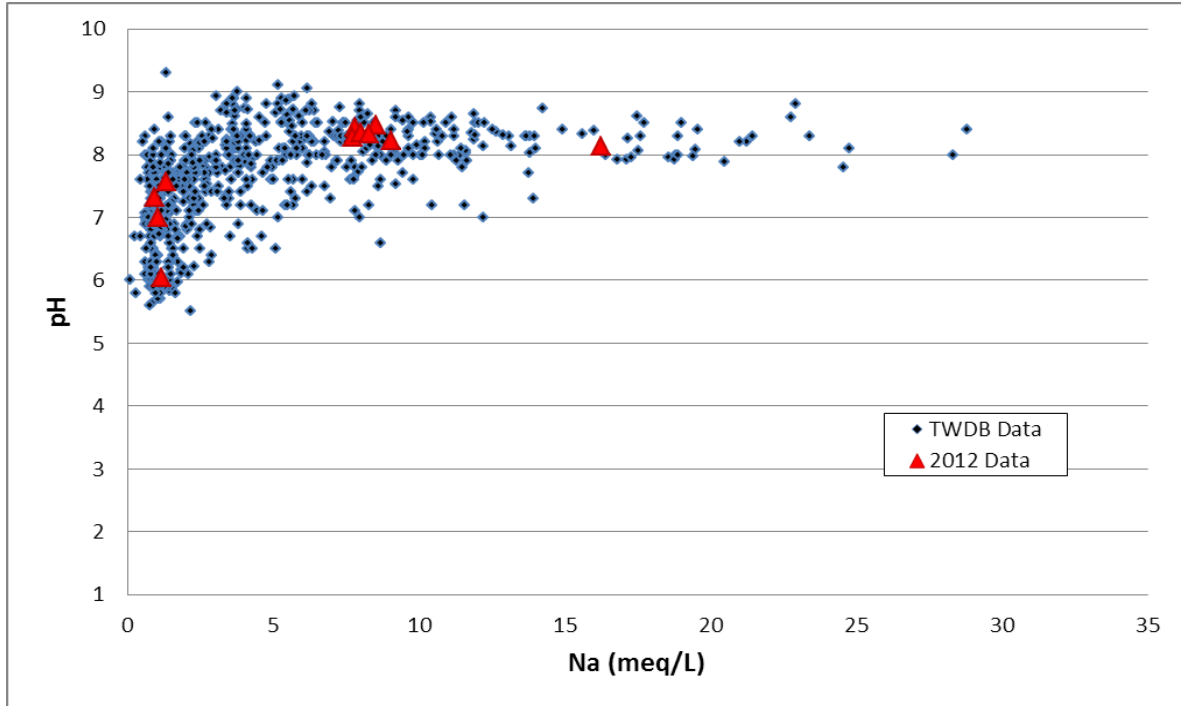


Figure 7-96. pH versus sodium (Na) measured in milliequivalents per liter (meq/L), Wilcox Group of the Carrizo-Wilcox Aquifer, Central Transect, Groundwater Management Area 12.

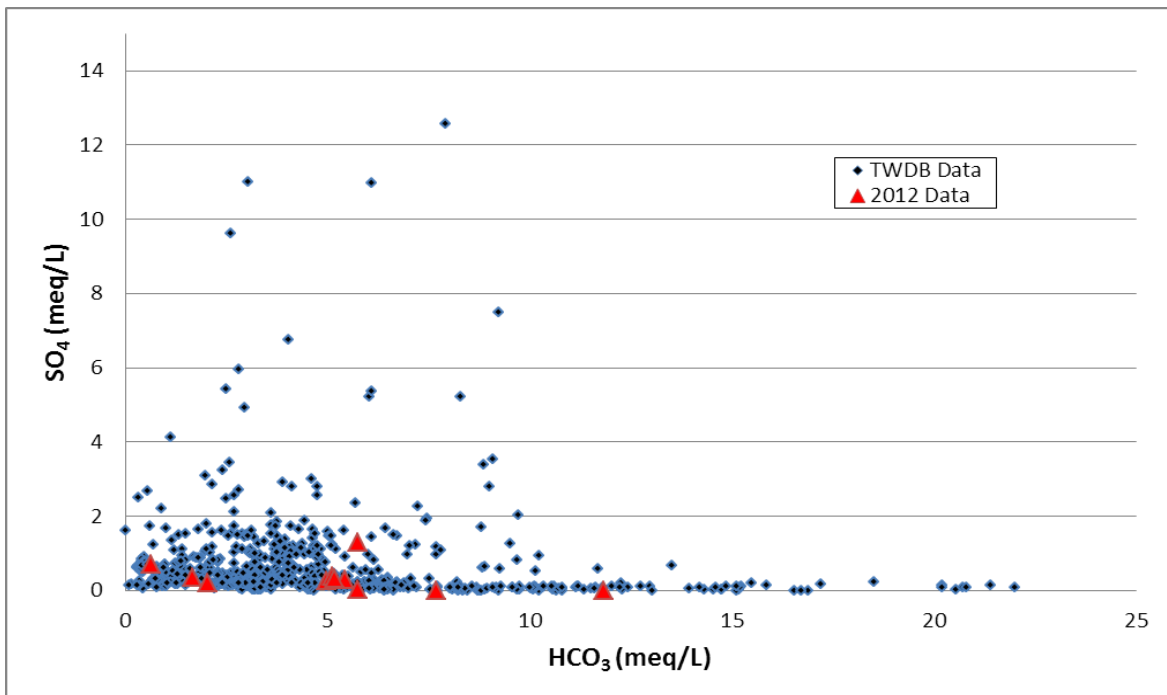


Figure 7-97. Sulfate (SO<sub>4</sub>) versus bicarbonate (HCO<sub>3</sub>) measured in milliequivalents per liter (meq/L), Wilcox Group of the Carrizo-Wilcox Aquifer, Central Transect, Groundwater Management Area 12.

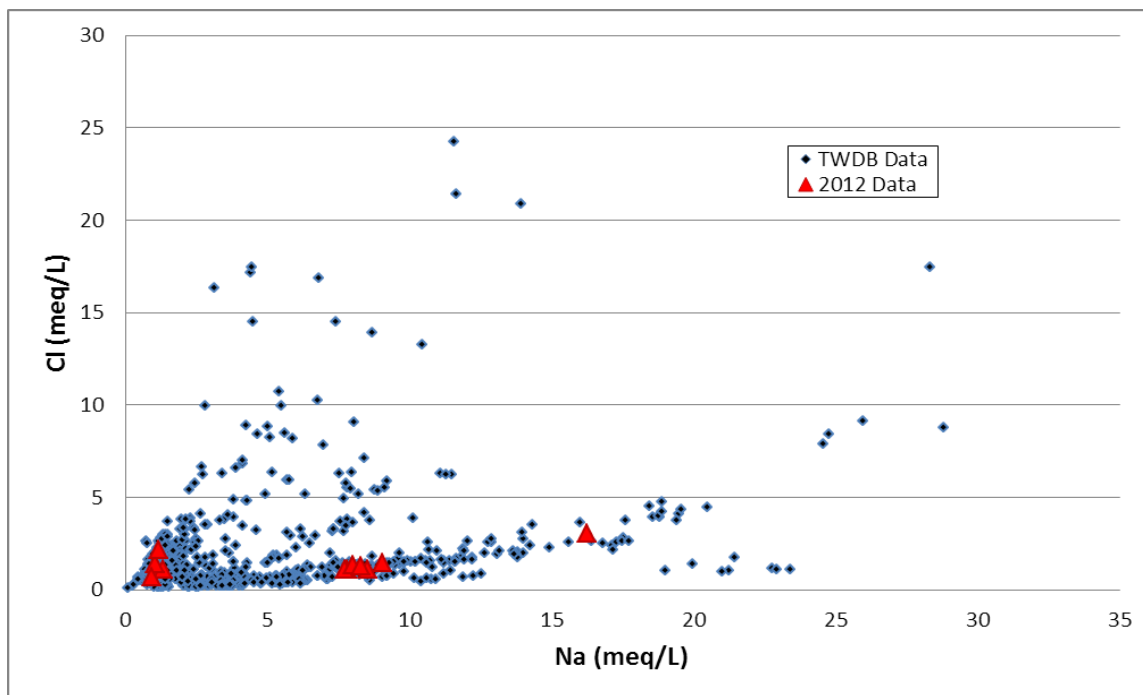


Figure 7-98. Chloride (Cl) versus sodium (Na measured in milliequivalents per liter (meq/L)), Wilcox Group of the Carrizo-Wilcox Aquifer, Central Transect, Groundwater Management Area 12.

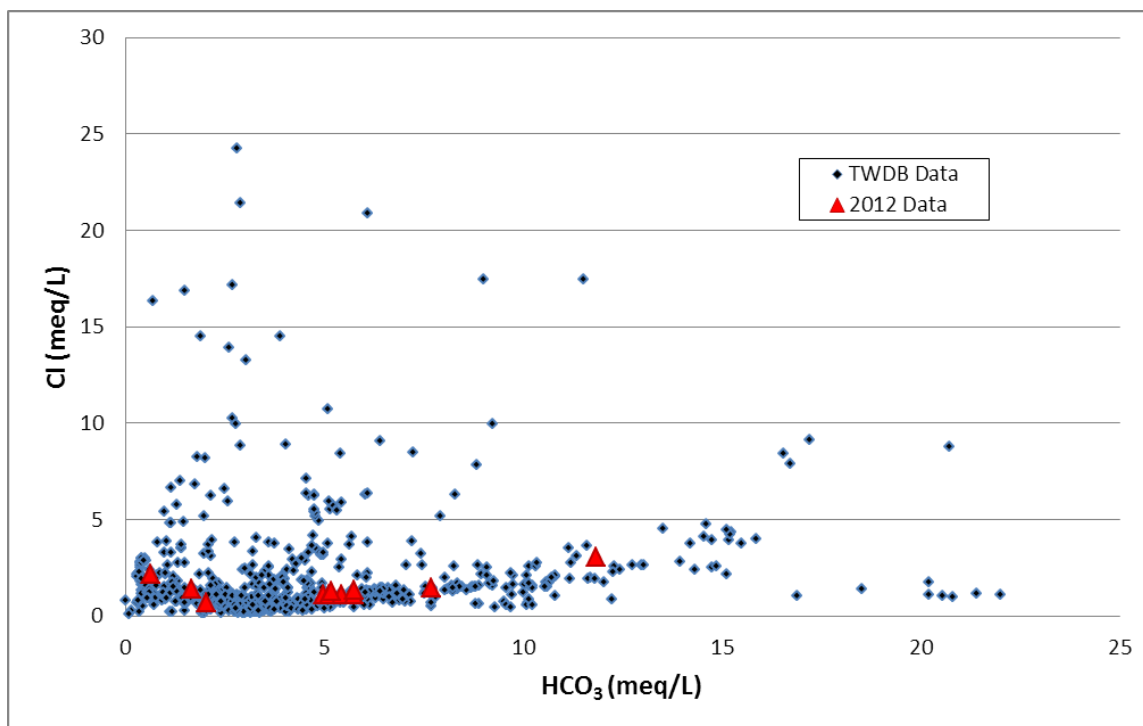


Figure 7-99. Chloride (Cl) versus bicarbonate ( $\text{HCO}_3$ ) measured in milliequivalents per liter (meq/L), Wilcox Group of the Carrizo-Wilcox Aquifer, Central Transect, Groundwater Management Area 12.

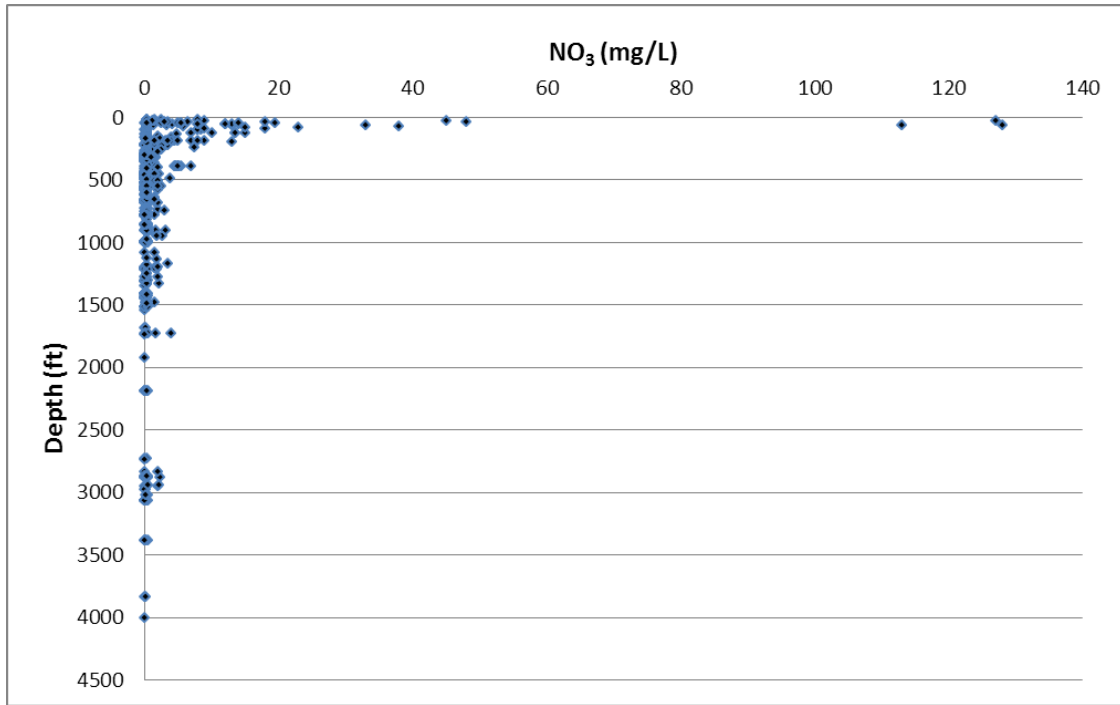


Figure 7-100. Depth measured from land surface in feet (ft) versus nitrate (NO<sub>3</sub>) measured in milligrams per liter (mg/L), Wilcox Group of the Carrizo-Wilcox Aquifer, Central Transect, Groundwater Management Area 12.

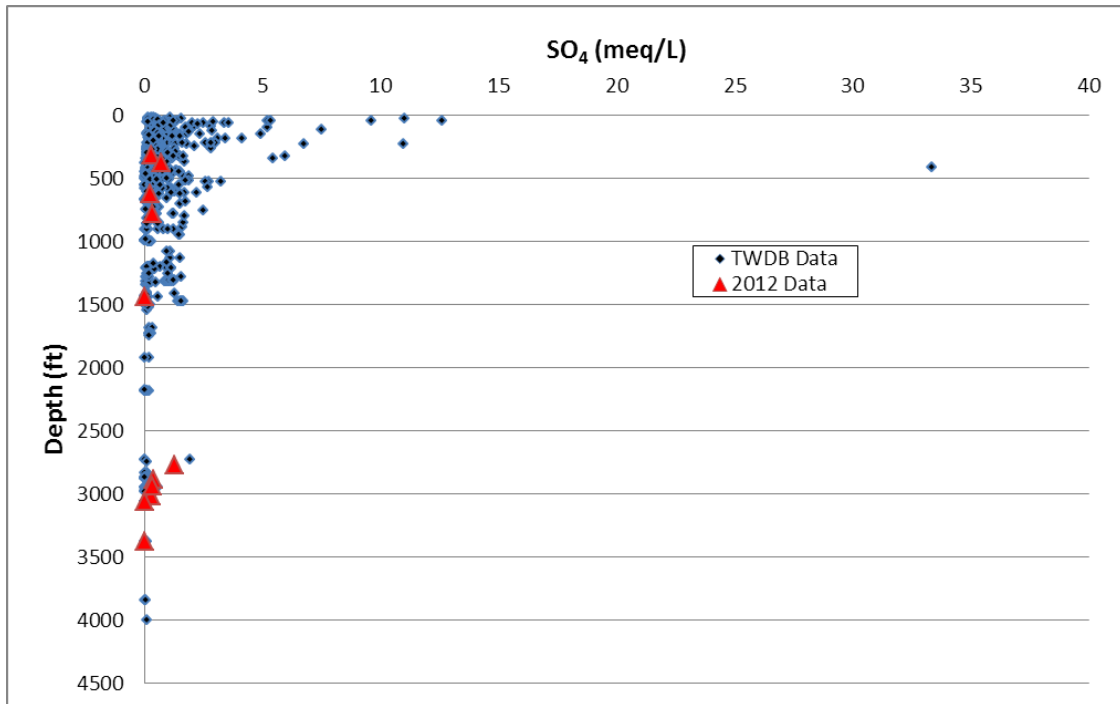
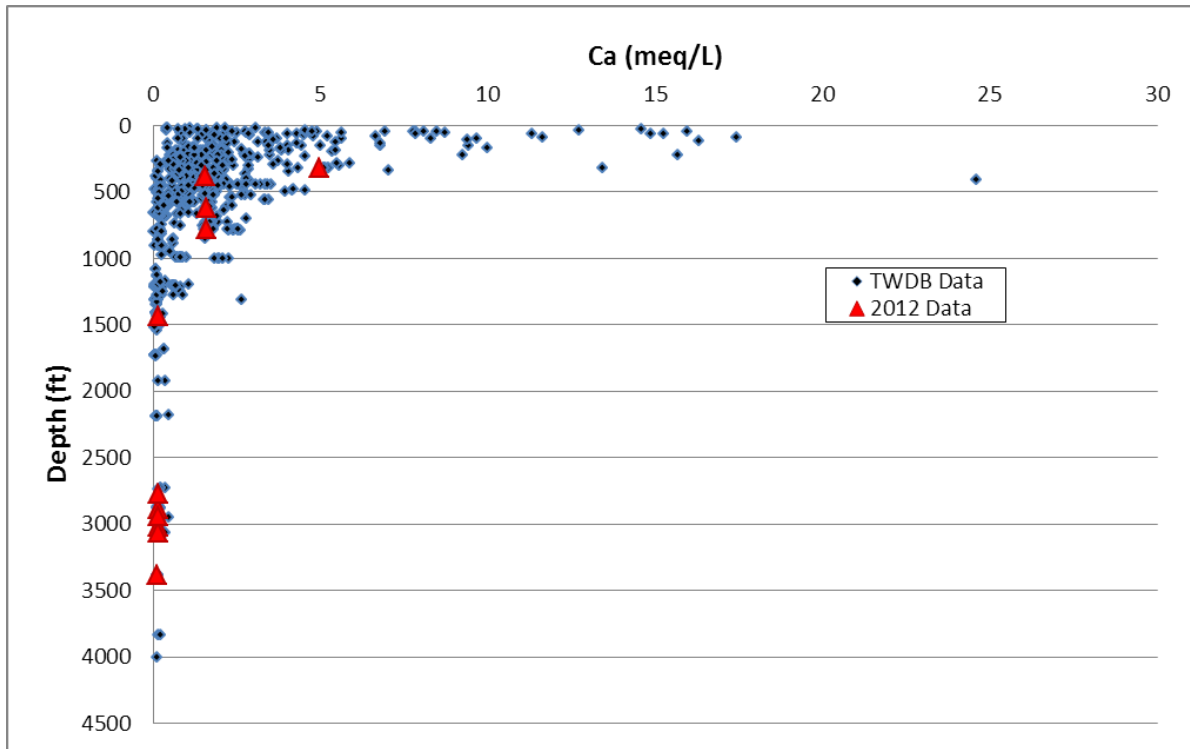
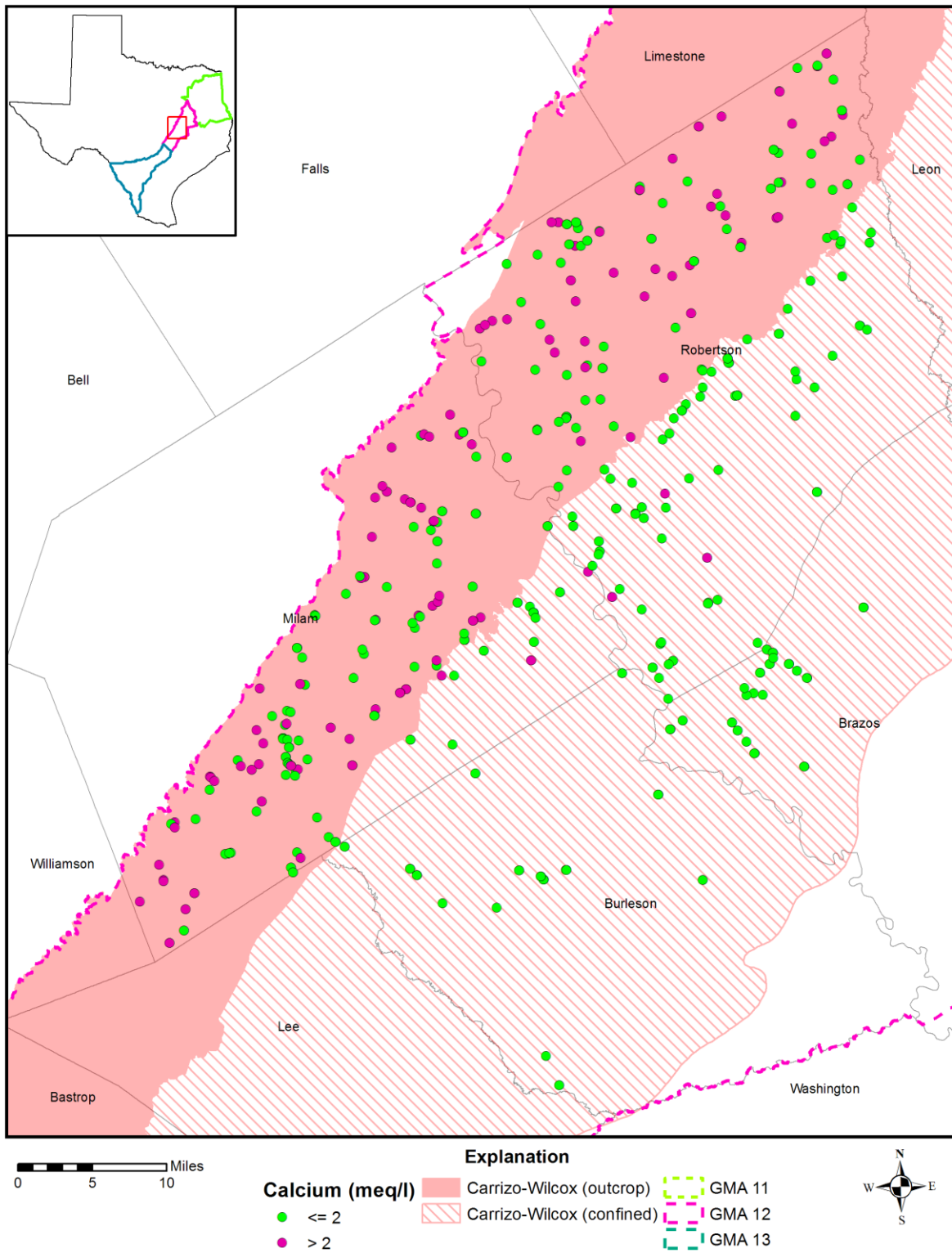


Figure 7-101. Depth measured from land surface in feet (ft) versus sulfate (SO<sub>4</sub>) measured in milliequivalents per liter (meq/L), Wilcox Group of the Carrizo-Wilcox Aquifer, Central Transect, Groundwater Management Area 12.



**Figure 7-102.** Depth measured from land surface in feet (ft) versus calcium (Ca) measured in milliequivalents per liter (meq/L), Wilcox Group of the Carrizo-Wilcox Aquifer, Central Transect, Groundwater Management Area 12.



**Figure 7-103. Calcium concentrations measured in milliequivalents per liter (meq/L) in the Wilcox Group of the Carrizo-Wilcox Aquifer, Central Transect, Groundwater Management Area (GMA) 12.**

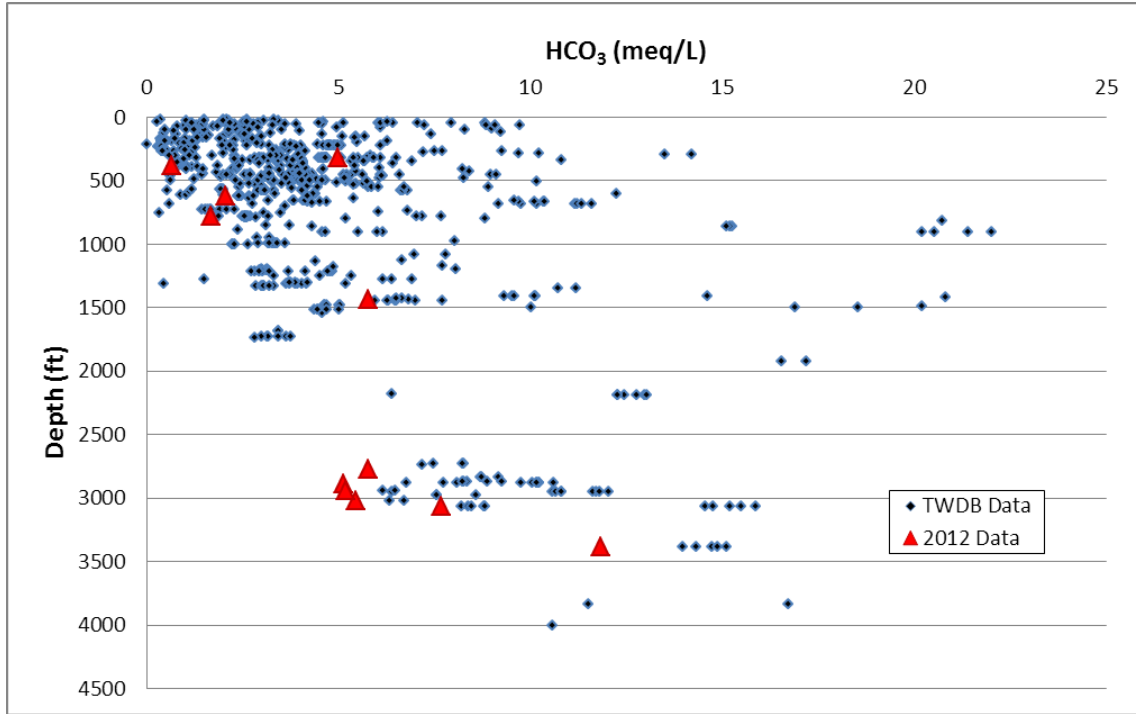


Figure 7-104. Depth measured from land surface in feet (ft) versus bicarbonate ( $\text{HCO}_3^-$ ) measured in milliequivalents per liter (meq/L), Wilcox Group of the Carrizo-Wilcox Aquifer, Central Transect, Groundwater Management Area 12.

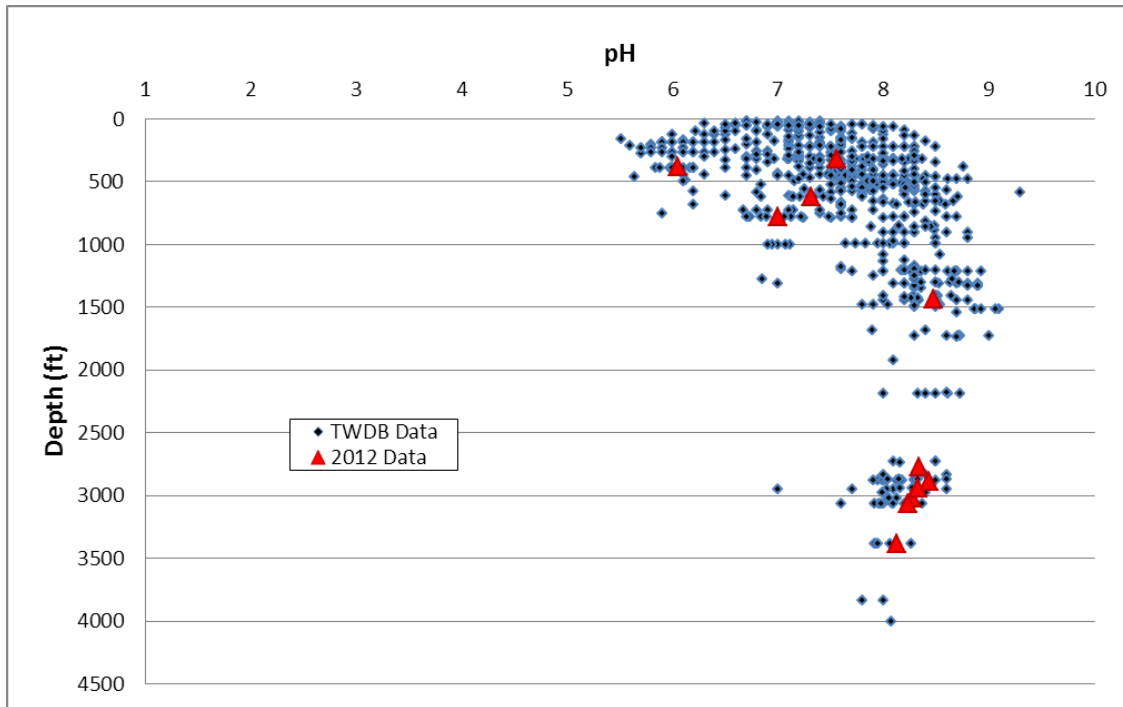


Figure 7-105. Depth measured from land surface in feet (ft) versus pH, Wilcox Group of the Carrizo-Wilcox Aquifer, Central Transect, Groundwater Management Area 12.

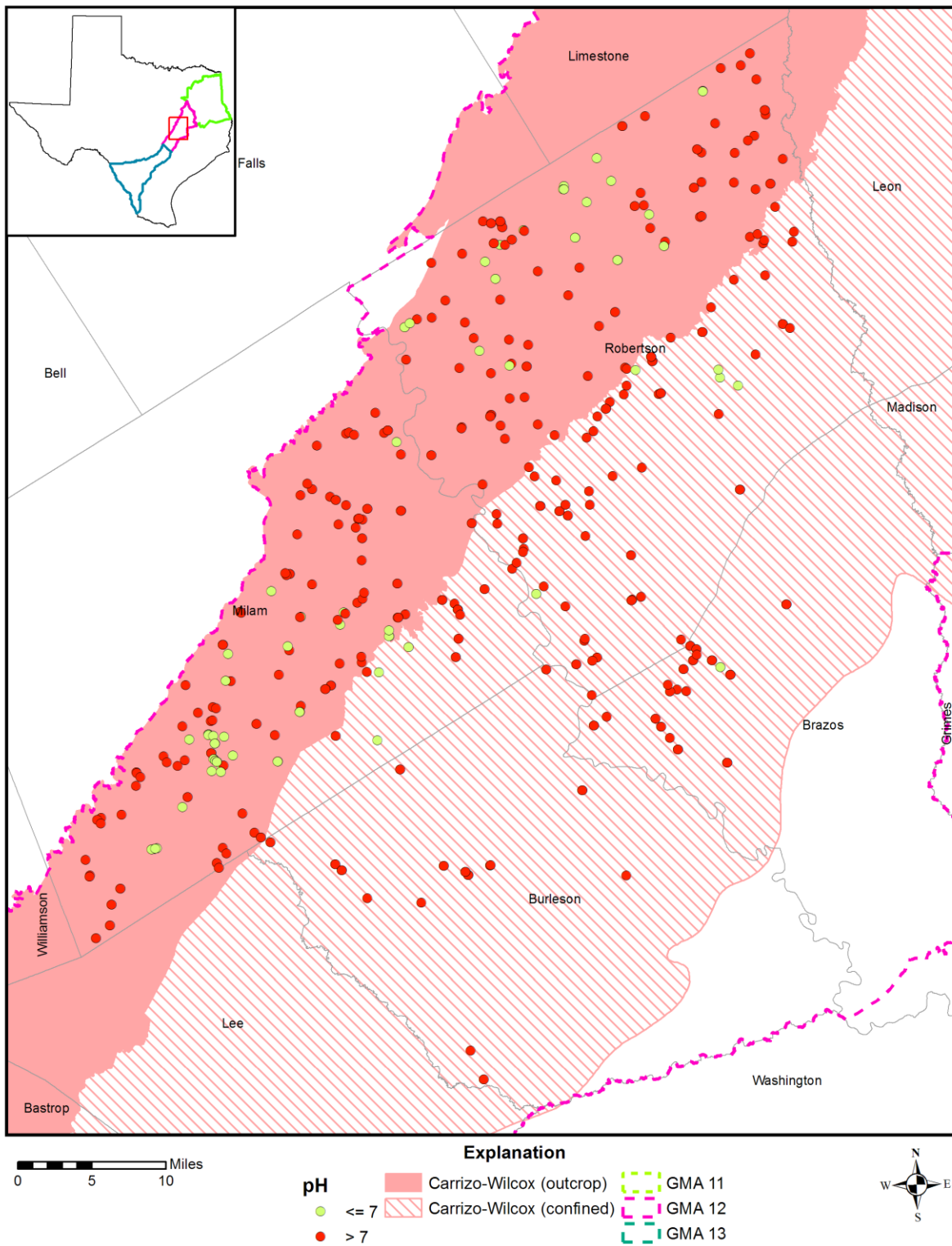


Figure 7-106. pH in the Wilcox Group of the Carrizo-Wilcox Aquifer, Central Transect, Groundwater Management Areas (GMA) 12.

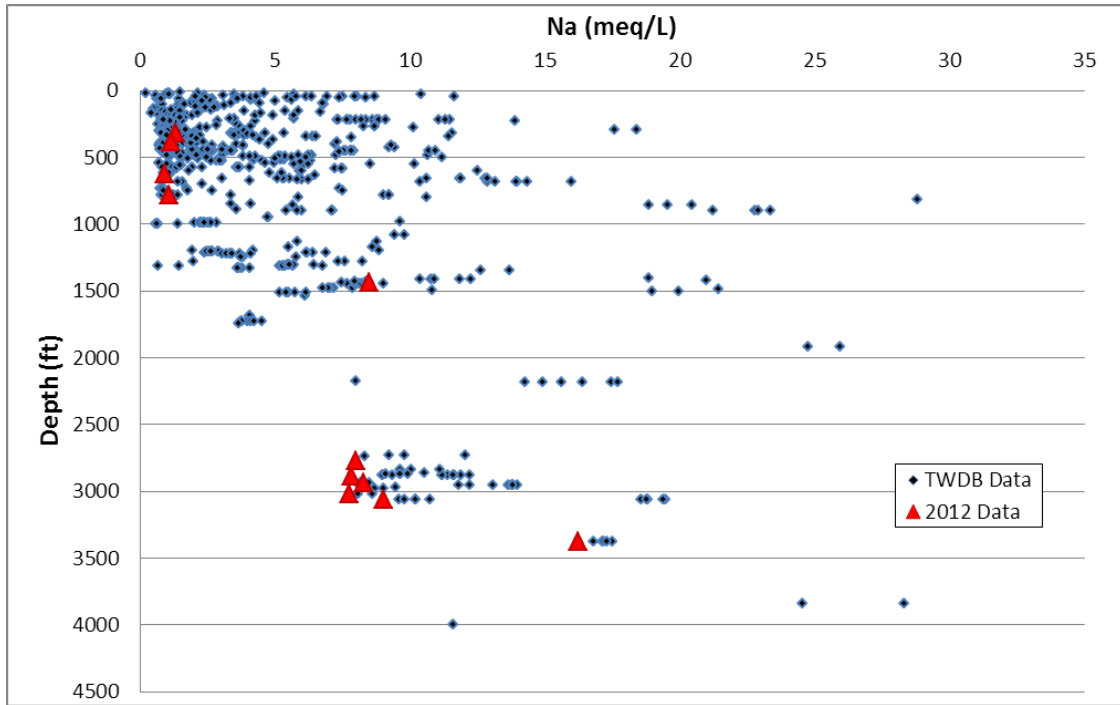


Figure 7-107. Depth measured from land surface in feet (ft) versus sodium (Na) measured in milliequivalents per liter (meq/L), Wilcox Group of the Carrizo-Wilcox Aquifer, Central Transect, Groundwater Management Area 12.

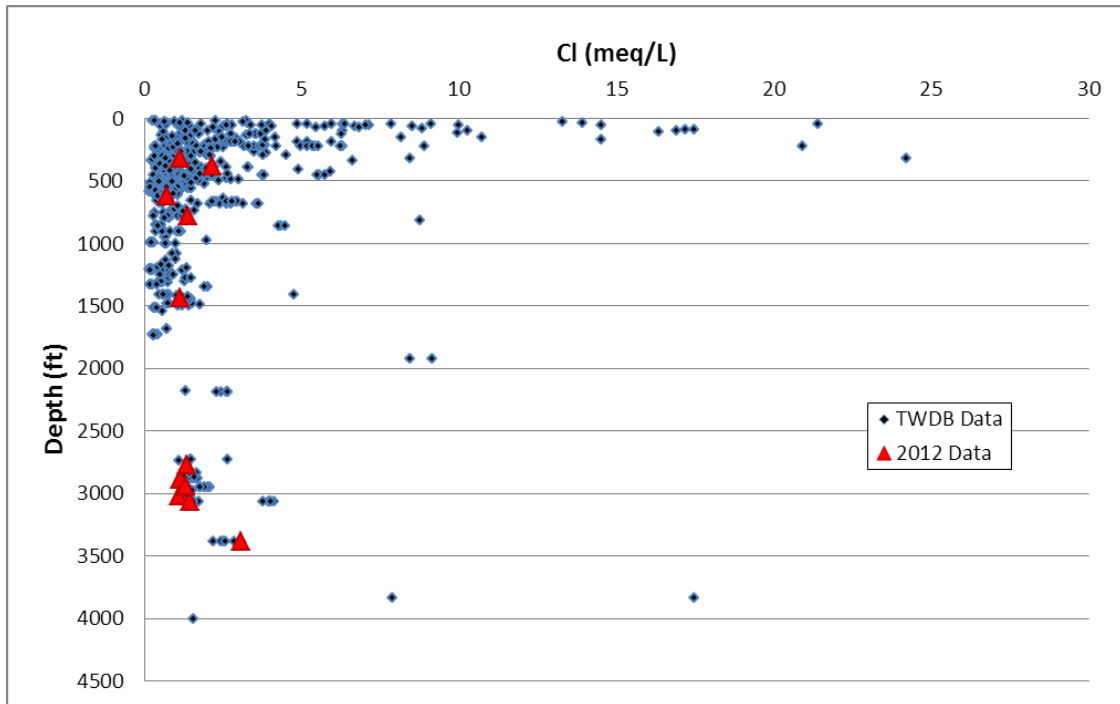
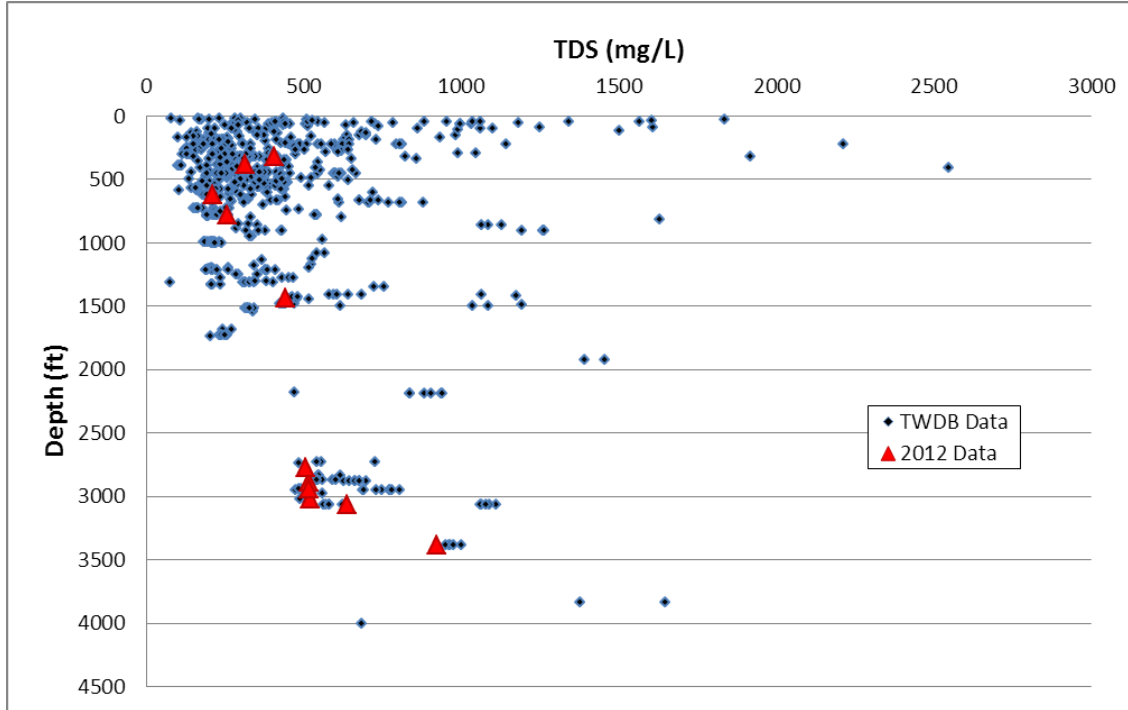


Figure 7-108. Depth measured from land surface in feet (ft) versus chloride (Cl) measured in milliequivalents per liter (meq/L), Wilcox Group of the Carrizo-Wilcox Aquifer, Central Transect, Groundwater Management Area 12.



**Figure 7-109.** Depth measured from land surface in feet (ft) versus total dissolved solids (TDS) measured in parts per million (ppm), Wilcox Group of the Carrizo-Wilcox Aquifer, Central Transect, Groundwater Management Area 12.

### Queen City Aquifer

The Queen City Aquifer is a minor aquifer in the Central Transect. The outcrop strikes from southwest to northeast across the county (Figure 7-110) and dips to depths of about 1,200 feet (TWDB, 2013) along the southeast downdip side of the aquifer. Total width of the aquifer in the outcrop is about 10 miles wide. The water level data (Figure 7-111) indicates groundwater flow from the outcrop into the confined section. There are less water level and water chemistry data for the aquifer in comparison to the Wilcox Group of the Carrizo-Wilcox Aquifer for this transect.

#### Piper Diagram

The cation triangle of the Piper diagram (Figure 7-112) shows a general trend of a mixed (calcium-magnesium-sodium) cation and (chloride-sulfate) anion at shallow depths evolving to sodium-bicarbonate type water at depth.

#### Bicarbonate versus Sodium Plot

A plot of bicarbonate versus sodium (Figure 7-113) shows general increase in sodium and bicarbonate at about a 1:1 ratio. At low sodium values (less than five milliequivalents per liter) bicarbonate is increasing independent from sodium.

#### Sodium versus Calcium Plot

A plot of sodium versus calcium (Figure 7-114) shows an inverse correlation between sodium and calcium. Calcium increases independent of sodium at low sodium concentrations. Sodium increases independent of calcium at low calcium concentrations.

#### Bicarbonate versus Calcium Plot

A plot of bicarbonate versus calcium (Figure 7-115) shows an inverse correlation between calcium and bicarbonate. Similar to sodium versus calcium (Figure 7-114), calcium increases independent of bicarbonate at low bicarbonate concentrations and bicarbonate increases independent of calcium at low calcium concentrations.

#### pH versus Bicarbonate Plot

The plot of pH versus bicarbonate (Figure 7-116) shows two limbs, on one limb pH rises from about a pH of five to eight with increasing bicarbonate. The second limb shows bicarbonate rising independent of pH.

#### pH versus Sodium Plot

The plot of pH versus sodium (Figure 7-117) shows two parts of a curve: 1) increases in pH with small increases in sodium and 2) increases in sodium independent of pH. This graph is similar to the pH versus bicarbonate plot (Figure 7-116).

#### Sulfate versus Bicarbonate Plot

A plot of sulfate versus bicarbonate (Figure 7-118) shows higher sulfate values at low bicarbonate. Sulfate “disappears” at bicarbonate values greater than about 12 milliequivalents per liter.

#### Chloride versus Sodium Plot

The plot of chloride versus sodium (Figure 7-119) shows three trends: a) slight increase of chloride with sodium for sodium concentrations less than about 15 milliequivalents per liter, b) increase in chloride for sodium concentrations greater than 15 milliequivalents per liter and c) random high chloride values for low sodium values.

#### Chloride versus Bicarbonate Plot

The plot of chloride versus bicarbonate (Figure 7-120) shows three similar trends to chloride versus sodium (Figure 7-119).

#### Depth versus Nitrate Plot

The plot of depth versus nitrate (Figure 7-121) shows higher nitrate values occur in those wells less than 800 feet.

#### Depth versus Sulfate Plot

The plot of depth versus sulfate (Figure 7-122) shows that no major pattern is observed with this data.

#### Depth versus Calcium Plot

The plot of depth versus calcium (Figure 7-123) shows higher calcium concentrations are observed at depth shallower than about 800 feet.

#### Depth versus Bicarbonate Plot

The plot of depth versus bicarbonate (Figure 7-124) shows that bicarbonate increases with depth.

#### Depth versus Sodium Plot

The plot of depth versus sodium (Figure 7-125) shows that sodium increases with depth.

#### Depth versus pH Plot

The plot of depth versus pH (Figure 7-126) shows general pH increases with depth.

#### Depth versus Chloride Plot

The plot of depth versus chloride (Figure 7-127) shows chloride increases at shallow depths and at depths greater than 800 feet.

#### Depth versus Total Dissolved Solids Plot

The plot of depth versus total dissolved solids (Figure 7-128) shows total dissolved solids increases with depth. Most of the increased total dissolved solids are from bicarbonate, although there is some chloride increase that contributes to the higher total dissolved solids.

#### Discussion

The cation triangle for the Queen City Aquifer shows mixed cation type water in the outcrop evolving to a sodium dominated water in the downdip sections (Figure 7-112). The anion triangle shows mixed anion chemistry in the outcrop and a bicarbonate water downdip. The Queen City Aquifer waters show a similar evolution to sodium-bicarbonate water as observed in the underlying Wilcox Group of the Carrizo-Wilcox Aquifer. Although much of the increase in salinity downdip is from the development of a sodium-bicarbonate water, some of the salinity is derived from additional chloride.

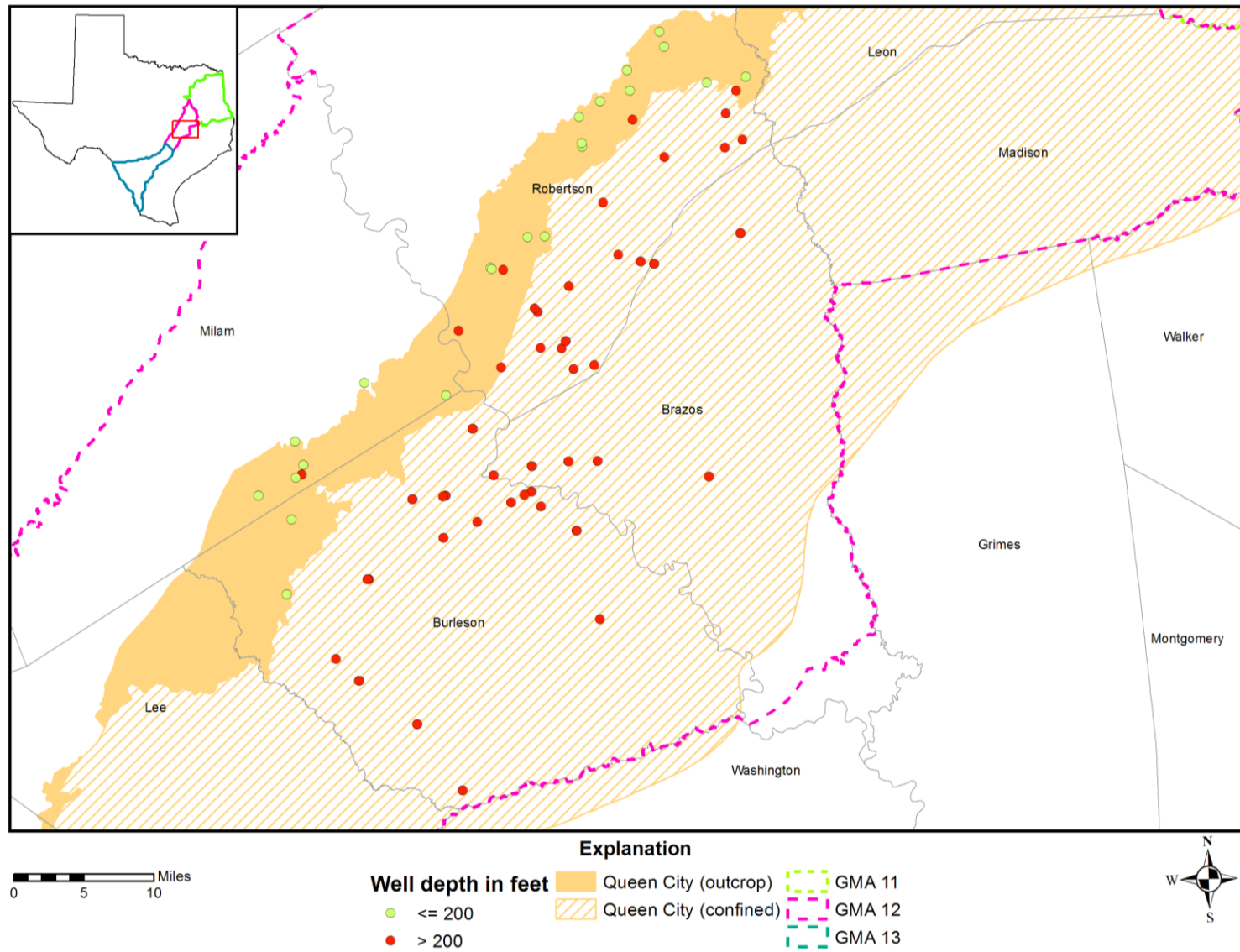


Figure 7-110. Well depths measured from land surface in feet in the Queen City Aquifer, Central Transect, Groundwater Management Area (GMA) 12.

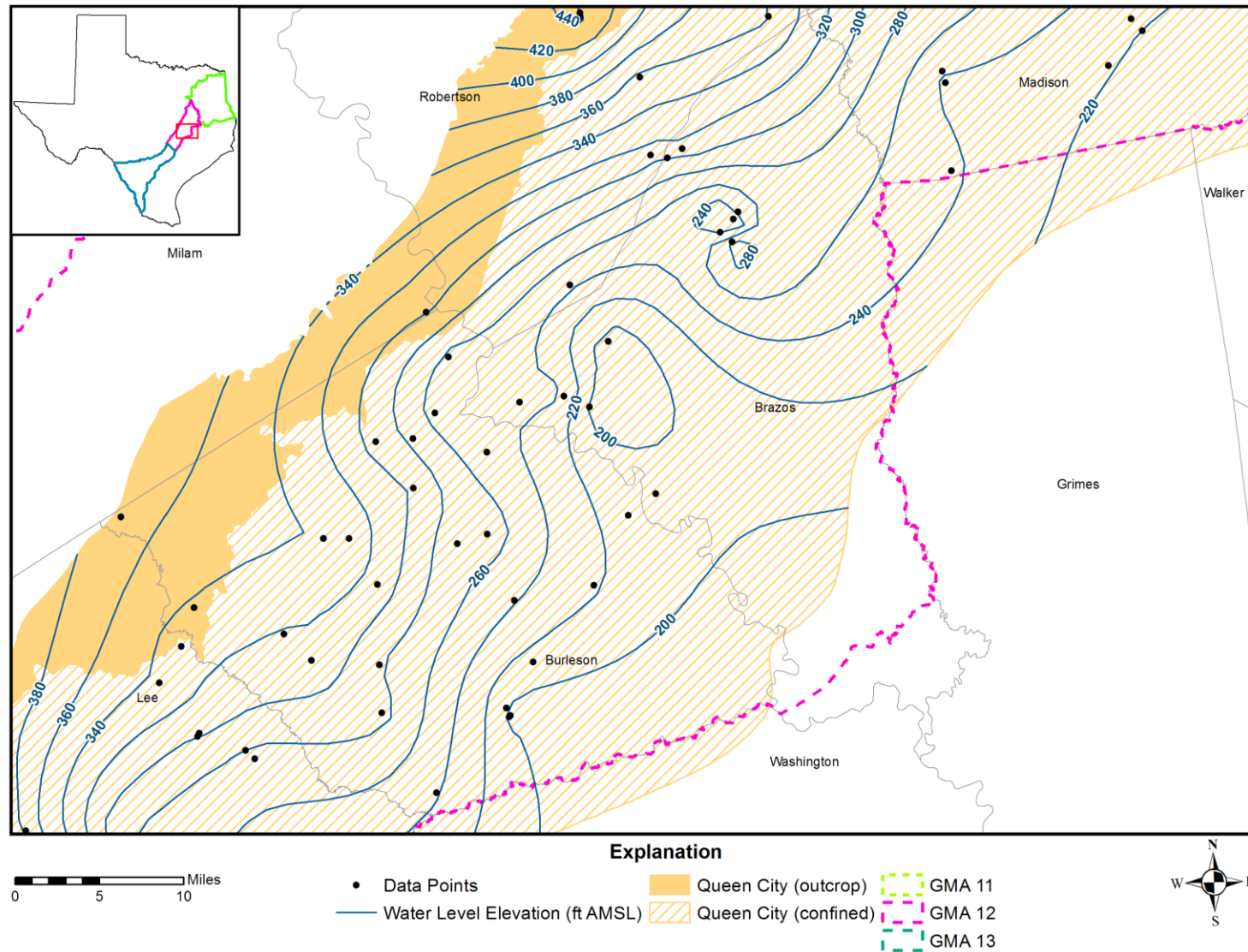


Figure 7-111. Potentiometric surface of the Queen City Aquifer using water level data measured in feet above mean sea level (ft AMSL) from 1990 to 2011 in the Central Transect, Groundwater Management Area (GMA) 12.

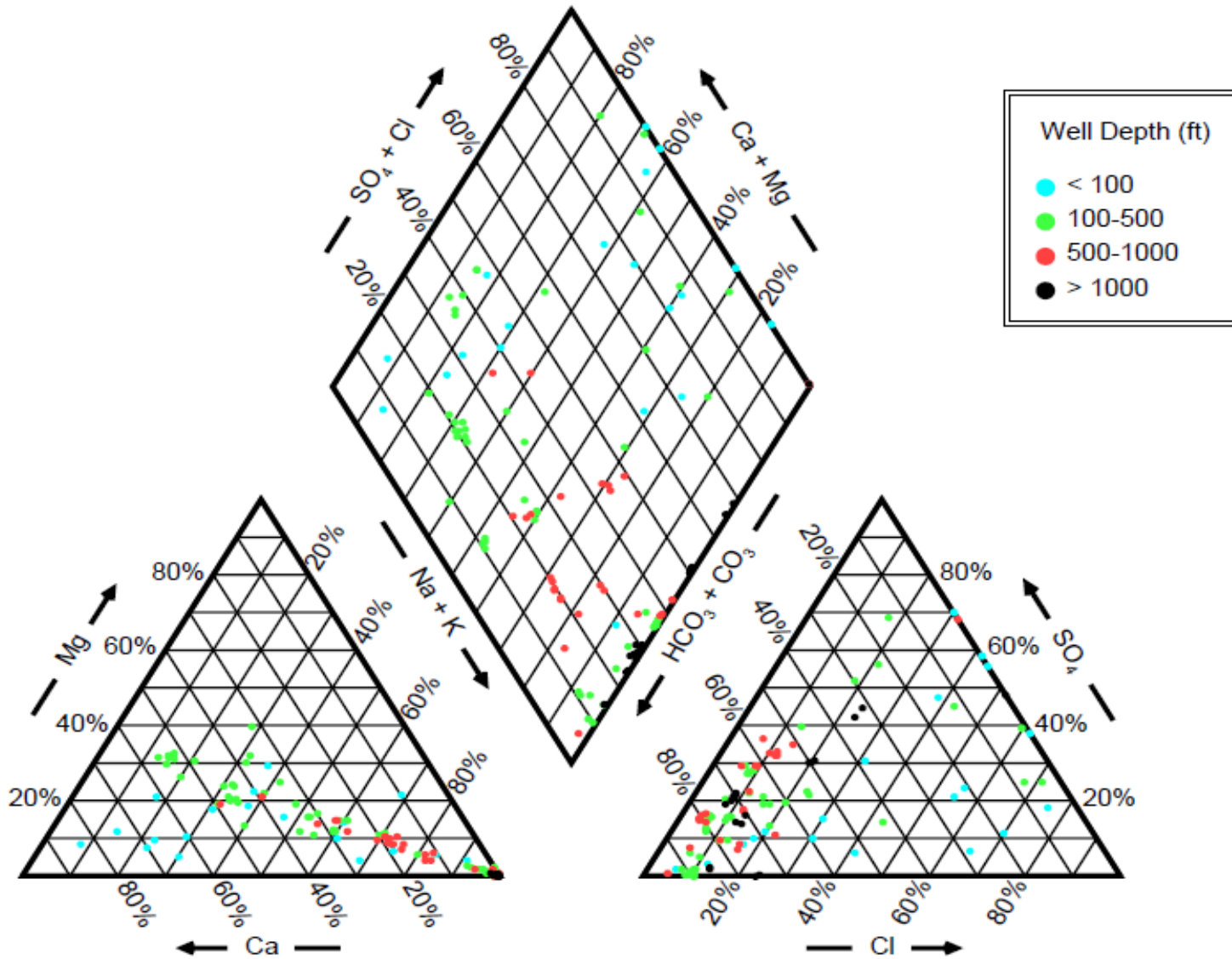


Figure 7-112. Piper diagram showing chemistry of the Queen City Aquifer wells in Central Transect by well depth measured from land surface in feet (ft).

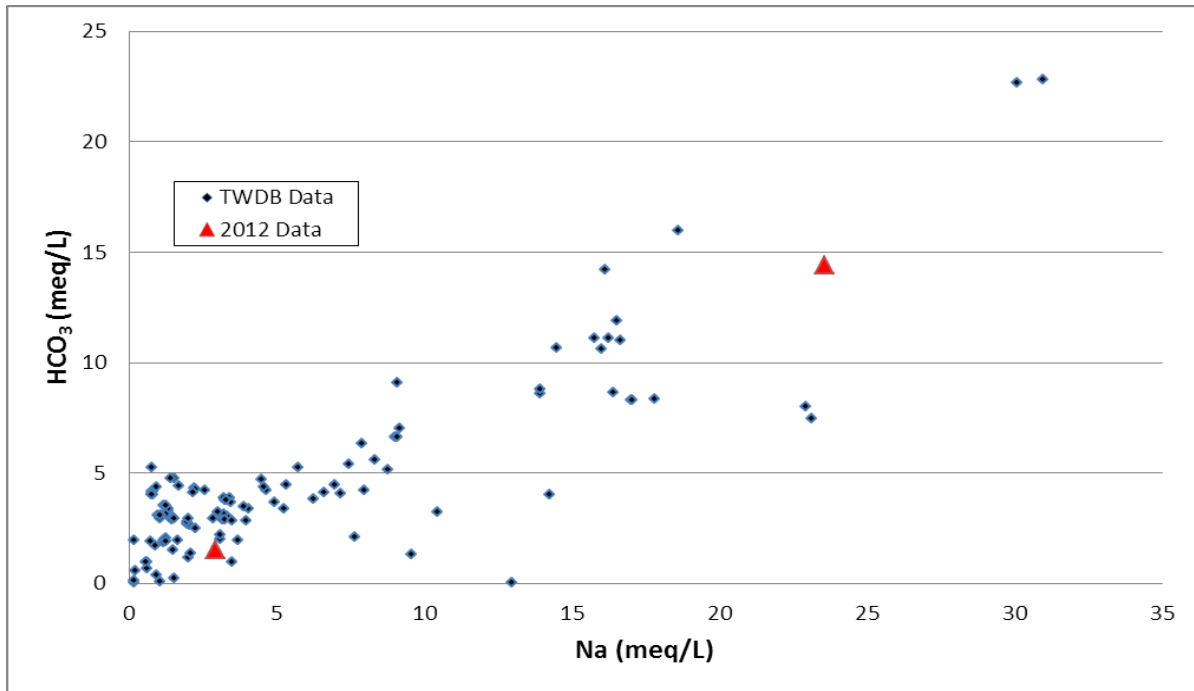


Figure 7-113. Bicarbonate (HCO<sub>3</sub>) versus sodium (Na) measured in milliequivalents per liter (meq/L), Queen City Aquifer, Central Transect, Groundwater Management Area 12.

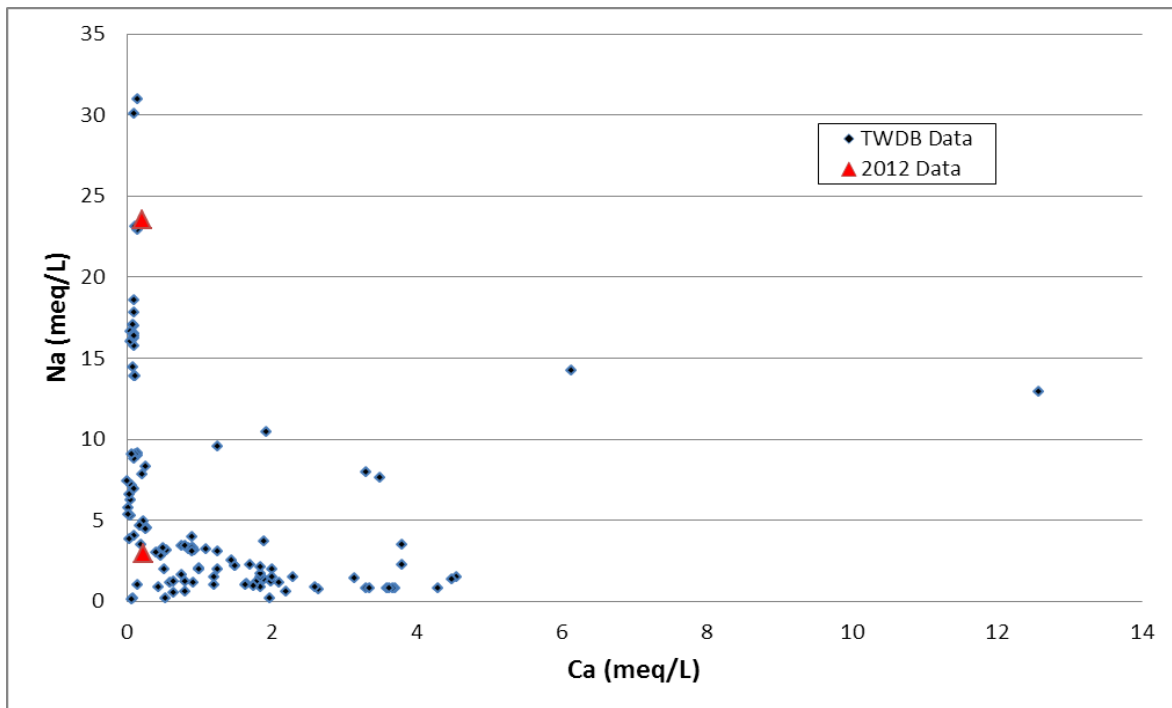


Figure 7-114. Sodium (Na) versus calcium (Ca) measured in milliequivalents per liter (meq/L), Queen City Aquifer, Central Transect, Groundwater Management Area 12.

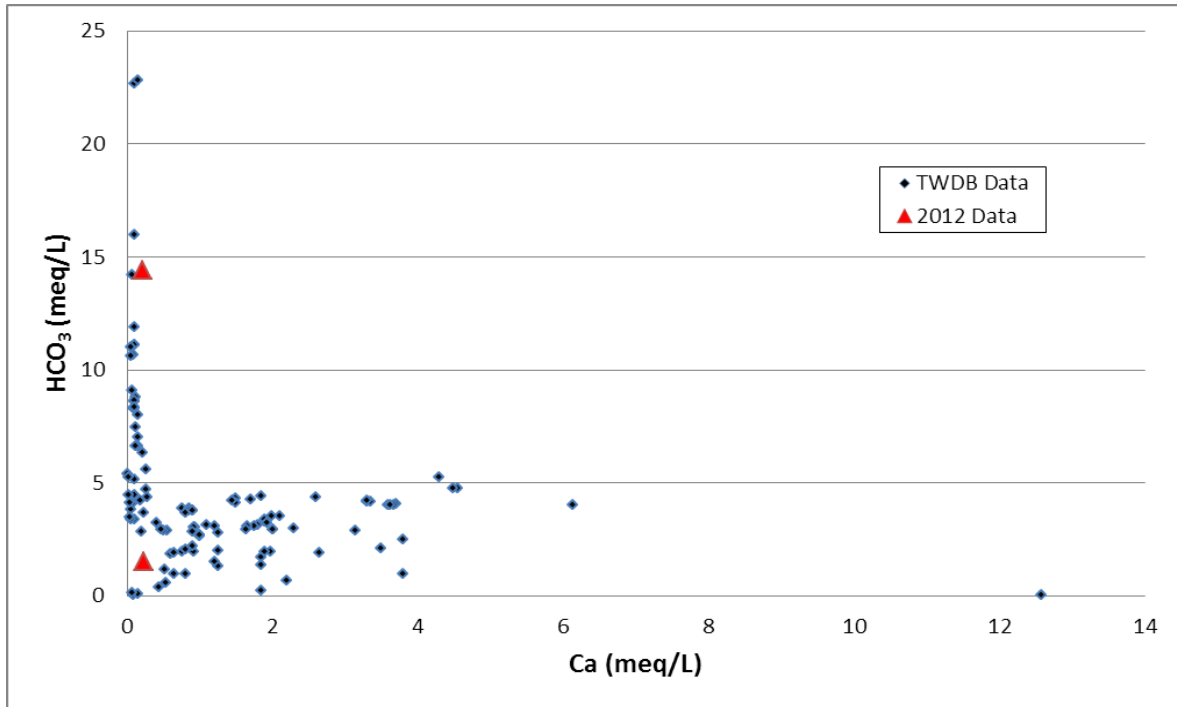


Figure 7-115. Bicarbonate (HCO<sub>3</sub>) versus calcium (Ca) measured in milliequivalents per liter (meq/L), Queen City Aquifer, Central Transect, Groundwater Management Area 12.

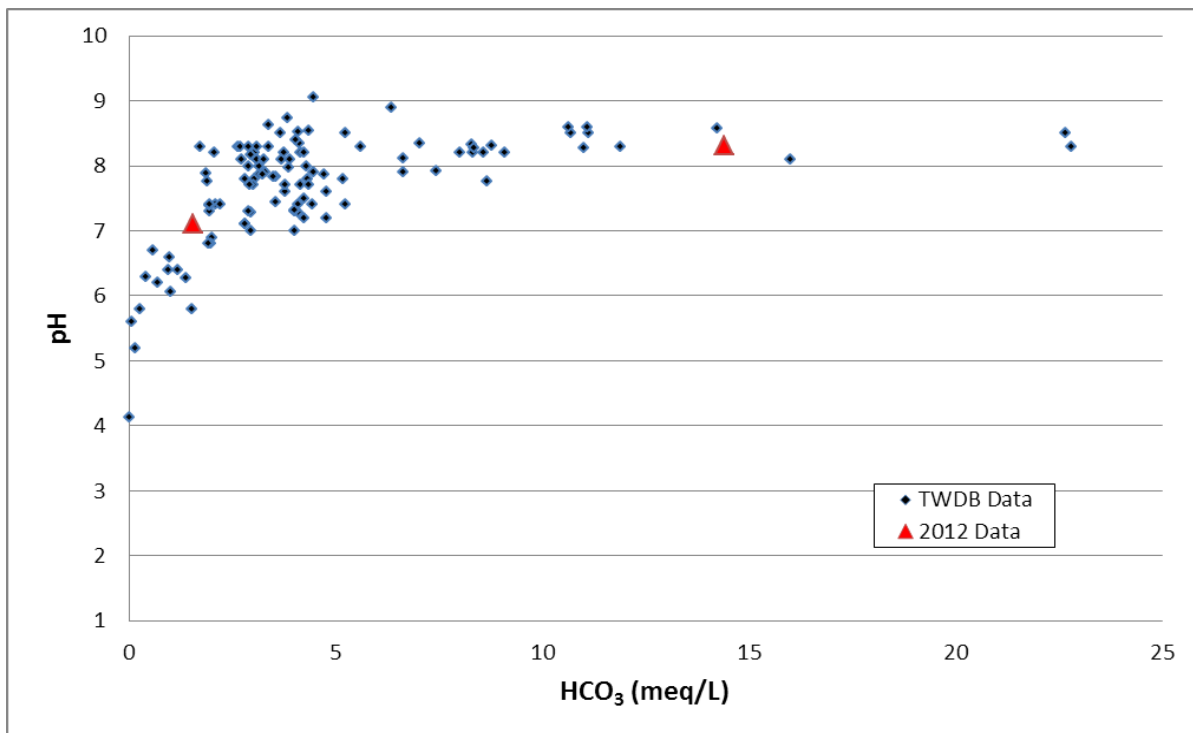


Figure 7-116. pH versus bicarbonate (HCO<sub>3</sub>) measured in milliequivalents per liter (meq/L), Queen City Aquifer, Central Transect, Groundwater Management Area 12.

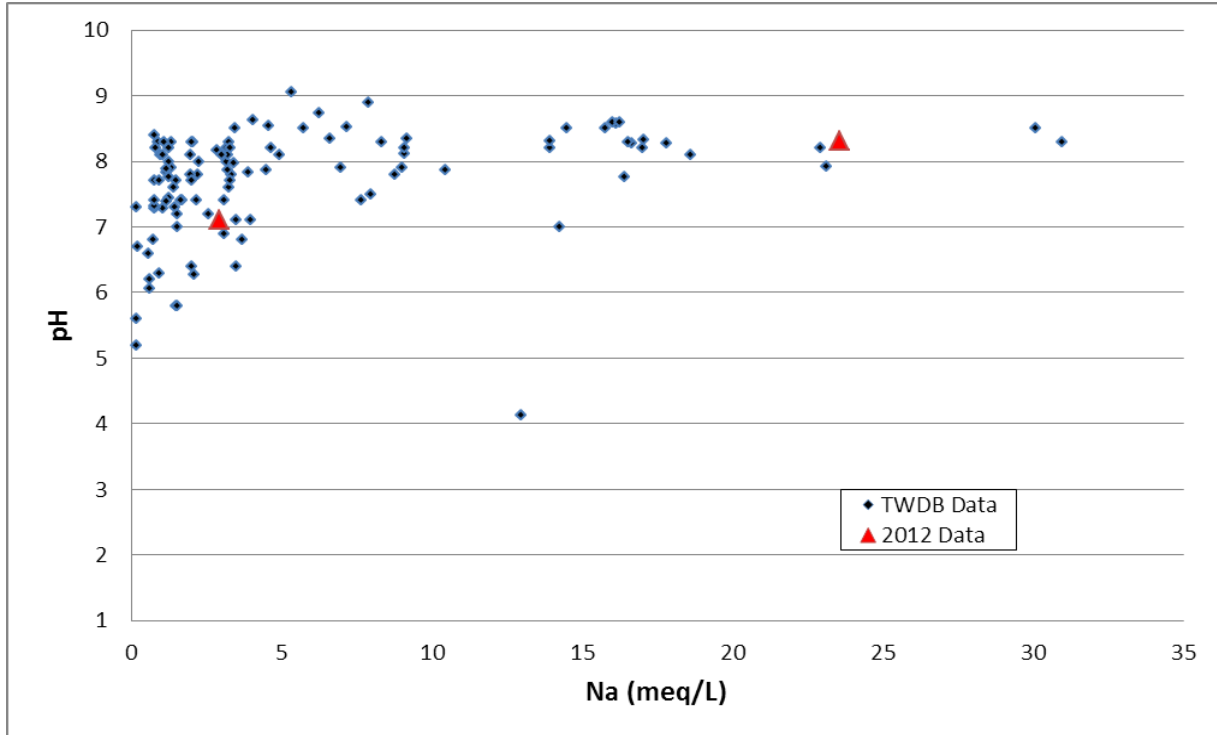


Figure 7-117. pH versus sodium (Na) measured in milliequivalents per liter (meq/L), Queen City Aquifer, Central Transect, Groundwater Management Area 12.

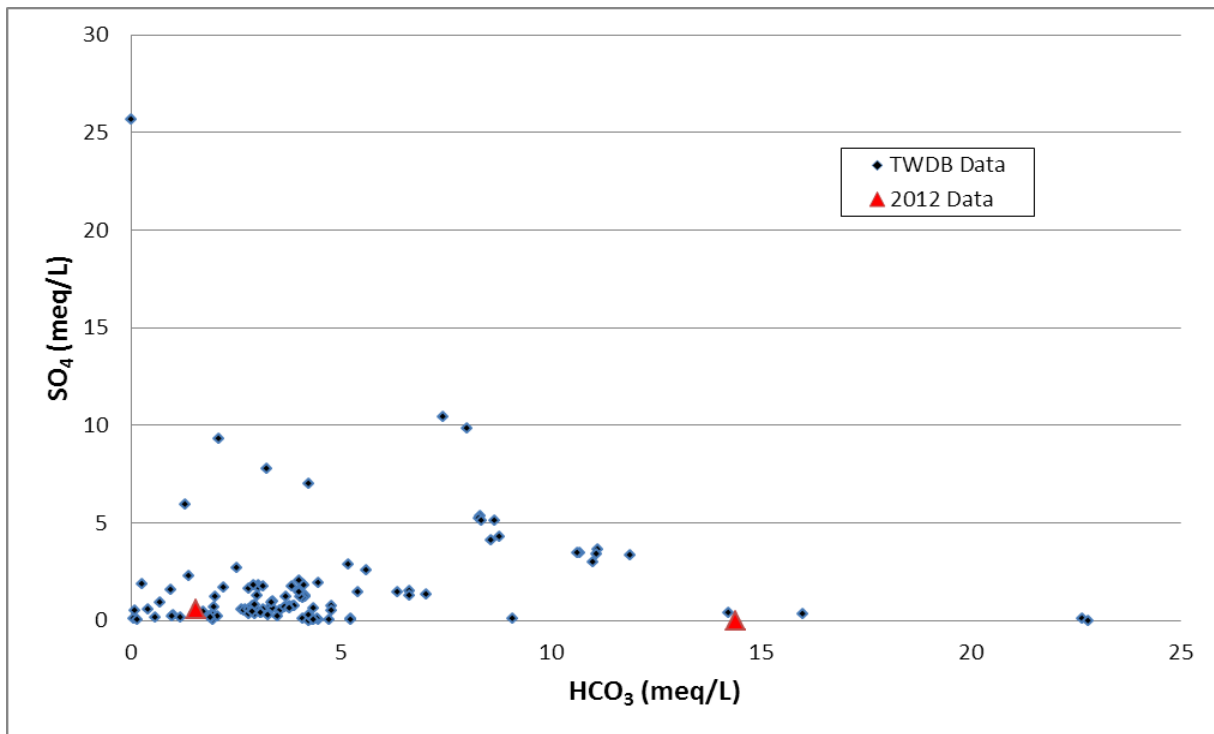


Figure 7-118. Sulfate (SO<sub>4</sub>) versus bicarbonate (HCO<sub>3</sub>) measured in milliequivalents per liter (meq/L), Queen City Aquifer, Central Transect, Groundwater Management Area 12.

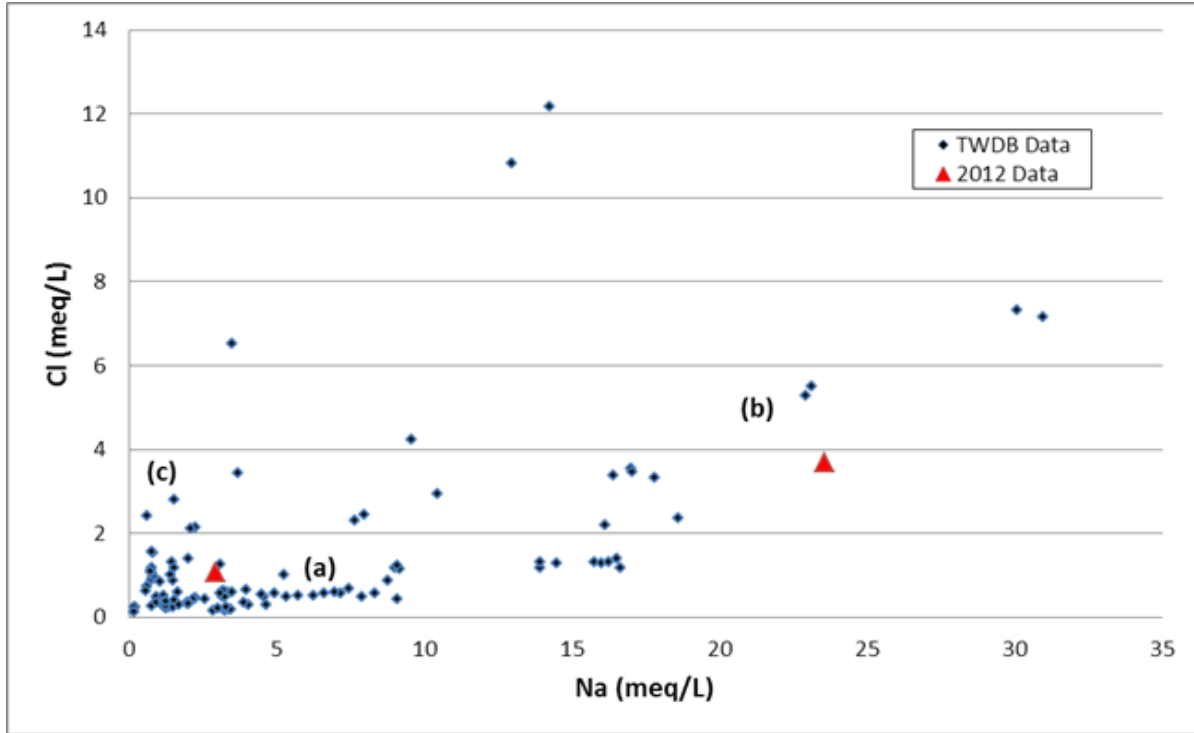


Figure 7-119. Chloride (Cl) versus sodium (Na) measured in milliequivalents per liter (meq/L), Queen City Aquifer, Central Transect, Groundwater Management Area 12.

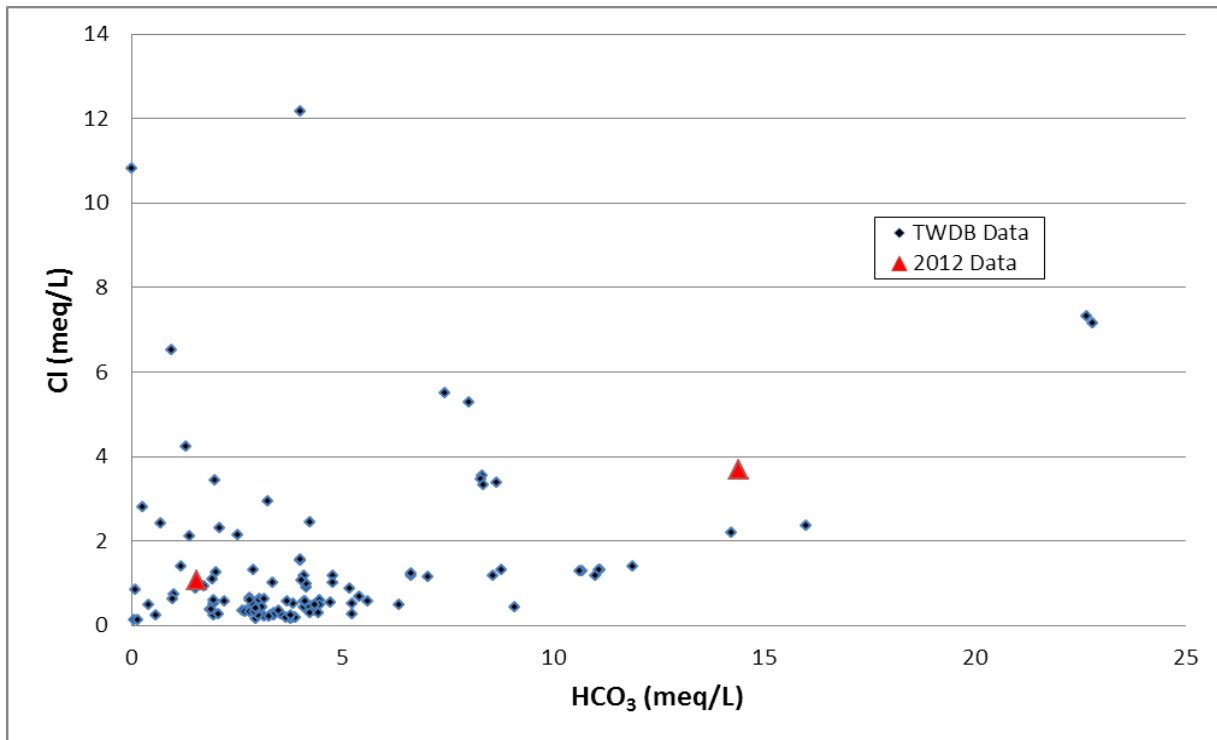


Figure 7-120. Chloride (Cl) versus bicarbonate ( $\text{HCO}_3$ ) measured in milliequivalents per liter (meq/L), Queen City Aquifer, Central Transect, Groundwater Management Area 12.

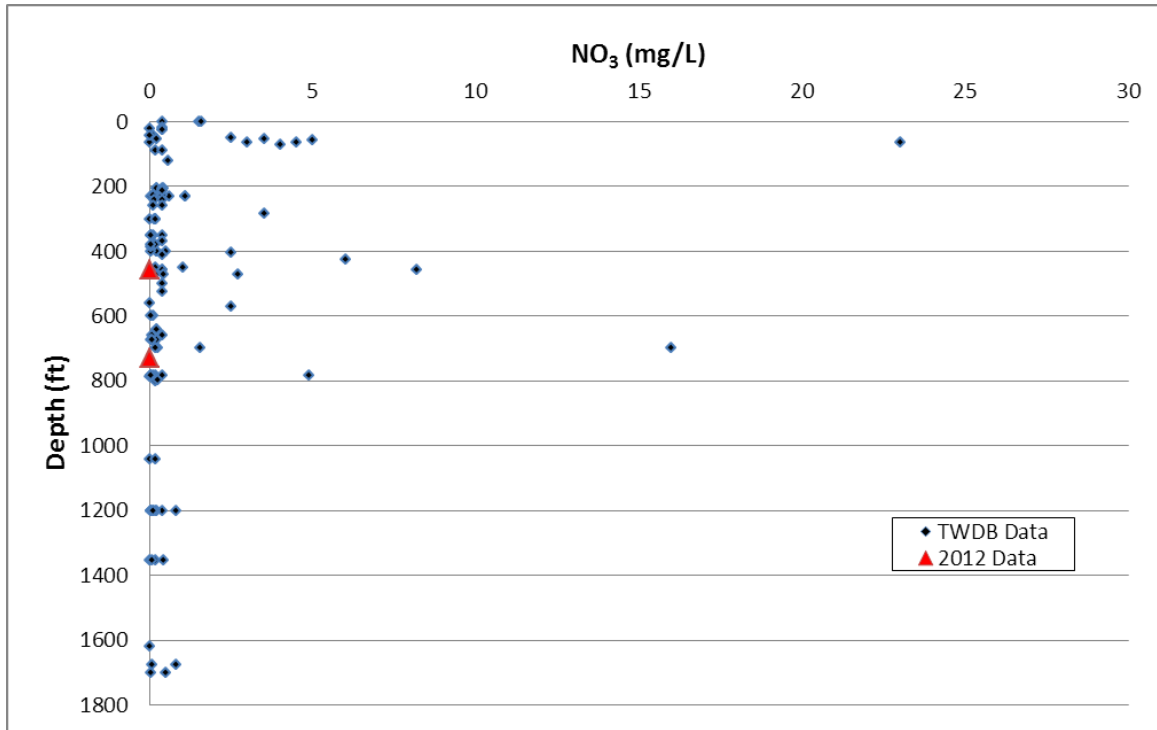


Figure 7-121. Depth measured from land surface in feet (ft) versus nitrate (NO<sub>3</sub>) measured in milligrams per liter (mg/L), Queen City Aquifer, Central Transect, Groundwater Management Area 12.

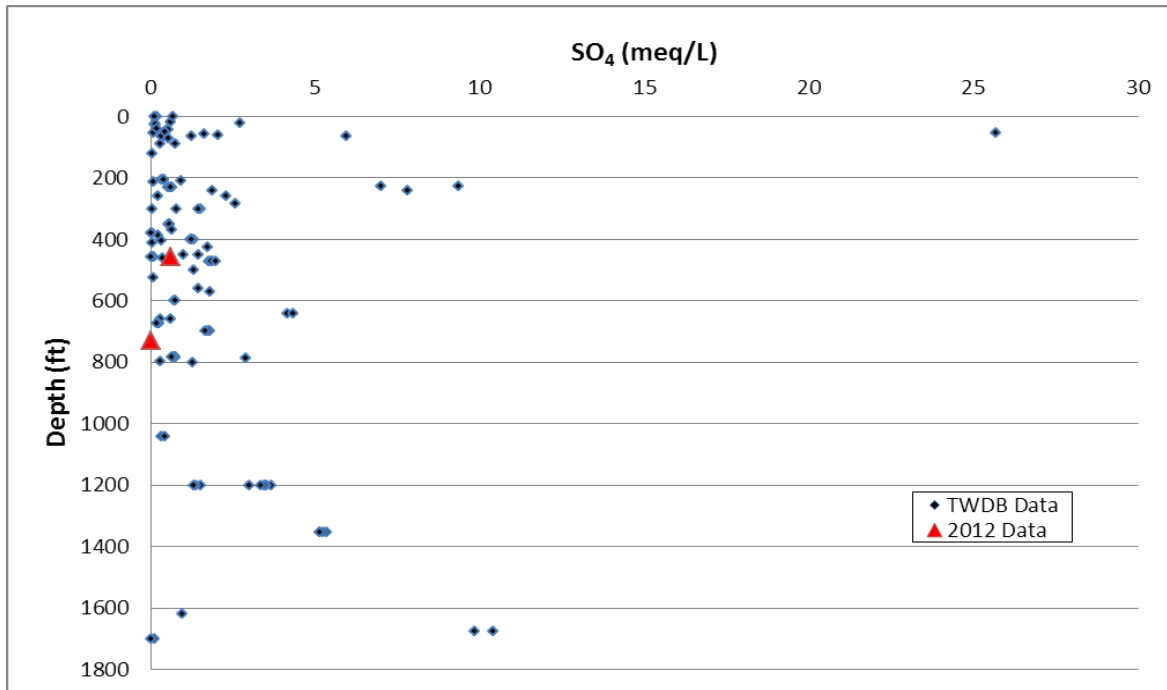


Figure 7-122. Depth measured from land surface in feet (ft) versus sulfate (SO<sub>4</sub>) measured in milliequivalents per liter (meq/L), Queen City Aquifer, Central Transect, Groundwater Management Area 12.

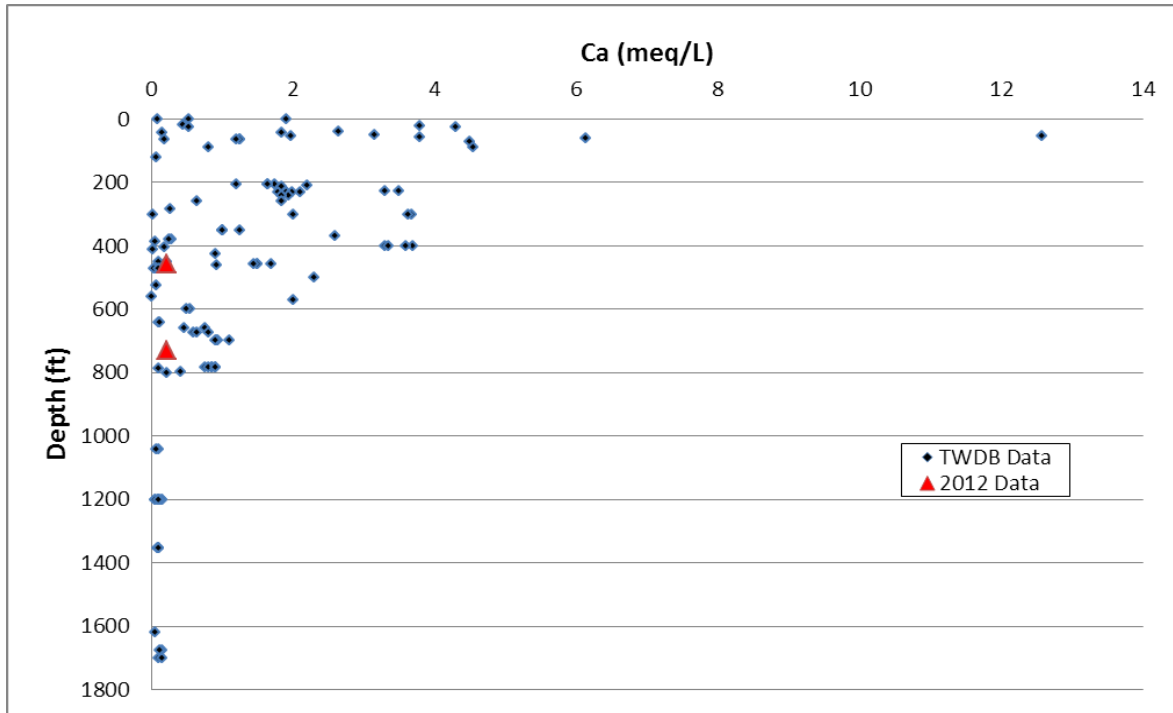


Figure 7-123. Depth measured from land surface in feet (ft) versus calcium (Ca) measured in milliequivalents per liter (meq/L), Queen City Aquifer, Central Transect, Groundwater Management Area 12.

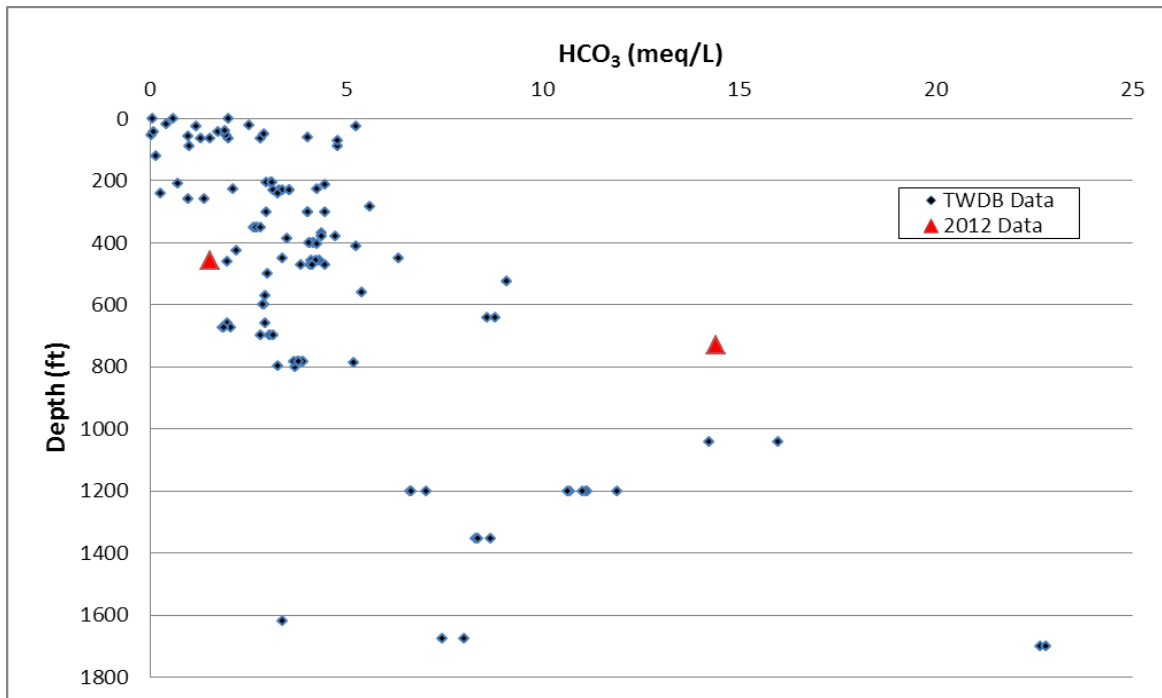


Figure 7-124. Depth measured from land surface in feet (ft) versus bicarbonate ( $\text{HCO}_3$ ) measured in milliequivalents per liter (meq/L), Queen City Aquifer, Central Transect, Groundwater Management Area 12.

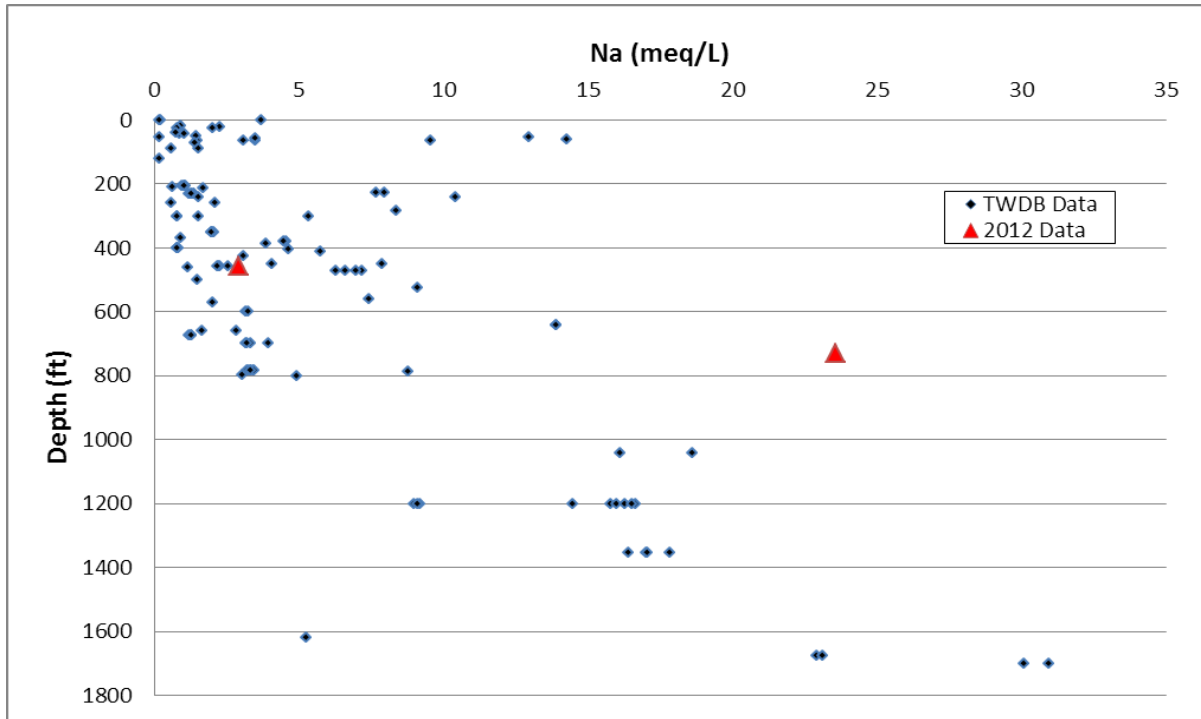


Figure 7-125. Depth measured from land surface in feet (ft) versus sodium (Na) measured in milliequivalents per liter (meq/L), Queen City Aquifer, Central Transect, Groundwater Management Area 12.

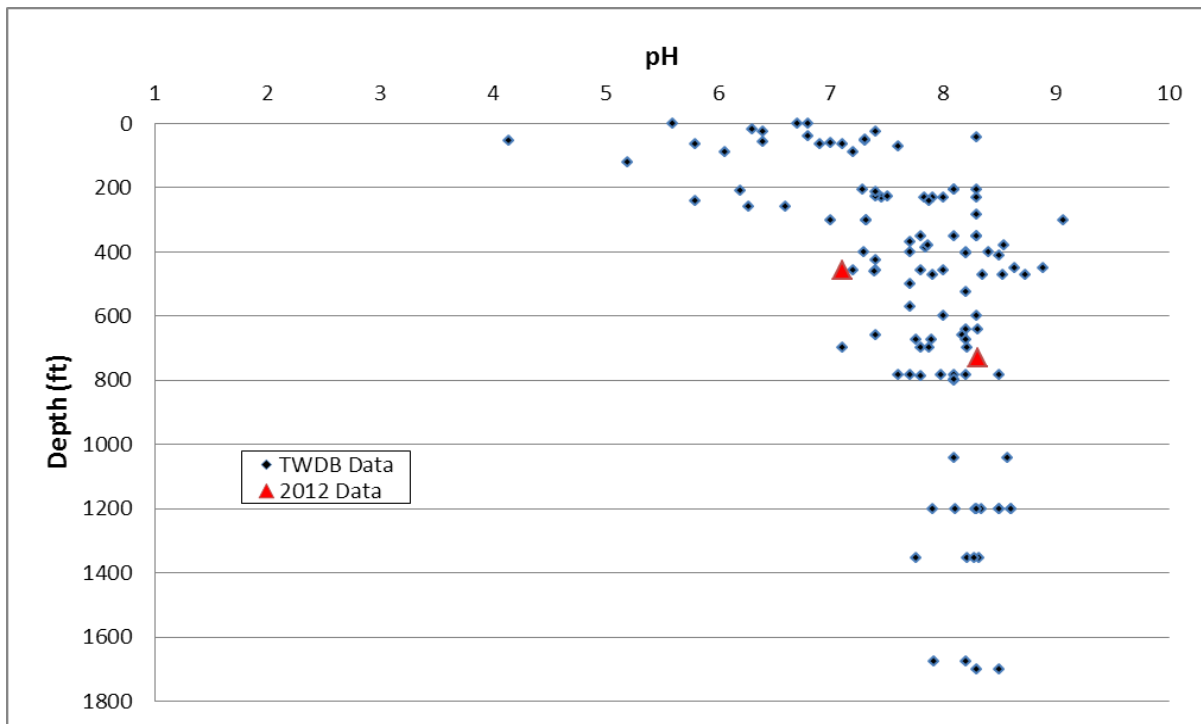


Figure 7-126. Depth measured from land surface in feet (ft) versus pH, Queen City Aquifer, Central Transect, Groundwater Management Area 12.

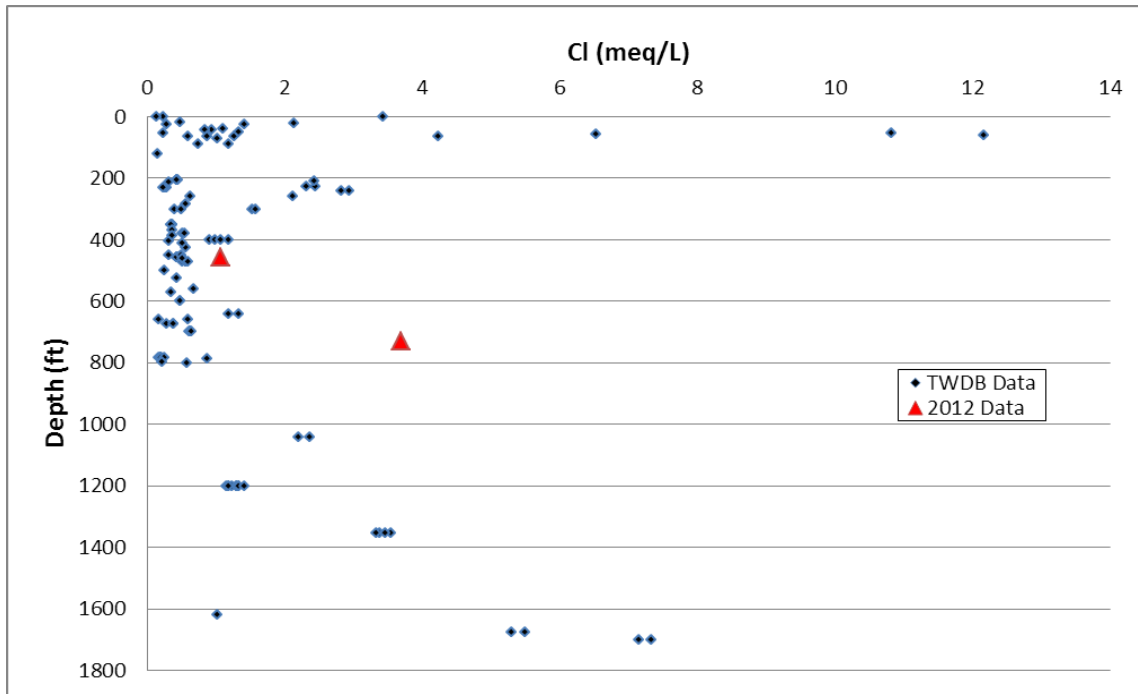


Figure 7-127. Depth measured from land surface in feet (ft) versus chloride (Cl) measured in milliequivalents per liter (meq/L), Queen City Aquifer, Central Transect, Groundwater Management Area 12.

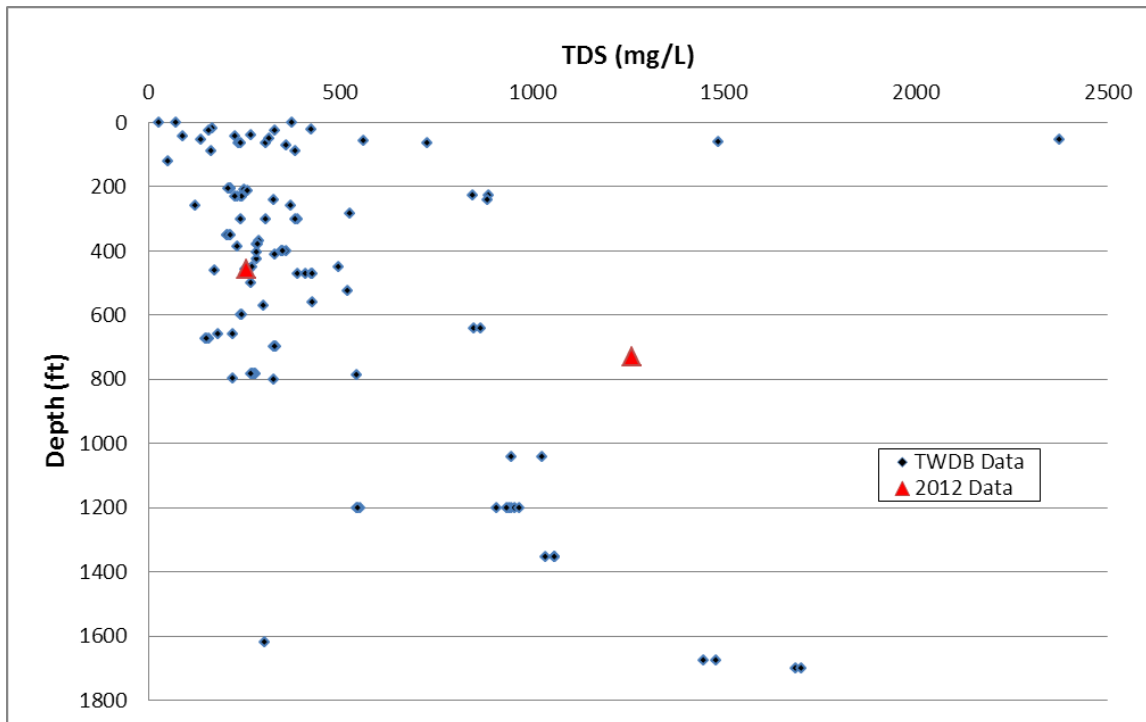


Figure 7-128. Depth measured from land surface in feet (ft) versus total dissolved solids (TDS) measured in parts per million (ppm), Queen City Aquifer, Central Transect, Groundwater Management Area 12.

## **Sparta Aquifer**

The Sparta Aquifer is a minor aquifer which extends southwest to northeast across the Central Transect. There is data available both in the outcrop and downdip for this aquifer. Well depths are less than 500 feet in the outcrop to greater than 2,000 feet downdip (Figure 7-129). The potentiometric surface dips from elevations of about 350 feet in the outcrop to elevations of about 200 feet in the confined section (Figure 7-130).

### Piper Diagram

The cation triangle for the Piper diagram for the Sparta Aquifer (Figure 7-131) shows a mixed (calcium-sodium-magnesium) cation and a mixed (chloride-bicarbonate-sulfate) anion composition in the outcrop, trending to a sodium-bicarbonate dominated composition at depths in the confined aquifer greater than 500 feet.

### Bicarbonate versus Sodium Plot

A plot of bicarbonate versus sodium (Figure 7-132) shows a linear increase in sodium and bicarbonate at a rate of about 1:1.

### Sodium versus Calcium Plot

A plot of sodium versus calcium (Figure 7-133) shows two separate limbs: 1) a calcium limb with low sodium and 2) a sodium limb with low calcium.

### Bicarbonate versus Calcium Plot

A plot of bicarbonate versus calcium (Figure 7-134) shows a similar relationship having two limbs between bicarbonate versus calcium as is observed for sodium versus calcium (Figure 7-133).

### pH versus Bicarbonate Plot

The plot of pH versus bicarbonate (Figure 7-135) shows three limbs: 1) pH rises independent of bicarbonate from five to seven, 2) pH increase to about eight with increasing bicarbonate and 3) bicarbonate increases independent of pH.

### pH versus Sodium Plot

The plot of pH versus sodium (Figure 7-136) is similar to pH versus bicarbonate (Figure 7-135), but does not show three distinct limbs for the data.

### Sulfate versus Bicarbonate Plot

The plot of sulfate versus bicarbonate (Figure 7-137) for the Sparta Aquifer shows higher sulfate values at bicarbonate concentrations less than about five milliequivalents per liter and low sulfate concentrations at bicarbonate values greater than ten milliequivalents per liter.

### Chloride versus Sodium Plot

The plot of chloride versus sodium (Figure 7-138) shows small increases in chloride at higher sodium concentrations.

### Chloride versus Bicarbonate Plot

The plot of chloride versus bicarbonate (Figure 7-139) shows a small increase of chloride with bicarbonate, suggesting a small addition of a sodium-chloride water.

#### Depth versus Sulfate Plot

The plot of depth versus sulfate (Figure 7-140) shows higher sulfate concentrations in the upper 500 feet and then declining to low concentrations of about 1,000 feet and then increase to about 1,500 feet.

#### Depth versus Calcium Plot

The plot of depth versus calcium (Figure 7-141) shows higher calcium concentrations in the upper 500 feet and then declining to low concentrations at depths greater than 500 feet.

#### Depth versus Bicarbonate Plot

The plot of depth versus bicarbonate (Figure 7-142) shows a general increase in bicarbonate with depth.

#### Depth versus Sodium Plot

The plot of depth versus sodium (Figure 7-143) shows a general increase of sodium with depth.

#### Depth versus pH Plot

The plot of depth versus pH (Figure 7-144) shows a general increase in pH with depth.

#### Depth versus Chloride Plot

The plot of depth versus chloride (Figure 7-145) shows a trend of a small increase in chloride with depth greater than 1,000 feet, with some random higher chloride throughout the samples depth range.

#### Depth versus Total Dissolved Solids Plot

The plot of depth versus total dissolved solids (Figure 7-146) shows a general increase of total dissolved solids with depth. The increase in total dissolved solids is primarily from increasing concentrations of sodium and bicarbonate and not increases in chloride.

#### Discussion

The cation triangle shows a mixed cation type water at shallower depths in the outcrop and sodium dominated water at depth (Figure 7-132 and Figure 7-144). The anion triangle shows a mixed-anion type water in the outcrop. Down dip the anion composition is dominated by bicarbonate. The Sparta Aquifer groundwater chemistry shows the typical evolution of sodium-bicarbonate water as seen in the underlying Queen City Aquifer and Wilcox Group of the Carrizo-Wilcox Aquifer. The chemical changes seen at depth may be accounted for by an intra-aquifer geochemistry and do not require cross-formational leakage from adjacent aquifers to account for the sodium-bicarbonate waters in the confined section. However, the possibility cannot be ruled out that mixing with the chemically similar groundwater in the underlying aquifers may occur and geochemistry alone may not be enough to differentiate the two.

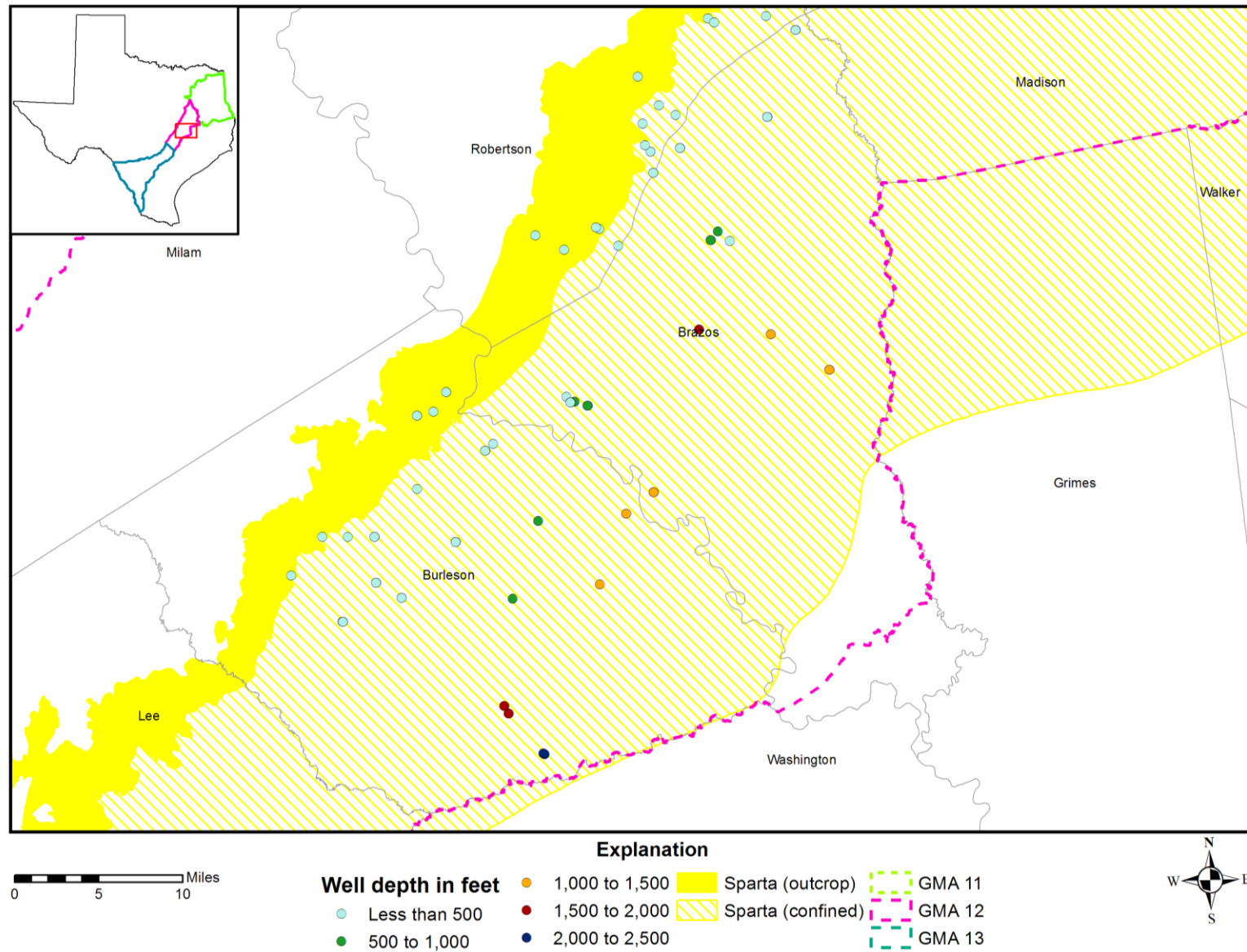


Figure 7-129. Well depths measured from land surface in feet in the Sparta Aquifer, Central Transect, Groundwater Management Area (GMA) 12.

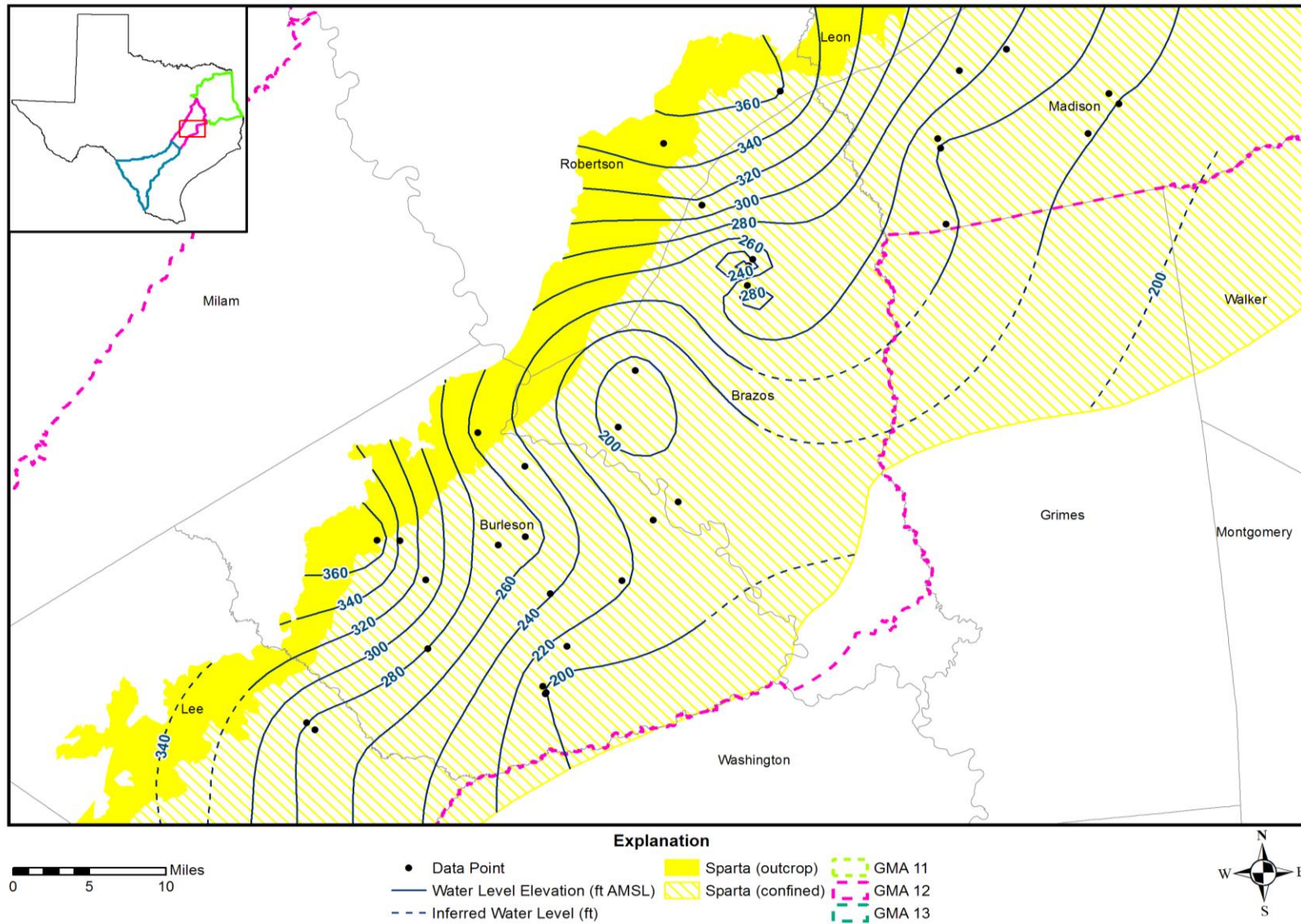


Figure 7-130. Potentiometric surface of the Sparta Aquifer using water level data measured in feet above mean sea level (ft AMSL) from 1990 to 2011 in the Central Transect, Groundwater Management Area 12.

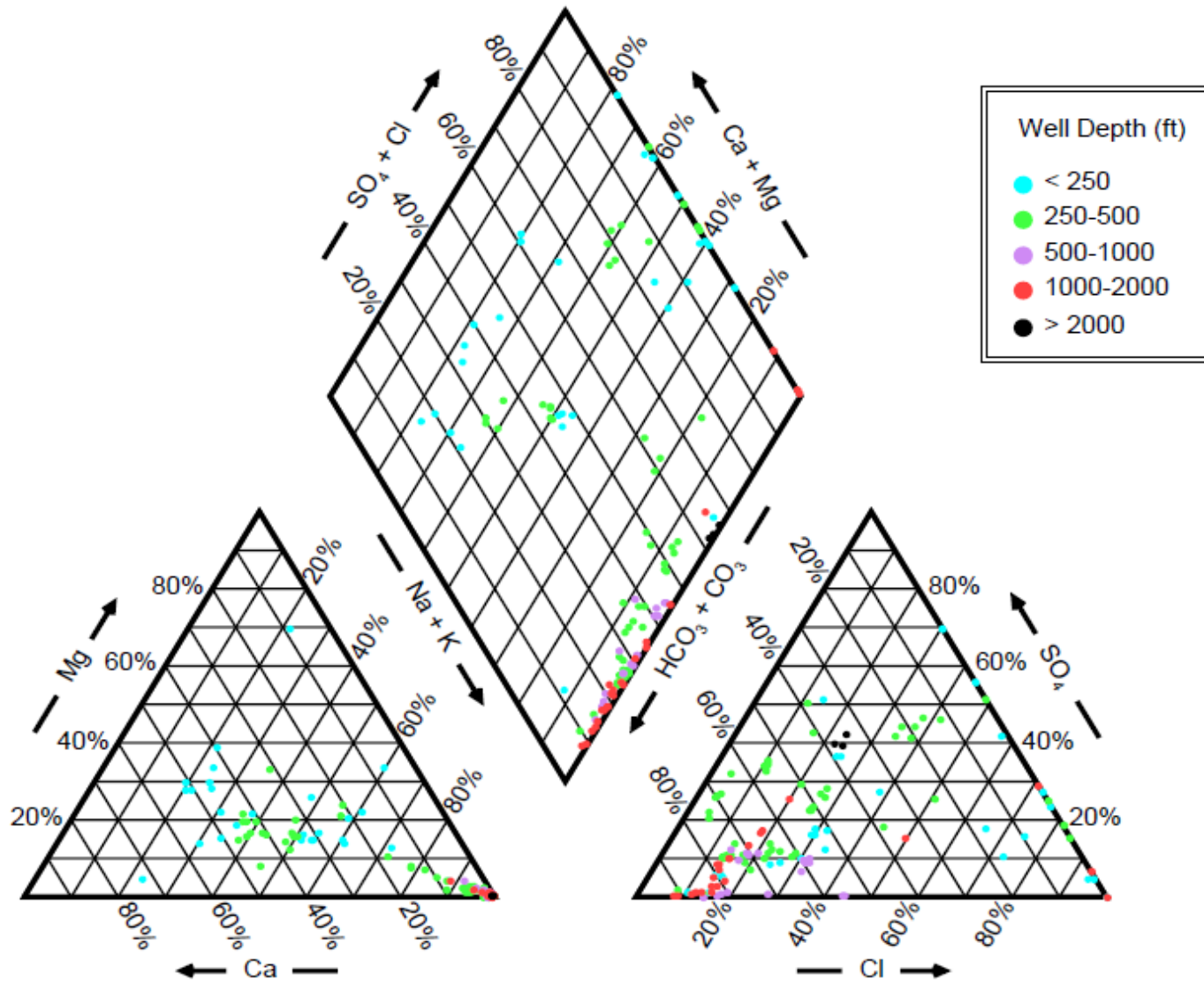


Figure 7-131. Piper diagram showing chemistry of the Sparta Aquifer wells in the Central Transect by well depth measured from land surface measured in feet (ft).

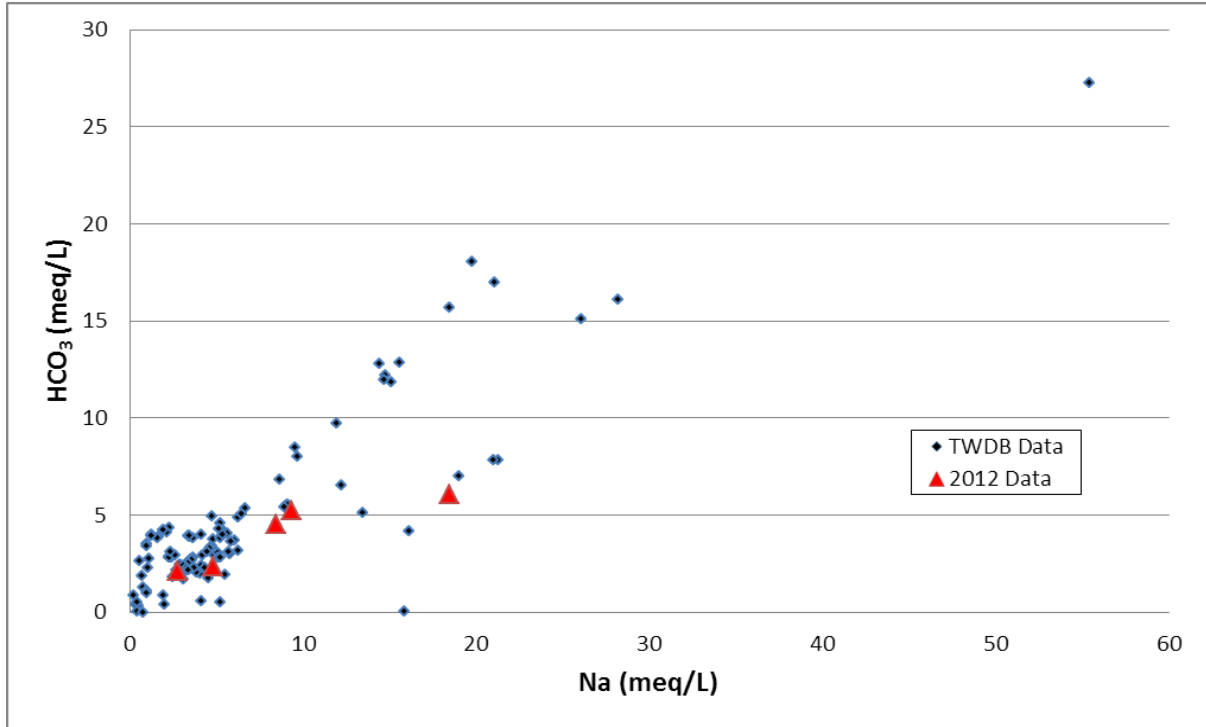


Figure 7-132. Bicarbonate ( $\text{HCO}_3$ ) versus sodium (Na) measured in milliequivalents per liter (meq/L), Sparta Aquifer, Central Transect, Groundwater Management Area 12.

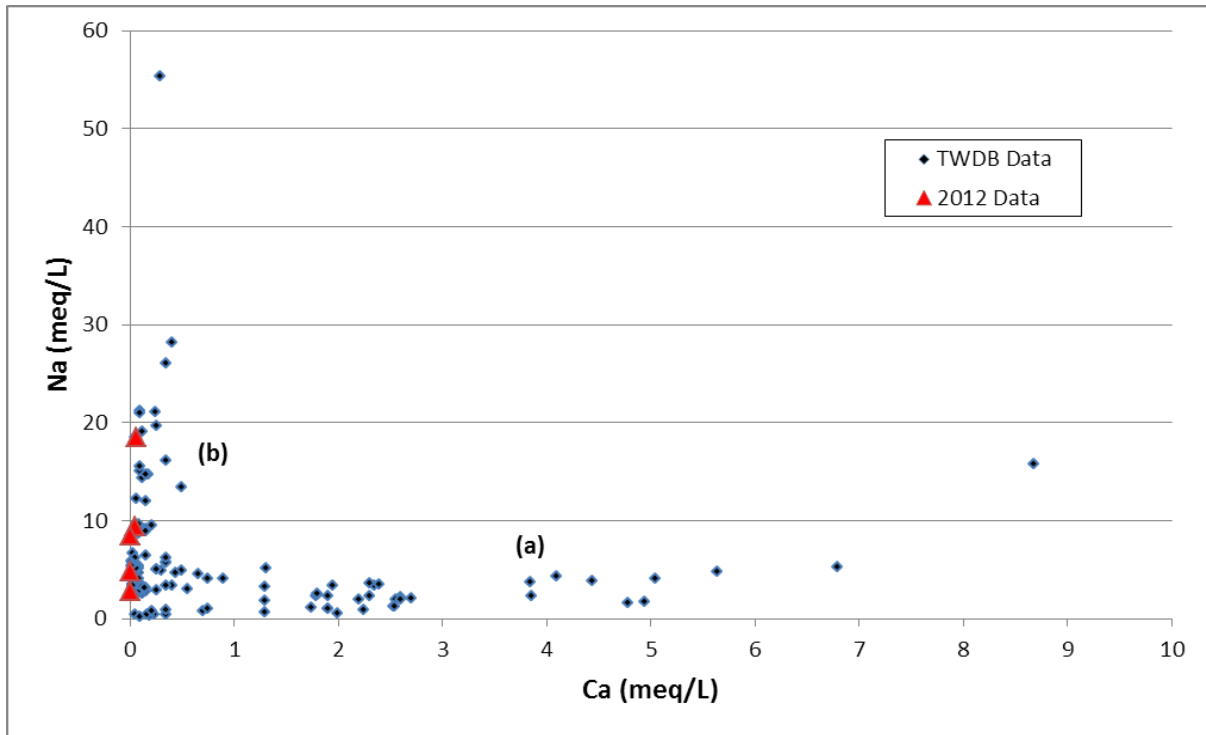


Figure 7-133. Sodium (Na) versus calcium (Ca) measured in milliequivalents per liter (meq/L), Sparta Aquifer, Central Transect, Groundwater Management Area 12.

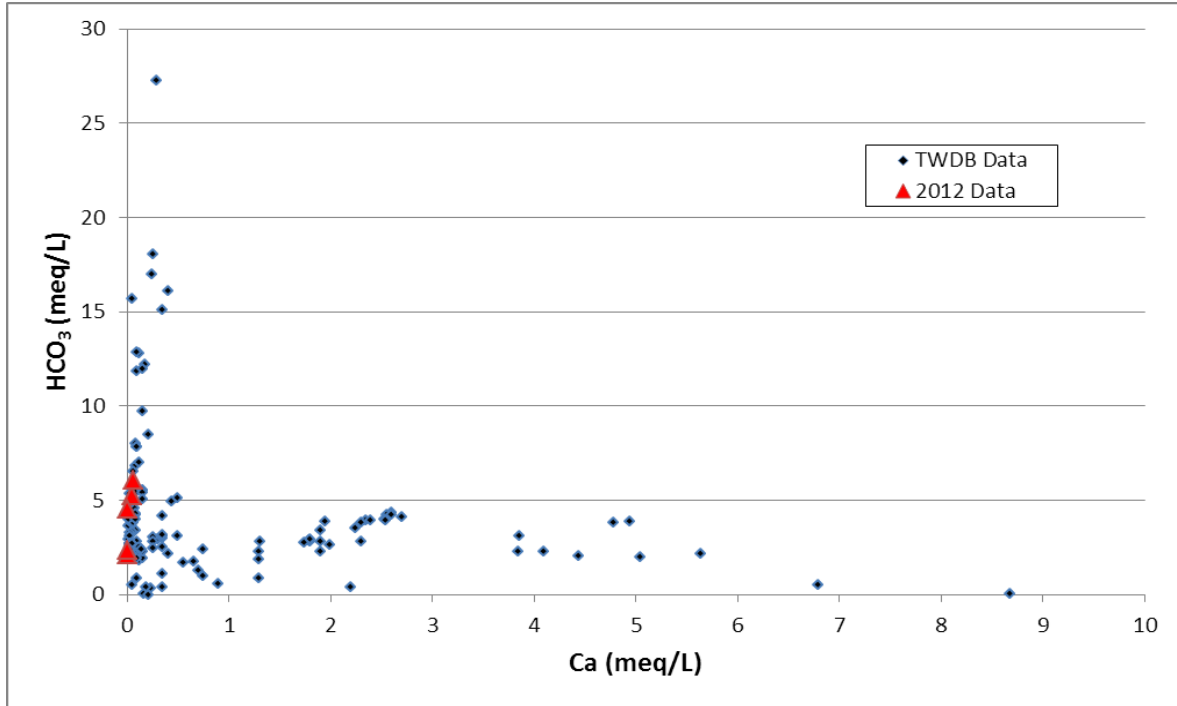


Figure 7-134. Bicarbonate (HCO<sub>3</sub>) versus calcium (Ca) measured in milliequivalents per liter (meq/L), Sparta Aquifer, Central Transect, Groundwater Management Area 12.

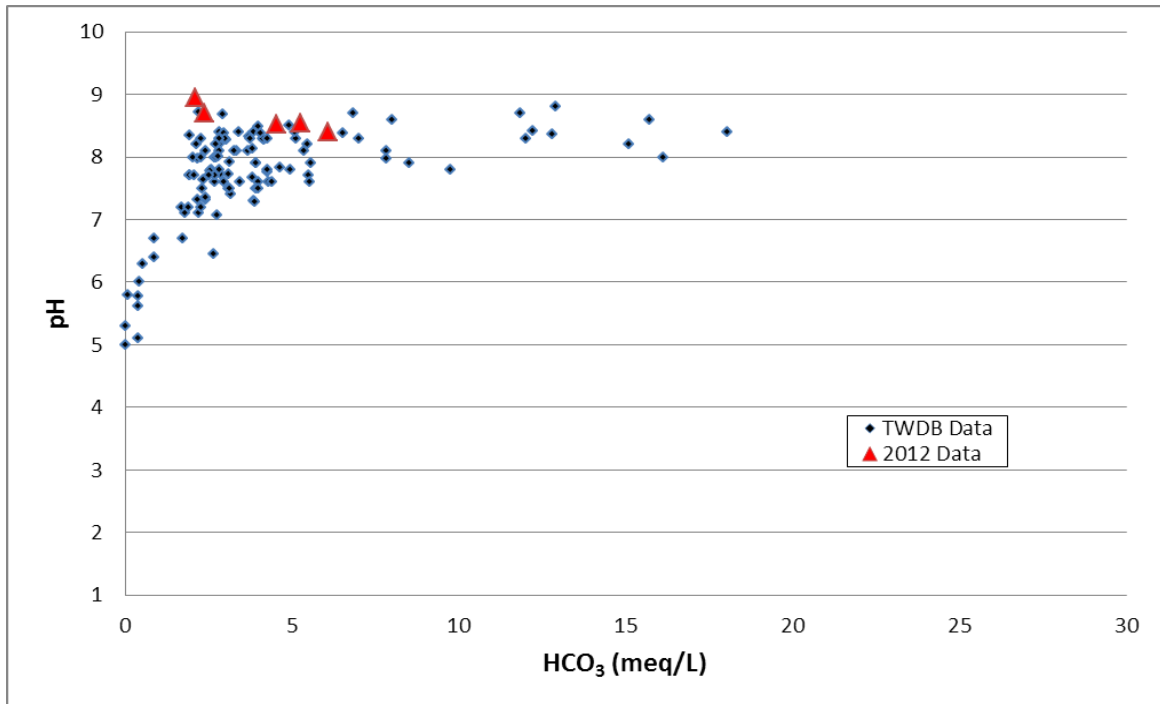


Figure 7-135. pH versus bicarbonate (HCO<sub>3</sub>) measured in milliequivalents per liter (meq/L), Sparta Aquifer, Central Transect, Groundwater Management Area 12.

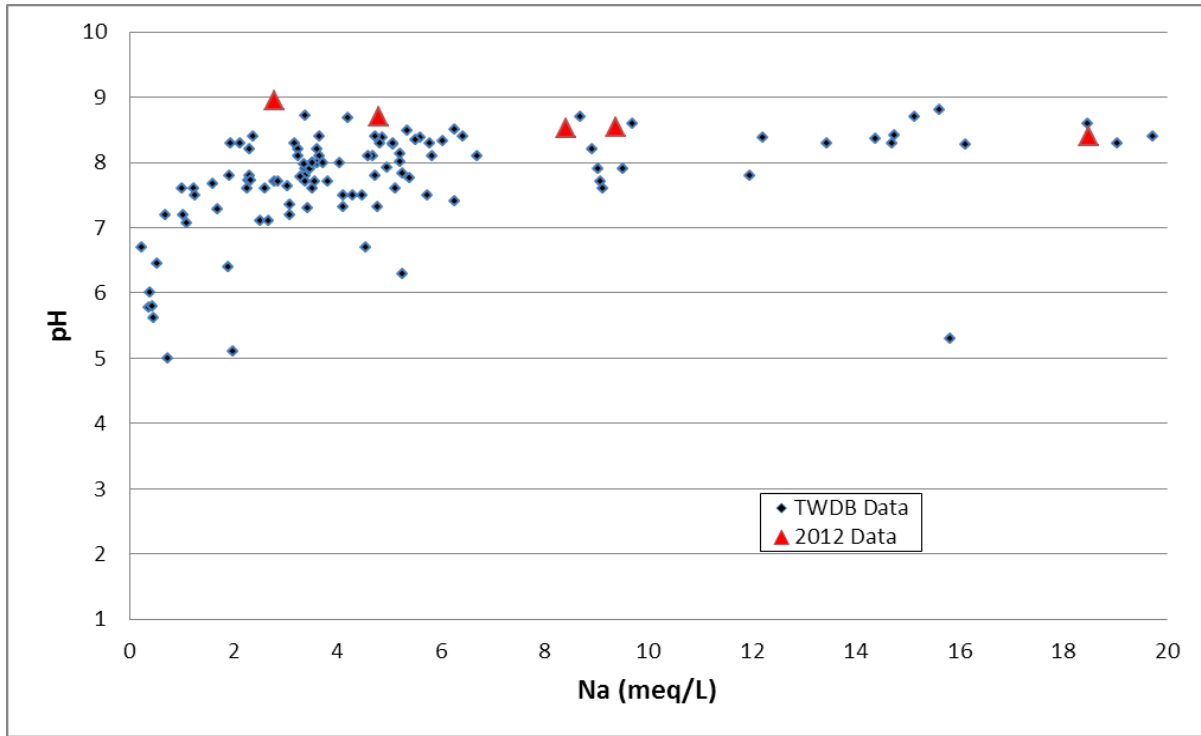


Figure 7-136. pH versus sodium (Na) measured in milliequivalents per liter (meq/L), Sparta Aquifer, Central Transect, Groundwater Management Area 12.

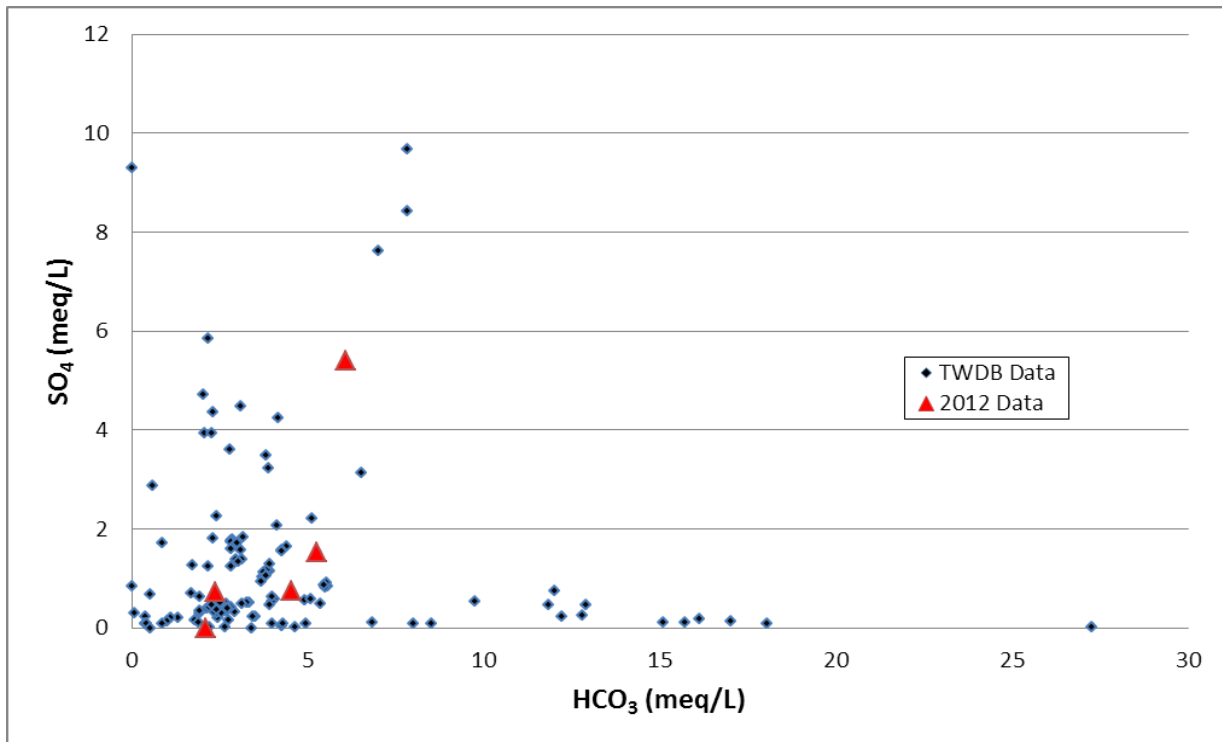


Figure 7-137. Sulfate (SO<sub>4</sub>) versus bicarbonate (HCO<sub>3</sub>) measured in milliequivalents per liter (meq/L), Sparta Aquifer, Central Transect, Groundwater Management Area 12.

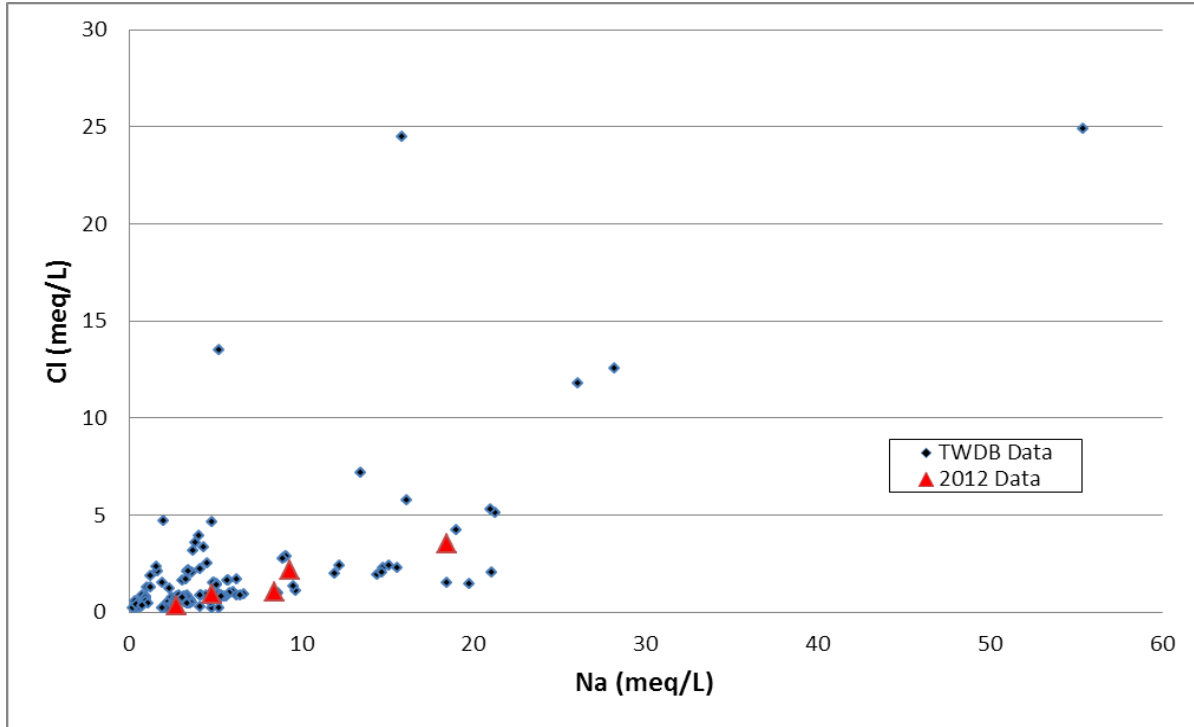


Figure 7-138. Chloride (Cl) versus sodium (Na) measured in milliequivalents per liter (meq/L), Sparta Aquifer, Central Transect, Groundwater Management Area 12.

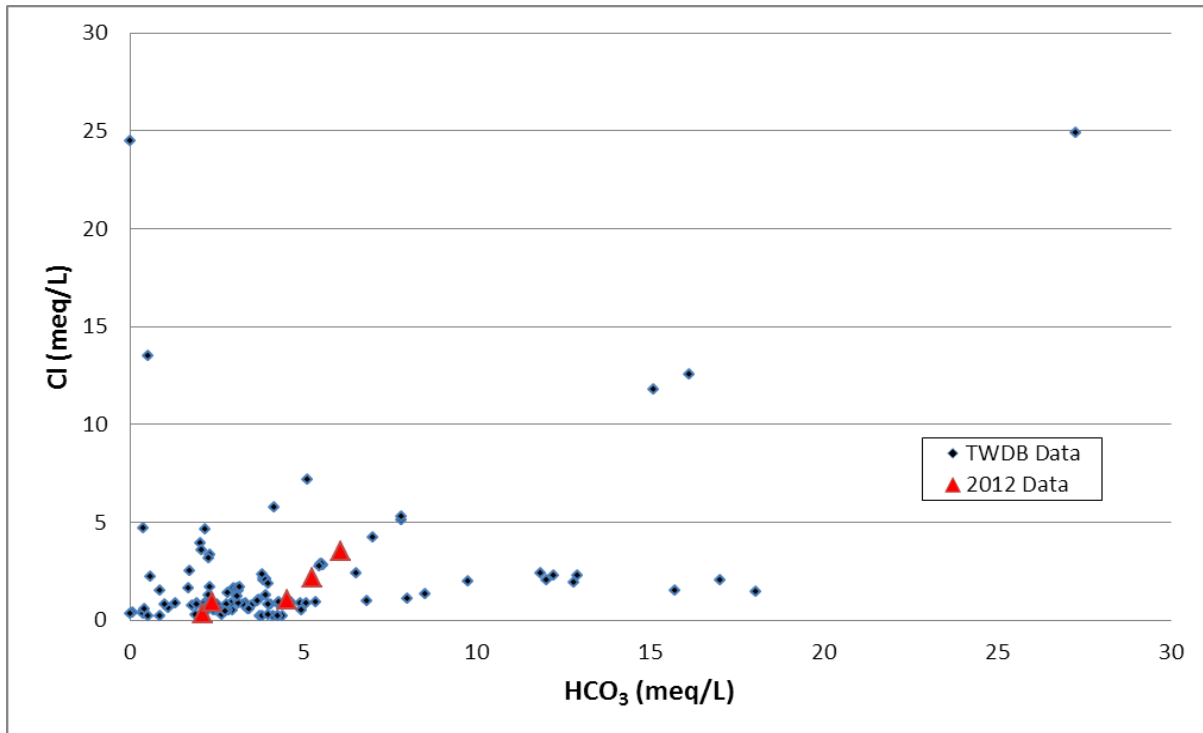


Figure 7-139. Chloride (Cl) versus bicarbonate (HCO<sub>3</sub>) measured in milliequivalents per liter (meq/L), Sparta Aquifer, Central Transect, Groundwater Management Area 12.

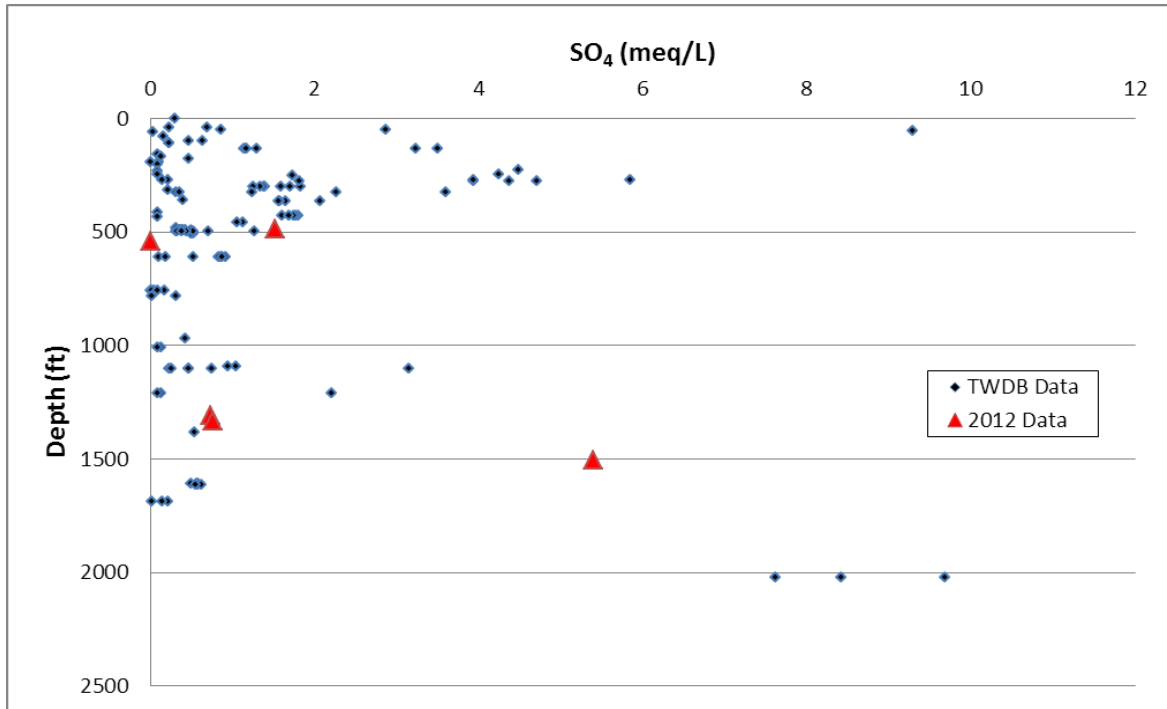


Figure 7-140. Depth measured from land surface in feet (ft) versus sulfate ( $\text{SO}_4$ ) measured in milliequivalents per liter (meq/L), Sparta Aquifer, Central Transect, Groundwater Management Area 12.

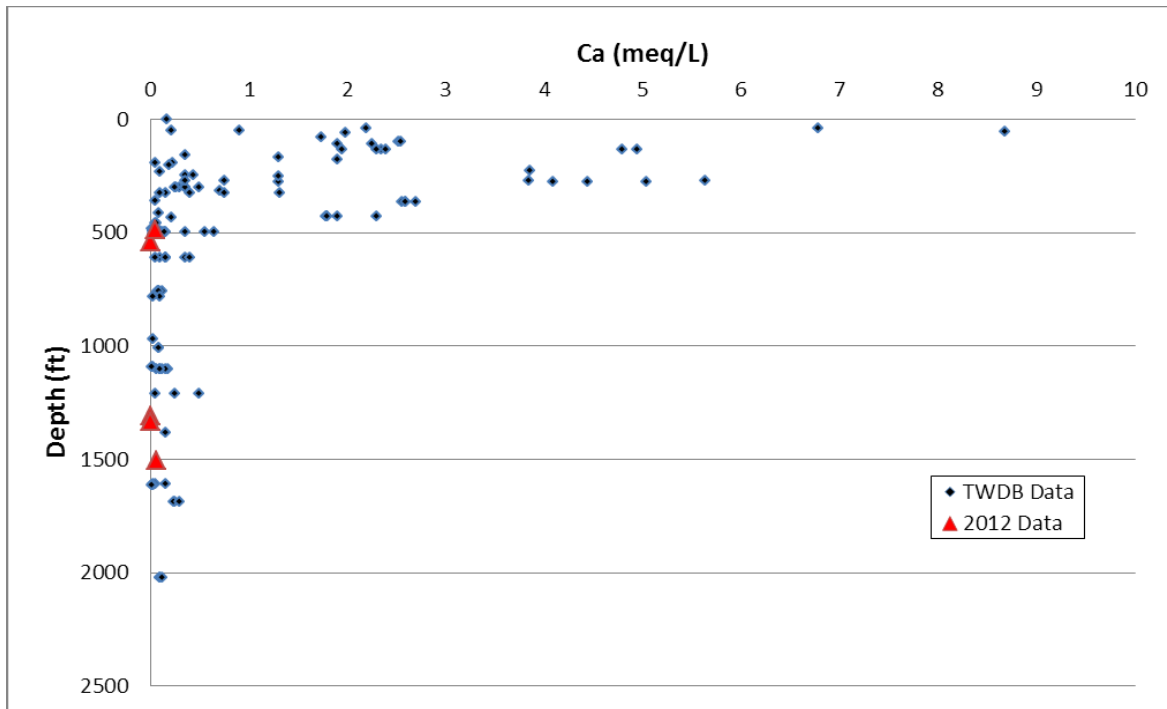


Figure 7-141. Depth measured from land surface in feet (ft) versus calcium (Ca) measured in milliequivalents per liter (meq/L), Sparta Aquifer, Central Transect, Groundwater Management Area 12.

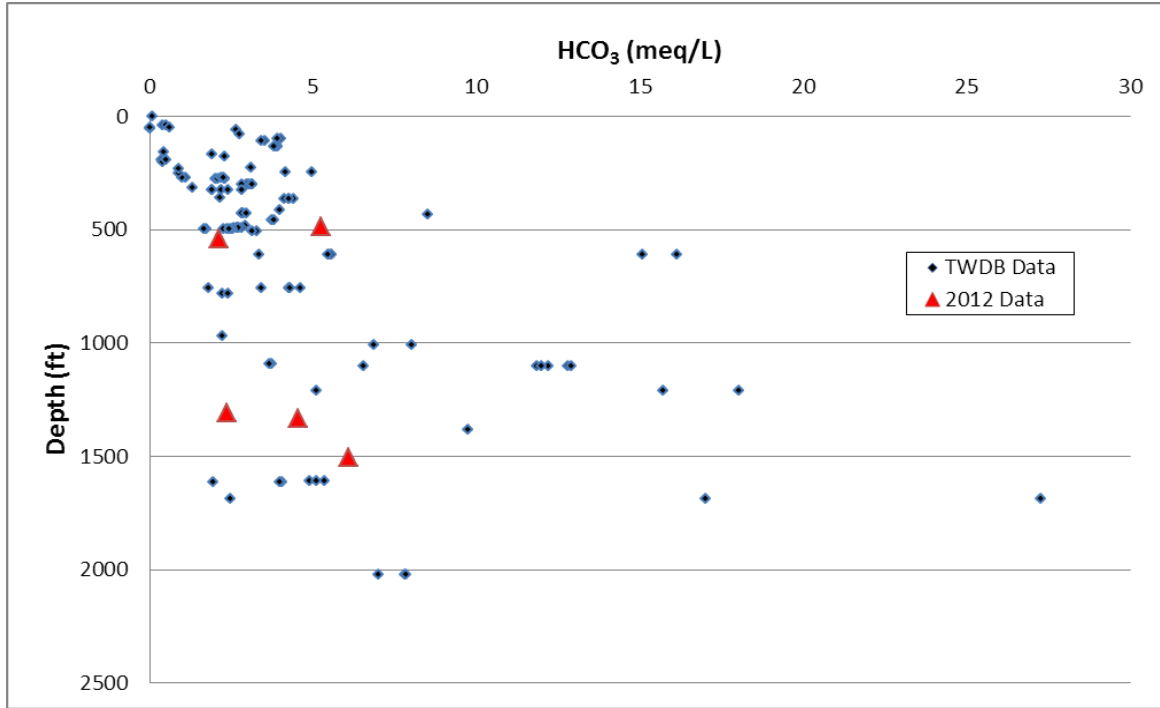


Figure 7-142. Depth measured from land surface in feet (ft) versus bicarbonate ( $\text{HCO}_3$ ) measured in milliequivalents per liter (meq/L), Sparta Aquifer, Central Transect, Groundwater Management Area 12.

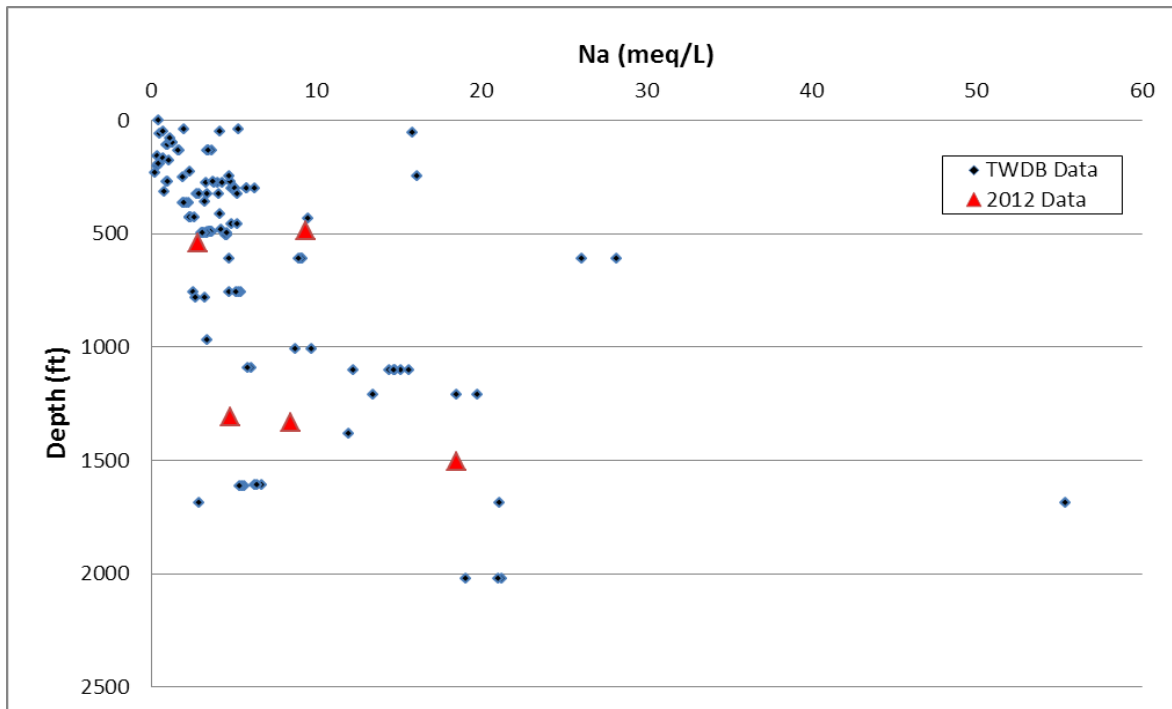


Figure 7-143. Depth measured from land surface in feet (ft) versus sodium (Na) measured in milliequivalents per liter (meq/L), Sparta Aquifer, Central Transect, Groundwater Management Area 12.

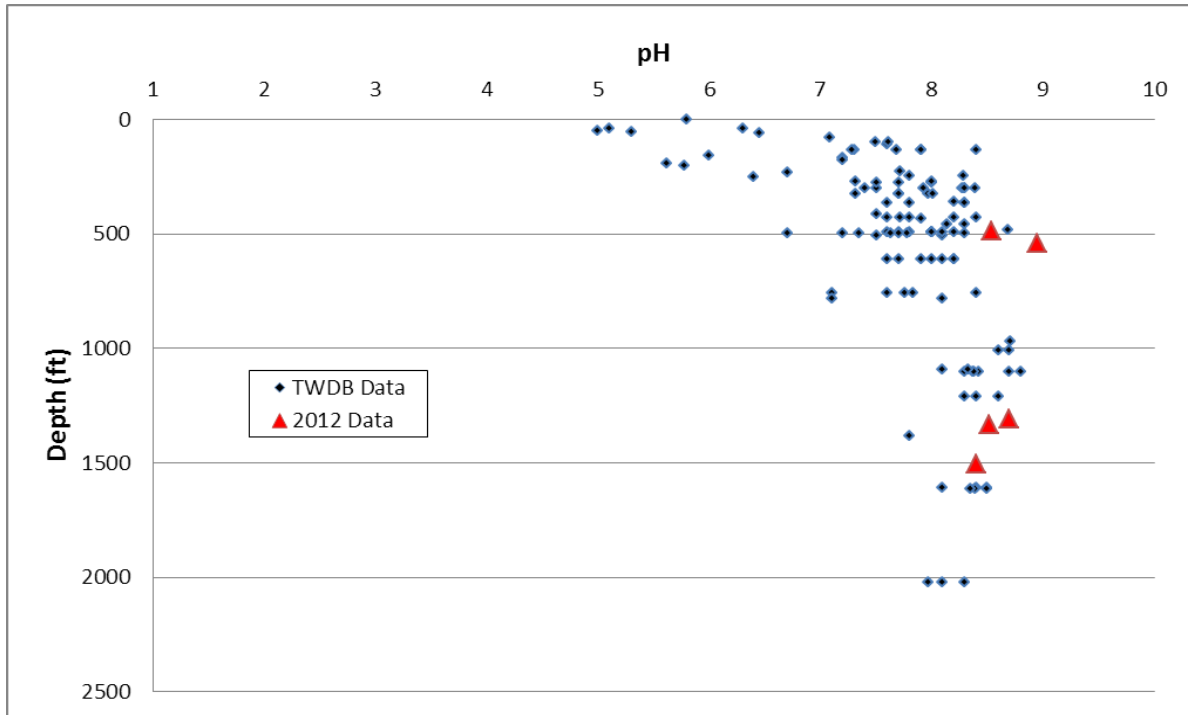


Figure 7-144. Depth measured from land surface in feet (ft) versus pH, Sparta Aquifer, Central Transect, Groundwater Management Area 12.

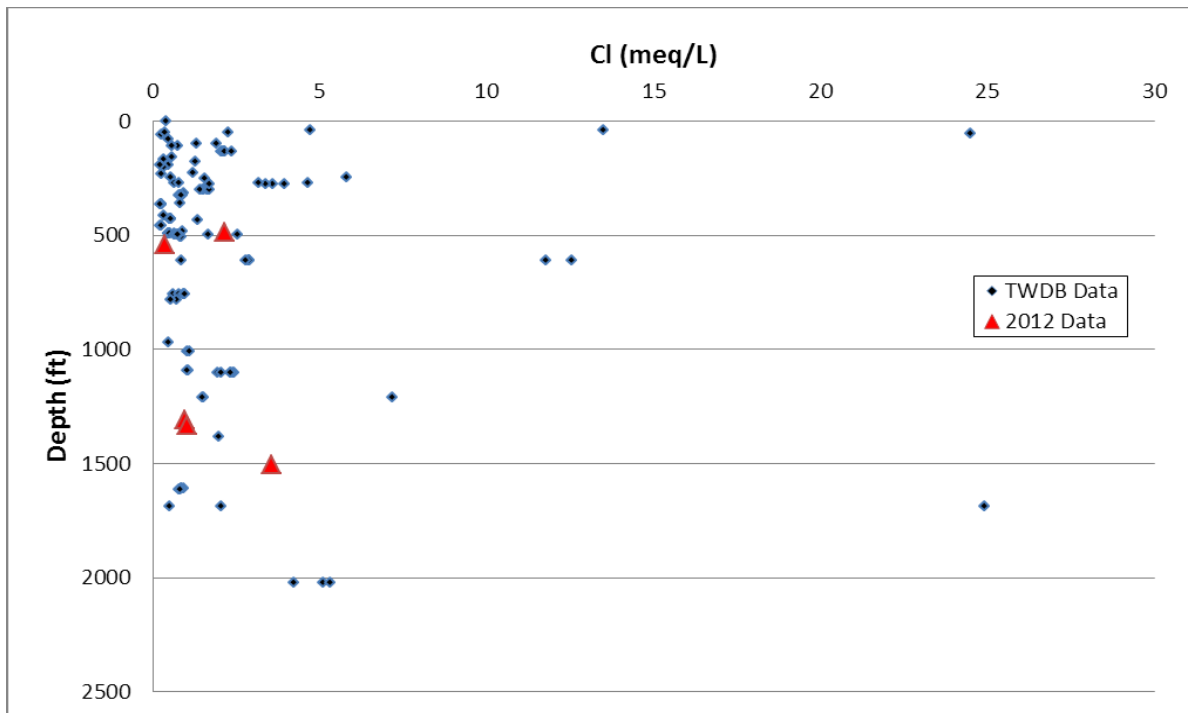
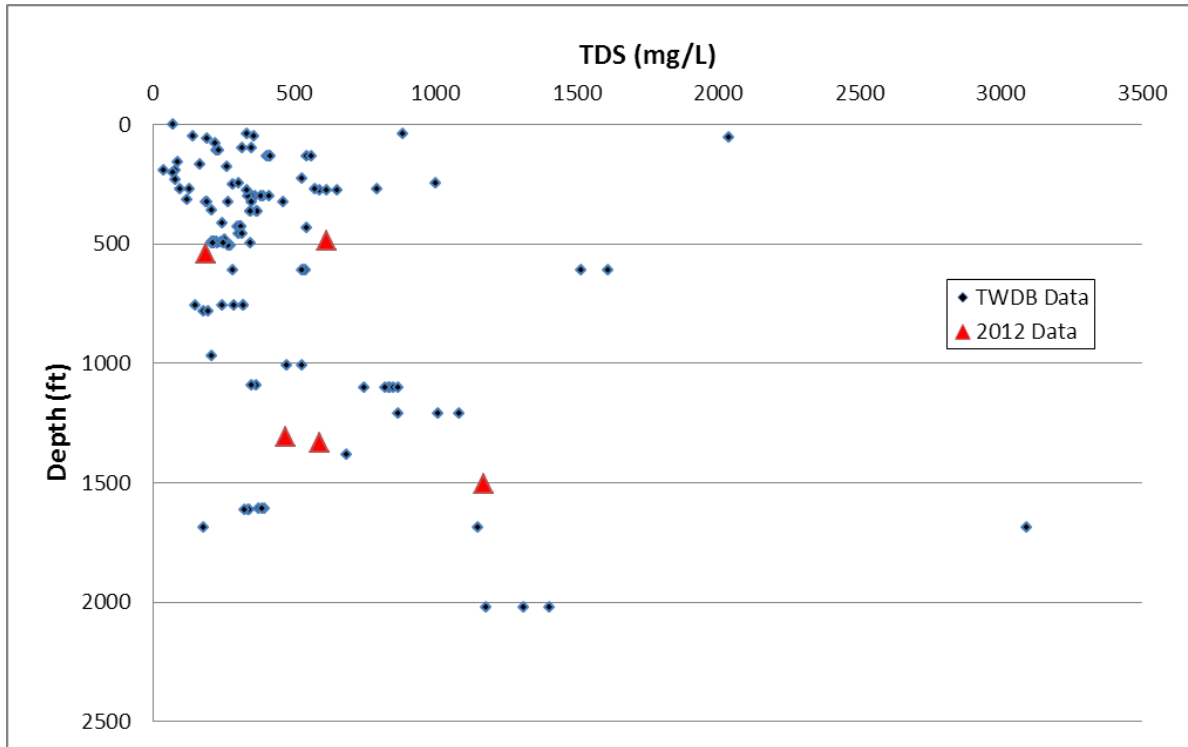


Figure 7-145. Depth measured from land surface in feet (ft) versus chloride (Cl) measured in milliequivalents per liter (meq/L), Sparta Aquifer, Central Transect, Groundwater Management Area 12.



**Figure 7-146.** Depth measured from land surface in feet (ft) versus total dissolved solids (TDS) measured in parts per million (ppm), Sparta Aquifer, Central Transect, Groundwater Management Area 12.

### Yegua-Jackson Aquifer

The Yegua-Jackson Aquifer outcrop is in Brazos and Burleson counties (Figure 7-147). There are only a limited number of wells in the outcrop. Most of the data from this analysis are from the TWDB database. Two Yegua-Jackson Aquifer wells were sampled in 2012. There are no wells in the TWDB database for the downdip confined section of the Yegua-Jackson Aquifer.

#### Well Depths

Well depths in the outcrop of the Yegua-Jackson Aquifer are generally less than 600 feet (Figure 7-147).

#### Water Levels

Water levels in the Yegua-Jackson Aquifer range from about 260 to 200 feet (Figure 7-148).

#### Piper Diagram

The Piper diagram for the Yegua-Jackson Aquifer in the Central Transect (Figure 7-149) shows a sodium type water in the cation triangle and a mixed chloride-sulfate-bicarbonate water in the anion triangle. This Piper diagram represents the outcrop water chemistry. There are no downdip Yegua-Jackson Aquifer wells.

#### Bicarbonate versus Sodium Plot

A plot of bicarbonate versus sodium (Figure 7-150) shows both bicarbonate and sodium increasing but at a sodium to bicarbonate ratio of about 2:1.

#### Sodium versus Calcium Plot

A plot of sodium versus calcium (Figure 7-151) shows general increases in both sodium and calcium, but sodium is increasing at a rate much higher than calcium. This relationship is different than observed for other aquifers in this transect.

#### Bicarbonate versus Calcium Plot

A plot of bicarbonate versus calcium (Figure 7-152) shows no relationship between calcium and bicarbonate.

#### pH versus Bicarbonate Plot

The plot of pH versus bicarbonate (Figure 7-153) shows pHs in the seven to nine range. Bicarbonate concentrations do not appear related to pH.

#### pH versus Sodium Plot

The plot of pH versus sodium (Figure 7-154) shows no relationship between the two constituents.

#### Sulfate versus Bicarbonate Plot

No relationship is observed between sulfate and bicarbonate for a limited database (Figure 7-155). If data were available down dip a sulfate to bicarbonate inverse relationship might be effected as seen for other aquifers.

#### Chloride versus Sodium Plot

The plot of chloride versus sodium (Figure 7-156) shows a general quasi-linear relationship between sodium and chloride. This aquifer appears dominated by sodium and chloride.

#### Depth versus Sulfate Plot

No correlation is observed (Figure 7-157).

#### Depth versus Calcium Plot

No correlation is observed (Figure 7-158).

#### Depth versus Sodium Plot

No correlation is observed (Figure 7-159).

#### Depth versus Chloride Plot

No correlation is observed (Figure 7-160).

#### Depth versus Total Dissolved Solids Plot

No correlation is observed (Figure 7-161).

#### Discussion

Potable groundwater in the Yegua-Jackson Aquifer in the Central Transect is restricted to its outcrop. Based on its Piper diagram the water chemistry is sodium mixed (chloride-sulfate-bicarbonate) type of water. This composition is similar to the water compositions for the Yegua-Jackson Aquifer in the other transects but dissimilar to the chemical water composition of the underlying aquifers: the Wilcox Group of the Carrizo-Wilcox, Queen City and Sparta in the

Central Transect where sodium-bicarbonate water is present. General total dissolved solids values in the Yegua-Jackson Aquifer are higher than underlying aquifers. Based on the water chemistry of the Yegua-Jackson Aquifer, groundwaters from the underlying Wilcox Group, Queen City or Sparta aquifers do not appear to be mixing with the Yegua-Jackson Aquifer waters.

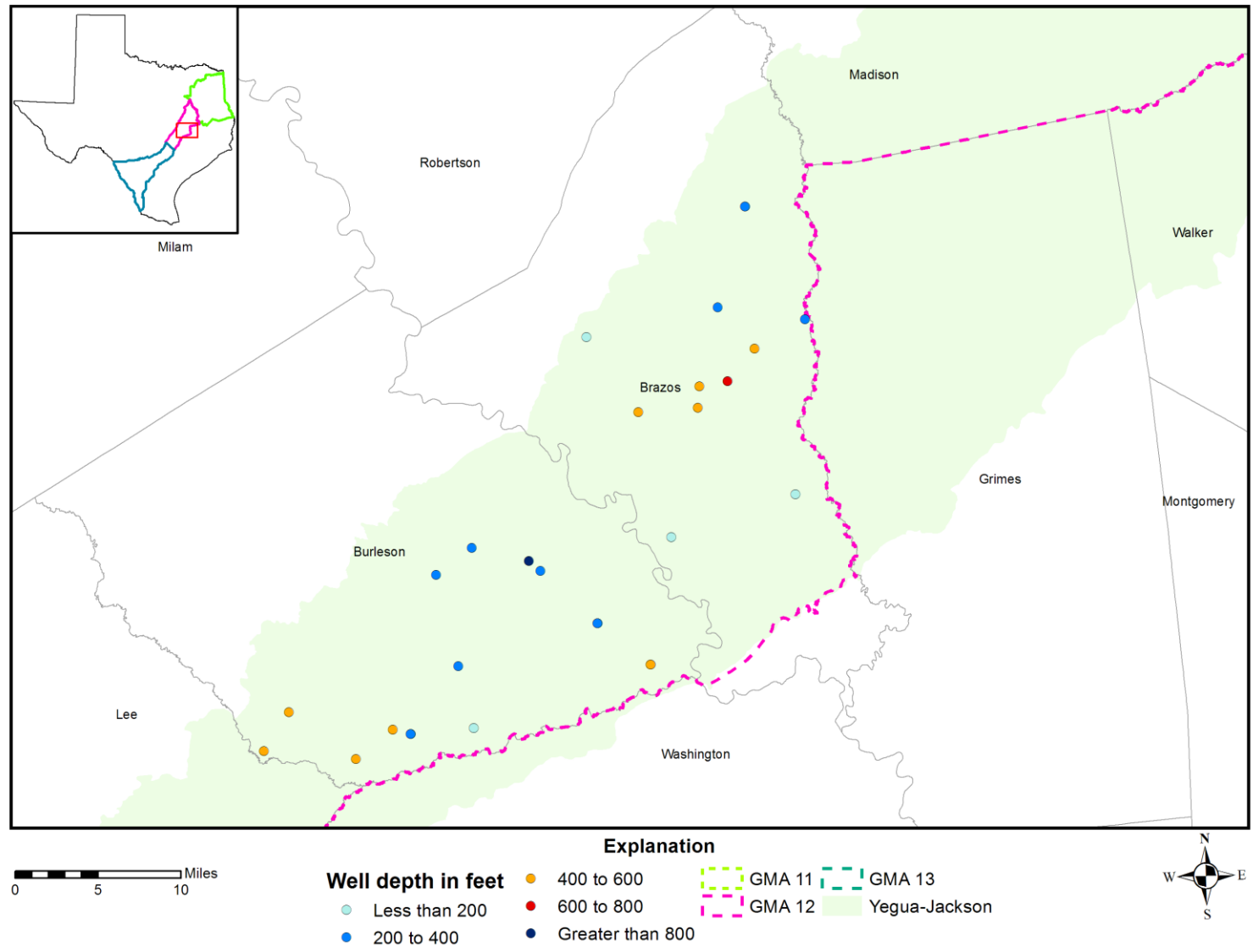


Figure 7-147. Well depths measured from land surface in feet in the Yegua-Jackson Aquifer, Central Transect, Groundwater Management Area (GMA) 12.

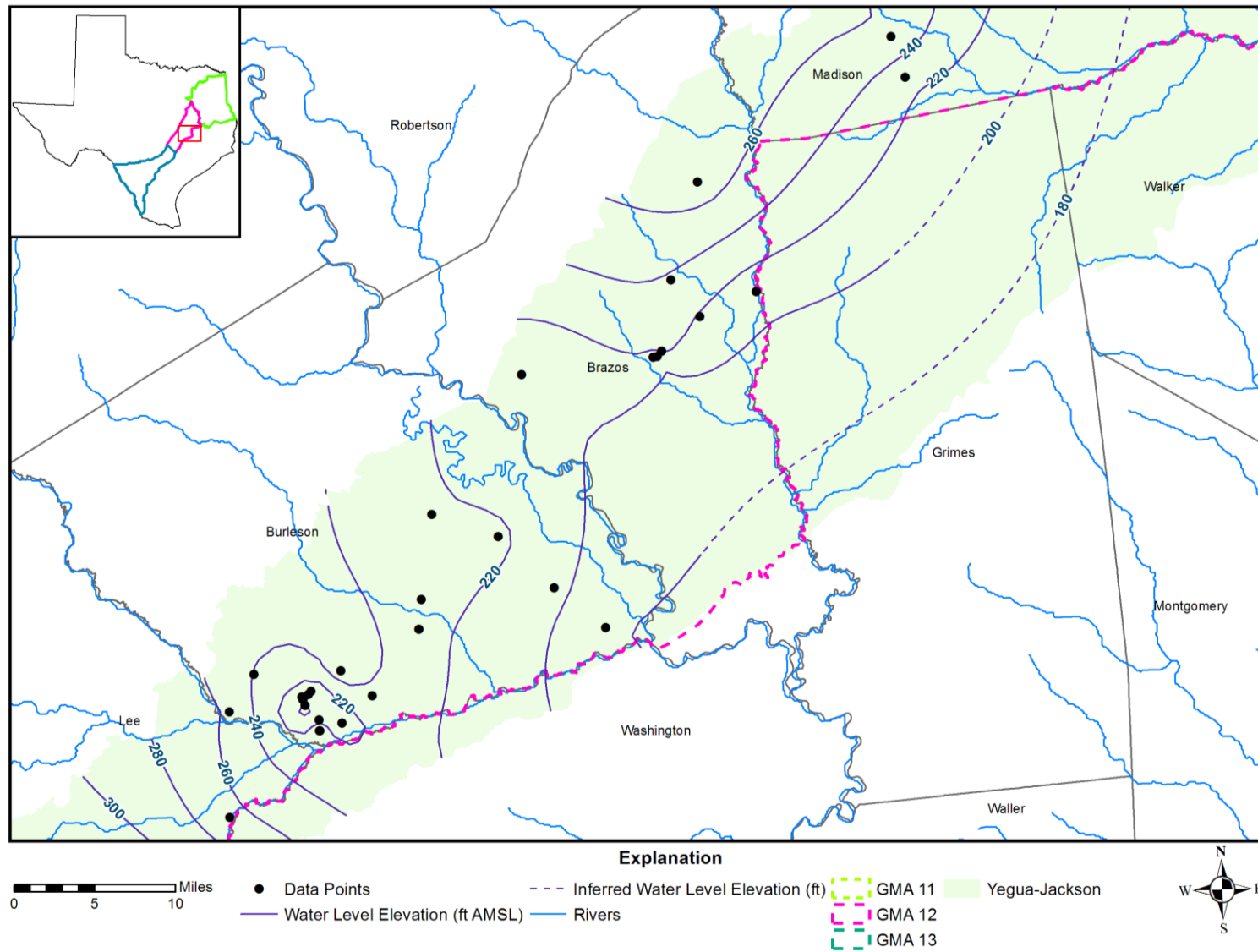


Figure 7-148. Potentiometric surface of the Yegua-Jackson Aquifer using water level data measured in feet above mean sea level (ft AMSL) from 1980 to 2011 in the Central Transect, Groundwater Management Area 12.

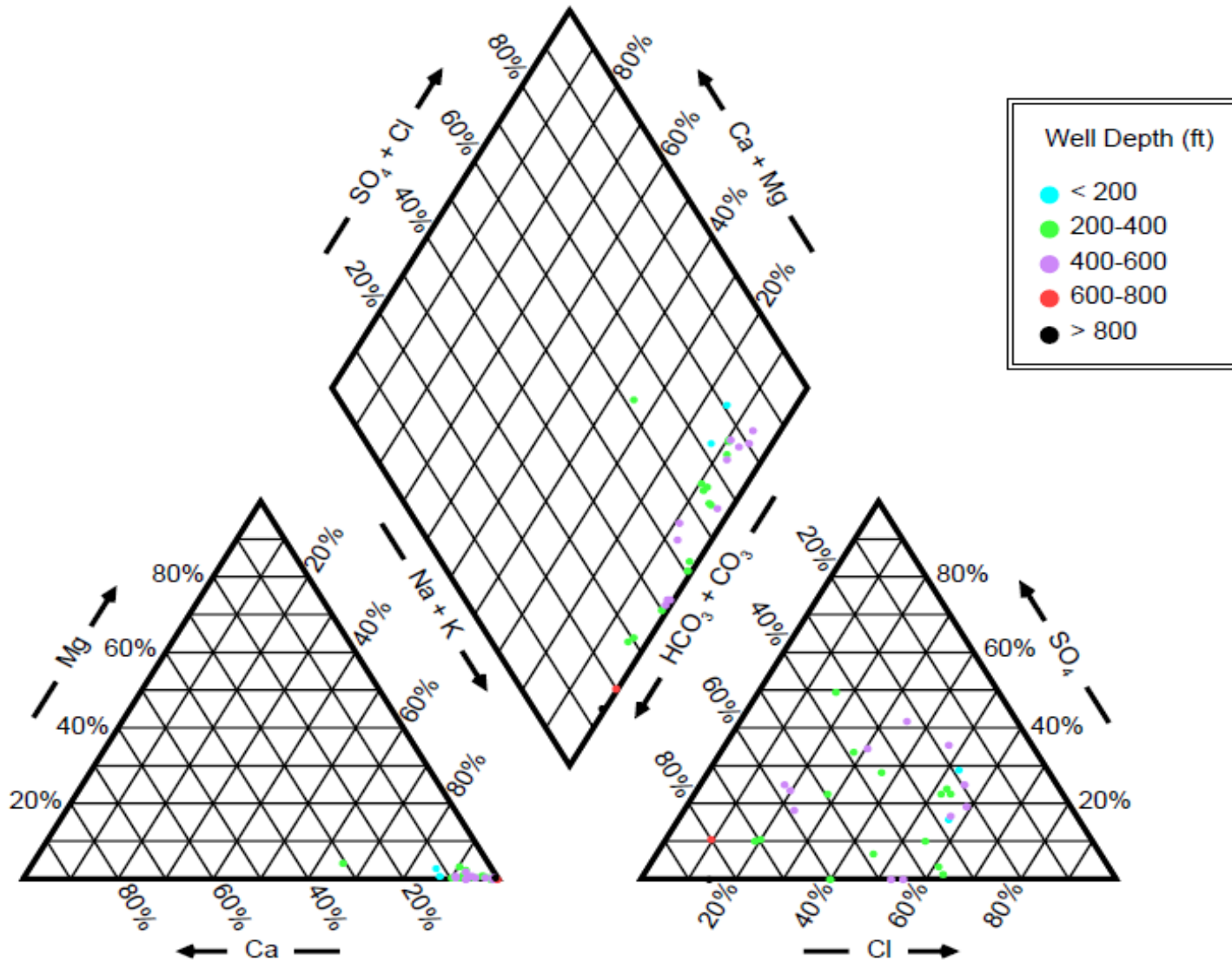


Figure 7-149. Piper diagram showing chemistry of the Yegua-Jackson Aquifer wells in the Central Transect by well depth measured from land surface in feet (ft).

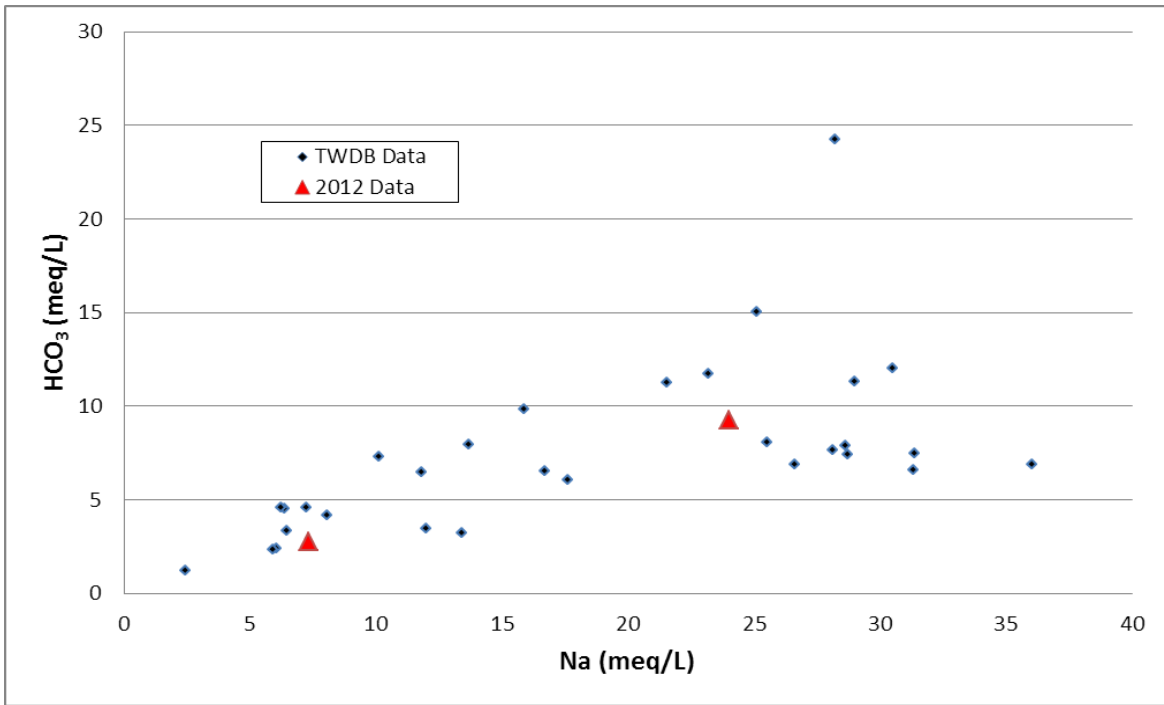


Figure 7-150. Bicarbonate (HCO<sub>3</sub>) versus sodium (Na) measured in milliequivalents per liter (meq/L), Yegua-Jackson Aquifer, Central Transect, Groundwater Management Area 12.

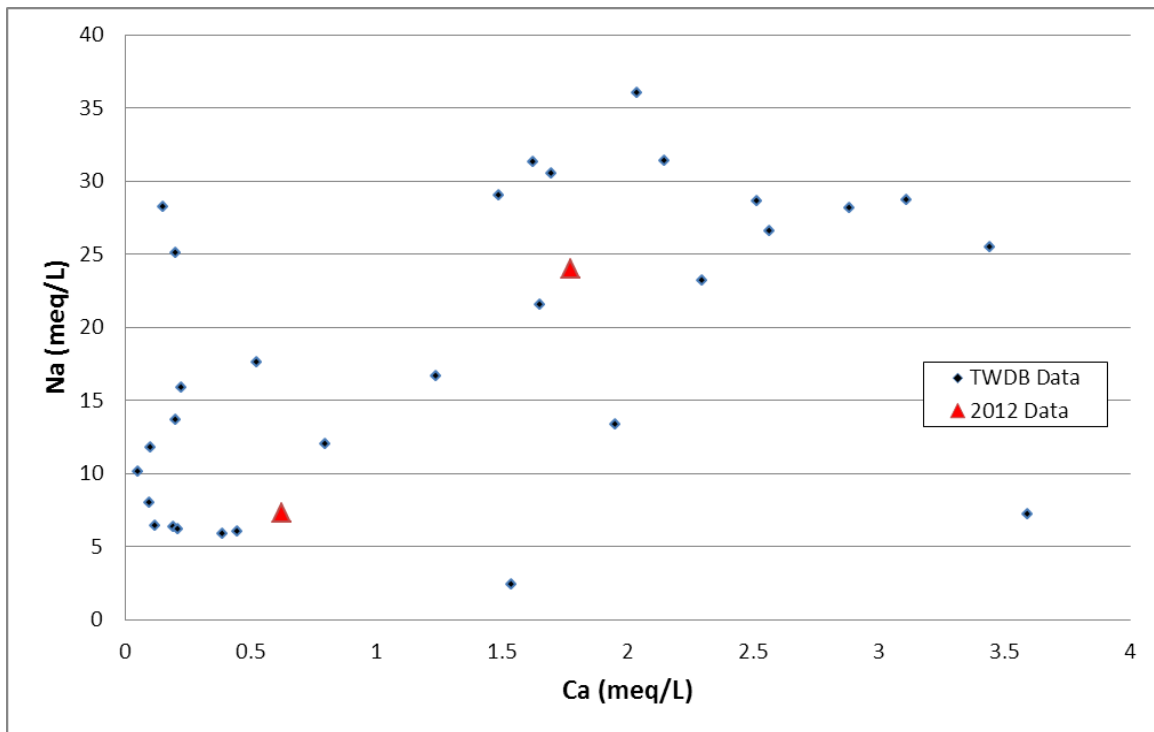


Figure 7-151. Sodium (Na) versus calcium (Ca) measured in milliequivalents per liter (meq/L), Yegua-Jackson Aquifer, Central Transect, Groundwater Management Area 12.

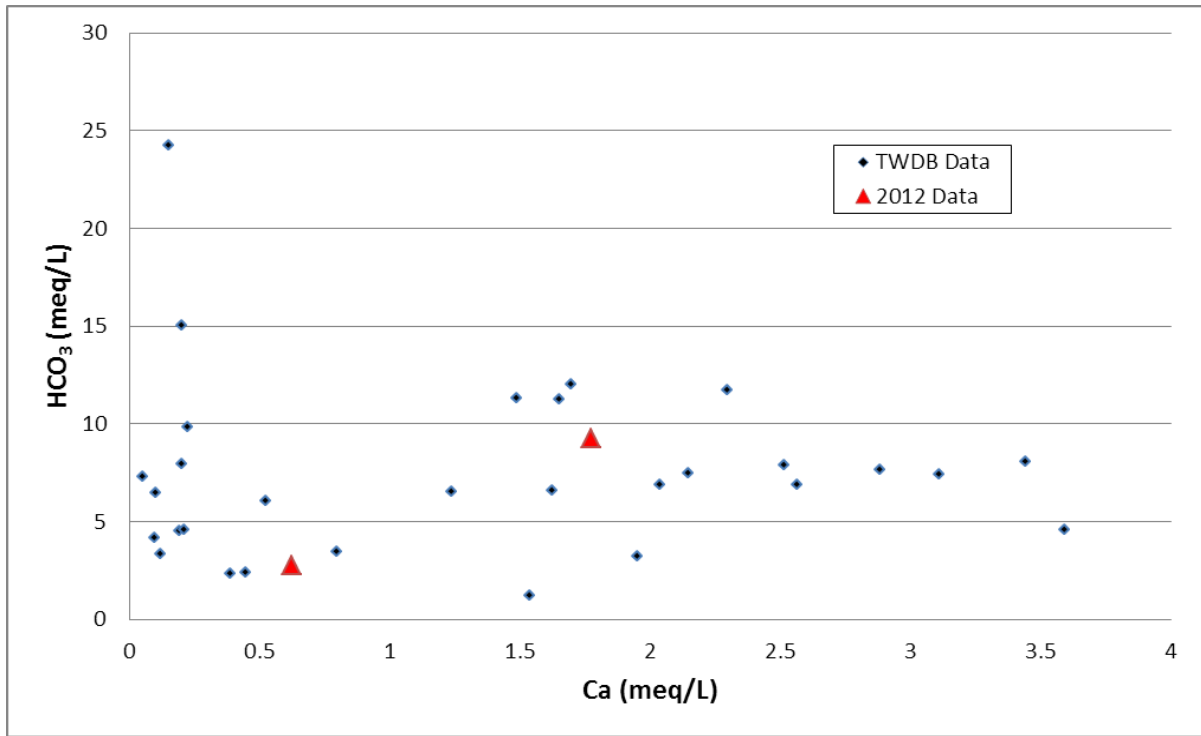


Figure 7-152. Bicarbonate (HCO<sub>3</sub>) versus calcium (Ca) measured in milliequivalents per liter (meq/L), Yegua-Jackson Aquifer, Central Transect, Groundwater Management Area 12.

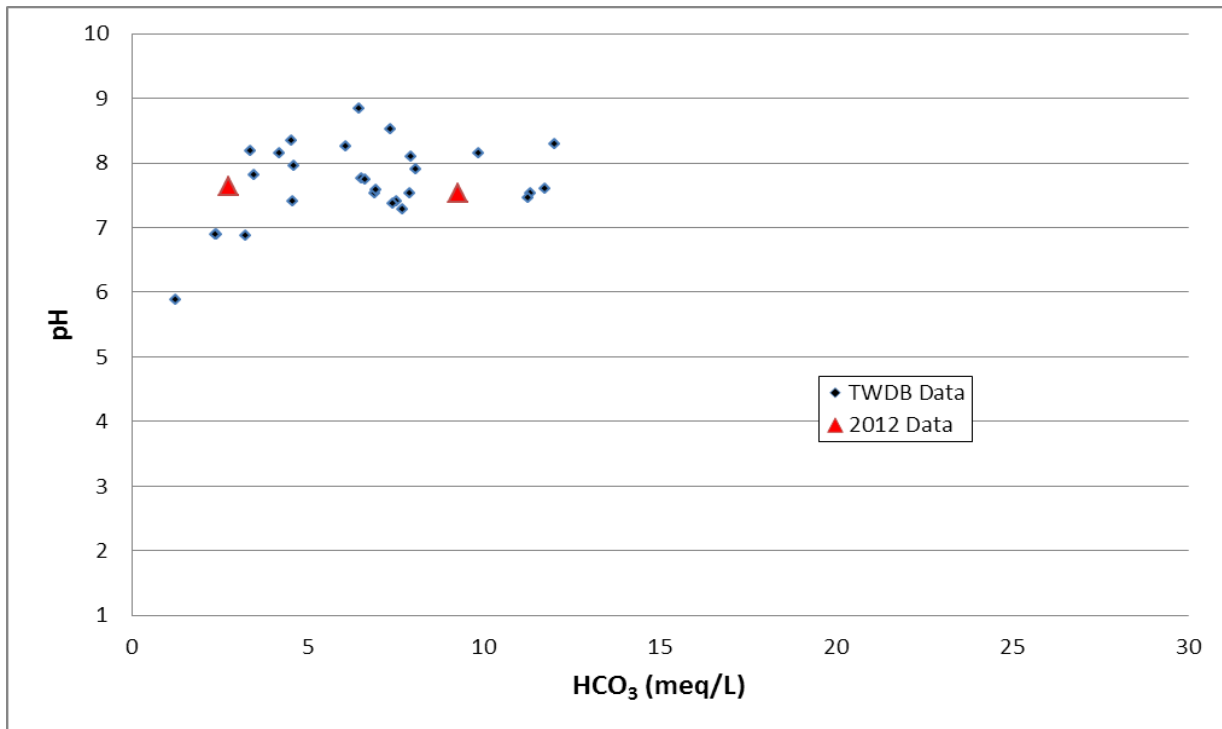


Figure 7-153. pH versus bicarbonate (HCO<sub>3</sub>) measured in milliequivalents per liter (meq/L), Yegua-Jackson Aquifer, Central Transect, Groundwater Management Area 12.

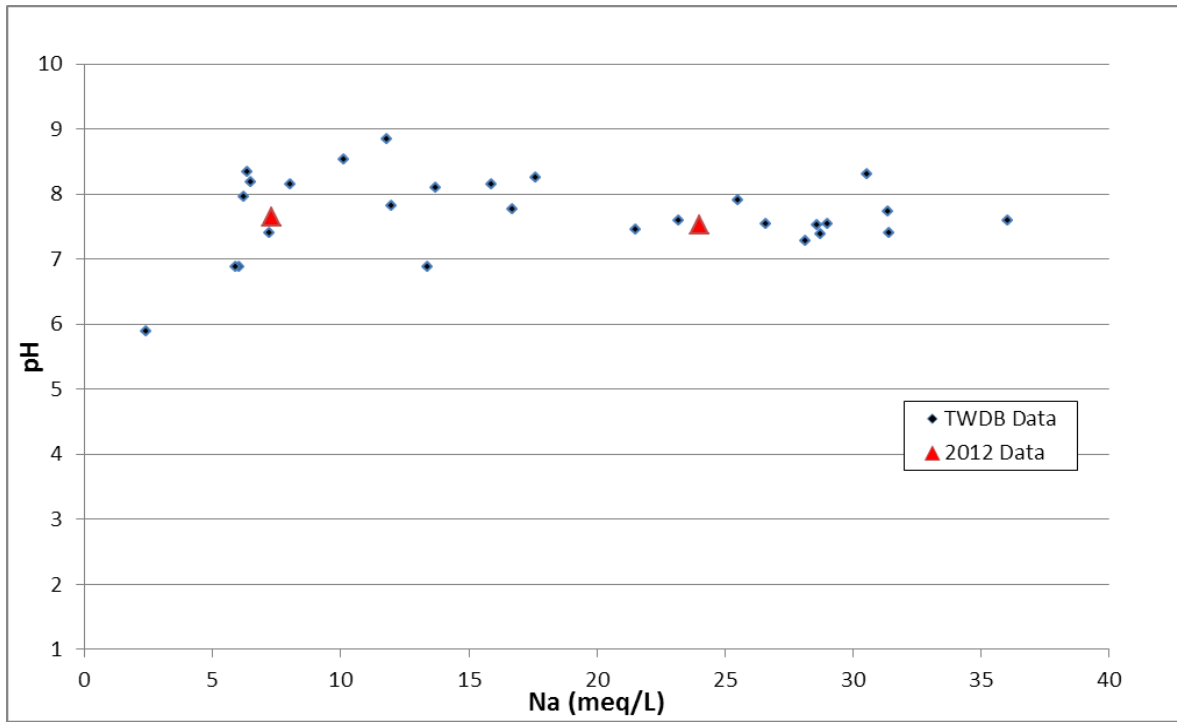


Figure 7-154. pH versus sodium (Na measured in milliequivalents per liter (meq/L)), Yegua-Jackson Aquifer, Central Transect, Groundwater Management Area 12.

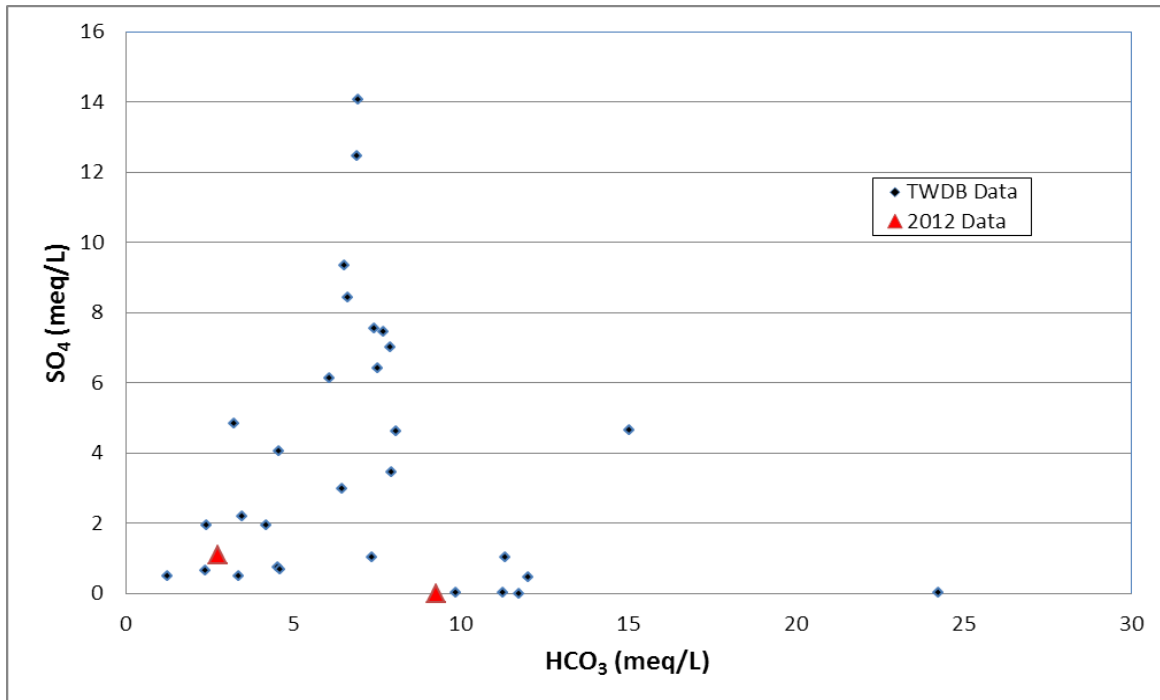


Figure 7-155. Sulfate (SO<sub>4</sub>) versus bicarbonate (HCO<sub>3</sub>) measured in milliequivalents per liter (meq/L), Yegua-Jackson Aquifer, Central Transect, Groundwater Management Area 12.

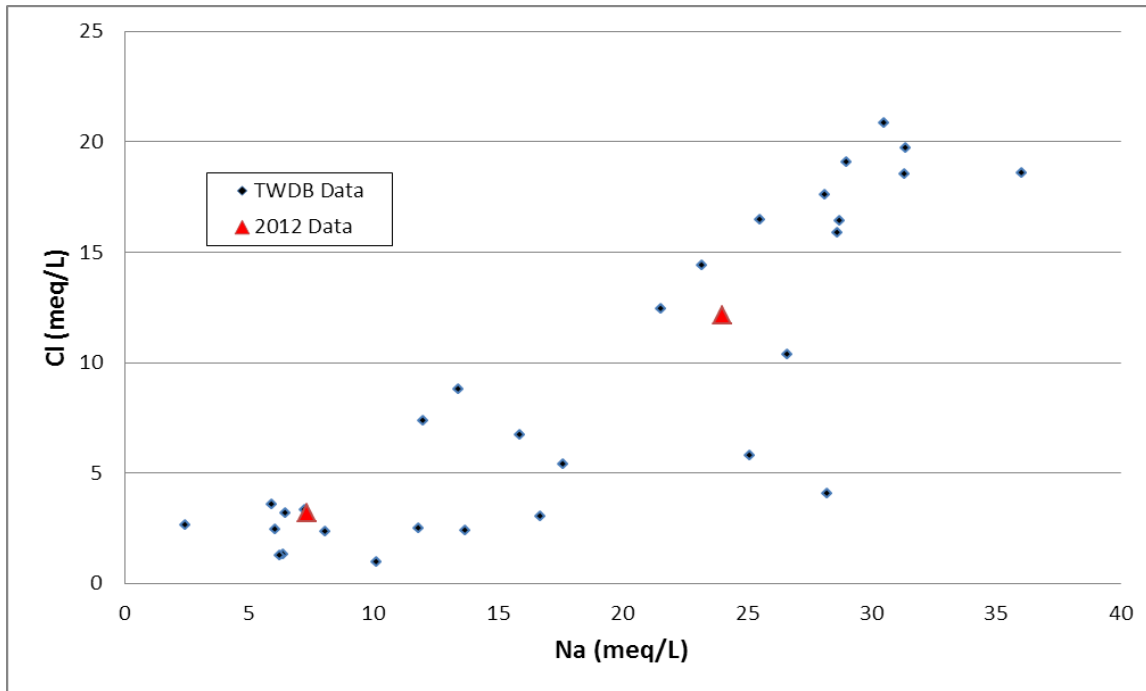


Figure 7-156. Chloride (Cl) versus sodium (Na) measured in milliequivalents per liter (meq/L), Yegua-Jackson Aquifer, Central Transect, Groundwater Management Area 12.

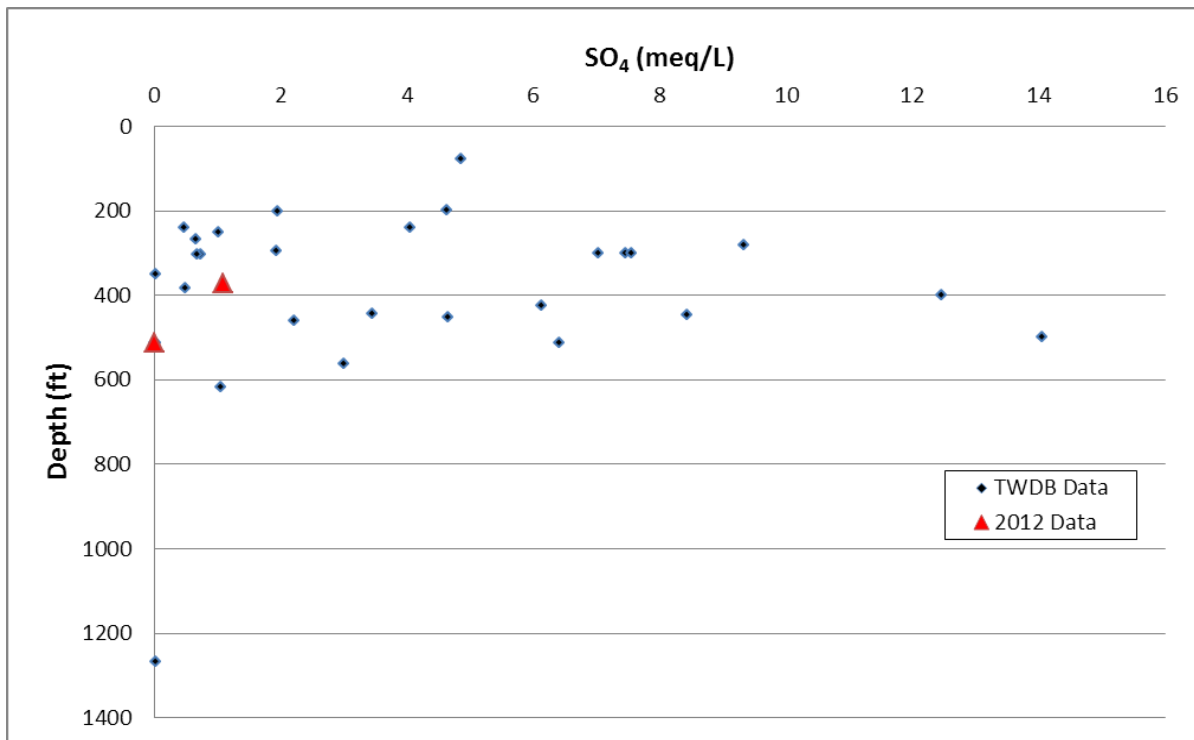


Figure 7-157. Depth measured from land surface in feet (ft) versus sulfate (SO<sub>4</sub>) measured in milliequivalents per liter (meq/L), Yegua-Jackson Aquifer, Central Transect, Groundwater Management Area 12.

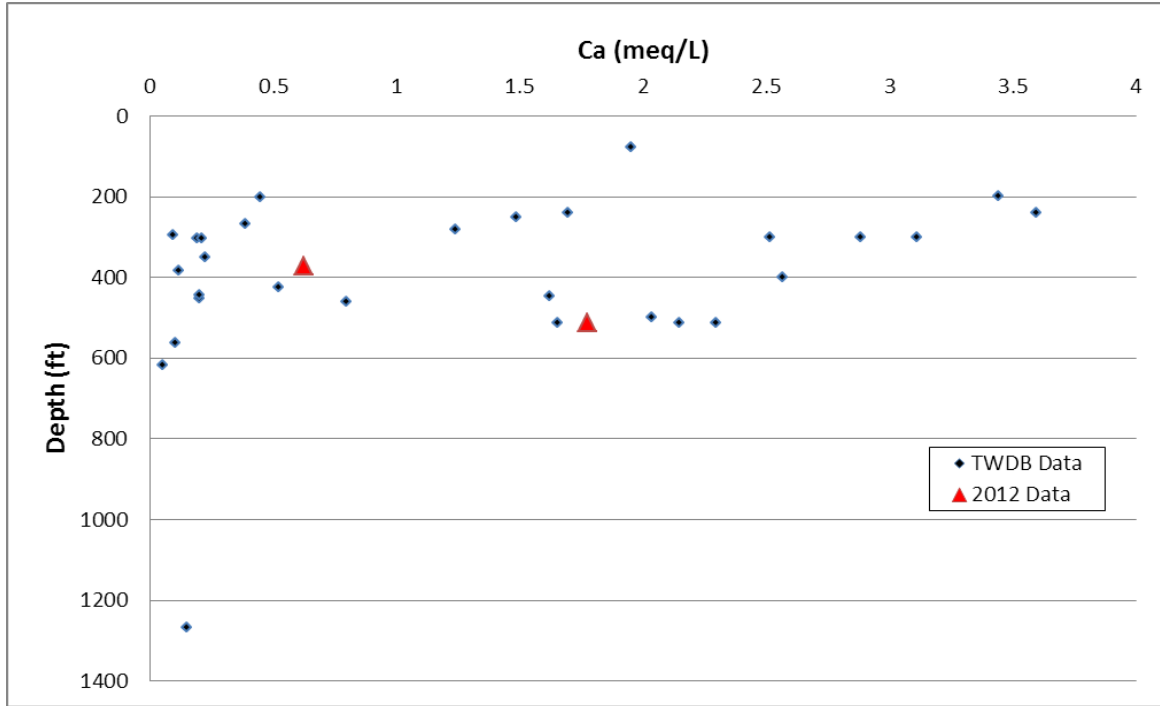


Figure 7-158. Depth measured from land surface in feet (ft) versus calcium (Ca) measured in milliequivalents per liter (meq/L), Yegua-Jackson Aquifer, Central Transect, Groundwater Management Area 12.

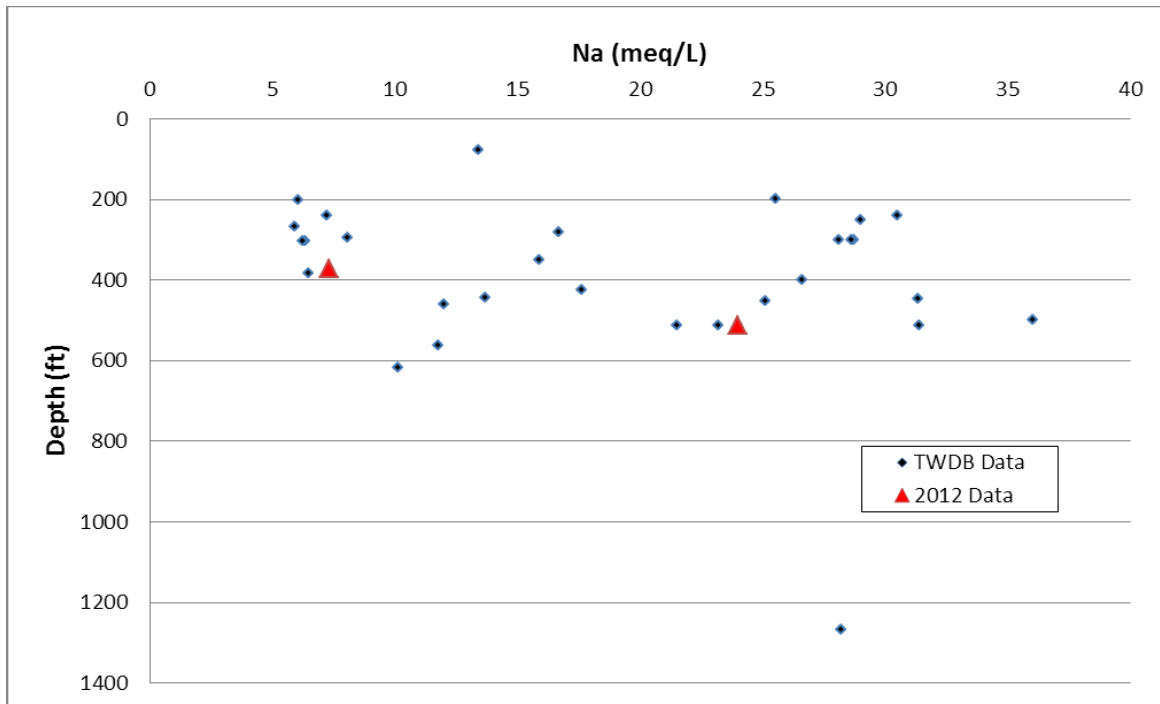


Figure 7-159. Depth measured from land surface in feet (ft) versus sodium (Na) measured in milliequivalents per liter (meq/L), Yegua-Jackson Aquifer, Central Transect, Groundwater Management Area 12.

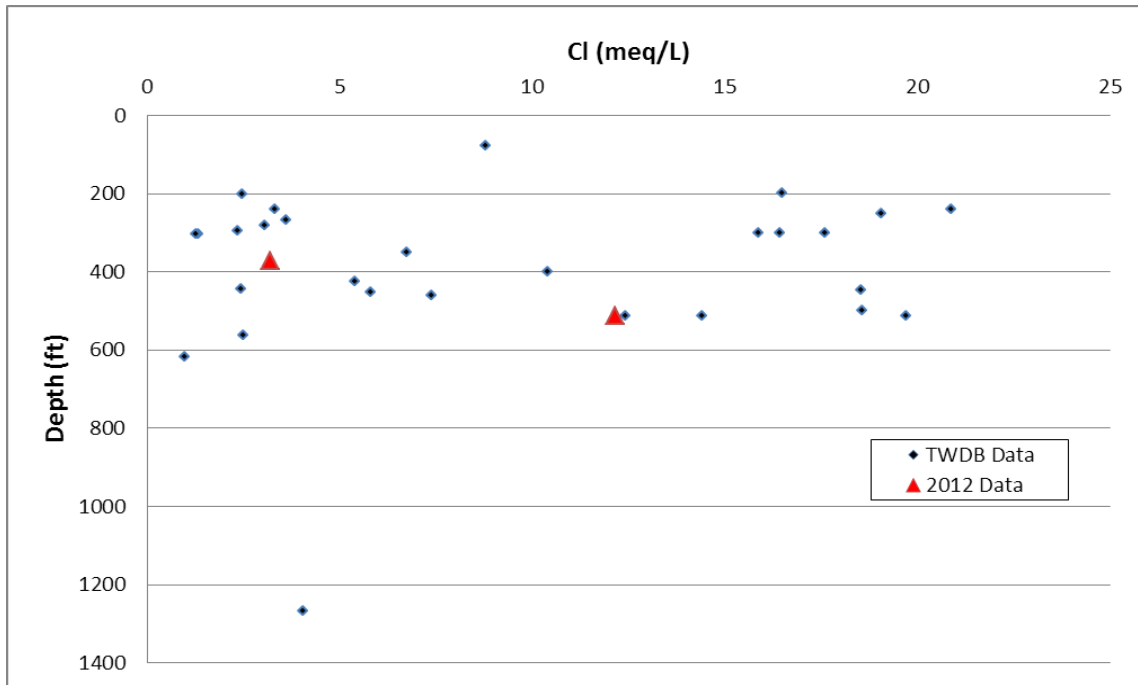


Figure 7-160. Depth measured from land surface in feet (ft) versus chloride (Cl) measured in milliequivalents per liter (meq/L), Yegua-Jackson Aquifer, Central Transect, Groundwater Management Area 12.

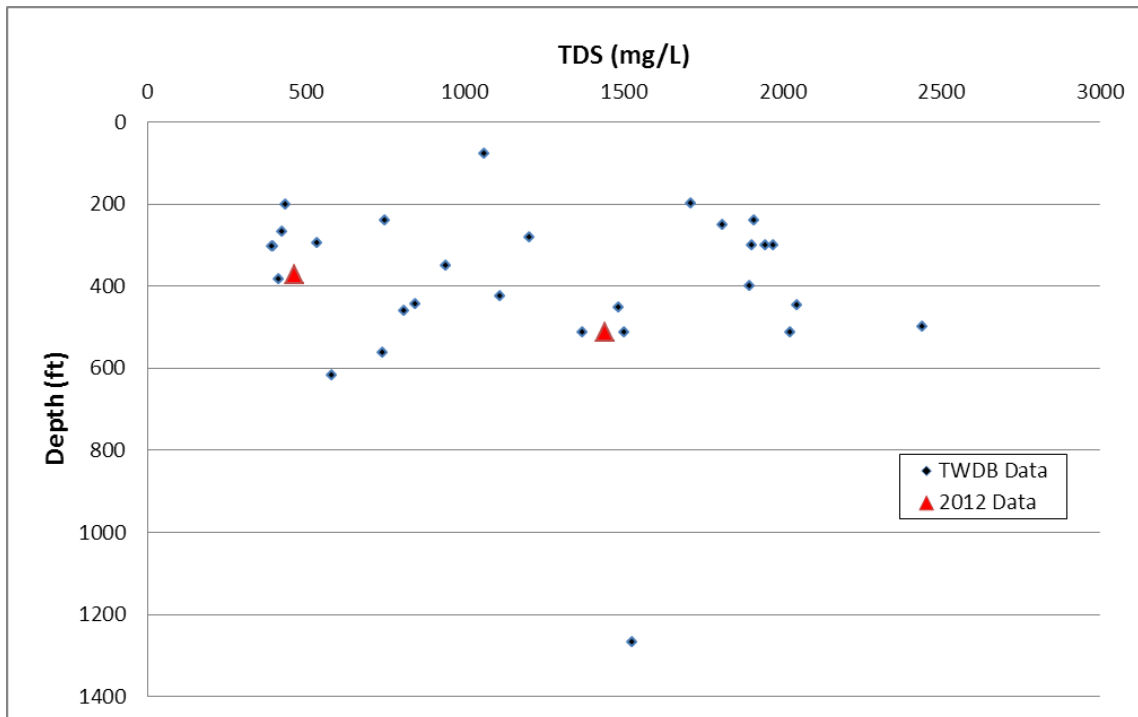


Figure 7-161. Depth measured from land surface versus total dissolved solids (TDS) measured in parts per million (ppm), Yegua-Jackson Aquifer, Central Transect, Groundwater Management Area 12.

## **Brazos River Alluvium Aquifer**

The Brazos River Alluvium Aquifer extends along the Brazos River from the northwest extent of Milam County to the boundary on the southern side of Brazos and Burleson counties. The Brazos River Alluvium Aquifer is designated as a minor aquifer by the TWDB. The aquifer is prolific but of limited lateral extent. Most of the wells in the aquifer are for agricultural use. There is an extensive TWDB database for wells in this aquifer (Figure 7-162). During the 2012 groundwater sampling, one Brazos River Alluvium Aquifer well was sampled.

### Well Depths

Based on the well depth map, the upper 100 feet of the Brazos River Alluvium Aquifer is screened for water production (Figure 7-162). The U.S. Geological Survey study of the Brazos River Alluvium Aquifer structure indicates that the maximum thickness of the alluvium is 168 feet based on current data (Shah and others, 2007)

### Potentiometric Surface

The potentiometric surface for the Brazos River Alluvium Aquifer is at about 260 feet on the northwest side of Groundwater Management Areas 11, 12 and 13 (Milam County) and declines to about 185 feet on the southern extent of the aquifer in southern Burleson and Milam counties (Figure 7-163). Water levels in the aquifer follow water levels in the Brazos River. Kelley and others (2004) and Dutton and others (2003) indicate that flow from surrounding aquifers such as the Carrizo-Wilcox Aquifer are generally toward the alluvium.

### Piper Diagram

The Piper diagram for the Brazos River Alluvium Aquifer (Figure 7-164) shows a general chemical composition of a calcium-magnesium type water for the cations and a bicarbonate (to bicarbonate-chloride-sulfate) water for the anion water chemistry.

### Bicarbonate versus Sodium Plot

No correlation is observed (Figure 7-165). These are not bicarbonate-sodium waters as typically seen in the Tertiary-aged aquifers.

### Sodium versus Calcium Plot

A plot of sodium versus calcium (Figure 7-166) shows a weak correlation between sodium and calcium, and different than seen for Tertiary-aged aquifers.

### Bicarbonate versus Calcium Plot

No correlation is observed (Figure 7-167).

### Sulfate versus Bicarbonate Plot

No correlation is observed (Figure 7-168).

### Chloride versus Sodium Plot

The plot of chloride versus sodium (Figure 7-169) shows linear increases in both chloride and sodium at a ratio of about 1:1.

### Chloride versus Sulfate Plot

The plot of chloride versus sulfate (Figure 7-170) shows a general increase in chloride and sulfate, although chloride is increasing more rapidly than sulfate.

### Magnesium versus Calcium Plot

The plot of magnesium versus calcium (Figure 7-171) shows linear increases in magnesium and calcium. The ratio for magnesium and calcium is about 2:1.

### Sulfate versus Calcium Plot

The plot of sulfate versus calcium (Figure 7-172) shows general increase in both sulfate and calcium. Sulfate and calcium increase at a ratio of about 1:1.

### Discussion

The Piper diagram (Figure 7-164) of the Brazos River Alluvium Aquifer has a general calcium-magnesium-sodium (mixed) cation bicarbonate dominated anion composition. This general composition of the Brazos River Alluvium Aquifer differs from the Tertiary-aged aquifers that underlie the Brazos River Alluvium Aquifer either as subcrop directly beneath the Brazos River Alluvium Aquifer or as the confined portion of these aquifers. The aquifers that underlie the Brazos River Alluvium Aquifer are the Wilcox Group of the Carrizo-Wilcox, the Queen City, the Sparta and the Yegua-Jackson. The Wilcox Group has a calcium-magnesium-chloride-sulfate type water in outcrop and sodium-bicarbonate water downdip. The Queen City Aquifer water chemistry distribution between outcrop and downdip sections is similar to the Wilcox Group. The chemical composition of the Queen City Aquifer is calcium-magnesium-chloride-sulfate water in the outcrop and sodium-bicarbonate water in the confined section. The Sparta Aquifer waters are calcium-magnesium-chloride-sulfate waters in the outcrop and sodium-bicarbonate water downdip. The Yegua-Jackson Aquifer water occurs only in the outcrop and is sodium-chloride-bicarbonate type waters.

Comparison of the potentiometric surface for the Brazos River Alluvium Aquifer (Figure 7-163) to the potentiometric surfaces for the underlying Tertiary-aged aquifer (Figure 7-90, Figure 7-111, Figure 7-130 and Figure 7-148) would suggest a potential for upward flow from these deeper formations in the Brazos River Alluvium Aquifer. However, if there is upward leakage from any of these formations either from subcrop directly beneath the Brazos River Alluvium Aquifer or as upward leakage from the confined portions of these aquifers then the upward leaking groundwater should have both a cation and anion composition of calcium-magnesium and bicarbonate, since the dominant water chemistry of the Brazos River Alluvium Aquifer is calcium-magnesium-bicarbonate water. None of the aquifers beneath the Brazos River Alluvium Aquifer have both a calcium-magnesium (cation) and bicarbonate (anion) composition within the same water. Comparison of the Brazos River Alluvium Aquifer Piper diagram to the Piper diagrams of the Tertiary-aged aquifers that underlie the Brazos River Alluvium Aquifer therefore do not support the concept of significant upward leakage from these deeper aquifers into the Brazos River Alluvium Aquifer. One sample from the Brazos River Alluvium Aquifer collected in 2012 had a carbon-14 percent modern of 98 percent modern water. These conclusions agree with the observations of Chowdhury and others (2010) that there is no significant upward leakage of groundwater from the Tertiary-aged aquifers into the Brazos River Alluvium Aquifer.



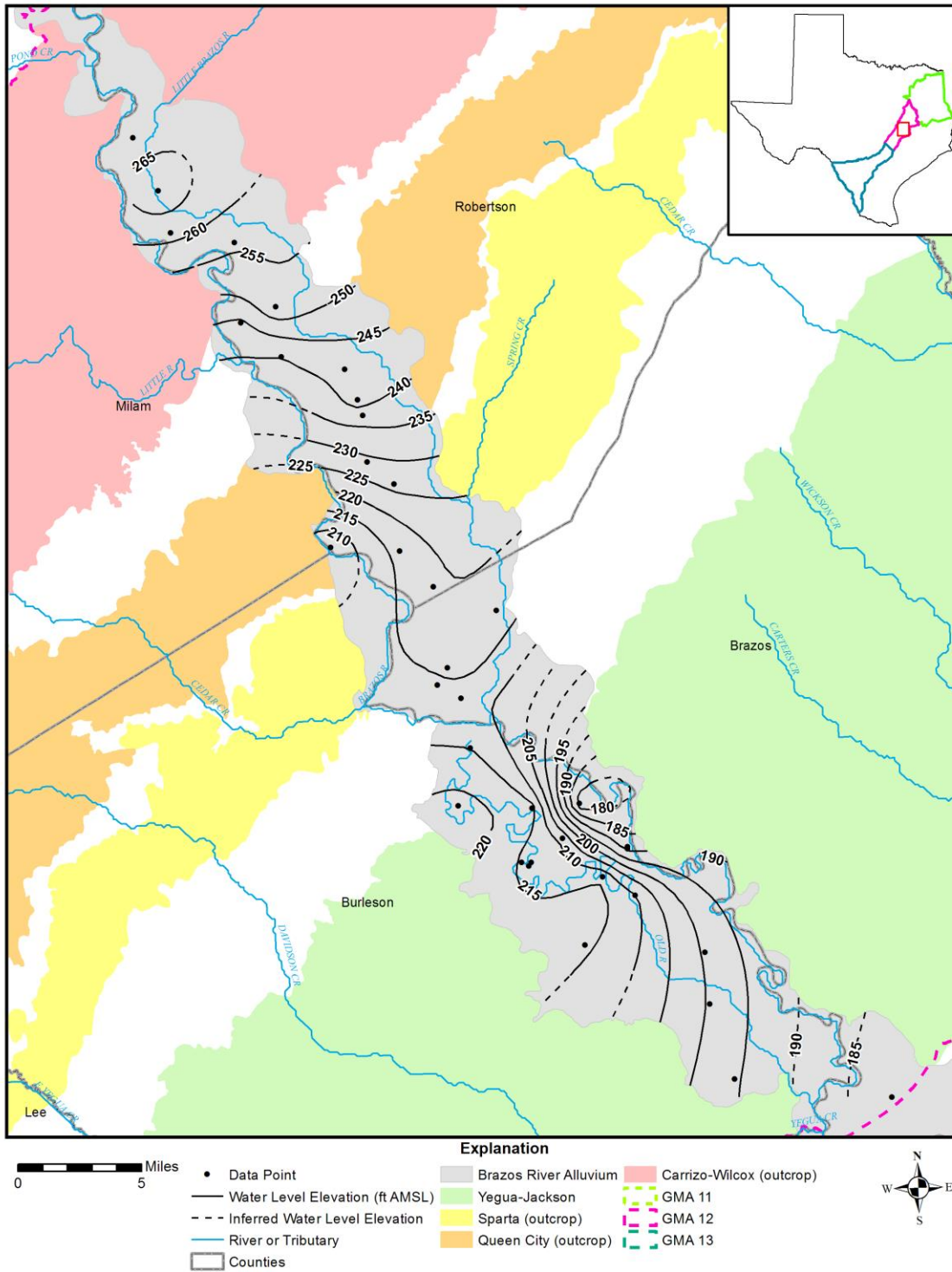


**Figure 7-163. Potentiometric surface of the Brazos River Alluvium Aquifer using water well data measured in feet above mean sea level (ft AMSL) from 1990 to 2011 in the Central Transect, Groundwater Management Area 12.**

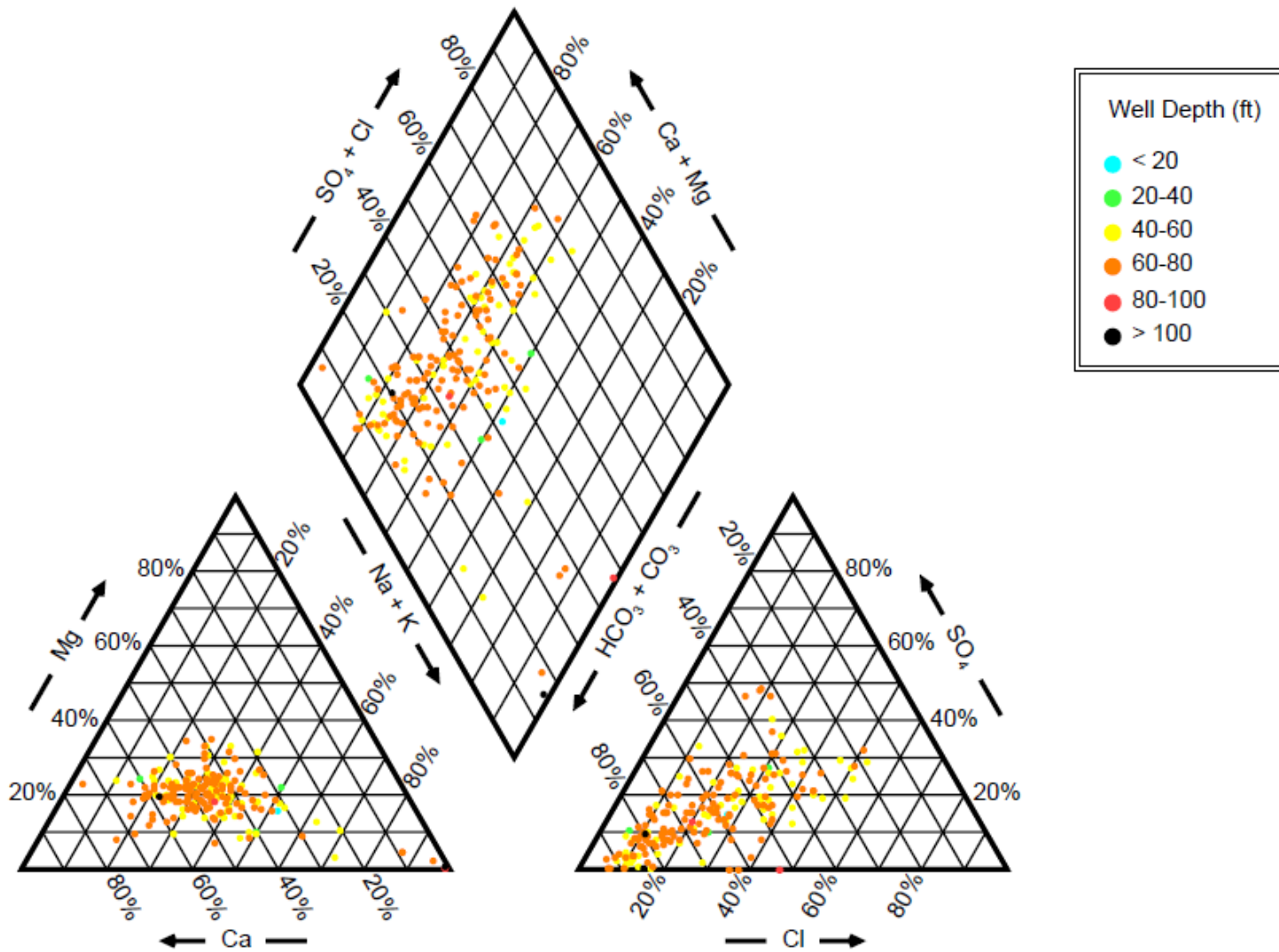


Figure 7-164. Piper diagram showing chemistry of the Brazos River Alluvium Aquifer wells in the Central Transect by well depth measured from land surface measured in feet (ft).

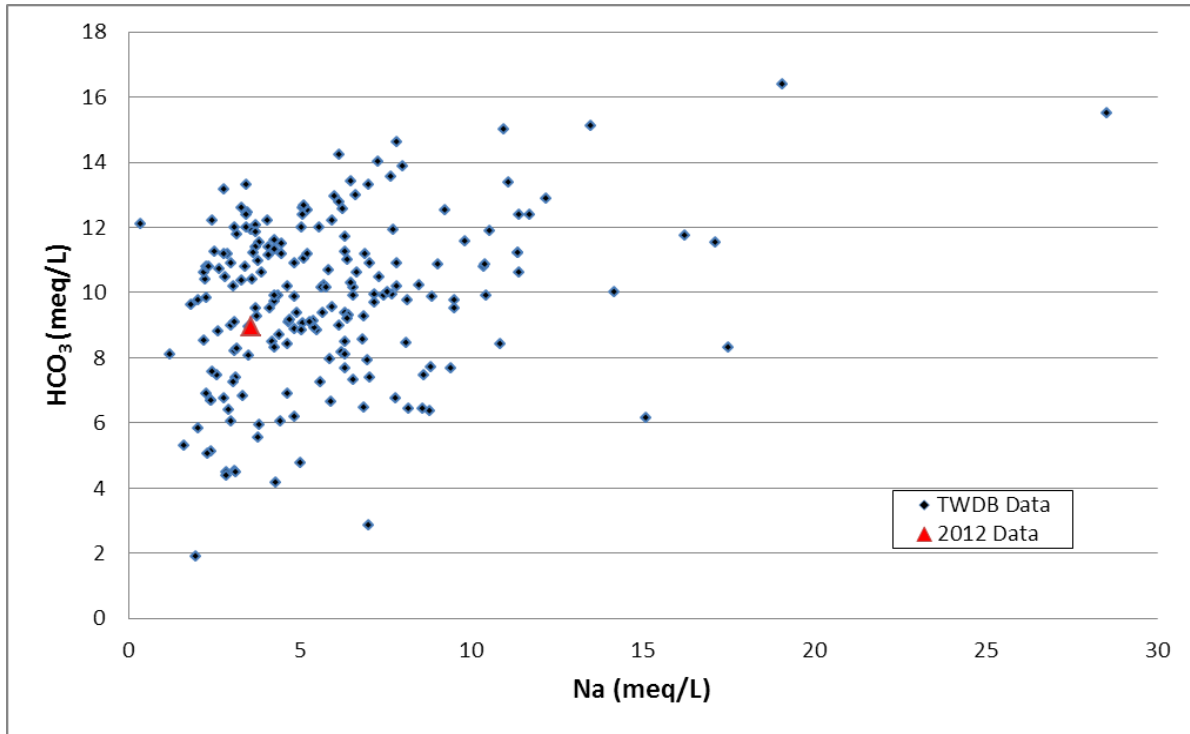


Figure 7-165. Bicarbonate (HCO<sub>3</sub>) versus sodium (Na) measured in milliequivalents per liter (meq/L), Brazos River Alluvium Aquifer, Central Transect, Groundwater Management Area 12.

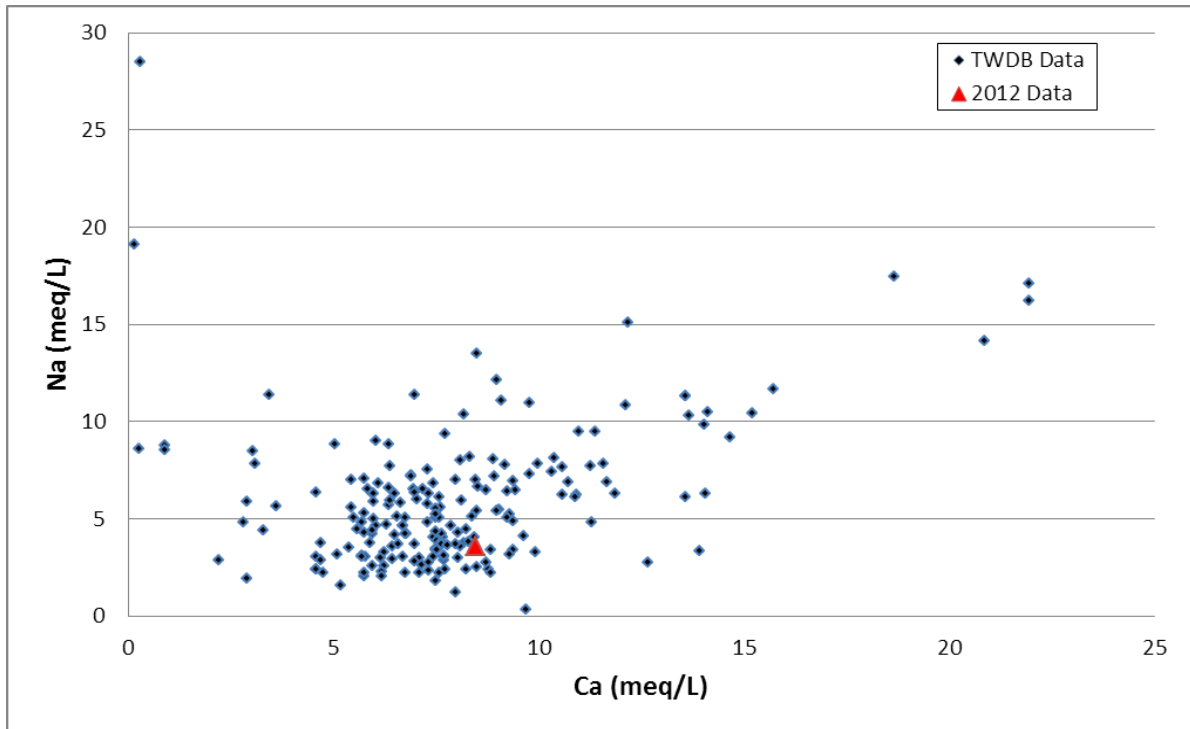


Figure 7-166. Sodium (Na) versus calcium (Ca) measured in milliequivalents per liter (meq/L), Brazos River Alluvium Aquifer, Central Transect, Groundwater Management Area 12.

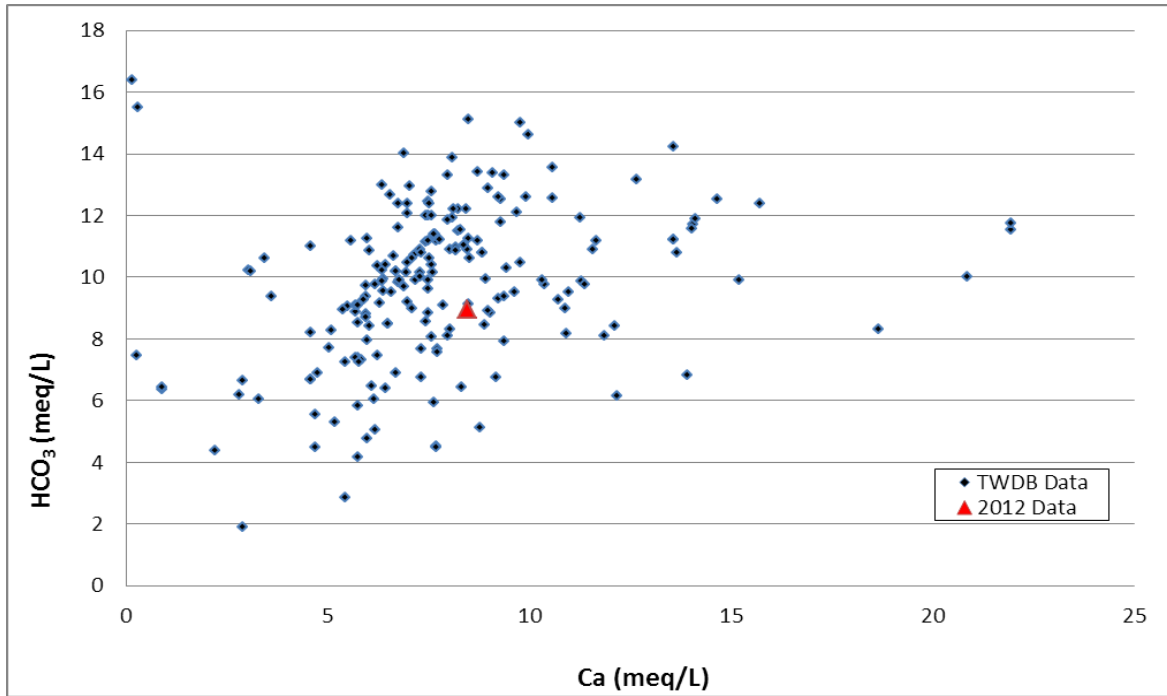


Figure 7-167. Bicarbonate (HCO<sub>3</sub>) versus calcium (Ca) measured in milliequivalents per liter (meq/L), Brazos River Alluvium Aquifer, Central Transect, Groundwater Management Area 12.

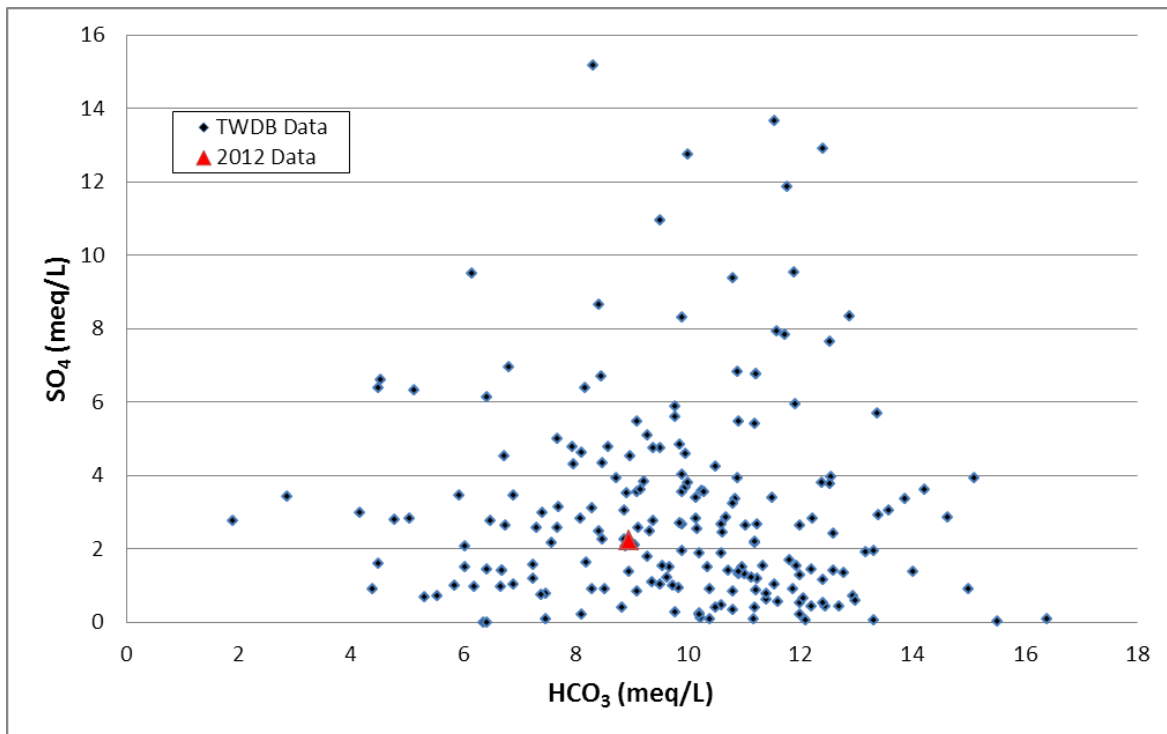
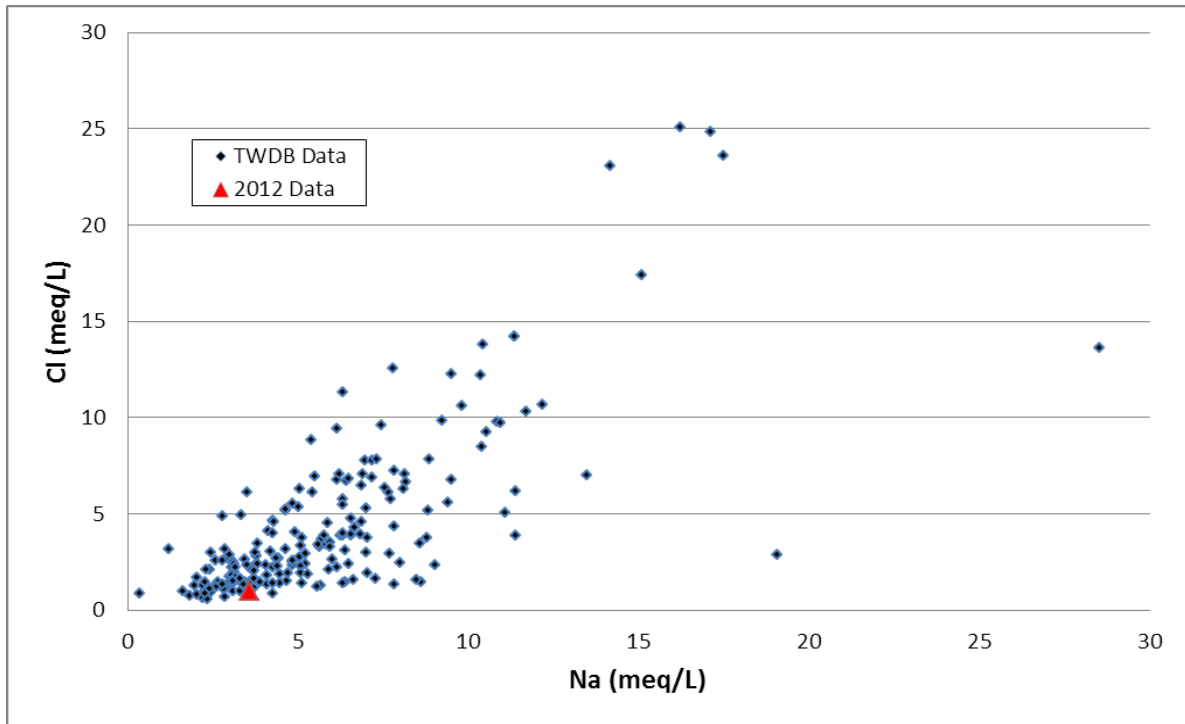
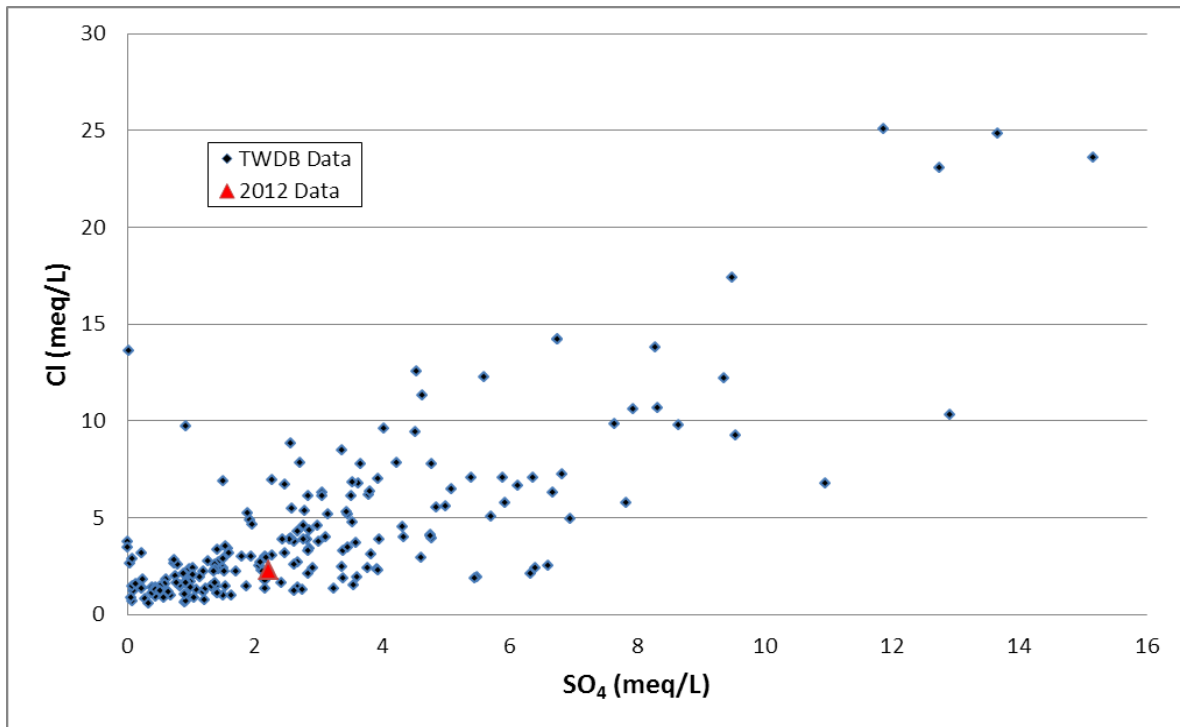


Figure 7-168. Sulfate (SO<sub>4</sub>) versus bicarbonate (HCO<sub>3</sub>) measured in milliequivalents per liter (meq/L), Brazos River Alluvium Aquifer, Central Transect, Groundwater Management Area 12.



**Figure 7-169. Chloride (Cl) versus sodium (Na) measured in milliequivalents per liter (meq/L), Brazos River Alluvium Aquifer, Central Transect, Groundwater Management Area 12.**



**Figure 7-170. Chloride (Cl) versus sulfate (SO<sub>4</sub>) measured in milliequivalents per liter (meq/L), Brazos River Alluvium Aquifer, Central Transect, Groundwater Management Area 12.**

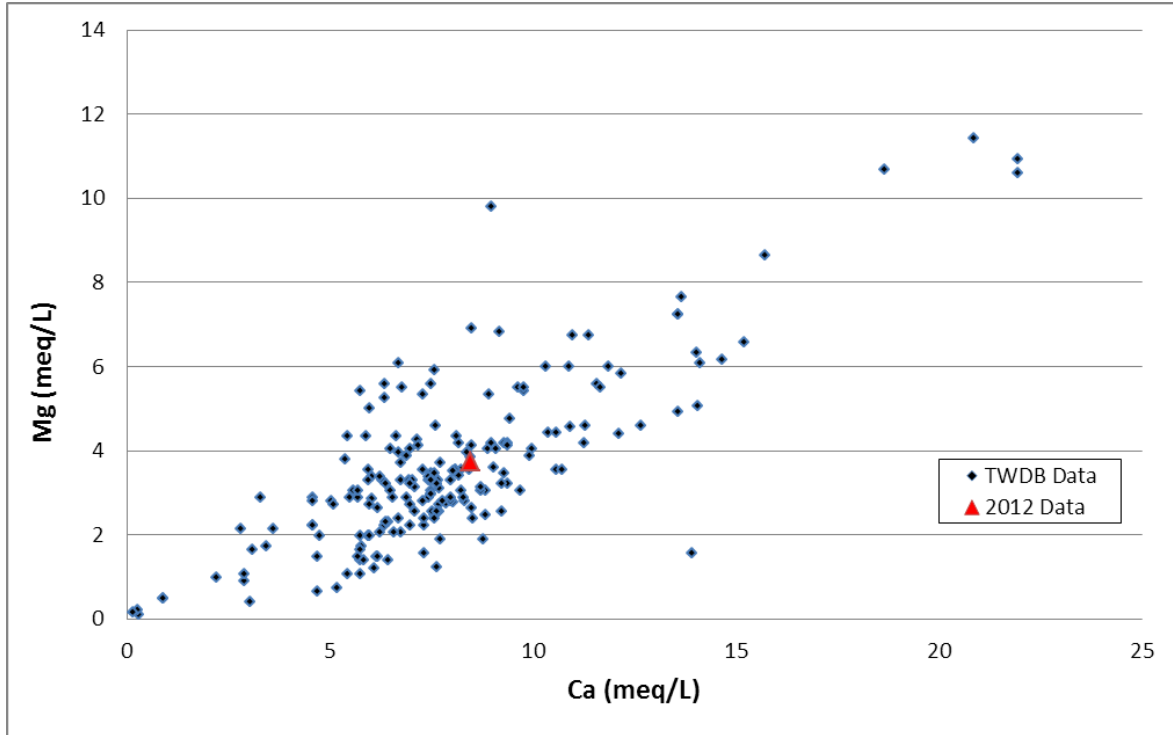


Figure 7-171. Magnesium (Mg) versus calcium (Ca) measured in milliequivalents per liter (meq/L), Brazos River Alluvium Aquifer, Central Transect, Groundwater Management Area 12.

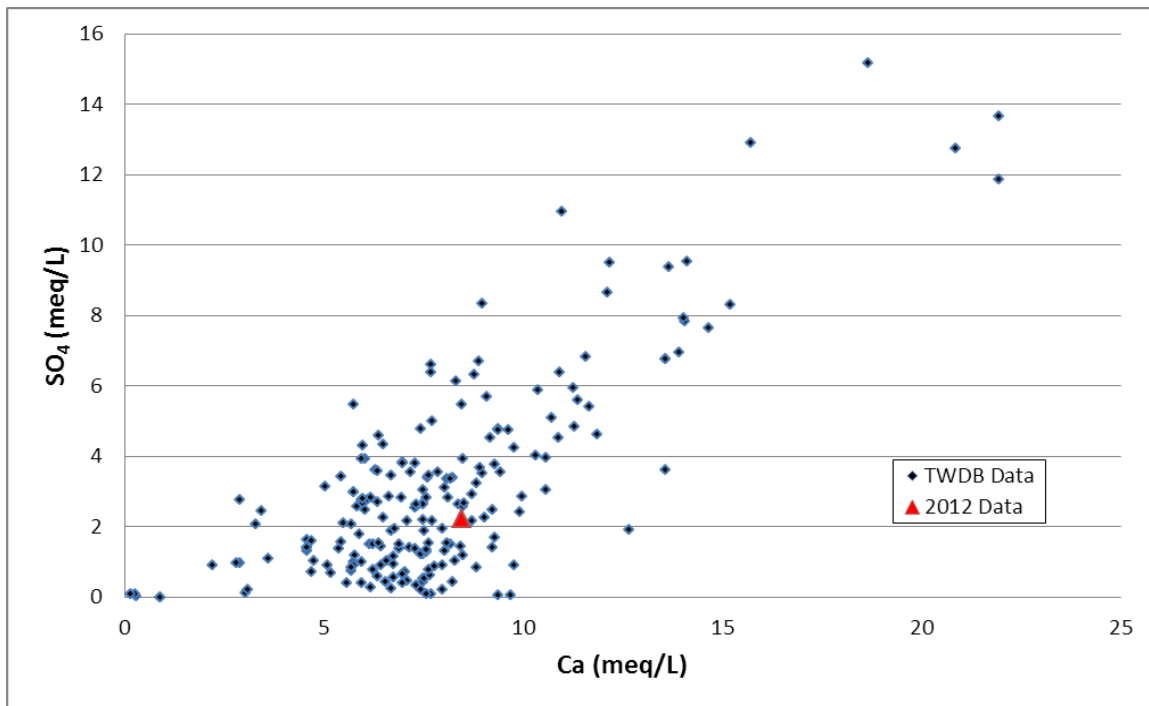


Figure 7-172. Sulfate (SO<sub>4</sub>) versus calcium (Ca) measured in milliequivalents per liter (meq/L), Brazos River Alluvium Aquifer, Central Transect, Groundwater Management Area 12.

### 7.2.2 *Geochemical Modeling*

A total of 19 new radiocarbon (carbon-14) samples were collected for this transect from six aquifers: Carrizo-Wilcox (1), Wilcox Group of the Carrizo-Wilcox Aquifer (8), Queen City (2), Sparta (5), Yegua-Jackson (2) and the Brazos River Alluvium (1). All analytical results are provided in Table 7-2 and Appendix A. Sample locations are in Figure 7-86. The dip profile A-A' is oriented toward the southeast near the Brazos and Burleson county line (Figure 7-87) and the strike profile B-B' crosses Milam and Robertson counties (Figure 7-88). Uncorrected ages are given for the strike profile (Table 7-3). Geochemical modeling was done for the Simsboro Formation (Wilcox Group) of the Carrizo-Wilcox Aquifer for a dip profile in the counties of Brazos, Burleson, Robertson, and Milam (Table 7-3).

#### **Aquifer Composition and Estimation of Age**

Modeling was performed to evaluate probable aquifer composition and reactions necessary to match the water chemistry and ages at the end of the conceptualized flowlines. There are 11 Wilcox Group wells that range in depth from 315 to 3,380 feet below land surface and are distributed from the outcrop area to approximately 11 miles downgradient (Figure 7-86 and Figure 7-87). Consideration was given to screen intervals, alignment with flow, and the circumstance of several wells being located essentially in the same area; the result was a selection of five wells deemed representative of the flow system for use in the carbon-14 assessment (Figure 7-86, Figure 7-88, Figure 7-89 and Table 7-1). The composition of major constituents increases steadily along the flow path as would be expected, except for the final well which may be mixing with more saline water.

The first three wells of the dip section are modeled as before using the Pearson and White correction, with NETPATH and the results are given in Table 7-3. The final two wells of the dip section have no measureable radiocarbon, so an age using the NETPATH approach cannot be estimated. Two approaches were taken with NETPATH, in the first approach (Mass Balance Method 1, Table 7-3), the age at the first well was corrected using the Pearson and White correction, followed by the two well inverse model approach from Well 1 to Well 2, and Well 1 to Well 3. The well to well inverse method did not yield plausible results. In the second approach (Mass Balance Method 2, Table 7-3), the mass balance option was used in which the computation is made from recharge area, to Well 1, and then using Well 1 composition the age correction is made for Well 2. This method was repeated with Well 1 to Well 3, bypassing well two for the correction at Well 3. All computed ages are given in Table 7-3 for comparison.

Simulations were made considering ion exchange, calcite and lignite reactions, and for the Simsboro the effects of methanogenesis were required for a solution, in which methane and carbon dioxide are products of lignite oxidation. In all cases the thermodynamic states were honored, and the computed and measured  $\delta^{13}\text{C}$  values matched at the final well.

These general trends can be seen in the plots of major ions with distance along the transect (Figure 7-173 and Figure 7-174). The mass balance modeling required the generation of methane and carbon dioxide to satisfy the match of  $\delta^{13}\text{C}$  of the total dissolved carbon between measured and calculated values. Figure 7-175 depicts the changes in other indicator isotopic values that support methanogenesis, which is the oxidation of organic substrates such as lignite, generating methane with a depleted  $\delta^{13}\text{C}$  value and carbon dioxide with an enriched value. Sulfate becomes the electron acceptor and is reduced leaving a more enriched  $\delta^{34}\text{S}$  value in the residual sulfate. Note the methane mole percent is increasing significantly, in part from possible thermogenic gas

from deeper zones, but the  $\delta^{13}\text{C}$  is progressively more depleted than the more typical value of approximately -50 ‰ for thermogenic gas, indicating contribution of biogenic methane. Additionally the  $\delta^{34}\text{S}$  is progressively enriched from -1 to almost 30 ‰ clearly indicating sulfate is being reduced.

All these reactions support the first approach and result of correction for the initial wells in the Wilcox Group of the Carrizo-Wilcox Aquifer dip transect; whereas the final two wells are of old but indeterminate age due to low, zero, radiocarbon content (Table 7-3).

Two additional Carrizo-Wilcox Aquifer wells were sampled in the TWDB defined outcrop (Figure 7-86 and Figure 7-88) confirming the young age of the water in the outcrop (Table 7-3). Wells BBMR 18 and 2 have carbon-14 percent modern of 83.38 percent modern and 69.2 percent modern respectively indicating younger ages of the groundwater in the outcrop.

The age of the waters in the outcrop for wells BBMR 1, 2 and 18 appear to be much younger than these waters immediately downdip. BBMR 14, approximately four miles downdip from the Carrizo-Wilcox Aquifer outcrop is 21,515 years before present.

## Discussion

The geochemical composition of groundwater in each aquifer in the Central Transect is one of three types. In the Wilcox Group, Queen City and Sparta aquifers, the water chemistry evolves from a mixed-cation mixed-anion water in the outcrop to a sodium-bicarbonate water downdip. All the water chemistry types observed in these aquifers can be explained by intra-aquifer geochemical processes. Cross-formational flow from one aquifer to another is not needed to explain the chemistry, but this does not eliminate the possibility of cross-formational flow. We believe the data indicate that the quantity of cross-formational flow is relatively small.

The water chemistry of the Yegua-Jackson Aquifer is dissimilar to the chemistry in the other aquifers. As observed for the Yegua-Jackson in the Northeast Transect, the Yegua-Jackson Aquifer (in the Central Transect) chemistry is a sodium-mixed anion water and cannot result by cross-formational leakage from underlying aquifers. The total dissolved solids for the Yegua-Jackson Aquifer is also higher than for the other aquifers.

The water chemistry in the Brazos River Alluvium Aquifer is generally a calcium-magnesium mixed anion type water different than the waters in outcrop or downdip for any of the four aquifers which may underlie the Brazos River Alluvium Aquifer. Although there is some overlap in the Piper diagrams for each water-bearing unit, no cross-formational water from another aquifer is needed to explain its chemistry.

The carbon-14 corrected ages for the Wilcox Group groundwaters increase very rapidly downdip. Elevated calcium and low pH waters are also primarily in the outcrop, suggesting most of the active flow in the aquifer may be within the outcrop rather than into the downdip confined part of the Wilcox Group. Uncorrected carbon-14 ages for the Queen City, Sparta and Yegua-Jackson aquifers also indicate old ages (less than 10,000 years before present) for waters in these aquifers. The youngest uncorrected carbon-14 ages were for water from the Brazos River Alluvium Aquifer. The uncorrected ages for this water were 200 years.

Figure 7-177 and Figure 7-178, display downdip graphical cross sections along the Central Transect, with analytical data posted for sodium and carbon 14 (expressed as percent modern) at the appropriate well location.

Figure 7-177 visually displays increasing trends in sodium with depth which are consistent with cation exchange along the flow path from the outcrop to the confined downdip section of the aquifer. This trend is consistent across the Wilcox Group, Queen City, and Sparta aquifers, but is not evident in data from the Yegua-Jackson Aquifer. Figure 7-177 affirms the data trends presented graphically in Figure 7-107.

Figure 7-178 presents trends in carbon-14 analytical data, expressed as percent modern fraction. The percent modern fraction is an expression of the age of the groundwater; the higher the modern fraction, the younger the groundwater. This figure affirms the conceptual model of the age of groundwater increasing along the flow paths from the outcrop to the confined downdip section.

**Table 7-3. Summary of age estimates for the Wilcox Group of the Carrizo-Wilcox Aquifer.**

<b>Model No.</b>	<b>Location Name</b>	<b>Report Sample No.</b>	<b>Well Depth (ft)</b>	<b>Cl (mg/L)</b>	<b>Alk (mg/L)<sup>(1)</sup></b>	<b>TDS (mg/L)</b>	<b>δ<sup>13</sup>C ‰ (DIC)</b>	<b><sup>14</sup>C<sub>OBS</sub> (pmc)</b>	<b><sup>14</sup>C<sub>OBS</sub> (ybp)</b>	<b><sup>14</sup>C<sub>ADJ</sub> (ybp)<sup>(2)</sup> Pearson &amp; White (1969)</b>	<b><sup>14</sup>C<sub>ADJ</sub> (ybp) Mass Balance Method 1</b>	<b><sup>14</sup>C<sub>ADJ</sub> (ybp) Mass Balance Method 2</b>
<b>Strike Section</b>												
1	Rockdale #10	BBMR-18	380	76.9	40.0	312	-24.2	83.38	1,460			
2	N. Millano WSC #3	BBMR-1	315	39.8	312	407	11.2	69.2	2,950			
3	Robertson WSC #3	BBMR-2	783	49.5	104	256	-19.7	32.94	8,920	7,006	7,006	
<b>Dip Section</b>												
1	RCWSC #3	BBMR-2	783	49.5	104	256	-19.7	32.94	8,920	7,006	7,006	Mass balance
2	Hearne #2	BBMR-14	1,433	40.5	360	442	-11.2	1.83	32,140	25,690	24,600	21,515
3	Col. Sta. #5	BBMR-5	2,884	40.3	320	516	-5.4	0.90	37,830	25,520	27,356 <sup>(4)</sup>	27,335 <sup>(4)</sup>
4	TAMU #7A	BBMR-12	3,060	51.4	480	638	-9.3	0	>43,500	35,556	No <sup>14</sup> C data	No <sup>14</sup> C data
5	Brushy WSW #2	BBMR-17	3,380	109 <sup>(3)</sup>	740	922	-6.7	0	>43,500	32,922	No <sup>14</sup> C data	No <sup>14</sup> C data

**NOTES:**

(1) Alkalinity as CaCO<sub>3</sub>.

(2) Correction using Pearson and White (1967) with δ<sup>13</sup>C soil CO<sub>2</sub> = -25 ‰, and calcite = 0 ‰.

(3) Elevated chloride concentrations indicate mixing with a deeper brine of unknown composition.

(4) Reaction directly between BBMR-2 and BBMR-5 not considering BBMR-14.

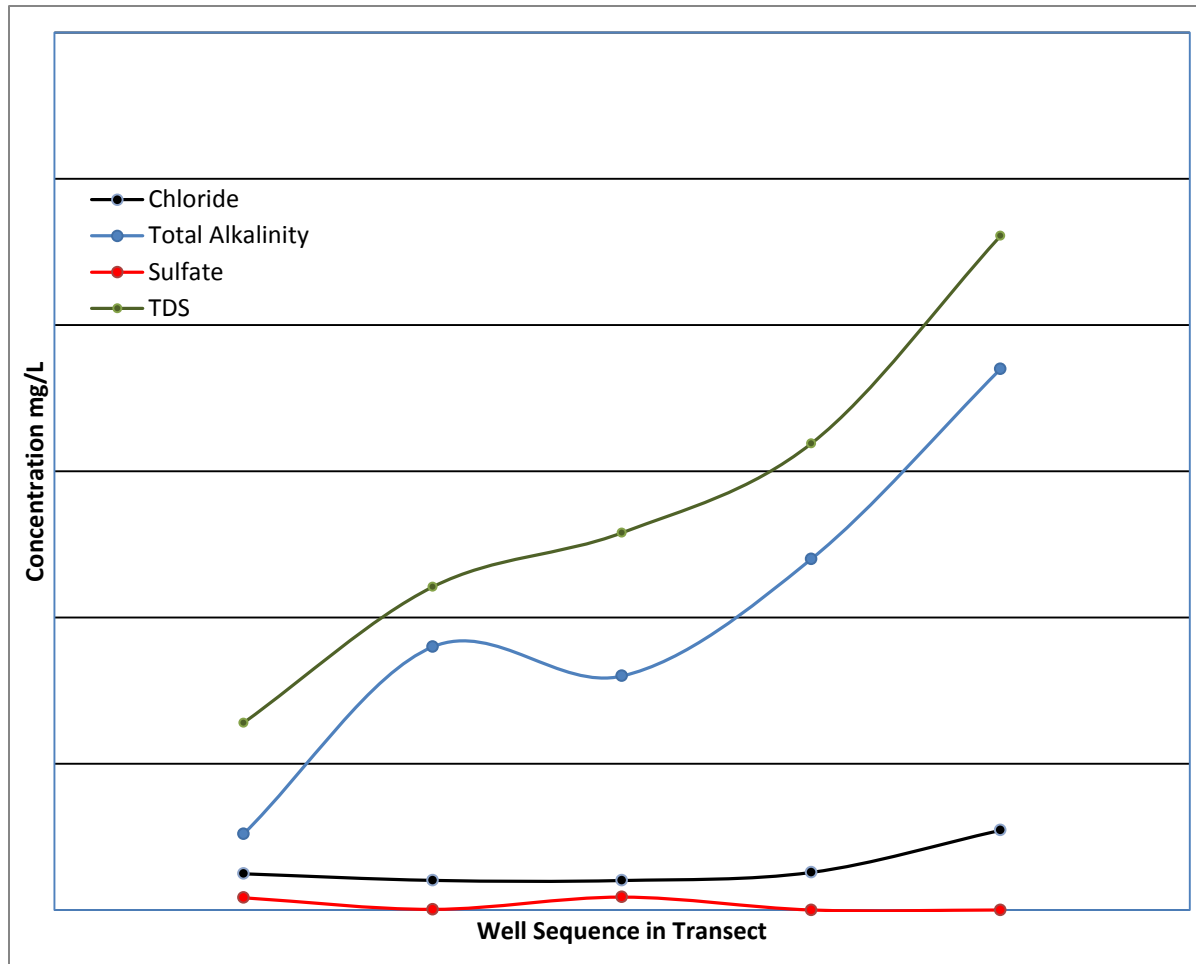


Figure 7-173. Relative concentrations of major anions and total dissolved solids in the evolution of the Simsboro Formation (Wilcox Group) of the Carrizo-Wilcox Aquifer along this transect.

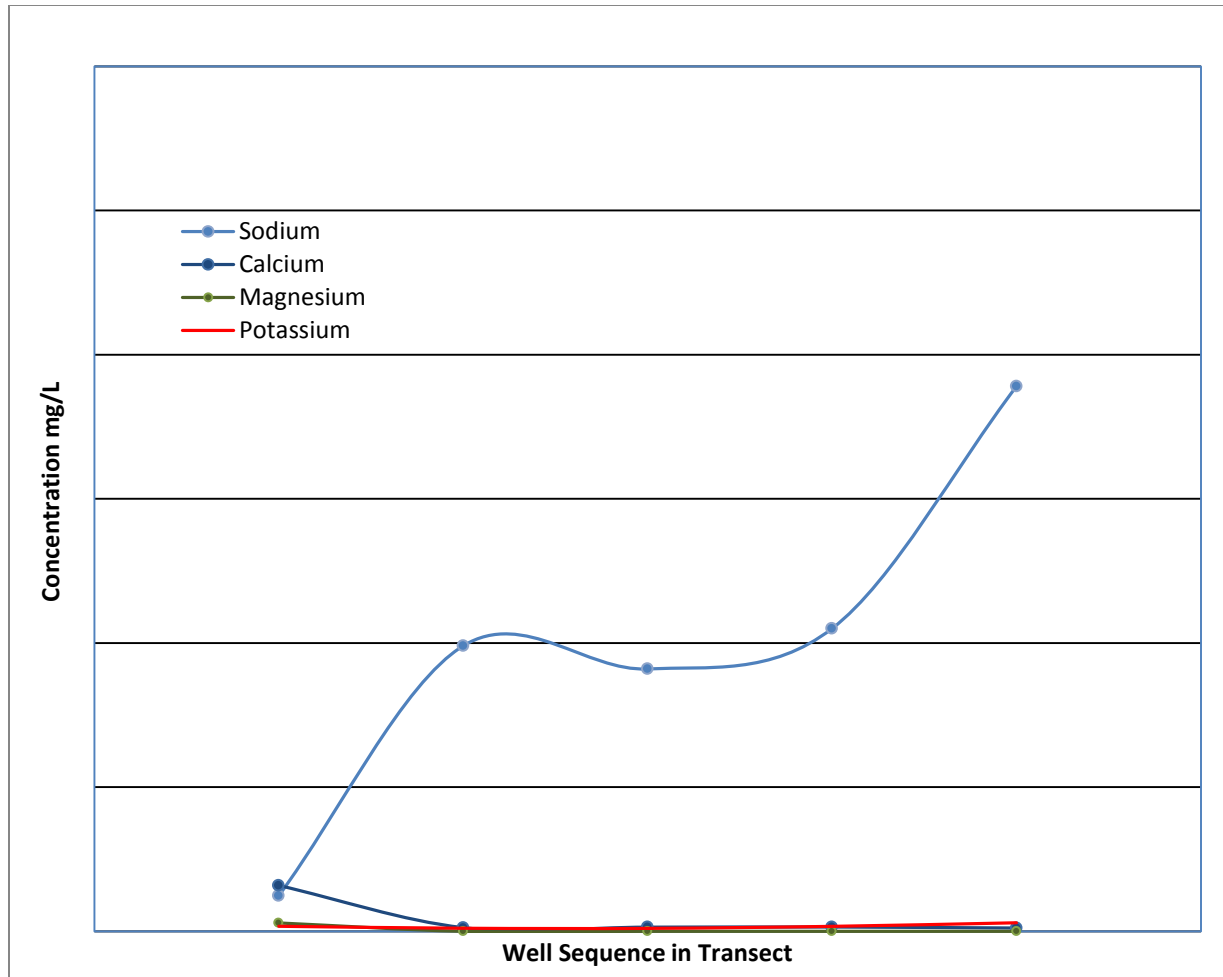


Figure 7-174. Relative concentrations of major cation in the evolution of the Simsboro Formation (Wilcox Group) of the Carrizo-Wilcox Aquifer along this transect.

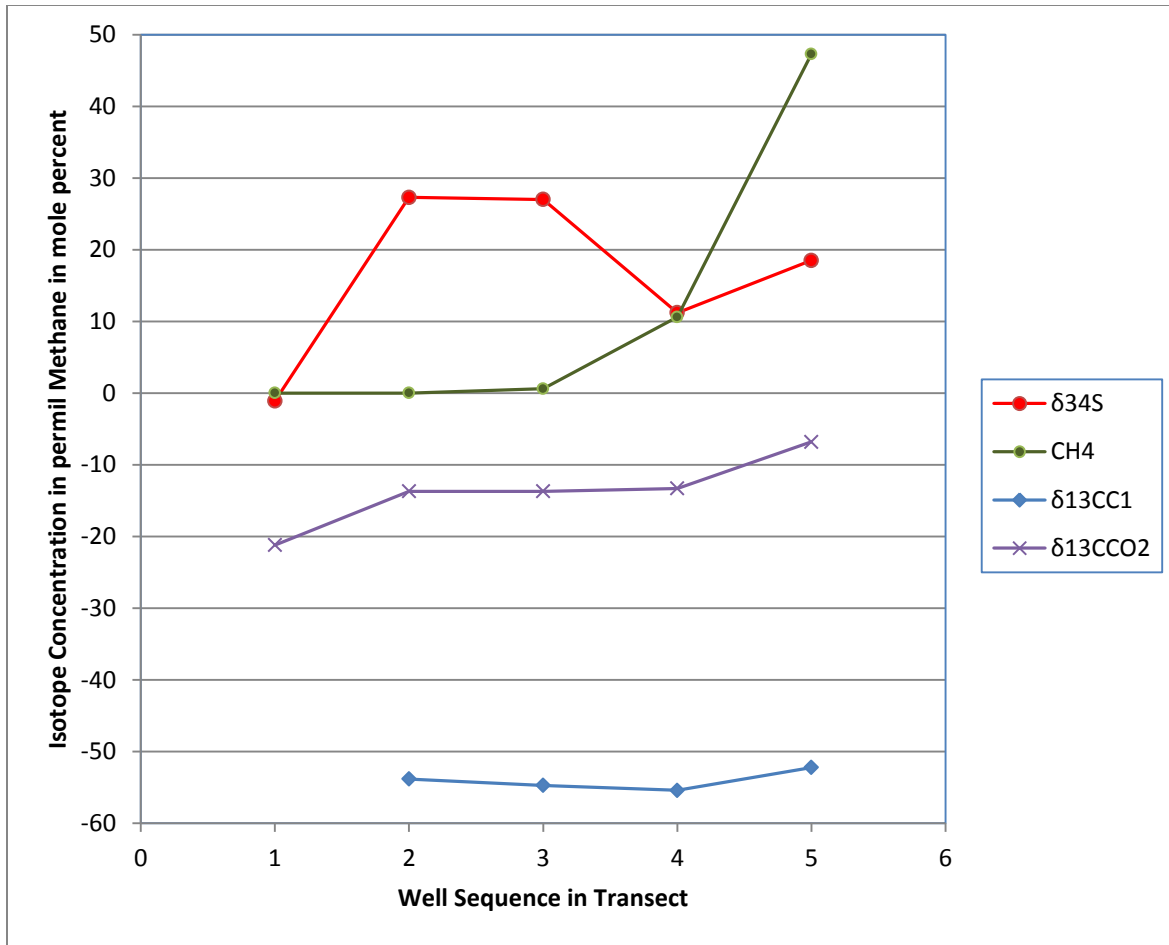
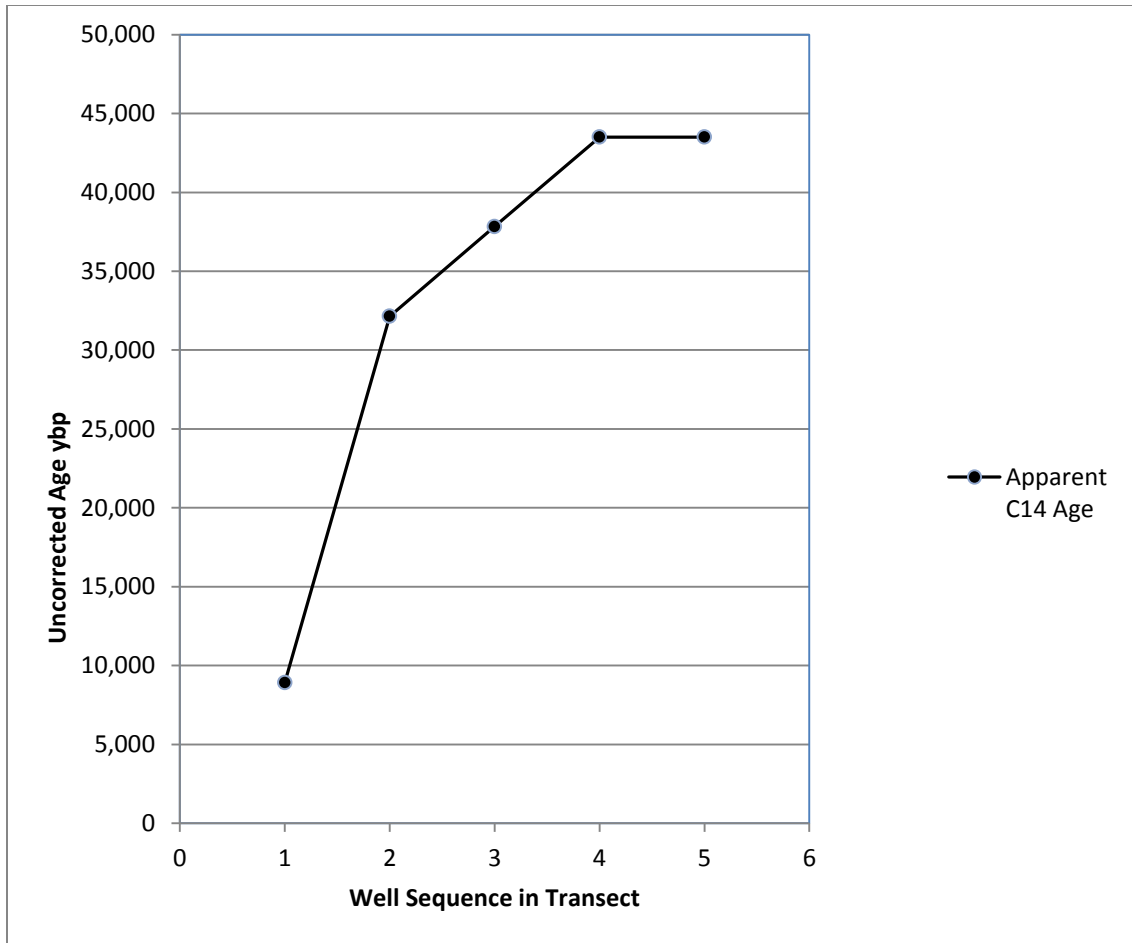
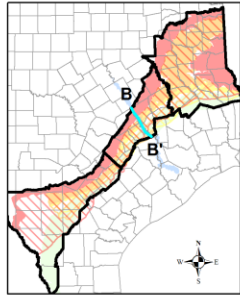


Figure 7-175. Stable isotope values and methane mole percent of fixed gas in the Simsboro Formation (Wilcox Group) of the Carrizo-Wilcox Aquifer along this transect.



**Figure 7-176. Relative measured radiocarbon age in the evolution of the Simsboro Formation (Wilcox Group) of the Carrizo-Wilcox Aquifer along this transect.**



Profile B-B' Showing Sodium (meq/L)  
at Recorded Well Depth  
GMA 12

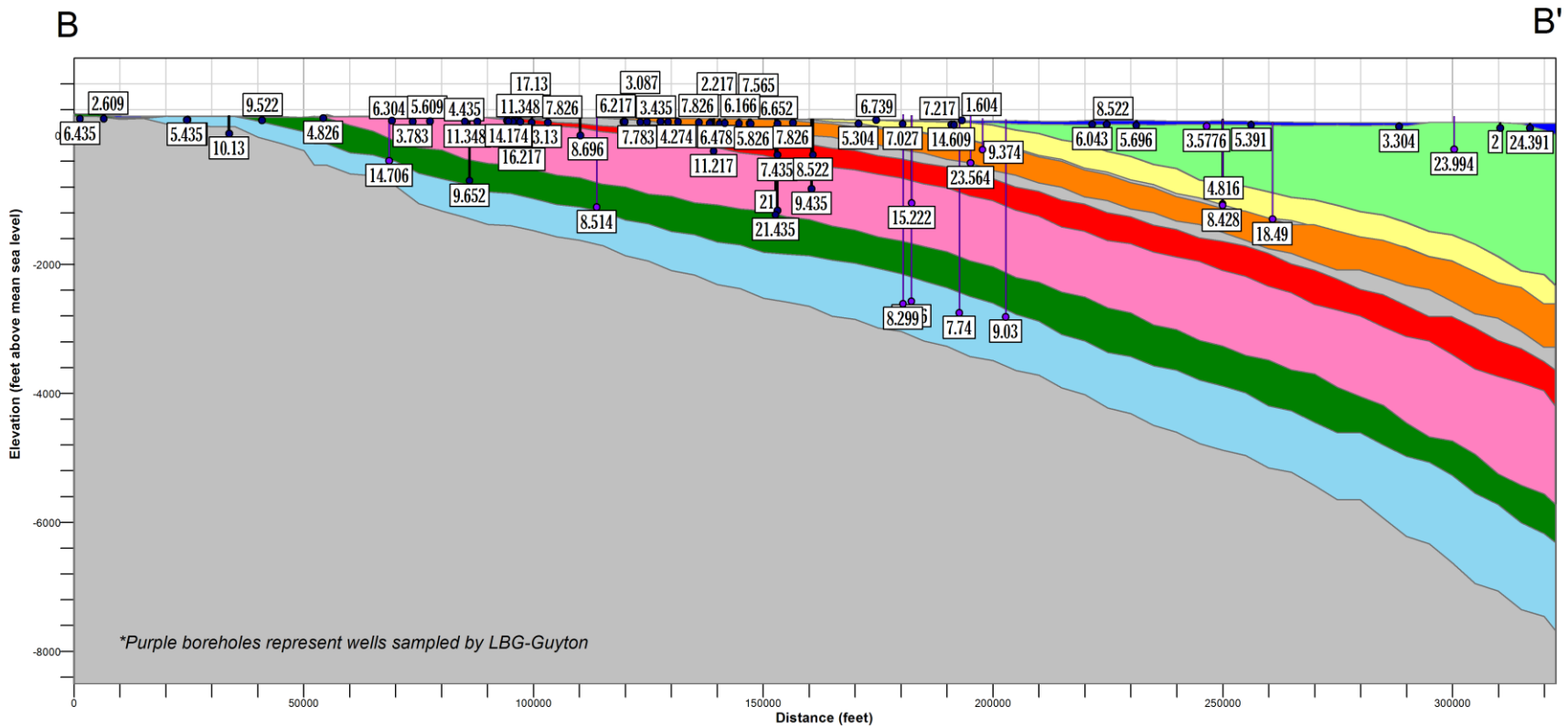
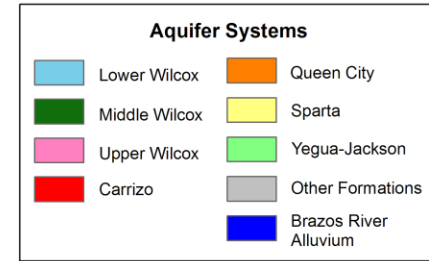
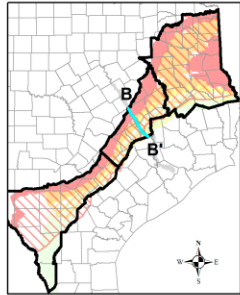


Figure 7-177. Central Transect cross section with sodium analytical data measured in milliequivalents per liter (meq/L).



Profile B-B' Showing Carbon-14  
Percent (%) Modern at Recorded Well Depth  
GMA 12

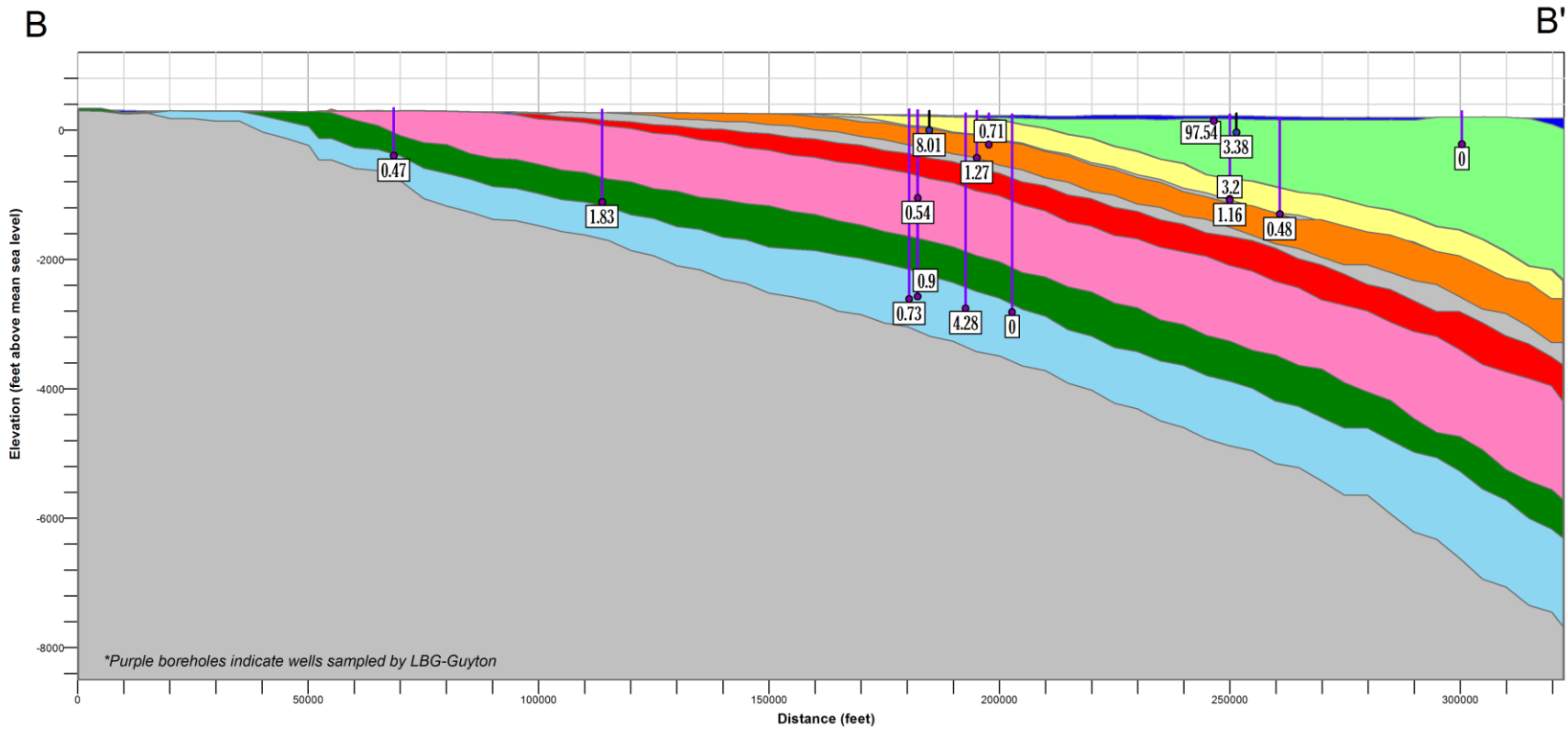
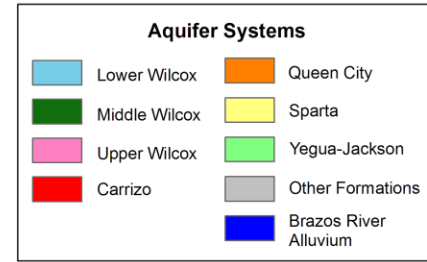


Figure 7-178. Central Transect cross section with carbon-14 analytical data measured in percent modern carbon.

### **7.3 Gonzales Transect**

An excellent database from the TWDB groundwater database exists for water wells, water chemistry and water levels in the Carrizo-Wilcox, Queen City, Sparta and Yegua-Jackson aquifers in Guadalupe, Gonzales and Caldwell counties (Figure 7-179). In addition twenty-three wells were sampled for this project in 2012 in the Carrizo-Wilcox, Queen City and Sparta for basic inorganic chemistry, gas chemistry and isotope chemistry. The 2012 chemistry data are in Table 7-4 and locations of the sampled wells on Figure 7-180. A geologic dip-oriented cross section from northwest to southeast shows the geology and location of the wells sampled in 2012 (Figure 7-181). The TWDB chemistry data by aquifer are in Appendix A.

#### **7.3.1 General Geochemical Trends**

##### **Carrizo Sand Formation of the Carrizo-Wilcox Aquifer**

The Carrizo Sand Formation of the Carrizo-Wilcox Aquifer is the primary aquifer in Guadalupe, Gonzales and Caldwell counties. The most extensive groundwater database is available for the Carrizo Sand Formation. The distribution of data for the Carrizo Sand Formation are shown on Figure 7-182.

##### Well Depths

Based on Figure 7-182, the dip-oriented cross section for the transect, well depths in the outcrop are less than 200 feet and increase to well depths greater than 2,000 feet in east to southeast Gonzales County.

##### Potentiometric Surface

The Carrizo Sand Formation potentiometric surface for the transect (based on most recent data) (Figure 7-183) shows water levels in the outcrop greater than 400 feet (above mean sea level) to water levels downdip in the east and southeast section of Gonzales County of about 300 feet or less. From this map two directions of non-anthropogenic groundwater flow can be inferred: 1) along strike in the outcrop toward the rivers and creeks that cross the outcrop and 2) down the structured dip of the Carrizo Sand Formation from outcrop to the deep subsurface. Downdip wells in the confined section may be “flowing” wells (Figure 7-184).

##### Piper Diagram

The Piper diagram for the Carrizo Sand Formation in the Gonzales Transect shows a mixed cation (calcium-sodium) mixed anion (sulfate-chloride-bicarbonate) water at shallower depth evolving to a sodium-bicarbonate-chloride water at depth (Figure 7-185).

##### Bicarbonate versus Sodium Plot

A plot of bicarbonate versus sodium (Figure 7-186) for all the TWDB data and the 2012 data show two trends. For bicarbonate values less than approximately three milliequivalents per liter, bicarbonate increases independent of sodium. For bicarbonate concentrations greater than three milliequivalents per liter, both sodium and bicarbonate increase linearly at an approximate ratio of 1:1, with a slight concave upward bend to the data.

### Sodium versus Calcium Plot

A plot of sodium versus calcium for all data (Figure 7-187) show an interesting relationship between sodium and calcium. At low concentrations of sodium, sodium values are independent of calcium. Conversely at low concentrations of calcium, sodium is independent of calcium.

### Bicarbonate versus Calcium Plot

A plot of bicarbonate versus calcium (Figure 7-188) shows a distribution of data similar to the pattern of sodium and calcium (Figure 7-187) with a slight difference, calcium and bicarbonate (at low concentrations) appear to increase linearly to about three milliequivalents per liter. Calcium then decrease to zero calcium as bicarbonate increases to over 30 milliequivalents per liter.

### pH versus Bicarbonate Plot

The plot of pH versus bicarbonate (Figure 7-189) shows three limbs to this curve: a) pH rises from less than five with very low bicarbonate, b) from pH seven to eight, bicarbonate concentrations rise to about five milliequivalents per liter and c) above a pH of approximately seven and a half, bicarbonate increases independent of pH. There might even be a slight decline in pH at bicarbonate concentrations greater than 15 milliequivalents per liter.

### pH versus Sodium Plot

The plot of pH versus sodium (Figure 7-190) shows a similar distribution of data to the pH versus bicarbonate plot (Figure 7-189).

### Sulfate versus Bicarbonate Plot

The plot of sulfate versus bicarbonate (Figure 7-191) shows higher sulfate concentrations at bicarbonate concentrations less than ten milliequivalents per liter. There are very low sulfate concentrations at bicarbonate concentrations greater than ten milliequivalents per liter.

### Chloride versus Sodium Plot

The plot of chloride versus sodium (Figure 7-192) shows sodium increasing independent of chloride for sodium concentrations less than ten milliequivalents per liter. Chloride starts increasing slowly at higher sodium concentrations from ten to 30 milliequivalents per liter at a ratio of about 1:1 for sodium concentrations greater than about 30 milliequivalents per liter.

### Chloride versus Bicarbonate Plot

The plot of chloride versus bicarbonate (Figure 7-193) shows three trends: a) bicarbonate increases independent of chloride or bicarbonate values from zero to ten milliequivalents per liter, b) there is a general increase in both bicarbonate and chloride from bicarbonate concentrations of ten to 30 milliequivalents per liter and c) there are also a set of higher chloride values at lower bicarbonate concentrations.

### Depth versus Sulfate Plot

The plot of depth versus sulfate (Figure 7-194) shows the highest concentrations of sulfate at the shallowest depths and declining to negligible concentrations below 2,500 feet.

### Depth versus Calcium Plot

The plot of depth versus calcium (Figure 7-195) shows the highest concentrations of calcium at the shallowest depths and not declining to negligible values until depths greater than about 2,500 feet.

### Map of Calcium

The map of calcium (Figure 7-196) concentration decreases from outcrop to the deeper confined parts of the aquifer. Higher calcium concentrations occur deep into the aquifer and are not restricted only to the Carrizo Sand Formation of the Carrizo-Wilcox Aquifer outcrop.

### Depth versus Sodium Plot

The plot of depth versus sodium (Figure 7-197) shows increases in sodium at depths greater than about 1,800 feet.

### Depth versus Bicarbonate Plot

The plot of depth versus bicarbonate (Figure 7-198) shows higher bicarbonate concentrations at depths greater than about 1,500 feet.

### Map of Bicarbonate

The map of bicarbonate (Figure 7-199) shows low bicarbonate values occur in the outcrop, but also extend into the deeper confined parts of the aquifer. The highest bicarbonate values are in the deeper parts of the aquifer.

### Depth versus pH Plot

The plot of depth versus pH (Figure 7-200) shows a general increase in pH with depth.

### Map of pH

The map of pH (Figure 7-201) in the Carrizo Sand Formation shows the lowest pH's in the updip section although low pH values (less than seven) are not restricted only to the outcrop area. Low pH waters extend deep into the aquifer.

### Depth versus Chloride Plot

The plot of depth versus chloride (Figure 7-202) shows some higher chloride concentrations at depth less than 500 feet and higher concentrations at depths greater than about 1,700 feet. There is a general trend showing nominal increases in chloride to depths of 3,000 feet.

### Map of Chloride

The map of chloride (Figure 7-203) shows most of the high chloride concentrations occur in the deepest downdip parts of the aquifer with a few higher chloride waters near the outcrop.

### Depth versus Total Dissolved Solids Plot

The plot of depth versus total dissolved solids (Figure 7-204) shows higher total dissolved solids waters at depths greater than about 1,700 feet.

### Discussion

Groundwater in the Carrizo Sand Formation in the Gonzales Transect is recharged and discharged in the outcrop or flows into the deeper subsurface. The groundwater chemistry

evolves from a mixed calcium-sodium and sulfate-chloride cation water in the outcrop to a sodium-bicarbonate with some chloride and no sulfate down gradient. The earlier part of the flow in the confined part of the aquifer is not dominated by sodium-bicarbonate water. The sodium-bicarbonate type water only occurs deeper in the aquifer. The implication is that there is minimal sodium-montmorillonite in the shallower portion of the Carrizo Sand Formation in this area to provide exchange sites to replace the dissolved calcium with sodium. This is in contrast to the distribution of calcium in the Central Transect where elevated calcium occurs only in the outcrop (Figure 7-103). The increase in bicarbonate with no change in pH suggests that coalification of organics in the deeper parts of the aquifer are an additional source of bicarbonate. The higher chloride concentrations at depth suggest that a saline source of water is leaking into the aquifer. The increase in salinity to total dissolved solids values is greater than 1,000 milliequivalents per liter, however are caused by increases in both chloride and bicarbonate. The eastern extent of meteoric groundwater has not been reached based on water chemistry data from these wells.

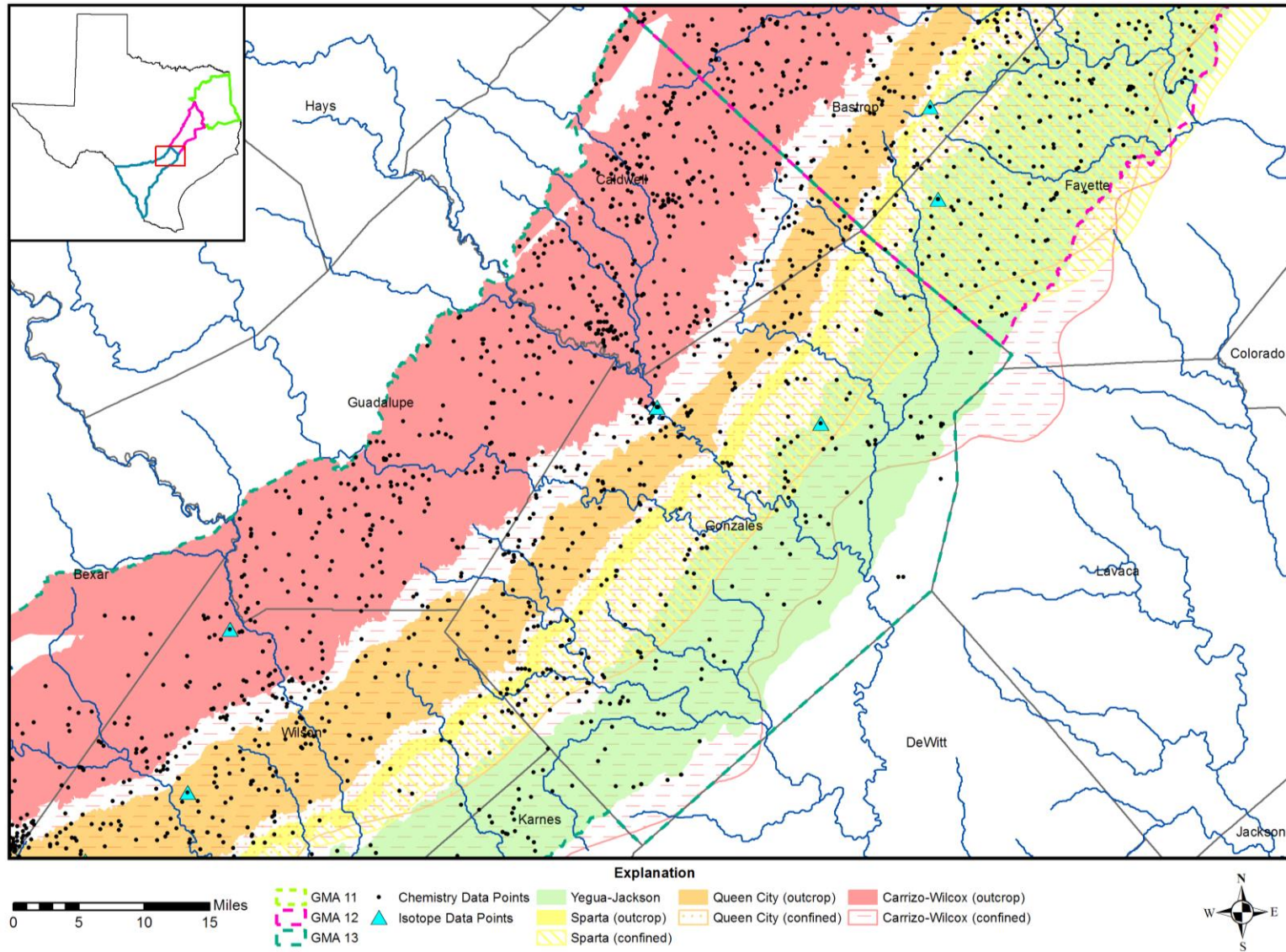


Figure 7-179. Data distribution of wells with outcrop and downdip extent (up to 3,000 milliequivalents per liter total dissolved solids) of the Carrizo-Wilcox, Queen City, Sparta and Yegua-Jackson aquifers in the Gonzales Transect Groundwater Management Area (GMA) 13.

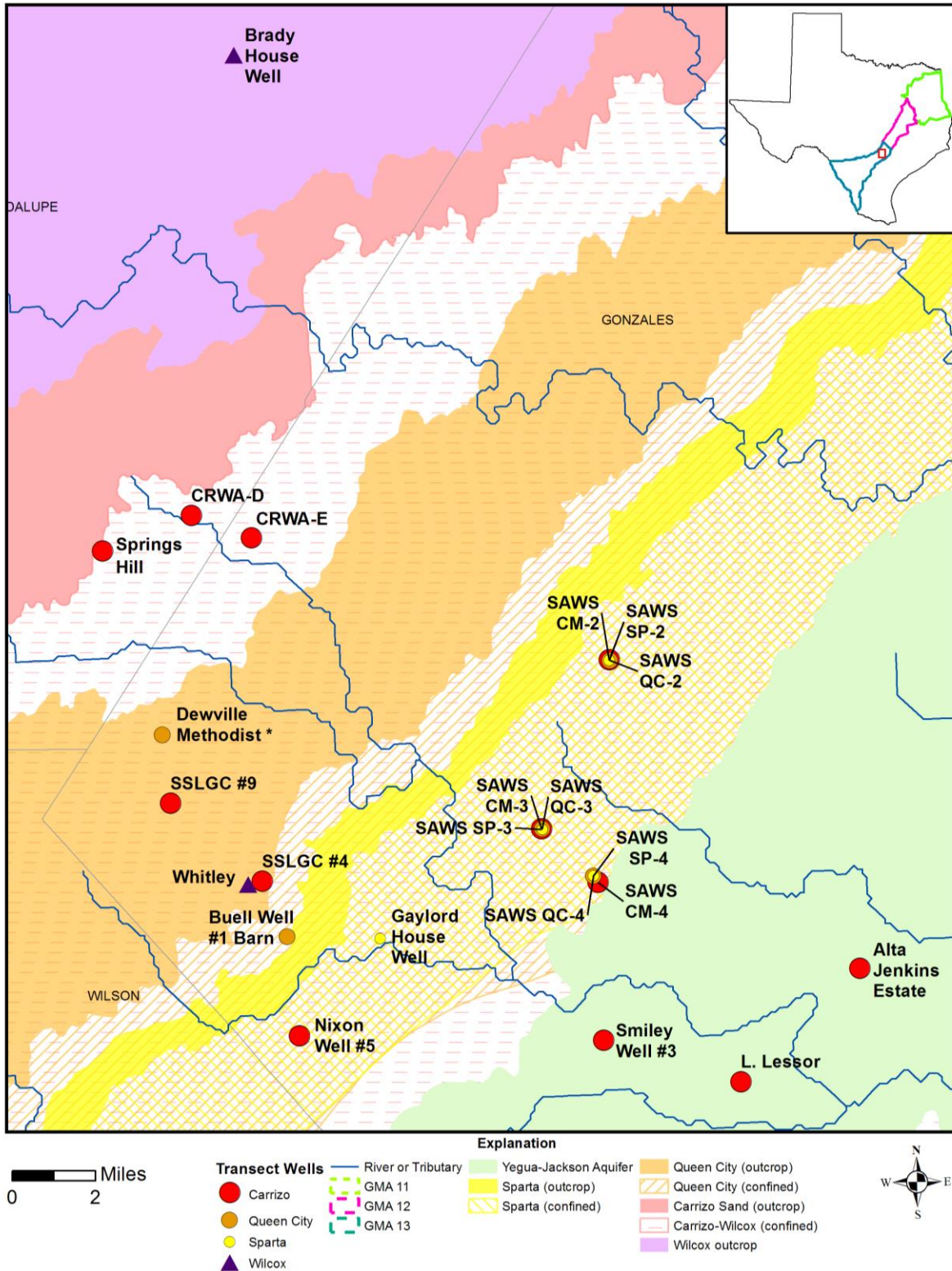
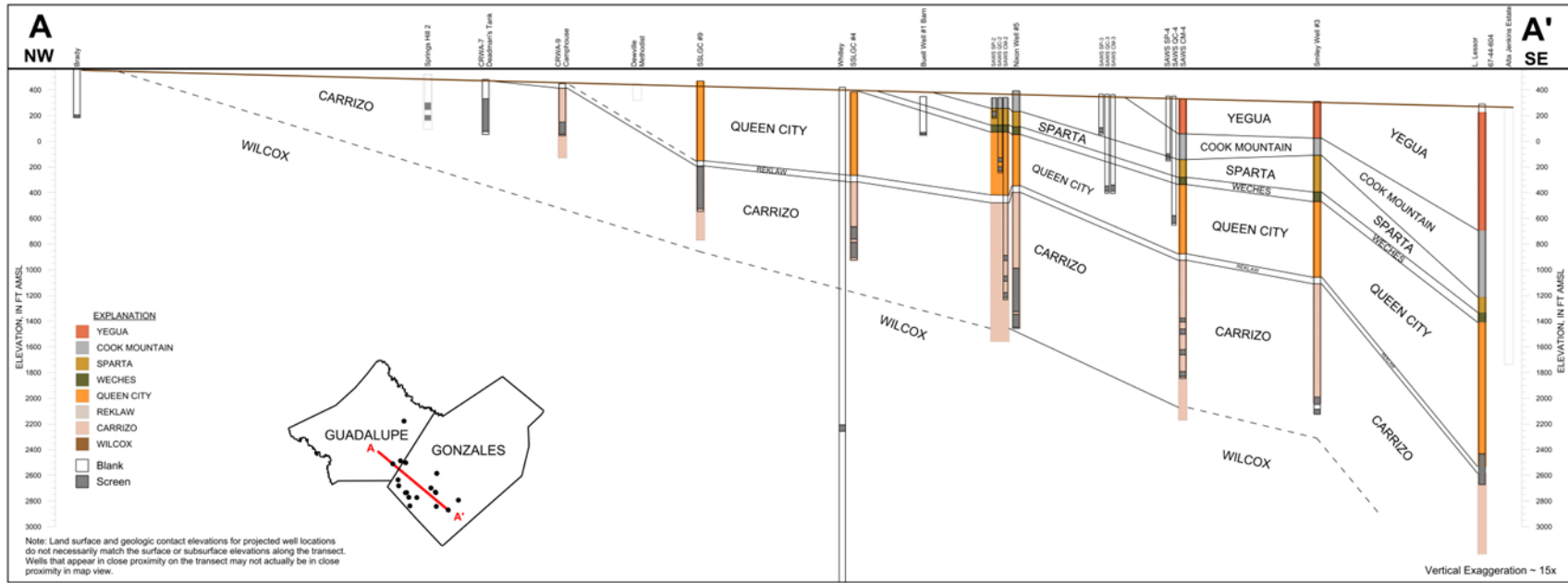


Figure 7-180. Gonzales Transect sampled well locations, Groundwater Management Area (GMA) 13.

Evaluation of Hydrochemical and Isotopic Data in Groundwater Management Areas 11, 12 and 13



See 'Figure 7-181 GUGZ dip section.pdf' for the full-scale version of the cross-section (included as a separate document).

Figure 7-181. Cross-section A-A' in dip direction of the Gonzales Transect, Groundwater Management Area 13.

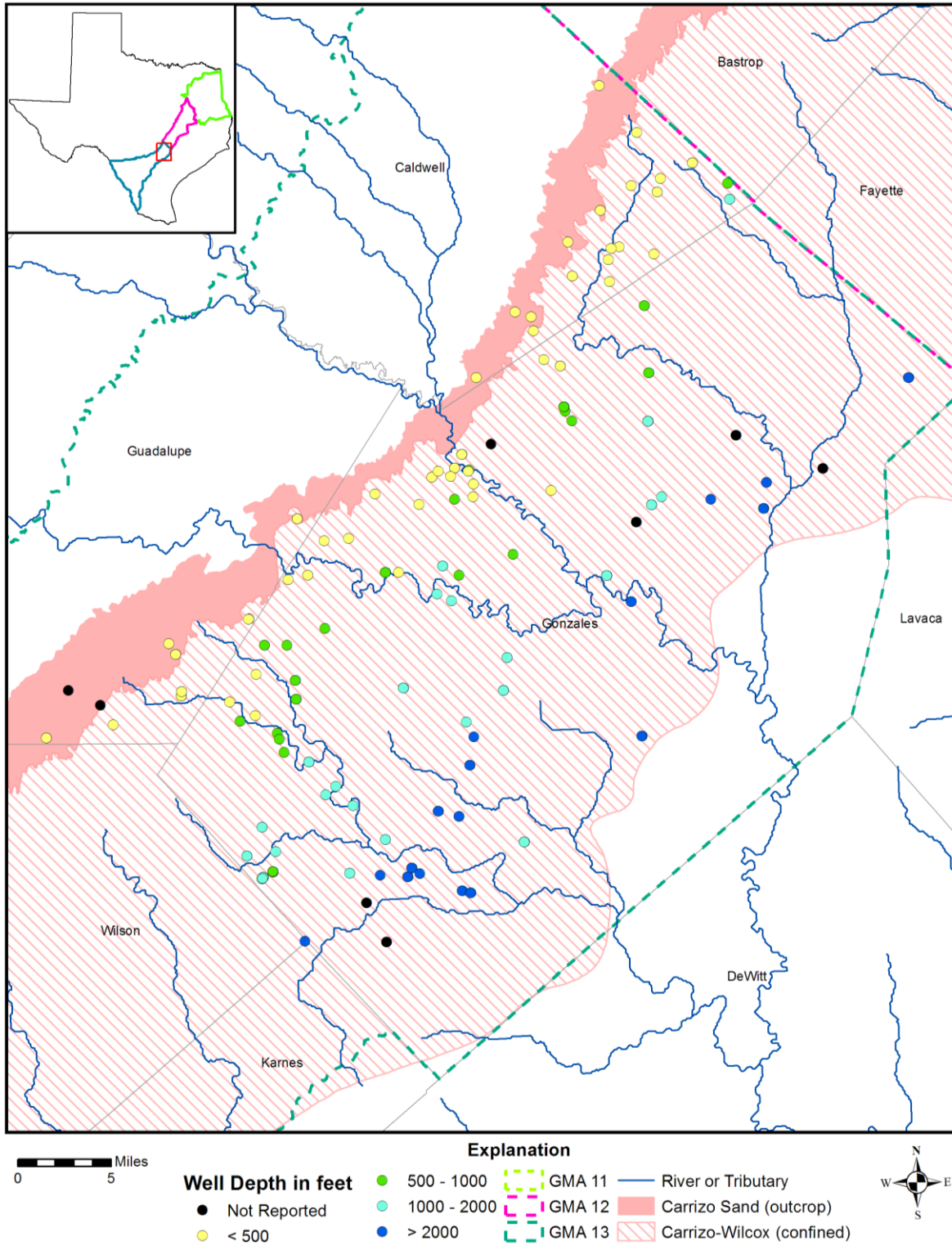
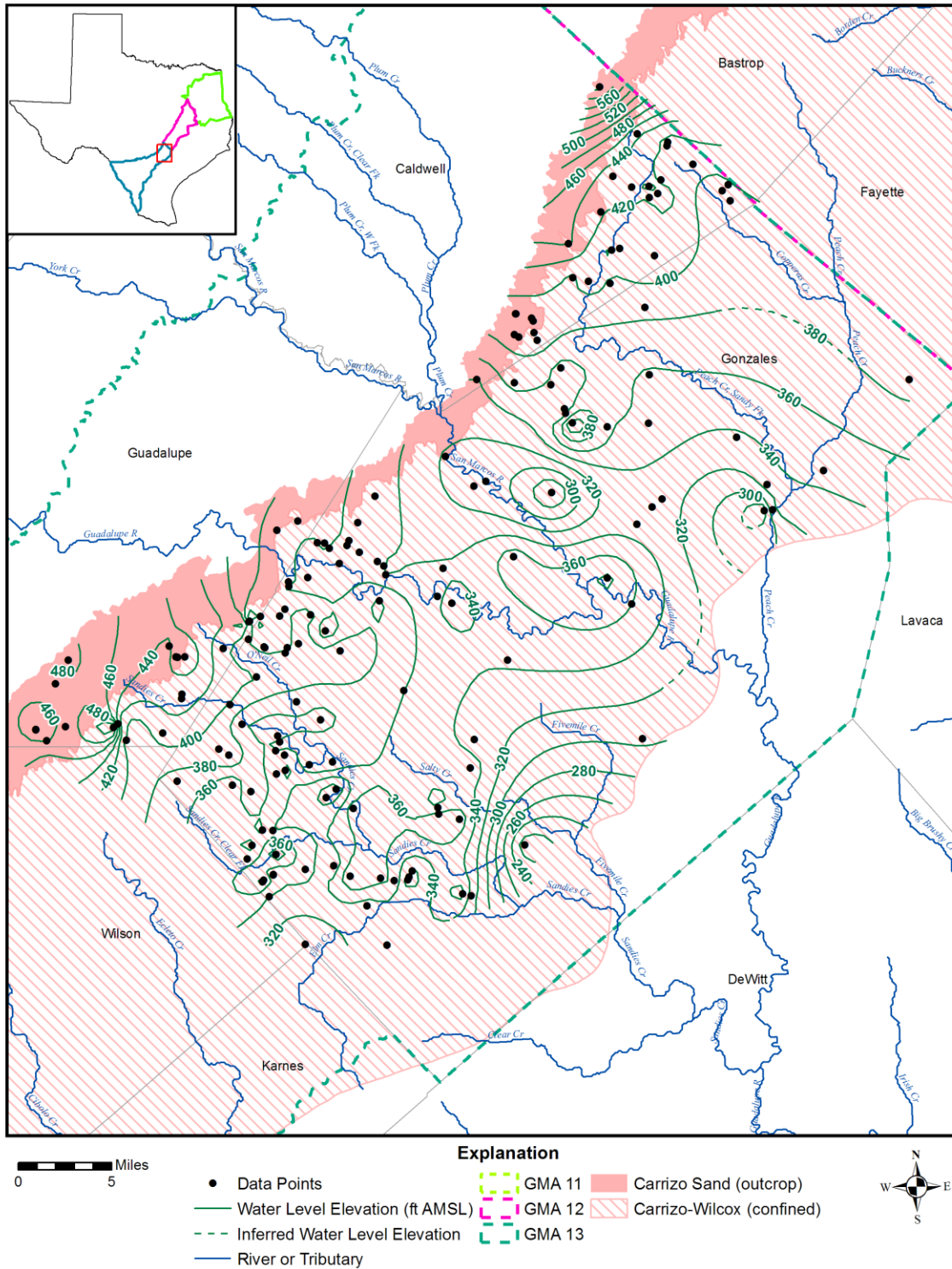


Figure 7-182. Well depths measured from land surface in feet (ft) in the Carrizo Sand Formation of the Carrizo-Wilcox Aquifer, Gonzales Transect, Groundwater Management Area (GMA) 13.



**Figure 7-183.** Potentiometric surface of the Carrizo Sand Formation of the Carrizo-Wilcox Aquifer using water level data measured in feet above mean sea level (ft AMSL) from 1931 to 2010 in the Gonzales Transect, Groundwater Management Area (GMA) 13.

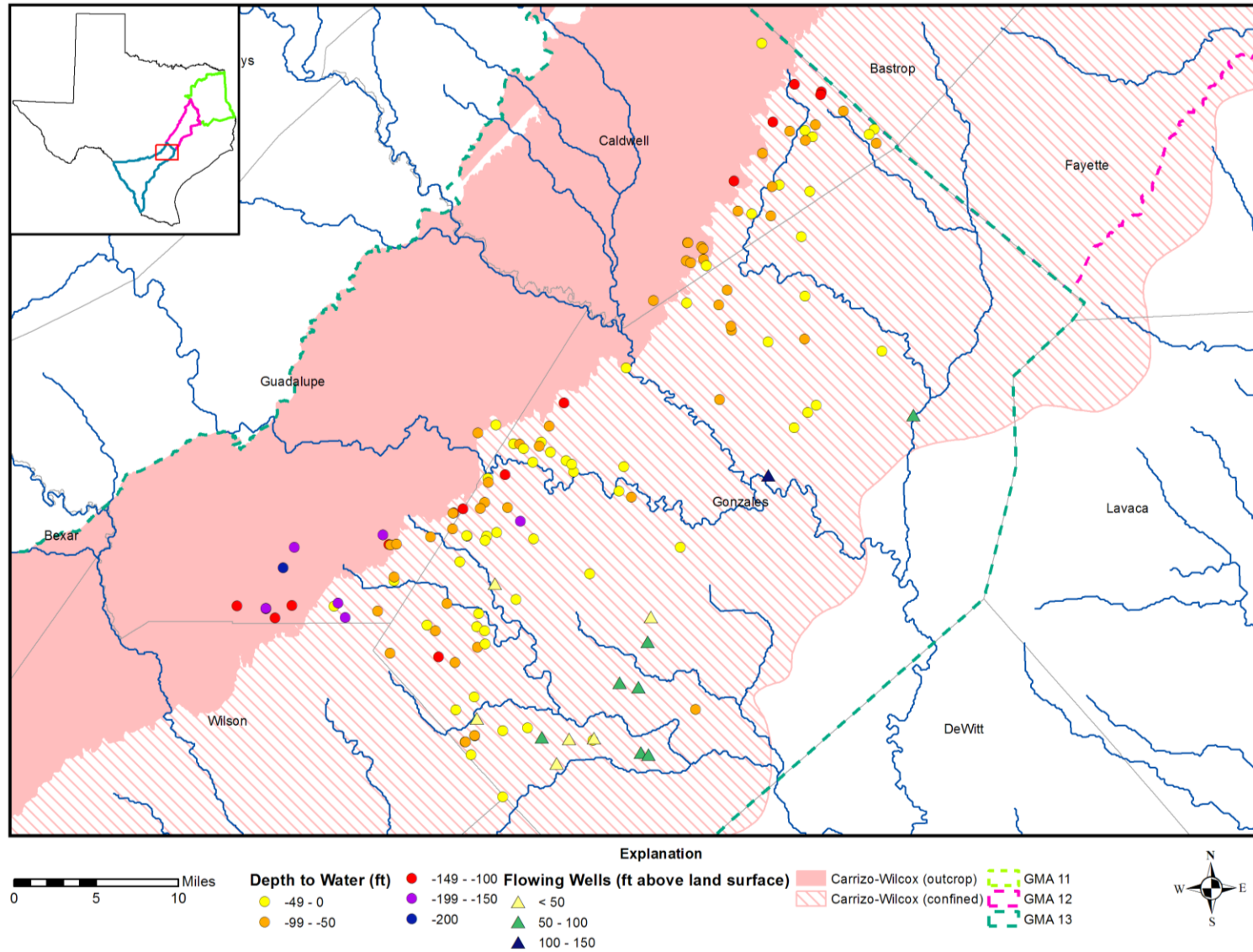


Figure 7-184. Depth to water in flowing and non-flowing wells in the Carrizo Sand Formation of the Carrizo-Wilcox Aquifer, Gonzales Transect, Groundwater Management Area (GMA) 13.

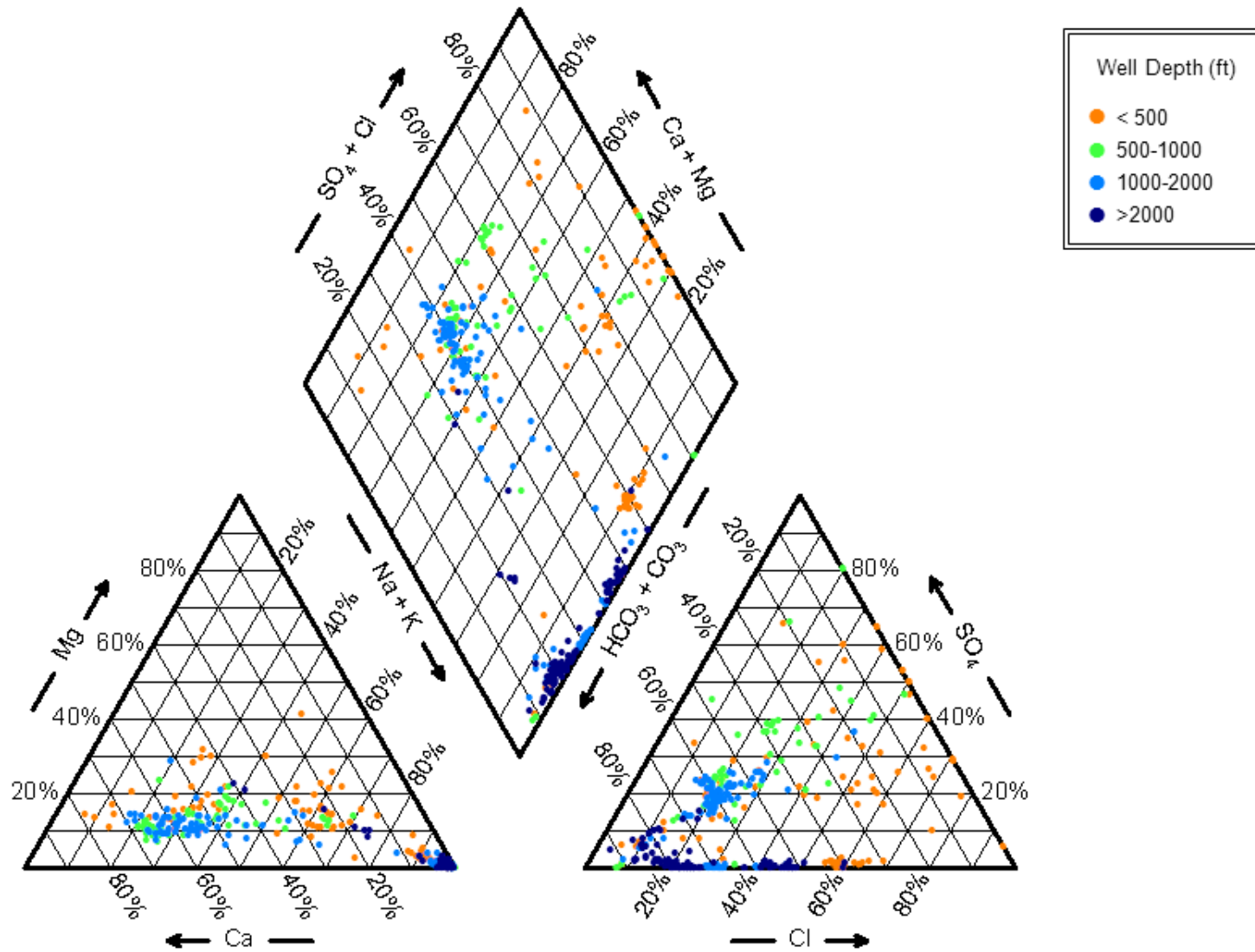


Figure 7-185. Piper diagram showing chemistry of the Carrizo Sand Formation of the Carrizo-Wilcox Aquifer wells in the Gonzales Transect by well depth measured from land surface in feet (ft).

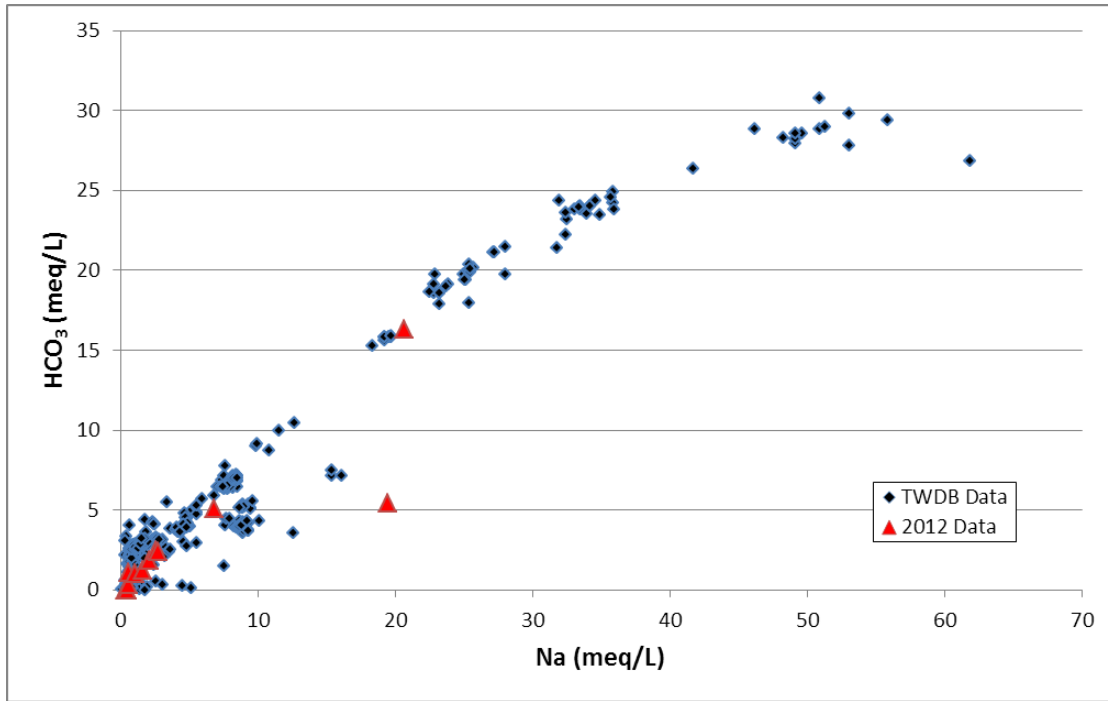


Figure 7-186. Bicarbonate (HCO<sub>3</sub>) versus sodium (Na) measured in milliequivalents per liter (meq/L), Carrizo Sand Formation of the Carrizo-Wilcox Aquifer, Gonzales Transect, Groundwater Management Area 13.

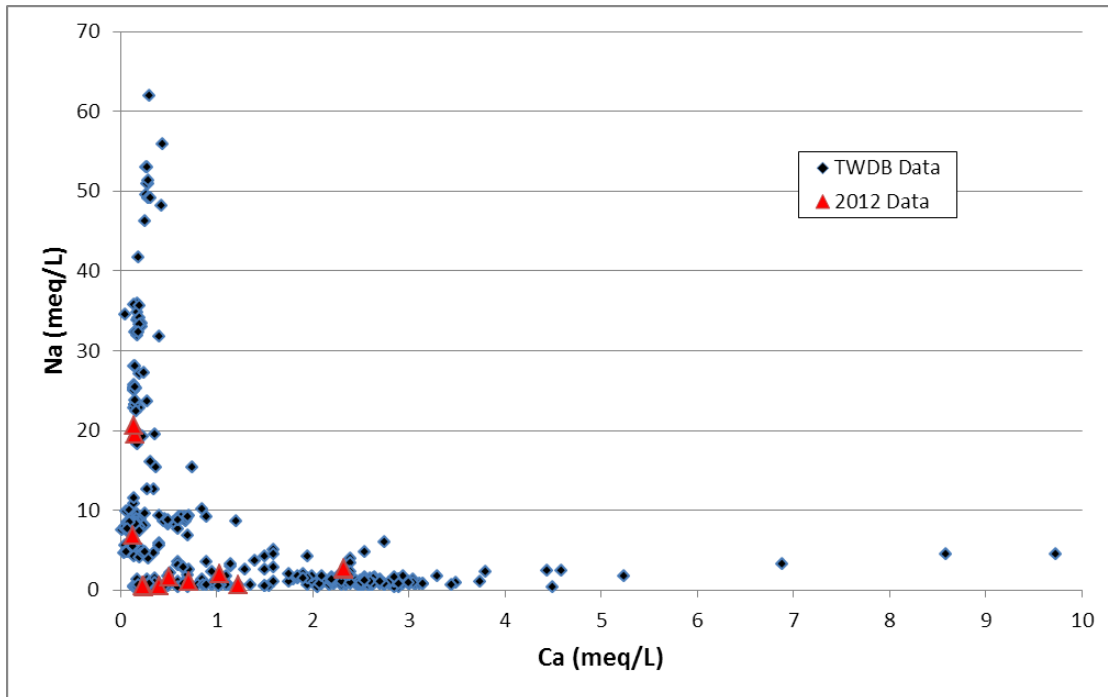


Figure 7-187. Sodium (Na) versus calcium (Ca) measured in milliequivalents per liter (meq/L), Carrizo Sand Formation of the Carrizo-Wilcox Aquifer, Gonzales Transect, Groundwater Management Area 13.

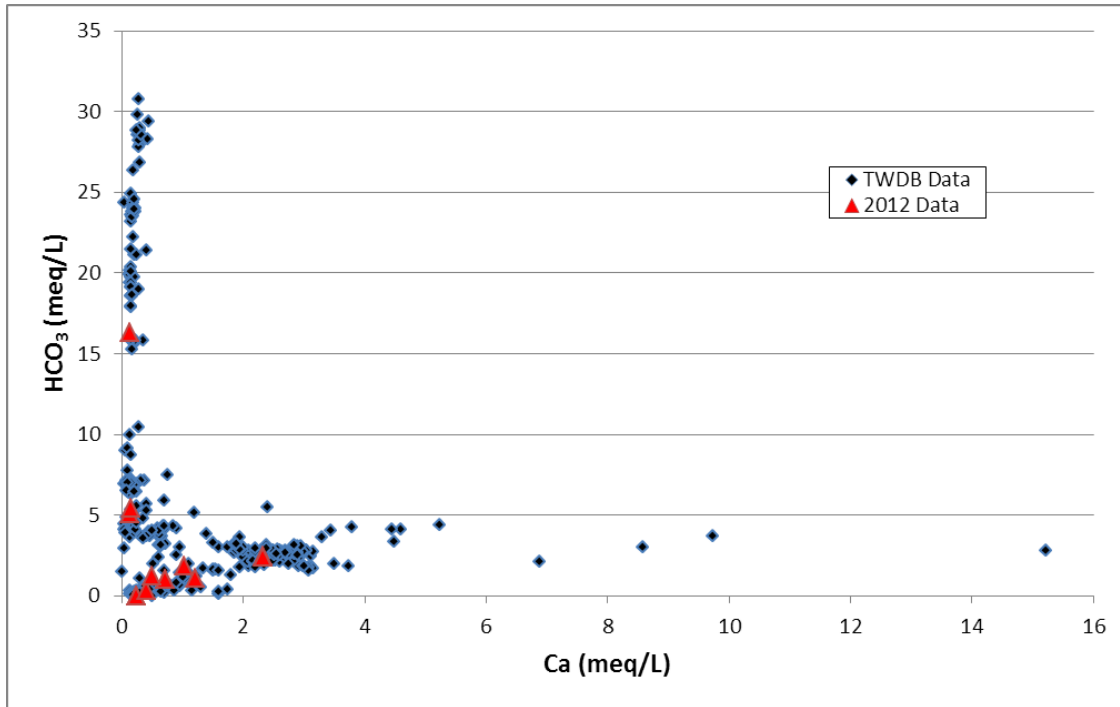


Figure 7-188. Bicarbonate ( $\text{HCO}_3^-$ ) versus calcium (Ca) measured in milliequivalents per liter (meq/L), Carrizo Sand Formation of the Carrizo-Wilcox Aquifer, Gonzales Transect, Groundwater Management Area 13.

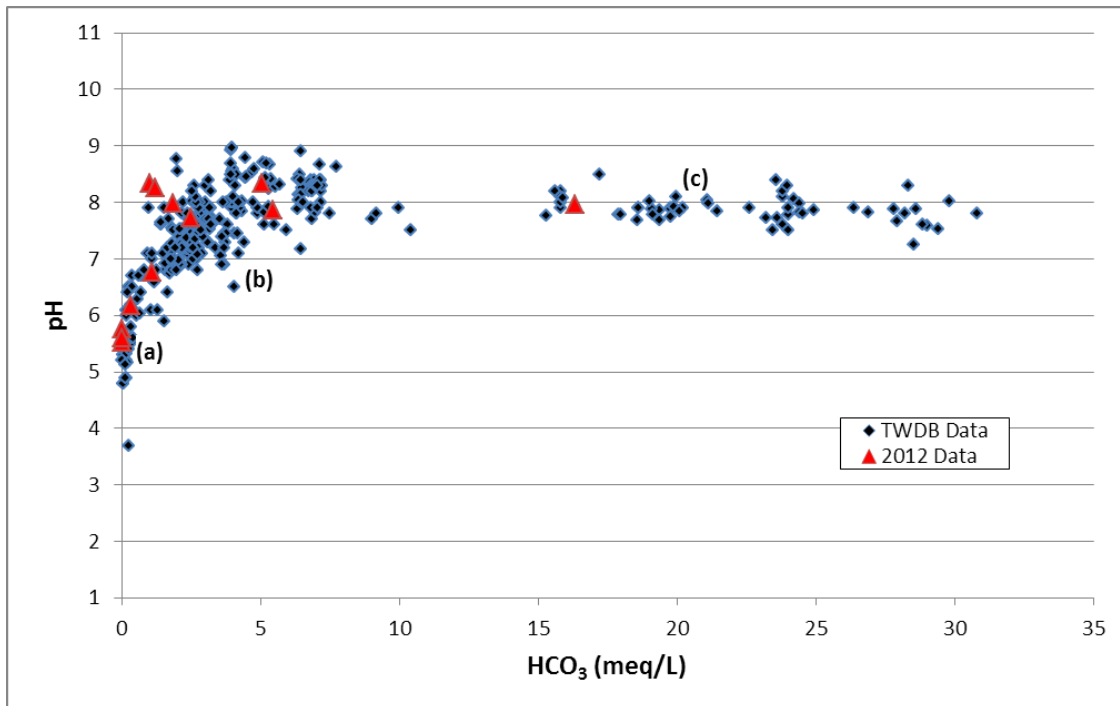


Figure 7-189. pH versus bicarbonate ( $\text{HCO}_3^-$ ) measured in milliequivalents per liter (meq/L), Carrizo Sand Formation of the Carrizo-Wilcox Aquifer, Gonzales Transect, Groundwater Management Area 13.

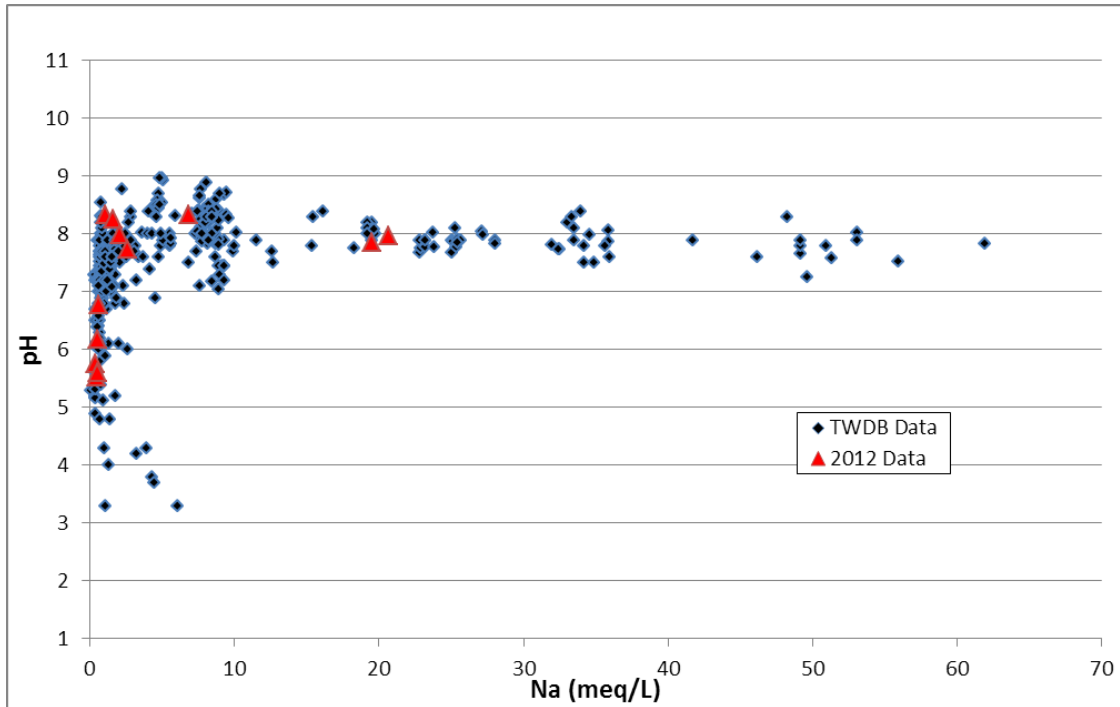


Figure 7-190. pH versus sodium (Na) measured in milliequivalents per liter (meq/L), Carrizo Sand Formation of the Carrizo-Wilcox Aquifer, Gonzales Transect, Groundwater Management Area 13.

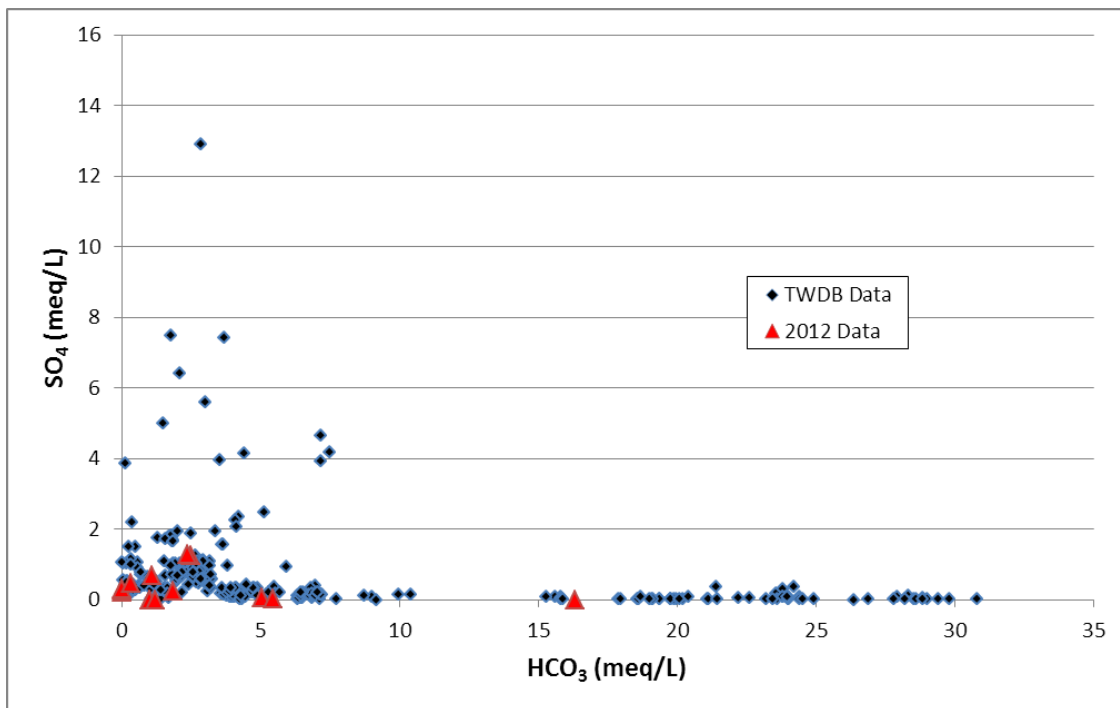
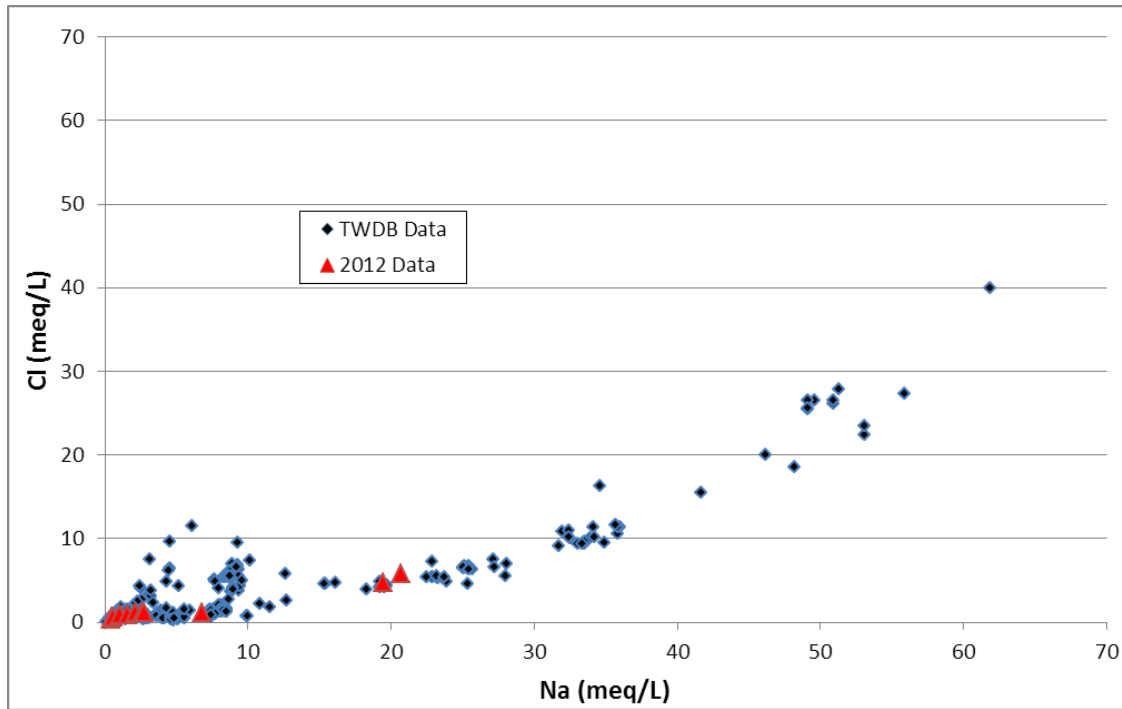
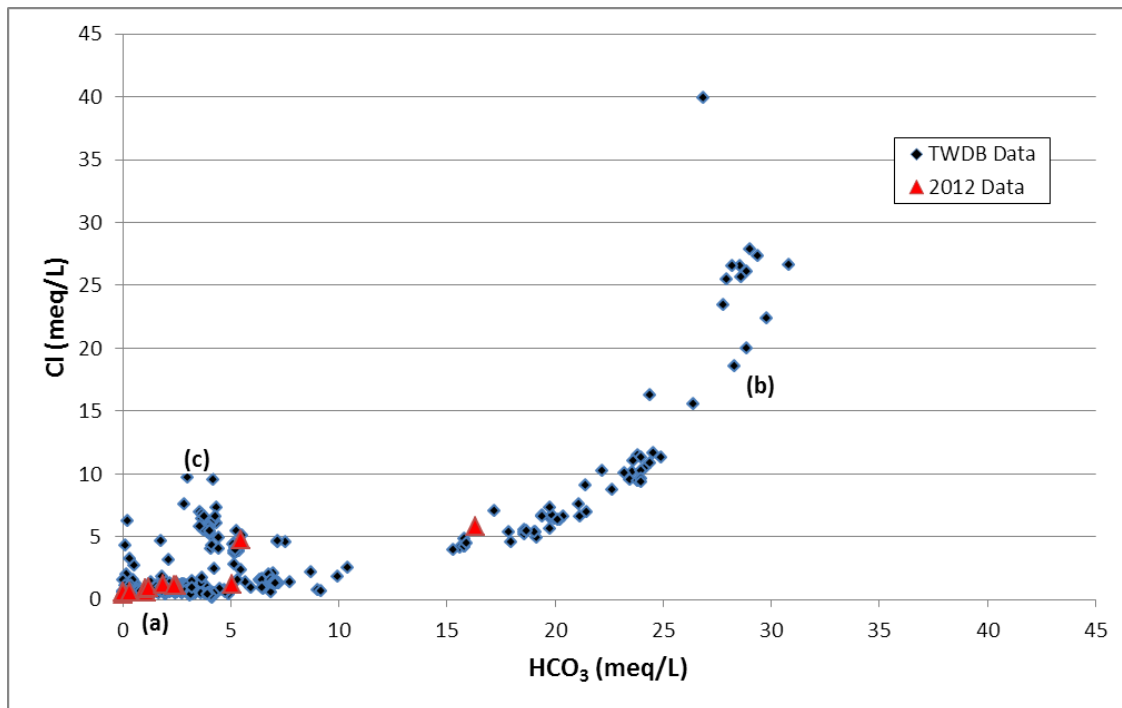


Figure 7-191. Sulfate (SO<sub>4</sub>) versus bicarbonate (HCO<sub>3</sub>) measured in milliequivalents per liter (meq/L), Carrizo Sand Formation of the Carrizo-Wilcox Aquifer, Gonzales Transect, Groundwater Management Area 13.



**Figure 7-192.** Chloride (Cl) versus sodium (Na) measured in milliequivalents per liter (meq/L), Carrizo Sand Formation of the Carrizo-Wilcox Aquifer, Gonzales Transect, Groundwater Management Area 13.



**Figure 7-193.** Chloride (Cl) versus bicarbonate ( $\text{HCO}_3$ ) measured in milliequivalents per liter (meq/L), Carrizo Sand Formation of the Carrizo-Wilcox Aquifer, Gonzales Transect, Groundwater Management Area 13.

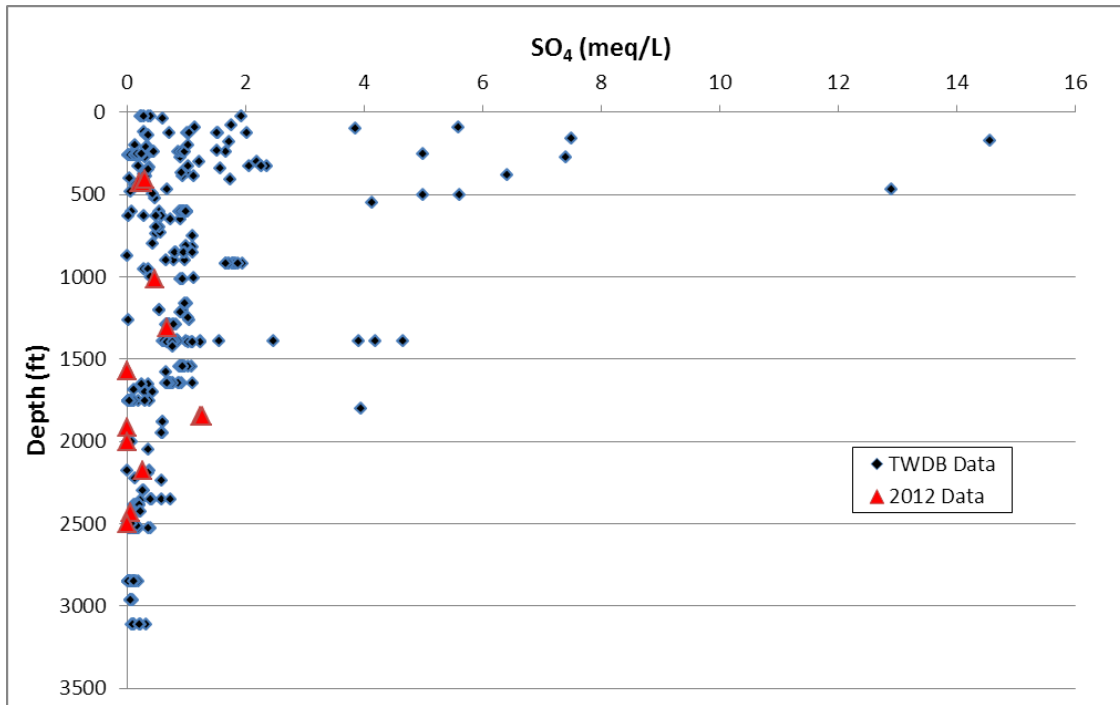


Figure 7-194. Depth measured from land surface in feet (ft) versus sulfate (SO<sub>4</sub>) measured in milliequivalents per liter (meq/L), Carrizo Sand Formation of the Carrizo-Wilcox Aquifer, Gonzales Transect, Groundwater Management Area 13.

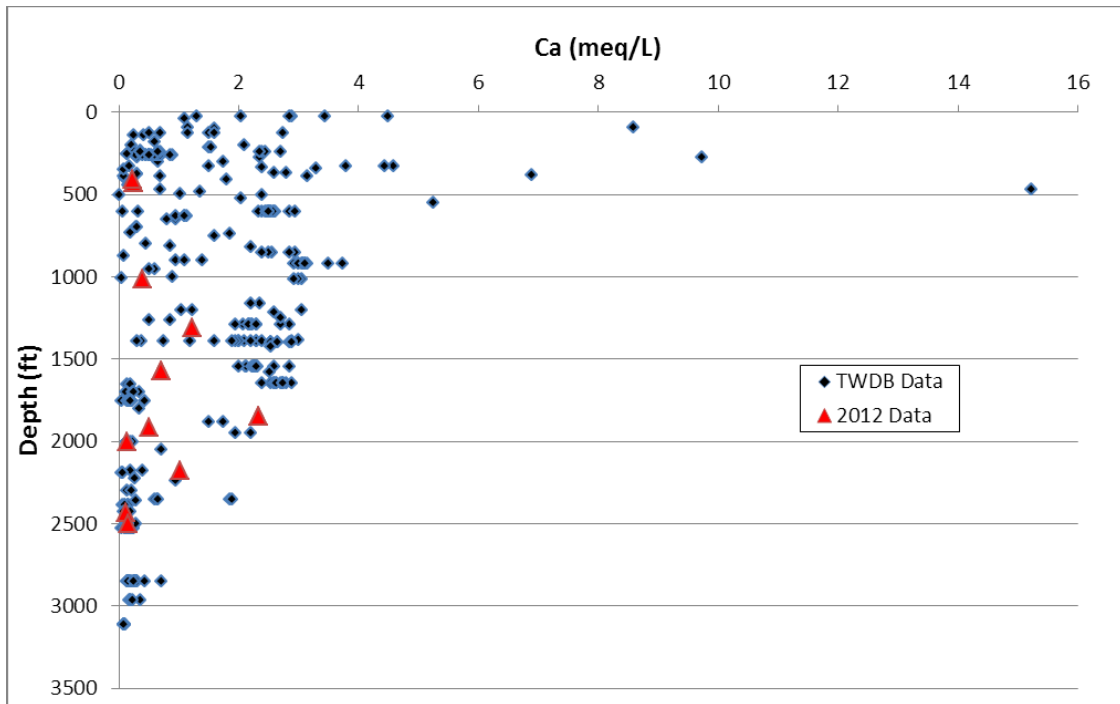


Figure 7-195. Depth measured from land surface in feet (ft) versus calcium (Ca) measured in milliequivalents per liter (meq/L), Carrizo Sand Formation of the Carrizo-Wilcox Aquifer, Gonzales Transect, Groundwater Management Area 13.

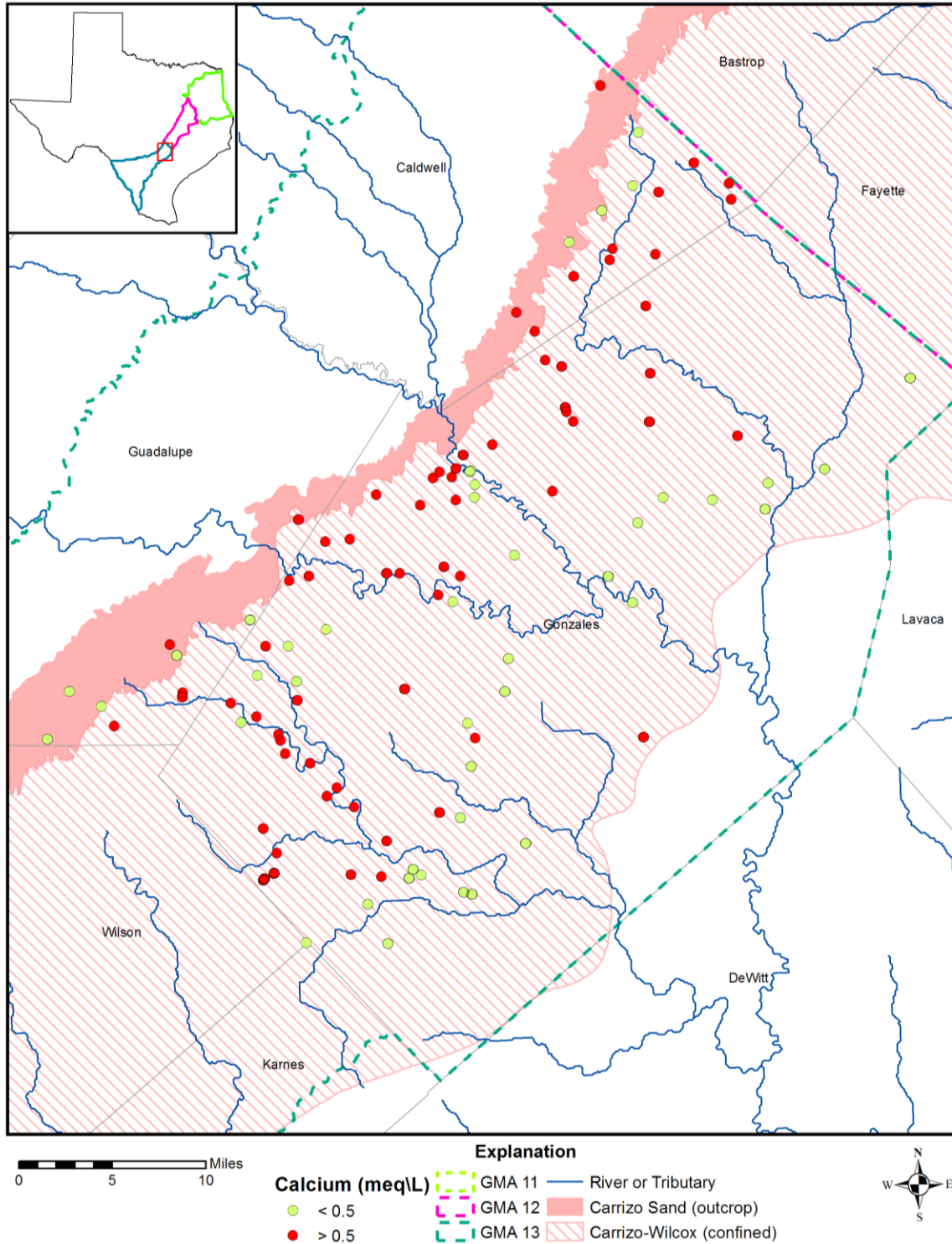


Figure 7-196. Calcium concentrations measured in milliequivalents per liter (meq/L) in the Carrizo Sand Formation of the Carrizo-Wilcox Aquifer, Gonzales Transect, Groundwater Management Area (GMA) 13.

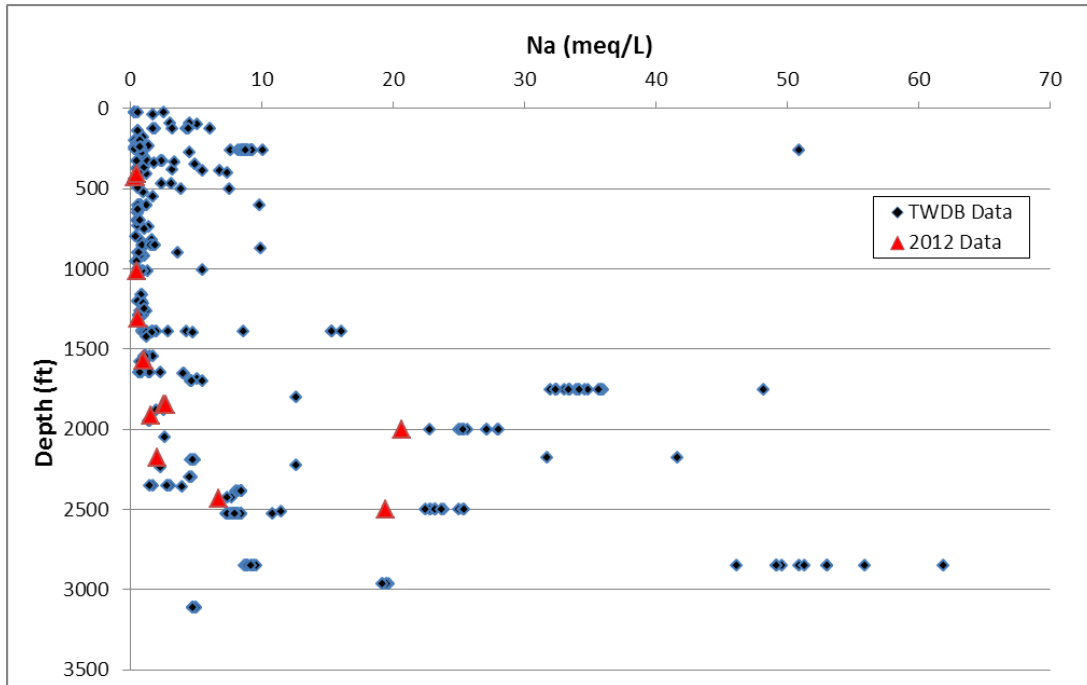


Figure 7-197. Depth measured from land surface in feet (ft) versus sodium (Na) measured in milliequivalents per liter (meq/L), Carrizo Sand Formation of the Carrizo-Wilcox Aquifer, Gonzales Transect, Groundwater Management Area 13.

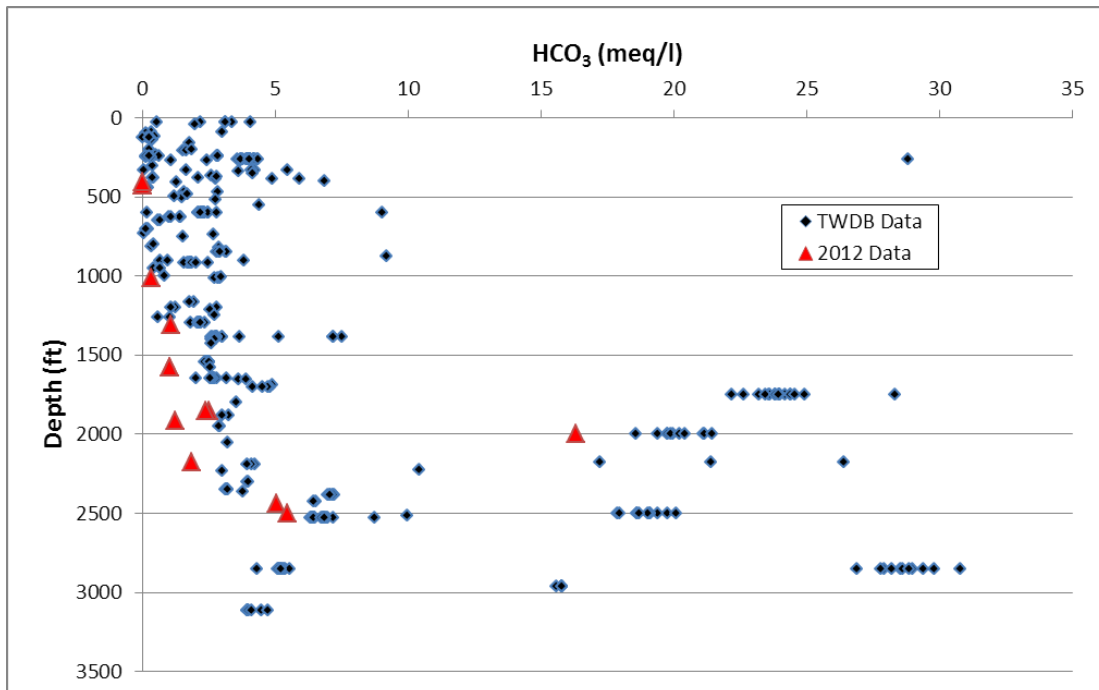
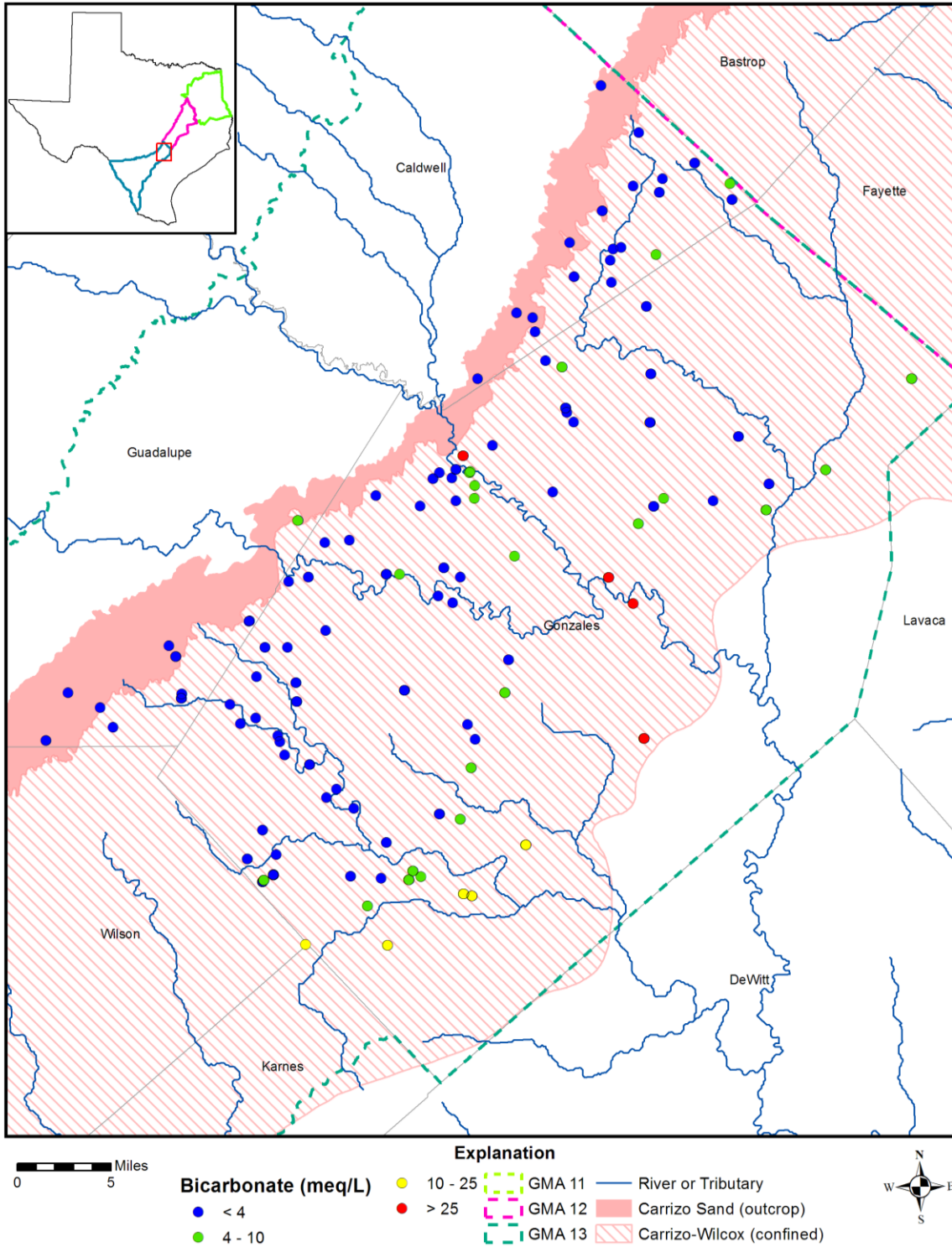


Figure 7-198. Depth measured from land surface in feet (ft) versus bicarbonate ( $\text{HCO}_3$ ) measured in milliequivalents per liter (meq/L), Carrizo Sand Formation of the Carrizo-Wilcox Aquifer, Gonzales Transect, Groundwater Management Area 13.



**Figure 7-199. Bicarbonate ( $\text{HCO}_3$ ) concentrations measured in milliequivalents per liter (meq/L) in the Carrizo Sand Formation of the Carrizo-Wilcox Aquifer, Gonzales Transect, Groundwater Management Area (GMA) 13.**

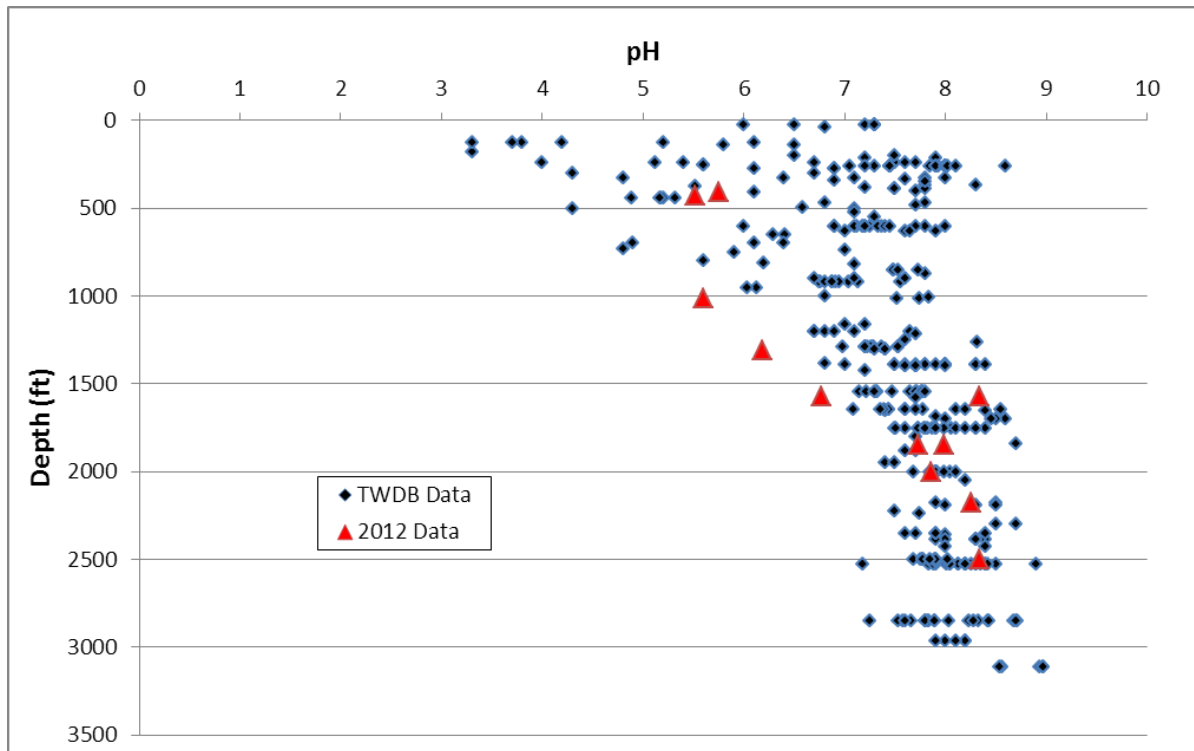


Figure 7-200. Depth measured from land surface in feet (ft) versus pH, Carrizo Sand Formation of the Carrizo-Wilcox Aquifer, Gonzales Transect, Groundwater Management Area 13.

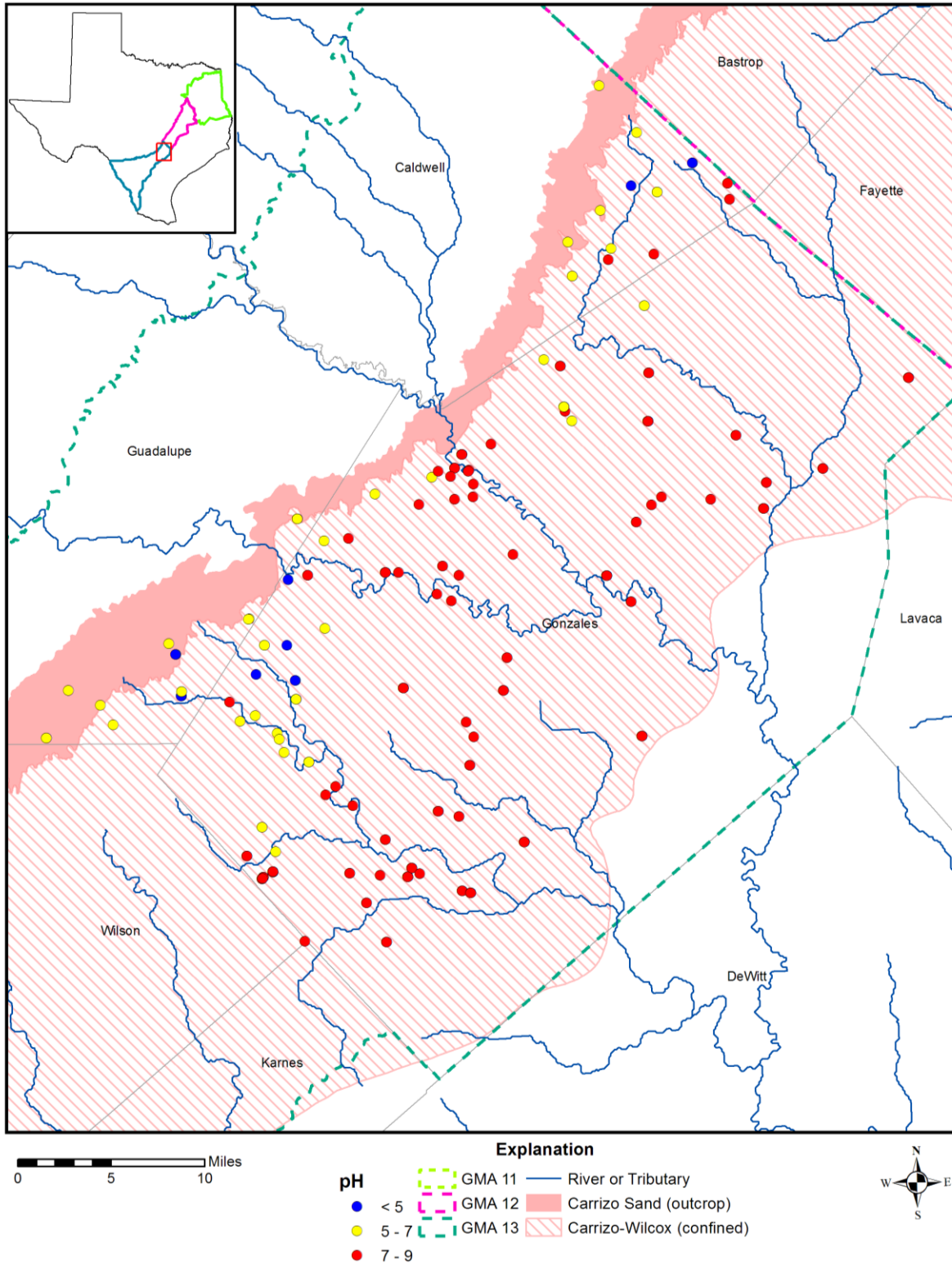
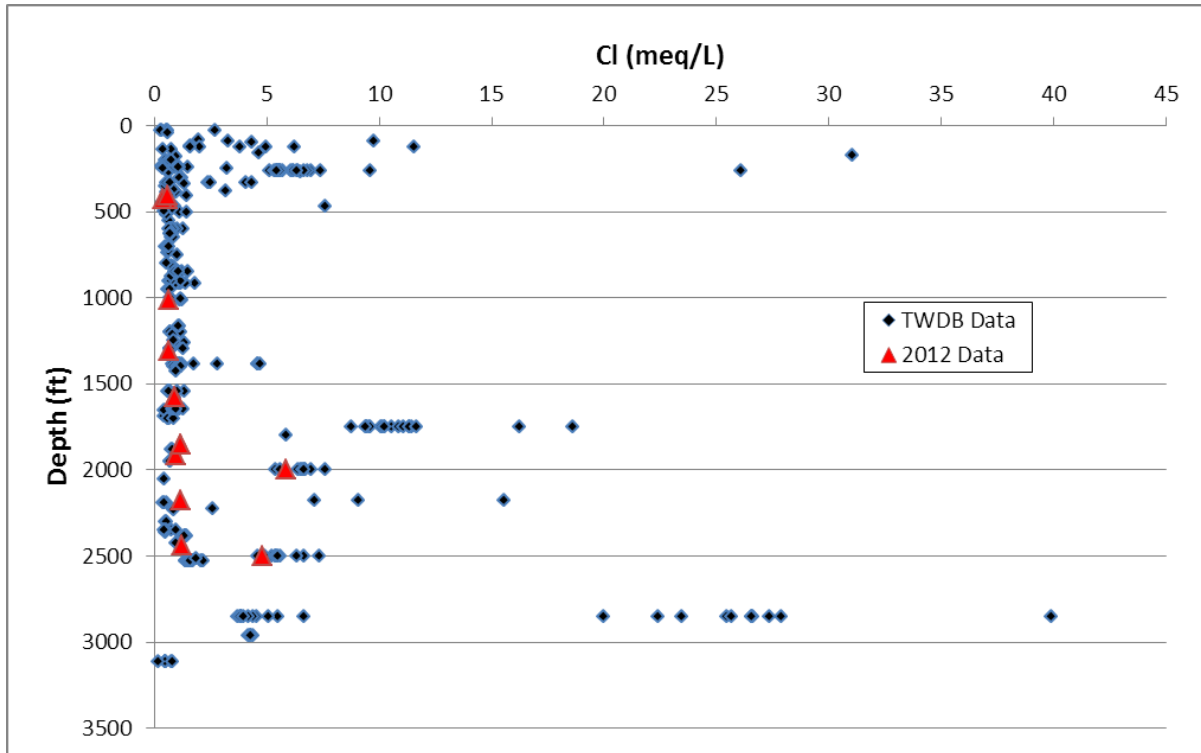
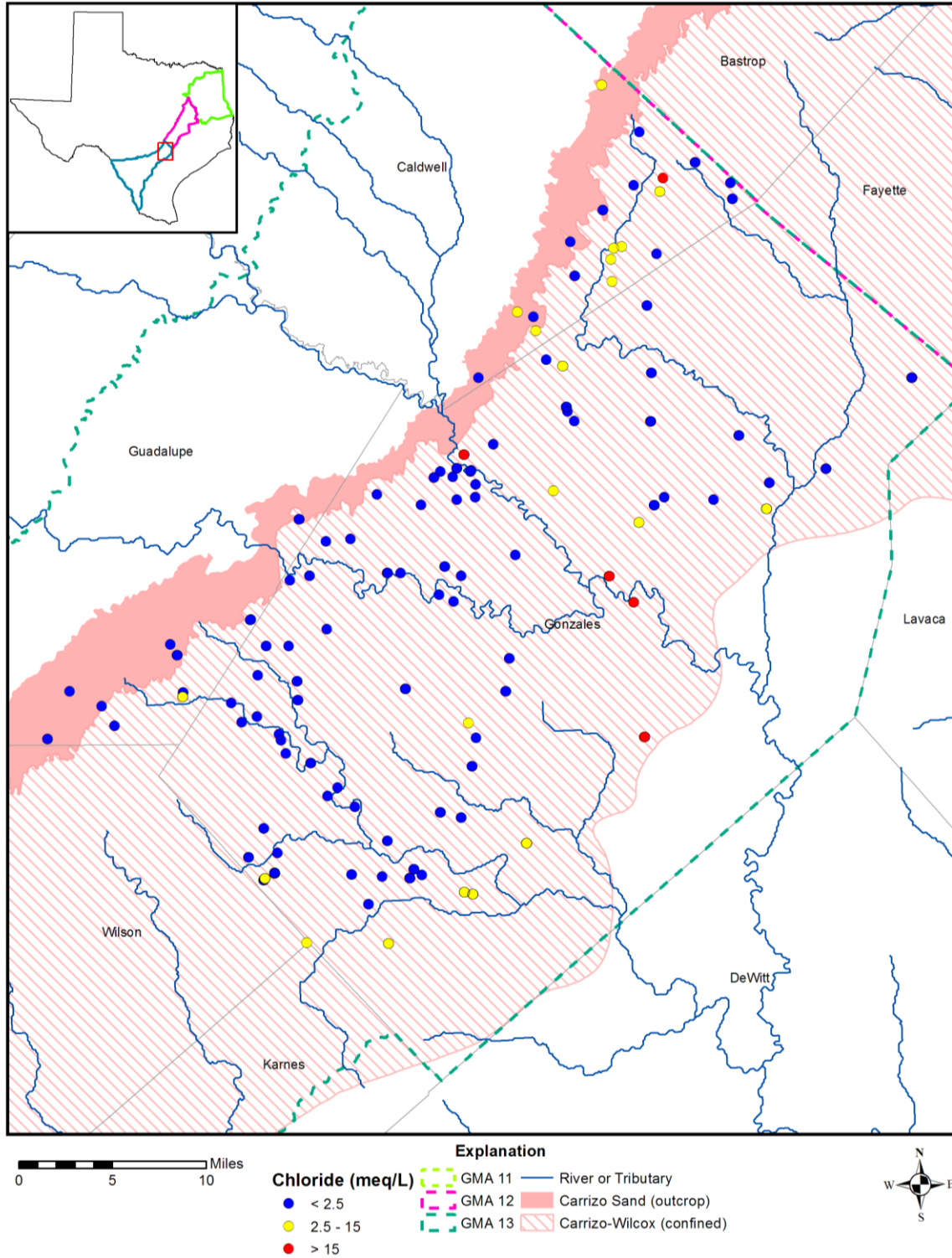


Figure 7-201. pH in the Carrizo Sand Formation of the Carrizo-Wilcox Aquifer, Gonzales Transect, Groundwater Management Area (GMA) 13.



**Figure 7-202.** Depth measured from land surface versus chloride (Cl) measured in milliequivalents per liter (meq/L), Carrizo Sand Formation of the Carrizo-Wilcox Aquifer, Gonzales Transect, Groundwater Management Area 13.



**Figure 7-203. Chloride (Cl) concentrations measured in milliequivalents per liter (meq/L) in the Carrizo Sand Formation of the Carrizo-Wilcox Aquifer, Gonzales Transect, Groundwater Management Area 13.**

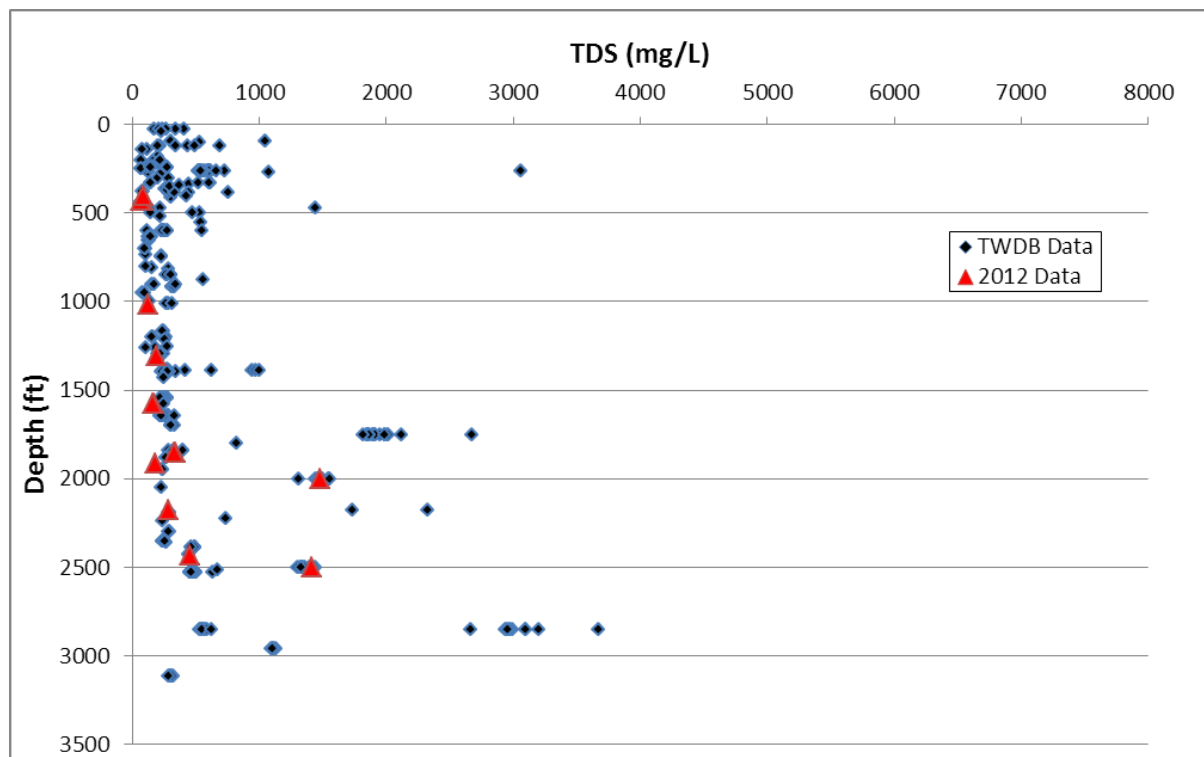


**Figure 7-204.** Depth measured from land surface in feet (ft) versus total dissolved solids (TDS) measured in parts per million (ppm), Carrizo Sand Formation of the Carrizo-Wilcox Aquifer, Gonzales Transect, Groundwater Management Area 13.

### Queen City Aquifer

The Queen City Aquifer is a minor aquifer in Gonzales County. The outcrop strikes from southwest to northeast across the county and dips to depths of about 800 feet along the southeast downdip side of the aquifer (Figure 7-205). Total width of the aquifer is about 10 miles wide. There is a limited amount of water level data and water chemistry data for the aquifer. The water level data (Figure 7-206) indicates groundwater flow from the outcrop into the confined section.

#### Piper Diagram

The cation triangle for the Piper diagram (Figure 7-207) shows a general trend of a mixed cation to a sodium-dominated water type. The deeper waters appear to be more sodium-rich. The plot of anion percent in the anion triangle shows a bicarbonate-sulfate mixed composition. Most of the water chemistry analyses are in the outcrop rather than downdip.

#### Bicarbonate versus Sodium Plot

A plot of bicarbonate versus sodium (Figure 7-208) shows general increases of sodium and bicarbonate, but not a 1:1 ratio. There is an additional source of sodium for these waters.

#### Sodium versus Calcium Plot

A plot of sodium versus calcium (Figure 7-209) shows an inverse correlation between sodium and calcium.

### Chloride versus Sodium Plot

The plot of chloride versus sodium (Figure 7-210) shows two possible trends where sodium-chloride is being added to the waters: 1) increasing sodium and chloride starting at low concentrations of both and 2) increasing chloride at high sodium values.

### Discussion

The cation triangle for the Queen City Aquifer Piper diagram shows mixed (calcium-magnesium-sodium) cation type water to sodium dominated water (Figure 7-207). The anion triangle shows a mixed anion chemistry that does not migrate to the bicarbonate corner. The water chemistry in the Queen City Aquifer is different than in the underlying Carrizo Sand Formation portion of the Carrizo-Wilcox Aquifer. The Queen City Aquifer waters do not show the evolution to sodium-bicarbonate water as observed in the Carrizo Sand Formation. Most of the Queen City Aquifer waters are in the outcrop.

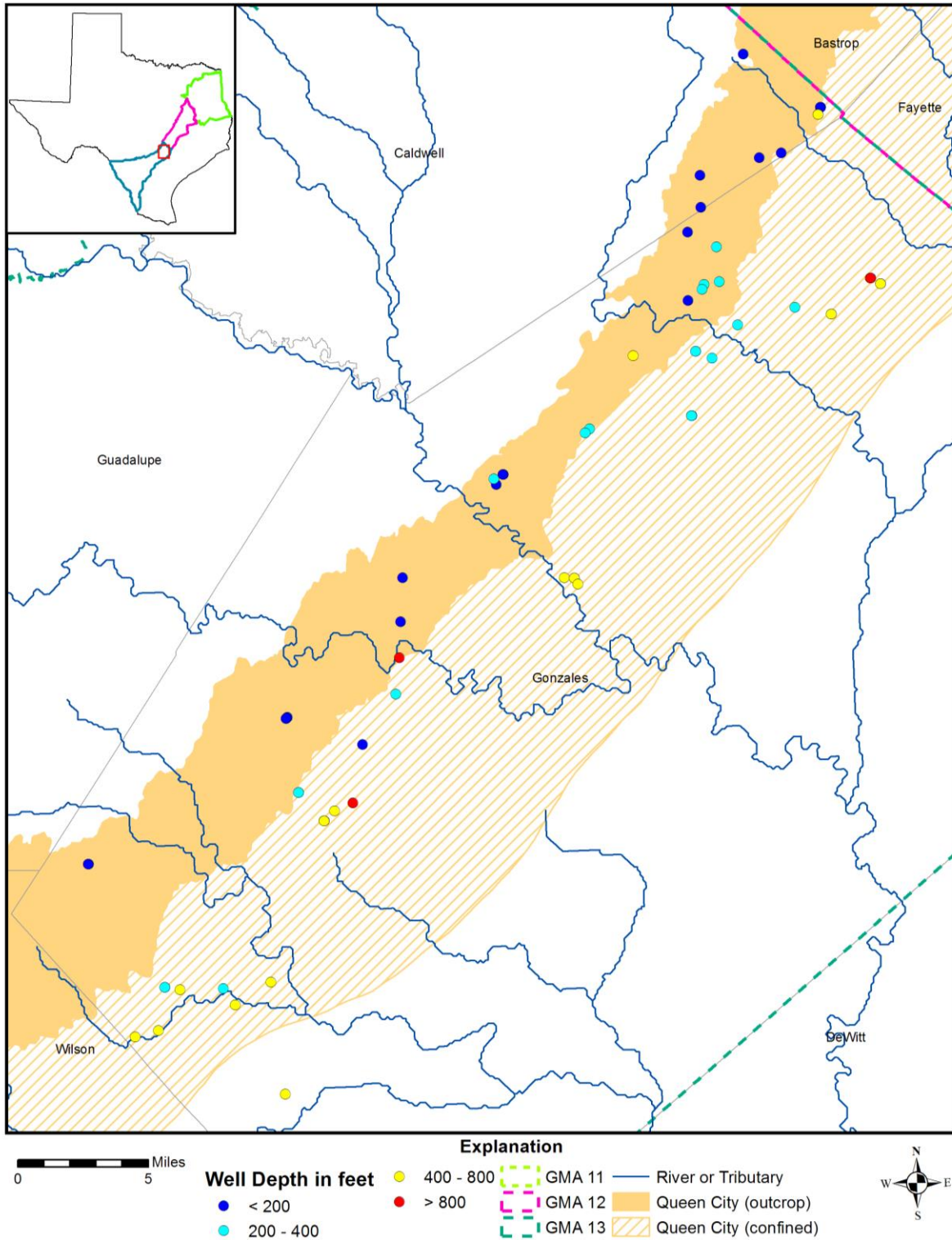
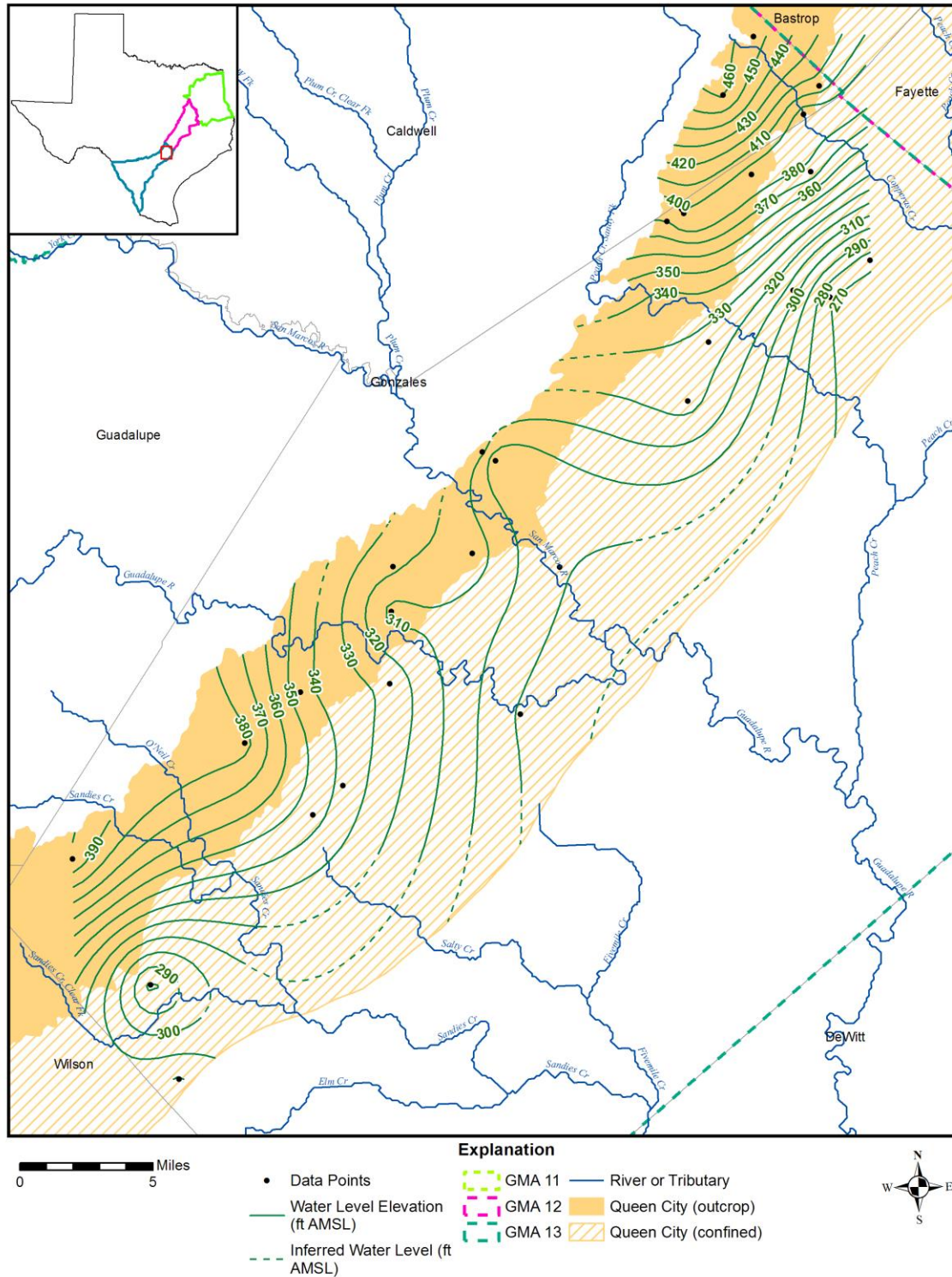


Figure 7-205. Well depths measured from land surface in feet in the Queen City Aquifer, Gonzales Transect, Groundwater Management Area (GMA) 13.



**Figure 7-206. Potentiometric surface of the Queen City Aquifer using water level data measured in feet above mean sea level (ft AMSL) from 1980 to 2011 in the Gonzales Transect, Groundwater Management Area 13.**

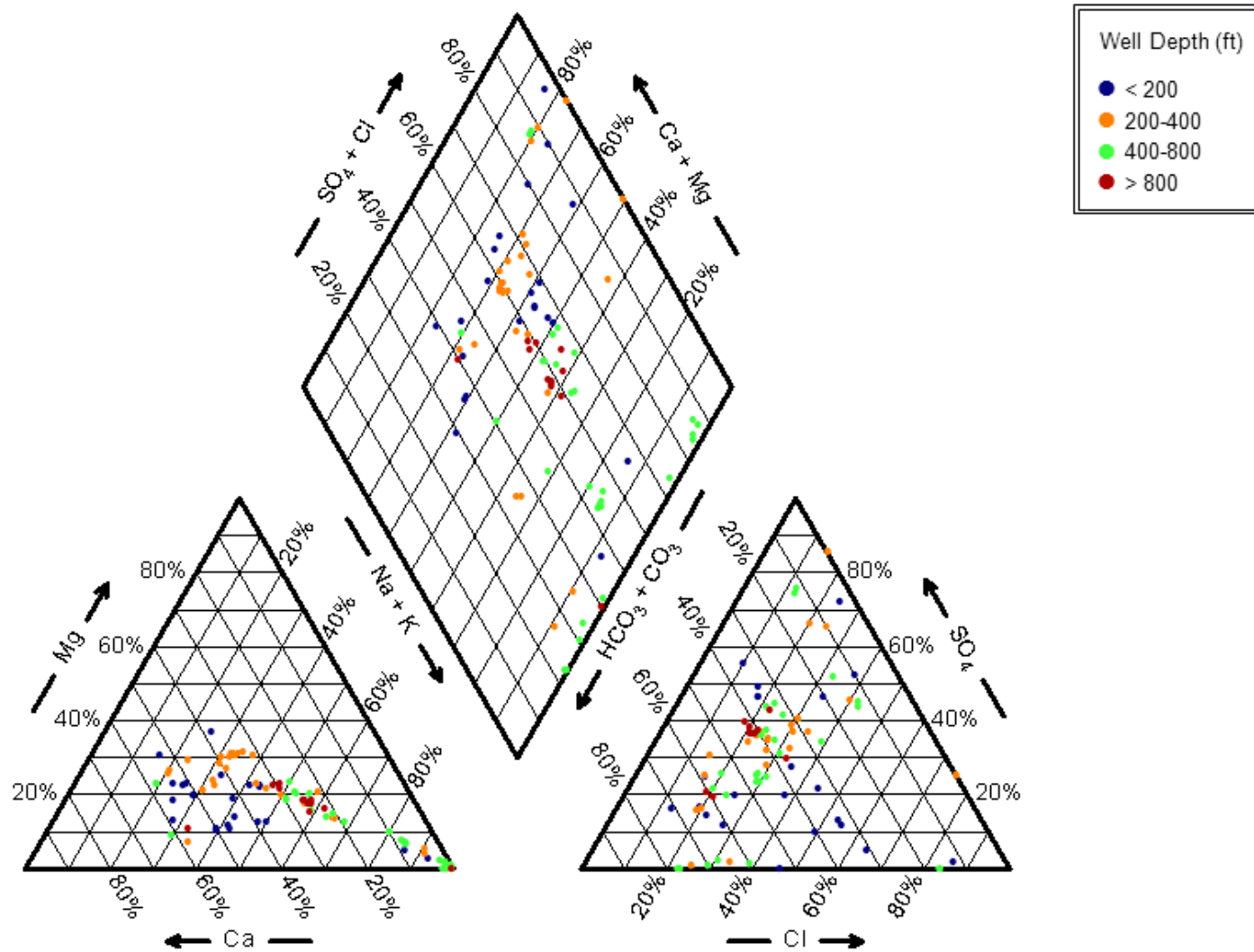


Figure 7-207. Piper diagram showing chemistry of the Queen City Aquifer wells in the Gonzales Transect by well depth measured from land surface in feet (ft).

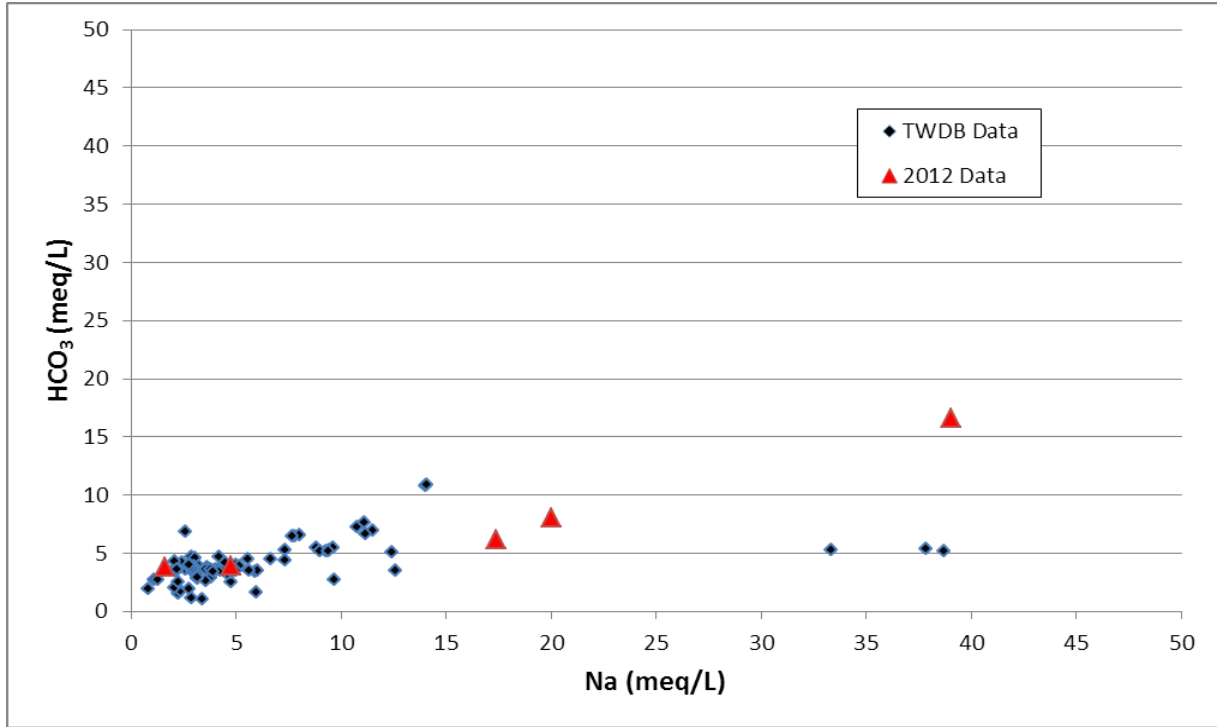


Figure 7-208. Bicarbonate (HCO<sub>3</sub>) versus sodium (Na) measured in milliequivalents per liter (meq/L), Queen City Aquifer, Gonzales Transect, Groundwater Management Area 13.

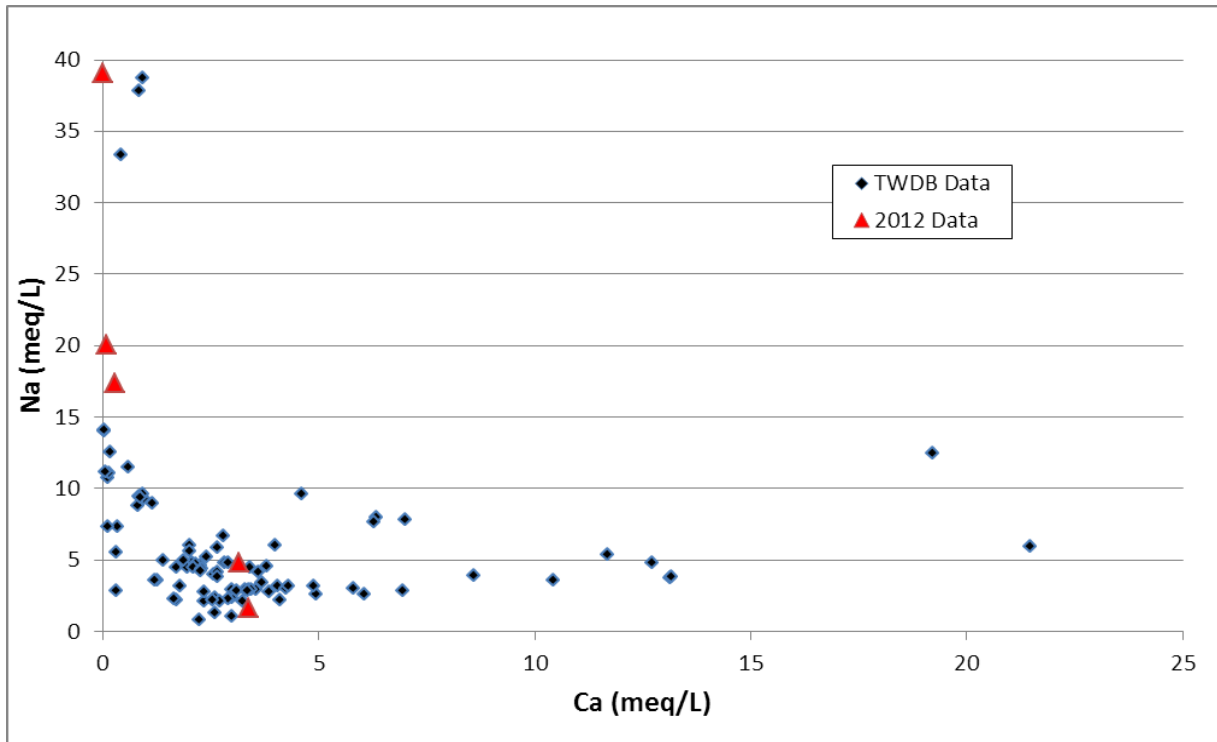


Figure 7-209. Sodium (Na) versus calcium (Ca) measured in milliequivalents per liter (meq/L), Queen City Aquifer, Gonzales Transect, Groundwater Management Area 13.

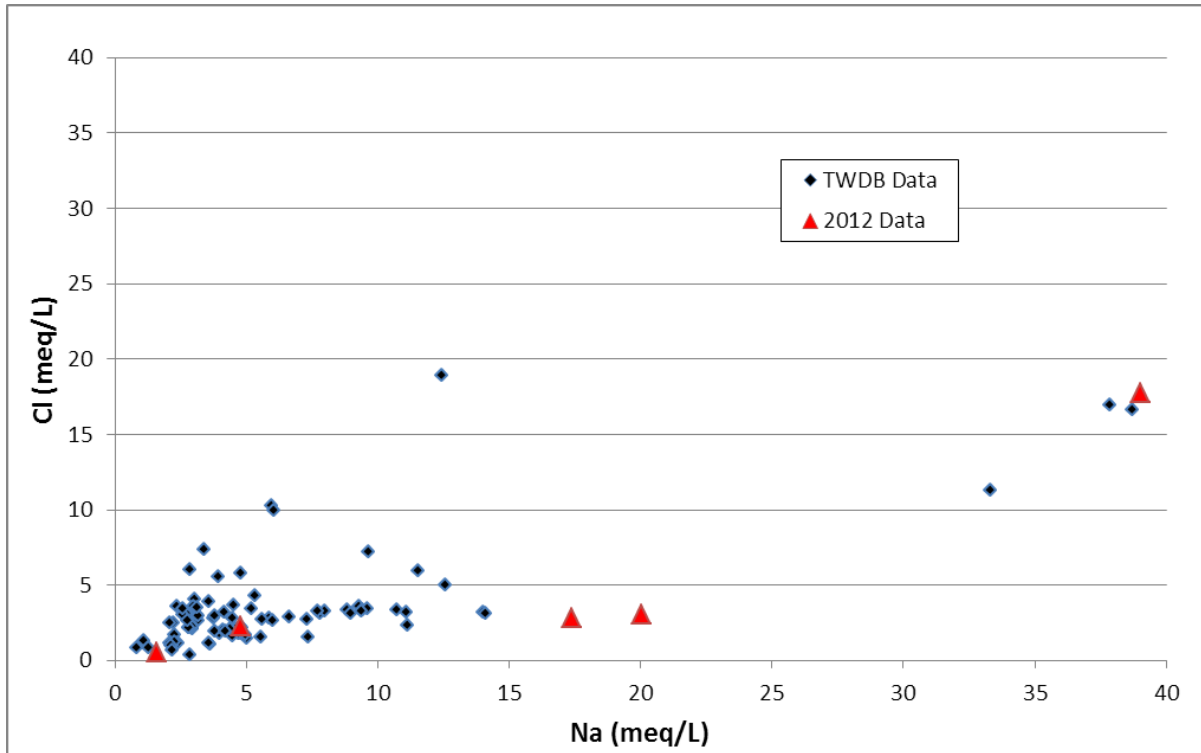


Figure 7-210. Chloride (Cl) versus sodium (Na) measured in milliequivalents per liter (meq/L), Queen City Aquifer, Gonzales Transect, Groundwater Management Area 13.

### Sparta Aquifer

The Sparta Aquifer is a minor aquifer which extends southwest to northeast across Gonzales County. There is a very limited amount of data available for this aquifer. Well depths are less than 200 feet in the outcrop to greater than 600 feet downdip (Figure 7-211). The potentiometric surface (Figure 7-212) shows dips from elevations of about 300 feet in the outcrop to elevations of about 250 feet in the confined section.

#### Piper Diagram

The cation triangle for the Sparta Aquifer Piper diagram (Figure 7-213) shows a mixed cation composition trending to a sodium dominated composition. The anion triangle shows a mixed chloride-sulfate water. There are no sodium-bicarbonate waters in the samples analyzed in the Sparta Aquifer in Gonzales County.

#### Bicarbonate versus Sodium Plot

A plot of bicarbonate versus sodium (Figure 7-214) shows a small linear increase in sodium with bicarbonate but sodium is increasing much more rapidly than the bicarbonate. This is not a sodium-bicarbonate water.

#### Sodium versus Calcium Plot

A plot of sodium versus calcium (Figure 7-215) shows an inverse correlation.

### Chloride versus Sodium Plot

The plot of chloride versus sodium (Figure 7-216) shows a direct correlation between the concentrations of sodium and chloride.

### Depth versus Chloride Plot

The plot of depth versus chloride (Figure 7-217) shows high chloride concentrations at depth.

### Depth versus Total Dissolved Solids Plot

The plot of depth versus total dissolved solids (Figure 7-218) in the Sparta Aquifer is generally high. Highest (2,000 to 11,000 milligrams per liter) values are seen at depths greater than 400 feet.

### Discussion

The cation triangle of the Sparta Aquifer Piper diagram shows a mixed cation type water to sodium dominated water (Figure 7-213). The anion triangle shows a chloride-sulfate type water. The higher chloride concentrations are deeper in the aquifer. The water chemistry shows a strong sodium-chloride influence and not a sodium-bicarbonate type of water that occurs in the underlying Carrizo Sand Formation portion of the Carrizo-Wilcox Aquifer. Most of the aquifer contains high total dissolved solids waters. Leakage from deeper aquifers such as the Carrizo Sand Formation is not apparent.

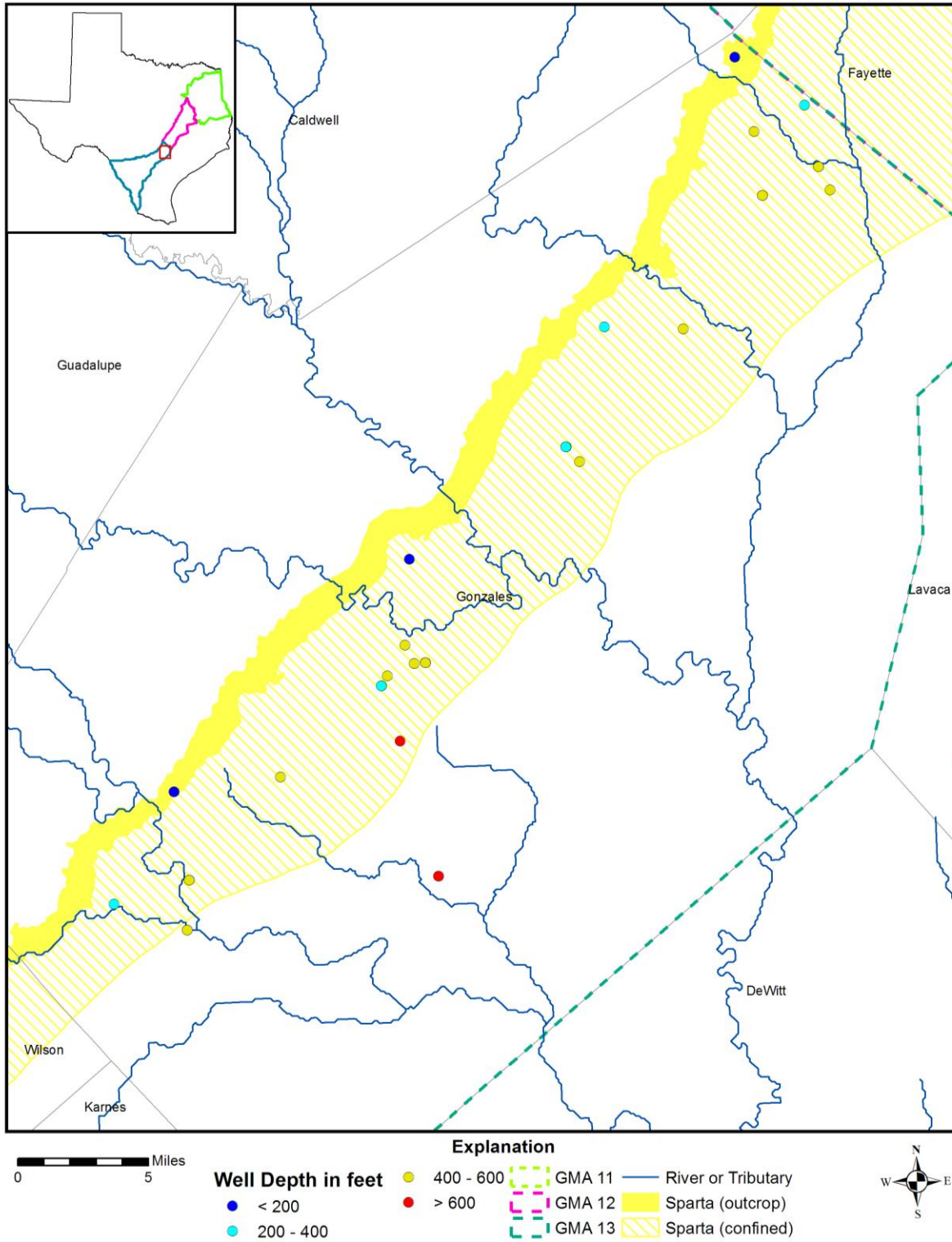


Figure 7-211. Well depths measured from land surface in feet in the Sparta Aquifer, Gonzales Transect, Groundwater Management Area (GMA) 13.

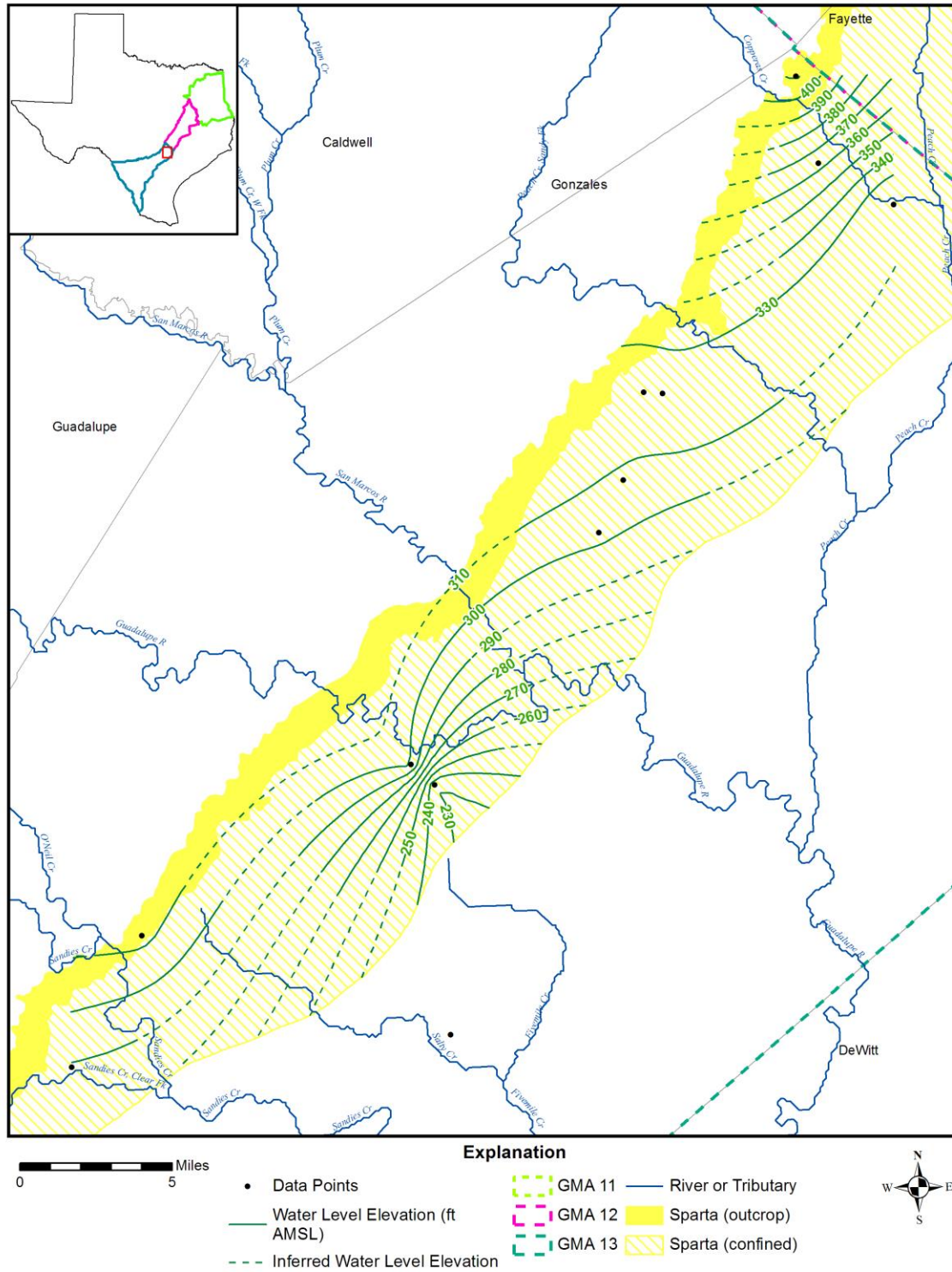


Figure 7-212. Potentiometric surface of the Sparta Aquifer using water level data measured in feet above mean sea level (ft AMSL) from 1980 to 2011 in the Gonzales Transect, Groundwater Management Area (GMA) 13.

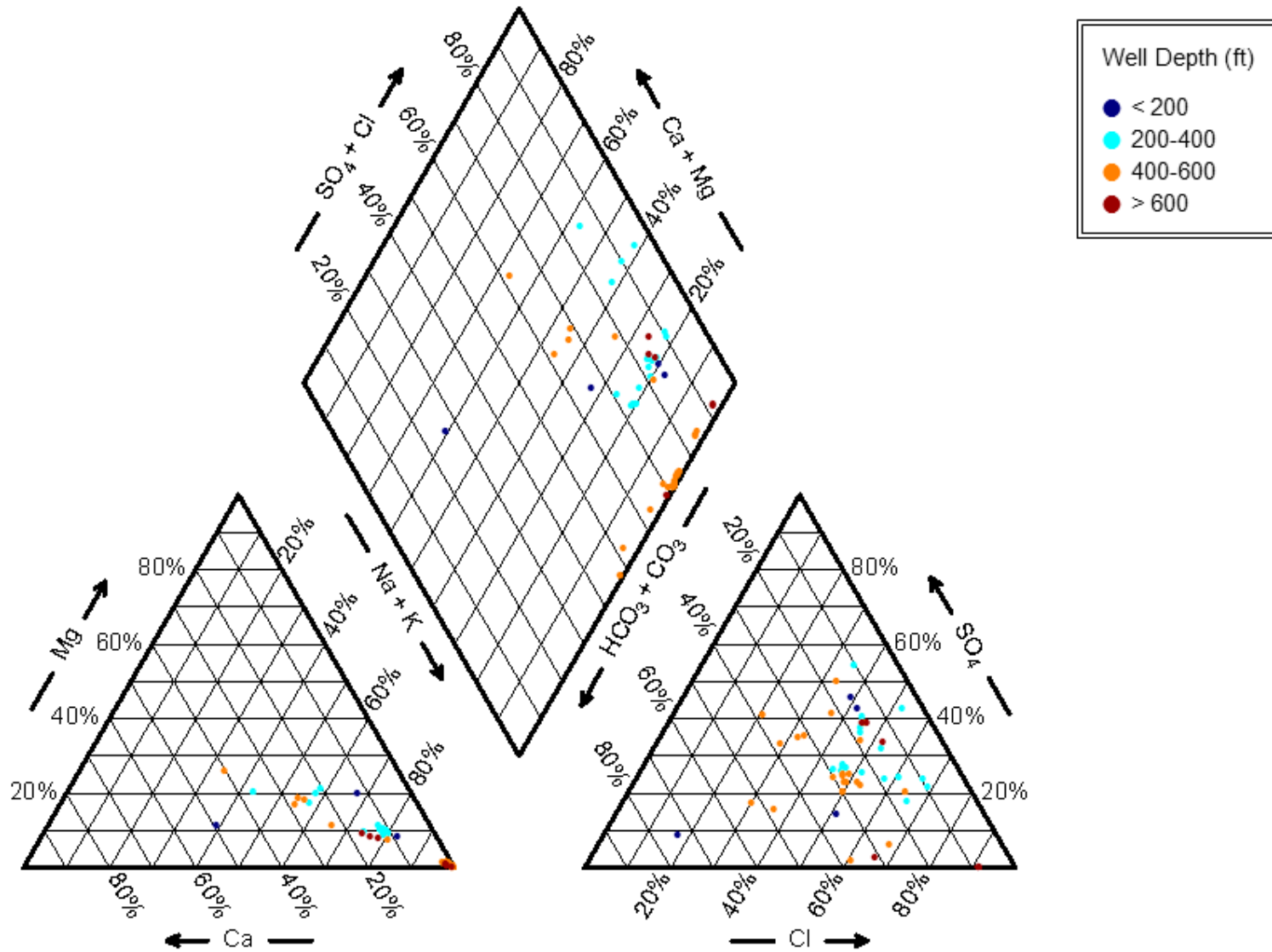


Figure 7-213. Piper diagram showing chemistry of the Sparta Aquifer wells in the Gonzales Transect by well depth measured from land surface in feet (ft).

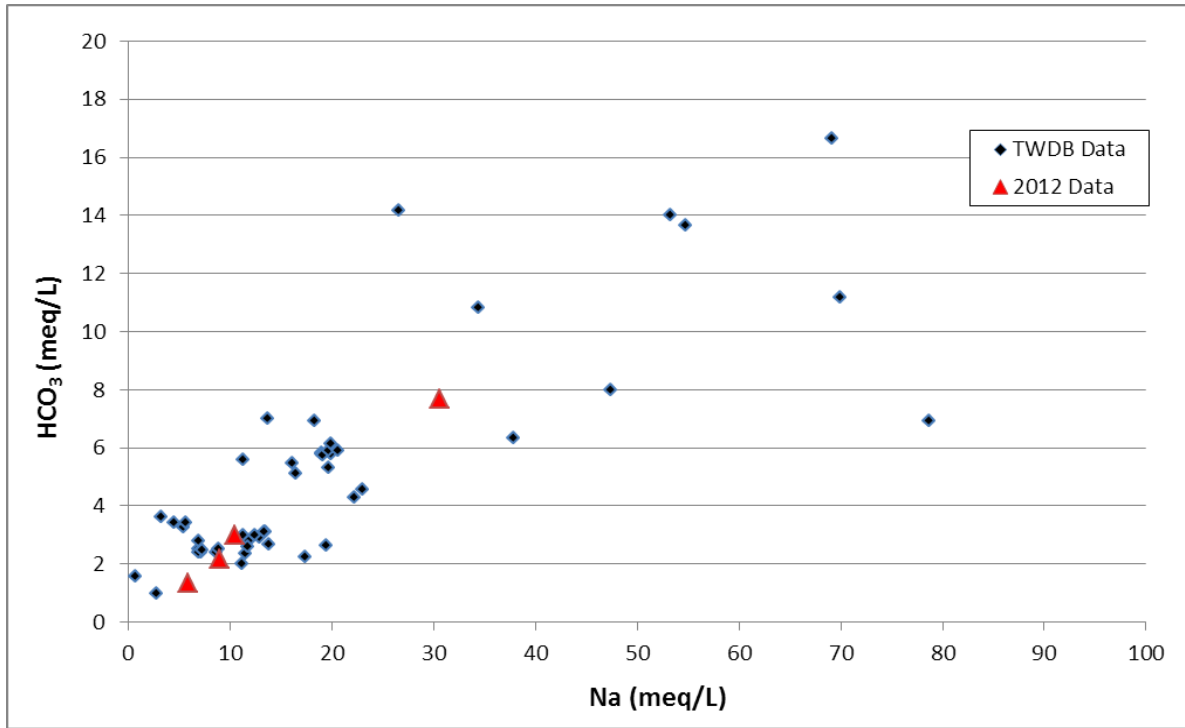


Figure 7-214. Bicarbonate ( $\text{HCO}_3$ ) versus sodium (Na) measured in milliequivalents per liter (meq/L), Sparta Aquifer, Gonzales Transect, Groundwater Management Area 13.

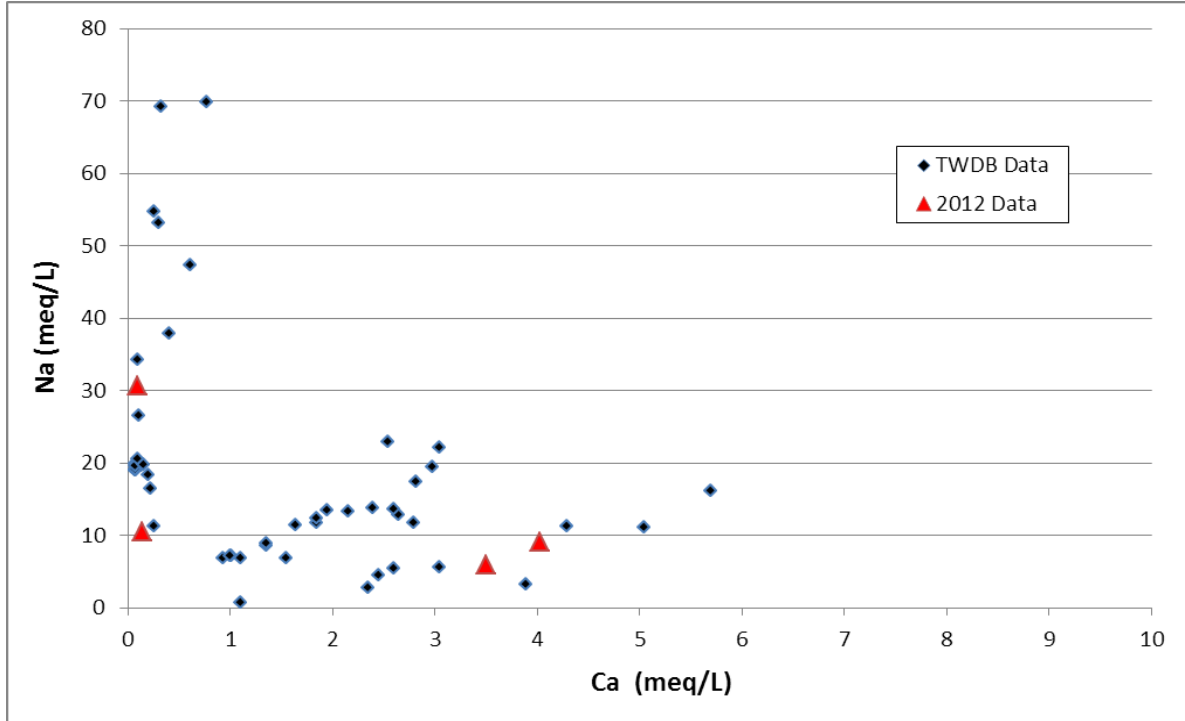


Figure 7-215. Sodium (Na) versus calcium (Ca) measured in milliequivalents per liter (meq/L), Sparta Aquifer, Gonzales Transect, Groundwater Management Area 13.

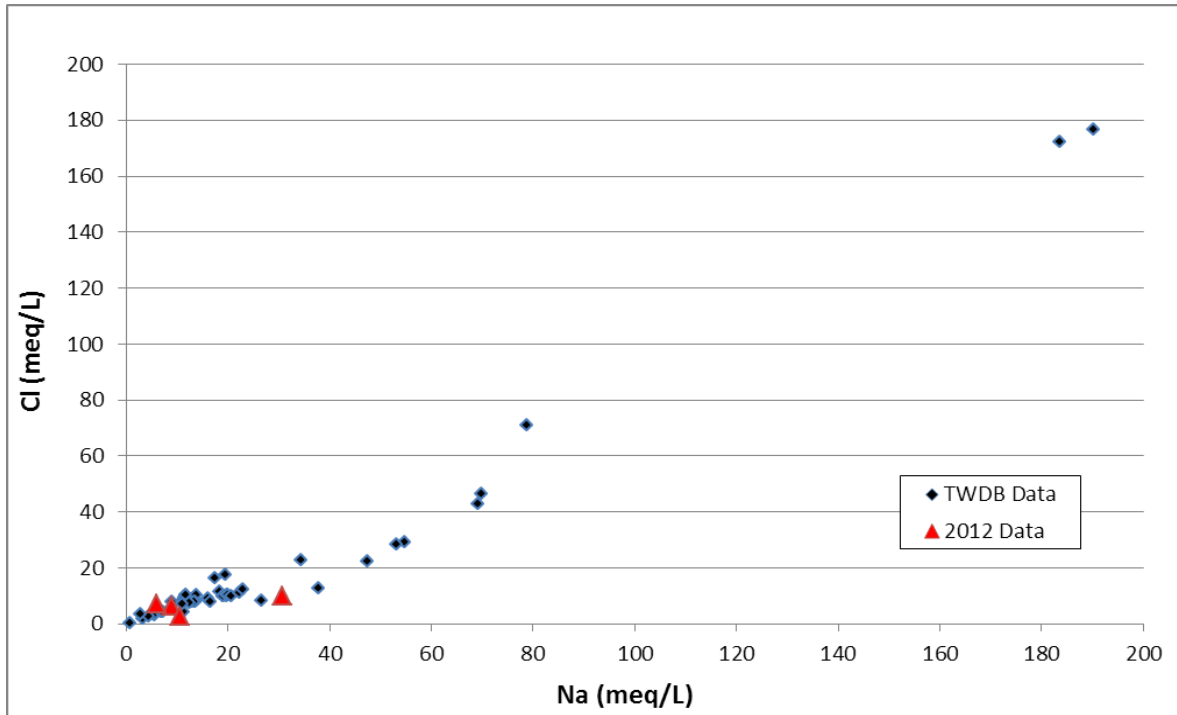


Figure 7-216. Chloride (Cl) versus sodium (Na) measured in milliequivalents per liter (meq/L), Sparta Aquifer, Gonzales Transect, Groundwater Management Area 13.

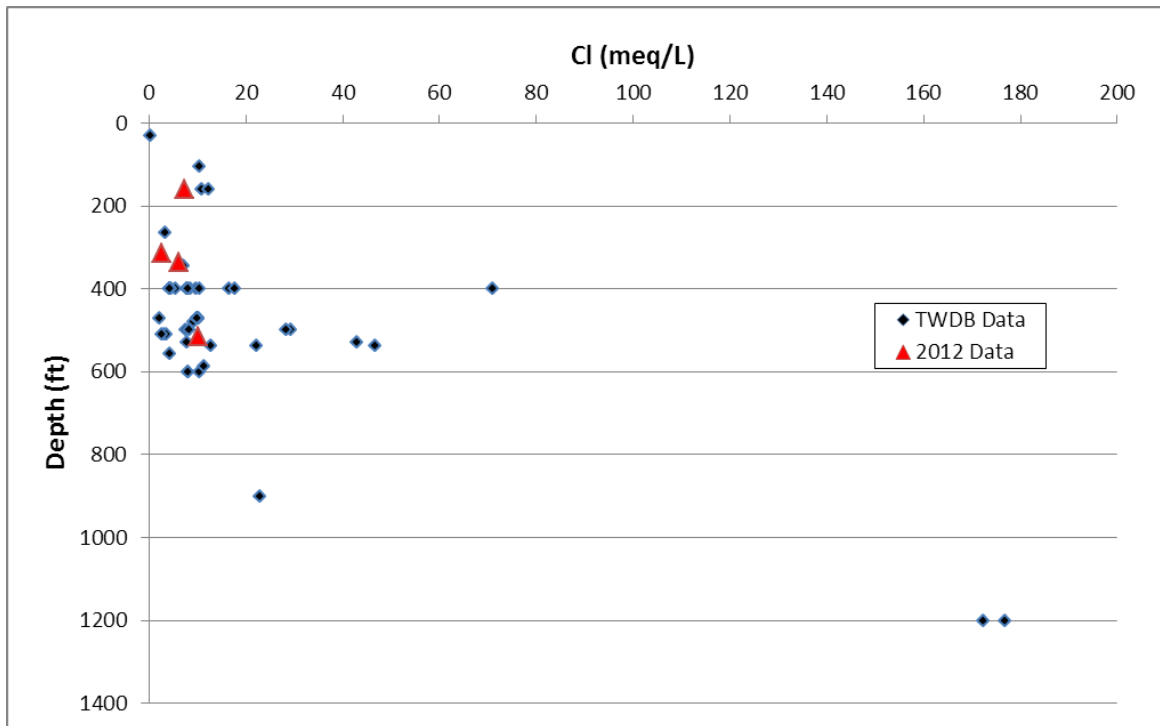
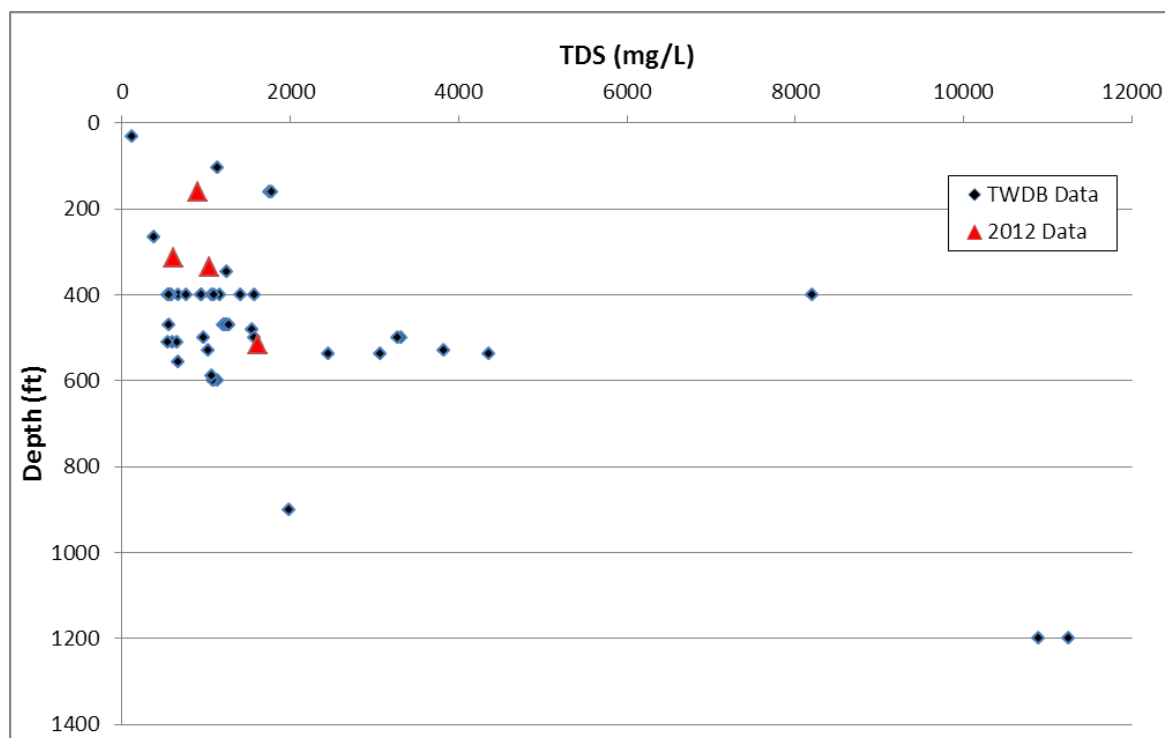


Figure 7-217. Depth measured from land surface in feet (ft) versus chloride (Cl) measured in milliequivalents per liter (meq/L), Sparta Aquifer, Gonzales Transect, Groundwater Management Area 13.



**Figure 7-218.** Depth measured from land surface in feet (ft) versus total dissolved solids (TDS) measured in parts per million (ppm), Sparta Aquifer, Gonzales Transect, Groundwater Management Area 13.

### Yegua-Jackson Aquifer

The Yegua-Jackson Aquifer in Gonzales County has a limited number of wells and therefore limited water level data and water chemistry data. Nearly all wells in the TWDB database are located in the outcrop. Most of the wells are shallower than 300 feet (Figure 7-219). Water levels in the aquifer range from about 300 feet to 215 feet (Figure 7-220). No wells were sampled in the Yegua-Jackson Aquifer in 2012.

#### Piper Diagram

The cation triangle for the Yegua-Jackson Aquifer Piper diagram (Figure 7-221) shows a calcium-sodium trend with low magnesium. The anion triangle shows a mixed composition dominated by chloride and sulfate. There are no sodium-bicarbonate water observed in the Yegua-Jackson Aquifer.

#### Bicarbonate versus Sodium Plot

No correlation is observed (Figure 7-222).

#### Chloride versus Sodium Plot

The plot of chloride versus sodium (Figure 7-223) shows a general increase in sodium to chloride.

### Depth versus Total Dissolved Solids Plot

The plot of depth versus total dissolved solids (Figure 7-224) shows total dissolved solids values ranging from about 500 parts per million to about 4,500 parts per million. This aquifer is primarily brackish.

### Discussion

The cation triangle for the Yegua-Jackson Aquifer Piper diagram (Figure 7-221) shows calcium-sodium type water at shallower depths and predominant sodium type water at greater depths. The anion triangle shows mixed chloride-sulfate water with minimal bicarbonate. Most of the production from Yegua-Jackson Aquifer is from the outcrop and most wells contain brackish waters. The Yegua-Jackson Aquifer does not contain sodium-bicarbonate waters. There is no chemical evidence for upward leakage from an underlying freshwater aquifer such as the Carrizo-Wilcox Aquifer.

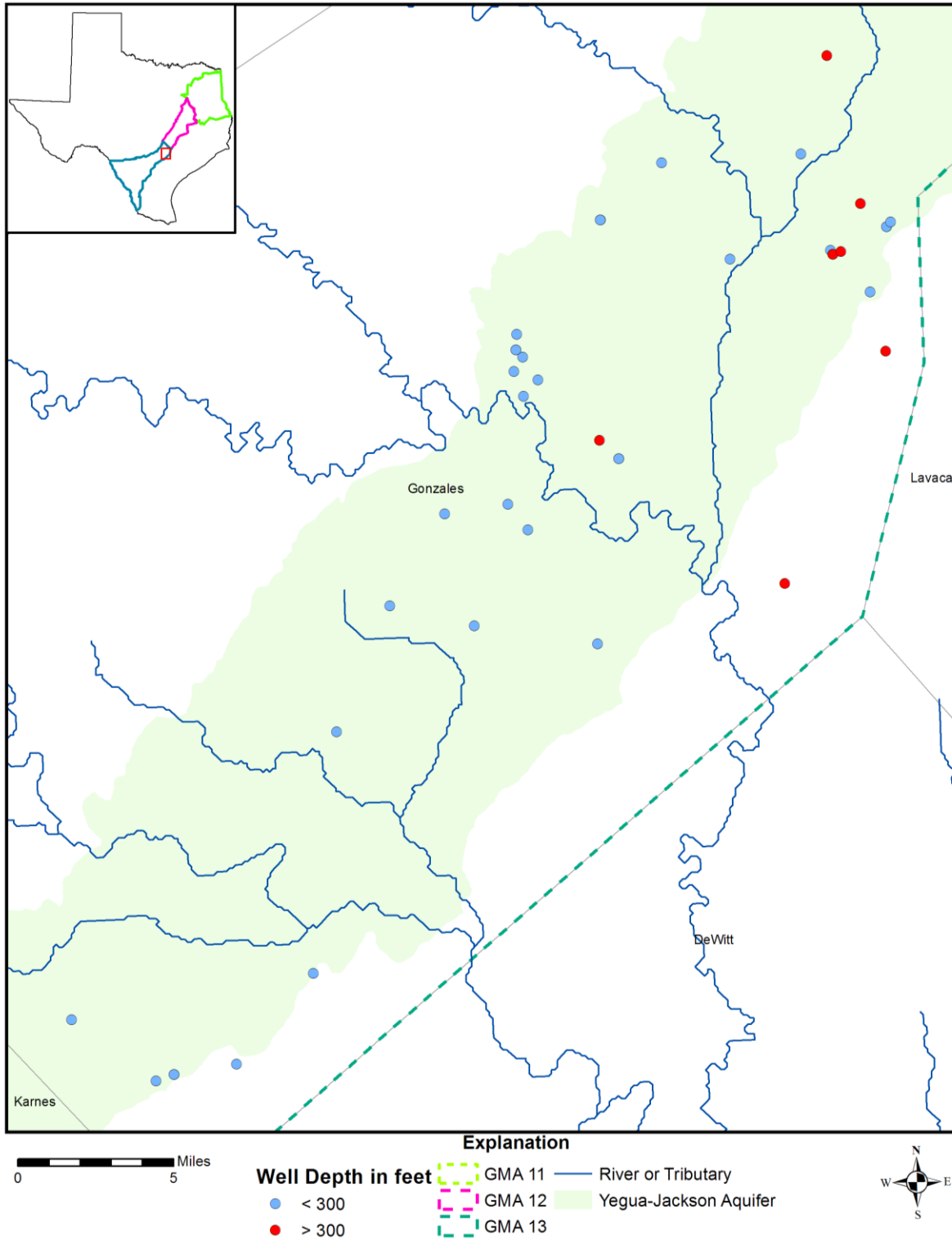
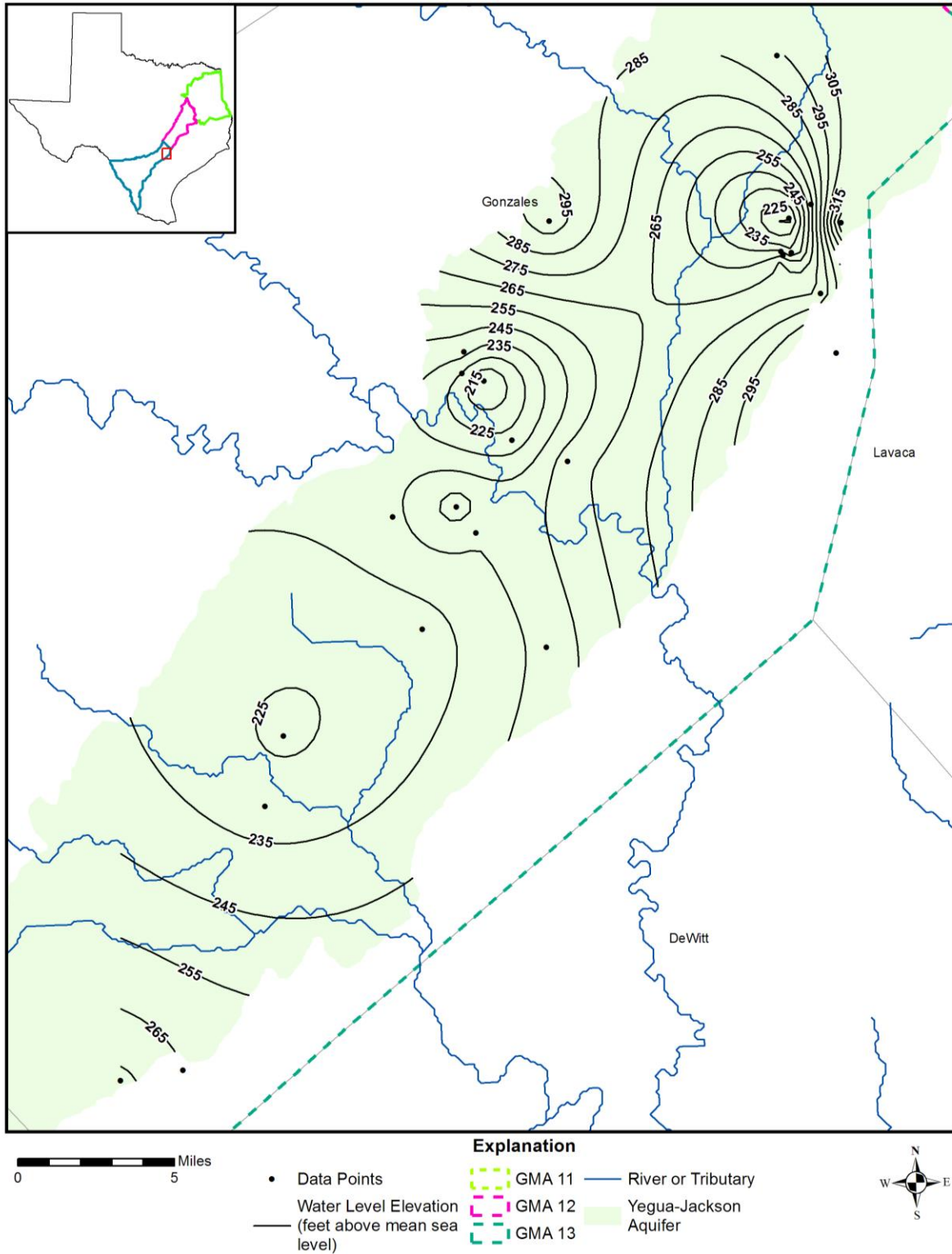


Figure 7-219. Well depths measured from land surface in feet in the Yegua-Jackson Aquifer, Gonzales Transect, Groundwater Management Area (GMA) 13.



**Figure 7-220. Potentiometric surface of the Yegua-Jackson Aquifer using water level data measured in feet above mean sea level (ft AMSL) from 1921 to 2002 in the Gonzales Transect, Groundwater Management Area (GMA) 13.**

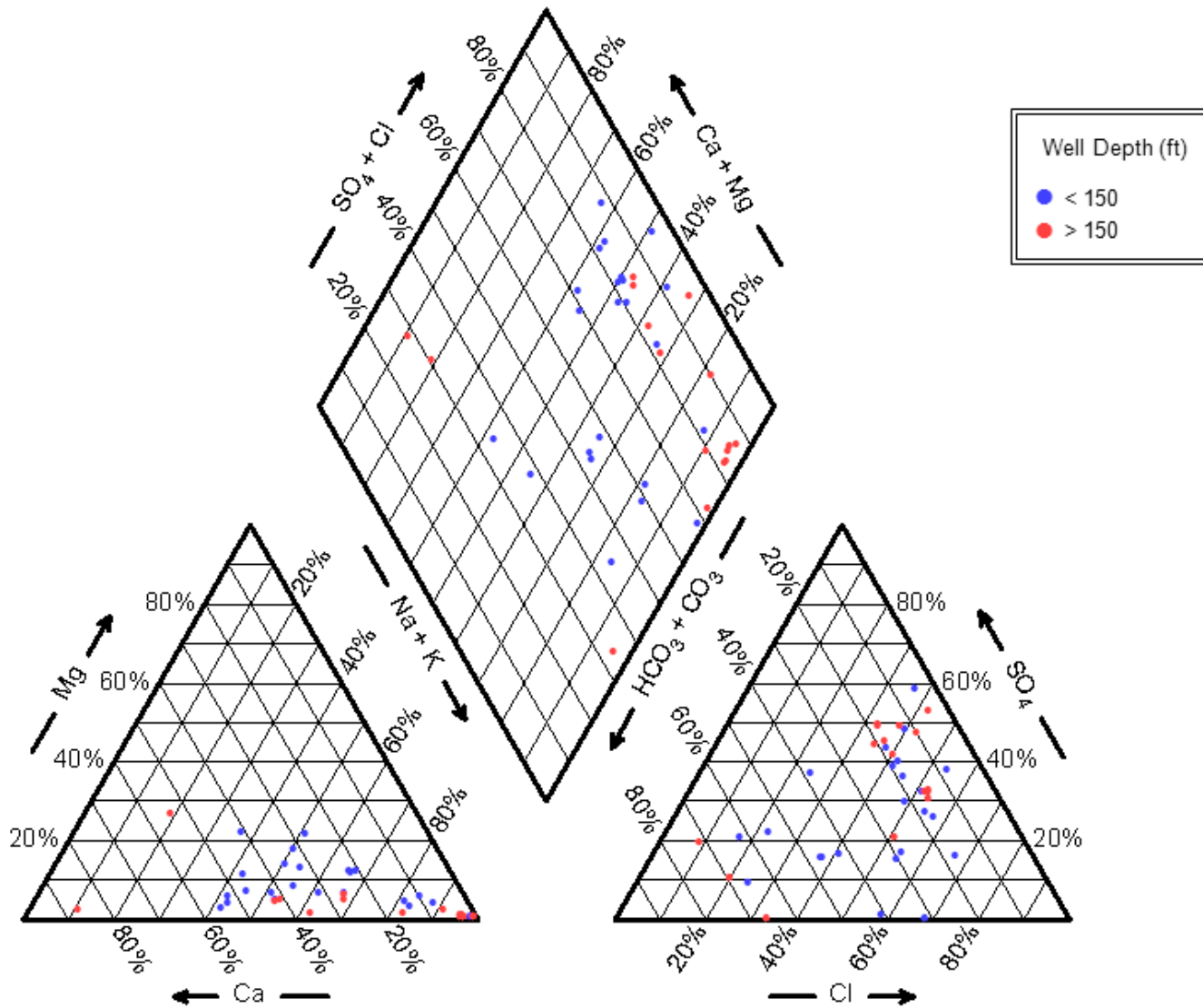


Figure 7-221. Piper diagram showing chemistry of the Yegua-Jackson Aquifer wells in the Gonzales Transect by well depth measured from land surface in feet (ft).

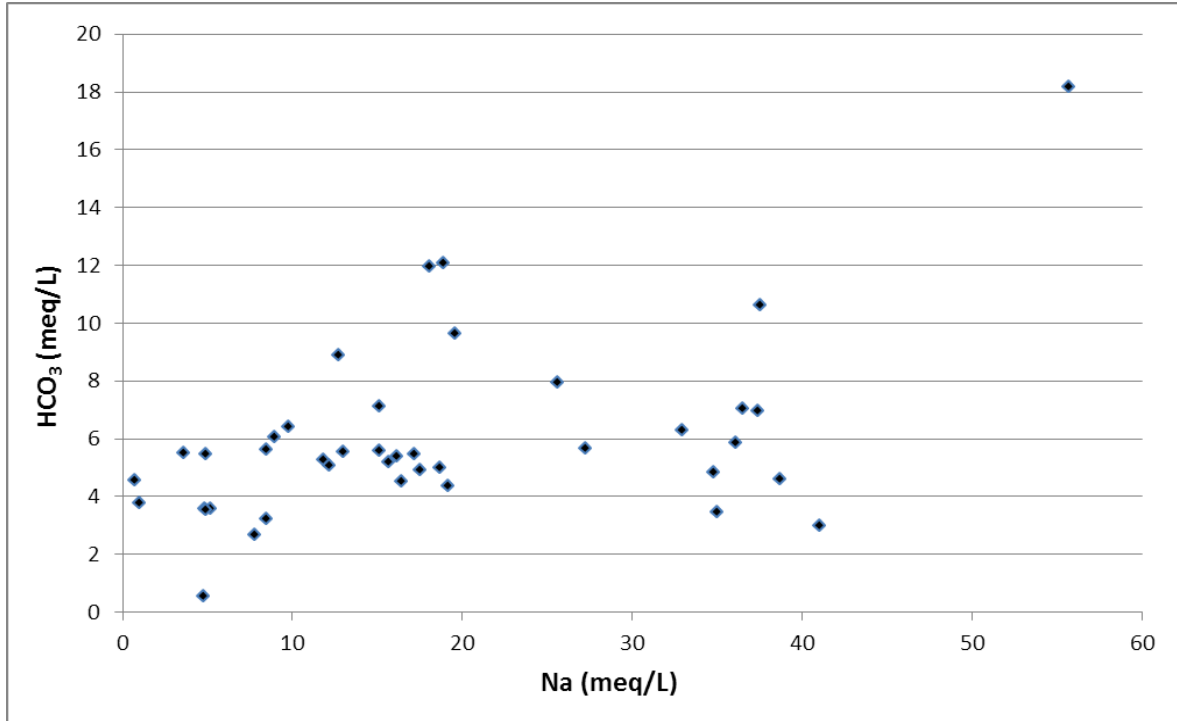


Figure 7-222. Bicarbonate (HCO<sub>3</sub><sup>-</sup>) versus sodium (Na) measured in milliequivalents per liter (meq/L), Yegua-Jackson Aquifer, Gonzales Transect, Groundwater Management Area 13.

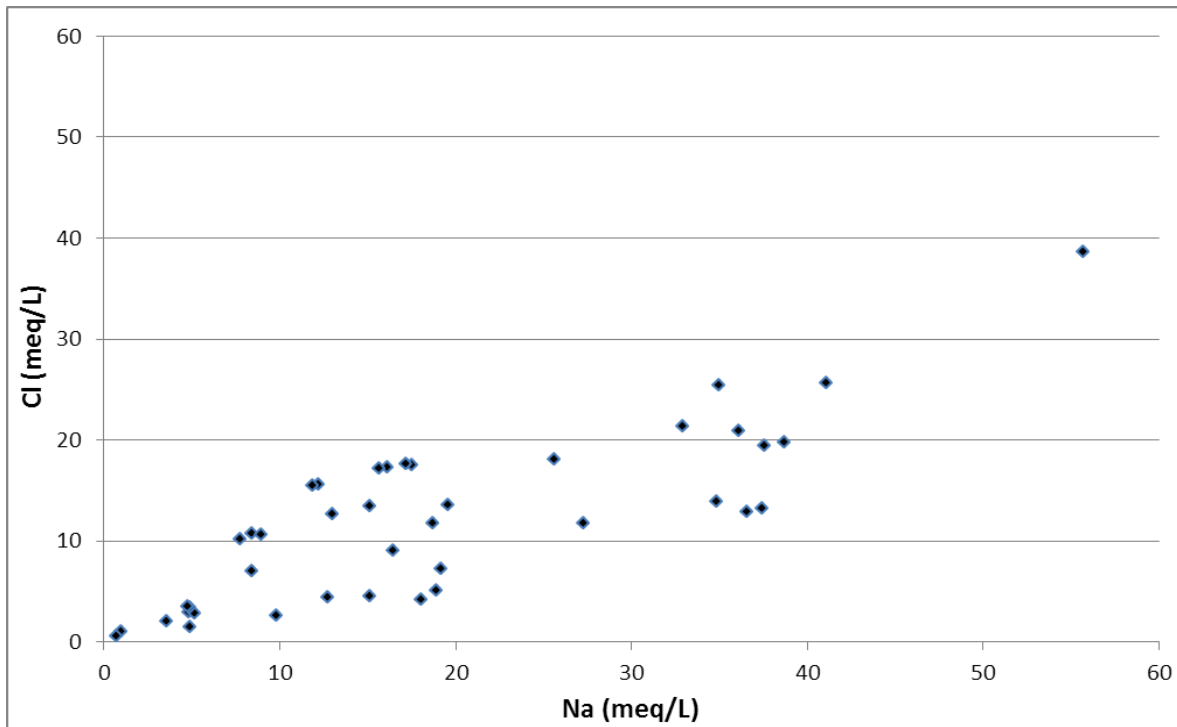
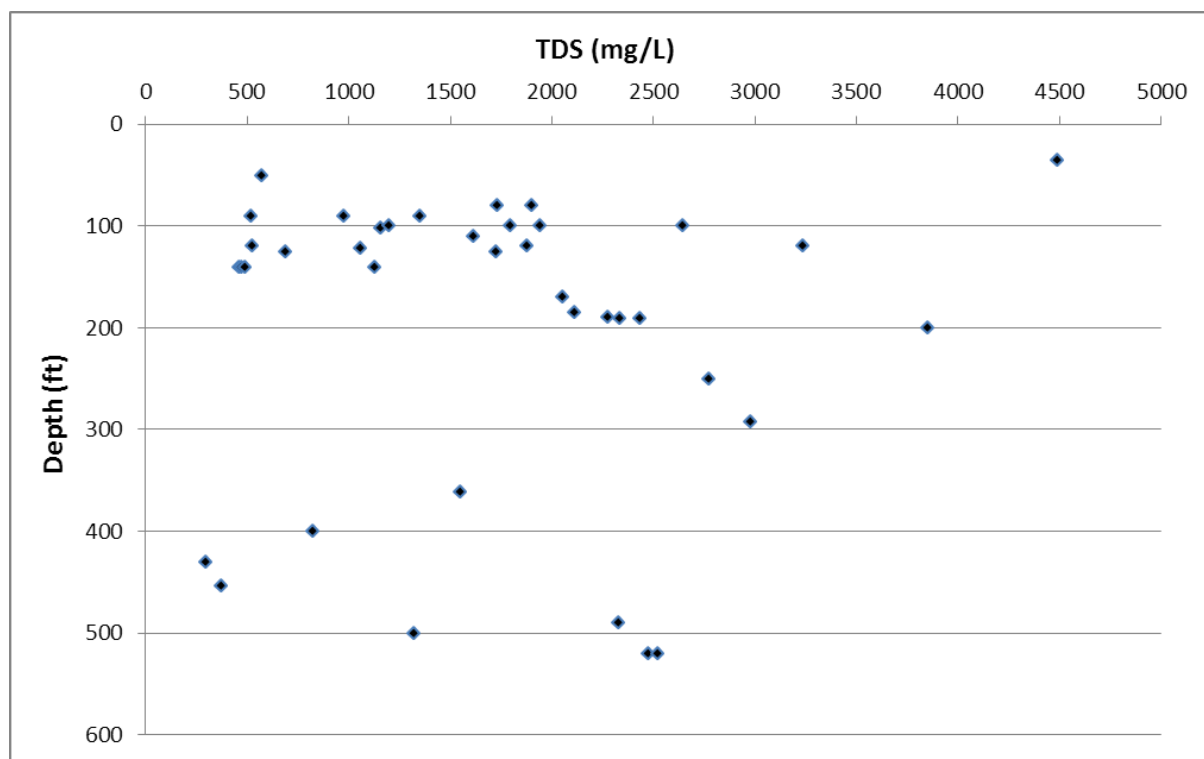


Figure 7-223. Chloride (Cl<sup>-</sup>) versus sodium (Na) measured in milliequivalents per liter (meq/L), Yegua-Jackson Aquifer, Gonzales Transect, Groundwater Management Area 13.



**Figure 7-224.** Depth measured from land surface in feet (ft) versus total dissolved solids (TDS) measured in parts per million (ppm), Yegua-Jackson Aquifer, Gonzales Transect, Groundwater Management Area 13.

### Well Nests

San Antonio Water System has constructed nests of wells at four locations in southern Gonzales County to monitor the impact of water levels in the Carrizo Sand Formation, Queen City and Sparta aquifers associated with the future production of the Carrizo Sand Formation groundwater from their Buckhorn well field (HDR, 2004). Nest location 1 does not include a well monitoring the Sparta Aquifer. Therefore this location was omitted from the sampling program because it represented a less complete vertical sampling of the aquifers in question than nest locations 2, 3, and 4. Nest locations 2, 3, and 4 all have individual wells monitoring the Sparta, Queen City and Carrizo Sand Formation aquifers. This presents an opportunity to evaluate and compare geochemical composition of groundwater in different aquifers at the same location. Samples were collected and analyzed from nine wells in nest locations 2, 3 and 4 for general chemistry and isotopes to determine if there were similarities in chemistry that might indicate upward cross-formational flow from the Carrizo Sand Formation into the Queen City and Sparta aquifers. The chemical data for these nested wells (in addition to the data for all the wells sampled along this transect) are in Table 7-4 and are identified as GUGZ-11 through GUGZ-19.

The nested data are plotted on four Piper diagrams. Figure 7-225 compiles all analyses from the three nests. Figure 7-226 is a Piper diagram for Nest 2. Figure 7-227 is a Piper diagram for Nest 3. Figure 7-228 is a Piper diagram for Nest 4. The locations of the well nests are shown on Figure 7-180. Figure 7-229 and Figure 7-230 plot the carbon-14 percent modern and  $\delta^{13}\text{C}$  respectively for the three nests for each formation.

The Piper diagrams all indicate that the water chemistry for Carrizo Sand Formation water, the Queen City Aquifer water and the Sparta Aquifer water are geochemically different from each other. The  $\delta^{13}\text{C}$  and carbon-14 data also indicate the waters in each aquifer are different from each other. There is no chemical evidence from these well nests of the Carrizo Sand Formation waters leaking into the Queen City Aquifer.

Evaluation of Hydrochemical and Isotopic Data in Groundwater Management Areas 11, 12 and 13

**Table 7-4. Chemical and isotopic results from samples collected in the Gonzales Transect during 2012.**

Sample Number	GUGZ-1	GUGZ-2	GUGZ-3	GUGZ-4	GUGZ-5	GUGZ-6		
Well Owner	Mr. Brady	Springs Hill WSC	Canyon Regional	CRWA Wells Ranch	Dewville Methodist	Schertz-Seguin L.G.C.		
Well Number	Brady House Well	Springs Hill	CRWA-D Well #7	CRWA-E Well #9	Dewville Methodist	SSLGC #9		
Well Depth (ft)	380	430	428	405	128	1014		
Screened interval <sup>1</sup> (feet below ground surface)	360-380	220-357	150-405	300-395	--	664-994		
Aquifer	Wilcox	Carrizo	Carrizo	Carrizo	Queen City	Carrizo		
Sample Date	8/30/2012	9/25/2012	9/25/2012	9/25/2012	8/23/2012	8/30/2012		
<b>Stabilized Field Readings</b>		<b>Units</b>						
Temp (deg C)	°C	26.3	23.3	24.6	24.5	24.1	26.4	
pH		7.25	5.52	5.75	5.60	7.19	6.18	
Conductivity (mS)	µS	1266	94.4	86.2	101.6	546	136.4	
<b>SAT Lab Results: Analyte</b>		<b>Units</b>						
General Chemistry	Total Alkalinity	mg/L	308	<20.0	<20.0	<20.0	236	20.0
	HS <sup>-</sup> (Bisulfide ion)	mg/L	<0.050	<0.050	<0.050	<0.050	<0.050	<0.050
	Bromide	mg/L	<0.500	<0.500	<0.500	<0.500	<0.500	<0.500
	Hydrogen Sulfide	mg/L	<0.050	<0.050	<0.050	<0.050	<0.050	<0.050
	Fluoride	mg/L	1	<0.100	<0.100	<0.100	0.411	<0.100
	Chloride	mg/L	157	21	13.9	20.7	19.5	22.0
	Nitrite as N	mg/L	<0.50	<0.50	<0.50	<0.50	<0.50	<0.50
	Nitrate as N	mg/L	<0.50	<0.50	<0.50	<0.50	1.01	<0.50
	TOC	mg/L	2	21	4.00	7.10	3.90	1.60
	Sulfate	mg/L	76	10	13.1	14.8	26.2	22.4
	Specific Conductance	µmhos/cm	1,460	138	114	135	615	202
	TDS	mg/L	730	82	70.0	85.0	358	122
	pH	pH units	7	6	5.36	5.69	7.05	5.75
	pH @ Temperature	°C	15	16	16	14	22	15
	Calcium	mg/L	96	5	4.80	4.68	67.6	8.00
	Iron	mg/L	0	<0.050	0.44	0.511	<0.050	0.970
Magnesium	mg/L	28	2	1.35	1.73	6.17	2.28	
Potassium	mg/L	7	5	5.59	5.64	4.83	7.30	
Sodium	mg/L	133	11	8.73	12.1	37.2	12.6	
<b>Zymax Lab Results: Analyte</b>		<b>Units</b>						
Fixed Gas	O <sub>2</sub> + Ar	% Volume	11.6	14.1	13.5	11.3	13.2	16.3
	N <sub>2</sub>	% Volume	81.4	74.8	78.4	78.8	79.6	77.2
	CH <sub>4</sub>	% Volume	<0.1	<0.1	<0.1	<0.1	<0.1	<0.1
	CO	% Volume	<0.1	<0.1	<0.1	<0.1	<0.1	<0.1
	CO <sub>2</sub>	% Volume	7	11.2	8.1	9.9	7.2	6.4
Gas in headspace	C1	ppmv	134.4	160.3	48.5	85.4	11.1	84.1
	C2	ppmv	37.1	1.4	0.9	<1.0	11.7	16.7
	C3	ppmv	4.9	1.5	1.7	<1.0	1.7	2.6
	i-C4	ppmv	<1.0	<1.0	<1.0	<1.0	<1.0	<1.0
	n-C4	ppmv	2.7	1.4	<1.0	<1.0	2.4	2.3
	i-C5	ppmv	<1.0	<1.0	<1.0	<1.0	<1.0	<1.0
Gas in water	n-C5	ppmv	1.3	<1.0	<1.0	<1.0	<1.0	1.4
	C1	µg/L	7.6	<1.0	<1.0	0.9	0.5	7.5
	C2	µg/L	<1.0	<1.0	<1.0	<1.0	<1.0	<1.0
Isotope Analysis	C3	µg/L	<1.0	<1.0	<1.0	<1.0	<1.0	<1.0
	δ <sup>13</sup> C <sub>C1</sub>	‰ VPDB	-51.2	ND <sup>5</sup>	ND	ND	ND	-50.8
	δ <sup>13</sup> C <sub>CO2</sub>	‰ VPDB	-19.4	-19.95	-19.92	-19.94	-18.5	-19.5
	δ <sup>13</sup> C <sub>C2</sub>	‰ VPDB	ND	ND	ND	ND	ND	ND
	δD <sub>C1</sub>	‰ VSMOW	ND	ND	ND	ND	ND	ND
	δD <sub>C2</sub>	‰ VSMOW	ND	ND	ND	ND	ND	ND
Beta Lab Results: Analyte	δ <sup>18</sup> O <sub>H2O</sub>	‰ VSMOW	-4.1	-4.8	-4.8	-4.8	-4.4	-4.8
	δD <sub>H2O</sub>	‰ VSMOW	-25.1	-26.6	-27.9	-28.2	-25.6	-28.3
<b>Beta Lab Results: Analyte</b>		<b>Units</b>						
Radiometric Analysis	Apparent <sup>14</sup> C Age	YBP	10,020	1,060	1,650	1,620	101	3,600
	Apparent Age Error	+/- yrs	50	30	30	30	0.3	30
	<sup>13</sup> C/ <sup>12</sup> C Ratio	‰	-16.4	-21.6	-21.6	-21.5	-15.7	-21.6
	Fraction Modern	%	28.7%	87.6%	81.4%	81.7%	101.4%	63.9%
	Fmnd Error	+/- %	0.18%	0.32%	0.30%	0.30%	0.25%	0.24%
<b>U. of AZ Lab Results: Analyte</b>		<b>Units</b>						
Sulfate Isotope	δ <sup>34</sup> S	‰	2.8	-2.2	-1.8	3.1	8.5	6.8
	δ <sup>18</sup> O (SO <sub>4</sub> )	‰	11.2	9.2	9.1	8.1	1.9	7.5

1) Represents top of highest screen interval to bottom of lowest screen interval.  
 -- = No screen data available

3) Well was originally completed to 5750 for oil and gas, and subsequently plugged back to 2676 feet below ground surface.

4) \* indicates that field notes suggest that measurements are unreliable due to possibly malfunctioning field meters.

5) ND = Target component's concentration too low to obtain reliable isotope data.

<sup>a</sup> = Laboratory Note: Estimate for target components at low concentrations

<sup>b</sup> = Laboratory Note: Estimate due to low concentration, 3xSTDEV applies

<sup>c</sup> = Laboratory Note: Qualitative measure of hydrocarbon gas during isotope analysis

**Table 7-4. Chemical and isotopic results from samples collected in the Gonzales Transect during 2012 (Continued).**

Sample Number		GUGZ-7	GUGZ-8	GUGZ-9	GUGZ-10	GUGZ-11	GUGZ-12	
Well Owner	Schertz-Seguin L.G.C.	W. Whitley	J. Buell	T. Gaylord	SAWS	SAWS		
Well Number	SSLGC #4	Whitley	Buell Well #1 Bam	Gaylord House Well	SAWS SP-2	SAWS QC-2		
Well Depth (ft)	1310	5750 <sup>3</sup>	310	335	160	585		
Screened Interval <sup>1</sup> (feet below ground surface)	1050-1290	2626-2676	280-300	--	105-145	470-570		
Aquifer	Carrizo	Wilcox	Queen City	Sparta	Sparta	Queen City		
Sample Date	8/30/2012	8/23/2012	8/23/2012	8/23/2012	11/20/2012	11/20/2012		
<b>Stabilized Field Readings</b>		<b>Units</b>						
Temp (deg C)	°C	28.9	26.2	24.3	23.5	23.8	25.5	
pH		6.77	8.66	7.79	7.98	6.39	8.44	
Conductivity (mS)	µS	289	2360	979	1699	130 <sup>4</sup>	180 <sup>4</sup>	
<b>SAT Lab Results: Analyte</b>		<b>Units</b>						
General Chemistry	Total Alkalinity	mg/L	68.0	580	244	136	84.0	388
	HS <sup>-</sup> (Bisulfide ion)	mg/L	<0.050	<0.050	<0.050	<0.050	<0.050	<0.050
	Bromide	mg/L	<0.500	1.81	<0.500	<0.500	0.846	<0.500
	Hydrogen Sulfide	mg/L	<0.050	<0.050	<0.050	<0.050	<0.050	<0.050
	Fluoride	mg/L	<0.100	0.692	<0.100	<0.100	0.400	0.394
	Chloride	mg/L	23.1	384	79.5	220	258	100
	Nitrite as N	mg/L	<0.50	<0.50	<0.50	<0.50	<0.50	<0.50
	Nitrate as N	mg/L	<0.50	<0.50	<0.50	<0.50	<0.50	<0.50
	TOC	mg/L	1.10	5.90	3.50	3.2	4.60	10.9
	Sulfate	mg/L	32.4	247	147	389	130	158
	Specific Conductance	µmhos/cm	333	2980	1090	1890	1460	1580
	TDS	mg/L	186	1590	582	1040	905	978
	pH	pH units	6.73	8.57	7.71	7.74	6.57	8.68
	pH @ Temperature	°C	16	21	20	19	14	15
	Calcium	mg/L	24.4	1.80	63.3	80.6	69.9	5.76
	Iron	mg/L	1.48	0.174	0.215	0.215	8.27	<0.050
Magnesium	mg/L	4.66	0.613	27.6	34	28.5	2.91	
Potassium	mg/L	9.44	4.89	11.8	18	6.24	3.74	
Sodium	mg/L	13.9	626	111	210	138	404	
<b>Zymax Lab Results: Analyte</b>		<b>Units</b>						
Fixed Gas	O <sub>2</sub> + Ar	% Volume	17.5	11.5	21.5	11.8	7.6	5.6
	N <sub>2</sub>	% Volume	79.7	88.1	76.8	87.5	83.7	94.0
	CH <sub>4</sub>	% Volume	<0.1	<0.1	<0.1	<0.1	<0.1	<0.1
	CO	% Volume	<0.1	<0.1	<0.1	<0.1	<0.1	<0.1
Gas in headspace	CO <sub>2</sub>	% Volume	2.8	0.4	1.7	0.7	8.7	0.4
	C1	ppmv	16.5	154.3	20.3	143.9	129.4	176.0
	C2	ppmv	17.7	44.8	10.4	32.7	2.5	<1.0
	C3	ppmv	2.8	6.7	<1.0	5.2	3.3	<1.0
	i-C4	ppmv	<1.0	<1.0	<1.0	<1.0	<1.0	<1.0
	n-C4	ppmv	2.2	5.0	<1.0	4.0	2.3	<1.0
Gas in water	i-C5	ppmv	<1.0	<1.0	<1.0	<1.0	<1.0	<1.0
	n-C5	ppmv	1.0	2.3	<1.0	<1.0	0.8	<1.0
	C1	µg/L	0.8	5.7	1.1	8.4	7.1	11.0
	C2	µg/L	<1.0	<1.0	<1.0	<1.0	<1.0	<1.0
	C3	µg/L	<1.0	<1.0	<1.0	<1.0	<1.0	<1.0
Isotope Analysis	δ <sup>13</sup> C <sub>C1</sub>	‰ VPDB	ND	ND	ND	ND	<sup>a</sup> -51.3	-52.9
	δ <sup>13</sup> C <sub>CO2</sub>	‰ VPDB	-20.1	-17.9	-19.1	-22.1	-11.8	-10.0
	δ <sup>13</sup> C <sub>C2</sub>	‰ VPDB	ND	ND	ND	ND	ND	ND
	δD <sub>C1</sub>	‰ VSMOW	ND	ND	ND	ND	ND	ND
	δD <sub>C2</sub>	‰ VSMOW	ND	ND	ND	ND	ND	ND
	δ <sup>18</sup> O <sub>H2O</sub>	‰ VSMOW	-4.8	-4.6	-4.8	-4.3	-4.6	-4.7
δD <sub>H2O</sub>	‰ VSMOW	-27.7	-27.6	-26.3	-24.8	-25.5	-25.7	
<b>Beta Lab Results: Analyte</b>		<b>Units</b>						
Radiometric Analysis	Apparent <sup>14</sup> C Age	yBP	9,040	31,380	25,350	20,580	4,620	38,890
	Apparent Age Error	+/- yrs	40	200	130	90	30	440
	<sup>13</sup> C/ <sup>12</sup> C Ratio	‰	-18.9	-13.9	-16.5	-21.6	-17.9	-9.2
	Fraction Modern	%	32.5%	2.0%	4.3%	7.7%	56.3%	0.8%
	Fmdn Error	+/- %	0.16%	0.05%	0.07%	0.09%	0.21%	0.04%
<b>U. of AZ Lab Results: Analyte</b>		<b>Units</b>						
Sulfate Isotope	δ <sup>34</sup> S	‰	6.3	14.7	6.8	-3.2	-9.2	7.4
	δ <sup>18</sup> O (SO <sub>4</sub> )	‰	8	16.3	9.5	9.1	9.3	10.9

1) Represents top of highest screen interval to bottom of lowest screen interval.  
 -- = No screen data available

3) Well was originally completed to 5750 for oil and gas, and subsequently plugged back to 2676 feet below ground surface.

4) \* indicates that field notes suggest that measurements are unreliable due to possibly malfunctioning field meters.

5) ND = Target component's concentration too low to obtain reliable isotope data.

<sup>a</sup> = Laboratory Note: Estimate for target components at low concentrations

<sup>b</sup> = Laboratory Note: Estimate due to low concentration, 3σSTDEV applies

<sup>c</sup> = Laboratory Note: Qualitative measure of hydrocarbon gas during isotope analysis

**Table 7-4. Chemical and isotopic results from samples collected in the Gonzales Transect during 2012 (Continued).**

Sample Number		GUGZ-13	GUGZ-13D	GUGZ-14	GUGZ-15	GUGZ-16	GUGZ-17	GUGZ-18	
Well Owner		SAWS	SAWS	SAWS	SAWS	SAWS	SAWS	SAWS	
Well Number		SAWS CM-2	SAWS CM-2	SAWS SP-3	SAWS QC-3	SAWS CM-3	SAWS SP-4	SAWS QC-4	
Well Depth (ft)		1575	1575	315	769	1915	515	1005	
Screened Interval <sup>1</sup> (feet below ground surface)		1230-1560	1230-1560	260-300	714-754	1700-1900	460-500	930-990	
Aquifer		Carrizo	Carrizo	Sparta	Queen City	Carrizo	Sparta	Queen City	
Sample Date		11/21/2012	11/21/2012	11/20/2012	11/20/2012	11/20/2012	11/20/2012	11/20/2012	
<b>Stabilized Field Readings</b>		<b>Units</b>							
Temp (deg C)		°C	24.7	24.7	25.1	25.6	25.7	27.3	26.2
pH			8.34	8.3	8.58	8.56	8.26	8.71	8.91
Conductivity (mS)		µS	250	250	910	1450	140	2250	130*
<b>SAT Lab Results: Analyte</b>		<b>Units</b>							
General Chemistry	Total Alkalinity	mg/L	64.0	64	188	500	76.0	480	1040
	HS <sup>-</sup> (Bisulfide ion)	mg/L	<0.050	<0.050	<0.050	<0.050	<0.050	<0.050	<0.050
	Bromide	mg/L	<0.500	<0.500	<0.500	<0.500	<0.500	1.17	1.8
	Hydrogen Sulfide	mg/L	<0.050	<0.050	<0.050	<0.050	<0.050	<0.050	<0.050
	Fluoride	mg/L	<0.100	<0.100	0.428	0.482	<0.100	0.842	1.90
	Chloride	mg/L	31.6	31.6	90.8	110	34.3	360	633
	Nitrite as N	mg/L	<0.50	<0.50	<0.50	<0.50	<0.50	<0.50	<0.50
	Nitrate as N	mg/L	<0.50	<0.50	<0.50	<0.50	<0.50	<0.50	<0.50
	TOC	mg/L	2.60	2.40	5.00	10.7	2.30	11.0	21.2
	Sulfate	mg/L	<0.50	<0.50	101	112	<0.50	106	<0.50
	Specific Conductance	µmhos/cm	276	280	1050	1670	304	2570	4120
	TDS	mg/L	174	159	607	1040	179	1620	2680
	pH	pH units	8.41	8.49	8.88	8.95	8.68	9.08	9.12
	pH @ Temperature	°C	17	18	16	15	14	15	15
	Calcium	mg/L	14.3	14.2	2.80	1.52	10.1	1.86	<1.00
Iron	mg/L	<0.050	<0.050	<0.050	0.087	<0.050	0.548	0.256	
Magnesium	mg/L	5.16	5.15	1.47	<0.500	6.56	0.648	<0.500	
Potassium	mg/L	9.60	9.47	2.91	2.3	8.66	3.32	4.69	
Sodium	mg/L	25.0	23.9	244	466	37.5	712	908	
<b>Zymax Lab Results: Analyte</b>		<b>Units</b>							
Fixed Gas	O <sub>2</sub> + Ar	% Volume	8.2	8.4	8.9	7.9	8.3	7.9	5.6
	N <sub>2</sub>	% Volume	86.4	86.4	91.1	91.8	87.4	91.5	43.9
	CH <sub>4</sub>	% Volume	5.4	5.3	<0.1	<0.1	3.7	0.3	50.3
	CO	% Volume	<0.1	<0.1	<0.1	<0.1	0.5	0.3	<0.1
	CO <sub>2</sub>	% Volume	<0.1	<0.1	<0.1	0.3	0.1	0.1	0.2
Gas in headspace	C1	ppmv	16014.0	16270.8	118.5	200.0	11863.1	784.3	See Fixed
	C2	ppmv	30.8	30.3	6.2	7.4	25.0	18.5	79.5
	C3	ppmv	2.8	9.1	5.5	5.4	9.9	10.8	7.4
	i-C4	ppmv	<1.0	<1.0	<1.0	<1.0	<1.0	<1.0	<1.0
	n-C4	ppmv	2	4.9	3.6	<1.0	6.1	7.0	3.9
	i-C5	ppmv	<1.0	<1.0	<1.0	<1.0	<1.0	<1.0	<1.0
	n-C5	ppmv	<1.0	<1.0	1.1	2.4	<1.0	2.2	<1.0
Gas in water	C1	µg/L	1005.8	1119.1	4.8	10.2	732.4	44.4	11,867.80
	C2	µg/L	<1.0	<1.0	<1.0	<1.0	<1.0	<1.0	<1.0
	C3	µg/L	<1.0	<1.0	<1.0	<1.0	<1.0	<1.0	<1.0
Isotope Analysis	δ <sup>13</sup> C <sub>C1</sub>	‰ VPDB	-89.7	-90.6	<sup>a</sup> -50.8	-52.0	-90.6	-52.6	-69.9
	δ <sup>13</sup> C <sub>CO2</sub>	‰ VPDB	ND	ND	-11.8	-6.0	ND	-19.6	ND
	δ <sup>13</sup> C <sub>C2</sub>	‰ VPDB	ND	ND	ND	ND	ND	ND	ND
	δD <sub>C1</sub>	‰ VSMOW	-209	-212	ND	ND	-214	ND	-210
	δD <sub>C2</sub>	‰ VSMOW	ND	ND	ND	ND	ND	ND	ND
	δ <sup>18</sup> O <sub>H2O</sub>	‰ VSMOW	-4.9	-5	-4.6	-4.7	-4.9	-4.3	-4.4
	δD <sub>H2O</sub>	‰ VSMOW	-27.4	-29.5	-26.0	-25.6	-27.6	-24.7	-25.5
<b>Beta Lab Results: Analyte</b>		<b>Units</b>							
Radiometric Analysis	Apparent <sup>14</sup> C Age	YBP	14,630	14,330	14,680	27,390	14,660	20,000	43,300
	Apparent Age Error	+/- yrs	60	60	50	140	60	80	720
	<sup>13</sup> C/ <sup>12</sup> C Ratio	‰	-15.7	-15.2	-15.8	-8.3	-16.2	-19.9	-9.1
	Fraction Modern	%	16.2%	16.8%	16.1%	3.3%	16.1%	8.3%	0.5%
	FmDn Error	+/- %	0.12%	0.12%	0.10%	0.06%	0.12%	0.08%	0.04%
<b>U. of AZ Lab Results: Analyte</b>		<b>Units</b>							
Sulfate Isotope	δ <sup>34</sup> S	‰	1.7	14.6	-5.6	14.6	Insufficient SO <sub>4</sub>	9.6	2.2
	δ <sup>18</sup> O (SO <sub>4</sub> )	‰	Insufficient SO <sub>4</sub>	Insufficient SO <sub>4</sub>	11.9	13.1	6.5	15.9	7.8

1) Represents top of highest screen interval to bottom of lowest screen interval.

-- = No screen data available

3) Well was originally completed to 5750 for oil and gas, and subsequently plugged back to 2676 feet below ground surface.

4) \* indicates that field notes suggest that measurements are unreliable due to possibly malfunctioning field meters.

5) ND = Target component's concentration too low to obtain reliable isotope data.

<sup>a</sup> = Laboratory Note: Estimate for target components at low concentrations

<sup>b</sup> = Laboratory Note: Estimate due to low concentration, 3xSTDEV applies

<sup>c</sup> = Laboratory Note: Qualitative measure of hydrocarbon gas during isotope analysis

Evaluation of Hydrochemical and Isotopic Data in Groundwater Management Areas 11, 12 and 13

**Table 7-4. Chemical and isotopic results from samples collected in the Gonzales Transect during 2012 (Continued).**

	Sample Number	GUGZ-19	GUGZ-20	GUGZ-20D	GUGZ-21	GUGZ-22	GUGZ-23	
	Well Owner	SAWS	City of Nixon	City of Nixon	City of Smiley	L. Lessor	Alta Jenkins Estate	
	Well Number	SAWS CM-4	Nixon Well #5	Nixon Well #5	Smiley Well #3	L. Lessor	Alta Jenkins Estate	
	Well Depth (ft)	2175	1850	1850	2435	2500	2000	
	Screened Interval <sup>1</sup> (feet below ground surface)	1705-2160	1380-1840	1380-1840	2302-2435	--	--	
	Aquifer	Carrizo	Carrizo	Carrizo	Carrizo	Carrizo	Carrizo	
	Sample Date	11/21/2012	8/8/2012	8/8/2012	8/8/2012	8/8/2012	8/8/2012	
<b>Stabilized Field Readings</b>		<b>Units</b>						
	Temp (deg C)	°C	26.2	32.7	32.7	42.4	>50	
	pH		7.99	7.73	7.73	8.34	7.86	
	Conductivity (mS)	µS	417	633	633	787	2150	
<b>SAT Lab Results: Analyte</b>		<b>Units</b>						
General Chemistry	Total Alkalinity	mg/L	116	156	148	316	340	
	HS <sup>-</sup> (Bisulfide ion)	mg/L	<0.050	<0.050	<0.050	0.97	<0.050	
	Bromide	mg/L	<0.500	<0.500	<0.500	<0.500	0.697	
	Hydrogen Sulfide	mg/L	<0.050	<0.050	<0.050	3.22	<0.050	
	Fluoride	mg/L	<0.100	0.122	<0.100	0.401	1.52	
	Chloride	mg/L	42.3	40.8	41.4	43.8	17.1	
	Nitrite as N	mg/L	<0.50	<0.50	<0.50	<0.50	<0.50	
	Nitrate as N	mg/L	<0.50	<0.50	<0.50	<0.50	<0.50	
	TOC	mg/L	2.80	<1.00	<1.00	1.80	3.50	
	Sulfate	mg/L	12.4	59.0	60.5	3.05	0.68	
	Specific Conductance	µmhos/cm	467	635	617	824	2410	
	TDS	mg/L	280	342	335	450	1410	
	pH	pH units	7.91	7.34	7.55	8.30	8.02	8.15
	pH @ Temperature	°C	19	23	23	23	23	23
	Calcium	mg/L	20.6	46.5	46.5	2.52	3.02	2.74
Iron	mg/L	0.256	<0.050	<0.050	<0.050	<0.050	0.163	
Magnesium	mg/L	11.0	6.81	7.04	0.677	0.830	0.744	
Potassium	mg/L	9.03	10.7	10.8	4.54	9.71	10.5	
Sodium	mg/L	48.8	60.7	63.9	158	453	481	
<b>Zymax Lab Results: Analyte</b>		<b>Units</b>						
Fixed Gas	O <sub>2</sub> + Ar	% Volume	8.5	16.4	17.8	14.0	10.1	
	N <sub>2</sub>	% Volume	8.5	82.9	81.5	74.9	45.6	
	CH <sub>4</sub>	% Volume	3.1	<0.1	<0.1	10.9	42.6	
	CO	% Volume	0.5	<0.1	<0.1	<0.1	<0.1	
	CO <sub>2</sub>	% Volume	0.4	0.7	0.7	0.3	1.8	
Gas in headspace	C1	ppmv	9294.2	35.2	36.1	See Fixed	See Fixed	
	C2	ppmv	22.4	16.5	20.1	22.9	23.3	
	C3	ppmv	8.3	1.7	2.2	3.5	6.9	
	i-C4	ppmv	<1.0	<1.0	<0.1	<1.0	<1.0	
	n-C4	ppmv	4.2	1.6	1.9	1.0	1.8	
Gas in water	i-C5	ppmv	<1.0	<1.0	<0.1	<1.0	<1.0	
	n-C5	ppmv	1.3	<1.0	<0.1	<1.0	<1.0	
	C1	µg/L	626.5	2.5	2.2	7381.7	19,729.10	
	C2	µg/L	<1.0	<1.0	<1.0	0.9	7.5	
	C3	µg/L	<1.0	<1.0	<1.0	<1.0	<1.0	
Isotope Analysis	δ <sup>13</sup> C <sub>C1</sub>	‰ VPDB	-73.3	ND	ND	-51.6	-47.2	
	δ <sup>13</sup> C <sub>C02</sub>	‰ VPDB	-1	-21.8	-21.9	-14.7	-11.1	
	δ <sup>13</sup> C <sub>C2</sub>	‰ VPDB	ND	ND	ND	ND	ND	
	δD <sub>C1</sub>	‰ VSMOW	-197	ND	ND	-296	-255	
	δD <sub>C2</sub>	‰ VSMOW	ND	ND	ND	ND	ND	
	δ <sup>18</sup> O <sub>H2O</sub>	‰ VSMOW	-5.1	-5.0	-5.0	-4.9	-4.3	
δD <sub>H2O</sub>	‰ VSMOW	-28.9	-29.3	-28.0	-28.7	-27.2		
<b>Beta Lab Results: Analyte</b>		<b>Units</b>						
Radiometric Analysis	Apparent <sup>14</sup> C Age	YBP	13,490	17,780	17,910	35,010	> 43,500	
	Apparent Age Error	+/- yrs	50	70	70	310		
	<sup>13</sup> C/ <sup>12</sup> C Ratio	‰	-18.3	-18.8	-18.1	-10.7	-6.6	
	Fraction Modern	%	18.7%	10.9%	10.8%	1.3%	0.0%	
	Fmdn Error	+/- %	0.11%	0.09%	0.09%	0.05%	0.00%	
<b>U. of AZ Lab Results: Analyte</b>		<b>Units</b>						
Sulfate Isotope	δ <sup>34</sup> S	‰	39.8	6.2	6.4	6.3	9.1	
	δ <sup>18</sup> O (SO <sub>2</sub> )	‰	18.3	10.5	10	7.3	-2.5	

1) Represents top of highest screen interval to bottom of lowest screen interval.

-- = No screen data available

3) Well was originally completed to 5750 for oil and gas, and subsequently plugged back to 2676 feet below ground surface.

4) \* indicates that field notes suggest that measurements are unreliable due to possibly malfunctioning field meters.

5) ND = Target component's concentration too low to obtain reliable isotope data.

<sup>a</sup> = Laboratory Note: Estimate for target components at low concentrations

<sup>b</sup> = Laboratory Note: Estimate due to low concentration, 3xSTDEV applies

<sup>c</sup> = Laboratory Note: Qualitative measure of hydrocarbon gas during isotope analysis

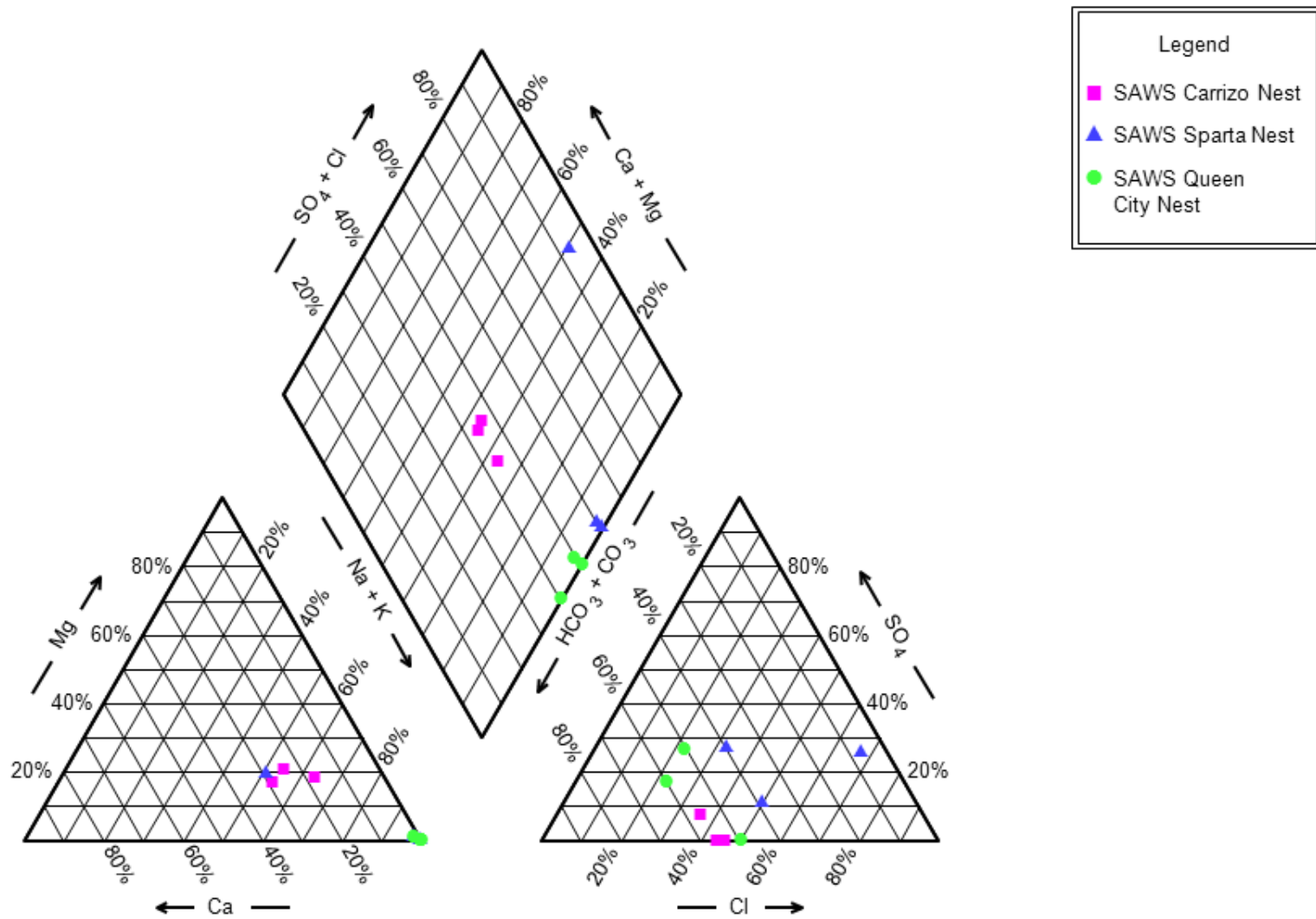


Figure 7-225. Piper diagram showing chemistry of all the San Antonio Water System well nests in the Gonzales Transect by aquifer.

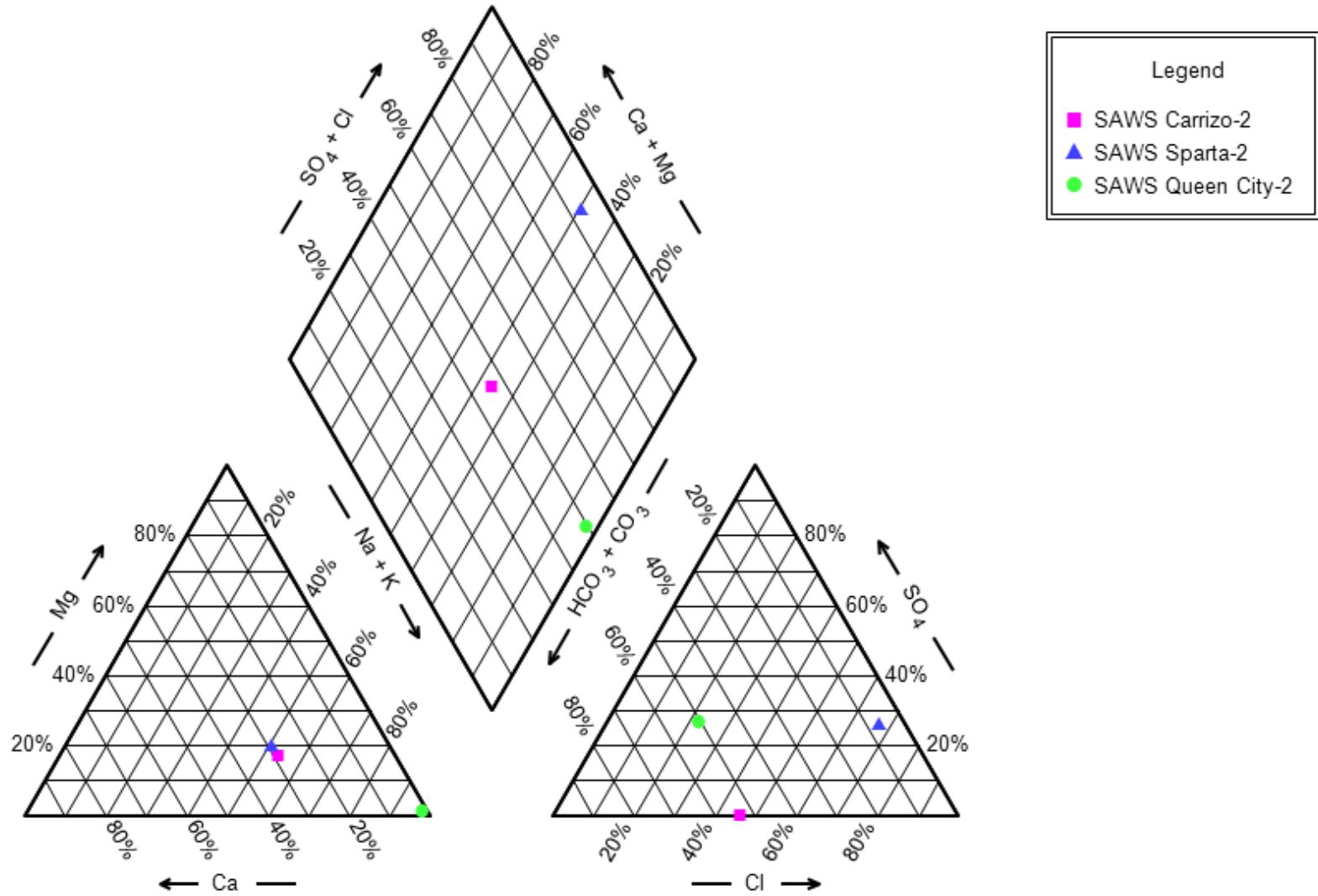


Figure 7-226. Piper diagram showing chemistry of the San Antonio Water System well Nest 2 in the Gonzales Transect.

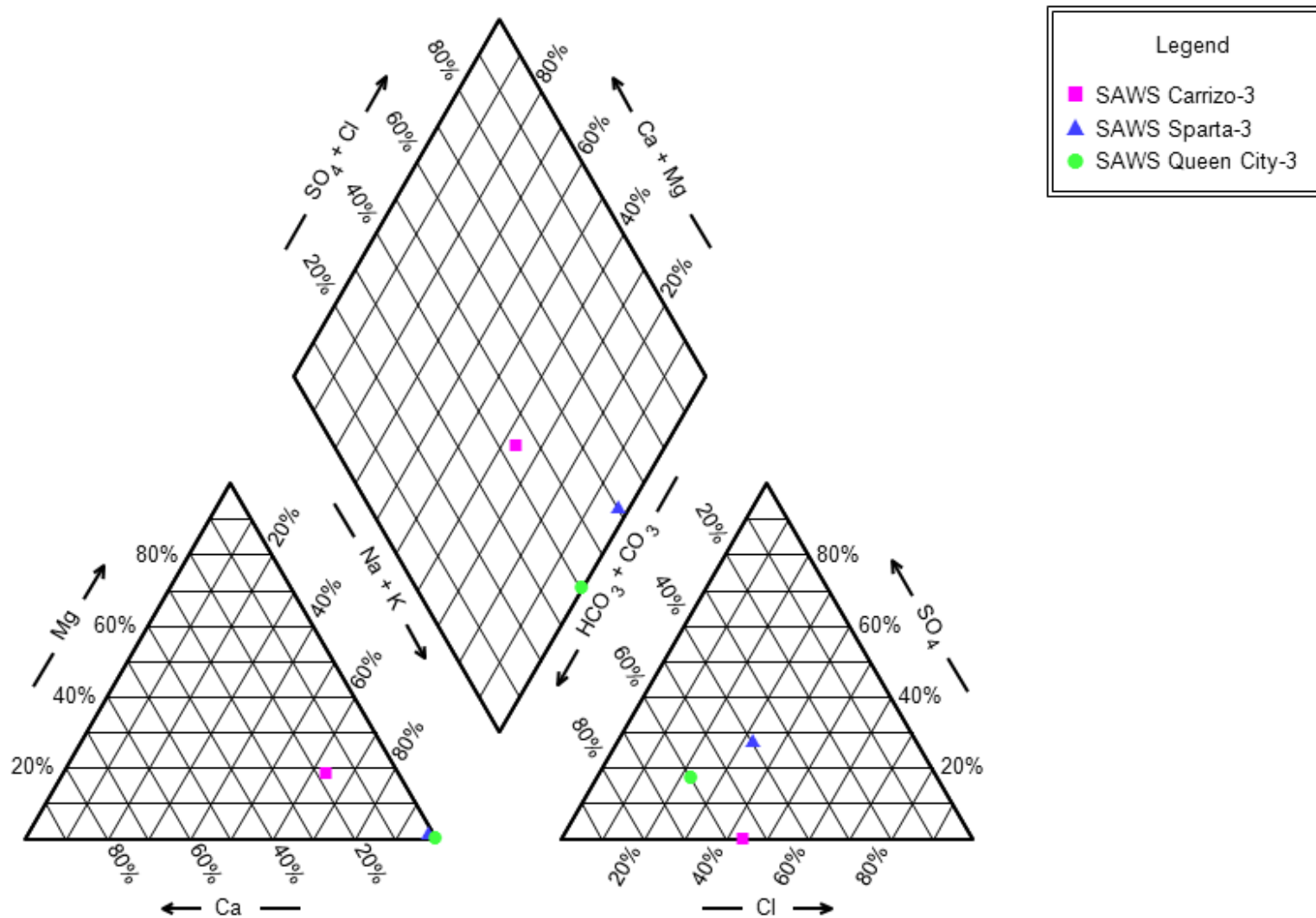


Figure 7-227. Piper diagram showing chemistry of the San Antonio Water System well Nest 3 in the Gonzales Transect.

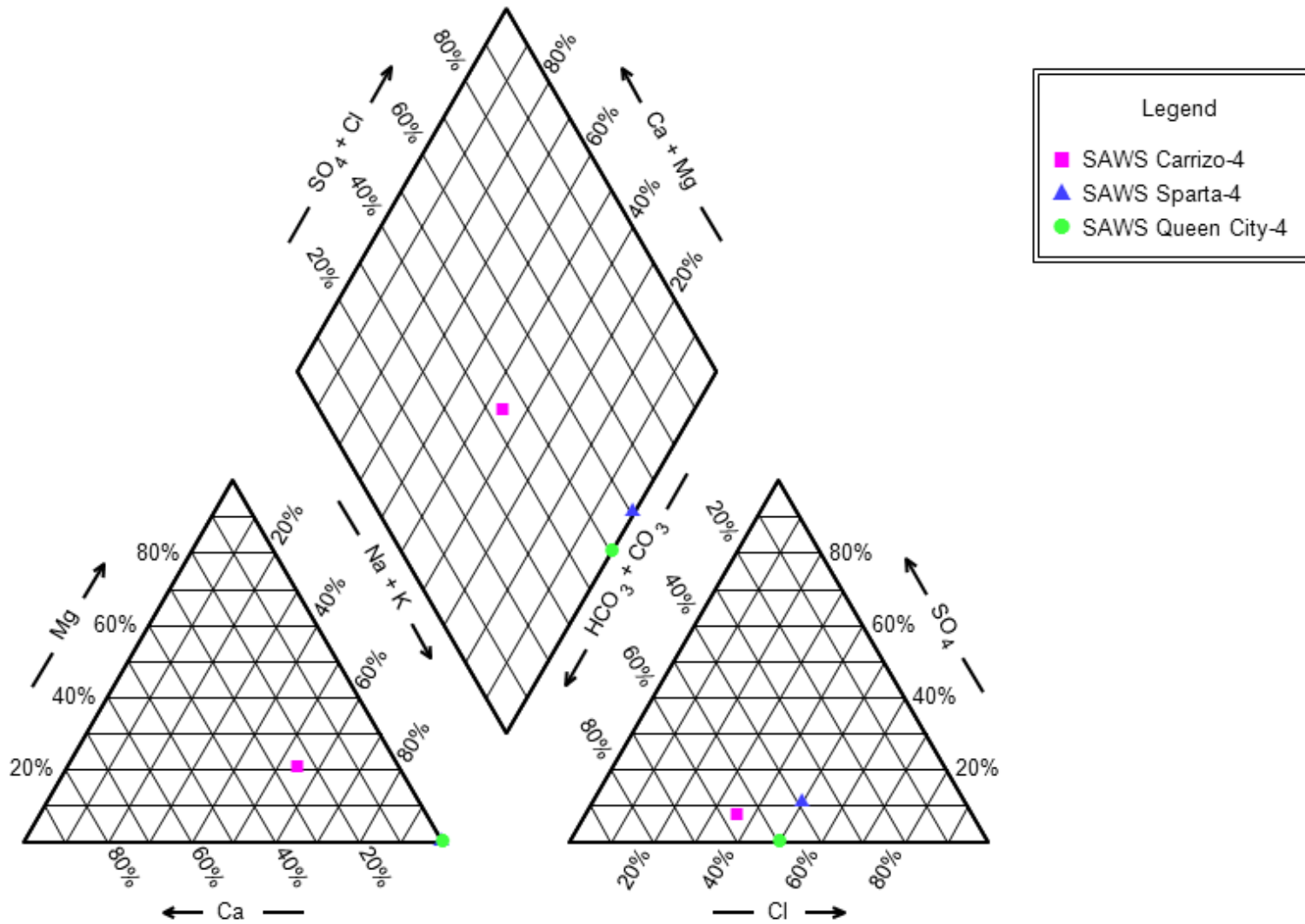


Figure 7-228. Piper diagram showing chemistry of the San Antonio Water System well Nest 4 in the Gonzales Transect.

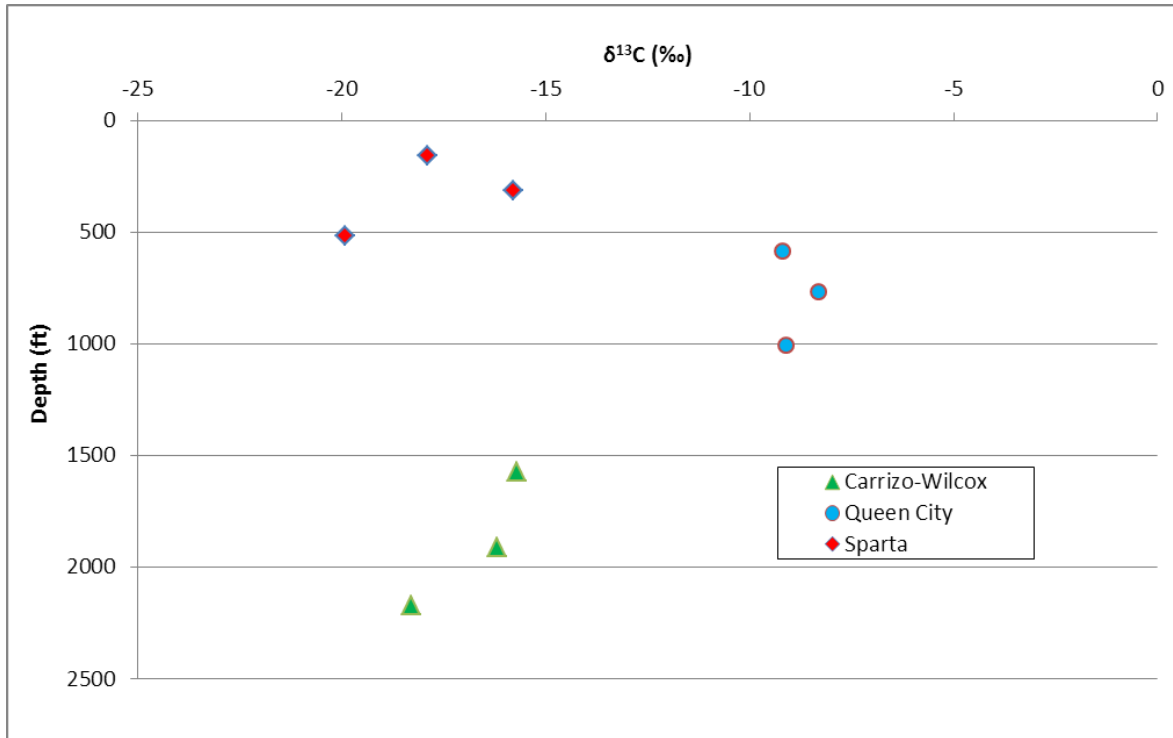


Figure 7-229. Depth measured in feet (ft) versus δ<sup>13</sup>C, San Antonio Water System well nests, Gonzales Transect, Groundwater Management Area 13.

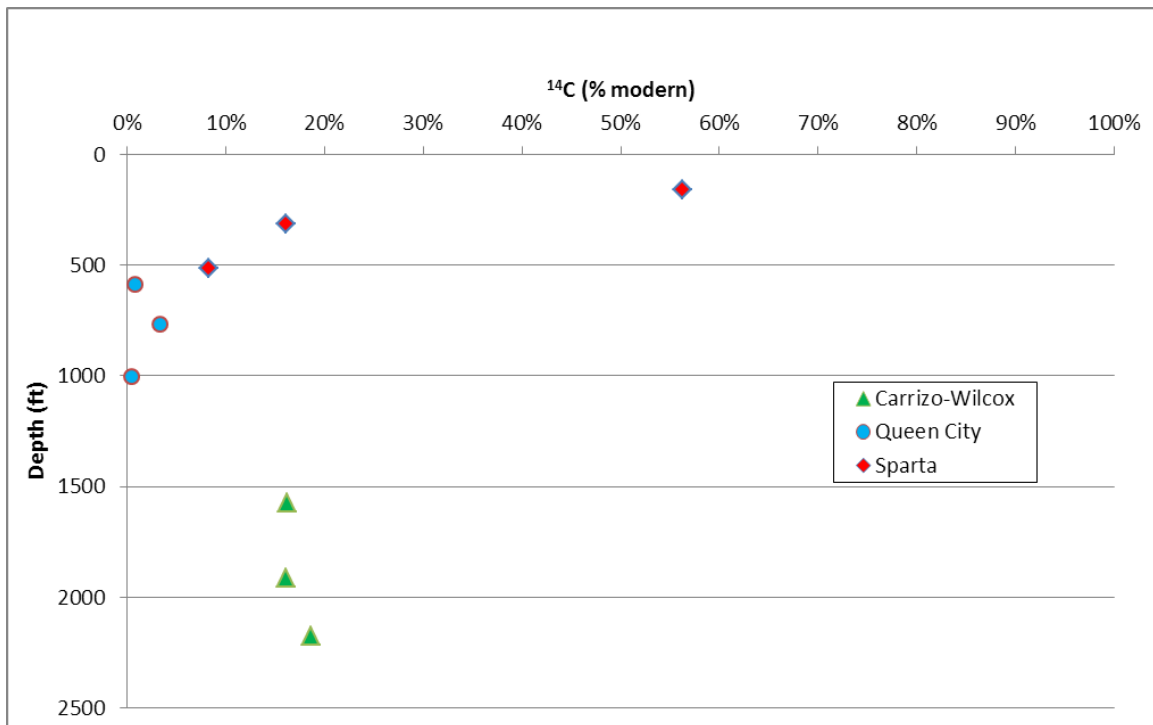


Figure 7-230. Depth measured in feet (ft) versus carbon-14 percent modern (¹⁴C %), San Antonio Water System well nests, Gonzales Transect, Groundwater Management Area 13.

### 7.3.2 *Geochemical Modeling*

The estimation of the groundwater age in the Carrizo Sand Formation portion of the Carrizo-Wilcox Aquifer along the Gonzales Transect is a two-step process. The first step is to determine quantitatively the geochemical evolution of a groundwater as it flows from outcrop to downdip along a flowpath defined by a set of wells with known chemistry. The second step is to calculate a corrected carbon-14 age with this well-defined geochemical pathway. Table 7-5 shows the age estimates of these waters.

#### **Aquifer Composition**

Geochemical modeling for the Gonzales Transect (Figure 7-180) is based on samples collected in 2012 for this project; these analytical results are included in Appendix A and Table 7-4. A total of 23 wells were sampled and analyzed from the Carrizo Sand Formation (12), the Wilcox Group (2), the Queen City (5) and the Sparta (4) aquifers. It should be noted that TWDB aquifer designations were used for these assignments and the accuracy of such assignments cannot be proven otherwise. These analyses are intended to provide radiocarbon measurements for use in estimating the age of groundwater at points along groundwater flow paths, to provide general chemistry to define water composition along the groundwater flow path, to determine geochemical processes affecting local compositional changes and to evaluate data for evidence of cross-formational flow. In addition to the measurement of the stable isotopic content of the dissolved constituents and the water itself, samples of dissolved gas were also analyzed for identification, quantification and isotopic content.

Twelve groundwater samples from the Carrizo Sand Formation are from wells broadly aligned in a northwest to southeast orientation, following the general down dip direction of groundwater flow (Figure 7-183). These wells sample discrete intervals within the Carrizo Sand Formation and predominantly represent the confined section of the aquifer. The shallowest three wells (Model well numbers 2, 3 and 4, Table 7-5) are within two miles of the Carrizo Sand Formation outcrop and have depths of 405 to 430 feet below land surface. The deepest well along this transect has a total depth of 2,500 feet below land surface and is producing from the confined portion of the Carrizo Sand Formation (Table 7-5 and Figure 7-181).

The Carrizo Sand Formation is a relatively clean fluvial sand separated from the underlying Wilcox Group of the Carrizo-Wilcox Aquifer and the overlying Queen City Aquifer by mudstone aquitards. It was initially assumed that the aquifer composition defined by these wells would represent an evolutionary path of shallow recharge water modified along the flow path by mineral reactions generally well understood for this region. The predominant change is from a calcium-bicarbonate to a sodium-bicarbonate water type until the deeper section evidences mixing with a deeper sourced higher total dissolved solids and sodium chloride brine.

These general trends can be seen even in cross-plots using all available data (please note that since two samples are duplicates, not all samples may be visible in the plot due to proximity) for the Carrizo Sand Formation in Guadalupe and Gonzalez counties from the TWDB database. For example, Figure 7-233 and Figure 7-234 are plots comparing sodium, bicarbonate, pH, chloride, calcium, sulfate, total dissolved solids and  $\delta^{34}\text{S}$  with depth to illustrate the expected overall compositional change. More instructive are the compositional changes indicated by the analyses of the Carrizo Sand Formation wells sampled in 2012 for the transect (Figure 7-235 through Figure 7-238). The trends observed for total dissolved solids, sodium, chloride, and alkalinity are remarkably consistent for wells sampled over a 25 mile transect considering the data are from 12

wells from the Carrizo Sand Formation and rather broadly spaced (Figure 7-181). The data fit the conceptual model; however there is an obvious difference in the three San Antonio Water System wells (Model well numbers 13, 16 and 19 on Table 7-5) which are located on the north edge of the sampled set of wells. This break in consistency is more obvious when highlighted with the dashed lines especially with respect to other more reactive constituents (Figure 7-235 through Figure 7-238).

The inconsistent trend in constituents when the San Antonio Water System wells (Table 7-5) are included is indicative of a problem with the conceptual model of flow; however when these three wells are removed, the same flow path seems consistent and plausible (Figure 7-235 through Figure 7-238). The solution to this inconsistency may be that the chemistry of the groundwater is indicating the San Antonio Water System wells are far enough removed to the north to be part of a separate flow path. Although, in general, the water composition for chloride, sodium, total dissolved solids,  $^{14}\text{C}_{\text{OBS}}$  etc., of the San Antonio Water System wells fit with the expected changes with respect to overall profile chemistry, there exists a significantly different geochemical environment at the depth and region surrounding the San Antonio Water System wells. The San Antonio Water System wells are different in that the sulfate concentration drops to zero, indicating active sulfate reduction; simultaneously the methanogenesis is generating biogenic methane with depleted  $\delta^{13}\text{C}$  and  $\delta\text{D}$  values of -73.3 ‰ to -90.6 ‰ and -197 ‰ to -214 ‰ respectively, as well as enriched  $\delta^{13}\text{C}$  in the carbon dioxide (-1.0 ‰). In Transect 1, significant sulfate still remains in the groundwater and without methanogenesis only thermogenic gas is seen with much lower concentration (Figure 7-238). The thermogenic gas has a more enriched  $\delta^{13}\text{C}$  and  $\delta\text{D}$ , as well as wetter gas fractions ( $\text{C}_1$ ,  $\text{C}_2$ ,  $\text{C}_3$  and  $\text{n-C}_4$ ), and the expected more depleted  $\delta^{13}\text{C}$  of carbon dioxide (-19.5 ‰ to -20.1 ‰) derived from soil zones and virtually identical to the  $\delta^{13}\text{C}$  of the total dissolved carbon (-18.9 ‰ to -21.6 ‰).

The San Antonio Water System well nests have such active methanogenesis that methane is detectable in the fixed gas analysis and the oxygen content in that analysis is low for those wells (Appendix A). It should be noted that the San Antonio Water System wells do contain measurable quantities of the wetter hydrocarbon gases, but in similar concentrations to that observed for the main transect; whereas the biogenic methane has increased the total methane by two orders of magnitude (Appendix A). The main transect is referred to as Transect 1 and the San Antonio Water System well nests as Transect 2 for the Gonzales Transect (Figure 7-231). The reason for the localized difference in environmental conditions between the transects may be an aquifer condition at that depth. Lignites were identified in these wells during construction.

Comparison of these well locations to the estimated potentiometric surface given in the Queen City and Sparta Aquifers GAM report (Figure 7-232) indicates that separating these wells into two flow paths is a reasonable alternative.

### **Estimation of Age**

Fourteen of the Carrizo Sand Formation groundwater samples (including two duplicates) were collected from locations selected to represent the expected groundwater flowpath from outcrop to the deepest downgradient locations screened in the Carrizo Sand Formation portion of the Carrizo-Wilcox Aquifer (Figure 7-181 and Figure 7-231). The hydrogeology for this transect is relatively well defined and the assumption is that the corrected radiocarbon data will be correlative with velocities computed using physical flow models of the Carrizo Sand Formation. There are an additional 11 radiocarbon samples from the adjacent Wilcox Group, Queen City

and Sparta aquifers that may be useful in assessing evidence of cross-formational flow from the Carrizo Sand Formation. The measured  $\delta^{13}\text{C}$  and the carbon-14 activities are given in Table 7-5 and the chloride and alkalinity concentrations are provided for reference. Uncorrected  $^{14}\text{C}_{\text{OBS}}$  ages range from 1060 years before present to 43,500 years before present.

The  $^{14}\text{C}_{\text{OBS}}$  values require correction to more realistic computed ages and the Pearson and White (1967) procedure as well as the inverse modeling approach of NETPATH were used to estimate the best and most representative groundwater age. The three shallowest and least concentrated samples (Model well numbers 2, 3, and 4) are not candidates for the more comprehensive NETPATH simulation, because the alkalinity measurement for each was below the laboratory quantification limit (Appendix B, Table 7-6). A measurement or estimate for bicarbonate concentration is essential for NETPATH simulations, because the inverse method accounts for the differences between wells both in concentrations of dissolved constituents, and isotopic measurement in order to define the contribution from mineral and gas reactions.

The first three wells are similar in depth, composition and uncorrected age. The approach taken here was to use only one of the three shallow wells as the initial well for the NETPATH calculations and in the absence of a measured value for alkalinity, the mid-point of the reporting limit for alkalinity (ten milliequivalents per liter) was selected as a reasonable estimate. The corrected age for each of the first three wells was computed using the Pearson and White (1967) procedure which considers only calcite and carbon dioxide as the reactants and carbon sources and only requires the  $\delta^{13}\text{C}$  value of the soil gas and calcite. The computed ages range from modern to 476 years before present (Table 7-5). Model well number 3 was selected as the first well to be used for the NETPATH simulation, because Well 1 was deemed contaminated by modern recharge, and Well 2 was out of sequence in terms of measured and estimated age and additionally had a much larger open screen interval. The NETPATH simulation requires an initial (Well 3) and final well (Well 4) for the inverse calculation to determine the adjusted age. NETPATH results corrected the  $^{14}\text{C}_{\text{OBS}}$  to 1,633 years between model well number 3 and 4, with a total age from recharge to model well number 4 of 2,041 years before present, which is about 30 percent younger than the measured value of 3,600 years before present (Table 7-5).

For the nine wells used in Transect 1, the initial three wells were evaluated for carbon-14 age using the Pearson and White procedure, which yielded ages from modern to 430 years before present. The final two deep wells in the profile (Model well numbers 22 and 23) do not have measurable radiocarbon concentrations and thus represent water apparently older than about 45,000 years before present. Each of the four intermediate wells were considered by pairs using NETPATH to make the age adjustments and the results are given in Table 7-5. Because dissolved sulfate concentrations are high, and no biogenic methane, or enriched carbon dioxide is observed, along Transect 1, then it is assumed that no significant methanogenesis is occurring. The NETPATH simulations were successful by considering only carbon dioxide, calcite, lignite, calcium, magnesium, and sodium ion exchange. The sulfate source with  $\delta^{34}\text{S}$  similar to gypsum, but undoubtedly simply seawater derived sulfate in the clays and mudstones. All reacting minerals were monitored for violations in thermodynamic solubility requirements, and the computed  $\delta^{13}\text{C}$  matched the measured value at each final well of the modeled well pair. The last two wells (Model well numbers 22 and 23) cannot be modeled without considering mixing from some additional water source, probably a brine, to account for the elevated chloride which by model well number 23 is five times the chloride value seen in the upgradient wells. The computed corrected ages ( $^{14}\text{C}_{\text{ADJ}}$ ) are given in Table 7-5.

Secondary reactions of sulfate sources and silicate hydrolysis were considered during modeling and shown to not contribute any significant modification to the age calculation and were considered unimportant for this assessment. The calculation performed in NETPATH is constrained by two important procedures. First, the change in groundwater composition between wells must be accounted for by reaction with minerals, gasses or ion exchange, if this cannot result in a solution, then the pathway is not considered correct, either because of incorrect reaction formulation or possibly the effect of mixing with water sources not yet identified. Secondly, the thermodynamic reaction state of minerals must be monitored such that the model does not, for example, allow precipitation of a phase which is actually undersaturated. This calculation of thermodynamic reaction state is done as part of the NETPATH approach by using the geochemical equilibrium model, WATEQ.

The same procedure could not be followed for the second transect because not only were the initial wells without a measured alkalinity, the San Antonio Water System wells have an unacceptably high charge imbalance that cannot be explained. To provide at least an estimate of correction the method of Pearson and White was used and the resultant values are shown in Table 7-5; on average the ages are corrected by about 23 percent to younger ages. The wells along Transect 1 show a consistent decrease in carbon-14 percent from outcrop to the farthest downdip well and a consistent increase in age from modern waters in the outcrop to 33,176 in model well number 21 to no measurable carbon-14 in model well numbers 22 and 23.

Two wells were sampled from the Wilcox Group that directly underlies the Carrizo Sand Formation. The first well is a calcium-sodium-bicarbonate-chloride type water, but by the time groundwater reaches the region of the second sample the water has become a dominantly sodium-chloride water type. This elevation along the flow path is suggestive of progressive mixing of the recharged Wilcox Group water or either with a deeper brine. It is important to note that the increased concentration of sodium chloride is a common occurrence in the deeper sections of aquifers in this region. A plot of the chloride concentration with respect to the actual distance downgradient from the initial well in the transect illustrates the appearance of elevated chloride (Figure 7-239). The chloride concentration in the Wilcox Group is elevated all along the transect but significantly so by model well number 8. It should also be noted that the appearance of elevated chloride in the Carrizo Sand Formation and Queen City aquifers are at significantly different places along the transect. Of course, there is no guarantee that the two wells on the same flow path. In fact, it is almost guaranteed that the two wells are not on the same flowpath. Even with available head data, there is no guarantee that the wells are on the same flowpath unless the assumption of homogeneity and isotropy in hydraulic properties is employed, and that the wells that are used to collect water level measurements in the 3-dimensional aquifer system appropriately represent the aquifer in the area. This discussion is meant to serve as a general description of what type of changes are occurring if one assumes the wells are generally located on the same flowpath.

The measured ages for the two wells of the Wilcox Group are 10,020 and 31,380 years before present; however, corrections for measured ages cannot reliably be done because of possible mixing. Without knowing the mixing percentage or composition, the estimate of corrected age is not possible at present.

The Queen City Aquifer directly overlays the Carrizo Sand Formation and the Sparta Aquifer is above the Queen City Aquifer. Both of these shallow aquifers, and the deeper Wilcox Group are generally more saline, with lower quality water than the Carrizo Sand Formation at many points

along the transect (Figure 7-240). By mile 15 along the transect all three have total dissolved solids values greater than 1,500 milligrams per liter while the Carrizo Sand Formation is consistently below 500 milligrams per liter total dissolved solids. In a general sense the chloride, bicarbonate and sodium increase along the flow path for both aquifers indicating that the same general conversion to a sodium-bicarbonate type water is occurring, but with significant input of chloride into the aquifer as well.

The increase in bicarbonate is accompanied by a progressive enrichment of the  $\delta^{13}\text{C}$  of the total dissolved carbon (Figure 7-241). This indicates that calcite is progressively dissolving, and with no significant loss in sulfate or appearance of biogenic methane then methanogenic reactions are not indicated (Appendix B). Although there are eight measured  $^{14}\text{C}_{\text{OBS}}$  values, the ages cannot be corrected using NETPATH. The chloride is widely variable indicating mixing and perhaps surface infiltration, wells do not align along a flow path, the depths and well locations are not screened and located such that they can be projected onto a single transect. The uncorrected ages are inconsistent and the use of a simple correction method such as the Pearson and White procedure, does not improve the trend of data to suggest a plausible flow path (Figure 7-242 and Table 7-6).

The Carrizo Sand Formation is the highest quality aquifer from recharge to depth as compared to the Wilcox Group, Queen City or Sparta aquifers along this transect. The samples are best defined by two transects which are similar in general chemical composition; however Transect 2 has three wells (San Antonio Water System) that have a significantly reducing environment. This environmental change is most evident by the appearance of methanogenesis, biogenic methane, sulfate reduction and generation of carbon dioxide with enriched  $\delta^{13}\text{C}$ .

Shallow aquifer samples in the Carrizo Sand Formation have a modern age carbon-14. The deepest well samples at the end of the transects have no measurable carbon-14. The ages increase progressively from a few thousand years to about 35,000 years. The chloride concentration is also increasing and without some indication of mixing percentages, a corrected age for these waters cannot be made

The carbon-14 corrected ages (Pearson and White, 1967) values for the Sparta, Queen City and Wilcox Group aquifers range from modern to 35,000 years before present.

## **Discussion**

The geochemical composition of groundwater in each aquifer in the Gonzales Transect is one of two types. The Carrizo Sand Formation portion of the Carrizo-Wilcox and the Queen City aquifers contain waters that have evolved from a mixed cation and mixed anion type water in the outcrop to a sodium-bicarbonate water, some chloride addition in the downdip waters. The water chemistry in these aquifers can be explained by intra-aquifer geochemical reactions (i.e., calcite dissolution and cation exchange, plus other associated reactions). Plus the mixing of sodium-chloride either at shallow depths or in the deepest sections for the aquifers. Cross-formational leakage of waters from other aquifers is not needed to account for the general observed chemistry.

The water chemistry in the Sparta and Yegua-Jackson aquifers are different than the underlying Carrizo Sand Formation and Sparta aquifers. Both these aquifers contain calcium-sodium-chloride-sulfate-bicarbonate waters; they do not show the evolution of sodium-bicarbonate water as observed in the Carrizo Sand Formation and Queen City aquifers. Both the Sparta and Yegua-

Jackson aquifers show linear increases in sodium and chloride. The Yegua-Jackson Aquifer is typically more brackish than the underlying aquifers. The chemistry of these two aquifers does not indicate an upward cross-formational flow.

A comparison of the water chemistry from the three San Antonio Water System nest of wells in the Carrizo Sand Formation, Queen City and Sparta (Gonzales County) aquifers shows the total dissolved solids, the general chemistry (Piper diagrams) and  $\delta^{13}\text{C}$  and carbon-14 percent modern are different for each aquifer in each nest but similar to each aquifer for the three nests. These chemical data do not indicate cross-formational flow.

The carbon-14 corrected ages for the Carrizo Sand Formation shows a continual increase in age from the outcrop where water is considered to be modern to the deepest wells in eastern Gonzales County where the groundwaters contain no measurable carbon-14 and waters may be 40,000 years or older. High concentrations of calcium also occur deep into the Carrizo Sand Formation. The gradual increase in age and gradual decrease in carbon-14 age indicates downdip groundwater flow from outcrop to depths of 3,000 feet. This is contrary to our chemical interpretation in the Central Transect where groundwater flow appears to primarily be in the outcrop and there appears to be less flow into the deep subsurface.

Total dissolved solids concentrations are increasing in the deep subsurface. Most of the increase is related to increases in sodium and bicarbonate though some of the increase is attributable to the addition of sodium-chloride water. The high bicarbonate is attributed to organic carbon maturation. The increase in chloride is attributed to updip migration of saline water from the geopressed zone (Galloway, 1982 and Dutton and others, 2006).

Figure 7-243 and Figure 7-244 display downdip graphical cross sections along the Gonzales Transect, with analytical data posted for sodium and carbon 14 (expressed as percent modern fraction) at the appropriate well locations. Figure 7-243 visually displays increasing trends in sodium with depth which are consistent with cation exchange along the flow path from the outcrop to the confined downdip section of the aquifer, and some mixing with sodium-chloride waters, as previously discussed. This trend is consistent across the Carrizo Sand Formation, the Wilcox Group and the Queen City aquifers. The Sparta and the Yegua-Jackson aquifers do not show the evolution of sodium-bicarbonate water as observed in the Carrizo Sand Formation and Queen City aquifers.

Figure 7-244 visually presents trends of carbon-14 analytical data, expressed as percent modern fraction. The percent modern fraction is an expression of the age of the groundwater; the higher the modern fraction, the younger the groundwater. This figure affirms the conceptual model of the age of groundwater increasing along the flow paths from the outcrop to the confined downdip section. It is noteworthy that in the locations of the San Antonio Water System nested wells, the apparent age of the Queen City Aquifer groundwater is significantly greater than in either the Sparta or the Carrizo Sand Formation aquifers, indicating a longer travel time for a comparable flow path length.

**Table 7-5. Summary of results for the Carrizo Sand Formation portion of the Carrizo-Wilcox Aquifer groundwater age estimates from geochemical modeling<sup>(6)</sup>.**

Model No.	Location Name	Well Internal Well No.	Well Depth (ft)	Cl (mg/L)	Alk (mg/L) <sup>(1)</sup>	$\delta^{13}\text{C}$ ‰ (DIC)	<sup>14</sup> C <sub>OBS</sub> (pmc)	<sup>14</sup> C <sub>OBS</sub> (ybp)	<sup>14</sup> C <sub>ADJ</sub> (ybp) <sup>(2)</sup> <i>Pearson &amp; White (1969)</i>	<sup>14</sup> C <sub>ADJ</sub> (ybp) <i>Mass Balance Transect 1</i>	<sup>14</sup> C <sub>ADJ</sub> (ybp) <i>Mass Balance Transect 2</i>
2	Springs Hill	GUGZ-2	430	20.7	<20	-21.6	87.64	1,060	modern	<sup>(3)</sup>	-
3	CRWA-D	GUGZ-3	428	13.9	<20	-21.6	81.43	1,650	476	<sup>(3)</sup>	-
4	CRWA-E	GUGZ-4	405	20.7	<20	-21.5	81.74	1,620	408	<sup>(3)</sup>	-
6	SSLGC #9	GUGZ-6	1,014	22	20	-21.6	63.88	3,600	2,426	2,041	-
7	SSLGC #4	GUGZ-7	1,310	23.1	68	-18.9	32.45	9,040		8,171	-
13	SAWS CM-2	GUGZ-13	1,575	31.6	64	-15.7	16.18	14,630		-	10,893 <sup>(2,4)</sup>
13-D	SAWS CM-2	GUGZ-13D	1,575	31.6	64	-15.2	16.8	14,330		-	10,333 <sup>(2,4)</sup>
16	SAWS CM-3	GUGZ-16	1,915	34.3	76	-16.2	16.12	14,660		-	11,175 <sup>(2,4)</sup>
19	SAWS CM-4	GUGZ-19	2,175	42.3	116	-18.3	18.65	16,490		-	13,984 <sup>(2,4)</sup>
20	Nixon Well #5	GUGZ-20	1,850	40.8	156	-18.8	10.93	17,780		17,384	-
20-D	Nixon Well #5	GUGZ-20D	1,850	41.4	148	-18.1	10.76	17,910		<sup>(3)</sup>	-
21	Smiley Well #3	GUGZ-21	2,433	43.8	316	-10.7	1.28	35,010		33,176	-
22	L. Lessor	GUGZ-22	2,500	171	340	-6.6	0	>45,000		<sup>(5)</sup>	-
23	Alta Jenkins	GUGZ-23	2,000	203	1,020	-5.2	0	>45,000		<sup>(5)</sup>	-

NOTES:

- (1) Alkalinity as CaCO<sub>3</sub>.
- (2) Correction using Pearson and White (1967) with  $\delta^{13}\text{C}$  soil CO<sub>2</sub> = -25 ‰, and calcite = 0 ‰.
- (3) <sup>14</sup>C correction calculation were not performed because of missing analyses and charge balance errors in the analyses.
- (4) Sample was not modeled using NETPATH because of the large charge imbalance (>10%) and no upgradient wells were sampled.
- (5) Elevated chloride concentrations indicate mixing with a deeper brine of unknown composition.
- (6) A total of 23 wells were sampled for the Gonzales Transect: the 12 wells interpreted as producing from the Carrizo Sand Formation portion of the Carrizo-Wilcox Aquifer are listed in this table. The complete well list with all data is provided in Table 7-4 and Appendix A.
- (7)  $\delta^{13}\text{C}$  ‰ is a measure of the ratio of stable isotope carbon-13 to carbon-12.

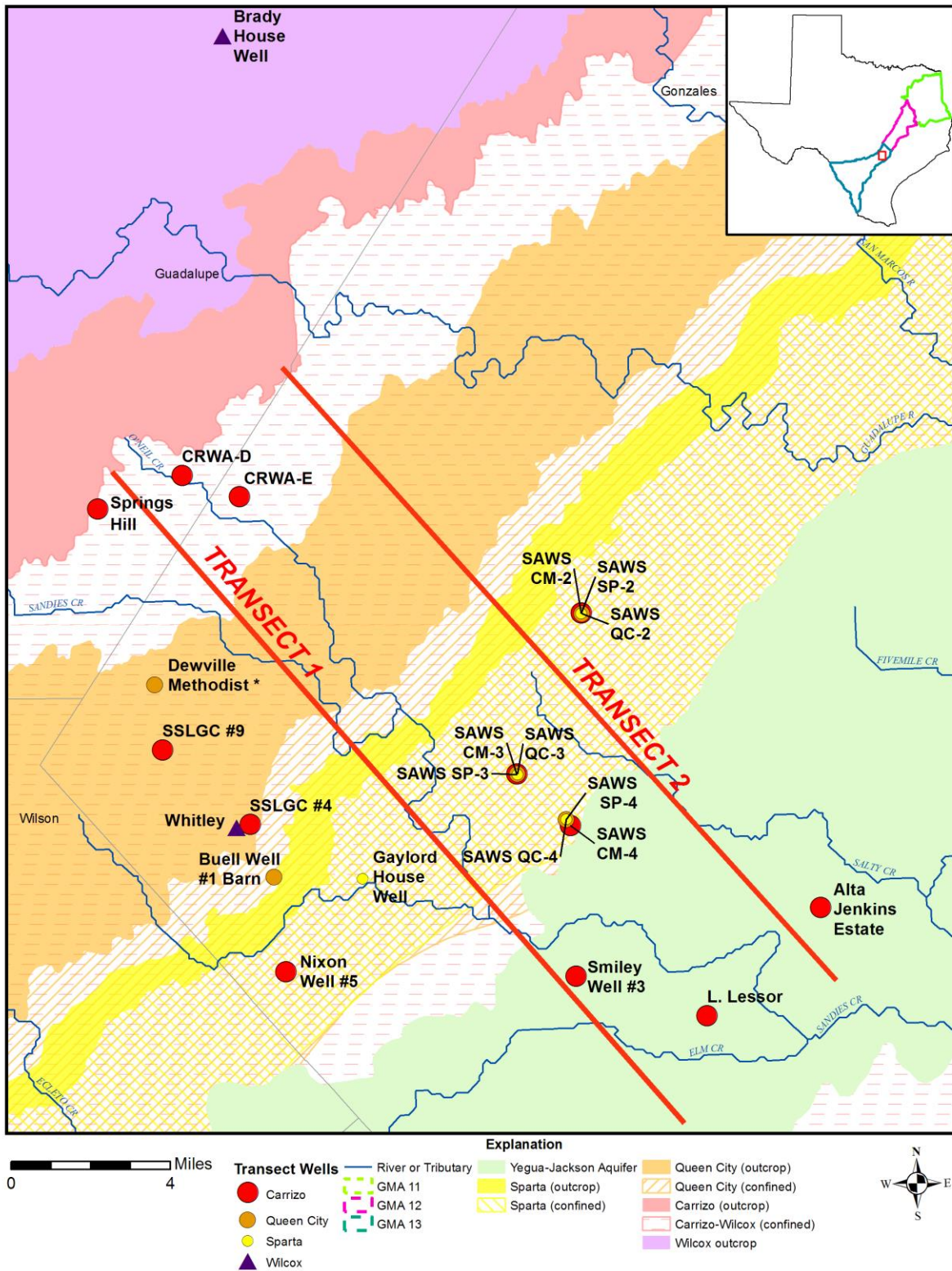


Figure 7-231. Gonzales Transect sampled well locations, Groundwater Management Area (GMA) 13.



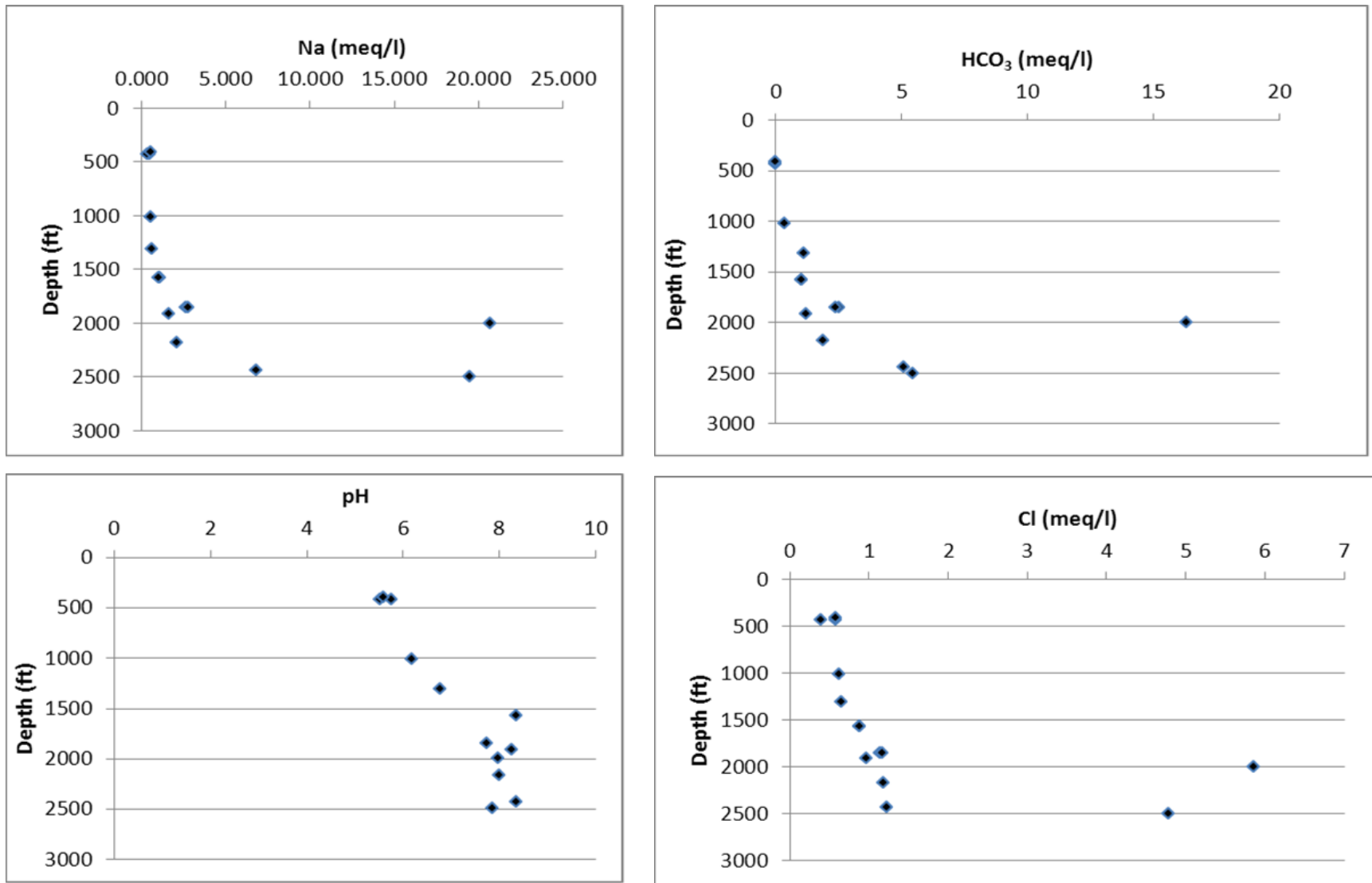


Figure 7-233. Regional compositional changes in the Carrizo Sand Formation portion of the Carrizo-Wilcox Aquifer using the existing TWDB database.

Evaluation of Hydrochemical and Isotopic Data in Groundwater Management Areas 11, 12 and 13

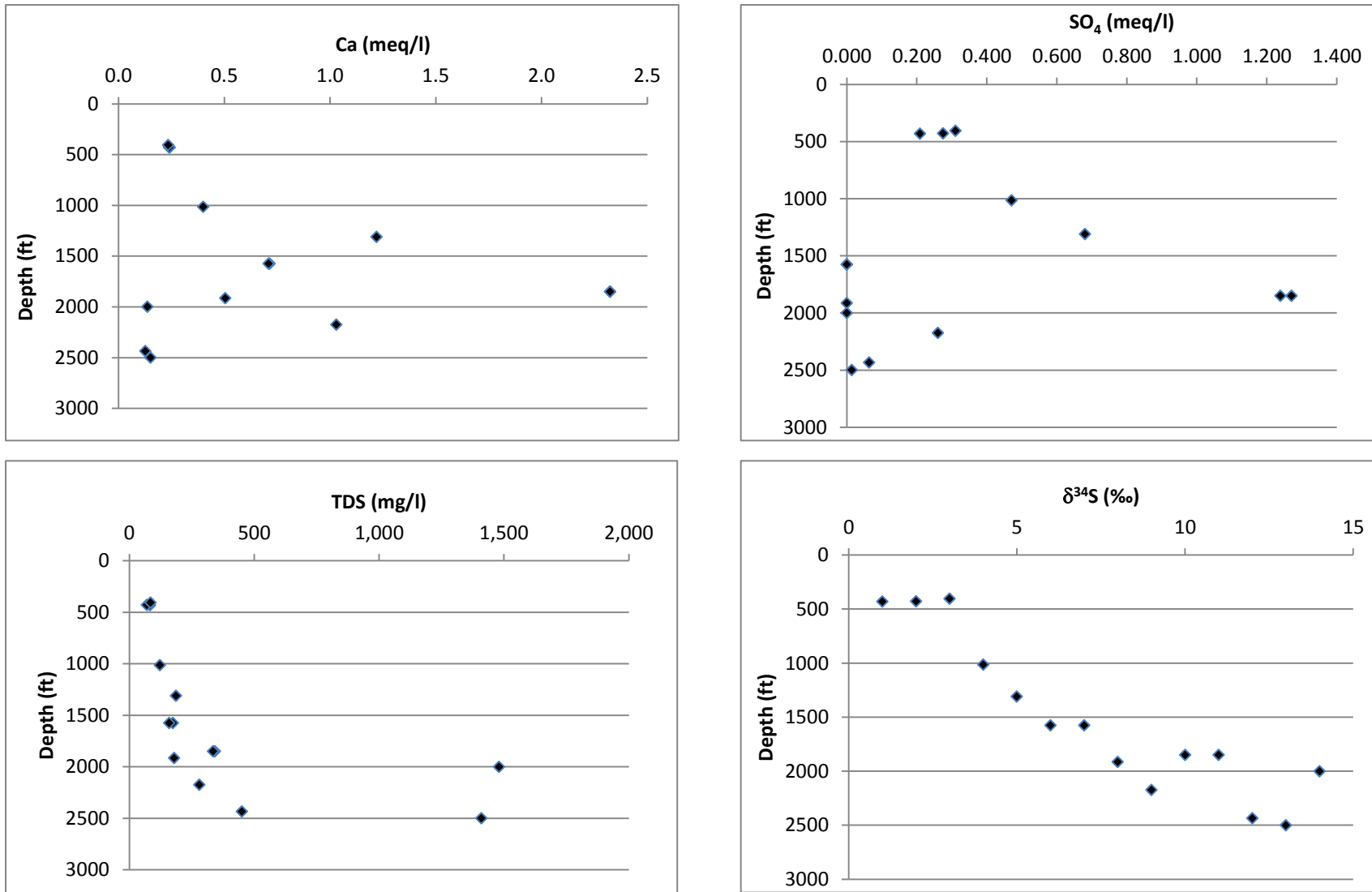


Figure 7-234. Regional compositional changes in the Carrizo Sand Formation portion of the Carrizo-Wilcox Aquifer using the existing TWDB database.

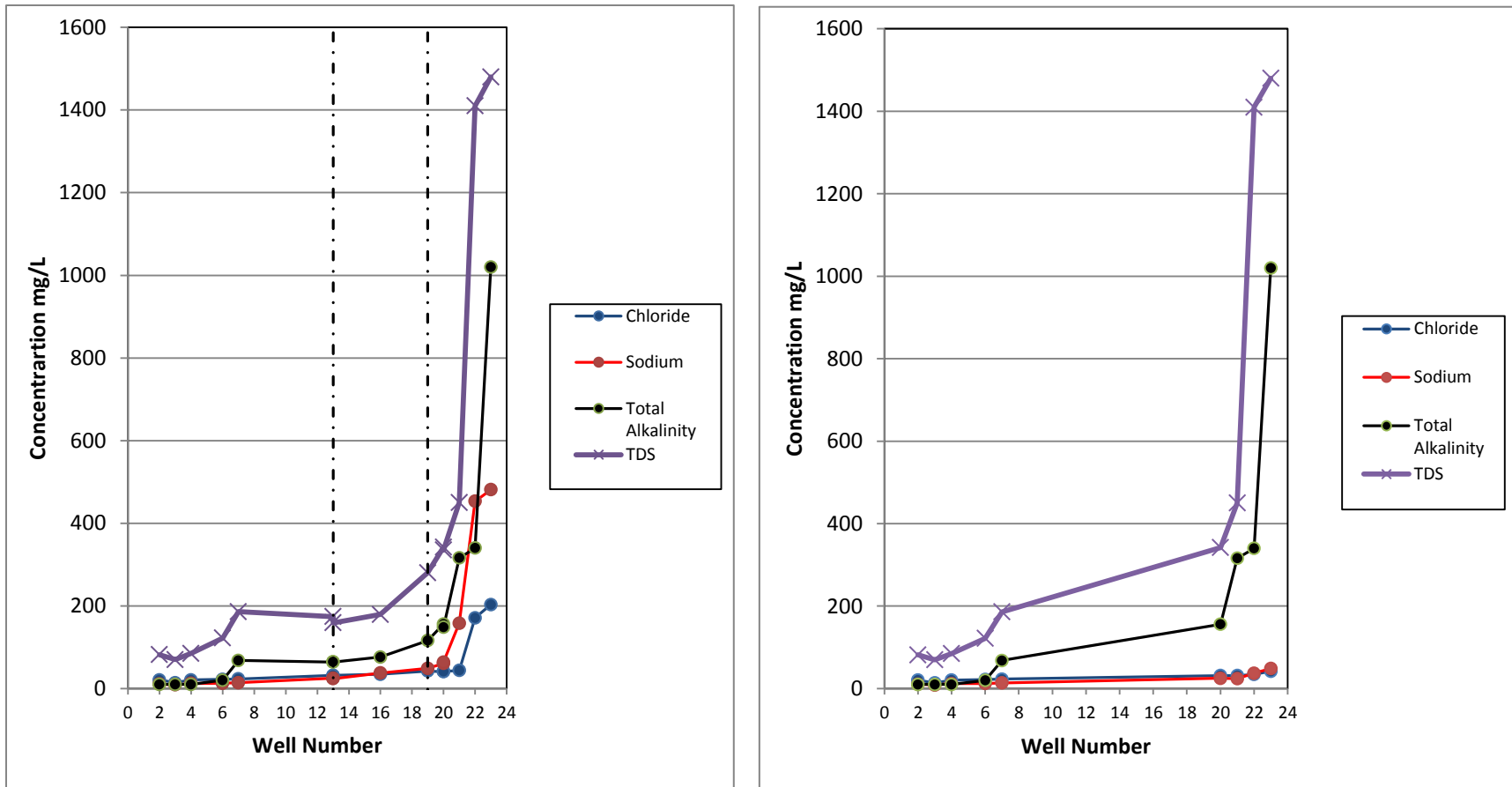


Figure 7-235. Anion concentrations along Transect 1 that includes Transect 2 wells indicated by the region between the dashed lines with (left) and excluded Transect 2 wells (right).

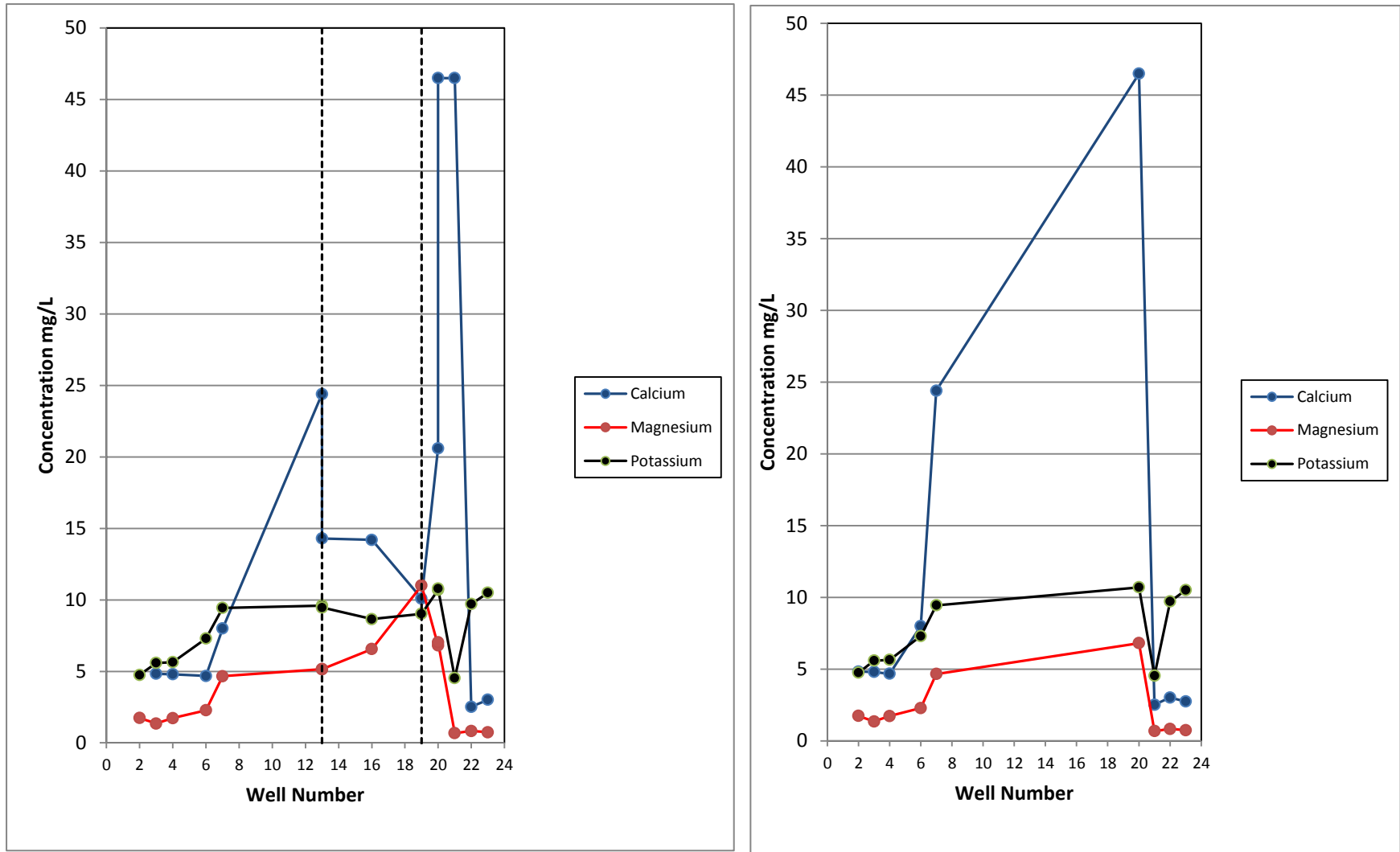


Figure 7-236. Cation concentrations along Transect 1 that in the first case includes the Transect 2 wells indicated by the region between the dashed lines (left) and excludes the Transect 2 wells (right).

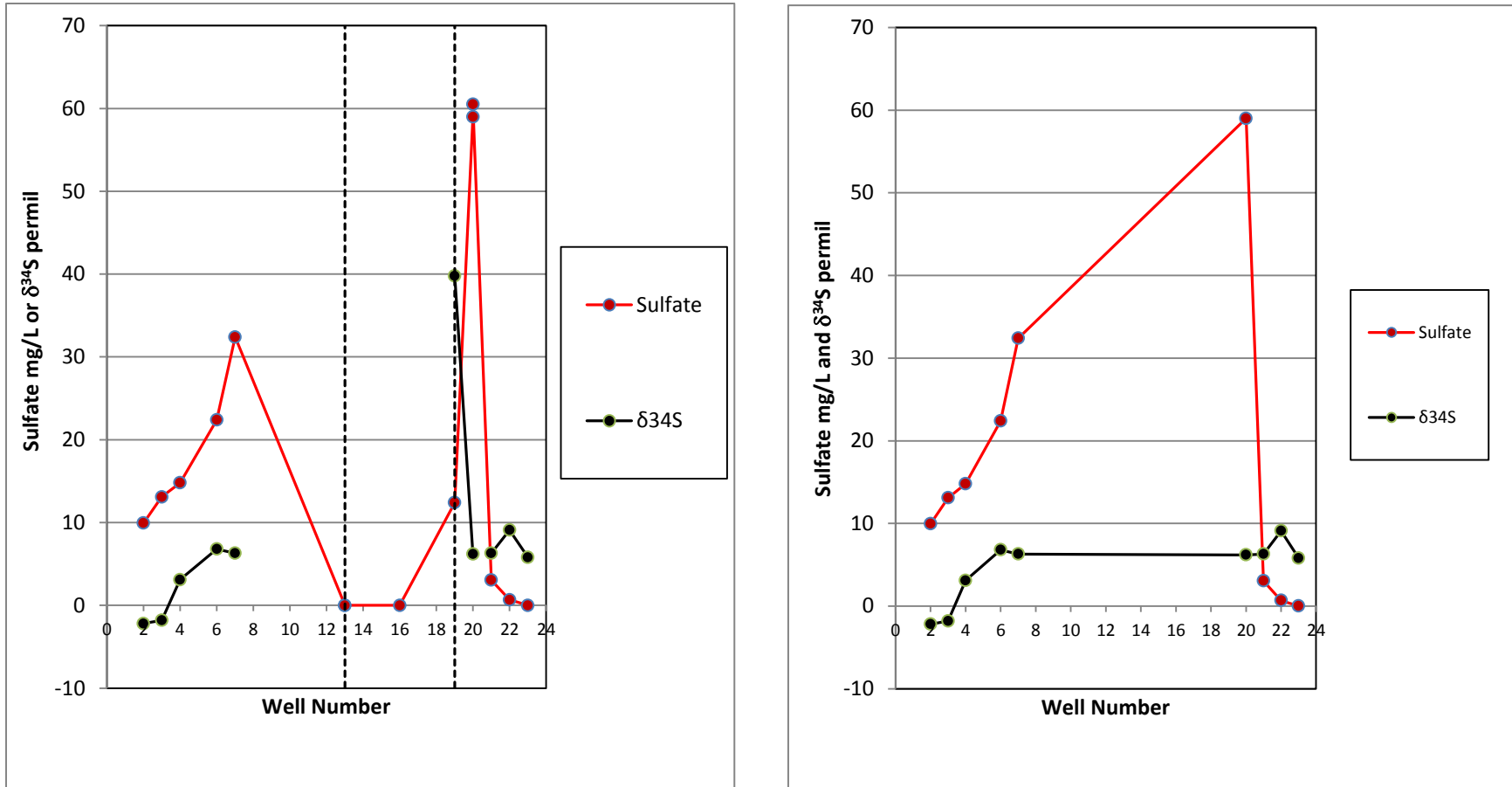


Figure 7-237. Sulfate concentrations and sulfur isotope values along the profile by well with (left) and without (right) Transect 2 wells.

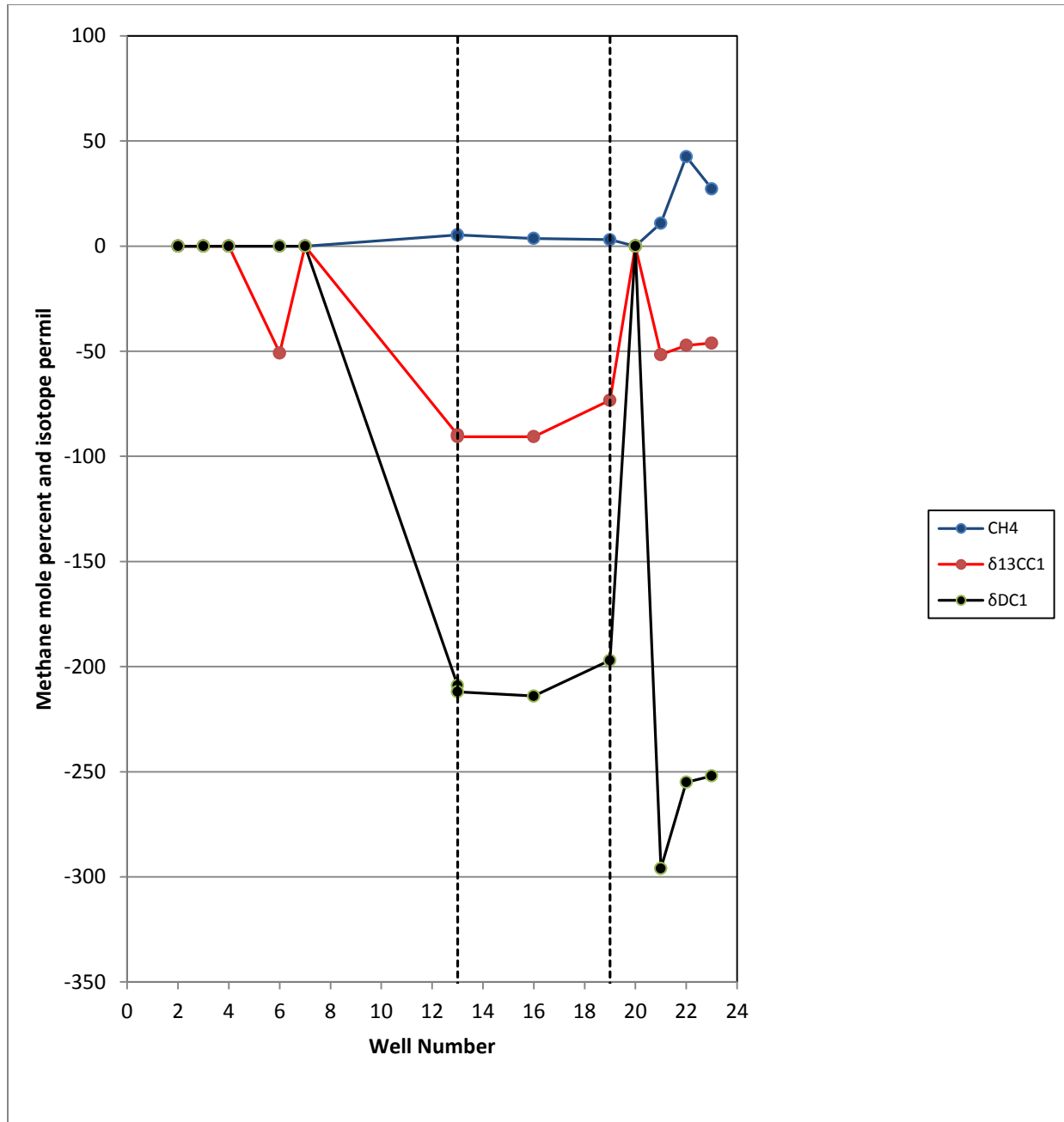


Figure 7-238. Methane mole percent of dissolved gas and the methane isotopic values.

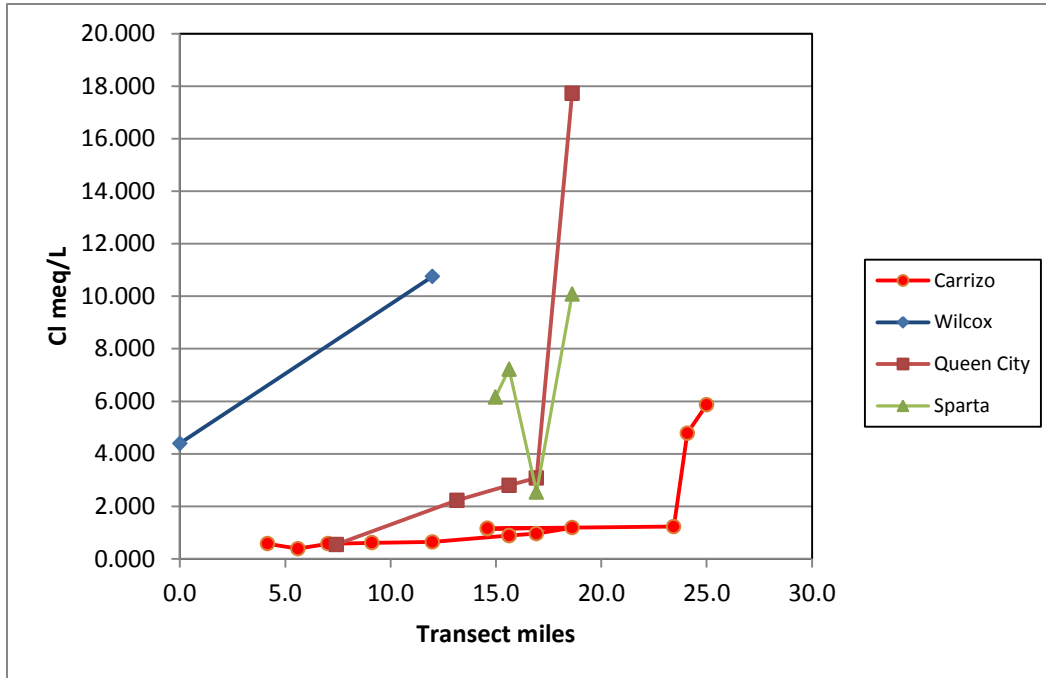


Figure 7-239. Chloride (Cl) concentration measured in milliequivalents per liter (meq/L) in all four aquifers with transect distance from model well number 1 (Wilcox Group recharge area).

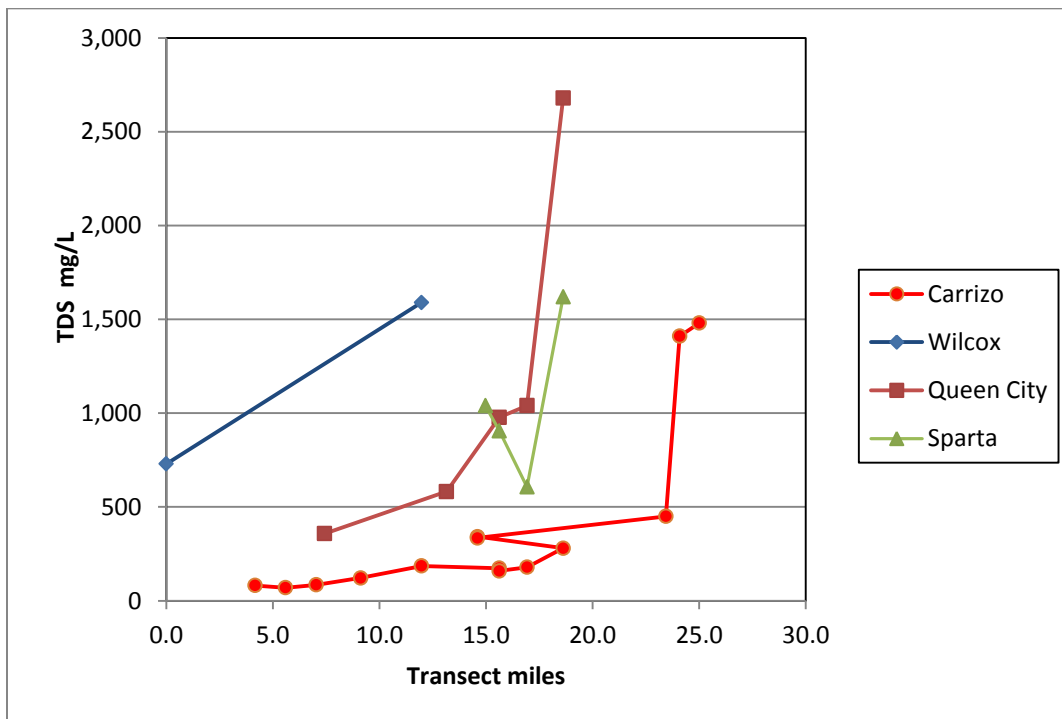


Figure 7-240. The comparison of total dissolved solids (TDS) measured in milligrams per liter (mg/L) content with transect distance among the four aquifers in the transect.

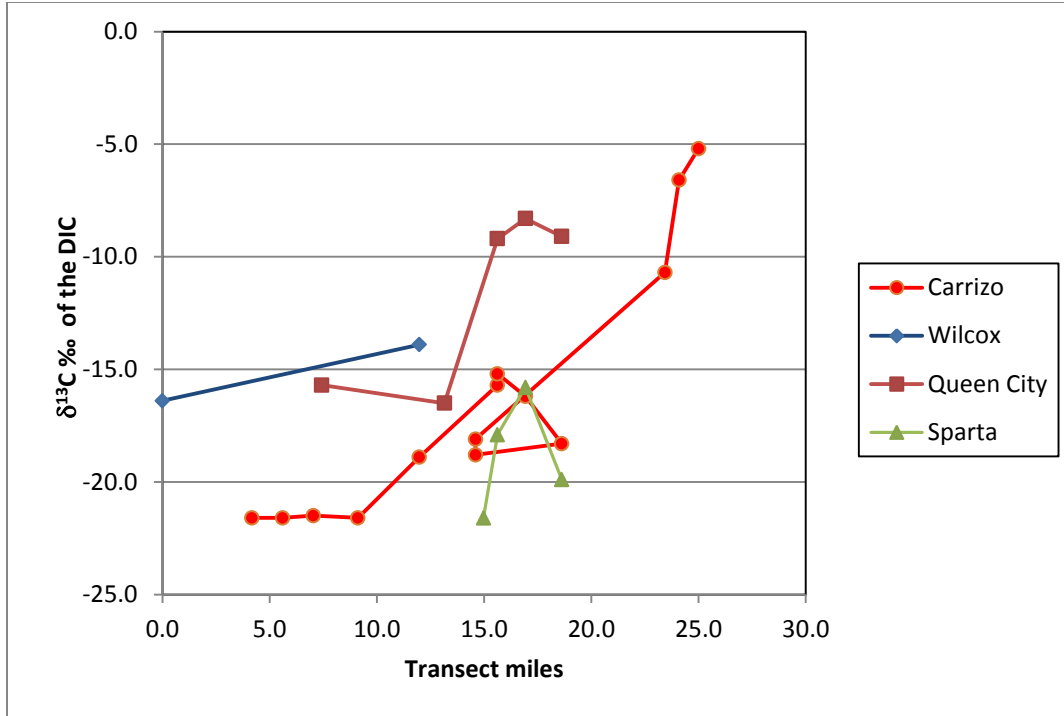


Figure 7-241. The comparison of  $\delta^{13}\text{C}$  of the total dissolved carbon with transect distance among the four aquifers in the transect.

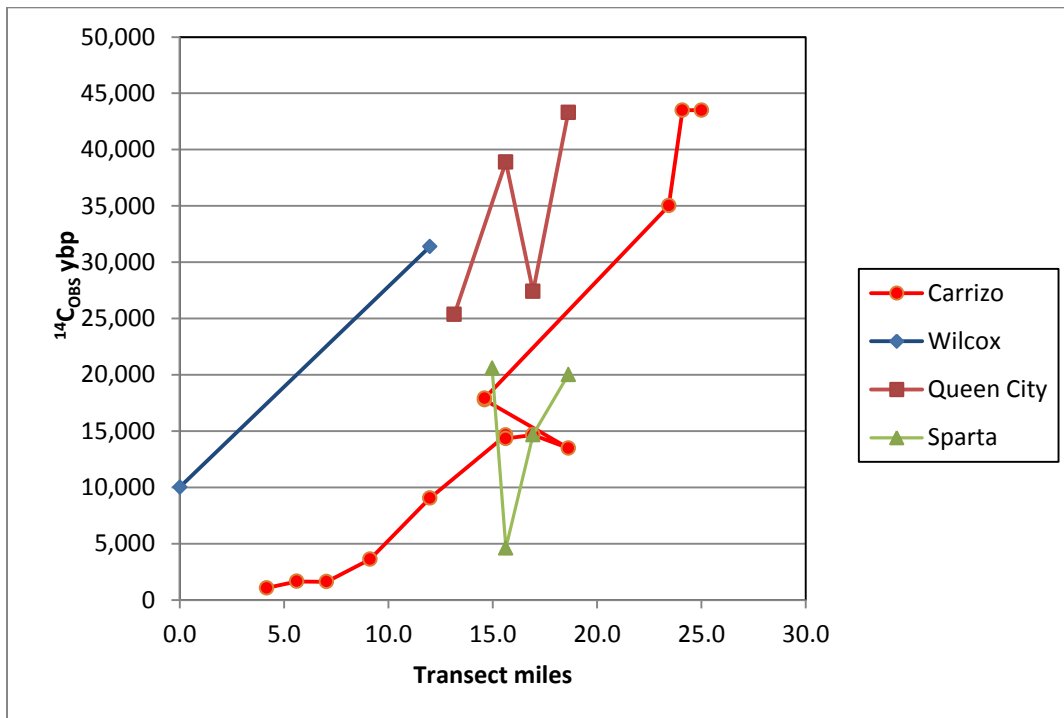


Figure 7-242. The comparison of  $^{14}\text{C}_{\text{OBS}}$  years before present of total dissolved carbon with transect distance among the four aquifers in the transect (compare with Table 7-5 and Table 7-6 for  $^{14}\text{C}_{\text{ADJ}}$ ).

**Table 7-6. Summary of results for the Queen City and Sparta aquifer groundwater age estimates.**

Model No.	Location Name	TWDB Well No.	Well Depth (ft)	Cl (mg/L)	Alk (mg/L) <sup>(1)</sup>	$\delta^{13}\text{C}$ ‰ (DIC)	<sup>14</sup> C <sub>OBS</sub> (pmc)	<sup>14</sup> C <sub>OBS</sub> (ybp)	<sup>14</sup> C <sub>ADJ</sub> (ybp) <sup>(2)</sup> <i>Pearson &amp; White (1967)</i>
Sparta Aquifer									
10	Gaylord Hse	GUGZ-10	335	220	136	-21.6	7.72	20,580	19,406
11	SAWS-SP2	GUGZ-11	160	258	84	-17.9	56.26	4,620	1,936
14	SAWS-SP3	GUGZ-14	315	91	188	-15.8	16.08	14,680	10,994
17	SAWS-SP4	GUGZ-17	515	360	480	-19.9	8.29	20,000	18,167
Queen City Aquifer									
5	Dewville	GUGZ-5	128	19.5	236	-15.7	modern	modern	modern
9	Buell	GUGZ-9	310	80	244	-16.5	4.26	23,350	20,012
12	SAWS-QC2	GUGZ-12	585	100	388	-9.2	0.79	38,890	30,860
15	SAWS-QC3	GUGZ-15	769	110	500	-8.3	3.31	27,390	18,533
18	SAWS-QC4	GUGZ-18	1005	633	1040	-9.1	0.46	43,300	35,182

**NOTES:**

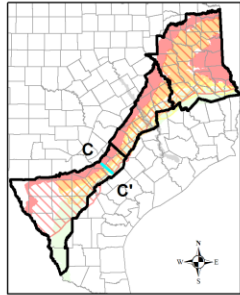
 (1) Alkalinity as CaCO<sub>3</sub>.

 (2) Correction using Pearson and White (1967) with  $\delta^{13}\text{C}$  soil CO<sub>2</sub> = -25 ‰, and calcite = 0 ‰.

 (3) <sup>14</sup>C correction calculation could not be performed because of missing analyses and charge balance errors in the analyses.

(4) Sample was not modeled using NETPATH because of the large charge imbalance (&gt;10%) and no upgradient wells were sampled.

(5) Elevated chloride concentrations indicate mixing with a deeper brine of unknown composition.



### Profile C-C' Showing Sodium (meq/L) at Recorded Well Depth GMA 13

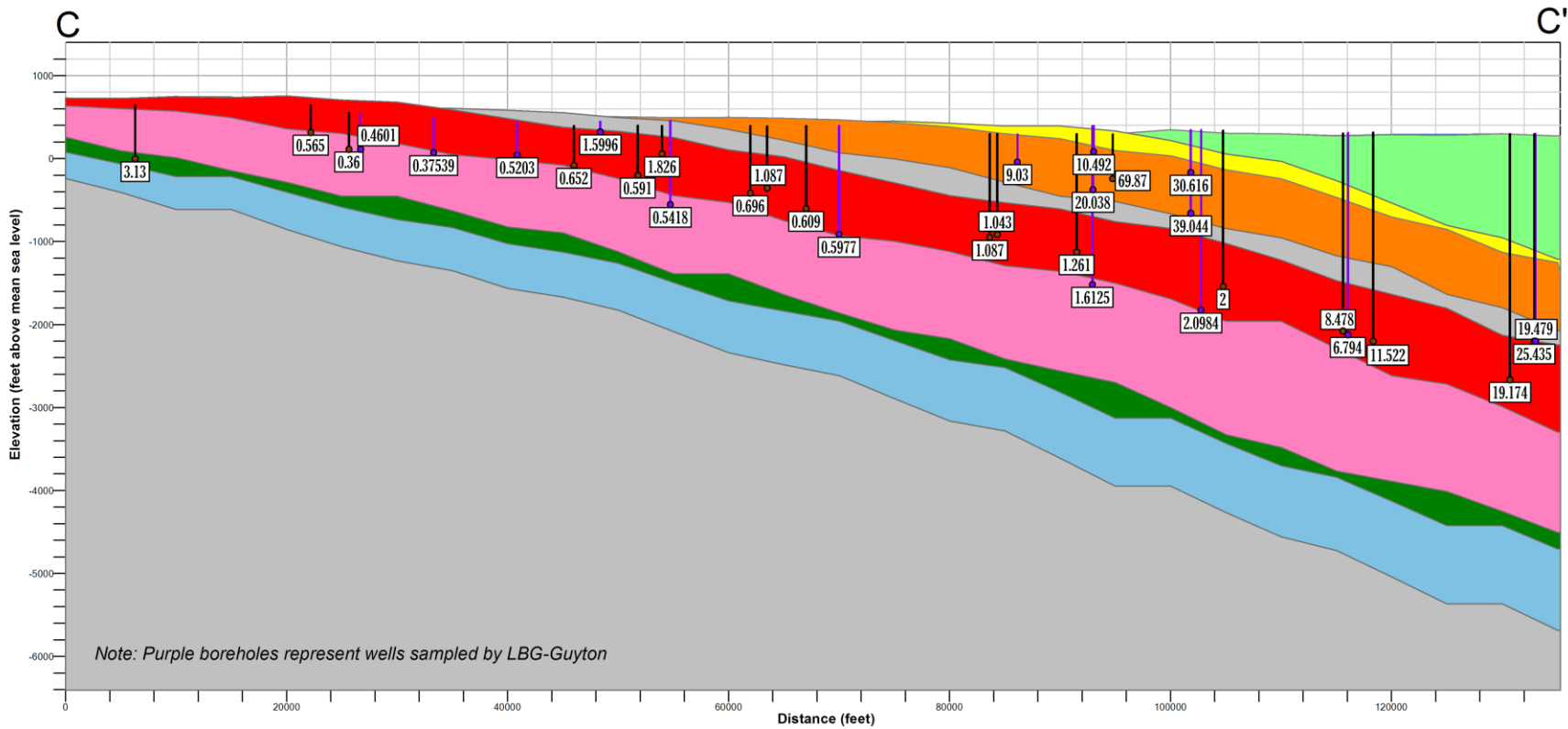
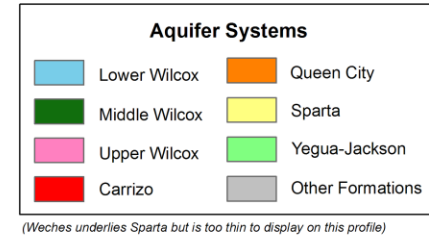


Figure 7-243. Gonzales Transect cross section with sodium analytical data.

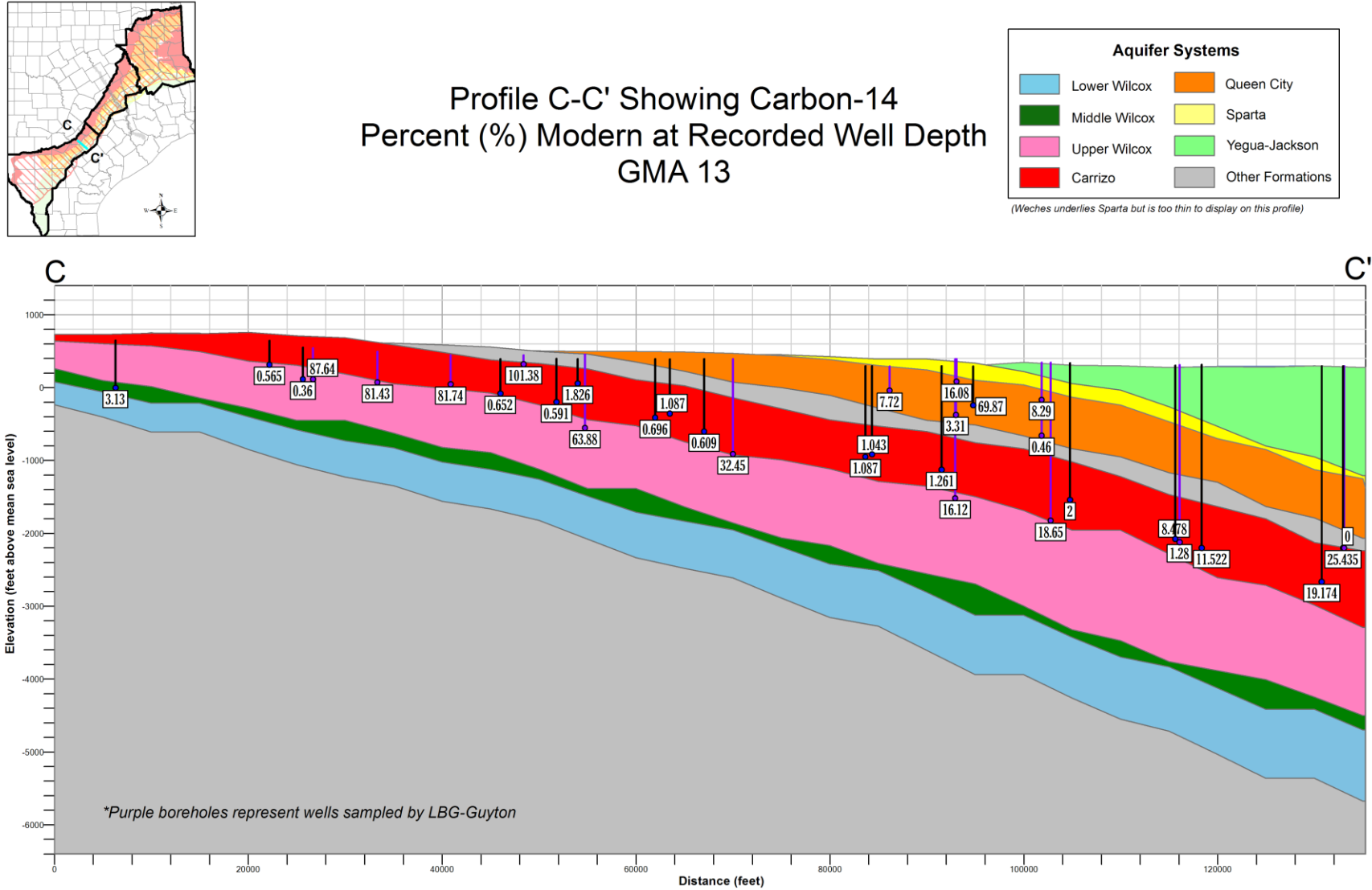


Figure 7-244. Gonzales Transect cross section with carbon-14 analytical data.

## 7.4 South Transect

An excellent database from the TWDB exists for water wells, water chemistry and water levels in the Carrizo-Wilcox, Queen City, Sparta and Yegua-Jackson aquifers in Bexar, Atascosa and McMullen counties. The locations of wells in the TWDB database are shown in Figure 7-245. No new (2012) data were collected in this transect area. Pearson (1966) and Pearson and White (1967) conducted research of age dating of groundwater in the Carrizo Sand Formation portion of the Carrizo-Wilcox Aquifer in Bexar, Atascosa and McMullen counties.

### 7.4.1 General Geochemical Trends

#### **Carrizo Sand Formation portion of the Carrizo-Wilcox Aquifer**

The Carrizo Sand Formation is the primary aquifer in southern Bexar, Atascosa and McMullen counties. The Carrizo Sand Formation is the fresh water section of the Carrizo-Wilcox Aquifer in south Texas. The Wilcox Group is typically brackish even in the outcrop. The most extensive groundwater database for this area is primarily for the Carrizo Sand Formation. The distribution of data for the Carrizo Sand Formation is shown in Figure 7-246.

#### Well Depths

Based on Figure 7-246, a dip oriented transect for the three counties, water wells in the outcrop are less than 1,000 feet in southern Bexar and northern Atascosa counties to well depths greater than 5,000 feet in McMullen County.

#### Potentiometric Surface

The Carrizo Sand Formation potentiometric surface (Figure 7-247) for the three county transect shows most recent water levels for each well in southern Bexar County are at an average of about 500 feet. Water levels decline to about 300 feet in Atascosa County and are as low as 140 feet to 200 feet in McMullen County. This dips from north to south down the structured dip of the Carrizo Sand Formation. Groundwater therefore flows from the outcrop in Bexar County into the deep subsurface.

A set of faults partially offset the Carrizo Sand Formation portion of the Carrizo-Wilcox Aquifer along the Charlotte, Jourdanton and Pleasanton Trough (Figure 7-248) (Hargis, 2009). As shown in this figure, this set of faults forms a graben between the upthrown and downthrown blocks in the area. This graben (Figure 7-246) may impede down gradient flow in the Carrizo Sand Formation. Hargis (2009) shows displacements on individual faults up to 100 feet.

#### Piper Diagram

The Piper diagram for the Carrizo Sand Formation in the South Transect (Figure 7-249) shows mixed (calcium-sodium) cation composition at shallower depths in southern Bexar and northern Atascosa counties evolving to a sodium-bicarbonate as well depths increase from about 2,000 to 3,000 feet to depths greater than 5,000 feet.

#### Bicarbonate versus Sodium Plot

A plot of bicarbonate versus sodium (Figure 7-250) for the TWDB data shows two trends. For bicarbonate values from zero to five milliequivalents per liter, bicarbonate increases independent of sodium. From bicarbonate concentrations greater than about five milliequivalents per liter, bicarbonate and sodium are at a ratio of about 1:1.

### Sodium versus Calcium Plot

A plot of sodium versus calcium for the TWDB data (Figure 7-251) shows an inverse relationship between sodium and calcium. At low concentrations of sodium, calcium appears independent of sodium. The trend shifts at higher sodium, such that sodium increases independent of calcium.

### Bicarbonate versus Calcium Plot

A plot of bicarbonate versus calcium (Figure 7-252) for the TWDB data shows a distribution similar to the sodium versus calcium plot (Figure 7-251), but with an interesting difference. Calcium and bicarbonate appear to increase linearly to about four to five milliequivalents per liter and then calcium decreases to zero. At bicarbonate concentrations greater than six milliequivalents per liter, bicarbonate concentrations increase independent of calcium to 20 milliequivalents per liter.

### pH versus Bicarbonate Plot

The plot of pH versus bicarbonate (Figure 7-253) shows three trends. pH rises from less than five with very low bicarbonate from pH seven to eight, bicarbonate rises to about seven milliequivalents per liter above bicarbonate concentrations of seven and bicarbonate increases independent of pH to bicarbonate values greater than 30 milliequivalents per liter.

### pH versus Sodium Plot

The plot of pH versus sodium (Figure 7-254) shows a similar distribution of data to the pH versus bicarbonate graph (Figure 7-253).

### Sulfate versus Bicarbonate Plot

The plot of sulfate versus bicarbonate (Figure 7-255) shows two trends: 1) higher sulfate values at bicarbonate concentrations and 2) bicarbonate increasing independent of sulfate for bicarbonate values greater than about 12 milliequivalents per liter.

### Chloride versus Sodium Plot

The plot of chloride versus sodium (Figure 7-256) shows two trends: 1) sodium increasing independent of chloride and 2) sodium and chloride increasing at approximately 1:1 ratio.

### Chloride versus Bicarbonate Plot

The plot of chloride versus bicarbonate (Figure 7-257) shows three trends: 1) bicarbonate increases independent to chloride for bicarbonate concentrations ranging from zero up to about seven milliequivalents per liter, 2) chloride increases for bicarbonate concentrations greater than about seven and 3) higher random concentrations of chloride for bicarbonate concentrations less than ten milliequivalents per liter.

### Depth versus Sulfate Plot

The plot of depth versus sulfate (Figure 7-258) shows the highest sulfate concentrations at the shallowest depths and then declining to the lowest concentrations at depths greater than 5,000 feet.

### Depth versus Calcium Plot

The plot of depth versus calcium (Figure 7-259) shows the highest concentrations of calcium at the shallowest depths (less than 1,000 feet). Calcium concentrations remain high to depth of about 3,000 feet. Calcium concentrations below 3,000 feet are very low.

### Map of Calcium

Calcium concentration (Figure 7-260) in the Carrizo Sand Formation does not decline to very low concentrations until the middle of Atascosa County. This is the approximate locations of Hargis (2009) faulting in the Carrizo Sand Formation (Figure 7-246). Offsets created by the faulting of the Carrizo Sand Formation may limit the downdip flow in the Carrizo Sand Formation and, therefore inhibit distribution of calcium by advection to the southeast.

### Depth versus Sodium Plot

The plot of depth versus sodium (Figure 7-261) shows a trend of increasing sodium at depths greater than about 2,500 feet. This increase occurs approximately at the same depth as the decrease in calcium with depth (Figure 7-259).

### Depth versus Bicarbonate Plot

The plot of depth versus bicarbonate (Figure 7-262) shows bicarbonate increases with depth in three steps. Bicarbonate remains low at depths below 1,000 feet. A second step occurs between 1,000 to 3,000 feet where bicarbonate concentrations are approximately five milliequivalents per liter. A third step occurs from 3,000 feet to depths greater than 5,000 feet, bicarbonate continues to increase.

### Map of Bicarbonate

A map of bicarbonate (Figure 7-263) shows low bicarbonate values occur in the outcrop and consistently increase to much higher values in McMullen County.

### Depth versus pH Plot

The plot of depth versus pH (Figure 7-264) shows a general increase in pH with depth.

### Map of pH

A map of pH (Figure 7-265) in the Carrizo Sand Formation shows a consistent increase in pH with greater depth.

### Map of Sodium

A map of sodium (Figure 7-266) shows low concentrations in the Carrizo Sand Formation in most of Atascosa County. Sodium increases significantly in McMullen County.

### Depth versus Chloride Plot

The plot of depth versus chloride (Figure 7-267) shows two trends: 1) a shallow trend and 2) increasing chloride at depths greater than about 3,000 feet.

### Map of Chloride

A map of chloride (Figure 7-268) shows a shallow trend of higher values are primarily in northern Atascosa County. The deeper high chloride waters are along the downdip extent of deep wells in McMullen County.

### Depth versus Total Dissolved Solids Plot

The plot of depth versus total dissolved solids (Figure 7-269) shows several trends. At depths less than 1,000 feet, total dissolved solids can be variable. Either total dissolved solids can be very high or be gradually increasing. From about 750 feet to about 3,500 feet total dissolved solids continues to increase gradually. From depth greater than about 3,500 feet, total dissolved solids increases significantly. Much of the increase in total dissolved solids with depth is from increases in sodium and bicarbonate (Figure 7-261 and Figure 7-262) and not chloride (Figure 7-267).

### Map of Total Dissolved Solids

A map of total dissolved solids (Figure 7-270) shows a general increase from the outcrop in northern Bexar County to central McMullen County where the highest total dissolved solids values occur.

### Discussion

Groundwater in the Carrizo Sand Formation in the South Transect is recharged in the outcrop and flows into the deeper subsurface. The groundwater chemistry evolves from mixed calcium-sodium and sulfate-chloride water in the outcrop to a sodium-bicarbonate with some chloride and no sulfate down gradient. The earlier part of the flow system is not dominated by a sodium-bicarbonate water. This only occurs deeper in the aquifer. The implication is that there is minimal sodium-Montmorillonite in the Carrizo Sand Formation outcrop to provide exchange sites to replace the dissolved calcium with sodium. Figure 7-252, the plot of bicarbonate versus calcium shows three trends: 1) a linear increase in calcium and bicarbonate from about 0.5 milliequivalents per liter to about five milliequivalents per liter, 2) decreases in calcium with increases in sodium and 3) increases in sodium independent of calcium. In stage one, calcite is being dissolved. In stage two, calcium is being exchanged for sodium in an initial phase. In stage three, sodium becomes dominant by cation exchange. The downdip extent of high calcium waters appears to coincide with the Charlotte, Jourdanton and Pleasanton Trough. This faulting in the Carrizo Sand Formation may create a partial barrier to downdip flow in the Carrizo Sand Formation. The increase in bicarbonate with no change in pH suggests that coalification or organics in the deeper parts of the aquifer is an additional source of bicarbonate. Some higher chloride concentrations in the deepest parts of the Carrizo Sand Formation suggest that a saline source of water is leaking into the aquifer. The increase in salinity is compared to the total dissolved solids values greater 1,000 milligrams per liter; however it is primarily from bicarbonate and not chloride. The increase in salinity that is often mapped for these upper coastal plain aquifers is inferred to represent the downdip extent of meteoric outcrop recharge groundwater. This may be incorrect. Meteoric groundwater may extend much further downdip in the high transmissivity sands, such as the Carrizo Sand Formation, than had previously been interpreted (e.g., Dutton and other, 2009).

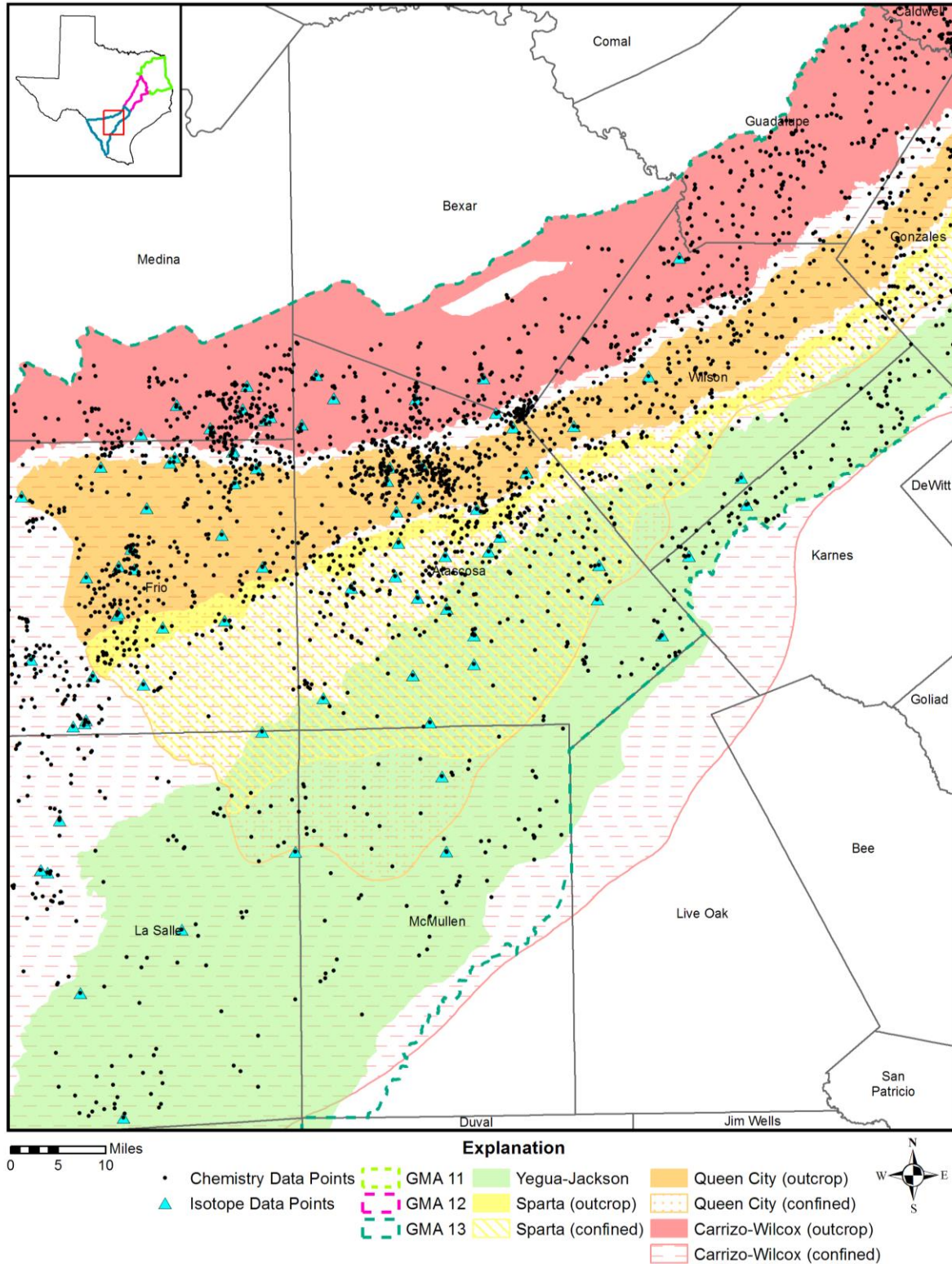


Figure 7-245. Data distribution of wells with outcrop and downdip extent (up to 3,000 milligrams per liter total dissolved solids) of the Carrizo Sand Formation portion of the Carrizo-Wilcox Aquifer, Queen City, Sparta and Yegua-Jackson aquifers in the South Transect.

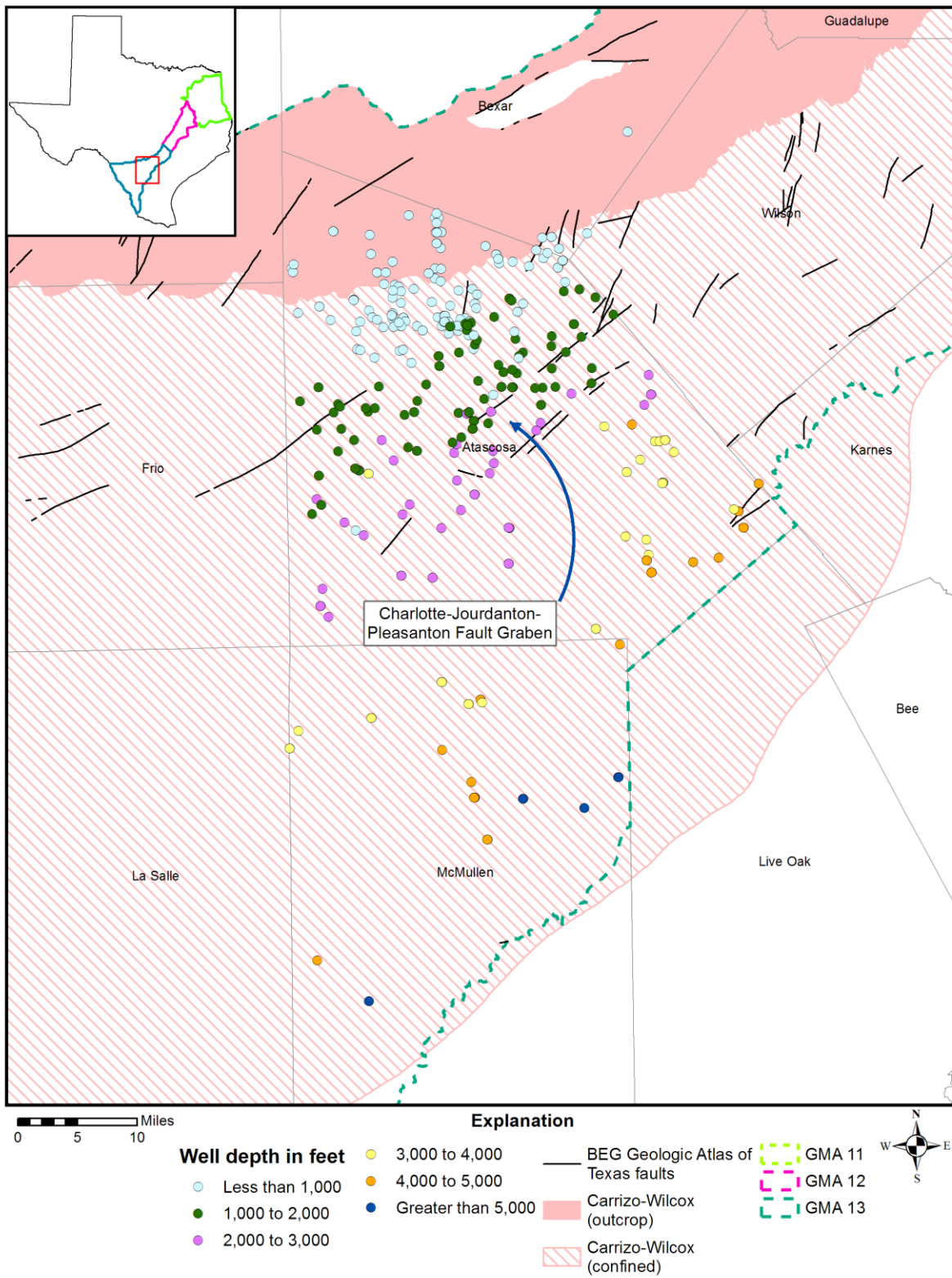


Figure 7-246. Well depths measured from land surface in feet in the Carrizo Sand Formation portion of the Carrizo-Wilcox Aquifer, South Transect, Groundwater Management Area (GMA) 13.

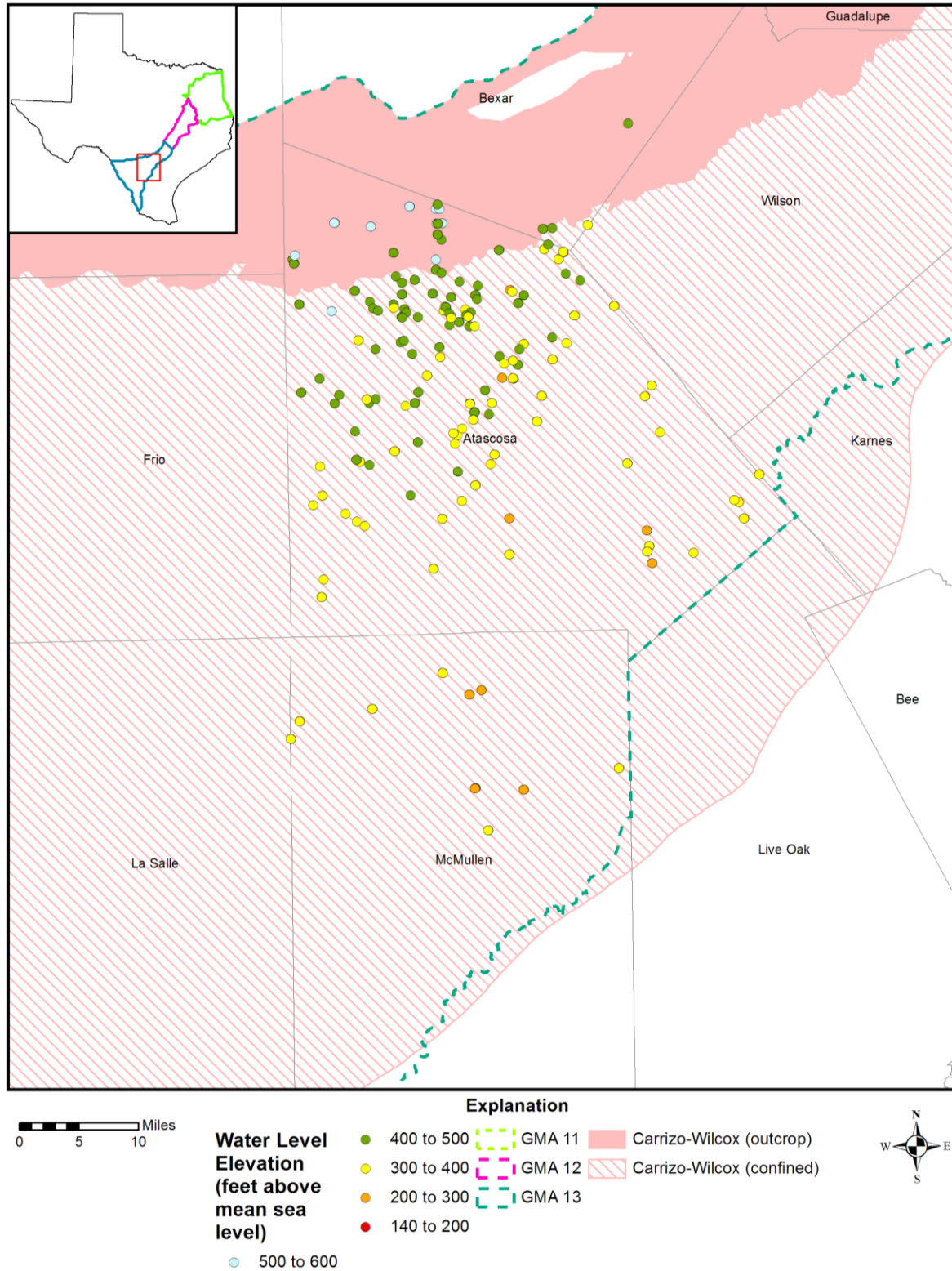


Figure 7-247. Water level elevations from 1929 to 2010 measured in feet above mean sea level (ft AMSL) in the Carrizo Sand Formation portion of the Carrizo-Wilcox Aquifer, South Transect, Groundwater Management Area (GMA) 13.

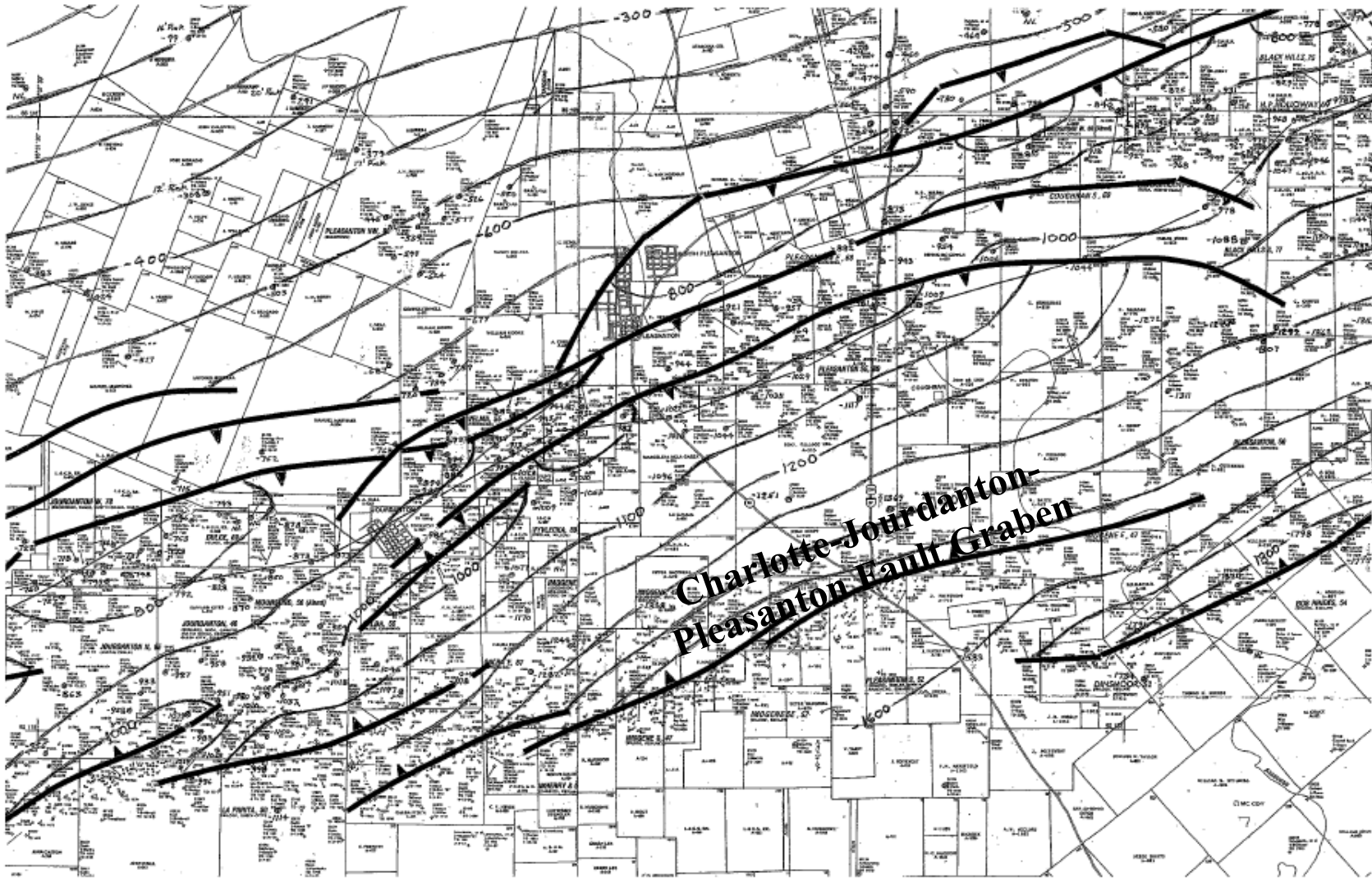


Figure 7-248. Carrizo Sand Formation portion of the Carrizo-Wilcox Aquifer faults in Charlotte, Jourdanton and Pleasanton Trough, Atascosa County, Texas (from Hargis, 2009).

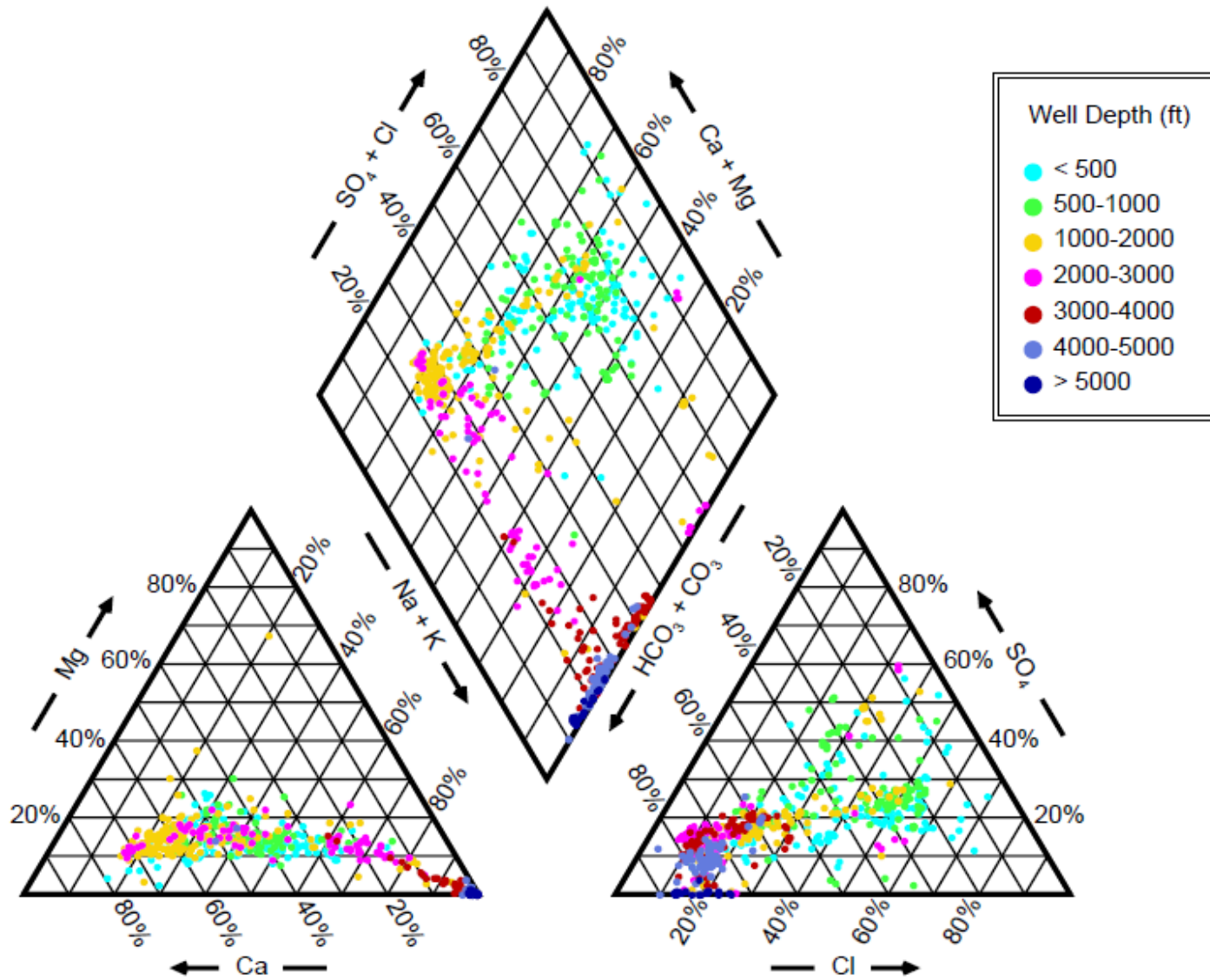


Figure 7-249. Piper diagram showing chemistry of the Carrizo Sand Formation portion of the Carrizo-Wilcox Aquifer wells in the South Transect by well depth measured from land surface in feet (ft).

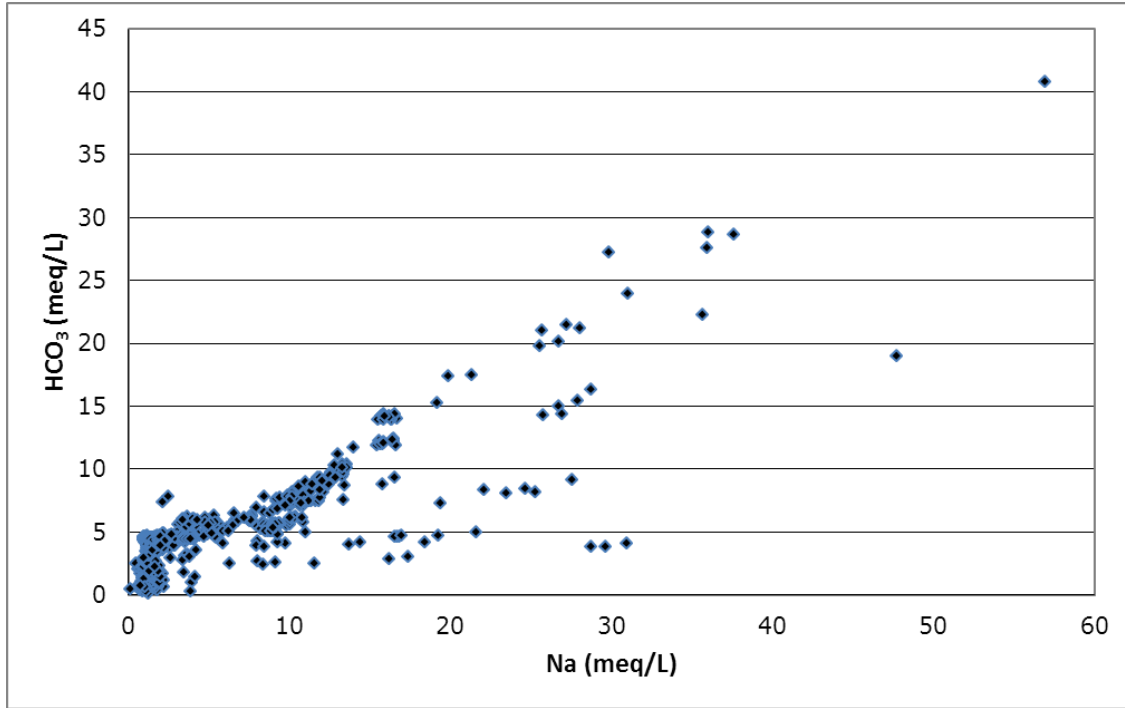


Figure 7-250. Bicarbonate (HCO<sub>3</sub>) versus sodium (Na) measured in milliequivalents per liter (meq/L), Carrizo Sand Formation portion of the Carrizo-Wilcox Aquifer, South Transect, Groundwater Management Area 13.

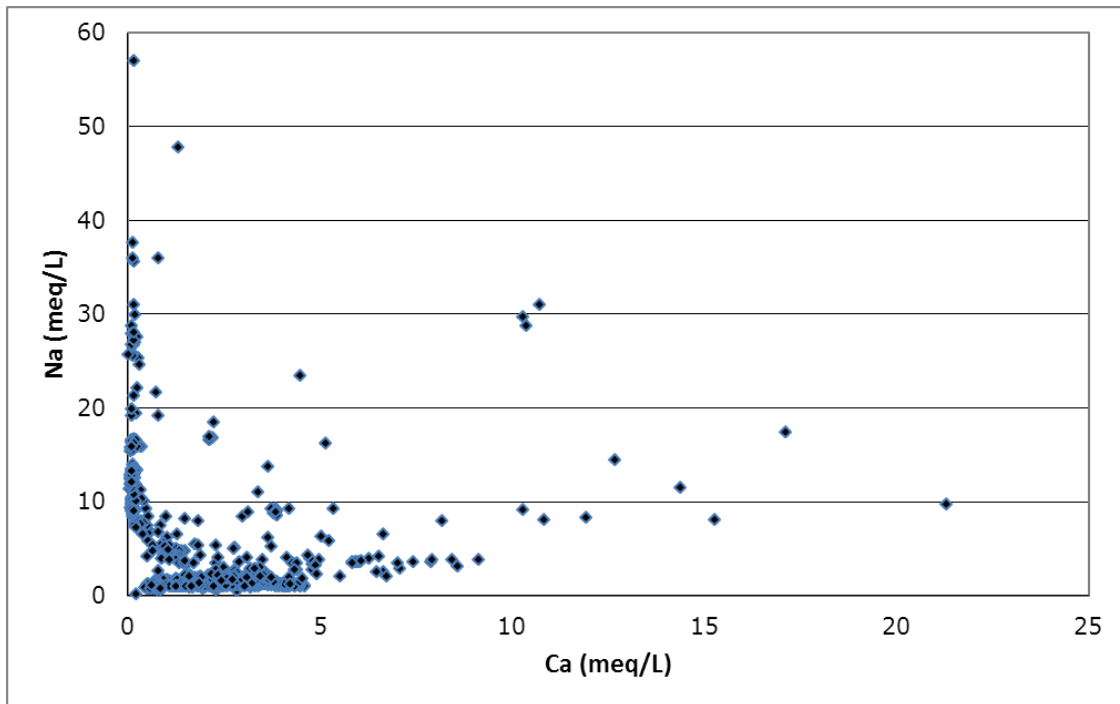


Figure 7-251. Sodium (Na) versus calcium (Ca) measured in milliequivalents per liter (meq/L), Carrizo Sand Formation portion of the Carrizo-Wilcox Aquifer, South Transect, Groundwater Management Area 13.

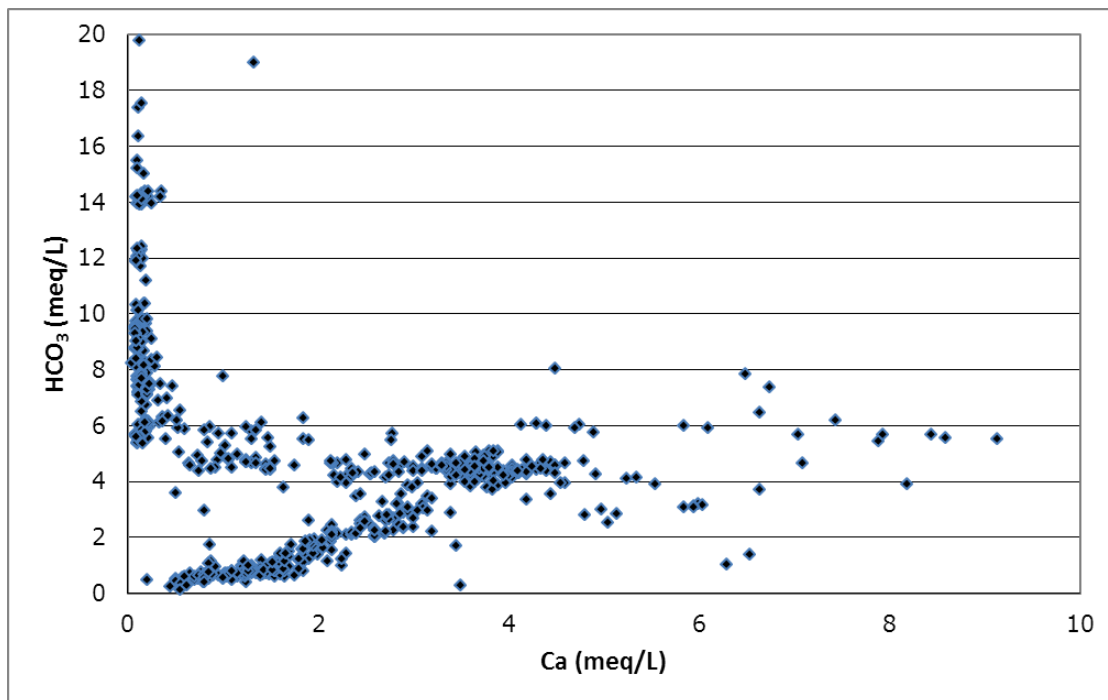


Figure 7-252. Bicarbonate ( $\text{HCO}_3$ ) versus calcium (Ca) measured in milliequivalents per liter (meq/L), Carrizo Sand Formation portion of the Carrizo-Wilcox Aquifer, South Transect, Groundwater Management Area 13.

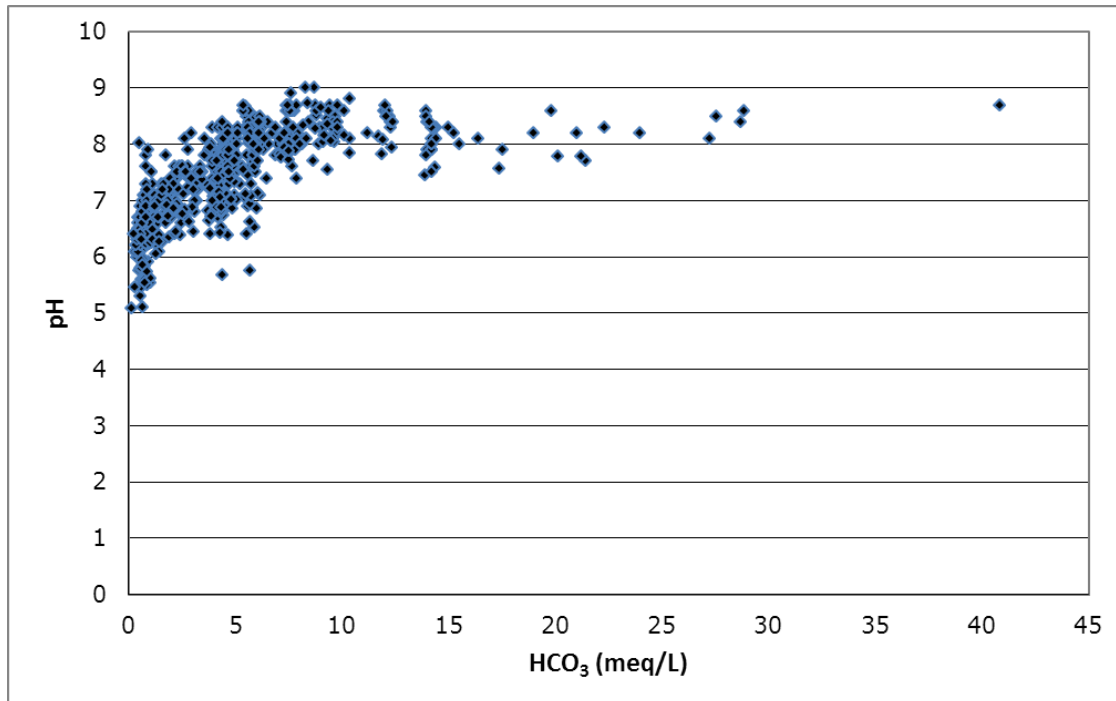


Figure 7-253. pH versus bicarbonate ( $\text{HCO}_3$ ) measured in milliequivalents per liter (meq/L), Carrizo Sand Formation portion of the Carrizo-Wilcox Aquifer, South Transect, Groundwater Management Area 13.

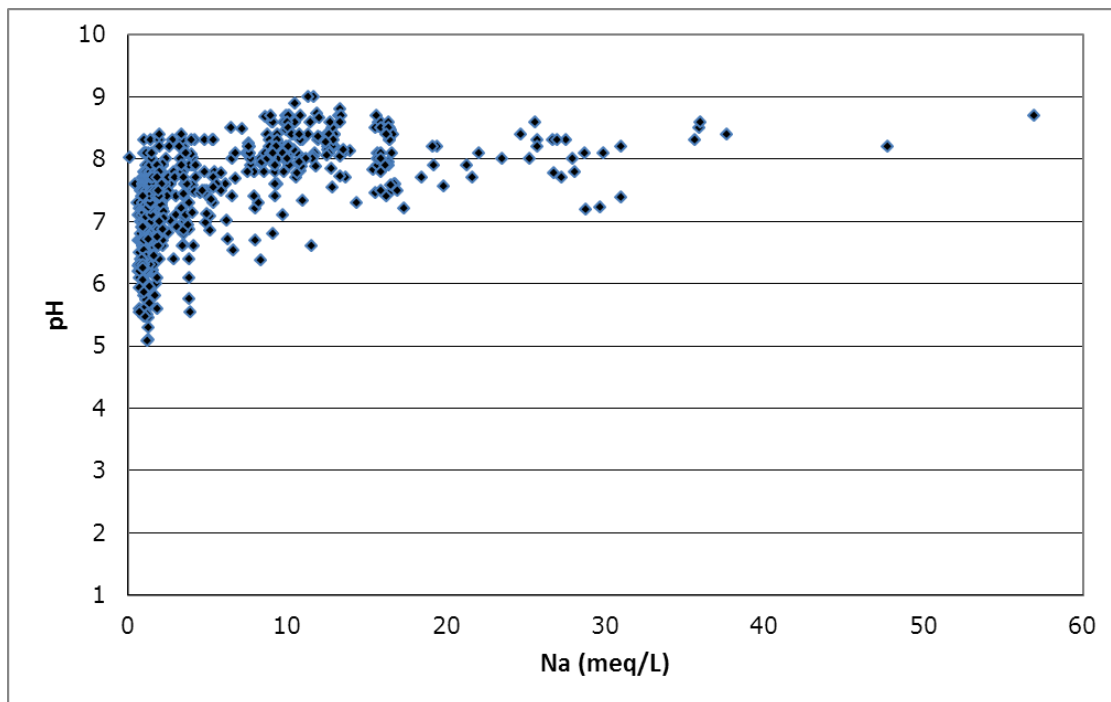


Figure 7-254. pH versus sodium (Na) measured in milliequivalents per liter (meq/L), Carrizo Sand Formation portion of the Carrizo-Wilcox Aquifer, South Transect, Groundwater Management Area 13.

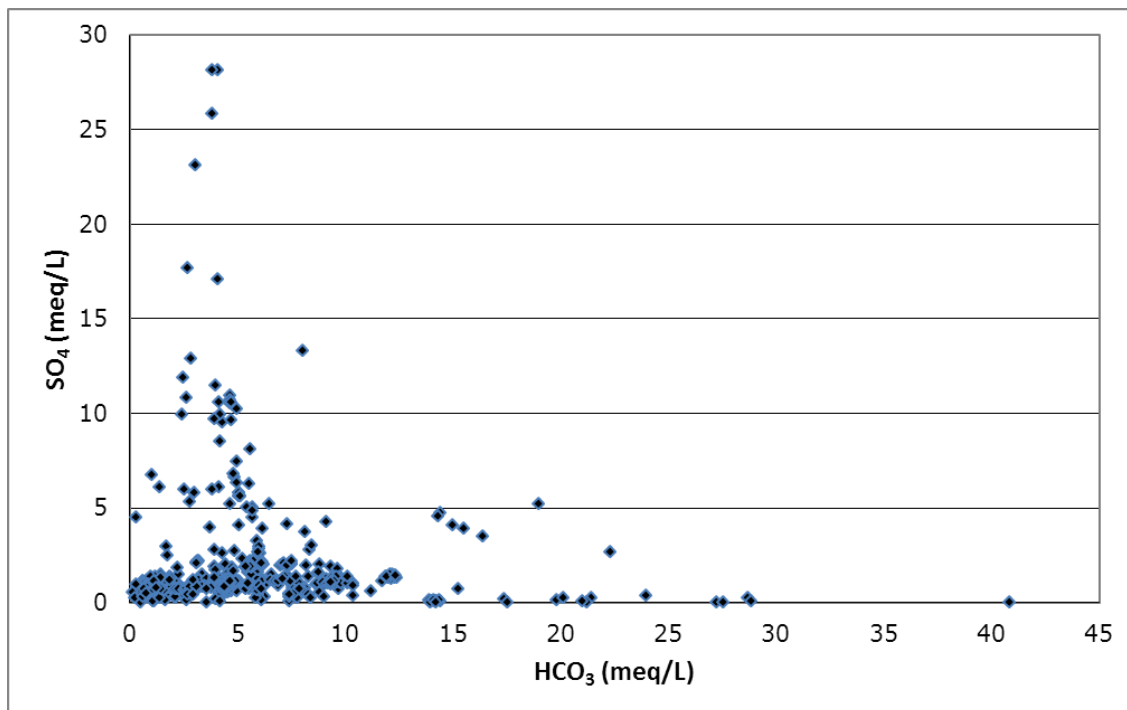


Figure 7-255. Sulfate (SO<sub>4</sub>) versus bicarbonate (HCO<sub>3</sub>) measured in milliequivalents per liter (meq/L), Carrizo Sand Formation portion of the Carrizo-Wilcox Aquifer, South Transect, Groundwater Management Area 13.

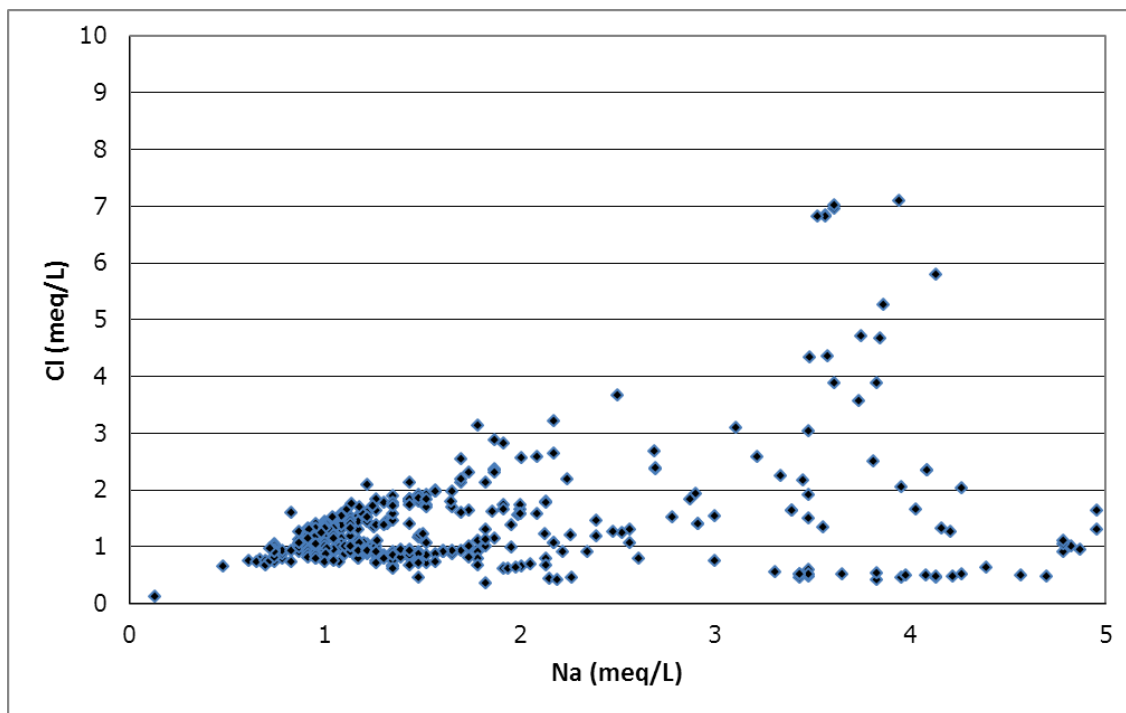


Figure 7-256. Chloride (Cl) versus sodium (Na) measured in milliequivalents per liter (meq/L), Carrizo Sand Formation portion of the Carrizo-Wilcox Aquifer, South Transect, Groundwater Management Area 13.

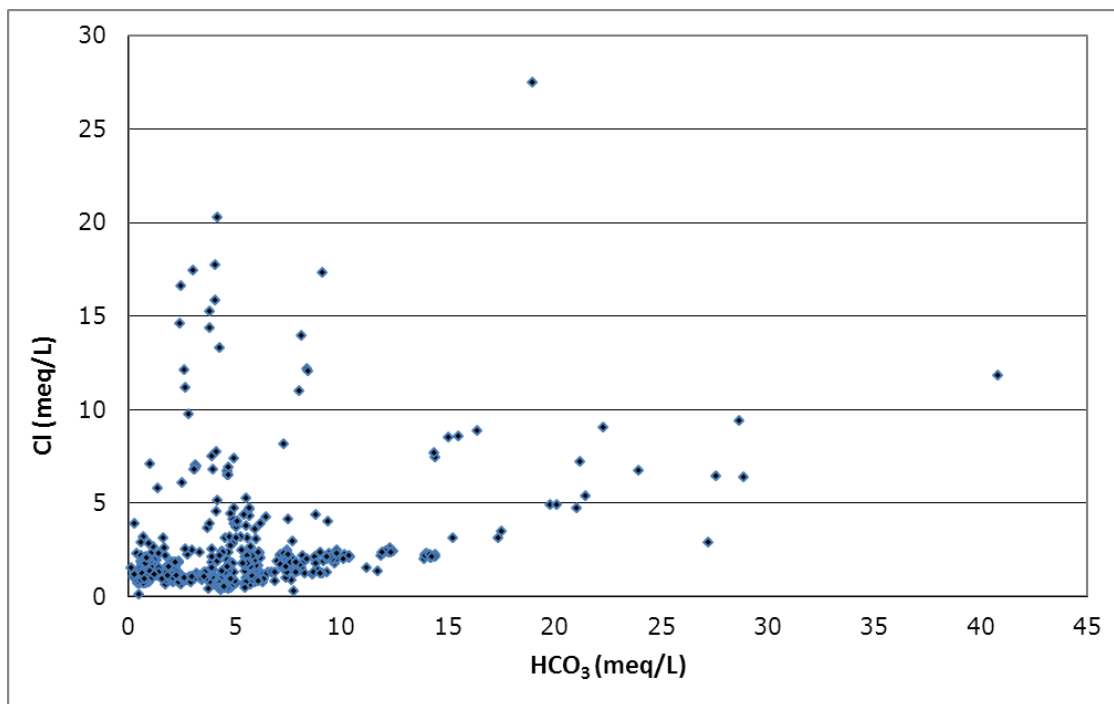


Figure 7-257. Chloride (Cl) versus bicarbonate ( $\text{HCO}_3$ ) measured in milliequivalents per liter (meq/L), Carrizo Sand Formation portion of the Carrizo-Wilcox Aquifer, South Transect, Groundwater Management Area 13.

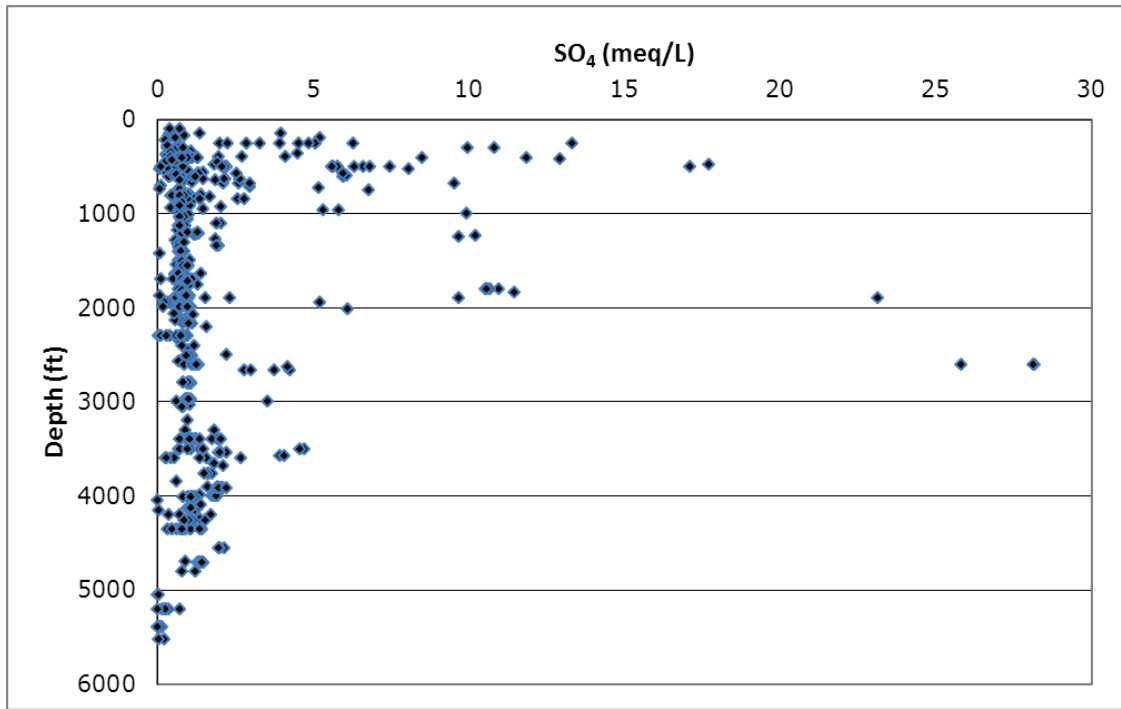


Figure 7-258. Depth measured from land surface in feet (ft) versus sulfate (SO<sub>4</sub>) measured in milliequivalents per liter (meq/L), Carrizo Sand Formation portion of the Carrizo-Wilcox Aquifer, South Transect, Groundwater Management Area 13.

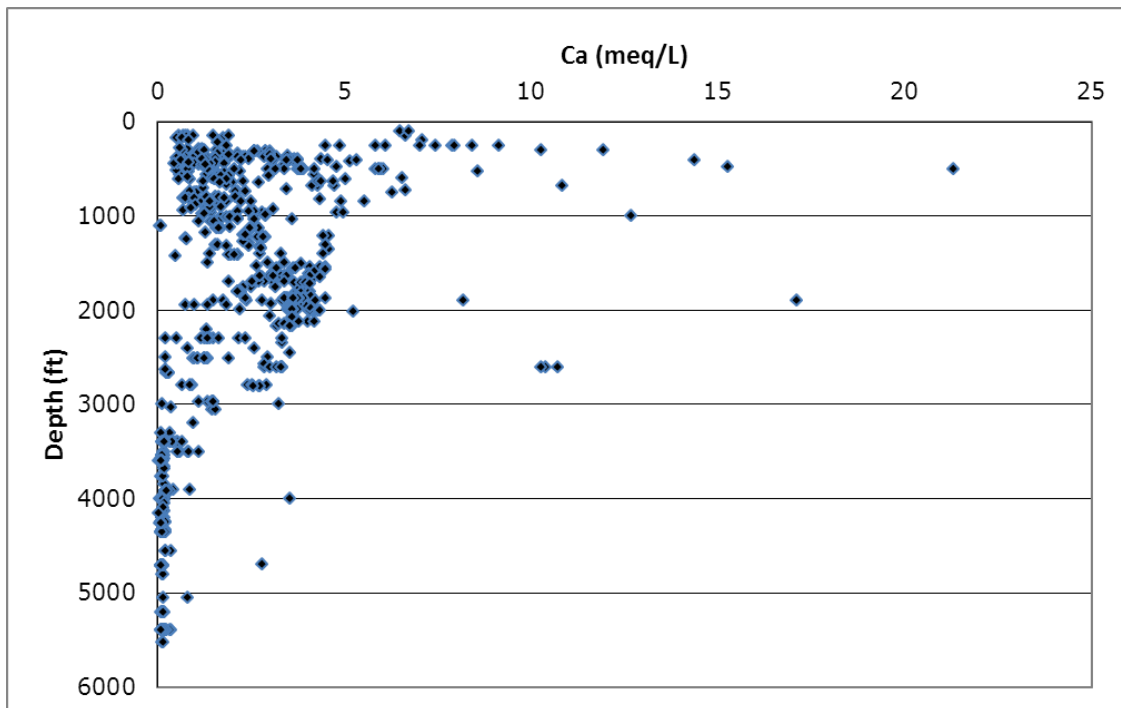
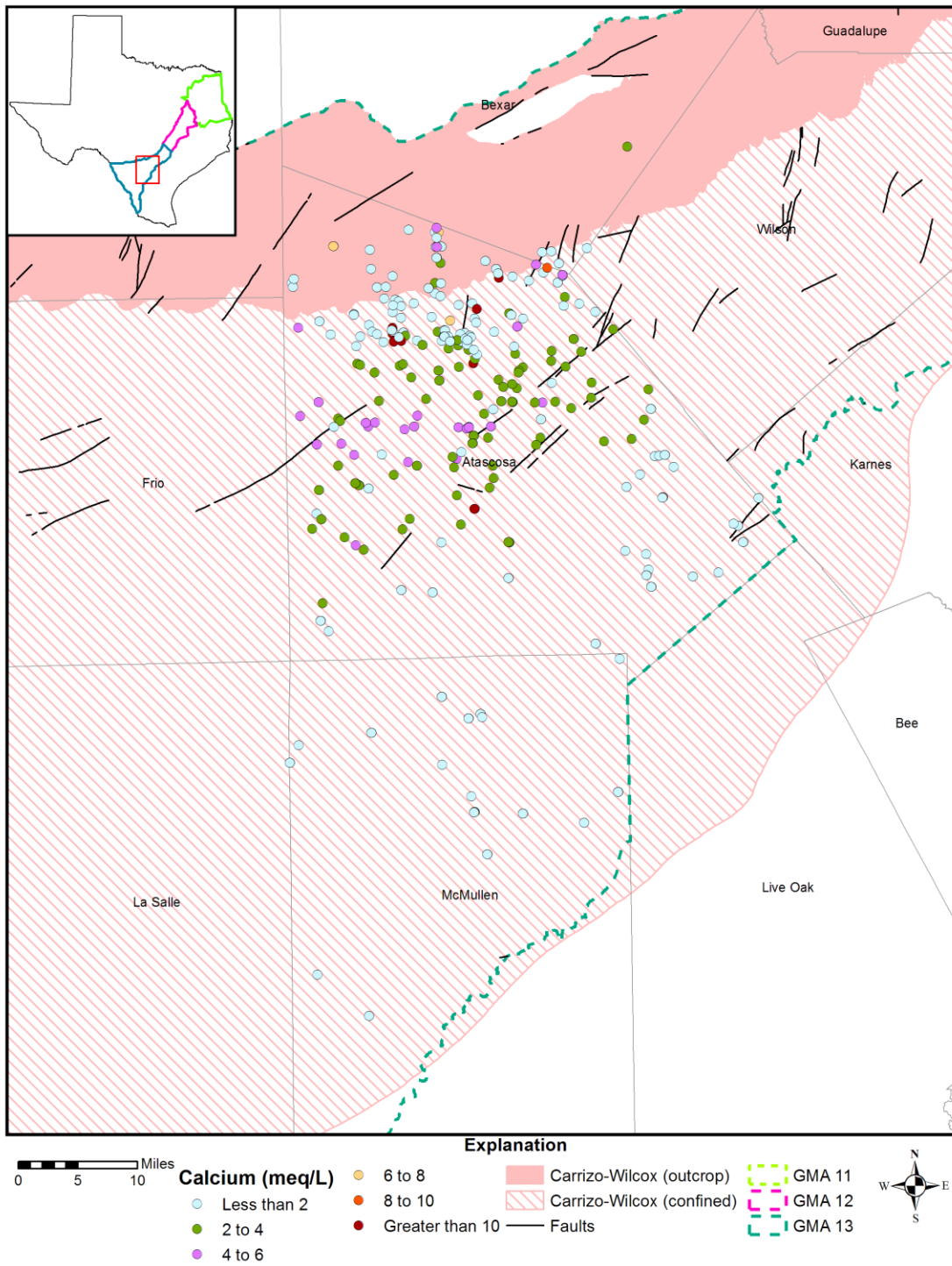


Figure 7-259. Depth measured from land surface in feet (ft) versus calcium (Ca) measured in milliequivalents per liter (meq/L), Carrizo Sand Formation portion of the Carrizo-Wilcox Aquifer, South Transect, Groundwater Management Area 13.



**Figure 7-260. Calcium concentrations measured in milliequivalents per liter (meq/L) in the Carrizo Sand Formation portion of the Carrizo-Wilcox Aquifer, South Transect, Groundwater Management Area (GMA) 13.**

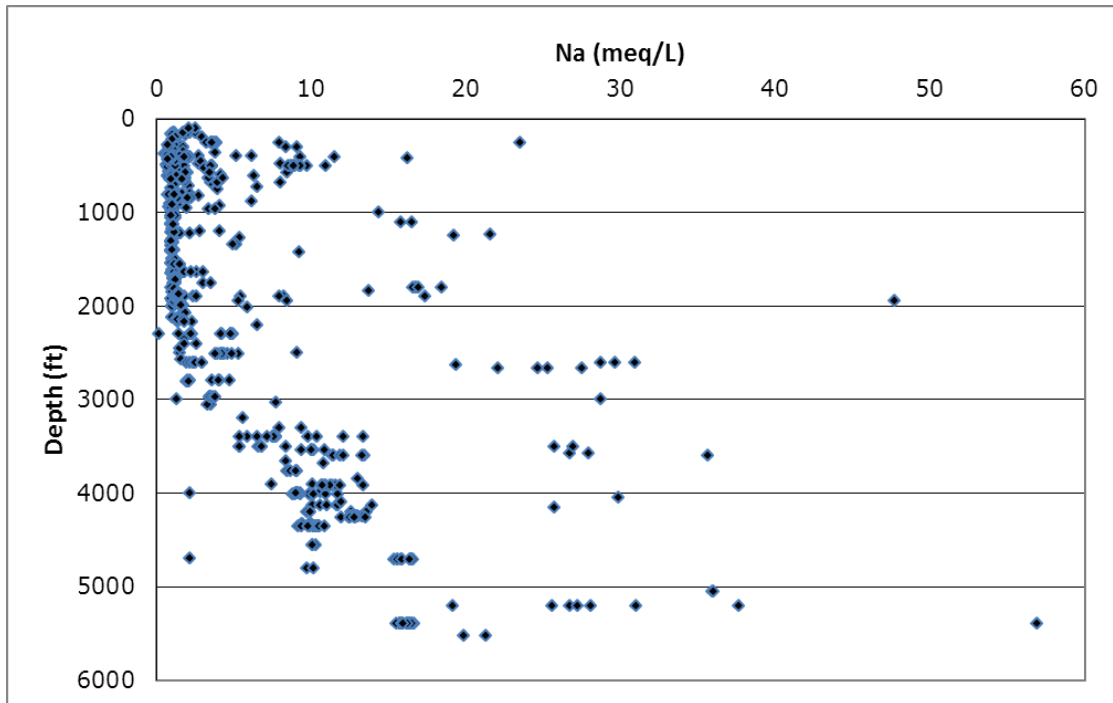


Figure 7-261. Depth measured from land surface in feet (ft) versus sodium (Na) measured in milliequivalents per liter (meq/L), Carrizo Sand Formation portion of the Carrizo-Wilcox Aquifer, South Transect, Groundwater Management Area 13.

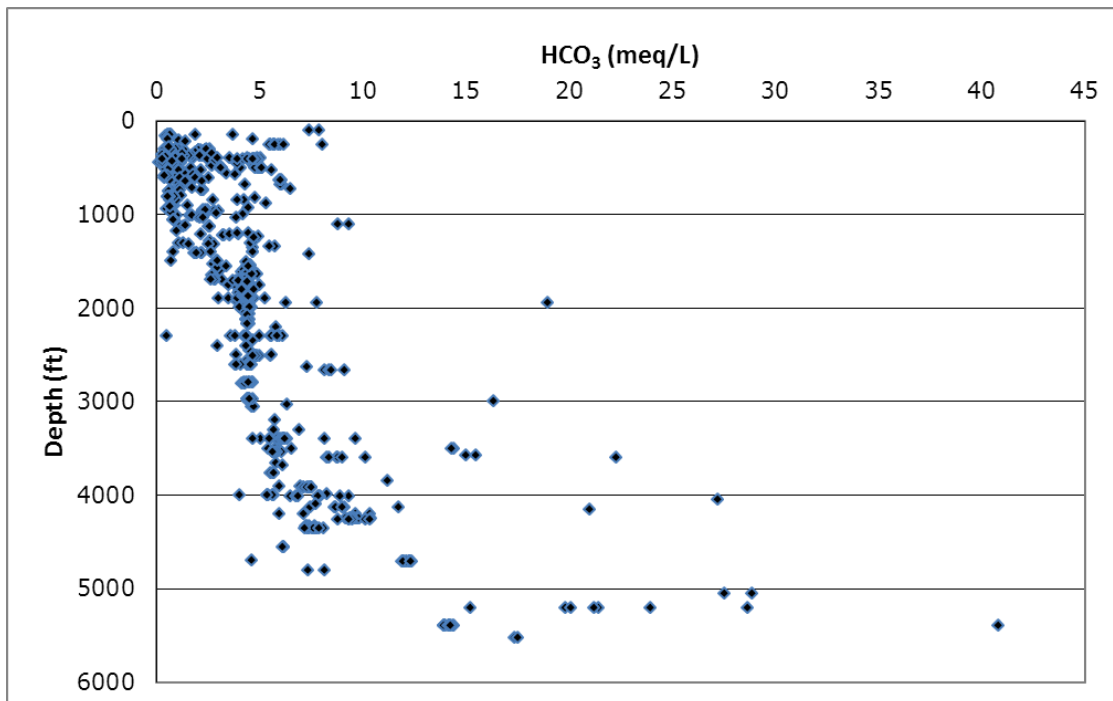


Figure 7-262. Depth measured from land surface versus bicarbonate (HCO<sub>3</sub>) measured in milliequivalents per liter (meq/L), Carrizo Sand Formation portion of the Carrizo-Wilcox Aquifer, South Transect, Groundwater Management Area 13.

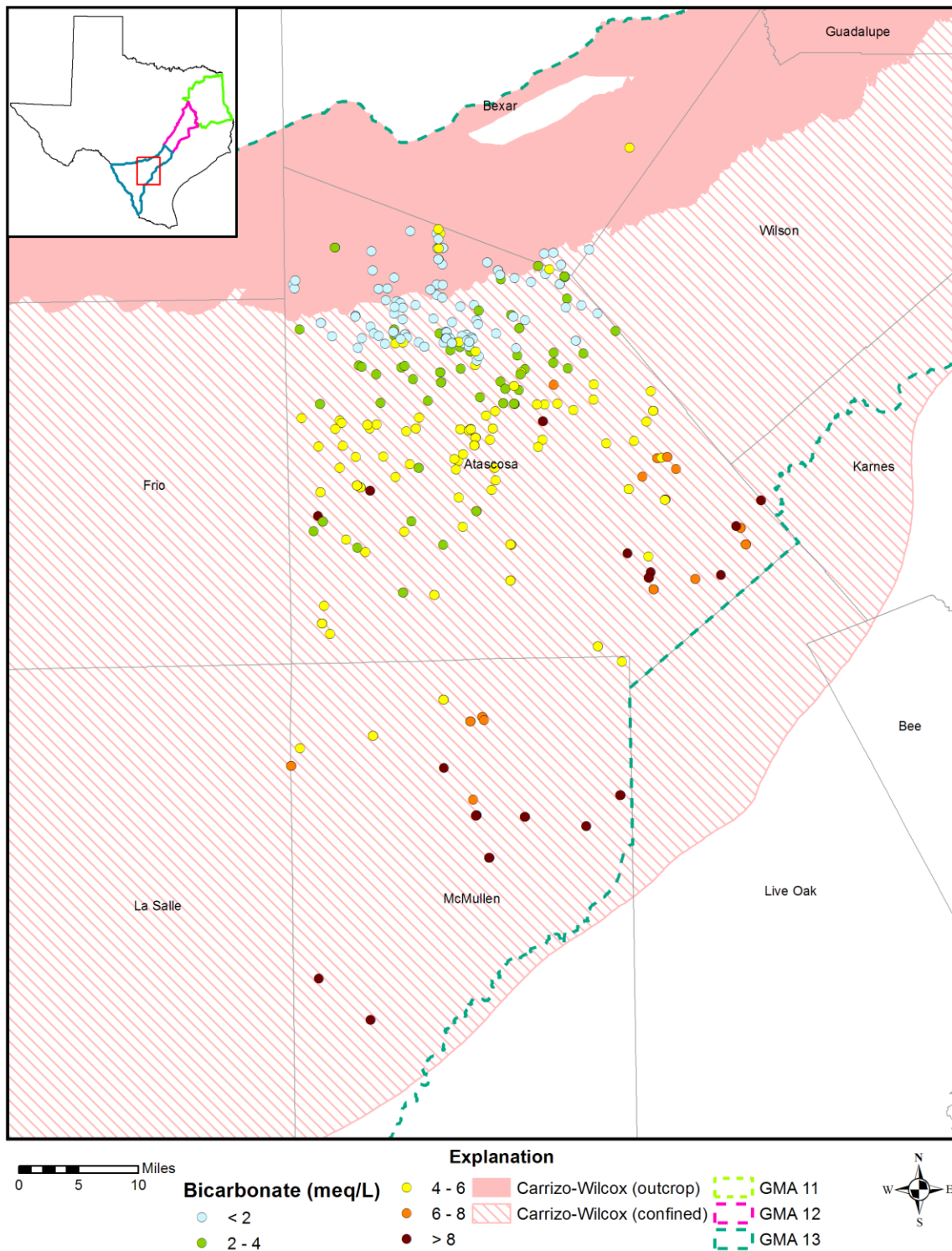
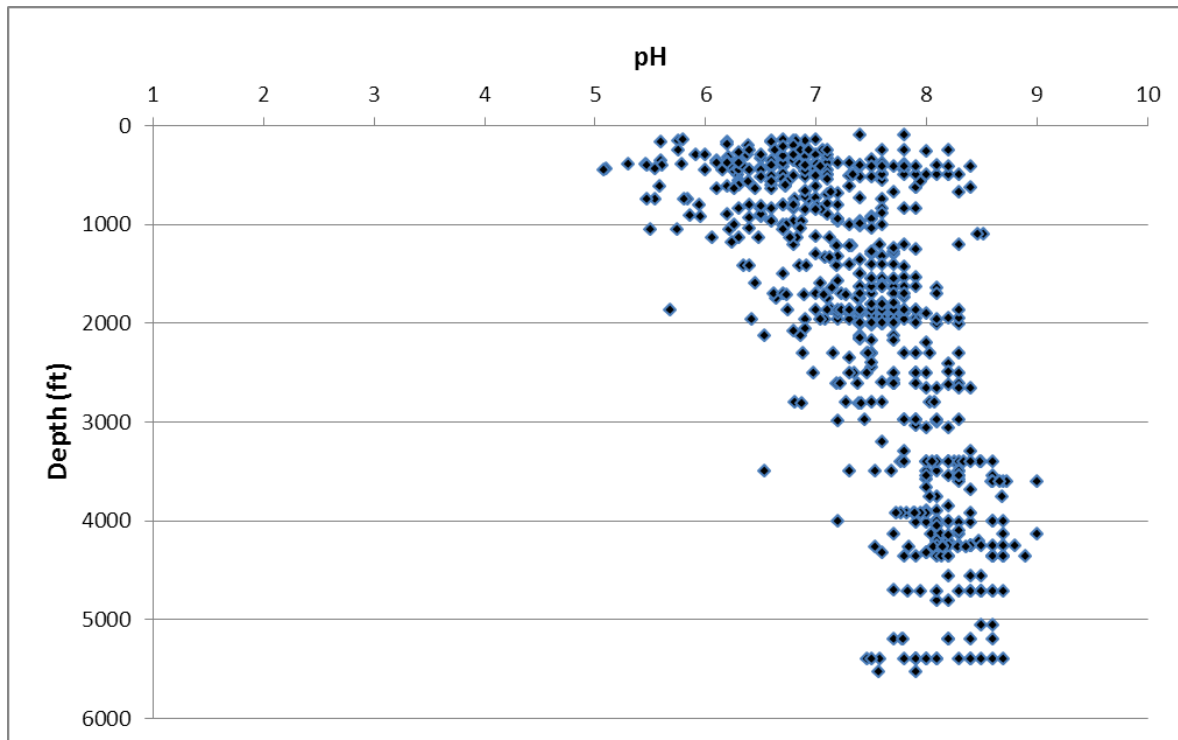


Figure 7-263. Bicarbonate concentrations measured in milliequivalents per liter (meq/L) in the Carrizo Sand Formation portion of the Carrizo-Wilcox Aquifer, South Transect, Groundwater Management Area (GMA) 13.



**Figure 7-264.** Depth measured from land surface in feet (ft) versus pH, Carrizo Sand Formation portion of the Carrizo-Wilcox Aquifer, South Transect, Groundwater Management Area 13.

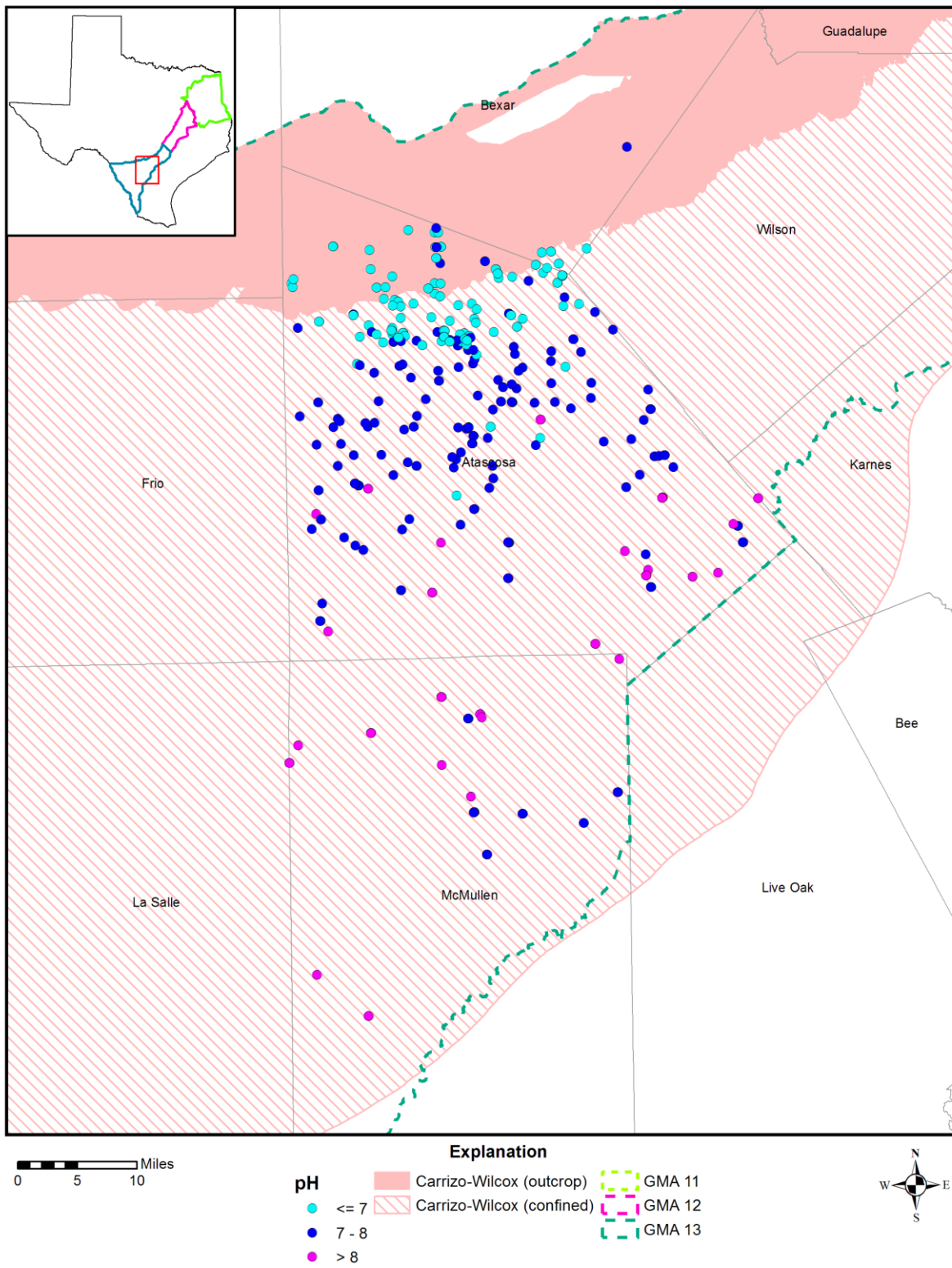
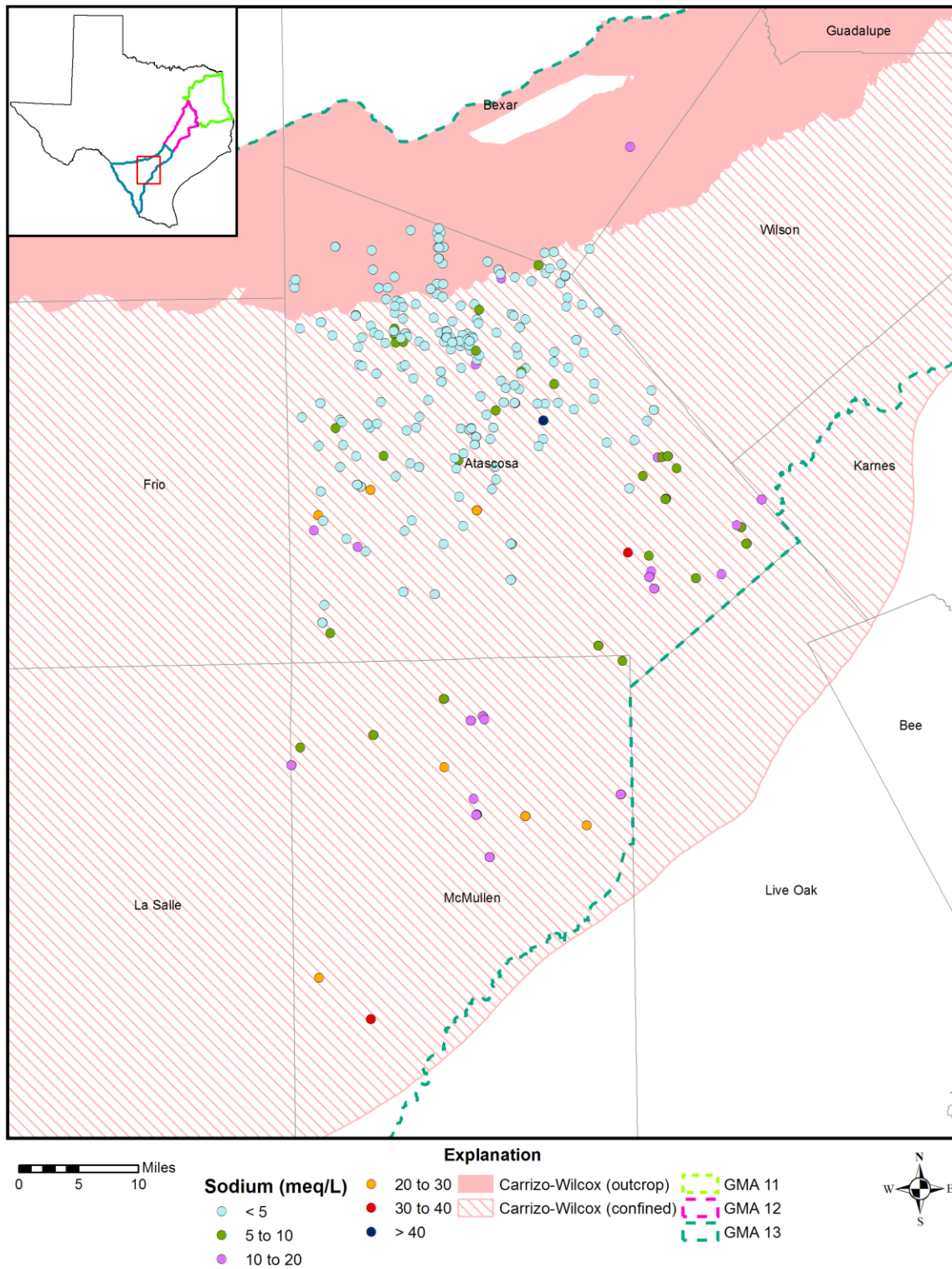
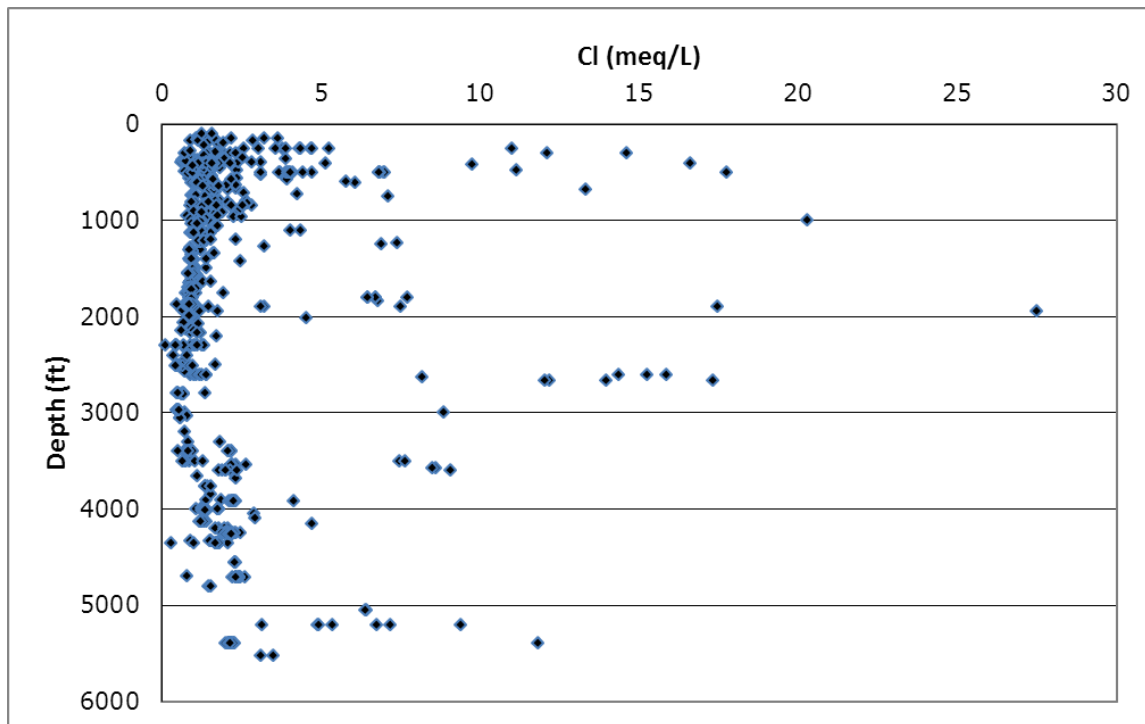


Figure 7-265. pH concentrations in the Carrizo Sand Formation portion of the Carrizo-Wilcox Aquifer, South Transect, Groundwater Management Area (GMA) 13.



**Figure 7-266. Sodium concentrations measured in milliequivalents per liter (meq/L) in the Carrizo Sand Formation portion of the Carrizo-Wilcox Aquifer, South Transect, Groundwater Management Area (GMA) 13.**



**Figure 7-267.** Depth measured from land surface versus chloride (Cl) measured in milliequivalents per liter (meq/L), Carrizo Sand Formation portion of the Carrizo-Wilcox Aquifer, South Transect, Groundwater Management Area 13.

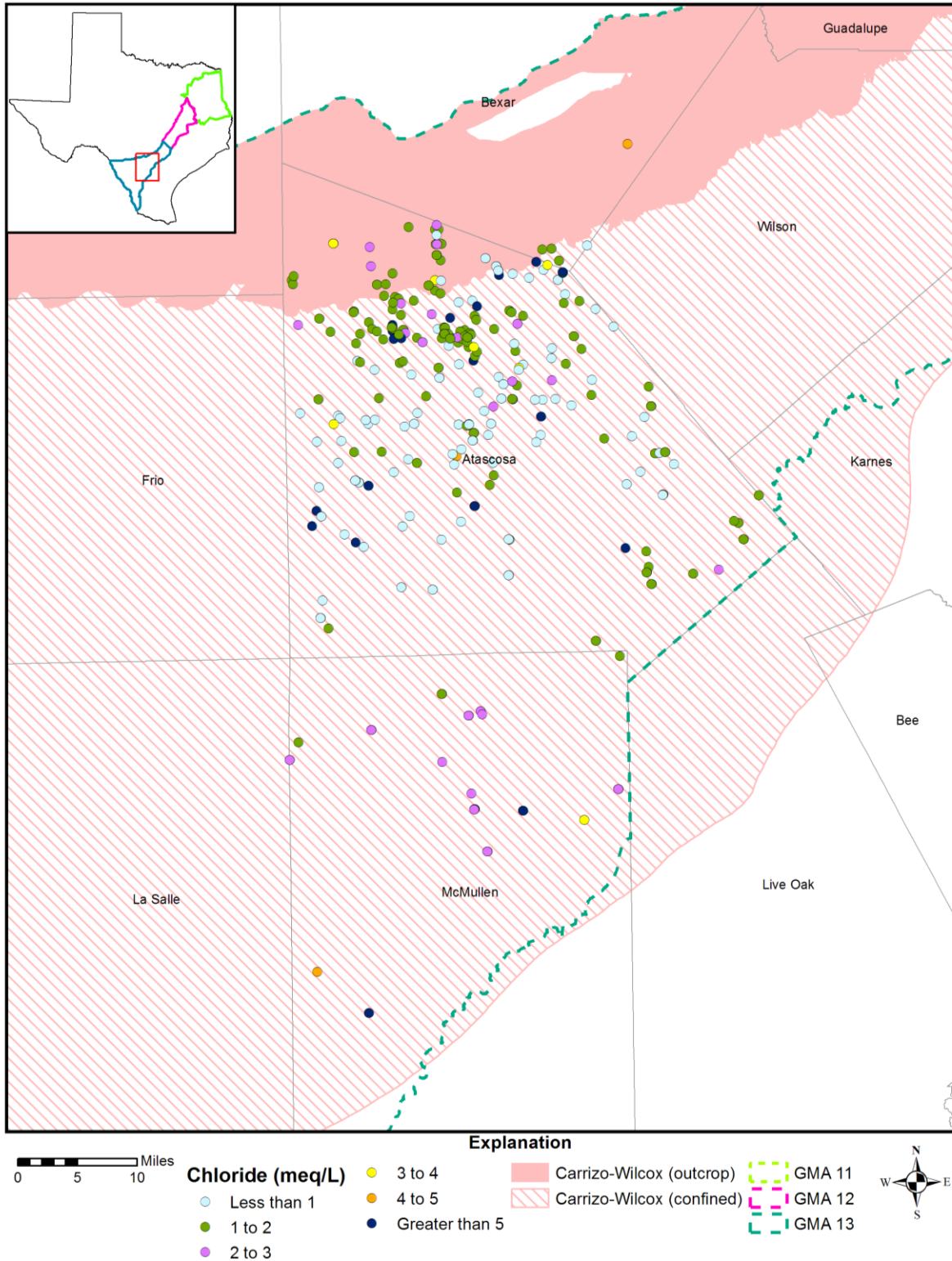
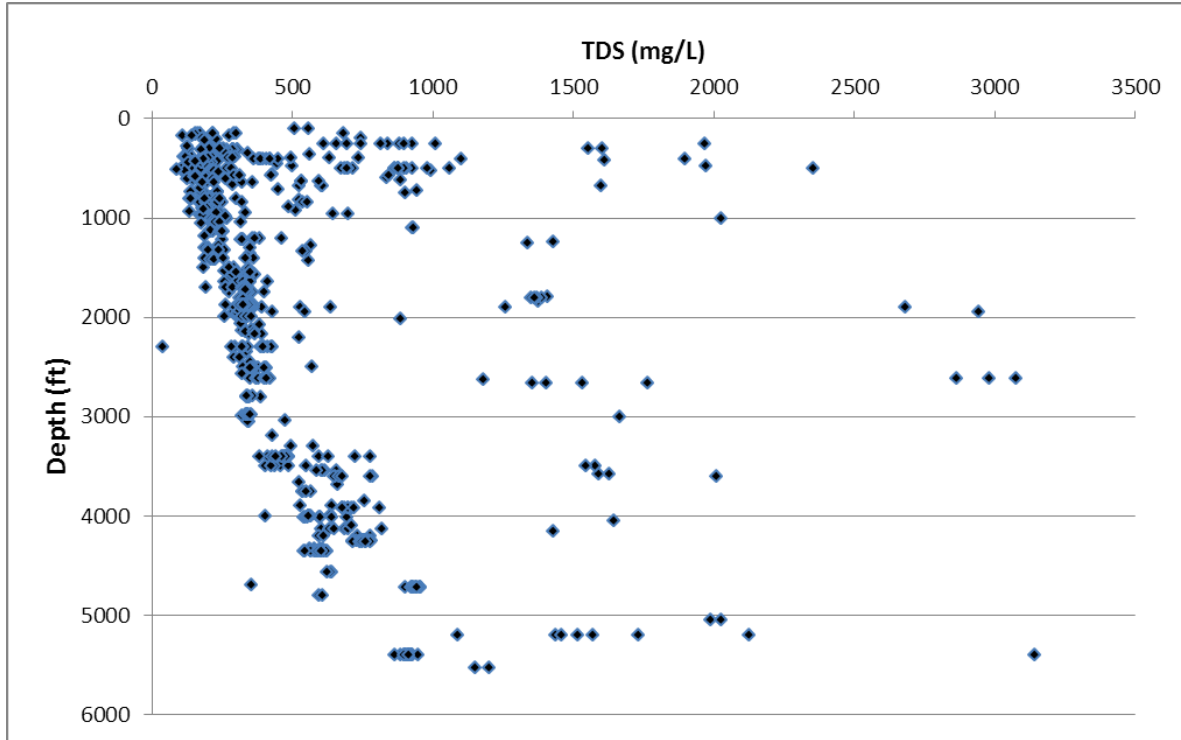


Figure 7-268. Chloride concentrations measured in milliequivalents per liter (meq/L) in the Carrizo Sand Formation portion of the Carrizo-Wilcox Aquifer, South Transect, Groundwater Management Area (GMA) 13.



**Figure 7-269.** Depth measured from land surface measured in feet (ft) versus total dissolved solids measured in parts per million (ppm), Carrizo Sand Formation portion of the Carrizo-Wilcox Aquifer, South Transect, Groundwater Management Area 13.

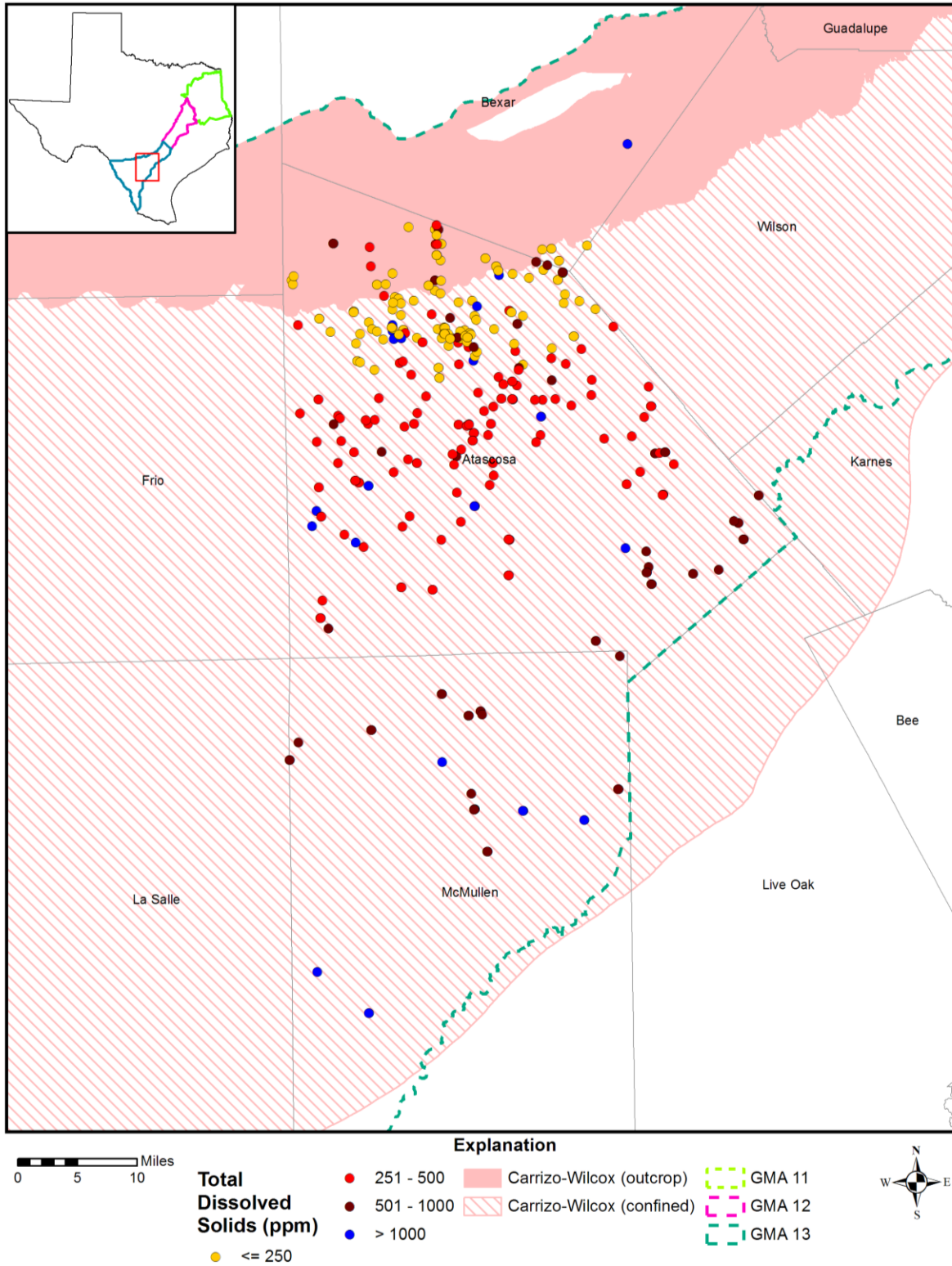


Figure 7-270. Total dissolved solids measured in parts per million (ppm) in the Carrizo Sand Formation portion of the Carrizo-Wilcox Aquifer, South Transect, Groundwater Management Area (GMA) 13.

## **Queen City Aquifer**

A moderate-sized database from the TWDB exists for water wells, water chemistry and water levels in the Queen City Aquifer in the South Transect. The Queen City Aquifer is a minor aquifer, secondary to the Carrizo Sand Formation portion of the Carrizo-Wilcox Aquifer in this transect.

### Well Depths

Depths of the aquifer extend from less than 500 feet in the outcrop in northern Atascosa County to depths greater than 3,000 feet in central McMullen County (Figure 7-271).

### Potentiometric Surface

The Queen City Aquifer potentiometric surface shows water wells in the outcrop as high as 400 to 450 feet (above mean sea level) in the outcrop to elevations of 300 to 350 feet downdip. Direction of groundwater flow appears to be from the outcrop down the structural dip to the south (Figure 7-272) except for the area in northeast Atascosa County where there is depression in the water level surface. However, it is assumed that this depression has only existed since pumping began and it may not be representative of long-term flow paths.

### Piper Diagram

The Piper diagram (Figure 7-273) for the Queen City Aquifer in the South Transect shows a mixed cation composition (calcium-sodium) evolving to a sodium water downdip. The anion triangle shows sulfate-chloride-bicarbonate water in updip regions to bicarbonate water with some chloride (20 to 40 percent) in the downdip section. The composition of and evolution of the Queen City Aquifer, water is similar to the underlying Carrizo Sand Formation but based on fewer available data.

### Bicarbonate versus Sodium Plot

A plot of the bicarbonate versus sodium (Figure 7-274) for the Queen City Aquifer from the TWDB data shows a linear increasing trend with a sodium-bicarbonate ratio of slightly greater than 1:0.

### Sodium versus Calcium Plot

A plot of sodium versus calcium (Figure 7-275) shows an inverse relationship between sodium and calcium, at low sodium values calcium increases independent of sodium. The trend shifts at higher sodium concentrations, which are then independent of calcium. This relationship for the Queen City Aquifer appears similar to the sodium versus calcium plot (Figure 7-251) for the underlying Carrizo Sand Formation.

### Bicarbonate versus Calcium Plot

A plot of bicarbonate versus calcium (Figure 7-276) for the Queen City Aquifer shows a distribution similar to the sodium versus calcium plot (Figure 7-275). This relationship is also similar to the bicarbonate versus calcium plot for the Carrizo Sand Formation (Figure 7-252) except that there are no chemical analyses where sodium in the Queen City Aquifer is less than five milliequivalents per liter. There are only a few sampled wells in the outcrop of the Queen City Aquifer.

#### pH versus Bicarbonate Plot

The plot of pH versus bicarbonate (Figure 7-277) exhibits a trend similar to the Carrizo Sand Formation, but lacks the low pH values seen in the Carrizo Sand Formation (Figure 7-253). As stated above, this may occur because of a lack of wells sampled for water chemistry in the Queen City Aquifer outcrop.

#### pH versus Sodium Plot

The plot of pH versus sodium (Figure 7-278) shows a similar distribution of data to the pH bicarbonate plot (Figure 7-277).

#### Sulfate versus Bicarbonate Plot

The plot of sulfate versus bicarbonate (Figure 7-279) shows higher sulfate concentrations at bicarbonate less than seven milliequivalents per liter. At higher bicarbonate values bicarbonate increases independent of sulfate, although the sulfate never decreases to negligible concentrations as observed in the Carrizo Sand Formation (Figure 7-255).

#### Sodium versus Chloride Plot

The plot of sodium versus chloride (Figure 7-280) shows two trends: 1) for sodium less than 20 milliequivalents per liter, sodium increases independent of chloride and 2) for sodium greater than 20 milliequivalents per liter, both sodium and chloride are increasing indicating the addition of an sodium-chloride source.

#### Chloride versus Bicarbonate Plot

The plot of chloride versus bicarbonate (Figure 7-281) shows two trends: 1) bicarbonate increases independent of chloride from bicarbonate concentrations of about five to 13 milliequivalents per liter and 2) at higher bicarbonate values, chloride values are increasing suggesting the addition of a sodium-chloride source.

#### Depth versus Sulfate Plot

The plot of depth versus sulfate (Figure 7-282) shows higher sulfate values at depth shallower than about 750 feet.

#### Map of Sulfate

A map of sulfate (Figure 7-283) in the Queen City Aquifer shows higher sulfate concentrations in the outcrop than in the downdip portion of the aquifer.

#### Depth versus Calcium Plot

The plot of depth versus calcium (Figure 7-284) shows higher calcium concentrations at depths less than about 1,200 feet. At greater depth calcium concentrations are negligible.

#### Map of Calcium

A map of calcium (Figure 7-285) in the Queen City Aquifer shows higher calcium values toward the outcrop in northern Atascosa County. Lower calcium concentrations occur in southern Atascosa and McMullen counties.

### Depth versus Bicarbonate Plot

The plot of depth versus bicarbonate (Figure 7-286) shows increasing bicarbonate with depth, primarily at depth greater than 1,000 feet.

### Map of Bicarbonate

A map of bicarbonate (Figure 7-287) in the Queen City Aquifer shows higher concentrations farther to the south as the aquifer deepens from less than 1,000 feet in Atascosa County to greater than 1,000 feet in McMullen County.

### Depth versus pH Plot

The plot of depth versus pH (Figure 7-288) shows higher pH values with depth.

### Depth versus Sodium Plot

The plot of depth versus sodium (Figure 7-289) shows increasing sodium with depth. The greater changes are deeper in the aquifer.

### Depth versus Chloride Plot

The plot of depth versus chloride (Figure 7-290) shows no general trends of increasing chloride.

### Depth versus Total Dissolved Solids Plot

The plot of depth versus total dissolved solids (Figure 7-291) shows minor increases in total dissolved solids depth greater than about 1,000 feet and greater increases at depth greater than 2,000 feet.

### Discussion

Groundwater in the Queen City Aquifer in the South Transect is recharged in the outcrop and flows into the deeper confined parts of the aquifer. The groundwater chemistry evolves from a mixed calcium-sodium cation and sulfate-chloride anion water updip to sodium-bicarbonate water down dip. There are only a few samples in the outcrop, so a typical composition of groundwater in the outcrop cannot be determined. The downdip waters have evolved to a sodium-bicarbonate type of water similar to those observed in the underlying Carrizo Sand Formation. The chemical processes in the Queen City Aquifer are considered similar to those for the Carrizo Sand Formation. The higher calcium waters in the Queen City Aquifer only extend to a depth of about 1,200 feet, whereas the higher calcium water in the Carrizo Sand Formation extend to 3,000 feet. Similarly the deepest wells in the Queen City Aquifer are about 3,500 feet, where the deepest wells in the Carrizo Sand Formation along this transect extend to 5,500 feet. The Queen City Aquifer is considered less permeable and may have higher clay content than the Carrizo Sand Formation portion of the Carrizo Sand Formation, which may explain the shallower maximum depth and slight differences in water chemistry.

The water chemistry of the Queen City Aquifer and its chemical evolution appears to result from intra aquifer reaction rather than the leakage of groundwater from the underlying Carrizo Sand Formation. Cross-formational leakage from the underlying Carrizo Sand Formation is not needed to explain the Queen City Aquifer water chemistry.

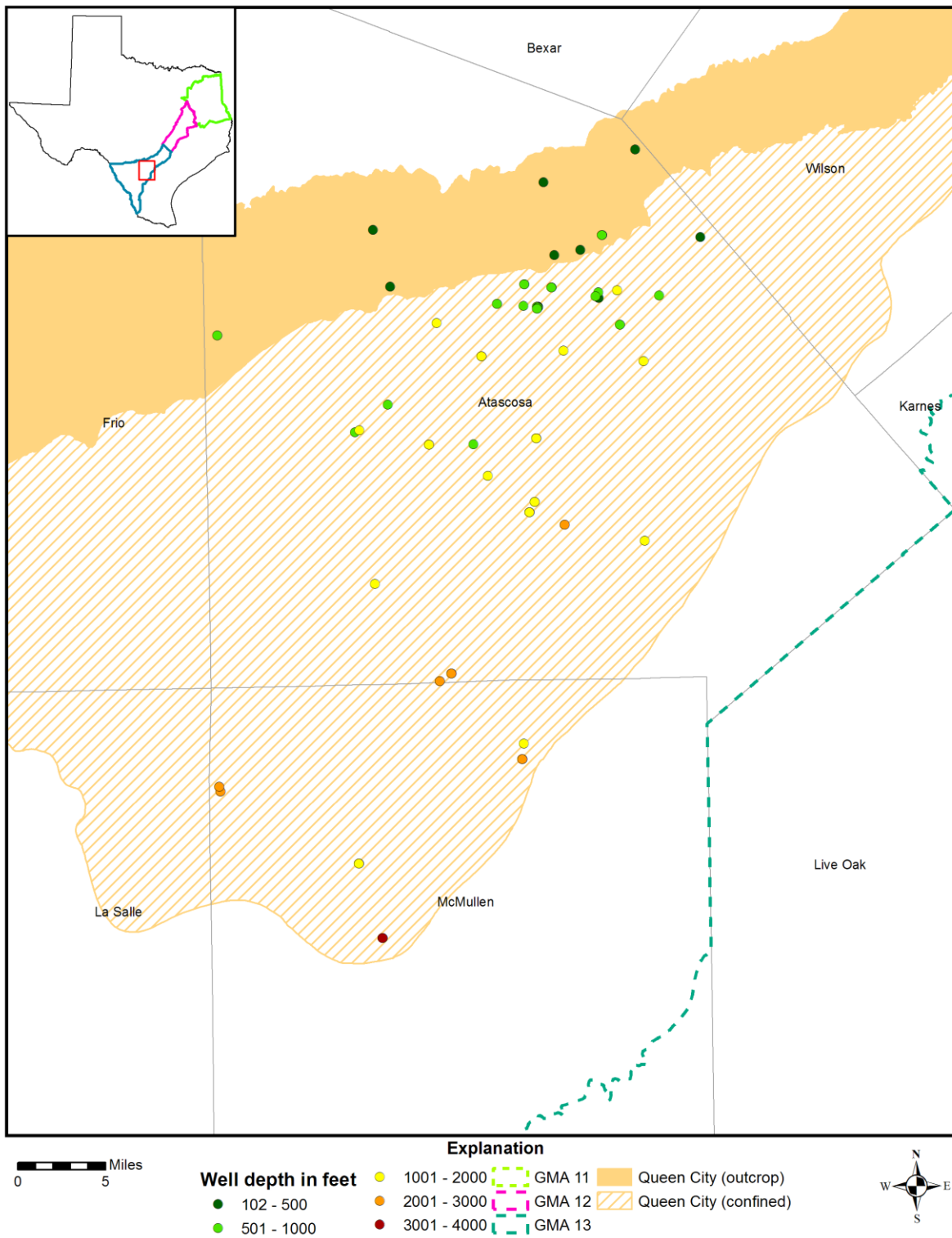


Figure 7-271. Well depths measured from land surface in feet in the Queen City Aquifer, South Transect, Groundwater Management Area (GMA) 13.

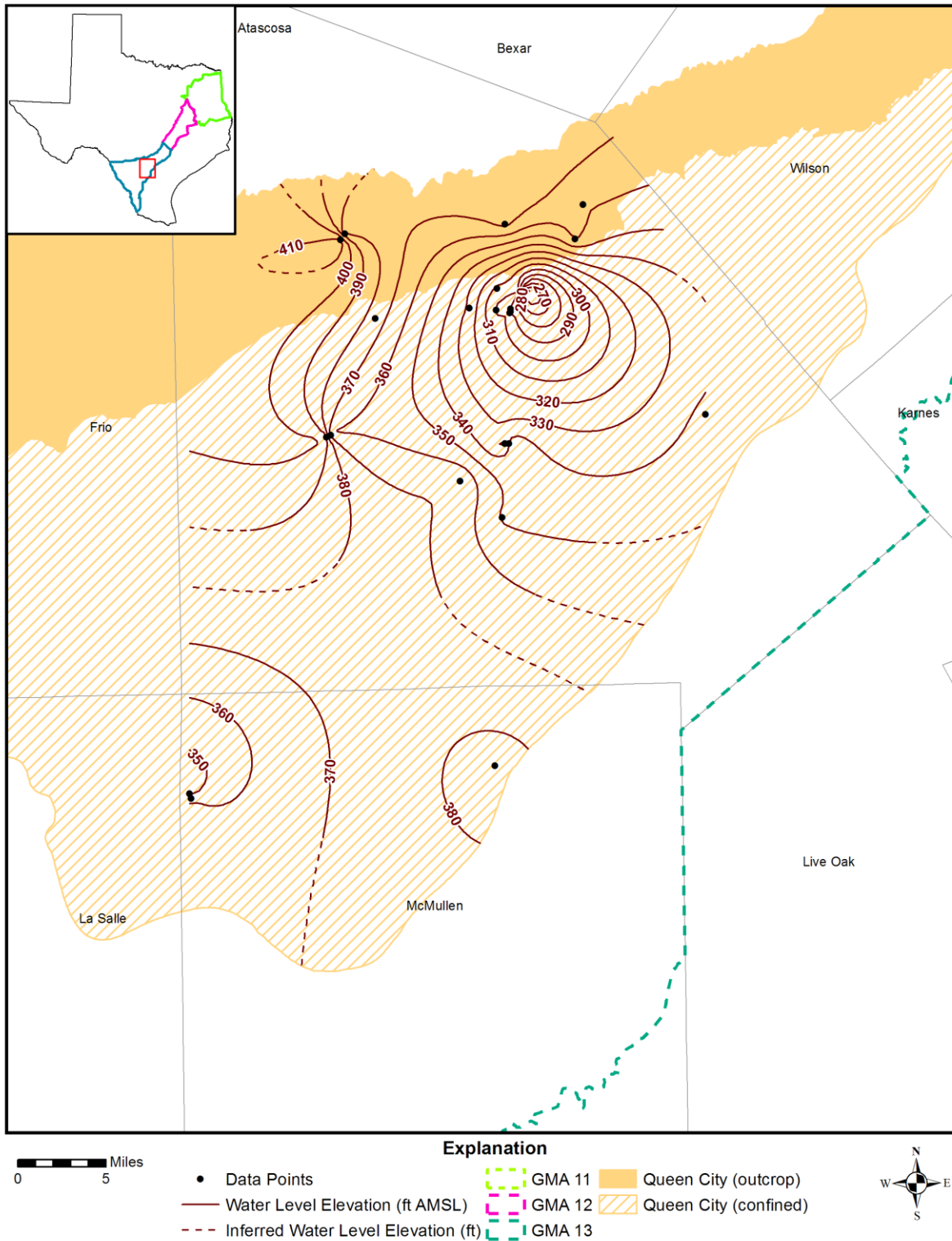


Figure 7-272. Water level elevations from 1971 to 2011 measured in feet above mean sea level (ft AMSL) in the Queen City Aquifer, South Transect, Groundwater Management Area (GMA) 13.

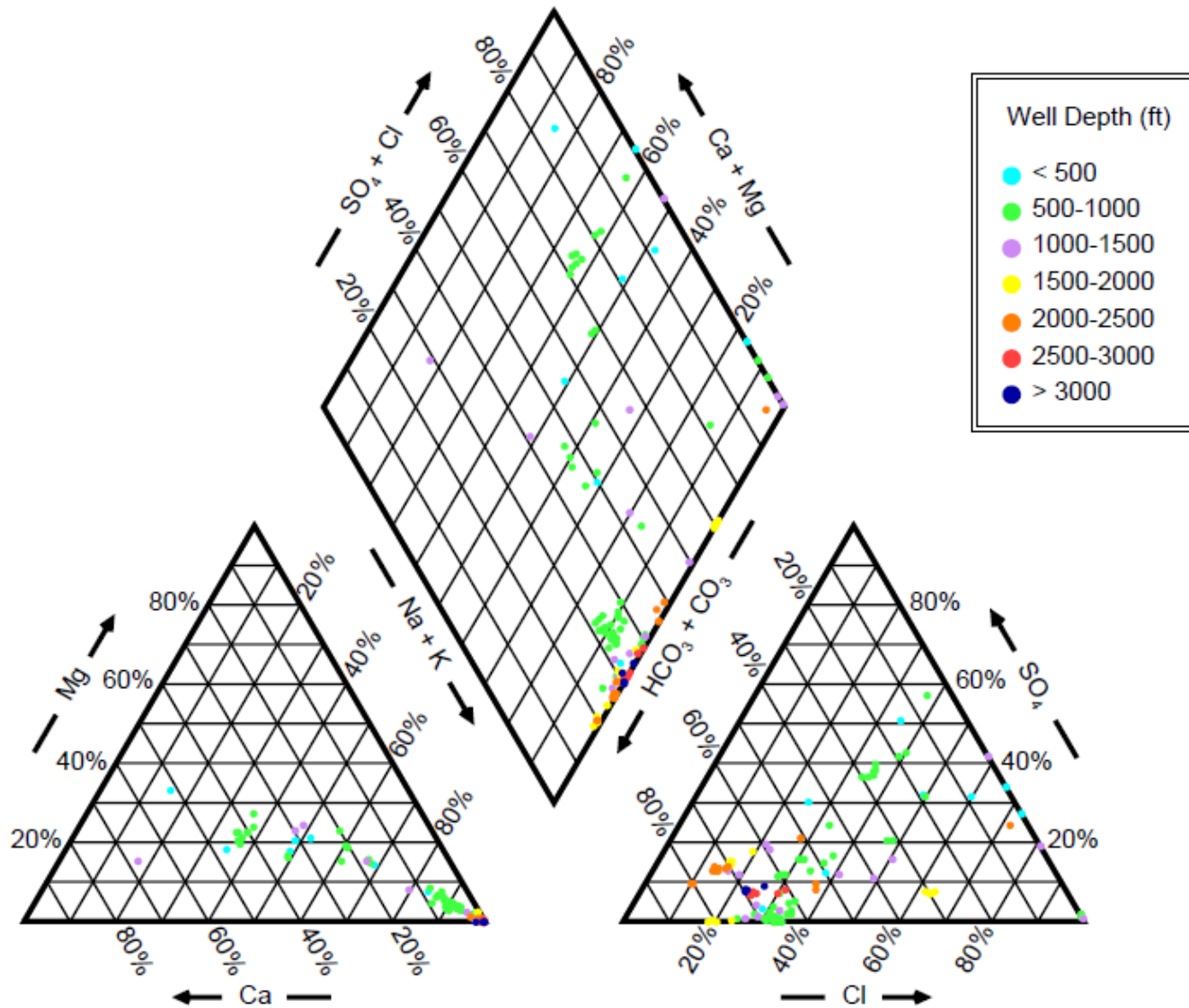


Figure 7-273. Piper diagram showing chemistry of the Queen City Aquifer wells in the South Transect by well depth measured from land surface in feet (ft).

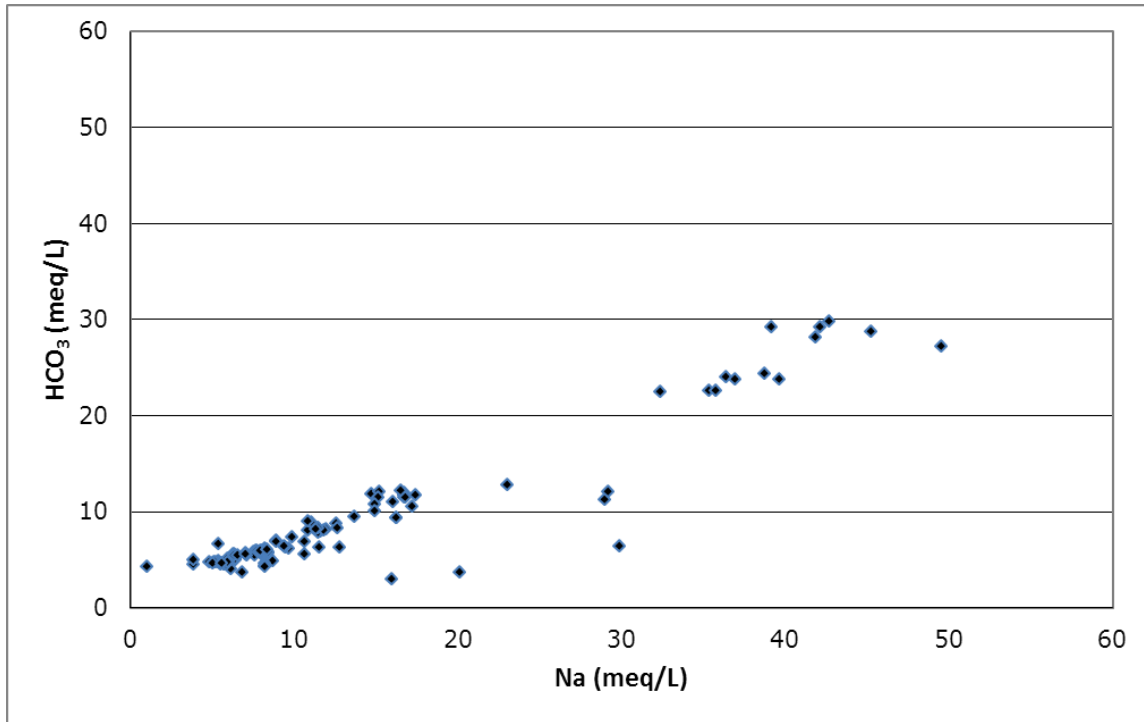


Figure 7-274. Bicarbonate (HCO<sub>3</sub>) versus sodium (Na) measured in milliequivalents per liter (meq/L), Queen City Aquifer, South Transect, Groundwater Management Area 13.

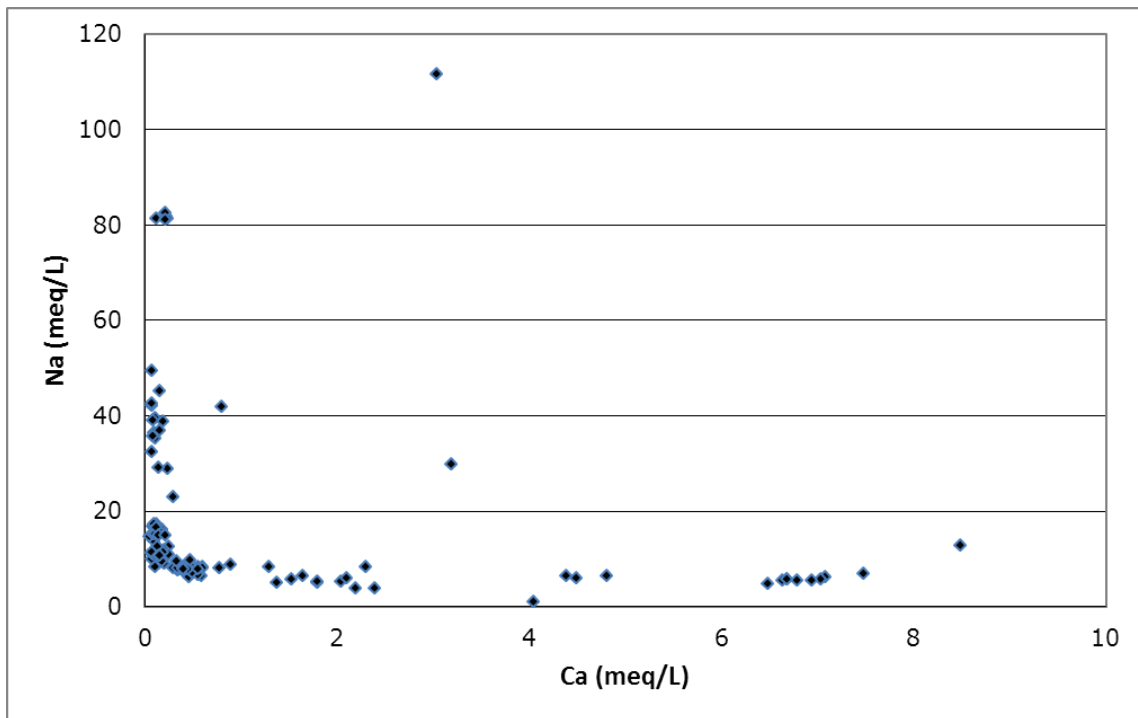


Figure 7-275. Sodium (Na) versus calcium (Ca) measured in milliequivalents per liter (meq/L), Queen City Aquifer, South Transect, Groundwater Management Area 13.

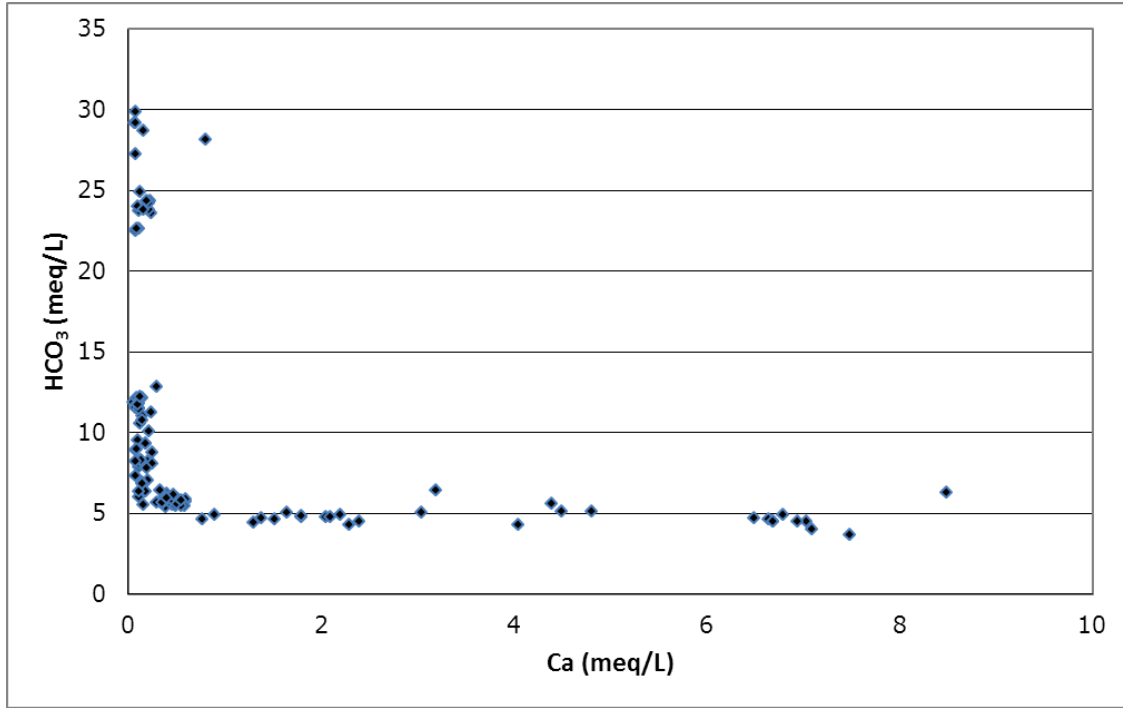


Figure 7-276. Bicarbonate (HCO<sub>3</sub>) versus calcium (Ca) measured in milliequivalents per liter (meq/L), Queen City Aquifer, South Transect, Groundwater Management Area 13.

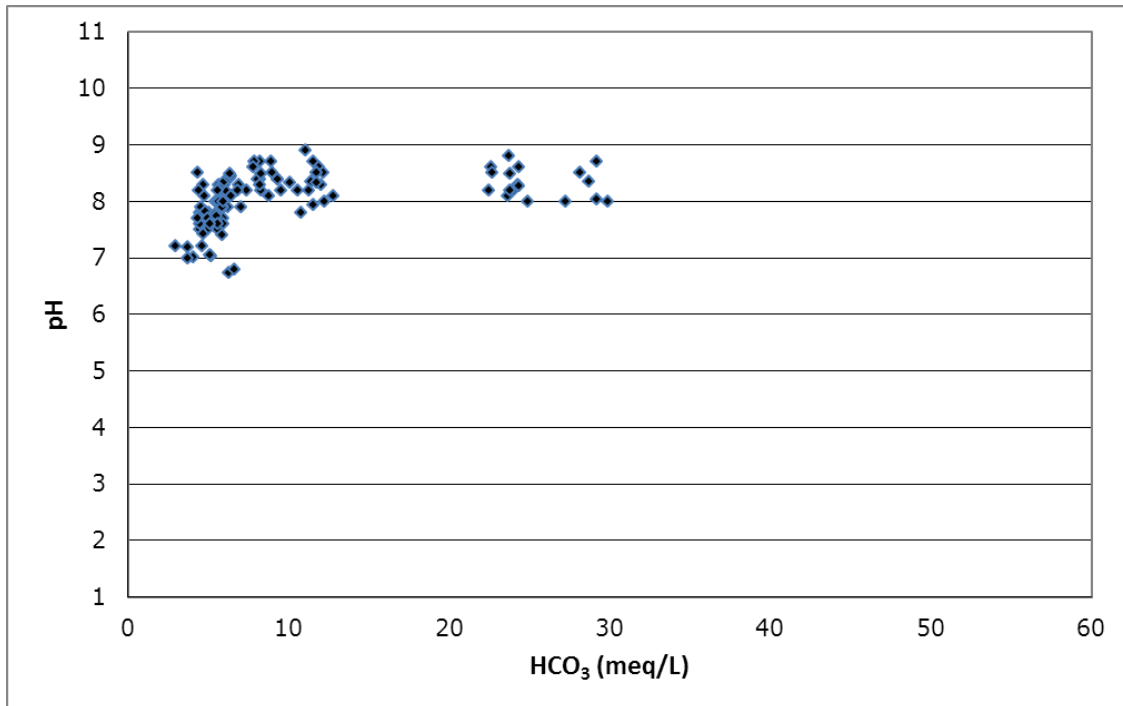


Figure 7-277. pH versus bicarbonate (HCO<sub>3</sub>) measured in milliequivalents per liter (meq/L), Queen City Aquifer, South Transect, Groundwater Management Area 13.

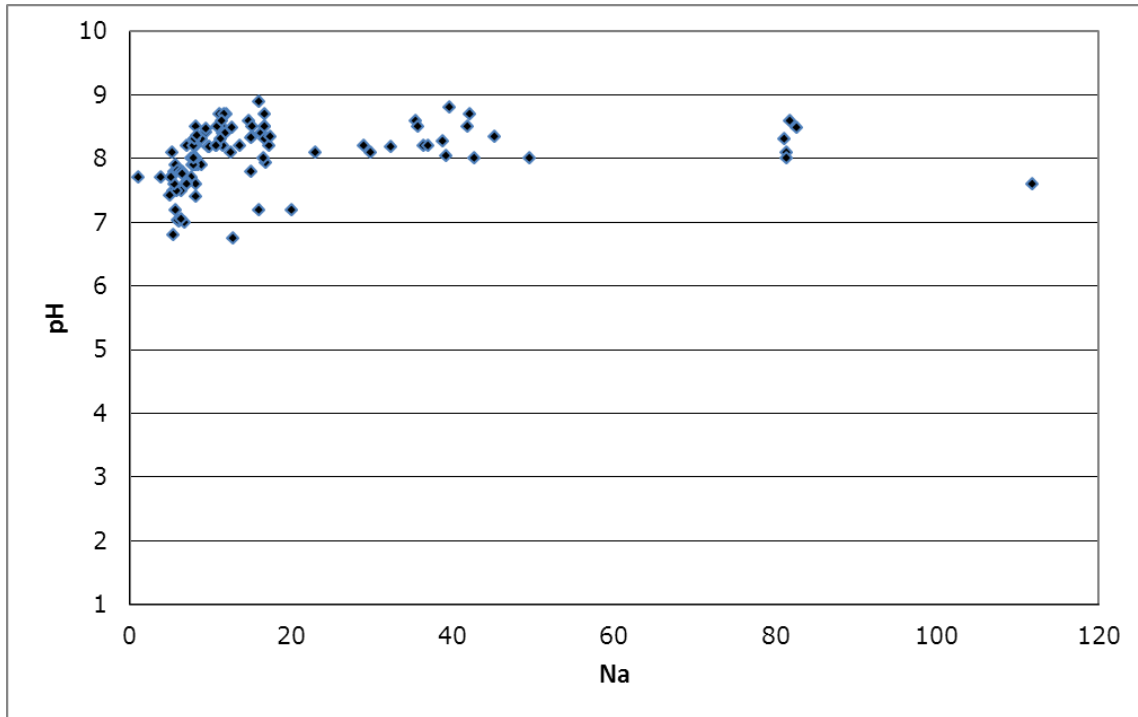


Figure 7-278. pH versus sodium (Na) measured in milliequivalents per liter (meq/L), Queen City Aquifer, South Transect, Groundwater Management Area 13.

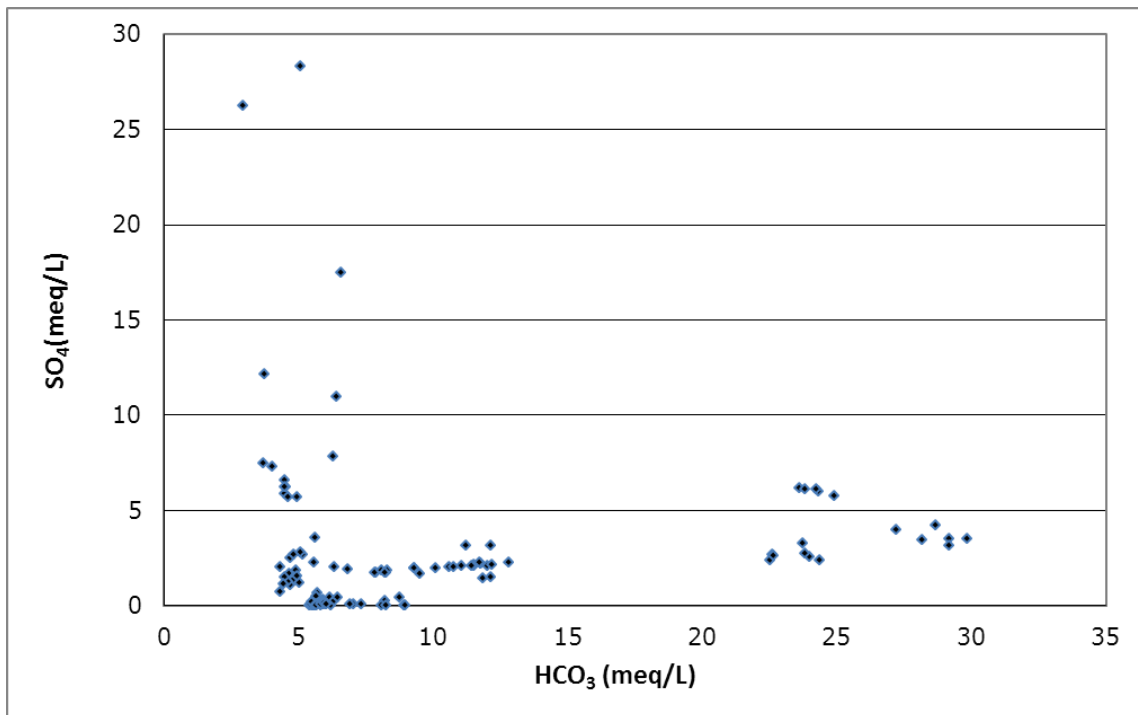


Figure 7-279. Sulfate (SO<sub>4</sub>) versus bicarbonate (HCO<sub>3</sub>) measured in milliequivalents per liter (meq/L), Queen City Aquifer, South Transect, Groundwater Management Area 13.

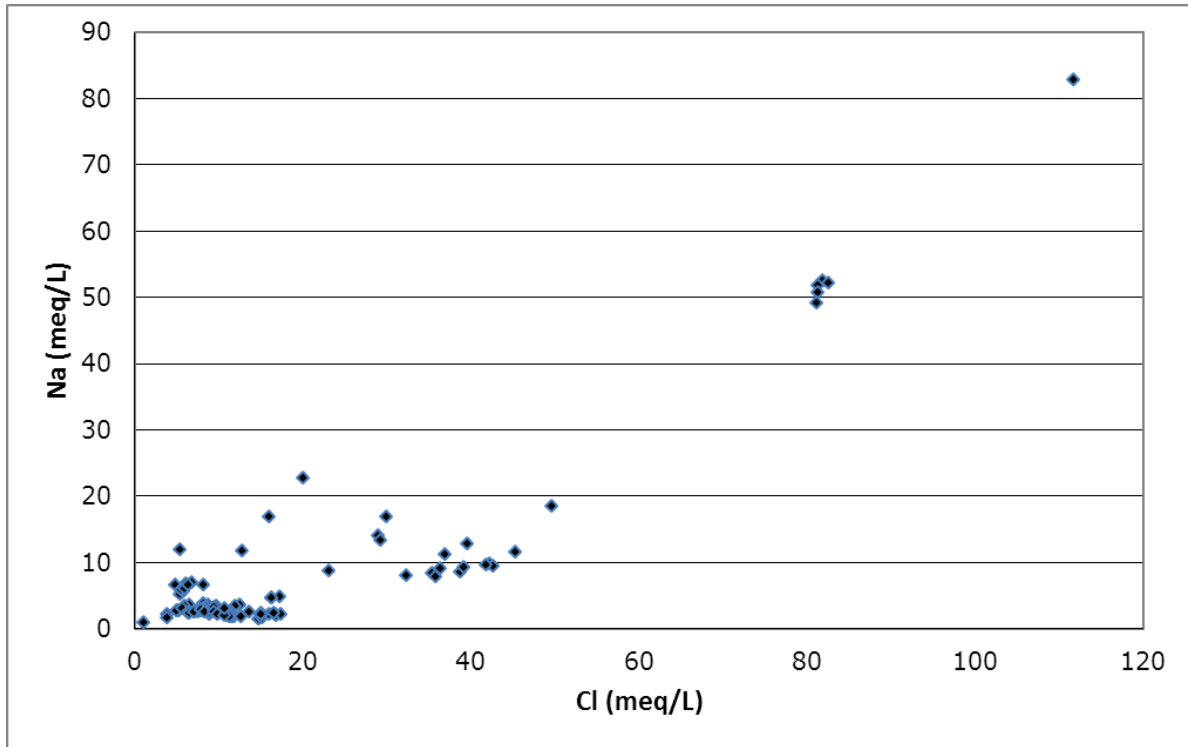


Figure 7-280. Sodium (Na) versus chloride (Cl) measured in milliequivalents per liter (meq/L), Queen City Aquifer, South Transect, Groundwater Management Area 13.

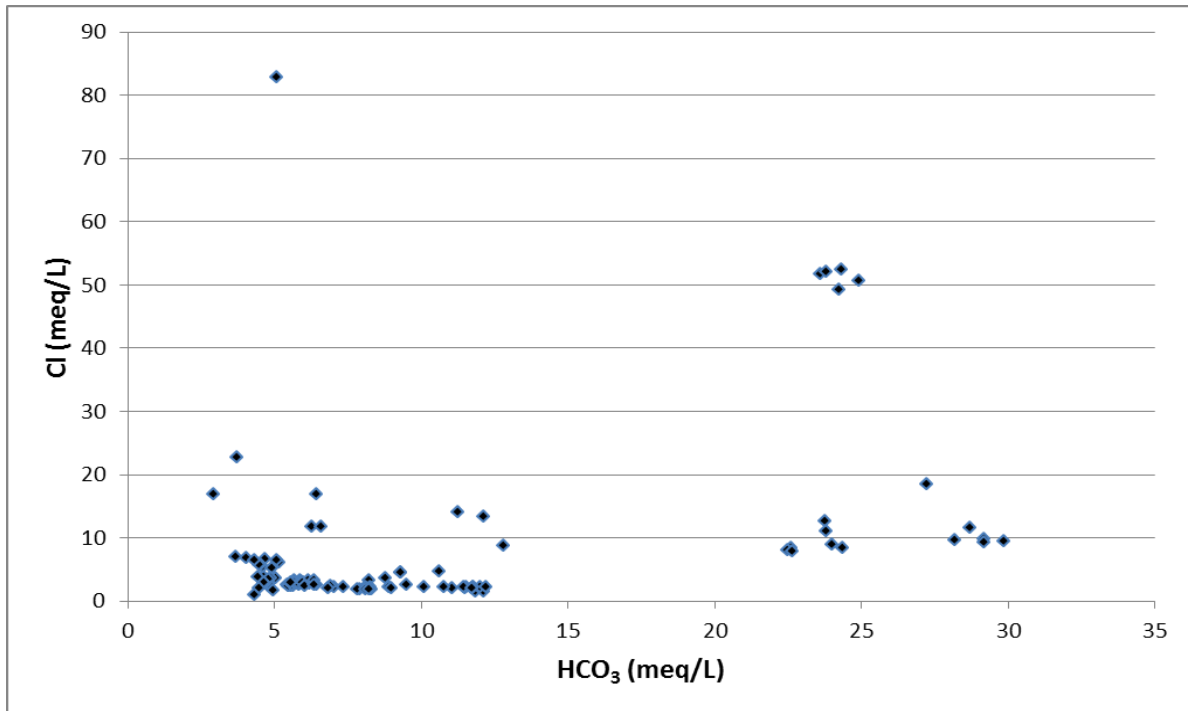


Figure 7-281. Chloride (Cl) versus bicarbonate ( $\text{HCO}_3$ ) measured in milliequivalents per liter (meq/L), Queen City Aquifer, South Transect, Groundwater Management Area 13.

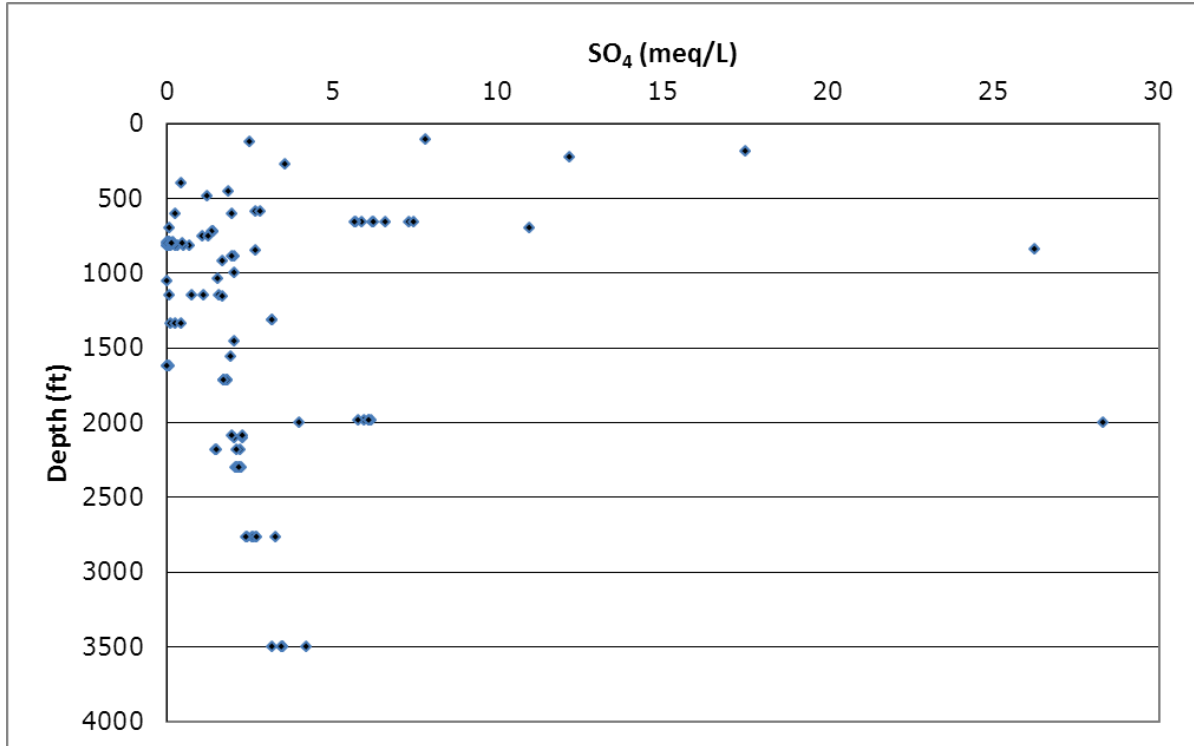
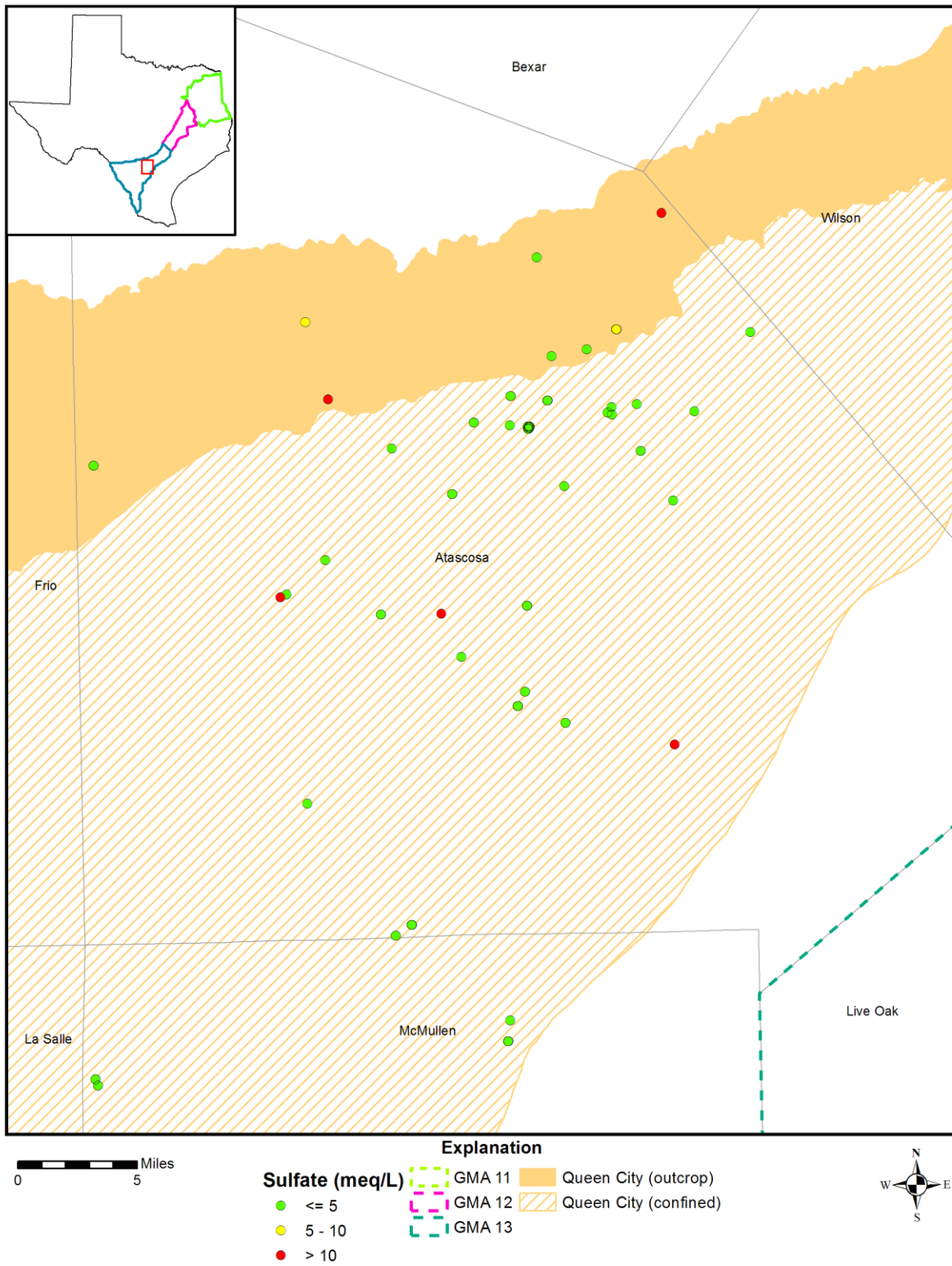
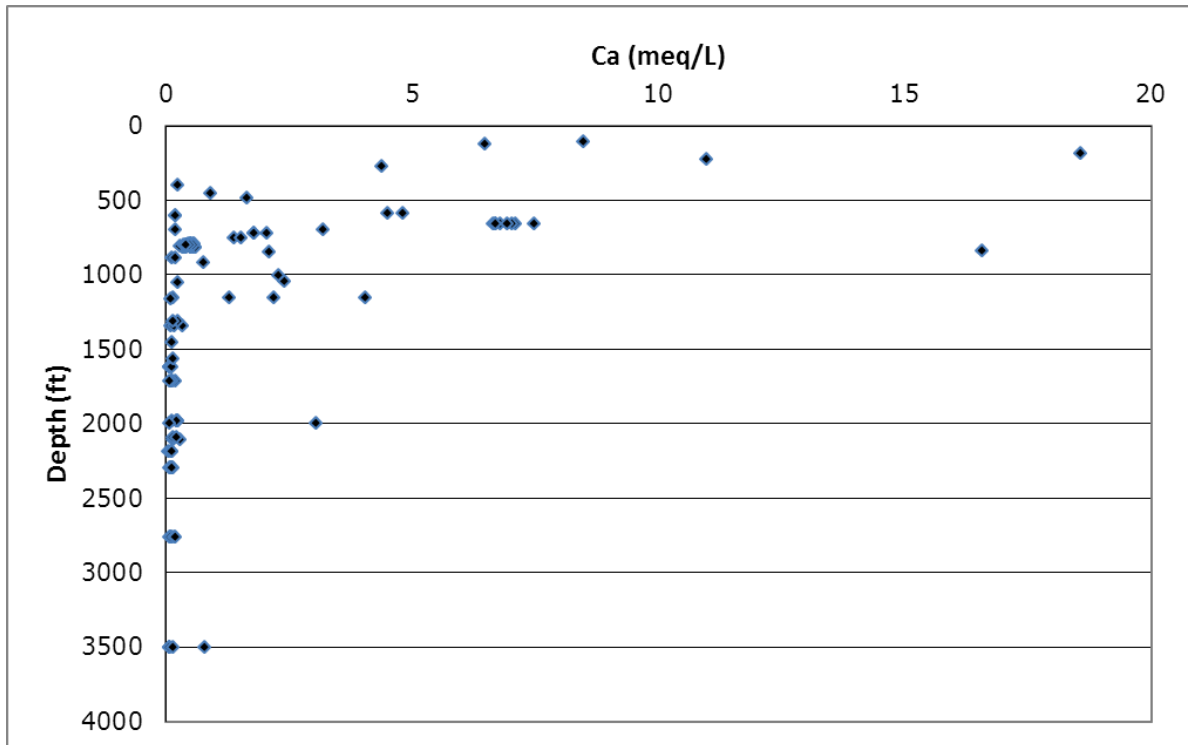


Figure 7-282. Depth measured from land surface in feet (ft) versus sulfate (SO<sub>4</sub>) measured in milliequivalents per liter (meq/L), Queen City Aquifer, South Transect, Groundwater Management Area 13.



**Figure 7-283. Sulfate concentrations measured in milliequivalents per liter (meq/L) in the Queen City Aquifer, South Transect, Groundwater Management Area (GMA) 13.**



**Figure 7-284. Depth measured from land surface in feet (ft) versus calcium (Ca) measured in milliequivalents per liter (meq/L), Queen City Aquifer, South Transect, Groundwater Management Area 13.**

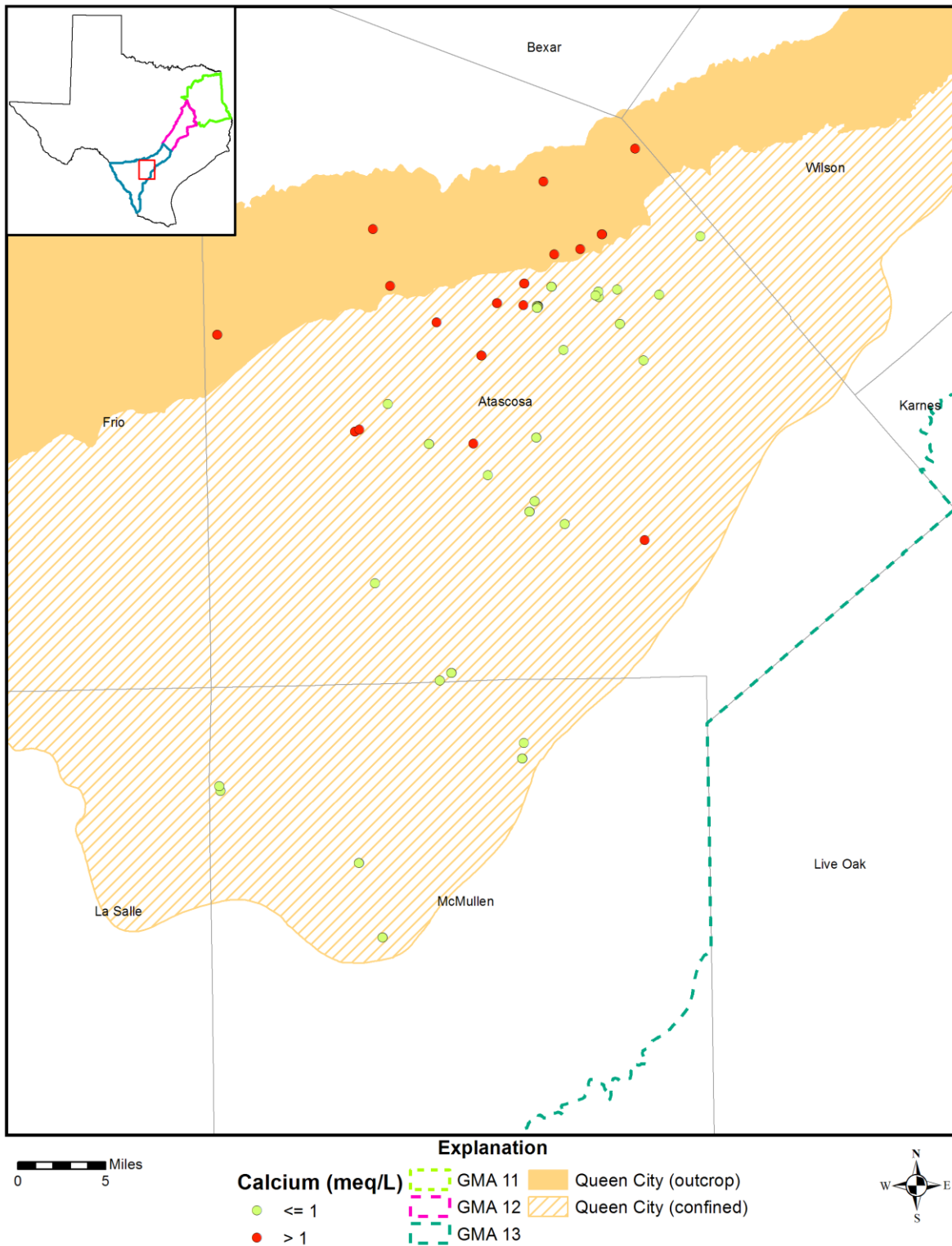


Figure 7-285. Calcium concentrations measured in milliequivalents per liter (meq/L) in the Queen City Aquifer, South Transect, Groundwater Management Area (GMA) 13.

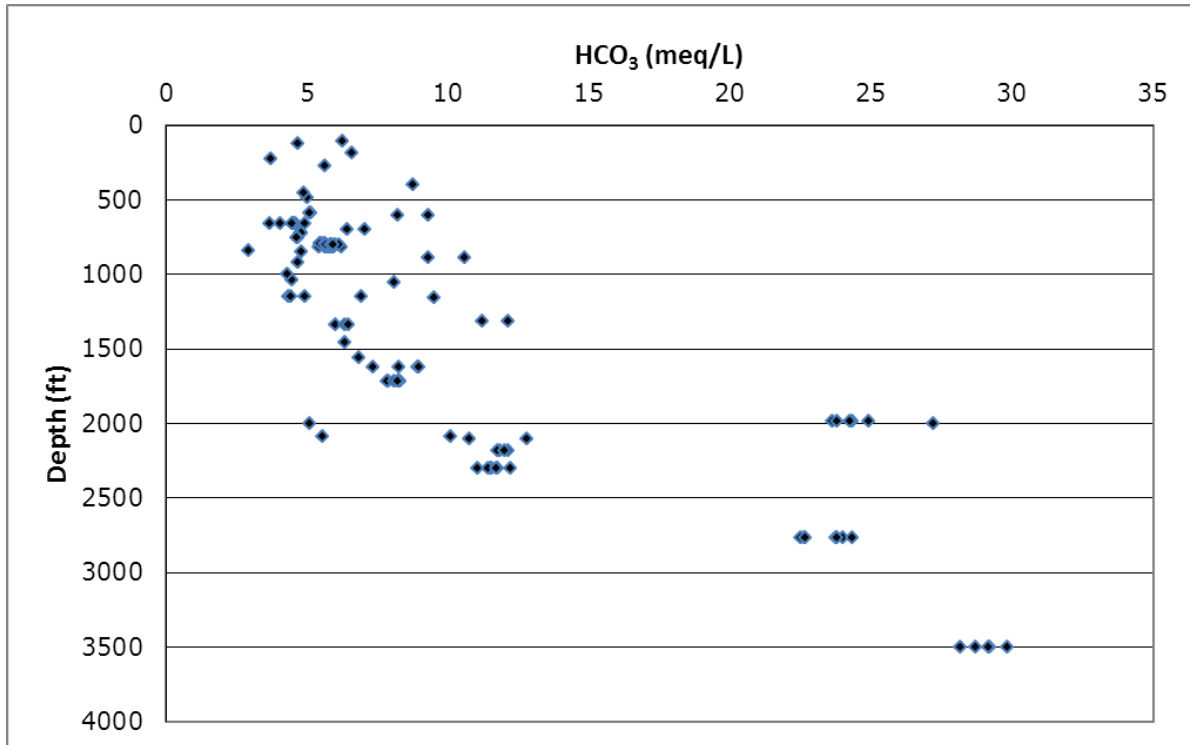


Figure 7-286. Depth measured from land surface in feet (ft) versus bicarbonate ( $\text{HCO}_3^-$ ) measured in milliequivalents per liter (meq/L), Queen City Aquifer, South Transect, Groundwater Management Area 13.

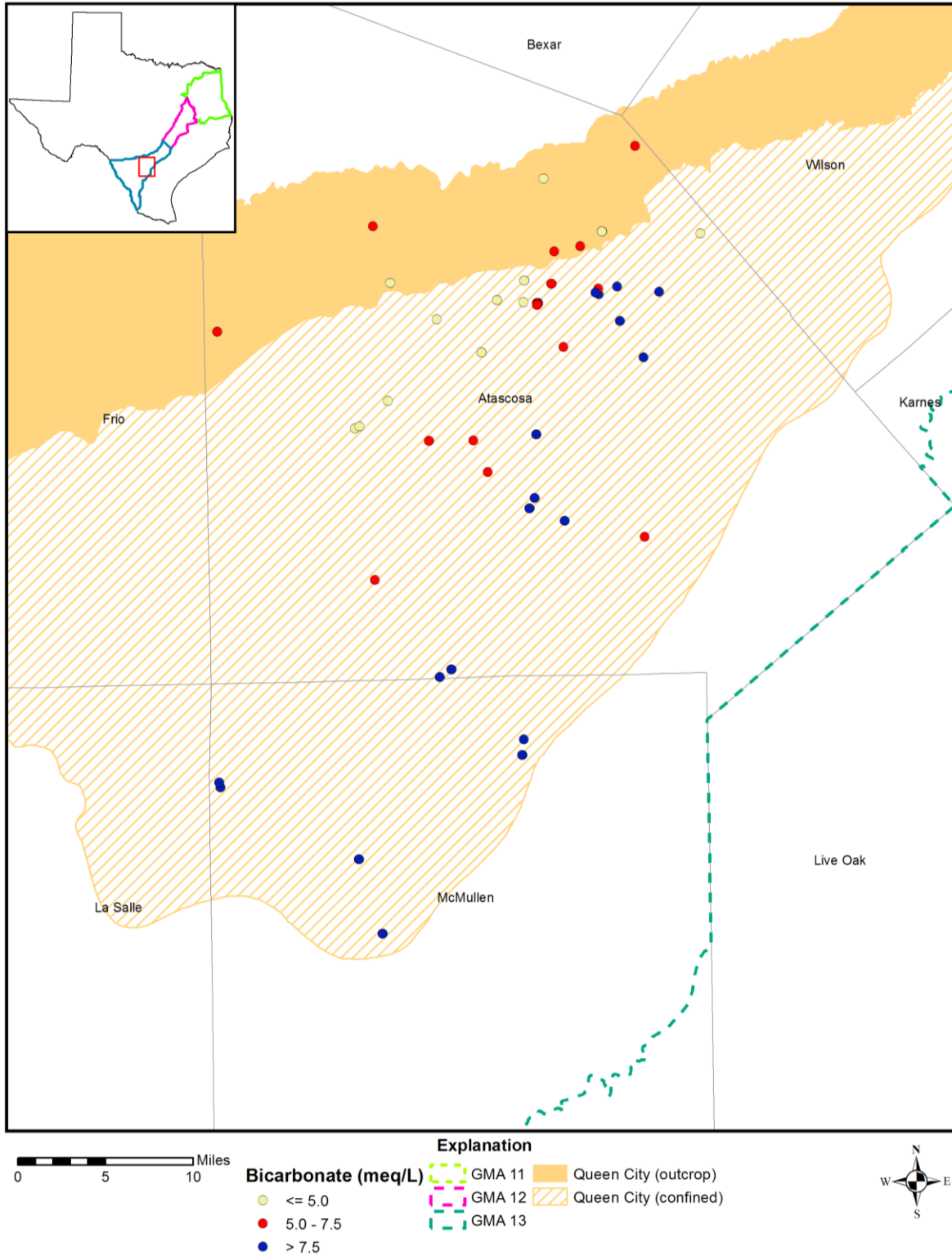


Figure 7-287. Bicarbonate concentrations measured in milliequivalents per liter (meq/L) in the Queen City Aquifer, South Transect, Groundwater Management Area (GMA) 13.

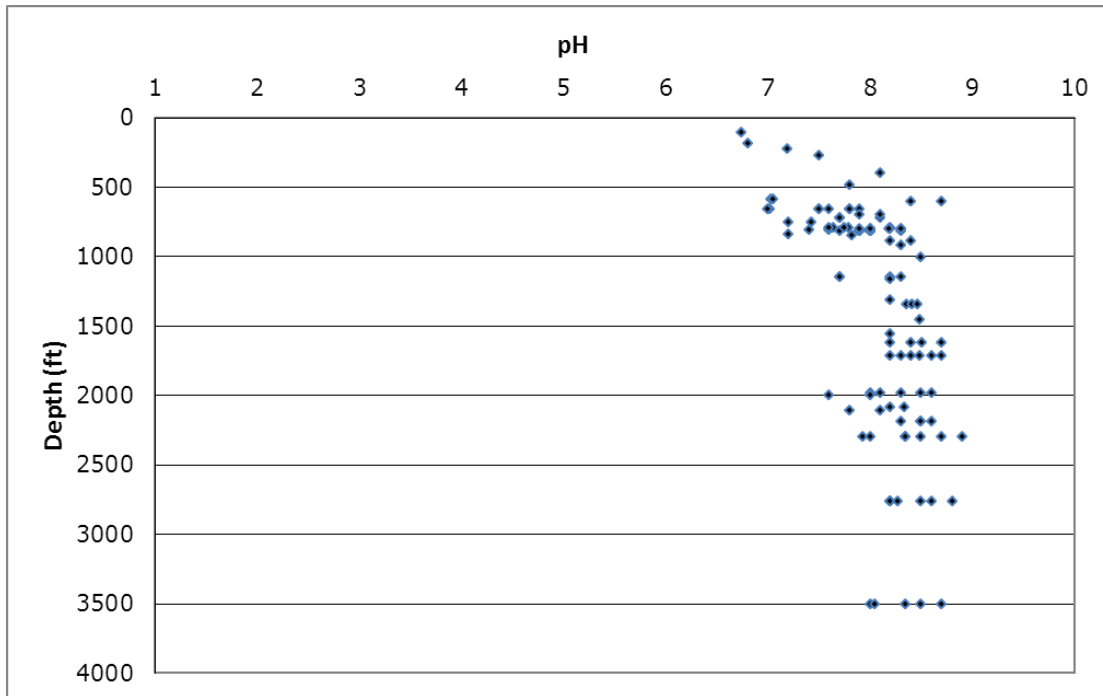


Figure 7-288. Depth measured from land surface in feet (ft) versus pH, Queen City Aquifer, South Transect, Groundwater Management Area 13.

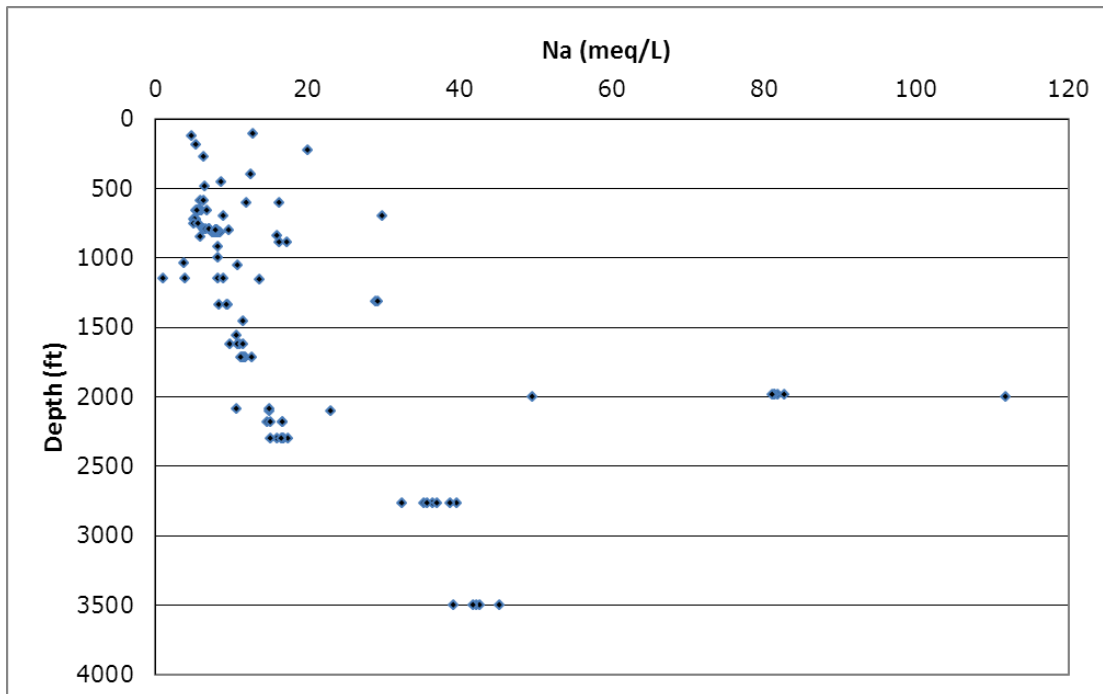


Figure 7-289. Depth measured from land surface in feet (ft) versus sodium (Na) measured in milliequivalents per liter (meq/L), Queen City Aquifer, South Transect, Groundwater Management Area 13.

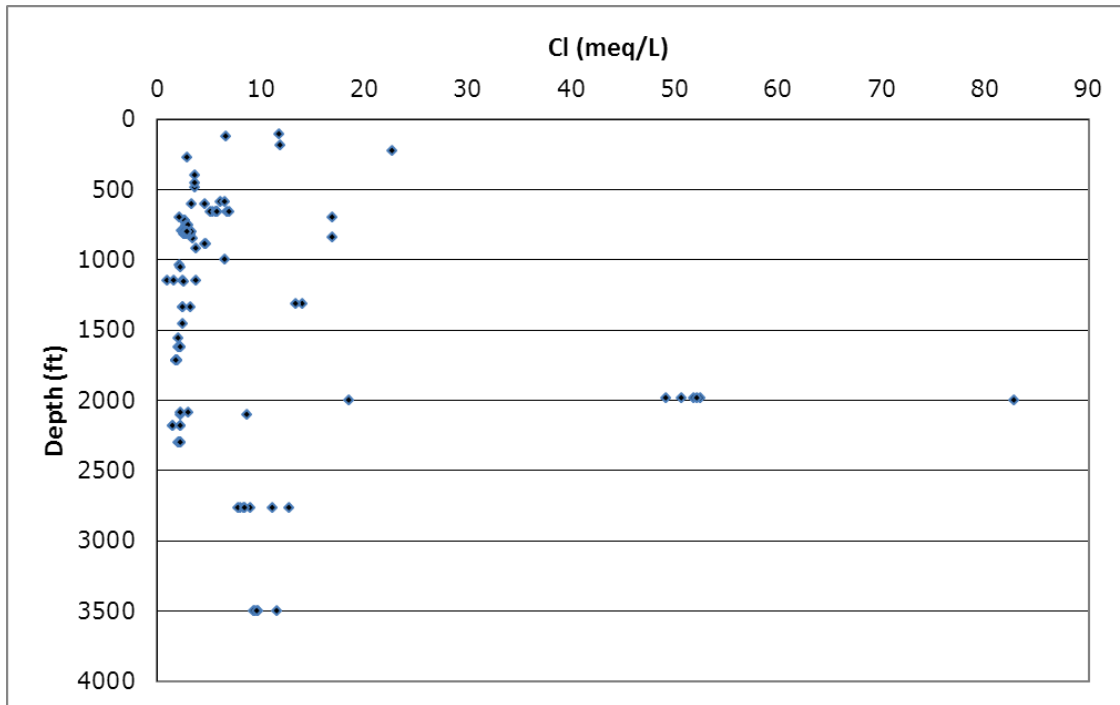


Figure 7-290. Depth measured from land surface in feet (ft) versus chloride (Cl) measured in milliequivalents per liter (meq/L), Queen City Aquifer, South Transect, Groundwater Management Area 13.

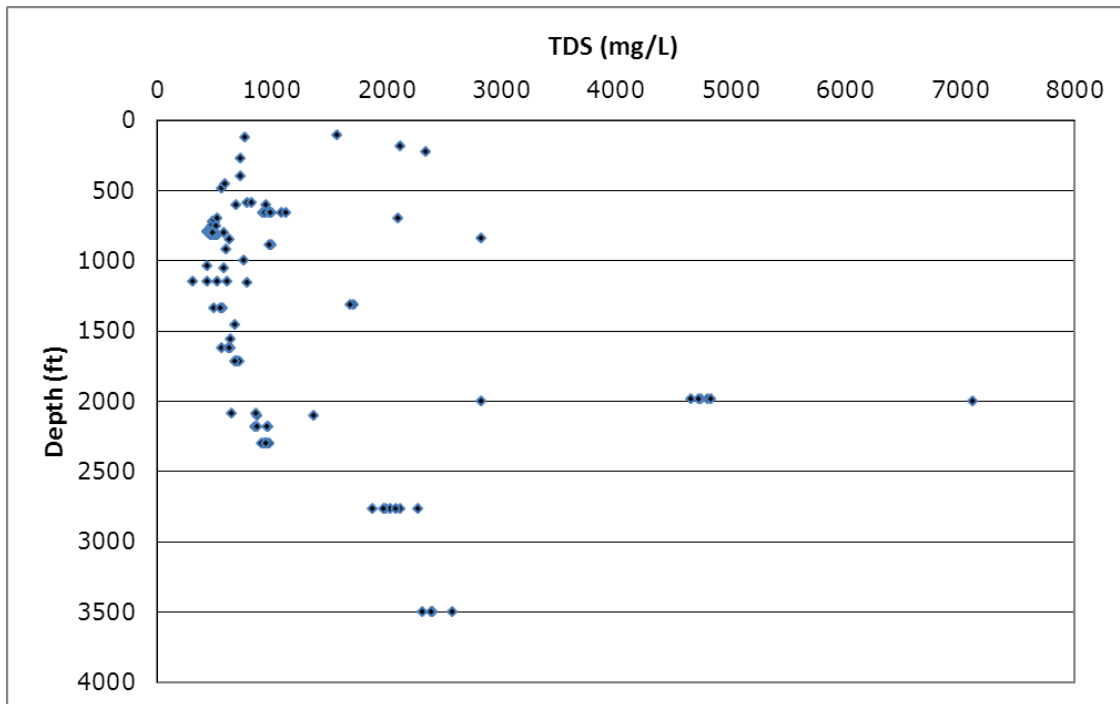


Figure 7-291. Depth measured from land surface in feet (ft) versus total dissolved solids (TDS) measured in parts per million (ppm), Queen City Aquifer, South Transect, Groundwater Management Area 13.

## **Sparta Aquifer**

A small database exists for the TWDB groundwater data for water wells, water chemistry and water levels for the Sparta Aquifer in the South Transect. The Sparta Aquifer is a minor aquifer in south Texas. There are no groundwater data for the Sparta Aquifer in its outcrop area in the South Transect. All data are in the confined portion of the aquifer.

### Well Depth

Depths of wells (Figure 7-292) extend from less than 500 feet just downdip from the outcrop to maximum depths of about 1,000 feet in central Atascosa County.

### Potentiometric Surface

Water level data (Figure 7-293) are considered too limited to develop a potentiometric surface and determine direction of groundwater flow. It is presumed to be from the outcrop into the deeper subsurface.

### Piper Diagram

The Piper diagram for the Sparta Aquifer (Figure 7-294) in the South Transect shows a mixed cation (calcium-magnesium-sodium) composition and mixed anion (sulfate-chloride) composition water for wells shallower than 1,000 feet. For the deeper wells, the cation composition is dominated by sodium and the anion composition has a wide range of chloride-bicarbonate waters.

### Bicarbonate versus Sodium Plot

A plot of bicarbonate versus sodium (Figure 7-295) shows no general pattern as observed for the underlying Queen City or Carrizo Sand Formation portion of the Carrizo-Wilcox aquifers. There are no sodium-bicarbonate type waters in the Sparta Aquifer.

### Sodium versus Calcium Plot

A plot of sodium versus calcium (Figure 7-296) for the Sparta Aquifer exhibits a slight inverse relationship between sodium and calcium as observed for the underlying Queen City and Carrizo Sand Formation aquifers. The calcium concentrations are higher than in most of the aquifers studied.

### Bicarbonate versus Calcium Plot

A plot of bicarbonate versus calcium (Figure 7-297) for the Sparta Aquifer exhibits an inverse relationship between calcium and bicarbonate as observed for the underlying Queen City and Carrizo Sand Formation aquifers. This inverse relationship may not be the same in the other aquifers, because all the samples are from downdip in the aquifer. This inverse relationship between calcium versus bicarbonate for those aquifers evolving into a sodium-bicarbonate water occurs where there are samples in both the outcrop and downdip.

### pH versus Bicarbonate Plot

A plot of pH versus bicarbonate (Figure 7-298) exhibits no relationship between the two constituents. There is no “low pH” limb in this curve as seen in other aquifers, possibly because there are no samples from the outcrop.

#### Sulfate versus Bicarbonate Plot

The plot of sulfate versus bicarbonate (Figure 7-299) shows an inverse relationship between sulfate and bicarbonate. The sulfate concentrations for the Sparta Aquifer in the South Transect are some of the highest observed for any of the aquifers from this study.

#### Chloride versus Sodium Plot

The plot of chloride versus sodium (Figure 7-300) for the Sparta Aquifer exhibits increases in both sodium and chloride but not at a 1:1 ratio. Sodium is increasing more rapid and the rapid increase of sodium to chloride suggests the addition of bicarbonate and chloride sources.

#### Depth versus Sulfate Plot

The plot of depth versus sulfate (Figure 7-301) shows lower sulfate concentrations with depth.

#### Depth versus Calcium Plot

The plot of depth versus calcium (Figure 7-302) shows lower calcium with depth. Calcium may be exchanging with sodium at greater depths. Higher calcium concentrations are not found at depth greater than about 600 feet.

#### Depth versus Bicarbonate Plot

The plot of depth versus bicarbonate (Figure 7-303) shows increasing bicarbonate with depth.

#### Depth versus Sodium Plot

The plot of depth versus sodium (Figure 7-304) shows no trends.

#### Depth versus Chloride Plot

The plot of depth versus chloride (Figure 7-305) generally shows no trends.

#### Depth versus Total Dissolved Solids Plot

The plot of depth versus total dissolved solids (Figure 7-306) shows a total dissolved solids range from about 1,000 parts per million to about 4,000 parts per million. Their concentrations are higher than observed for most of the groundwater in the underlying Carrizo Sand Formation or the Queen City Aquifer for the South Transect.

#### Discussion

Water quality of the Sparta Aquifer in the South Transect characteristically is poor with an average total dissolved solids of 1,000 parts per million or greater. The Piper diagram shows a wide range of chemistry. The anion (chloride-sulfate-bicarbonate) composition shows a wide range with more waters as sulfate-chloride type water than bicarbonate type water, whereas the underlying Queen City and Carrizo Sand Formation aquifers have anion composition predominantly in the bicarbonate corner. Water chemistry in the Sparta Aquifer is dissimilar to water chemistry in the underlying aquifers. This dissimilarity does not support the concept of upwards leakage from the Carrizo Sand Formation to the Queen City Aquifer to the Sparta Aquifer on a regional basis. Similarly the Sparta Aquifer has total dissolved solids values higher than the Queen City and Carrizo Sand Formation aquifers. Their higher total dissolved solids values in the shallower Sparta Aquifer do not support a hypothesis of upward leakage by cross-formational flow from deeper formations.

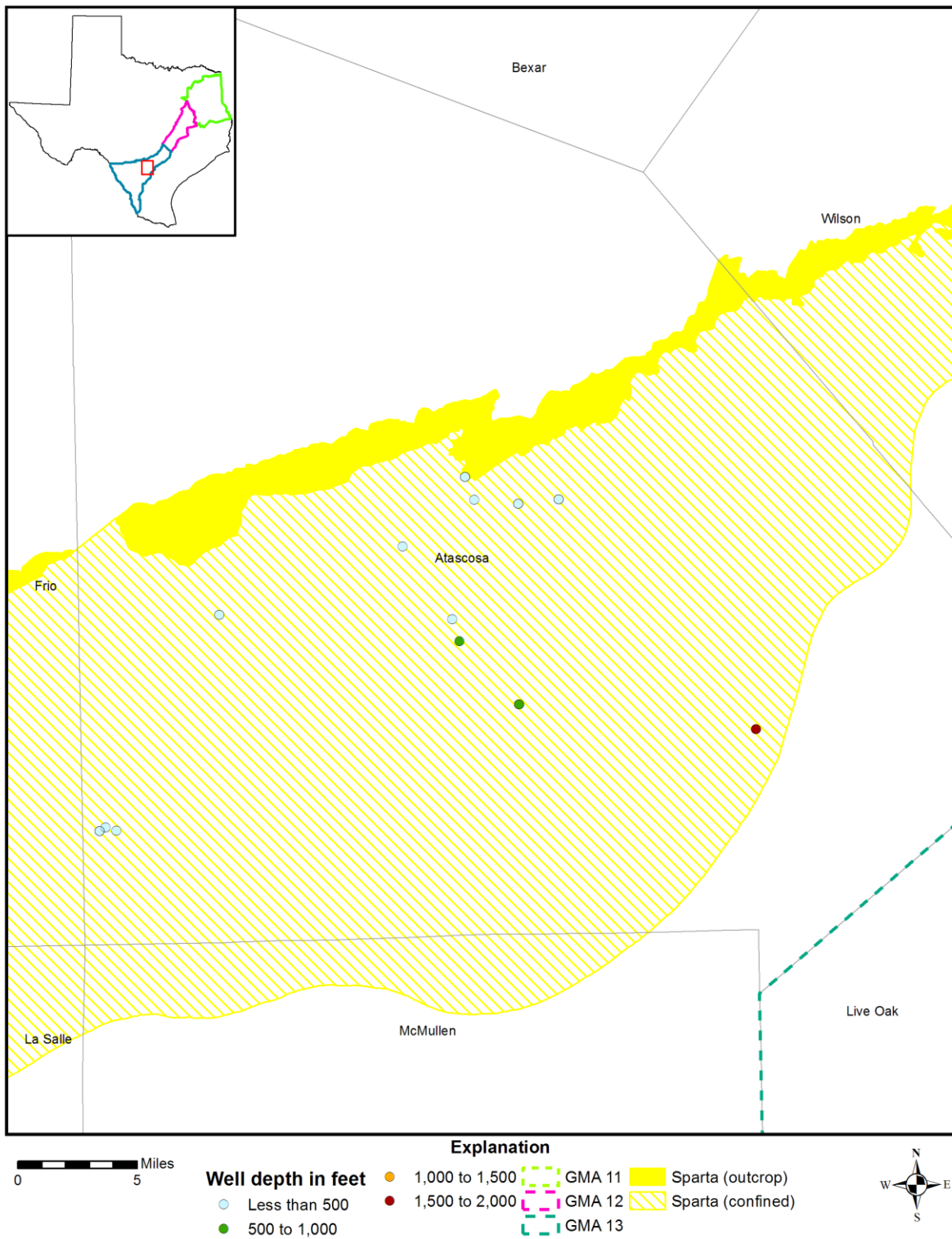


Figure 7-292. Well depths measured in feet from land surface in the Sparta Aquifer, South Transect, Groundwater Management Area (GMA) 13.

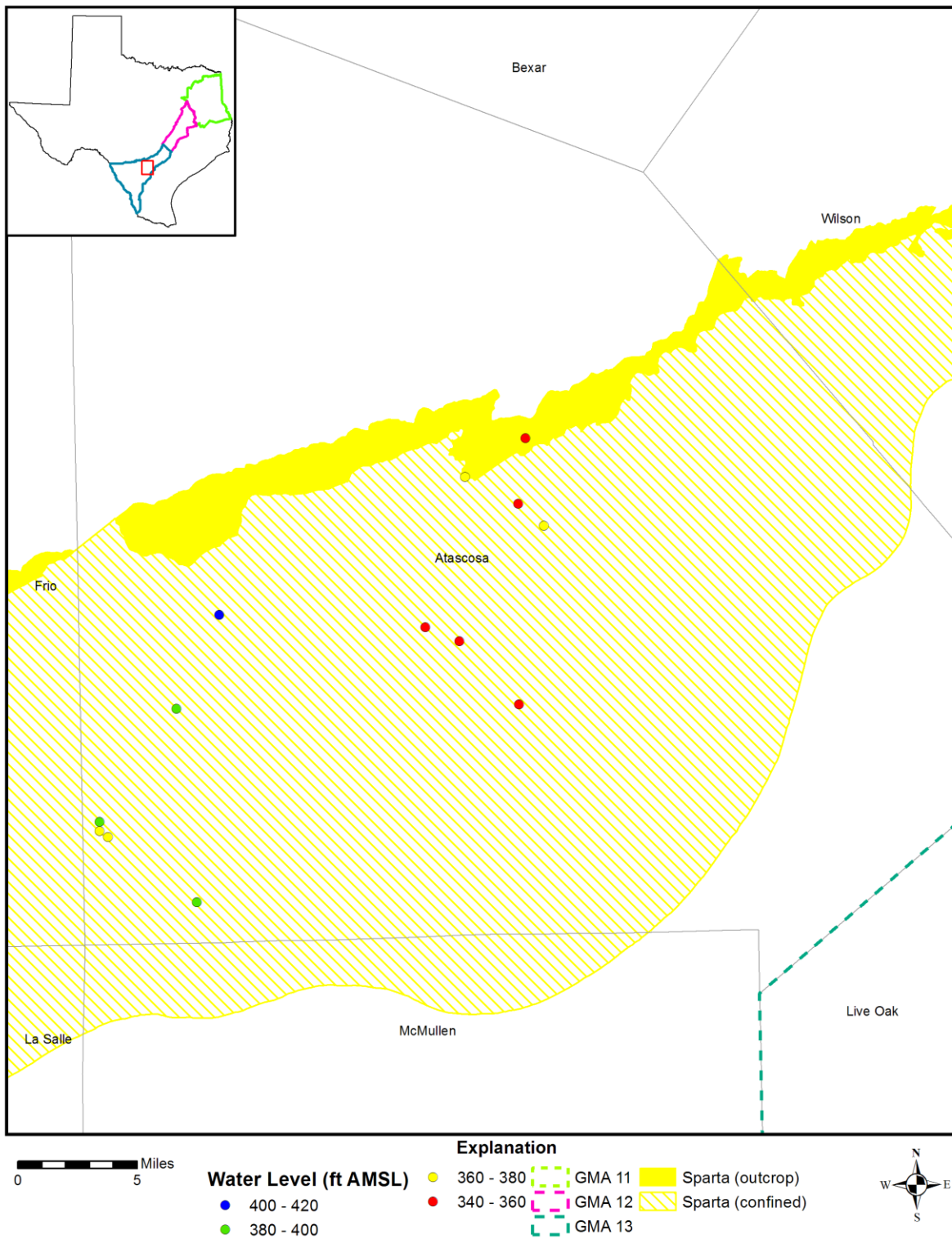


Figure 7-293. Water level elevations from 1942 to 2010 measured in feet above mean sea level (ft AMSL) in the Sparta Aquifer, South Transect, Groundwater Management Area (GMA) 13.

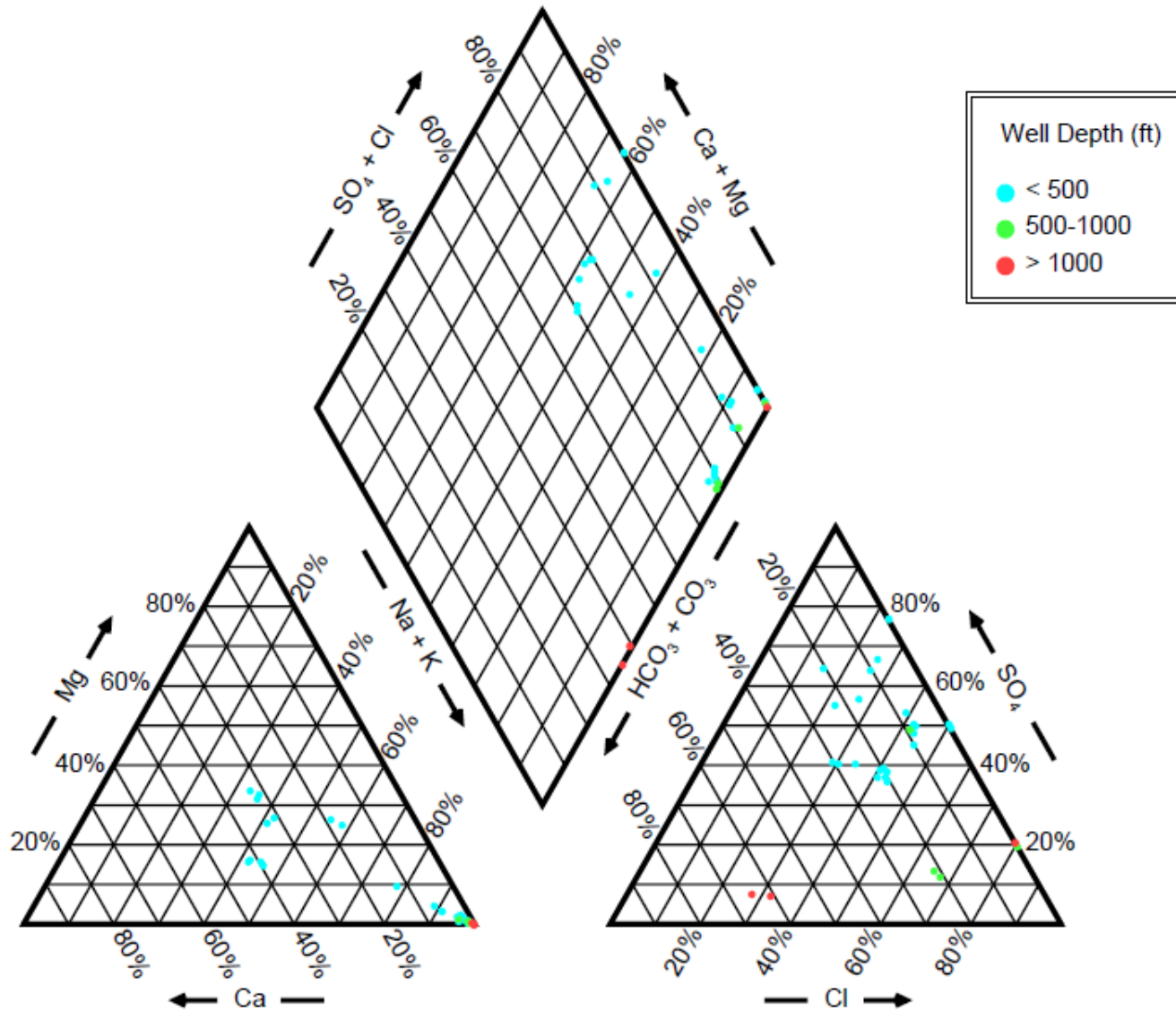


Figure 7-294. Piper diagram showing chemistry of the Sparta Aquifer wells in the South Transect by well depth measured from land surface in feet (ft).

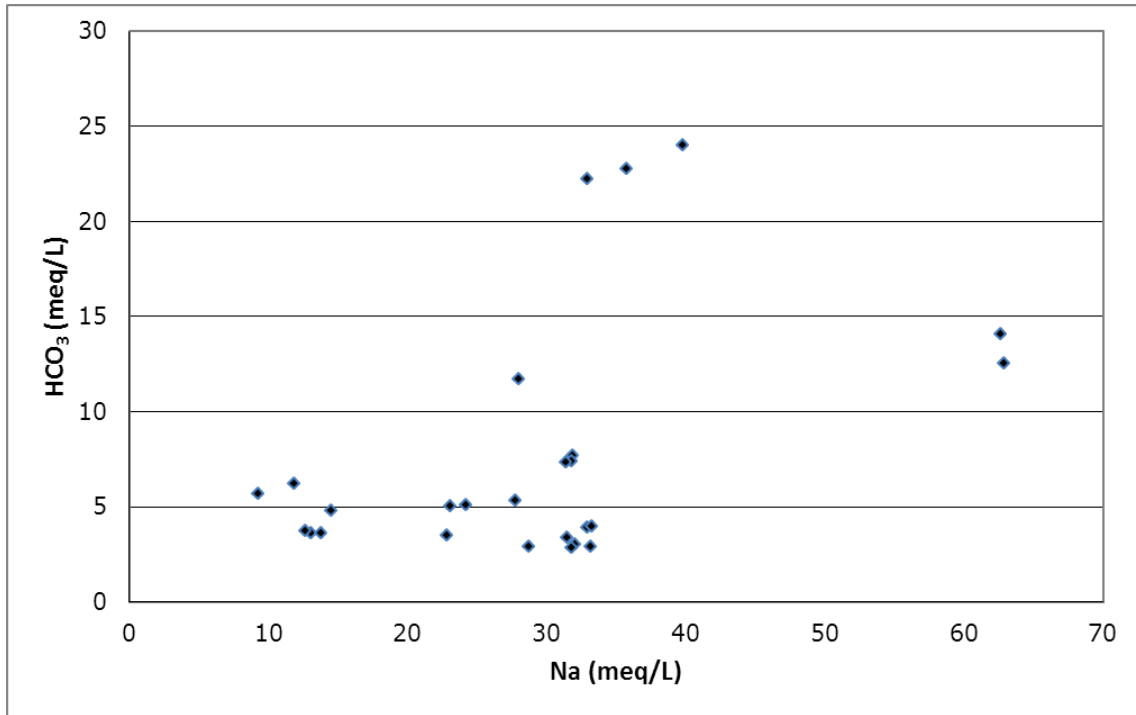


Figure 7-295. Bicarbonate ( $\text{HCO}_3$ ) versus sodium (Na) measured in milliequivalents per liter (meq/L), Sparta Aquifer, South Transect, Groundwater Management Area 13.

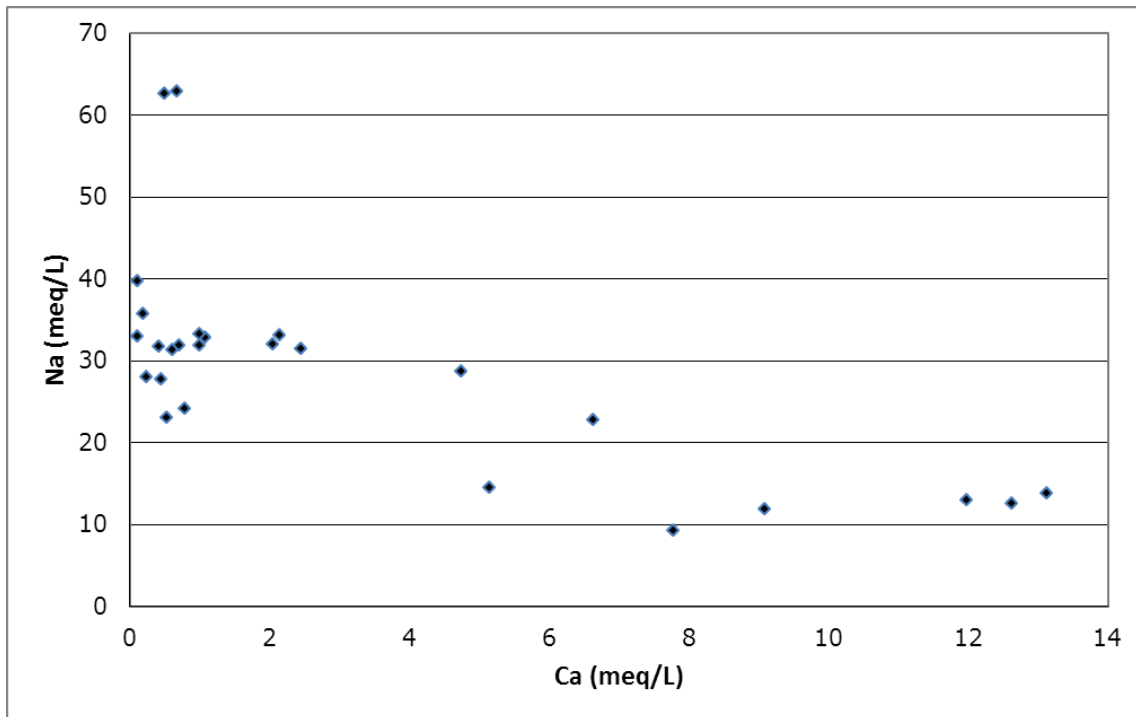


Figure 7-296. Sodium (Na) versus calcium (Ca) measured in milliequivalents per liter (meq/L), Sparta Aquifer, South Transect, Groundwater Management Area 13.

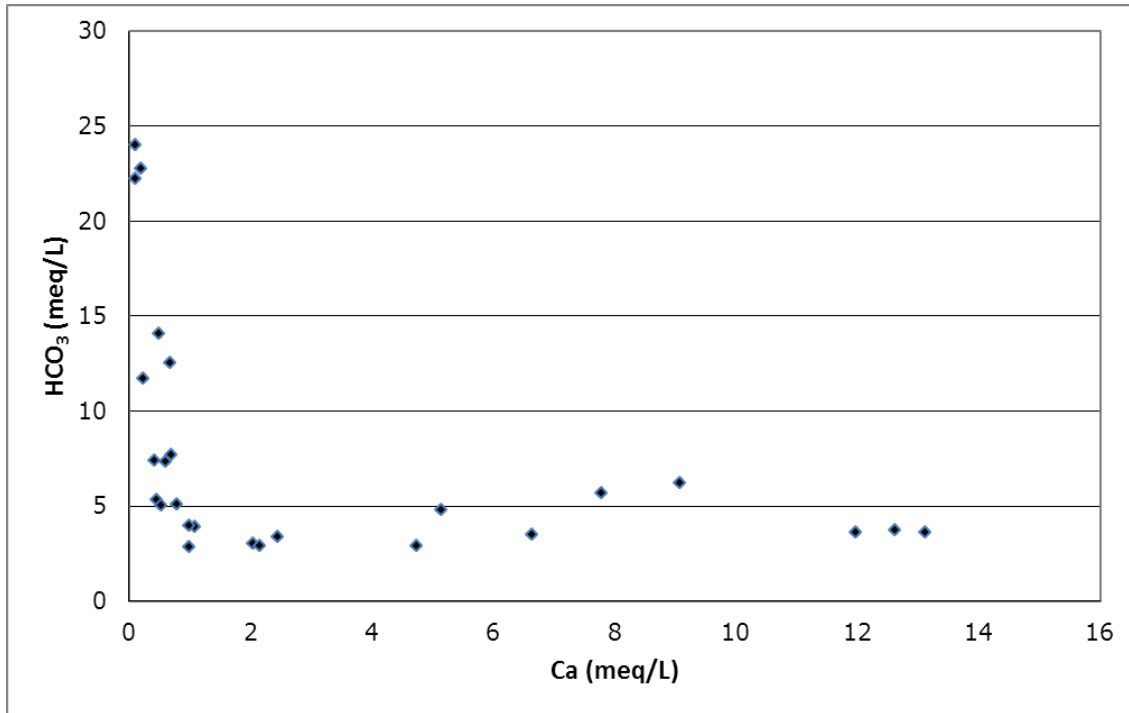


Figure 7-297. Bicarbonate (HCO<sub>3</sub><sup>-</sup>) versus calcium (Ca) measured in milliequivalents per liter (meq/L), Sparta Aquifer, South Transect, Groundwater Management Area 13.

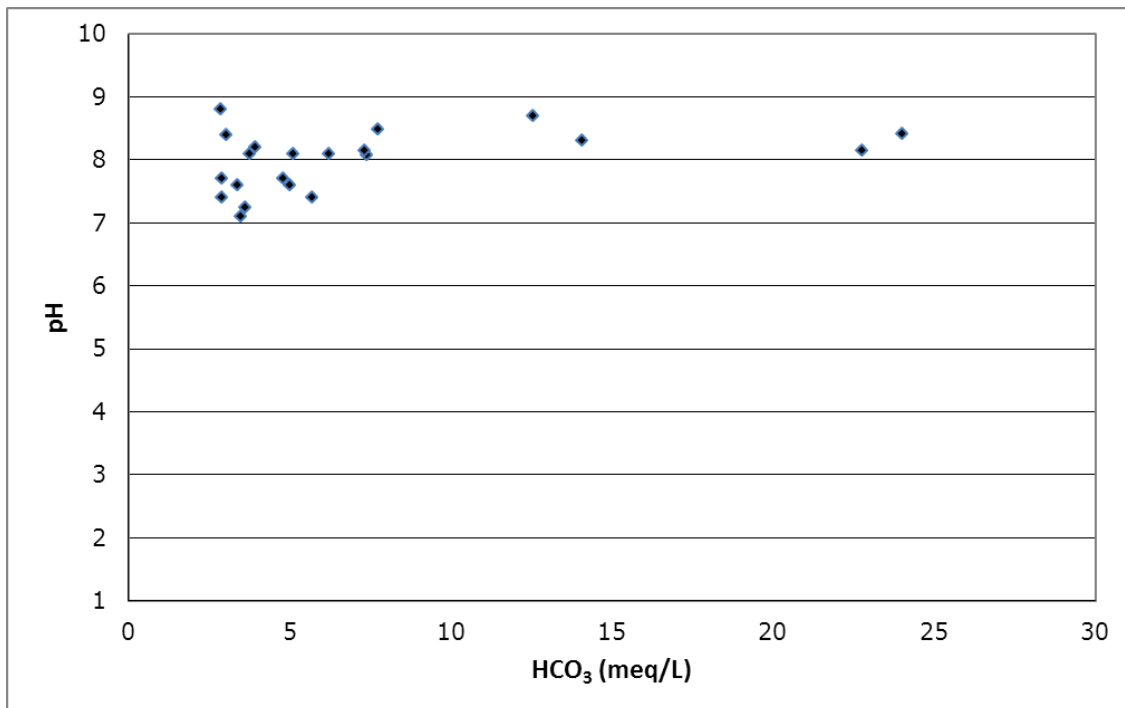


Figure 7-298. pH versus bicarbonate (HCO<sub>3</sub><sup>-</sup>) measured in milliequivalents per liter (meq/L), Sparta Aquifer, South Transect, Groundwater Management Area 13.



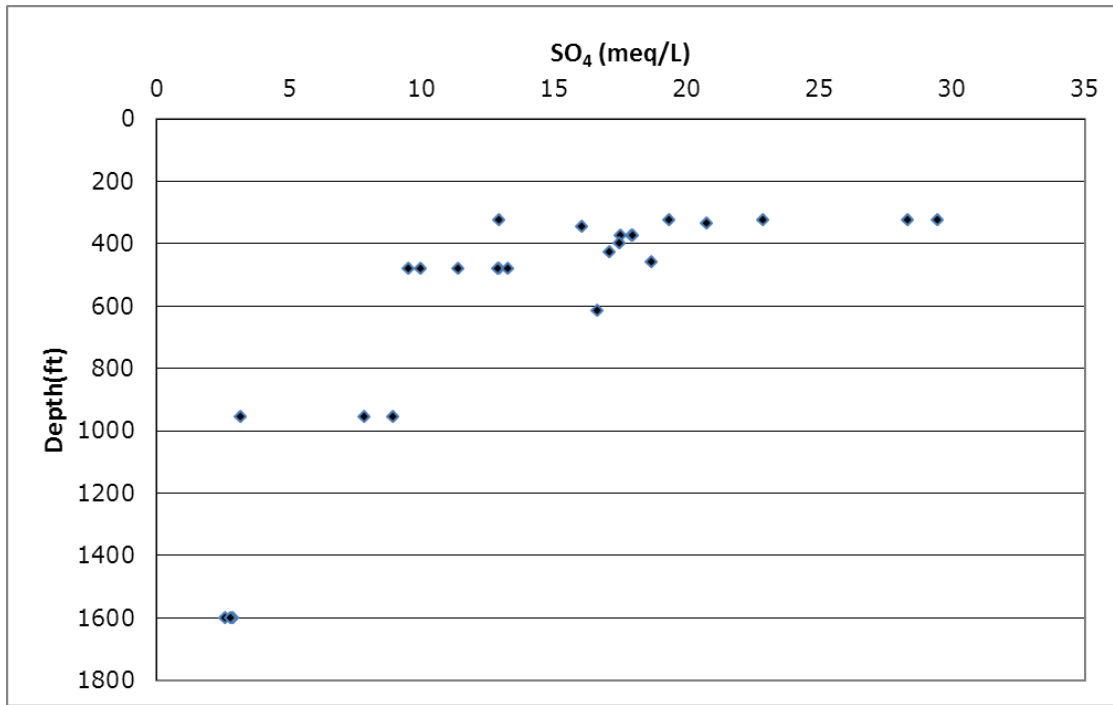


Figure 7-301. Depth measured from land surface in feet (ft) versus sulfate (SO<sub>4</sub>) measured in milliequivalents per liter (meq/L), Sparta Aquifer, South Transect, Groundwater Management Area 13.

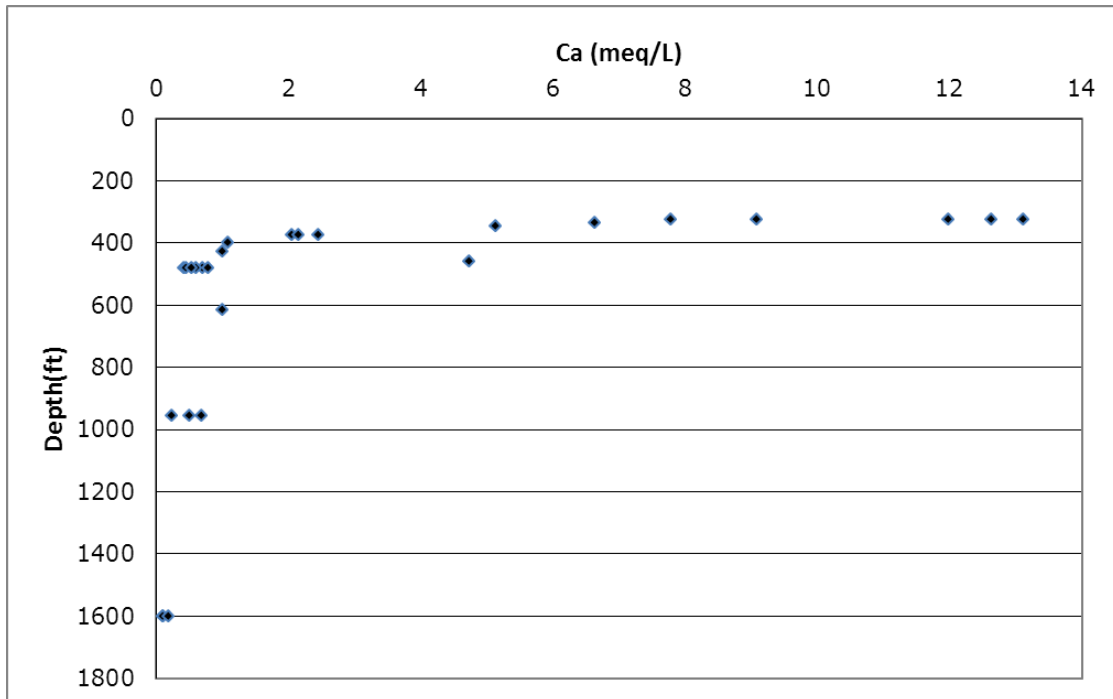


Figure 7-302. Depth measured from land surface in feet (ft) versus calcium (Ca) measured in milliequivalents per liter (meq/L), Sparta Aquifer, South Transect, Groundwater Management Area 13.

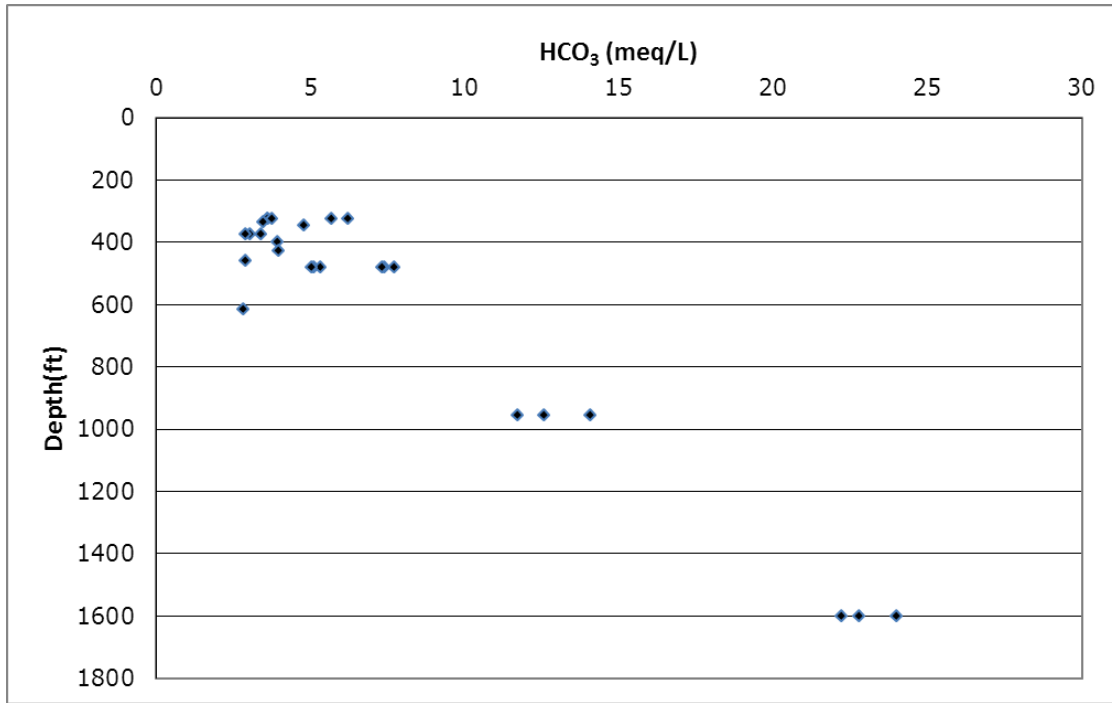


Figure 7-303. Depth measured from land surface in feet (ft) versus bicarbonate (HCO<sub>3</sub>) measured in milliequivalents per liter (meq/L), Sparta Aquifer, South Transect, Groundwater Management Area 13.

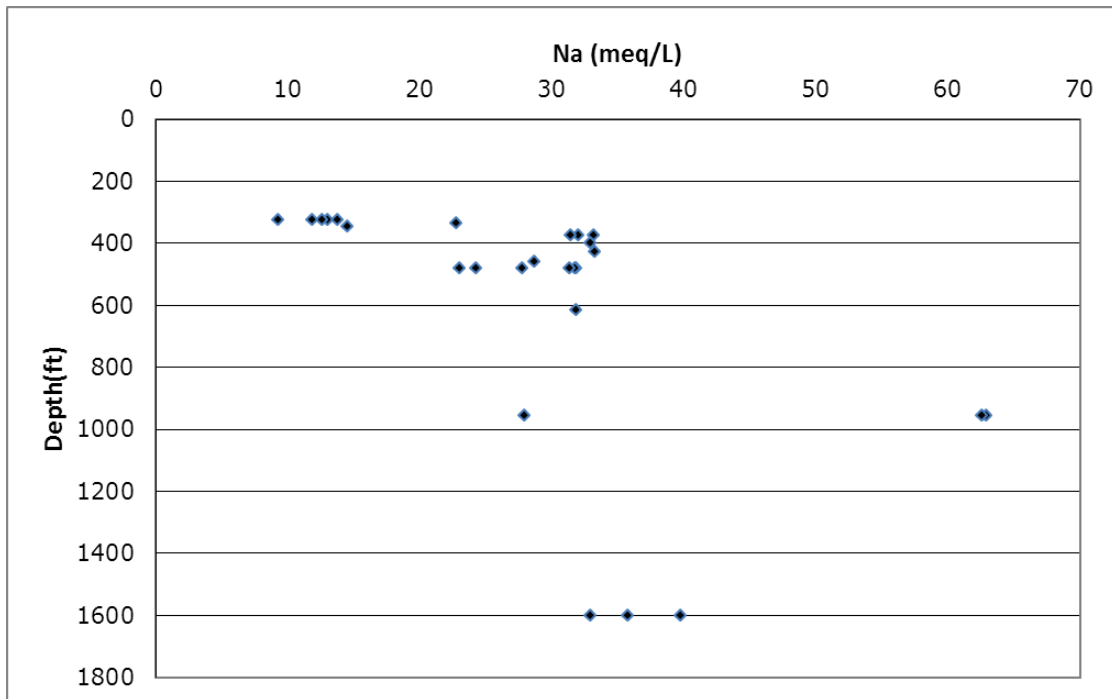


Figure 7-304. Depth measured from land surface in feet (ft) versus sodium (Na) measured in milliequivalents per liter (meq/L), Sparta Aquifer, South Transect, Groundwater Management Area 13.

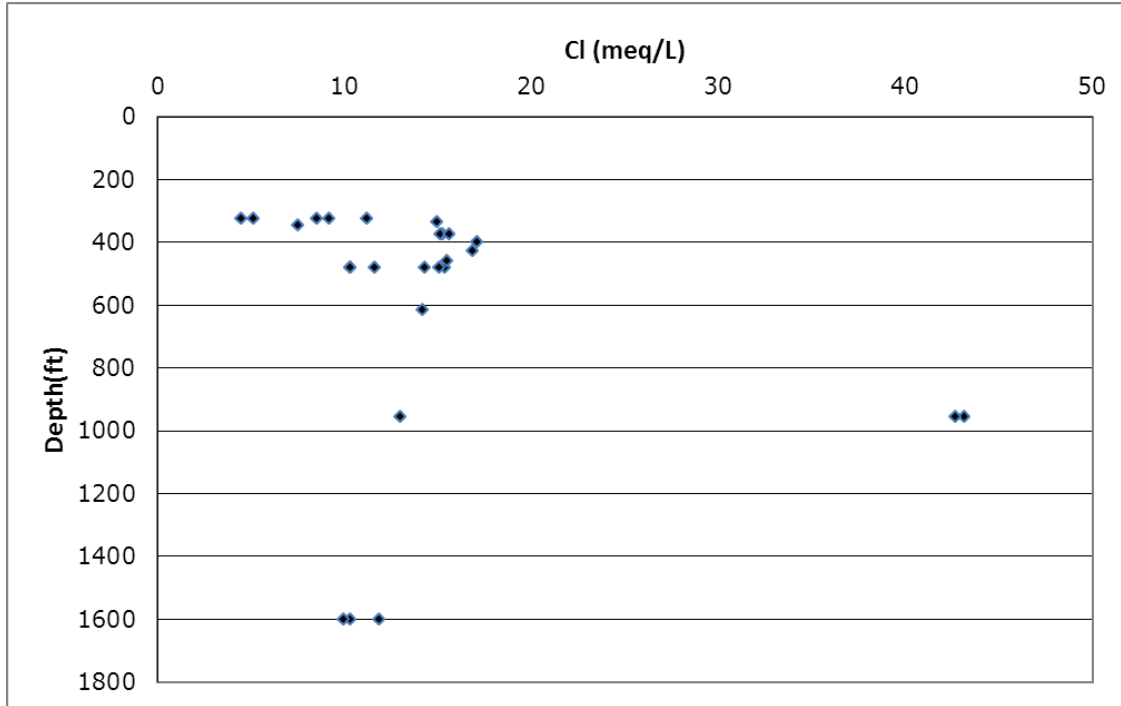


Figure 7-305. Depth measured from land surface in feet (ft) versus chloride (Cl) measured in milliequivalents per liter (meq/L), Sparta Aquifer, South Transect, Groundwater Management Area 13.

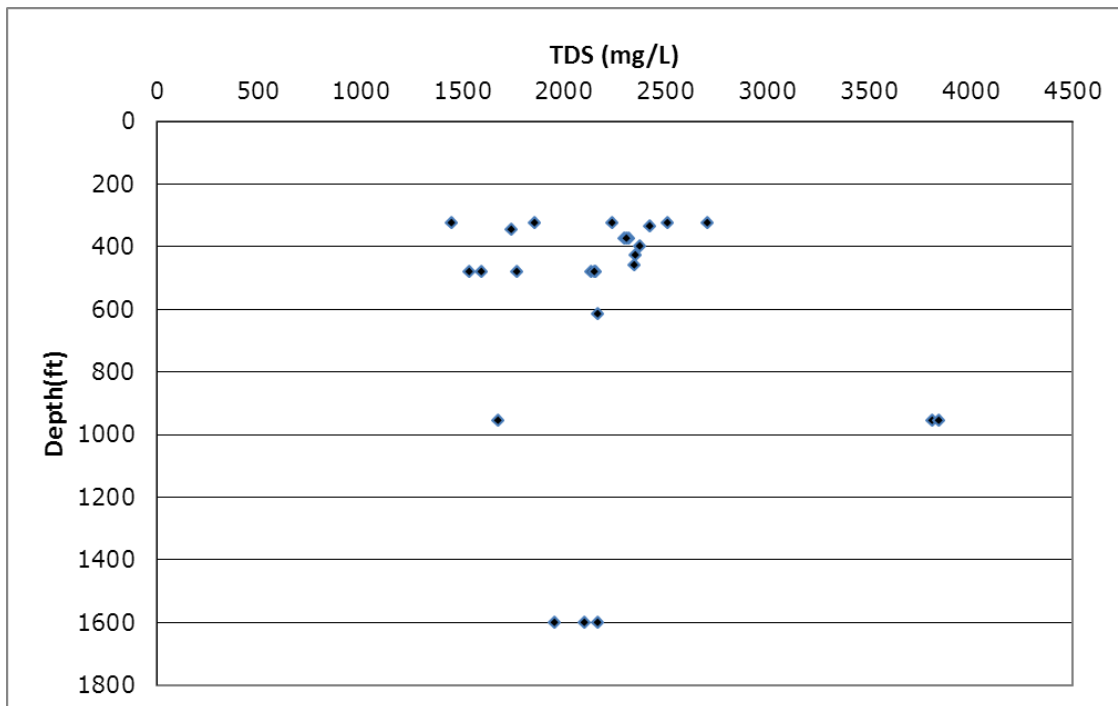


Figure 7-306. Depth measured from land surface in feet (ft) versus total dissolved solids (TDS) measured in parts per million (ppm), Sparta Aquifer, South Transect, Groundwater Management Area (GMA) 13.

## **Yegua-Jackson Aquifer**

A small database for the TWDB groundwater data exist for the Yegua-Jackson Aquifer in the South Transect.

### Well Depth

The TWDB database indicates well depth in the Yegua-Jackson Aquifer range from about 50 feet to over 800 feet. All wells in the TWDB database indicate the Yegua-Jackson Aquifer production is within the outcrop (Figure 7-307).

### Potentiometric Surface

Water levels vary from about 150 feet to greater than 300 feet (Figure 7-308). There is too little data to develop a potentiometric surface and discern a general direction of groundwater flow.

### Piper Diagram

The Piper diagram for the Yegua-Jackson Aquifer (Figure 7-309) shows a transition from calcium-sodium type water to a sodium type for the cation triangle. There is very little magnesium in these waters as compared to the other aquifers. From shallower to deeper waters, the chemistry of the water for the ions shifts from a sulfate-chloride water to a chloride water at greater depths. There are no bicarbonate-dominated waters at any depth. This is in contrast to the Carrizo Sand Formation and the Queen City Aquifer for the South Transect.

### Chemistry Plots

Most of the comparisons between two ionic constituents show no correlations and therefore are not included here. This included sodium versus bicarbonate, pH versus bicarbonate, sulfate versus bicarbonate, chloride versus sulfate and most relationships between depth and an ionic constituent. The only chemical constituents that do correlate are sodium versus chloride, sodium versus calcium, depth versus calcium and depth versus chloride and are shown below.

#### Sodium versus Calcium Plot

The plot of sodium versus calcium (Figure 7-310) for the Yegua-Jackson Aquifer primarily has one limb (the sodium limb) of the sodium-calcium relationship observed for many of the other aquifers.

#### Chloride versus Sodium Plot

The plot of chloride versus sodium (Figure 7-311) shows a linear correlation with both sodium and chloride concentrations increasing to about 150 milliequivalents per liter for sodium and chloride.

#### Depth versus Calcium Plot

The plot of depth versus calcium (Figure 7-312) for the Yegua-Jackson Aquifer shows higher calcium at shallow depths and decreasing to negligible concentrations at depths greater than 200 feet.

#### Depth versus Chloride Plot

The plot of depth versus chloride (Figure 7-313) for the Yegua-Jackson Aquifer shows a general increase of chloride with depth to high concentrations.

### Depth versus Total Dissolved Solids Plot

The plot of depth versus total dissolved solids (Figure 7-314) shows total dissolved solids concentrations in the Yegua-Jackson Aquifer range from 1,000 to about 9,500 parts per million. Concentrations appear to increase with depth and all waters are brackish.

### Discussion

Water quality of the Yegua-Jackson Aquifer in the South Transect characteristically is poor with total dissolved solids concentrations from 1,000 parts per million to greater than 10,000 parts per million. The Piper diagram (Figure 7-309) shows a transition in the cation triangle from calcium-sodium water at shallow depths to sodium water for the deeper waters. The anion triangle shows a transition from sulfate-chloride water at shallow depths to chloride water at greater depths. There are no bicarbonate waters in this aquifer. This is in contrast to the dominance of sodium-bicarbonate water in the underlying Queen City and Carrizo Sand Formation aquifers. From the water chemistry, there is no evidence of upward leakage from underlying permeable aquifers such as the Queen City and Carrizo Sand Formation aquifers into the Yegua-Jackson Aquifer.

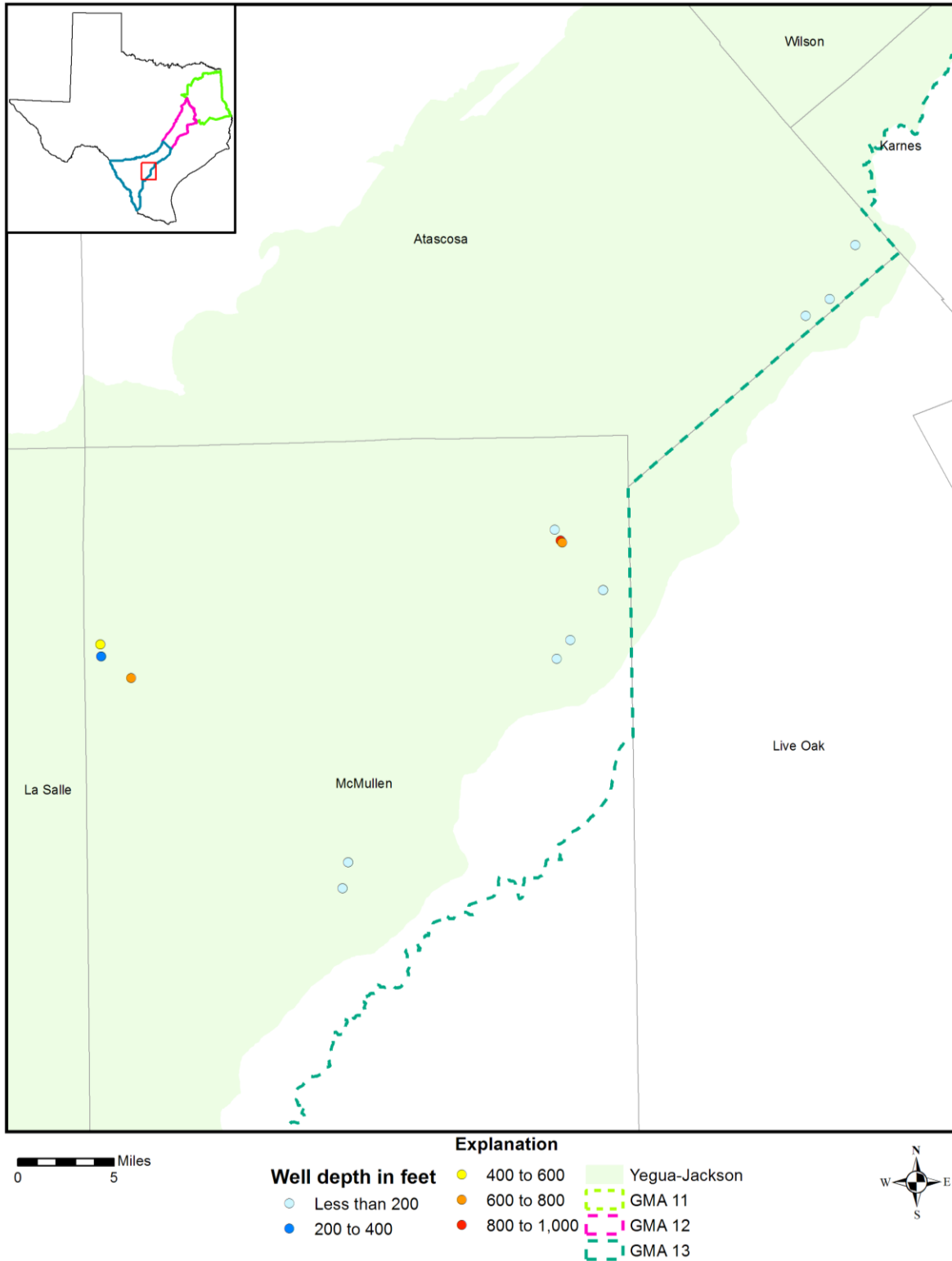


Figure 7-307. Well depths measured from land surface in feet in the Yegua-Jackson Aquifer, South Transect, Groundwater Management Area (GMA) 13.

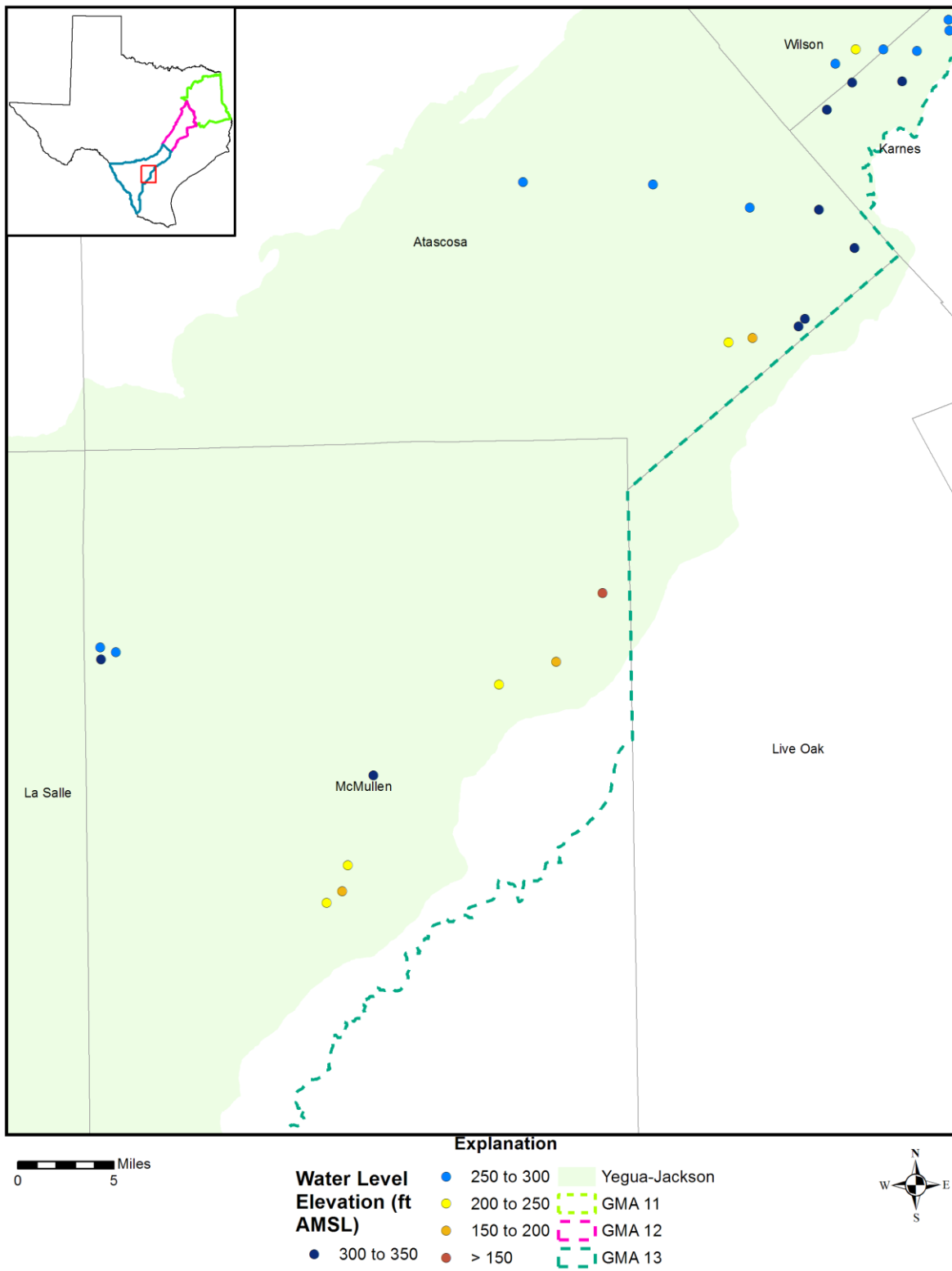


Figure 7-308. Water level elevations from 1921 to 2010 measured in feet above mean sea level (ft AMSL) in the Yegua-Jackson Aquifer, South Transect, Groundwater Management Area (GMA) 13.

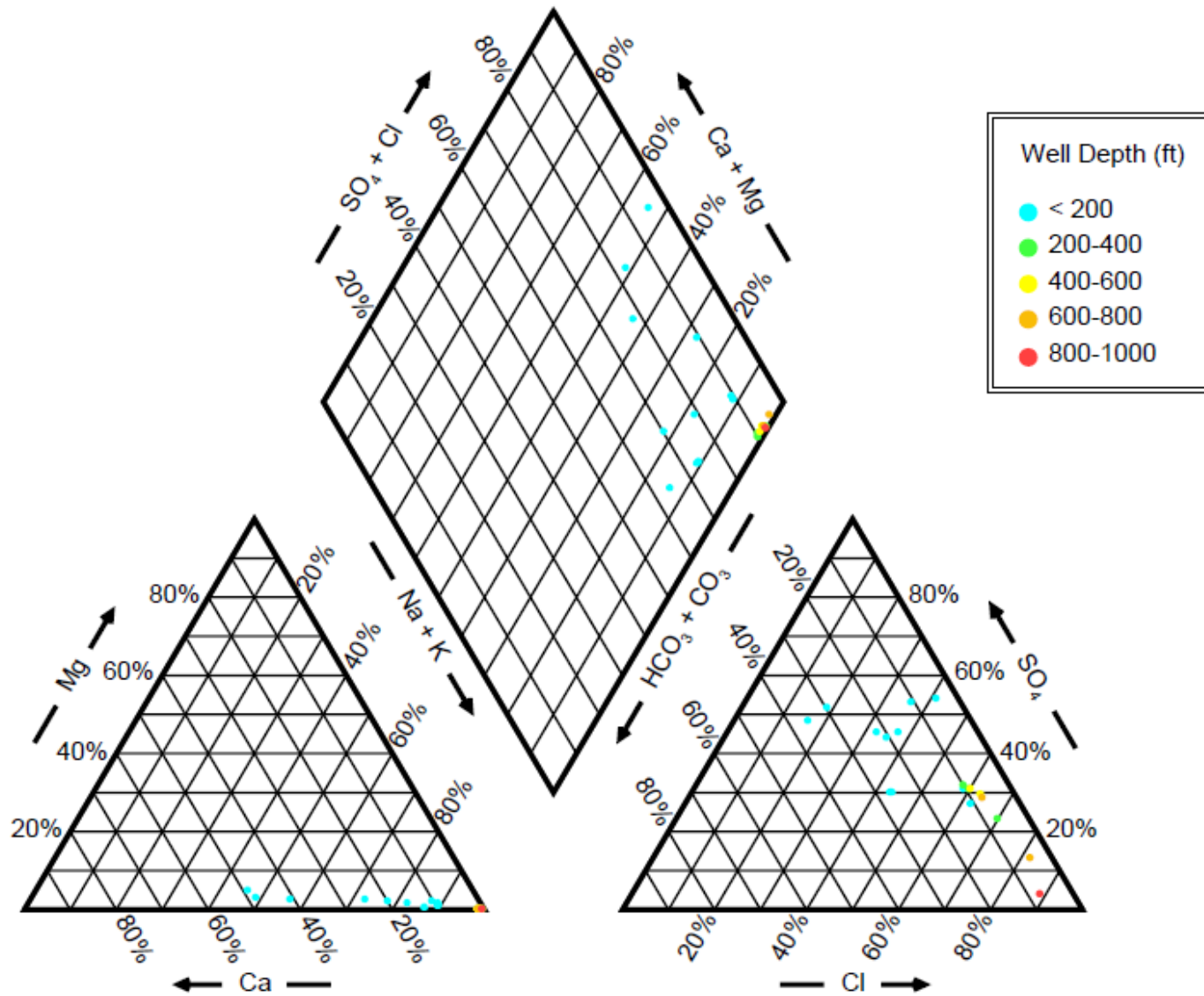


Figure 7-309. Piper diagram showing chemistry of the Yegua-Jackson Aquifer in the South Transect by well depth measured from land surface in feet (ft).

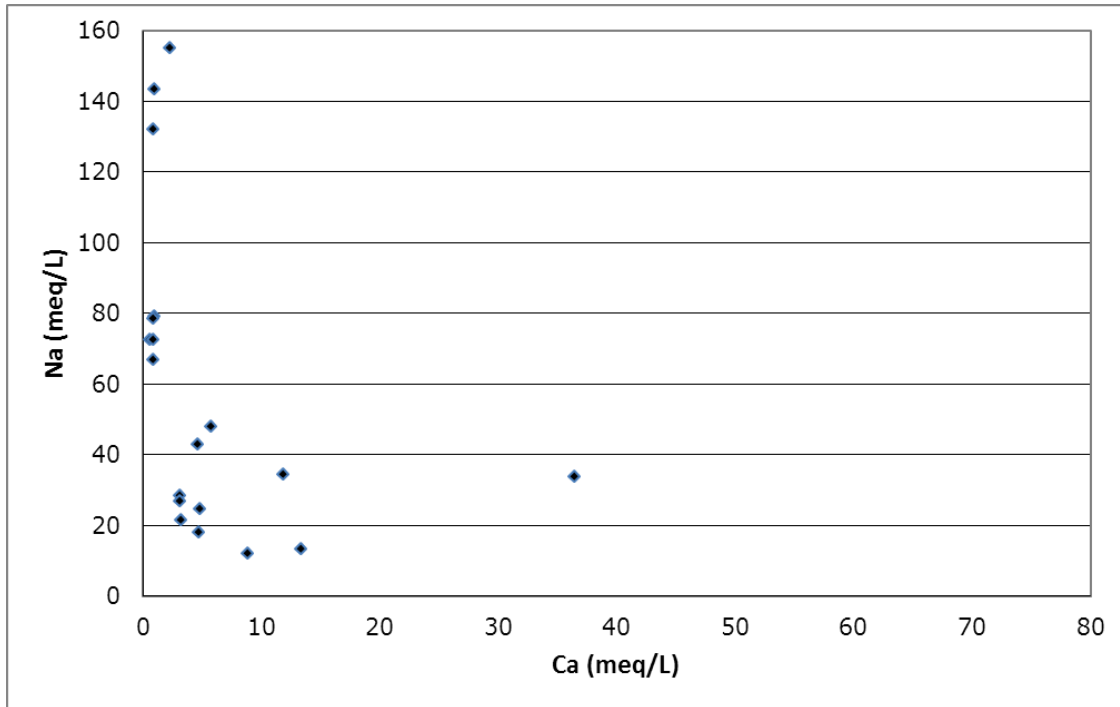


Figure 7-310. Sodium (Na) versus calcium (Ca) measured in milliequivalents per liter (meq/L), Yegua-Jackson Aquifer, South Transect, Groundwater Management Area 13.

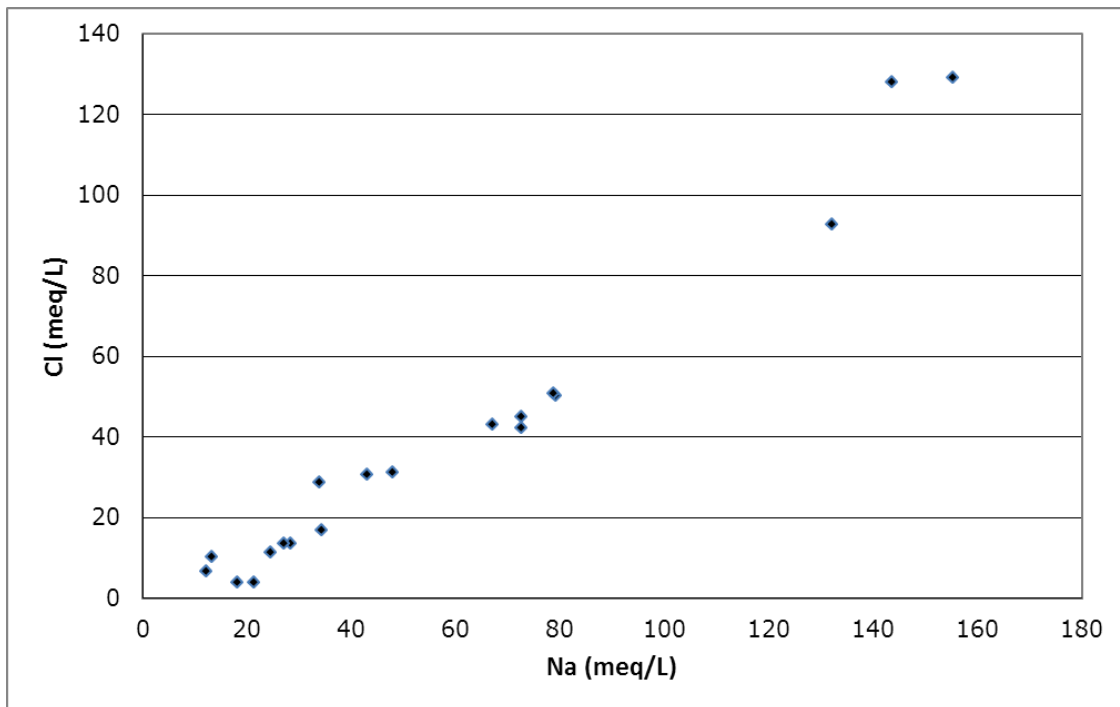


Figure 7-311. Chloride (Cl) versus sodium (Na) measured in milliequivalents per liter (meq/L), Yegua-Jackson Aquifer, South Transect, Groundwater Management Area 13.

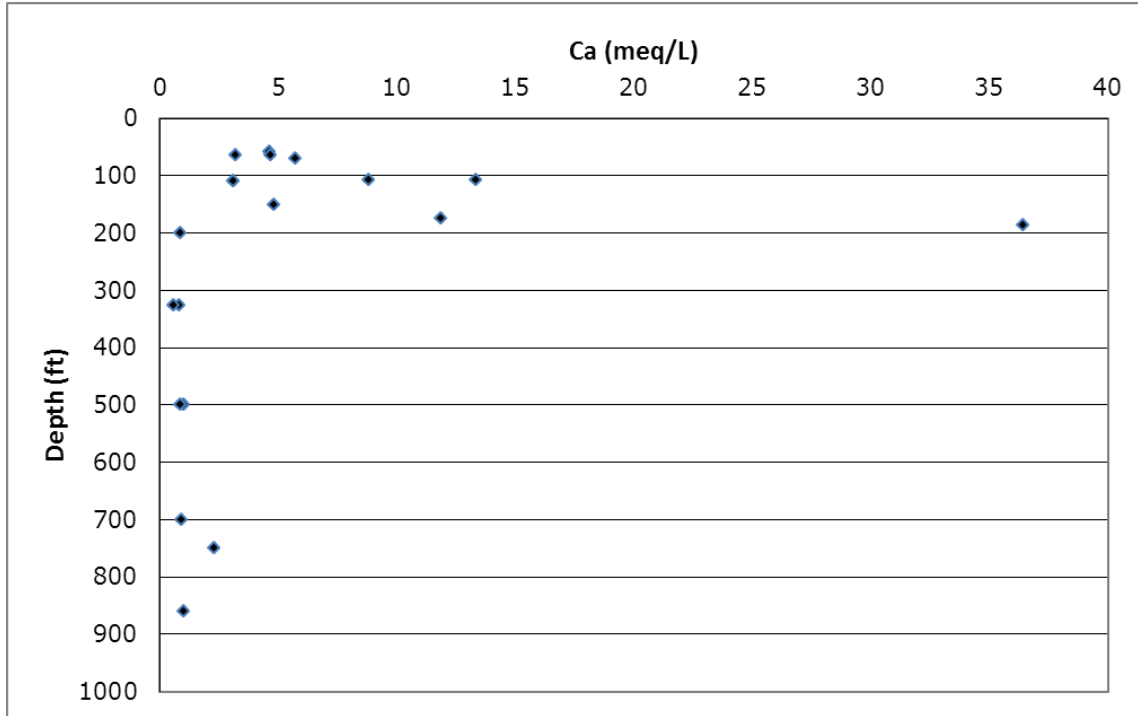


Figure 7-312. Depth measured from land surface in feet (ft) versus calcium (Ca) measured in milliequivalents per liter (meq/L), Yegua-Jackson Aquifer, South Transect, Groundwater Management Area 13.

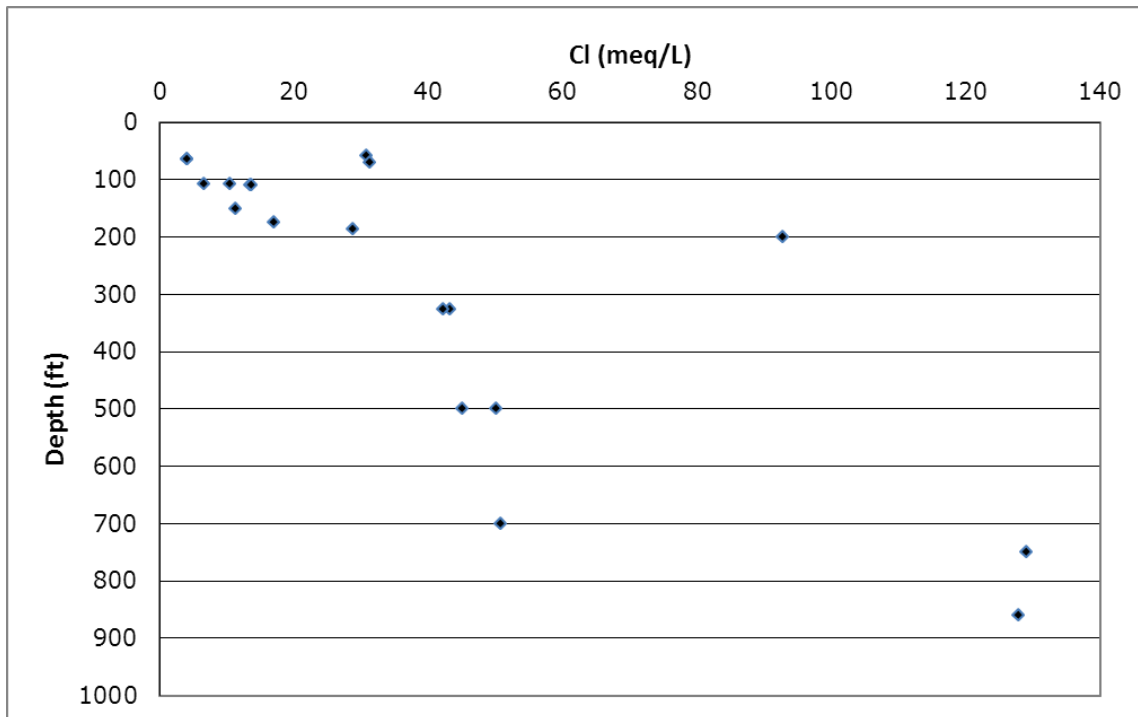
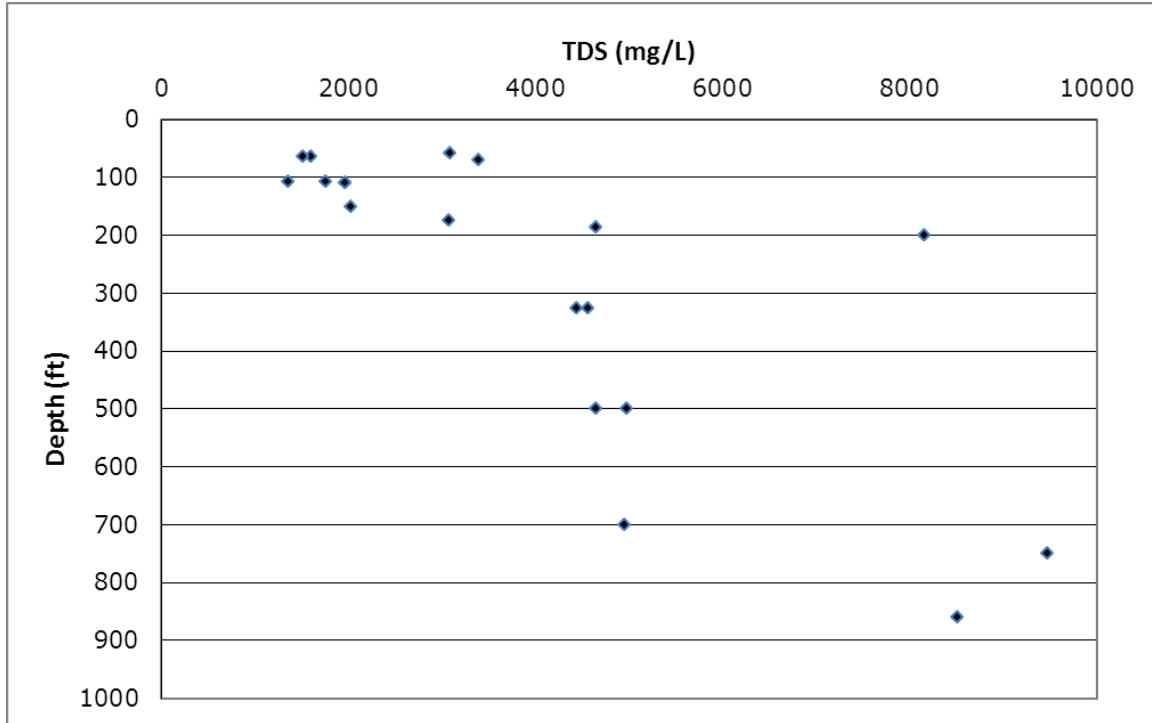


Figure 7-313. Depth measured from land surface versus chloride (Cl) measured in milliequivalents per liter (meq/L), Yegua-Jackson Aquifer, South Transect, Groundwater Management Area 13.



**Figure 7-314.** Depth measured from land surface in feet (ft) versus total dissolved solids (TDS) measured in parts per million (ppm), Yegua-Jackson Aquifer, South Transect, Groundwater Management Area 13.

#### 7.4.2 Geochemical Modeling

The South Transect follows generally the same line of section originally investigated by Pearson and White (1967), who sampled wells in the Carrizo Sand Formation from the recharge area in Atascosa County down gradient for 50 miles to McMullen and Live Oak counties for chemical, stable carbon isotope and radiocarbon analysis (Figure 7-315 and Figure 7-316). Their conclusions were that the radiocarbon ages of total dissolved carbon were generally reflecting the age of the groundwater and that because of mineral dissolution, the carbon content was being modified along the flow path, resulting in an apparent age that is slightly older than the probable actual age. Consequently, they proposed equations to account for both the reactions in the soil zone of the recharge area and reactions along the flow path in which carbonate minerals were dissolving and adding mass without changing the radiocarbon concentration in the water.

Although chemical analyses are widely available from wells throughout the region, the available radiocarbon data are much fewer in number but represent the most directly applicable analyses addressing the objective of independently testing the conceptual model of flow paths and rate of movement of water in the Carrizo Sand Formation. For this study, potential flow paths, both directionally and vertically, were considered by: 1) evaluation of previously reported hydrogeologic and geochemical data, 2) from interpreting thermodynamically constrained mass-balance reactions from the NETPATH geochemical modeling program (Plummer and others, 1994) and 3) comparing results to previous studies, including that of Pearson and White (1967).

Previous studies have provided information of groundwater flow direction and flow rates within the Carrizo Sand Formation in the Atascosa County area. Pearson and White (1967) used carbon-

<sup>14</sup>C age data of groundwater to estimate flow rates. The Carrizo-Wilcox Aquifer (southern portion) GAM (Deeds and others, 2003) report provides a regional evaluation of flow direction. Hydrogeologic data from nearly 100 wells in Atascosa County and adjacent counties were used to evaluate the potentiometric surface (Deeds and others, 2003). Geochemical data from over 290 wells were evaluated to determine changes in groundwater chemistry as a function of distance along the transect line defined for this study based on estimated principal flow directions. Geochemical and carbon isotopic data from 15 wells were used as input into the NETPATH modeling program.

The corrected carbon-14 age is almost always different than the analytical value, generally a younger age. This is the case for all wells investigated in this transect. No new samples were collected for this transect; the calculations rely on the re-evaluation of the radiocarbon analyses and correction factors proposed by Pearson and White (1967) for an area of the Carrizo Sand Formation that adequately represents the transect of interest for this study.

Pearson and White (1967) estimated groundwater flow rates in the Carrizo Sand Formation using groundwater ages as determined from the carbon-14 content of the carbonate dissolved in the groundwater. Figure 7-316 shows the location of the wells and their estimated age contours of groundwater in the Carrizo Sand Formation. The outcrop of the Carrizo Sand Formation was identified as being located in the northern portion of Atascosa County and is assumed to be the principal recharge area for the aquifer, with subsequent progressively confined flow in the thickening, but lithologically well-defined fluvial-deltaic system. Sampling methods in 1967 for chemical composition and for carbon-14 analyses were different and much more difficult than the methods used today, and consequently at least two samples were suspected by the authors of field sampling problems as a result of sampling complications. The remaining 13 analyses of groundwater radiocarbon dates range from modern age in the outcrop to greater than 30,000 years before present in McMullen County (Figure 7-316).

The current study uses the same geochemical and carbon isotopic data as Pearson and White (1967) for the NETPATH modeling inputs. Well locations shown on Figure 7-315 display both state well numbers and laboratory numbers for clarity and to facilitate comparison to the figures in Pearson and White (1967; Figure 2).

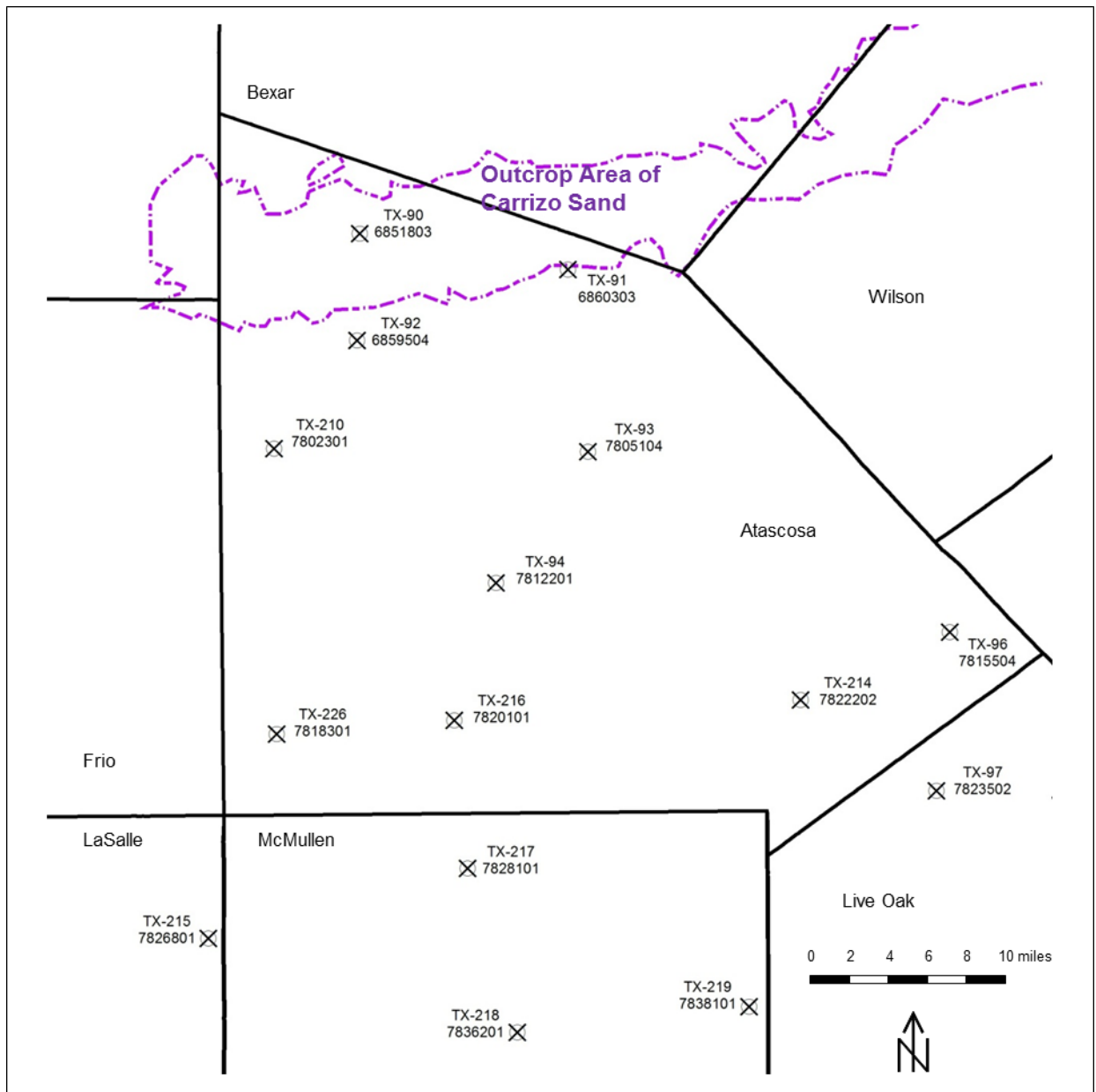


Figure 7-315. Study area showing locations of wells used in geochemical modeling (Pearson and White, 1967).

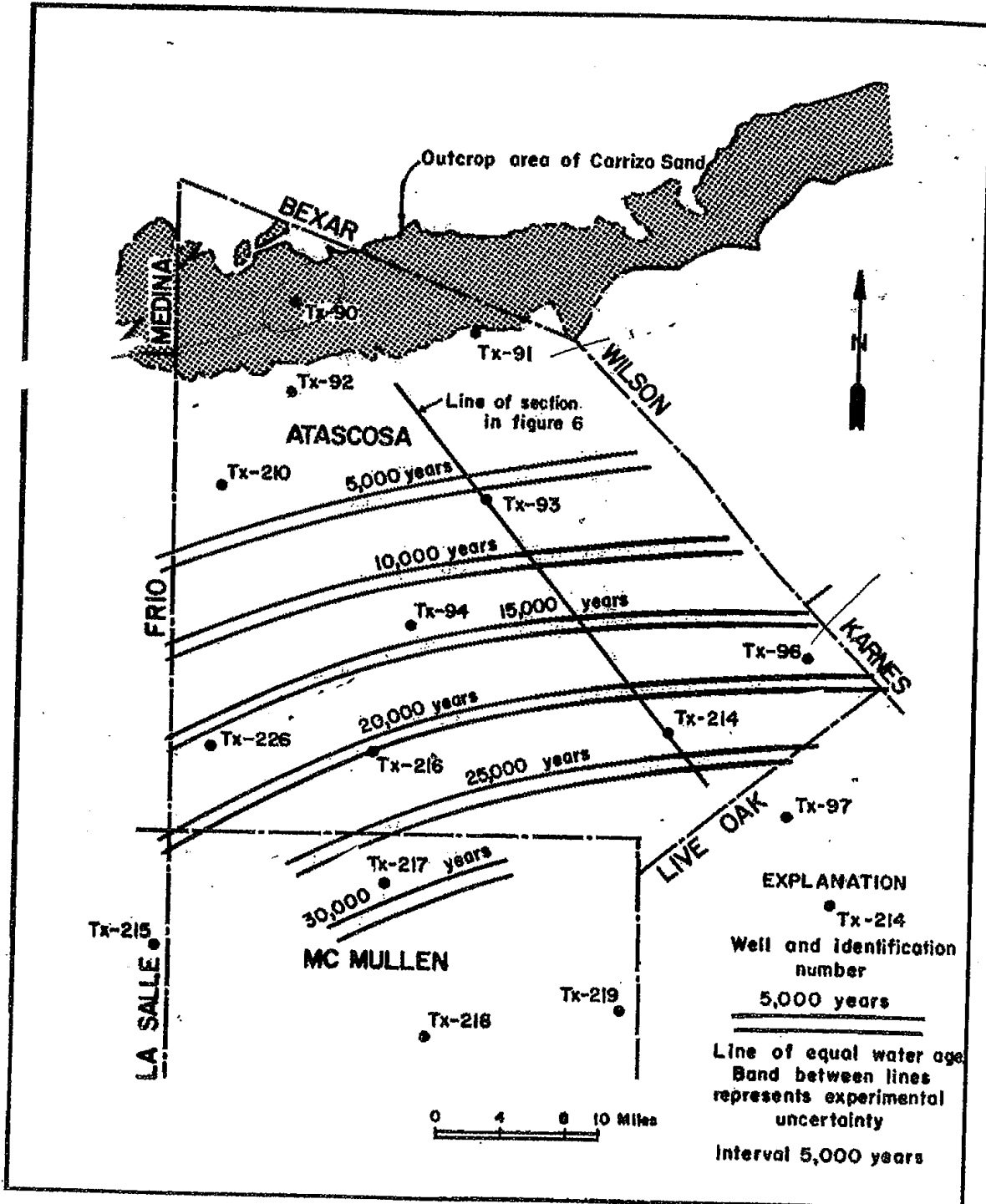


Figure 7-316. Ages of groundwater in the Carrizo Sand Formation portion of the Carrizo-Wilcox Aquifer (Figure 5 from Pearson and White (1967)).

### Hydrogeology and Hydrochemistry

The Carrizo Sand Formation crops out in a band that is subparallel to the Gulf of Mexico coastline from northeastern to southwestern Texas. The formation dips southeast and as a part of

the Carrizo-Wilcox Aquifer system, is one of the major water supplies in Texas, with fresh water at depths as great as 5,000 feet. Details of the regional hydrogeology of the Carrizo Sand Formation are documented in the Carrizo-Wilcox Aquifer (southern portion) GAM (Deeds and others, 2003) report and are consequently not within the scope of this study.

The formation crops out in northern Atascosa County as a landscape of rolling hills six to eight miles wide (Figure 7-315). The Carrizo Sand Formation section increases in thickness from 600 to 700 feet near the outcrop to up to 1,300 feet in the southeastern portion of the county. The Carrizo Sand Formation is fairly uniform, consisting mostly of fine to medium grained quartz sand with minor amounts of clay, lignite, calcite and pyrite.

The regional groundwater flow in the Carrizo Sand Formation is to the southeast initially under water-table conditions in the outcrop then artesian conditions down dip of the outcrop (Deeds and others, 2003). Water level data from nearly 100 wells in Atascosa County and adjacent counties were used to generate the groundwater elevation contours. Water level data were limited to that prior to 1970 and if multiple data for a single well exists, the data collected nearest to 1963 was used. Kriging statistical methods were used to generate the groundwater elevations contours. In general, groundwater flow in Atascosa County is concordant with the regional flow to the southeast. Hydrologic troughs, roughly corresponding to the position of the Atascosa River and its tributaries, exist in the central and southwestern portions of the county (Figure 7-317). The presence of these hydrologic lows creates local changes in the groundwater flow direction, for example groundwater elevation contours indicate the inferred flow path in the northeastern part of the county is slightly to the south (Figure 7-317).

It should be noted that although the Carrizo-Wilcox Aquifer (southern portion) GAM is in general similar to the flow directions assumed by Pearson and White (1967) there are subtle but significant differences when evaluating flow relationships between wells. Clearly the wells do not align along a single specific flow line, thus numerous flow lines from outcrop to depth are assumed and tested. Furthermore, the composition of the recharge water is important; however in the absence of detailed water composition from wells across the recharge area, the assumption is made that lateral changes in chemical composition along strike from any given recharge location are minimal. Nevertheless, flow along different flowlines could reasonably be expected to have a chemical evolution histories that are similar in process but occur at different rates depending of hydraulic head, permeability, and cross-formational flow; these subtle differences are possible explanations for differences in flow paths, but data are still too sparse to address this on anything but a regional scale.

The changes in concentrations of major groundwater chemical constituents in the wells with isotope data, including alkalinity, calcium, chloride, magnesium, sodium, and sulfate, were examined as a function of distance along the transect line (Figure 7-318, Figure 7-319 and Figure 7-320). The evolution of composition is consistent with what is seen along other transects in the Carrizo-Wilcox Aquifer; that being the development of a sodium bicarbonate type water evolving to high levels of dissolved solids eventually reaching significant enough depths to begin mixing with deeper brines. Chemical analyses from these wells are used in the NETPATH modeling of reactions that impact composition as the water migrates from well to well, and in the determination of the corrected carbon-14 estimates of age. It is interesting to note that the early portion of the flow path is the region of calcium and sulfate influence which diminishes along the transect but at different rates as sodium and bicarbonate clearly increase. This behavior is

captured even in the plots of all data (Figure 7-318) and confirms that the subset of chemical analyses used in the model is representative of the aquifer processes in general.

Chemical data from over 290 wells from Bexar, Atascosa and McMullen counties (Appendix A) were used in the evaluation. Well distances along the transect line were calculated by projecting the well location perpendicularly back to transect line. While in general there is an increase in well depth along the transect, these wells are completed at a variety of depths; therefore constituent concentrations can be affected not only by the lateral distance from the outcrop but also the vertical position of the well within the aquifer. Although there are a number of wells that have compositions which are outliers to the general trends and may represent shallow well influence from anthropogenic activity, or co-mingling with other aquifers, the trends in chemical evolution are clear and consistent with the wells investigated for radiocarbon ages in this study (Figure 7-318).

Groundwater in the northwestern part of Atascosa County, south of the Carrizo Sand Formation outcrop, is of the magnesium calcium-bicarbonate type. Alkalinity ranges from about 50 to 300 milliequivalents per liter, calcium is generally between about 25 and 80 milliequivalents per liter, while sodium is less than 50 milliequivalents per liter (Figure 7-319 and Figure 7-320).

In a zone approximately 30 miles south of the Carrizo Sand Formation outcrop is the region in which the sodium content increases rapidly and the calcium correspondently decreases by ion exchange. South of this transition zone, calcium concentrations are generally less than five milliequivalents per liter, while sodium is generally over 200 milliequivalents per liter. A rapid increase in both sodium and chloride concentrations in the southernmost wells in the study area (Figure 7-319) is most likely due to the mixing with more saline water, perhaps saline geothermal brine, a mixture of remnant seawater, or brine from salt dissolution, etc. At present the options of sources of water for mixing are speculative and would benefit from analyses of deep brine samples. Deeper sampling would also help define how far downdip meteoric water has flowed.

### **NETPATH Modeling**

NETPATH modeling was performed between all wells that could be representative of the more general flow paths for the sub-regions in this Atascosa County area (Figure 7-317). The simulations determined if a chemical reaction path between the sampled wells was valid, given the geochemical and isotopic changes between the wells. Assuming no errors in geochemical or isotopic data and that the mineral suite is known, a result of no valid models between two adjacent wells, would indicate that either a direct flow between locations along the transect with the composition represented by those wells does not occur, or that water or gases from one or more additional sources are introduced into the flow path and are unaccounted for in the modeling. The modeled pathways are used to investigate the possibility of reactions that could account for the chemical changes; these reaction pathways indicated in Figure 7-318 are not intended to depict actual flow paths. The flow path would likely be generally downgradient from outcrop too deep in the section and the well compositions would be projected along strike for limited distances to the location of a regional groundwater flow line.

Modeled reaction pathways included simulated recharge water to the upgradient wells in or nearest to the outcrop, and subsequently from those wells to the nearest downgradient well, continuing to the southernmost wells in the study area. Modeled reaction paths were generally

south to southeast from well-to-well given the inferred flow paths discussed previously. Across gradient pathways were not modeled.

The simulations rely on solid phases and gases previously identified for the Carrizo Sand Formation: carbon dioxide, methane, calcite, gypsum, halite (a surrogate for chloride and sodium coming from clays), pyrite, and clay minerals for ion exchange, lignite or other organic material associated with the clay fraction of the aquifer (Pearson and White, 1967). Primary silicates such as feldspars, amphiboles, and phyllosilicates are omitted since their inclusion does not affect age calculations in this system significantly. Plummer and others (1994) state it is commonly observed that the concentration of dissolved iron is very low during sulfate reduction because of the very low solubility of iron sulfide phases. If sulfate reduction were occurring (in the absence of iron reactions) all the hydrogen sulfide produced would be found in solution, generating a noticeable amount of hydrogen sulfide, considering the amount of carbon dioxide that must be produced. Therefore, if sulfate reduction is occurring in the aquifer, there must be source and sink for sulfur and iron. Our models assume sulfate reduction is occurring which explains the significant decline in sulfate concentration (Figure 7-320) along the transect containing the wells listed in Table 7-7, and thus goethite is considered as the source for iron that mitigates the production of dissolved hydrogen sulfide. The question of the source of sulfate at elevated concentrations across most of the flow regime remains, given that gypsum is not found in the formation. Studies have indicated that calcium sulfate water in pore fluids in coastal plain aquifers (Chapelle and McMahon, 1991) or sulfate substituting in the lattice of marine calcite (Busenberg and Plummer, 1985) may provide sources of sulfate without gypsum being present. In our models below, gypsum is included proxy to provide a source of sulfur. Additionally, model assumptions include:

- Initial soil calcite has a  $\delta^{13}\text{C}_{\text{soil}}$  of 0 ‰ and  $^{14}\text{C}$  is 0 pmc
- Initial soil organic material ( $\text{CH}_2\text{O}$  or lignite) has a  $\delta^{13}\text{C}_{\text{soil}}$  of -25 ‰ and  $^{14}\text{C}$  of 0 pmc
- Initial soil  $\text{CO}_2$  has a  $\delta^{13}\text{C}_{\text{soil}}$  of -25 ‰ and  $^{14}\text{C}$  of 100 pmc

Several sources of error may lead to erroneous model results. These include:

- Lack of knowledge of the stratigraphy. An assumption is made that the strata is homogeneous throughout the study area and to all well depths. Variations in the properties of the strata, including but not limited to mineralogy, grain size, porosity, and hydraulic conductivity, may create unaccounted for geochemical reactions or flow pathways.
- Limited well screening vertically or lack of nested well screening, geochemical data from each well comes from a vertically limited portion of the aquifer. Furthermore, data are limited to the shallow aquifer in the northern portion of the transect, the middle aquifer in the center of the transect, and to the deep aquifer from the southern portion of the transect. Potential other sources or flow paths cannot be evaluated and therefore are not included as a part of the model.

The two wells located in the outcrop area, TX 90 and TX 91, are not compatible with any of the downgradient wells (Figure 7-318 and Table 7-7). Both wells are shallow and the measured carbon-14 was pre-modern indicating potential atmospheric contamination during sampling. In addition, the chloride concentration of TX 90 is twice that of the downgradient wells suggesting the groundwater may be receiving infiltration of surface water that has had significant

evaporation. The third well along the transect, TX-92, is just down gradient from the Carrizo-Sand Formation outcrop and the fourth well (TX-210) is clearly the first well representative of the confined aquifer, isolated from the effects of the soil and atmospheric carbon-14 (Figure 7-315, Figure 7-317 and Figure 7-321). Mass balance simulation for these two wells from the soil zone in the outcrop, through well TX-92 to TX-210 yields a corrected carbon-14 age of 1,618 years before present, which is similar to the corrected age of 1,730 years before present obtained by Pearson and White (1967). The measured age of 8,758 years before present is an overestimate because of all the calcite that has dissolved in the groundwater that added total dissolved carbon but diluted the carbon-14 (Table 7-7).

Well TX-210 is located in the western region of Atascosa County, but is the only sampled well that is between the outcrop area and the much deeper Carrizo Sand Formation wells. The chemical and isotopic composition are reasonable for that distance along the transect, and the assumption is made that this well represents the starting point for all subsequent simulations downgradient and the composition of the Carrizo Sand Formation at that point is effectively representative of the aquifer along a line of strike from the location of the TX-210 well. Four simulated transects were considered reasonable for this region and all simulation begin with the well TX-210 composition (Table 7-7).

Inverse modeling using NETPATH was performed from well to well along all potential flow paths that generally aligned with the water level contours for the region (Figure 7-317). The success of a well to well simulation is based on matching the changes in chemical and isotopic composition with plausible mineral and gas sources, and the requirement of not violating any thermodynamic restrictions. As might be expected to be the case, it was not possible to select a single line of transect to which all well compositions could be projected along strike and then generate successful models from well to well. This indicates that the reaction progress along a specific flow line occurs at different rates even though the mineral and gas reactants, and the specific reactions are the same. This became evident when successful models were compared. There are at least four decipherable flow paths or transects that are based on valid inverse models. Each begin with the composition of well TX-210, conform to the general water level decline, and rely on essentially the same mineral and gas reactant combination (Figure 7-317 and Table 7-7). The computed adjusted ages are in agreement with the trend observed initially by Pearson and White (1967) but are rigorously constrained.

The selected reaction pathways are displayed as solid lines but alternative pathways were found to be options and those are shown as dashed lines. It is important to reiterate that the reaction paths indicate that the changes in water chemical and isotopic compositions between these wells can be explained, but that the actual flow line would be consistent with the potentiometric surface. The modeling was accomplished by considering dissolution of calcite and goethite, oxidation of organic phases such lignite, precipitation of small amounts of pyrite, generation of absorption of carbon dioxide, and ion exchange between calcium, magnesium, and sodium. Constraints were imposed that required the  $\delta^{13}\text{C}$  of the computed final water match the measured  $\delta^{13}\text{C}$  of the total dissolved carbon.

Results of the various models along the indicated pathways shown in Figure 7-317 are given in Table 7-7 and the detailed mass balance accounting is given in Table 7-7.

## Discussion

Hydrogeologic data, geochemical data and NETPATH modeling is used to determine likely groundwater flow paths and potential sources of inflow into the Carrizo Sand Formation in Atascosa and adjacent counties. Evaluation of water levels indicate that the flow in the study area is generally to the south-southeast, however variations in the potentiometric surface create some localized changes in the flow path direction to the south-southwest. Geochemical data indicate a significant change in the water type, from a calcium bicarbonate type in the northwestern portion of the Atascosa County to a sodium bicarbonate type in the southwestern portion and adjacent counties.

The plausibility of flow paths between any two wells was evaluated using NETPATH modeling. A summary of model transects is provided in Figure 7-317. Model reaction paths with valid results are shown with either a solid or dashed line; a selection is made primarily based on conformance with expected groundwater flow, but either reaction pathway is geochemically justifiable. Only one well, TX-217, cannot be modeled as part of a transect using the assumptions established for this study. Valid reaction paths are largely in the same direction as the inferred groundwater flow; all measured  $^{14}\text{C}_{\text{OBS}}$  values required correction as the result of dissolution of calcite or organic material, or the incorporation of carbon-14 from carbon dioxide.

In the southernmost portion of the transect, Live Oak and McMullen counties, invalid reaction paths or modeling results occur. No valid reaction paths were modeled to either well TX-97 or TX-219. These wells measure abnormally elevated constituents such as chloride and very old groundwater ages; this is not easily explained by mineral dissolution, but could reasonably be accounted for by mixing with deeper brines or remnant seawater.

The vertical position of wells may also serve to explain the lack of valid flow paths or inconsistent ages in the southernmost portion of the study area. As shown on Figure 7-321, Figure 7-322, Figure 7-323 and Figure 7-324 an inferred shallow groundwater flow path is initially derived from the recharge area. Valid reaction models occur between wells that vertically remain within this shallow flow path. Model results and geochemical data from the deeper and more southern wells are indicative of a mixing with other groundwater sources.

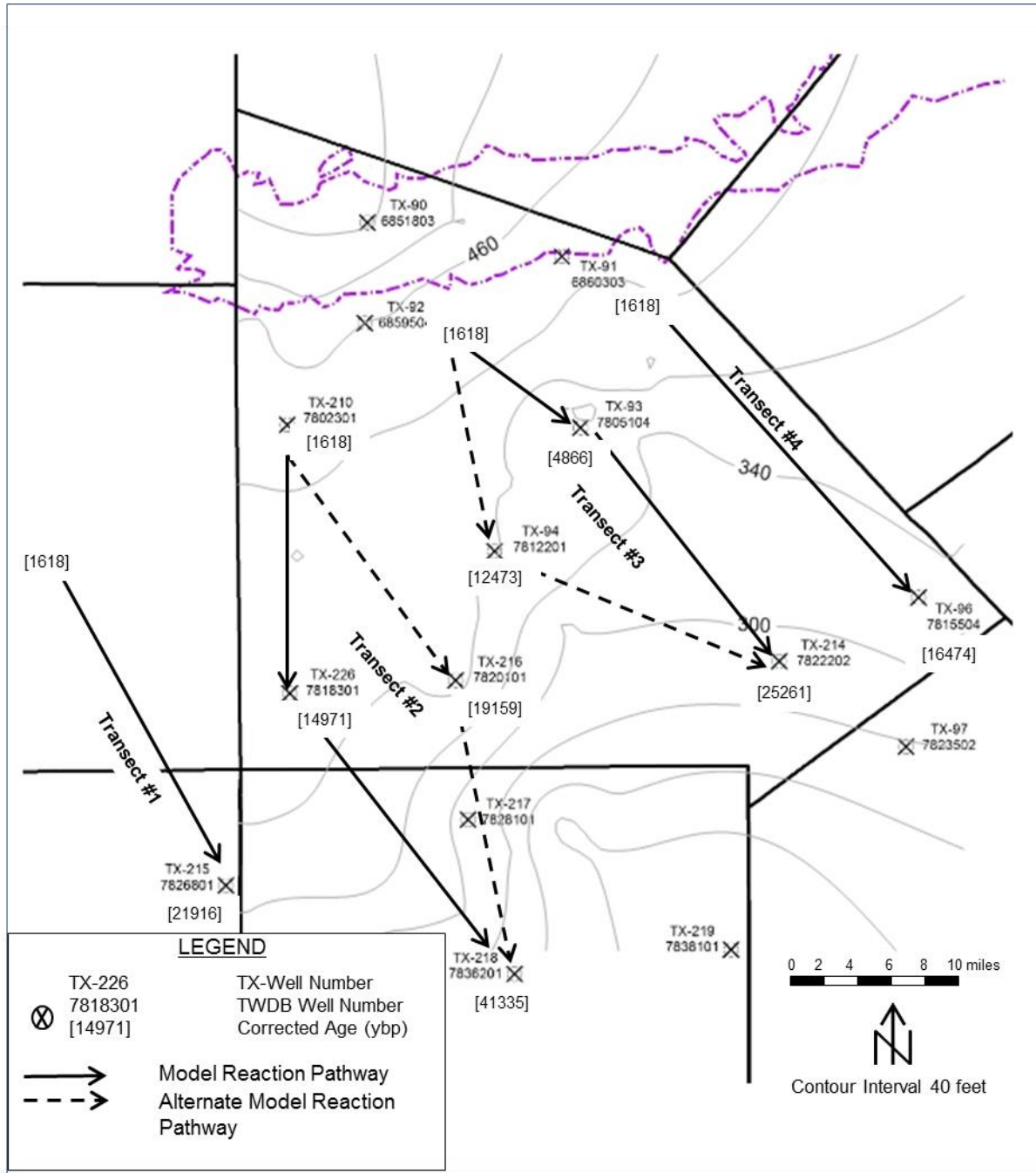


Figure 7-317. Groundwater elevation contours, model transect lines and corrected groundwater ages.

Evaluation of Hydrochemical and Isotopic Data in Groundwater Management Areas 11, 12 and 13

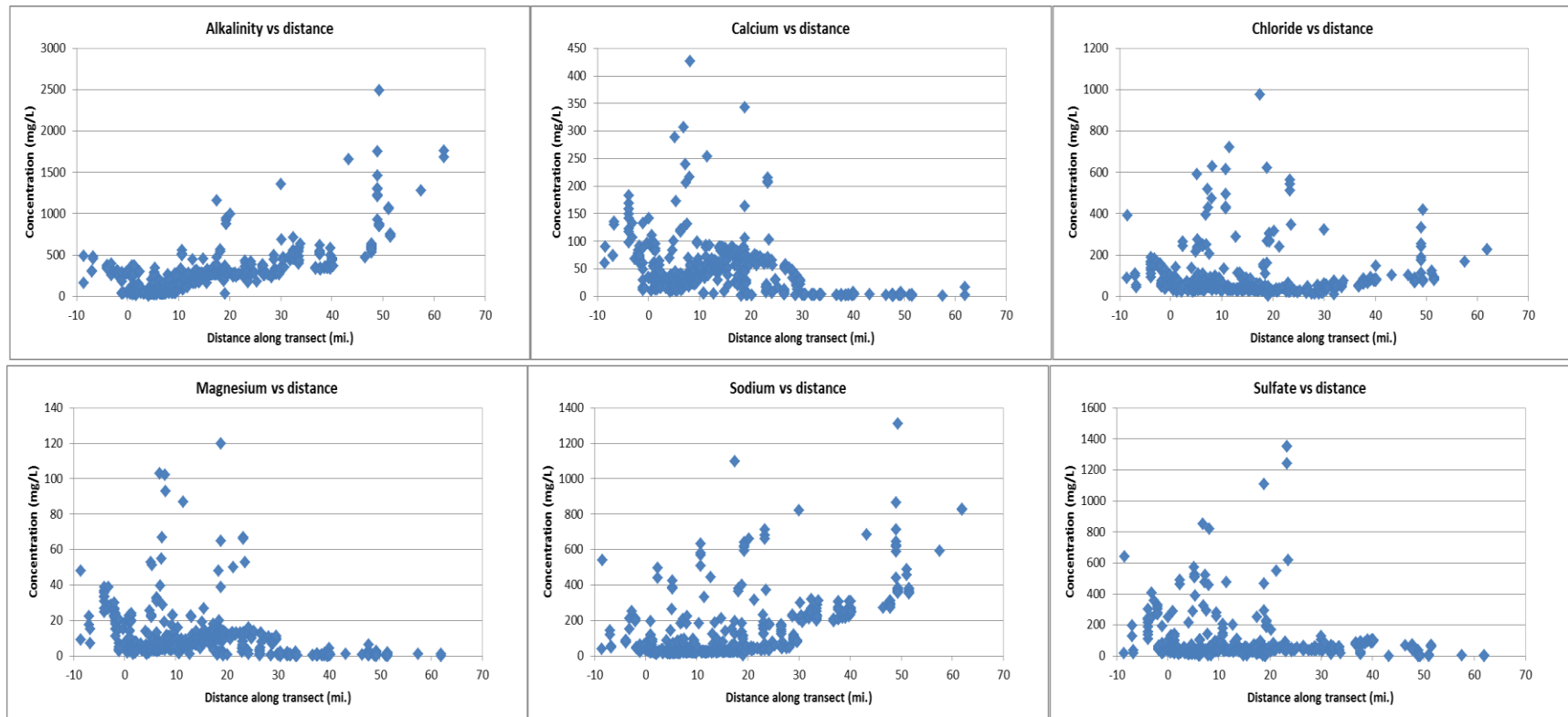


Figure 7-318. Concentrations measured in milligrams per liter (mg/L) of major geochemical constituents of alkalinity, calcium, chloride, magnesium, sodium and sulfate as a function of distance along the transect line measured in miles (mi).

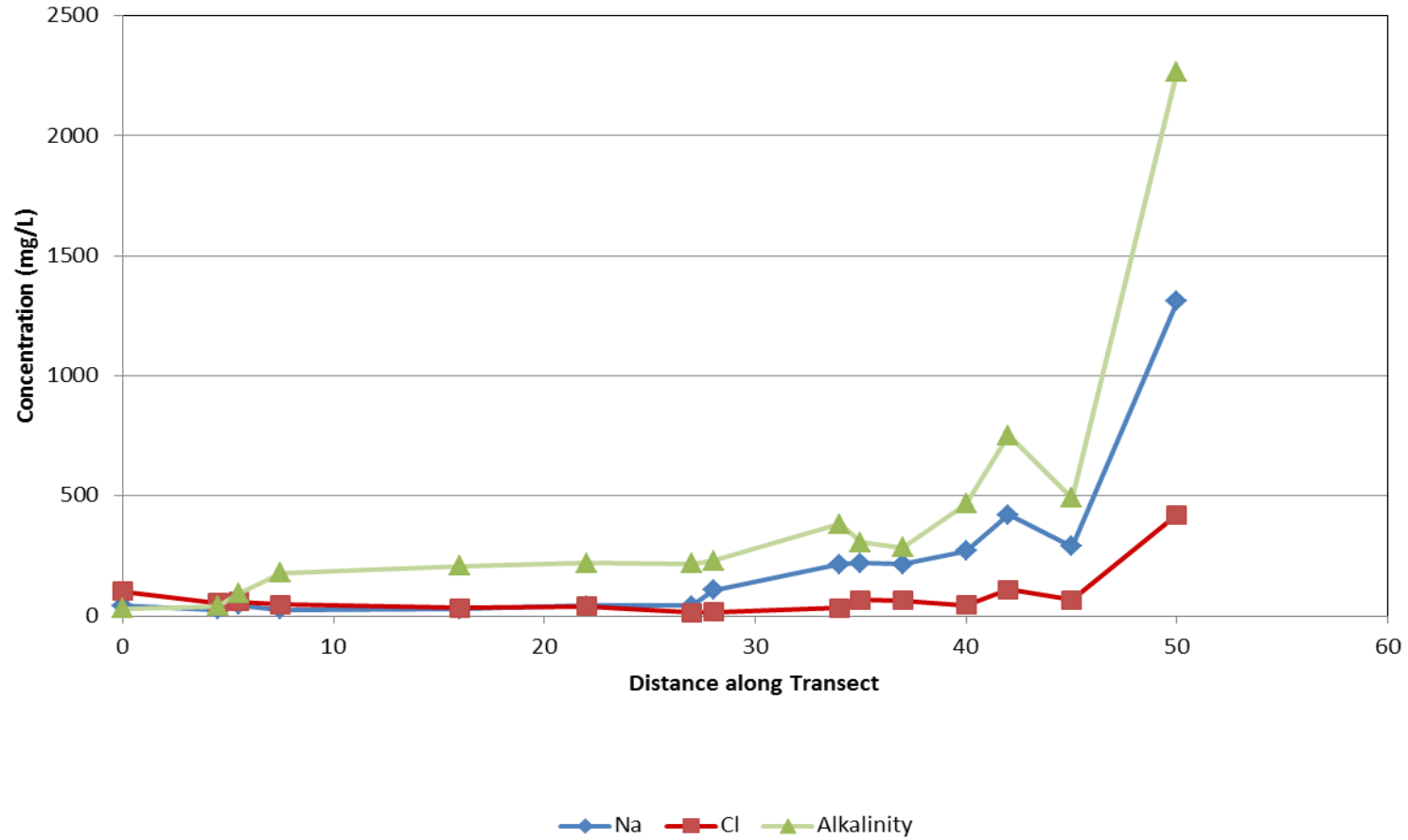


Figure 7-319. Sodium, chloride and alkalinity concentrations measured in milligrams per liter (mg/L) as a function of distance along the transect line in wells used for NETPATH modeling.

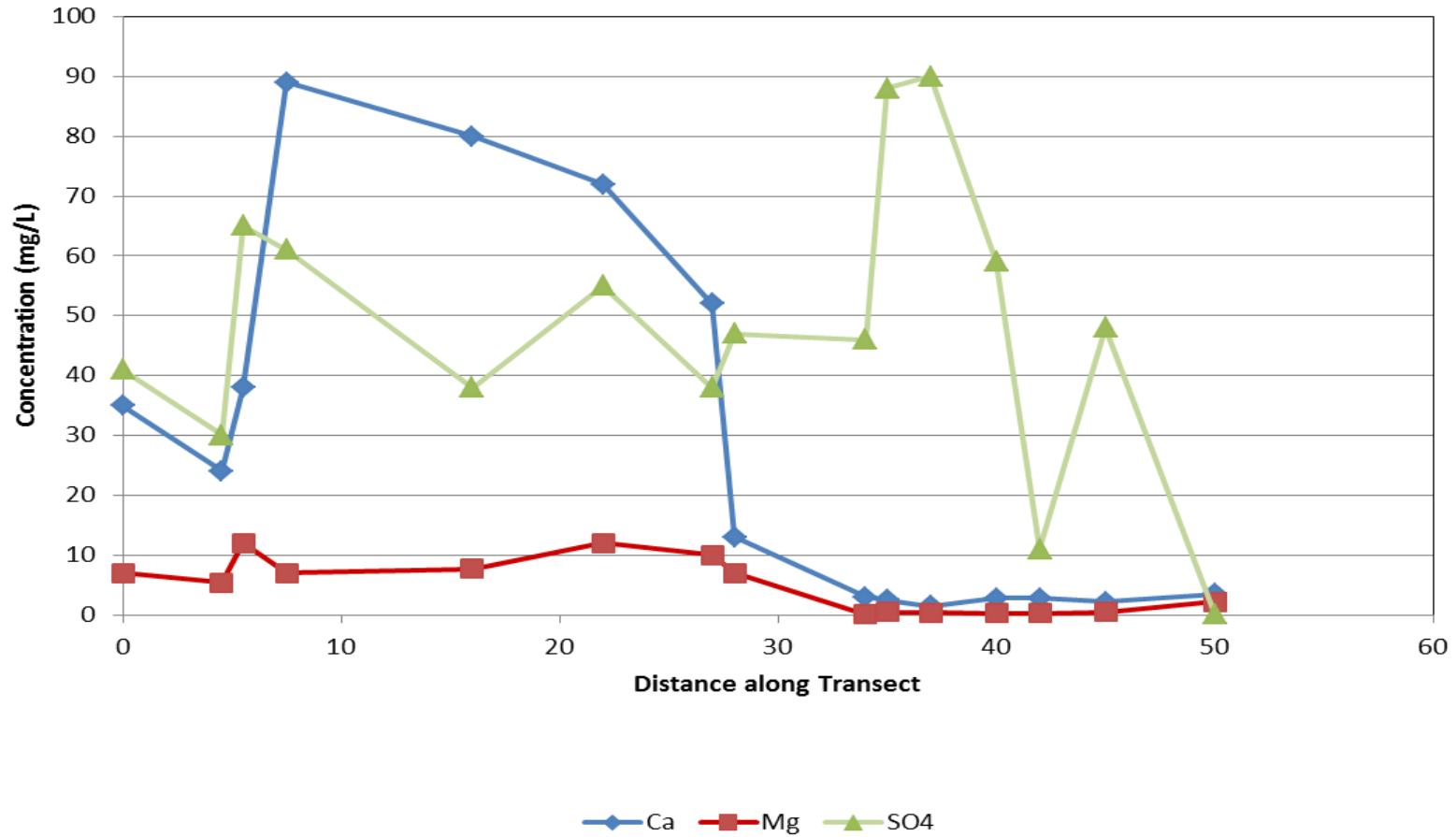


Figure 7-320. Calcium, magnesium and sulfate concentrations measured in milligrams per liter (mg/L) as a function of distance along the transect line in wells used for NETPATH modeling.

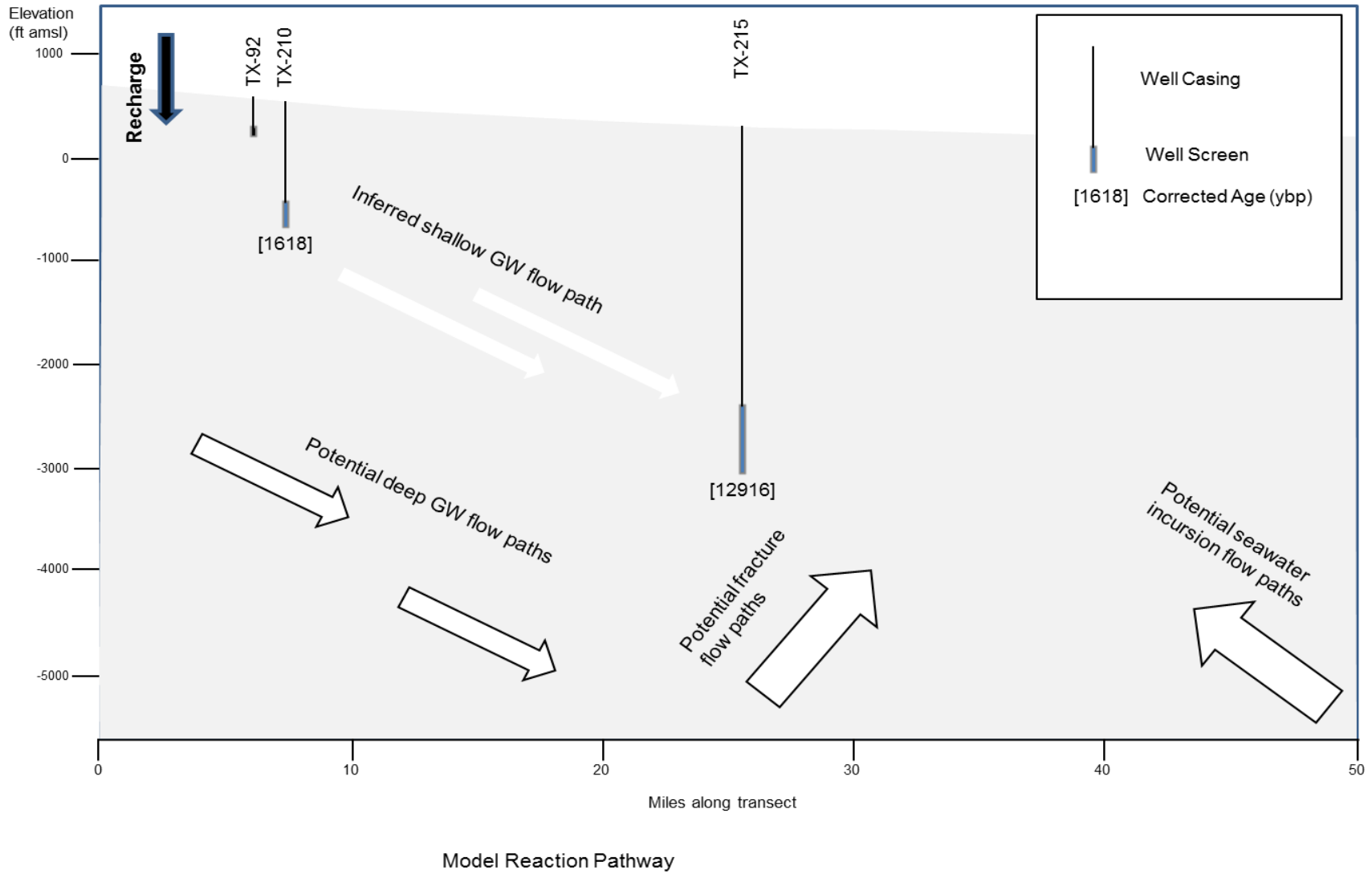


Figure 7-321. Vertical profile along Transect line 1 showing well, well screen depths and inferred and potential water flow pathways.

**Table 7-7. Summary of results for groundwater age estimates from geochemical modeling.**

TWDB Well No.	Well TX No.	Well Depth (ft)	Chloride (mg/L)	Alkalinity (mg/L) <sup>(1)</sup>	$\delta^{13}\text{C}$ ‰ (DIC)	<sup>14</sup> C <sub>OBS</sub> (ybp)	<sup>14</sup> C <sub>ADJ</sub> (ybp) <sup>(2)</sup>	<sup>14</sup> C <sub>ADJ</sub> (ybp) Transect 1 <sup>(3)</sup>	<sup>14</sup> C <sub>ADJ</sub> (ybp) Transect 2 <sup>(4)</sup>	<sup>14</sup> C <sub>ADJ</sub> (ybp) Transect 3 <sup>(5)</sup>	<sup>14</sup> C <sub>ADJ</sub> (ybp) Transect 4 <sup>(6)</sup>	Non-Transect Wells
6851803	TX-90	166	102	31.15	-18.9	2,109	98.1	-	-	-	-	(11)
6860303	TX-91	145	59	93.44	-18.5	2,321	90.1	-	-	-	-	(11)
6859504	TX-92 <sup>(7)</sup>	411	54	40.16	-17.9	5,550	3,750	-	-	-	-	
7802301	TX-210 <sup>(8)</sup>	1,205	47	178	-11.5	8,758	1,730	1,618	1,618	1,618	1,618	
7818301	TX-226	2,400	13	217.26	-8.8	22,099	16,200	-	14,971	-	-	
7820101	TX-216	2,794	17	229.51	-11.7	26,495	20,200	-	19,159	-	-	
7828101	TX-217	3,998	64	283.61	-9.5	35,719	28,200	-	-	-	-	(12)
7826801	TX-215	3,300	66	304.92	-9.1	31,176	>22,000	21,916	-	-	-	
7836201	TX-218	4,250	67	490	-10.7	40,818	>28,200	-	41,401 <sup>(9)</sup>	-	-	
7805104	TX-93	1,700	34	209	-11.8	14,182	6,300	-	-	4,866	-	
7812201	TX-94	2,075	41	218.85	-9.9	21,446	14,000	-	12,473	-	-	
7822202	TX-214	4,132	46	466.39	-9.8	34,510	22,900	-	-	25,261 <sup>(10)</sup>	-	
7815504	TX-96	4,326	32	383.5	-15.0	29,494	18,900	-	-	-	16,474	
7823502	TX-97	4,842	110	752.25	-3.7	35,583	>18,000	-	-	-	-	(13)
7838101	TX-219	5,400	420	2,267.06	-10.6	40,316	>24,300	-	-	-	-	(13)

NOTES:

- (1) Alkalinity as TDIC
- (2) Pearson & White (1967)
- (3) TX-210 to TX-215
- (4) TX-210 to TX-226 to TX-218 (alternate pathway TX-210 to TX-216 to TX-218)
- (5) TX-210 to TX-93 to TX-214 (alternative pathway TX-210 to TX-94 to TX-214)
- (6) TX-210 to TX-96
- (7) Used in mass balance modeling from recharge to upgradient well (TX-210)
- (8) Groundwater used as upgradient well proxy for all transects
- (9) Age via alternate pathway = 45,687 ybp
- (10) Age via alternate pathway = 32,868 ybp
- (11) Not representative of recharge
- (12) Anomalous Well –not included in any transect pathways
- (13) Mixing occurring with deeper groundwater-not included in any transect pathways

Evaluation of Hydrochemical and Isotopic Data in Groundwater Management Areas 11, 12 and 13

**Table 7-8. Results of modeling reaction paths.**

<b>Model Results<sup>(1)</sup></b>						
	Recharge to Upgradient Well	Transect 1	Transect 2		Transect 2 (Alternate Path)	
	Recharge to TX92 to TX210 (mass balance)	Recharge to TX210 to TX215 (user defined)	Recharge to TX210 to TX226 (user defined)	Recharge to TX226 to TX218 (user defined)	Recharge to TX210 to TX216 (user defined)	Recharge to TX216 to TX218 (user defined)
<b>Plausible phases<sup>(2)</sup></b>	Mass Transfer (millimoles per kilogram H <sub>2</sub> O)					
Calcite	1.63418	1.96747	0.98226	2.59665	0.60120	2.96139
CO <sub>2</sub> (g)	0.85350	NA	-0.08161	NA	NA	NA
Mg/Na exchange	-0.06589	0.26747	-0.12345	0.39091	-0.00001	0.26747
Ca/Na exchange	0.01155	4.12600	1.90585	3.83966	2.49824	3.23095
K/Na exchange	0.10896	-0.38647	-2.86856	2.29461	-1.42791	0.88661
Lignite	NA	0.57906		2.52870	0.58336	1.87962
SI calcite	-1.6 to 0.6	0.6 to -0.4	0.6	0.6 to 0.09	0.6	0.03 to 0.09
<b>Isotope Data</b>						
d <sup>13</sup> C computed	-11.5000	-9.1000	-8.5000	-10.7000	-11.7000	-10.7000
d <sup>13</sup> C observed	-11.5000	-9.1000	-8.9515	-10.7000	-11.7000	-10.7000
<sup>14</sup> C <sub>OBS</sub> (pmc)	33.60	2.06	6.38	0.62	3.69	0.62
<sup>14</sup> C <sub>ADJ</sub> (pmc)	40.87	24.00	32.09	15.05	30.80	15.35
<sup>14</sup> C <sub>OBS</sub> (ybp)	8758	31176	22099	40818	26495	40818
<sup>14</sup> C <sub>ADJ</sub> (ybp)	1618	20298	13353	26364	17541	26528
<b>Adjusted Age</b>						
Well ID	TX210	TX 215	TX 226	TX 218	TX 216	TX 218
Age (yrs)	1618	21916	14971	41335	19159	45687

(1) Model inputs are d13C = 0 ‰ and 14C = 0 % modern for calcite, d13C = -25 ‰ and 14C = 0 % modern for lignite, d13C = -20 ‰ and 14C = 0 % modern for CO2(g), except for the Recharge to Upgradient Well model, which used d13C = -25 ‰ and 14C = 100 % modern for CO2(g)

(2) Minimal elements and phases used to define carbonate system. Fe, Na, S, Mg, Cl, K omitted as not essential or not measured

NA = Phased not used in model

**Table 7-8. Results of modeling reaction paths (continued).**

	<b>Model Results<sup>(1)</sup></b>				
	Transect 3		Transect 3 (Alternate Path)		Transect 4
	Recharge to TX210 to TX93 (user defined)	Recharge to TX93 to TX214 (user defined)	Recharge to TX210 to TX94 (user defined)	Recharge to TX94 to TX214 (user defined)	Recharge to TX210 to TX96 (user defined)
<b>Plausible phases<sup>(2)</sup></b>	Mass Transfer (millimoles per kilogram H <sub>2</sub> O)				
Calcite	1.13023	2.52934	1.52028	2.13930	1.22193
CO <sub>2</sub> (g)		NA	NA	NA	NA
Mg/Na exchange	-0.02881	0.30451	-0.20578	0.48148	0.28393
Ca/Na exchange	1.08170	4.45631	1.94453	3.86667	3.36857
K/Na exchange	-2.01875	1.01539	-2.73760	1.18788	0.96622
Lignite	1.09272	0.86146	0.61276	1.34141	3.10120
SI calcite	0.6 to -0.5	-0.5 to 0.1	0.6 to -0.5	-0.5 to 0.1	0.6 to -0.3
<b>Isotope Data</b>					
d <sup>13</sup> C computed	-11.8000	-9.8000	-9.9000	-9.8000	-15.0000
d <sup>13</sup> C observed	-11.8000	-9.8000	-9.9000	-9.8000	-15.0000
<sup>14</sup> C <sub>OBS</sub> (pmc)	17.10	1.36	6.92	1.36	2.54
<sup>14</sup> C <sub>ADJ</sub> (pmc)	25.33	16.03	25.73	16.03	15.32
<sup>14</sup> C <sub>OBS</sub> (ybp)	14182	34510	21446	34510	29494
<sup>14</sup> C <sub>ADJ</sub> (ybp)	3248	20395	10855	20395	14856
<b>Adjusted Age</b>					
Well ID	TX 93	TX 214	TX 94	TX 214	TX 96
Age (yrs)	4866	25261	12473	32868	16474

(1) Model inputs are d13C = 0 ‰ and 14C = 0 ‰ modern for calcite, d13C = -25 ‰ and 14C = 0 ‰ modern for lignite, d13C = -20 ‰ and 14C = 0 ‰ modern for CO<sub>2</sub>(g), except for the Recharge to Upgradient Well model, which used d13C = -25 ‰ and 14C = 100 ‰ modern for CO<sub>2</sub>(g)

(2) Minimal elements and phases used to define carbonate system. Fe, Na, S, Mg, Cl, K omitted as not essential or not measured

NA = Phased not used in model

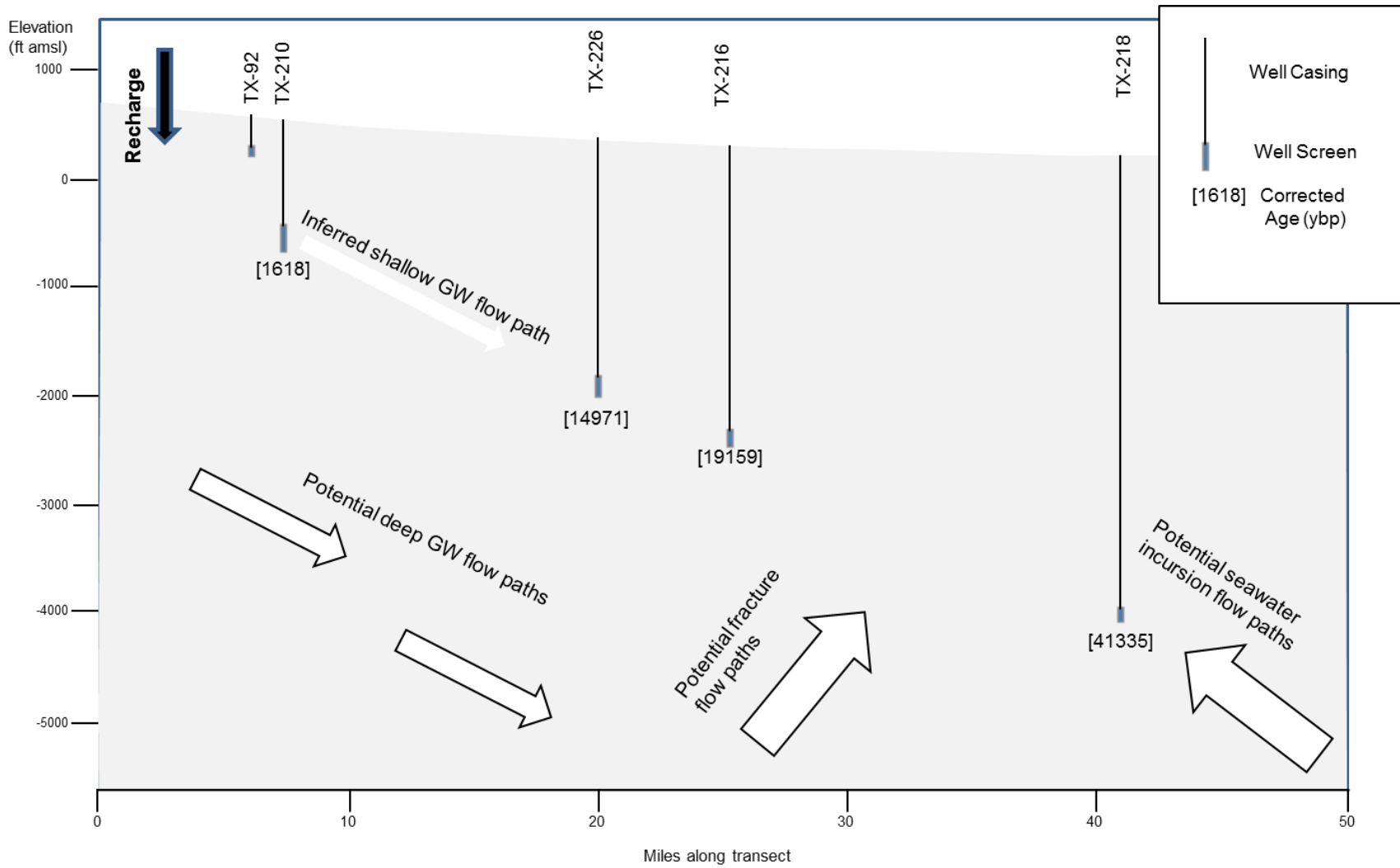


Figure 7-322. Vertical profile along Transect line 2 showing well, well screen depths and inferred and potential groundwater flow pathways.

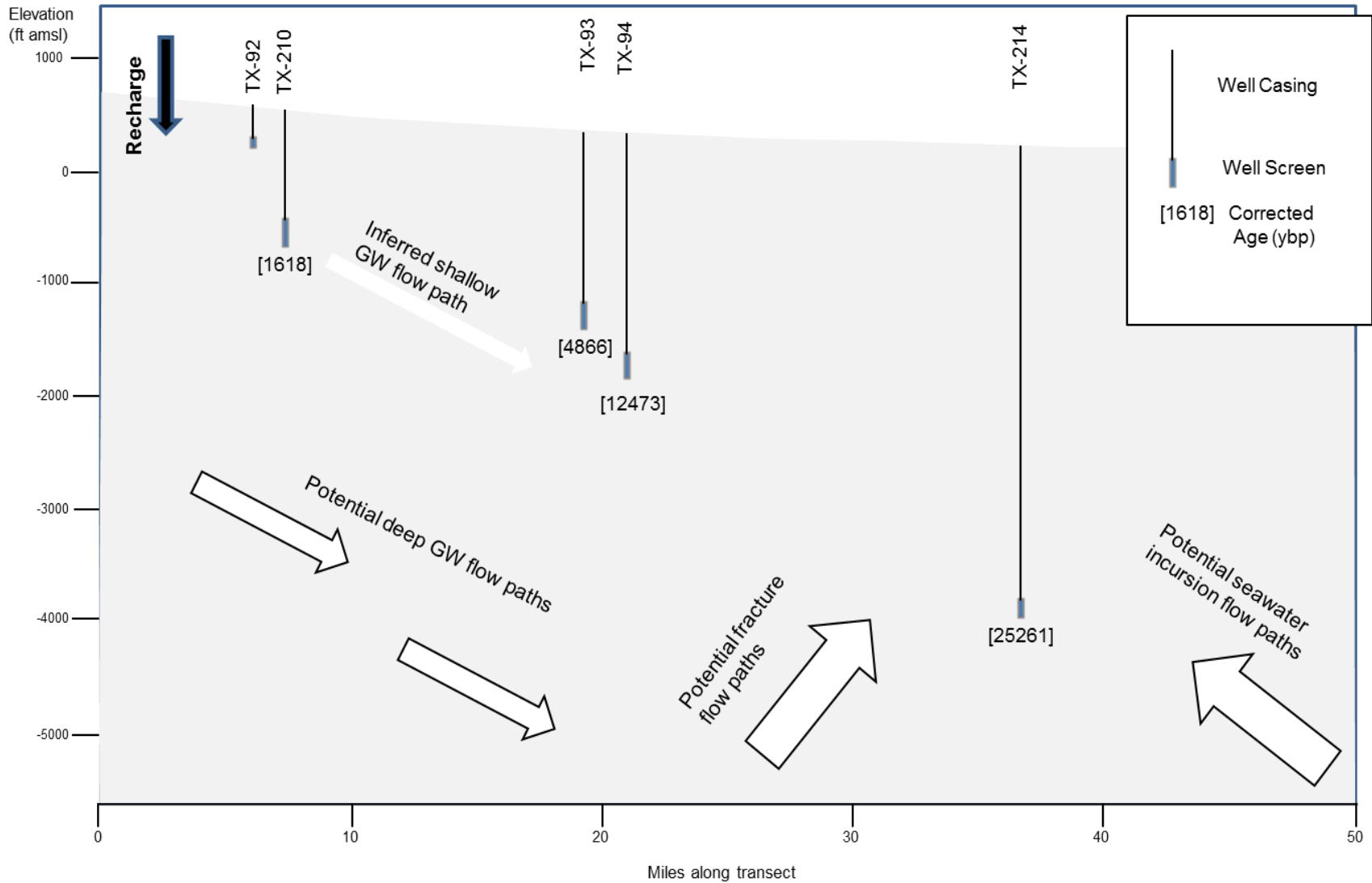


Figure 7-323. Vertical profile along Transect line 3 showing well, well screen depths and inferred and potential groundwater flow pathways.

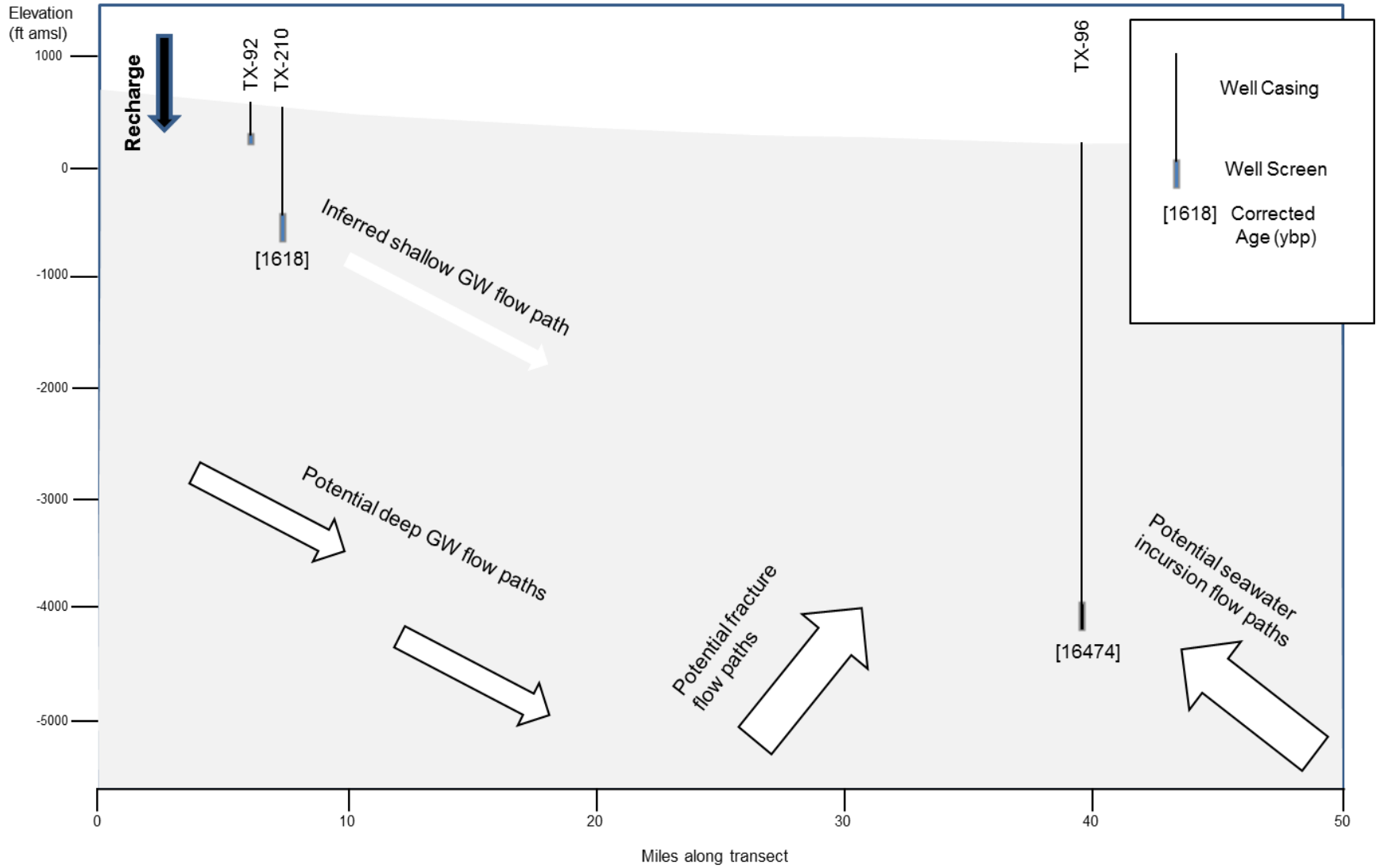


Figure 7-324. Vertical profile along Transect line 4 showing well, well screen depths and inferred and potential groundwater flow pathways.

### **7.4.3 Brackish Lower Wilcox Group**

Brackish groundwater in the Carrizo-Wilcox, Queen City, Sparta and Yegua-Jackson aquifers in Texas represents an important part of the aquifers studied for this project. LBG-Guyton (2003) in a state-wide assessment mapped the presence of brackish groundwater in Groundwater Management Areas 11, 12 and 13 as being primarily in their downdip extent. The Carrizo-Wilcox, however, was one aquifer where the presence of brackish water occurred far updip in the confined section and in the outcrop. In Gonzales County, fresh groundwater in the Carrizo-Wilcox Aquifer did not extend downdip from the outcrop. In southern Bexar County brackish groundwater is present as well in the outcrop. Brackish groundwater is often defined as having a total dissolved solid from 1,000 milliequivalents per liter to 10,000 milliequivalents per liter (Richter and Kreitler, 1993). Typically only total dissolved solids are measured and interpreted from geophysical log data. The specific ionic composition of the brackish water is not determined and possible origin is not made.

The San Antonio Water System is currently developing a brackish groundwater well for the City of San Antonio (Kreitler and Morrison, 2009). They conducted preliminary chemical analysis for test wells in the Carrizo-Wilcox Aquifer in southern Bexar and northern Atascosa counties. The Bexar County wells had a total dissolved solids range of 1,200 to 1,500 milligrams per liter. TW-3, the Atascosa test well had total dissolved solids values from 1,500 to 1,700 milligrams per liter.

The chemical composition for the Bexar County test wells was a sodium-sulfate water with relatively low chloride. TW-3, the Atascosa County well was a sodium-chloride water with lower sulfate (Table 7-9).

For this study five Carrizo-Wilcox Aquifer wells were sampled from the outcrop in southern Bexar County to northern Atascosa County plus an injection well in the downdip section of the Carrizo-Wilcox Aquifer in Webb County. Inorganic chemistry, isotope and gas analyses were done to develop a better understanding of the chemistry and origin of brackish waters.

Because of the geologic setting of the Carrizo-Wilcox Aquifer and the chemical evolution seen at the other transects, the following conceptual hydrogeologic model was anticipated.

1. Because of the characteristically lower permeability of the Carrizo-Wilcox Aquifer in south Texas, the age of these waters would be older than observed in the other transects.
2. Regardless of age, groundwater flowed from the outcrop downdip into deeper parts of the aquifer and geochemical evolution of the groundwater chemistry should occur from shallow to deep.
3. Because of its deltaic to marine depositional origin, hydrocarbon gases would be present.
4. Its brackish nature might result from an updip migration of more saline water.

#### **Aquifer Composition**

The chemical compositions of all six wells sampled in 2012 in the Bexar and Atascosa county area for the brackish Lower Wilcox Group are given in Table 7-10. The first four wells are in Bexar County and range in depth from 240 to 1,804 feet below land surface, the fifth well is in Atascosa County and is 2,660 feet below land surface, but all five wells are close enough to project to an essentially north to south transect line (Figure 7-325 through Figure 7-327). The

sixth well is much deeper and is actually completed in the Lower Wilcox Group section in Webb County and is not shown on Figure 7-326. It is an injection well for Shell Oil for which we were offered the opportunity to sample and is included for comparison to the five transect wells.

All wells were sampled in 2012 and have both chemical and isotopic analyses (Table 7-10). The screened intervals for the wells have been projected along strike to the designated cross-section line (Figure 7-327) and the profile should be representative of hypothetical Carrizo-Wilcox Aquifer flow system down the structural dip. The chemical data do not depict a chemical evolution seen in the other aquifers. The chemical composition is a sodium-sulfate to a sodium-chloride water type (Figure 7-328), and the shallowest well (in the outcrop) is already significantly saline with a total dissolved solids of 1,600 milligrams per liter, which is unusual for a well only 240 feet deep. The groundwater chemistry for alkalinity, sulfate, chloride and calcium changes little along the transect line (Figure 7-329 and Figure 7-330). The changes observed on the Piper diagram for the other aquifers in this study show greater chemical changes.

The sulfate concentration is 580 milligrams per liter in the first sample and 432 milligrams per liter in the last well in the profile; apparently there is neither an additional sulfate source along the flow path nor is sulfate reduction or methanogenesis evident. The  $\delta^{34}\text{S}$  values for sulfate are almost invariant along the flow path, ranging from  $\delta^{34}\text{S}$  of 2.6 ‰ to 3.3 ‰, suggesting that the sulfate is derived from the outcrop area (Figure 7-330). Similarly the chloride concentration is relatively constant with distance across the first four wells but Well 5 (Atascosa County) as in other transects has evidence of mixing with a brine at depth that has elevated the sodium and chloride (Figure 7-329). The sixth well is an injection well drilled to about 10,000 feet below land surface to the deeper Carrizo-Wilcox Aquifer zones, but the location is two counties away to the southwest (Figure 7-326 and Figure 7-327). The chloride concentration is 4,750 milligrams per liter and could be an indication that the deeper Lower Wilcox Group in this transect is mixing with the Lower Wilcox Group at depth. The fifth sample in the transect (TW3, Atascosa County) has a chloride concentration of 695 milligrams per liter and the sulfate is lower than the preceding wells indicating perhaps that some sulfate reduction is occurring. The sulfur isotopic measurement in TW3 is extremely enriched to a  $\delta^{34}\text{S}$  value of + 40.8 ‰, significantly above the prior values of 2.6 to 3.3 ‰, also indicating sulfate reduction is occurring, leaving an enriched sulfate isotopic signature. The  $\delta^{34}\text{S}$  for the Lower Wilcox Group sample is also enriched, but only to a  $\delta^{34}\text{S}$  of 10.6 ‰, but that may be a local difference rather than a regional signature. The other exception is the third well which does have lower sulfate and higher sodium and chloride, but for no obvious reason (Figure 7-328).

Methane is detected in low concentrations in the fixed gas measurements; the hydrocarbon fraction analysis of the dissolved gas qualitatively indicates various low concentrations of  $\text{C}_1 - \text{C}_6$  content in all samples (Table 7-10). The  $\delta^{13}\text{C}$  measurement of methane for TW-3 yields a value of -27.9 ‰, along with the evidence of higher gas fractions suggests trace concentrations of thermogenic and not biogenic hydrocarbon gas. The deep Carrizo-Wilcox Aquifer sample in Webb County had significant thermogenic hydrocarbon gas content and may be the source for the thermogenic gas in the Carrizo-Wilcox Aquifer (Figure 7-330).

### Estimation of Age

The five Carrizo-Wilcox Aquifer groundwater samples have measured carbon-14 contents that range from 5.08 percent modern carbon (23,940 years before present) in the updip Borrego well to 1.96 percent modern carbon (31,580) in the deepest well in Atascosa County (TW-3, Table

7-11); however all three San Antonio Water System wells in southern Bexar County measure slightly older ages. The  $\delta^{13}\text{C}$  is consistent from -15.5 ‰ to -16.8 ‰ and the alkalinity is nearly constant from 220 to 284 milligrams per liter. There is no evidence that the aquifer is dissolving calcite to any significant extent along the flow path, and calculations with WATEQ indicate that the groundwater from the San Antonio Water System wells is essentially at equilibrium with calcite at all four well locations. The saturation index values range from +0.06 to +0.25 which is generally considered within the range expected for indication of equilibrium, especially with the potential for loss of carbon dioxide during sampling as samples are brought to the surface from depth, which could significantly impact the measured field pH and thus the saturation calculation. (Table 7-12) These small variations in concentrations and isotopic values suggest that the aquifer composition is not changing with mineral or gas reactions from well to well in a linear fashion; and thus corrections for additional carbon entering the groundwater are not warranted, and corrections using NETPATH are not useful. It is suggested that the differences in ages for the wells are due different pathways for each well from recharge to the well location, that the primary reactions occur early in the flowpath, and that only an estimate from a simple method like the Pearson and White procedure is useful. This correction is minimal and is given in Table 7-11.

It is noteworthy that the deep Carrizo-Wilcox Aquifer sample in Webb County is much more saline and has an uncorrected age of 36,120 years before present, but the flow path is not defined and a correction procedure is not possible without additional information about the upgradient wells and aquifer composition. It is surprising that the Webb County sample with its higher total dissolved solids and chloride had measurable carbon-14.

The chemical composition of the brackish groundwater along an outcrop to downdip transect in Bexar and Atascosa county is primarily a sodium-sulfate water to a sodium-chloride water, but there is no obvious evolution of the chemistry from outcrop into the confined section. This is in contrast to the other aquifers investigated for this study where a chemical evolution pathway is well defined. Similarly, the corrected carbon-14 ages (Pearson and White, 1967) were all old (20,000 to 33,000 years before present) regardless of a sample location in the outcrop to the deepest well at 2,660 feet. These values are dissimilar to the typical sodium-bicarbonate water seen in most of the aquifers in this study. As more brackish wells are constructed and tested, for brackish water development, complete chemical and isotopic analyses are needed to determine whether this chemistry of the brackish Lower Wilcox Group is anomalous.

## **Discussion**

The geochemical composition in each aquifer on the South Transect is one of two types. Both the Carrizo-Wilcox Aquifer and the Queen City Aquifer evolve from a mixed cation mixed anion water at shallow depths to a sodium-bicarbonate water at depth. The Queen City Aquifer appears to add more chloride at depth in comparison to the Carrizo-Wilcox Aquifer. The water chemistry for both aquifers can be explained by intra-aquifer geochemical processes (i.e., formation of a sodium-bicarbonate water). The previously described set of geochemical reactions of calcite dissolution, cation exchange downdip sulfate reduction and pH change seen in the northeast, central and Gonzales Transect are applicable for the Carrizo-Wilcox and Queen City aquifers. The addition of sodium-chloride at depth from presumable updip migration of saline water is also occurring. There is no evidence of cross-formational leakage.

The water chemistry of the Sparta Aquifer evolves from a sodium-calcium-chloride-sulfate water at shallower depths to chloride-bicarbonate water at depth and has a different chemistry as observed in the underlying Carrizo-Wilcox Aquifer and the Queen City Aquifer. The Sparta Aquifer waters are brackish. The chemical origin of this water is not known but does not appear to result from cross-formational flow from the underlying Carrizo-Wilcox Aquifer or the Queen City Aquifer.

The water chemistry in the Yegua-Jackson Aquifer is dissimilar to the underlying Carrizo-Wilcox and the Queen City aquifers. There are similarities between the Yegua-Jackson Aquifer and the Sparta Aquifer, although the Yegua-Jackson Aquifer waters are lower in magnesium and higher in chloride than the Sparta Aquifer. The Yegua-Jackson Aquifer waters have higher total dissolved solids values for the underlying aquifer. The water chemistry of the Yegua-Jackson Aquifer does not suggest cross-formational flow from underlying aquifers.

The carbon-14 corrected ages for the Carrizo-Wilcox Aquifer show a continual increase in age from northern Atascosa to McMullen counties. Ages increase from modern in the outcrop to possible ages of 40,000 plus. Higher concentrations of calcium occur as far south as the Charlotte, Jourdanton and Pleasanton Trough. This downdip movement of calcium and gradual increase in carbon-14 ages is contrary to the rapid increase in carbon-14 age and decreasing calcium concentration as seen in the Wilcox Group of the Carrizo-Wilcox Aquifer in the Central Transect.

In the South Transect, as well as in the Gonzales Transect, groundwater is flowing from the outcrop into the deep subsurface. Based on accepted hydrogeologic concepts of groundwater flow down the hydraulic gradient fresh groundwater is moving into the deep subsurface of the Carrizo-Wilcox Aquifer, but the chemistry of the aquifers overlying the Carrizo-Wilcox Aquifer does not indicate upward leakage.

Evaluation of Hydrochemical and Isotopic Data in Groundwater Management Areas 11, 12 and 13

**Table 7-9. Selected chemical constituents for the brackish test and monitor wells (Kreitler and Morrison, 2009).**

Well ID	Sample Date	Field Parameters			Lab	Lab Parameters												
		pH	Temp	Conductance		TDS	Turbidity	Calcium	Magnesium	Sodium	Potassium	Total Iron	Total Alk	Bicarbonate	Chloride	Sulfate	Fluoride	Silica
		(s.u.)	(deg C)	(umhos/cm)		(mg/L)	NTU	(mg/L)	(mg/L)	(mg/L)	(mg/L)	(mg/L)	(mg/L)	(mg/L)	(mg/L)	(mg/L)	(mg/L)	(mg/L)
<b>MW-1</b>																		
	11/14/06	7.7	31.0	2,160	LCRA	1,410	NP	44.8	22.8	424	9.38	0.647	207	207	274	508	NP	NP
					ELI	1,240	1.0	43.7	22.5	415	8.90	0.667	243	296	100	545	1.26	15.6
<b>TW-1</b>																		
	4/20/07	7.5	33.0	1,970	LCRA	1,360	NP	42.8	23.4	389	8.64	0.324	236	233	230	508	NP	19.1
					ELI	1,324	<0.1	43.2	23.0	391	8.60	0.300	248	303	285	508	1.36	17.6
	3/4/08	7.6	33.0	2,040	LCRA	1,390	1.5	44.2	22.4	386	7.91	0.306	233	233	238	526	NP	21.1
	3/12/08	7.6	33.5	2,040	LCRA	1,380	1.6	43.2	22.4	384	8.38	0.241	232	232	239	513	NP	20.9
	3/18/08	7.5	33.0	2,060	LCRA	1,380	1.1	42.7	21.9	381	7.78	0.238	232	232	230	506	NP	21.8
	3/26/08	7.5 <sup>1</sup>	33.0 <sup>1</sup>	1,900 <sup>1</sup>	ELI	1,427	1.4	44.6	24.5	406	9.20	0.265	256	312	242	498	0.28	12.7
<b>MW-2</b>																		
	12/28/06	7.7	29.0	2,070	LCRA	1,380	NP	14.8	7.4	497	5.84	NP	247	246	263	491	NP	NP
					ELI	1,188	4.0	12.9	7.1	455	5.60	1.970	263	320	240	511	0.84	15.7
<b>TW-2</b>																		
	4/13/07	7.9	29.5	1,980	LCRA	1,310	NP	15.7	7.6	442	5.20	0.133	236	236	245	464	NP	15.1
					ELI	1,437	1.0	15.5	7.4	433	5.00	0.167	230	281	260	492	2.22	14.4
<b>TW-3</b>																		
	6/13/07 <sup>2</sup>	8.3	38.5	3,040	LCRA	1,700	3.8	5.1	1.6	633	4.27	0.201	456	443	615	204	0.50	27.4
	8/24/07	8.4 <sup>3</sup>	-	2,580 <sup>3</sup>	LCRA	1,520	22.8	6.1	2.0	567	4.33	NP	422	404	427	144	0.75	NP
	1/8/08	8.0	38.5	2,480	LCRA	1,520	0.7	5.8	1.7	581	4.04	ND	407	373	496	180	0.53	19.7
	2/14/08	8.1	38.0	2,290	LCRA	1,380	0.2	5.0	1.5	508	3.75	ND	418	398	432	134	NP	19.4
					ELI	1,680	0.2	5.4	1.6	510	4.10	0.153	462	564	506	152	2.16	15.8
<b>TCEQ Secondary Standard</b>																		
		≥7	NS	NS		1,000	1.0 <sup>4</sup>	NS	NS	NS	NS	0.3	NS	NS	300	300	2.00	NS

NOTES:

- ND = non detect
- NP = not performed
- NS = no secondary standard for this constituent
- 1) Measured in field by Carollo
- 2) Sample was retrieved from temporary well screened from 2,520 to 2,550 feet depth
- 3) Measured at lab
- 4) Standard for treated water

Evaluation of Hydrochemical and Isotopic Data in Groundwater Management Areas 11, 12 and 13

**Table 7-10. Chemical and isotopic composition of the brackish Lower Wilcox Group water samples.**

	Sample Number	BXAT-1	BXAT-2	BXAT-3	BXAT-4	BXAT-5	Webb County	
	Well Owner	SAWS	SAWS	SAWS	SAWS	Alfred Borrego	Shell Oil	
	Well Number	SAWS TW-1	SAWS TW-2	SAWS TW-3	SAWS BGD-1	Borrego Well	Injection Well	
	Well Depth (ft)	1,796	1,250	2,660	1,330	240	3,500	
	Screened Interval <sup>1</sup> (feet below ground surface)	1,240-1,786	752-1,230	1965-2,640	855-1310	170-240	--	
	Aquifer	Wilcox	Wilcox	Wilcox	Wilcox	Wilcox	Wilcox	
	Sample Date	5/31/2012	5/31/2012	5/31/2012	6/1/2012	6/7/2012	--	
<b>Stabilized Field Readings</b>		<b>Units</b>						
	Temp	°F	78.6	84.9	79.2	87.4	80.6	NA <sup>3</sup>
	pH		7.36	7.56	7.73	7.31	7.19	NA
	Conductivity	mS	2.10	1.93	2.79	1.93	1.81	NA
<b>SAT Lab Results: Analyte</b>		<b>Units</b>						
General Chemistry	Total Alkalinity	mg/L	244	216	284	224	220	1209
	HS <sup>-</sup> (Bisulfide ion)	mg/L	1	<0.050	<0.050	<0.050	<0.050	NA
	Bromide	mg/L	1	1	1	1	1	NA
	Hydrogen Sulfide	mg/L	1	<0.050	<0.050	<0.050	<0.050	NA
	Fluoride	mg/L	0	0	1	0	0	2
	Chloride	mg/L	252	211	695	222	176	4750
	Nitrite as N	mg/L	<0.50	<0.50	<0.50	<0.50	<0.50	NA
	Nitrate as N	mg/L	<0.50	<0.50	<0.50	<0.50	<0.50	BRL
	TOC	mg/L	5	4	21	5	2	52
	Sulfate	mg/L	580	446	104	436	432	16
	Specific Conductance	µmhos/cm	2500	2200	3170	2210	2170	177,000
	TDS	mg/L	1600	1400	2000	1420	1450	10,400
	pH	pH units	8	8	8	8	8	7.76
	pH @ Temperature		24	24	23	24	15	--
	Calcium	mg/L	45	18	17	20	64	22.1
Iron	mg/L	0	0	0	0	0	BRL	
Magnesium	mg/L	24	8	2	9	32	5.97	
Potassium	mg/L	13	7	7	9	12	16	
Sodium	mg/L	341	329	478	357	238	2290	
<b>Zymax Lab Results: Analyte</b>		<b>Units</b>						
Gas in water	C1	µg/L	1.6	1.8	3.6	1.2	1.1	NA
	C2	µg/L	<1.0	<1.0	<sup>a</sup> 0.2	<1.0	<1.0	NA
	C3	µg/L	<1.0	<1.0	<sup>a</sup> 0.2	<1.0	<1.0	NA
<sup>c</sup> Gas in headspace	C1	ppmv	98.5	45.7	501.2	51.6	32.6	NA
	C2	ppmv	12.8	<1.0	235.4	7.7	<1.0	NA
	C3	ppmv	15.3	6.4	14.1	9.0	<1.0	NA
	i-C4	ppmv	8.8	<1.0	<1.0	2.7	<1.0	NA
	n-C4	ppmv	12.8	2.5	4.2	6.0	<1.0	NA
	i-C5	ppmv	5.3	<1.0	<1.0	4.8	<1.0	NA
	n-C5	ppmv	3.8	<1.0	<1.0	2.8	<1.0	NA
C6+	ppmv	63.5	41.1	1784.1	66.4	16.3	NA	
Fixed Gas	O <sub>2</sub> + Ar	% Volume	7.7	18.3	12.1	17.2	15.2	NA
	N <sub>2</sub>	% Volume	91.1	81.5	86.0	82.5	83.5	NA
	CH <sub>4</sub>	% Volume	<0.1	<0.1	<0.1	<0.1	<0.1	6220 mg/L
	CO	% Volume	<0.1	<0.1	1.4	<0.1	<0.1	NA
	CO <sub>2</sub>	% Volume	1.2	0.2	0.5	0.3	1.3	NA
Isotope analysis	δ <sup>13</sup> C <sub>C1</sub>	‰ VPDB	ND	ND	-27.9	ND <sup>4</sup>	ND	-46.9
	δ <sup>13</sup> C <sub>CO2</sub>	‰ VPDB	-19.8	-20.4	-22.4	-18.5	-21.0	-16.4
	δ <sup>13</sup> C <sub>C2</sub>	‰ VPDB	ND	ND	<sup>b</sup> -33.1	ND	ND	NA
	δD <sub>C1</sub>	‰ VSMOW	ND	ND	<sup>b</sup> -204	ND	ND	-268.7
	δD <sub>C2</sub>	‰ VSMOW	ND	ND	ND	ND	ND	NA
	δ <sup>18</sup> O <sub>-H2O</sub>	‰ VSMOW	-4.6	-4.8	-4.5	-4.9	-4.5	-3.1
δD <sub>-H2O</sub>	‰ VSMOW	-27.7	-28.0	-26.8	-29.1	-27.6	-20	
<b>Beta Lab Results: Analyte</b>		<b>Units</b>						
Radiometric Analysis	Apparent <sup>14</sup> C Age	YBP	36,430	36,130	31,580	38,330	23,940	36,120
	Apparent Age Error	+/- yrs	360	370	230	450	120	320
	<sup>13</sup> C/ <sup>12</sup> C Ratio	‰	-15.5	-14	-16.8	-12.5	-15.5	-11.3
	Fraction Modern	‰	1.1%	1.1%	2.0%	0.9%	5.1%	1.1%
Fmdn Error	+/- %	0.05%	0.05%	0.06%	0.05%	0.07%	0.04%	
<b>U. of AZ Lab Results: Analyte</b>		<b>Units</b>						
Sulfate Isotope	δ <sup>34</sup> S	‰	2.6	2.7	40.8	2.8	3.3	NA
	δ <sup>18</sup> O (SO <sub>4</sub> )	‰	9.3	10.2	17.0	9.4	10.6	-3.1

1) Represents top of highest screen interval to bottom of lowest screen interval.

-- = No screen data available

3) NA = Not Analyzed

4) ND = Target component's concentration too low to obtain reliable isotope data.

<sup>a</sup> = Laboratory Note: Estimate for target components at low concentrations

<sup>b</sup> = Laboratory Note: Estimate due to low concentration, 3xSTDEV applies

<sup>c</sup> = Laboratory Note: Qualitative measure of hydrocarbon gas during isotope analysis

Evaluation of Hydrochemical and Isotopic Data in Groundwater Management Areas 11, 12 and 13

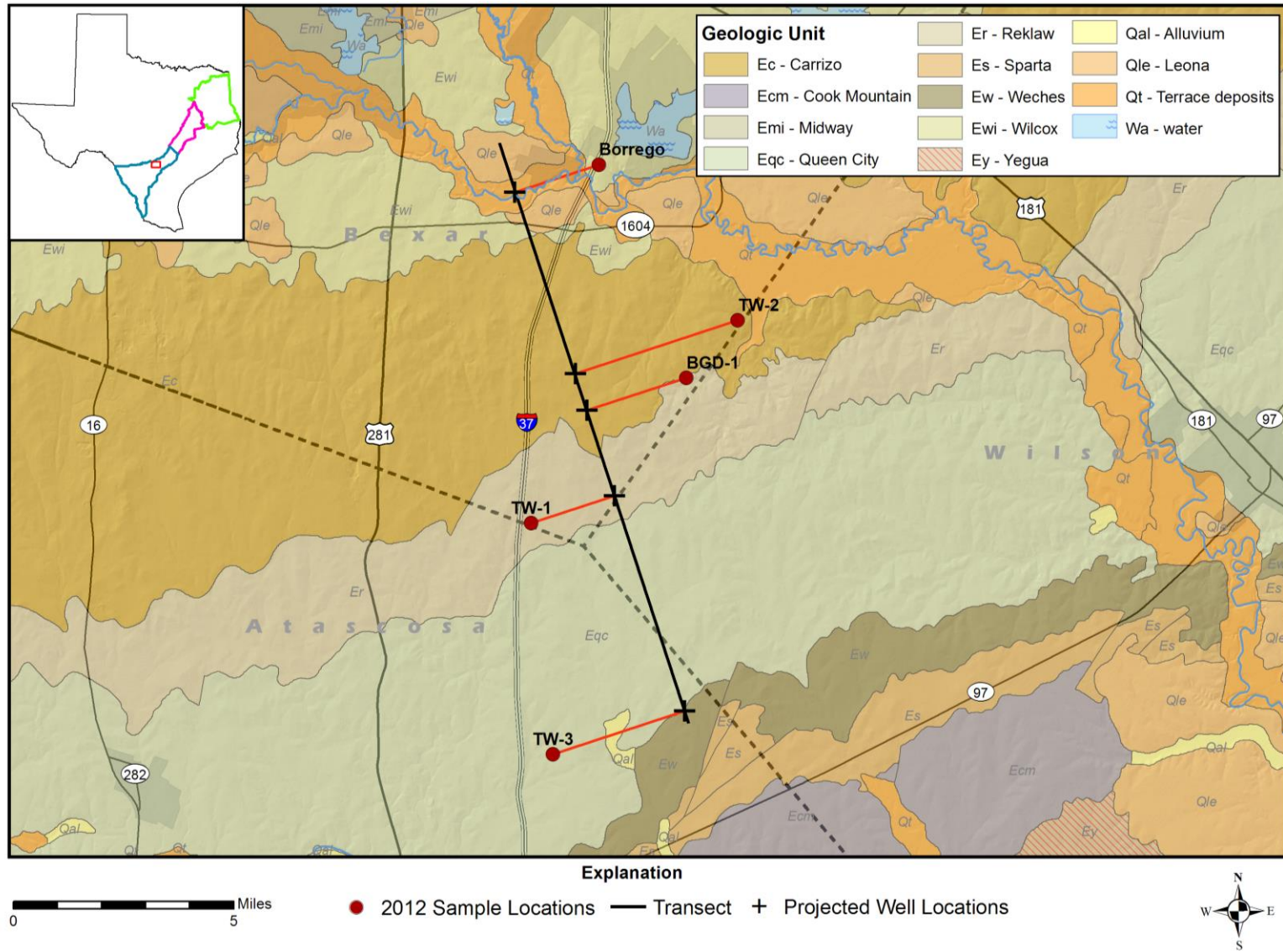


Figure 7-325. Location map for the brackish Lower Wilcox Group wells sampled in 2012 in Bexar and Atascosa counties.

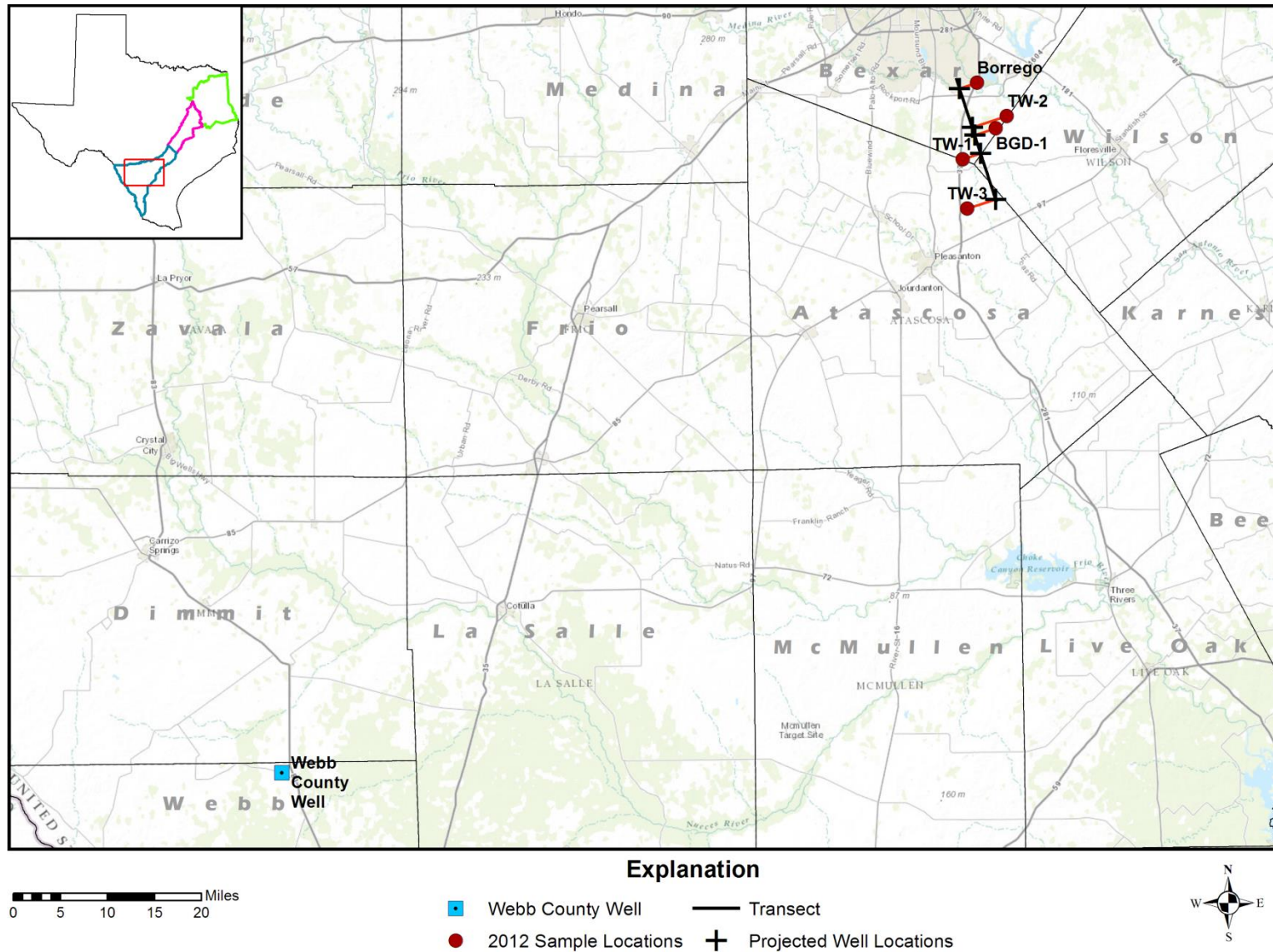
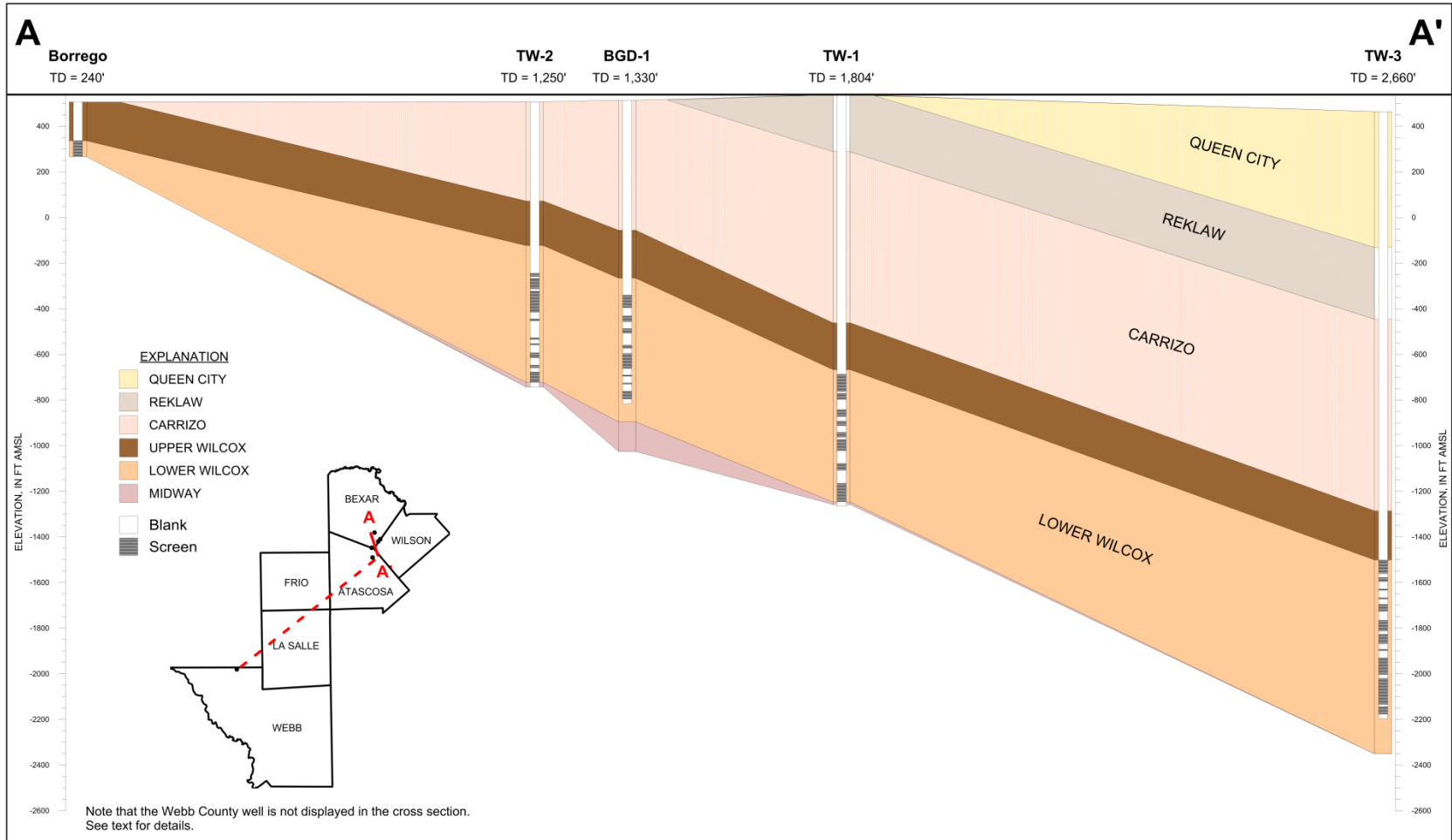


Figure 7-326. Location map for the brackish Lower Wilcox Group wells sampled in 2012 in Bexar, Atascosa and Webb counties.



See 'Figure 7-327 BXAT dip section.pdf' for the full-scale version of the cross-section (included as a separate document).

Figure 7-327. Cross-section A-A' of wells sampled in the brackish Lower Wilcox Group in 2012 in Bexar and Atascosa counties.

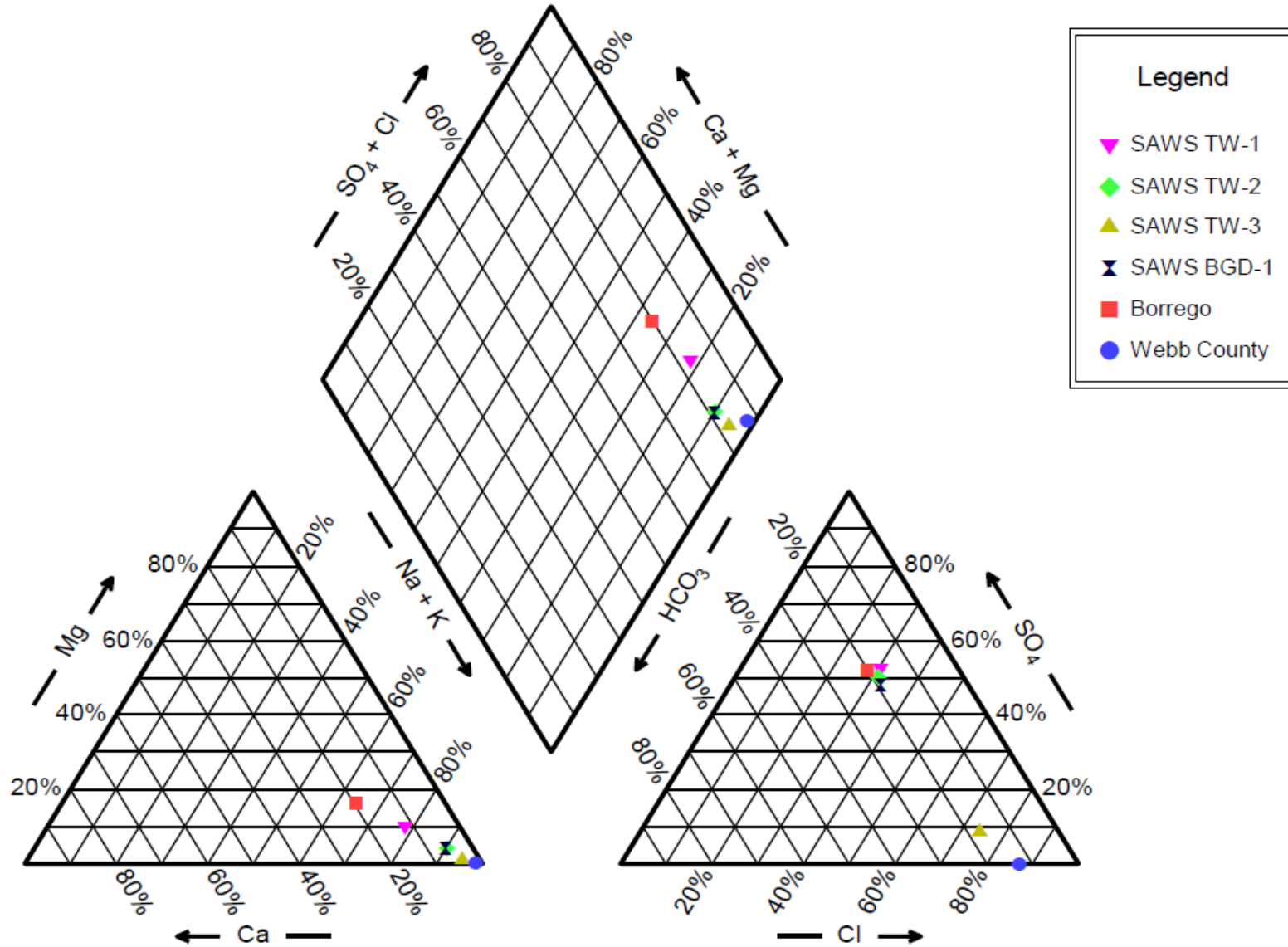


Figure 7-328. Piper diagram for the brackish Lower Wilcox Group wells.

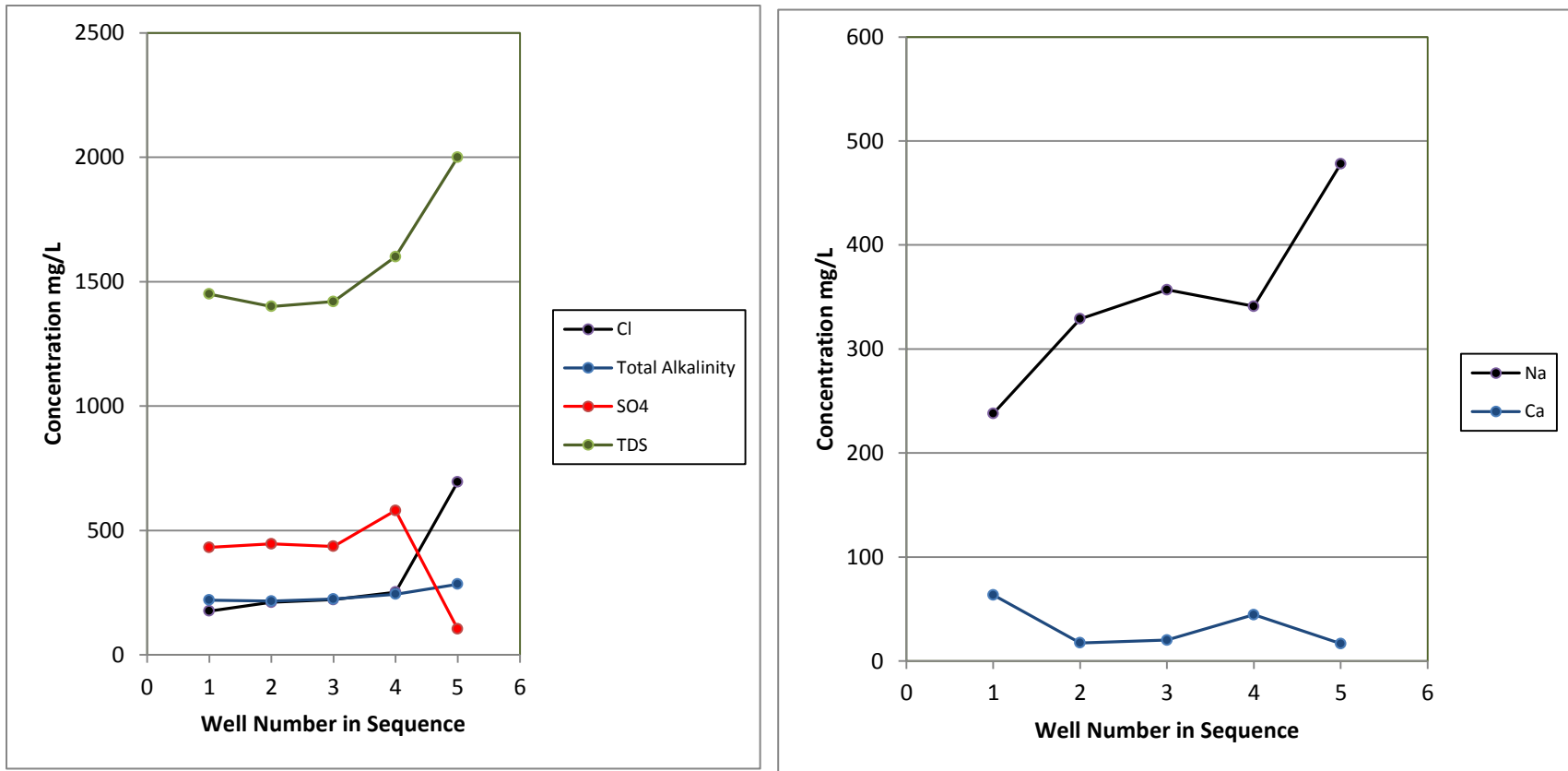


Figure 7-329. Concentrations of major cations measured in milligrams per liter (mg/L), anions and total dissolved solids with respect to well location in the transect.

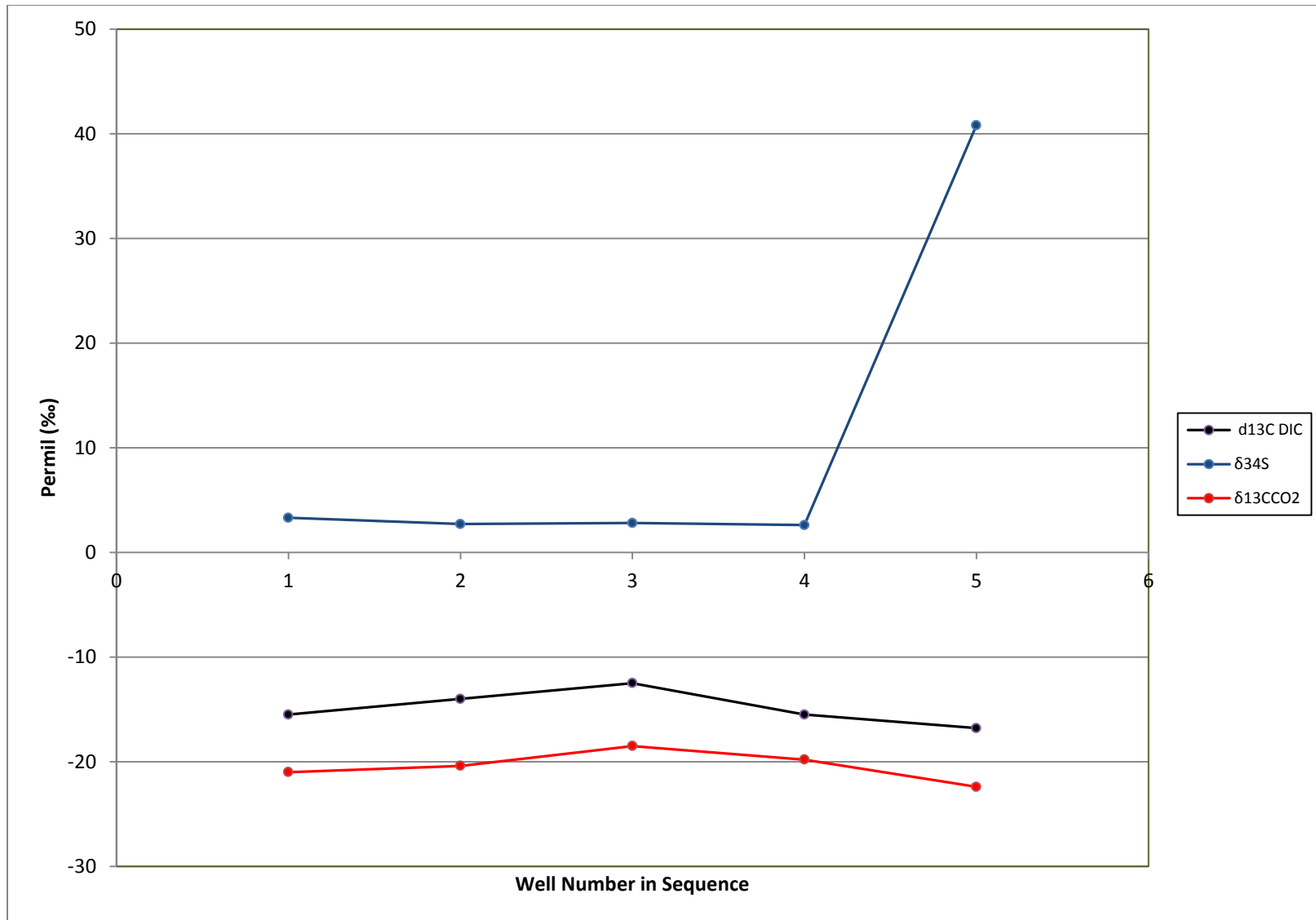


Figure 7-330. Stable isotopes along the transect.

**Table 7-11. Summary of results for the brackish Lower Wilcox Group groundwater age estimates.**

Model No.	Location Name	Internal Well No.	Well Depth (ft)	Cl (mg/L)	Alk (mg/L) <sup>(1)</sup>	$\delta^{13}\text{C}$ ‰ (DIC)	<sup>14</sup> C <sub>OBS</sub> (pmc)	<sup>14</sup> C <sub>OBS</sub> (ybp)	<sup>14</sup> C <sub>ADI</sub> (ybp) <sup>(2)</sup> <i>Pearson &amp; White (1969)</i>
1	Borrogo	BXAT-5	240	176	220	-15.5	5.08	23,940	20,100
2	SAWS-TW2	BXAT-2	1250	211	216	-14.0	1.11	36,130	31,472
3	SAWS BGD-1	BXAT-4	1330	222	224	-12.5	0.85	38,330	32,762
4	SAWS TW-1	BXAT-1	1804	252	244	-15.5	1.07	36,430	32,590
5	SAWS TW-3	BXAT-3	2660	695	284	-16.8	1.96	31,580	28,387
6	Shell	WEBB	3500	4750 <sup>(3)</sup>	1209	-11.3	1.11	36,120	29,741

## NOTES:

 (1) Alkalinity as CaCO<sub>3</sub>

 (2) Correction using Pearson and White (1967) with  $\delta^{13}\text{C}$  soil CO<sub>2</sub> = -25 ‰, and calcite = 0 ‰

(3) Elevated chloride concentrations indicate mixing with a deeper brine of unknown composition

**Table 7-12. Summary of results for the brackish Lower Wilcox Group groundwater pH and saturation indices.**

Model No.	Location Name	Internal Well No.	Well Depth (ft)	pH (field)	pH (lab)	Saturation Index (SI)
1	Borrogo	BXAT-5	240	7.73	7.5	0.91
2	SAWS-TW2	BXAT-2	1250	7.19	7.6	0.25
3	SAWS BGD-1	BXAT-4	1330	7.56	8	0.24
4	SAWS TW-1	BXAT-1	1804	7.31	8.1	0.2
5	SAWS TW-3	BXAT-3	2660	7.36	7.8	0.06
6	Shell	WEBB	3500	*	7.76	1

## 8 Numerical Modeling for Central and Gonzales Transects

### 8.1 Overview of Existing Models

An objective of the current study is to confirm, refine, or modify the conceptual model of groundwater flow within each aquifer and the possible interaction between aquifers in the study area. Because, the Groundwater Availability Models have differing grid orientations and differing boundary conditions representing the Cook Mountain Formation, combining the Groundwater Availability Models into one three-dimensional model would be complicated and require resources beyond the scope of this study. Instead, existing Groundwater Availability Models are combined into two-dimensional transect models. The following aquifers were combined in two-dimensional transects based on the existing Groundwater Availability Model considerations: Carrizo-Wilcox, Queen City, Sparta and Yegua-Jackson.

An overview of the stratigraphic units composing the examined hydrogeologic system is given in Table 8-1 and explained briefly in the following section from oldest unit to youngest. These aquifers span Texas from the Rio Grande in south Texas northeastward through the Sabine River in east Texas. The Carrizo-Wilcox, Queen City and Sparta aquifers have been therefore divided into three areas, each modeled separately. These form the southern portion of the Sparta, Queen City, and Carrizo-Wilcox aquifers (Deeds and others, 2003); central portion of the Sparta, Queen City, and Carrizo-Wilcox aquifers (Dutton and others, 2003); and northern portion of the Sparta, Queen City, and Carrizo-Wilcox aquifers (Fryar and others, 2003) as shown in Figure 8-1. Additionally, the Yegua-Jackson Aquifer has been modeled with a single Groundwater Availability Model spanning the entire extent of the aquifer in Texas from south to east as depicted in Figure 8-1. The development and application of these models are documented in detail in the corresponding Groundwater Availability Model reports submitted to the TWDB.

**Table 8-1. Generalized stratigraphic profile for the Carrizo-Wilcox, Queen City, Sparta (QCSP) and Yegua-Jackson (YEG) aquifers in the investigated area.**

<b>Formation</b>	<b>Aquifer/Aquitard</b>	<b>Age</b>	<b>GAM</b>
Catahoula	minor aquifer	Oligocene	YEG
Upper Jackson (Whitsett)	minor aquifer	Eocene-Oligocene	YEG
Lower Jackson (Manning, Wellborn, Caddell)	minor aquifer	Upper Eocene	YEG
Upper Yegua	minor aquifer	Middle Eocene	YEG
Lower Yegua	minor aquifer	Middle Eocene	YEG
Cook Mountain	aquitard	Middle Eocene	-
Sparta	minor aquifer	Middle Eocene	QCSP
Weches	aquitard	Middle Eocene	QCSP
Queen City	minor aquifer	Middle Eocene	QCSP
Reklaw	aquitard	Middle Eocene	QCSP
Carrizo	main aquifer	Middle Eocene	QCSP
Upper Wilcox / Calvert Bluff	main aquifer	Lower Eocene	QCSP
Middle Wilcox / Simsboro	main aquifer	Lower Eocene	QCSP
Lower Wilcox / Hooper	main aquifer	Upper Paleocene	QCSP

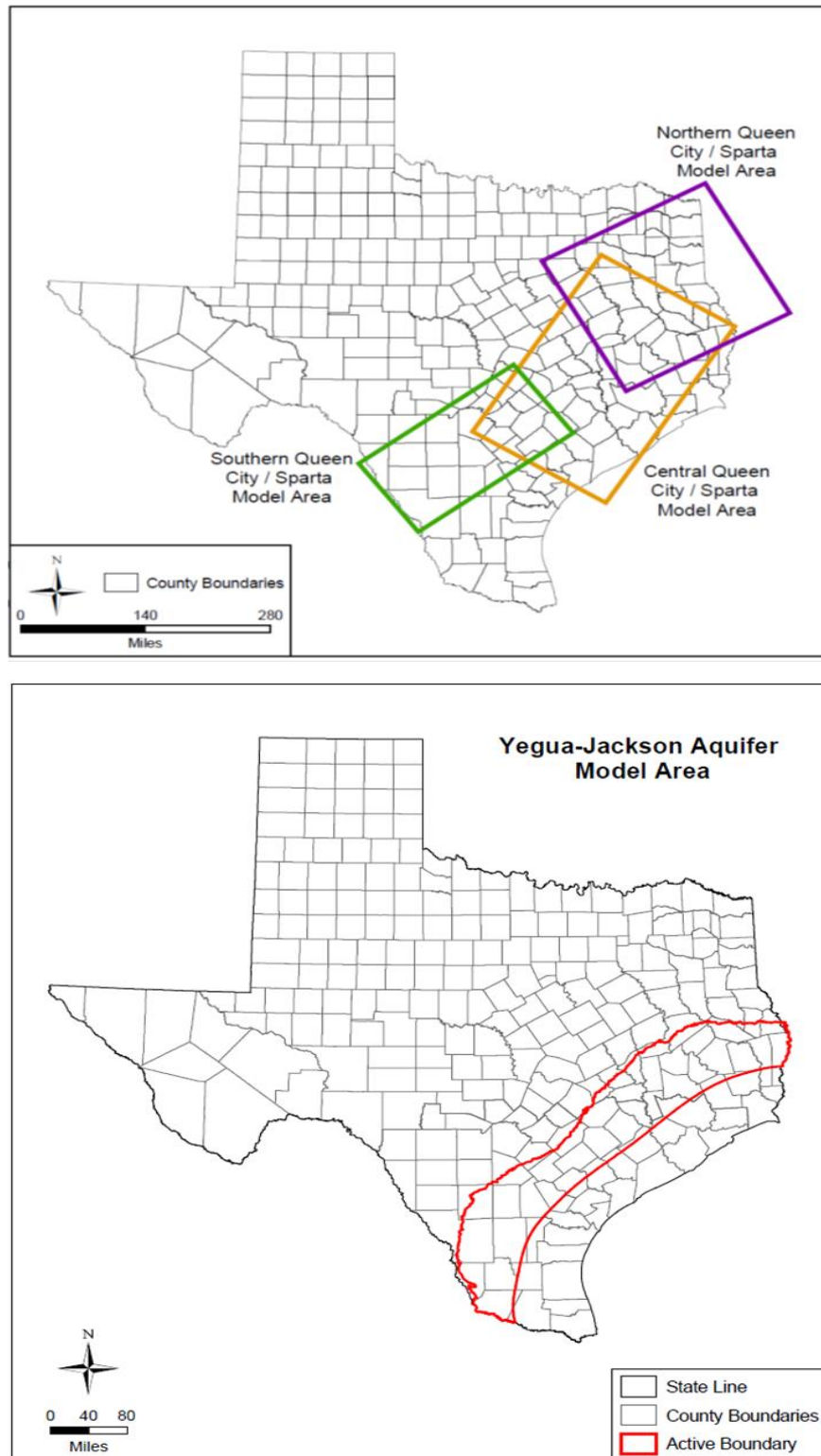


**Figure 8-1.** Location of the three Groundwater Availability Models for the Sparta, Queen City and Carrizo-Wilcox aquifers (top) and the Groundwater Availability Model for the Yegua-Jackson Aquifer (bottom).

### ***8.1.1 Yegua-Jackson Aquifer Groundwater Availability Model***

The three-dimensional groundwater model for the Yegua-Jackson Aquifer was developed in MODFLOW based on a rectilinear grid with cells of 1 mile by 1 mile. Figure 8-2 shows the Yegua-Jackson Aquifer model grid and the outline of active cells in the model. The model grid consists of 337,250 cells in total, oriented along the strike and approximately parallel to the coast. The model grid origin is located at Texas Groundwater Availability Model coordinate system 17,786,114.1 feet north and 5,353,874.5 feet east with the x-axis oriented 0.78 radians north of east. The model has 475 columns and 142 rows for a total of 67,450 grid cells per layer and comprises five layers dipping towards the gulf from the outcrop. After clipping each layer to the proper dimensions of the corresponding geological formations, layer 1 has 31,454 active cells whereas layers 2 through 5 have 29,607 active cells each.

Model layers in MODFLOW are differentiated using the IBOUND index. Layer 1 in the Yegua-Jackson Aquifer model represents the shallow portion of the Yegua-Jackson Aquifer and the younger overlying formations including the Catahoula Formation where the Yegua-Jackson Aquifer is confined. Layers 2 through 5 represent the Upper Jackson Unit, the Lower Jackson Unit, the Upper Yegua Unit and the Lower Yegua Unit, respectively. Figure 8-3 illustrates a typical dip-oriented cross-section of the Yegua-Jackson Aquifer model. The first layer in the model is extended to overlie the rest of the layers and include the shallow outcrop section of the Yegua-Jackson Aquifer.

The model incorporates the structure, hydrostratigraphy and hydraulic properties relevant to the modeled aquifer system, as well as flows relevant to surface-water, recharge, discharge, evapotranspiration and pumping imposed at the model boundaries. The implemented geometry has been used both for steady-state as well as transient simulations. In the current work scope, simulations are run solely in steady-state and boundary conditions are defined based on the steady-state model. Three types of boundary conditions are generally available: specified head (Dirichlet), specified flow (Neumann), and head-dependent flow (Cauchy). A no-flow boundary is a special case of a Neumann boundary condition. In the Yegua-Jackson Aquifer model the bottom boundary corresponding to the base of the Lower Yegua Unit (layer 5) is assigned a no-flow boundary condition. The lateral boundaries are defined by the extent of the Yegua-Jackson Aquifer at the southwest and northeast of the region and can be therefore considered as no-flow boundaries as well. Similarly, the down-dip boundary of the model near the coast reaches the extent of the known structure and is assumed to be a no-flow boundary condition. The portion of layer 1 that represents the Catahoula Formation is assigned a general head boundary condition based on hydraulic heads of the Jasper Aquifer extracted from the existing northern, central and southern Gulf Coast Aquifer Groundwater Availability Models. Surface water acts as a head-dependent flow boundary condition at the active cells of layer 1 corresponding to the outcrop. For the implementation of surface water bodies, the reservoir package (Fenske and others, 1996) and the stream package (Prudic, 1988) for MODFLOW were used. Precipitation-based recharge is assigned at the outcrop using a scaled topographic factor. Evapotranspiration is applied to cells neighboring stream cells in the Yegua-Jackson Aquifer outcrop using the evapotranspiration package for MODFLOW. Pumping discharge is assigned as prescribed flow boundary conditions based on a localized pumping categorization for wells available from the TWDB database. A qualitative description of the model geometry and boundary conditions is illustrated in Figure 8-4. A more detailed description of the development, application and analysis of the Yegua-

Jackson Aquifer Groundwater Availability Model is described in the report submitted to the TWDB (Deeds and others, 2010).

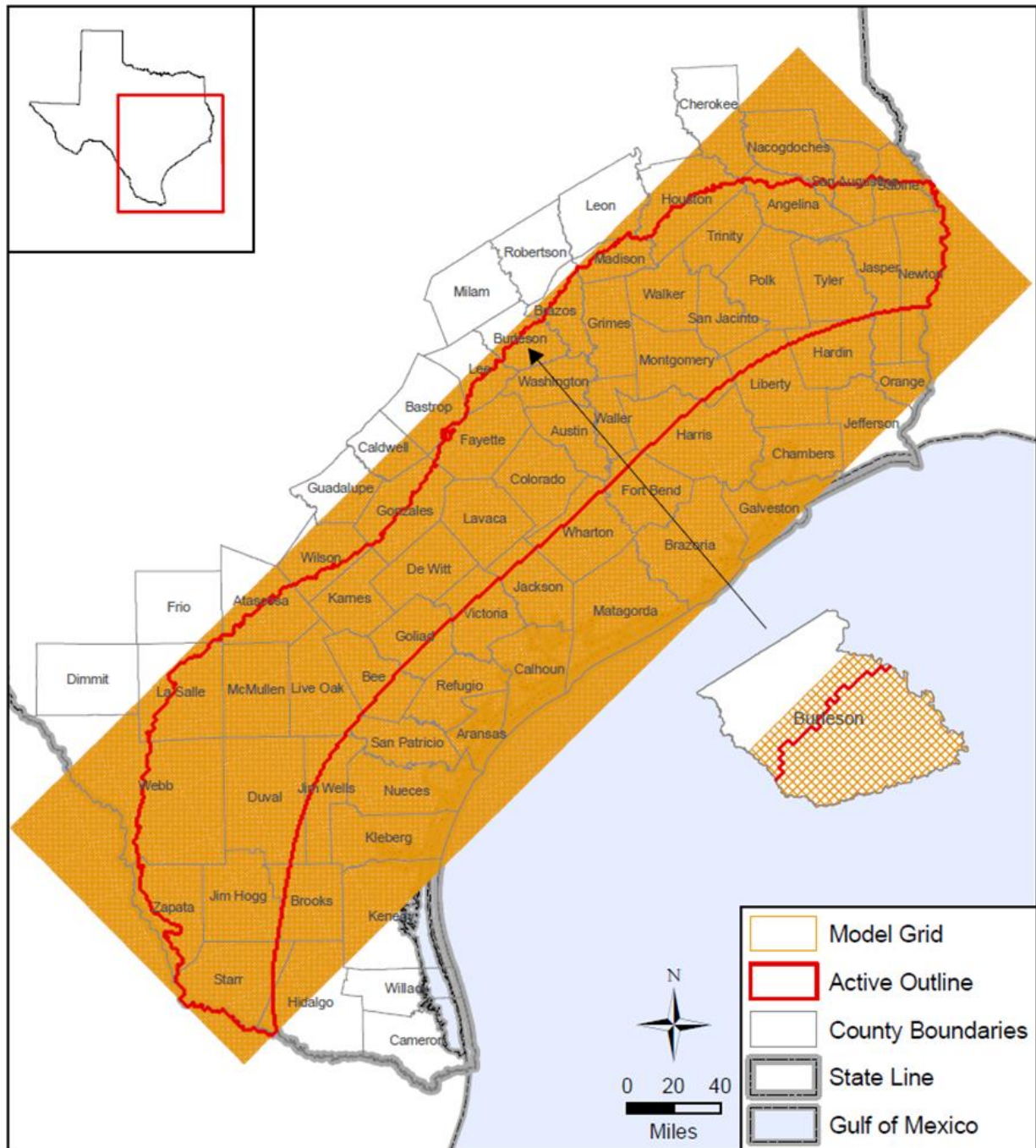


**Figure 8-2.** Plan-view of spatial grid and outline of active cells in the Groundwater Availability Model for the Yegua-Jackson Aquifer (Deeds and others, 2010).

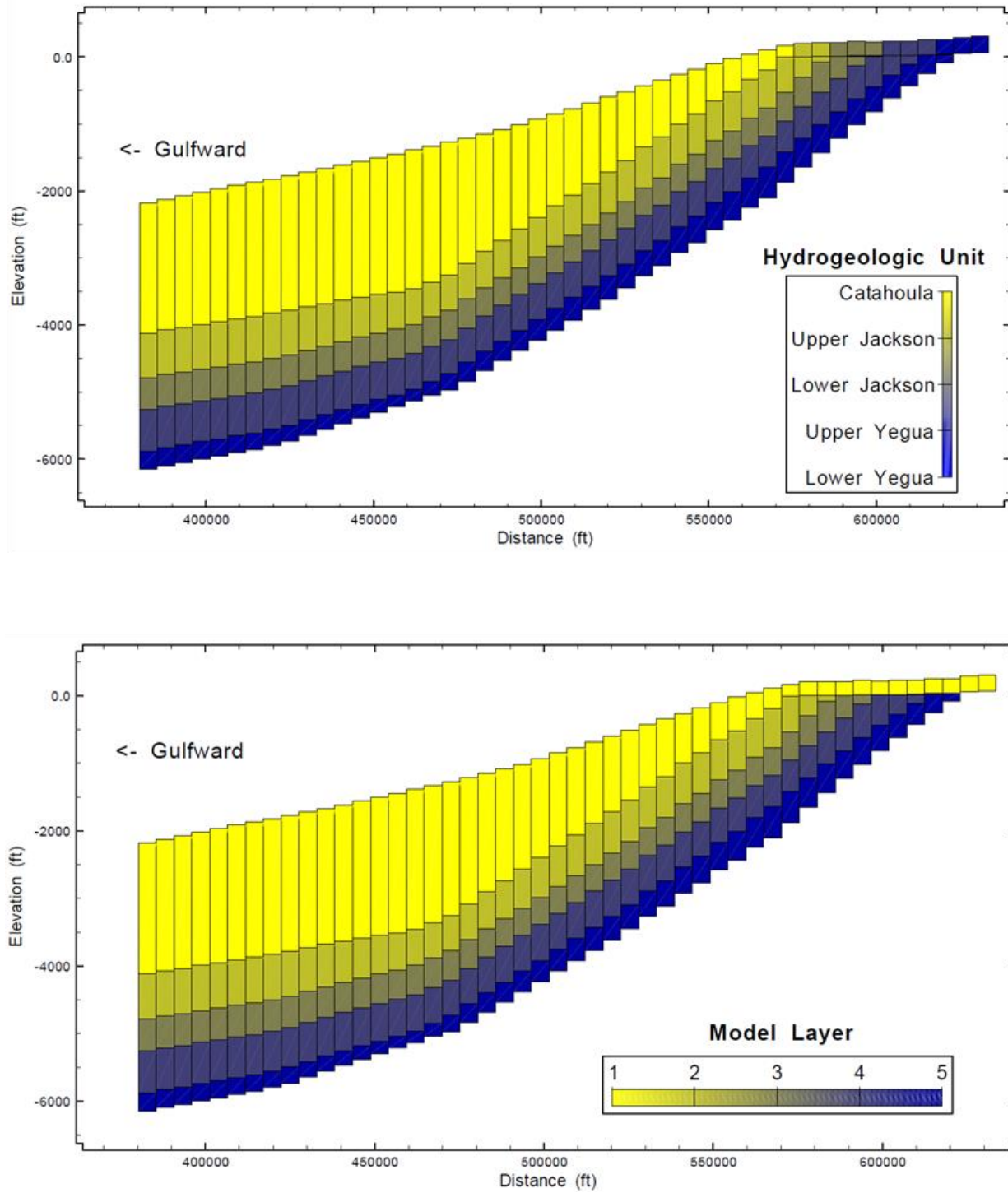


Figure 8-3. Cross-section of hydrogeologic units and corresponding layer indexes in the Groundwater Availability Model for the Yegua-Jackson Aquifer (Deeds and others, 2010).

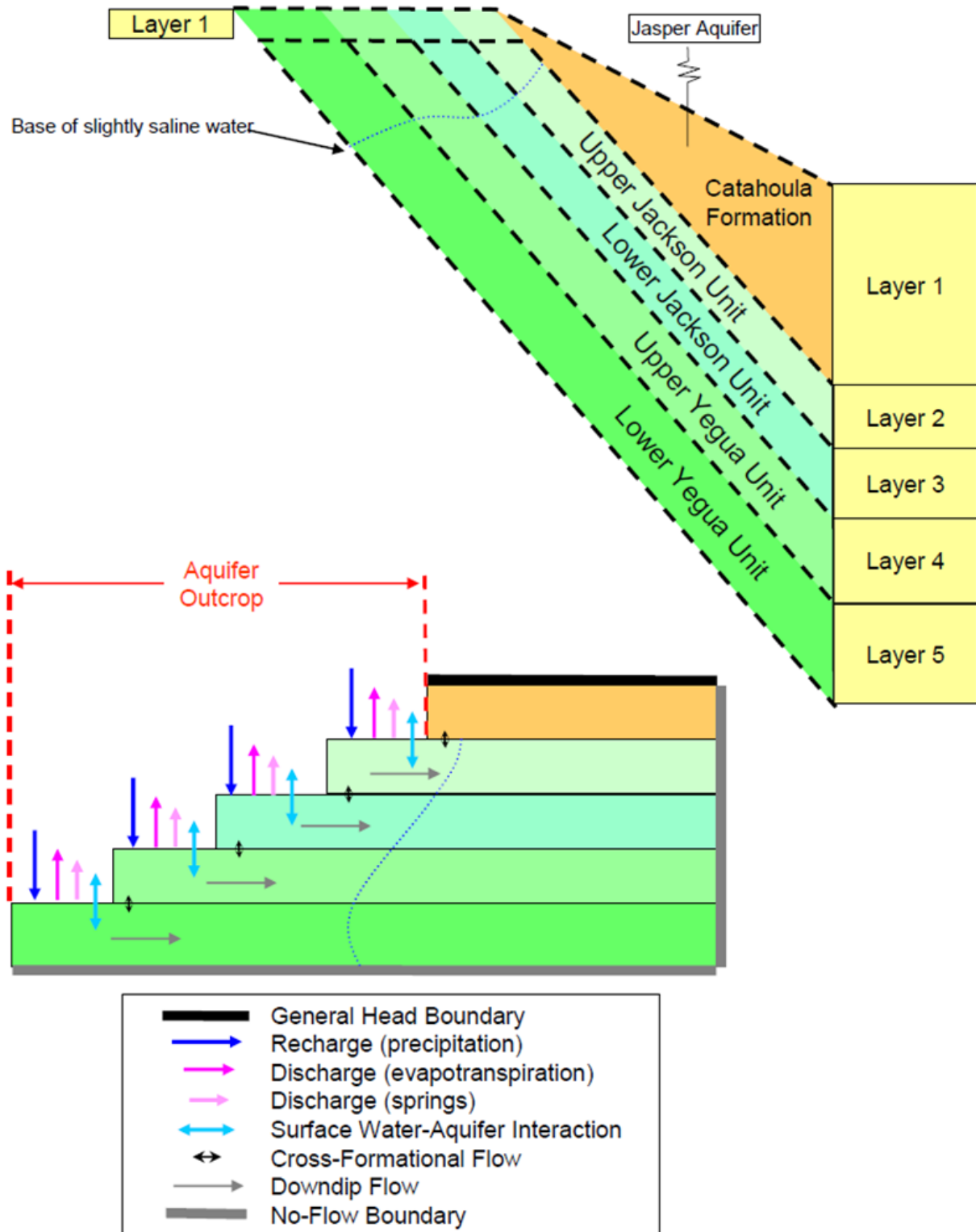


Figure 8-4. Qualitative profile and model conceptualization of the Groundwater Availability Model for the Yegua-Jackson Aquifer (from Deeds and others, 2010).

### **8.1.2 *Queen City and Sparta Aquifers Groundwater Availability Model***

The three-dimensional groundwater models for the Sparta, Queen City and Carrizo-Wilcox aquifers were developed in MODFLOW based on rectilinear grids with discretization of 1 mile by 1 mile (Kelley and others, 2004). In order to cover the entire extent of the aquifers, three models were developed; the southern portion of the Queen City and Sparta Aquifers Groundwater Availability Model, central portion of the Queen City and Sparta aquifers Groundwater Availability Model and the northern portion of the Queen City and Sparta aquifers Groundwater Availability Model. Plan-views of the model grids and outlines of the active grid cells for the southern and central portions of the Sparta, Queen City and Carrizo-Wilcox aquifers Groundwater Availability Models are shown in Figure 8-5. The model grid for the southern portion of the Sparta, Queen City and Carrizo-Wilcox aquifers originates at Texas Groundwater Availability Model coordinate system 18,280,000 feet north and 5,062,000 feet east with the x-axis rotated by 36.727 degrees north of east. The model for the southern portion of the Sparta, Queen City and Carrizo-Wilcox aquifers has 112 rows and 217 columns resulting in 24,304 grid cells per layer. The model grid origin for the central portion of the Sparta, Queen City and Carrizo-Wilcox aquifers is located at Texas Groundwater Availability Model coordinate system 18,977,220 feet north and 5,382,716 feet east with the x-axis rotated by 58° north of east. The model for the central portion of the Sparta, Queen City and Carrizo-Wilcox aquifers has 177 rows and 273 columns for a total of 48,321 grid cells in each layer. The models comprise eight model layers that were cropped to the outcrop or down-dip boundary to delineate the active grid cells. Cells west of the Rio Grande are also considered inactive as the river is assumed to represent a regional groundwater flow divide. Each layer includes a different number of active cells depending on the extent of the corresponding formation.

The implemented layers dip towards the gulf from the outcrop and represent the Sparta, Queen City and Carrizo-Wilcox aquifers as well as the intervening Weches and Reklaw aquitards. IBOUND indices are assigned per model layer, with layer 1 corresponding to the Sparta Aquifer and layer 8 to the Lower Wilcox. Cells representing the outcrop of a formation are assigned the IBOUND value of the corresponding formation layer.

The models take into account available information on the structure, hydrostratigraphy and hydraulic properties of the formations, as well as flows relevant to interaction with surface water, recharge and evapotranspiration estimates at the outcrop and discharge caused by pumping. The Queen City and Sparta aquifers Groundwater Availability Models have been used for transient as well as steady-state simulations. Model runs in the current work scope restrict to steady-state conditions, and boundary conditions for use in the transect models will be extracted from the steady-state models for the Sparta, Queen City and Carrizo-Wilcox aquifers. The boundary conditions in the models for the Sparta, Queen City and Carrizo-Wilcox aquifers are categorized into specified head conditions (Dirichlet), specified flow (Neumann) and head-dependent flow conditions (Cauchy). The bottom of layer 8 (Lower Wilcox) is assigned a no-flow boundary condition representing the marine shales of the Midway Formation. No-flow boundaries are also assigned to the down-dip and lateral boundaries, as well as the lateral boundary of the model for the southern portion of the Sparta, Queen City and Carrizo-Wilcox aquifers that coincides with the Rio Grande. In down-dip portions of the model where the Cook Mountain Formation or Yegua-Jackson Aquifer overlie the Sparta Aquifer, these sediments are represented by a general head boundary condition (Cauchy) based on harmonic averages of hydraulic conductivities of the overlying hydrostratigraphic units (Galloway and others, 1994) and water table estimates.

Surface water bodies are implemented as head-dependent flow boundary conditions using the stream-routing package (Prudic, 1988) and the reservoir package (Fenske and others, 1996). Precipitation-based recharge was determined based on functions between precipitation and recharge corrected by scaling factors accounting for topography and geology. Evaporation was estimated using a Soil-Water Assessment Tool (SWAT, USDA Agricultural Research Service) and implemented as a head-dependent flow boundary with the evapotranspiration package of MODFLOW. Pumping discharge was implemented as a cell dependent specified flow boundary. A qualitative profile of the stratigraphic units and boundary conditions taken into account in the models is given in Figure 8-6 (from Kelley and others, 2004). A more detailed description is given in the groundwater model availability report for the Sparta, Queen City and Carrizo-Wilcox aquifers submitted to the TWDB.

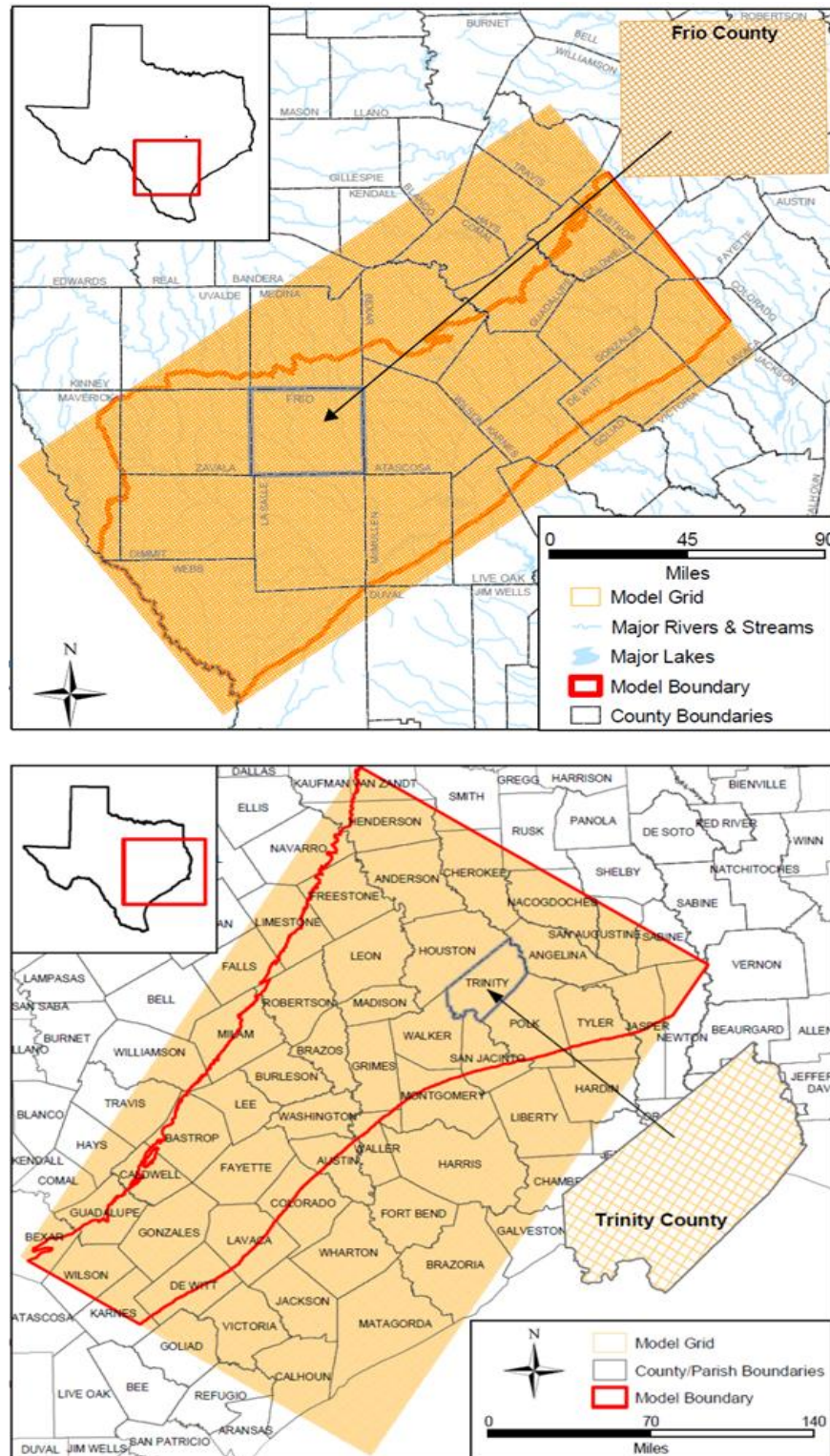


Figure 8-5. Spatial grid plan-views and model boundaries of the Groundwater Availability Models for the southern portion of the Sparta, Queen City and Carrizo-Wilcox aquifers (top) and central portion of the Sparta, Queen City and Carrizo-Wilcox aquifers (bottom) (Kelley and others, 2004).

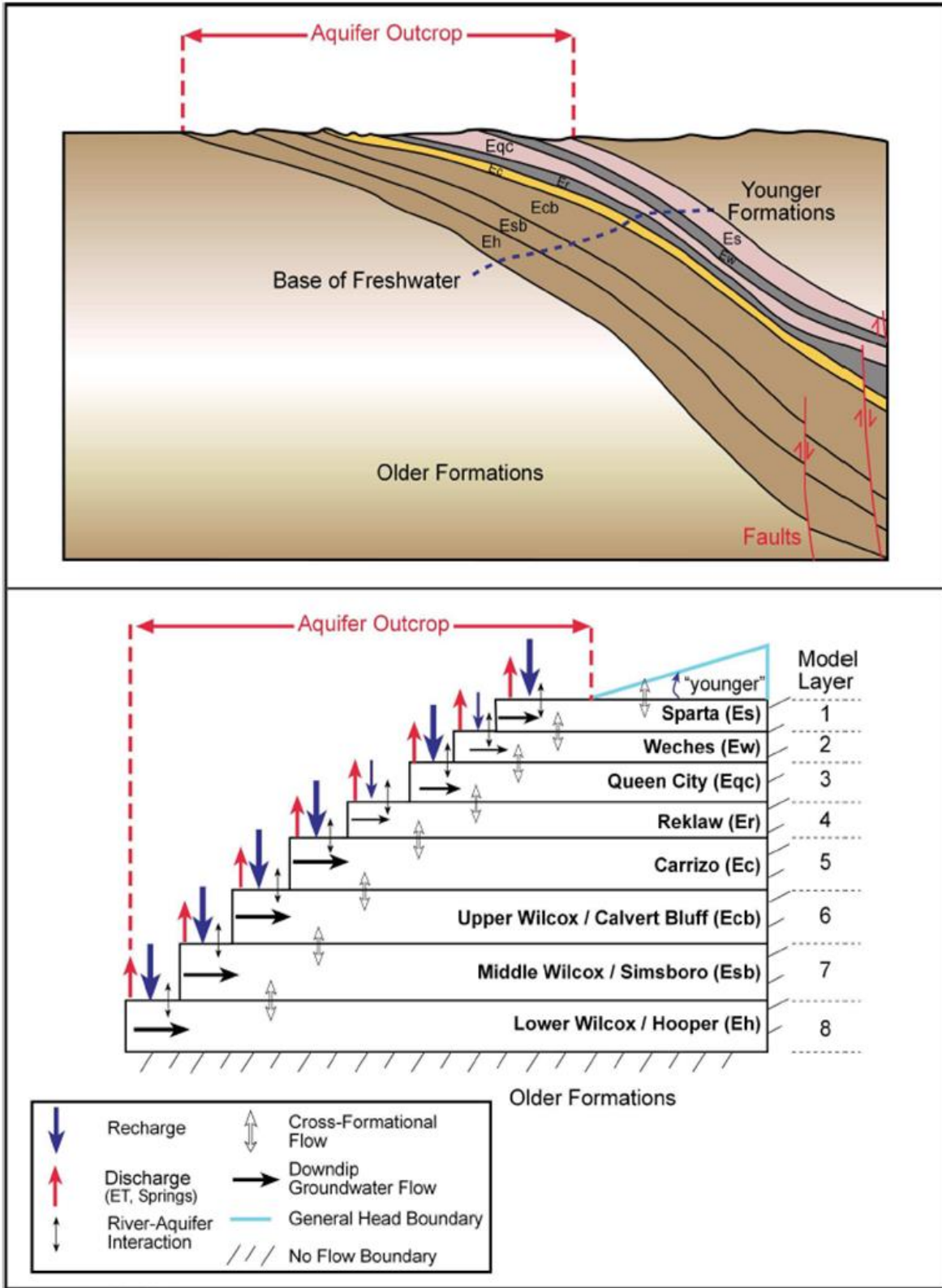


Figure 8-6. Qualitative profile and model conceptualization of the Groundwater Availability Models for the Sparta, Queen City and Carrizo-Wilcox aquifers (from Kelley and others, 2004).

## 8.2 Model Extraction and Design

The conceptual models of the Yegua-Jackson, Queen City, Sparta and Carrizo-Wilcox aquifers described in Section 8.1 are herein combined in two-dimensional transect models comprising the units from the top of the Catahoula Formation through the bottom of the Lower Wilcox. Two locations are selected to delineate the transect models as shown in Figure 8-7. The two transects are oriented almost parallel to dip towards the gulf of the formations at their respective locations. Layering and hydraulic properties from the three-dimensional models are extracted to the two-dimensional transects. Any faults within the three-dimensional models are ignored in the two-dimensional transects because the lateral flow around the faults cannot be easily converted to a two-dimensional model. The exclusion of the faults would tend to underestimate the degree of resistance to downdip flow and underestimate simulated groundwater ages.

The first transect, referred to as the Gonzales Transect Model, spans from the Lower Wilcox outcrop in Guadalupe County to the down-dip edge of the Yegua-Jackson Aquifer Groundwater Availability Model near the coast. The exact coordinates of the first and last grid cell along the Gonzales Transect are given in Table 8-2. The intersection of the transect line with the Yegua-Jackson, Sparta, Queen City and Carrizo-Wilcox aquifers outcrop is entirely located within the Guadalupe River basin and within the boundaries of Guadalupe County and Gonzales County. The model outcrop is therefore located in the transition between the Subtropical Humid climate zone and the Subtropical Subhumid climate zone (TDWR, 1983).

The second transect, referred to as the Central Transect Model, is roughly parallel to the first transect and spans from the Lower Wilcox outcrop in Burleson County to the down-dip edge of the Yegua-Jackson Aquifer Groundwater Availability Model. The exact coordinates of the first and last grid cell of the Central Transect Model are given in Table 8-2. The selected transect line intersects the Yegua-Jackson, Sparta, Queen City, Carrizo-Wilcox aquifer outcrops entirely within the Brazos River basin and within the boundaries of Milam County and Burleson County.

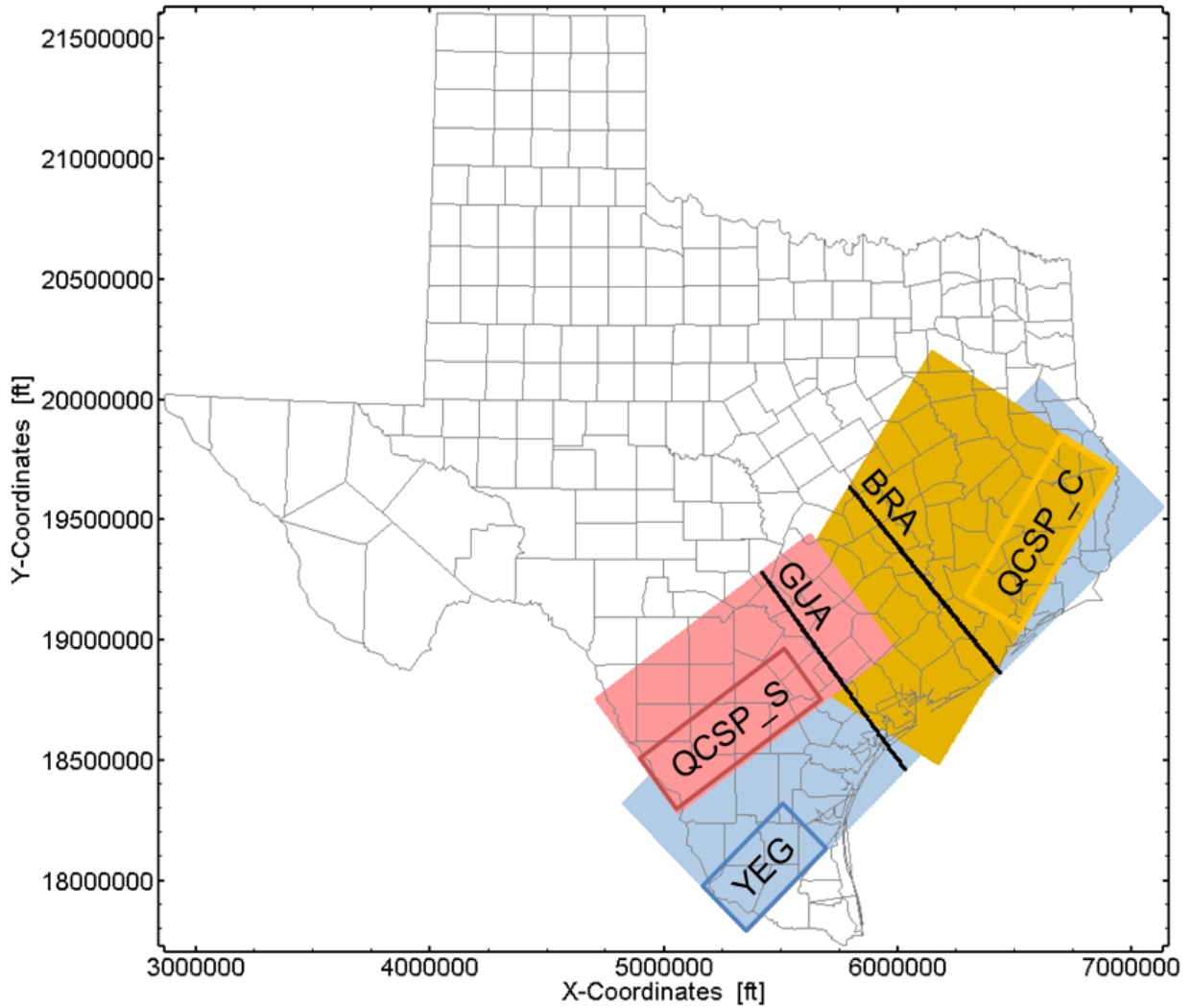


**Figure 8-7.** Locations of the Gonzales (GUA) and Central Transect (BRA) lines compared to three-dimensional spatial grid plan-views of the Groundwater Availability Model for the Yegua-Jackson Aquifer (YEG), southern portion of the Sparta, Queen City and Carrizo-Wilcox aquifers (QCSP\_S) and central portion of the Sparta, Queen City and Carrizo-Wilcox aquifers (QCSP\_C) (coordinates in Groundwater Availability Model projection).

**Table 8-2.** Locations of the first grid cell at the outcrop and last grid cell at the down-dip boundary in the two transect lines at Texas Groundwater Availability Model coordinates.

	First grid cell coordinates (outcrop)		Last grid cell coordinates (down-dip boundary)	
	X1	Y1	X2	Y2
Guadalupe	5418805	19280711	6033206	18462035
Brazos	5794543	19631806	6438543	18863134

### **8.2.1 Development of the Gonzales Transect Model**

The Gonzales Transect Model model is constructed by combining the hydrostratigraphic units as represented in the models of the Yegua-Jackson Aquifer and the southern portion of the Sparta, Queen City and Carrizo-Wilcox (Figure 8-4 and Figure 8-6). Model cells from the three-dimensional models are cropped out using the Gonzales Transect Model line (Figure 8-8). The line is parallel to the y-axis of the model for the southern portion of the Sparta, Queen City, and Carrizo-Wilcox aquifers, thus the corresponding single row of model cells is selected. Consequently, cells of all 8 layers corresponding to the selected row are extracted to construct a cross-section of the model for the southern portion of the Sparta, Queen City, and Carrizo-Wilcox aquifers. On the other hand, the Yegua-Jackson Aquifer Groundwater Availability Model orientation is rotated with respect to the Gonzales Transect Model line, therefore grid cells are selected based on the minimum distance to the transect. The extracted Yegua-Jackson Aquifer cross-section therefore combines cells from several rows extended to the 5 layers of the model.

The cross-sections extracted from the Yegua-Jackson Aquifer and Queen City and Sparta aquifers models are illustrated in Figure 8-9. It is observed that the bottom of the Yegua-Jackson Aquifer cross-section and the top of the Queen City and Sparta aquifers cross section do not coincide, as the Cook Formation aquitard separating the Yegua-Jackson and Sparta aquifers is missing. In order to merge the cross-sections into a unified transect model, the Cook Mountain Formation has been implemented assuming it has a thickness equal to the distance between the bottom of the Yegua-Jackson Aquifer and the top of the Queen City and Sparta aquifers cross-section. Figure 8-9 additionally indicates that the deeper section of the Queen City and Sparta aquifers cross-section does not extend as far as the edge of the Yegua-Jackson Aquifer cross-section, owing to the different spatial extents of the original three-dimensional models (Figure 8-7). The layers of the Queen City and Sparta aquifers cross-section are therefore extended underneath the Yegua-Jackson Aquifer layers by keeping layer thicknesses and hydraulic properties constant and equal to those from the corresponding last cell at the down-dip edge of the cross-section. Layer elevations in the extended part are draped to the bottom of the Lower Yegua.

For the development of the transect model, an additional modification is implemented for the Yegua-Jackson outcrop. A portion of layer 1 in the Yegua-Jackson Aquifer model was used to represent the Yegua-Jackson Aquifer outcrop. After extracting the Yegua-Jackson Aquifer cross-section along the Gonzales Transect Model line the cells of the surficial layer representing the shallow flow system in the Yegua-Jackson aquifer were merged with the underlying cells of the corresponding aquifer unit. In this way, deep recharge is represented and a horizontal conductivity connects these outcrop cells with the other cells representing the same aquifer unit.

The resulting transect has in total 995 cells with 761 active cells defined by the formation boundaries according to the three-dimensional models. The distribution of model layer indexes, horizontal conductivity and leakance is shown in Figure 8-9. The two-dimensional transect model consists of 14 layers representing the Yegua-Jackson Aquifer units (Catahoula, Upper Jackson, Lower Jackson, Upper Yegua, Lower Yegua), the Cook Mountain Formation, and the the Queen City and Sparta aquifers units (Sparta, Weches, Queen City, Reklaw, Carrizo, Upper Wilcox/Calvert Bluff, Middle Wilcox/Simsboro, Lower Wilcox/Hooper).

Similarly to the original three-dimensional models, no-flow boundaries are assigned to the down-dip model boundary, as well as the bottom boundary of the transect corresponding to the bottom

of the Lower Wilcox unit (Figure 8-10). Grid cells of the modified Catahoula Formation are assigned a general head boundary condition. For this, hydraulic head and vertical conductivity values are extracted from the original Yegua-Jackson Aquifer model and assigned to the corresponding grid cells of the transect model. Surface water, precipitation-based recharge, evapotranspiration and pumping recharge are not assigned explicitly at the outcrop cells of the transect model. Instead, a net recharge is prescribed at the outcrop, corresponding to the net deep recharge that infiltrates after balancing for recharge, interaction with surface water, evapotranspiration and pumping. A more detailed analysis on the amount of net deep recharge assigned at the outcrop is presented in Section 8.3.

An overview of layer IBOUND indexes, active cells and layer averages of hydraulic properties in the Gonzales Transect Model model as well as properties assigned to the Cook Mountain layer are given in Table 8-3.

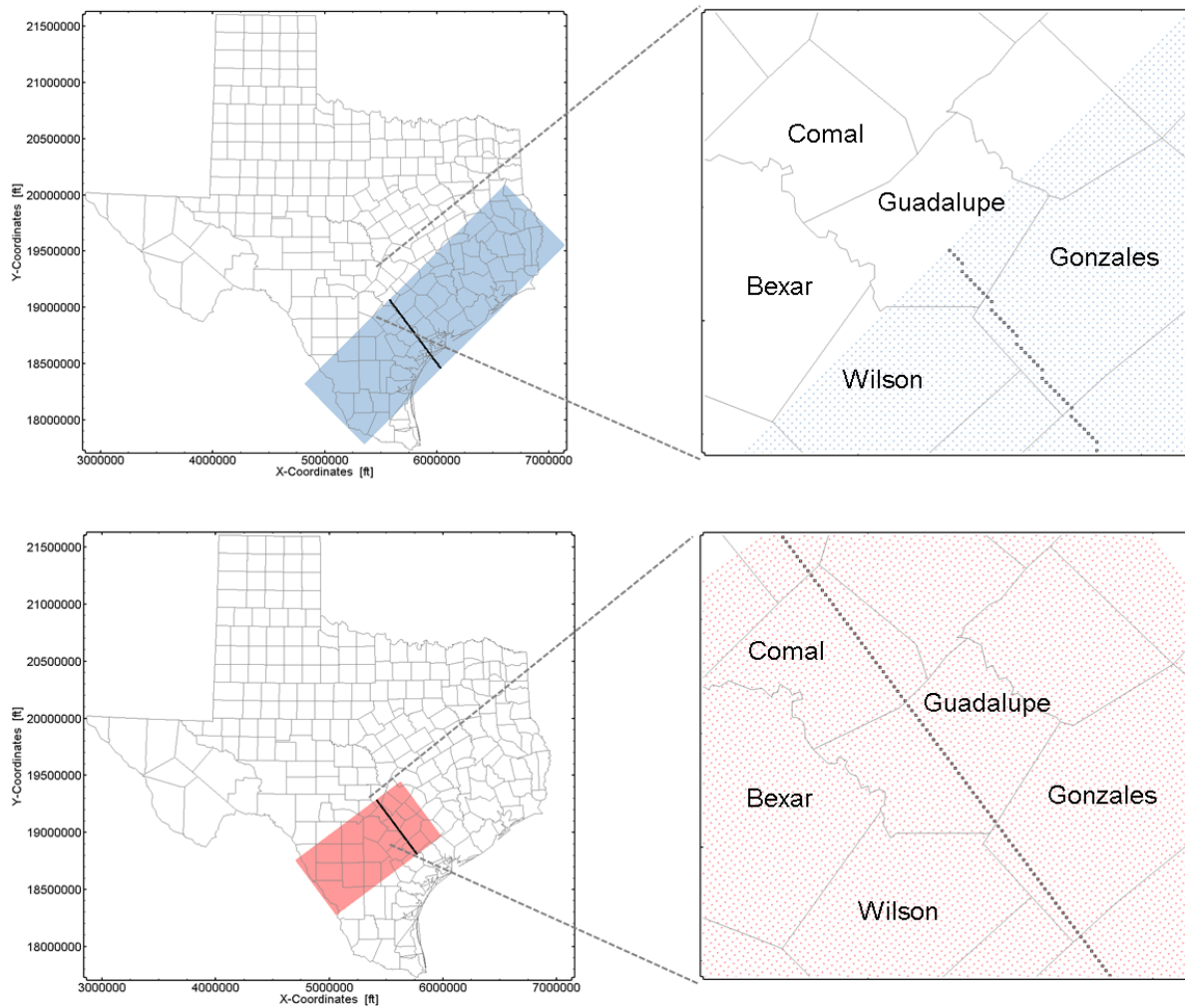


**Figure 8-8.** Extraction of the Yegua-Jackson Aquifer and Queen City and Sparta aquifers cross-sections by intercepting the Gonzales Transect Model line with the three-dimensional spatial grids used in the Yegua-Jackson Aquifer and Queen City and Sparta aquifers Groundwater Availability Models. The two cross-sections are consequently combined to create the Guadalupe transect model.

Evaluation of Hydrochemical and Isotopic Data in Groundwater Management Areas 11, 12 and 13

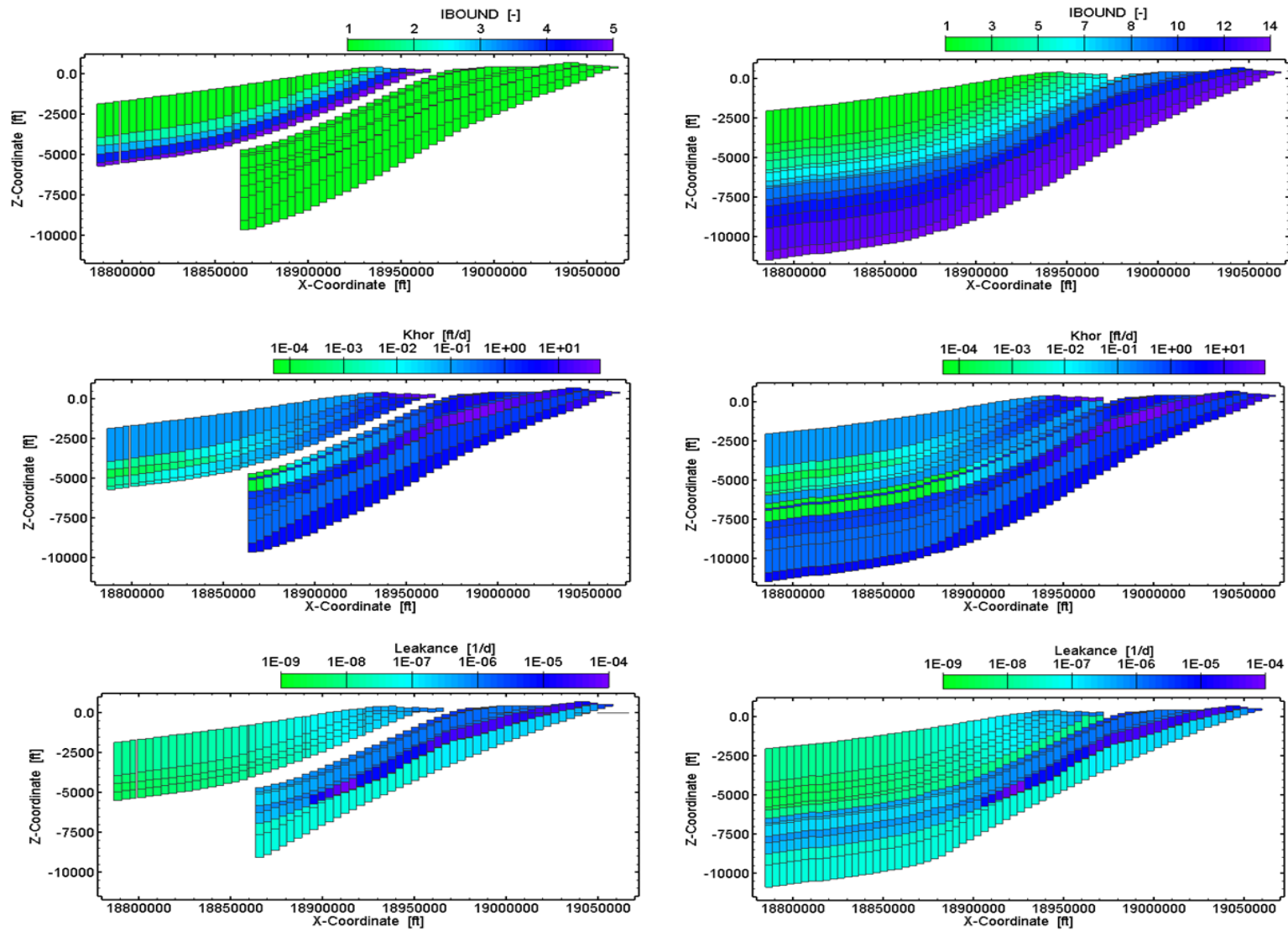


Figure 8-9. The Yegua-Jackson Aquifer and Queen City and Sparta aquifers cross-sections extracted from the three-dimensional Groundwater Availability Models (left) compared to the resulting Gonzales Transect Model model (right): distributions of layer indexes (top), horizontal conductivity (middle) and leakance (bottom).

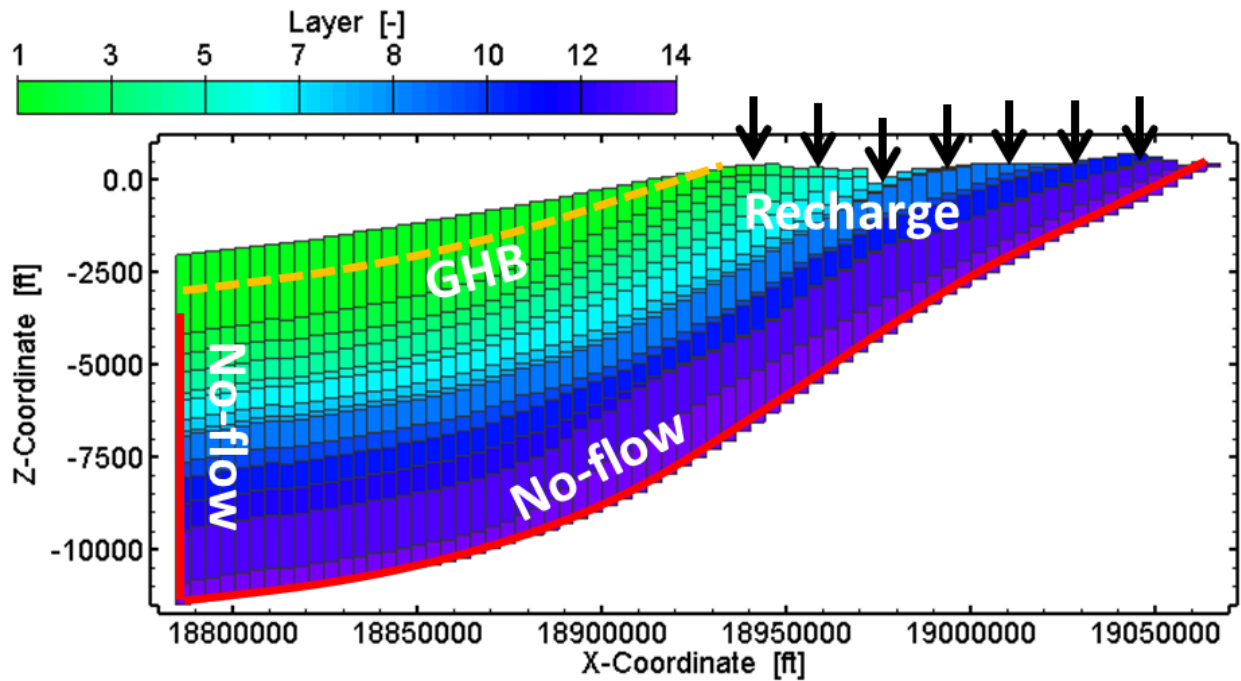


Figure 8-10. Boundary conditions used in the Gonzales Model Transect model.

Table 8-3. IBOUND indexes, number of active cells, mean layer horizontal conductivity and leakance in the Gonzales Transect Model model.

Layer	Layer in 3D model	IBOUND in 2D transect	No. of active cells in 2D transect	Mean horizontal conductivity (ft/d)	Mean leakance (1/d)
Catahoula	YEG 1	1	39	1.000E-01	3.093E-08
Upper Jackson	YEG 2	2	40	1.820E-02	2.034E-08
Lower Jackson	YEG 3	3	42	7.993E-03	1.741E-08
Upper Yegua	YEG 4	4	44	4.706E-02	1.946E-08
Lower Yegua	YEG 5	5	47	5.728E-02	2.475E-08
Cook Mountain	-	6	47	1.000E-01	1.000E-08
Sparta	QCSP_S 1	7	53	4.051E-03	8.606E-07
Weches	QCSP_S 2	8	54	1.000E+00	5.572E-07
Queen City	QCSP_S 3	9	59	9.278E-03	4.437E-07
Reklaw	QCSP_S 4	10	62	1.000E+00	9.659E-07
Carrizo	QCSP_S 5	11	67	3.470E+00	3.281E-06
Upper Wilcox	QCSP_S 6	12	67	5.474E-01	7.082E-08
Middle Wilcox	QCSP_S 7	13	68	4.819E-01	7.739E-08
Lower Wilcox	QCSP_S 8	14	72	3.426E+00	-

### 8.2.2 Development of the Central Transect Model

The Central Transect Model model is constructed using the grids and stratigraphy of the Yegua-Jackson Aquifer Groundwater Availability Model and the central portion of the Queen City and

Sparta aquifers Groundwater Availability Model (Figure 8-4 and Figure 8-6). Similarly to the previous section, the transect line is mapped on both three-dimensional grids, and the cells nearest to the line are selected in each model (Figure 8-11). These are extended to all layers in order to extract a cross-section from the Yegua-Jackson Aquifer model and a cross-section from the model for the central portion of the Sparta, Queen City and Carrizo-Wilcox aquifers. The extracted cross-sections are illustrated in Figure 8-12.

Similar to the Gonzales Transect Model model, elevation differences between the bottom of the Yegua-Jackson Aquifer and top of the Queen City and Sparta aquifers cross-section indicate the apparent extent and thickness of the Cook Mountain aquitard between the Yegua-Jackson and Sparta aquifers. A layer representing the Cook Mountain Formation is implemented between the two cross-sections in order to combine them into the Central Transect Model model.

Furthermore, as seen in Figure 8-12, the top elevations of the Sparta Aquifer cells located down-dip in the Queen City and Sparta aquifers cross-sections exceed the bottom elevations of the Yegua-Jackson Aquifer cross-section. Elevations of the 4 lowermost cell columns in the Queen City and Sparta aquifers cross-section were therefore shifted to match those of the Yegua-Jackson Aquifer bottom. Similarly to the Gonzales Transect Model model, the deeper section of the Queen City and Sparta aquifers cross-section does not reach the down-dip edge of the Yegua-Jackson Aquifer model. The Queen City and Sparta aquifers layers are extended based on the layer thicknesses of the lowermost cell column and draped under the bottom layer elevations of the Yegua-Jackson Aquifer cross-section.

Similar to the procedure followed in the development of the Gonzales Transect Model model, the cells of the surficial layer representing the shallow flow system in the Yegua-Jackson aquifer were merged with the underlying cells of the corresponding aquifer unit. In this way, deep recharge is represented and a horizontal conductivity connects these outcrop cells with the other cells representing the same aquifer unit.

Merging the two cross-sections according to this procedure yields the Central Transect Model grid that consists of 1400 grid cells out of which 1119 cells are active. The distributions of model layer indexes, horizontal conductivity and leakance are shown in Table 8-4. Similarly to the Gonzales Transect Model, the two-dimensional transect model in the Central Transect Model incorporates a total of 14 layers that include the Catahoula, Upper Jackson, Lower Jackson, Upper Yegua, Lower Yegua, Cook Mountain, Sparta, Weches, Queen City, Reklaw, Carrizo, Upper Wilcox/Calvert Bluff, Middle Wilcox/Simsboro, Lower Wilcox/Hooper units.

The boundary conditions are incorporated from the three-dimensional models and are shown in Figure 8-13. The down-dip boundary and bottom of the model corresponding to the bottom of the Lower Wilcox unit are assigned no-flow boundary conditions. A general head boundary is used for the cells of the modified Catahoula layer according to the general head boundary and vertical conductivity values extracted from the corresponding cells of the original three-dimensional Yegua-Jackson Aquifer model. The head-dependent and fixed-flow conditions of surface water bodies, precipitation-based recharge, evapotranspiration and pumping recharge are extracted from the three-dimensional models but are not transferred directly as boundary conditions at the transect outcrop. Instead a net deep recharge will be used to represent, in an averaged sense, the balance of these flows. This net recharge will be determined through calibration. An overview of IBOUND indexes for the individual formation layers, as well as the number of active cells and layer averages of hydraulic properties in the Central Transect Model model are given in Table 8-4.

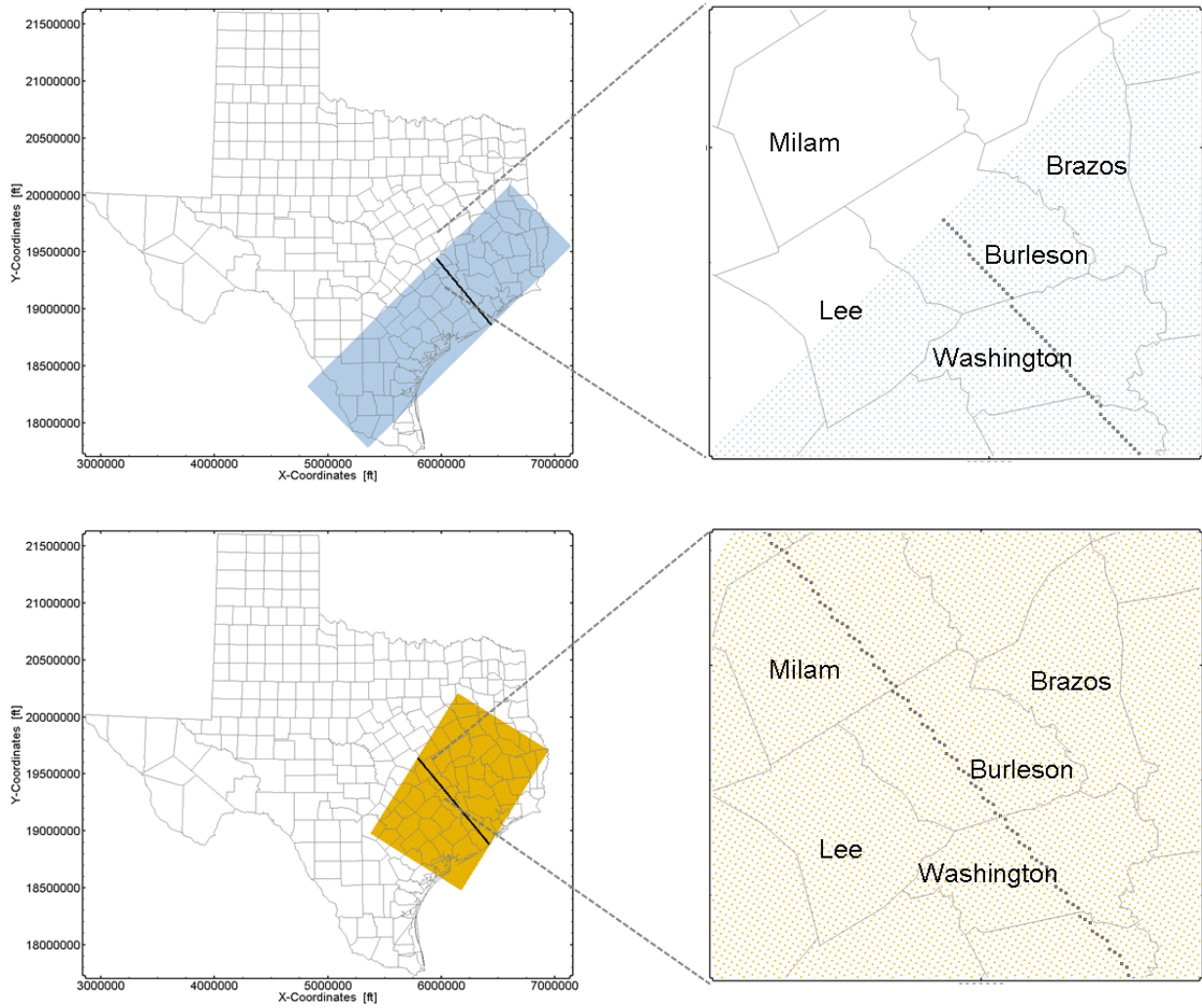


**Figure 8-11.** Extraction of the Yegua-Jackson Aquifer and the Queen City and Sparta aquifers cross-sections by intercepting the Central Transect Model line to the three-dimensional spatial grids used in the Yegua-Jackson Aquifer and the Queen City and Sparta aquifers Groundwater Availability Models. The two cross-sections are consequently combined to create the Central Transect Model model.

Evaluation of Hydrochemical and Isotopic Data in Groundwater Management Areas 11, 12 and 13

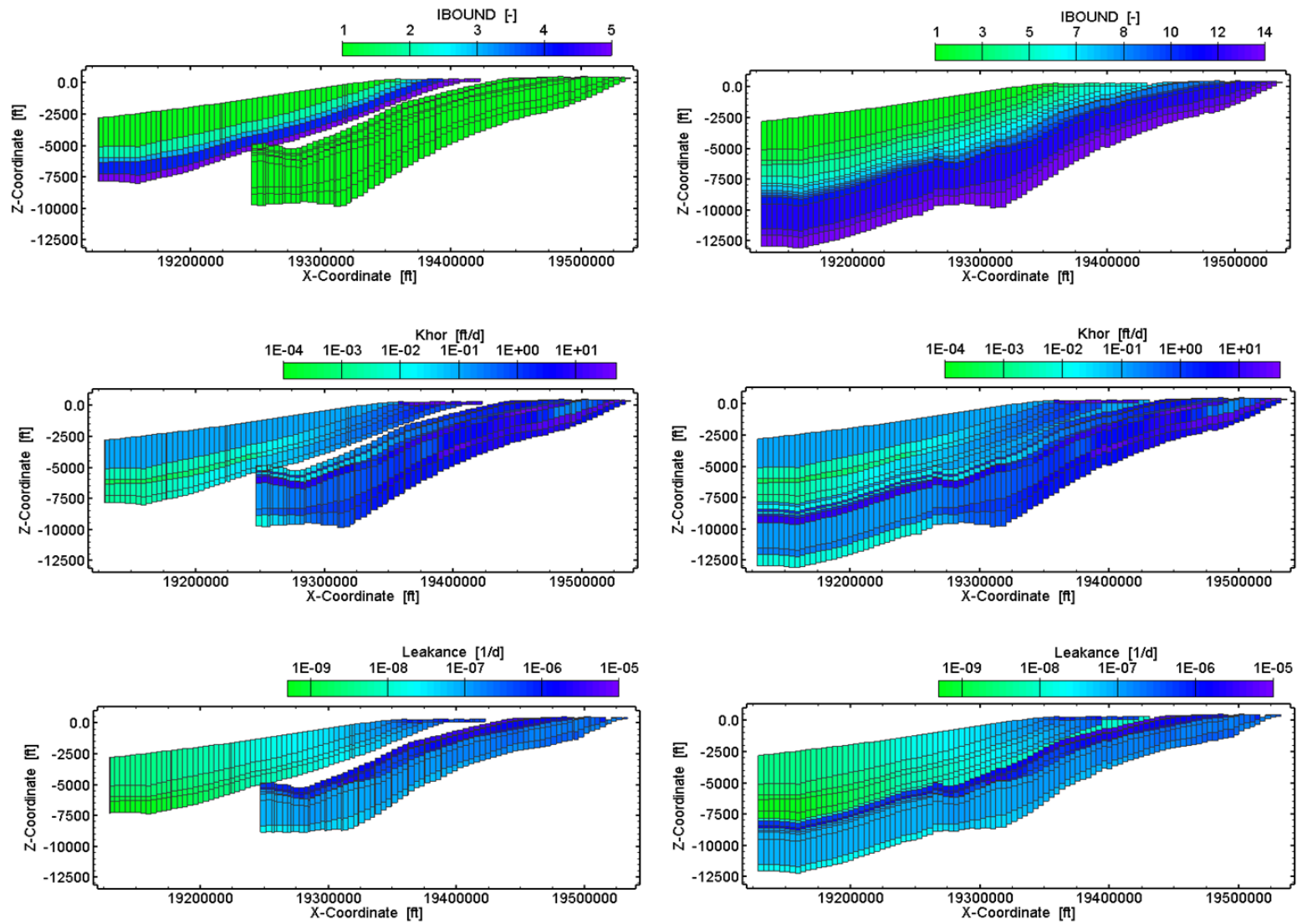


Figure 8-12. The Yegua-Jackson Aquifer and the Queen City and Sparta aquifers cross-sections extracted from the three-dimensional Groundwater Availability Models (left) compared to the resulting Central Transect Model model (right): distributions of layer indexes (top), horizontal conductivity (middle) and leakage (bottom).

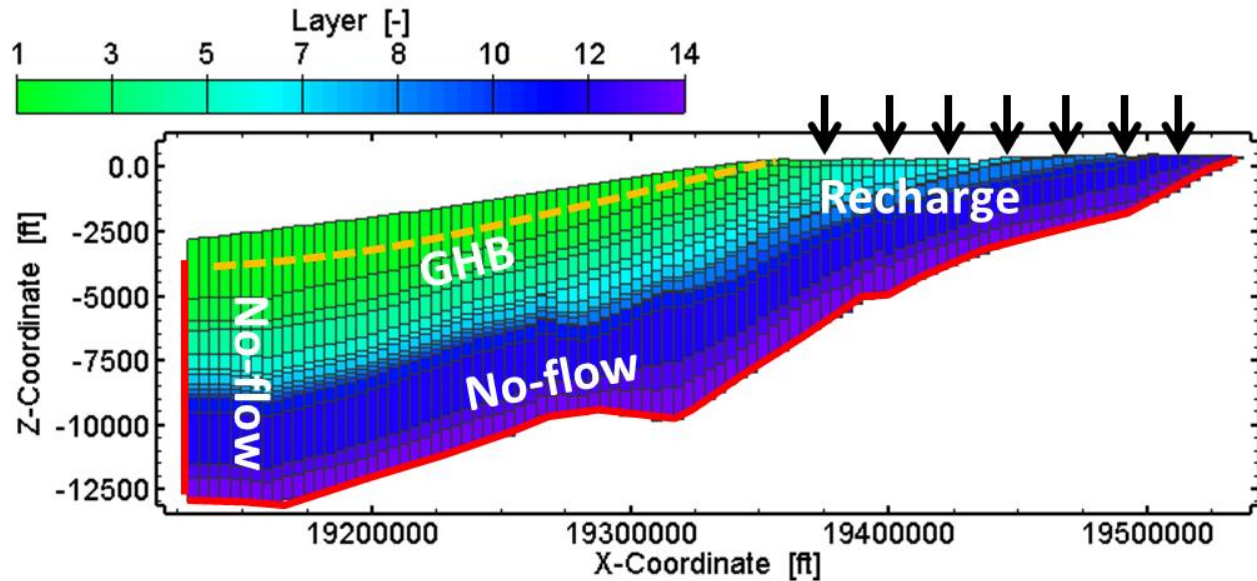


Figure 8-13. Boundary conditions used in the Central Transect Model model.

Table 8-4. IBOUND indexes, number of active cells, mean layer horizontal conductivity and leakance in the Central Transect Model model.

Layer	Layer in 3D model	IBOUND in 2D transect	# of active cells in 2D transect	Mean horizontal conductivity (ft/d)	Mean leakance (1/d)
Catahoula	YEG 1	1	56	1.000E-01	1.535E-08
Upper Jackson	YEG 2	2	58	2.197E-02	1.219E-08
Lower Jackson	YEG 3	3	61	1.262E-02	8.979E-09
Upper Yegua	YEG 4	4	65	6.203E-02	8.891E-09
Lower Yegua	YEG 5	5	72	6.796E-02	1.236E-08
Cook Mountain	-	6	74	1.000E-01	1.000E-8
Sparta	QCSP_C 1	7	81	1.170E-01	1.310E-06
Weches	QCSP_C 2	8	84	1.000E+00	1.747E-06
Queen City	QCSP_C 3	9	89	1.490E-01	4.769E-07
Reklaw	QCSP_C 4	10	91	1.000E+00	4.799E-07
Carrizo	QCSP_C 5	11	92	6.973E+00	1.176E-07
Upper Wilcox	QCSP_C 6	12	97	5.375E-01	1.279E-07
Middle Wilcox	QCSP_C 7	13	99	2.009E+00	6.047E-08
Lower Wilcox	QCSP_C 8	14	100	3.452E-01	-

### 8.3 Modeling Approach

The three-dimensional groundwater models for the Yegua-Jackson, the Sparta and the Queen City aquifers provided predictions of a steady-state head distribution based on available data and estimates of hydraulic properties, recharge, discharge, evapotranspiration, and exchange with surface water bodies. These model variables vary through the entirety of the three-dimensional model domains. Therefore the hydraulic heads predicted by the models may vary depending on local boundary conditions and hydraulic properties, but are also determined by the regional-scale conditions and imposed gradients. This poses a challenge for the development of representative two-dimensional transect models that can realistically capture the flow conditions and patterns prevailing in the three-dimensional system. Despite the fact that hydraulic properties may be

transferred directly to a two-dimensional model based on the stratigraphy at the transect location, this does not necessarily apply for boundary conditions and inputs of fluxes such as recharge. For example, a two-dimensional transect model may not intercept a nearby local stream that recharges the aquifers and therefore affects the hydraulic heads in the area. Therefore, developing a representative local-scale two-dimensional modeling approach requires the incorporation of calibrated boundary conditions that re-produce the hydraulic heads predicted by the regional-scale three-dimensional models at the location of interest.

To demonstrate these effects, an analysis of mass balance in the outcrop is performed using flows extracted from steady-state simulations of the Yegua-Jackson, Queen City and Sparta aquifers Groundwater Availability Models and are presented in this section. Two areas are selected for the analysis of the Gonzales and Central Transect Model locations bounded by the Guadalupe River basin and the Brazos River basin, respectively. The areas are delineated based on the river basin boundaries as shown in Figure 8-14. Consequently they are cropped such that they encompass the Yegua-Jackson Aquifer as well as the Sparta, Queen City and Carrizo-Wilcox aquifers outcrop. The Yegua-Jackson Aquifer and Queen City and Sparta aquifers outcrops in the investigated areas are shown in Figure 8-15. Steady-state flows for the Yegua-Jackson Aquifer and southern portion of the Queen City and Sparta aquifers model cells within the delineated area for Gonzales Transect Model, and the Yegua-Jackson Aquifer and central portion of the Queen City and Sparta aquifers model cells within the delineated area for the Central Transect Model are used to derive the following data:

- Net deep recharge at the outcrop, corresponding to the net result after balancing recharge, stream leakage (corresponding to mass exchange with surface water bodies), evapotranspiration and drains (corresponding to pumping) at the outcrop cells.
- Vertical flow from outcrop cells into underlying cells connected to the bottom of the outcrop cells.
- Transverse lateral flow between lateral faces of the outcrop cells and lateral faces of non-outcrop cells of the formations within the delineated areas.
- Transverse lateral flow between lateral faces of outcrop cells located inside the delineated basin area and lateral faces of cells located outside it.

A qualitative illustration of this procedure is given in Figure 8-16. The flow values extracted from the steady-state simulations are listed in Table 8-5. In a first approach, one may consider the net recharge (Figure 8-16) as an appropriate measure for quantifying a fixed flow boundary condition at the outcrop of the transect model. Based on a simplified approach, the total net recharge in the outcrop across the basin may be scaled to the area covered by the outcrop cells of the two-dimensional transect model. For the investigated area within the Guadalupe River basin, the total net recharge at the outcrops equals 10,660 ft<sup>3</sup>/d and -804,200 ft<sup>3</sup>/d for the Yegua-Jackson Aquifer and the Queen City and Sparta aquifers outcrop, respectively. The direction of flow is considered positive downwards, so that a positive value indicates recharge and a negative value indicates discharge. Scaled to the area of the transect outcrop this yields 175.4 ft<sup>3</sup>/d and -11,910 ft<sup>3</sup>/d for the Queen City and Sparta aquifers and Yegua-Jackson Aquifer, respectively. The analysis of the Brazos River basin bounds a significantly larger area, yielding a total net recharge of 2,760,000 ft<sup>3</sup>/d and -965,300 ft<sup>3</sup>/d for the Yegua-Jackson Aquifer and the Queen City and Sparta aquifers outcrop, respectively. Scaled to the outcrop area of the Central Transect

Model model this corresponds to 22,680 ft<sup>3</sup>/d and -13,140 ft<sup>3</sup>/d for the Yegua-Jackson Aquifer and the Queen City and Sparta aquifers, respectively.

The differences in net recharge between the Yegua-Jackson Aquifer and Queen City and Sparta aquifers parts of the outcrop within the same river basin, as well as between the Guadalupe and the Brazos River basins indicate that the flow regime in the investigated areas cannot be described with a simplified extrapolation of net recharge infiltrating or discharge exfiltrating vertically through the outcrop. Indeed, the values of lateral flows given in Table 8-5 indicate that these constitute a significant part of the total mass balance. Transverse lateral flow between outcrop and non-outcrop cells is larger than net recharge by an order of magnitude in the southern portion of the Queen City and Sparta aquifers Groundwater Availability Model. Similarly, transverse lateral flow into the outcrop through the basin boundaries is of the same magnitude as the net recharge in the Yegua-Jackson Aquifer Groundwater Availability Model. Consequently this is depicted in the values of vertical flow from the outcrop cells to the formation cells below them, resulting in flows infiltrating the formations significantly different from the net recharge calculated at the outcrops (Table 8-5). The hydraulic heads extracted from the three-dimensional models at the cross-sections are thus significantly influenced by the lateral flows through the cross-sections. A validation of this effect on a local scale for the extracted cross-sections would confirm that hydraulic heads and flow patterns in the extracted cross-sections cannot be consistently re-produced by recharge locally assigned at the cross-section outcrop cells. This is demonstrated by extracting flows from the three-dimensional model along the transects. Figure 8-17 shows the amount of lateral flow through the lateral face of the southern and central portion of the Queen City and Sparta Aquifers cross-sections (1,200,000 ft<sup>3</sup>/d and 1,600,000 ft<sup>3</sup>/d, respectively) compared to flow leaving the Queen City and Sparta aquifers vertically through the general head boundary imposed at the Sparta Formation cells along the transects (23,000 ft<sup>3</sup>/d and 23,000 ft<sup>3</sup>/d, respectively). Lateral flow across the model face exceeds vertical outflow through the boundary by two orders of magnitude, indicating that the hydraulic head distribution in the transects cannot be consistently described by the local distribution of net recharge alone.

To compensate for the conceptual differences between flow patterns in the two-dimensional and the three-dimensional models, net recharge at the outcrops of the transect models is replaced by calibrated recharge values. Calibration is therefore the first step of the current modeling approach. Calibrated recharge corresponds to the net deep recharge infiltrating the model cells through the outcrops after balancing for recharge, discharge, surface water interaction, evapotranspiration and pumping. In the calibration approach used here, recharge at the Yegua-Jackson Aquifer outcrops was varied separately from recharge at the Sparta, Queen City and Carrizo-Wilcox aquifer outcrops. Additionally to recharge, vertical conductivity (described with leakance in the MODFLOW model) of the Cook Mountain Formation was calibrated. As described previously, this formation is an aquitard acting as a confining layer between the Yegua-Jackson and the Sparta aquifers. It therefore defines the hydraulic connection between the Yegua-Jackson Aquifer, the Queen City and Sparta aquifers and determines the resulting hydraulic heads across the transect model domain for a given amount of recharge. As mass exchange between the Yegua-Jackson Aquifer, Queen City and Sparta aquifers parts of the transects occurs mainly through flow in the vertical direction, leakance is the parameter determining the degree of confinement between the two systems. The Cook Mountain Formation was not included explicitly in the three-dimensional Yegua-Jackson Aquifer, the Queen City and Sparta aquifers models, thus leakance needs to be considered as a calibration parameter. The

method used for the calibration is manual calibration, also referred to as the “trial-and-error” method. The objective of the calibration approach was to adjust recharge at the outcrops and leakance of Cook Mountain Formation layer in order to improve the overall agreement of predicted head values to those from the three-dimensional models. However the calibration approach indicated the following common aspects for both transects:

- Layers 7 through 14, representing the units of the Queen City and Sparta aquifers cross-section (Sparta, Weches, Queen City, Reklaw, Carrizo, Upper Wilcox, Middle Wilcox and Lower Wilcox) are characterized by an almost uniform distribution of hydraulic heads. The range of hydraulic head differences throughout the entire extent of these layers is typically in the order of 10 feet. Consequently, hydraulic heads in the Queen City and Sparta aquifers layers respond with a uniform increase or decrease to any change of recharge and/or leakance of the Cook Mountain Formation. In general, an increase of recharge introduces a uniform shift of hydraulic heads to higher values. Whether this increase further propagates into the Yegua-Jackson Aquifer cells is determined by the leakance of the Cook Mountain Formation.
- Hydraulic heads in layers 1 through 5, representing the units of the Yegua-Jackson Aquifer cross-section (Catahoula, Upper Jackson, Lower Jackson, Upper Yegua and Lower Yegua) are strongly influenced by the general head boundary condition prescribed in the Catahoula. Furthermore, with increasing vicinity to the Cook Mountain Formation, hydraulic heads in Yegua-Jackson Aquifer cells are affected by heads in the Queen City and Sparta aquifers. Cells located in the Yegua-Jackson Aquifer layers are strongly influenced by inflow coming from the Queen City and Sparta aquifers layers, typically demonstrating hydraulic heads converging to those in the Queen City and Sparta aquifers. In general, increases of recharge introduce increases in hydraulic heads. Leakance of the Cook Mountain Formation is the parameter that determines whether a change in the Yegua-Jackson Aquifer hydraulic heads propagates into the Queen City and Sparta aquifers layers.
- As a confining layer between the Yegua-Jackson Aquifer and the Queen City and Sparta aquifers layers of the transect, the Cook Mountain Formation unit limits the exchange of fluxes between these. If the Cook Mountain Formation unit is considered to have a very low leakance, any increase in recharge at the Queen City and Sparta aquifers outcrop results in significant uniform increase of hydraulic heads in layers 7 through 14. On the other hand, increasing the leakance of the Cook Mountain Formation unit allows vertical cross-formational flow, so that increases of recharge at the Queen City and Sparta aquifers outcrop can cause an increase of hydraulic heads further into the Yegua-Jackson Aquifer part of the transect. A highly conductive Cook Mountain Formation unit allows hydraulic heads across the entire transect to equilibrate, with exception of heads bound to the general head boundary prescribed in the Catahoula layer.

The calibration aims to re-produce the hydraulic head distribution in an averaged sense for the Yegua-Jackson Aquifer, Queen City and Sparta aquifers rather than re-producing the detailed distribution throughout the transect. The resulting parameters fit by the calibration are given in Table 8-6.

Once calibration of recharge and Cook Mountain Formation leakance is complete, the two transect models are used to investigate sensitivity of water ages to model input parameters such as formation horizontal conductivity, leakance and recharge. Water age is determined as particle

travel time using backward particle tracking from the model cells to the outcrop. For each model layer, the input parameters were systematically decreased and increased from their calibrated values while the change in water ages was monitored. Four simulations were completed for each parameter sensitivity, where recharge was varied according to

A: (new parameter) = (old parameter) \* factor

or

B: (new parameter) = (old parameter) \* 10 ^ (factor-1)

using the factors of 0.5, 0.9, 1.1, and 1.5. Recharge was varied according to *A* while horizontal conductivity and leakance were varied according to *B*. For 3 parameters (recharge, horizontal conductivity and leakance), 4 factors and 14 model layers, this procedure results in a total of 168 runs for each transect model. However the number of runs is slightly smaller in each case, as no sensitivity analysis can be performed for parameters that are not defined for a layer (i.e., sensitivity of recharge at the Cook Mountain Formation layer is not examined as it is assumed that this formation has no outcrop). The sensitivity analysis was performed through comparison of each simulation run to a reference simulation where water ages were calculated using the calibrated input parameters. To quantify this sensitivity, the analysis was limited to water ages from selected cells of the transect models corresponding to well locations and depths with available water age measurements. For water ages derived for these selected observation points, the average was calculated and used as a comparative measure to the calculated average of the reference case.

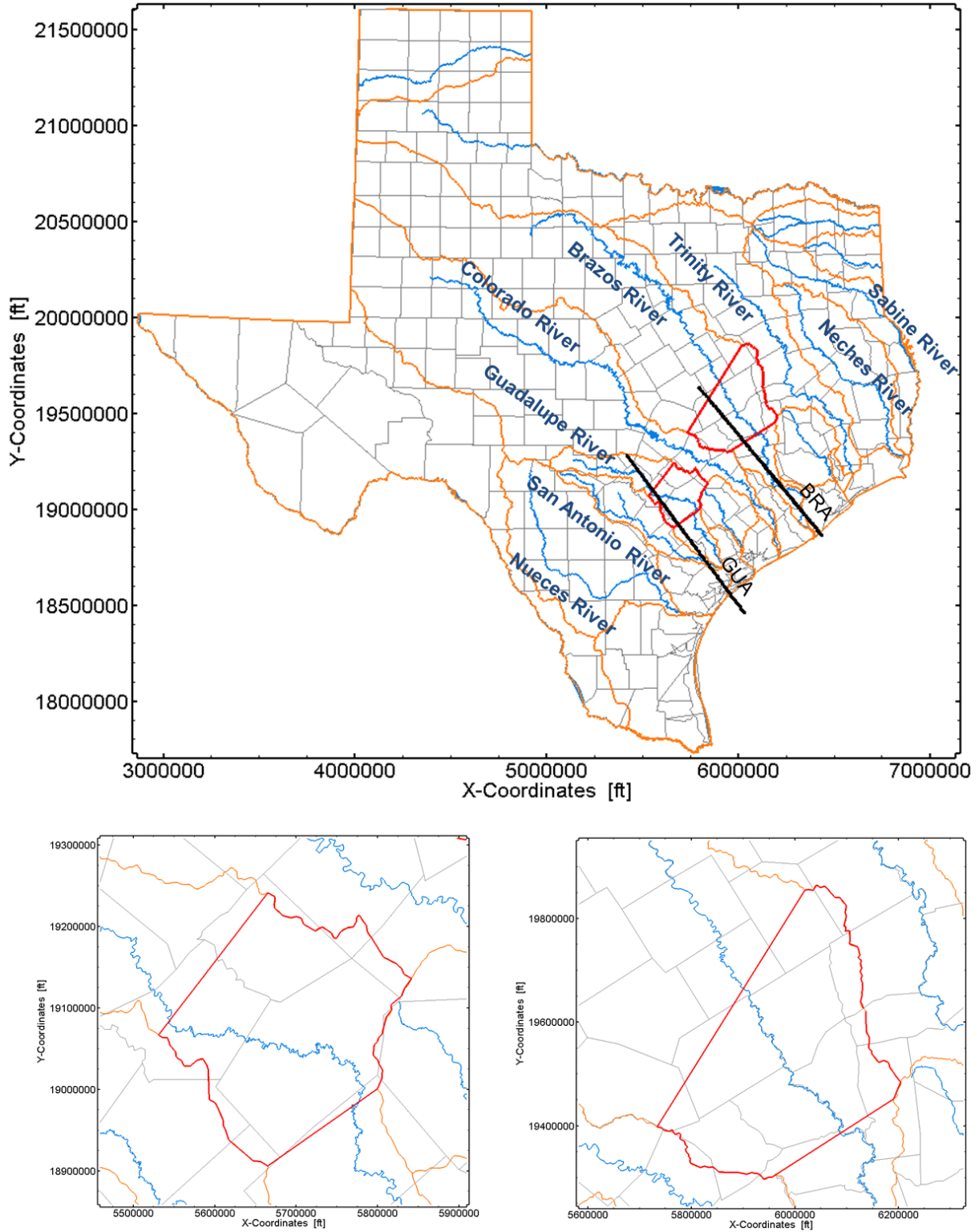


**Figure 8-14.** Delineation of areas used for the outcrop mass balance using the Guadalupe River and the Brazos River basins. The basins are subsequently cropped to the outcrop locations.

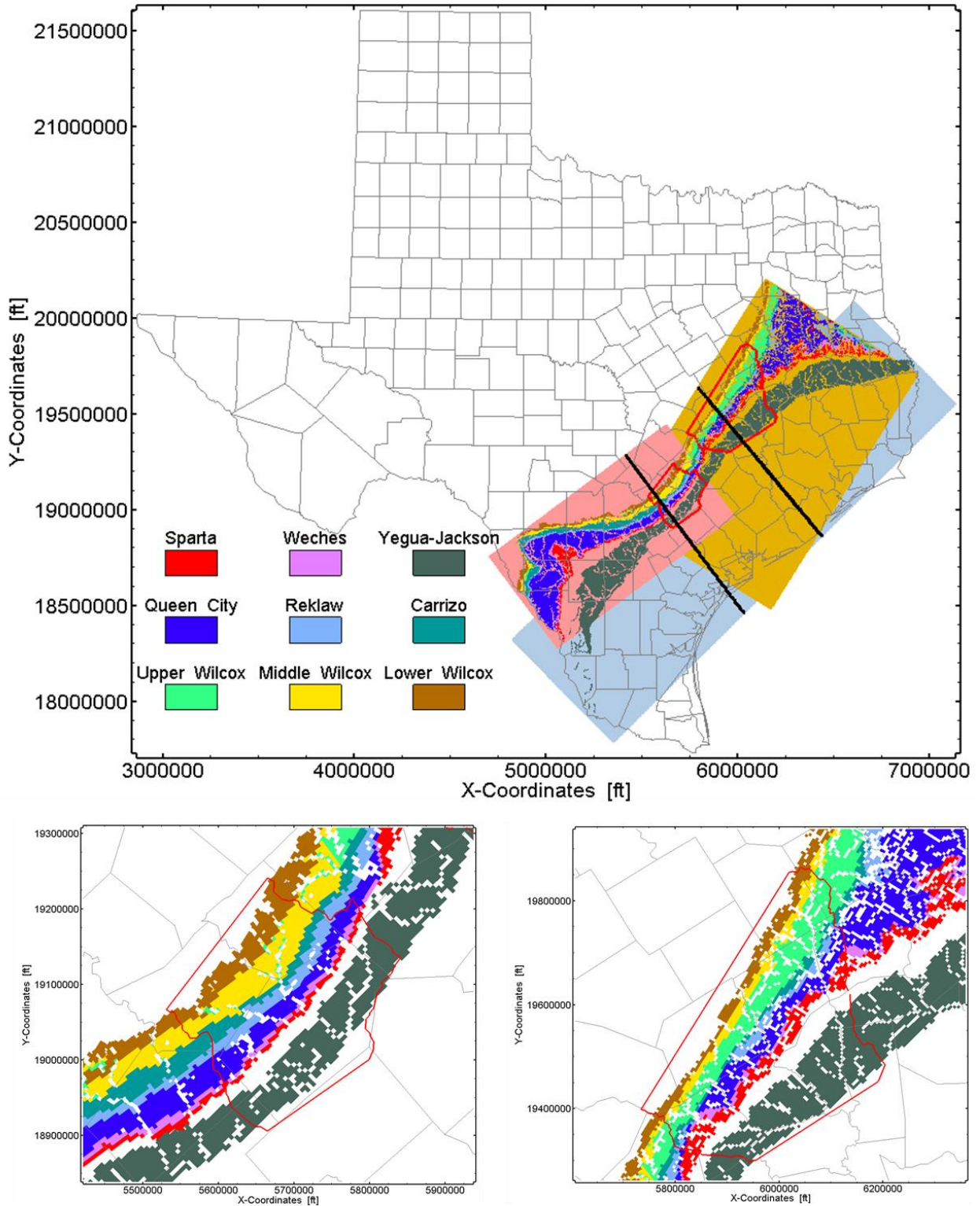


**Figure 8-15.** Formation outcrops in the Groundwater Availability Models for the Yegua-Jackson Aquifer, southern portion of the Queen City, Sparta and Carrizo-Wilcox aquifers and central portion of the Queen City, Sparta and Carrizo-Wilcox aquifers and river basins cropped to the outcrops.

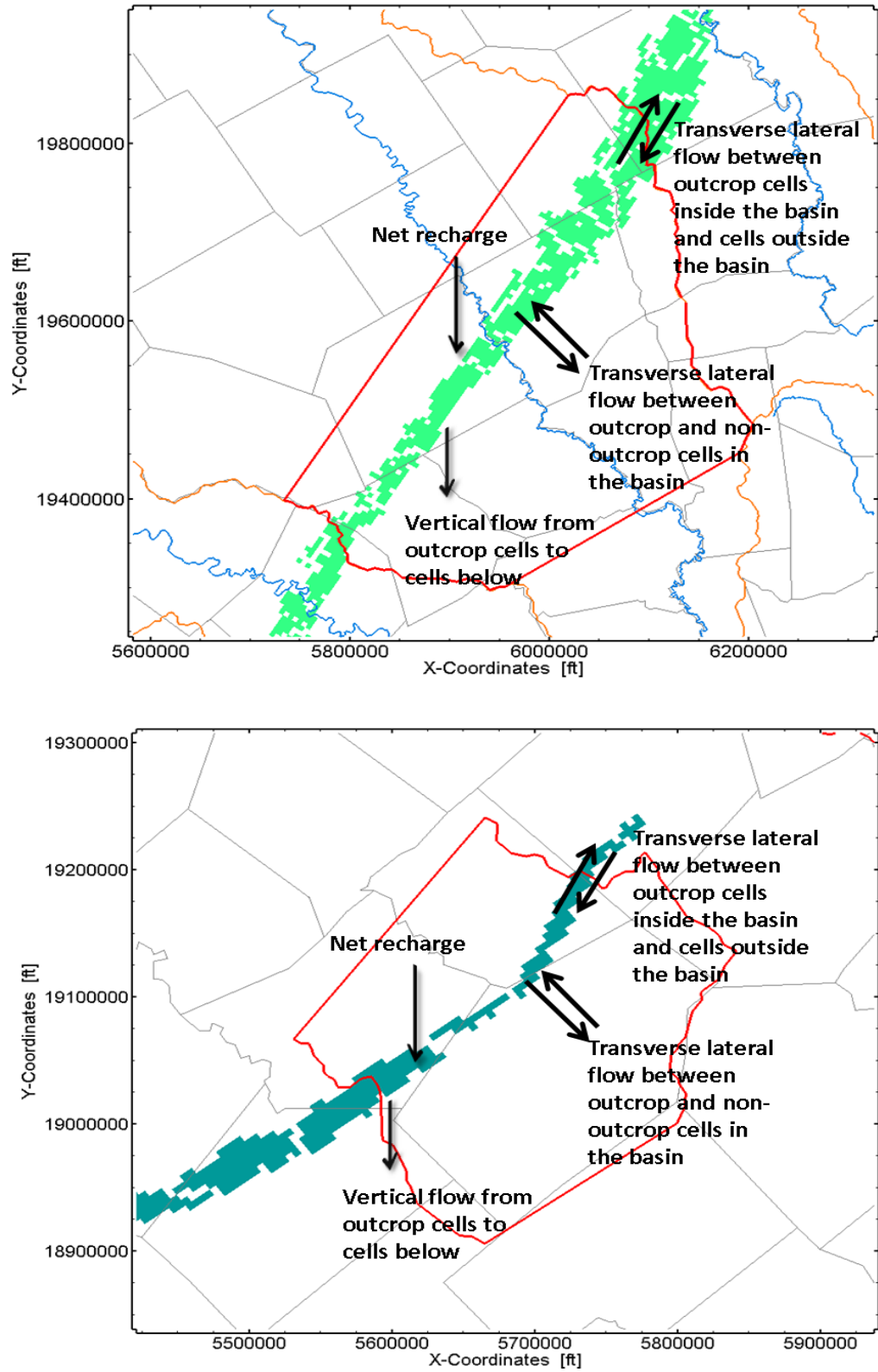


Figure 8-16. Extraction of fluxes from the Upper Wilcox outcrop in the Brazos basin area (top) and fluxes from the Carrizo-Wilcox Aquifer outcrop in the Guadalupe basin area (bottom).

**Table 8-5. Mass balance derived for the investigated areas of the Guadalupe and the Brazos River basin.**

	Guadalupe Basin		Brazos Basin	
	Southern Portion of the Queen City and Sparta Aquifers	Yegua-Jackson Aquifer	Central Portion of the Queen City and Sparta Aquifers	Yegua-Jackson Aquifer
Number of outcrop cells 2D	17	8	22	16
Number of outcrop cells 3D	1033	540	2677	1175
Net recharge [ft <sup>3</sup> /d]	1.066E+04	-8.042E+05	2.760E+06	-9.653E+05
Net recharge [ft/d]	3.701E-07	-5.342E-05	3.698E-05	-2.947E-05
Net recharge [inches/year]	1.621E-03	-2.339E-01	1.619E-01	-1.29E-01
Transverse lateral flow between outcrop and non-outcrop cells in the basin [ft <sup>3</sup> /d]	-2.903E+05	1.621E+04	-1.125E+06	5.251E+04
Transverse lateral flow between outcrop cells inside the basin and cells outside the basin [ft <sup>3</sup> /d]	3.092E+04	6.907E+05	-3.509E+05	7.605E+05
Vertical flow from outcrop cells to cells below [ft <sup>3</sup> /d]	2.654E+05	9.723E+04	-1.342E+06	1.284E+05

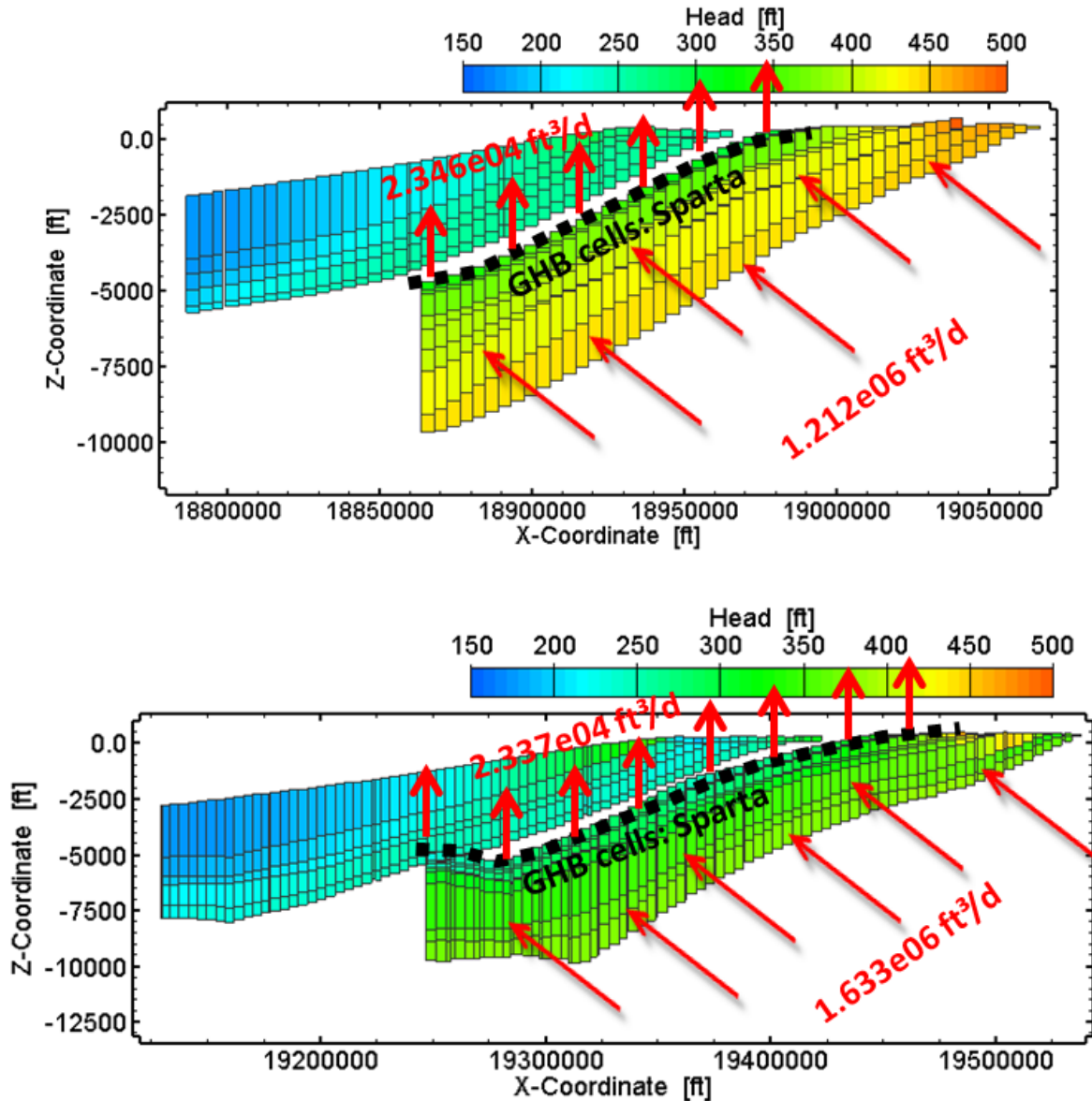


Figure 8-17. Comparison of transverse lateral flow to vertical flow through the general head boundary conditions for the models of the Sparta, Queen City and Carrizo-Wilcox aquifers in the Gonzales (top) and the central (bottom) cross-sections.

Table 8-6. Calibrated parameters for the Gonzales and the Central Transect models.

	Gonzales Transect Model	Central Transect Model
Cook Mountain Formation Leakance [1/d]	1.000E-08	4.000E-06
Cook Mountain Formation Horizontal Conductivity [ft/d]	1.000E-01	1.000E-01
Recharge Queen City and Sparta Aquifers [ft/d]	1.500E-06	5.000E-07
Recharge Queen City and Sparta Aquifers [ft³/d]	4.181E+01	1.393E+01
Recharge Yegua-Jackson Aquifer [ft/d]	5.500E-07	2.500E-07
Recharge Yegua-Jackson Aquifer [ft³/d]	1.533E+01	6.969E+00

## 8.4 Gonzales Transect Model

This section presents a discussion of the numerical simulation results using the Gonzales Transect model. The analysis begins with the steady-state flow simulations carried out with MODFLOW based on the geometry and boundary conditions. Hydraulic properties of the layered formation system are extracted from the three-dimensional models as described in Section 8.2. Net recharge at the outcrops and leakance of the Cook Mountain Formation are calibrated according to the modeling approach. The simulated hydraulic heads and flow field are consequently used for particle tracking simulations for the estimation of groundwater ages. The discussion on the particle tracking simulations is extended to the analysis of groundwater age sensitivity to input parameters.

### 8.4.1 Results of Flow Simulations

The extracted cross-sections of hydraulic heads modeled with the three-dimensional models for the Yegua-Jackson Aquifer and the southern portion of the Sparta, Queen City and Carrizo-Wilcox aquifers are shown in Figure 8-18. In general, hydraulic heads in the southern portion of the Sparta, Queen City and Carrizo-Wilcox aquifers decrease with depth within each layer, and increase layer-wise descending from the Sparta Aquifer to the Lower Wilcox. Hydraulic heads in the Sparta Aquifer range from 301 feet at the outcrop, which is also the lowest head in the entire cross-section, to 365 feet near the middle of the layer. Hydraulic heads in the Lower Wilcox are more uniform, with a minimum value of 438 feet at the down-dip edge of the model and a maximum value of 454 feet at the outcrop. The maximum head in the southern portion of the Queen City and Sparta aquifers cross-section is observed at the outcrop of the Carrizo-Wilcox Aquifer and equals 601 feet. Heads in the Yegua-Jackson Aquifer are generally lower. Hydraulic head reaches a minimum of 169 feet and a maximum of 287 feet at the down-dip end and near the outcrop of the Catahoula Formation, respectively. In the Lower Yegua, hydraulic heads decrease to 186 feet at the down-dip end and increase to 261 feet below the outcrop.

Figure 8-18 further illustrates the hydraulic head distribution modeled with the Gonzales Transect model. A main feature of the transect model results is that hydraulic heads change uniformly in the Queen City and Sparta aquifer system, affecting the Yegua-Jackson Aquifer system through the confining layer representing the Cook Mountain Formation. This feature gives a characteristic pattern of hydraulic heads sharply changing at the transition between the two systems. The calibration of recharge at the outcrop and Cook Mountain Formation leakance for the Gonzales Transect results in hydraulic heads ranging between 392 and 400 feet in the Queen City and Sparta aquifers. On the other hand, in the Yegua-Jackson Aquifer layers of the model hydraulic heads vary between 174 feet at the down-dip edge of the Catahoula Formation and 321 feet in the Lower Yegua below the outcrop (Figure 8-18). The wider range of hydraulic heads in the Yegua-Jackson Aquifer occurs due to the general head boundary condition prescribed in the cells of the Catahoula layer.

A verification exercise for the hydraulic heads predicted with the Guadalupe transect model has been carried out using head data measured in wells. Available state wells were selected from the state well database available on the TWDB website based on their location and vicinity to the Guadalupe transect line (Figure 8-19). The selected wells were consequently projected to the transect line to select the model column, and the layer corresponding to the aquifer screened in the well was selected. Only five wells were available in the vicinity of the Guadalupe transect model capturing hydraulic heads for a limited range of depths and layers. The cross-plots in

Figure 8-19 show qualitative agreement between modeled and measured hydraulic heads for these locations. However the amount and distribution of data is not sufficient for estimating the goodness of the Guadalupe transect model calibration. The modeled heads are therefore additionally evaluated through comparison to the three-dimensional models that have been calibrated using targets that span across the entire area of the investigated aquifers rather than the immediate vicinity of the Guadalupe transect.

In order to quantify the differences in results between the two models, three columns have been selected in each of the Yegua-Jackson Aquifer and the Queen City and Sparta aquifers parts near the down-dip model boundaries, the outcrop and the middle of the transect. The resulting 39 observation points are used to extract hydraulic heads for comparison between the three-dimensional and two-dimensional models. The locations of these columns and observation points (Figure 8-21) have been selected in order to provide a qualitatively representative range of hydraulic heads at different depths of the modeled formations. A detailed listing of the selected model cell IDs, simulated heads and resulting differences and relative errors in simulated heads between the two models is given in Table 8-9. Cross-plots of the extracted hydraulic heads predicted with the three-dimensional models and the Gonzales Transect model are given in Figure 8-21. The red points in the plot represent observation points in the Queen City and Sparta aquifers, whereas yellow points represent observation points in the Yegua-Jackson Aquifer. It is observed that despite a variation of hydraulic heads between 300 and 450 feet in the three-dimensional southern portion of the Queen City and Sparta aquifers model, observation points in the Queen City and Sparta aquifers layers of the transect model have an almost uniform head of 400 feet. On the other hand, hydraulic heads in the Yegua-Jackson Aquifer show a good agreement in average. Hydraulic heads in the Yegua-Jackson Aquifer provide better agreement between the two models due to the close proximity to the general head boundary prescribed at the Catahoula Formation in both models. The errors of simulated hydraulic head differences relative to hydraulic heads simulated with the transect model are illustrated versus depth in Figure 8-22. For the layers representing Catahoula Formation through Lower Yegua, it is indicated that the lowest errors occur near the surface (thus near the general head boundaries). Relative errors in the Yegua-Jackson Aquifer increase with depth and layer. For layers representing Sparta Aquifer through Lower Wilcox, Figure 8-22 illustrates that the range of hydraulic heads predicted with the transect model agree well to the heads of the Reklaw Formation in the three-dimensional model. Relative errors in the Queen City and Sparta aquifers increase with increasing distance from the Reklaw Formation.

When the hydraulic head computed for a grid cell in MODFLOW drops below its bottom elevation the cell is assumed to be dried out. The steady-state simulation using the calibrated input parameters results in drying out 1 outcrop cell of the Reklaw Formation, 2 outcrop cells of the Carrizo-Wilcox Aquifer and 2 cells of the Upper Wilcox that do not belong to the outcrop. Table 8-10 gives the number of outcrop cells per layer as well as the recharge assigned to each cell after the calibration. Red-colored fonts in the table indicate outcrop cells of layers 10 and 11 where one or more outcrop cells dry out during the simulation. The implementation in MODFLOW allows the recharge assigned to a dried-out cell to be transferred to the underlying cell. Therefore 41.81 ft<sup>3</sup>/d from the Reklaw Formation and 41.81 ft<sup>3</sup>/d from the Carrizo-Wilcox Aquifer outcrop are transferred to the outcrop of the Middle Wilcox.

Table 8-10 further gives a comparison of the total recharge assigned at the outcrop per layer compared to the total flow per layer through the bottom faces of the layer cells and through the

upper faces of the layer cells. The Lower Wilcox has a no-flow boundary of the transect model and is not assigned any recharge, therefore the current model configuration imposes conditions such that a net flow of zero occurs between the Lower and Middle Wilcox under steady-state conditions. The Middle Wilcox is assigned recharge of 125.45 ft<sup>3</sup>/d which corresponds to the same amount of total flow through the upper faces of the Middle Wilcox cells. Therefore, the steady-state condition, the inflow at the outcrop essentially flows through the Middle Wilcox and eventually moves upward through the interface to the Upper Wilcox layer. The equivalent effect is observed in each layer, with the difference between bottom and top vertical flows balancing the recharge at the layer outcrop. Vertical flow therefore accumulates the imposed recharge in each layer that finally discharges 833.56 ft<sup>3</sup>/d through the general head boundary prescribed at the Catahoula. This flow pattern is essentially driven by the boundary conditions that impose inflow at the outcrop, no-flow conditions at the bottom and the down-dip edge of the model and finally a head-dependent flux at the top layer. Table 8-10 indicates that the amount of flow through the Cook Mountain Formation unit in the Gonzales Transect model is 710.9 ft<sup>3</sup>/d. The top boundary condition in the three-dimensional southern portion of the Queen City and Sparta aquifers model was a general head boundary assigned to the top layer of the model that corresponded to the Sparta Aquifer. Extracting the corresponding flow through the general head boundary in the Queen City and Sparta aquifers cross-section used for the construction of the transects results 23,460 ft<sup>3</sup>/d of vertical flow leaving the model domain through the Sparta Aquifer. On the other hand, the bottom of the original Yegua-Jackson Aquifer model corresponded to a no-flow boundary prescribed at the Lower Yegua layer. Thus no vertical flow was allowed in and out of the domain through the bottom boundary of the cross-section. In the transect model, these mutually exclusive boundary conditions are compromised by imposing a cross-formational flow of 710.9 ft<sup>3</sup>/d through the Cook Mountain Formation layer. This discrepancy, illustrated in Figure 8-23, indicates that removing the general head boundary from the Queen City and Sparta aquifers and merging it with the Yegua-Jackson Aquifer cross-section constitutes the two-dimensional transect model as a compromise between the original models.

Model layers describing the Sparta Aquifer through the Lower Wilcox in the Queen City and Sparta aquifers cross-section were extended down-dip to coincide with the extent of the overlying Yegua-Jackson Aquifer layers extracted from the Yegua-Jackson Aquifer model. This procedure introduces uncertainty in the model calculations as it imposes assumptions on the stratigraphy and relevant hydraulic properties in the extended part of the model. Despite the fact that a quantitative analysis of this uncertainty is beyond the scope of this work, an indicative measure can be drawn by the mass balance in the transect model. The transect model domain can be divided into three portions as illustrated in Figure 8-24: a portion corresponding to the formation layer extensions added the Queen City and Sparta aquifers (A), a portion corresponding to the original extent of the Queen City and Sparta aquifers (B), and finally the portion corresponding to the Yegua-Jackson Aquifer that remained unchanged in the development of the transect model (C). For each of these three portions, the sum of absolute flows through model cell bottom faces is calculated as a measure of vertical flow across the model domain. Similarly, the sum of absolute flows through model cell right faces indicates the amount of horizontal flow across the model domain. The corresponding values computed for portions A, B and C are given in Table 8-11. The same table provides the derived percentages of vertical and horizontal flow occurring in portion B with respect to the entire transect domain and to the Queen City and Sparta aquifers layers of the model. The values indicate that only a 12.18

and 4.8 percent of the total vertical and horizontal flow, respectively, corresponds to flow within portion A.

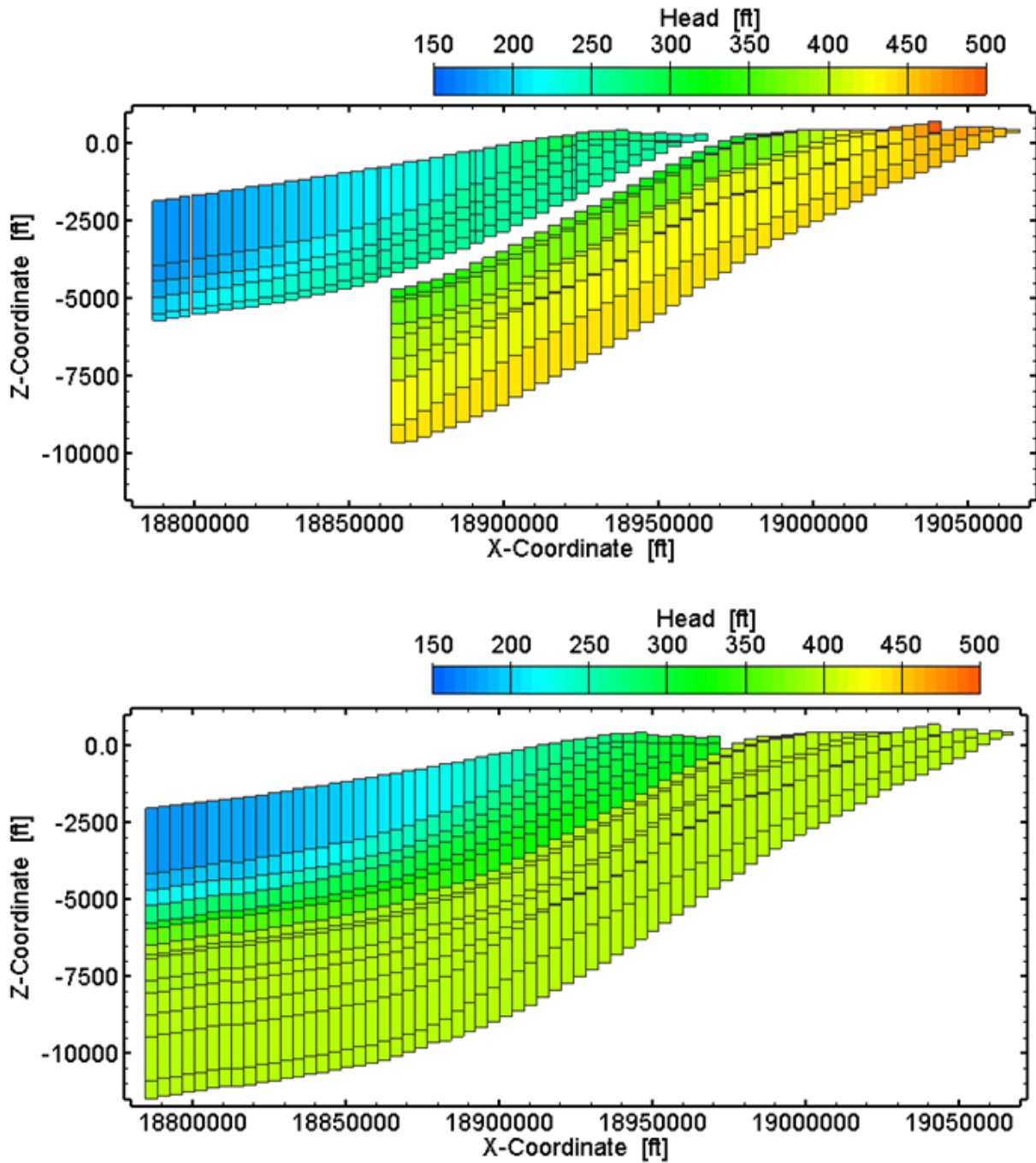


Figure 8-18. Comparison of hydraulic heads predicted with the three-dimensional models of the Yegua-Jackson Aquifer and southern portion of the Sparta, Queen City and Carrizo-Wilcox aquifers (top) to those predicted with the Gonzales Transect model (bottom).

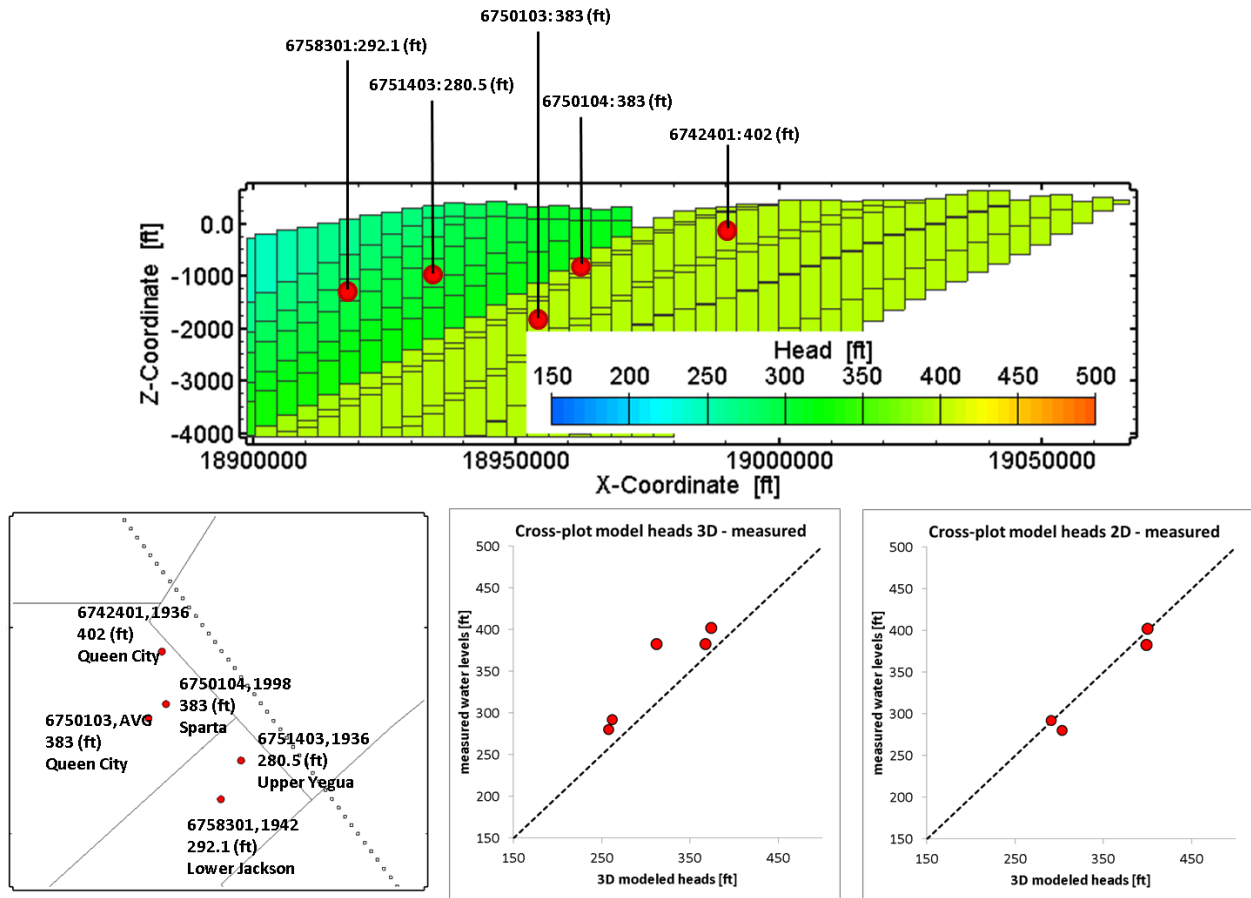


Figure 8-19. Cells corresponding to water level measurements (top) based on projections of well locations to the Gonzales Transect model (bottom, left), and cross-plots between measurements and heads modeled with the 3D (bottom, middle) and the 2D models (bottom, right). State well number (TWDB database), measured water level and corresponding aquifer are indicated next to the well locations.

Table 8-7 State wells with available water level measurements near the Gonzales Transect mode coordinates, measured water levels and modeled heads at cells corresponding to well locations and depths.

State Well No.	County	X-Coord. [ft]	Y-Coord. [ft]	Aquifer	Head modeled 2D [ft]	Head modeled 3D [ft]	Head measure d [ft]
6758301	Karnes	5636234	18916610	Lower Jackson	290.9	262.3	292.1
6751403	Karnes	5646036	18935426	Upper Yegua	303.2	257.8	280.5
6750104	Wilson	5609552	18962824	Sparta	398.6	312.5	383.0
6742401	Wilson	5607550	18988385	Queen City	400.1	373.8	402.0
6750103	Wilson	5601103	18955982	Queen City	398.9	367.7	383.0

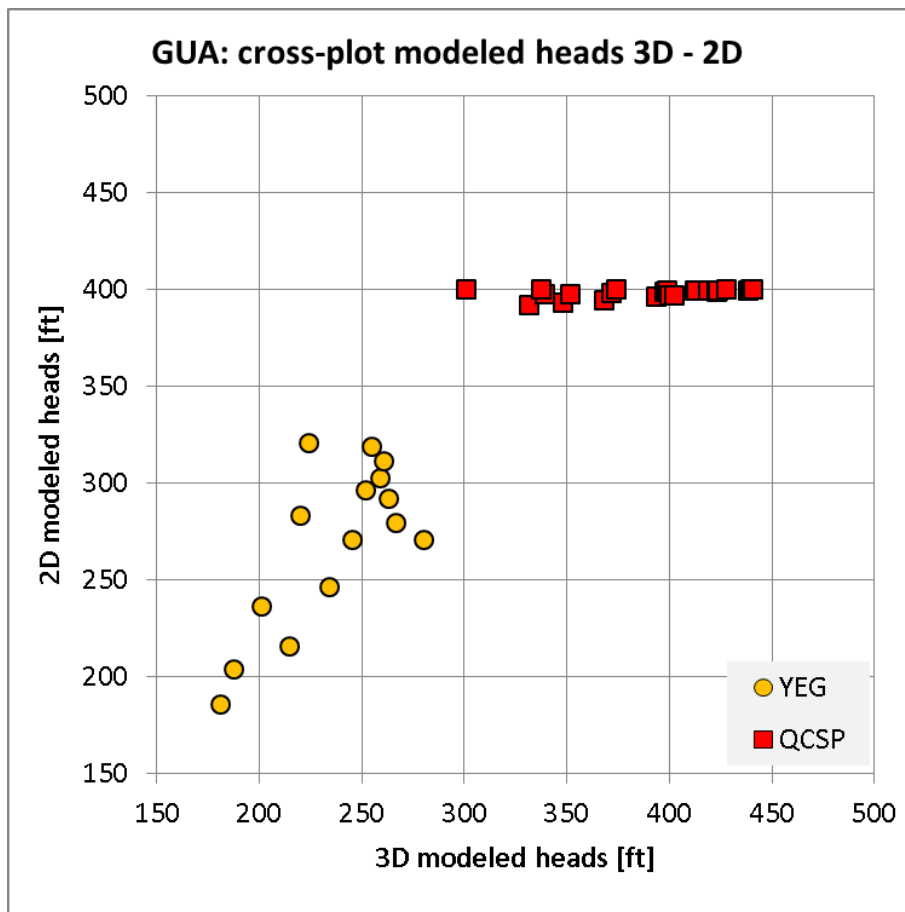
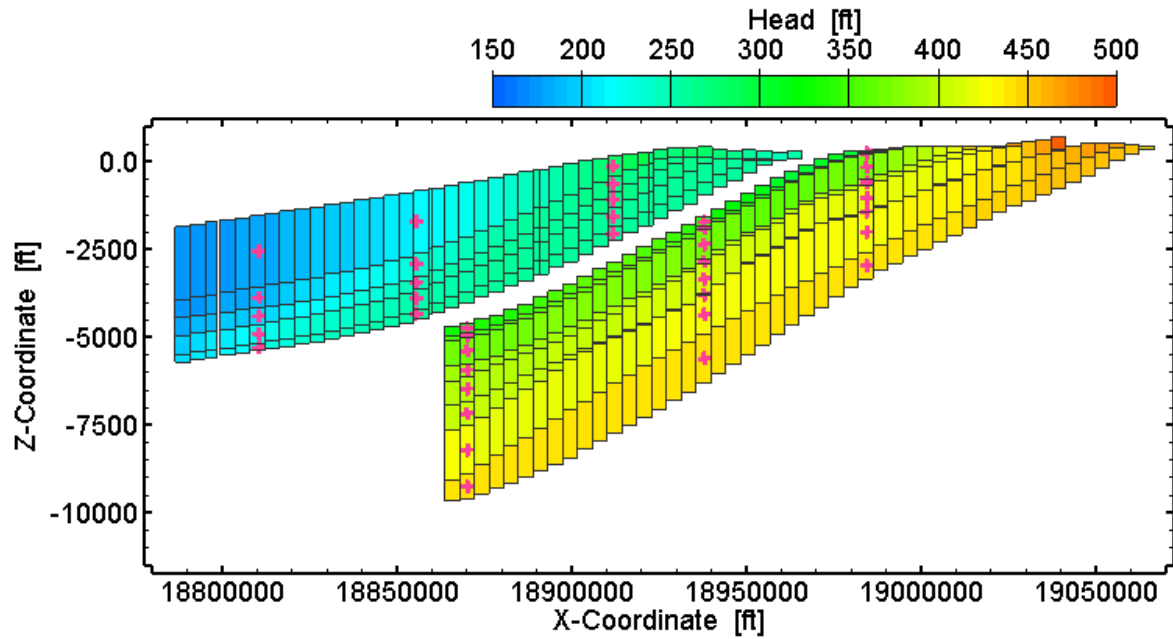


Figure 8-20. Cross-plots of hydraulic heads modeled with the three-dimensional Groundwater Availability Models and the Gonzales Transect model at locations selected as representative for deep and shallow parts of the modeled formations.

**Table 8-8. Selected model cells and their hydraulic heads used for comparison between the Gonzales Transect model and the three-dimensional Yegua-Jackson Aquifer and southern portion of the Queen City and Sparta aquifers models.**

<b>Formation</b>	<b>Cell 3D</b>	<b>Cell 2D</b>	<b>Z-Coord. [ft]</b>	<b>Head 3D [ft]</b>	<b>Head 2D [ft]</b>	<b>difference [ft]</b>	<b>rel. error [%]</b>
Catahoula	193:060:1	61:001:1	-2.55E+03	180.91	185.66	4.75	2.63
Catahoula	194:049:1	50:001:1	-1.70E+03	214.66	215.81	1.15	0.54
Catahoula	196:036:1	37:001:1	-1.25E+02	279.95	270.91	-9.04	3.23
Upper Jackson	193:060:2	61:001:2	-3.87E+03	187.51	203.69	16.17	8.63
Upper Jackson	194:049:2	50:001:2	-2.92E+03	234.28	246.14	11.85	5.06
Upper Jackson	196:036:2	37:001:2	-6.40E+02	266.67	279.26	12.59	4.72
Lower Jackson	193:060:3	61:001:3	-4.39E+03	201.10	236.28	35.17	17.49
Lower Jackson	194:049:3	50:001:3	-3.43E+03	245.33	271.07	25.74	10.49
Lower Jackson	196:036:3	37:001:3	-1.08E+03	263.17	291.86	28.69	10.90
Upper Yegua	193:060:4	61:001:4	-4.91E+03	220.26	283.39	63.13	28.66
Upper Yegua	194:049:4	50:001:4	-3.90E+03	251.92	296.65	44.73	17.76
Upper Yegua	196:036:4	37:001:4	-1.57E+03	259.18	302.80	43.61	16.83
Lower Yegua	193:060:5	61:001:5	-5.28E+03	224.34	320.81	96.47	43.00
Lower Yegua	194:049:5	50:001:5	-4.32E+03	255.13	318.74	63.61	24.93
Lower Yegua	196:036:5	37:001:5	-2.05E+03	260.67	311.36	50.69	19.45
Sparta	168:098:1	47:001:7	-4.74E+03	331.58	392.24	60.66	18.30
Sparta	168:082:1	31:001:7	-1.70E+03	339.49	397.43	57.94	17.07
Sparta	168:071:1	20:001:7	2.82E+02	301.01	400.24	99.22	32.96
Weches	168:098:2	47:001:8	-4.95E+03	348.30	393.30	45.01	12.92
Weches	168:082:2	31:001:8	-1.89E+03	351.39	397.84	46.45	13.22
Weches	168:071:2	20:001:8	2.27E+02	337.57	400.15	62.58	18.54
Queen City	168:098:3	47:001:9	-5.38E+03	368.35	394.73	26.38	7.16
Queen City	168:082:3	31:001:9	-2.36E+03	371.92	398.47	26.55	7.14
Queen City	168:071:3	20:001:9	-1.55E+02	373.84	400.06	26.22	7.01
Reklaw	168:098:4	47:001:10	-5.93E+03	393.49	396.52	3.03	0.77
Reklaw	168:082:4	31:001:10	-2.84E+03	397.86	398.99	1.13	0.28
Reklaw	168:071:4	20:001:10	-5.85E+02	398.68	399.83	1.15	0.29
Carrizo	168:098:5	47:001:11	-6.47E+03	400.24	397.16	-3.08	0.77
Carrizo	168:082:5	31:001:11	-3.34E+03	412.73	399.30	-13.43	3.25
Carrizo	168:071:5	20:001:11	-1.04E+03	418.81	399.62	-19.18	4.58
Upper Wilcox	168:098:6	47:001:12	-7.17E+03	402.55	397.32	-5.23	1.30
Upper Wilcox	168:082:6	31:001:12	-3.78E+03	412.79	399.30	-13.49	3.27
Upper Wilcox	168:071:6	20:001:12	-1.42E+03	418.85	399.63	-19.23	4.59
Middle Wilcox	168:098:7	47:001:13	-8.21E+03	423.12	398.79	-24.33	5.75
Middle Wilcox	168:082:7	31:001:13	-4.35E+03	423.70	399.62	-24.08	5.68
Middle Wilcox	168:071:7	20:001:13	-2.01E+03	427.85	399.97	-27.88	6.52
Lower Wilcox	168:098:8	47:001:14	-9.25E+03	438.55	399.75	-38.81	8.85
Lower Wilcox	168:082:8	31:001:14	-5.60E+03	439.69	399.92	-39.76	9.04
Lower Wilcox	168:071:8	20:001:14	-2.96E+03	440.67	400.09	-40.58	9.21

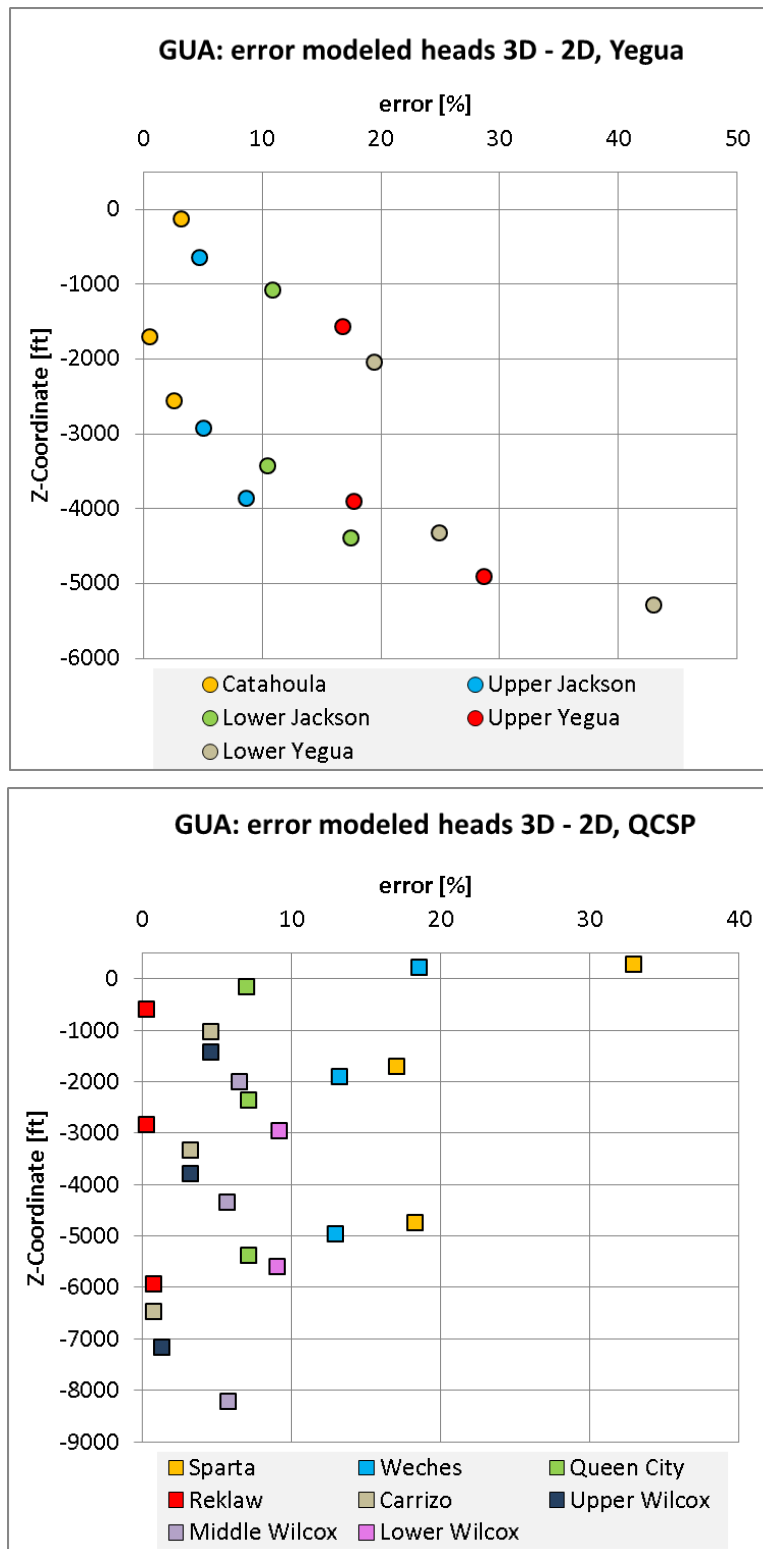


Figure 8-21. Comparison of hydraulic heads between the Gonzales Transect model and Groundwater Availability Models: plots of relative error versus depth for the Yegua-Jackson Aquifer (top) and the Sparta, Queen City and Carrizo-Wilcox aquifers (bottom).

**Table 8-9. Overview of recharge assigned to outcrop cells per layer in the Gonzales Transect model. Red colors indicate dried-out cells where recharge is transferred to the cells of the underlying layer.**

Layer	Layer ID	Outcrop cells (#)	Recharge per cell (ft <sup>3</sup> /d)	Recharge per layer (ft <sup>3</sup> /d)	Total flow bottom faces (ft <sup>3</sup> /d)	Total flow upper faces (ft <sup>3</sup> /d)
Catahoula	1	0	0.0	0.0	833.56	0.0
Upper Jackson	2	1	15.33	15.33	818.23	-833.56
Lower Jackson	3	2	15.33	30.66	787.56	-818.23
Upper Yegua	4	2	15.33	30.66	756.89	-787.56
Lower Yegua	5	3	15.33	45.99	710.89	-756.89
Cook Mountain	6	0	0.0	0.0	710.89	-710.89
Sparta	7	2	41.81	83.63	627.26	-710.89
Weches	8	1	41.81	41.81	585.44	-627.26
Queen City	9	5	41.81	209.08	376.35	-585.44
Reklaw	10	3	41.81	83.63	292.72	-376.35
Carrizo	11	5	41.81	167.27	125.45	-292.72
Upper Wilcox	12	0	0.0	0.0	125.45	-125.45
Middle Wilcox	13	1	41.81	125.45	0.0	-125.45
Lower Wilcox	14	0	0.0	0.0	0.0	0.0

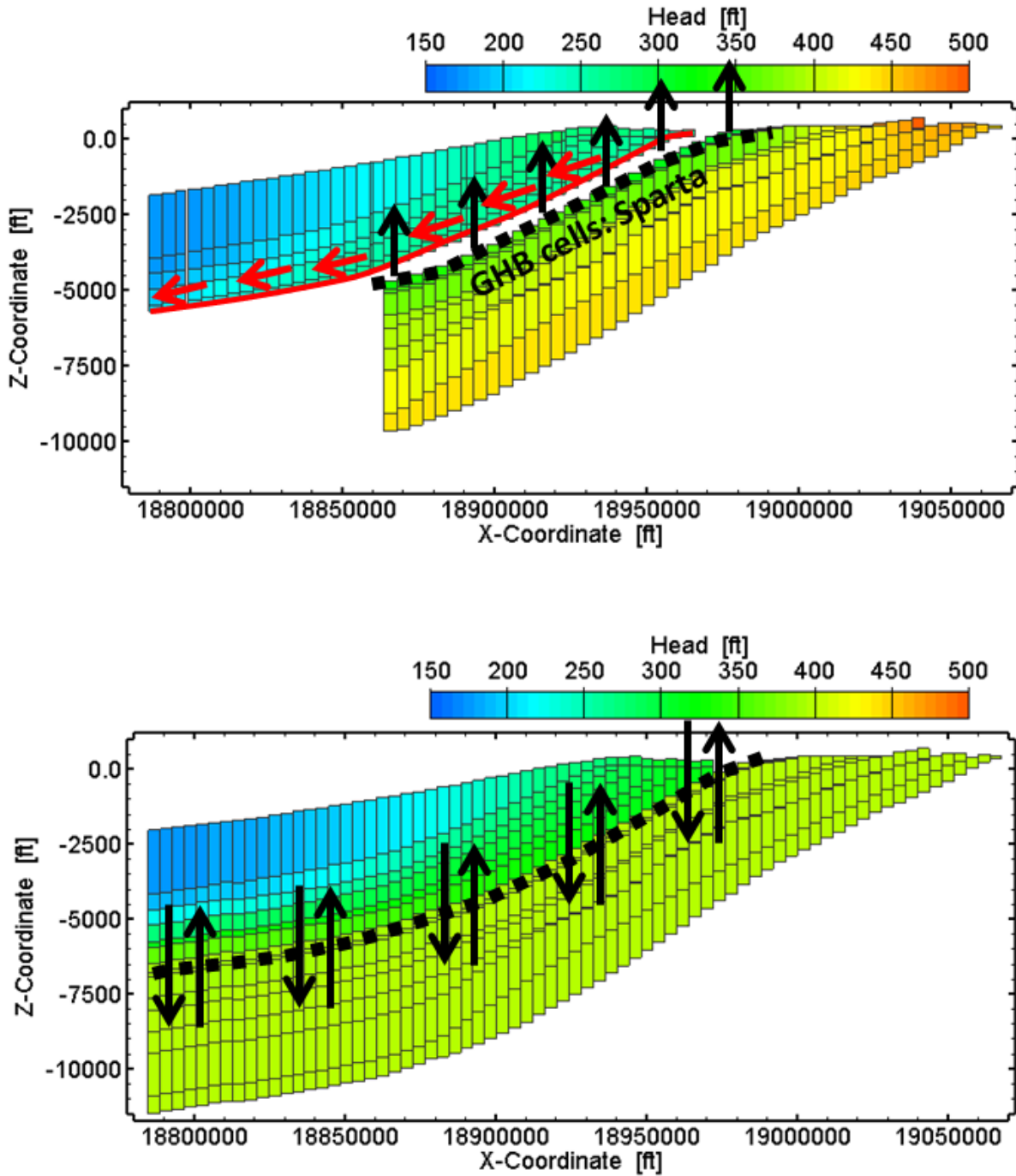


Figure 8-22. Illustration of the conceptual difference in boundary conditions used in the three-dimensional models and the two-dimensional transect: the original Yegua-Jackson Aquifer Groundwater Availability Model treats the base of the Lower Yegua unit as a no-flow boundary whereas in the transect model water flows in vertically through the Cook Mountain Formation. Similarly, the Queen City and Sparta Aquifers Groundwater Availability Model treats the Sparta Aquifer unit as a general head boundary whereas hydraulic heads in the Sparta Aquifer unit of the transect model depend strongly on recharge and general head boundary conditions imposed at the outcrop and the Catahoula.

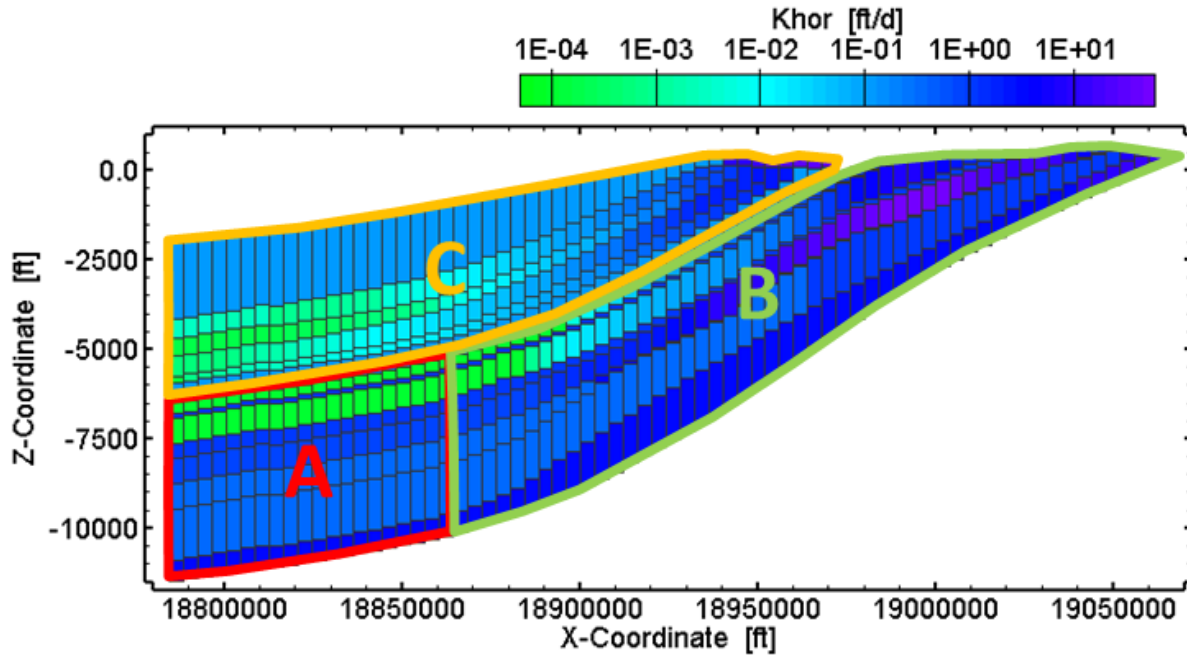


Figure 8-23. Portions of the Gonzales transect model corresponding to extended (A) and, original (B) layers from the Queen City and Sparta aquifers Groundwater Availability Models and layers from the Yegua-Jackson Aquifer Groundwater Availability Model (C).

Table 8-10. Percentage of water balance that occurs in the deep portions where the Queen City and Sparta aquifers Groundwater Availability Models layers were extended in the Gonzales Transect model. Vertical flows correspond to the sum of absolute values of flows through the bottom face of the model cells in the corresponding portion of the model (A, B, and C). Horizontal flows correspond to the sum of absolute values of flows through the right face of the model cells in the corresponding portion of the model (A, B, and C).

GUA transect portion	SUM vertical flow [ft <sup>3</sup> /d]	SUM horizontal flow [ft <sup>3</sup> /d]	Percentage of water balance vertical flow [%]	Percentage of water balance horizontal flow [%]
A + B + C	7.783E+03	4.723E+04	-	-
A + B	3.165E+03	2.198E+04	-	-
A	9.485E+02	2.272E+03	-	-
A / (A + B + C)	-	-	12.2	48.1
A / (A + B)	-	-	30.0	10.3

### 8.4.2 Age and Sensitivity Analysis

The velocity field calculated with the steady-state two-dimensional MODFLOW simulation is used for particle tracking simulations using MODPATH. Water ages are computed as backward travel times of particles from a cell to the outcrop. Figure 8-24 shows the simulated travel times for the Gonzales Transect using the original hydraulic properties extracted from the three-dimensional models, with the calibrated recharge and Cook Mountain Formation leakance. For illustrative purposes, the same figure shows backward particle pathlines extracted for two vertical grid cell columns of the model. The color of the pathlines changes with location indicating the particle travel time at the corresponding location. The lowest groundwater ages are

observed in the Catahoula layer (10,000 to 100,000 years), which is attributed to the general head boundary condition assigned in this layer. Groundwater ages between 100,000 and 1,000,000 years are observed in the shallow parts of the Yegua-Jackson Aquifer and the shallow and deeper parts of the Sparta, Queen City and Carrizo-Wilcox aquifers. Particles traced back from the shallow portion of the Upper and Lower Jackson (right column of grid cells) flow almost parallel to the surface, vertically through the Cook Mountain Formation, and along the Sparta layer to the origin at the Sparta Formation outcrop. On the other hand, particles from the shallower parts of the Upper and Lower Yegua (right column of grid cells) follow longer paths through deeper portions of the Yegua Formation, passing almost vertically through the Cook Mountain Formation and the Sparta Aquifer, and flowing along the Queen City Aquifer layer from the origin at the Queen City Aquifer outcrop. Similarly, particles placed in the shallower parts of the Cook Mountain Formation, Sparta Aquifer, Weches Formation, Queen City Aquifer and Reklaw Formation cells (right column of grid cells) originate from the Queen City Aquifer outcrop with a large portion of their flowpath located along the Queen City Aquifer layer. In the deeper parts of the transect model (left column of grid cells) ground water ages in the Yegua-Jackson, Sparta and Queen City aquifers vary between 1,000,000 and 10,000,000 years. Particles placed in these cells generally show a longer flow path through deeper parts of the transect and parallel to the dip along the Carrizo and Middle Wilcox. It is observed that all particles placed in the deeper parts of the transect originate from the Carrizo-Wilcox and Middle Wilcox outcrop. Groundwater ages are clearly increased in the Carrizo-Wilcox Aquifer, exceeding 1,000,000 years already at shallower locations and 10,000,000 years in the deeper parts. Particles placed in the shallow and deep parts of Carrizo and Wilcox layers are characterized by flow paths almost parallel to the dip, and also originate from the outcrop of the Middle Wilcox.

This simulation will be referred to as the reference case and will be used for comparison of water ages for each incremental change in input parameters during the sensitivity analysis. The sensitivity analysis is carried out for horizontal conductivity (Khor), leakance (Vcont) and recharge (RCH) in each of the 14 model layers. Sensitivity runs are not performed for combinations of parameters and layers that are not definable in the reference case. This results in 148 sensitivity runs in total as shown in Table 8-11.

Table 8-12 gives a list of 23 well locations where water age measurements are available and will form the basis for the comparison. The locations of these wells were mapped on the Guadalupe River basin and then projected onto the Gonzales Transect line to obtain the model columns corresponding to the X-Y well locations. Consequently, model cells were assigned to each well measurement based on the model layer and aquifer corresponding to the measurement. The map of well locations and the corresponding cells in the Gonzales Transect model are illustrated in Figure 8-25. The water ages predicted with the reference case are compared to the corresponding water age measurements in Table 8-12. Only 22 of the wells are used for the sensitivity analysis, as *Brady Well* lies out of the extent of the transect model.

Comparison of the measured ages of groundwater and the simulated ages of groundwater from the cross-sectional models in Table 8-12 indicate significant differences ranging from one to three orders of magnitude. One of the groundwater samples from the outcrop has a measured age of “modern”. The laboratory-measured ages from 20 of the other samples ranges from 1060 to 43,300 years and two samples were estimated to be greater than 43,500 years old. The simulated ages range from 37,779 to 4,922,000 years old. Thirteen of the 23 samples (57%) have simulated ages greater than 1,000,000 years old and seventeen (74%) have simulated ages greater than

100,000 years old. The old simulated ages are the result of the small hydraulic gradients that exist in the calibrated cross-sectional model.

The sensitivity analysis was carried out by varying the input parameters for each layer separately. The average water age of the 22 observation points was used as a measure for comparing each sensitivity run to the reference case. Figure 8-26 through Figure 8-28 show the water age sensitivity to formational horizontal conductivity, leakance and recharge, respectively. The results are presented separately for sensitivity to the Yegua-Jackson Aquifer input parameters (top image) and to input parameters of the Queen City and Sparta aquifers (bottom image).

Figure 8-25 indicates that all observation points in the Gonzales Transect model lie within the Queen City and Sparta aquifers layers. Therefore sensitivity to input parameters assigned to the Yegua-Jackson Aquifer is generally lower compared to sensitivity with respect to input in layers Sparta through Lower Wilcox (Figure 8-26 through Figure 8-28).

The plots of sensitivity to horizontal conductivity (Figure 8-26) indicate that the highest sensitivity is with respect to Weches and the Middle Wilcox. An increase of horizontal conductivity in these layers increases the average water age by more than 1,000,000 years. In general, increasing horizontal conductivity in the Yegua-Jackson Aquifer layers introduces an increase of predicted water ages within a range of 70,000 years (Figure 8-26); with a single exception in the sensitivity to the Upper Yegua that demonstrates the opposite behavior. Variations of horizontal conductivity in the Queen City and Sparta aquifers layers induce different responses depending on the layer. Increasing horizontal conductivity in the Sparta, Weches, Queen City and Reklaw layers generally produces a decrease in water ages whereas changing horizontal conductivity in the Carrizo, Upper Wilcox, Middle Wilcox and Lower Wilcox layer produces the opposite effect.

The highest sensitivity to leakance is observed for varying the leakance of the Cook Mountain Formation and the Middle Wilcox (Figure 8-27). An increase of leakance of the Cook Mountain Formation by a factor of 1.5 results in water ages decreased by more than 1,000,000 years. On the other hand, a similar increase of Middle Wilcox leakance produces an increase of the average water age by almost 1,000,000 years. In general, increasing leakance by a factor of 1.5 in the Yegua-Jackson Aquifer increases the average water age up to 500,000 years. Increasing leakance by a factor of 1.5 in the Queen City and Sparta aquifers layers in general increases the average water age within a range of 200,000 years, with water age increase reaching 400,000 and 900,000 years for Reklaw Formation and Middle Wilcox leakance, respectively.

Figure 8-28 indicates that the highest sensitivity to recharge corresponds to recharge assigned to the Middle Wilcox and the Carrizo. An increase of recharge by a factor of 1.5 in the Middle Wilcox or the Carrizo decreases the average water age by 700,000 and 1,200,000 years, respectively. It should be pointed out that changes in recharge during the sensitivity analysis correspond to recharge values assigned to individual grid cells of the outcrop. Therefore variations of recharge in formations with several outcrop cells proportionally result in larger absolute variations of total recharge in the model compared to formations with a smaller number of outcrop cells. The number of outcrop cells in each layer and resulting recharge after correcting for dried-out cells are given in Table 8-9. It is observed that, despite the fact that the maximum recharge corresponds to the Queen City Aquifer outcrop, its sensitivity is less pronounced compared to sensitivity to the Carrizo or Middle Wilcox outcrops. Sensitivity to recharge

assigned at the Yegua-Jackson Aquifer outcrop (Figure 8-28) shows a water age decrease within a range of 15,000 years when recharge is increased by a factor of 1.5. Sensitivity patterns to recharge assigned in the Queen City and Sparta aquifers are different depending on the layer. Water age decreases when recharge in the Carrizo and Middle Wilcox is increased, while it increases with recharge assigned Weches, Reklaw and Queen City layers. This is likely because the Carrizo and Wilcox layers have higher horizontal hydraulic conductivities and, therefore, greater recharge penetration depth than the layers with respectively lower horizontal hydraulic conductivities.

In general, the sensitivity plots show consistent monotonic behavior in water age as a response to an incremental change to input parameters. However some runs produce “kinks” where one value does not agree with the trend indicated by the other three values in a parameter sensitivity, or responses resulting in extreme increases or decreases in water age. These cases are the following:

- 111\_K2 (sensitivity to Carrizo Formation horizontal conductivity, fraction of base value 0.9): water ages from the individual observation points indicate that some observation points are characterized by an increase in water age for increasing conductivity while other observation points behave in the opposite fashion. Despite the fact that water ages from the individual observation points change monotonically with conductivity, averaging ages from all points results in a non-monotonic behavior due to different magnitudes of water age increase and decrease at different locations.
- 112\_K4 (sensitivity to Upper Wilcox horizontal conductivity, fraction of base value 1.5): water ages in the individual observation points increase monotonically with conductivity. However the magnitude of increase is significantly larger for observation points in the Carrizo formation, with a pronounced increase for a base value of 1.5. It should be noted that 12 out of the 22 observation points are located in the Carrizo layer.
- 113\_V4 (sensitivity to Middle Wilcox horizontal conductivity, fraction of base value 1.5): water ages at the observation points increase monotonically with conductivity. Similarly to the Upper Wilcox sensitivity, the magnitude of increase is significantly larger for observation points in the Carrizo formation resulting in a pronounced increase for a base value of 1.5.
- 13\_V1 (sensitivity to Lower Jackson leakance, fraction of base value 0.5): water ages increase monotonically with leakance. However, the observation points located in the Carrizo formation indicate pronounced sensitivity when decreasing the Lower Jackson leakance by a factor of 0.5.
- 19\_R4 (sensitivity to Queen City recharge, fraction of base value 1.5): the magnitude of change in water ages in the Carrizo formation is significantly larger compared to the rest of the observation points. These increase with Queen City recharge for fraction base values 0.5 through 1.1 and then decrease significantly for a fraction base value of 1.5.
- 19\_K2 (sensitivity to Queen City horizontal conductivity, fraction of base value 0.9): some observation points indicate an increase in water age for increasing conductivity, while other observation points indicate the opposite. Despite the fact that water ages from the individual observation points change monotonically with conductivity, the average water age behaves non-monotonically due to different magnitudes of water age changes at different locations.

In general, groundwater ages respond in very different ways at every observation point. A change in an input parameter may induce an increase of groundwater age at a certain location in an aquifer and, at the same time, a decrease in groundwater age at a different location in the same aquifer. In some cases, responses to monotonic increases of an input parameter appear to be non-monotonic changes of water age. Similarly, some cases demonstrate extreme sensitivity to an incremental change to an input parameter by demonstrating abrupt changes in groundwater age up to 6 million years. Such effects can be explained with the tortuous flow paths indicated by the particle tracking simulations (Figure 8-24). For example, pathlines ending in the Lower Jackson and the Upper Yegua (Figure 8-24, right column of marked grid cells) reveal very different flow paths and, therefore, different travel times despite the proximity of these two observation points. It becomes clear that any change in input parameters may affect the flow pattern in a way that these pathlines change entirely and shift either towards greater depths or closer to the surface. The high, and in some cases, seemingly non-consistent sensitivity of water ages is therefore attributed to the high sensitivity of flow paths.

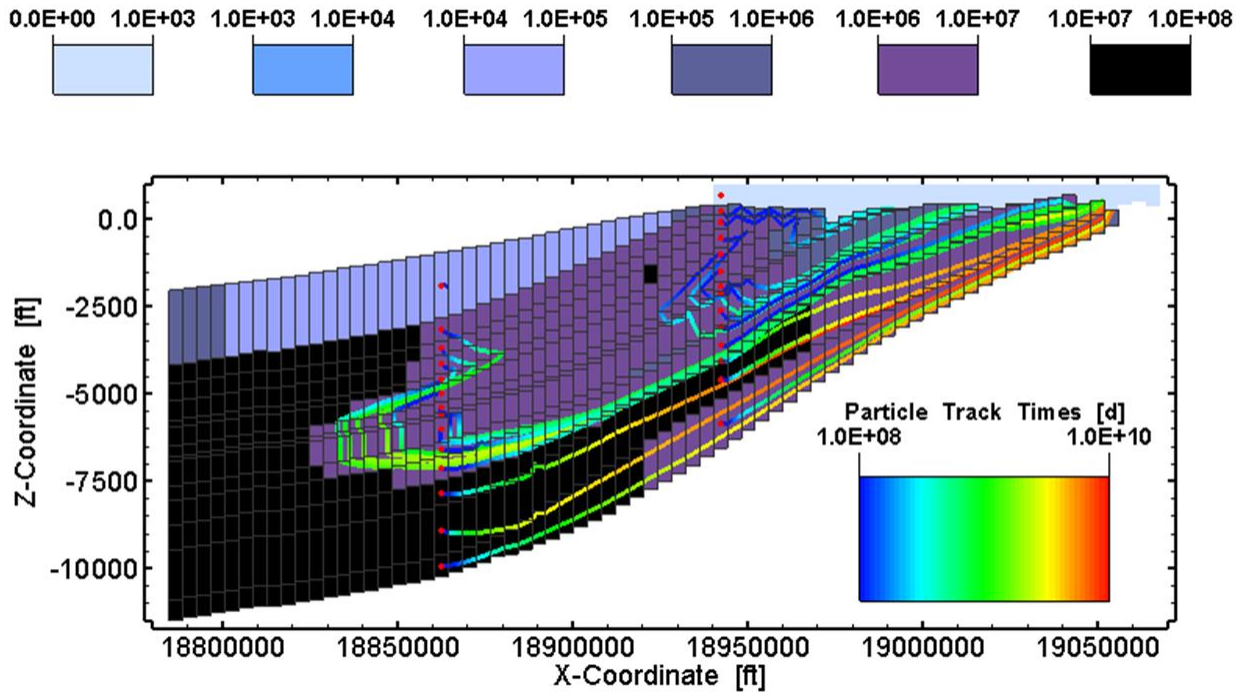


Figure 8-24. Groundwater ages and particle pathlines computed with the reference simulation of the Gonzales Transect model.

**Table 8-11. Overview of water age sensitivity runs carried out with the Gonzales Transect model.**

Parameter	Horizontal conductivity				Leakance				Recharge			
	0.5	0.9	1.1	1.5	0.5	0.9	1.1	1.5	0.5	0.9	1.1	1.5
Layer												
Catahoula	11_K1	11_K2	11_K3	11_K4	11_V1	11_V2	11_V3	11_V4	-	-	-	-
Upper Jackson	12_K1	12_K2	12_K3	12_K4	12_V1	12_V2	12_V3	12_V4	12_R1	12_R2	12_R3	12_R4
Lower Jackson	13_K1	13_K2	13_K3	13_K4	13_V1	13_V2	13_V3	13_V4	13_R1	13_R2	13_R3	13_R4
Upper Yegua	14_K1	14_K2	14_K3	14_K4	14_V1	14_V2	14_V3	14_V4	14_R1	14_R2	14_R3	14_R4
Lower Yegua	15_K1	15_K2	15_K3	15_K4	15_V1	15_V2	15_V3	15_V4	15_R1	15_R2	15_R3	15_R4
Cook Mountain	16_K1	16_K2	16_K3	16_K4	16_V1	16_V2	16_V3	16_V4	-	-	-	-
Sparta	17_K1	17_K2	17_K3	17_K4	17_V1	17_V2	17_V3	17_V4	17_R1	17_R2	17_R3	17_R4
Weches	18_K1	18_K2	18_K3	18_K4	18_V1	18_V2	18_V3	18_V4	18_R1	18_R2	18_R3	18_R4
Queen City	19_K1	19_K2	19_K3	19_K4	19_V1	19_V2	19_V3	19_V4	19_R1	19_R2	19_R3	19_R4
Reklaw	110_K1	110_K2	110_K3	110_K4	110_V1	110_V2	110_V3	110_V4	110_R1	110_R2	110_R3	110_R4
Carrizo	111_K1	111_K2	111_K3	111_K4	111_V1	111_V2	111_V3	111_V4	111_R1	111_R2	111_R3	111_R4
Upper Wilcox	112_K1	112_K2	112_K3	112_K4	112_V1	112_V2	112_V3	112_V4	-	-	-	-
Middle Wilcox	113_K1	113_K2	113_K3	113_K4	113_V1	113_V2	113_V3	113_V4	113_R1	113_R2	113_R3	113_R4
Lower Wilcox	114_K1	114_K2	114_K3	114_K4	-	-	-	-	-	-	-	-

**Table 8-12. Overview of wells with available water age measurements and comparison to water ages modeled using particle tracking in the Gonzales Transect.**

<b>Well ID</b>	<b>X-Coord. [ft]</b>	<b>Y-Coord. [ft]</b>	<b>Aquifer</b>	<b>GUA Model Cell ID</b>	<b>Remarks</b>	<b>Water Age Measured [yrs]</b>	<b>Water Age Simulated [yrs]</b>
Brady Well	5626720	19096600	Wilcox	-		10,020	-
Springs Hill #2	5608880	19033600	Carrizo	9:01:11		1,060	1.457E+06
CRWA-D (#7 Deadman Tank)	5621320	19038100	Carrizo	10:01:11		1,650	1.459E+06
CRWA-E (#9-Camphouse)	5628840	19035300	Carrizo	11:01:11		1,620	1.623E+06
Dewville Methodist	5617800	19010400	Queen City	14:01:09	Outcrop	Modern	5.691E+04
SSLGC #9	5618740	19001600	Carrizo	15:01:11		3,600	2.615E+06
SSLGC #4	5630340	18991700	Carrizo	18:01:11		9,040	3.131E+06
Whitley Well	5628890	18991300	Wilcox	18:01:13		31,380	4.071E+06
Buell #1 Barn	5633570	18984600	Queen City	19:01:09		25,350	3.993E+05
Gaylord Well,	5645300	18984400	Sparta	21:01:07		20,580	3.779E+04
SAWS SP-2.	5674340	19019700	Sparta	19:01:07		4,620	0.000E+00
SAWS QC-2.	5674430	19019700	Queen City	19:01:09		38,890	3.993E+05
SAWS CM-2	5674340	19019800	Carrizo	19:01:11		14,630	3.325E+06
SAWS SP-3	5665870	18998300	Sparta	21:01:07		14,680	3.779E+04
SAWS QC-3	5665870	18998400	Queen City	21:01:09		27,390	5.261E+05
SAWS CM-3	5665780	18998400	Carrizo	21:01:11		14,660	3.782E+06
SAWS SP-4	5672360	18992300	Sparta	23:01:07		20,000	1.362E+05
SAWS QC-4	5672360	18992300	Queen City	23:01:09		43,300	6.721E+05
SAWS CM-4	5672910	18991500	Carrizo	23:01:11		13,490	4.329E+06
Nixon #5	5635060	18972100	Carrizo	21:01:11		17,780	3.782E+06
Smiley #3	5673530	18971600	Carrizo	26:01:11		35,010	4.922E+06
Lessor Well	5691160	18966200	Carrizo	29:01:11		>43,500	4.155E+06
Jenkins Well	5706130	18980600	Carrizo	28:01:11		>43,500	4.516E+06

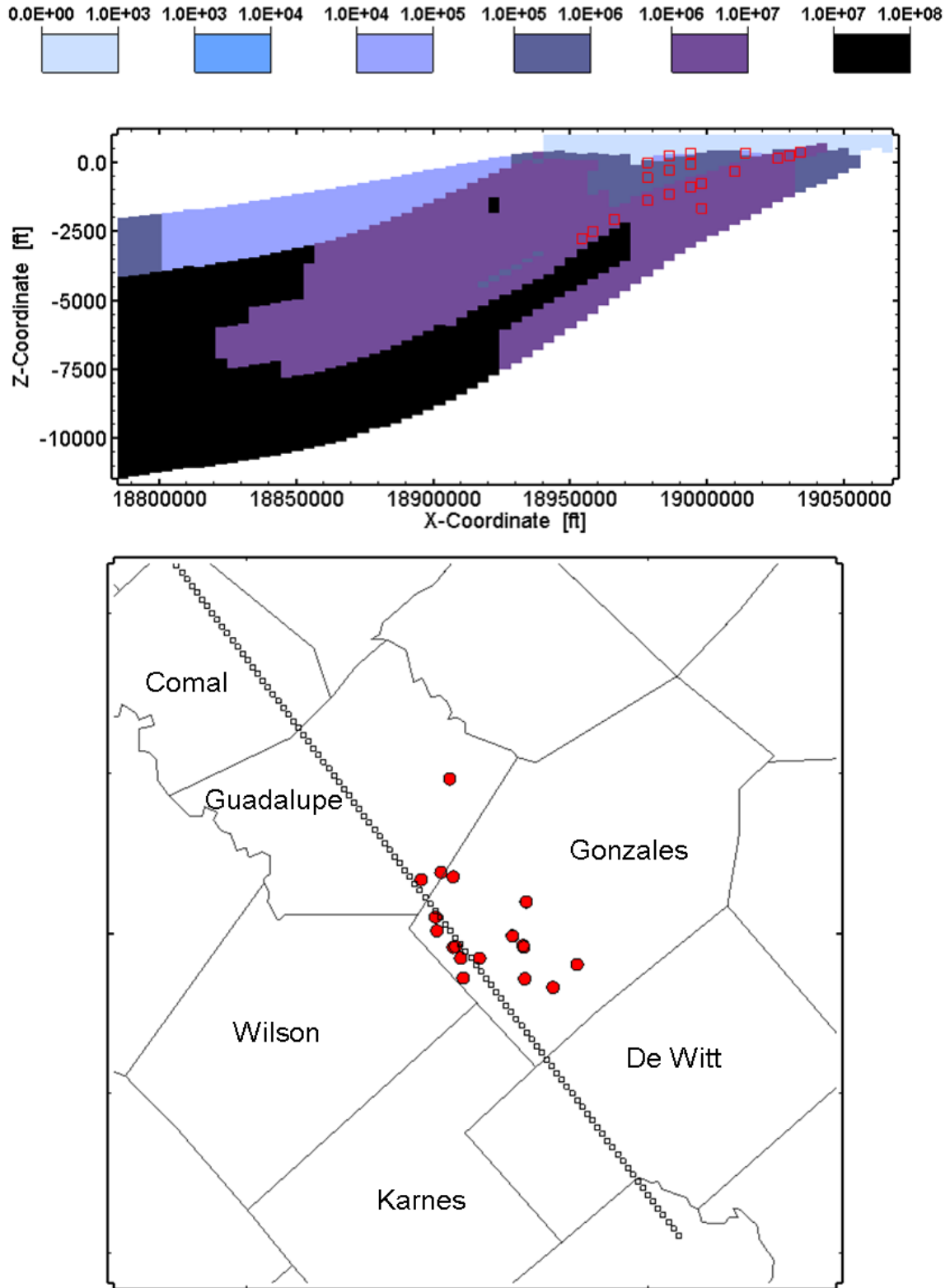


Figure 8-25. Model cells corresponding to water age measurements projected locations and depths in the Gonzales Transect.

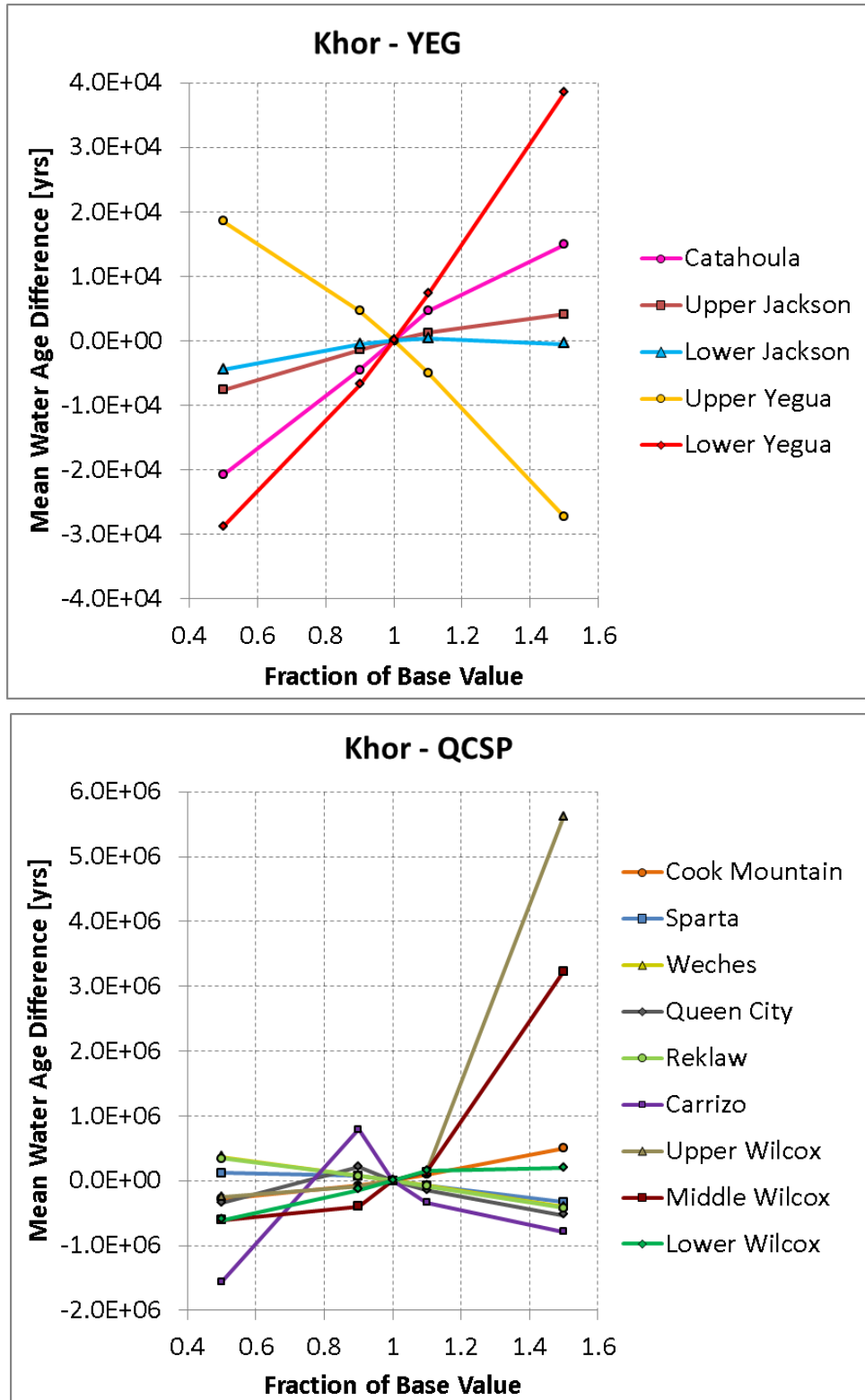


Figure 8-26. Water age sensitivity to layer horizontal conductivity, Gonzales Transect model.

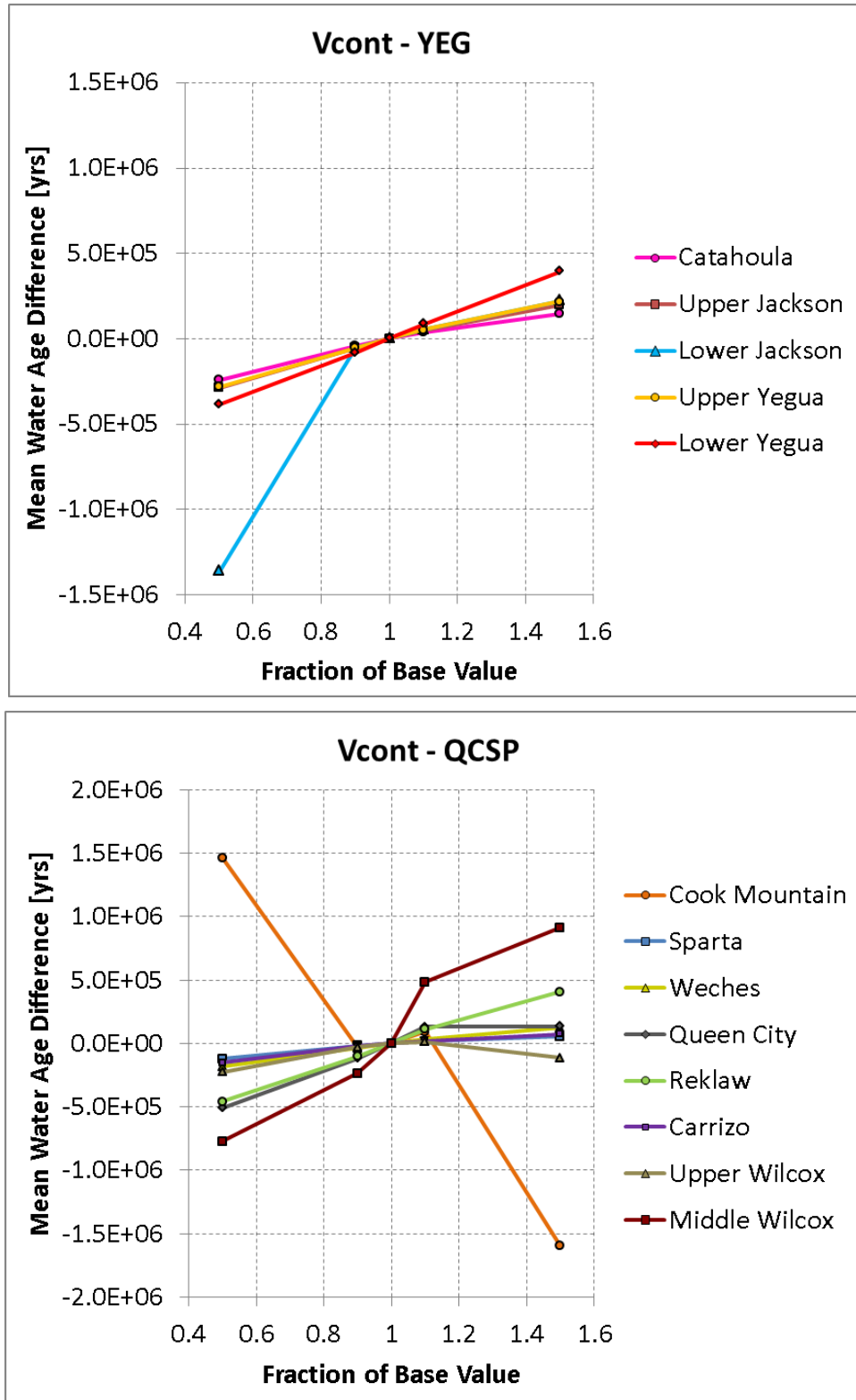


Figure 8-27. Water age sensitivity to layer leakage, Gonzales Transect model.

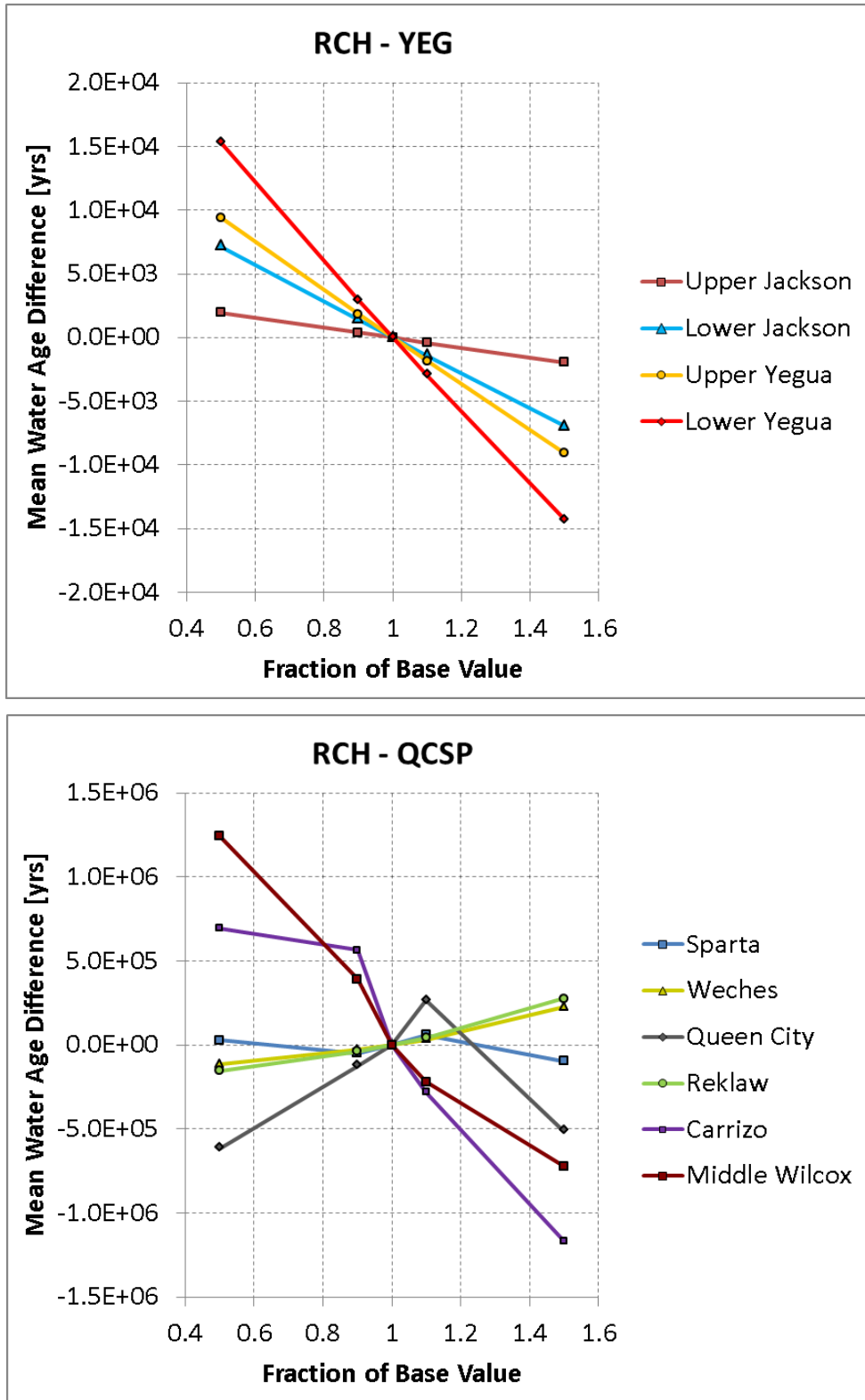


Figure 8-28. Water age sensitivity to recharge at layer outcrop, Gonzales Transect model.

## 8.5 Central Transect Model

In the following section, the analysis carried out with the Central Transect model will be presented. The first part of the discussion gives an overview of the results from the steady-state flow simulations based on the geometry and hydraulic properties extracted from the three-dimensional models, and the boundary conditions that have been partly defined based on the existing boundaries in the three-dimensional models and partly based on the calibration approach. Hydraulic head distributions and flows predicted with the Central Transect model are extensively compared to those extracted from the three-dimensional models. These are consequently used for estimating groundwater ages through particle tracking simulations. The particle tracking simulations and the analysis of groundwater age sensitivities to input parameters is given.

### 8.5.1 Results of Flow Simulations

Hydraulic heads predicted with the three-dimensional Yegua-Jackson Aquifer and central portion of the Queen City and Sparta aquifers models at the extracted cross-sections are shown in Figure 8-29. Hydraulic heads in the central portion of the Queen City and Sparta aquifers cross-section vary between a minimum of 228 feet at the down-dip edge of the Sparta Aquifer and a maximum of 526 feet at the outcrop of the Carrizo-Wilcox Aquifer. In general, hydraulic heads increase for descending layers from the Sparta Aquifer to the Lower Wilcox. Within each formation layer, hydraulic heads decrease with depth. Hydraulic heads in the Sparta Aquifer vary between 228 feet and 365 feet near the middle of the layer. The corresponding range in the Lower Wilcox is from 439 feet at the down-dip boundary to 454 feet below the formation outcrop. Similarly to the observations in the Gonzales Transect, hydraulic heads in the Yegua-Jackson Aquifer are generally lower. The general head boundary in the Catahoula Formation introduces the lowest hydraulic head of 173 feet at the down-dip model boundary and the highest hydraulic head of 340 feet below the model outcrops. In the Lower Yegua, heads increase from 226 feet at the down-dip edge to 315 feet at the formation outcrop.

Figure 8-29 also illustrates the corresponding heads simulated with the Central Transect model after the calibration of input parameters. Similarly to the Gonzales Transect model, calibration of the Central Transect results in an almost uniform hydraulic head distribution in the Queen City and Sparta aquifers ranging between 331 and 333 feet. Hydraulic heads in the Queen City and Sparta aquifers influence the Yegua-Jackson Aquifer through the Cook Mountain Formation that acts as a confining layer between the two systems. As shown in Table 8-6, the leakance of the Cook Mountain Formation in the Central Transect is significantly higher compared to the value calibrated in the Gonzales Transect simulations. As a result, the hydraulic connection between Yegua-Jackson Aquifer and Queen City and Sparta aquifers portions of the model is more conductive and allows propagation of hydraulic heads across the model domain. It is observed that the shallow parts of the Yegua-Jackson Aquifer layers are characterized by hydraulic heads ranging between 320 and 332 feet determined, on the one hand, by general head boundary heads in the Catahoula and, on the other hand, by the connection to the underlying Queen City and Sparta aquifers layers. In the deeper section of the Yegua-Jackson Aquifer, head values assigned to the general head boundary differ significantly from simulated heads in the Queen City and Sparta aquifers. Therefore the contrast of hydraulic heads between the Catahoula, Upper Jackson, Lower Jackson and Upper Yegua Formations, and the Queen City and Sparta aquifers becomes apparent in the deeper parts of the Yegua-Jackson Aquifer.

The modeled hydraulic heads can be verified through comparison to measured well head data. For that purpose, wells in the vicinity of the Central Transect Model line have been selected and projected onto the transect model as shown in Figure 8-30. The comparison to hydraulic heads predicted with the three-dimensional models indicates agreement as shown in the corresponding cross-plot given in Figure 8-30 (Table 8-13). On the other hand, it is observed that the uniform heads predicted with the Brazos transect model do not capture the distribution of measured heads that range between 189 and 456 ft. It is further indicated that due to the limited amount of well data the comparison only gives insights for the shallow parts of the model near the outcrop. A more systematic evaluation of the transect model predictions is performed in the following through comparison to the calibrated three-dimensional models.

In order to facilitate a comparison between hydraulic heads predicted with the two-dimensional and the three-dimensional models, three cell columns in the each of the Yegua-Jackson Aquifer and the Queen City and Sparta aquifers cross-sections near the down-dip model boundary, the outcrop and the middle of the transect were analyzed. The locations of these columns were selected to yield representative values of hydraulic heads at different formation depths. Hydraulic heads are consequently extracted at the 39 observation points corresponding to the model cells of the selected columns. The locations of the observation points are given in Figure 8-32. The same figure presents the resulting cross-plots of simulated and observed hydraulic heads. Simulated hydraulic heads in the Queen City, Sparta and Carrizo-Wilcox aquifer system at the selected cells of the three-dimensional model vary between 230 and 390 feet. Combined with the uniform heads modeled with the Central Transect model, this results in an almost horizontal cross-plot distribution for the Queen City and Sparta aquifers with the best agreement in hydraulic heads of the Upper and Middle Wilcox (Table 8-15). On the other hand, the general head boundary condition prescribed in both models at the Catahoula provides a better agreement for the Yegua-Jackson Aquifer system. Figure 8-33 illustrates the corresponding relative error between the two models for the Yegua-Jackson Aquifer and the Queen City and Sparta aquifers separately. In the Yegua-Jackson Aquifer, the minimum errors are observed in the Catahoula with increasing values for increasing depth and, respectively, distance from the general head boundary condition. The minimum error in the Queen City, Sparta and Carrizo-Wilcox aquifer system is observed in the Middle, Upper and Lower Wilcox. On the other hand, heads modeled with the three-dimensional central portion of the Queen City and Sparta aquifers model at observation cells in the Sparta Aquifer and Weches vary between 235 and 351 feet, resulting in relative errors up to 50 percent (Figure 8-33 and Table 8-15).

The steady-state MODFLOW simulation using the calibrated parameters results in hydraulic heads below the bottom elevations at several grid cells. In these cases, the grid cells are assumed to be dried-out and any recharge assigned to them is transferred to the underlying cells. The Central Transect simulation results in 1 cell drying out in the Sparta Aquifer, 3 cells in the Weches, 2 cells in the Queen City Aquifer, 1 cell in the Reklaw Formation, 2 cells in the Carrizo and 1 cell in the Middle Wilcox. The number of outcrop cells per formation in the Central Transect, the recharge assigned according to the calibration results and the mass balances derived per formation are given in Table 8-16. Red fonts indicate one dried-out cell of the Sparta Aquifer and one dried-out cell of the Weches that correspond to the outcrop. Consequently, recharge rates of 13.93 ft<sup>3</sup>/d assigned to each of these two cells is transferred to the underlying cells of the Queen City Aquifer and Upper Wilcox Groups, respectively.

Next to recharge per layer, Table 8-15 also shows the amount of total vertical flow through the bottom and top cell faces for each layer. The Lower Wilcox layer has no outcrop and also no inflows through the no-flow boundaries at the bottom and the down-dip edge, resulting in a net flow of zero between the Lower and Middle Wilcox under steady-state conditions. The Middle Wilcox receives 27.87 ft<sup>3</sup>/d of water through recharge at the outcrop. The same amount of water flows vertically through the upper faces of the Middle Wilcox cells and into the Upper Wilcox. Consequently, this accumulates with flow from recharge at the Upper Wilcox outcrop (83.63 ft<sup>3</sup>/d) to move further upwards through the interface to the Carrizo (111.51 ft<sup>3</sup>/d). The same flow pattern occurs in the rest of the model layers so that, finally, a total flow of 418.7 ft<sup>3</sup>/d discharges through the general head boundary of the Catahoula. This behavior is dictated by the boundary conditions of the model that drive the inflow at the outcrop through the formation layers and towards the general head boundaries, since the bottom and down-dip edge model boundaries are no-flow boundaries.

The general head boundary assigned to the Sparta Aquifer in the three-dimensional central portion of the Queen City and Sparta aquifers model is removed in the development of the Central Transect. Similarly, the no-flow boundary of the Yegua-Jackson Aquifer bottom is substituted by a hydraulic connection to the Yegua-Jackson aquifers through the Cook Mountain semi-confining layer. In the original central portion of the Queen City and Sparta aquifers model, flow through the general head boundary prescribed at the Sparta Aquifer grid cells is equal to 23,380 ft<sup>3</sup>/d whereas zero flow occurs through the no-flow bottom boundary of the three-dimensional Yegua-Jackson Aquifer model (Figure 8-34). Table 8-16 indicates that flow through the semi-confining layer of Cook Mountain Formation equals 306.7 ft<sup>3</sup>/d. This corresponds to only 1.3 percent of the 23,380 ft<sup>3</sup>/d flowing through the Queen City and Sparta aquifers top boundary, indicating that flow in the Central Transect model has to constitute a compromise between the mutually exclusive boundaries and imposed flow conditions in the different three-dimensional models.

Figure 8-35 shows a schematic illustration of the different portions that make up the Central Transect model geometry. The first portion (A) corresponds to the part of the Queen City and Sparta aquifers layers that was absent in the original central portion of the Queen City and Sparta aquifers model and was implemented in the Central Transect by extending the Queen City and Sparta aquifers layers below the Yegua-Jackson Aquifer cross-section. The second (B) and third (C) portion correspond to the original Queen City and Sparta aquifers and Yegua-Jackson Aquifer cross-sections. The uncertainty introduced in the Central Transect model through the assumptions made for the stratigraphy and hydraulic properties assigned to portion (A) of the model is qualitatively described in the mass balance. Table 8-17 summarizes the sums of absolute flows through grid cell bottom faces (sum vertical flow) and absolute flows through grid cell right faces (sum horizontal flow) across all grid cells of the Central Transect. A comparison to the sums of flow corresponding to the entire transect indicates that vertical and horizontal flow occurring in portion (A) constitutes only 5.01 and 1.18 percent of the total vertical and horizontal flow, respectively.

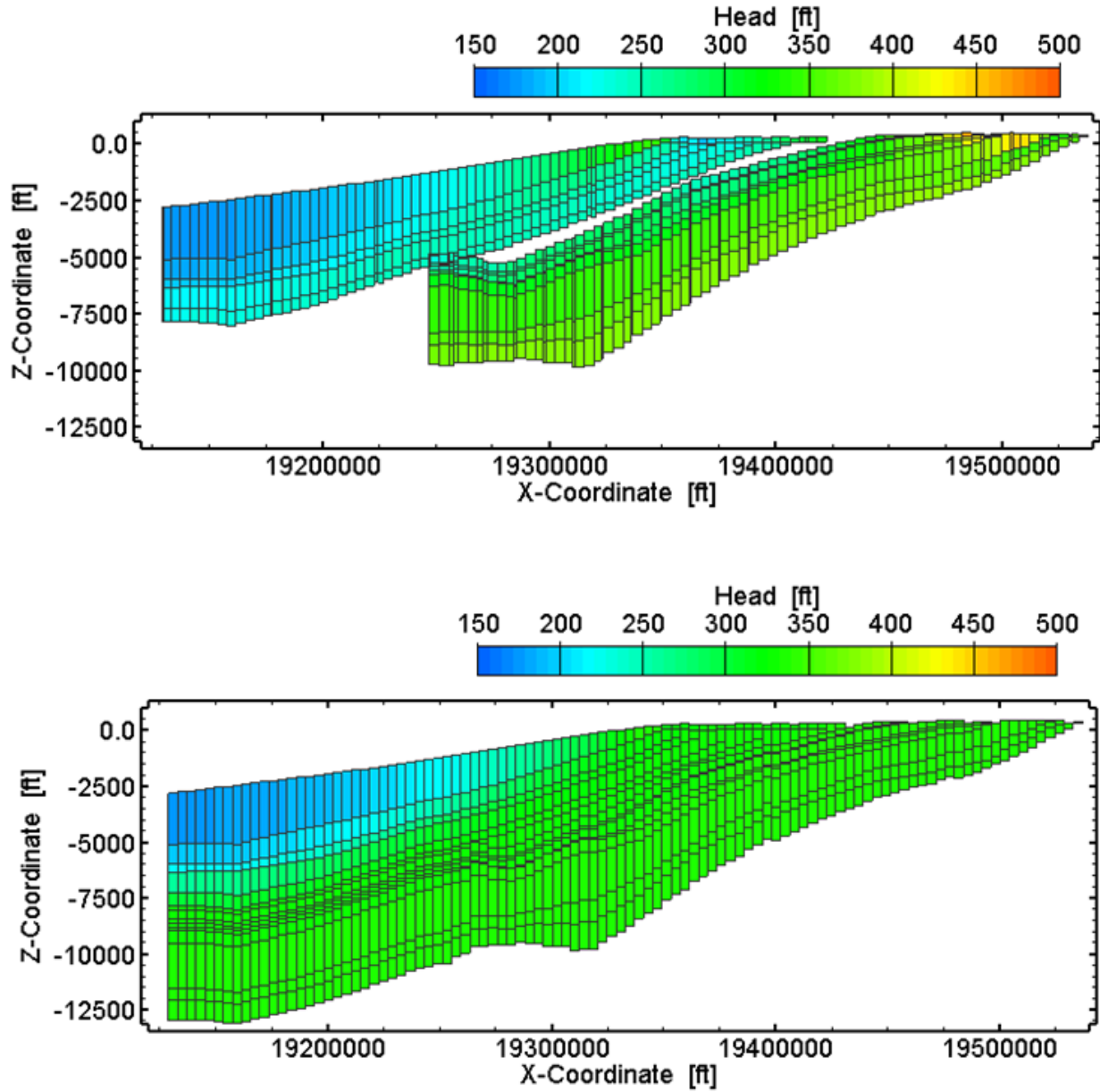


Figure 8-29. Comparison of hydraulic heads predicted with the three-dimensional models of the Yegua-Jackson Aquifer and the central portion of the Sparta, Queen City and Carrizo-Wilcox aquifers cross sections (top) to those predicted with the Central Transect model (bottom).

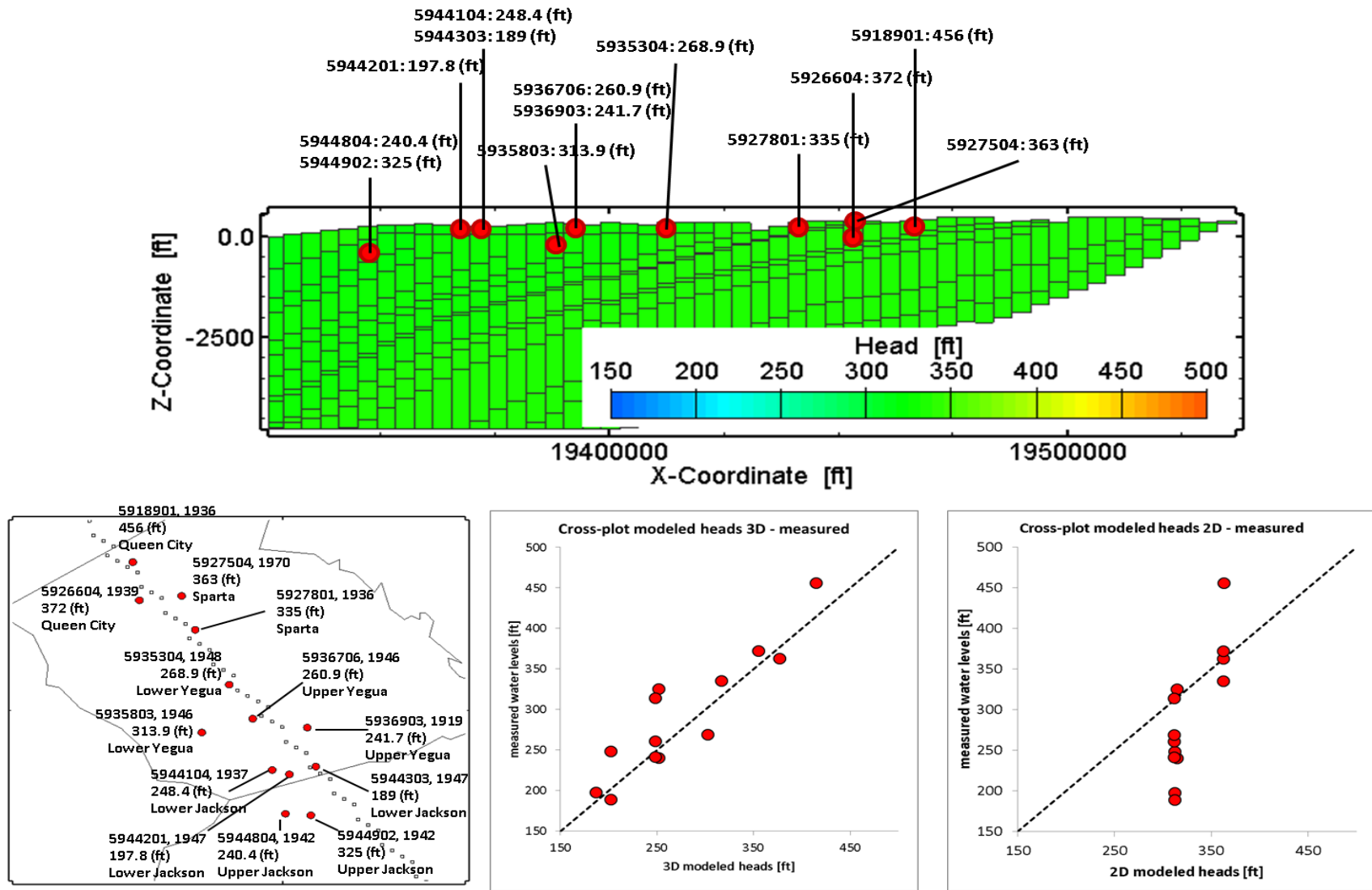


Figure 8-30. Cells corresponding to water level measurements (top) based on projections of well locations to the Central Transect model (bottom, left), and cross-plots between measurements and heads modeled with the 3D (bottom, middle) and the 2D models (bottom, right). State well number (TWDB database), measured water level and corresponding aquifer are indicated next to the well locations.

**Table 8-13. State wells with available water level measurements near the Central Transect model coordinates, measured water levels and modeled heads at cells corresponding to well locations and depths.**

<b>State Well No.</b>	<b>County</b>	<b>X-Coord. [ft]</b>	<b>Y-Coord. [ft]</b>	<b>Aquifer</b>	<b>Head modeled 2D [ft]</b>	<b>Head modeled 3D [ft]</b>	<b>Head measured [ft]</b>
5944804	Washington	6001221	19348581	Upper Jackson	314.5	252.2	240.4
5944902	Washington	6012452	19347817	Upper Jackson	314.5	252.2	325.0
5944104	Burleson	5995383	19370378	Lower Jackson	312.4	202.2	248.4
5944201	Burleson	6002976	19368183	Lower Jackson	312.4	186.9	197.8
5944303	Burleson	6014666	19372093	Lower Jackson	312.4	202.2	189.0
5936706	Burleson	5986726	19395939	Upper Yegua	311.7	248.2	260.9
5936903	Burleson	6010908	19391522	Upper Yegua	311.7	248.2	241.7
5935304	Burleson	5976330	19412941	Lower Yegua	311.8	302.5	268.9
5935803	Burleson	5964287	19389081	Lower Yegua	311.8	248.1	313.9
5927801	Burleson	5961357	19440242	Sparta	362.8	317.1	335.0
5927504	Burleson	5955352	19457180	Sparta	362.8	377.3	363.0
5918901	Burleson	5933740	19474065	Queen City	362.9	415.1	456.0
5926604	Burleson	5936652	19455008	Queen City	362.8	355.4	372.0

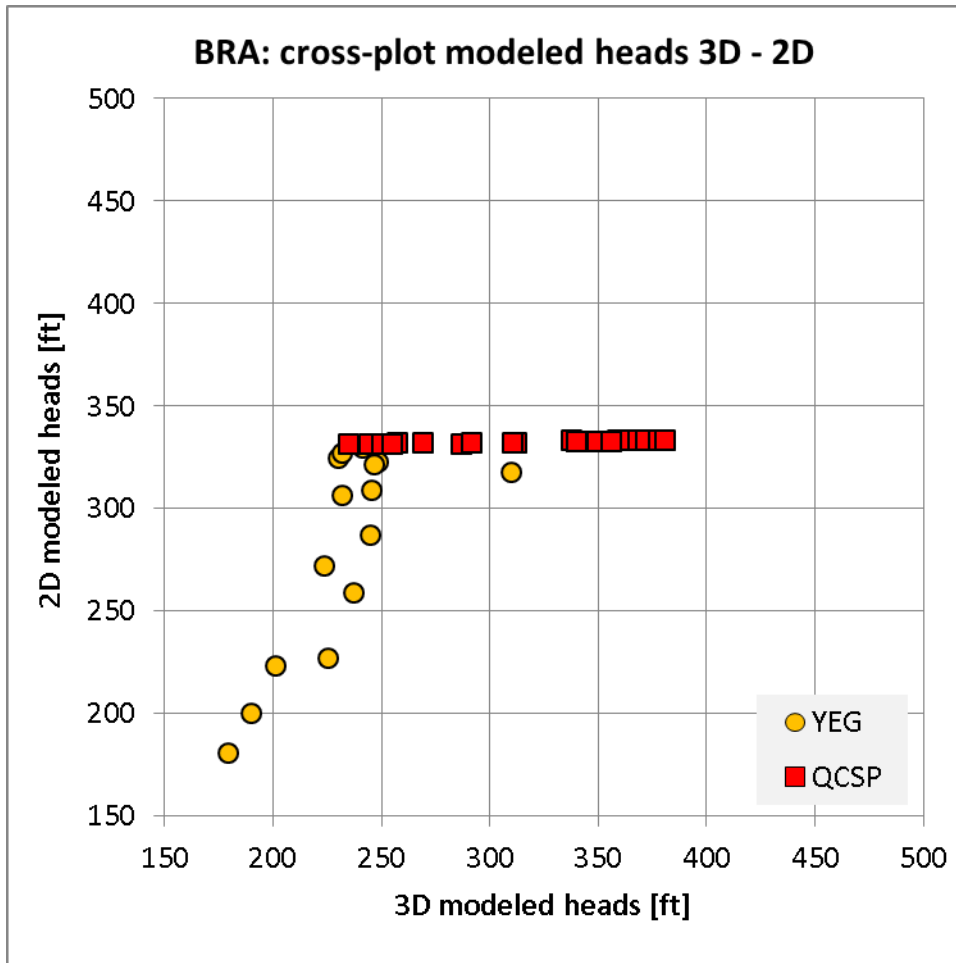
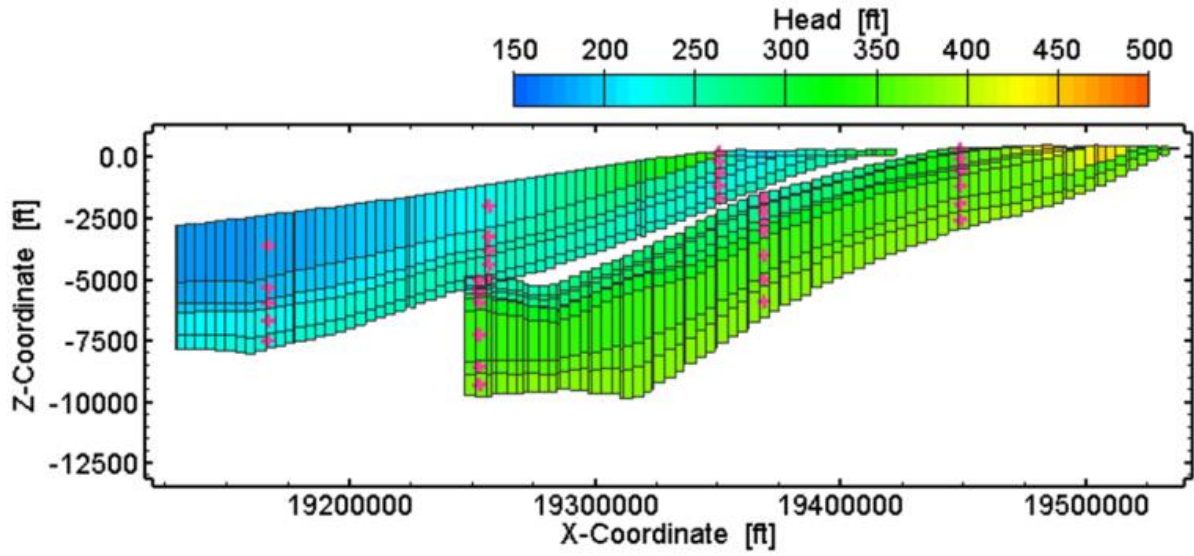


Figure 8-31. Cross-plots of hydraulic heads modeled with the three-dimensional Groundwater Availability Models and the Central Transect model at locations selected as representative for deep and shallow parts of the modeled formations.

**Table 8-14. Selected model cells and their hydraulic heads used for comparison between the Central Transect model and the three-dimensional model Groundwater Availability Models.**

<b>Formation</b>	<b>Cell 3D</b>	<b>Cell 2D</b>	<b>Z-Coord. [ft]</b>	<b>Head 3D [ft]</b>	<b>Head 2D [ft]</b>	<b>Difference [ft]</b>	<b>Rel. Error [%]</b>
Catahoula	296:067:1	91:001:1	-3.62E+03	179.24	181.02	1.78	0.99
Catahoula	298:045:1	69:001:1	-1.99E+03	225.33	226.94	1.61	0.71
Catahoula	300:022:1	46:001:1	1.68E+02	310.11	317.55	7.45	2.40
Upper Jackson	296:067:2	91:001:2	-5.34E+03	189.77	199.88	10.11	5.33
Upper Jackson	298:045:2	69:001:2	-3.25E+03	237.31	259.09	21.78	9.18
Upper Jackson	300:022:2	46:001:2	-1.86E+02	248.54	322.59	74.04	29.79
Lower Jackson	296:067:3	91:001:3	-5.98E+03	201.20	223.34	22.14	11.00
Lower Jackson	298:045:3	69:001:3	-3.81E+03	244.65	287.17	42.52	17.38
Lower Jackson	300:022:3	46:001:3	-6.61E+02	230.29	324.46	94.17	40.89
Upper Yegua	296:067:4	91:001:4	-6.68E+03	223.55	271.84	48.29	21.60
Upper Yegua	298:045:4	69:001:4	-4.39E+03	245.73	308.99	63.26	25.74
Upper Yegua	300:022:4	46:001:4	-1.19E+03	231.97	327.10	95.13	41.01
Lower Yegua	296:067:5	91:001:5	-7.51E+03	231.82	306.22	74.40	32.10
Lower Yegua	298:045:5	69:001:5	-4.98E+03	246.85	321.43	74.58	30.21
Lower Yegua	300:022:5	46:001:5	-1.71E+03	241.30	329.49	88.19	36.55
Sparta	118:090:1	70:001:7	-5.69E+03	235.18	331.34	96.16	40.89
Sparta	127:063:1	42:001:7	-1.66E+03	244.41	331.75	87.34	35.73
Sparta	133:044:1	22:001:7	3.14E+02	351.37	332.92	-18.45	5.25
Weches	118:090:2	70:001:8	-5.97E+03	250.18	331.45	81.27	32.48
Weches	127:063:2	42:001:8	-1.91E+03	257.07	331.82	74.75	29.08
Weches	133:044:2	22:001:8	2.33E+02	344.52	332.94	-11.58	3.36
Queen City	118:090:3	70:001:9	-6.15E+03	254.79	331.49	76.69	30.10
Queen City	127:063:3	42:001:9	-2.24E+03	268.96	331.91	62.96	23.41
Queen City	133:044:3	22:001:9	-5.17E+01	340.10	332.96	-7.13	2.10
Reklaw	118:090:4	70:001:10	-6.28E+03	286.63	331.75	45.12	15.74
Reklaw	127:063:4	42:001:10	-2.65E+03	291.80	332.12	40.32	13.82
Reklaw	133:044:4	22:001:10	-3.70E+02	341.84	332.99	-8.85	2.59
Carrizo	118:090:5	70:001:11	-6.60E+03	312.40	331.99	19.59	6.27
Carrizo	127:063:5	42:001:11	-3.04E+03	310.55	332.33	21.79	7.02
Carrizo	133:044:5	22:001:11	-5.83E+02	337.91	333.03	-4.88	1.44
Upper Wilcox	118:090:6	70:001:12	-7.91E+03	339.97	332.46	-7.51	2.21
Upper Wilcox	127:063:6	42:001:12	-4.02E+03	349.52	332.93	-16.59	4.75
Upper Wilcox	133:044:6	22:001:12	-1.17E+03	359.00	333.17	-25.83	7.20
Middle Wilcox	118:090:7	70:001:13	-9.22E+03	355.96	332.80	-23.16	6.51
Middle Wilcox	127:063:7	42:001:13	-5.02E+03	364.71	333.37	-31.35	8.60
Middle Wilcox	133:044:7	22:001:13	-1.90E+03	368.37	333.57	-34.79	9.45
Lower Wilcox	118:090:8	70:001:14	-9.95E+03	372.25	333.06	-39.19	10.53
Lower Wilcox	127:063:8	42:001:14	-5.90E+03	377.59	333.51	-44.08	11.67
Lower Wilcox	133:044:8	22:001:14	-2.56E+03	380.68	333.58	-47.09	12.37

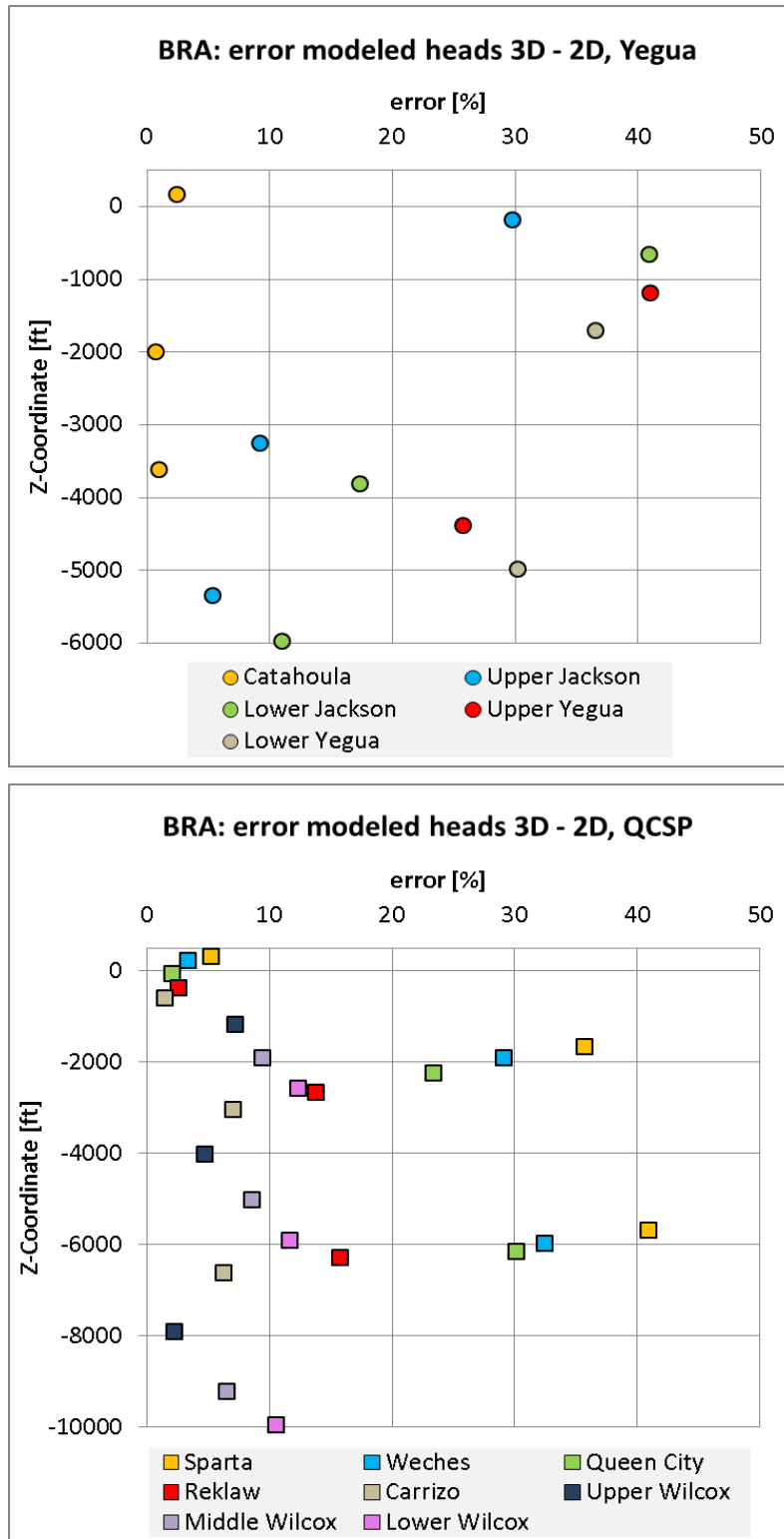


Figure 8-32. Comparison of hydraulic heads between Central Transect model and Groundwater Availability Models: plots of relative error versus depth for the Yegua-Jackson Aquifer (top) and the Sparta, Queen City and Carrizo-Wilcox aquifers (bottom).

**Table 8-15. Overview of recharge assigned to outcrop cells per layer in the Central Transect model. Red colors indicate dried-out cells where recharge is transferred to the cells of the underlying layer.**

<b>Layer</b>	<b>Layer ID</b>	<b>Outcrop Cells (#)</b>	<b>Recharge per Cell (ft<sup>3</sup>/d)</b>	<b>Recharge per Layer (ft<sup>3</sup>/d)</b>	<b>Total Flow Bottom Faces (ft<sup>3</sup>/d)</b>	<b>Total Flow Upper Faces (ft<sup>3</sup>/d)</b>
Catahoula	1	0	0.0	0.0	418.17	0.0
Upper Jackson	2	2	6.96	13.93	404.23	-418.17
Lower Jackson	3	3	6.96	20.90	383.32	-404.23
Upper Yegua	4	4	6.96	27.87	355.44	-383.32
Lower Yegua	5	7	6.96	48.78	306.66	-355.44
Cook Mountain	6	0	0.0	0.0	306.66	-306.66
Sparta	7	4	13.93	41.81	264.84	-306.66
Weches	8	3	13.93	27.87	236.96	-264.84
Queen City	9	5	13.93	83.63	153.33	-236.96
Reklaw	10	2	13.93	27.87	125.45	-153.33
Carrizo	11	1	13.93	13.93	111.51	-125.45
Upper Wilcox	12	5	13.93	83.63	27.63	-111.51
Middle Wilcox	13	2	13.93	27.87	0.0	-27.87
Lower Wilcox	14	0	0.0	0.0	0.0	0.0

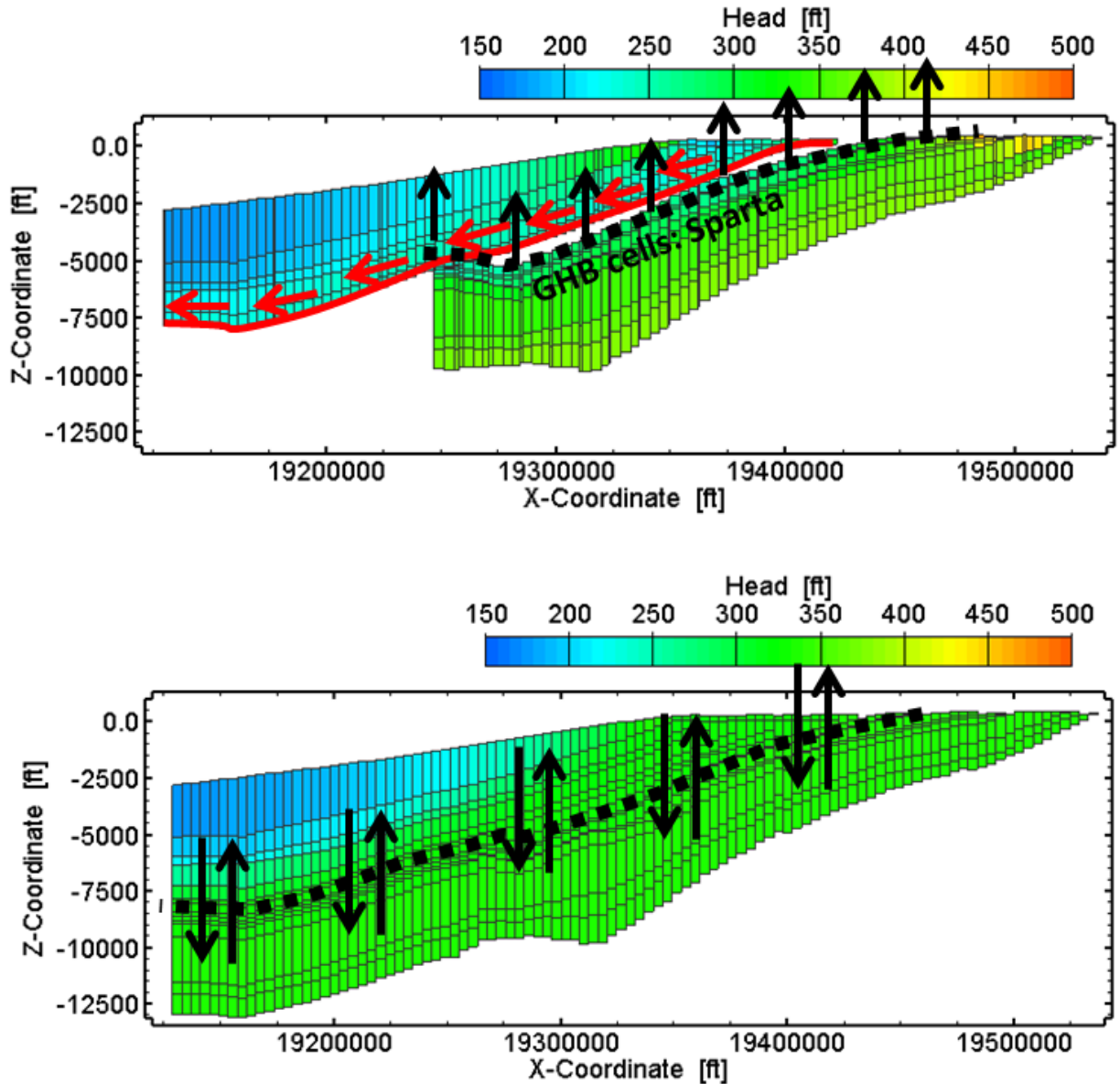


Figure 8-33. Illustration of conceptual differences in the boundary conditions used in the 3D models and the 2D transect: the original Yegua-Jackson Aquifer Groundwater Availability Model treats the base of the Lower Yegua unit as a no-flow boundary whereas, in the transect model, water flows in vertically through the Cook Mountain Formation. Similarly, the Queen City Sparta Aquifers Groundwater Availability Model treats the Sparta Aquifer unit as a general head boundary whereas hydraulic heads in the Sparta Aquifer unit of the transect model depend strongly on recharge and general head boundary conditions imposed at the outcrop and the Catahoula.

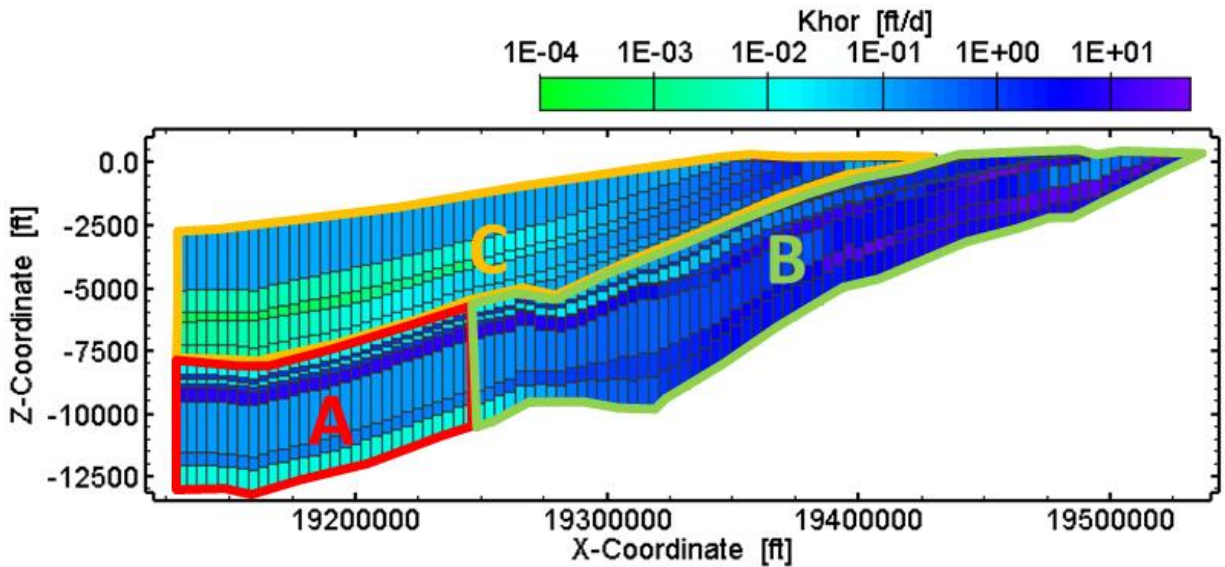


Figure 8-34. Portions of the Central Transect model corresponding to extended (A) and original Queen City and Sparta aquifers Groundwater Availability Model layers (B) and the Yegua-Jackson Aquifer Groundwater Availability Model layers (C).

Table 8-16. Percentage of the water balance that occurs in the deep portions where the Queen City and Sparta aquifers Groundwater Availability Model layers were extended in the Central Transect model. Vertical flows correspond to the sum of absolute values of flows through the bottom face of the model cells in the corresponding portion of the model (A, B, and C). Horizontal flows correspond to the sum of absolute values of flows through the right face of the model cells in the corresponding portion of the model (A, B, and C).

Central Transect Portion	SUM Vertical Flow [ft <sup>3</sup> /d]	SUM Horizontal Flow [ft <sup>3</sup> /d]	Percentage of Water Balance Vertical Flow [%]	Percentage of Water Balance Horizontal Flow [%]
A + B + C	3.922E+03	4.339E+04	-	-
A + B	1.344E+03	8.771E+03	-	-
A	1.968E+03	5.123E+02	-	-
A / (A + B + C)	-	-	5.0	1.2
A / (A + B)	-	-	1.4	5.8

### 8.5.2 Age and Sensitivity Analysis

The sensitivity analysis is carried out by means of backward particle tracking simulations using MODPATH. Groundwater age at individual model cells is evaluated as the travel time from the cell backwards to the outcrop. The hydraulic head distribution and resulting velocity field computed with the Central Transect model forms the basis for the reference particle tracking simulation. Water ages simulated with the reference case are illustrated in Figure 8-35. The same figure shows pathlines from backward particle tracking for two vertical columns of grid cells selected in the model. The color of each pathline varies indicating the time travelled of a particle at the corresponding location. Travel times computed for the Catahoula cells are affected by the general head boundary assigned at these cells. Groundwater ages in the shallow parts of the Yegua-Jackson Aquifer are generally high, varying between 1,000,000 and 10,000,000 years with some exceptions of groundwater ages below 1,000,000 years located mostly in the Upper

Jackson. The reason behind the high groundwater ages even at the cells near or at the outcrop of the Yegua-Jackson Aquifer is indicated by the pathlines of particles placed in the Lower Jackson and Upper Yegua (left column grid cells). These particle tracks do not show origination from the Yegua-Jackson Aquifer outcrop. Instead, the particles originate from the Sparta and the Queen City aquifers outcrop, flowing at first along these aquifers and then almost parallel to the surface and into the Lower Jackson and Upper Yegua. Groundwater ages in the shallower parts of the Sparta, Queen City and Carrizo-Wilcox aquifers vary between 100,000 and 1,000,000 years and increase above 10,000,000 years with increasing depth. Particles placed in the shallow parts of the Lower Yegua, Sparta, Queen City and Carrizo (left column grid cells) originate from the Carrizo and Upper Wilcox outcrop with a large portion of their flow paths occurring along the dip direction and through the Carrizo and Upper Wilcox layers. On the other hand, all particles placed in the deeper parts of the transect (right column grid cells) originate from the outcrops of the Upper and Middle Wilcox layers. Pathlines ending at the deeper parts of the Upper Jackson, Lower Jackson and Upper Yegua indicate flow almost parallel to the dip direction in the deeper parts of the Yegua, vertical flow through the Sparta, Queen City and Carrizo-Wilcox aquifers, and flow along the Upper Wilcox layer. Particles placed in the deeper parts of the Lower Yegua, Sparta, Queen City and Carrizo-Wilcox layers mostly originate from the Middle Wilcox outcrop flowing parallel to the dip. Groundwater ages in the shallow portion of the Wilcox vary between 1,000,000 and 10,000,000 years, increasing up to 1,000,000,000 years in the deeper parts of the Central Transect.

All subsequent simulations of water age sensitivity to variations in input parameters will be compared to the reference case. The sensitivity analysis is carried out for horizontal conductivity (Khor), leakance (Vcont) and recharge (RCH) varied individually for each of the 14 model layers where these input parameters are applicable. This results in 152 sensitivity runs that are listed in Table 8-17.

Comparison to the sensitivity runs is then performed for selected cells of the model. These correspond to locations and depths of wells where water age measurements are available, projected to the Central Transect line. A complete list of the available wells, their coordinates, screened aquifers, corresponding model cells and measured versus modeled water ages is given in Table 8-18. Only 17 of the total 23 wells are used for the current sensitivity analysis, as projections of six wells to the transect line result in inactive model cells outside the modeled area. An overview of the well locations with respect to the Central Transect model as well as the model cells assigned to these locations is given in Figure 8-36.

Comparison of the measured ages of groundwater and the simulated ages of groundwater from the cross-sectional models in Table 8-16 indicate significant differences ranging from one to three orders of magnitude. The laboratory-measured ages from 19 of the samples ranges from 200 to 43,070 years and four samples were estimated to be greater than 43,500 years old. The simulated ages range from 1,418,000 to 8,511,000 years old. The old simulated ages are the result of the small hydraulic gradients that exist in the calibrated cross-sectional model for the Central Transect.

The sensitivity analysis was carried out by varying the input parameters separately in each layer. For each sensitivity run, water ages from the 17 selected model cells were used to derive the average that is then used as a comparative measure to the reference case. The resulting sensitivity to formation horizontal conductivity, leakance and recharge is shown in Figure 8-37 through

Figure 8-39. Each figure presents the summarized water age sensitivity separately for the Yegua-Jackson Aquifer (top image) and the Queen City and Sparta aquifers input (bottom image).

It should be noted that only one observation cell is located in the Jackson, while the remaining 16 cells are scattered among the Sparta, Queen City, Carrizo and Middle Wilcox cells. Therefore, sensitivity to input parameters assigned to the Yegua-Jackson Aquifer layers are less pronounced compared to sensitivity to parameters of the Queen City and Sparta aquifers layers.

The plots of sensitivity to horizontal conductivity (Figure 8-37) indicate a maximum sensitivity for the Carrizo and the Queen City layers. An increase in the horizontal conductivity of the Carrizo results in an increase of average groundwater ages by approximately 4,900,000 years. On the other hand, increasing the Queen City Aquifer conductivity by a factor of 1.5 produces a decrease of water ages by approximately 680,000 years. Sensitivity to horizontal conductivity in the Yegua-Jackson Aquifer is essentially limited to the Upper Jackson and the Lower Jackson layers. These demonstrate opposite responses; water age decreases with increasing conductivity of the Upper Jackson and with decreasing conductivity of the Lower Jackson. Sensitivity to horizontal conductivity of the Queen City and Sparta aquifers differs for every layer and does not indicate patterns or a consistent behavior that would allow obvious conclusions about the effect of horizontal conductivity on water ages for the selected observation points. In general, water age differences from the reference case vary between -300,000 and 300,000 years with the exception of the “kinks” in the sensitivity plots that will be described in detail later in this section.

Sensitivity to leakance (Figure 8-38) behaves in a more consistent and uniform manner. Increasing the leakance either in the Yegua-Jackson Aquifer or Queen City and Sparta aquifers layers induces an increase in average groundwater age. Leakance of the Cook Mountain Formation layer appears to be the most sensitive with a water age increase of 890,000 years for an increase in leakance by a factor of 1.5. An increase in leakance by a factor of 1.5 in the Yegua-Jackson Aquifer produces an average groundwater age increase within a range of 150,000 to 300,000 years. Similarly, increasing the leakance by the same factor in the Queen City and Sparta aquifers results in an average groundwater age increase within the range of 24,000 to 380,000 years.

Figure 8-39 indicates that the highest sensitivity to recharge corresponds to recharge assigned to the Middle Wilcox and the Weches outcrop. Average water age decreases by 100,000 years for a decrease in recharge at the Weches by a factor of 0.5. Similarly, water age decreases or increases by 500,000 years for increases or decreases in recharge at the Middle Wilcox of 50 percent. Sensitivity to recharge indicates an almost linear behavior for the Yegua-Jackson Aquifer layers, with water ages increasing when increasing recharge at the Yegua-Jackson Aquifer outcrop. The largest range of water age difference from the reference case observed is -440,000 to 440,000 years for recharge in the Lower Jackson outcrop. On the other hand, increases of recharge in the Queen City and Sparta aquifers tend to decrease the simulated water ages.

As indicated by the sensitivity plots, water ages change in a general monotonic fashion for increases or decreases of input parameters. However some exceptions produce “kinks” in the sensitivity plots, meaning that, in some cases, a parameter change by a certain factor induces a response that does not agree with the trend indicated by responses to similar changes of the same parameter by different factors. These cases are discussed separately in the following:

- 111\_K4 (sensitivity to Carrizo Formation horizontal conductivity, fraction of base value 1.5): some observation points indicate an increase of water age with increasing

conductivity while other observation points indicate the opposite. Averaging the water ages from all points results in a non-monotonic behavior due to the different magnitudes of water age change at the different locations. The extreme increase of the average age for a factor of 1.5 is mainly due to significant increases of travel times from the observation point in the Jackson Formation (Clay WSC #1 well) and two observation points in the Sparta Formation (Col Sta Sparta #1 and TAMU Well #2).

- 17\_K1 - 17\_K4 (sensitivity to Sparta Formation horizontal conductivity): water ages from the majority of observation points evolve non-monotonically. No representative behavior can be established from the observation points.
- 17\_R4 (sensitivity to Sparta Formation recharge, fraction of base value 1.5): water ages from several observation points evolve non-monotonically. Different magnitudes of water age change at the different locations influence the average sensitivity. For a recharge increase factor of 1.5, the decrease in water ages is mainly driven by the observation point in the Jackson (Clay WSC #1) and an observation point in the Sparta (Snook #2).
- 19\_K1 - 19\_K4 (sensitivity to Queen City Formation horizontal conductivity): water ages of observation points in the Queen City (Smetana Forest and Lakewood Estates) decrease monotonically with increasing conductivity. The averaging procedure for the other observation points induces non-monotonicity in the sensitivity plot. However, given the magnitude difference of water age change between factors of 0.5 and 1.5, and factors of 0.9 and 1.1, an overall decrease of water age with increasing horizontal conductivity of the Queen City Formation can be concluded.
- 19\_R1 (sensitivity to Queen City Formation recharge, fraction of base value 0.5): in contrast to the general trend, water age is decreased significantly for a factor of 0.5 at observation points in the Jackson (Clay WSC #1), the Carrizo (Col Sta Carrizo #1) and the Middle Wilcox (Bryan #18 and Rockdale #10).
- 110\_K1 - 110\_K4 (sensitivity to Reklaw Formation horizontal conductivity): while water ages from several observation points behave monotonically, different magnitudes of conductivity change induce non-monotonicity in the average. For a factor of 0.5, water age is driven lower by the observation point in the Carrizo (Col Sta Carrizo #1). For a factor of 1.5, water age is significantly decreased at two observation points of the Middle Wilcox (Bryan #18 and Rockdale #10).
- 112\_K1 - 112\_K4 (sensitivity to Upper Wilcox horizontal conductivity, fraction of base value 1.5): different magnitudes of water age increase and decrease at the different observation points lead to the non-monotonic sensitivity of the averaged water age.
- 112\_V4 (sensitivity to Upper Wilcox leakance, fraction of base value 1.5): in general, water ages in the observation points increase with increasing leakance. However, five observation points in the Middle Wilcox (TAME Well #A7, Bryan #18, Bryan #19, Brushy WSC #2 and Rockdale #10) indicate a decrease of water age when changing the factor from 1.1 to 1.5.
- 113\_K1 - 113\_K4 (sensitivity to Middle Wilcox horizontal conductivity): all observation points from the Carrizo, Sparta, Jackson and Queen City Formations indicate consistent increases or decreases for increasing horizontal conductivity. On the other hand, the observation points from the Middle Wilcox do not indicate any consistent pattern in the water age response to sensitivity.

- 16\_V4 (sensitivity to Cook Mountain Formation leakance, fraction of base value 1.5): the average water age from observations is consistently characterized by increasing age values for increasing leakance of the Cook Mountain Formation. However, for a factor of 1.5 a single observation point that belongs to the Jackson layer (Clay WSC #1) and is located near the surface demonstrates an extremely high and unrealistic water age of 12,000,000 years. Compared to the water age predicted with run 16\_V3, this corresponds to an increase of almost two orders of magnitude. The difference of average water age after removing this single value is reduced to 150,000 years.

Similarly to Gonzales sensitivity analysis, the behavior of groundwater ages computed with the Central Transect model depend strongly on the locations of the observation points. Observation points located in the same aquifer layer may demonstrate the opposite response of water age to a change in a given parameter. Similarly, water ages from observation points in neighboring layers behave differently despite their proximity. Once more, this type of sensitivity can be explained as a pronounced sensitivity of pathlines to the input parameters. Figure 8-33 shows that particles tracked backwards from two neighboring cells in the shallow parts of the Upper Yegua and the Lower Yegua follow very different flow paths originating from the Queen City Aquifer and the Carrizo-Wilcox Aquifer outcrop, respectively. Similarly, particles placed in deeper parts of the same layers can be tracked back to the Wilcox outcrop, however following very different flow paths. This implies that changes in parameters within a formation layer may alter groundwater age at one point while not affecting it at all at the neighboring point despite their proximity.

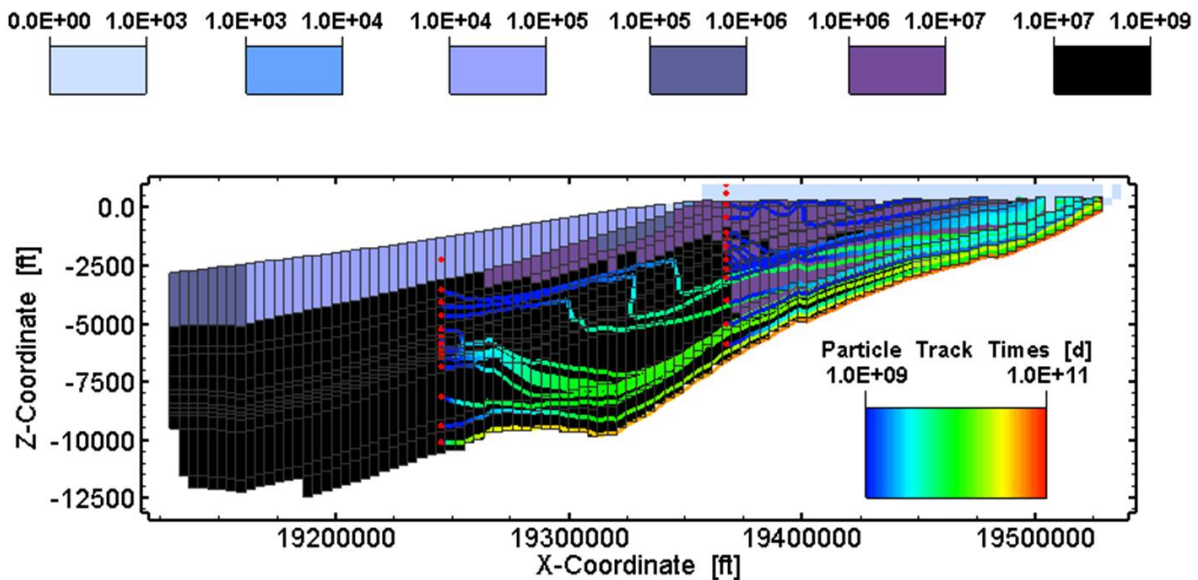


Figure 8-35. Groundwater ages (in years) and particle pathlines computed with the reference simulation of the Central Transect model.

**Table 8-17. Overview of water age sensitivity runs carried out with the Central Transect model.**

Parameter	Horizontal Conductivity				Leakance				Recharge			
	0.5	0.9	1.1	1.5	0.5	0.9	1.1	1.5	0.5	0.9	1.1	1.5
<b>Layer</b>												
Catahoula	11_K1	11_K2	11_K3	11_K4	11_V1	11_V2	11_V3	11_V4	-	-	-	-
Upper Jackson	12_K1	12_K2	12_K3	12_K4	12_V1	12_V2	12_V3	12_V4	12_R1	12_R2	12_R3	12_R4
Lower Jackson	13_K1	13_K2	13_K3	13_K4	13_V1	13_V2	13_V3	13_V4	13_R1	13_R2	13_R3	13_R4
Upper Yegua	14_K1	14_K2	14_K3	14_K4	14_V1	14_V2	14_V3	14_V4	14_R1	14_R2	14_R3	14_R4
Lower Yegua	15_K1	15_K2	15_K3	15_K4	15_V1	15_V2	15_V3	15_V4	15_R1	15_R2	15_R3	15_R4
Cook Mountain	16_K1	16_K2	16_K3	16_K4	16_V1	16_V2	16_V3	16_V4	-	-	-	-
Sparta	17_K1	17_K2	17_K3	17_K4	17_V1	17_V2	17_V3	17_V4	17_R1	17_R2	17_R3	17_R4
Weches	18_K1	18_K2	18_K3	18_K4	18_V1	18_V2	18_V3	18_V4	18_R1	18_R2	18_R3	18_R4
Queen City	19_K1	19_K2	19_K3	19_K4	19_V1	19_V2	19_V3	19_V4	19_R1	19_R2	19_R3	19_R4
Reklaw	110_K1	110_K2	110_K3	110_K4	110_V1	110_V2	110_V3	110_V4	110_R1	110_R2	110_R3	110_R4
Carrizo	111_K1	111_K2	111_K3	111_K4	111_V1	111_V2	111_V3	111_V4	111_R1	111_R2	111_R3	111_R4
Upper Wilcox	112_K1	112_K2	112_K3	112_K4	112_V1	112_V2	112_V3	112_V4	112_R1	112_R2	112_R3	112_R4
Middle Wilcox	113_K1	113_K2	113_K3	113_K4	113_V1	113_V2	113_V3	113_V4	113_R1	113_R2	113_R3	113_R4
Lower Wilcox	114_K1	114_K2	114_K3	114_K4	-	-	-	-	-	-	-	-

**Table 8-18. Overview of wells with available water age measurements and comparison to water age modeled using particle tracking in the Brazos transect.**

Well ID	X-Coord [ft]	Y-Coord [ft]	Aquifer	GUA Model Cell ID	Remarks	Water Age Measured [yrs]	Water Age Simulated [yrs]
N. Milam WSC #2	5906470	19570600	Carr-Wilcox	-		2,950	-
Robertson WSC #3	6006860	19656100	Carr-Wilcox	-		8,920	-
Robertson WSC #4	6035210	19695700	Carr-Wilcox	-		14,330	-
Col Sta Carrizo #1	6022450	19501500	Carrizo	24:01:11		41,870	2.042E+06
Col Sta #5	6022440	19501500	Simsboro	24:01:13		37,830	2.368E+06
Col Sta Sparta #1	6034080	19501900	Sparta	25:01:07		16,490	8.134E+05
Clay WSC #1	6070900	19392400	Jackson	43:01:02		>43,500	7.337E+06
Smetana Forest	6027640	19489700	Queen City	26:01:09		35,050	1.926E+06
Lakewood Estates	6026960	19511600	Queen City	22:01:09		11,200	1.418E+06
Snook #3	6029560	19425600	Sparta	34:01:07		27,640	2.977E+06
TAMU Well #7	6022420	19489800	Simsboro	23:01:13		25,320	2.307E+06
TAMU Well #A7	6028350	19481500	Simsboro	27:01:13		>43,500	2.722E+06
Calvert #4	5961720	19600700	Simsboro	2:01:13	outcrop	43,070	0.000E+00
Hearne #2	5989200	19564800	Simsboro	11:01:13		32,140	2.019E+06
Bryan #18	6025580	19511900	Simsboro	22:01:13		>43,500	3.637E+06
Bryan #19	6024810	19504700	Simsboro	23:01:13		39,560	2.307E+06
Brushy WSC #2	6046000	19476800	Simsboro	30:01:13		>43,500	3.114E+06
Rockdale #10	5863770	19484100	Simsboro	6:01:13		1,460	1.858E+06
TAMU Well #2	6024040	19485000	Sparta	26:01:07		39,770	8.511E+05
Snook #2	6031280	19425100	Sparta	36:01:07		35,780	3.399E+06
Ramblewood #1	6048110	19477000	Yegua	-		14,560	-
TAMU Farm Well	6044350	19440600	Alluvial	-		200	-
TDJC Buffalo Ranch	6055750	19438900	Alluvial	-		42,880	-

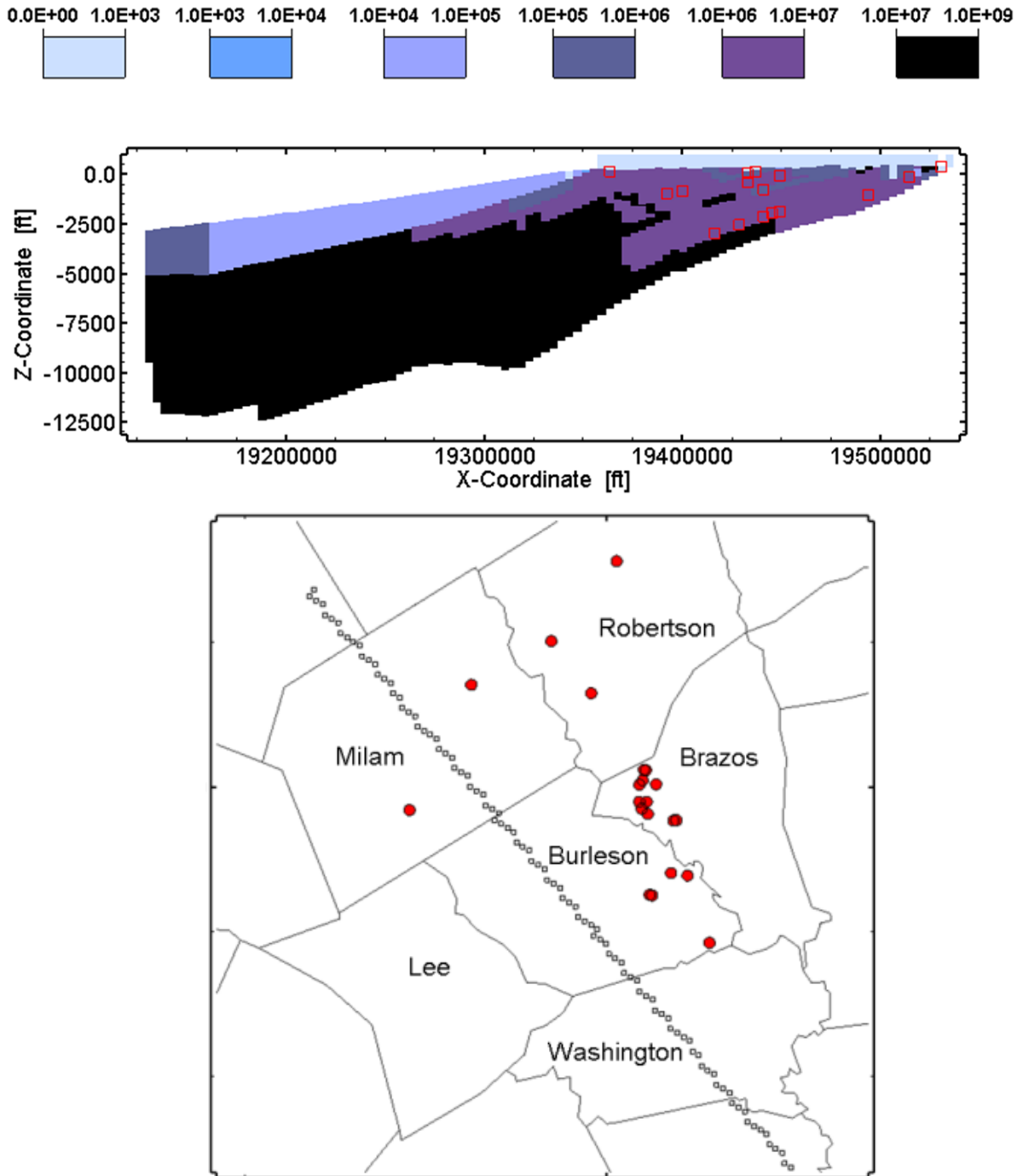


Figure 8-36. Model cells corresponding to water age measurements projected locations and depths in the Central Transect.

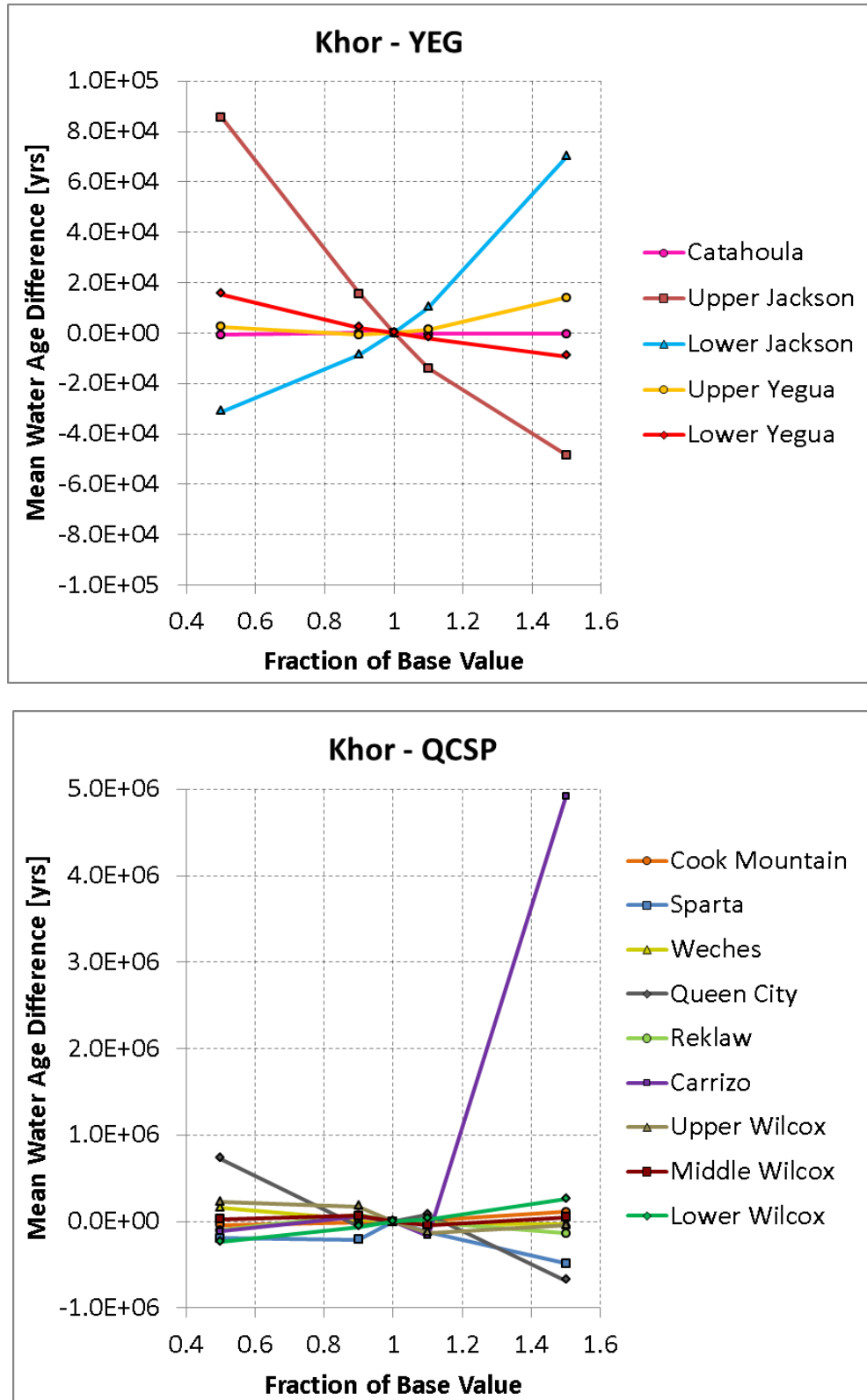


Figure 8-37. Water age sensitivity to layer horizontal conductivity, Central Transect model.

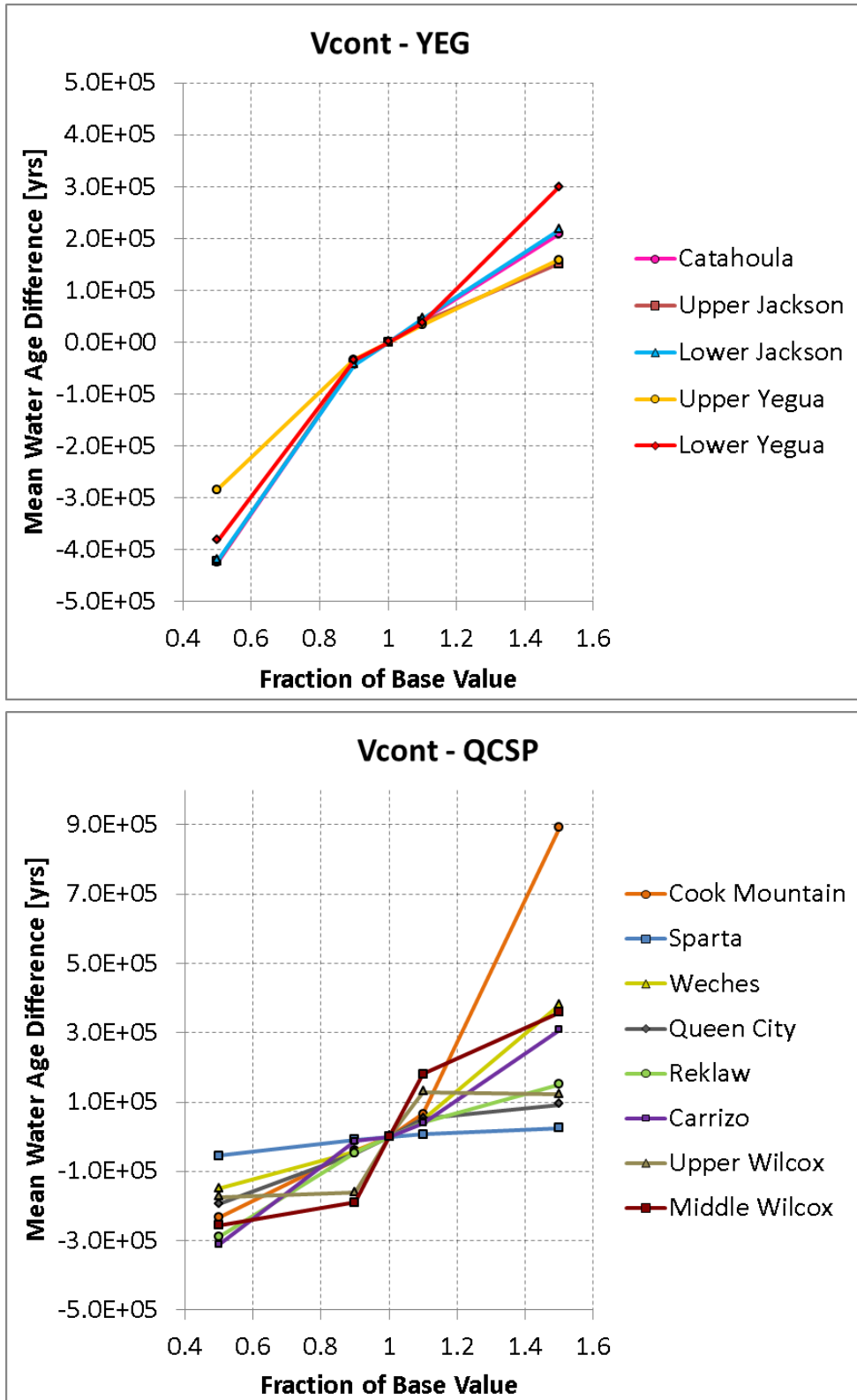


Figure 8-38. Water age sensitivity to layer leakance, Central Transect model.

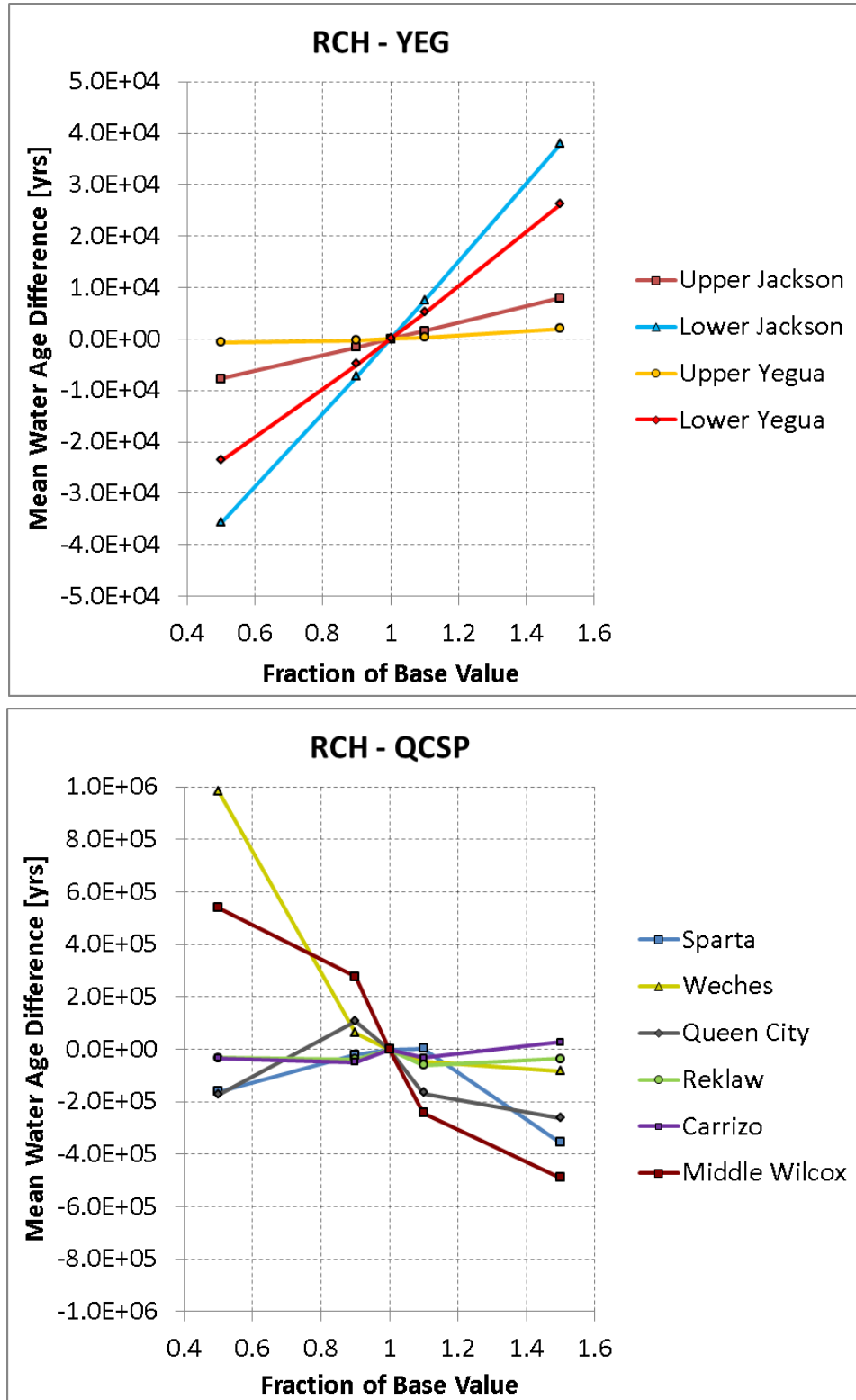


Figure 8-39. Water age sensitivity to recharge at layer outcrop, Central Transect model.

## 8.6 Modeling Discussion

Two-dimensional transect models of the Yegua-Jackson, Sparta, Queen City and Carrizo-Wilcox aquifers were developed to assess groundwater ages and downgradient movement of water. The transect models were developed based on geometries and data extracted from the existing three-dimensional Groundwater Availability Models of the Yegua-Jackson, Sparta, Queen City and Carrizo-Wilcox aquifers.

The Yegua-Jackson Aquifer model comprises model layers representing the Catahoula, Upper Jackson, Lower Jackson, Upper Yegua and Lower Yegua units. The models include the Sparta, Weches, Queen City, Reklaw, Carrizo, Upper Wilcox, Middle Wilcox and Lower Wilcox units. These Groundwater Availability Models were used to extract cross-sections at two selected transect lines intersecting the aquifer outcrops in the area of Guadalupe County and in the area of Brazos County. The extracted cross-sections were combined to form the two transect models in the Guadalupe and Brazos river basins by implementing the confining Cook Mountain Formation between the Lower Yegua bottom and the Sparta Aquifer top and, where necessary, by extending the cross-sections accordingly to match the down-dip extent of the Yegua-Jackson Aquifer Groundwater Availability Model. The Cook Mountain Formation in the transect models therefore substituted the general head boundary prescribed at the Sparta Aquifer in the Queen City and Sparta Aquifers Groundwater Availability Model and the no-flow boundary assigned to the bottom of the Lower Yegua in the Yegua-Jackson Aquifer Groundwater Availability Model. Additionally, some uncertainty was introduced through the cross-section extensions.

Using the original Groundwater Availability Models, steady-state simulations were used to derive a mass balance at the aquifer outcrops delineated in the Guadalupe River and the Brazos River basins. The analysis has shown that net recharge calculated locally at the transect outcrops cannot adequately reproduce the flow conditions in the subsurface, as these are dictated by three-dimensional flow patterns imposed by the boundary conditions and flow gradients on a regional scale. Flows lateral to the transect plane have a pronounced effect compared to flows that infiltrate the grid cells through the outcrop and eventually discharge through the Catahoula flowing upwards and vertically to the younger formations.

The first step of the current modeling approach was therefore a calibration of the transect models with respect to net recharge at the outcrop after balancing for precipitation recharge, evapotranspiration and interaction with surface water bodies. In parallel, leakance of the Cook Mountain Formation that determines the level of confinement or hydraulic connection between the Yegua-Jackson Aquifer and Sparta, Queen City and Carrizo-Wilcox aquifers was also calibrated. The calibration showed that the range of hydraulic heads in the Queen City and Sparta aquifers is very narrow in the transect models, an effect that partly extends into the Yegua-Jackson Aquifer depending on the Cook Mountain Formation leakance. Consequently hydraulic heads in the Yegua-Jackson Aquifer were determined by the interplay between the general head boundary prescribed at the Catahoula and the amount of inflow from the Queen City and Sparta aquifers through the Cook Mountain Formation. Changes in the calibrated parameters produced shifting of hydraulic head values without increasing the variance of their distribution. Since hydraulic heads behave in a significantly more uniform fashion in the transect models, the calibration resulted in distributions of hydraulic heads for the Yegua-Jackson Aquifer and the Queen City and Sparta aquifers matching those of the original three-dimensional models only in an averaged sense.

The analyses of mass balances from the two-dimensional transect models showed that the flow patterns are dictated by the boundary conditions. Water mass infiltrating as recharge at the outcrops flows through the model layers generally down dip and also vertically upwards crossing the model layers until it is discharged through the general head boundary of the Catahoula. This cross-formational vertical flow is imposed by the no-flow boundary conditions at the bottom of the models and at the down-dip edge of the transect model domain. Analysis of the mass balance further showed that the amount of flow occurring in the portions of the transects that were extended after extraction from the original Groundwater Availability Models to connect the aquifers is small compared to the overall flow in the transects. The associated uncertainty with this modification is negligible. However, the amount of vertical flow through the Cook Mountain Formation layer indicates that the transect models can only constitute a compromise between the original models and their boundary conditions. This compromise does not allow a reproduction of the hydraulic heads in the three-dimensional models by the two-dimensional transect models. Note that the Cook Mountain is treated as a general-head boundary condition in the Groundwater Availability Model for the Sparta, Queen City and Carrizo-Wilcox aquifers while it is treated as a no-flow boundary in the Groundwater Availability Model for the Yegua-Jackson Aquifer. Therefore, any combination of the Groundwater Availability Models cannot agree with both of the models.

The hydraulic head distribution and relevant flow fields computed with the steady-state transect model simulations are used to estimate groundwater ages based on particle tracking simulations. The reference cases using the calibrated parameters for Gonzales and Central Transect models show groundwater ages varying between 100,000 and 1,000,000 years in the shallow portions of the aquifers, and between 1,000,000 and 100,000,000 years in the deeper portions of the aquifers with water ages reaching 1,000,000,000 years in the deepest parts near the down-dip edge of the models. Particle pathlines indicate that groundwater ages in the shallow portions of the aquifers are determined to a great extent by flow paths originating at the outcrops of the Sparta and the Queen City aquifers, whereas groundwater ages in the deeper parts are dictated by flow paths originating from the outcrops of the Carrizo-Wilcox Aquifer.

The models were additionally used to investigate the sensitivity of groundwater ages to formation horizontal conductivity, leakance and recharge at the outcrop. The sensitivity was analyzed with incremental changes of these input parameters per layer while monitoring the change in the predicted-groundwater age at selected locations of the transect corresponding to available water age measurements in the area. The sensitivity analysis consistently showed that input parameters for the Queen City and Sparta aquifers are more sensitive to changes in average groundwater age than those parameters assigned to the Yegua-Jackson Aquifer portions of the transects. In some cases, incremental changes in formation parameters induced changes in the average groundwater age on the order of millions of years. The analysis further indicated that groundwater ages responded in very different ways at the different observation points. For example, groundwater ages at certain depths within an aquifer may increase for a given incremental change to an input parameter, the opposite may apply for a different depth within the same aquifer. Similarly, in some cases, changes in water age did not respond monotonically to monotonic increases or decreases of an input parameter. Such effects are attributed to the significant sensitivity of flow paths within the transects. The analysis showed that, for both transects, flow paths of neighboring points can be significantly different, such that incremental changes in input parameters may entirely change the particle travel path that groundwater would have to follow to reach a given monitoring location.

There is a clear discrepancy between the simulated groundwater ages in the three-dimensional Queen City and Sparta aquifers models and that in the two-dimensional models. This results from the explicit incorporation of the overlying Yegua-Jackson Aquifer units in the two-dimensional model. For the equivalent down-dip flow observed in the three-dimensional model to occur in the two-dimensional model, the observed heads in the Yegua-Jackson Aquifer units would be violated with simulated heads being approximately 100 feet too high. The indications from the two-dimensional models are that, to simultaneously match the heads in the Sparta Aquifer units and the Yegua-Jackson Aquifer units, significantly less down-dip flow must occur than that in the three-dimensional Queen City and Sparta aquifers models. However, the simulated groundwater ages from the three-dimensional Queen City and Sparta aquifers model in Atascosa County compares well with age estimates based on geochemistry by Pearson and White (1967) as shown in Kelley and others, (2004). A possible outcome of this is that the three-dimensional model over predicts (scales) hydraulic conductivity and leakance of confining units to increase velocities down dip over what may truly be the current integrated travel path velocity.

One explanation for this discrepancy may be due to the hydrologic conditions which resulted in the observed groundwater ages. Harrison and Summa (1991) show that past conditions affecting the entire Gulf Coast Aquifer system can result in deeper penetration of meteoric water into the down-dip portions of the aquifers than that expected under current conditions. They indicate that sea levels in the Gulf of Mexico were 200 meters lower than present levels during Oligocene times and estimate that, under these conditions, meteoric water can be expected to flow down-dip an additional 75 kilometers within the Wilcox Group of the Carrizo-Wilcox Aquifer compared to what would be expected under current sea levels. Harrison and Summa (1991) also estimate that the recent development of geopressures which restrict the penetration of meteoric water under current conditions were not present in Miocene and earlier times when a smaller compactional force allowed deeper invasion of meteoric water. Given that sea levels level during the last glacial low stand (18,000 years before present) were approximately 130 meters lower than present levels and 40 to 50 meters lower just 10,000 years ago, a significantly greater penetration of meteoric water would be expected than under present conditions.

In other words, groundwater ages in the confined or deeper portions of the Tertiary-aged aquifers, particularly those in excess of 10,000 years may be a result of very different hydrologic conditions than exist today. Therefore, the general-head-boundaries used in the three-dimensional Queen City and Sparta aquifers models – which are a surrogate for sea water levels representing the exit avenue of down-dip groundwater outflow – may be more representative of ancient conditions rather than current conditions for groundwater simulated to be tens of thousands of years old or greater. Furthermore, the amount of down-dip flow simulated in the two-dimensional models may be more representative of current conditions. Ultimately, the concept of steady-state conditions existing over time scales of more than tens of thousands of years may be unfounded. It follows that the comparison of steady-state groundwater model simulations to observed groundwater ages may be equally unfounded. The sediments that comprise the aquifers being simulated were deposited between 60 and 32 million years before present. Since that time, there have been 12 major depositional episodes that would also correlate to major eustatic changes (Galloway and others, 2000).

Simulated ages within the two-dimensional transect models are extremely sensitive to changes in the recharge to the Carrizo-Wilcox Aquifer and to changes in the leakance of the Cook Mountain Formation confining unit. For example, increasing either by a factor of 1.5 can result in a

reduction in the mean groundwater age on the order of 1,000,000 years in the Gonzales Transect. Since both of these parameters are poorly constrained, there is significant uncertainty in the simulated groundwater ages.

## 9 Conclusions

There are three general water chemistries in the major and minor aquifers in Groundwater Management Areas 11, 12 and 13. They are sodium-bicarbonate type water, sodium-sulfate-chloride type water and calcium-magnesium-sodium-bicarbonate water.

The occurrence of sodium-bicarbonate type water is common in Tertiary-aged aquifers, Carrizo-Wilcox, Queen City and Sparta, along the Texas gulf coast from east Texas to south Texas. The Yegua-Jackson Aquifer typically is not a sodium-bicarbonate water, but a sodium-sulfate-chloride water. The Brazos River Alluvium Aquifer in Groundwater Management Area 12 is a mixed cation (calcium-magnesium-sodium) bicarbonate type water.

The sodium-bicarbonate waters are most common in that they are the dominant water type in the most prolific and most transmissive aquifers in Groundwater Management Areas 11, 12 and 13. These are the Carrizo-Wilcox Aquifer in east Texas, the Wilcox Group of the Carrizo-Wilcox Aquifer in central Texas (primarily the Simsboro Formation) and the Carrizo Sand Formation portion of the Carrizo-Wilcox Aquifer, the Queen City and the Sparta in east and central Texas. The Queen City and Sparta aquifers are less productive farther to the south.

The sodium-bicarbonate waters originate as a calcium-magnesium-chloride-sulfate in the outcrop (recharge zone). As they flow into the deeper confined sections between these aquifers they “evolve” to a sodium-bicarbonate water. Several geochemical reactions of the groundwater and the aquifer lithology cause the formation of the sodium-bicarbonate water. Each step is listed below and is evident in several graphs for each aquifer in each of the regions (transects) investigated in this study. The water chemistry for each aquifer in each of the four transect regions was evaluated in detail to better understand the important geochemical reactions that result in the sodium-bicarbonate type water. It was surprising how the same set of chemical reactions occurred in the different aquifers, whether they are in the Wilcox Group of the Carrizo-Wilcox Aquifer, the Carrizo Sand Formation portion of the Carrizo-Wilcox Aquifer, the Queen City Aquifer or possibly the Sparta Aquifer.

1. Where the process starts in in the outcrop, where calcite is dissolved. Calcium and bicarbonate concentrations increase and pH begins to rise.
2. Presumably the availability of cation-exchange sites on clays is very small, such that the exchange of sodium for calcium is minor and the water stays a calcium-type water. The available exchange sites in the outcrop may have been depleted over time.
3. As groundwater flows down the hydraulic gradient from the outcrop into the confined section, the low pH groundwater encounters enough clay with available exchange sites. The cation exchange of sodium for calcium begins.
4. The exchange of sodium on the clays for calcium on the water keeps the waters slightly under saturated with respect to calcite, so more calcite can then be dissolved. These two chemical reactions cause the sodium and bicarbonate and pH to rise.
5. Deeper within the aquifer, organic material may begin to “coalify” generating methane and carbon dioxide. This additional carbon dioxide converts to bicarbonate and permits the sodium and bicarbonate concentrations to increase to high concentrations with little or no pH change. This reaction creates more reducing conditions. Nitrate and sulfate which may be present in the outcrop will be reduced to negligible amounts.

6. These reactions that are associated with the formation of the sodium-bicarbonate water (increasing sodium and bicarbonate, increasing and flattening of pH, loss of calcium, loss of nitrate and sulfate) are evident in: a) the Wilcox Group of the Carrizo-Wilcox Aquifer in east Texas, the Simsboro Formation (Wilcox Group) of the Carrizo-Wilcox Aquifer in central Texas and the Carrizo Sand Formation portion of the Carrizo-Wilcox Aquifer in the Gonzales Transect and the South Transect, b) the Queen City Aquifer in the east transect, the Central Transect (along the Brazos River) and the South Transect and c) the Sparta Aquifer in the east and Central Transects but not in the Gonzales or the South Transects. These processes are consistent for each of their aquifers and consistently occur with both increasing depth and location of the well whether it be in the outcrop or in the downdip confined part of an aquifer. That is, the groundwater evolves from a low-pH, oxidizing, calcium, magnesium, sulfate, chloride type water in the outcrop to a reduced high pH, sodium-bicarbonate water down the hydraulic gradient into the deep subsurface.
7. Because of the consistency of the water chemistry and its location within the aquifer, the chemistry of the water in these sodium-bicarbonate waters can be accounted for by intra-aquifer geochemical reactions. The occurrence of the sodium-bicarbonate type does not require the addition of a new water from an external source (e.g., cross-formational flow).

The Queen City Aquifer in the Gonzales Transect does not evolve to a bicarbonate dominated water. Similarly the Sparta Aquifer in the Gonzales and South Transect remains a chloride-sulfate type water. These three aquifers in their different transect areas are underlain by the very fresh sodium-bicarbonate water in the Carrizo Sand. The water chemistry for these aquifers do not support the concept of significant leakage of the underlying Carrizo Sand into these aquifers.

The Yegua-Jackson Aquifer from central Texas to south Texas is predominantly a sodium-chloride-sulfate type water. Groundwater production is primarily in the outcrop and not downdip. The source of this chemistry is not known, but it has not been impacted by the leakage of a deeper sodium-bicarbonate water. The total dissolved solids for the groundwater in the Yegua-Jackson often is higher than underlying aquifers. Underlying aquifers therefore are not leaking into the Yegua-Jackson Aquifer and causing lower total dissolved solids waters.

The Brazos River Alluvium Aquifer along the Brazos River in Groundwater Management Area 12 has a calcium-magnesium-bicarbonate composition. None of the Tertiary-aged aquifers beneath the Brazos River Alluvium Aquifer, Carrizo-Wilcox, Queen City, Sparta or Yegua-Jackson have that type of water either in their subcrop immediately beneath the alluvium or within their confined section beneath the alluvium. Therefore there is no water chemistry evidence of upward leakage from deeper Tertiary-aged aquifers into the Brazos River Alluvium Aquifer. The water chemistry from the three nests of San Antonio Water System wells in Gonzales County further documents the lack of cross formation flow between the Carrizo-Wilcox, the Queen City and the Sparta aquifers. The water chemistry and isotope chemistry for each of these nests of wells are different for the different aquifers, but consistent for the Carrizo-Wilcox, Queen City and Sparta aquifers for all three nests.

This observation that overlying or underlying adjacent aquifers do not impact the water chemistry of an aquifer does not take into account possible chemistry changes that may occur as water leaks through aquitards on its way from one aquifer to another. Aquitards are not typically produced as a groundwater supply, therefore there is no chemistry databased for the typical

aquitard (e.g., the Reklaw Formation or Queen City Aquifer, Calvert Bluff or Cook Mountain Formation). This is a limiting factor in trying to see cross-formational flow.

Total dissolved solids for most of the aquifers increase with depth. Much of the increase is caused by sodium and bicarbonate though some is also attributable to the addition of sodium-chloride. This can best be seen on the graphs for the Carrizo-Wilcox Aquifer in the Gonzales Transect and the South Transect where increases in chloride occur in the deeper parts of the aquifer. Historically, the downdip extent of meteoric water has been mapped as a 1,000 or 3,000 mg/L contour waters farther downdip were considered to be formation waters of much higher total dissolved solids that have possibly migrated updip by geopressure forces deeper in these formations.

The increase in chloride indicates the presence of a mixing zone of meteoric groundwater (updip) and deeper more saline water (downdip). The 1,000 mg/L total dissolved solids contour is caused primarily by increases in bicarbonate and not increases in chloride. There has to be a downdip extent of meteoric groundwater, but it is not defined as a total dissolved solids contour of 1,000 mg/L. It is deeper than has previously been mapped.

The carbon-14 ages of groundwater characteristically are younger in the outcrop and older downdip in the confined section of an aquifer. A “correct” estimate of the age of a water requires knowing more than just the activity of carbon-14. These waters are waters that chemically evolved from the outcrop to their dip parts by the addition of sodium and bicarbonate.

Bicarbonate concentrations may increase from less than 50 parts per million to 500 parts per million. Part of this increase in bicarbonate is through the addition of “dead” (no carbon-14) from the aquifer matrix itself. The addition of dead carbon will result in an older carbon-14 age if the carbon-14 age is not corrected to subtract this dead addition. The corrected carbon-14 dates in this report are the best that are technically available. This is achieved either with a  $\delta^{13}\text{C}$  correction technique or a  $\delta^{13}\text{C}$  plus geochemical modeling approach. Where enough data were available to describe quantitatively the chemical reactions of the water, then this modeling approach was used. When only a  $\delta^{13}\text{C}$  value was available to correct the date then this approach followed. If the  $\delta^{13}\text{C}$  did not help in the correction, the only apparent carbon-14 value is given.

Through the text of this report, the approach used to estimate the age is given. Most of the efforts in age dating of the water were for the Wilcox Group in east Texas, the Simsboro Formation in the Central Transect, the Carrizo Sand Formation in the Gonzales and South Transects, where we had the best understanding of the geochemical reactions involved in the formation of sodium-bicarbonate waters. Ages increased from the outcrop, where a carbon-14 date was modern to the farthest downdip wells sampled that had no measurable carbon-14 and an inferred age of at least 40,000 years before present. In large part the Carrizo-Wilcox to Yegua-Jackson aquifers contain old water.

The “best” carbon-14 dates are estimated where there is enough well data to construct flow paths and where the evolution of chemistry can be evaluated, where only one or two wells could be sampled for an aquifer in a region less interpretation of age can be made.

There is an interesting comparison between the carbon-14 ages of the Carrizo Sand Formation waters in the Gonzales Transect and the South Transect. For both transects there is a gradual increase in age from the outcrop to measurable carbon-14 values at intermediate depths to very low carbon-14 percent modern at the deepest wells. In contrast, the carbon-14 ages for the

Simsboro Formation (Wilcox Group) of the Carrizo-Wilcox Aquifer in wells in the Central Transect gets old (20,000 years plus) immediately (4 miles) downdip from the outcrop.

A comparison of the downdip extent of the higher calcium in the Carrizo Sand Formation versus the Simsboro Formation is similar to the carbon-14 age distribution just discussed. In the Gonzales Transect and the South Transect higher calcium values are observed about 20 miles downdip from the outcrop. For the Central Transect, the higher calcium values occur primarily in the outcrop and not downdip in the confined section.

A hydrogeologic implication to this difference of carbon-14 ages and downdip measurement of calcium between the South and Central Transects is that Carrizo Sand Formation groundwater in the South Transect is actively flowing from the outcrop into the deep subsurface. In the South Transect the more active part of the flow system is partly blocked by the faulting through the Carrizo Sand Formation in the Charlotte, Jourdanton and Pleasanton Trough in Atascosa County. In the Central Transect, much of the active flow may be contained to the outcrop with discharge to the numerous streams and rivers that cross or headwater in the outcrop. Faulting in or near the Wilcox Group outcrop may also limit downdip flow. There may only be limited flow into the deeper confined parts of the aquifer.

This concept of more recharge flowing to the confined section of the aquifer in south Texas is counterintuitive to the idea of more precipitation and less evapotranspiration in east Texas than in south Texas. The much higher transmissivities for the Carrizo Sand Formation in south Texas than for the Simsboro Formation or Wilcox Group in those areas north of the Colorado River may permit more recharge to occur into the deeper subsurface in south Texas and more lateral flow in the outcrop to occur in central and east Texas.

Groundwater is flowing from the outcrop into the subsurface of the Carrizo Sand Formation for the Gonzales Transect and the South Transect. This observation is based on the potentiometric surface, the presence of elevated calcium in the confined section and the gradual increase in carbon-14 ages for both the South Transect and in the Gonzales Transect. Although there is no obvious geochemical evidence for cross formation flow from deeper units to shallower units, groundwater is flowing from shallower to deep, leaving us with the inexorable problem of how to discharge the buildup of groundwater at depth when it intersects the deep saline formation waters that must be flowing up the structural dip from deeper geopressed zones (Galloway, 1982 and Dutton and others, 2006).

The water chemistry in the brackish Lower Wilcox Group wells in the Bexar and Atascosa counties appears unique in comparison to other aquifers studied in this project. The sodium-sulfate water type for the brackish wells is similar only to waters in Yegua-Jackson Aquifer. The carbon-14 percent modern indicates “old” water in both the outcrop and downdip. No chemical or isotopic evolution is observed for the water chemistry for the brackish Lower Wilcox Group as was observed in the other aquifers in this study.

The results of this study generally confirm the conceptual models for the Queen City and Sparta and Yegua-Jackson GAMs. However, there are several questions that have not been answered by evaluating the hydrochemical and isotopic data. First, due to lack of sufficient and/or appropriate deep wells for sampling, the downdip flow conditions in all the aquifers is still in question. The estimates of groundwater age generally confirm the conceptual model assumption that recharge occurs on the outcrop of the aquifers and that some portion of that recharge moves downdip over time. However, the nature of the flow deep in the aquifers is still not fully understood and this

study has not provided any hard evidence regarding the conceptualization of the downdip boundary condition for the aquifers.

Groundwater age estimates from the two-dimensional cross-sectional flow models did not compare well to estimated carbon-14 age estimates. It is uncertain why there is such a discrepancy between the groundwater age estimated from the 2-dimensional modeling and the isotopic data. Factors might include bad modeling assumptions, parameters and/or boundary conditions, as well as sea level changes and the dynamics of overburden that were not accounted for in the models.

Determining the volume of vertical flow between aquifers based on the hydrochemical and isotopic data is complicated by that fact that there is no well definable chemical signature specific to one aquifer. The chemical evolutionary pathways must be evaluated to see whether the chemistry on an intra-aquifer basis is consistent or can only be explained by the addition of a new groundwater with a distinct chemical signature. The addition of this new chemistry from another aquifer in large part was not seen during this study, which indicates either it is not occurring in volume that can be identified in the hydrochemical and isotopic data or that the chemistry is not the best tool to discern cross-formational flow. Aquitard chemistry could impact water chemistry patterns, but there is a paucity of chemical data from the aquitards. The aquifer chemistry data does not disprove cross-formational flow, but conversely it does not necessarily help quantify the amount of cross-formational flow.

*This page is intentionally blank.*

## **10 Acknowledgements**

LBG-Guyton would like to acknowledge the many people and organizations without whom this project would not have been possible. Our gratitude is extended to the Texas Water Development Board for providing the funding for this project. Specifically, would like to thank Cindy Ridgeway, who served as the TWDB contract manager, and Larry French, the director of the Groundwater Division of the TWDB for their input during the technical review process and the review of the draft report.

This project could not have been completed without the dedication and effort of the project team and its members. Our thanks to Rosemary Wyman and staff at Baer Engineering, Inc., for organizing and directing the field work involving sampling of over 50 wells for this project; to the numerous municipalities and water supply corporations who provided and coordinated access to their wells for the sampling effort; and to the laboratory staff at San Antonio Testing Labs, Zymax Laboratory, Beta Analytic, and the University of Arizona.

Thanks also to Marcie Pellegrino for review and assembly of the draft and final reports; Kristie Laughlin for developing hydrogeologic cross-sections; and to Radu Boghici for helping assimilate data and performing quality control on the databases.

*This page is intentionally blank.*

## 11 References

- Boghici, R., 2009, Water quality in the Carrizo-Wilcox aquifer 1990-2006: Texas Water Development Board Report 372, 33 p.
- Busenberg, N.E., and Plummer, L., 1985, Kinetic and thermodynamic factors controlling the distribution of SO<sub>3</sub><sup>2-</sup> and Na<sup>+</sup> in calcites and selected aragonites: *Geochimica et Cosmochimica Acta*, Vol 49, Iss. 3, p. 713-725.
- Chapelle, F.H., and McMahon, P.B., 1991, Geochemistry of dissolved inorganic carbon in a Coastal Plain aquifer. 1. Sulfate from confining beds as an oxidant in microbial CO<sub>2</sub> production: *Journal of Hydrology*, Vol. 127, p. 85-108.
- Chowdhury, A.H., Osting, T., Furnans, J., and Mathews, R., 2010, Groundwater-surface water interaction in the Brazos river basin: evidence from lake connection history and chemical and isotopic compositions: Texas Water Development Board Report 375, 61 p.
- Cronin, J.G., and Wilson, C.A., 1967, Groundwater in the flood-plain alluvium of the Brazos river, Whitney Dam to vicinity of Richmond, Texas: Texas Water Development Board Report 41, 206 p.
- Deeds, N.E., Fryar, D., Dutton, A.R., Nicot, J., 2009, Hydrogeology of the Carrizo-Wilcox Aquifer *in* Hutchison, W.R., Davidson, S.C., Brown, B.J., and Mace, R.E., eds., *Aquifers of the Upper Coastal Plains of Texas*: Texas Water Development Board Report 374, p. 35-60.
- Deeds, N., Kelley, V., Fryar, D., Jones, T., Whallon, A.J., and Dean, K.D., 2003, Groundwater Availability Model for the Southern Carrizo-Wilcox Aquifer: contract report by Intera and Parsons to the Texas Water Development Board, 529 p.
- Deeds, N.E., Yan, T., Singh, A., Jones, T.L., Kelley, V.A., Knox, P.R., and Young, S.C., 2010, Final Report: Groundwater Availability Model for the Yegau-Jackson aquifer: prepared for the Texas Water Development Board, March 2010, 582 p.
- Dutton, A.R., Nicot, J., and Kier, K.S., 2006, Hydrodynamic convergence of hydropressured and geopressured zones, Central Texas, Gulf of Mexico Basin, USA: *Hydrogeology Journal* v. 14, issue 6, p. 859-867.
- Dutton, A.R., Harden, B., Nicot, J., and O'Rourke, D., 2003, Groundwater Availability Model for the central part of the Carrizo-Wilcox aquifer in Texas: contract report by R. W. Harden and Associates, Inc., HDR Engineering Services, Inc., and the Bureau of Economic Geology, The University of Texas at Austin to the Texas Water Development Board, 295 p.
- Fenske, J.P., Leake, S.A. and Prudic, D.E., 1996. Documentation of a Computer Program (RESI) to Simulate Leakage from Reservoirs Using the Modular Finite-Difference Ground-Water Flow Model (MODFLOW). U.S. Geological Survey Open-File Report 96-364, 51 p.
- Fogg, G.E., and Kreitler, C.W., 1982, Ground-water hydraulics and hydrochemical facies in Eocene aquifers of the East Texas Basin. The University of Texas at Austin, Bureau of Economic Geology Report of Investigations No. 127, 75 p.
- Fogg, G.E., Kaiser, W.R., and Ambrose, M.L., 1991, The Wilcox Group and the Carrizo Sand (Palogene) in the Sabine Uplift Area, Texas: Ground-water Hydraulics and Hydrochemistry: Bureau of Economic Geology, The University of Texas at Austin, 70 p.

- Fogg, G.E., Seni, S.J., and Kreitler, C.W., 1983, Three-Dimensional ground water modeling in depositional systems, Wilcox Group, Oakwood salt dome area, East Texas: The University of Texas at Austin, Bureau of Economic Geology Report of Investigations No. 133, 55 p.
- Foster, M.D., 1950, The origin of high sodium bicarbonate waters in the Atlantic and Gulf Coastal Plains: *Geochem. Cosmochim. Acta*, vol. 1, p. 33-48.
- Fryar, D., Senger, R., Deeds, N., Pickens, J., Jones, T., Whallon, A.J., and Dean, K.D., 2003, Groundwater Availability Model for the Carrizo-Wilcox aquifer: contract report by Intera and Parsons to the Texas Water Development Board, 529 p.
- Galloway, W.E., Ganey-Curry, Li and Butler, 2000, Cenozoic depositional history of the Gulf of Mexico basin: *American Association of Petroleum Geologists Bulletin*, Vol. 84, No. 11, p. 1743-1774.
- Galloway, W.E., 1982, Epigenetic zonation and fluid flow history of uranium-bearing fluvial aquifer systems, South Texas uranium province: The University of Texas at Austin, Bureau of Economic Geology, Report of Investigations No. 119, 31 p.
- Galloway, W.E., Liu, X., Travis-Neuberger, D., and Xue, L., 1994, Reference high-resolution correlation cross sections, Paleogene section, Texas coastal plain: Bureau of Economic Geology, The University of Texas at Austin, 19 p. + 6 Figs.
- Grossman, E.L., Hahn, R.W., and Fritz, S.J., 1986, Origin of gaseous hydrocarbons in the Sparta aquifer in Brazos and Burleson counties, Texas: *Gulf Coast Association of Geologic Societies*, Vol. 36, p 457-470.
- Grossman, E.L., Coffman, B.K., Fritz, S.J., and Wada, H., 1989, Bacterial production of methane and its influence on ground-water chemistry in east-central Texas aquifers: *Geology*, Vol. 17, p 495-499.
- Guevara, E.H., and Garcia, R., 1972, Depositional systems and oil-gas reservoirs in the Queen City formation (Eocene), Texas: *Gulf Coast Association of Geological Societies Transactions*, Vol. 22, 22 p.
- Hamlin, H.S., 1988, Depositional and ground-water flow systems of the Carrizo-Upper Wilcox, South Texas: The University of Texas at Austin, Bureau of Economic Geology, Report of Investigations No. 175, 61 p.
- Hargis, R., 2009, Stratigraphic investigation of the Wilcox Group, South Texas: contract report for Underground Water Conservation District.
- Harrison, W.J. and Summ, L.L., 1991, Paleohydrology of the Gulf of Mexico basin. *American Journal of Science*, Vol. 291, p. 109-176.
- HDR Engineering, Inc., 2004, South-central Carrizo system groundwater model, SAWS Gonzales-Carrizo project: prepared for San Antonio Water Systems, 211 p.
- Hem, J.D., 1986, Study and interpretation of the chemical characteristics of natural water, (3<sup>rd</sup> ed.): U. S. Geological Survey Water-Supply Paper 2254, variously paginated.
- Henry, C.D., Basciano, J.M., and Duex, T.W., 1980, Hydrology and water quality of the Eocene Wilcox Group: significance for lignite development in East Texas: Bureau of Economic Geology, The University of Texas at Austin, *Geologic Circular* 80-3, 9 p.

- Kaiser, W.R., 1978. Depositional systems in the Wilcox Group (Eocene) of east-central Texas and the occurrence of lignite *in* proceedings 1976 Gulf Coast Lignite Conference: Geology, Utilization, and Environmental Aspects, W.R. Kaiser, ed. The University of Texas at Austin, Bureau of Economic Geology, Report of Investigations No. 90, p. 283.
- Kelley, V.A., Deeds, N.E., Fryar, D.G., Nicot, J-P. and others., 2004, Groundwater Availability Models for the Queen City and Sparta aquifers: contract report by Intera Inc., and the Bureau of Economic Geology, The University of Texas at Austin to the Texas Water Development Board, October 2004, 867 p.
- Kelly, V., Fryar, D., and Deeds, N.E., 2009, Hydrogeology of the Queen City and Sparta aquifers with an emphasis on regional mechanisms of discharge *in* Hutchison, W.R., Davidson, S.C., Brown, B.J., and Mace, R.E., eds., Aquifers of the Upper Coastal Plains of Texas: Texas Water Development Board Report 374, p. 87-116.
- Klemt, W.B., Duffin, G.L., Elder, G.R., 1976, Ground-water resources of the Carrizo aquifer in the Winter Garden area of Texas, Vol. 1, Texas Water Development Board Report 210, 30 p.
- Kreitler, C.W., 1989, Hydrogeology of sedimentary basins: Bureau of Economic Geology, The University of Texas at Austin, Journal of Hydrology, Vol 106, pp. 29-53.
- Kreitler, C.W., Guevera, E., Granata, G., and McKalips, D., 1977, Hydrogeology of the Gulf Coast aquifers, Houston-Galveston area, Texas: Transactions—Gulf Coast Association of Geological Societies, Vol. 27, p. 72–89.
- Kreitler, C.W., and Morrison, K.H., 2009, Evaluation of the brackish groundwater resources of the Wilcox aquifer in the San Antonio, Texas area *in* Hutchison, W.R., Davidson, S.C., Brown, B.J., and Mace, R.E., eds., Aquifers of the Upper Coastal Plains of Texas: Texas Water Development Board Report 374, p. 167-178.
- Kreitler, C.W. and Pass, D., 1980, Carbon-14 dating of Wilcox aquifer groundwater *in* Kreitler, C.W. and others., Geology and Geohydrology of the East Texas Basin: Bureau of Economic Geology, The University of Texas at Austin, Geologic Circular 80-12, p. 79-82.
- Kreitler, C.W. and Senger, R.K., 1991, Wellhead protection strategies for confined aquifer settings: contract report, Ground-water Protection Division, Office of Ground Water and Drinking Water, U.S. Environmental Protection Agency, 183 p.
- Kreitler, C.W. and Wuerch, U., 1981, Carbon-14 dating of ground water near Oakwood Dome *in* Kreitler, C.W. and others., Geology and Geohydrology of the East Texas Basin: Bureau of Economic Geology, The University of Texas at Austin, Geologic Circular 81-7, p. 156-161.
- LBG-Guyton Associates, 2003, Brackish groundwater manual for Texas regional water planning groups: Report prepared for the Texas Water Development Board, Austin, Texas, 188 p.
- LBG-Guyton Associates, 2008, Data from test wells for SAWS brackish Wilcox groundwater investigation southern Bexar and northern Atascosa counties, Texas: prepared for the San Antonio Water System, 16 p. + 30 Figs.
- McCoy, W.T., 1991, Evaluation of ground-water resources of the western portion of the Winter Garden area, Texas: Texas Water Development Board Report 334, 64 p.

- Meisler, H., Miller, J.A., Knobel, L.L., and Wait, R.L., 1988, Region 22, Atlantic and Eastern Gulf Coastal plain: The Geology of North America, Vol. O-2, Hydrogeology, The Geological Society of America, 524 p. + 3 plates.
- Nance, H.S. III., 2010, Controls on and uses of hydrochemical and isotopic heterogeneity in the Plateau aquifer system, contiguous aquifers, and associated surface water, Edwards Plateau region, Texas: Ph.D. Dissertation, The University of Texas at Austin, 2010, 300 p.
- Pearson, F.J., Jr., 1966, Ground-water ages and flow rates by the carbon-14 method: Ph.D. Dissertation, The University of Texas at Austin, p. 97.
- Pearson, F.J., Jr., and White, D.E., 1967, Carbon-14 ages and flow rates of water in Carrizo Sand, Atascosa County, Texas: Water Resources Research, Vol. 3, p. 251-261.
- Plummer, L.N., Busby, J.F., Lee, R.W., and Hanshaw, B.B. 1990, Geochemical modeling of the Madison aquifer in parts of Montana, Wyoming, and South Dakota: Water Resources Research Vol. 26, 1981-2014.
- Plummer, L.N, Prestemon, E.C., and Parkhurst, D., 1994, An interactive code (NETPATH) for modeling NET geochemical reactions along a flow PATH, version 2: U. S. Geological Survey, Water Resources Investigation Report 94-4169, 130p.
- PRISM (2000). Average Annual Precipitation. Prism.oregonstate.edu. Retrieved February 17, 2013, from <http://www.prism.oregonstate.edu/pub/prism/maps/Precipitation/Total/States/TX/tx.gif>
- Prudic, D.E., 1988, Documentation of a computer program to simulate stream-aquifer relations using a modular, finite-difference, ground-water flow model: U.S. Geological Survey, Open-File Report 88-729, 113 p.
- Reedy, R.C., Nicot, J., Scanlon, B.R., Deeds, N.E., Kelley, V., and Mace, R.E., 2009, Recharge in the Carrizo-Wilcox aquifer *in* Hutchison, W.R., Davidson, S.C., Brown, B.J., and Mace, R.E., eds., Aquifers of the Upper Coastal Plains of Texas: Texas Water Development Board Report 374, p. 161-166.
- Richter, B.C. and C.W. Kreitler, 1993, Geochemical techniques for identifying sources of ground-water salinization: Boca Raton, FL, CRC Press, Inc., 258p.
- Sanford, W.E. and Selnick, D.L., 2013, Estimation of evapotranspiration across the conterminous United States using a regression with climate and land-cover data: Journal of the American Water Resources Association, Vol. 49, No. 1, February 2013.
- Saunders, G.P., 2009, Low-flow gain-loss study of the Colorado River in Bastrop county, Texas *in* Hutchison, W.R., Davidson, S.C., Brown, B.J., and Mace, R.E., eds., Aquifers of the Upper Coastal Plains of Texas: Texas Water Development Board Report 374, p. 161-166.
- Shah, S.D., Houston, N.A., and Braun, C.L., 2007, Hydrogeologic Characterization of the Brazos River Alluvium Aquifer, Bosque County to Fort Bend County, Texas
- Texas Water Development Board, 2013, Groundwater Database, <http://www.twdb.state.tx.us/groundwater/data/gwdbbrpt.asp>.
- Thorkidsen, D., and Price, R.D., 1991, Ground-Water Resources of the Carrizo-Wilcox Aquifer in the Central Texas Region: Texas Water Development Board Report 332.

TDWR, 1983, Climatic Atlas of Texas, Larkin, T.J. and G.W. Bomar, Report LP-192,  
William F. Guyton and Associates, 1970, Groundwater Conditions in Angelina and Nacogdoches  
Counties, Texas: Texas Water Development Board Report 110.

## **Appendix A**

### **Chemical Analysis**

**(Includes Data Collected Previously by TWDB & New Data  
Collected During This Study)**

**Electronic Deliverables Only**

*This page is intentionally left blank*

## **Appendix B**

### **Field Notes and Lab Reports Electronic Deliverables Only**

*This page is intentionally left blank*